



**EUROPEAN HYDROGEN ENERGY
CONFERENCE 2014**

Proceedings

Organizer

AeH₂

Spanish Hydrogen Association
www.aeh2.org

Under the auspices of

EHA
EUROPEAN HYDROGEN ASSOCIATION



EUROPEAN HYDROGEN
ENERGY CONFERENCE 2014

Organizer



Spanish Hydrogen
Association

Platinum sponsor

ABENGOA HIDROGENO

Gold sponsor



Silver sponsor



Collaborators



Media partners



Chairman Welcome Letter

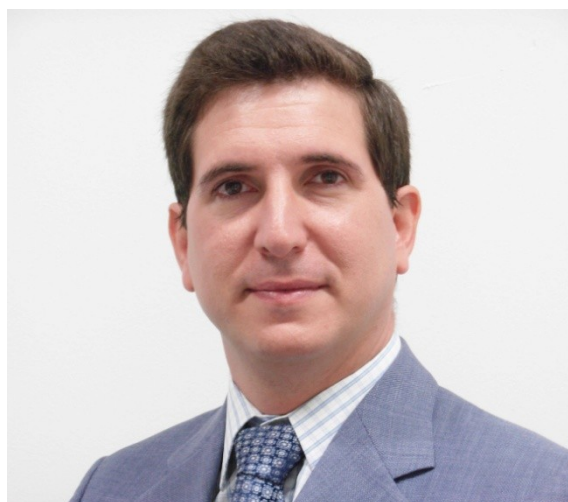
Dear friends and colleagues from the hydrogen and fuel cell sector, as Chairman of the Organizing Committee of EHEC 2014, and of the Spanish Hydrogen Association, it is my pleasure to invite you to this edition of the event, held from 12th to 14th of March 2014 in our beautiful city of Seville.

The European Hydrogen Energy Conference is, without doubt, the European reference framework for updates on hydrogen and fuel cell related technologies, and the best setting to present the advances in research, products and projects we are all developing in the sector.

With the more traditional economic activities in a crisis situation, there can be no doubt that our technologies are going to contribute to the creation of markets, prosperity and opportunities and, unquestionably, new jobs in our home countries and regions. We must demonstrate that we have viable projects, mature technologies and products that provide solutions. It is the great opportunity we have been waiting for and we want to share it with you at EHEC 2014!

Led by the Scientific Committee, we have selected the fields and subjects we believe will be of most interest to our community. In this respect, the plenary sessions are sure to arouse the expectations of all, for their topicality and relevance.

As a native of Seville, I would also like to inform you that March is one of the nicest months to visit the city, when orange blossom and jasmine are in bloom; I would encourage some sightseeing in this ancient city whenever this exciting conference is not occupying all your time here.



Very truly yours...

Javier Brey Sánchez

Chairman of the Spanish Hydrogen Association

The Spanish Hydrogen Association

The Spanish Hydrogen Association (AeH2) is a non-profit organization that has as main aim the promotion of hydrogen technology development as an energy carrier, and its use in industrial and commercial applications.



AeH2 members are the most active Spanish companies, public and private institutions and researchers in hydrogen technology, with a common interest: opening markets and social and environmental benefits of introducing hydrogen and fuel cells in the energy systems.

AeH2 members have developed strong capabilities in hydrogen and fuel cell technologies.

The AeH2 has shown itself as an important and visible actor in the hydrogen community in Spain and abroad and will play an important role in this emerging industry.

The Spanish Hydrogen Association supports research, development, demonstration and market introduction of hydrogen energy. To reach its aims the AeH2 carries out different activities:

- Information and dissemination.
- Expertise and promotion.
- Organization and participation in conferences, seminars and meetings.
- Promotion and education.
- Lobby work for hydrogen and fuel cells.
- Facilitates contacts to companies from Spain and abroad.
- Provides networking forums for the exchange of ideas.

The AeH2 has promoted the creation of the AEN/CTN 181 of “Hydrogen Technologies” and participates in the International Committee ISO/TC 197 “Hydrogen Technologies”.

AeH2 cooperate with other Associations from Europe and abroad. AeH2 is a member of:

- European Hydrogen Association – EHA
- International Association for the Hydrogen Energy – IAHE
- Partnership for Advancing the Transition to Hydrogen - PATH
- AeH2 collaborate with the Canadian Hydrogen and Fuel Cell Association.

The Association plays an important role promoting activities for the hydrogen community and its relations with organizations or authorities, either international or Spanish, and in strategic, legislative and regulatory issues.

The AeH2 has promoted the Spanish Technological Platform for Hydrogen and Fuel Cells, active since May 2005. The Platform works on the national strategic policy in technological fields for hydrogen and fuel cells.

For more info www.aeh2.org / www.ptehpc.org

Plenary Sessions

All Plenary Sessions will take place in the Main Hall (Room A).

Plenary Session 1:

Transport applications - H2 infrastructure deployment in Europe

Wednesday March 12th, 10:30-12:00h

Chairperson Plenary 1: Mr. Bert De Colvenaer (FCH JU Executive Director)

- **Dr Joan M. Ogden (Univ. California-Davis): Analysis of the hydrogen infrastructure deployment in USA**

Dr. Joan Ogden is Professor of Environmental Science and Policy at the University of California, Davis and Director of the Sustainable Transportation Energy Pathways Program at the campus's Institute of Transportation Studies. Her primary research interest is technical and economic assessment of new energy technologies, especially in the areas of alternative fuels, fuel cells, renewable energy and energy conservation. Her recent work centers on the use of hydrogen as an energy carrier, hydrogen infrastructure strategies, and applications of fuel cell technology in transportation and stationary power production. She has served on California state committees on hydrogen and greenhouse gas issues, the USDOE Hydrogen Technical Advisory Committee, the IPCC panel on Renewable Energy, and on National Academies committees assessing hydrogen fuel cell and plug-in hybrid vehicles. She holds a BS in mathematics from the University of Illinois, and a Ph.D. in theoretical physics from the University of Maryland.



- **Dr Steffen Moller-Holst (Sintef): Hydrogen infrastructure deployment in Europe- towards full coverage in 2050?**

Dr. Steffen Møller-Holst earned his PhD on PEM Fuel Cells (1996), was engaged at Los Alamos National Laboratory, NM, USA 1997-99, and has since 2001 been employed at SINTEF with responsibility for a significant project portfolio within H₂ & Fuel Cell. Currently, Møller-Holst is (N.ERGHY)-Chair for the Transport Pillar (FCH2 JU) and Chairman for the Hydrogen Council and thereby advisor to the Norwegian Government.



- **Dr. Jörg Wind (Daimler AG EU-Projects and Energy Systems Analyses): “Progress on FCEV development and conditions for FCEV market introduction”**

Dr. Jörg Wind has studied physics at the Technical University of Munich (TUM). After doing his Ph.D. in the field of semiconductor physics and sensor technology at the TUM in 1992, he started working in the field of fuel cells and hydrogen. As a project manager, he was responsible for material development for high temperature fuel cells and exhaust aftertreatment at DASA and DaimlerChrysler from 1992 until 1998. From 1998 until 2002, he was responsible for PEM stack development at DaimlerChrysler. Since 2002, he is responsible for strategic energy projects and EC funded projects, comprising projects in the field of fuel cell vehicles and battery electric vehicles (including energy systems analyses and WTW-analyses). He has been involved in the setup of the FCH JU from the beginning on and is currently vice chair of the NEW-IG transportation committee.



- **Dr. Lars Peter Thiesen (General Motors): " Electric Mobility with Hydrogen – Five Years of Experience in Field Operation"**

Dr. Lars Peter Thiesen began his career at Opel in 1998 at the Fuel Cell Activities department (FCA). Since then, he held various positions and responsibilities, including GM/Opel’s hydrogen and fuel cell deployment strategy for Europe. Currently, he is responsible for future mobility, technology strategy and regulations within General Motors’ European public policy department. Prior to his career at Opel, Lars Peter Thiesen worked as a scientist at the University of Kiel, Germany specialized in renewable energies. He holds a PhD in Natural Sciences (Physics).



Plenary Session 2:

Programmatic situation - from Joint Undertaking to Horizon 2020

Wednesday March 12th, 12:00-12.40h

- **Mr Bert de Colvenaer (FCH JU Executive Director): The Fuel Cells and Hydrogen Joint Undertaking : Towards the Deployment of Fuel Cells and Hydrogen Technologies.**

Bert De Colvenaer was appointed as the Executive Director of the Fuel Cells and Hydrogen Joint Undertaking as from 1 September 2010. As Executive Director, he is the legal representative of the FCH JU and the chief executive responsible for the day-to-day management of the FCH JU, in accordance with the decisions of the Governing Board. Supported by the staff of the Programme Office, this includes : manage the launch of the calls for project proposals and the evaluation and selection of projects; monitor and update the Multi-Annual Implementation Plan of the FCH JU; coordinate with other relevant programmes at national and regional levels; and communicate information on FCH JU activities.

Bert De Colvenaer has been involved for more than 20 years in the automotive industry in the field of power-train production engineering and advanced research. He has been working on fuel cell research from the early 90's and was involved in high level group activities and major EU research projects. In 2002 he established and led the Advanced Technology Division of Toyota Europe, focusing on breakthrough research in the field of robotics, fuel cell and hydrogen and new automotive production technologies.

Bert De Colvenaer's academic background is in mechanical engineering and industrial management.



Plenary Session 3:

H2&FC opportunities in the Mediterranean area

Thursday March 13th, 08:30-10:00h

Chairperson Plenary 3: Ms. Marieke Reijalt (EHA Executive Director)

- **Mr Vicente Fernandez Guerrero, Secretary General of Industry (JUNTA DE ANDALUCÍA)**

Vicente Fernández Guerrero was born in Malaga in 1973. He has a degree in law from the University of Seville and entered by public examination in the Lawyers Team of the Andalusian Government in 1999. Currently he is the General Secretary of Innovation, Industry and Energy of the regional ministry of Economy, Innovation, Science and Employment. He has been at the forefront of law offices of the regional ministries of Tourism and Sport; Education and Science; Economy and Finance; and Economics, Innovation, Science and Employment. He has also worked at the Tax Agency of Andalusia and at the Advisory Area of the Andalusian Government. Vicente Fernandez is also the president of the Andalusian Energy Agency.



- **Dr Athanasios Konstandopoulos (APT Laboratory, CPERI/CERTH): Carbon Neutral Solar Fuel Technology**

Dr. Konstandopoulos is a specialist in aerosol technology and structured reactors for energy, environmental and biotech applications. He has coordinated and managed numerous research projects, funded by the European Commission and leading international industries. He is the recipient of the 2006 European Descartes Prize, the 2010 European Research Council Advanced Grant, a Fellow of the Society of Automotive Engineers, author of numerous widely cited publications and member of the Board of Governors of the European Commission's Joint Research Center.



- **Mr Khalid Benhamou (Sahara Wind Inc.): The role of Hydrogen from the trade winds in North Africa's broader renewable energy transition**

As Engineer from California Polytechnic (1992), Khalid Benhamou installed in 1994 Morocco's first hybrid wind/diesel system on the Sahara trade windblown coastline. With co-funding from NATO in support of the large Sahara Wind 5 GW-HVDC transmission Project, he conducted regional wind measurements and deployed Africa's first wind-hydrogen systems in Morocco and Mauritania's universities.



Plenary Session 4:

Generation & Storage Energy

Friday March 14th, 08:30-10:00h

Chairperson Plenary 4:TBC

- **Dr Ulrich Bünger (Ludwig-Bölkow-Systemtechnik GmbH): Large –scale storage of hydrogen. Problem of energy storage. Analysis of the European situation**

Dr. Ulrich Bünger M.Sc., Dr.-Ing., is with LBST since 1990. His fields of experience are: project management of techno-economic feasibility studies on hydrogen energy and fuel cell systems, well-to-wheel studies on alternative vehicle fuels and co-ordination of international strategy projects for industry and politics. Coordinator of the WtW analysis for the German Transport Energy Strategy (TES), analysis of hydrogen vehicle storage systems and market potential of small residential fuel cell systems for Germany. Coordination of the European projects Thematic Network on Hydrogen Energy (HyNet), the European Hydrogen Energy Roadmap project (HyWays) and the planning activity for future European Transport Demonstration Projects (HyLights). Degrees in mechanical engineering from Hannover University (Germany), Georgia Institute of Technology (USA) with sabbaticals at Purdue University (USA) and Technical University of Norway. From 2002 until 2012 Associate Professor for hydrogen energy systems at the Technical University of Norway in Trondheim.



- **Mr Anthony Leo: (Vice President -Applications Engineering and Advanced Technology Development. Fuel Cell Energy): Stationary Power Generation with Fuel Cells**

Anthony (Tony) Leo has played key leadership roles in development and commercialization of electrochemical systems for more than 30 years. He is currently responsible for Application Engineering and Advanced Technology Development at FuelCell Energy, Inc., an integrated fuel cell company which manufactures, installs, and services fuel cell powerplants around the world.



- **Dr Michael Hirscher (Max Planck Institute for Intelligent Systems): State of the art and trends in material development for hydrogen storage**

Michael Hirscher is group leader “Hydrogen storage” at the Max Planck Institute for Intelligent Systems, Stuttgart, Germany. He studied physics at University of Stuttgart, Germany and Oregon State University, USA, and was awarded the Otto Hahn Medal of the Max Planck Society in 1988. Recently, he edited the “Handbook of Hydrogen Storage” and is operating agent of IEA-HIA Task 32 “Hydrogen-based energy storage” since 2013.



Organizing Committee

Entity		Name
Abengoa Hidrógeno		Mr. José Javier Brey Sánchez (Chairman)
Fundación para el Desarrollo de Nuevas Tecnologías del Hidrógeno en Aragón (FHa)		Ms. María Alamán Herbera
Universidad Pablo de Olavide		Mr. Raúl Brey Sánchez
Abengoa Hidrógeno		Ms. África Castro Rosende
Fundación para el Desarrollo de Nuevas Tecnologías del Hidrógeno en Aragón (FHa)		Mr. Luis Correas Usón
Centro Nacional de Experimentación de Tecnologías de Hidrógeno y Pilas de Combustible (CNH2)		Mr. Daniel Esteban Bechtold
Instituto Nacional de Técnica Aeroespacial (INTA)		Mr. Antonio González García-Conde
Centro de Investigaciones Energéticas, Medioambientales y Tecnológicas (CIEMAT)		Mr. Tomás González Ayuso
Junta de Andalucía. Secretaría General de Innovación Industria y Energía		Ms. María de Leyva
ARIEMA Energía y Medioambiente		Mr. Rafael Luque Berruezo
Asociación Española del Hidrógeno (AeH2)		Ms. Sagrari Miguel Montalvá
Consejo Superior de Investigaciones Científicas (CSIC)		Mr. Miguel Antonio Peña Jiménez

Scientific Committee

Organizers would like to especially acknowledge the work and dedication of all members in the Scientific Committee, helping to ensure the excellent quality of all scientific contents of the conference.

- Stéphane Abanades, (France)
- Francisco Alcaide, (Spain)
- Jose Manuel Andujar, (Spain)
- Ermete Antolini, (Italy)
- Pedro Luis Arias, (Spain)
- Alfonso Arnedo, (Spain)
- Gurutze Arzamendi Manterola, (Spain)
- Félix Barreras, (Spain)
- Nigel P. Brandon, (UK)
- Javier Brey, (Spain)
- Raúl Brey Sánchez, (Spain)
- Ulrich Bünger, (Germany)
- José F. Cambra, (Spain)
- Lorenzo Castrillo, (Spain)
- África Castro, (Spain)
- Fabrizio Cavani, (Italy)
- Antonio Chica, (Spain)
- Luis Correas Usón, (Spain)
- András Erdőhelyi, (Hungary)
- José Francisco Fernández, (Spain)
- Ana Fernández Carazo, (Spain)
- Francesco Frusteri, (Italy)
- Luis Gandía Pascual, (Spain)
- Carmen García, (Spain)
- Gonzalo García, (Spain)
- José Luis García Fierro, (Spain)
- Francisco García Peña, (Spain)
- Raquel Garde, (Spain)
- Antonio González, (Spain)
- Domingo Guinea, (Spain)
- Björn Christian Hauback, (Norway)
- Kas Hemmes, (The Netherlands)
- Patricia Hernández-Fernández, (Denmark)
- Michael Hirscher, (Germany)
- Narcís Homs, (Spain)
- Fernando Isorna, (Spain)
- Søren Knudsen Kær, (Denmark)
- Dimitris Kondarides, (Greece)
- Hubert Landinger, (Germany)
- Maria Jesús Lázaro, (Spain)
- Xianguo Li, (Canada)
- Yong Dan Li, (China)
- Justo Lobato, (Spain)
- Eduardo López, (Spain)
- Rosa Maria Magalhães Rego, (Portugal)
- Adélio Mendes, (Portugal)
- Oscar Miguel, (Spain)
- Pierre Millet, (France)
- Claude Mirodatos, (France)
- Rafael Moliner, (Spain)
- Antonio Mónzón, (Spain)
- Nazim Z. Muradov, (USA)
- Jens Oluf Jensen, (Denmark)
- Victor M. Orera, (Spain)
- Henri Paillère, (France)
- Deepak Pant, (Belgium)
- Elena Pastor, (Spain)
- Johannes M.L. Penninger, (The Netherlands)
- José Ángel Peña, (Spain)
- Miguel A. Peña, (Spain)
- Francisco José Pérez-Alonso, (Spain)
- Covadonga Pevida, (Spain)
- Pilar Ramírez de la Piscina, (Spain)
- Carmen M. Rangel, (Portugal)
- Enrique Rodríguez Castellón, (Spain)
- Martin Roeb, (Germany)
- Sergio Rojas, (Spain)
- Felipe Rosa, (Spain)
- Fernando Rubiera, (Spain)
- Günter Schiller, (Germany)
- David Serrano, (Spain)
- Giancarlo Sioli, (Italy)
- Robert Steinberger-Wilckens, (UK)
- Francisco Tinaut, (Spain)
- Panagiotis Tsiakaras, (Greece)
- Andrei V.Tchouvelev, (Canada)
- Reinhold Wurster, (Germany)

Abstracts Index

HYDROGEN PRODUCTION: REFORMING.....	26
Glycerol Reforming For Hydrogen Production: Structured Nanocomposite Perovskite-Like Materials (HPR1-1)	27
Ethanol and glycerol steam reforming using Co/SBA-15 catalysts: Effect of the incorporation of Ce, La and Zr (HPR1-2).....	31
Exergetic Study of Catalytic Steam Reforming of Bio-ethanol over Pd-Rh/CeO ₂ with Hydrogen Purification in a Membrane Reactor (HPR1-3).....	35
Hydrogen production from biogas reforming process: study of catalyst deactivation in the presence of H ₂ S (HPR1-4)	40
Environmental and economic assessment of technologies for the production of biohydrogen and its distribution (HPR2-1).....	44
Hydrogen Production from Biomass via Steam Reforming of Bio-Oil Components (Furfural). Effect of Support Materials and Method of Incorporation of Active Metal (Ni). (HPR2-2)	48
Hydrogen production from a bio-oil model compound over alumina and modified alumina nickel catalysts (HPR2-3)	52
Hydrogen Production From Coal And Biomass Co-Gasification. Elcogas Experience On The Field (HPR2-4)	55
Effect of biodiesel derived impurities on the catalytic steam reforming of glycerol in a fluidized bed reactor (HPR2-5).....	58
Hydrogen production from supercritical water reforming of glycerol (HPR2-6).....	62
Steam reforming of sulfur-containing liquid fuels: dodecane/ diesel on a Rh-Pt bimetallic catalyst for H ₂ production (HPR3-1)	66
Production of H ₂ generated from hydrocarbons in-situ with CO ₂ disposal (HPR3-2)	69
Thermocatalytic Decomposition of LPG as Hydrogen Source for Fuel Cells (HPR3-3).....	71
Behaviour Of Nickel-Alumina Spinel (NiAl ₂ O ₄) Catalysts For Isooctane Steam Reforming (HPR3-4)	74
Improvement of Steam Reforming of Toluene by CO ₂ Capture using Fe/CaO-Ca ₁₂ Al ₁₄ O ₃₃ Bi-functional Materials. (HPR4-1).....	78
Using 2-D TDLAS to Improve Efficiency and Reliability in Steam Methane Reforming (HPR4-2)	83

MODELING OF METHANE STEAM REFORMING IN MEMBRANE CATALYTIC REACTOR (HPR4-3)	86
CO ₂ -free hydrogen production by methane catalytic decomposition over pure silica materials (HPR4-4)	89
Selection of the acid function for a bifunctional catalyst based on CuFe ₂ O ₄ spinel for dimethyl ether steam reforming (HPR4-5)	92
Influence of Ni environment of supported catalysts on its reactivity in the acetone steam reforming reaction for hydrogen production from Bio-Oil (HPR4-6)	95
H ₂ -production from CO ₂ -assisted ethanol steam reforming; the regeneration of Ni-based catalysts (HPR5-1)	100
Reforming Of Ethanol On Co/Al ₂ O ₃ Catalysts Reduced At Different Temperatures (HPR5-2)	104
The Chemical-loop Reforming of Ethanol on Spinel Ferrites (HPR5-3)	107
Micro-reformer for hydrogen-rich gas generation from ethanol for a portable micro-SOFC system (HPR5-4)	110
Doped copper-manganese oxide catalysts for the production of hydrogen via steam reforming of methanol (HPR5-5)	115
Mechanistic studies of methanol reforming on Co-MnO catalysts (HPR5-6)	120
HYDROGEN PRODUCTION: OTHERS	124
Polymer Electrolyte Membrane Water Electrolysis : status, perspectives and technological developments. (HPO1-1)	125
Characterization of IrO ₂ and IrRuO ₂ Electrocatalysts for the O ₂ Evolution Reaction in SPE Water Electrolyzers (HPO1-2)	127
High pressure PEM electrolyzers and their application for renewable energy systems (HPO1-3)	129
Electrodeposited catalysts and anion exchange membranes for alkaline water electrolysis (HPO1-4)	131
Improvements to Integrate High Pressure Alkaline electrolyzers for Electricity/H ₂ production from Renewable Energies to Balance the GRID – ELYGRID Project (HPO1-5)	136
Ti based-Supports for Unitized Regenerative Fuel Cells (HPO1-6)	139
Fabrication and characterization of microtubular SOEC in coelectrolysis mode (HPO2-1)	141
Development and Characterisation of Solid Oxide Electrolyser Cells (SOEC) (HPO2-2)	143

Peak hydrogen power plant based on SOEC/SOFC---the system configuration (HPO2-3)	145
Dual Atmosphere Study Of The K41X Stainless Steel For Interconnet Application In High Temperature Water Vapour Electrolysis (HPO2-4).....	147
Optimization of SO ₂ crossover and water transport in SO ₂ -depolarized electrolyser for hydrogen production (HPO2-5).....	149
Design and Manufacturing of Catalytic Membrane Reactors by developing new nano-architected catalytic and selective membrane materials (HPO2-6)	151
Cartridges for Controlled Hydrogen Generation based on Galvanic Zn Water Reaction (HPO3-1)	154
Scale-up experiences of microbial electrolysis cells (MECs) for hydrogen production and wastewater treatment (HPO3-2).....	158
Production of Biohydrogen through the Combination of Two Stage Fermentation Processes Using Salt-Rich Substrates (HPO3-3)	161
Promotion Effect Of Precious Metals On Ni/ γ -Al ₂ O ₃ Catalyst In Selective Co Methanation (HPO3-4).....	163
Microreactors technology for Hydrogen Production and Purification (HPO3-5).....	166
CO preferential oxidation over Co ₃ O ₄ -CeO ₂ catalysts synthesized by freeze-drying method (HPO3-6)	169
Effects of preparation method, carriers and promoters on the reactivity of cadmium and zinc sulfide systems in the water splitting reaction under visible light irradiation (HPO4-1)	173
Effect of temperature used in the solvothermal synthesis on the structure and photoactivity of CdS for hydrogen production under visible light (HPO4-2).....	177
Solar Hydrogen Production from Cellulose Biomass with Enzymatic and Artificial Photosynthesis System (HPO4-3)	181
Photocatalytic water splitting using CNT-inorganic hybrid materials (HPO4-4)	183
Dynamic Model of a Solar Water Splitting Process based on a Two Step Thermochemical Cycle (HPO4-5).....	185
Water-gas shift activity over catalysts based on ceria-copper inverse configurations and influence of the presence of O ₂ in the reactant mixture (HPO4-6).....	187
Experimental assessment of the cyclability of the Mn ₂ O ₃ /MnO thermochemical cycle for solar hydrogen production (HPO5-1).....	189
Hydrogen From Synthetic Biogas Via Sip Using NiAl ₂ O ₄ Catalyst: Reduction Stage (HPO5-2)...	193

Acceleration of Redox Reaction of Metal Oxide with Oxide Ion Conducting Support Materials and Application to Hydrogen Production (HPO5-3)..... 198

Techno-environmental evaluation of Steam-Iron as an alternative process for hydrogen storage or purification (HPO5-4)..... 202

High Temperature water gas shift reaction over catalysts containing one activity promoter (HPO5-5)..... 205

Enhancement of CO conversion in a novel Electroless Pore-Plated Pd membrane reactor for H₂ production via Water Gas Shift (HPO5-6) 208

HYDROGEN STORAGE.....211

Hydrogen storage by sodium borohydride: Development of versatile and fast responding reactors for the release of Hydrogen in mobile applications (HS1-1)..... 212

Understanding the role of additives/catalysts in H₂ storage processes based on borohydride materials (HS1-2)..... 215

Electrochemical Hydrogen Compressor Performance Based On Speek And Nafion Membranes (HS1-3)..... 219

BMW Hydrogen Storage Technology – Current Status and Future Trends (HS1-4) 222

Hydrogen as a solution for storing intermittent renewable energy (HS1-5) 224

Energy evaluation of a solar hydrogen storage facility (HS1-6)..... 226

Experimental and simulated results for the desorption process in a complex hydride hydrogen storage reactor with addition of metal hydride (HS2-1)..... 228

Modified Hydrogen Storage Performance Of Mg(NH₂)₂/LiH Composite (HS2-2) 232

Long-Term Atomistic Simulation of Hydrogen Diffusion in Metals (HS2-3)..... 234

Thermal decomposition of ammonia borane impregnated in the pores of activated bentonite (HS2-4)..... 238

Synthesis of trimetallic core-shell catalysts composed of transition metals for the hydrolysis of ammonia borane (HS2-5) 240

Type Approval of Composite Gas Cylinders – Probabilistic Analysis of rc&s Concerning Minimum Burst Pressure (HS2-6)..... 242

FUEL CELL COMPONENTS AND STACKS245

Enabling low temperature fuel cells via improved Pt-alloy cathode catalysts (FCC1-1)..... 246

Array of Self-Supported Platinum Nanotubes as PEM fuel cell electrode (FCC1-2)	248
Scaling-up and characterization of ultralow-loading MEAs made-up by electrospray (FCC1-3)	251
Impact of PTFE content in GDLs on PEFC performance evaluated by neutron radiography combined with pulsed helox analysis (FCC1-4)	255
A Dissipative Particle Dynamics Approach to Evaluate Structures and Transport Phenomena (FCC1-5)	258
Electrically Induced Thermal Evolution Of Graphene-Based Vanadium Oxide Semiconducting Films For Self-Thawing Of Fuel Cell Engines (FCC1-6)	262
Order Reduction of a Distributed Parameter PEM Fuel Cell Anode Gas Channel Model (FCC2-1)	265
Investigation of the liquid water distribution in a 50 cm ² PEM Fuel Cell: effects of reactants relative humidity, oxygen/air feed, and current density. (FCC2-2).....	273
Fuel cell current density distribution analysis: comparison between a 3D model and experimental data (FCC2-3).....	277
Ageing studies of PEM Fuel Cells developed for reformat fuel operation in μ CHP units (FCC2-4)	280
Lanthanide nickelates: advanced oxygen electrode materials for solid oxide cells (SOFC/HTSE) (FCC3-1)	283
Advanced Solid Oxide Cells For Fuel-To-Power And Power-To-Fuel Conversion (FCC3-2).....	287
Development and performance analysis of a metallic passive Micro Direct Methanol Fuel Cell for portable applications (FCC3-3)	289
Noble metal oxide and valve metal oxide promoters of Pt for methanol oxidation (FCC3-4) ..	291
Catalytic electro-activation of the Pt-Ti interphase for CO and metanol oxidation (FCC3-5)....	293
Vibrating Wire Method With Semi-Circle Wire For Measuring Hydrogen Viscosity (FCC3-6) ...	295
Advanced Electrodes for SOFCs – a PhD approach (FCC4-1)	298
High performance microtubular Solid Oxide Fuel Cells for portable applications (FCC4-2).....	301
Infiltrated cathode materials for microtubular solid oxide fuel cells (FCC4-3)	304
Preparation And Characterisation Of Sulphonated Composite PBI-TiO ₂ Membranes For High Temperature PEMFCs (FCC4-4)	306

Influence of ammonia as contaminant on high temperature proton exchange membrane fuel cell performance (FCC4-5).....	308
Oxidation Behavior Of Ashless Coal In A Direct Carbon Fuel Cell (FCC4-6)	310
Supercritical synthesis of fuel cell catalysts on high surface area carbon substrates (FCC5-1). 313	
On the relationship between the amount of N and ORR performance of N/Carbon nanotube electrodes (FCC5-2)	317
Cation and anion binding effect on the oxygen reduction activity of Fe/N/C based catalysts (FCC5-3)	320
Effect of reformat H2 fuel and Air bleed mitigation on the durability of low temperature PEFCs for μ -CHP applications (FCC5-4)	325
Polymerization of protic ionic liquid for HTPEMFCs: study of ionic moieties and crosslinking effects (FCC6-1)	328
Development of anodic materials for HT-PEMFCs with higher tolerance to H2S (FCC6-2).....	332
Performance of a High-Temperature PEM Fuel Cell Operated with Oxygen Enriched Cathode Air and Hydrogen from Synthetic Reformate (FCC6-3)	336
Electrochemical performance of a HT-PEM fuel cell with bi-functional electro/reforming anode (FCC6-4)	339
Multi-scale modeling to boost fuel cell performance: From pore-scale simulations to better efficiency and durability (FCC6-5)	343
Optimization of HT-PEM fuel cells (FCC6-6).....	345
HYDROGEN AND FUEL CELL SYSTEMS AND APPLICATIONS	346
HyLIFT: projects on hydrogen powered fuel cell materials handling vehicles in Europe (FCA1-1)	347
Cost-efficient fuel cell hybrid systems for inner-city transport (FCA1-2)	351
A Compelling Value Proposition For Fuel Cell Buses (FCA1-3).....	353
CHIC – Clean Hydrogen In European Cities: demonstration of 55 FC hydrogen buses (FCA1-4)	354
Fuel Cell Control Unit – employ automotive reliability for fuel cell systems (FCA1-5)	357
Aeronautical Auxiliary Power Unit (APU) based on Fuel Cell (FCA1-6).....	360
Experimental results of a gasoline engine converted to run on hydrogen-rich synthetic gases (FCA2-1).....	363

Methanol Reformer - The next milestone for Fuel Cell powered submarines (FCA2-2)	365
Developments in the context of the hydrogen and fuel cell-based AIP system of the Spanish S-80 submarine (FCA2-3).....	369
DMFC and PEMFC/H ₂ performance under unmanned aerial vehicles environmental flight conditions (FCA2-4)	371
Fuel Cells for UAV(Unmanned Aerial Vehicle) applications (FCA2-5)	373
A Polymer Fuel cell stack breadboard development for lunar manned exploration mission (FCA2-6).....	375
Challenges in PEMFC stack development for mobile and stationary applications (FCA3-1)	377
Variable Configuration Converter In Stacked Microbial Fuel Cells (MFC) For Optimised Energy Harvesting And Cell Reversal Prevention (FCA3-2)	379
Electrolyser real-time control using the techno-economic optimization software Odyssey (FCA3-3).....	383
Investigations on a solid oxide cell after 6100 h operation in electrolysis mode (FCA3-4)	387
Hydrogen Thermophysical Properties Database Compiling a New Equation of State and Correlations Based on the Latest Experimental Data at High Temperatures and High Pressures (FCA4-1).....	390
Back-Up Systems For Telecommunications Installations Using Fuel Cells (FCA4-2).....	392
Autonomous solar-hydrogen-battery power supply for remote emergency telecommunication stations (FCA4-3)	394
Hydrogen storage in the geological underground – a first analysis of options for erection and operation (FCA4-4)	398
Simulation And Experimental Evaluation Of Operating Modes In A Hydrogen-Based Microgrid (FCA4-5).....	400
Assessment of Sustainability of the Direct Peroxide/Peroxide Fuel Cell (FCA4-6)	406
Recuperation of Exhaust Energy via Hydrogen Production Using a Steam Reforming Process – Fuel Saving Strategies for Natural Gas Combustion Engines (FCA5-1)	409
Exergy analyses of hydrogen-based energy storage systems comparing utilization of pure and methanated hydrogen in combined cycle power plants and fuel cell μ -CHP units (FCA5-2)	411
A multi-fuel processor test bench based on reforming coupled to a fuel cell as a previous stage to industrial scale-up (FCA5-3)	416

How to Put in Work a Fuel Cell System. Design, Implementation, Control and Cost Analysis of the Balance of Plant (FCA5-4).....	421
Residual heat use generated by a 12kW fuel cell in an electric vehicle heating system (FCA5-5)	427
Development of a Combined Heat and Power Plant Based on Molten Carbonate Fuel Cell Technology (FCA5-6)	429
HYDROGEN DISTRIBUTION AND FILLING STATIONS.....	431
Infrastructure Readiness For Hydrogen Fleet Deployments (DFS1-1)	432
Hydrogen Infrastructure for Transport – Hitting the road together (DFS1-2)	434
The next phase of Hydrogen infrastructure in Norway (DFS1-3).....	436
Hydrogen-Compressed Natural Gas Refueling Infrastructure in India (DFS1-4).....	437
An optimization approach for evaluating subsidies in the initial location of hydrogen refueling stations (DFS1-5)	438
Location of hydrogen fueling stations in urban areas (DFS1-6)	441
Assessment of a hydrogen refueling station (DFS2-1)	445
Rollout of hydrogen refuelling stations employing a strategy of fixed nodes and maximum flows (DFS2-2)	447
Electrochemical hydrogen compression and purification (DFS2-3).....	451
Effect of precooled inlet gas on temperature evolution during refueling (DFS2-4)	455
MARKET STRATEGIES	457
Analysis of the general public and stakeholder awareness and acceptance on hydrogen technologies (MS-1)	458
Hydrogen Transport in European Cities (HyTEC) (MS-2).....	461
H2FC European Infrastructure; Support Opportunities to Hydrogen and Fuel Cell Research (MS-3).....	463
European Electro-mobility Observatory-compiling and presenting EV data (MS-4)	466
COMMERCIALIZATION AND STRATEGIES	469

Pre-investigation of Water Electrolysis for Flexible Energy Storage at Large Scales: The Case of the Spanish Power System (CS-1).....	470
Water electrolysis as key enabler for power to gas accelerating renewable energy integration (CS-2)	476
Homologation of Fuel Cell Electric Vehicle (CS-3).....	478
The International Energy Agency Hydrogen Implementing Agreement (IEA HIA): Collaborative R,D&D to 2015 and Beyond (CS-4)	480
COUNTRIES AND ASSESSMENTS	483
Hydrogen as a Fuel and Energy Storage: Success Factors for the German Energiewende (CA-1)	484
The Fuel Cell and Hydrogen Network North Rhine-Westphalia (CA-2)	486
Aragon bet on Hydrogen and Fuel Cells (CA-3).....	488
Numerical analysis of hydrogen safety issues (CA-4).....	490
Application of Accident Modeling and Prediction Methodology to a Hydrogen Fuelling Station (CA-5).....	494
Life-cycle performance of hydrogen production via biofuel reforming (CA-6).....	497
POSTERS	500
State of Regulatory Framework for Hydrogen Infrastructures (P-3)	501
SMR Integration and Increase of CO ₂ Production (P-4)	506
Alkali and Alkaline-Earth Metal Borohydride Hydrazinates: Synthesis, Structures and Dehydrogenation (P-21).....	509
Hydrogen Production Technologies - Operational Challenges Of A Pressurized Alkaline Electrolyzer-Prototype (P-22).....	510
Improvement of the desorption kinetics and thermodynamics from CaH ₂ +AlB ₂ system by NbF ₅ doping (P-23).....	514
Advanced Alkaline Electrolyzer For Hydrogen Production; Design And Manufacturing (P-26). 515	
Water Management Studies In A Pem Fuel Cell: Fuel Cell Stack Design (P-28).....	518
Investigation on water distribution patterns featuring back-diffusion transport in a Polymer Electrolyte Membrane Fuel Cell with Neutron Imaging (P-47)	520

Hydrogen production system by steam reforming integrated in a solar parabolic disc (P-48) .	524
Eliminating hydrogen inventories for green energy storage using liquid metal technology (P-50)	527
Hydrogen from biomass derived oxygenates: Thermodynamic comparison between bio-oil and ethanol steam reforming (P-56).....	530
Preparation and Characterization of Sulfonated Poly(phenylene)s Containing Cis/Trans Mixture of Bis(4-chlorophenyl)-1,2-diphenylethylene for Proton Exchange Membrane (P-63)	533
Synthesis and properties of sulfonated grafting copolymer via superacid-catalyzed polyhydroxyalkylation reaction (P-64)	535
Hydrogenation Behaviors of MgH_x -Graphene Composites by Reactive Mechanical Grinding (P-70).....	537
Evaluations of Hydrogen Permeability on SCZY/SHP/Ni Composites Membrane (P-71).....	540
Non-Platinum Electrocatalysts for Hydrogen Oxidation in Alkaline Media (P-75).....	543
Low Temperature Hydrogen Oxidation over Platinum Free Electrocatalysts: PEMFC vs AEMFC (P-76)	544
A review of electrocatalysts for PEM water electrolysis applications (P-78).....	545
Hydrogen production from methane steam reforming in combustion heat assisted novel micro-channel reactor with catalytic stacking: A CFD simulation study (P-83).....	547
Effects of Electrode/Electrolyte Thickness on the Performance of Micro-tubular Solid Oxide Fuel Cells Made by Sequential Aqueous Electrophoretic Deposition (P-85)	550
Effects of the filler compositions of micro porous layer for anode on the performance of direct highly concentrated methanol fuel cell (P-88).....	551
DMFC for auxiliary power supply in a river buoy (P-90)	553
Development of degradation and optimization model for PBI based high temperature PEMFCS (P-97)	555
Durability analysis of high temperature PEM fuel cell for DSS test using EIS (P-98)	557
Excellent catalytic effects of Ni- and graphene-based catalysts on hydrogenation/dehydrogenation of magnesium hydride (P-101).....	558
Valorization of biogas produced in WWTP by means of PEM fuel cells (P-103).....	560
Hydrogen adsorption on Co/Ni mixed-metal MOF-74-type materials (P-106).....	563

Synthesis and characterization of new nano-composites membranes based in polysulfone/ ZnAl-heptamolibdate LDH (P-107)	565
Synthesis and characterization of quaternary ammonia polysulfone nanocomposite membranes for H ₂ /O ₂ alkaline fuel cell applications: An electrochemical study (P-108).....	568
Study of Hydrogen production from wind power in Adrar (P-112)	571
Electrochemical analysis of WNi-CeO ₂ cermet as sulphur tolerant SOFC anode (P-116)	575
Combined XPS and DRIFTS study of the reduction under CO of Cu/CeO ₂ CO-PROX catalysts (P- 117).....	578
Synthesis of CuO/Al ₂ O ₃ films onto stainless steel microgrids for CO preferential oxidation (P- 123).....	580
Optimizing the synthesis method of ZrO ₂ -supported NiFe ₂ O ₄ for solar hydrogen production by thermochemical water splitting (P-125)	585
Control and Monitoring Tools Developed for Hydrogen Based Systems (P-133).....	590
High-purity hydrogen from acidic fractions of bio-oil by "steam-iron" (P-149)	595
Hydrogen sensing properties of anodically synthesized porous TiO ₂ film coated with Pd thin film and its mechanical enhancement by the bottom electrode configuration (P-151).....	600
LIFE+ ZEROHYTECHPARK: "experiencie on low power pem fuel cell UPS systems for central servers" (P-153).....	605
Hydrogen fuel cell power pack design (P-154).....	608
The Catalytic Activity of Carbon Nanotube Loaded Carbon Paper towards Oxygen Reduction Reaction in PEMFC (P-161).....	611
RF-Sputtered Gd-doped ceria (GDC) Thin Film as electrolyte for micro-SOFC (P-162).....	612
Ag-Modified Cu-Ceria Anode for SOFC directly fuelled with simulated biogas mixtures (P-164)	613
Photocatalytic hydrogen production from methanol over Cu-TiO ₂ catalysts (P-166)	616
High V.LO-City: speeding up fuel cell hybride bus deployment in European cities (P-168)	621
Reinforced Polymeric Ionic Liquid Membranes for HT PEMFCs (P-174).....	623
Hydrogen generation by hydrolysis of sodium borohydride with bentonite supported Co-B catalyst (P-175).....	626
The grain size effects on stress assist hydrogen transport in polycrystalline Nickel (P-177).....	629

Porous Ni-YSZ and Ni-GDC anode buffer layers prepared by magnetron sputtering for Solid Oxide Fuel Cells (P-186).....	630
EFFECT OF GAS CHANNELS FLOW PATTERNS ON COLD-START BEHAVIORS OF POLYMER ELECTROLYTE FUEL CELLS (PEFCs) (P-188)	632
Development of ultralight and thin bipolar plate based on EPOXY-Carbon fiber prepregs-graphite composite (P-189).....	634
Advanced Multi-Fuel Reformer for Fuel Cell CHP Systems (P-194)	637
Numerical simulations of the two-phase flow in the anode channel of a PEMFC using the VOF method (P-196)	641
Mo ₂ C electrocatalysts for hydrogen evolution: effect of carbon-support (P-199)	644
Phosphoric Acid Doped Cross-linked Porous Polybenzimidazole Membranes for Proton Exchange Membrane Fuel Cells (P-201).....	646
Development of high performance membrane electrode assemblies using a non-platinum catalyst for alkaline membrane fuel cells (P-205).....	648
H ₂ uptake capacities on materials incorporating cyanometalate building blocks (P-209)	650
Preparation and characterization OF Pd-Ag-Au alloy membranes for hydrogen separation (P-214).....	652
Comparison between electroless plating and PVD-magnetron sputtering techniques for preparation of Pd-Ag membranes for hydrogen separation (P-217).....	654
Steam Reforming Process for manufacturing of Hydrogen in Solid Oxide Fuel Cell using Biogas (P-222)	656
Global hydrogen systems analysis. IEA HYDROGEN ANNEX 30 (P-223).....	659
Preparation of Pd-Ag pore filled membranes for hydrogen separation (P-225)	661
Structural and electrical characterization of the novel SrCo _{1-x} M _x O _{3-δ} perovskites (M= Ti, V, Nb) : evaluation as SOFC cathode materials (P-232)	663
Dehydrogenation kinetics of magnesium hydride under different experimental conditions (P-234).....	666
Thermal Integration possibilities with SOFC exhaust gases and heat transfer (P-237)	668
Effect of carbon dioxide on proton exchange membrane fuel cell performance: Influence of the operating temperature (P-240).....	671

Numerical modeling of the degradation rate for membrane electrode assembly in high temperature proton exchange membrane fuel cells and analyzing operational effects of the degradation (P-242)	674
Study on the Sulfur adsorption properties of Mesoporous Material for Fuel Cell (P-247)	676
Development of Steam Methane Reformer for 5kW PEMFC Stationary Fuel Cell System (P-249)	678
Hydrogen production from biogas through dry and steam reforming (P-250)	680
New catalysts based on chalcophanite promoted with Ni applied to steam reforming of bioethanol (P-255).....	684
Oxidative steam reforming of methane over nickel catalysts supported on La ₂ O ₃ -CeO ₂ -Al ₂ O ₃ (P-266)	688
Open Source control in PEM Fuel Cells (P-268)	691
Advances in Hydrogen Production by Sorption Enhanced Reforming. Process and materials development (P-269).....	693
Effect of exposure time to organometallic precursors for the preparation of Pt Nanocatalysts on a Nafion-coated Carbon BLACK (P-270)	695
Effect of graphite fiber on electrical conductivity of an epoxy/carbon composite used for a bipolar plate in a fuel cell (P-271)	698
Preparation of Pt Nanopatterning for PEMFC on a Self Assembled Copolymer Thin Film using a drying process (P-272).....	701
Multi factors influence analysis on the development and marketplace of hydrogen technologies. Students dissemination (P-277).....	703
The use of waste hydrogen for energy purposes in Poland (P-279)	707
A semi-analytical model for droplet dynamics on the GDL surface of a PEM fuel cell cathode (P-281).....	711
Hydrogen production through sodium borohydride ethanolysis (P-291).....	714
Evaluation of sepiolite-supported catalysts for biogas reforming to hydrogen production (P-292)	717
Experimental evaluation of cell components affecting the performance of an air-breathing PEM fuel cell (P-295).....	721
Integration of an electrolyzer into a minigrid (P-296)	724

PEM fuel cell performance analysis: static and dynamic behaviour and its integration with a supercapacitor (P-298).....	727
Nanosized Fe-doped ceria samples synthesized by freeze-drying precursor method (P-300)..	731
Development of simple method for measuring quantity of hydrogen permeation through thick metals using sensor gas chromatograph (P-301).....	735
Air-breathing pem fuel cell system for golf cart (P-305).....	738
A study on degradation of high-temperature PEMFC (P-308).....	741
Poisoning intermediates on the ethanol electrooxidation reaction over Pt-based catalysts (P-316).....	743
Numerical predictions and experimental validation of DEFC performance: AEM vs. PEM (P-322).....	746
Hybrid Chitosan-Carbon as New Electrocatalyst Support for Direct Methanol Fuel Cells (P-325).....	749
The Unique Role of CaO in Stabilizing the Pt/Al ₂ O ₃ Catalyst for the Dehydrogenation of Cyclohexane (P-327).....	751
Photoinduced Hydrogen Production with Photosensitization of Zn Chlorophyll Analog Dimer as a Photosynthetic Special pair Model (P-329).....	753
The performance of an ionic liquid functionalized carbon supported Pt-Ru catalyst for pem fuel cells (P-335).....	755
Temperature and Pressure effects on hydrogen separation from unconverted shift gas mixture using a Palladium Membrane Reactor (P-338).....	758
Renewable hydrogen production from steam reforming of glycerol using Ni-Cu-Mg-Al mixed oxides obtained from hydrotalcite-like compounds (P-340).....	762
Hydrogen production by bio oil reforming over nickel aluminates (P-342).....	766
Novel materials for a HT-PEMFC stack for operation as automotive range extender (P-343) ..	770
Improvement of fuel cells' cost and performance by application of nanotechnology: a review (P-345).....	772
A multi dimension approach for fast analysis of Polymer Electrolyte Membrane Fuel Cells (P-346).....	774
An overview of H ₂ FC SUPERGEN, the UK's inclusive Hydrogen & Fuel Cell research network and UK Hydrogen & Fuel Cell activities (P-348).....	778

Theoretical Study on the Effects of the Magnesium Hydride Doping with Cobalt and Nickel on the Hydrogen Release (P-354).....	780
Hydrogen in Mobile Applications – the Path of Latvia to Carbon Free Economy (P-356)	782
Specific technical requirements for hydrogen storage systems on underwater vehicles intended for exploration of the world ocean (P-357).....	784

Hydrogen production: reforming

Glycerol Reforming For Hydrogen Production: Structured Nanocomposite Perovskite-Like Materials (HPR1-1)

Ksenia PARKHOMENKO¹, Sadio CISSE¹, Anne-Cécile ROGER¹,
Natalia MEZENTSEVA^{2,3}, Ekaterina SMAL^{2,3}, Vladislav SADYKOV^{2,3}

¹ ICPEES, UMR7515 CNRS, University of Strasbourg, FRANCE, parkhomenko@unistra.fr

² Borekov Institute of Catalysis, RUSSIA, sadykov@catalysis.nsk.su

³ Novosibirsk State University, RUSSIA

INTRODUCTION

The biodiesel is commercially produced by transesterification reaction between triglycerides (vegetable oils) and an alcohol, usually in the presence of a basic or acid catalyst [1]. During the transesterification, the different types of triglycerides, derived from different types of feedstock like palm, soy or rapeseed, are transformed to their respective ester and as co-product glycerol is formed. For each mole of biodiesel formed one mole of glycerol is produced, which corresponds approximately to 10 wt. % of the amount of biodiesel produced. The increase in the biodiesel production, derived by different governmental policies, has created a glut of glycerol in the market [2]. The excess of glycerol has led to new researches in order to transform and what is more important valorize the glycerol coming from the biodiesel production [3].

The production of hydrogen by glycerol steam reforming is an alternative proposed to valorize the glycerol originated from the biodiesel production as well as an alternative of H₂ production from the residual fractions of a global process (biodiesel production). This process follows the novel concept of biorefinery [4], where biomass is attempt to fulfill the place of crude oil in the conventional refineries, obtaining a spectrum of valuable products (including H₂) and fuels. So far, few works have been performed in H₂ production from glycerol steam reforming. There is still a scope for finding an efficient catalyst for the process. The reaction conditions are not yet well defined, varying the reaction temperature (350 °C to 700 °C), the water to glycerol feed ratio (12:1), GHSV, etc. Besides, the formation of carbon deposits has been reported as a major problem.

In this research project, coming from French-Russian collaboration, glycerol steam reforming was studied for selective hydrogen production using nanocomposite active components based on Ln-Mn-Cr-Pr perovskite-like oxides synthesized by modified Pechini route, with addition of active metals and aluminum oxide. The use of perovskite-like oxides as the catalyst precursors is an attractive option for the formation of highly dispersed active metal (Ni, Ru and their alloys) fixed in oxide non-reducible matrix that occurs as a result of perovskite reduction. The structural and thermal stability as well as catalytic activity of such systems can be adjusted by substitution with various cations (Y, Sm, Pr, Zr etc), the participation of this cations in generating the oxygen mobility of oxide matrix during the reaction might prevent the catalyst from coking and increase even more its activity and stability [5].

EXPERIMENTAL

Nanocomposite active components were comprised of Ln-Mn-Cr-Pr perovskite-like oxides prepared via modified Pechini route [6] with addition of active metals (up to 2 wt.% of Ru and up to 10 wt.% of Ni) and aluminum oxide. Mixed manganite-chromite was synthesised using metal nitrates, $\text{Ru}(\text{OH})\text{Cl}_3$, citric acid, ethylene glycol and ethylenediamine as reagents [6]. Citric acid and metal salts were dissolved in ethylene glycol at 80 °C and in distilled water at room temperature, respectively. The prepared solutions were mixed together under stirring followed by addition of ethylenediamine. The mixed solution was stirred for 60 min and then heated at 70 °C for 24 h till the gel formation. The gel was calcined under air at 600 °C for 2 h, obtained solid was ground and annealed at 900 °C. Active metals (Ni and Ru) were supported on powdered nanocomposites by insipient wetness impregnation followed by drying and calcinations at 800 °C. Structural features of materials were studied by BET, XRD, H_2 -TPR, TEM with EDX analysis. Carbon deposits were determined by TPO. The surface/bulk oxygen mobility was measured using oxygen isotope heteroexchange in both isothermal and temperature-programmed experiments. In the case of repeated red-ox cycles, samples were reoxidized in the flow of O_2 for 1 h at 500 °C.

Catalytic experiments were carried out in a quartz continuous flow reactor (internal diameter 7 mm). The catalyst mixed with SiC was placed in-between two plugs of quartz wool. Before reaction, the catalyst is reduced, then H_2 is flush out of the reactor using a flow of inert gases. During the purge period, the reaction temperature was adjusted. The water:glycerol solution was fed using a micropump and introduced into the reactor evaporation zone before the catalyst bed. The reaction begins when the dosage device is introduced into the reactor. The non-condensable gas products were analysed by online gas-phase chromatography. The condensable products were collected after 5, 8 and 25h of the reaction and analyzed later on. The catalyst activity was evaluated by means of three different conversions: the global conversion of glycerol (X), the conversion to gaseous products (X_G), and the conversion to liquid products (X_L). The comparison between the different catalysts was based on their hydrogen production expressed as moles of H_2 per mole of glycerol introduced ($\text{mol}_{\text{H}_2} \cdot \text{mol}_{\text{Gly.in}}^{-1}$).

RESULTS AND CONCLUSIONS

Structured perovskite-like materials possess a specific surface area from 12 to 90 m^2g^{-1} . The phase composition of the prepared samples depends on the substitution cation nature. H_2 -TPR experiments showed the presence of two reduction zones: lower temperature zone may be attributed to the reduction of Ru and Ni that form metal alloyed nanoparticles strongly interacting with perovskite support due to a good epitaxy (confirmed by XRD and TEM). A broad peak in higher temperature zone was assigned to reduction of NiO admixture present in samples according to XRD data. The data of oxygen isotope exchange experiments showed a high rate of oxygen mobility even after reforming reaction – around one third stays mobile at the temperatures higher than 600 °C.

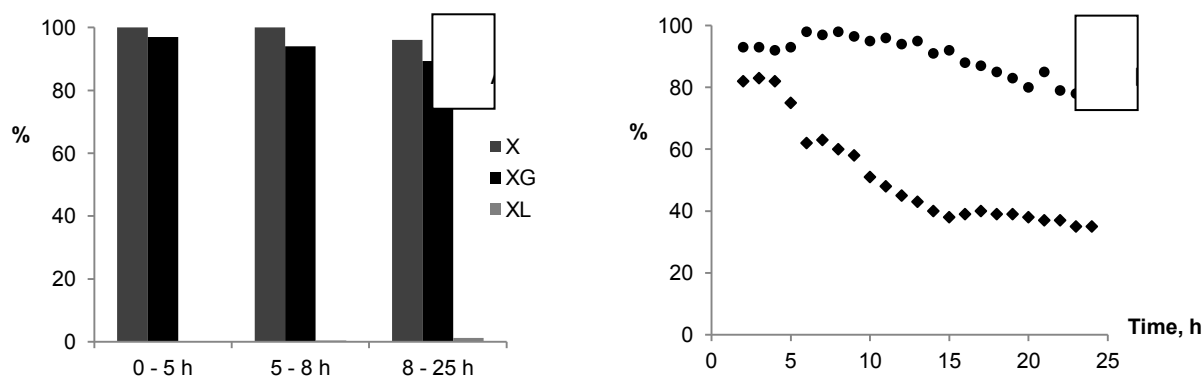


Fig.1. A) Glycerol conversion over Ru+Ni/LaPrCrMn/YSZ catalyst (650 °C, in presence of oxygen). B) Glycerol conversion into non-condensable gas products over Ru+Ni/LaPrCrMn/YSZ catalyst: ◆ - steam reforming conditions, ● - oxy-steam reforming conditions.

Glycerol steam reforming was performed in isothermal conditions during 24-25h for all catalysts – with/without addition of small amounts of oxygen. The effect of the oxygen introduction was observed beneficial for all catalysts (Fig. 1). The data of O₂-TPO, performed in order to study the types and quantity of deposited carbonaceous species, was used for establishing overall carbon balance of a reaction. As follows from comparison of catalysts performance in glycerol steam or oxy-steam reforming, mixed manganite-chromite/YSZ nanocomposite as support provides specific activity of Ru+Ni alloy nanoparticles higher than that for other perovskite-like supports [7]. Ru-doped catalysts demonstrated a better performance, which can be explained by prevention of coking and less sintering of Ni clusters stabilized in bimetallic alloys. A higher activity was obtained for Pr-containing catalysts, which suggests importance of these redox cations providing higher oxygen mobility in the oxide support.

Synthesis of complex perovskite precursors containing transition metal cations with broadly varying redox properties such as easily reduced to metal Ni and Ru cations and much less prone to reduction Cr and Mn cations is an efficient approach to design efficient and stable to coking nanocomposite catalysts of glycerol steam reforming for hydrogen production. Under reaction conditions, these perovskites are transformed into nanocomposites comprised of metal/alloy nanoparticles and oxide patches epitaxially bound with disordered perovskite particles. High catalytic activity and coking stability are provided by tuning the oxygen mobility in complex oxide supports with Cr, Mn cations in perovskites and/or by adding fluorite-like oxides with high oxygen mobility. Strong metal-oxide support interaction provides also stability of metal nanoparticles to sintering in real operation conditions.

[1] S. Fernando, S. Adhikari, K. Kota, and R. Bandi, *Fuel* 86 (2007) 2806-2809

[2] K.S. Tyson, J. Bozell, R. Wallace, E. Petersen, and L. Moens (2004) *Biomass Oil Analysis: Research Needs and Recommendations*. NREL/TP-510-34796

[3] C.-H. Zhou, J.N. Beltramini, Y.-X. Fan, and G.Q. Lu, *Chemical Society Reviews* 37 (2008) 527-549

[4] a) S. Fernando, S. Adhikari, C. Chandrapal, and N. Murali, *Energy & Fuels* 20 (2006) 1727-1737;
b) P. Ramirez de la Piscina, and N. Homs, *Chemical Society Reviews* 37 (2008) 2459-2467

[5] a) Valderrama, G.; Kienneman, A. and Goldwasser, M. R. *Catalysis Today* 133 (2008) 142-148;
b) Sadykov, V.; Mezentseva, N.; Alikina, G.; Bunina, R.; Rogov, V.; Krieger, T.; Belochapkine, S.; Ross, J. *Catalysis Today* 145 (2009) 127-137

[6] a) Pechini, M. P. US Patent 3 (1967) 330, 697; b) Kuznetsova, T. G.; Sadykov, V. A.; Moroz, E. M.; Trukhan, S. N.; Paukshtis, E. A.; Kolomiichuk, V. N.; Burgina, E. B.; Zaikovskii, V. I.; Fedotov, M. A.; Lunin V. V.; and Kemnitz, E. *Studies in Surface Science and Catalysis* 143 (2002) 659-667

[7] V. A. Sadykov, S. N. Pavlova, G. M. Alikina et al. *Perovskite-based Catalysts for Transformation of Natural Gas and Oxygenates into Syngas*, 2013, in press

Ethanol and glycerol steam reforming using Co/SBA-15 catalysts: Effect of the incorporation of Ce, La and Zr (HPR1-2)

A.J. Vizcaíno, L. García-Moreno, J.A. Calles, A. Carrero.

Department of Chemical and Energy Technology, ESCET. Rey Juan Carlos University, c/Tulipán s/n, 28933 Móstoles (Madrid), Spain.

INTRODUCTION

Currently, the reduction of emissions of pollutants, such as CO₂, NO_x, SO₂, and solid particles to atmosphere by the utilization of fossil fuels is an issue of increasing interest. Furthermore, fossil fuels are limited resources, so it is necessary to search alternative, clean and renewable energy systems [1], where plant-based fuels and hydrogen as an energy vector are outstanding [2]. Moreover, the possibility of hydrogen to be obtained from a wide variety of feedstocks makes it quite interesting since every region may be able to produce much of their own energy [3]. Among the different hydrogen production alternatives, steam reforming of bio-oils, oxygenated hydrocarbons or bio-alcohols is very suitable from both the environmental and energy efficiency point of view [4]. Bioethanol is a good candidate since it has not to be fully purified if used in steam reforming, so avoiding the high dehydration costs of current bioethanol production processes [5]. Glycerol is also a good candidate because it can be generated as a by-product in biodiesel production and the amount of glycerol available is planned to be high. In this mean it is necessary to find alternative uses of glycerol in order to reduce biodiesel production costs [6]

Catalysts for steam reforming processes are currently a research subject, focusing on the catalytic activity, the selectivity to hydrogen and the resistance to coke formation. This last issue is one of the main problems for catalyst deactivation together with sintering of metal particles. Steam reforming is usually carried out at high temperature with conventional catalyst. However, cobalt-based catalysts exhibit a good performance even at low temperature, which is mainly related to the reducibility of cobalt species [8]. Besides, the addition of other metals, such as La, Ce and Zr, has improved catalyst stability, attributed to the reduction of coke formation [7-9]. The choice of a catalytic support is also very important, and in this mean SBA-15 has shown good characteristics for accommodating metallic particles due to its controllable pore size, pore volume, and high surface area [7].

Thus, in this work, we have studied the effect of Zr, Ce and La incorporation into SBA-15 silica as support of Co catalysts on their catalytic properties for steam reforming of ethanol and glycerol.

EXPERIMENTAL

Four catalysts with 7 wt% Co supported on SBA-15 mesostructured material were prepared by incipient wetness impregnation, three of them containing 10 wt% of Ce, La or Zr. Catalysts were characterized by Thermogravimetric Analysis (TGA), Inductively Coupled Plasma Atomic Emission Spectroscopy (ICP-AES), X-ray Powder Diffraction (XRD), Hydrogen Temperature Programmed Reduction (TPR) and Nitrogen Physisorption analysis (N₂-BET).

The experimental installation to carry out the ethanol and glycerol steam reforming test was a MICROACTIVITY-PRO unit. Previous to the reaction, catalyst was in situ reduced under flowing pure hydrogen (30 mL/min) at 700 °C for 4.5 h with a heating rate of 2 °C/min. After the catalyst activation, the reaction temperature was fixed at 500, 600 or 700 °C and, catalytic test was carried out isothermally at atmospheric pressure under nitrogen-diluted conditions. A liquid reaction mixture with water/ethanol = 3.7 or water/glycerol = 6 molar ratio was introduced at a flow rate of 0.075 mL/min, vaporized at 150 °C and further eluted by N₂ (60 mL/min). Weight hourly space velocity (WHSV_{ethanol} = 16.4 h⁻¹ and WHSV_{glycerol} = 7.7 h⁻¹) was defined as the ratio between the inlet feed mass flow rate and the mass of catalyst. The composition of the output gas and liquid streams were determined by gas chromatography.

RESULTS AND DISCUSSION

Physisorption analyses showed that the incorporation of promoters to the catalyst causes lower values of both surface area and pore volume as compared with Co/SBA-15 catalyst.

Fig. 1.a. shows the X-ray diffraction patterns of the calcined catalysts. It can be clearly seen the peaks corresponding to Co₃O₄. In addition, the X-ray diffraction pattern of Co/Ce/SBA-15 catalyst shows a peak corresponding to CeO₂, which indicates that these species are not finely dispersed over the support. In the case of Co/Ce/SBA-15, Co/Zr/SBA-15 and Co/La/SBA-15 catalysts, the intensity of the Co₃O₄ reflections was reduced, indicating smaller crystallites. In fact, the diameter of the Co₃O₄ crystals calculated from XRD both for the calcined and the reduced samples indicated that the addition of Ce, La and Zr helps to form smaller Co₃O₄ particles, in the order: Co/SBA-15 > Co/Ce/SBA-15 ≈ Co/Zr/SBA-15 > Co/La/SBA-15.

Fig. 1.b. shows the H₂-TPR profiles of the calcined samples. All curves show two reduction zones: (i) at low temperatures (250-400°C), corresponding to the reduction of Co₃O₄ particles with low metal-support interaction; (ii) at high temperatures (above 400°C), corresponding to the reduction of the Co phase strongly interacting with the support. It can be observed that the incorporation of Ce, La and Zr causes the reduction temperature to shift towards higher values, due to stronger interaction between the metal phase and the support, in the order: Co/SBA-15 < Co/Ce/SBA-15 < Co/Zr/SBA-15 < Co/La/SBA-15.

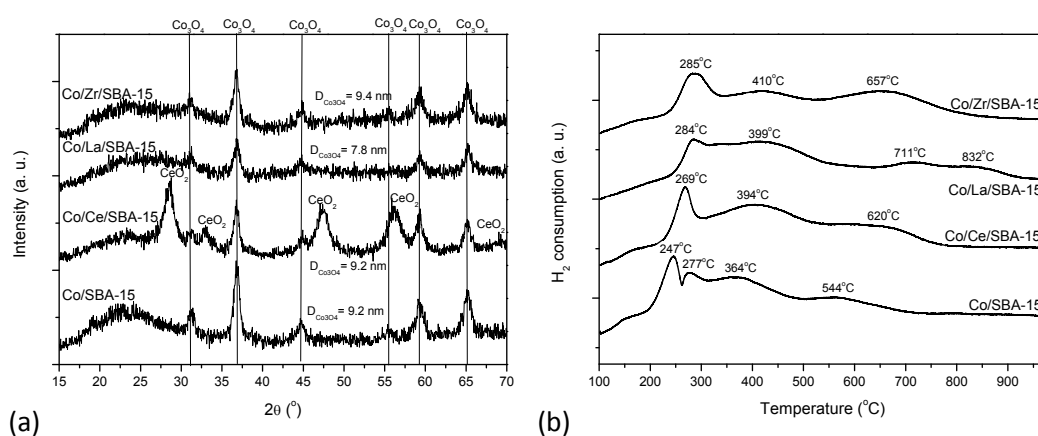


Figure 1. Catalysts characterization: (a) X-ray diffraction patterns; (b) H₂-TPR profiles.

Regarding catalytic tests in ethanol steam reforming, the best results were obtained for the Co/SBA-15 catalyst, which achieved 58.7% of ethanol conversion, followed by Co/Zr/SBA-15 with a 54.8% conversion of ethanol working at low temperatures. All catalyst showed low selectivities to gaseous products, below 45%, being more selective Co/SBA-15. As temperature was increased, conversions and selectivities grew in a different grade for each catalyst, depending on different reducibility properties. As a consequence, Co/Ce/SBA-15 shows good results at intermediate temperature. At high temperatures (Figure 2.a), it was observed that all catalysts increased the conversion of ethanol to almost 100%. In terms of gas stream selectivity, catalysts reached values above 63%, being Co/La/SBA-15 the sample with the highest selectivity towards gas products. Besides, Co/Zr/SBA-15 showed high conversion to ethanol, but the acidity of ZrO_2 led to ethylene and thus low hydrogen production. The Co/La/SBA-15 achieved better results at high temperatures, because this catalyst exhibits the strongest metal-support interaction.

In the case of glycerol (Figure 2 (b)), conversion values between 83.4 and 97.1% were achieved at low temperatures with Co/Ce/SBA-15 reaching the highest value. Under these conditions, the catalysts showed low selectivities to gaseous products, being Co/Ce/SBA-15 the most selective with 64.3% of gas selectivity. At high temperatures, the conversion to glycerol was almost 100% for all catalysts, except for Co/SBA-15, which was 92.1%. Gas selectivity increased with temperature in all cases and the highest selectivity (72.8%) was obtained with Co/Ce/SBA-15.

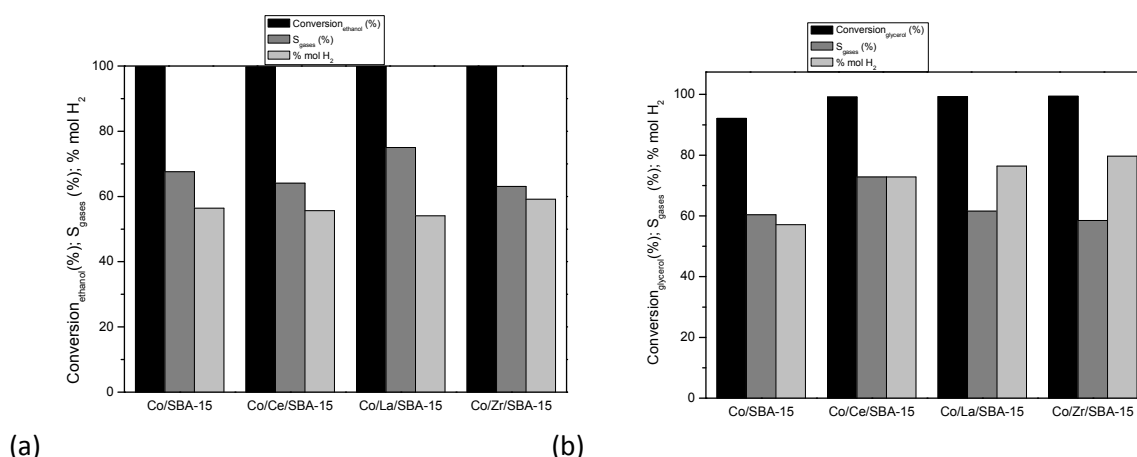


Figure 2. Catalytic results on: a) ethanol steam reforming ($T=700^\circ\text{C}$, $H_2O/EtOH$: 3.7, $WHSV$: 16.4 h^{-1}) and b) glycerol steam reforming (T : 600°C , $H_2O/Glycerol$: 6, $WHSV$: 7.7 h^{-1}).

Acknowledgements

The authors acknowledge the financial support from the “Ministerio de Educación y Ciencia” through the project ENE2007-66959 and from the “Comunidad de Madrid” through the RESTOENE project (S2009/ENE-1743).

REFERENCES

I. S. Nashawi, A. Malallah, M. Al-Bisharah, *Energy fuels* 24 (2010) 1788.

A. J. Vizcaíno, A. Carrero, J. A. Calles, *Int. J. Hydrogen Energy*, 32 (2007) 1450.

J.D. Holladay, J. Hu, D.L. King, Y. Wang, *Catal. Today* 139 (2009) 244.

A. Tanksale, J.N. Beltramini, G.Q. Max Lu, *Renew. Sust. Energy Rev.* 14 (2010) 166.

P. Ferreira-Aparicio, M.J. Benito, J.L. Sanz, *Catal. Rev.* 47 (2005) 491

M. Gupta, N. Kumar, *Renew. Sust. Energ. Rev.* 16 (2012) 4551.

Lin, S. S.-Y., Kim, D. H., Ha, S. Y., *Appl. Catal. A: Gen.*, 355 (2009) 69.

Llorca, J., Homs, N., Sales, J., Ramírez de la Piscina, P., *J. Catal.*, 209 (2002) 306.

Haga, F., Nakajima, T., Miya, H., Mi Shima, S., *Catal. Lett.*, 48 (2013) 223.

Exergetic Study of Catalytic Steam Reforming of Bio-ethanol over Pd-Rh/CeO₂ with Hydrogen Purification in a Membrane Reactor (HPR1-3)

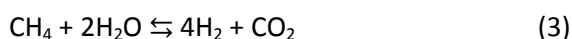
Ali Hedayati^{1,2}, Olivier Le Corre², Bruno Lacarriere², Jordi Llorca¹

¹Institut de Tècniques Energètiques, Universitat Politècnica de Catalunya, Diagonal 647, ed. ETSEIB, 08028 Barcelona, Spain

²DSEE, Ecole des Mines de Nantes, 4 rue A. Kastler, BP 20722, F44307 Nantes Cedex 01, France

Introduction

Ethanol Steam Reforming (ESR) process is one of the promising methods for hydrogen production to feed fuel cells. During the ESR process, ethanol is converted to hydrogen and carbon oxides over a catalyst in the presence of steam at temperatures typically between 823 and 1123 K, according to the following reactions:



The special properties of ethanol such as hydrogen to carbon ratio of 3 and high hydrogen content per unit volume in liquid form have put ESR in the center of attention for direct production of H₂ [1]. Bio-ethanol is a renewable fuel that can be directly used for reforming processes since it already contains water.

Regarding the need for the hydrogen purification in steam reforming units, the application of catalytic membrane reactors (CMR) is beneficial. In a CMR, the shift effect to the product side for more hydrogen production is favorable. If dense metallic membranes are used in CMRs, a pure H₂ stream is directly obtained and no other purification units are needed, meaning a drastic decrease in the cost and energy consumption [2]. Among all types of membranes, palladium-based membranes are able to deliver hydrogen in 99.999% purity, very suitable for PEMFCs feeding.

In this work, an exergy analysis of the ESR system is done based on experimental data obtained over a Pd-Rh supported on ceria catalyst in a Pd-based membrane reactor. Exergy analysis is a powerful tool to obtain deeper insight into the ESR process and its optimization. Both chemical and physical exergy for chemical species, together with heat loss calculations are considered to evaluate the exergy efficiency of the process. Different operational conditions ranging from 873 to 923 K and 4 to 12 bar, using a 50 – 50% volume of distilled water and ethanol (steam to carbon ratio of 1.6) have been explored.

Experimental

Catalyst preparation

Catalytic honeycombs loaded with 0.5Rh-0.5Pd/CeO₂ were prepared according to [3, 4]. Cordierite monoliths of 2 cm diameter and length were first coated with ca. 250 mg of cerium oxide using an aqueous solution of Ce(NO₃)₂·6H₂O (Fluka). Then the monoliths were dried and calcined at 773 K. Noble metals were added by wetness impregnation using an aqueous solution of 0.5% Pd – 0.5% Rh made of PdCl₂ and RhCl₃ in distilled water. The monoliths were dried at 373 K and calcined at 673 K for 2 hours. Prior to the experiments, the catalytic monoliths were reduced at 550 K (10% H₂ in N₂) for 1 hour.

Membrane fuel reformer

The reactor used was 10 in. tall and 1 in. in diameter and was equipped with 4 metallic membrane rods selective to hydrogen made up of Pd-Ag; each one 3 in. tall and 1/8 in. diameter [3]. The membrane consisted on a 30 μm layer of Pd – Ag supported on PSS support. To perform the experiments, five monoliths in series were placed inside the reactor before the membrane rods.

Exergy analysis

To evaluate the exergetic performance of the system, the physical and chemical exergy of the inlet and outlet streams are considered. The physical exergy is calculated according to equation 4.

$$\Psi^{PH} = (H - H_0) - T_0(S - S_0) \quad (4)$$

The boundary of the system is taken to be around the whole reformer setup. Figure 1 presents the scheme of the reformer system. 'W_{el}' is the power supplied to the heating band. 'Q' represents the heat released to the atmosphere (or used in preheating the fuel) by the hot gases exiting the reactor.

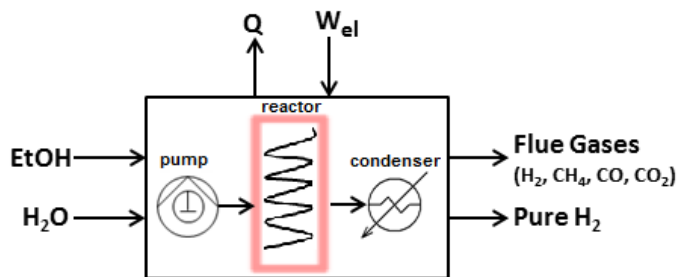


Figure 1 – The Reformer System

The Reformer system was considered in two ways. First, the system was studied considering only the ESR process without any hydrogen purification and, second, with the metallic membrane in use for hydrogen separation. In case of sole ESR process, the exergy efficiency of hydrogen production is defined as:

$$\text{ESR exergetic efficiency} = \eta_{\text{ex.tot}} = \frac{\Psi_{\text{Hydrogen}} + \Psi_{\text{waste gas}}}{\Psi_{\text{water}} + \Psi_{\text{EtOH}} + \Psi_{\text{el}}} \quad (5)$$

When the metallic membrane is in use, pure hydrogen is produced. To evaluate the membrane effect, another factor is defined, which is the Hydrogen Separation Exergetic Efficiency (Ψ_{HS}):

$$\Psi_{HS} = \frac{\Psi_{\text{pure separated hydrogen}}}{\Psi_{\text{total converted hydrogen}}} \quad (6)$$

This factor makes it possible to measure the overall exergetic efficiency of the reforming process by merging the equations 5 and 6, so that:

$$\eta_{\text{ex.reforming}} = \eta_{\text{ex.tot}} \times \Psi_{HS} \quad (7)$$

Thermal efficiency

The thermal efficiency of the system is based on the input and output of the energy flow. For ethanol and gaseous products the Higher Heating Value (HHV) is considered.

$$\eta_{\text{Thermal}} = \frac{HHV_{\text{Products}} + \Delta H_{\text{COOLING}}}{HHV_{\text{EtOH}} + Q_{EL}} \quad (8)$$

Products accounts for the permeated hydrogen and the flue gases. $\Delta H_{\text{cooling}}$ represents the heat released during the cooling process from the reaction temperature to 298.15 K.

Results

The fuel flow rate showed a significant effect on the exergetic efficiency of the ESR process; ESR exergetic efficiency increases linearly with the increase in the fuel flow rate. The maximum ESR exergetic efficiency reaches 33% at 10 bars and 923 K. As the fuel flow rate increases, the fraction of hydrogen in the produced gases increases in coincidence with the increase in total produced hydrogen. Regarding the pressure and temperature, not a notable effect was seen. Nevertheless, the hydrogen fraction in produced gases was significantly decreased at higher pressures which is described according to the equilibrium reaction of methane steam reforming that is shifted to the reactants side.

When the metallic membrane is in use, the hydrogen separation process is known to be energy free from exergetic point of view due to the physical nature of permeation phenomenon. Hence, the effect of separation process on the whole system is taken into account only in terms of the production of pure hydrogen, aiming for feeding a fuel cell. At higher pressure, the hydrogen separation exergetic efficiency is markedly higher, which is attributed to the dependency of the hydrogen separation on the partial pressure of the hydrogen around the membrane (Sieverts' Law). Ψ_{HS} increases from ~30 to ~70% as the pressure increases from 4 to 12 bar at the highest flow rate at 923 K. The effect of fuel flow rate is more obvious at lower pressures.

Both pressure and temperature had a positive effect on the overall exergetic efficiency of the reforming system, while again the effect of temperature is not considerable. The effect of fuel rate on the ESR exergy efficiency, hydrogen separation exergetic efficiency, and the overall exergy efficiency of the reforming system is shown in figure 2.

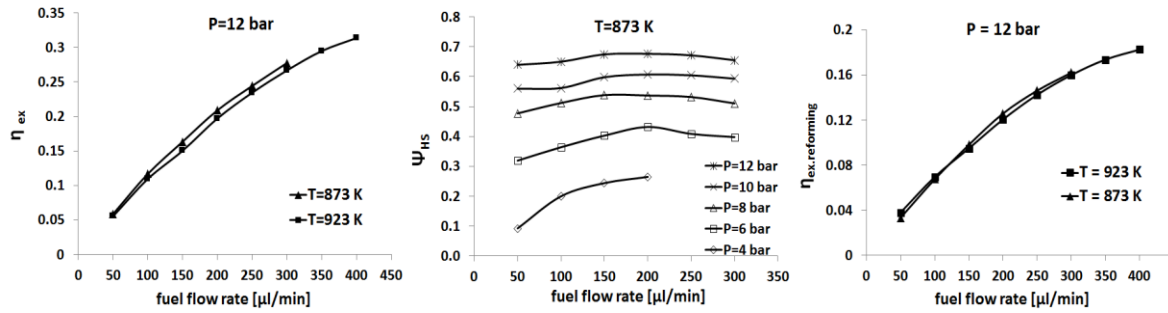


Figure 2 – effect of fuel flow rate on the exergy efficiency factors

It is worthy to mention that although the diverse effects of higher pressure on the hydrogen yield and higher fuel flow rate on the hydrogen separation exergetic efficiency were stated, the overall performance of the system is improved when both pressure and fuel flow rate increase. On one hand more fuel is available for conversion to hydrogen at higher fuel flow rates and on the other hand more hydrogen is able to permeate through the membrane at higher pressures.

The heat loss study of the system showed that if the reactor walls are insulated ideally, the overall exergetic efficiency of the reformer system increases significantly and can reach values up to 40%. Another interesting result is that the effect of fuel flow rate on the exergetic efficiency is nearly ignorable in case of discounting the heat losses.

The evaluation of the thermal efficiency of the reforming process shows a high dependency upon inlet fuel flow rate and the reaction temperature while it is nearly independent of the pressure changes. The thermal efficiency significantly increases from 6% to 35% as the fuel flow rate increases from 50 to 400 μl/min at 923 K. Thermal efficiency of the reforming system represents higher values compared to the exergetic efficiency. At 12 bar and 923 K the exergetic efficiency of the reforming process is around 20%, while the thermal efficiency is 35% at the same conditions. Generally, the thermal efficiency is up to five times more than the exergetic efficiency. Nevertheless, taking into account the second law of thermodynamics and considering the final states of the products, exergetic evaluation gives better idea on the performance of the system and its approach to the ideality.

Conclusion

The exergy of the catalytic steam reforming of ethanol was studied using a Pd-Rh/CeO₂ catalyst in a metallic membrane reactor. Two scenarios were studied, i.e. the ESR process itself and the purification of hydrogen via the metallic membranes. The effects of operational conditions on the exergetic factors were studied and it was concluded that fuel flow rate and pressure have significant effects on the exergetic efficiency. Also it was determined that the heat loss effect on the overall exergetic efficiency of the reformer is considerable and in case of full insulation of the reactor vessel, the overall exergetic efficiency is ~40% under the operational conditions tested. The process is optimized at 8 bars both exergetically and operationally in terms of production of hydrogen.

References

Luis M. Gandia, Gurutze Arzamendi and Pedro M. Dieguez, Renewable Hydrogen technologies; Production, Purification, Storage, Applications and Safety, Elsevier, 2013, chap. 1

Diego Mendes, Silvano Tosti, Fabio Borgognoni, Adelio Mendes, Luis M. Madeira, Integrated analysis of a membrane-based process for hydrogen production from ethanol steam reforming, Catalysis Today, 2010 156; 107–117

Eduardo Lopez, Nuria J. Divins, Jordi Llorca, Hydrogen production from ethanol over Pd–Rh/CeO₂ with a metallic membrane reactor, Catalysis Today, 2012, 193; 145– 150

Hicham Idriss, Morgan Scott, Jordi Llorca, Sze C. Chan, William Chiu, Po-Yo Sheng, Anna Yee, Mark A. Blackford, Steve J. Pas, Anita J. Hill, Faisal M. Alamgir, Robert Rettew, Cole Petersburg, Sanjaya D. Senanayake, Mark A. Barteau, A Phenomenological Study of the Metal–Oxide Interface: The Role of Catalysis in Hydrogen Production from Renewable Resources, ChemSusChem, 2008, 1; 905-910

Hydrogen production from biogas reforming process: study of catalyst deactivation in the presence of H₂S (HPR1-4)

U. Izquierdo, V.L. Barrio, J. Requies, M.B. Güemez, J.F. Cambra, P.L. Arias

Dept. of Chemical and Environmental Engineering, School of Engineering. University of the Basque Country UPV/EHU

INTRODUCTION

Europe needs a clean, safe, reliable and guaranteed energy supply that enables the high quality of life and sustainable development. Its current energy system is based on fossil fuels and is showing clear signs of exhaustion and their use presents evident and negative environmental impacts. Therefore, the use of sustainable energy resources, such as biogas, provides solutions to the problems derived from the use of fossil fuels as well as to the existing increasing energy consumption [1].

The aim of this work is the production of hydrogen, an energy vector of great interest, from a renewable resource like biogas by a tri-reforming process. Special emphasis was dedicated to study the influence of hydrogen sulfide on the catalyst activity and to catalysts regeneration through several processes [2,3].

EXPERIMENTAL METHODOLOGY

A bench-scale Microactivity plant (PID Eng&Tech), was used for activity tests. The fed gaseous mixture flows were adjusted by electronic controllers and a HPLC-Gilson liquid pump was used for the deionized water injection. Before running the activity tests, each catalyst was reduced at 1073 K, using 350 NmL/min of a N₂:H₂=3:1 mixture during 4 h. The effluent stream was cooled down in a partial condenser. The condensed aqueous phase was collected and weighted, and the gas phase was online analyzed by a Micro GC equipped with a TCD detector.

Several Ni-based catalysts and a bimetallic Rh-Ni catalyst supported on alumina modified with CeO₂ and ZrO₂ oxides were prepared. For all the experiments, at first a synthetic biogas consisting of 60% CH₄ and 40% CO₂ (vol.) was fed to the catalytic fixed bed reactor under tri-reforming conditions (S/C=1.0 and O/C=0.25 [4]) and after 1 hour of stable operation, 25 ppm of H₂S were added to the model biogas in order to study catalysts deactivation phenomena. Then, two types of regeneration processes were carried out, a self-regeneration and a low temperature oxidation, with the aim of testing the feasibility of tri-reforming catalysts regeneration when sulfur poisoning occurs.

RESULTS AND DISCUSSION

Several characterization techniques were used in order to study the physico-chemical properties of the catalysts. In Table 1 the catalysts textural properties (BET), chemical compositions (ICP/AES) and H₂ chemisorption and XRD results are summarized. In addition to those techniques, TPR profiles were obtained for all the catalysts and both fresh calcined and spent catalysts surfaces were also characterized through XPS measurements.

Very high conversions, near to the ones predicted by thermodynamical equilibrium, were achieved by all tested catalysts at the beginning when the model biogas was fed. Then, after 1 hour of stable operation, when 25 ppm of H₂S were continuously added to the feed all the catalysts suffered from deactivation. Therefore, two different regeneration processes were carried out.

Table 1: Surface area (Sa), Pore volume (Pv), Pore size (Ps) and chemical composition of calcined catalysts. Hydrogen chemisorption results of reduced catalysts: Metal surface area (Ma), Dispersion (Disp.) and Ni crystallite size (Cs). Ni average Cs measured by XRD.

Catalyst	Textural properties			Chemical composition (ICP/AES)		H ₂ chemisorption			XRD	
	Sa (m ² / g)	Pv (cm ³ / g)	Ps (Å)	Nominal / real (wt.%)		Ma (m ² / g)	Disp. (%)	Ni Cs (nm)	Ni Cs (nm)	
Commercial	21.6	0.09	169.5	-/12.4 (Ni)	-/0.4 (Ca)					
Ni/Ce-Al ₂ O ₃	163.3	0.59	143.7	13.0/10.8 (Ni)	6.0/3.3 (Ce)	5.6	6.4	16	8	
Ni/Zr-Al ₂ O ₃	166.6	0.62	146.3	13.0/11.4 (Ni)	8.0/5.5 (Zr)	-	-	-	-	
Ni/Ce-Zr-Al ₂ O ₃	151.0	0.60	153.2	13.0/10.6 (Ni) 4.0/3.6 (Zr)	3.0/2.7 (Ce)	5.1	7.3	14	7	
Rh-Ni/Ce-Al ₂ O ₃	156.8	0.60	150.1	13.0/10.0 (Ni) 6.0/3.6 (Ce)	1.0/0.9 (Rh)	8.0	11.6	88	5	

In the case of the commercial catalyst, no regeneration was observed after the deactivation using any of the two regeneration processes studied. For the Ni/Ce-Al₂O₃ and Ni/Zr-Al₂O₃ catalysts results are presented in Figure 1. The self-regeneration (the graphs in top of Figure 1) consisted of just removing the H₂S injection. It was carried out after full deactivation and when the process was stable. If the results obtained are compared, the CeO₂ containing catalysts almost recovered the initial catalytic activity while the ones containing ZrO₂ experimented a very small activity recovery.

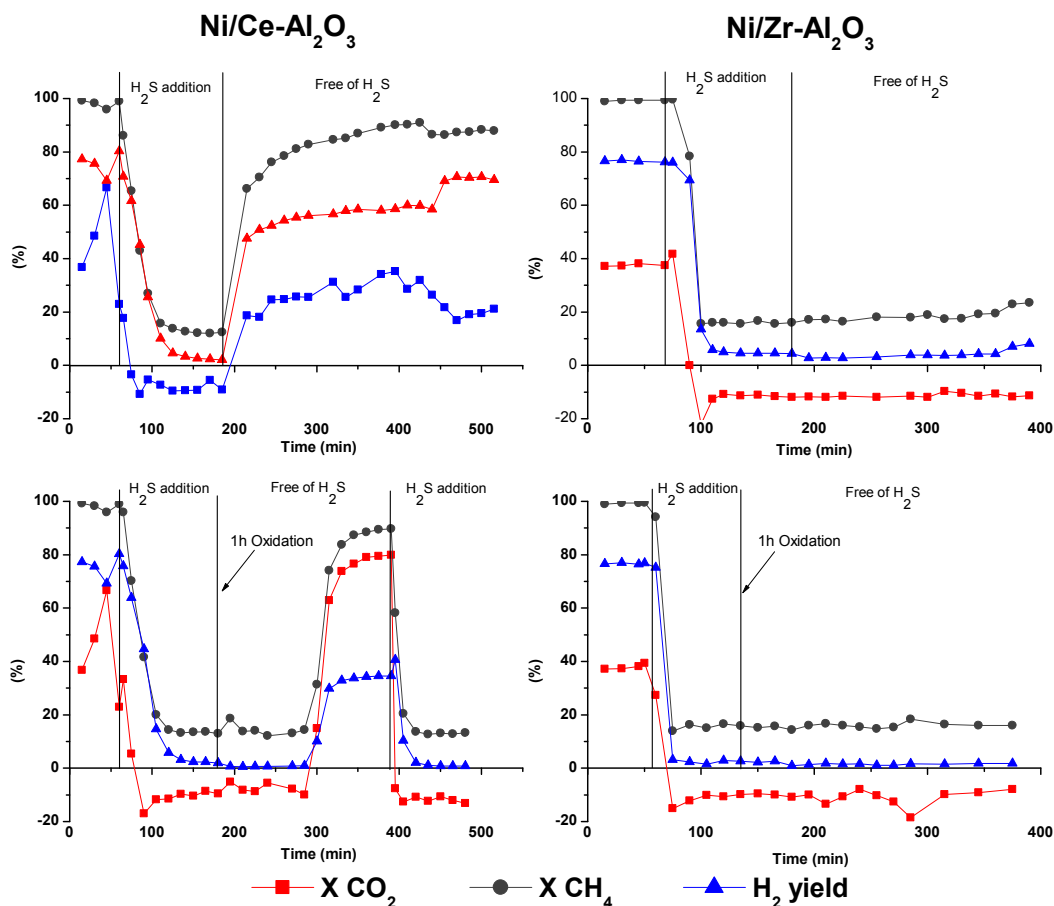


Figure 1: Ni/Ce-Al₂O₃ and Ni/Zr-Al₂O₃ catalysts activity results. Top left: self-regeneration of the Ni/Ce-Al₂O₃ catalyst. Bottom left: Regeneration by oxidation of the Ni/Ce-Al₂O₃ catalyst. Top right: self-regeneration of the Ni/Zr-Al₂O₃ catalyst. Bottom right: Regeneration by oxidation of the Ni/Zr-Al₂O₃ catalyst.

The regeneration by low temperature oxidation (the graphs at the bottom of Figure 1) was carried out passing a mixture of O₂:N₂=1:3 (vol.) at 500°C during 1 h. After this regeneration process the initially used model biogas stream was again fed. For the ZrO₂ containing catalyst, no regeneration took place. However, in the case of the CeO₂ containing catalyst, after two hours of fully deactivated operation, the low temperature oxidation regenerated its reforming capacity. As a result CH₄ conversion reached values similar to the ones obtained before the sulfur addition and CO₂ conversion reached higher values than the ones initially measured. The regeneration process by low temperature oxidation seems to promote the CO₂ conversion. Finally, H₂S was added again to the reactant stream in order to study a second deactivation process, which occurred quicker. For the CeO₂-ZrO₂ catalyst the same behavior as for the CeO₂ catalyst was observed. Characterization results provide evidences about how ceria facilitated regeneration.

For the bimetallic catalyst, the Rh-Ni/Ce-Al₂O₃, the presence of a noble metal implied that deactivation took longer time. Specially, in the case of just self-regeneration high methane and CO₂

conversions were reached. Thus, the presence of a small amount of Rh allows increasing deactivation catalyst resistance.

CONCLUSIONS

In this work, Ni-catalysts reactivation after sulfur poisoning while being used to reform biogas was studied using two different regeneration processes. In the case of the commercial and Ni/Zr-Al₂O₃ catalysts, they did not recover their activity using any of the two regeneration processes.

Ni/Ce-Al₂O₃ and Ni/Ce-Zr-Al₂O₃ catalysts recovered most of their initial activity. Furthermore, in the case of the regeneration under oxidative conditions at low temperature, the CO₂ conversion achieved after regeneration was significantly higher than the one obtained before sulfur poisoning. This effect could be attributed to the support modification with CeO₂ and to the higher selectivity achieved for the reverse water gas shift reaction.

As it would be expected, the bimetallic Rh-Ni/Ce-Al₂O₃ catalyst showed higher resistance to deactivation and its sulfur poisoning seems to be reversible.

REFERENCES

[1] Ryckebosch E, Drouillon M, Vervaeren H. Techniques for transformation of biogas to biomethane. *Biomass bioenerg* 35 (2011) 1633-45.

[2] Fidalgo B, Muradov N, Menéndez JA. Effect of H₂S on carbon-catalyzed methane decomposition and CO₂ reforming reactions. *J Catal* 276 (2010) 6-15.

[3] Albertazzi S, Basile F, Brandin J, Einvall J, Fornasari G, Hulteberg C, et. al. Effect of fly ash and H₂S on a Ni-based catalyst for the upgrading of a biomass-generated gas. *Biomass bioenerg* 32 (2008) 345-53.

[4] Izquierdo U, Barrio VL, Requies J, Cambra JF, Güemez MB, Arias PL. Tri-reforming: A new biogas process for synthesis gas and hydrogen production. *Int J Hydrogen Energ* 38 (2013) 7623-31.

ACKNOWLEDGEMENTS

The authors gratefully acknowledge the support from the University of the Basque Country and edp company.

Environmental and economic assessment of technologies for the production of biohydrogen and its distribution (HPR2-1)

Konstantin Zech[□], Stefan Rönsch[□], Elias Grasemann[□], Katja Oehmichen[□],
Julia Michaelis[§], Simon Funke[§]

- [□] Deutsches Biomasseforschungszentrum gGmbH (DBFZ), Torgauer Straße 116, D-04347 Leipzig,
[§] Fraunhofer Institute for Systems and Innovation Research ISI, Breslauer Straße 48, D-76139
Karlsruhe

INTRODUCTION

The conversion of biomass is considered an important option for supplying the future mobility sector with sustainable hydrogen. In the study “Hy-NOW - Evaluation of processes and technologies for the provision of hydrogen based on biomass”, various processes and technologies were evaluated which are suitable for a biomass-based production of hydrogen. This includes thermochemical processes like the gasification of biomass in fixed bed, fluidized bed and entrained-flow gasification systems and the reforming of secondary bioenergy carriers (e.g. biogas) as well as biochemical processes like the fermentation of biomass to hydrogen or the photolysis of water. After a fundamental pre-screening of these processes, three of them were identified as being most promising for a short or medium-term realization within a demonstration plant. Plant and distribution concepts for these three processes were then defined and subsequently analyzed in detail.

PLANT CONCEPTS

Two of these plant concepts are based on allothermal fluidized bed gasification, with production capacities of 9 MWH₂ (270 kg/h H₂ – concept 1) and 3 MWH₂ (90 kg/h H₂ – concept 2). In these concepts, wood chips are gasified in a twin bed reactor using a circulating bed material to provide the required reaction heat. The raw gas leaving the gasifier is cooled down in a heat exchanger, dedusted in a pre-coated bag house filter and fed into a sulphur resistant raw gas shift reactor to raise the hydrogen content of the gas. Tars are removed in an oil-based washing system, the gas is compressed and carbon dioxide is removed in a pressurised water washing. Remaining methane from the gasification is separated from hydrogen by a pressure swing adsorption and reformed afterwards. Figure 1 depicts the plant setup of concept 1 exemplarily.

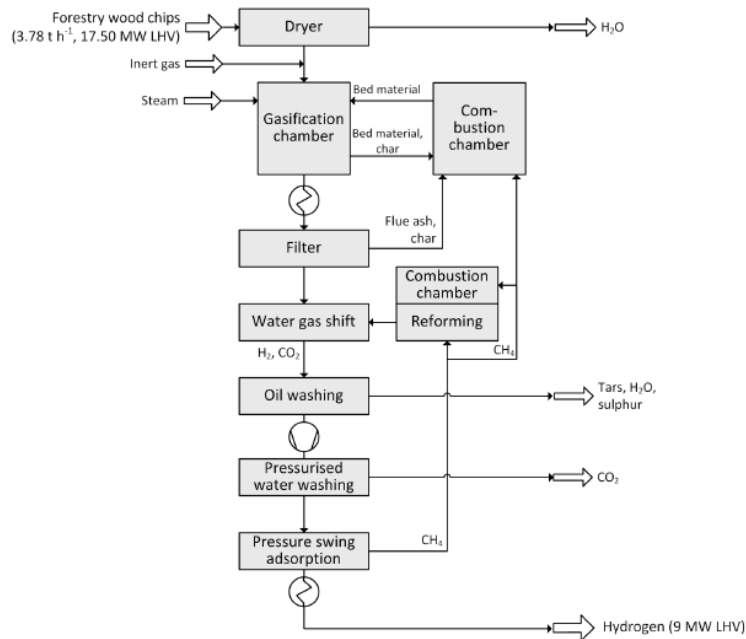


Figure 1: Process scheme of concept 1

The third concept (not depicted) is based on the steam reforming of biogas and has a production capacity of 6 MW H₂ (180 kg/h H₂). The assumed raw material, a mixture of maize silage, manure and organic waste, is mashed and anaerobically digested to biogas. After cleaning, the methane fraction of the biogas is converted to hydrogen using an allothermal steam reforming reactor and a water-gas-shift process.

In both plant concepts, a pressure swing adsorption is used to separate hydrogen with high purity.

DISTRIBUTION CONCEPTS

With regard to plant capacities, it is assumed that transport is realized through trailers with pressure cylinders of 500 bar and a capacity of 1 ton of hydrogen per trailer. The distribution concept includes compression and storage, transport and distribution of hydrogen at the filling station. Since neither the production site nor the filling station is considered as a specific location, a mean transport distance of 150 km is assumed.

A capital intensive transport using a pipeline might only be feasible in isolated cases within the short or medium term.

TECHNICAL ASSESSMENTS

Within the technical analysis, the energetic efficiency is evaluated based on a detailed mass and energy flow analysis. These are calculated by flow-sheet simulation. Figure 2 shows the resulting energy flow diagram of plant concept 1 exemplarily.

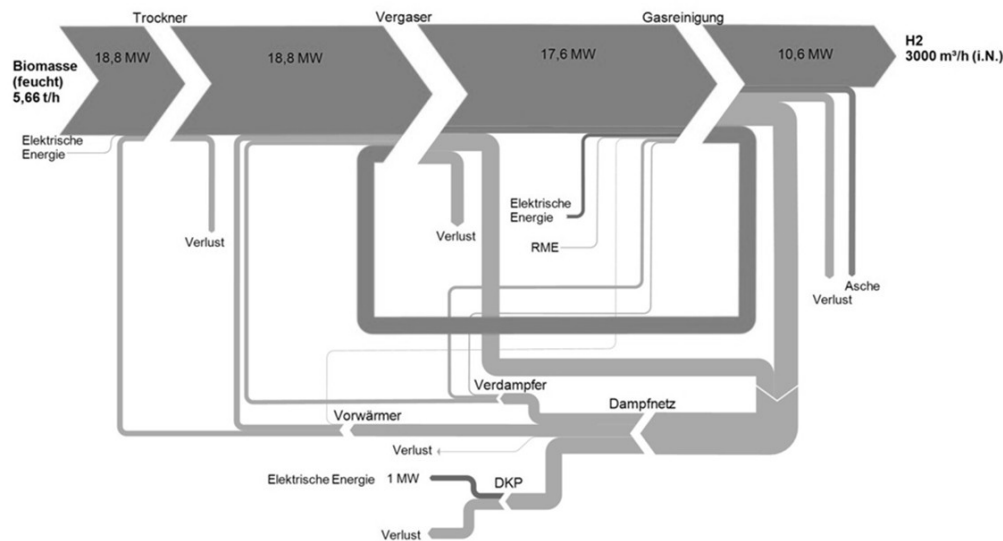


Figure 2: Energy flow diagram of plant concept 1 (in German)

The technical assessment shows disadvantages for the fermentation-based plant concept in the net efficiency of the hydrogen production, i.e. the conversion efficiency from biomass to hydrogen. The net efficiency ranges from 50 % for concept 1 to 39 % for concept 3. Under consideration of thermodynamic criteria, gasification-based concepts appear advantageous, since they are characterized by smaller losses – especially for plants with higher outputs.

Taking the energy demand related to the distribution of hydrogen into account, the overall efficiency decreases further to between 43 % for concept 1 and 34 % for concept 3.

ECONOMIC ASSESSMENTS

The hydrogen production costs were calculated based on an approach defined in the guideline number 6025 by the association of German engineers. For the gasification-based concept 1 specific hydrogen provision costs of 59 EUR/GJ H₂ (7.1 EUR/kg H₂) were calculated. These costs correspond to the fermentation-based concept 3 with provision costs of 54 EUR/GJ H₂ (6.5 EUR/kg H₂). With 76 EUR/GJ H₂ (9.1 EUR/kg H₂) the gasification-based concept 2 has about 30 % higher provision costs mostly related to scaling. Generally, 30 to 40 % of the provision costs are caused by the distribution of the hydrogen.

Regarding both financial risks and biofuel production costs total capital investments (TCI) are an important factor. These were estimated to amount to 32 mill. EUR for concept 1 (3 555 EUR/kW H₂), 14.6 mill. EUR for concept 2 (4 875 EUR/kW H₂) and 21.3 mill. EUR for concept 3 (3 544 EUR/kW H₂).

ENVIRONMENTAL ASSESSMENTS

The life cycle assessment shows a high influence of the hydrogen distribution on the emissions, energy consumption and greenhouse gas mitigation potentials. The utilization of electric power for

the hydrogen compression is the driving impact herein, when the German electricity mix is assumed. The differences in the life cycle assessments are small for the raw material conversion. There are, however, differences in the feedstock supply. Residual forest wood is assumed as feedstock for the gasification-based concepts, whereas a substrate containing 60 % energy crops is assumed for the fermentation-based process. Therefore, the gasification-based concepts 1 and 2 reach the target that biofuels have to fulfill by 2017, demanding a greenhouse gas mitigation of 50 %. The fermentation-based concept 3 does not reach this target under the assumptions made.

The specific greenhouse gas emissions amount to ca. 34 gCO₂-Eq./MJ (4,08 kgCO₂-Eq./kg H₂ resp.) for the gasification-based concepts 1 and 2 whereas ca. 44 gCO₂-Eq./MJ (5,28 kgCO₂-Eq./kg H₂ resp.) were calculated for the fermentation-based concept 3. Through a larger share of renewable energy in the future electricity mix, the greenhouse gas emissions of all three concepts could be lowered substantially.

CONCLUSION

Considering the specific costs of the hydrogen provision, concepts 1 and 3 are on a similar level. Since the TCI are an important factor determining the financial risk, concept 2 has advantages despite the relatively high hydrogen provision costs. Furthermore, the lower raw material requirements ease its supply with an adequate-priced feedstock.

The gasification-based concepts 1 and 2 have significantly lower greenhouse gas emissions compared to the fermentation-based concept 3. This is due to the assumed raw material being consisting mostly of energy crops as opposed to forestry residues. However, the largest share of the greenhouse gas emissions comes from the hydrogen compression within the distribution process.

Since the distribution makes up 30 – 40 % of the total hydrogen provision costs and the larger part of the greenhouse gas emissions, it is a key element for the feasibility of a hydrogen provision concept based on biomass.

ACKNOWLEDGEMENT

The work presented here was part of the collaborative project “Hy-NOW: Evaluation of processes and technologies for the provision of hydrogen based on biomass”. The project was funded by the National Organisation Hydrogen and Fuel Cell Technology (NOW GmbH) within the National Innovation Programme Hydrogen and Fuel Cell Technology (NIP).

Hydrogen Production from Biomass via Steam Reforming of Bio-Oil Components (Furfural). Effect of Support Materials and Method of Incorporation of Active Metal (Ni). (HPR2-2)

S.Sayas, A. Chica*

Instituto de Tecnología Química (UPV-CSIC), Universidad Politécnica de Valencia, Consejo Superior de Investigaciones Científicas, Avenida de los naranjos s/n, 46022 Valencia, Spain

(*) corr. author: achica@itq.upv.es Fax: +34 96 387 78 13 Tel: +34 96 387 70 00 ext.: 78508

INTRODUCTION

Hydrogen can be considered one of the most environmentally friendly fuels that can be efficiently used for power generation [1]. At present, the most favourable route to hydrogen production is based on natural gas and naphtha catalytic steam reforming (SR), or coal gasification, as its main sources. Consequently, hydrogen production based on fossil fuels is a net contributor to CO₂ emissions and the greenhouse effect. Thus, a new eco-friendly reservoir of hydrogen is needed for a clean and sustainable production of energy. Currently, hydrogen production by SR of liquid products from fast pyrolysis has attracted considerable attention [2]. Bio-oil from biomass pyrolysis is a complex mixture, whose major components are oxygenated compounds such as alcohols, acids, aldehydes and ketones, as well as more complex carbohydrates and lignin derived materials [3-5]. This bio-oil can be reformed as a whole or separated by water extraction into two fractions: an organic fraction with lignin derived materials that can be used for the production of more valuable products [6-8], and a water soluble fraction with an industrial limited use, which could be catalytically steam reformed for hydrogen production. In order to select the best operating conditions for hydrogen production by catalytic SR of the aqueous fraction of bio-oil, model compounds can be used for preliminary studies. In this work furfural has been chosen as model compound. In general, biomass derived-compounds to hydrogen through SR highly depend on the type of metal catalyst used, type of precursors, preparation methods, type of catalyst support, presence of additives, and operating conditions [9-11]. Among them, support plays an important role in steam reforming since it helps in the dispersion of metal catalyst and enhances metal catalyst activity via metal-support interaction [9,11]. In the present work we have explored the SR of furfural (SRF) on Ni supported over various supports. It is found that the best results are obtained with double laminar hydroxides (DLHs) as support. Two methods for the Ni incorporation are also explored finding that the incorporation of Ni during the synthesis of DLHs lead to furfural steam reforming materials with high catalytic performance.

EXPERIMENTAL

Seven commercial supports [SiO₂ (BASF), Al₂O₃ (Merck), ASA (Crossfield catalysts), MgO (Fluka), MgAl₂O₃ (Alfa Aesar), ZnO (Fluka), TiO₂ (Aldrich)] and one based on Zn-DLH synthesized in the our laboratory have been used to support the Ni. The incorporation of Ni was accomplished by incipient wetness impregnation with an aqueous solution containing the required amount of Ni (NO₃)₂ 6H₂O (Aldrich, 98%) to achieve a nominal concentration of 20 wt% of Ni. Moreover, another incorporation method of Ni (co-precipitation method) was performed. In this method the Ni was incorporated

during the Zn-DLH synthesis. After Ni incorporation, catalysts were calcined in muffle oven at 600°C for 3 h before reaction. The nickel content in the samples was determined by atomic absorption spectrophotometry (AAS). N₂ adsorption-desorption, X-ray, TEM and TPR have been used as characterization techniques. Steam reforming experiments were carried out in a continuous fixed bed reactor at atmospheric pressure, H₂O/FUR molar ratio of 18, contact time between 0.35 and 2.9 h and a range of temperatures between 400°C and 600°C. Before reaction the catalysts were reduced "in situ" in flow of H₂ at 600°C for 2 hours.

RESULTS AND DISCUSSION

Table 1 shows the catalytic activity and products selectivity for all catalytic materials prepared in this work.

Table 1. Catalytic conversion of furfural and products selectivity. Reaction conditions: 400°C, 1atm, contact time 0.72 h, and H₂O/furfural of 18 (mol/mol).

Catalyst	FUR. Conv., mol %	Products Selectivity, %mol				
		H ₂	CO	CH ₄	CO ₂	C ₃ H ₆ O
Ni/SiO ₂	61.9	54.8	16.8	0.7	23.4	3.9
Ni/Al ₂ O ₃	33.1	58.5	6.2	1.2	28.5	4.0
Ni/ASA	19.8	56.0	8.7	0.2	27.3	7.6
Ni/MgO	0.5	56.6	3.2	0.0	37.0	0.0
Ni/MgAl ₂ O ₃	53.2	52.7	17.4	0.6	21.5	5.7
Ni/ZnO	25.3	57.8	17.0	0.5	19.7	4.2
Ni/TiO ₂	21.8	52.7	16.3	0.4	21.0	8.3
Ni/Zn-DLH	62.4	57.5	5.8	1.0	29.3	5.8

As it can be seen Ni incorporated on Zn-DLH, prepared by us, exhibits the best catalytic performance (Ni/Zn-DLH), according to its higher activity and selectivity to hydrogen. Nevertheless, the products distribution obtained with this material could be still improved. Specifically it would be desirable to increase the hydrogen production and decrease the formation of CO, CH₄ and acetone. Thus, a second method for the incorporation of Ni in the Zn-DLH support was explored. This method consisted in the Ni incorporation during the Zn-DLH synthesis (co-precipitation method).

As it can be seen in Figure 1, the Zn-DLH based catalyst containing Ni incorporated by co-precipitation (NiZn-DLH) improved the catalytic performance. Specifically, it can be seen a significant improvement in the activity at low reaction temperatures (400°C) and in the production of non-desirable products such a CO and CH₄.

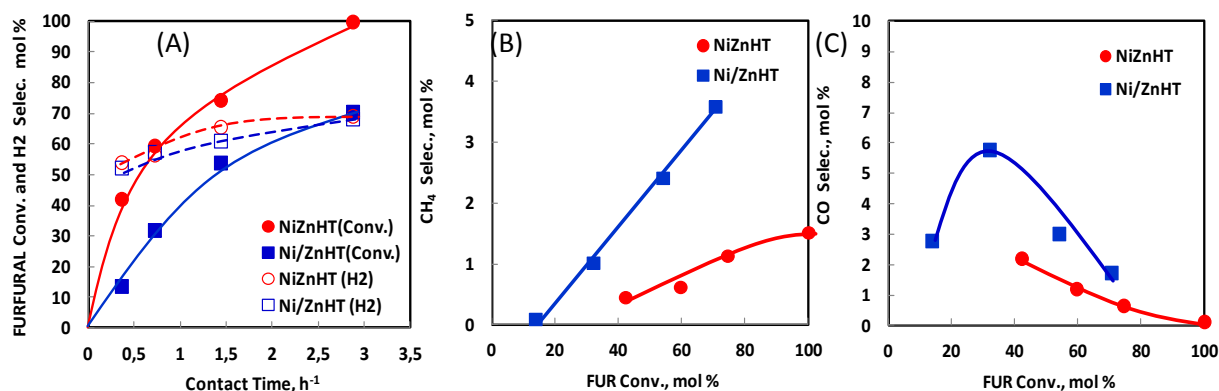


Figure 1. Catalytic performance of the two samples of Zn-DLH where the Ni has been incorporated using two different methods (incipient wetness impregnation and co-precipitation). Reaction conditions: T=400°C; P=1atm; H₂O/FUR =18; different contact times. (A) Furfural conversion and hydrogen selectivity versus contact time; (B) CH₄ selectivity versus furfural conversion and (c) CO selectivity versus furfural conversion.

BET surface area and size of the Ni metallic particles (calculated by XRD and TEM) were determined. Co-precipitation method led to a Ni-based catalyst with larger BET area and significantly smaller nickel metallic particles (45 m²/g and 13 nm, and 20 m²/g and 32 nm, respectively). These features are very important from the catalytic performance point of view since smaller Ni metallic particles would increase the number of active sites available to carry out the SRF. This characterization results could explain the better catalytic performance exhibited by the sample prepared by co-precipitation (NiZn-DHL).

Together to the activity another important features of a good catalyst is the stability. It is well known that the stability of a reforming catalyst is strongly influenced by the coke deposition and metal sinterization. Catalytic activity, carbon deposited and level of sinterization of metallic nickel particles were study after 24 hours of reaction at 400°C. Ni/Zn-DHL catalysts presented a higher deactivation over time (7,2% of deactivation for the sample Ni/Zn-DHL against 2,8% for NiZn-DHL sample). This deactivation level could be explained by the higher amount of deposited carbon and especially by the stronger level of sinterization of the nickel metallic particles found for this sample (15.2 wt.% of deposited carbon and 24% of sinterization level for sample NiZn-DHL against 18.3 wt.% of deposited carbon and 45% of sinterization level for sample Ni/Zn-DHL).

CONCLUSIONS

Different supports promoted with Ni have been tested in the SRF. Among them, Zn-DLH-based catalyst exhibited the best catalytic performance. Two methods of Ni incorporation over the Zn-DLH support have been also studied. Co-precipitation method has allowed to prepare a NiZn-DLH-based material with improved catalytic behaviors in the SRF. Characterization of this material suggests that it's higher BET area and lower Ni metallic particles are the main responsible of its enhanced catalytic performance. Lower coke deposition and Ni sinterization are also detected in the sample prepared by co-precipitation what would justify the higher stability exhibited by this sample.

ACKNOWLEDGEMENTS

Financial support by the Polytechnic University of Valencia and Spanish Council for Scientific Research (CSIC) is gratefully acknowledged.

REFERENCES

- S.G. Chalk, J.F. Miller, *J. Power Sources* 159 (2006) 73.
- S. Ayalur Chattanathan, S. Adhikari, and N. Abdoulmoumine, *Renewable Sustainable Energy Rev.* 16 (2012) 2366.
- F. Xu, Y. Xu, H. Yin, X. F. Zhu, and Q. X. Guo, *Energy Fuels* 23 (2009) 1775.
- J. Piskorz, D.S. Scott, D. Radlein, *ACS Symp. Ser.* 376 (1988) 167.
- A. Oasmaa, D. Meier, in: A.V. Bridgwater (Ed.), *Fast Pyrolysis of Biomass: A Handbook*, vol. 2, CPL Press, Newbury, 2002, p. 41.
- J. Piskorz, D.S. Scott, D. Radlein, *ACS Symp. Ser.* 376 (1988) 167-178.
- S.Czernik, D. Wang, D. Montane, E. Chornet, *E. Dev. Thermochem. Biomass Convers.* 1 (1997) 672-686.
- S.S. Kelley, X.M. Wang, M.D. Myers, D.K. Johnson, J.W. Scahill, *Dev. Thermochem. Biomass Convers.* 1 (1997) 557-572.
- A. Chica, S. Sayas, *Catal. Today* 146 (2009) 37-43.
- Huber, G.W., Corma, A., *Synergies between bio- and oil refineries for the production of fuels from biomass*, *Angew. Chem. Int. Ed.*, 46, pp. 7184-7201, 2007.
- J. F. Da Costa-Serra, R. Guil-López, A. Chica, *Inter J Hydrogen Energy* 13 (2010) 6709-6716.

Hydrogen production from a bio-oil model compound over alumina and modified alumina nickel catalysts (HPR2-3)

K. Bizkarra, V.L. Barrio, J. Requies, A. Yartu, P.L. Arias, J.F. Cambra

*Dept. of Chemical and Environmental Engineering, School of Engineering
University of the Basque Country UPV/EHU
c/Alameda Urquijo s/n, 48013 Bilbao, Spain*

INTRODUCTION

Hydrogen production is a hot topic in the energy area and it has attracted great interest as a future clean energy fuel because of its potential applications in transportation and production of electricity. It can be produced from various sources, like fossil fuels and sustainable resources. Nevertheless, the use of hydrocarbons and coal for hydrogen production fails to provide a solution to deal with the huge amount of carbon dioxide emissions produced during hydrogen production processes.

Therefore, the development of a technology using biomass resources to produce hydrogen attracts much attention, as they are considered renewable, available, and carbon-neutral. Biomass derived bio-oils such as alcohols and organic acids are easily obtained and are recognized as appropriate fuels for hydrogen production.

In this study, the steam reforming (SR) of a model compound (n-butanol), representative of biomass derived pyrolysis liquid or bio-oil -renewable resource- was selected as hydrogen production process. Both fresh and used catalysts were characterized using inductively coupled plasma atomic emission spectrometry (ICP-AES), N₂ physisorption, temperature programmed reduction (TPR), H₂ chemisorption, X-ray diffraction (XRD) and X-ray photoelectron spectroscopy (XPS) techniques. These results are correlated with the obtained activity results.

ACTIVITY TESTS

A bench-scale Microactivity plant (PID Eng&Tech), was used for activity tests. The fed gaseous mixture flows were adjusted by electronic controllers and two HPLC-Gilson liquid pumps were used for the bio-oil model compound and deionised water injection. A 316-L stainless-steel fixed bed reactor (9 mm i.d. and 30.5 cm length) was used in all the experiments, as a conventional reaction system. The reaction products were cooled in a partial condenser.

The condensed liquid was collected, weighted and offline analyzed with a gas chromatograph equipped with TDC and FID detectors. The gas phase was online analyzed with another gas chromatograph equipped with the same detectors. Two columns were used in a series arrangement for the complete separation of the components of the gas phase, such as hydrogen, methane, carbon monoxide and carbon dioxide.

Different nickel based catalysts, supported on alumina and alumina modified with CeO₂, La₂O₃ and MgO, were prepared. The presence of nickel is an important parameter for the catalytic process

because metallic nickel activates the organic molecule, breaking O-H, C-C y C-H bonds and promotes the reaction of organic fractions with the OH groups of water. The modifiers were selected based on their high oxygen mobility and storage capacity (Ce) and their ability to neutralize acidic sites of the support (La and Mg). A commercial Ni/Al₂O₃ catalyst was used for comparison purposes.

Before running the activity tests, each catalyst was reduced at 1073 K, using 225 NmL/min of a 4:1 N₂:H₂ mixture during 4 h. Four hours activity tests were carried out at 1073, 973 and 873 K and then the reaction temperature was raised until 1073 K again for two hours to compare results with the initial ones to check whether catalysts suffered deactivation or not. Finally, blank and bare supports tests were also performed.

All tests were carried out at atmospheric pressure, feeding the bio-oil model compound (n-butanol) and water to achieve a steam to carbon ratio (S/C) of 5.0.

RESULTS AND DISCUSSION

All catalysts achieved complete conversions of n-butanol in activity tests at different temperatures, except the commercial one in the SR test at 873 K. However, the measured hydrogen yields showed differences between the tested catalysts.

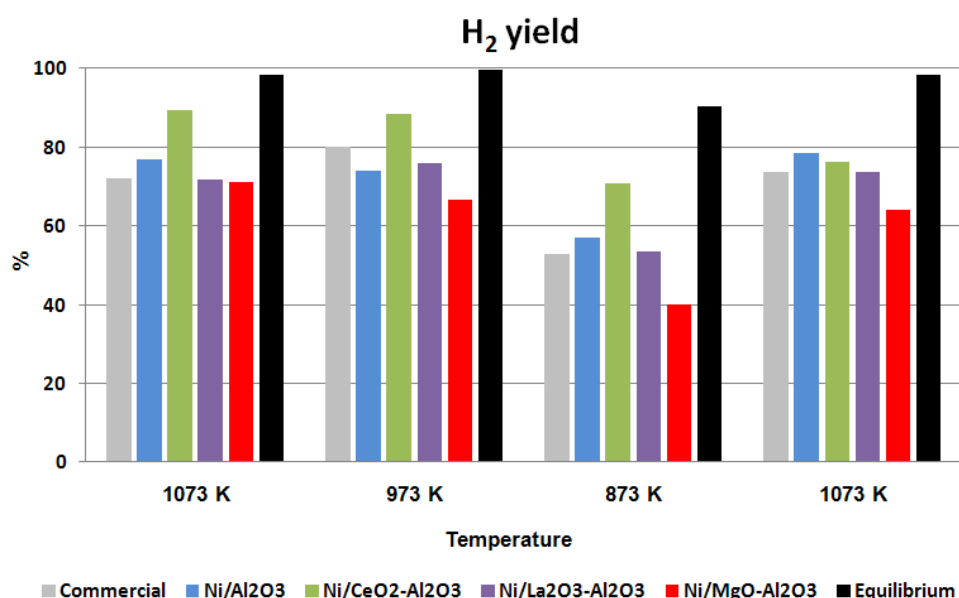


Figure 3. Comparison of hydrogen yields achieved during the activity test under different experimental conditions compared with the equilibrium values.

The equilibrium H₂ yield reaches a maximum value at 973 K. These equilibrium yields were not achieved by any of the tested catalyst. Besides, the experimental hydrogen yields are much lower than the equilibrium hydrogen yields. The difference is due to the presence of C₂, C₃ and C₄ species in the reaction gas product, which do not appear in equilibrium conditions. The higher hydrogen yield was reached in the SR process with the Ni/CeO₂-Al₂O₃ fresh catalyst at 1073 K.

The commercial catalyst showed in general a lower H₂ yield compared with the prepared Ni/Al₂O₃ catalysts. When support modified catalysts were tested, the reached hydrogen yield varied significantly in the cases of Ni/CeO₂-Al₂O₃ and Ni/MgO-Al₂O₃ catalysts, which showed a higher and lower hydrogen yields than the nickel catalyst supported on bare alumina, respectively, in all tested conditions. Ni/La₂O₃-Al₂O₃ catalyst showed a similar behaviour to the commercial catalyst.

When reaction temperature was raised again to 1073 K, three catalysts maintained the initial hydrogen yield values (Commercial, Ni/Al₂O₃ and Ni/La₂O₃-Al₂O₃), while other two catalysts evidenced clear deactivation signs. However, despite the deactivation, Ni/CeO₂-Al₂O₃ catalyst continues achieving one of the highest hydrogen yields. Correlation between activity data and characterization results will be described.

CONCLUSIONS

In this work the effect of the temperature in steam reforming of n-butanol at S/C = 5.0 was studied using several catalysts prepared in the laboratory, as well as a commercial one. The obtained results show a hydrogen yield improvement using prepared Ni/Al₂O₃ catalysts instead of the commercial one.

Ni/CeO₂-Al₂O₃ catalyst achieved the higher hydrogen yield in all 4 hour duration tests, and it continues being one of the catalysts with the higher hydrogen yield when reaction temperature was raised again to 1073 K. Therefore, the modification of the support of the nickel catalyst with cerium oxide is beneficial for in order to obtain a more active catalyst.

Ni/Al₂O₃ and Ni/La₂O₃-Al₂O₃ catalysts showed a high stability. This stability will be correlated with the characterization data.

Hydrogen Production From Coal And Biomass Co-Gasification. Elcogas Experience On The Field (HPR2-4)

Pedro Caseroa, Francisco García Peñaa, Pilar Cooaa

aELCOGAS S.A. R&D Department, Ctra.Calzada de Calatrava, km 27, Puertollano, 13500 Spain

ELCOGAS S.A. is a Spanish company shared by European electrical companies and equipment suppliers. It operates the Puertollano 335 MWe ISO IGCC demonstration power plant, the largest IGCC in the world using solid fuel in a single pressurised entrained flow gasifier. It is in commercial operation since 1998 with syngas being its design fuel a mixture 50:50 of coal (45% ash) and pet-coke (6 % sulphur).

The ELCOGAS R&D activities are based on the opportunity that an operative IGCC plant offers to fuel flexibility, multi-production and zero emissions. Current largest investment in R&D activities is focused on CO₂ capture and Hydrogen production, aiming at demonstrating the feasibility of CO₂ capture coupled with Hydrogen production in an IGCC that uses solid fossil fuels and wastes as feedstock. A significant milestone was the construction of a 14 MWth pilot plant fed by a 2% slip-stream of the Puertollano IGCC (3,600 Nm³/h) and able to capture 100 t/d of CO₂ while producing 2 t/d of high purity Hydrogen, using proven and commercial technology. The feeding gas can be “sweet” or “sour” (free or not from sulphur compounds). The process consists on a two-step shifting unit to convert CO into CO₂, a CO₂ separation unit through chemical absorption and a Hydrogen purification unit through PSA technology which provides 99.99% purity hydrogen at 15 bar and 40°C. Auxiliary systems and process control are completely integrated in the existing IGCC. The plant was commissioned in 2010 (see figure 1).

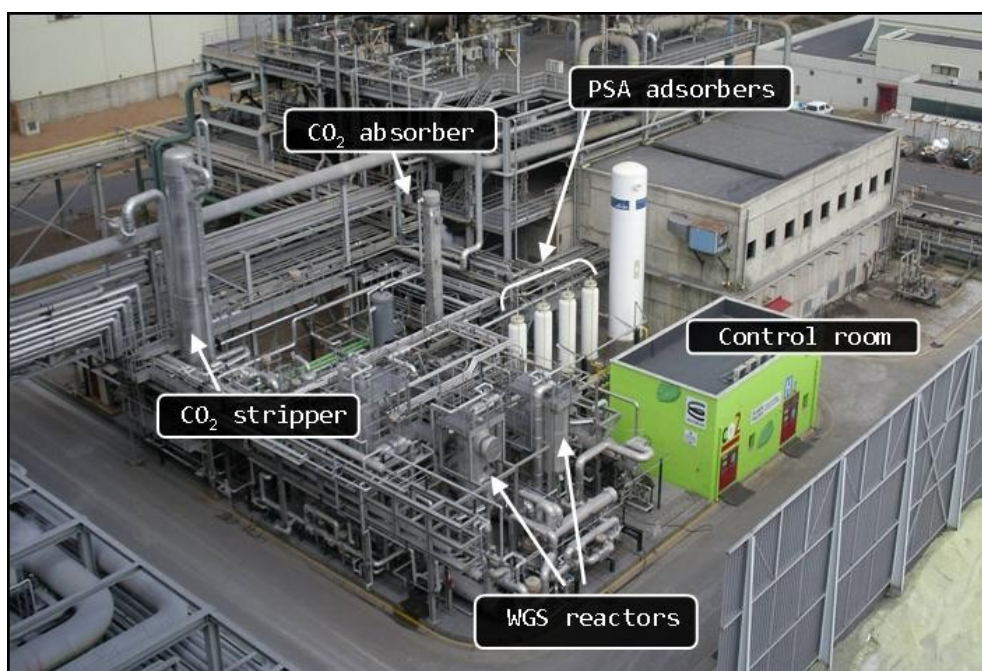


Figure 1. CO₂ capture and H₂ Production Pilot Plant at Elcogas.

One of the main assets of this kind of plant (industrial pilot) is that allows realistic economic estimates in various scenarios, like electricity and H₂ co-production. This issue was tackled through the elaboration of the breakeven link between the market price for the electricity generated in Puertollano IGCC plant, and the equivalent market price for the hydrogen that could be sold, based on the penalty on electricity generation derived from hydrogen production. Such curve therefore provides with a tool allowing taking the decision whether sell electricity or hydrogen. As a case of study (see Figure 2), considering an electricity market price of 44.3 €/MWh (the average in Spanish electricity market during 2013), this tool provides that the equivalent selling price for the H₂ produced in the IGCC plant is 1,6 €/kg (for H₂ at conditions at the outlet of the PSA purification unit). Namely the decision whether to sell H₂ or electricity is at such values. Another application of this tool is to obtain the marginal cost of H₂ production at ELCOGAS. The average marginal electricity production cost for ELCOGAS in IGCC mode in 2013 was 21.2 €/MWh, which gives an average marginal H₂ production cost of 0.61 €/kg. This value is considering CO₂ capture (but not transport or storage) but without H₂ conditioning.

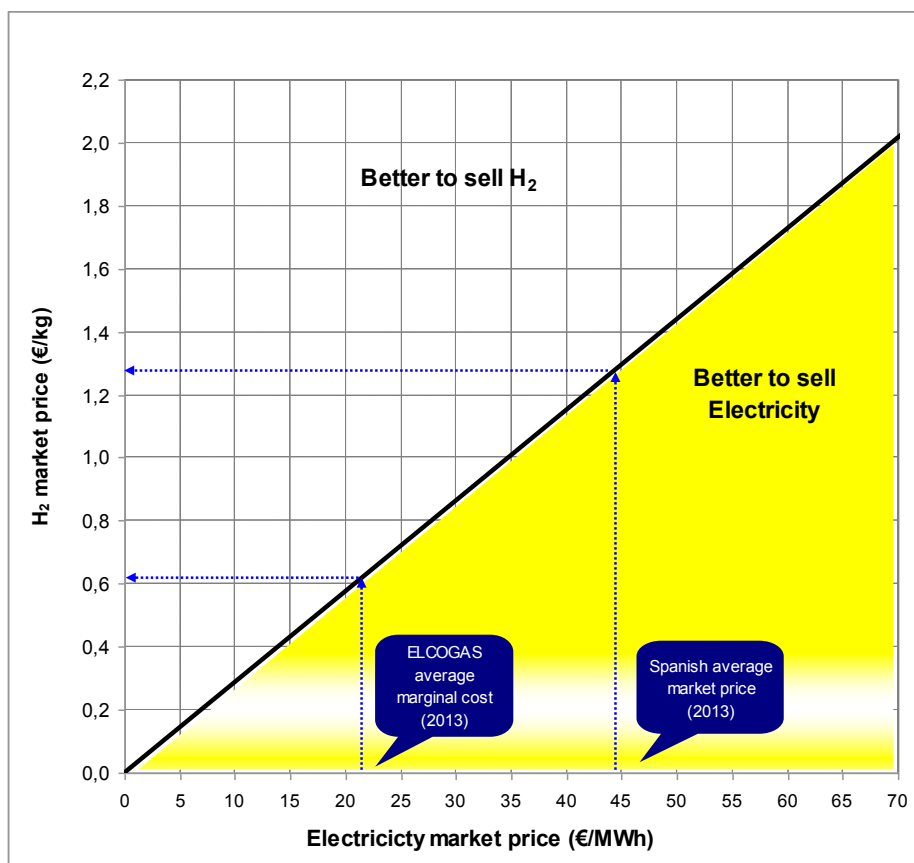


Figure 2. Breakeven curve of electricity market price and H₂ market price.

H₂ is envisaged as an alternative fuels in the near future, and the application to transport is taking shape in the two main elements of the chain: fuel cell vehicles start to hit the roads, and H₂ station

are being deploying. The location of Puertollano offers interesting synergies for this purpose at national level, for example in a hypothetical North-South hydrogen route linking two hydrogen filling stations currently active in Spain: Seville (300 km from Puertollano) and Huesca (600 km from Puertollano). So this is a nice scenario for assessing the competitiveness of the H₂ that could be produced at ELCOGAS. The range of prices currently dispensed in existing H₂ stations vary from 8 to 15 €/kg. To compare this price with the H₂ at ELCOGAS, it is required to take into account the cost of compression, storage and dispensing, which is in the range of 1-2 €/kg for a capacity of 100 t/d. Therefore the total dispensing marginal cost of the H₂ that could be produced in ELCOGAS is between 2 and 3 €/kg, which allows concluding that H₂ produced via gasification of fossil fuels would be competitive.

The most recent experience is related to the integration of this plant using biomass co-gasification, under FECUNDUS project (RFCS Programme) in which the biomass influence in the CO conversion and CO₂/H₂ separation process is being studied through different co-gasification tests: 2 & 4% of orujillo (olive residue) and 2 & 4% of grape seed meal. The CO₂ capture & H₂ Production pilot plant behaved as expected taking into account the working conditions in the conversion and separation units as a whole: The conversion unit was operated in sour conditions with design steam/CO ratios and variable reactors inlet temperatures, showing a satisfactory performance.

Technical achievements of the different tests campaigns carried out in the pilot plant will be reported. Several economic assessments have been done using results coming from this real project, which will also be reported giving special attention to co-production of electricity and Hydrogen scenarios.

Effect of biodiesel derived impurities on the catalytic steam reforming of glycerol in a fluidized bed reactor (HPR2-5)

Javier Remón, Víctor Mercado, Lucía García, Jesús Arauzo

Thermochemical Processes Group (GPT), Aragon Institute for Engineering Research (I3A), Universidad de Zaragoza, Mariano Esquillor S/N, 50018 Zaragoza, Spain

ABSTRACT

In the present work, the specific effect of the presence of three of the impurities most commonly found in glycerol derived from biodiesel manufacturing on the catalytic steam reforming process has been studied. The influence of the concentration of CH₃OH (0-5 wt.%), CH₃COOH (0-3 wt.%) and KOH (0-2.8 wt.%) on the catalytic steam reforming of a solution of glycerol (30 wt.%) at 550 °C has been evaluated using a three factor-two level design of experiments with statistical analysis of the results. The results show that the presence of the aforementioned impurities has a significant impact on the reforming process. Depending on the concentration of the impurities considered in this work, the carbon conversion to gas varies from 76 to 100 %. The gas phase was composed of a mixture of H₂ (68 vol.%), CO₂ (26 vol.%), CO (4 vol.%) and CH₄ (2 vol. %), being the liquid condensate a complex mixture of alcohols, carboxylic acids, ketones, furans and phenols.

1. INTRODUCTION

The production of 10 kg of biodiesel yields approximately 1 kg of crude glycerol. This glycerol discharged from the biodiesel production plants consists not only of glycerol but of many other chemicals as well. These include water, organic and inorganic salts used as catalyst, soaps, alcohol, traces of glycerides and vegetables [1]. In order to diminish the biodiesel production costs, a viable alternative consists of upgrading this glycerol phase towards other valuable products and/or energy.

A promising strategy to upgrade this glycerol derived from biodiesel production is the catalytic steam reforming. There are many works where the catalytic steam reforming of glycerol has been proved appropriate for the valorisation of this by-product. However, in the vast majority of these works, a reagent grade glycerol was used, and there are few works employing crude glycerol. In this context, prior to upgrade crude glycerol, it is very important to understand how the presence of the impurities affects the process in order to select the best refining conditions. This allows reaching a compromise between the prior refining process of the biodiesel-derived glycerol and its posterior upgrading. Taking this information into account, in the present work, the effect of the presence of CH₃COOH (one of the possible acids used in the acidification step), KOH (one of the homogeneous catalyst commonly employed in the biodiesel production) and CH₃OH (an alcohol generally used in the biodiesel production as well as during the liquid-liquid extraction in the purification step) has been studied on the feasibility of upgrading crude glycerol solutions by catalytic steam reforming.

2. EXPERIMENTAL

The catalytic steam reforming experiments were carried out in a fluidized bed reactor at atmospheric pressure and at a temperature of 550 °C, for 3 hours using a W/mglycerol (mass of

catalyst/glycerol mass flow) of 15 g catalyst min/g glycerol. An u/umf ratio of 6 was used. A coprecipitated Ni-Co/Al-Mg, having 28% (relative atomic percentage) of Ni expressed as Ni/(Ni+Al+Mg+Co), an atomic Mg/Al ratio of 0.26 and a Co/Ni atomic ratio of 0.10, was selected for this work. Further information about the experimental system and the catalyst preparation method as well as about the characterization of the catalyst can be found in our previous communication [2].

The influence of the presence of different amounts of CH₃OH (0-5 wt.%), CH₃COOH (0-3 wt.%), and KOH (0-2.8 wt.%) in a 30 wt.% glycerol solution was studied experimentally using a three factors two levels full factorial design of experiments with statistical analysis of the results by means of an analysis of variance (ANOVA) test with a confidence level of 95%. For the experimental design of this work, different 30 wt.% glycerol solutions were prepared according to a full factorial design of experiments. Table 1 shows the composition and the pH of the solutions employed.

Table 1. Acetic acid, methanol, potassium hydroxide (wt.%) content and pH (mean ± standard deviation) of the 30 wt.% glycerol solutions.

Experiment	CH ₃ COOH	CH ₃ OH	KOH	pH
1	0	0	0	5.76 ± 0.22
2	3	0	0	2.46 ± 0.06
3	0	5	0	6.46 ± 0.30
4	3	5	0	2.53 ± 0.22
5	0	0	2.8	13.29 ± 0.41
6	3	0	2.8	11.84 ± 0.31
7	0	5	2.8	13.40 ± 0.47
8	3	5	2.8	11.93 ± 0.37
9,10,11	1.5	2.5	1.4	6.50 ± 0.06

3. RESULTS AND CONCLUSIONS

The presence of the impurities has been evaluated on the carbon conversion to gas, the gas phase composition and the carbon conversion to liquid as well as on the composition of the liquid condensate.

Figure 1 shows the experimental carbon conversion to gas obtained during the reforming experiments. For each experiment, the overall carbon conversion achieved in each one of the three hours of experiment has been calculated and represented in Figure 1. From the experimental results, it was found that the carbon conversion to gas statistically depended on the presence of the biodieselderived impurities studied in this work. Figure 1 shows how the carbon conversion to gas varied from 76 to 100 %, depending on the concentration of CH₃COOH, CH₃OH and KOH. The evolution over time of the carbon conversion to gas revealed catalytic stability for experiments 1 to 4. In contrast, an increase in the carbon conversion to gas with time was observed for experiments 5, 8 and 9, due to the presence of potassium in the solutions, which might have a positive catalytic effect.

The gas phase was composed of a mixture of H₂ (68 vol.%), CO₂ (26 vol.%), CO (4 vol.%) and CH₄ (2 vol. %). It was found that the presence of the impurities has a negligible effect on the composition of the gas phase. The liquid condensates were collected, and analyzed offline by means of total organic carbon content and chemical composition by means of GC-MS. This liquid phase was constituted by a mixture of different organic compounds such as alcohols (methanol and ethanol), acids (acetic acid), aldehydes (acetaldehyde) ketones (1-hydroxy-2-propanone, acetone), furans and phenols (phenol, phenol-2-methyl, phenol-3-methyl) among others. The composition of the liquid phase was statistically dependent on the presence of the impurities studied in this work.

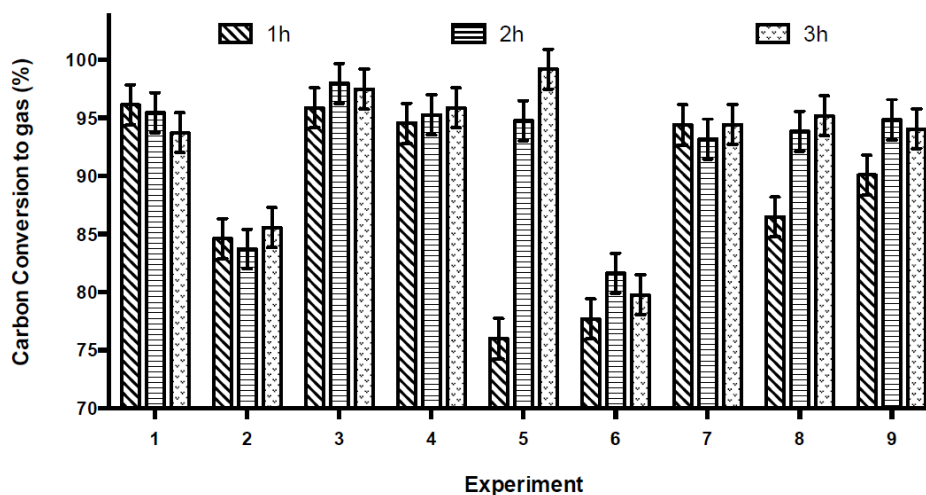


Figure 1. Overall carbon conversion to gas obtained in each of the three hours for the catalytic steam reforming experiments. Results are presented as mean \pm 0.5 LSD interval with 95 % confidence.

All these results have been analyzed in depth making use of a three-factor, two-level design of experiments with statistical analysis of the results. Significant interactions between impurities were detected. The different concentrations of CH₃COOH, CH₃OH and KOH as well as their interactions explain the results obtained in this work. In addition, the effect of the presence of these impurities on the thermodynamic equilibrium values (gas yields and gas compositions) has also been studied using the Gibbs free energy minimization method, employing different thermodynamic packages. Statistically empirical models were created from the thermodynamic results. These models revealed that the presence of the impurities has a statistically significant influence on the thermodynamic equilibrium values at the temperature employed in this work. This influence, although statistically significant, was not very important from a practical point of view. A comparison between the equilibrium values and the experimental results revealed that the differences observed in this work might be kinetic rather than thermodynamic.

4. ACKNOWLEDGEMENTS

The authors wish to express their gratitude to the Spanish MICINN (project ENE-2010-18985) for providing financial support and the FPI grant awarded to Javier Remón Núñez (BES- 2011-044856).

5. REFERENCES

- [1] R. Manosak, S. Limpattayanate, M. Hunsom, Fuel Processing Technology 92 (2011) 92-99.
- [2] J. Remón, J.A. Medrano, F. Bimbela, L. García, J. Arauzo, Applied Catalysis B: Environmental 132-133 (2013) 433-444.

Hydrogen production from supercritical water reforming of glycerol (HPR2-6)

F.J. Gutiérrez Ortiz, P. Ollero, A. Serrera, P. G. Aguilera

*Departamento de Ingeniería Química y Ambiental, Universidad de Sevilla
Camino de los Descubrimientos, s/n. 41092 Sevilla, Spain*

INTRODUCTION

This paper summarizes the overall study on supercritical water reforming of glycerol carried out by our research group during the last four years.

The transformation of glycerol by reforming into an energy carrier (syngas or hydrogen) is one of the most attractive routes of valorization.

The main possible catalytic reforming processes -steam reforming, aqueous phase reforming and autothermal reforming- have been extensively studied, and an evaluation of these could appear attractive. However, as an emerging and promising media, supercritical water (SCW) could be also used to obtain hydrogen due to its relevant thermophysical properties such as a high capability to solubilize gaseous organic molecules and high reactivity, among others, and because the reactions in SCW are conducted in a single phase. As a result, it may be possible to perform the process in the absence of a catalyst, which would be a big advantage as compared with the rest of reforming processes.

The study can be divided in two parts: theoretical and experimental.

THEORETICAL STUDY

The theoretical study was performed using AspenPlus™ as simulation tool in three steps: (1) thermodynamic analysis, (2) energy and exergy analysis of a conceptual design of the process, and (3) optimization of the final proposed process.

The thermodynamic analysis provides information on conditions that are advantageous for hydrogen production. Firstly, a discussion about the most suitable thermodynamic method to be used for the simulation of the supercritical state was carried out, concluding that it was the predictive Soave-Redlich-Kwong (PSRK) equation of state, because it provides the most accurate binary interaction parameters, gives more satisfactory results for mixtures of non-polar and polar components and shows the minimum deviation between the liquid and vapor curves in the supercritical state. By a sensitivity analysis, it was verified that an optimum hydrogen efficiency of 88% (respect to the theoretical maximum) is achieved for a glycerol feed concentration of 5 wt%, at 800 °C and 240 bars.

In a second step, a first conceptual design for producing maximum electrical power in an energy self-sufficient system was proposed and assessed by an analysis of energy and exergy. The design involves a heat exchanger network in order to improve the energy use, as well as an expander at the

reformer outlet to get maximum available work from the huge pressure energy of reformat product. The heat needed in the reformer is delivered by the combustion of the product gas or an external fuel. It was verified that a glycerol feed concentration of almost 22 wt% is necessary to achieve an energy self-sufficient system (a support fuel is not needed), at 800 °C and 240 bars. A net electrical power of 1.3 MW per ton/h is obtained, but burning all the hydrogen generated (about 75 kg/h).

Finally, the design was optimized to maximize power and hydrogen production as follows: the expanded product gas is conditioned by two water gas shift reactors (WGS) and a pressure swing adsorption unit (PSA), so a hydrogen-rich gas stream (with a purity of 99.999%) is sent to a proton exchange membrane fuel cell (PEMFC) to be converted into electrical energy, and the PSA off-gas stream is used as fuel gas to provide the thermal energy required by the reforming process. Figure 1 shows the heat-integrated flow-sheet of the final proposed process. At 800 °C and 240 bars, it was obtained a power of 1.6 MW per ton/h of glycerol with a feed concentration of 26.5 wt.% (874 kW in the PEM fuel cell), resulting in overall exergy and energy efficiencies of 33.8% and 35.8%, respectively.

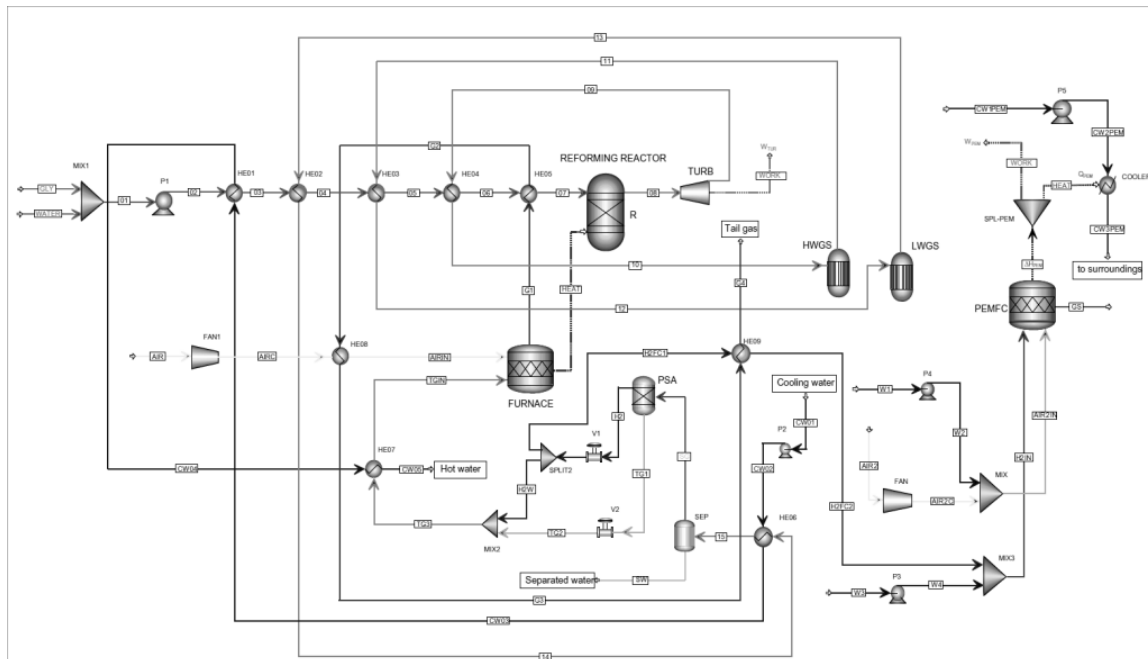


Fig. 1. Process for producing H₂ and power from SCW reforming of glycerol

EXPERIMENTAL STUDY

The possibility of performing the process of glycerol reforming using SCW without adding a catalyst needed to be experimentally verified. In addition, the experimental results make it possible to contrast the previous theoretical results from simulation to get an approach to chemical equilibrium.

Figure 2 illustrates a photo of a part of the pilot plant, which includes its main components. On the front, the electrical furnace is depicted and in the backward, it can be seen the cooler, the first back-pressure control valve, pressure transmitters, liquid-gas knock-out drum, and gas mass flow meter. The reforming process of glycerol using SCW was carried out in an empty tubular reactor. A fraction of the product gas was derived to the gas chromatograph (GC), and some liquid samples were taken from the bottom of the gas-liquid knock-out drum, and cooled-saved for high performance liquid chromatography (HPLC) analysis.

The experimental tests were carried out at 240 bars, temperatures of 750-850 °C, glycerol feed concentrations of 5-30 wt.%, feed flow-rates of 0.5-1.5 L/h, and all of them lasted 3-6 hours.



Fig. 2. General picture of the pilot plant

The results showed that the glycerol conversion was almost complete, except at the highest glycerol feed concentration, in which the conversion was of 88%. Almost all of the product gas (>98 vol.%) was always H₂, CO₂, CO and CH₄. However, in a few cases, it was detected a small concentration of C₂ (<2 vol.%), identified as ethylene or ethane, both with similar retention times in the GC. The mean error of the carbon balance was less than 10%, for all of the valid experiments. It was demonstrated that the use of a glycerol concentration as high as 30 wt.% produces a gas with high hydrogen yield, and other fuel gas (CO+CH₄), when the residence time was 2-3 minutes, matching well the simulation results assuming chemical equilibrium. Hydrogen yields from 2 to 4 mol H₂/mol glycerol were obtained at high and low glycerol feed concentrations, respectively, when operating at high temperature and residence time, although requiring a much higher residence time at a high glycerol concentration. Thus, the equilibrium conversion was not reached when there was insufficient residence time (<1 minute). In addition, the reactor material (made of Inconel 625) seems to show a catalytic activity that decreases to become steady after operating about 50 h. Carbon

nanotubes were encountered in the carbonaceous residues, detecting the presence of nickel particles, whose source could be the own wall of the reactor.

Currently, more experiments are being carried out with the addition of a heterogeneous catalyst, in order to check its activity, stability and selectivity, and to compare with the previous results above mentioned. In this way, lower temperatures are being tested in order to reduce the severity of the operating conditions. Some preliminary results have been obtained using commercial catalysts based on ruthenium and nickel supported on alumina and silica. Apparently, catalysts based on nickel present a better process performance than those based on ruthenium. The catalyst stability is being processed and assessed, because this may be a weak point in the use of catalysts in SCW reforming, so new developments could be recommendable. The selectivities to hydrogen or methane are competitive each other, depending on the catalyst and the operating temperature. These results and some more will be completed in two months, so we will be able to expose these results as a novelty in our current research.

Steam reforming of sulfur-containing liquid fuels: dodecane/ diesel on a Rh-Pt bimetallic catalyst for H₂ production (HPR3-1)

Qinghe Zheng *a*, Christiane Janke *b*, Robert Farrauto *a*, *

a Columbia University, New York, NY 10027, United States

b BASF SE, Ludwigshafen 67056, Germany

Introduction

The steam reforming (SR) of hydrocarbon liquid fuels is accompanied by the WGS reaction and preferential oxidation to produce fuel cell- quality hydrogen [1]. The catalytic reforming of liquid fuels such as diesel is complicated by the tendency for coking and poisoning by sulfur compounds [2]. Coking can be minimized by injection of high concentrations of steam (high S/C ratio) into the feed but an energy penalty is created due to the heat consumption for water vaporization. Precious metal catalysts were widely used in SR and were known to be more active, coke and sulfur tolerant than base metal catalysts such as Ni [3]. The present study was aimed at the exploration of a Rh-Pt bimetallic catalyst in SR of sulfur- containing liquid fuels. Compared to previous studies that also investigated precious metal catalysts in SR of hydrocarbon liquid fuels, new processes were performed in the present study. The SR of dodecane (C₁₂H₂₆) for H₂ production with and without sulfur as a surrogate for diesel fuel was firstly studied. Commercially available diesel was later applied to the catalytic SR infrastructure. The catalyst and process showed the feasibility of simultaneously reducing S/C ratios and sustaining catalytic performance.

Experimental

Catalytic SR of dodecane and diesel reactions were conducted over a Rh-Pt/ ZrO₂-SiO₂ catalyst supplied by BASF. The catalyst was secured in a fixed bed quartz tube reactor (ID of 10.5 mm, OD of 12.7 mm) at GHSV= 40, 910 h⁻¹, 690 °C and 1 atm. 0.3 mL of catalyst particles (600 μm– 710 μm in diameter) were diluted with 1 mL quartz particles (600 μm–710 μm in diameter). Dodecane solution (Signal-Aldrich®) with and without sulfur, water and N₂ were pumped separately and continuously into the heated reaction system. The N₂ was used as an internal standard. Thiophene was added to the dodecane feed as a source of organic sulfur. SR of sulfur-free dodecane tests with S/C ratio of 1.6, 1.8 and 2.5 were conducted for the exploration of appropriate catalytic conditions. Catalyst stability/deactivation was studied by SR (with 74 ppm-sulfur) of dodecane with 50 min-, 100 min-, and 200min- TOS. SR of dodecane (with 29 or 74 ppm-sulfur) – air regeneration cycle tests (pre-emptive regeneration) with the same TOS sequences were studied to alleviate some catalyst deactivation. A similar test sequence was also applied to ultra- low sulfur diesel fuel (Shell®). Characterization measurements including SEM (HITACHI® S-4700 I), TPO (Quantachrome® ChemBET Pulsar), Raman Spectroscopy (HORIBA® LabRAM ARAMIS) were carried out to study the catalyst properties before and after testing.

Result and Discussion

Catalytic performance for SR of sulfur-free dodecane was improved with increasing S/C ratio above stoichiometric (S/C= 1). Rapid catalyst deactivation was observed with S/C= 1.6, while

relatively stable catalytic performance was achieved when $S/C \geq 1.8$. To sustain catalytic stability, ensure water sufficiency for WGS reaction, and minimize energy consumption, $S/C = 1.8$ was chosen as the condition for the dodecane/ diesel tests.

Successful catalytic performance of dodecane with 74 ppm sulfur was achieved, with initial mole fractions of main products (H_2 , CO , CO_2 , CH_4) reaching equilibrium. However, catalyst deactivation was observed with longer TOS. SEM and TPO together revealed the formation of coke on the spent catalyst surface. Raman Spectra showed that higher graphitization of coke was accompanied with longer TOS. Coke formation was responsible for catalyst deactivation.

Preemptive air regeneration [4], for various TOS, was found to sustain the catalytic activity by combusting coke before it began to deactivate the catalyst. Lower rates of catalyst deactivation were achieved with shorter cycles of TOS between pre-emptive regenerations. Compared to that with 74 ppm sulfur present, more stable catalytic performance was observed with pre-emptive regeneration of dodecane with 29 ppm sulfur (Fig. 1). Sulfur was hence considered another influential factor of catalyst deactivation by accelerating coke formation as reported earlier [5].

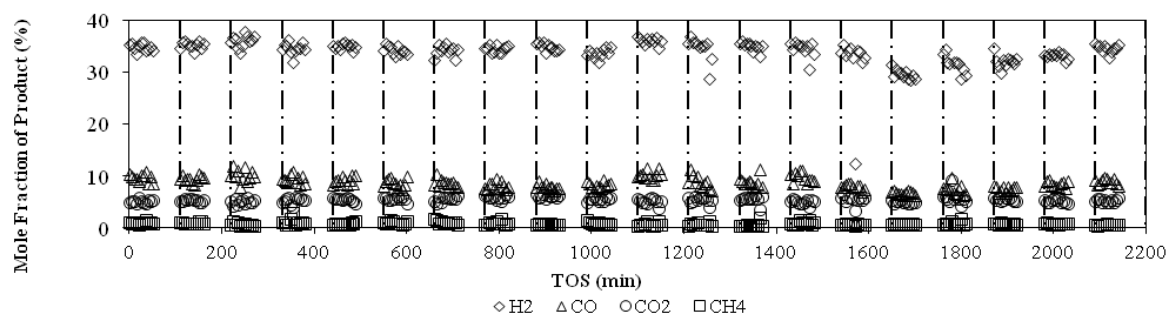


Fig. 1 Mole fraction of main products (H_2 , CO , CO_2 , CH_4) as a function of TOS for 50 min- SRD (29 ppm sulfur) -air regeneration cycle tests, GHSV= 40910 h⁻¹, $S/C = 1.8$, at 690 oC and 1 atm.

Ultra low sulfur diesel was successfully reformed with the current catalyst under the same reaction conditions for the SR of dodecane tests (Fig. 2). Preemptive air regeneration was also found effective in alleviating catalyst deactivation during the first three cycles. However, rapid catalyst deactivation was observed after 600 min TOS. Rather than just sulfur the presence of varied carbon species (C12-C18) in diesel fuel was believed to require some process changes in S/C and the pre-emptive regeneration cycle for achieving more sustained catalytic performance.

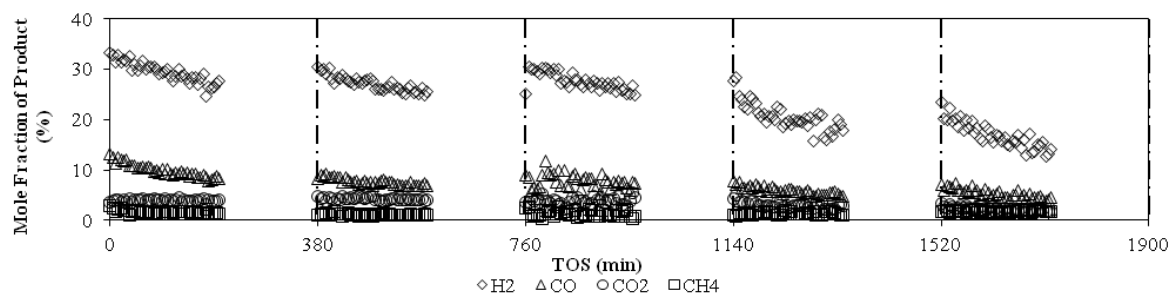


Fig. 2 Mole Fraction of main products (H₂, CO, CO₂, CH₄) as a function of TOS for SR (200min) - air regeneration cycle test of diesel fuel (ULSD, Shell®), GHSV= 40910 h⁻¹, S/C= 1.8, at 690 oC and 1 atm.

References

- [1] R. J. Farrauto, Y. Liu, W. Ruettinger, O. Ilinich, L. Shore, T. Giroux. *Catalysis Reviews*. 49 (2007) 141-196.
- [2] N. B. Klinghoffer, F. Barrai, M. J. Castaldi. *Journal of Power Sources*. 196 (2011) 6374-6381.
- [3] Q. Ming, T. Healey, L. Allen, P. Irving. *Catalysis Today*. 77 (2002) 51-64.
- [4] T. Giroux, E. Waterman, R. J. Farrauto, inventors; BASF Corporation, assignee. Reforming sulfur-containing hydrocarbons using a sulfur resistant catalyst. US patent 7, 901, 565 B2. 2011 Mar 8.
- [5] A. Simson, R. Farrauto, M. Castaldi. *Applied Catalysis B: Environmental*. 106 (2011) 295-303.

Production of H₂ generated from hydrocarbons in-situ with CO₂ disposal (HPR3-2)

Leonid Surguchev, LUKOIL Overseas North Shelf AS

and

Roman Berenblyum, International Research Institute of Stavanger (IRIS)

ABSTRACTS

Hydrogen has a great potential as an environmentally clean energy fuel. The drawback, however, is that the modern methods of hydrogen production require significant amounts of energy and generate large volumes of CO₂. The most common way of producing hydrogen today is a staged process including natural hydrocarbon gas production, its transport and processing, steam reforming and storage, followed by further transport and management of by-products such as CO₂. A process allowing for generating hydrogen from hydrocarbons in situ could open a new immense source of clean hydrogen energy for commercial use.

In the proposed novel concept the hydrogen generation process is carried out directly in the hydrocarbon reservoir. The reservoir is then converted into a ready to produce high pressure hydrogen storage cell. Hydrocarbon processing and transportation stages on the surface are therefore abated. The energy required for hydrogen production is significantly reduced with CO₂ being captured and stored in-situ. In the “conventional” process capturing and storing CO₂ from a power plant alone can increase the energy cost by up to 60%. In addition to energy saving the emissions of green house gases is wed out.

In order to validate the concept of in situ hydrogen generation process several laboratory experiments were performed. The CO₂ flooding experiments in the sandstone core at reservoir conditions indicated gravitational segregation of CO₂ in the methane-carbon dioxide system. The hydrogen conversion experiment demonstrated feasibility of the suggested process. Catalytic experiments without optimising reaction conditions showed that resulted gas compositions can contain up to 55% of hydrogen. Thermodynamic calculations using experimental data allowed to evaluate relative importance of the reactions that may take place at given conditions.

For the in-situ process a water soluble precursor can be placed in the reservoir using dedicated injection wells. Steam reforming temperatures may be reached with either steam injection or in-situ combustion resulting in required increase of reservoir temperatures. High thermal energy generated in situ may be utilised later by temporally using the injection wells as geothermal ones. Circulating water into these wells will allow to bring this thermal energy to the surface and to reduce the temperature in the reservoir. Reduction of the reservoir temperature from steam-vapour condition at hydrogen generation stage to conditions corresponding to condensation of water will have positive effect for separation of hydrogen in situ and CO₂ dissolution in water. CO₂ solubility in water is almost 700 times higher than solubility of H₂. At cooler temperatures gravity segregation will effectively contribute to hydrogen segregation and accumulation of it in the upper parts of the geological structure.

The commercial application of in-situ generation of hydrogen from hydrocarbons may be particularly relevant to

- tight gas and shale gas reservoirs,
- coal bed methane deposits.

The process could also be modified to be coupled with in-situ oil upgrade in depleted and waterflooded oil fields, heavy oil, bitumen and shale oil deposits (in the form of in-situ upgrading of oil).

Thermocatalytic Decomposition of LPG as Hydrogen Source for Fuel Cells (HPR3-3)

Stefan Neuberg, Helmut Pennemann, Athanassios Ziogas, Gunther Kolb

Institut für Mikrotechnik Mainz GmbH (IMM), Mainz, Germany

INTRODUCTION

Fuel cell technology bears significant advantages for the power supply of de-centralized, mobile and portable applications such as Auxiliary Power Units (APU) [1]. However, the hydrogen supply is a critical issue, especially when long-term operation is considered, because compressed and liquid hydrogen show significant drawbacks concerning power density and boil-off respectively. For Liquefied Petroleum Gas (LPG), which is a mixture of propane and butane, a well-established distribution grid exists. LPG is an attractive fuel owing to its low storage pressure and high hydrogen content.

The thermocatalytic decomposition of light hydrocarbon fuels is a viable alternative to more conventional hydrocarbon production techniques such as steam reforming [2,3], partial oxidation [4] and, in between, autothermal reforming. A significant advantage of the thermocatalytic decomposition is the high hydrogen content of the product gas, because the hydrocarbon is decomposed over heterogeneous catalyst producing ideally only carbon apart from the hydrogen. However, the catalyst obviously accumulates large amounts of coke on its surface and therefore requires periodic regeneration by air treatment.

The target of the current development work is to investigate the potential of thermocatalytic decomposition for a small scale fuel cell APU operated with high temperature PEM technology and with a power output in the range of few hundred Watts. This has been subject of only few publications in the past [5,6].

EXPERIMENTAL AND RESULTS

More than 15 catalyst samples were prepared and tested in the scope of the current work. The catalysts under investigation were prepared by an impregnation procedure applying alumina carrier in most cases. The catalysts were then ground and sieved to gain a particle size fraction between 300 μm and 400 μm . The samples were introduced into a small scale fixed bed reactor and tested at reaction temperatures between 700 °C and 1,100 °C in 100 K steps applying pure propane as model feed. After each reaction temperature a regeneration cycle by exposure to air followed the test. Fig. 1 shows the product gas composition for 700°C, 1,000°C and 1,100°C reaction temperature for a Ni/Al₂O₃ catalyst containing 10% Ni. The first measurement is obviously not representative for the product composition but rather reflects incomplete exchange of gases in the sample lines. While significant amounts of methane in the range of 25 Vol.% were still formed at 700°C, the hydrogen content in the product exceeded 90 Vol.% at 1,100°C. However, the content of carbon monoxide in the product increased from less than 1 Vol.% to values in the range of 2 Vol.% at the higher temperature. These values can be easily tolerated by high temperature PEM fuel cell technology envisaged here. At 1,000°C reaction temperature, the catalyst showed on the short term increasing

formation of methane. This could be suppressed by increasing the reaction temperature to 1,100°C. To investigate the medium term stability of the catalyst, repeated decomposition and regeneration cycles were performed, which are shown in Fig. 2. The values shown are average values gathered during 20 min reaction time of each cycle. Regeneration in air was performed for the same duration between the cycles. They confirmed the tendency of the catalyst towards increased methane formation with time at least at a reaction temperature of 1,000°C.

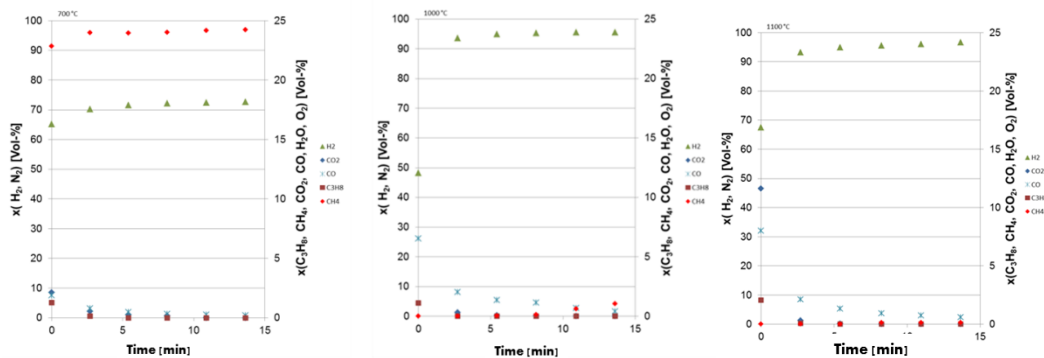


Fig. 1. Product gas composition as determined for the thermocatalytic decomposition of propane at 700°C (left), 1,000°C (centre) and 1,100 °C (right) reaction temperature; feed flow rate 6.7 ml/min; catalyst mass 2.1 g.

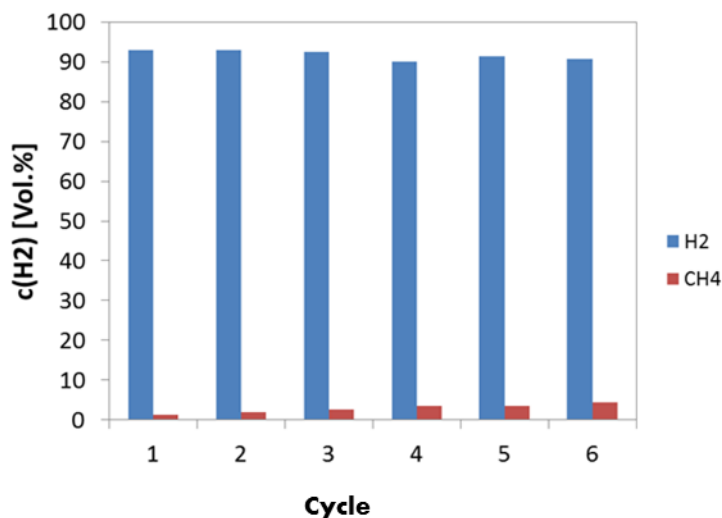


Fig. 2. Hydrogen and methane concentration in the product gas during the thermocatalytic decomposition of propane at 1,000 °C reaction temperature over Ni/Al₂O₃ catalyst containing 10% Ni; feed flow rate 6.7 mL/min; catalyst mass 2,118g; regeneration cycles of 20 min duration were performed between the measurements shown here.

OUTLOOK

The catalyst formulations will be further optimized regarding their selectivity and long term stability. For a practical system, the periodic operation of the process requires two reactors to be operated in parallel, one reactor producing hydrogen, while the second reactor is operated under conditions of regeneration. A close coupling of both reactors is recommended to allow the heat transfer between the exothermic regeneration and the endothermic decomposition reactions. As a first step towards the realization of a prototype system, an ASPEN model has been set up. It revealed that the unconverted hydrogen and other gases contained in the fuel cell anode feed cannot be further utilized in the system but should be rather combusted in a monolithic afterburner.

REFERENCES

- [1] Kolb, G.; Fuel Processing for Fuel Cells, 1 Ed.; Wiley-VCH, Weinheim (2008).
- [2] Kolb, G., Zapf, R., Hessel, V., Löwe, H.; "Propane steam reforming in micro-channels - results from catalyst screening and optimisation", Appl. Catal. A 277, (2004) pp. 155-166.
- [3] Wichert, M., Men, Y., O'Connell, M., Tiemann, D., Zapf, R., Kolb, G., Butschek, S., Frank, R., Schiegl, A.; "Self-sustained operation and durability test of a 300 W-class micro-structured LPG fuel processor", Int. J. Hydrogen Energy 36, (2011) pp. 3496-3504.
- [4] Pennemann, H., Hessel, V., Kolb, G., Löwe, H., Zapf, R.; "Partial oxidation of propane using a micro structured reactor", Chem. Eng. J. 135, 1 (2008) pp. S66-S73.
- [5] Ledjeff-Hey, K., Kalk, T., Mahlendorf, F., Niemzig, O., Trautmann, A., Roes, J.; "Portable PEFC generator with propane as fuel", J. Power Sources 86, (2000) pp. 166-172.
- [6] Ledjeff-Hey, K., Formanski, V., Kalk, T., Roes, J.; "Compact hydrogen production systems for solid polymer fuel cells", J. Power Sources 71, (1998) pp. 199-207.

Behaviour Of Nickel-Alumina Spinel (NiAl_2O_4) Catalysts For Isooctane Steam Reforming (HPR3-4)

C. Jiménez-González, Z. Boukha, B. de Rivas,
J.I. Gutiérrez-Ortiz, J.R. González-Velasco, R. López-Fonseca

*Chemical Technologies for Environmental Sustainability Group,
Department of Chemical Engineering, Faculty of Science and Technology,
Universidad del País Vasco UPV/EHU, P.O. Box 644, E-48080 Bilbao, Spain*

(* Corresponding author: ruben.lopez@ehu.es)

Keywords: Hydrogen, isooctane, nickel aluminate, steam reforming, synthesis gas

Introduction

Liquid fuels, derived from either fossil or renewable sources, represent an attractive source of hydrogen since their distribution infrastructure is readily available. Steam reforming is the most effective method to produce hydrogen from liquid hydrocarbons with a high yield in comparison with autothermal reforming and partial oxidation. Noble metal-based catalysts are more efficient because of their long-term activity and coke resistance, but their cost is high. In contrast, nickel-based catalysts appear to be a good alternative although they may undergo severe deactivation due to carbon deposition. Activity is mainly governed by the size of the Ni particles.

In our previous research it was shown that NiAl_2O_4 spinel can be a promising precursor to develop suitable Ni/ Al_2O_3 catalysts with a high activity and a marked stability for various methane reforming processes such as steam reforming or partial oxidation [1,2]. In this work the attention has been focused on the optimisation of the preparation methodology, using coprecipitation instead of conventional coimpregnation, and the nickel loading for the synthesis of both bulk and alumina supported nickel-alumina spinel catalysts. Particularly the effect of the existence of a pure NiAl_2O_4 crystalline phase or a mixture of the spinel phase together with a NiO phase was analysed on the performance of the resultant reduced catalyst for the steam reforming of isooctane, which was used as a surrogate for gasoline.

Experimental

Three different nickel spinel samples were prepared by the coprecipitation method. The process was conducted by the drop-by-drop addition under constant stirring of a 0.6 M solution of NH_4OH into an aqueous solution of a mixture of $\text{Ni}(\text{CH}_3\text{-COO})_2 \cdot 4\text{H}_2\text{O}$ and $\text{Al}(\text{NO}_3)_3 \cdot 9\text{H}_2\text{O}$ (1:2 Ni/Al molar ratio). The procedure was followed for preparing either a bulk spinel (CP) or two alumina ($133 \text{ m}^2 \text{ g}^{-1}$) supported spinel catalysts (CP/A). The temperature was kept at 25 °C during the precipitation and the pH was fixed at 8, after that the precipitates were aged for 30 minutes before being filtered and washed with hot deionised water. The three catalysts were labelled as CP(32), CP/A(24) and CP/A(17) and the corresponding nickel loadings were 32, 24 and 17 wt.%, respectively. Also a pure NiO bulk catalyst was prepared by simple calcination in air of $\text{Ni}(\text{CH}_3\text{-COO})_2 \cdot 4\text{H}_2\text{O}$. All the samples were dried at 110 °C overnight and then calcined at 850 °C in static air for 4 h at a heating rate of 10 °C min⁻¹. Their characterisation involved BET, XRD,

H₂-TPR, XPS and UV-visible-NIR. In addition, the used catalysts were preliminary analysed by XRD and TGA-MS.

The catalytic tests (steam reforming of isooctane) were performed, on 125 mg of catalyst, in a flow reactor operating at atmospheric pressure. The reaction mixture was composed of 1.95 vol% C₈H₁₈ and H₂O (H₂O/C=3) diluted in N₂ and a total flow rate equal to 800 cm³ min⁻¹. Prior to the reaction, the catalysts were activated by reduction with 5%H₂/N₂ at 850 °C for 2 h. The experiments were carried out at constant temperature (600 °C) for 31 h. For comparative purposes the activity of a commercial Rh/A (1 wt.%Rh, Aldrich Chemical Co.) catalyst was also examined

Results and discussion

[Table 1](#) summarises the characterisation results obtained on the prepared catalysts. Nitrogen adsorption-desorption measurements showed that all the samples exhibited IV-type isotherms, indicating the existence of well-developed mesopores, with significantly reduced hysteresis loops for all the catalysts. Note that, although being a bulk catalyst, the surface area of the CP(32) sample was relatively high. On the other hand, a marked decrease in surface area with respect to the bare alumina was found for the supported catalysts. This was more notable for the CP/A(24) sample.

Table 1. Characterisation and activity results of reduced nickel catalysts.

Catalyst	Ni, wt. %	S _{BET} , m ² g ⁻¹	Ni ⁰ size, nm ^(a)	NiO/NiAl ₂ O ₄ ^(b)	Yield				H ₂ /CO	CO/CO ₂	Coke, %
					H ₂	CO	CO ₂	CH ₄			
CP(32)	32	55	14	0.1	0.70	0.05	0.16	0.05	14.8	0.33	61
CP/A(24)	24	57	12	0.08	0.96	0.08	0.22	0.06	14.3	0.34	83
CP/A(17)	17	84	8	0.06	0.96	0.09	0.22	0.07	12.0	0.41	67
Rh/A	-	126	-	-	0.80	0.16	0.14	0.06	5.6	1.18	2
Equilibrium					2.15	0.35	0.56	0.09	1.6	0.61	

Values determined by (a) XRD and (b) H₂-TPR.

X-ray diffraction patterns of all the calcined samples showed peaks assignable to nickel aluminate phase (19.5°, 31.7°, 37.5°, 45.3°, 60.2° and 65.8°) and evidenced the disappearance of the signals attributed to the alumina structure. The presence of the NiO phase was not apparently observed in the patterns probably owing to its small particle size and/or its low concentration. This was in contrast with the results found for spinel catalysts prepared by impregnation since a mixture of free NiO together with NiAl₂O₄ was observed [2]. Consequently, the synthesis route based on precipitation led to more structurally homogeneous catalysts. All these results were further corroborated by UV-visible-NIR diffuse reflectance. Hence, the bands at 380 nm, 420 nm and 720 nm (with a very low intensity) were assigned to the octahedrally coordinated Ni²⁺ species in NiO lattice, whilst those at 550 nm and in the range of 600–645 nm were related to the tetrahedrally coordinated Ni²⁺ species in the nickel aluminate lattice. The surface Ni²⁺ composition of calcined

samples was also analysed by XPS. The fitting of the experimental data revealed the presence of a single type of Ni species, NiAl₂O₄.

The H₂-TPR profiles exhibited two visible reduction bands. The first band was centred at 400-450 °C and corresponded to the reduction of free γ -NiO species. The main reduction feature was considerably more intense and broader and could be deconvoluted into two signals located at 650-700 and 800 °C. These were related to the reduction of γ -NiO species (defect/non-stoichiometric spinel phase) and γ -NiO species (stoichiometric spinel phase), respectively. From the NiO/NiAl₂O₄ ratios it could be deduced that all the samples prepared by coprecipitation contained mostly the spinel phase with a low contribution of γ -NiO species (lower than 9%). This was in concordance with the previous characterisation results. Also noteworthy was that the reducibility was promoted at slightly lower temperatures for the supported catalysts in comparison with the bulk sample.

After a severe reduction step (850 °C/2 h), the samples revealed that Ni²⁺ was completely converted into metallic Ni (peaks at 44.6°, 52° and 76.5°) with a simultaneous re-construction of the alumina structure. Accordingly, the UV-vis-NIR bands attributed to Ni²⁺ were not visible. The average size of Ni particles, as estimated by XRD, was relatively small decreased from 14 to 8 nm with the following order CP(32) > CP/A(24) > CP/A(17). This suggested that the coprecipitation route could be adequate for obtaining reduced particle sizes, especially for alumina supported NiAl₂O₄ samples.

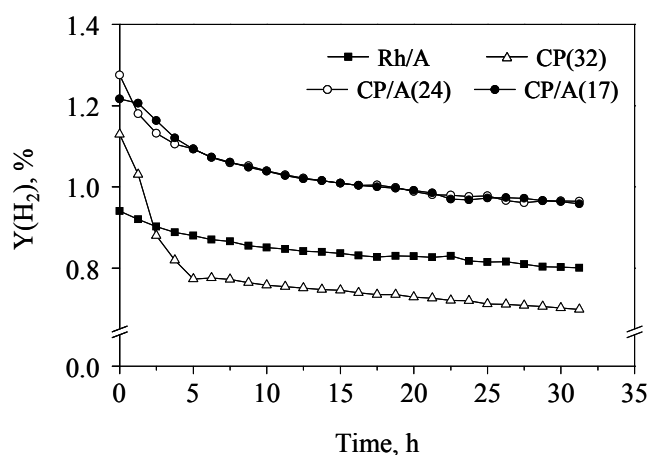


Fig. 1. Evolution of yield of H₂ with time for the various nickel catalysts at 600 °C.

The catalytic performance for steam reforming of isooctane at 600 °C after 31 h is shown in Table 1 in terms of yields of the main reforming products (H₂, CO, CO₂ and CH₄). Both supported NiAl₂O₄ catalysts were markedly more active than bulk NiAl₂O₄. Despite having a significantly lower Ni content the yield of hydrogen of CP/A(17) was virtually identical to that of CP/A(24). It seemed that the higher Ni content was compensated for by a smaller crystallite size and a higher surface area. Moreover, these two catalysts favoured a higher conversion of the hydrocarbon to H₂ in comparison with the commercial Rh/A sample (Fig. 1). On the other hand, all the nickel catalysts showed a slight deactivation (more evident for CP(32)) during the first 5 h of reaction probably due to a notable coke formation as revealed by XRD and TGA-MS (Table 1).

Acknowledgements

The financial support for this work provided by the Spanish Ministerio de Ciencia e Innovación (CTQ2010-16752/PPQ) and Gobierno Vasco (PRE_2013_2_453) are gratefully acknowledged.

References

- [1] R. López-Fonseca, C. Jiménez-González, B. de Rivas, J.I. Gutiérrez-Ortiz. Appl. Catal. A 437-438 (2012) 53-62.
- [2] C. Jiménez-González, Z. Boukha, B. de Rivas, J.J. Delgado, M.A. Cauqui, J.R. González-Velasco, J.I. Gutiérrez-Ortiz, R. López-Fonseca, Appl. Catal. A 466 (2013) 96-104.

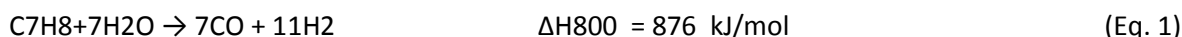
Improvement of Steam Reforming of Toluene by CO₂ Capture using Fe/CaO-Ca₁₂Al₁₄O₃₃ Bi-functional Materials. (HPR4-1)

I. ZAMBONI, Y. ZIMMERMANN, A. KIENNEMANN and C. COURSON

ICPEES – UMR CNRS 7515 – ECPM, 25 rue Becquerel, 67087 Strasbourg Cedex 2, France

INTRODUCTION

Hydrogen production from biomass gasification is an attractive way to provide sustainable energy and reduce the use of fossil sources and so the emission of greenhouse gases. Nevertheless, biomass gasification leads to syngas (H₂ and CO) production associated to CO₂, methane and heavy aromatic hydrocarbons known as tar [1]. In this context, steam reforming (Eq. 1) is a solution to eliminate tar during biomass gasification and improve hydrogen yield. This endothermic reaction is always associated with the exothermic water gas shift reaction (Eq. 2). Iron (oxide or metal) which is not toxic, abundant and cheap, is known for its ability to promote the breaking of C-C and C-H bonds in organic compounds [2], its activity in water gas shift reaction at high temperature and its low selectivity to carbon formation.



The production of a H₂ rich gas by steam reforming of tar can be improved by in-situ capture of CO₂ using a sorbent (Eq. 3), thanks to the displacement of the equilibrium of the water gas shift reaction towards H₂ production. Among CO₂ sorbents, calcium oxide is the most suitable material because of its sorption capacity at high temperature (650-700°C near gasification temperature) and its regenerability. However, CaO sintering linked to multiple carbonations and calcinations (regenerations) leads to a decrease in sorption capacity [3]. To avoid the deterioration of CaO sorbent morphology, Ca₁₂Al₁₄O₃₃ can be used as binder and the new material CaO-Ca₁₂Al₁₄O₃₃ permits to increase the CO₂ access to the sorption sites [4].



Afterwards, the bi-functional material Fe/CaO-Ca₁₂Al₁₄O₃₃ could be an interesting choice to favor the steam reforming of toluene (model molecule of tar), as well as the water gas shift reaction and the CO₂ sorption. In this work two iron precursors are used in order to study the effect of the different species of iron on the steam reforming of tar. To validate the efficiency of the proposed materials, Fe/CaO system is also studied as reference.

EXPERIMENTAL

The reference system Fe/CaO is prepared by mechanical mixture according to the method described in previous work [5] using iron acetate (FeAc) or nitrate (FeN) and calcium acetate (Cc) as

precursors. The method used to prepare the CaO-Ca₁₂Al₁₄O₃₃ phase (denoted Cc-CaAl) is a modification of the method described by Li et al. [6]. The appropriate amounts of aluminum nitrate and calcium acetate to obtain a CaO/Ca₁₂Al₁₄O₃₃ weight ratio of 85/15 were dissolved in distilled water. After evaporation, the white solid was dried and calcined at 750°C for 4 hours. The solid was then rehydrated, dried and calcined again at 900°C.

The bi-functional materials Fe/CaO-Ca₁₂Al₁₄O₃₃ were synthesized by mechanical mixing method. The amount of iron acetate or iron nitrate to obtain a chosen final product containing 10wt% of iron was mixed with the CaO-Ca₁₂Al₁₄O₃₃ (Cc-CaAl) sorbent. The mixture was calcined for 4 hours at 750°C after a temperature rate of 3°C/min. The two bi-functional materials are denoted as FeAc/Cc-CaAl and FeN/Cc-CaAl. The particle size of all materials is in the range of 120-125µm.

X-ray diffraction (XRD), temperature programmed reduction (TPR) and Mossbauer spectroscopy analyses were carried out to characterize the bi-functional materials. Thermo-gravimetric analyses (carbonation-calcination cycles) and sorption tests were performed at 650°C or 700°C to evaluate the sorption capacity and stability of the sorbents.

In order to study the activity of the bi-functional materials, toluene steam reforming was carried out in a fixed bed reactor as a function of temperature. The gas composition at the outlet of the reactor was monitored by gas chromatography.

RESULTS AND DISCUSSION

DRX, TPR and Mossbauer characterizations of the materials showed that the Ca₂Fe₂O₅ mixed phase is formed when iron nitrate is added to CaO. The addition of iron acetate favors the formation of the Fe₂O₃ phase in presence of calcium acetate precursor. In the same manner, the main phase of iron in the material FeAc/Cc-CaAl is hematite (α-Fe₂O₃), while in the FeN/Cc-CaAl, Ca₂Fe₂O₅ is the principal phase.

Regarding to the sorption test, the results showed that in FeAc/Cc-CaAl and FeN/Cc-CaAl, mayenite stabilizes CaO phase, in addition, the sorption capacity of FeAc/Cc-CaAl (0.66 gCO₂/gCaO) is greater than the sorption capacity of FeN/Cc-CaAl (0.52 gCO₂/gCaO). The formation of Fe₂O₃ phase instead of Ca₂Fe₂O₅ phase allows the availability of a more important amount of CaO.

The catalytic activity is presented as H₂ production rate. In figure 1, the H₂ production rate of FeAc/Cc, FeN/Cc, FeAc/Cc-CaAl and FeN/Cc-CaAl bi-functional materials and the corresponding sorbent (Cc and Cc-CaAl) are shown. Hydrogen production depends on the sorbent and the iron oxide. The latter is necessary to overcome the activation step of CaO in the first minutes of reaction. The catalytic stability in steam reforming of toluene is improved for FeAc/Cc (Fig. 1a).

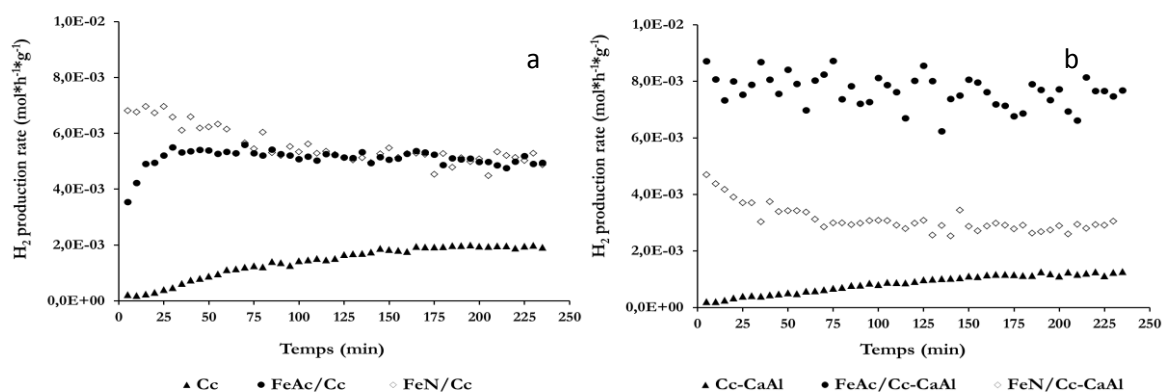


Figure 1. Hydrogen production rate of the bi-functional materials a) Fe/CaO and b) Fe/CaO-Ca₁₂Al₁₄O₃₃ and their correspondent sorbents in steam reforming of toluene at 700°C.

The presence of Ca₁₂Al₁₄O₃₃ phase represents an advantage over the bi-functional materials only when iron is present in α -Fe₂O₃ form (FeAc/Cc-CaAl) and not as Ca₂Fe₂O₅ (FeN/Cc-CaAl) (Fig. 1b). The activity of the FeAc/Cc-CaAl is explained thanks to the characterizations; TPR showed that at a temperature of about 600°C, the Fe₂O₃ are readily reducible and longer available for the steam reforming and water gas shift reactions. The efficiency of CO₂ sorption in catalytic steam reforming of toluene at 700°C was detected in an indirect way through the absence of CO and the presence of CO₂ produced from water gas shift reaction.

Characterizations after catalytic test show that the Fe₃O₄ phase is present as a consequence of redox reactions. The selectivities in carbonaceous products were also used as parameters to evaluate the efficiency of the materials. FeAc/Cc-CaAl shows a high selectivity towards CO₂ and CH₄ while the selectivity towards benzene is lower and CO is not produced. In the case of FeN/Cc-CaAl the selectivity to benzene is high and CO₂ and CH₄ are lower.

The gas mixture obtained from steam reforming of toluene is analyzed as a function of temperature between 650°C and 825°C. Figure 2 shows the selectivity towards carbonaceous products, hydrogen yield and conversion of toluene for FeAc/Cc-CaAl material. This material led to a conversion of 95% of toluene at 825°C and to a low benzene production. At this temperature, the CaO-Ca₁₂Al₁₄O₃₃ phase does not act as sorbent but more as catalyst. The literature concerning the catalytic activity of CaO has shown the effectiveness of this phase in steam reforming at high temperature [7].

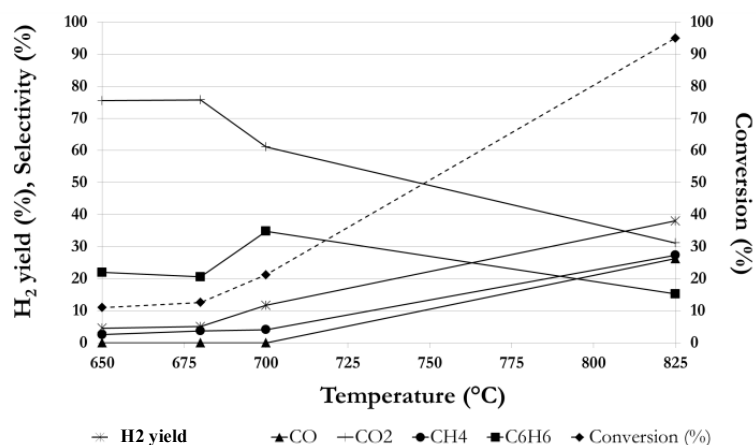


Figure 2. The gas mixture obtained from steam reforming of toluene in presence of FeAc/Cc-CaAl as a function of temperature between 650 and 825°C.

Finally, the effect of the Cc-CaAl and FeAc/Cc-CaAl in water gas shift reaction at 700°C is also evaluated. In presence of these materials, the rate of hydrogen production in water gas shift reaction is greater than in steam reforming of toluene which suggests that at 700°C the WGS is limited by the rate of the steam reforming of toluene.

CONCLUSION

In conclusion, the FeAc/CaO-Ca₁₂Al₁₄O₃₃ bi-functional material presents the best properties for the simultaneous steam reforming of toluene and CO₂ capture. The results showed that hydrogen production is improved thanks to the redox reactions from α -Fe₂O₃. The CaO sorbent stabilizes the rate of hydrogen production and favors the CO₂ capture. In presence of Ca₁₂Al₁₄O₃₃ phase, the surface properties of CaO and its ability to absorb CO₂ are stable. FeAc/CaO-Ca₁₂Al₁₄O₃₃ is then a potential material for steam reforming and simultaneous carbonation in the gasification step and decarbonation in the combustion zone of a dual fluidized bed reactor.

Acknowledgements

We acknowledge the French National Center of Scientific Research (CNRS) – PIE Program and Alsace Region for the financial support to carry out this work.

References

- [1] T.A. Milne, R.J. Evans, N. Abatzoglou, Biomass Gasifier “Tars”: Their Nature, Formation, and Conversion. National Renewable Energy Laboratory Report NREL/TP-570-23357, 1998.
- [2] S.S. Tamhankar, K. Tsuchiya, J.B. Riggs, Applied Catalysis 16 (1985) 103.
- [3] J. Adanez, L.F. de Diego, F. Garcia-Labiano, Fuel 78 (1999) 583.
- [4] C.S. Martavaltzi, A.A. Lemonidou, Chemical Engineering Science 65 (2010) 4134.

- [5] I. Zamboni, C. Courson, A. Kiennemann, *Catalysis Today* 176 (2011) 197.
- [6] Z.-S. Li, N.-S. Cai, Y.-Y. Huang, H.-J. Han, *Energy & Fuels* 19 (2005) 1447.
- [7] G. Taralas, M.G. Kontominas, *Fuel* 83 (2004) 1235.

Using 2-D TDLAS to Improve Efficiency and Reliability in Steam Methane Reforming (HPR4-2)

David M. Giltner, Andrew Sappey, Jim Howell, Pat Masterson, Mike Estes, Xavier Dubert

Zolo Technologies, Inc.

4946 N.63rd Street

Boulder, CO

80301

Steam methane reformers (SMRs) require tight temperature and excess air control to achieve optimal efficiency and reliability. Because of this, SMRs typically have many sensors to measure and control their operation. However, very few sensors are available for making temperature and oxygen measurements inside the firebox, where the combustion and reforming processes actually take place and safety is most critical (see figure). Thermocouples are not reliable when installed permanently inside the combustion chamber. Attempts have been made to use IR cameras for measuring temperature, but accurate quantitative results are difficult to achieve with this technology. Conventional O₂ sensors will not survive in the harsh environment of the combustion chamber, so they are typically located in the convection section. If multiple sensors are used, this approach can provide an acceptable average excess O₂ value for controlling the reformer, but it is not a reliable method for identifying pockets of high or low O₂, nor does it clearly tell the plant operator which burners are contributing to the O₂ imbalance.

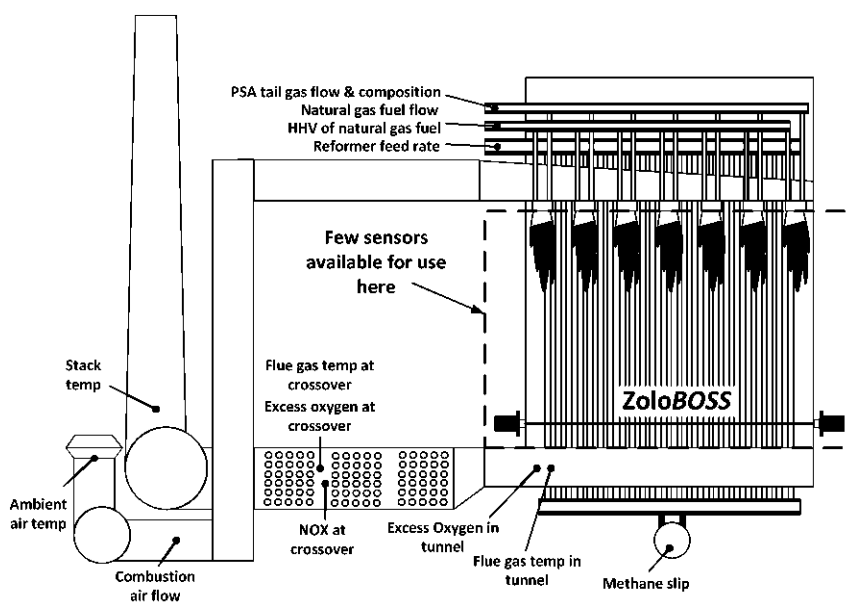


Figure 4: TDLAS is the only sensor technology capable of providing reliable and quantitative results directly in the firebox.

Tunable Diode Laser Absorption Spectroscopy (TDLAS) is a very attractive technology for providing accurate and actionable measurements directly inside the firebox. This technology is capable of measuring temperature, O₂, H₂O and CO in real-time, directly inside the furnace. It does not

require the insertion of probes into the furnace, and there are no extraction tubes to clog or delay measurement response.

The ZoloBOSS combustion monitoring system employs TDLAS technology in a wavelength-multiplexed fiber-coupled architecture. This approach allows multiple species to be detected with a single laser beam, and therefore a single path through the furnace. Multiple paths may be installed on the furnace to create a 2-dimensional profile that provides actionable data to allow plant operations to balance both temperature and O₂. The fiber coupled architecture allows the lasers and associated electronics to be located away from the harsh environment of the furnace. In addition, because TDLAS is based on molecular absorption parameters which do not change, the ZoloBOSS does not drift or require periodic field calibration.

We present results from ZoloBOSS TDLAS systems installed on two different SMRs. These demonstrations provided 2-dimensional profiles of the O₂, CO, and temperature inside the operating SMR furnace, and also provided high resolution measurements of temporal variations in the combustion process. By adjusting the air and fuel distribution to groups of burners it was demonstrated that improving the combustion balance using the ZoloBOSS data is straightforward and reliable. Results showed that the temperature variations across the furnace can be reduced by as much as 80% (see figure).

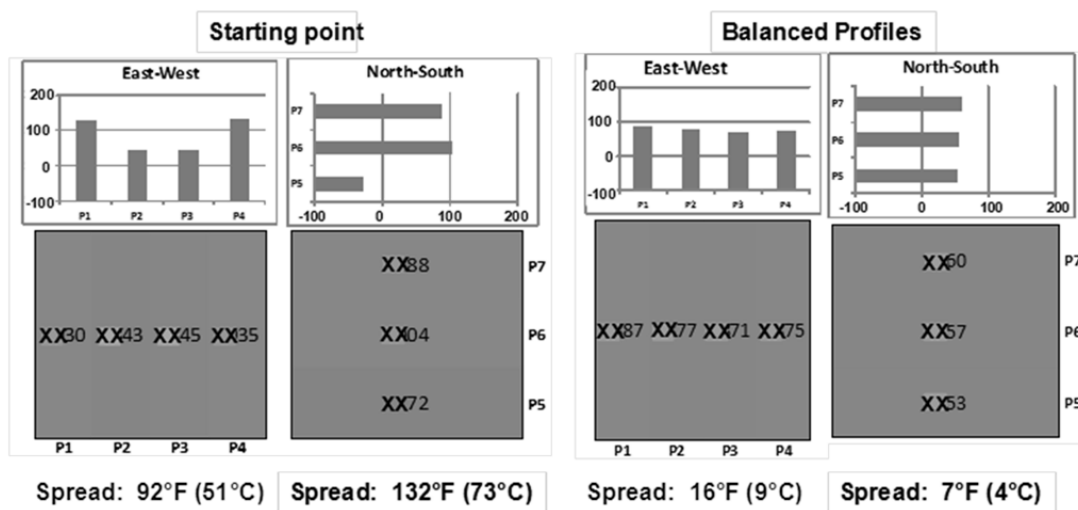


Figure 5: Temperature data from a ZoloBOSS demonstration on a Steam Methane Reformer showing the temperature variations before and after balancing.

The value of balancing combustion in an SMR includes contributions from improved combustion and process efficiency, longer tube life, lower risk of early tube failure, increased catalyst life, reduced emissions, and improved safety. In addition, the ZoloBOSS allows remote monitoring of the combustion, indicating any change in combustion status or health. Results at both nominally well-run plants indicate that: 1) significant combustion profile imbalances were initially present in both furnaces upon installation, 2) the data provided by the ZoloBOSS can be used to improve balance by

manually tuning burners, and 3) significant ROI will be realized as a result of long-term implementation and optimization.

MODELING OF METHANE STEAM REFORMING IN MEMBRANE CATALYTIC REACTOR (HPR4-3)

*Shashi Kumar, Jay Agrawal, Sandeep Kumar, and Surendra Kumar**

*Department of Chemical Engineering, Indian Institute of Technology Roorkee
Roorkee - 247667, Uttarakhand, India*

**Corresponding author- E-mail: skumar.iitroorkee@gmail.com*

With the growing concerns of environmental impacts of fossil fuels, interest in the field of research on hydrogen production technologies is growing. Combustion of hydrogen is environmentally innocuous and its heat of combustion is very high (-286 kJ/mol) four times as compared to -74.87 kJ/mol for methane. Thus, it is being touted as the fuel for future. Methane steam reforming is currently the most widely used industrial process to produce hydrogen on the large scale. Being endothermic process, it has to be operated at high temperature (850°C-1000°C) for substantial conversion of methane. Steam reforming operation is generally performed in catalyst filled tubes kept inside the furnace. At such a high temperature, number of challenges like choking of the tube, rupture of tube due to thermal stresses, high energy loss in heat transfer operations and lower operational safety are faced. Membrane Technology provides a promising alternative. As produced hydrogen permeates continuously to the permeate section in a membrane reactor, equilibrium is shifted forward, and the thermodynamic limit is circumvented. Thus higher methane conversion is achieved in fixed bed membrane reactor for steam reforming operation as compared to traditional reactor for the same operating temperature. Use of perm-selective membrane like palladium membrane or microporous membranes in steam methane reforming has been reported to have substantially increased conversion [1].

This research paper presents the comprehensive modeling study of steam methane reforming in two reactors-traditional reactor and membrane reactor. Traditional reactor is a conventional cylindrical packed bed reactor, while membrane reactor is an annular double tube type of reactor with catalyst packed on the annular side and sweep gas flowing in the tube side. Reactor dimensions have been chosen such that the flow area is same for both traditional and membrane reactors. In case of non-adiabatic operations heat flux for traditional and membrane reactors has been chosen such that total heat supplied is same for both the reactors. Besides, heat flux is chosen within the limits reported for industrial reforming process [2]. In the case of membrane reactor, Pd-Ag membrane has been considered.

The conservation equations have been formulated to develop one-dimensional isothermal model, one-dimensional non-isothermal model and two dimensional non-isothermal model for traditional and membrane reactors. Assumptions, which are common to all models are as follows: Axial dispersion is neglected; there is no deactivation of the catalyst; ideal gas law is applicable.

Kinetics of the steam reforming as reported by Xu and Froment [3] is used. The correlation reported by Shu et al. [1] has been used for the mass transport through Pd-Ag membrane.

For radial effective Peclet number correlation given by Kulkarni and Doraiswamy [4] has

been used. Effectiveness factor is taken as 0.02 as reported by Xu and Froment [5] in their research work carried out on diffusional limitations in steam methane reforming. For momentum balance equation, pressure drop is calculated by standard Ergun equation. For heat transfer in the bed, the heat transfer coefficient have been calculated by expressions reported by Wasch et al. [6] and Elnashaie et al. [7]. Physical properties for the calculation of coefficients and empirical parameters are taken at area averaged pressure and temperature conditions and their correlations are taken from Perry's Handbook [8].

Model equations constitute a set of ordinary differential equations or a set of partial differential equations or a combination of both which depends upon the dimensionality of reactor considered. One dimensional model equations have been solved by ODE45 solver of the MATLAB which uses Runge-Kutta class of methods. Two dimensional model equations have been discretized using central difference scheme and resulting equations have been solved by ODE15s solver of the MATLAB. This method is commonly called as method of lines.

Shu et al. (1995) [9] conducted experimental studies on the steam reforming of methane using Pd/Ag membrane reactor. Their results have been used to validate the models developed in this work. Predictions of the models have been found to be within $\pm 12\%$ deviation.

Detailed simulations have been performed on both the types of reactors. Effect of operating parameters/variables (Steam to methane ratio, Reaction side pressure, Permeation side pressure, and Sweep gas flow rate) on methane conversion, hydrogen yield, hydrogen recovery and average outlet temperature has been studied. Membrane reactor dimensions used are : length = 7 m, outside radius of the outer shell = 0.1 m, inside radius of the outer shell = 0.09 m, outside radius of the internal tube = 0.062 m, inside radius of the internal tube = 0.052 m, catalyst = Ni/MgAl₂O₃, porosity = 0.5).

For isothermal operation, the conversion in traditional reactor (29 %) is much lower than

that in a membrane reactor (99.95%) for operating variables namely, input stream temperature of 873 K, steam to methane ratio of 3, reaction side pressure 20 atm, permeation side pressure 1 atm and sweep gas to methane flow rate ratio of 4.

As expected, adiabatic operation is not preferable, because the methane conversion is low in both the reactors. For example at inlet temperature = 873 K, operating reaction side pressure = 20 atm, permeation side pressure = 1 atm and sweep gas to methane flow rate ratio = 4, methane conversion in traditional and membrane reactors are 7.42% and 20.96% respectively.

The surface plots of methane conversion and temperature with annular width (r) and membrane reactor length (l) have been prepared. Methane conversion profile over radial coordinates is almost flat and thus radial flux is not significant. Besides, methane conversion predicted by 2D model is 95.06 % as compared to 95.95 % in 1D model. Thus , the predictions of 1D model are very close to 2D model. Therefore, one dimensional model is adequate representation of the membrane reactor considered in the present study. However, two dimensional model developed in this work will be useful for membrane reactors having annular width more than 6 cm. This will also be useful for the traditional packed bed reactor for diameter more than 6 cm.

Based upon our study, it has been concluded that optimum conditions for annular membrane reactor considered are steam to methane ratio of 3, heat flux of 25 kW/m², inlet temperature 873 K, methane inlet flow rate 1.8 kmol/h and reactor pressure of 20 atm. For these conditions methane conversion is close to 100%, hydrogen yield is more than 92%, and hydrogen recovery is close to 96%.

It is our view that models developed in this work may be used for the analysis, design and simulation of methane steam reforming membrane reactors.

REFERENCES

- [1] J. Shu, B.P.A. Grandjean, S. Kaliaguine, Asymmetric Pd-Ag / stainless steel catalytic membranes for methane steam reforming, *Catal. Today*. 25 (1995) 327-332.
- [2] I. Dybkjaer, Tubular reforming and autothermal reforming of natural gas - an overview of available processes, *Fuel Process. Technol.* 42 (1995) 85-107.
- [3] J. Xu, G. Froment, Methane steam reforming, methanation and water gas shift: I. Intrinsic Kinetics, *AIChE J.* 35 (1989) 88-96.
- [4] B. Kulkarni, L. Doraiswamy, Estimation of effective transport properties in packed bed reactors, *Catal. Rev. Sci. Eng.* 22 (3) (1980) 431- 483.
- [5] J. Xu, G. Froment, Methane steam reforming. II. Diffusional limitations and reactor simulation, *AIChE J.* 35 (1) (1989) 97-103.
- [6] A. De Wasch, G. Froment, Heat transfer in packed beds, *Chem. Eng. Sci.* 27 (1972) 567-576.
- [7] S. Elnashaie, S. Elshishini, Modelling, simulation and optimization of industrial fixed bed catalytic reactors topics in Chemical Engineering, vol.7, Gordon and Breach Science Publisher, 1993.
- [8] R. Perry, D. Green, J. Maloney, Perry's Chemical Engineers' Handbook, 6th edition, Mc Graw Hill, New York, 1984.
- [9] F. Gallucci, L. Paturzo, A. Basile, A simulation study of the steam reforming of methane in a dense tubular membrane reactor, *Int. J. Hydrogen Energ.* 29 (2004) 611- 617.

CO₂-free hydrogen production by methane catalytic decomposition over pure silica materials (HPR4-4)

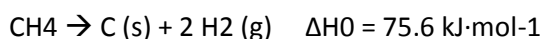
J.A. Botas¹, D.P. Serrano^{1,2}, P. Pizarro^{1,2} and G. Gómez¹

¹Department of Chemical and Energy Technology, ESCET, Rey Juan Carlos University, c/ Tulipán s/n, 28933, Móstoles, Madrid, Spain

²IMDEA Energy Institute, Avda. Ramón de la Sagra 3. 28935, Móstoles, Madrid, Spain

INTRODUCTION

Currently, most hydrogen is produced by steam methane reforming (SMR), which implies significant emissions of CO₂. Alternatively, hydrogen production via methane decomposition (DeCH₄) offers important environmental benefits since greenhouse emissions are avoided providing hydrogen and solid carbon as unique products, according to the following reaction [1]:



Two types of catalysts have been extensively explored until now in DeCH₄: metal and carbonaceous catalysts [2]. Among all of them, extremely high catalytic performance has been obtained over ordered mesoporous carbons due to a right balance between mesoporosity and amorphous pore walls [3,4]. Nevertheless, the synthesis of these mesostructured carbons is time-consuming and expensive. For these reasons, we decided to explore, for the first time, the use of another family of materials: pure silica solids. The pure silica samples investigated include one amorphous silica (am-SiO₂); two zeolites: silicalite 1 (silicalite-1) and hierarchical silicalite 1 (h-silicalite-1) and two ordered mesoporous silicas (MCM-41 and SBA-15).

EXPERIMENTAL

DeCH₄ reactions were performed using a thermobalance under isothermal conditions at 965 °C with a flow of 10 % CH₄ in argon. As the methane decomposition occurs, solid carbon is deposited over the silica particles allowing the reaction monitoring through the weight increase measurement.

Amorphous silica (am-SiO₂) was purchased from Aldrich and the rest of materials: MCM-41, silicalite-1, h-silicalite-1 and SBA-15 were synthesized following the procedures reported in literature [5-8].

RESULTS AND DISCUSSION

Table 1 summarizes the main properties of the silica samples studied in this work. Silicalite-1 is a zeolitic material with MFI type framework and the surface area is originated mainly by the presence of microporosity. H-silicalite-1 is a hierarchical pure silica MFI sample with bimodal porosity (micro and mesopores). On the other hand, MCM-41 and SBA-15 are ordered mesoporous silicas with different mean pore size (2 and 7 nm, respectively). Finally, am-SiO₂ is an amorphous silica sample without mesoscopic order and a broad pore size distribution.

Figure 1 (a) shows the evolution of the carbon formed from the reaction, and deposited on the catalysts, corresponding to the five silica samples under isothermal conditions at 965 °C, referred to the initial catalyst weight (C_{dep}/CO). It can be observed that the catalytic activity of silica samples present a certain induction time. The initial period of apparent inactivity observed for all silica samples suggest that these may be acting not as catalysts, but as promoters in the formation of catalytic sites through the reaction between methane molecules and the silanol groups located on their pore walls and external surface. On the other hand, Figure 1 (b) represents the carbon deposition rates which have been obtained as derivatives of the isothermal reactions. In all cases, after an initial rapid increase of the carbon generation rate, there is a sharp decay on the activity which is ascribed to the progressive deposition of carbon into the pore system of the catalysts leading to higher mass transfer limitations. It is remarkable that both zeolites exhibited the shortest induction times, but they are deactivated rapidly, due to their micropores blocking, showing very low carbon deposition rates at long reaction time. In the case of amorphous silica and mesostructured silica MCM-41, lower carbon deposition rates were observed. Among all the silica materials evaluated, SBA-15 showed a clearly superior carbon deposition rate at long reaction times. Moreover, it is remarkable that its activity remains stable even after 24 hours of reaction. This superior resistance to deactivation is attributed to the essentially mesoporous nature of SBA-15, with pore sizes large enough to keep a good accessibility to the active sites despite the carbon deposition. Therefore, it can be concluded that the properties of silica samples play an important role in their catalytic behavior for methane decomposition.

Table 1. Crystalline and textural properties of different silica samples.

Sample	Wall phase	$S_{BET} / m^2 \cdot g^{-1}$	$S_{MICRO} / m^2 \cdot g^{-1}$	$S_{EXT} / m^2 \cdot g^{-1}$	$V_{PORE} / cm^3 \cdot g^{-1}$
Silicalite-1	Crystalline	418	389	29	0.17
h-silicalite-1	Crystalline	617	392	225	0.18
MCM-41	Amorphous	1087	43	1044	0.82
SBA-15	Amorphous	755	346	409	1.04
am-SiO ₂	Amorphous	841	110	731	1.12

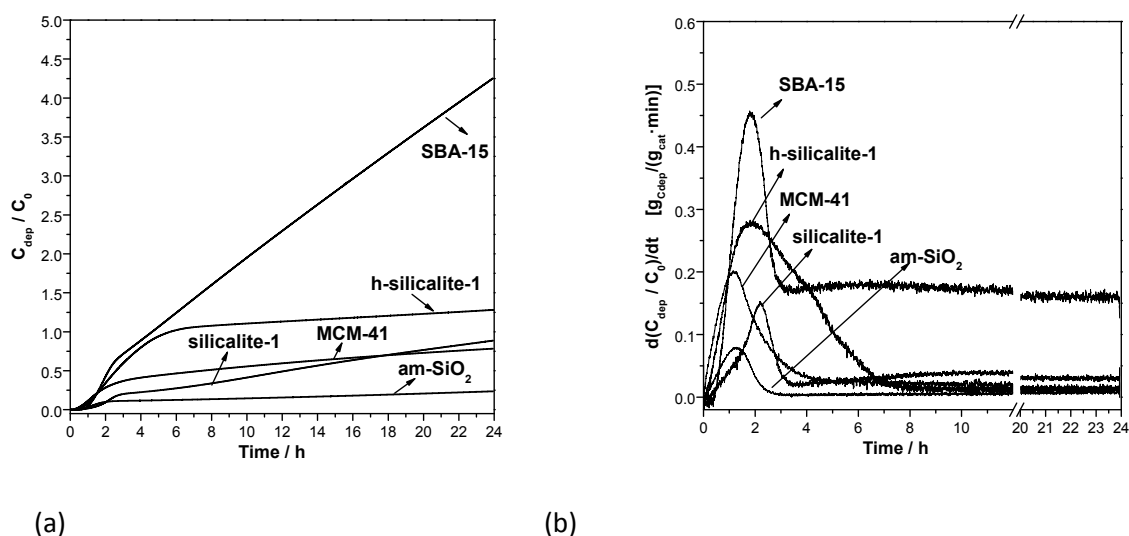


Figure 1. DeCH₄ over different silica materials: (a) evolution of catalyst weight increase in temperature programmed reaction, and (b) carbon deposition rates from reaction at 965 °C.

REFERENCES

- [1]. N. Muradov, *Int. J. Hydrogen Energy*, 26, 1165-1175 (2001).
- [2]. H. F. Abbas, W.M.A. Wan Daud, *Int. J. Hydrogen Energy*, 35, 1160-1190 (2010).
- [3]. D.P. Serrano, J.A. Botas, J.L.G. Fierro, R. Guil-López, P. Pizarro, G. Gómez, *Fuel*, 89, 1241-1248 (2010).
- [4]. D.P. Serrano, J.A. Botas, P. Pizarro, G. Gómez, *Int. J. Hydrogen Energy*, 38, 5671-5683 (2013).
- [5]. A. Matsumoto, K. Chen, K. Tsutsumi, M. Grün, K. Unger, *Microporous Mesoporous Mater.*, 32, 55-62 (1999).
- [6] D.P. Serrano, M.P. Uguina, G. Ovejero, R. Van Grieken, M. Camacho, *Microporous Mater.*, 4, 273-282 (1995).
- [7] D.P. Serrano, J. Aguado, J.M. Rodriguez, A. Peral, *Stud. Surf. Sci. Catal.*, 107, 282-288 (2007).
- [8] D. Zhao, J. Feng, Q. Huo, N. Melosh, G.H. Ferrickson, B.F. Chmelka, G.D. Stucky, *Science*, 279, 548-52 (1998).

Selection of the acid function for a bifunctional catalyst based on CuFe₂O₄ spinel for dimethyl ether steam reforming (HPR4-5)

L. Oar-Arteta, C. Montero, A.T. Aguayo, J. Bilbao, A.G. Gayubo

Dpto. Ingeniería Química, Universidad País Vasco, Apto. 644, 48080 Bilbao, Spain

Introduction

Dimethyl ether steam reforming (DME-SR) is an alternative process of growing interest to produce H₂ rich gas for low-temperature fuel cell systems, as DME is relatively inert, non-corrosive, non-carcinogenic and can be stored and handled as LPG, which means it is more readily used as a fuel and in fuel cells [1]. DME-SR proceeds over bifunctional catalysts, via hydrolysis of DME (over an acid function, such as γ -Al₂O₃ or HZSM-5 zeolites with different Si/Al ratio [2]), followed by methanol steam reforming (over a metallic function, such as Cu/ZnO/Al₂O₃ (CZA) [3]). In order to improve the regenerability of the catalyst, CuFe₂O₄ spinel has been proposed as the metallic function for DME-SR due to its high resistance to sintering [4], which is the main handicap of the CZA function. Nevertheless, CuFe₂O₄ spinel requires higher reaction temperature (usually above 350 °C) than CZA function for attaining high conversion in methanol steam reforming and it has lower mechanic resistance. Consequently, the use of a binder is advisable for preparing a bifunctional catalyst based on CuFe₂O₃ spinel, in order to confer it high resistance to attrition.

Boehmite (aluminum oxi-hydroxide, AlOOH) can be envisioned as an appropriate acid function for the bifunctional catalyst based on Cu spinel, as it can simultaneously act as a binder and acid function. In this paper, we have studied the kinetic behavior in DME hydrolysis (first step of DME-SR process) of AlOOH pure or modified by adding stronger acid solids for enhancing its activity, and the results have been compared with those corresponding to γ -Al₂O₃.

Experimental

The acid functions were prepared by wet physical mixing of AlOOH (Sasol) and the corresponding acid solid (80:20 mass ratio), and were calcined for 2h at 550 °C. The acid solids added include: HZSM-5 zeolites (denoted Z30, Z80 and Z280 according to their SiO₂/Al₂O₃ ratio); Z30 zeolite treated with NaOH 0.2 M (denoted A2Z30) or 0.4M (denoted A4Z30), in order to moderate its acidity; SAPO-5 (S-5) and SAPO18 (S-18). Kinetic runs were carried out in isothermal fluidized bed reactor (Microactivity Reference) connected on-line to a MicroGC Agilent 3000 (with four analytical channels) for product analysis. The operating conditions were: atmospheric pressure, increasing temperature steps from 300°C to 400°C, space time of 0.145 gcat-h/gMeOH and molar steam/MeOH ratio of 3.

Results

Fig. 1 shows the results of DME conversion (graph a) and hydrocarbons yield (graph b) obtained in the transformation of DME over pure γ -Al₂O₃ (A), pure boehmite (B) and mixtures of boehmite with different acid solids. It is observed that AlOOH is notably more active for DME hydrolysis than γ -

Al₂O₃ (Fig. 1a) and both solids completely avoid the formation of hydrocarbons even at high temperature (Fig. 1b).

The addition of the strongest acidic zeolites (Z30, Z80 and A2Z30) to AlOOH notably increases DME conversion (Fig 1a), but it also promotes high formation of hydrocarbons (Fig 1b), which is a handicap for DME-SR as it notably decreases H₂ yield [5]. The addition of weaker acidic zeolites (Z280, A4Z30) avoids the formation of hydrocarbons at temperatures lower than 375 °C, but it only improves slightly the conversion of DME in the 350-375 °C temperature range, required for attaining high conversion in methanol steam reforming over CuFe₂O₄ spinel. The addition of SAPO-5 does not significantly modify the kinetic behavior corresponding to pure AlOOH, and the addition of SAPO-18 gives way to the formation of a small amount of hydrocarbons.

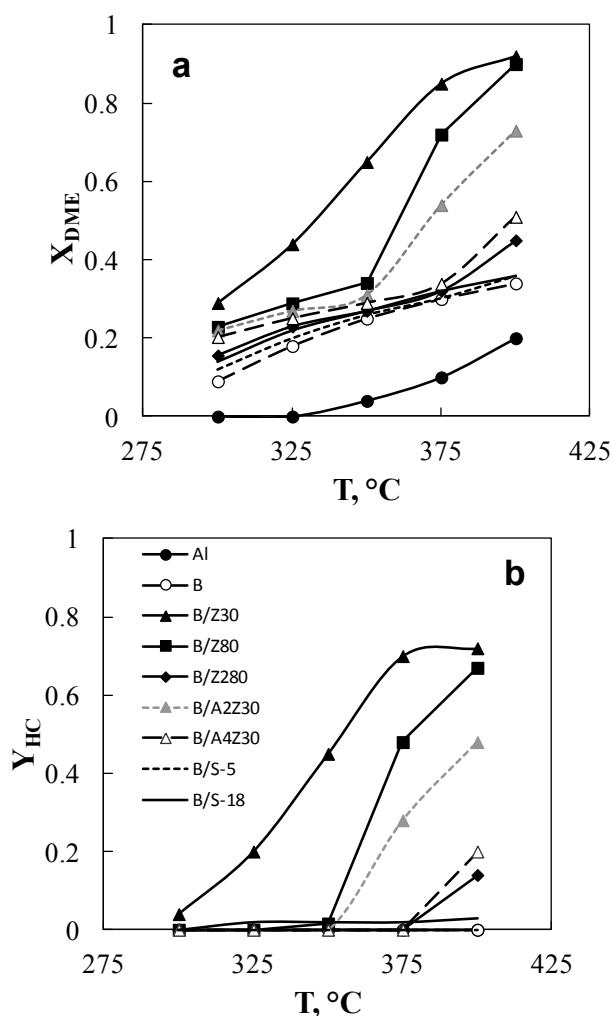


Fig 1. DME conversion (a) and hydrocarbons yield (b) obtained in DME hydrolysis over different acid functions.

Conclusions

AlOOH acid function promoted with strongly acidic solids is not a proper acid function for the bifunctional catalyst for DME-SR based on CuFe₂O₄ spinel, as it favors the formation of hydrocarbons. The addition to AlOOH of small amounts of moderately acid solids (such as Z280 or A4Z30) slightly improves the kinetic behavior of AlOOH acid function at temperatures below 375 °C. Nevertheless, taking into account the cost of these moderately acid solids and the small improvement they suppose to the performance in DME hydrolysis, it can be concluded that pure AlOOH is the most appropriate acid function for the bifunctional catalyst based on CuFe₂O₄ for DME-SR.

References

- Semelsberger, T.A., Borup, R.L., Greene, H.L. J. Power Sources, 2006, 156, 497-511.
- Shimoda, N., Faungnawakij, K., Kikuchi, R., Eguchi, K., Int. J. Hydrogen Energy, 2011, 36, 1433-1441
- Sá, S., Silva, H., Brandao, L., Sousa, J.M., Mendes, A., Appl. Catal. B, 2010, 99, 43-57.
- Faungnawakij, K., Fukunaga, T., Kikuchi, R., Eguchi, K., J. Catal, 2008, 256, 37-44
- Vicente, J. Gayubo, A.G., Ereña, J., Aguayo, A.T., Olazar, M., Bilbao, J. Appl. Catal. B, 2013, 130-131, 73-83.

Influence of Ni environment of supported catalysts on its reactivity in the acetone steam reforming reaction for hydrogen production from Bio-Oil (HPR4-6)

R.M. Navarro¹, R. Guil-Lopez¹, A.A. Ismail², S.A. Al-Sayari³, J.L.G. Fierro¹

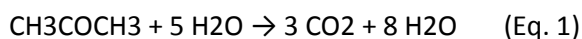
1 Grupo de Energía y Química Sostenibles, ICP-CSIC, C/Marie Curie 2, Cantoblanco, 28049-Madrid, Spain

2 Centre for Advanced Materials and Nanoengineering (CAMNE), Najran University, Najran 11001, Saudi Arabia

3 Advanced Materials Department, Central Metallurgical R&D Institute, CMRDI, Helwan 11421, Egypt

INTRODUCTION

There is an increasing interest in the development of technologies for the conversion of biomass derived hydrocarbons in hydrogen rich gas mixtures as a way to overcome the current technical limitations in hydrogen supply and storage. Recent developments in flash pyrolysis processes allow efficiently convert lignocellulosic biomass to a bio-oil (a complex mixture of aliphatic and aromatic oxygenates) which is easier for handling and transport [1]. Therefore, steam reforming of aqueous bio-oils fractions is an interesting alternative to produce hydrogen in a renewable way. Reforming of model oxygenate components is being studied due to complexity of steam reforming of bio-oils [2,3]. Most studies in literature are focused on the reforming of acetic acid with less attention on steam reforming of acetone, (SRA Eq. 1), although, acetone could be model of the carbonyl-containing compounds present on bio-oils (ketones and aldehydes).



The direct steam reforming of bio-oil generates high amount of undesirable by-products and high coke/oligomer deposition on the most common used Ni-catalyst, which quickly deactivates it. Given the influence of both the Ni particle size and nature of support on the reforming capacity of Ni based catalysts, a careful control of the interaction among Ni particles and supports is essential to develop catalysts stables for the reforming of bio-oils. Thus, it is important to study the influence of the environment of the active centre (Ni) in its catalytic performance from Ni-supported on alumina to ultra-stabilized Ni into the structure of a mixed oxide derived from hydrotalcite-like precursors [4,5], HT, $([\text{M}(\text{II})_{1-x}\text{M}(\text{III})_x(\text{OH})_2]_x \text{A}_x \text{Z}_z \cdot m\text{H}_2\text{O})_x$, where $\text{M}(\text{II})=\text{Ni}, \text{Mg}$ and, $\text{M}(\text{III})=\text{Al}$, and $\text{Az}=\text{CO}_3^{2-}, \text{Cl}^-$, etc.), passing through the interaction of Ni supported on alumina modified with different cations ($\text{La}^{+3}, \text{Ce}^{+4}, \text{Mg}^{+2}$, etc).

Within this research context, the aim of this study is to compare the catalytic behaviour of different Ni-catalysts (Ni-supported on different modified alumina and two Ni-Mg-Al mixed oxides from hydrotalcite catalysts) in the steam reforming of acetone reaction. The influence of the Ni-environment on the physicochemical properties and catalytic behaviour of catalysts have been studied. Careful investigation of the structure and nature of catalysts was done in an attempt to establish a relationship between activity and the changes in structural and surface characteristics of the supported and ex-HT materials induced by SRA-process.

EXPERIMENTAL

Ni-Mg-Al HT precursors were prepared by co-precipitation by urea hydrolysis method [5]. Mixed oxides with different Ni-loadings (ex-HT, 19-60 at.%) were obtained after calcination of HT precursors under a flow of air from room temperature to 850°C for 7 h (1°C min⁻¹). Ni supported on X-modified-Al₂O₃ catalysts (X=Mg, Ce, La) was also prepared by subsequent wet impregnations and calcined under a flow of air from room temperature to 500°C for 5 h (10°C min⁻¹). An additional Ni/Mg-Alcal sample was prepared by subsequent wet impregnations and calcined under a flow of air from room temperature to 850°C for 7 h (1°C min⁻¹). Table 1 summarizes the nomenclature and composition of catalysts studied in this work. Chemical composition was determined by ICP-AES spectroscopy using a Perkin-Elmer Optima 3300DV apparatus. Textural properties were obtained by N₂ adsorption-desorption at 77 K in a Micromeritics ASAP 2100 equipment. TPR experiments were carried out on a Micromeritics TPD/TPR 2900 apparatus. XRD-diffractograms of the catalysts were recorded in a Seifert XRD 3000P diffractometer (Cu K α radiation). X-ray photoelectron spectroscopy (XPS) was carried out with a VG Escalab 200R electron spectrometer equipped with MgK α X-ray source. Catalytic activity measurements were carried out in a fixed-bed reactor using 0.250 g of catalyst. The samples, reduced in situ at 600°C (for the supported samples) and 800°C (for ex-HT) for 2 h with 50 mL(STP)/min of a 10 vol% H₂/N₂ mixture, were tested in the steam reforming reaction under a GHSV = 10180 h⁻¹ at atmospheric pressure, with H₂O/CH₃COCH₃=6.0 and N₂ = 41 % vol. Activity tests were performed at 600°C maintaining the reaction for 10 h. The reaction products were analysed on-line by GC with TCD (Agilent) equipped with Porapack Q (CO₂, C₂H₆, C₂H₄, CH₂CO, water and acetone) and molecular sieve 5A (H₂, O₂, N₂, CO) packed columns connected in series, using He as carrier gas.

RESULTS AND DISCUSSION

Table 1 summarizes the chemical composition and the textural properties for the ex-HT mixed oxides (NM) and the supported catalysts. Atomic percentages of Ni, Mg and Al on all samples are close to that expected from nominal composition being indicative of the effectiveness of the corresponding preparation method used. The mixed oxide with higher Ni loading (NM-2) presented a slight decrease in both surface area and pore volume (Table 1) respect to that observed on the counterpart with lower Ni loading (NM-1). The decrease in the specific area and pore volume with the increase in the Ni loading is associated with the higher concentration of Ni(Mg)O species with lower-porosity respect to the Mg-Al mixed oxide matrix.

	Chemical composition (wt%)		Textural properties		XRD / phases		TPR reduction peaks (°C)	
	NiO	XO	S _{BET} (m ² /g)	V _{nores} (cm ³ /g Al ₂ O ₃)	Main	Secondary	Main	Secondary
ex-HT-1	20	44 (MgO)	90	0.502	spinel	NiO/MgO	770	575
ex-HT-2	60	14 (MgO)	69	0.362	NiO/MgO	[spinel]	590	475/645/850/940
Ni/MgAlcal	12	15 (MgO)	102	0.560	spinel	---	730	450/300
Ni/MgAl	12	15 (MgO)	110	0.412	NiO/MgO	spinel	522	811/290
Ni/CeAl	12	10 (CeO ₂)	177	0.650	CeO ₂	γ-Al ₂ O ₃	488	227/284/610
Ni/LaAl	12	15 (La ₂ O ₃)	149	0.612	γ-Al ₂ O ₃	N/D	605	297/415/495/777

Table 1. Characterization results of the ex-HT mixed oxides and supported catalysts

The diffraction patterns of ex-HT-1 and ex-HT-2 samples shows that Ni is distributed among NiO, Ni(Mg)Al₂O₄ and NiO-MgO solid solution phases depending on catalyst composition. The sample with lower Ni content, ex-HT-1, showed crystalline phases corresponding to NiO-MgO solid solutions and Ni-MgAl₂O₄ spinel, the latter with lower intensity respect to the solid solution. Although, the positions of the characteristic XRD peaks of MgO (JCPDS 78-0430) and NiO (JCPDS 78-0643) are very close, the peaks observed on ex-HT-1 sample is attributed to the formation of a NiO-MgO solution because calcination at high temperature produces the migration of Ni²⁺ and Mg²⁺ cations within the MgO or NiO lattices. X-ray diffractogram corresponding to ex-HT-2 sample shows diffraction peaks corresponding to NiO, NiO-MgO solid solutions and Ni(Mg)Al₂O₄ phases. The spinel phases in the ex-HT-2 was lower than in the ex-HT-1 counterpart as expected taking into account the lower Al content in the latter. The XRD-phases in the Ni/MgAl samples depend on the calcination temperature. Thus, the spinel phase is the main crystalline phase to increase the temperature of calcination.

Reducibility of ex-HTs-oxides and supported catalysts was studied by TPR. The reduction profile of ex-HT-1 presents only one reduction peak at 770°C characteristic of well-stabilized nickel species inside the NiO-MgO solid solution. The ex-HT-2 reduction profile showed a broad reduction peak in the 400-850°C range, which could be decomposed into five components (Table 1). The peak at low temperature is attributed to reduction of NiO species with weak interaction with other species, while the reduction peaks appearing at higher temperatures are related to the reduction of stabilized nickel species inside highly dispersed non-stoichiometric amorphous nickel aluminate spinels, NiO-MgO solid solutions and spinel phases, respectively. Ni/MgAlcal sample shows a similar reduction profile than ex-HT-1 with lower reduction temperatures which can be attributed at the reduction of well-stabilized Ni²⁺ inside the NiO-MgO solid solution with two small peaks at lower temperature caused by the reduction of NiO supported with different strength with the support. The Ni/MgAl (calcined at lower temperature, 500°C) shows the typical NiO supported reduction profile with strong interaction with the support. Additionally, a small component at higher temperature, assigned to the reduction of Ni²⁺ stabilized into the spinel phases, and another small component at lower temperature (typical NiO reduction) can be detected. The TPR profile of supported Ni/CeAl and Ni/LaAl catalysts show a complex reduction profile with several component caused by the reduction of NiO supported with different interaction with the support.

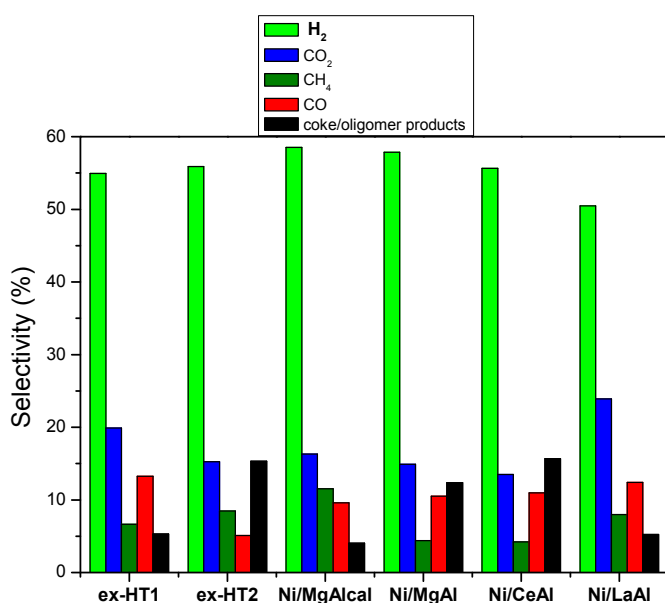


Figure 1. Selectivity toward products in acetone steam reforming after 10 hours on stream (600°C, H₂O/CH₃COCH₃ = 6.0, GHSV=10180 h⁻¹)

All catalysts converted all acetone (100% of conversion) mainly into the gasification gases (H₂, CO₂, CO and CH₄) with lower yields towards coke and carbon and products of condensations. Ex-HT-1 and Ni/MgAlcal converted acetone mainly into gasification gases with the lowest formation of coke/oligomer products (5.4 and 4.2%, respectively). Both catalysts show the highly stabilized NiO-MgO solid solution and spinel phases are the mainly crystalline ones, with highest reduction temperature (highest Ni stabilization). On comparing with these catalysts, the ex-HT-2 and Ni/CeAl samples showed lower capacity (81.9%) to transform the acetone into H₂, CO, CO₂ and CH₄.

Selectivity to gas products also depends on catalyst formulation (Table 1). The highest H₂ selectivity was obtained with both Ni/MgAl catalysts. This fact indicates an enhancement in the C-H bond breaking and water gas shift capacity respect to the rest of the catalysts. The differences in gasification of acetone into H₂, CO, CO₂ and CH₄ observed in the tested catalysts imply that the structure and Ni-environment on these catalysts modifies in different way the routes of acetone reforming. According to the chemistry of acetone under steam reforming conditions, both metal and support, play an essential role in the catalytic behaviour of supported Ni catalysts. The basic properties of the Mg-Al oxides, especially for the catalysts derived from hydrotalcites, may participate in the reforming mechanism of acetone since this molecule could react on these basic sites by means of condensation/oligomerization reactions. Likewise, gasification capacity of the four Mg-Al catalysts seem to be related with the basicity associated to NiO-MgO solid solution and spinel phases in the samples, due to the sample with lowest content of these phases, ex-HT-2, showed the lowest gasification activity. Moreover, higher Ni content is associated with higher Ni crystalline particle size, which favours carbon deposition. Therefore, the low gasification capacity of the ex-HT-2 catalyst suggests high carbon deposition on this sample.

CONCLUSIONS

The steam reforming of acetone (as model molecule of bio-oil) over Ni catalysts with different Ni-environment has been studied. The activity of catalysts clearly indicated the better performance of sample with lower Ni content in terms of gasification capacity as compared with the higher Ni-loading counterpart. Likewise, samples with the NiO-MgO solid solution and spinel phases seem to show a higher gasification capacity observed on the catalysts with these phases (). The higher Ni loading suggests higher carbon deposition on this sample associated to the higher Ni particle size developed in this sample.

ACKNOWLEDGEMENTS

This research was supported by the Ministry of Science and Innovation (Spain) and the Autonomous Government of Madrid, Madrid (Spain) under grants ENE2010-21198-C04-01 and S2009ENE-1743, respectively. Partial support to this work came from Najran University, The Kingdom of Saudi Arabia.

REFERENCES

- [1] X. Hu, L. Zhang, G. Lu, *Appl. Catal. A: Gen.* 427 (2012) 49.
- [2] E. Ch. Vagia, A. A. Lemonidou, *Appl. Catal. A: General*, *Appl. Catal. A: General* 351 (2008) 111-121.
- [3] C. Resini, L. Arrighi, M.C.H. Delgado, M.A.L. Vargas, L.J. Alemany, P. Riany, R.M. Berardinelli, G. Busca, *Int. J. Hydrogen Energ.* 31(1) (2006) 13-19.
- [4] A. Cavani, F. Trifiro and A. Vaccari, *Catal. Today* 11 (1991) 173–301.
- [5] R. Guil-Lopez, V. LaParola, M.A. Peña, J.L.G. Fierro, *Catal. Today* 116 (2006) 289-297.

H₂-production from CO₂-assisted ethanol steam reforming; the regeneration of Ni-based catalysts (HPR5-1)

LUKASZ BEDNARCZUK¹, PILAR RAMÍREZ DE LA PISCINA¹, NARCÍS HOMES^{1,2}

¹ Departament de Química Inorgànica and Institut de Nanociència i Nanotecnologia, Universitat de Barcelona, Martí i Franquès 1-11, 08028 Barcelona, Spain

² Catalonia Institute for Energy Research (IREC), 08930 Barcelona, Spain

INTRODUCTION

A main drawback of the use of nickel-based catalysts for H₂-production from the steam-reforming of ethanol is the formation of carbonaceous deposits, which could lead to the decay in the activity of catalysts. Many studies have been done with the aim of decrease the carbon deposition of these systems including the introduction of alkaline promoters, noble metals or the use of different supports [1-3]. Although the effect of oxygen introduction in the reactant mixture for decreasing the carbonaceous deposits on the catalysts has been largely studied, there are few studies concerning the introduction of other oxidants such as CO₂ [4-7]. Studies of combined steam reforming and dry reforming of ethanol over CeO₂-supported Rh- and Pt-based catalysts pointed to a possible effect of CO₂ co-feeding in the stability of catalysts due to decreasing of carbon deposits [6, 7]. It was suggested that CO₂ competes with ethanol for adsorption sites, suppressing the rate of formation of coke precursors. The aim of this work is the study of the effect of CO₂ on the ethanol steam reforming under low H₂O/ethanol ratios over nickel-based catalysts. For this purpose, Al₂O₃-, MgO-, Y₂O₃-, La₂O₃- and ZrO₂-supported Ni catalysts (promoted or not with K) were prepared, characterized and used in the CO₂-assisted ethanol steam reforming (CDES_R). Catalytic results of CDES_R were compared with those of ethanol steam reforming (ES_R) under similar conditions and analyzed as a function of the characteristics of the catalyst. The regeneration of catalysts by CO₂-treatment during ES_R was also studied in order to obtain information on the role of the CO₂ as reactant in the CDES_R process.

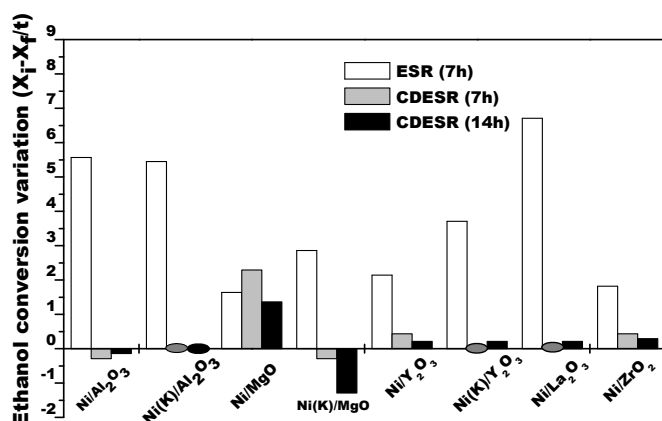
EXPERIMENTAL

Al₂O₃, MgO, Y₂O₃, La₂O₃ and ZrO₂ supports were prepared using a modified pseudo sol-gel method. Aqueous urea solutions of the corresponding nitrate precursors which contained activated carbon (20-40 mesh) were stirred for 50 h at 95°C. After filtration, the resulting solids were dried (100°C) and then calcined in a tubular reactor under an air flow at 600°C (4h). Catalysts containing Ni (ca. 8 % wt) and K (ca. 0.5 % wt) were prepared by incipient wetness impregnation using aqueous solutions of nitrate precursors. The resulting solids were dried (100°C) and then calcined at 450°C (5h). Calcined catalysts were characterized by chemical analysis (ICP), N₂ adsorption, XRD and TPR. Prior to catalytic test, samples were reduced in-situ with a 10 % vol. H₂/Ar flow at 600°C (2h). Reduced catalysts were characterized by XPS, CO₂-adsorption calorimetry and TPD-CO₂ experiments. Ethanol steam reforming (ES_R) was carried out at 600°C for 7 h with an EtOH/H₂O=1/1.6 (molar ratio) mixture. Then, the reactor was flushed with inert gas and following, CO₂-assisted ethanol reforming (CDES_R) experiments were carried out for 14 h under an EtOH/H₂O/CO₂=1/1.6/1.6 (molar ratio) mixture. The CO₂-treatments were carried out at 600 °C with a 10 % vol. CO₂/Ar mixture for

ca. 2 h. GHSV was always ca. 8100 h⁻¹ using about 200 mg of catalyst; the effluent was continuously monitored by on-line GC analysis using N₂ as internal standard. Post reaction catalysts were analyzed by XRD, Raman spectroscopy and TG-TPO experiments.

RESULTS AND DISCUSSION

From XRD analysis of calcined catalysts, only in Ni/ZrO₂ was possible to determine the crystallite size of the NiO cubic phase, which resulted in 27 nm. TPR results show that the presence of potassium led to a slight decrease of the reduction temperature of the supported nickel species. For the Y₂O₃- and La₂O₃-supported samples the calculated H₂-consumption points to a partial reduction of the supports. Surface Ni/M (M= support cation) XPS ratios of reduced catalysts were higher than those determined from chemical analysis; this effect was smaller for Al₂O₃- and ZrO₂-supported catalysts. For a given support, the presence of K-promoter doesn't greatly affect the Ni/M ratio. However, after reaction, a slight decrease on the Ni/Al and Ni/Y XPS ratios were determined for the Ni(K)/Al₂O₃ and Ni(K)/Y₂O₃ catalysts with respect to the corresponding non-promoted catalysts.



As expected, the heat of adsorption of CO₂ depended on the acidic-basic nature of the support used. For a given support, the presence of K-promoter results in an increase of the heat of adsorption and in the total amount of adsorbed CO₂; the lowest values were obtained for Ni/Al₂O₃ catalyst.

Figure 1. Variation of the ethanol conversion ($X_i - X_f$) per hour during ESR and CDESr experiments (0 means no change).

Under the reaction conditions used in the present work for ESR and CDESr (H₂O/ethanol= 1.6 molar ratio), besides H₂, the main products obtained were CO, ethylene and CH₄; acetaldehyde also was obtained as a function of the ethanol conversion achieved. Under CDESr conditions, the molar concentration of H₂ in the outlet reached values of about 55 %. Under ESR the catalysts showed decay on activity during the first 7h on stream (see Figure 1). When reaction was switched to CDESr conditions, the catalytic activity was maintained in most cases during 14 h; this was of particular relevance for Al₂O₃- and La₂O₃-supported catalysts which exhibited under ESR the highest deactivation. Only for Ni/MgO catalyst the behaviour was similar under ESR and CDESr conditions whereas the promoted Ni(K)/MgO sample improved its catalytic performance under CDESr.

In several post-reaction catalysts it was possible to determine the existence of NiO phase by XRD; for Ni/Al₂O₃ and Ni/ZrO₂, crystallite sizes of ca. 10 and 14 nm respectively were calculated. TG-TPO experiments carried out on CDESr post reaction catalysts allowed us to quantify the carbonaceous deposits; the Ni/La₂O₃ catalyst showed the lowest amount.

In a separate experiment, the effect of CO₂-treatment during ESR conditions was analyzed. In Figure 2A, the initial ethanol conversion and that determined after 14 h under ESR at 600°C for several catalysts is shown; in all cases, a diminution of ethanol conversion was found. During the CO₂-treatment process, the gaseous effluent was continuously monitored by on-line GC. After several minutes, CO was detected, and its concentration diminished with time; no longer was CO detected in the effluent after about 2 h. Then, Ar was flushed till CO₂ was not detected in the reactor effluent and the reaction mixture (EtOH/H₂O) was re-admitted. In general, the CO₂-treatment produced a regeneration of catalysts and a recovery of the catalytic performance was observed (see Figure 2A).

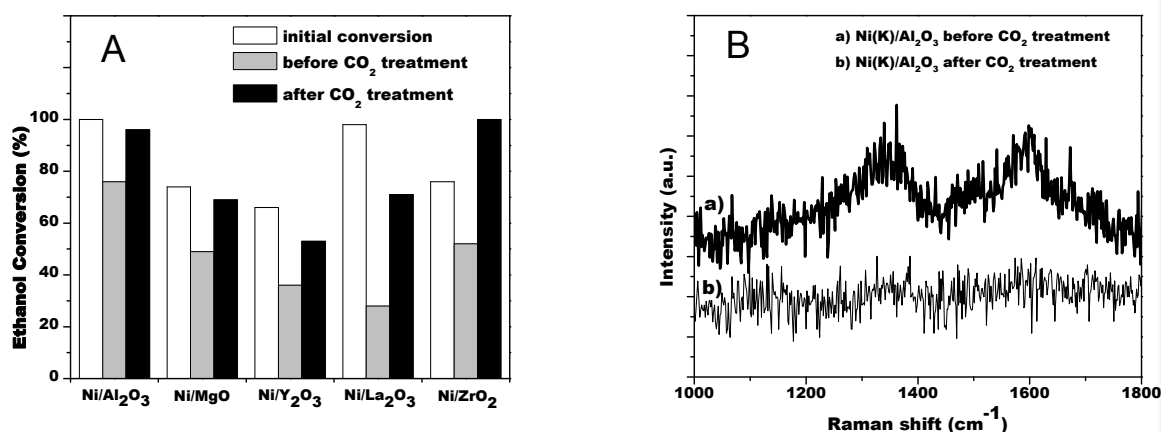


Figure 2. A) Effect of CO₂-treatment on ethanol conversion under ESR for several catalysts and, B) Raman spectra of Ni(K)/Al₂O₃ catalyst before and after the CO₂-treatment.

Raman spectroscopy was used for characterizing the carbonaceous deposits after the catalytic tests. Figure 2B shows the Raman spectra in the 1000–1800 cm⁻¹ region for the Ni(K)/Al₂O₃ catalyst; no bands due to carbonaceous deposits after the CO₂-treatment were found in contrast with those present in the spectrum registered before the CO₂-treatment. A clear effect of CO₂ on removal the carbonaceous deposits formed during the ESR reaction is determined for this catalyst; CO₂ could play a similar role during CDESr.

CONCLUSIONS

The CO₂-assisted ethanol steam reforming (CDESr) process for the production of H₂ can be effectively carried out over Ni-based catalysts using a low H₂O/EtOH ratio. The presence of CO₂ in the reactant mixture results in a positive effect preventing the catalyst deactivation. This process

results a function of the support and the presence of K promoter. A study of the deactivation/regeneration of catalysts found that a CO₂-treatment recovered the performance of deactivated Ni-catalysts.

REFERENCES

- [1] Navarro R. M., Peña M. A., Fierro J. L. G., Chem. Rev, 107 (2007) 3952
- [2] Ramirez de la Piscina, P., Homs, N., Chem. Soc. Rev., 37 (2008) 2459
- [3] Mattos L. V., Jacobs G., Davis B. H., Noronha F. B., Chem. Rev., 112 (2012) 4094
- [4] Bellido J. D. A., Tanabe E. Y., Assaf E. M., Appl. Catal. B, 90 (2009) 485
- [5] Bepalko N., Roger A.-C., Bussi J., Appl. Catal. A, 407 (2011) 204
- [6] de Lima S. M., da Silva A. M., Jacobs, G., Davis, B. H., Mattos, L. V., Noronha, F. B., Appl. Catal. B, 96 (2010) 387
- [7] da Silva A. M., de Souza K. R., Jacobs G., Graham U. M., Davis B. H., Mattos L. V., Noronha F. B., Appl. Catal. B, 102 (2011) 94

Reforming Of Ethanol On Co/Al₂O₃ Catalysts Reduced At Different Temperatures (HPR5-2)

Zsuzsa Ferencz, Kornélia Baán, Erika Varga, Albert Oszkó, András Erdőhelyi

Department of Physical Chemistry and Materials Science, University of Szeged, Hungary

Introduction

Noble metals are well known for their high catalytic activity and have been studied extensively in terms of ethanol steam reforming reactions [1,2]. Besides these samples the reforming of ethanol occurs with high efficiency over supported Co catalysts, and Co/Al₂O₃ exhibited one of the best performances [3]. The performance of the Co catalysts was influenced not only by the support [3] but by the precursor of the metal [4], by the preparation method of the catalyst [5], by the crystal size of the Co [6], and the morphology of the support [7]. In the present paper the effect of the reduction temperature on the efficiency of Co/Al₂O₃ in the ethanol + H₂O reaction was investigated.

Experimental

The catalysts were prepared by impregnating the Al₂O₃ support with the solution of Co(NO₃)₂ to yield a 11% metal content. The impregnated powders were dried and calcined at 973 K. Before each measurement the fragments of catalyst pellets were oxidized at 473 K and reduced at different temperatures from 773 to 1173 K. The steam reforming of ethanol was carried out in a fixed-bed continuous-flow reactor. In the reacting gas mixture the ethanol:water ratio was usually 1:3. The space velocity was 60000 h⁻¹. The products were analyzed by a gas chromatograph. The selectivity of H₂ and different other products were calculated separately. The amount and the reactivity of surface carbonaceous deposit formed in the catalytic reactions were determined by temperature-programmed hydrogenation. The infrared spectra during the reaction were recorded in a DRIFT cell (Spectra Tech) adapted to a BioRad FT-IR spectrometer. The acidic character of the samples was determined by NH₃ adsorption. The amount of surface Co atoms was measured by H₂ TPD after H₂ adsorption at 373 K. The BET surface and the temperature programmed reduction of the sample were determined by a BELCAT A instrument. The XRD study was carried out on a Rigaku Miniflex II powder X-ray diffractometer. The XP spectra were taken with a SPECS instrument. The samples were treated in a separate catalytic chamber which was connected directly to the analyzing device.

Results and discussion

On the XRD spectra of Co/Al₂O₃ diffraction peaks at 31.5°, 37.1°, 59.5°, and 65.5° were observed which belong to the spinel structure of CoAl₂O₄ or Co₃O₄. The presence of the diffraction peaks at 45.3° and 67.3° could be attributed to γ-Al₂O₃ with low crystallinity.

The TPR profile of the catalyst contains a broad peak between 580-980 K with three different maxima at 767, 823, and 858 K, and a high temperature reduction stage (T_{max}=1103 K) was also observed. The peak at low temperature corresponds to the reduction of large crystalline Co₃O₄ particles. The high temperature reduction stage corresponds to the reduction of CoO and CoAl₂O₄. The number of acidic sites, and the amount of surface Co atoms decreased as the calcination

temperature increased. The XP spectra of Co 2p in the 11% Co/Al₂O₃ sample shows the characteristic doublet (Co 2p_{3/2} at 782.1 eV) with satellite peaks both in the as received and the oxidized state, corresponding to Co²⁺ and Co³⁺. After reduction a strong shoulder, more precisely a nearly distinct peak depending on the reduction temperature appeared at the low binding energy side of the Co 2p_{3/2} component at 778.6 eV. This feature can be attributed to a more reduced cobalt state.

Catalytic measurements showed that the main products of ethanol reforming are H₂, CO, CO₂, C₂H₄ and acetaldehyde. The conversion at 873 K was nearly complete at the beginning of the reaction but then slightly decreased in time. The hydrogen selectivity was higher than 90% in the first minutes in all cases but it decreased in time as the reduction temperature of the catalyst decreased. On Co/Al₂O₃ reduced at 773 or 873 K the H₂ selectivity after 120 minutes of the reaction was below 50% while on the sample pretreated at 1173 K it was about 90%. Not only the H₂ but the CO₂ selectivity decreased with time of stream while that of ethylene and CO increased. It was found that the rate of H₂ and CO formation increased and that of C₂H₄ decreased as a function of the reduction temperature of the catalysts. On the sample reduced at 1173 K only traces of C₂H₄ was detected but in this case the CO selectivity increased up to 38%.

The TPR of surface carbon formed during the reaction at 823 K on a sample occurred in the same temperature range irrespective of the reduction temperature or the reaction temperature. For example on 11% CoAl₂O₃ the TPR peak maximum was at 820 K when the reaction was studied either at 823 or 973 K. Contrarily, the amount of surface carbonaceous deposit significantly depends on the reaction and on the reduction temperature, it increased with increasing either the reaction or reduction temperature.

According to the infrared spectra recorded during the catalytic reactions absorption bands were observed at 1579 and 1455 cm⁻¹ in all cases which could be assigned as the O-C-O vibrations of acetate species bonded to the alumina support. The intensities of these bands increased with time at 723 and at 823 K. These peaks were stable when the reactor was flushed with inert gas at the reaction temperature. When the catalyst was heated in the reaction mixture at low temperature absorption bands were detected at 1455, 1399, 1122, and 1053 cm⁻¹ which could be assigned as different vibrations of CH₃ and CO groups in the ethoxide species. The intensities decreased as the temperature increased and above 523 K these bands disappeared from the spectra and new peaks were detected which belong to the acetate species.

For comparison the decomposition of ethanol was also studied. It was found that in these cases additionally significant amount of diethyl ether was also formed. The selectivity of H₂ and CO formation which was less than in the presence of water significantly decreased but that of ethylene and acetaldehyde increased as a function of reaction time. The reduction temperature of the catalyst influenced the hydrogen and CO selectivity in the same way as in the reforming reaction. The formation rate of acetaldehyde first increased as a function of the calcination temperature and then decreased; the maximum selectivity was observed on the sample reduced at 873 K. Similar infrared spectra were recorded during the decomposition of ethanol as in the reforming reaction only the acetate band appeared at higher temperature.

These results clearly show that the reduction temperature significantly influences the product distribution, while the reduction degree and the structure of the Co species depend on the pretreatment of the sample.

References.

1. A. Erdőhelyi, J. Raskó, T. Kecskés, M. Tóth, M. Dömök, K. Baán, *Catal Today* 116, 367 (2006).
2. A. C. Basagiannis, P. Panagiotopoulou, X. E. Verykios, *Top Catal* 51, 2 (2008).
3. F. Haga, T. Nakajima, H. Miya, S. Mishima, *Catal Lett* 48, 223 (1997).
4. H. Song, B. Mirkenaloglu, U.S. Ozkan, *Appl. Catal. A:General* 382, 58 (2010).
5. S.R. Garcia, J.M. Assaf, *Modern Res. Catal.* 1, 52 (2012)
6. F. Haga, T. Nakajima, K. Yamashita S. Mishima, *React. Kinet. Catal Lett.* 63, 253 (1998).
7. I.I. Soykal, B. Bayram, H. Sohn, P. Gawade, J.T. Miller, U.S. Ozkan, *Appl. Catal. A:General* 449, 47 (2012).

The Chemical-loop Reforming of Ethanol on Spinel Ferrites (HPR5-3)

Cristian Trevisanut^{1,2}, Juliana Velasquez¹, Massimiliano Mari¹, Sigrid Yurena Arenas Urrea^{1,3}, Jean-Marc M. Millet², Fabrizio Cavani¹

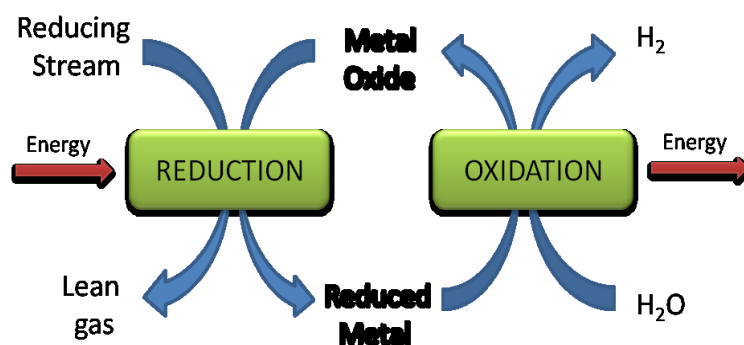
¹Dipartimento di Chimica Industriale "Toso Montanari", Università di Bologna, 40136 Bologna, Italy

²Institut de Recherches sur la Catalyse et l'Environnement de Lyon, IRCELYON, UMR 5256 CNRS-Université Claude-Bernard Lyon 1, F-69626 Villeurbanne Cedex, France

³Universidad de Las Palmas de Gran Canaria, 35002 Las Palmas, Spain

INTRODUCTION

Thermochemical water splitting is an option for producing high purity hydrogen. This process implies the reduction of a metal oxide as the first step, and its reoxidation with water in a second step, producing in this way pure hydrogen and restoring the original oxygen content of the metal oxide by means of a chemical-loop [1]. With the aim of decreasing the high temperatures generally required in the first step, a reducing fuel can be used (usually methane) [2]. However, bio-alcohols might be also considered as reducing stream for this process (Scheme 1) [3].



Scheme 1. The chemical-loop approach for alcohols reforming

In order to investigate the feasibility of a two-step cycle approach for the catalytic production of hydrogen from ethanol and water, different ferrites (Fe_3O_4 , CoFe_2O_4 , and NiFe_2O_4) were tested as electrons/ O_2^- carriers. The goal was to study the reactivity of materials with similar structure and composition, and to investigate the structural changes occurring on them during the chemical-loop [4].

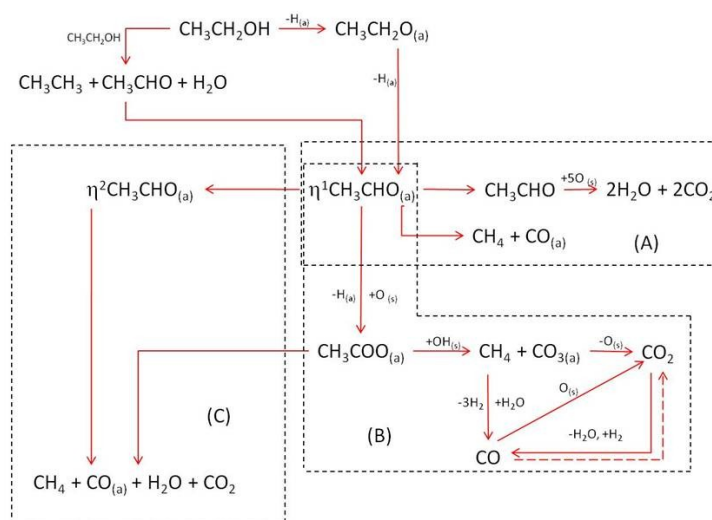
RESULTS AND DISCUSSION

The different ferrites were prepared by means of co-precipitation. Materials were first reduced with either pure ethanol or the azeotrope at 450°C (first step of the cycle); main products during this step were CO , CO_2 , CH_4 , H_2O , and H_2 , but also non-negligible amounts of C2-C4 chemicals were produced. The relative amount of each product was a function of the reaction time, which is related to the degree of reduction of the spinel. Co-feeding water during the first step led to different selectivity in C2-C4 compounds, less degree of reduction and lower reduction speed. An important

aspect was the accumulation of coke, which formed from the very beginning of the reaction. Co-feeding water was not helpful in reducing coke deposition as much as expected; however, the amount of coke formed could be minimized by controlling the chemical-physical features of the spinel, the process parameters and the reduction degree of the mixed oxide during the first step.

Materials were characterized by means of Mössbauer and X-ray Diffraction, both before and after reaction in order to understand the modifications occurred. The different characterization techniques revealed that the compounds were well reduced in the first step, but sintering and segregation of the co-cation occurred, which led to a change of reactivity during the successive cycles.

In-situ diffuse reflectance spectroscopy (DRIFTS) and mass spectrometry (MS) were also used with the aim of observing the surface species formed during the adsorption of the alcohol and its related gas products when increasing the temperature. In all the cases ethoxy species formed at low temperature and acetaldehyde produced by dehydrogenation. However, the transformation at middle and high temperatures differed depending on the catalyst used. It was found that acetates are important surface intermediates in the case of the Ni ferrite, whereas with the Co and Fe ferrites, more direct pathways to the oxidation products were evidenced but at higher temperatures. The set of reactions proposed for the transformation of ethanol on the different ferrites according to the evidence found is shown in Scheme 2 [4].



Scheme 2. Ethanol adsorption and transformation over CoFe₂O₄ (A) NiFe₂O₄ (B), and Fe₃O₄ (C).

CONCLUSIONS

The investigation allowed us to conclude that spinel-type mixed ferrites can be used as electrons and ionic oxygen carriers during the chemical-loop reforming of bio-ethanol. The chemical-physical characteristics of the oxides affected the reactivity behavior during both the reductive and the steam-oxidative steps. Coke formed during the former step, and its amount could be minimized, but not completely avoided, by tuning both the materials characteristics and the reaction conditions.

ACKNOWLEDGEMENTS

This work has been financed by the “Fondation Tuck”, Rueil-Malmaison Cedex (F), Project Enerbio.

[1] T. Kodama, N. Gokon, N. Chem. Rev. 107 (2007) 4048.

[2] P. Chiesa, G. Lozza, A Malandrino, M. Romano, V. Piccolo, Int. J. Hydr. En. 33 (2008) 2233.

[3] V. Crocellà, F. Cavani, G. Cerrato, S. Cocchi, M. Comito, G Magnacca, C. Morterra, J. Phys. Chem. C 116 (2012) 14998.

[4] J. Velasquez Ochoa, C. Trevisanut, J.-M. M. Millet, G. Busca, F. Cavani, J. Phys. Chem. C, in press.

Micro-reformer for hydrogen-rich gas generation from ethanol for a portable micro-SOFC system (HPR5-4)

D. Pla¹, M. Salleras², I. Garbayo², A. Morata¹, N. Sabaté², N. J. Divins³, M. Torrell¹, J. Llorca³ and A. Tarancón¹

1. Catalonia Institute for Energy Research (IREC), Department of Advanced Materials for Energy
Jardins de les Dones de Negre 1, 2nd floor

08930-Sant Adrià del Besòs, Barcelona /Spain

2. IMB-CNM (CSIC), Institute of Microelectronics of Barcelona,

National Center of Microelectronics, CSIC, Campus UAB,

08193 Bellaterra, Barcelona/ Spain

3. INTE, Institute of Energy Technologies,

Polytechnic University of Barcelona, Av. Diagonal 647, Ed. ETSEIB

08028 Barcelona/ Spain

One of the most promising applications of fuel cells is powering portable applications taking advantage of their high specific energy [1]. In particular, the development of micro power generation systems employing hydrogen-fed solid oxide fuel cells (SOFCs) is gaining interest because they may power consumer electronics even with higher energy densities than rechargeable lithium-ion batteries [2]. However, many challenges have to be overcome before introducing this technology into the market. The first, safely produce a continuous hydrogen flow from fuels easy to handle and store, e.g. liquid fuels. Catalytic fuel reformers using alcohols have become a realistic alternative as they can provide high energy density, low cost, safety, and easy transportation [3].

Interest in ethanol steam reforming (1) is growing rapidly, mainly because ethanol can be produced from renewable biomass (bio ethanol), it is liquid at atmospheric temperature and pressure, and it yields more hydrogen on a molar basis than other common fuels like for example methanol [4].



The state-of-the-art reformers are based on micro catalytic reactors with long micro- channels and external heating to meet the energy demand of the endothermic steam reforming reaction (ΔH_{SR} at 298K = 347.4 kJ/mole). This micro channel configuration has some problems associated to high pressure drop, non-modularity, high energy consumption and long start-up times.

This work reports the design, manufacturing and experimental results of a novel silicon-based micro-reactor for hydrogen-rich generation from ethanol. The current design is based on vertical micro-channels crossing a 500- μm silicon wafer. The projected area of the micro-reactor is 15 mm x 15 mm while the reactive area is more than 36 cm². This huge active surface per projected area (16 cm²/cm²) is achieved by more than 4x10⁴ vertical micro-channels (50 μm in diameter) perfectly aligned through which the fuel flows (Figure 1a). In addition, an integrated serpentine tungsten heater allows reaching the operation temperature autonomously. The micro-reactor is fabricated

with the mainstream microelectronics fabrication technologies (photolithography, wet etching, chemical vapor deposition and reactive ion etching) ensuring a cost-effective high reproducibility and reliability.

This vertical configuration, compared with other more conventional designs, allows reducing the pressure drop, i.e. the pressure required for the steam to flow. Moreover, the high surface-to-volume ratio of micro channels ($8 \times 10^4 \text{ m}^2/\text{m}^3$), loaded with catalytic material, leads to higher performances of the ethanol steam reforming reaction by achieving a larger specific contact area and a shorter diffusion length. The micro-channels are coated with the catalytic system, RhPd/CeO₂, by infiltration [5]. The cross-section images presented in Figure 1b clearly show that there is no significant tapering effect along the 500 μm thick wafer avoiding undesirable pressure drop due to bottlenecks.

The tungsten heater locally heats the active area to improve the thermal transfer. In addition, to improve the thermal efficiency of the device, the silicon micro-reactor has been encapsulated with an insulating glass cover by anodic bonding. A two-step glass wet-etching process has been developed for the glass cover fabrication in such a way that a well-defined deep cavity for the fluid flow and well-defined pathways for the external pads of the heater are achieved. Therefore, with this vertical configuration, an internal heating is possible and an efficient thermal coupling is achieved, allowing a managing of heat in a more compact configuration and a minimization of the thermal losses. This fact is crucial to combine a rapid-start up of the micro-reactor and a thermal sustaining of itself for the ethanol steam reaction.

The encapsulated micro-reformer has been tested for ethanol steam reforming under diluted feed conditions at the 923-1073K temperature (optimal operation temperatures for micro-SOFCs). A temperature external control system and an electrical power supply for the tungsten heater has been used during the tests. Results show the increase in contact area between fuel gas and catalyst that leads to reduced residence times and a high performance in small volumes. High specific hydrogen production rates, high ethanol conversions (>80%) and adequate selectivity profiles are achieved. (Figure 2)

This functional converter is the basis for a complete gas processing unit as a subsystem of an entire micro-SOFC system.

Figure 1. (a) Top view optical microscope image of the whole micro reformer and detail of the micro channels array and the heater pad (yellow line on the right), (b) Cross-section SEM images of the micro-channels of the reformer before and after catalyst filling.

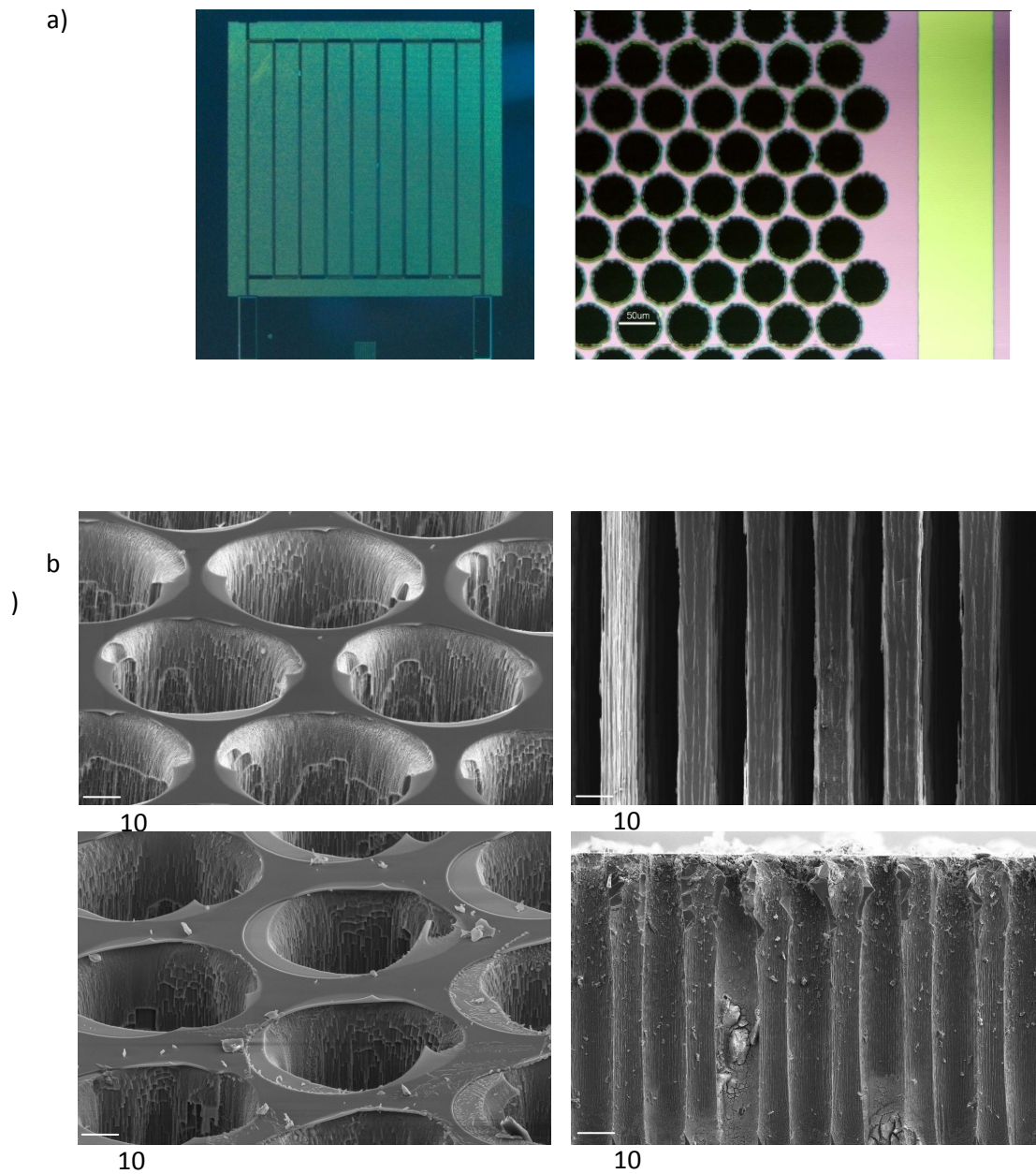
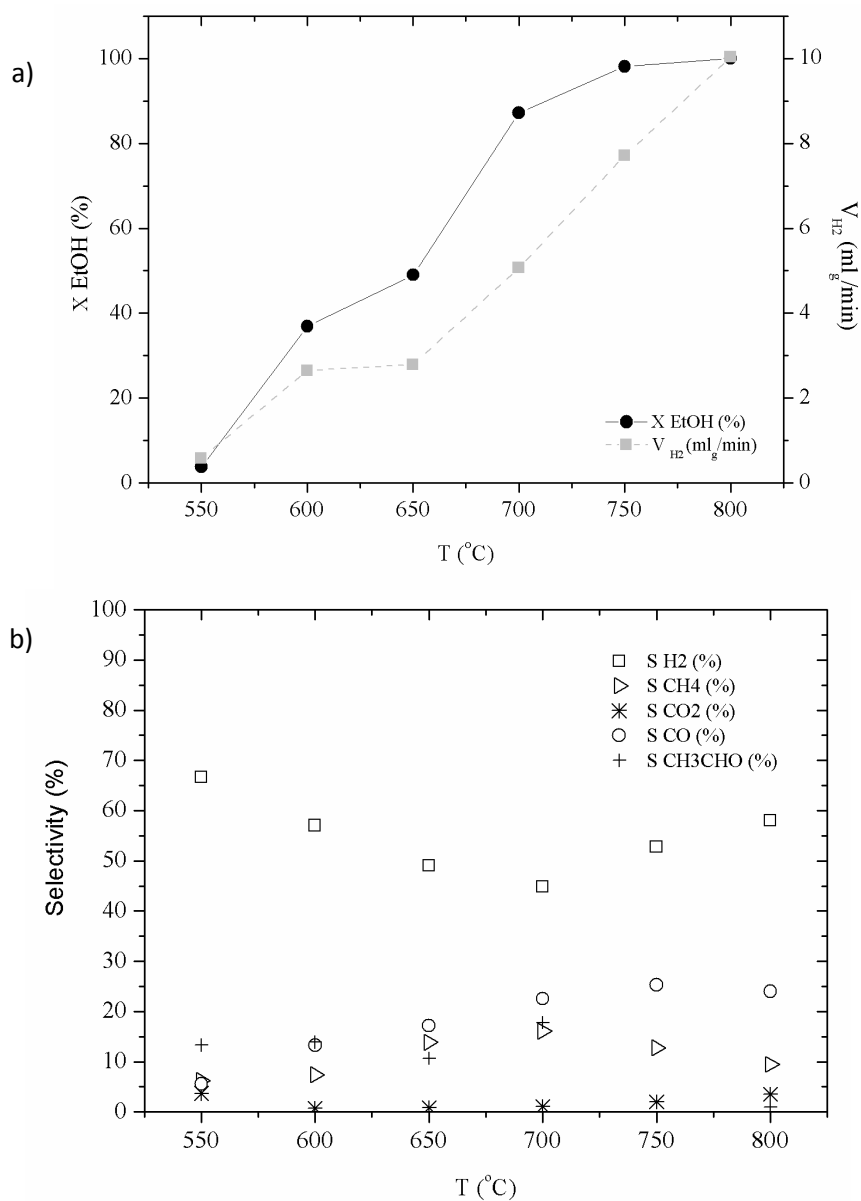


Figure 2. Ethanol conversion and hydrogen rate production (a) and selectivities (b) for the ethanol steam reforming at 923 – 1073K range, $p = 1$ bar, $S/C = 2$, $GHSV = 26$ h⁻¹.



[1] A. Bieberle-Hütter et al, A micro-solid oxide fuel cell system as battery replacement, *Journal of Power Sources*, 177, (2008), 123–130.

[2] B. Jiang et al, Design, fabrication and characterization of gas processing unit testing platform for micro-solid oxide fuel cells, *Procedia Engineering*, 25, (2011), 811–814.

[3] L.F. Brown, A comparative study of fuels on-board hydrogen production for fuel-cell-powered automobiles, *Internal Journal of Hydrogen Energy*, 26, (2001), 381-397

[4] J. Llorca et al, First use of macroporous silicon loaded with catalyst film for a chemical reaction: A microreformer for producing hydrogen from ethanol steam reforming, *Journal of Catalysis*, 255, (2008), 228-233.

[5] N. J. Divins et al, Bio-ethanol steam reforming and auto thermal reforming in 3- μm channels coated with RhPd/CeO₂ for hydrogen generation, *Chemical Engineering and Processing*, 64, (2013), 31– 37.

Doped copper-manganese oxide catalysts for the production of hydrogen via steam reforming of methanol (HPR5-5)

Joan Papavasiliou^{1,*}, George Avgouropoulos^{1,2} and Theophilos Ioannides¹

1 Foundation for Research and Technology-Hellas (FORTH), Institute of Chemical Engineering Sciences (ICE-HT), P.O. Box 1414, GR-26504 Patras, Greece

2 Department of Materials Science, University of Patras, GR-26504 Rio Patras, Greece

ABSTRACT

INTRODUCTION

The production of H₂-rich gas streams for PEM fuel cell systems can be done in a fuel processor unit by reforming a liquid fuel [1]. The resulting gas mixture contains significant amounts of CO and it is further processed with additional steam in a WGS reactor. The latter step can be avoided by using methanol as a starting fuel. An additional step of CO removal (e.g. preferential oxidation) is required in order to protect the anode electrocatalyst, thus complicating further the balance of plant of the fuel processor. Recent advances in the design and development of materials, such as polymer electrolyte membranes and electrocatalysts [2-4], allow the operation of PEMFCs at 180-220oC, whereas functionality of the anode is highly improved, so that it can operate at ~180oC with a reformat gas containing up to 2% CO. A challenge for fuel processing is the development of highly active and selective catalysts, which will be able to operate at temperatures as low as possible with minimal CO formation. Cu-Mn spinel oxide catalysts have been proven to be very efficient methanol steam reforming catalysts, and have been used for internal reforming methanol fuel cells operating at 200oC [3-7]. In this work steam reforming of methanol was carried out over a series of doped CuMnOx catalysts.

EXPERIMENTAL

The combustion method was used for the synthesis of doped Cu-Mn spinel oxide catalysts [3,4]. Urea and the corresponding nitrate salts were mixed in an alumina crucible in the appropriate molar ratios (dopants: Fe³⁺, Zn²⁺, Zr⁴⁺, Ce⁴⁺, Al³⁺; dopant/(dopant + Mn) = 0.10; Cu/(Cu+Mn) = 0.30; 75% excess of urea), according to previous results [3]. The mixed solutions were heated for a few minutes at 80oC, introduced in an open muffle furnace, preheated at 400-500oC, and autoignition took place yielding a foamy, voluminous powder. Structured catalysts were also prepared via the in-situ combustion synthesis of Cu-Mn mixed oxides supported on Cu metal foam. The catalysts were characterized with a variety of techniques including N₂ adsorption, XRD, XPS and H₂-TPR. Activity/selectivity measurements for steam reforming of methanol were carried out at atmospheric pressure in a fixed-bed reactor system. The standard catalyst weight was 0.3 g and the standard total flow rate of the reaction mixture was 70 cm³ min⁻¹ (W/F = 0.257 g s cm⁻³). The standard reaction feed was 5% MeOH, H₂O/MeOH = 1.5. Product and reactant analysis was carried out by gas chromatography.

RESULTS AND DISCUSSION

Addition of small amounts of dopant led to a significant increase of specific surface area (except for the Zn-doped sample), while the amount of consumed hydrogen in TPR slightly decreased. The undoped catalyst has a specific surface area of 8.6 m²/g, while the Al-doped sample has the highest value, i.e. 21.1 m²/g.

Analysis of XRD patterns showed that the spinel phase of Cu_{1.5}Mn_{1.5}O₄ is predominant in all samples. The co-appearance of Cu_{1.5}Mn_{1.5}O₄ and Mn₂O₃ or/and Mn₃O₄ phases is an indication of CuMn₂O₄ spinel decomposition. CuO, Cu₂O or dopant oxides were not detected in most cases, implying that copper or doping metal ions are (i) incorporated in the spinel lattice or/and (ii) finely dispersed as metal oxide clusters (XRD invisible due to small size) on the surface of spinel oxide. An increase of aluminium oxide loading resulted in decrease of Mn₃O₄ and Mn₂O₃ XRD peak intensities.

The reducibility of doped CuMnO_x catalysts was investigated via TPR measurements. The reduction profiles were characterized by a main peak at ~350–450°C, which was present in all cases at similar intensity, but its position shifted to lower temperatures in all doped samples. Thus, addition of the dopant promotes the reducibility of the spinel oxide.

XPS curve fitting analysis revealed that Mn(III), Mn(IV), Cu(II) and Cu(I) species are simultaneously present in the fresh, oxidized samples. The peak at 642 eV is assigned to Mn³⁺ and Mn⁴⁺ cations, in agreement with the literature [6]. The fact that the Mn 2p spectra did not contain any shake-up features at higher binding energies, suggests the absence of Mn²⁺ species from the catalyst surface. Copper in all as-prepared samples has its 2p_{3/2} main peak located at ~933.7 eV. In accordance with previous studies, this peak is assigned to Cu²⁺ cations, since it is accompanied by a strong shake-up line at ~942 eV. An additional peak-shoulder appears at 931 eV for all the samples and is assigned to Cu¹⁺, taking into account the corresponding kinetic energy spectra of Cu L₃VV electron. The binding energy of Cu(I), however, is strongly shifted negatively. These experimental observations are in agreement with the formation of Cu¹⁺ and Mn⁴⁺ ions as a result of the redox equilibrium Cu²⁺ + Mn³⁺ = Cu¹⁺ + Mn⁴⁺, which is expected on copper substitution. Doping metals are present in the Cu-Mn samples in a fully oxidized state, i.e. Ce⁴⁺, Zn²⁺, Al³⁺, Zr⁴⁺ and Fe³⁺. The results of the surface quantitative analysis showed that the addition of dopant results to a decrease in copper dispersion. Comparing XPS values for doping metal with the nominal compositions of the samples, it can be observed that they are much higher in most cases indicating that there is enrichment of the surface with dopant species, which have to be in a highly dispersed form to account for such higher surface coverages.

The addition of small amounts of oxides of Fe, Al, Zn, Zr and Ce had a beneficial effect on catalytic activity towards hydrogen production (Fig. 1), in agreement with TPR measurements. The Al- and Fe-doped catalysts showed the highest activity. The former sample could tolerate higher amounts of methanol as compared with Fe-doped sample, therefore more detailed tests were carried out over this sample. For the Al-doped catalysts, best results were obtained with the CuMnAlO_x sample having an atomic ratio Al/(Al+Cu+Mn) = 0.07. Additional tests under different methanol feeds showed that complete removal of methanol was achieved at 220°C (5% MeOH) and 240°C (20% MeOH) with the doped sample compared to 240°C (5% MeOH) and 300°C (20% MeOH) for the

undoped sample. At 200°C, the doped sample was almost two times more active than the undoped sample, while CO selectivities were less than 0.8% in all cases.

The activity of the CuMnAlO_x sample was also tested at various W/F ratios and MeOH/H₂O feeds (Fig. 2). A foam-based reformer was also employed in these activity measurements. With an increase in the methanol partial pressure in the feed, the methanol conversion decreased and higher contact times are required in order to overcome the negative effect of produced hydrogen. Nevertheless, a 500 h stability test showed that this catalyst can effectively operate at the temperature level of high temperature PEM fuel cells (i.e. 200°C) with a 17% decline in activity and achieve methanol conversions higher than 80% even in the presence of 30% MeOH in the feed. Concerning the activation procedure, Cu-Mn catalysts require a reductive activation step, which can be carried out either ex-situ with careful passivation before exposure to air (pyrophoric effect) or in-situ in the presence of the reaction mixture at temperatures lower than 280°C.

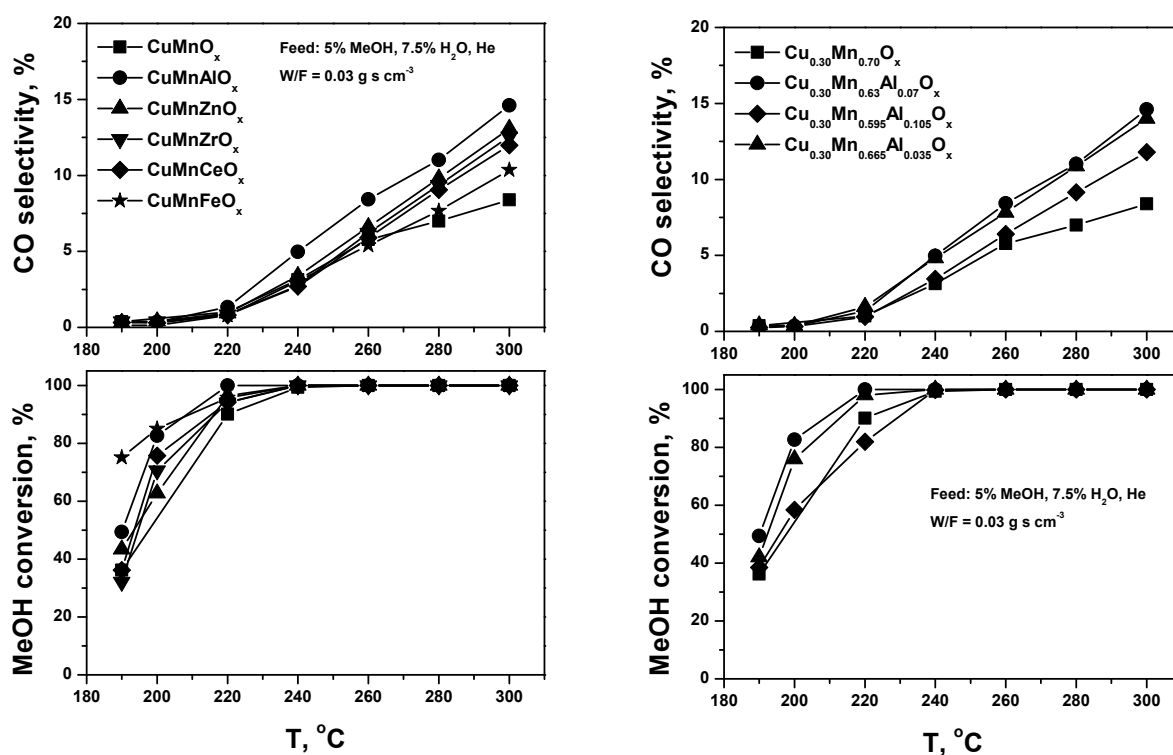


Figure 1. Activity and selectivity for steam reforming of methanol over combustion-synthesized doped CuMnO_x catalysts.

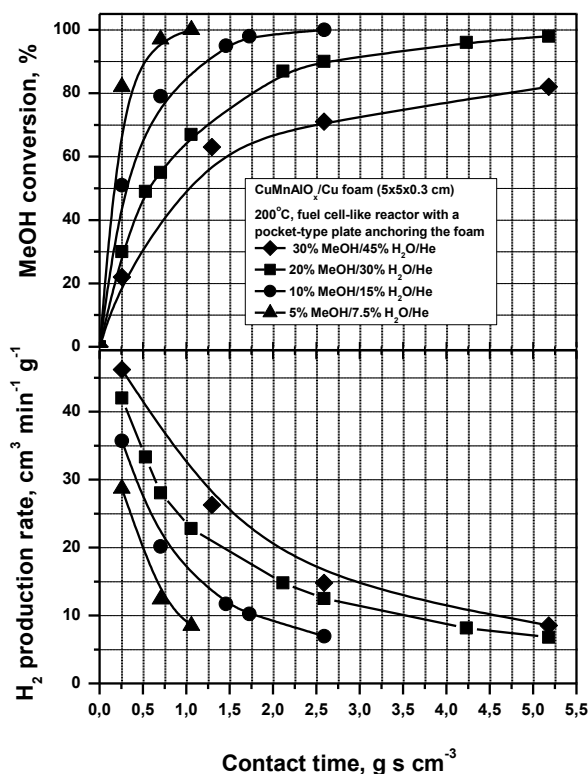


Figure 2. Effect of contact time (W/F) and MeOH/H₂O content on the activity of CuMnAlO_x catalyst

CONCLUSIONS

Doping of CuMnO_x catalyst has a beneficial effect on catalytic activity towards hydrogen production via low temperature steam reforming of methanol. Al- and Fe-doped catalysts showed the highest activity. CuMnAlO_x catalyst can effectively operate at 200°C for at least 500 h with methanol conversions higher than 80% in the presence of 30% MeOH in the feed.

REFERENCES

- G. Kolb, Fuel Processing for Fuel Cells, Wiley 2008.
- K.D. Papadimitriou, F. Paloukis, S.G. Neophytides, J.K. Kallitsis, Macromolecules 44 (2011) 4942-4951.
- G. Avgouropoulos, T. Ioannides, J.K. Kallitsis, S. Neophytides, Chem. Eng. J. 176-177 (2011) 95.
- G. Avgouropoulos, J. Papavasiliou, M.K. Daletou, J.K. Kallitsis, T. Ioannides, S. Neophytides, Appl. Catal. B: Environ. 90 (2009) 628.
- J. Papavasiliou, G. Avgouropoulos, T. Ioannides, Catal. Commun. 6 (2005) 497.

J. Papavasiliou, G. Avgouropoulos, T. Ioannides, J. Catal. 251 (2007) 7.

J. Papavasiliou, G. Avgouropoulos, T. Ioannides, Int. J. Hydrogen Energy 37 (2012) 16739.

Mechanistic studies of methanol reforming on Co-MnO catalysts (HPR5-6)

E. Papadopoulou^{1,2} and Theophilos Ioannides¹

1 Foundation for Research and Technology-Hellas (FORTH), Institute of Chemical Engineering Sciences (ICE-HT), P.O. Box 1414, GR-26504 Patras, Greece

2 Department of Chemical Engineering, University of Patras, Patras, Greece

ABSTRACT

INTRODUCTION

Hydrogen is considered as a major future energy carrier. There exist several routes for hydrogen production from primary fuels. A promising route is the steam reforming of methanol. Copper-based catalysts show high activity and CO₂ selectivity for the steam reforming of methanol [1]. On the other hand, cobalt-based catalysts have not been studied extensively for this particular reaction, although there exist numerous studies concerning ethanol steam reforming [2,3].

In this work, the steam reforming of methanol over CoMnO_x catalysts prepared through fumarate salt precursors has been investigated. CO, CO₂, H₂, H₂O and CH₃OH adsorption has been investigated with TPD experiments. TPSR and SSITKA experiments have been also performed to gain insight on the elementary steps of methanol reforming over the catalysts in question.

EXPERIMENTAL

The catalyst synthesis method involves the synthesis of the fumarate salts of the respective metal ions and their thermal decomposition (pyrolysis) under inert atmosphere. The synthesis parameters were the Co:Mn ratio (1/9, 1/2, 1/1) and the pyrolysis temperature (500, 600 or 700°C). Samples were also prepared via oxidative treatment of the organic salt precursors at 550°C.

The catalytic performance was examined in the reaction of steam reforming of methanol. The reduced form of the catalysts was made from the precursors in-situ right before the experiment. The catalysts were characterized with BET, XRD and H₂-TPR.

Activity/selectivity measurements for steam reforming of methanol were carried out at atmospheric pressure in a fixed-bed reactor system. The standard catalyst weight was 0.1 g mixed with 0.9g sand. The total flow rate of the reaction mixture was 100 cm³ min⁻¹ with standard reaction feed 5% MeOH and H₂O/MeOH = 1.5. Product and reactant analysis was carried out by gas chromatography.

CO, CO₂, H₂O and CH₃OH adsorption has been studied at room temperature while H₂O adsorption was also studied at 300°C. H₂ adsorption was examined at both 100 and 300°C.

RESULTS AND DISCUSSION

In-situ XRD measurements during pyrolysis of fumarate precursors showed that the fumarate structure is stable up to 400°C and subsequently decomposes. At 450 and 500°C, broad peaks of the

MnO phase are present, while at 550°C peaks of Co metal also appear in the pattern. The peaks of Co and MnO become more intense and sharper with further increase in temperature indicating sintering of the crystalline phases. It is evident that the reducing atmosphere prevailing during thermal treatment of the precursors, as well as the presence of solid carbon facilitates reduction of cobalt oxides towards metallic cobalt at temperatures above ~500°C. Thus, the reduced form of the catalyst, consisting mainly of metallic cobalt and MnO dispersed in a carbonaceous matrix (Co-MnO/C) can be prepared in a single step.

Catalytic tests showed that increase of cobalt loading leads to increase of methanol conversion, with CO being the primary carbon-containing product, while CO₂ is produced via the WGS reaction. Catalysts prepared by pyrolysis were more active than those prepared by calcination and did not require prereduction.

No significant CO adsorption was found on the catalysts following exposure to CO at room temperature, while CO₂ adsorption was significant showing both weak and strongly-bound states.

TPD after H₂ adsorption indicated the presence of multiple states of adsorbed hydrogen. Adsorption at room temperature (Fig. 1a) leads to population of weak and strongly bound species, while adsorption at high temperatures leads to population of an intermediate strength state, which corresponds to adsorption on both cobalt and MnO (Fig. 1b). Preoxidized catalysts which had been reduced prior to H₂ adsorption adsorbed less H₂ than the catalysts prepared by pyrolysis.

Water adsorption at 300°C was accompanied by H₂ production because of the reaction $\text{Co} + \text{H}_2\text{O} \rightarrow \text{CoO} + \text{H}_2$. This did not happen when the catalysts were exposed to H₂O at room temperature (Fig. 2). TPD profiles after water adsorption had common characteristics: one main peak with maximum at 90°C followed by a broad feature up to 400°C. The quantity of produced H₂ was less than the quantity of consumed water implying that part of the water was molecularly absorbed.

Methanol TPD showed molecular desorption of methanol at low temperatures and methanol decomposition to CO and H₂ at higher temperatures. CO₂ and water in smaller quantities were also detected. Higher pyrolysis temperature led to reduction of adsorbed methanol amount.

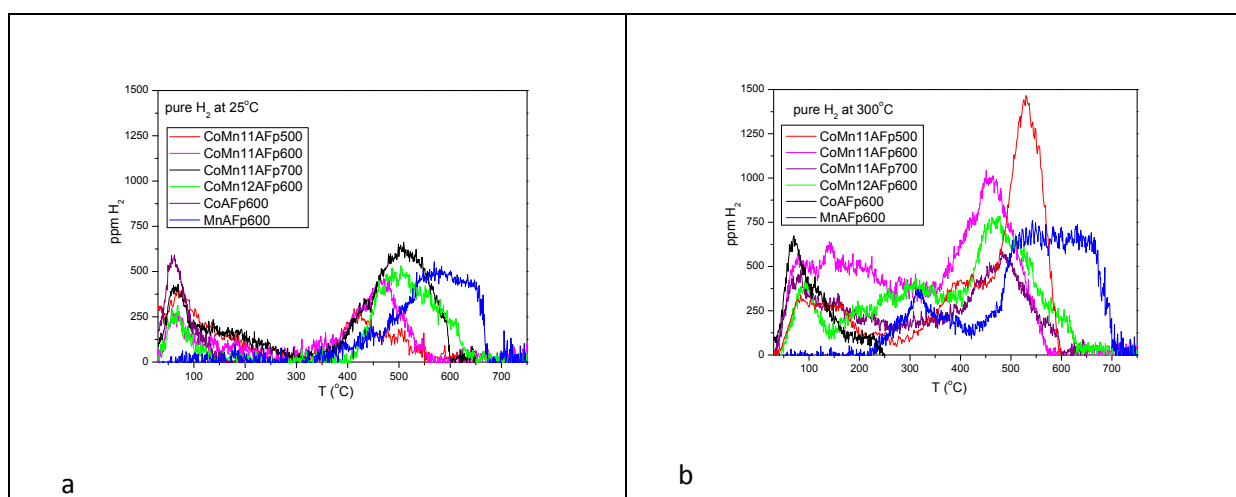


Figure 1. TPD H₂: a) after adsorption of pure H₂ at 25°C and b) after adsorption of pure H₂ at 300°C

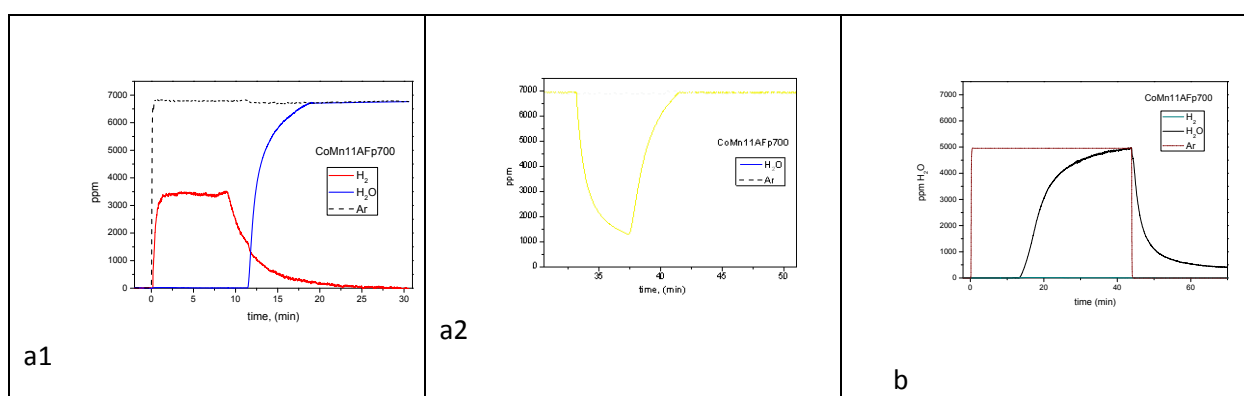


Figure 2. H₂O adsorption: a1) at 300°C, a2) during cooling from 300 to 25°C and b) at 25°C for CoMn11AFp700 catalyst

SSITKA experiments showed that water promotes the surface reaction of adsorbed methanol to CO and CO₂ but at the same time water competes for surface sites with methanol and lowers the concentration of reactive surface intermediates.

CONCLUSIONS

Co-MnO catalysts obtained by pyrolysis of fumarate precursors are more active than preoxidized ones in methanol steam reforming due to increased cobalt dispersion and higher concentration of active sites. Increase of cobalt loading leads to increased methanol conversion, while the pyrolysis temperature has a minor effect. The main reaction pathway is methanol decomposition, while carbon dioxide appears to be a secondary product of the water-gas shift reaction.

REFERENCES

- [1] Sáa S., Silva H., Brandão L., Sousa J.M, Mendesa A., Appl. Catal. B-Environ. 99:43 (2010).
- [2] De la Piscina P.R. and Homs N., Chem. Soc. Rev. 37:2459 (2008).
- [3] Llorca J., Homs N., Sales J., de la Piscina P.R., J. Catal. 209:306 (2002).

Hydrogen production: others

Polymer Electrolyte Membrane Water Electrolysis : status, perspectives and technological developments. (HPO1-1)

Pierre Millet^{1}, Fabien Auprêtre²*

1 Université Paris Sud 11, bât 410, 91405 Orsay Cedex France

2 CETH Co., 10 rue de la Prairie, 91140 Villebon-sur-Yvette, France

pierre.millet@u-psud.fr

In the industry sector, hydrogen is produced using CO₂-emitting processes (usually steam reforming of natural gas or gasification of fossil fuels). Water electrolysis offers an alternative path for the production of green-hydrogen in view of the so-called “hydrogen economy”. The purpose of this communication is to provide a review of technological developments in the field, to discuss some limitations of existing electrolyzers and to propose some perspectives [1].

State-of-art performances. A PEM water electrolysis cell operating at 1.8V and 1-2 A.cm⁻² (≈ 80% efficiency) is common good practice, at least at the laboratory scale. In the industry sector, 1.8 V @ 1 A.cm⁻² is commonly obtained on large (> 600 cm²) active area cell. Low pressure electrolyzers (1-50 bar) are appearing on the market whereas prototypes operating at pressures up to 150 bar have been developed and claims of operation up to 300 and even 700 bar have been reported. The technology is well-suited for operation using intermittent and fluctuating power sources and is therefore expected to play a significant role in the management of power-grids.

Limitations. Commercial PEM water electrolyzers are now competitive with their alkaline counterparts. In view of large scale deployment for energy storage applications, larger, more efficient, less expensive (≈ 500 \$/kW on-site) and more durable (50-100,000 h of operation with less than 10% efficiency loss) systems are required. On the short term, the main limitation will come from the limited production capacity of commercial systems (today in the 0 - 60 Nm³/h range). Larger capacities will be achieved by increasing cell areas as well as the number of cells mounted in electrolysis stack. Another limitation will come from the cost and performances of the membrane – electrode assemblies. Thinner, less resistive, more stable (at higher temperature) and less expensive membrane materials are required. Concerning electrocatalysis, stability on the long term and cost are two critical issues. More efficient (at higher current densities), less sensitive (to mineral and organic impurities), and less expensive catalysts materials are needed.

Potential for improvement & perspectives. Current performances of PEM water electrolysis can be significantly increased. Cells can be operated at much higher current densities (several A/cm²) in more compact systems with reduced capital expenses. Efficiencies of 70-80% can be obtained at > 1 A.cm⁻², by operating the cells at higher temperature (100-150 °C). Innovative materials are still required. New polymers and new catalytic compositions that could sustain such temperatures are needed. Concerning the anodic catalyst, there is a need to develop electronic carriers of large surface area stable under O₂ evolution and to develop catalytic compositions that could stabilize ruthenium. R&D on non-noble catalysts should be pursued to further reduce capital expenses. There is a need to replace bulk Ti bipolar plates and expensive porous current collectors. Improved durability (extension toward 50,000-100,000 h) and mean time before failure issues are also challenging. Improvement

requires the development of new diagnostic tools, process monitoring and maintenance strategy. R&D on high pressure electrolysis is still required and polymers with low gas solubility and permeability are needed.

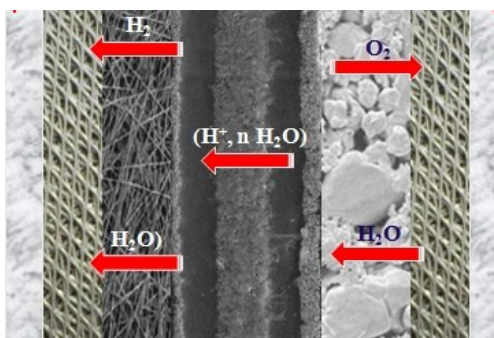


Fig. 1 : schematic diagram of a PEM water electrolysis cell.



Fig. 2 : photograph of a 5 Nm3 H2/hr 4-stack PEM water electrolysis system (CETH Co.).

References

[1] P. Millet, 2011, in : 'Electrochemical Technologies for Energy Storage and Conversion', chapter 8, Water electrolysis for hydrogen generation, R-S. Liu, X. Sun, H. Liu, L. Zhang and J. Zhang Eds, Wiley-VCH.

Characterization of IrO₂ and IrRuO₂ Electrocatalysts for the O₂ Evolution Reaction in SPE Water Electrolyzers (HP01-2)

S. Siracusano, V. Baglio, C. Alegre, A. S. Aricò

CNR-ITAE, Via Salita S. Lucia sopra Contesse 5-98126 Messina, Italy

Several processes and devices are currently developed for water electrolysis such as alkaline systems, solid oxide electrolyte and solid polymer electrolyte membrane (SPE)-based electrolyzers. SPE water electrolysis is considered the most promising method to produce hydrogen with a high degree of purity from renewable energy resources such as wind, photovoltaic and hydropower.

The rate determining step in SPE water electrolysis is associated with the oxygen evolution process occurring at the anode. The most common electrocatalysts for the oxygen evolution reaction (OER) beside being quite expensive noble metal oxides, e.g. IrO₂, RuO₂, are also currently used in the unsupported form at several mg cm⁻². Accordingly, they are characterized by low surface area and poor catalyst utilization. Moreover, the unsupported catalysts are more susceptible to sintering and agglomeration than supported catalysts.

In this work, IrO₂ and IrRuO₂ electrocatalysts were prepared and electrochemically characterized for the oxygen evolution reaction in a Solid Polymer Electrolyte (SPE) electrolyzer. The catalysts were synthesized through a sulfite-complex route. An amorphous iridium hydroxide hydrate precursor was obtained at ~ 80°C, which was, successively, calcined at 450 °C. The same procedure was applied for the iridium-ruthenium oxide. The physico-chemical characterization was carried out by X-Ray Diffraction (XRD) and Transmission Electron Microscopy (TEM). XRD was performed on the dry catalysts powders by a Philips X-Pert diffractometer equipped with a CuKα as radiation source. This diffractometer operated at 40 kV and 20 mA, with a scan rate of 0.5 2θ min⁻¹ and angular resolution of 0.005° 2θ. The diffraction patterns were fitted to Joint Committee on Powder Diffraction Standards (JCPDS). The morphology of the IrO₂ and IrRuO₂ catalysts was investigated by TEM using a Philips CM12 instrument. The specimen was prepared by ultrasonic dispersion of the catalyst in isopropyl alcohol and subsequently depositing a drop of the suspension on a carbon-coated Cu grid.

A Nafion 115 (Ion Power) membrane was used as the solid polymer electrolyte. The oxygen evolution catalysts based on IrO₂ and IrRuO₂ were directly deposited onto one side of the Nafion 115 by a spraycoating technique. Inks were composed of aqueous dispersions of catalyst, deionized water, Nafion® solution (5% Aldrich) and Ethanol (Carlo Erba); the anode catalyst loading was 2.5 mg·cm⁻². A Ti mesh was used as backing layer. A commercial 30% Pt/Vulcan XC-72 (ETEK, PEMEAS, Boston, USA) was used as the catalyst for the H₂ evolution. The cathode electrode was prepared by directly mixing in an ultrasonic bath a suspension of Nafion ionomer in water with the catalyst powder. The obtained cathode paste was spread on carbon cloth backings (GDL ELAT from ETEK) with a Pt loading of 0.6 mg·cm⁻². The ionomer content in both electrodes was 33 wt.% in the catalytic layer after drying. MEAs (5 cm² geometrical area) were directly prepared in the cell housing by tightening at 9 Nm using a dynamometric wrench.

The single cells were investigated by linear voltammetry, impedance spectroscopy and chrono-amperometric measurements. The electrochemical activity of these MEAs was analyzed in a temperature range from 25 °C to 80 °C.

The results have demonstrated promising performance and stability of these catalysts for application in an SPE electrolyzer.

ACKNOWLEDGEMENT

The authors acknowledge the financial support of the EU through the FCH JU ELECTROHYPEM Project. "The research leading to these results has received funding from the European Community's Seventh Framework Programme (FP7/2010-2013) for the Fuel Cells and Hydrogen Joint Technology Initiative under grant agreement Electrohypem n. 300081."

High pressure PEM electrolyzers and their application for renewable energy systems (HP01-3)

V. Fateev, P. Blach*, S. Grigoriev, A. Kalinnikov, V. Porembskiy

National Research Center «Kurchatov Institute», pl. Kurchatova, Moscow 123182, Russia; *TINA Systems S.L., c/Alcala n 59-5 floor, Madrid 28014, Spain

Last years we paid a lot of attention to high-pressure electrolyzers development. Different types of electrolysis stacks for pressure up to 300 bar were developed and tested. An obvious advantage of high-pressure systems is simplification of hydrogen storage problem as hydrogen practically does not need dehydration and hydrogen compressor could be excluded. But high pressure also results in decrease of current efficiency and gas purity due to an increase of speed of gases transportation through the membrane, increase of stack and plant construction materials interaction with hydrogen and oxygen.

In such a case the membrane is becoming to be a key issue. Tests of membranes (Nafion type) with different thickness at 30-300 bar showed that gas transport due to diffusion is mainly important for membranes with thickness less than 100 microns and at thickness about 200 microns hydrogen crossover with water flow is becoming more important. So membrane thickness 200-220 microns was chosen as further increase of the membrane thickness resulted mainly in cell voltage increase due to ohm losses in the membrane. Different types of membrane modification were carried out. It was shown that introduction of platinum catalysts in the membrane body (catalysts of hydrogen-oxygen interaction) practically do not increase the gases purity as reaction of dissolved gases on water covered catalyst is not efficient. Membrane modification with inorganic nanostructured proton conductors (mainly zirconium phosphate) appeared to be more efficient as permitted to decrease membrane gas permeability at operation conditions about 3 times.

As anode catalyst Ir, and mixed Ru-Ir-Sn oxides were used. Modification of the anode catalyst composition by Pt nanoparticle resulted in oxygen purity increase (for example from 96-97% to 97-98% at 130 bar) as hydrogen reaction with oxygen was rather efficient in gas phase at the electrode surface. Additional application of hydrogen-oxygen recombination systems inside the stack and at hydrogen and oxygen outlet from the electrolyzer provided hydrogen purity >99,99% and oxygen purity >99,98% even at 300 bar.

Nanostructural Pt-based electrocatalysts (2-10 nm) on nanostructured carbon carriers were developed for electrolyzer cathodes using plasma (magnetron-ion) sputtering technology of catalyst synthesis. Average particle size could be easier varied due to ion current density and time of sputtering. Pt catalyst with average particle size about 4-6 nm (specific surface up to 60 m²/g) demonstrated same activity at lower Pt loadings as catalysts synthesized by traditional technology – liquid phase reduction. Magnetron-ion sputtering was also used for bipolar plates and electrolyzer current collectors protection from oxidation and hydrogen saturation (for titanium components). Oxygen evolution catalysts base on mixed oxides demonstrated high activity (same activity as for iridium) with decreased (about 30%) platinum metals loading and good stability.

High efficient PEM electrolyzers operating at pressure 130 bar providing hydrogen purity 99,99% (energy consumption 4,0 – 4,2 kWh/m³, productivity up to 10 m³/h of hydrogen) were developed and successfully tested together with wind and solar power plants at Kurchatov institute and TINA facilities. Hydrogen was utilized in fuel cell or internal combustion engine. PEM electrolyzer for 300 bar with productivity 0,5 m³ of hydrogen also demonstrated good performance but here decrease of current efficiency was rather significant (up to 10% depending on operation conditions). Life-time tests demonstrated that electrolysis temperature about 60-70°C and current densities about 0,4-0,5 A/cm² are preferable to provide long life-time, good efficiency and gas purity. Use of sun irradiation for electrolyzer heating at start up procedure could be recommended. For northern climate, such electrolysis systems also could be efficient for heat production.

Reversible fuel cell-electrolyzer stacks with power up to 1 kW were developed and successfully tested. However, here operation at high pressure could be used for electrolysis mode only.

Electrodeposited catalysts and anion exchange membranes for alkaline water electrolysis (HP01-4)

Liliana Diaz, Graciela Abuina, Mariano Brunob, Federico Vivab, Horacio Cortib, Jaromír Hnátc, Martin Paidarc, Karel Bouzekc

a Centro de Procesos Superficiales, Instituto Nacional de Tecnología Industrial (INTI), Av. General Paz 5445, B1650KNA, San Martín, Buenos Aires, Argentina.

b Grupo Celdas de Combustible, Departamento de Física de la Materia Condensada, Centro Atómico Constituyentes, Comisión Nacional de Energía Atómica (CNEA), Av. General Paz 1499, B1650KNA, San Martín, Buenos Aires, Argentina.

c Department of Inorganic Technology, Institute of Chemical Technology Prague, Technická 5, 166 28 Prague 6, Czech Republic.

INTRODUCTION

Water electrolysis is an environmental friendly and versatile process for hydrogen production from non-fossil fuel primary energy sources. Water electrolysis technologies developed or under development include high-temperature steam electrolysis, proton exchange membrane electrolysis (PEME), anion exchange membrane electrolysis (AEME) and liquid alkaline electrolysis (LAE). From the above technologies AEME and LAE represent the most inexpensive alternatives, owing to the fact that relatively cheap materials are employed. This concerns particularly non-precious metals used as electrodes [1].

Zero gap electrolyzers employing hydroxide conducting polymer membrane electrolyte, with electrodes fabricated directly onto the membrane surfaces, as the membrane electrode assembly (MEA) in fuel cell technology [2], represent highly promising approach. On the other hand, well established and mature liquid alkaline electrolyzers are going to be used meanwhile emerging technologies are tested and they obtain wide acceptance to be considered as candidates to replace LAE in large scale applications.

However, in spite of its advantages, water electrolysis has to become more energy efficient and inexpensive in order to gain massive acceptance, as a technology suitable as one of the energy conversion step in the hydrogen economy.

Nickel is now universally used as electrodes for alkaline water electrolysis process, owing to its acceptable electrocatalytic properties and high stability in this environment; but efforts are being devoted to develop catalysts with lower overpotential for oxygen and hydrogen evolution reactions (OER and HER), in order to minimize the electrolyser operation voltage, and power consumptions as well.

Several Ni based materials have been studied as electrocatalysts for HER in the past. Significant overpotential reductions have been achieved with electrodes on the basis of NiMo alloys prepared by plasma spraying, thermal decomposition or electrodeposition [3-4] and NiZn alloy sintered or electrodeposited, with post dissolution of Zn in alkaline media [5]. RuO₂ and TiO₂/RuO₂ particles co-

deposited with Ni coatings represent an attractive option too even when the advantage of using inexpensive electrode materials is lost [6].

While it is possible to reach over-potential lower than 100 mV for HER in alkaline medium at temperature near 70 °C with appropriate catalysts, it seems not possible to develop catalysts with over-potential lower than 200 mV for OER under the same conditions.

Although an optimum HER catalyst is highly probably not at the same time the best one for OER and vice-versa, the use of the same material in both sides of bipolar electrodes, would lead to simpler and thus low cost fabrication techniques. Besides, since electrical resistance between elements of the bipolar electrode is an important issue during high current-density operation, a unique material as the anode and cathode of an electrolyser without any other electrical connections should represent the best choice for this design configuration [7].

Regarding AEME, the expected major improvements are likely to arise from the hydroxide conducting membrane, which is necessary, in order to meet requirements of mechanical stability, high conductivity and high durability [2]. Some of the materials studied for AEME applications are methylated melamine grafted poly vinyl benzyl chloride [8], self crosslinked quaternized polysulfone [9] and heterogeneous anion-selective based in styrene-divinyl benzene copolymer matrix [1].

The aim of this work is to investigate both, HER and OER, using electrodeposited NiZn and NiMo electrodes. Electrodeposition was selected as a convenient preparation method, considering that it can be easily applied at an industrial scale.

Moreover, the performance of the KOH doped ABPBI (poly (2,5)-benzimidazole) linear and crosslinked membranes were tested under alkaline water electrolysis conditions.

EXPERIMENTAL

NiZn and NiMo electrodes in a form of coatings of 10 µm thickness were prepared over steel substrates, with a Ni undercoat of 30 µm. NiZn deposition was completed using a bath containing Ni₂SO₄ 62 wt% and Zn₂SO₄ 38 wt% under a constant current density of 3 A dm⁻². Electrodeposited electrodes were activated by treating them with NaOH 20 wt% at room temperature for 24 hours. NiMo coatings were obtained from a bath of pH 10.5 containing NiSO₄·6H₂O 52 g·l⁻¹; Na₂MoO₄·2H₂O 73 g·l⁻¹; Na₃C₆H₅O₇·2H₂O 88 g·l⁻¹ and excess of NH₄OH. Applied current density of 16 A dm⁻² was used in this case.

ABPBI was prepared by condensation of 3,4-diaminobenzoic acid (DABA) monomer in polyphosphoric acid (PPA) following the procedure reported by Gómez Romero et al. [10]. Membranes were casted according to a procedure reported elsewhere [11], and immersed in 15 wt% KOH during 24 hours prior testing.

The morphology of the surfaces was examined by SEM (Philips 505) and the chemical composition determined by EDX.

Electrochemical measurements for electrocatalyst evaluation were carried out in a single compartment cell using a Gamry mod. Reference 3000 Potentiostat. A Pt foil was employed as

auxiliary electrode, Hg/HgO/OH⁻ as a reference one, and a 25 wt% KOH solution was used as electrolyte at room temperature.

A single alkaline laboratory electrolyzer was used to test the membrane performance under alkaline water electrolysis conditions. It is made of two Plexiglas blocks. Membrane-electrode assembly consisting of two Ni foam electrodes with an active area of 2 x 2 cm² attached from both sides directly to the membrane surface was squeezed between them. The electrodes were washed by a 15 wt% KOH solution representing at the same time ionically conductive phase, source of water and providing removal of the evolved gaseous phase.

RESULTS AND DISCUSSION

SEM images show that electrodeposited NiZn layers exhibit before Zn leaching a compact and uniform surface structure. After its leaching during electrode activation many cracks and pores occur on the electrode indicating a significant increase of its specific surface area. On the other hand, NiMo coatings show, directly after synthesis, a spherical (globular) and cauliflower-like pattern, with a considerably surface roughness.

The result of NiZn EDX analysis after Zn removal indicate Ni:Zn content in the electrode of 44:56 (atom %). In the case of NiMo 81:19 (atom %) ratio was observed.

Figure 1 shows the steady polarization curves for NiZn and NiMo coatings and for pure Ni for HER reaction electrodes.

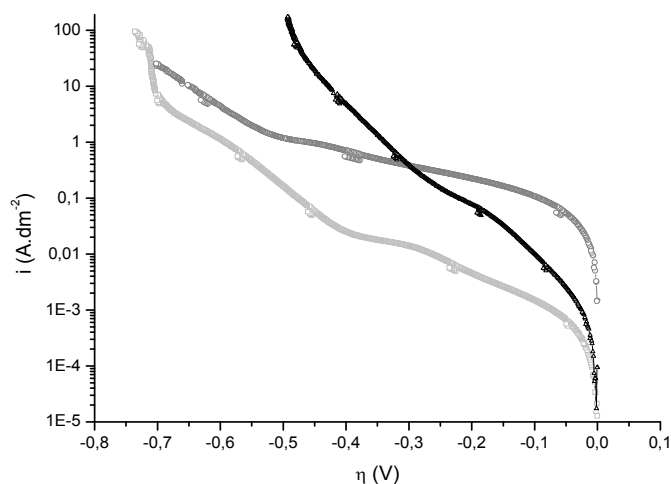


Figure 1: steady polarization curves of NiZn electrode (dark grey), NiMo electrode (black) and pure Ni electrode (light grey).

It can be seen that NiMo coating show the best electrocatalytic activity, providing a reduction in HER overpotential by 250 mV at a current density of 20 A dm⁻² when compared with pure Ni. The overpotential reduction is significantly smaller for NiZn coating at the same current density. On the

other hand, this electrode shows lower overpotential than Ni for OER, where no overpotential reduction is observed for NiMo electrode at a current density of 20 A dm⁻².

It is known that electrocatalysts performance depends on the composition of the catalyst and its specific surface area. The results presented indicate enhancement of the HER using the NiMo to be caused predominantly by the increase of Ni electrocatalytic activity by alloying it with Mo. In the case of NiZn electrode the overpotential reduction observed for both OER as well as for HER is related with the increase of the real surface area, and this can explain that NiZn is better catalyst than Ni for HER and also for OER.

Figure 2 shows the performance of ABPBI membranes in a laboratory alkaline water electrolyzer. It can be seen that membranes on a base of linear polymer show an increase in process efficiency compared with crosslinked ones. This is most probably related to the higher conductivity of these membranes related to their higher KOH solution uptake.

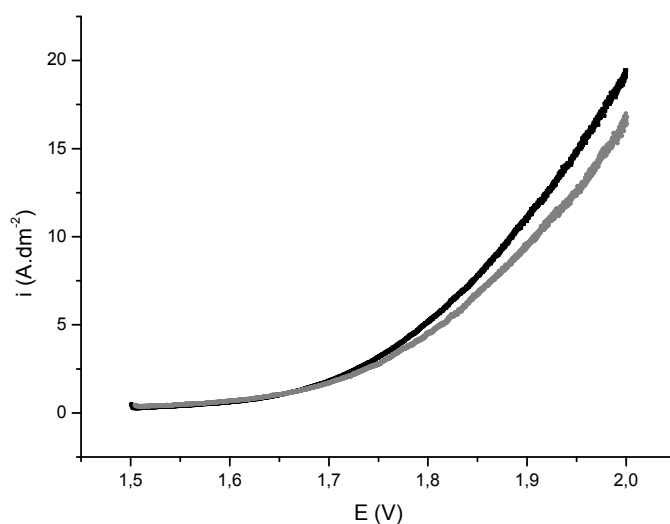


Figure 2: dependency of current density on cell voltage in alkaline laboratory electrolyzer at 50 °C in 15 wt% KOH solution with linear (black) and crosslinked (gray) alkali doped ABPBI membranes.

CONCLUSION

NiZn and NiMo coatings were tested as electrodes for bipolar liquid alkaline electrolyzers. NiMo showed a higher reduction in overpotential for HER, whereas NiZn showed a higher reduction in overpotential for OER compared with pure Ni.

Linear and crosslinked alkali doped ABPBI membranes showed a promising performance in alkaline water electrolysis test. As far as it is known to the authors, these are the first results reported for these type of membranes applied to AEME.

REFERENCES

-
- [1] Hnát J, Paidar M, Schauer J, Zitka J, Bouzek K. J. Appl. Electrochem. 2011; 41: 1043 – 1052.
- [2] Pletcher D, Li X. Int. J. Hydrogen Energy 2011; 36: 15089 – 15104.
- [3] Birry L, Lasia A. J Appl. Electrochem 2004; 34: 735 - 749.
- [4] Han Q, Cui S, Pu N, Chen J, Liu K, Wei X. Int. J. Hydrogen Energy 2010; 35: 5194 - 5201.
- [5] Solmaz R, Kardas G. Energy Conversion and Management, 2007; 48: 583 – 591.
- [6] Shibli S, Dilimon V. Int. J. Hydrogen Energy 2008; 33: 1104 – 1111.
- [7] Hu Ch, Wu Y. Mater. Chem. Phys., 2003; 82: 588–596.
- [8] Cao Y, Wu X, Scott K. Int. J. Hydrogen Energy 2011; 37: 9524 – 9528.
- [9] Xiao L, Zhang S, Pan J, Yang C, He M, Zhuang L, Lua J. Energy & Environmental Science, 2012, 5 7869.
- [10] Asensio JA, Borrós S, Gómez-Romero P. J. Polym. Sci. A: Polym Chem., 2002; 40: 3703–3710.
- [11] Diaz LA, Abuin GC, Corti HR. J. Membr. Sci., 2012; 35 – 44: 411– 412.

Improvements to Integrate High Pressure Alkaline electrolyzers for Electricity/H₂ production from Renewable Energies to Balance the GRID – ELYGRID Project (HPO1-5)

[AUTHORS: P. MARCUELLO FERNANDEZ, Aragon Hydrogen Foundation; D. EMBID GOMEZ, Aragon Hydrogen Foundation; E. ALBERTÍN MARCO, Aragon Hydrogen Foundation; G. GARCÍA JIMÉNEZ, Aragon Hydrogen Foundation; L. CORREAS USÓN, Aragon Hydrogen Foundation]

INTRODUCTION

ELYGRID Project aims at contributing to the reduction of the Total Cost of hydrogen produced via electrolysis coupled to Renewable Energy Sources, mainly wind turbines, and focusing on mega watt size electrolyzers (from 0,5 MW and up). The objectives are to improve the efficiency related to complete system by 20 % (10 % related to the stack and 10 % electrical conversion) and to reduce costs by 25%. The work has been structured in 3 different parts, namely: cells improvements, power electronics, and balance of plant (BOP). Two scalable prototype electrolyzers will be tested in facilities which allow feeding with renewable energies (photovoltaic and wind).

The main project objectives can be summarized below:

- Development (synthesis) of advanced materials for electrolysis cell diaphragms/membranes to be used for field testing. Increase the efficiency of the stack by increasing operation temperature and electrolyte concentration
- Identify technical improvements related to the Balance of Plant (BOP)
- Redesign power electronics, based on transistor instead of thyristor, less sensible to the electrical grid parameters.
- Field test of new stack with a 1,6 m diameter membrane
- Identification of technological market and local value-chain suppliers
- Outreach, social awareness and promotion of alkaline electrolysis coupled with renewable energy sources through demonstration projects, field testing and integration

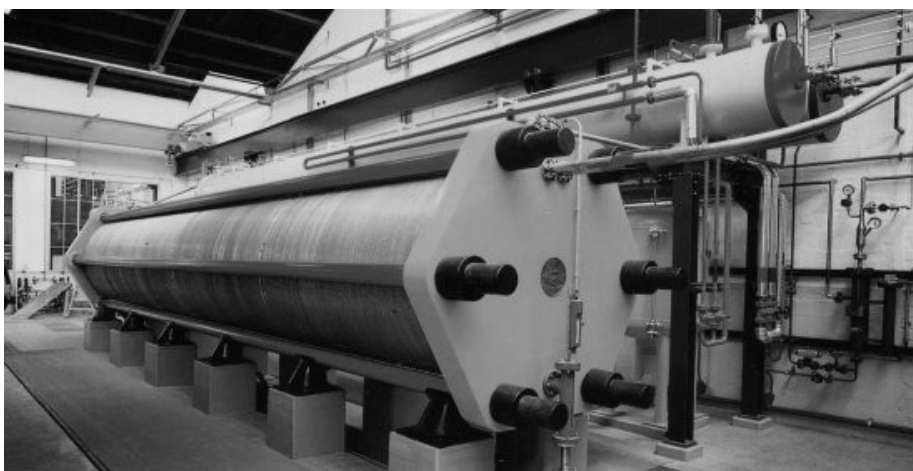


Illustration 1: Picture of the Type S-556 electrolyser of IHT

Industrie Haute Technologie (IHT) is the industrial partner inside the Consortium which is able to produce high pressure alkaline electrolyzers in big size per unit (3,5 MW / 760 Nm³/h). A new free asbestos membrane is being developed by the Consortium with the possibility of improving the performance and characteristics of the electrolyser. The current density used nowadays is 0,2 A/cm² and it is expected that the current can be increased up to 0,5 A/cm², doubling the actual value. The hydrogen capacity production per unit would be increased more than 3 Ton/day achieving in this way one of the goals described in MAIP 2008-2013 where the target in 2020 for the unit capacity is 3 Ton/day. On the other hand, the value of the energy consumption in the stack, 4,6 - 5 kWh/Nm³ H₂ at present, can be decreased with the new membrane. During the preliminary tests done in a lab test bench of 130 mm membrane diameter, the voltage per cell has been decreased from 1.9-2 V/cell up to 1,7 V/cell. Tests in a real scale (1,6 m membrane diameter) are being developed in the Aragon Hydrogen Foundation facilities.

Stable and durable membranes of the new composition have been manufactured by tape-casting at EMPA and by vertical coating at VITO. The materials investigated for using as composite membranes are synthetic or natural silicate based fillers supported in PPS. On the other hand, different concepts of membranes based on Zirfon have been developed.

The membranes are showing similar results concerning cell voltage, membrane conductivity and gas purity than asbestos and Zirfon[®] based membranes. The different membranes are being assessed in base on the new operation conditions (120°C and 30% KOH) in order to know its chemical stability.

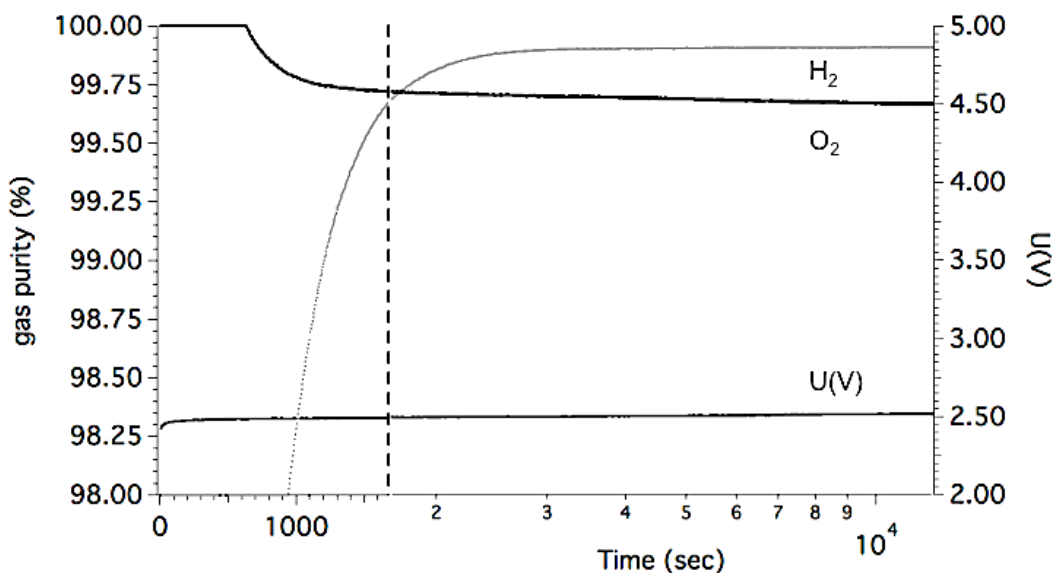


Illustration 2: Results of gas purity and voltage for one membrane tested

Other important task inside the Elygrid project is related to the improvement of the power electronics unit. This is a key matter since one of the main costs of an electrolyser during the lifetime is the electricity cost. Therefore a new topology concept of the rectifier is being developed in order

to try to increase the efficiency of the conversion from AC to DC power. A prototype in the range of MW of this new design will be built during the project. The coupling of the electrolyser together with the renewable energies, mainly wind energy, has been taken into consideration in the rectifier design.

Referring to the Balance of Plant, the main goal is to reduce the capital cost improving also some aspects regarding safety, maintenance and commissioning which must be taken into account when big units in the range of MW are being designed. It is expected to reduce this CAPEX around 25% with improvements in the mechanical design of head plates, tie rods and gas-liquid separators of the electrolyser. Furthermore, a review on field instrumentation and an easier operation is foreseen thanks to the development of an advanced control system.

Ti based-Supports for Unitized Regenerative Fuel Cells (HP01-6)

M.V. Martínez-Huerta¹, M. Roca-Ayats¹, E. Herreros¹, G. García^{1,2}, J.L. Galante¹ and M.A. Peña¹

1 Instituto de Catálisis y Petroleoquímica. CSIC. C/Marie Curie 2. 28049 Madrid, Spain.

2 Departamento de Química Física. Universidad de La Laguna. c/ Astrofísico F. Sánchez. 38071- La Laguna, Tenerife, Spain.

The so-called hydrogen economy is still being considered to promote the consumption of renewable and non polluting energy sources. Hydrogen from water could play the role of an energy carrier, chemicals being more easily stored and transported than any other energy vector. The interconversions of electricity into chemicals and viceversa require electrochemical devices: electrolyzers are used to convert electricity into hydrogen and H₂/air polymer electrolyte fuel cells (PEMFCs) are used to convert hydrogen fuel back into electricity. Unitized regenerative fuel cells (URFCs), a combination of both technologies, offer new perspectives to further bring down investment costs in the near future and to open the way to mass production for several specific applications [1].

In order to improve the round-trip efficiency of the URFC, one key issue is the fabrication of stable and highly active bi-operational oxygen electrode catalysts, which can be used for both oxygen reduction reaction (ORR) and oxygen evolution reaction (OER). Bi-operational electrocatalysts have been developed using a combination of unsupported metallic platinum and OER electrocatalysts such as ruthenium (oxide) and iridium (oxide) [2].

The importance of the support in electrocatalysis is well recognized. However, carbon black, the catalyst support widely used in fuel cells, is not suitable for URFC due to its facile corrosion at high voltage especially in water electrolysis mode.

In this study, we investigate titanium-based supports for URFCs as TiN, TiCN and TiC materials. Titanium carbides and nitrides materials present high melting points and corrosion resistance (typical properties of covalent substances such as diamond, boron, SiC, etc.) in combination with high thermal and electrical conductivities [3].

The present work reports on the synthesis of PtMe (Me = Ir, Ta, Ru) nanoparticles supported on TiC, TiCN and TiN materials (20 %wt. of noble metal loading) and their catalytic activity toward ORR and OER. Additionally, the corrosion resistance properties of the electrocatalysts under strongly oxidizing conditions (pH <1, applied potentials > 1.4 V and high oxygen concentration) have been investigated. Various physicochemical and electrochemical techniques such as XPS, XRD, TEM, in situ FTIRS, cyclic voltammetry (CV) and linear scan voltammetry (LSV) have been used in the present study.

The supported PtMe electrocatalysts were prepared by the ethylene glycol method (EGM) [4]. Appropriate amounts of metal precursors (IrCl₃, Johnson Matthey; PtCl₄, Alfa Aesar; RuCl₃, Alfa Aesar; C₁₀H₂₅O₅Ta, Aldrich) were employed to obtain nominal metal loading of 20 wt. % with a Pt:Me atomic ratio of 3:1 on the support material: TiC (Sigma-Aldrich, SA: 23 m²/g), TiC_{0.7}N_{0.3} (Sigma-Aldrich, SA: 22 m²/g) and TiN (ABO Switzerland Co., SA: 50 m²/g).

Results reveal the highest activity toward oxygen reduction and evolution reactions for the catalysts with TiCN as support, in addition to the best compromise between catalytic activity and stability (Fig. 1). TiC material appears to be the material with the worst performance and stability, while TiN support shows good activity towards ORR and OER, but with high passivation degree by dissolved oxygen. In this context, nitrogen loading appears to be an important factor for the catalyst performance and noble metal anchoring.

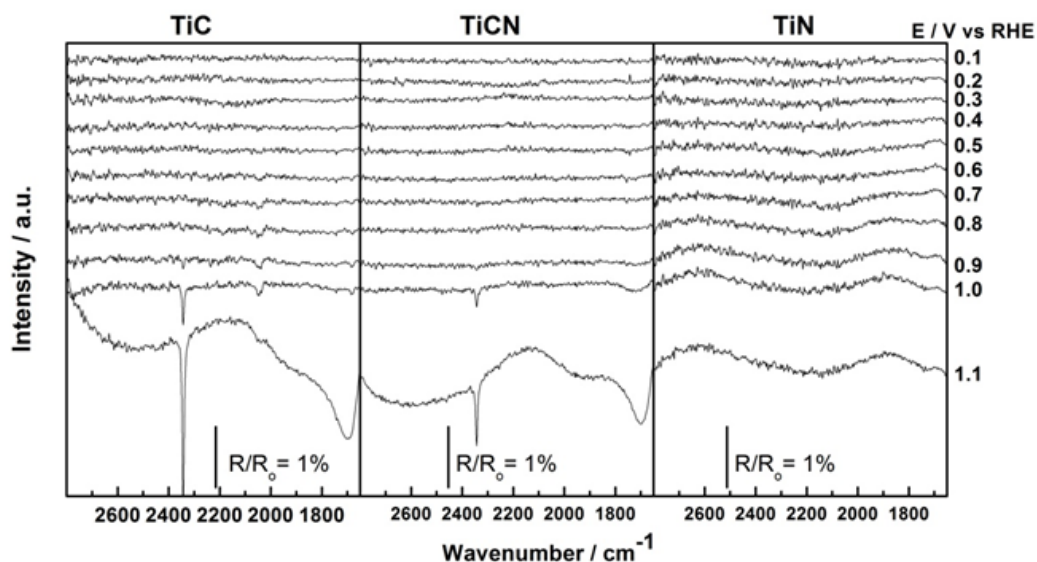


Figure 1. In situ FTIR spectra in 0.5 M H₂SO₄. The potential was set at 0.1 V and a reference spectrum R₀ was run. Then sample spectra R were measured every 0.1 V up to 1.1 V.

ACKNOWLEDGEMENTS

This work has been supported by the Spanish Science and Innovation Ministry under project ENE2010-15381.

REFERENCES

- [1] Petterson J, Ramsey B, Harrison D. J Power Sources 2006;157:28.
- [2] Park S, Shao Y, Liu J, Wang Y. Energy Environ Sci 2012;5:9331.
- [3] Oyama ST. Chemistry of Transition Metal Carbides and Nitrides. Editorial: Chapman & Hall, Great Britain 1996.
- [4] Bock C, Paquet C, Couillard M, Botton GA, MacDougall BR. J Am Chem Soc 2004; 126: 8028.

Fabrication and characterization of microtubular SOEC in coelectrolysis mode (HP02-1)

H. Monzón, M.A. Laguna-Bercero, V. M. Orera

Instituto de Ciencia de Materiales de Aragón (CSIC-Universidad de Zaragoza)

Simultaneous H₂O and CO₂ electrolysis, namely coelectrolysis, has been attracting attention lately as it offers the possibility of producing syngas from CO₂ waste and steam. High temperature electrolysis offers lower electricity consumption compared to conventional low temperature electrolysis. This technology is particularly advantageous when coupled with another process able to provide waste heat, as the higher the electrolysis temperature the higher the heat-to-electric energy ratio required for the process. Solid oxide electrolyser cells (SOEC) are basically solid oxide fuel cells (SOFC) operating in regenerative mode. We have fabricated a series of electrode supported microtubular cells based on optimized design from previous studies and characterized them in coelectrolysis mode.

Cathode support tubes based on nickel-yttria stabilized zirconia (Ni-YSZ) were shaped by plastic extrusion molding. YSZ electrolyte and LSM-YSZ (lanthanum-strontium doped manganite) cathode were added by successive dip coating and sintering steps at 1500°C and 1150°C, respectively. Cells were electrically contacted using platinum wire and paste and sealed to alumina tubes for gas input and output. Coelectrolysis was tested on a small tubular furnace at 850°C, feeding the cell with different gas flows containing steam, carbon dioxide, nitrogen and hydrogen in different compositions. Current density – voltage and electrochemical impedance spectra measurements were recorded using a VSP Potentiostat/Galvanostat (Princeton Applied Research, Oak Ridge, US). Output gas was analyzed using a gas chromatograph (Agilent Technologies MicroGC 900). Area specific resistance was calculated from recorded data as a function of inlet gas composition, yielding values ranging from 0.58 Ωcm² when steam and CO₂ rich flows are used to 2 Ωcm² when a diluted composition is used. Gas chromatography was used to examine the hydrogen and carbon monoxide content in the output gas, finding a good agreement with the gas shift reaction equilibrium. Faraday efficiency was close to 100% on the studied conditions, meaning that little or no conduction takes place through the electrolyte. Additionally the electrolyte conduction threshold was found close to 1.8V in the diluted feeding conditions.

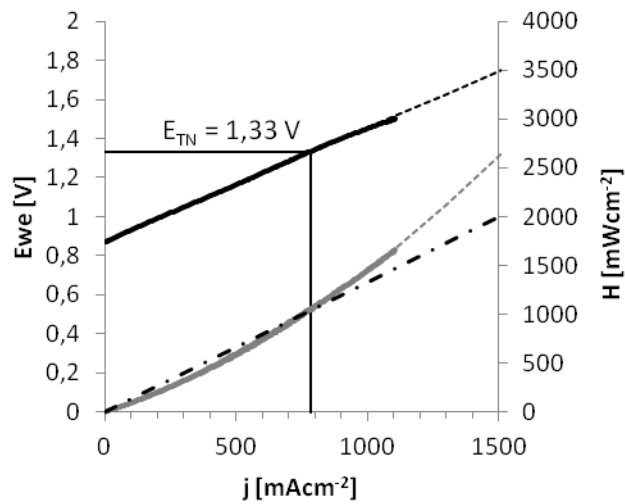


Figure 1: j-V (black lines), Heat generated during cell operation (grey) and calculated Heat consumed by the electrolysis (black dot and line). Thermo neutral voltage is found at the generated - consumed heat intersection.

Mild cell degradation was witnessed after several hours of operation at 600 mAcm⁻². The possible causes of this degradation will be discussed in the present work.

Development and Characterisation of Solid Oxide Electrolyser Cells (SOEC) (HP02-2)

1G. SCHILLER, 1M. HÖRLEIN, 2F. TIETZ

1Deutsches Zentrum für Luft- und Raumfahrt (DLR), D-70569 Stuttgart, Germany

2Forschungszentrum Jülich (JÜLICH), D-52425 Jülich, Germany

A reliable energy supply which is based on increasing shares of sustainable and renewable energy sources, such as wind power and solar energy, requires appropriate storage technologies. Hydrogen as energy carrier, produced by water electrolysis using electric current from regenerative energy sources, offers a high potential in this respect. A very efficient option to produce hydrogen in this way is high-temperature steam electrolysis based on solid oxide electrolyser cells (SOEC). This technology requires operating temperatures in the range of 700-1000 °C and offers some additional advantages compared to low temperature electrolysis techniques. The higher operating temperature results in faster reaction kinetics thus enabling potentially high energy efficiency. From a thermodynamic point of view, part of the energy demand for the endothermic water splitting reaction can be obtained from heat produced within the cell. The electric energy demand can be further significantly reduced if high temperature heat from renewable energy sources such as geothermal or solar thermal power or waste heat from industrial processes is available. Furthermore, it is possible with high temperature electrolysis to not only split water but also carbon dioxide or a mixture of both to produce synthesis gas (syngas) or other energy carriers such as methane or methanol by subsequent catalytic conversion. For a further development of this promising technology, development work on materials and cells as well as extensive operational experience is still needed. A main objective is to develop highly efficient and long-term stable cells and stacks using novel electrode materials and to improve the degradation behaviour by elucidating the relevant degradation mechanisms.

To this aim, German Aerospace Center (DLR) and Forschungszentrum Jülich (JÜLICH) who have both long experience in the development of SOFC/SOEC technology [1-3] started a joint project in the frame of the "Helmholtz Energy Alliance" on electrochemical energy storage and conversion. Cathode-supported cells containing novel perovskite-type air electrodes were fabricated by ceramic processing and sintering for electrochemical characterisation in electrolysis operating mode. The selection and preparation of electrode materials and the process of cell manufacturing is described. A new test bench has been installed which allows measuring polarisation curves of 4 cells simultaneously under relevant SOFC and SOEC conditions as well as performing long-term durability measurements. The experimental setup for electrochemical cell characterisation is described and results of electrochemical measurements performed at different operational conditions, such as different steam content and operating temperature, are presented. After operation the cells were investigated by post-test analytical methods; hereby special emphasis is put on the detailed investigation of degradation phenomena and mechanisms [4] by applying numerous characterisation techniques as well as the elaboration of mitigation strategies for the degradation processes.

References

Schiller G., Ansar A., Lang M., Patz O., 2009, J. Appl. Electrochem., vol. 39: pp. 293-301

Schiller G., Ansar A., Patz O., 2010, Advances in Science and Technology, vol. 72: pp. 135-143

Tietz F., Buchkremer H.-P., Stöver D., 2002, Solid State Ionics, vol. 152-153: pp. 373-381

Tietz F., Sebold D., Brisse A., Schefold J., 2013, J. Power Sources, vol. 223: pp. 129-135

Peak hydrogen power plant based on SOEC/SOFC---the system configuration (HP02-3)

Jaroslaw MILEWSKI, Marcin WOLOWICZ, Janusz LEWANDOWSKI

Institute of Heat Engineering at Warsaw University of Technology

Introduction

Fuel price inflation and a long-term increase in electricity consumption have provided added impetus to the search for ultra-effective power generation systems. Fuel cells generate power in electrochemical reactions with potentially ultra-high efficiency. High-temperature fuel cells (Solid Oxide Fuel Cell—SOFC and Molten Carbonate Fuel Cell—MCFC) are considered as highly efficient electricity sources. Solid Oxide Fuel Cells, next to the Molten Carbonate Fuel Cell belong to the group of fuel cells that can be used for energy purposes. Currently, these types of fuel cells are installed as supply hospitals and larger facilities where power stability is more important than cost. One can imagine a future in which fuel cells will be used on a wider scale. Housing estates, cottages agglomerations or industrial sites will have their own mini-power plants based on fuel cells. The fuel cell so that it can be considered as the upper heat source should work in a fairly high temperature. SOFCs are characterized by a temperature suitable for this purpose: 1,000°C. Hydrogen, Natural Gas, and biofuels are currently considered to be the main fuels for fuel cells. Hydrogen is an ideal fuel with respect to fuel cell working conditions. Unfortunately, hydrogen is not present in the environment in an uncombined form and must be generated for further utilization. Natural Gas, meanwhile, is considered to be an interim fuel due to limited resources. Fuel cells and hybrid systems look promising, but in order to meet demand, they require large amounts of hydrogen. Probably the cleanest method of producing hydrogen is electrolysis of water. In this area, the Solid Oxide Electrolysis Cell (SOEC) has attracted great interest in recent years as it has a potentially high power density and higher efficiency compared with conventional low-temperature electrolyzers. This paper contains an analysis of the considered system configurations for utilizing SOECs as hydrogen generators for storing electricity (eg. from renewable sources), for later utilization in SOFC for electricity generation, creating a peak-load hydrogen based power plant for small and medium size..

Peak hydrogen power plant based on SOEC/SOFC---the system configuration

A variant analysis of possibility configuration of peak-load system which based on SOEC/SOFC module and hydrogen storage was presented in the article. It seems that the most rational configuration of the power plant with the SOEC/SOFC can reach high total electricity-to-electricity conversion rate at small and medium size. The system can contain the minimum amount of devices when anode side of SOFC is exposed to the hydrogen storage directly. In this solution there is no compressors and pumps needed, and system contains no moving parts. Oxygen is then released surrounding or can be storage in the additional tank. In theory, it is possible to obtain higher efficiencies but this requires much higher capital expenditures (additional heat exchangers, gas turbines, set of heat regeneration heat exchangers, etc.) and much higher parameters of working media in the system (1,400°C, 30 bar).

The absolute efficient of the system depends on the assumptions made and the way in which the mathematical model was developed. It may change due to them, hence the presented analysis is rather qualitative than quantitative.

Acknowledgments

The project is financed from funds of National Centre for Science granted by a decision number DEC-2012/05/B/ST8/02849.

Dual Atmosphere Study Of The K41X Stainless Steel For Interconnect Application In High Temperature Water Vapour Electrolysis (HPO2-4)

M. R. Ardigo^a, L. Combemale^a, I. Popa^a, S. Chevalier^a, P. Girardon^b

^aICB, UMR 6303 CNRS-Université de Bourgogne, 21078 Dijon cedex, France

^bAPERAM, Centre de Recherche, 62330 Isbergues, France

High temperature water vapour electrolysis (HTE) is one of the most efficient technologies for mass hydrogen production. It works as an inverse fuel cell, using air at the anode side and water vapour at the cathode side. A major technical difficulty related to high temperature water vapour electrolysis is the development of interconnects working efficiently for a long period (25 000 hours).

From the electrical point of view, the interconnect must have a low contact resistance with the electrodes, that directly affects the electrochemical conversion efficiency (water into hydrogen) and can penalize the process. In this purpose, the interconnect has to get a slow oxidation kinetics and to form as less as possible electrical insulating oxides. From the chemical point of view, the interconnect has to be resistant against oxidation in an oxygen rich atmosphere (anode side) and hydrogen/water vapour rich atmosphere (cathode side).

The goal of this study is the development of interconnects with suitable properties for high temperature water vapour electrolysis. A ferritic stainless steel with 18% chromium content is tested in this purpose.

Isothermal oxidation tests were performed at 800°C in cathode (10%H₂+90%H₂O) and anode (95%O₂+5%H₂O) single atmospheres. Corrosion products of uncoated and coated samples were analysed by scanning electron microscopy equipped with energy dispersive X-ray analyses and X-ray diffraction. These characterisations allowed understanding interconnect degradation process. In both atmospheres, the formation of a duplex oxide scale was revealed. In H₂-H₂O, an inner layer consisting of protective chromia and an outer layer formed by a magnetite-type iron oxide was observed, while in O₂-H₂O a Cr-Mn spinel-type oxide grows in top of an inner chromia layer.

In parallel, electrical resistivity measurements were performed in both HTE atmospheres during 200 hours at 800°C. The area specific resistance (ASR) parameter reflects the resistance, the thickness, as well as the electrical properties of the oxide layers and should have a maximum limit value of 0.1 Ω·cm². A rather high, non-suitable, ASR parameter value (0.45 Ω·cm²) was obtained in the cathode atmosphere, while a rather good behaviour (0.1 Ω·cm²) was observed in the anode atmosphere.

In order to better approach HTE functioning conditions, very new and innovative additional tests were performed in dual atmosphere, the interconnect being exposed at one side to H₂-H₂O and at the other side to O₂-H₂O. The influence of the electrical current on the corrosion behaviour was tested by performing two types of experiments at 800°C during 100 hours, with and without applied current. A very interesting ASR parameter value was measured during the dual atmosphere experiment done under applied electrical current. The corrosion scales observed in both cases are identical: the electrical current doesn't seem to have any influence on the nature of the phases

formed at the interconnect surface. However, if the oxide layer obtained at the anode (air) side is the same as obtained previously in single atmosphere (Cr_2O_3 and $(\text{Cr,Mn})_3\text{O}_4$), a totally different situation was observed at the cathode ($\text{H}_2\text{-H}_2\text{O}$) side: the corrosion scale is now composed by inner chromia and outer $(\text{Cr,Mn})_3\text{O}_4$ protective oxides (instead of Cr_2O_3 and Fe_3O_4). A diffusion process of the chemical species from one side of the interconnect to the other seems to be the reason for this behaviour. This statement was confirmed by means of a third experiment performed with the dual atmosphere set-up, by applying $\text{H}_2\text{-H}_2\text{O}$ at both surfaces of the metallic material. The usual oxide layers previously obtained in the cathode single atmosphere were now revealed: Cr_2O_3 and Fe_3O_4 .

The results allowed identifying a promising solution for HTE metallic interconnect. Longer time tests will be done in order to confirm these very first results obtained in dual atmosphere.

Optimization of SO₂ crossover and water transport in SO₂-depolarized electrolyser for hydrogen production (HP02-5)

Annukka Santasalo-Aarnio, Michael M. Gasik

*Aalto University, School of Chemical Technology,
Department of Materials Science and Engineering,
Vuorimiehentie 2, P.O. Box 16200, 00076 Aalto, Finland*

Hydrogen production for application in fuel cells must fulfil several criteria of economic, technical and environmental sustainability. Water electrolysis powered by renewable power sources is traditionally considered technique, but it requires high overvoltages (the theoretical E_0 of the conventional water electrolysis 1.23 V vs. practical 1.7-2.2 V) and therefore leads to lower efficiency. Alternative process - sulfur dioxide depolarized electrolysis (SDE) - has been developed, where SO₂ is added to the anode space and it is oxidized electrochemically leading to sulfuric acid and hydrogen evolution at cathode. Such overall reaction $\text{SO}_2 + 2 \text{H}_2\text{O} \rightarrow \text{H}_2\text{SO}_4 + \text{H}_2$ requires only E_0 of ~0.16 V, i.e. significantly reduced overvoltage [1]. SDE is also a key component in the Outotec® Open Cycle for combined production of hydrogen and sulfuric acid [2].

Commonly, in SDEs proton conductive membrane (PEM) is used as a separator [3-5] because it has good proton but low electron conductivity. Nevertheless, SO₂ molecule as a small, non-charged molecule is able to transport through the water channels in PEM to the cathode causing unwanted side reactions and side products such as elemental sulfur. The side reactions decrease the overall efficiency, however, the solid side product can partially block the cathode surface changing the current distribution on the electrode plate and dramatically limiting the lifetime of the SDE. When in real industrial applications the current density is further increased, more protons are transported through the membrane resulting as more severe crossover.

In this work SDE tests with various current densities a bench-scale stack electrolyser were performed (Figure 1). In the testing facility the control over potential-current behavior is combined with the H₂ production, sulfuric acid as well as SO₂ concentrations at both electrolytes. With this methodology the overall balance of the whole electrolyser can be formulated. By altering the cell configuration, the water transport and the SO₂ crossover can be optimized and possibility to find a cathode cleaning cycles can be obtained. For this technology to become commercially viable the SO₂ crossover phenomenon needs to be controllable in an industrial scale electrolyser.

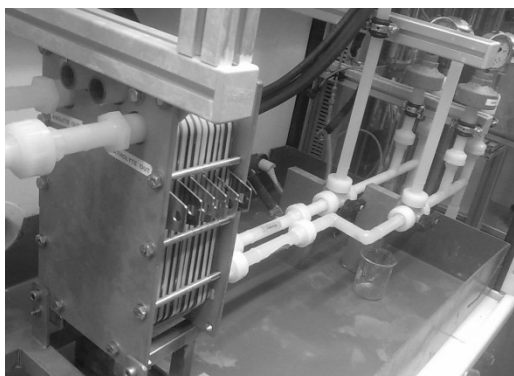


Figure 1. A bench-scale SO₂ depolarized electrolyser cells stack.

Support from the Fuel Cells and Hydrogen Joint Undertaking under project SOL2HY2 is greatly acknowledged.

References

- [1] Gorenssek, M.B., Staser, J.A., Stanford, T.G., Weidner, J.W., A thermodynamic analysis of the SO₂/H₂SO₄ system in SO₂-depolarized electrolysis, *Int. J. Hyd. Ene.* 34 (2009) 6089-6095.
- [2] Lökkiluoto, A., Taskinen, P.A., Gasik, M., Kojo, I.V., Peltola, H., Barker, M.H., Kleifges, K-H. Novel process concept for the production of H₂ and H₂SO₄ by SO₂-depolarized electrolysis. *Environment, Development and Sustainability* 14 (2012) p. 529-540, 2012.
- [3] Elvington, M.C., Colón-Mercado, H., McCatty, S., Stone, S.G., Hobbs, D.T., *J. Power Sources* 195 (2010) 2823-2829.
- [4] Sivasubramanian, P., Ramasamy, R.P., Freire, F.J., Holland, C.E., Weidner, J.W., *Int. J. Hydr. Ene.* 32 (2007) 463-468.
- [5] Xue, L., Zhang, P., Chen, S., Wang, L., Wang, J., *Int. J. Hydr. Ene.* 38 (2013) 11017-11022.

Design and Manufacturing of Catalytic Membrane Reactors by developing new nano-architected catalytic and selective membrane materials (HP02-6)

José Luis Viviente

Fundación Tecnalia Research & Innovation

Process Intensification (PI), which is defined as "any chemical engineering development that leads to a substantially smaller, cleaner, safer and more energy efficient technology", is likely to be the next revolution of the chemical industry. The need for more efficient processes, including further flexible engineering designs and, at the same time, increasing the safety and environmental impact of these processes, is pushing the industry to novel research in this field. The chemistry and related sectors have already recognised the benefits of PI and estimate a potential for energy saving of about 1000 kilo tonnes of oil equivalent (toe) per year using these processes.

The technology of membrane reactor plays an important role in PI and is based on a device combining a membrane based separation and a catalytic chemical reaction in one unit. Every catalytic industrial process can potentially benefit from the introduction of catalytic membranes and membrane reactors instead of the conventional reactors. According to SusChem (European Technology Platform for Sustainable Chemistry, Strategic Research Agenda 2005) more than 80% of the processes in the chemical industry worth approximately €1,500 billion, depend on catalytic technologies, and one of the shorter-term (5-10 years) objectives of this Platform is to "integrate reactor-catalyst-separation design: integration and intensification of processes requires the development of new catalytic concepts which break down the current barriers (for example, low flux in catalytic membranes)".

The DEMCAMER FP7 project (www.demcamer.org) proposes an answer to the paradigm met by the European Chemical Industry: increase the production rate while keeping the same products quality and reducing both production costs and environmental impacts. Through the implementation of a novel process intensification approach consisting on the combination of reaction and separation in a "Catalytic Membrane Reactor" single unit.

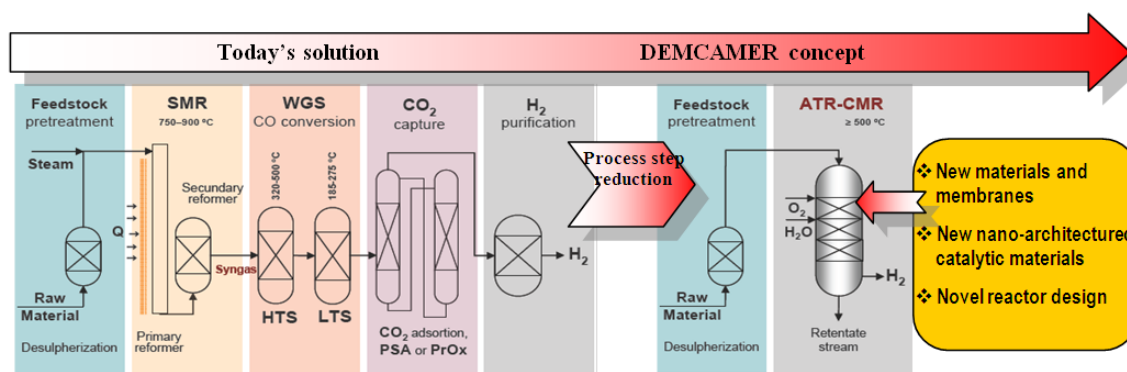


Figure 6. DEMCAMER project concept (ATR process)

The aim of DEMCAMER project is to develop innovative multifunctional Catalytic Membrane Reactors (CMR) based on new nano-architected catalysts and selective membranes materials to improve their performance, cost effectiveness (i.e.; reducing the number of steps) and sustainability (lower environmental impact and use of new raw materials) over four selected chemical processes ((Autothermal Reforming (ATR), Fischer-Tropsch (FTS), Water Gas Shift (WGS), and Oxidative Coupling of Methane (OCM)) for pure hydrogen, liquid hydrocarbons and ethylene production.

The scientific and technical objectives to achieve this general objective are the following

- To develop new membrane materials with improved separation properties, long durability, and with reduced cost.
- To develop new nano-architected catalysts with better performance and at reduced cost.
- To understand the fundamental physicochemical mechanisms and the relationship between structure/property/performance and manufacturing process in membranes and catalysts, in order to achieve radical improvements in membrane reactors.
- To design, model and build up novel more efficient (e.g. reducing the number of steps) membrane reactor configurations based on the new membranes and catalysts.
- To validate the new membrane reactor configurations, at semi-industrial prototype level, in four selected chemical process (Autothermal Reforming (ATR), Fischer-Tropsch (FTS), Water Gas Shift (WGS), and Oxidative Coupling of Methane (OCM)) for pure hydrogen, liquid hydrocarbons and ethylene production.
- To improve the cost efficiency of membrane reactors by increasing their performance, decreasing the raw materials consumption and the associated energy losses.
- To enable the use of new raw materials (i.e.; convert non-reactive raw materials)
- To assess the health, safety and environmental impact of the four CRM developed processes, a complete LCA of the developed technologies will be performed

The DEMCAMER scheduled work plan will comprise activities related to the whole product chain: i.e. development of materials/components (membranes, supports, seals, catalyst,..) through integration/validation at lab-scale, until development/validation of four semi-industrial pilot scale CMRs prototypes. Additionally, three research lines dealing with: 1) the collection of specifications and requirements, 2) modelling and simulation of the developed materials and processes, and 3) assessment of environmental, health & safety issues -in relation to the new intensified chemical processes- will be carried out.

For a maximum impact on the European industry this research, covering the complete value chain of catalytic membrane reactors, can only be carried out with a multidisciplinary and complementary team having the right expertise, including top level European Research Institutes and Universities (8 RES) working together with representative top industries (4 SME and 6 IND) in different sectors (from raw materials to petrochemical end-users).

Acknowledgements

The research under this project is receiving funding from the European Union Seventh Framework Programme (FP7/2007-2013) under grant agreement n° NMP3-LA-2011-262840.

Disclosure

Then present document reflects only the author's views and the Union is not liable for any use that may be made of the information contained therein.

Cartridges for Controlled Hydrogen Generation based on Galvanic Zn Water Reaction (HPO3-1)

ROBERT HAHN¹, Andreas Gabler¹, Axel Thoma¹, Fabian Glaw¹, Martin Krebs², Michael Schmalz², Petra Gehrke³, Joachim Helmke⁴, Matthias Arnold⁵, K.-D. Lang¹

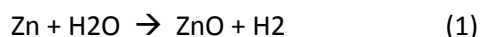
¹ Fraunhofer IZM, Berlin, Germany, ² Varta microbattery, Ellwangen, Germany

³ Grillo-Werke AG, Goslar, Germany, ⁴ gaskatel GmbH, Kassel, ⁵ Flexiva GmbH, Amtsberg, Germany

The main motivation underlying the development of micro fuel cells is the possibility to achieve higher energy densities in comparison to batteries. Hydrogen PEM micro fuel cell technology has been developed extensively over the last two decades. Nevertheless small, portable PEM fuel cells have not emerged on the market. The two greatest barriers for commercialization of large fuel cells are durability and cost [1]. For small, portable systems it is the lack of a light weight, reliable and low cost hydrogen source. Compressed gas or liquid hydrogen cannot be used for portable systems, reversible metal hydrides are still too costly and too heavy. Chemical hydrides require sophisticated peripheral components for hydrogen flow control.

THE PRINCIPLE

This paper describes galvanic cells which can be used as a hydrogen source as well. Hydrogen is produced by the reaction of zinc and water according to equation (1).



The system is somehow quite similar to the Zinc air primary battery. Here, the electrolyte contains additional water and the ingress of oxygen is prevented. Therefore the large energy density of the Zinc air battery can be maintained to a great extent while the life time of the system is much higher compared to Zinc air batteries. This is achieved by complete separation from ambient air. Zinc air batteries have an operational life time of only several weeks because of reaction with atmospheric gases.

The hydrogen producing cell consists of a gas-generating electrode (gas diffusion electrode, GDE) as cathode, a Zinc anode and it is filled with aqueous KOH electrolyte.

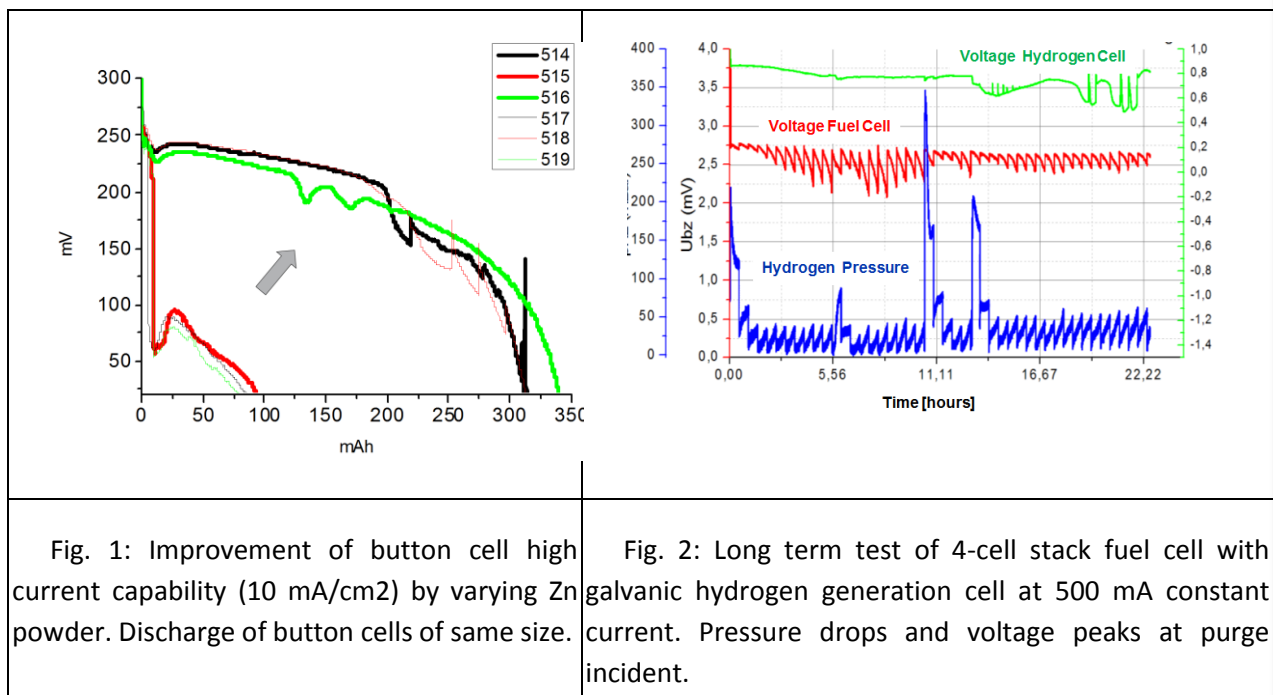
If the fuel cell and the galvanic cell are electrically connected in series, the galvanic cell produces the precise amount of hydrogen that the fuel cell consumes. Only minor leakages have to be compensated. Thus, a very low component overhead, in comparison to other known hydrogen generating systems, can be achieved, since pressure or flow controllers are not required. The system features two small hydrogen valves, one between the galvanic cell and the fuel cell and the other to purge the fuel cell anode. Depending on the current, the hydrogen-evolving cell yields a voltage between 0 and 0.4 volts. It produces not only hydrogen but adds ca. 10 to 20 percent of system voltage and thus electricity. An electrical circuit is used which controls the current of the galvanic cell and regulates the hydrogen pressure.

A major disadvantage of the galvanic hydrogen generation cells is the low hydrogen rate and the resultant low power density of the system. While the basic performance of the system has been studied previously [2] detailed investigations have been made to increase power density and to up-scale the system which will be presented in this paper. A model was used to predict the required hydrogen generation and hydrogen pressure as function of fuel cell power, hydrogen leakage and purge interval.

ANODE MATERIALS

Various types of Zn powders were fabricated using the mass fabrication technology dedicated to alkaline primary batteries. Both particle size and alloy content were varied. Experiments with regard to material optimization were made with help of standard button cells. Improvement of high power performance was achieved with sufficiently small particles (fig. 1).

Test cells have been used to measure the discharge capacity and discharge voltage as function of the current drain.



CATHODE

Well proven electrode fabrication technology including Raney-Nickel catalyst was used for preparation of the gas evolving cathode. The GDE have to serve several tasks simultaneously: it has to provide a large three phase boundary, hydrogen must be directed to the outside at high rate and prevented from entering the cell. The KOH electrolyte must stay inside the cell and not escape out of the package or through the hydrogen separation foil. Electrolyte diffusion must be sufficiently high inside the electrode and inside the separator.

The performance was further improved by increasing the separator adhesion which was achieved by laminating the separator foil onto the catalyst layer. These electrodes were successfully tested up to a current density of 50 mA/cm².

UPSCALING and SYSTEM TEST

Based on the material improvements and button cell tests larger demountable cells of 70 Ah capacity were designed and tested. These prismatic galvanic cells will be converted later on into a low cost hydrogen cartridge. Hydrogen flow was measured as function of current over time. Current-voltage curves and impedance was evaluated at an interval of 10 Ah during a continuous discharge at 500 mA. Current voltage characteristic and short circuit current remained stable until ca. 50 Ah discharge, then impedance and voltage drop increased steadily. After 60 Ah discharge only reduced currents can be drained or a break is required. As the cell performance is diffusion limited the V/I curve depends strongly on temperature.

A stack of four hydrogen evolving cells was connected to a micro fuel cell to evaluate the system performance. The fuel cell was optimized for lightweight portable application and passive humidity management [3].

An analytical model was developed to calculate the offset current to be imposed on the galvanic cell which is required to compensate for hydrogen leakages, hydrogen diffusion through the fuel cell membrane and fuel cell anode purges. Large purge intervals were investigated to save as much hydrogen as possible for electricity generation. For the same reason the hydrogen operation pressure was kept low. As can be seen in figure 2 the system can be operated at a pressure below 50 mbar with a purge interval of 30 minutes. On the other hand, to maintain high fuel cell voltage a slightly higher hydrogen production and shorter purge interval would be beneficial. Approximately 5% higher current of the gas evolving cell compared to the fuel cell is required for stable long term operation and practical leakage and purge rates.

APPLICATIONS

Even though impressive improvements with respect to hydrogen rate have been made, the system performs best at low to medium power density. An energy density near 1000 Wh/l similar to direct methanol fuel cells can be achieved at a discharge time not less than ca. one week. Therefore preferred applications are of grid charging stations for portable electronics which allows for example for 50 smart phone recharges. Other applications are related to energy autarkic remote sensors which may need a cartridge change once a year or less.

REFERENCES

[1] Yun Wang et al., A review of polymer electrolyte membrane fuel cells, Applied Energy 88 (2011) 981–1007

[2] Robert Hahn, Stefan Wagner, Steffen Krumbholz, Herbert Reichl, „Optimization of Efficiency and Energy Density of Passive Micro Fuel Cells and Galvanic Hydrogen Generators”, DTIP of MEMS & MOEMS 9-11 April 2008, ©EDA Publishing/DTIP 2008, ISBN: 978-2-35500-006-5

[3] S. Krumbholz, J. Kaiser, M. Weiland, R. Hahn, H. Reichl, Influences of current collector foils with different opening ratios in passive polymer electrolyte membrane fuel cells, Journal of Power Sources 196 (2011) 5277–5281

This research was funded by the German Federal Ministry of Economics and Technology under contract 03ET2028B

Scale-up experiences of microbial electrolysis cells (MECs) for hydrogen production and wastewater treatment (HPO3-2)

A. ESCAPA, L. GIL-CARRERA, A. MORÁN*

*Chemical and Environmental Bioprocess Engineering Group, Natural Resources Institute (IRENA),
University of Leon, Avda. de Portugal 41, Leon 24009, Spain*

Microbial electrolysis cells (MECs) are bio-electrochemical reactors that employ electrogenic bacteria to produce hydrogen by oxidizing organic matter (using the anode as an electron acceptor) through the hydrogen evolution reaction at the cathode (Gil-Carrera et al., 2013). This type of bioreactors represent a novel approach to harnessing the energy content of the organic matter in wastewater, and convert it to hydrogen gas, thus offsetting the operational costs of wastewater treatment plants. However, before practical implementation of bio-electrochemical reactors can be achieved, several techno-economic challenges need to be addressed: (i) the presence of bottlenecks in MECs scale-up and the need to develop approaches for resolving these issues, (ii) the absence of a clear cost estimation for MEC reactors, (iii) the determination of the most convenient architecture of MEC reactors (planar vs. tubular reactors).

In our communication we will try to offer an answer to the questions above with the hope that it will be helpful for developing cost-effective MEC manufacturing process and low cost materials. Firstly we will discuss those bottlenecks that most affect the scale-up process. At present the cathode materials and the cathodic reactions are limiting largely the performance of the MEC reactor and its scalability. In addition, the presence hydrogen consuming bacteria which are difficult to eradicate from the electrolyte of the MEC hamper the hydrogen recovery (Escapa et al., 2012).

Another issue that may prevent investor from spending funds on the MEC technology is that at present there is not clear estimation of MEC manufacturing costs. Researcher's initial efforts to come up with a future capital costs of bio-electrochemical reactors based on available laboratory materials, proposed costs in a broad range between €1137-3000 per cubic meter of reactor (m³R) (Rabaey and Verstraete, 2005; Fornero, Rosenbaum and Angenent, 2010; Rozendal et al., 2008; Pant et al., 2010). In our study we have found that if future MEC reactors could work at current densities of 5 amperes per squared meter of anode (A m²A) with an energy consumptions of 0.9 kilowatt-hour per kilogram of chemical oxygen demand reduced (kWh kg⁻¹-DQO), an acquisition costs of €1350 m³R represents a threshold at which the use of MECs in a domestic wastewater treatment plant would be justified.

In addition, practical implementation of MEC technology in wastewater treatment plants will require that the future design can compete with biological conventional treatments. We have identified three main constraints related to MEC architecture that need to be addressed, namely the footprint, wastewater composition and other technological constraints. The footprint impact can be minimized by reducing as much as possible the thickness of the MECs. In our studies we have come up with a thickness of 2.5 cm. Wastewater composition also has an influence over MEC architecture. Urban wastewaters usually present low conductivities; therefore, and in order to minimize ohmic losses in this type of reactors, both electrodes anode and cathode must be kept as close as possible. A

separation of around 1 mm has been successfully used in several studies (Escapa et al., 2012; Escapa et al., 2009; Tartakovsky et al., 2009; Tartakovsky et al., 2008). Another technical issue that deserves consideration is how the MEC reactors should be electrically connected. The most straightforward connection is the parallel connection of all the MEC units that made up the whole set-up. However this configuration would require the presence of a rectifier able to manage large currents, whose relative large purchase costs ($\sim\text{€}4 \text{ A}^{-1}$) would be prohibitive for practical application. Therefore a certain number of MEC units should be connected in series to minimize the circulating current. In Figure 1 we can see a cross section of the MEC reactor and the way they are connected in one stack. Moreover, and in order to further decrease the ohmic losses, these MEC units arranged in series might be connected through bipolar plates.

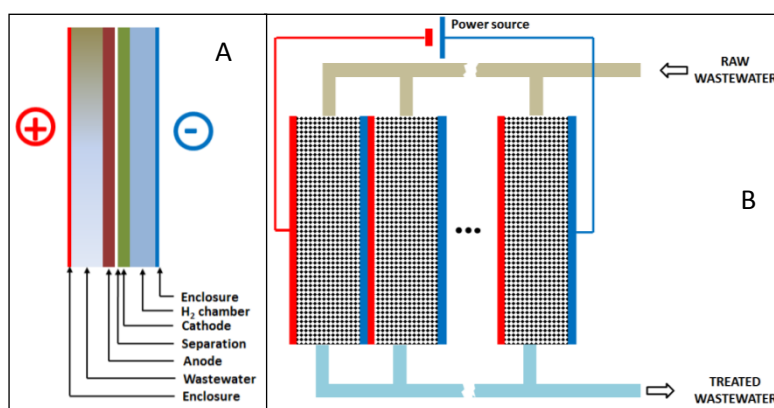


Figure 1. A: Cross section of an MEC unit. B: Cross section of a stack of MEC units connected hydraulically in parallel and electrically in series. Several stacks would complete the whole set-up of a MEC-based wastewater treatment in a wastewater treatment plant.

REFERENCES

- Escapa, A., Gil-Carrera, L., García, V., Morán, A., 2012. Performance of a continuous flow microbial electrolysis cell (MEC) fed with domestic wastewater, *Bioresour. Technol.* 117, 55-62.
- Escapa, A., Manuel, M.F., Morán, A., Gómez, X., Guiot, S.R., Tartakovsky, B., 2009. Hydrogen Production from Glycerol in a Membraneless Microbial Electrolysis Cell, *Energ. Fuel.* 23, 4612-4618.
- Fornero, J.J., Rosenbaum, M., Angenent, L.T., 2010. Electric Power Generation from Municipal, Food, and Animal Wastewaters Using Microbial Fuel Cells, *Electroanalysis.* 22, 832-843.
- Gil-Carrera, L., Escapa, A., Moreno, R., Morán, A., 2013. Reduced energy consumption during low strength domestic wastewater treatment in a semi-pilot tubular microbial electrolysis cell, *J. Environ. Manage.* 122, 1-7.
- Pant, D., Van Bogaert, G., De Smet, M., Diels, L., Vanbroekhoven, K., 2010. Use of novel permeable membrane and air cathodes in acetate microbial fuel cells, *Electrochim. Acta.* 55, 7710-7716.

Rabaey, K., Verstraete, W., 2005. Microbial fuel cells: novel biotechnology for energy generation, *Trends Biotechnol.* 23, 291-298.

Rozendal, R.A., Hamelers, H.V.M., Rabaey, K., Keller, J., Buisman, C.J.N., 2008. Towards practical implementation of bioelectrochemical wastewater treatment, *Trends Biotechnol.* 26, 450-459.

Tartakovsky, B., Manuel, M.F., Neburchilov, V., Wang, H., Guiot, S.R., 2008. Biocatalyzed hydrogen production in a continuous flow microbial fuel cell with a gas phase cathode, *J. Power Sources.* 182, 291-297.

Tartakovsky, B., Manuel, M.F., Wang, H., Guiot, S.R., 2009. High rate membrane-less microbial electrolysis cell for continuous hydrogen production, *Int. J. Hydrogen Energy.* 34, 672-677.

Production of Biohydrogen through the Combination of Two Stage Fermentation Processes Using Salt-Rich Substrates (HPO3-3)

Dayana Muzziotti¹, Alessandra Adessi^{1,2}, Andrea Sanchini¹, Laura Dipasquale³, Giuliana d'Ippolito³, Angelo Fontana³, Roberto De Philippis^{1,2}.

¹Department of Agrifood Production and Environmental Sciences (DISPAA), University of Florence, Florence, Italy.

²Institute of Chemistry of Organometallic Compounds (ICCOM), CNR, Florence, Italy.

³Institute of Biomolecular Chemistry (ICB), CNR, Pozzuoli (Naples), Italy.

Dark and Photofermentation are two promising processes for the production of biohydrogen. They are carried out by chemo- and photo- heterotrophic bacteria, respectively. The coupling of dark and photo- fermentation is currently under active study because, when these two processes are combined on a sequential mode, it is possible to approach the theoretical maximum yield of 12 mol of H₂ (mol glucose)⁻¹. In particular, the research on biological H₂ production processes is nowadays pointing towards the utilization of low cost substrates. Those media need to be as cheap and profusely available as possible. In this study the substrate tested for the combined process carried out by a marine thermophilic chemoheterotrophic bacterium and a photoheterotrophic purple non sulfur bacterium (PNSB) was artificial sea water supplemented with glucose, in order to assess the feasibility of using salt rich substrates for combined dark and photo fermentation processes. In particular, the aim of this work was to test the H₂ photo-evolution performances of PNSB growing on two synthetic spent media deriving from dark fermentation processes carried out by the marine thermophilic bacterium *Thermotoga neapolitana* DSM 4359T. Due to the presence of sea salts in the culture media, a first screening was performed on three PNSB strains belonging to the DISPAA's culture collection. The results obtained showed that only one strain, *Rhodospseudomonas palustris* 42OL, was capable of producing significant amounts of H₂ in presence of sea salts. The media utilized for dark fermentation experiments with *T. neapolitana* DSM 4359T were: ASW (Artificial Sea Water, containing 40 g/L of sea salts) and DASW (Diluted Artificial Sea Water, containing 10 g/L sea salts), both supplemented with glucose (5 g L⁻¹). The spent media deriving from dark fermentation were collected and analyzed to determine the amount of organic acids produced by *T. neapolitana* DSM 4359T. The two media contained lactic (2.84 and 2.71 g L⁻¹, respectively) and acetic acid (0.56 and 0.62 g L⁻¹, respectively). ASW was first used undiluted for photo-fermentation experiments, but no H₂ was produced and a scant growth was observed (0.990 ΔOD₆₆₀). The medium was then diluted 1:2 with distilled water. This dilution allowed a greater cell growth (2.977 ΔOD₆₆₀) but no H₂ was produced, yet. DASW medium was used undiluted, due to the lower amount of salts contained in the medium. In this case, *Rp. palustris* 42OL was able to produce H₂ and showed a mean H₂ production rate of 11.18±0.88 ml H₂ (L*h)⁻¹ with a 54.78 % substrate conversion. Moreover, a relevant increase in biomass was observed (2.675 ΔOD₆₆₀). With this medium, a yield of 4.74±0.37 mol H₂ per mol of glucose was obtained in the second phase of the combined process, which is much higher than typical yields obtained in the single process operating with *Rp. palustris* [0.21-2.76 mol H₂ (mol hexose)⁻¹]. The photo-fermentation of effluents derived from previous dark fermentations is a promising process, giving the possibility to recover energy from spent media that still contain reduced carbon sources. As it appears from the results, it was possible to obtain H₂ with a high yield

from a salt-rich medium, which usually is not suitable for growing PNSB. However, the concentration of salts plays a crucial role for the production of H₂ by photo-fermentation.

Acknowledgments. This study was supported by the Italian Ministry of the Environment (MATTM; PIRODE project) and by MIUR and CNR (EFOR project).

1 Patel S.K.S, Kumar P, Kalia V.C. Enhancing biological hydrogen production through complementary microbial metabolisms: Review. Int J Hydrogen Energy 2012; 37: 590- 603.

Promotion Effect Of Precious Metals On Ni/ γ -Al₂O₃ Catalyst In Selective CO Methanation (HPO3-4)

Woohyun Kim¹, Heung-ju Lee^{1,2}, Kee Young Koo¹, Wang Lai Yoon^{1*}

¹Hydrogen and Fuel Cell Department, New and Renewable Energy Research Division, Korea Institute of Energy Research (KIER), 152 Gajeong-ro, Yuseong-gu, Daejeon, 305-343, Republic of Korea

²Department of Chemical and Biomolecular Engineering, Yonsei University, 50 Yonsei-ro, Seodeamun-gu, Seoul 120-749, Republic of Korea

*corresponding author: wlyoon@kier.re.kr

Low temperature polymer electrolyte membrane fuel cells (PEMFCs) for distributed power use are vulnerable to carbon monoxide (CO) due to the irreversible adsorption of CO on platinum catalyst in the fuel cell stacks. Since an ordinary fuel processor producing hydrogen from natural gas combines steam reforming reaction and water-gas-shift reaction, the reformed gas contains approximately 1 % of CO. Thus, effective CO removal processes that can maintain the concentration of CO in hydrogen gas fed into the fuel cells below 10 ppm is necessary when the produced H₂ is fed into PEMFCs. The preferential oxidation (PrOx) of CO, selectively converting CO into carbon dioxide (CO₂) by oxidation, has been considered as one of the most successful CO removal processes for a fuel processor. However, the PrOx process can be the limitation to cost-effective design of fuel processors since the process requires the additional systems for air supply and has difficulty to control the excessive reaction heat.

To overcome the drawbacks of a PrOx process, selective CO methanation in the presence of CO₂ and H₂ can be an efficient CO-removal strategy for the fuel processors. Since the methanation process utilizes the reaction of CO and H₂ which exist in the reformed gas, any additional systems and materials are not required. Thus, selective CO methanation process can be the key to designing a compact fuel processor. To develop an effective selective CO methanation process, an appropriate catalyst has to be designed to meet the requirements as follows:

- Activity: The catalytic activity should be good enough to maintain the CO concentration of the reformed gas below 10 ppm.
- Selectivity: The side reactions (reverse water-gas-shift reaction and CO₂ methanation) unnecessarily consume hydrogen so CO selectivity should be higher than 50 %.
- Wide operating temperature: For the stable operation of the fuel processor, aforementioned requirements, both activity and selectivity, should be met under the wide operating temperature range of 200 – 250 °C.

In this work, we have selected nickel as the primary component of the selective CO methanation catalysts since commercial catalyst for CO methanation. However, the activity and selectivity of the nickel catalysts are not sufficient for the selective CO methanation of fuel processors so some modifications have been made to the basic nickel (Ni) catalyst. Firstly, we have prepared highly dispersed Ni-MgO/ γ -Al₂O₃ catalysts by deposition-precipitation method because the preparation method can improve metal loading with high dispersion and magnesium (Mg) is considered to

stabilize the highly dispersed nickel particles. Secondly, we have considered addition of novel metals in order to improve low-temperature activity and selectivity to CO. To select proper promoters, various chemical properties which may affect the activity and selectivity, e.g. adsorption intensity of CO/CO₂, H₂-spillover characteristics, etc., have been considered and four novel metals, Ru, Rh, Ir and Pt, have been chosen. The 1 wt% of these novel metals is added to the prepared Ni-based catalyst by impregnation method. All the prepared catalysts have been characterized by X-ray diffraction, BET surface area, H₂ chemisorption, CO/CO₂ temperature programmed desorption analyses. The catalytic performance tests have been carried out under the following experimental conditions which are similar to the reformed gas after water-gas-shift reaction:

- Gas hourly space velocity (GHSV): 2400 /h
- Gas composition: 1 vol% CO, 20 vol% CO₂, 15 vol% steam, 5 vol% nitrogen and hydrogen balance
- Reactor: a quartz tube (inner diameter: 1.04 cm)

Through the catalytic performance tests, the activity and selectivity have been analyzed with respect to temperature (see Figures 1 and 2). Thus, the promotion effect of precious metals to the nickel-based catalyst has been evaluated and this work will be contributed to the development of the cost-effective selective CO methanation catalysts for fuel processors.

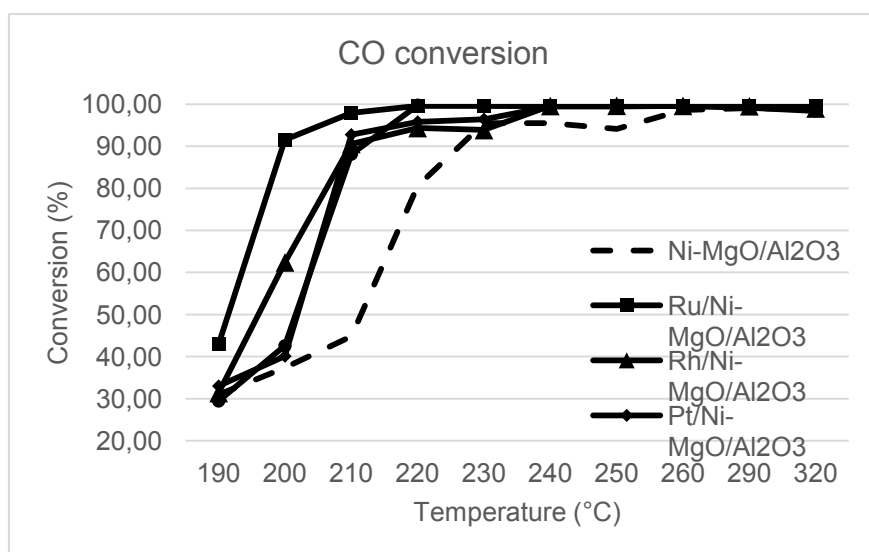
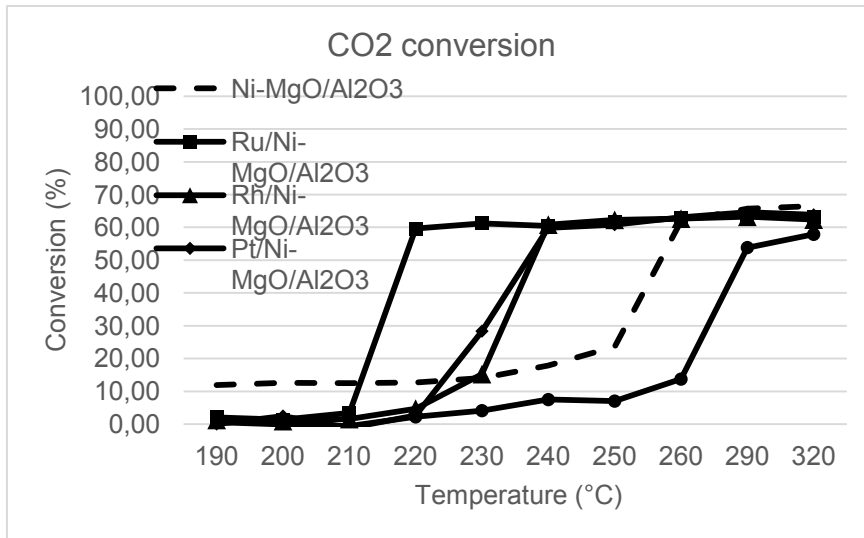


Figure 7. CO conversion

Figure 8. CO₂ conversion

Microreactors technology for Hydrogen Production and Purification (HP03-5)

*S. Palma, O.H. Laguna, A. Perez, S. Ivanova, F. Romero-Sarria, M.A. Centeno, J.A. Odriozola
Department of Inorganic Chemistry and Institute of Materials Science of Seville, University of Sevilla-
CSIC, Sevilla, Spain*

Nowadays the scientific interest in fuel cell (FC) technology is concentrated on the use of portable electronic devices to replace or supplement batteries for portable applications. FCs provides instant, environmentally clean and safe way to produce power with high energy densities (four to six times larger) as compared to Li-ion batteries. However, they have limited power capacity and cannot respond to the sudden changes in the load that may occur in some applications. These problems could be overwhelmed by the use of polymer electrolyte membrane fuel cells (PEMFCs) considered to enhance the energy density of the batteries, to possess a rapid start up time and low temperature operation regime. The PEMFCs are generally fueled by H₂ produced from hydrocarbons, ammonia or chemical hydrides, depending on the power requirements of the FC and between them the hydrocarbon reforming is the most viable H₂ production process. Usually, the steam reforming is preferred since it provides the highest hydrogen carbon monoxide (H₂/CO) molar ratio of 3. Although the fuel processing reactors are designed to maximize H₂ production through steam reforming, partial oxidation or autothermal reforming reactions also occur giving rise to other compounds such as H₂O, CO, CO₂ and some other molecules coming from hydrocarbons incomplete transformation [1].

The use of the FC for portable applications requires at first place diminution of the volume and weight of the reactors and when the PEMFCs are selected an additional and very important requisite takes the advantage, the lowering of the CO concentration to trace levels. Although, the hydrogen production is well known process and universally used in fixed bed catalytic reactors, the process intensification and the resolution of the volume and weight reactors limitation for a on board H₂ production is possible by applying the microreactor technology. The microreactors have the advantage of fast response time, easy integration, and small footprint, all of them ideal for portable power systems. The second and the most important problem of CO concentration could be solved by the application of the H₂ purification reaction, as water gas shift (WGS) followed by the preferential CO oxidation (CO-PROX) and methanation reaction if needed.

Nevertheless, when speaking about portable devices, generally the methanol is selected as a fuel for on-board reforming/purification H₂ production, due to the possibility for low CO production and the low temperature operating range of the reforming reaction. The use of methanol includes also and additional value the possibility to omit the WGS CO purification unit, known as the highest volume requiring unit. Then the CO-PROX reaction unit becomes the principal purification unit.

In this context, this work presents the description of the microreactor technology application to the CO-PROX reaction. The reactor using conventional CuO_x/CeO₂ is applied and the results are discussed in comparison to the use of fixed bed reactor and as a function of the methanol concentration in the reaction feed.

RESULTS

The CuOx/CeO₂ coated microreactor was successfully tested on the CO-PROX reaction under a simulated reformat feed. The maximum CO conversion was obtained at around 140°C for both fixed and microreactor, but the oxygen selectivity to CO₂ was higher when microreactor is used (Fig 1).

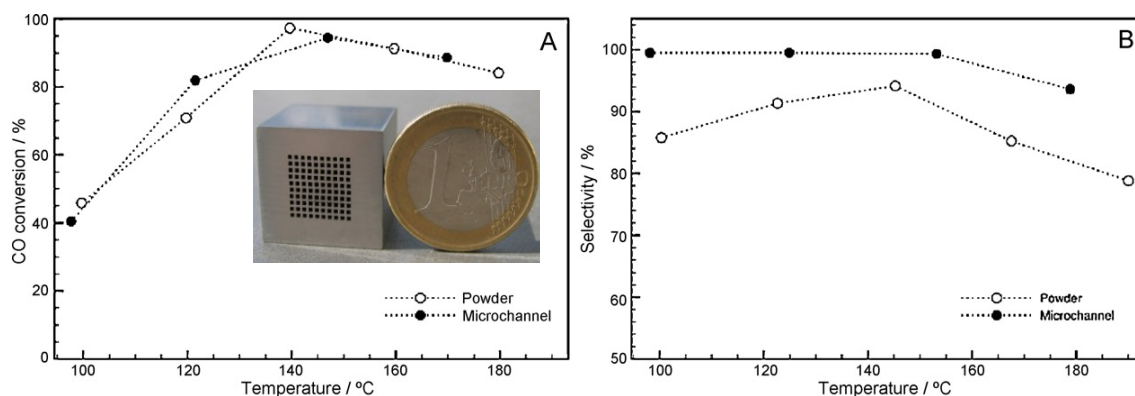


Figure 1. Microreactor vs. Fixed reactor

The modeling and the simulation of the microreactor using a computational fluid dynamics (CFD) was successfully validated for the first time with the experimental catalytic results and the influence of the catalysts loading was also considered. The kinetic parameters were included in the model and corroborated with the experimental results.

The integration of methanol reforming and PROX reaction involves the presence of non-converted methanol and water in the inlet stream of the PROX feed. Therefore, the effect of these products on the performance of the catalyst is essential for the integration of both processes. The influence of the methanol (MeOH) to the CO-PROX activity of the microreactor is presented in Figure 2. A negative effect on the CO-PROX activity was observed with the increase of the methanol concentration. A model CuOx-CeO₂ catalysts was also studied by in situ DRIFTS in order to explain its catalytic behavior in the presence of methanol and water. This correlation helped the identification of the reaction intermediates and allows the modification of the catalyst formulation, in order to achieve more robust catalysts in this process.

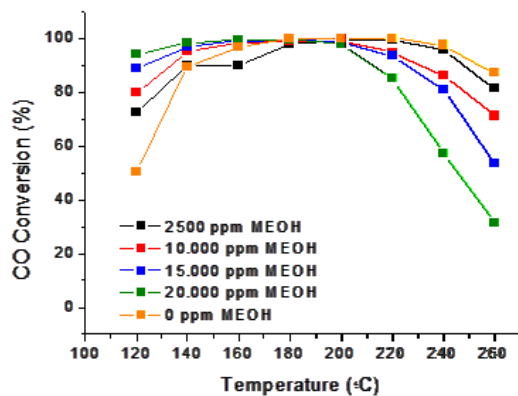


Figure 2. CO-PROX activity vs. methanol concentration

In summary this study evolves all the steps of the microreactor technology: from the microreactor arming through the catalyst washcoating to the evaluation of its activity in the harsh real conditions of potential on board application.

REFERENCES

[1] S. Ivanova, O.H. Laguna, M.A. Centeno, A. Eleta, M. Montes, J.A. Odriozola, in RENEWABLE HYDROGEN TECHNOLOGIES, (Eds. L. Gandia, G. Arzamendi, P. Dieguez), Elsevier 2013.

CO preferential oxidation over Co₃O₄-CeO₂ catalysts synthesized by freeze-drying method (HP03-6)

A. Arango-Díaz^a, J.A. Cecilia^a, J. Marreno-Jerez^b, P. Nuñez^b, J. Jiménez-Jiménez^a, A. Jiménez-López^a, E. Rodríguez-Castellón^a

^a Departamento de Química Inorgánica, Cristalografía y Mineralogía, Universidad de Málaga, Campus de Teatinos 29071, Málaga, Spain

^b Departamento de Química Inorgánica, Universidad de la Laguna, Av. Astrofísico Fco. Sánchez s/n 38206, La Laguna, Tenerife, Spain

Introduction

Hydrogen is a promising energy carriers for power generation, especially for proton exchange membrane fuel cells (PEMFCs) which have received much attention for mobile and small stationary power sources due to some advantages such as high efficiency, low temperature operation (, low cost, fast start-up, and environmental friendliness [1]. However, hydrogen-rich gas supplied to PEMFCs must be free from carbon monoxide (CO) due to the presence of CO poisons the Pt catalyst in the PEMFC anode. Among the popular methods for CO removal from the H₂-rich gases, the preferential catalytic oxidation of CO (CO-PROX) have been considered the most straightforward and cost effective method to decrease the CO concentration [2]. The CO-PROX catalysts can be classified in two categories. The first one is noble metal based catalysts as Au, Pt, Ru, Ag [3]. Nevertheless these catalysts have a poor availability and a high price. The other catalysts are non-precious based catalysts as Cu or Co, which associated to ceria CeO₂ leading to a catalytic systems with a high selectivity and stability in a wide temperature range for CO-PROX reaction due to its redox behavior. The literature recompiles a plethora of researchers of CuO-CeO₂ systems; however Co₃O₄-CeO₂ has been less studied in the literature [4]. This work describes the preparation of nanocrystalline CeO₂ based materials by freeze-drying method which presents advantages as the absence of diffusion process in their synthesis and their performance in the CO-PROX reaction at low temperatures (65-190 °C).

Experimental

Polycrystalline CuO-CeO₂ and Co₃O₄-CeO₂ were synthesized by freeze-drying method, using Ce(NO₃)₃·6H₂O, Cu(NO₃)₂·6H₂O and Co(NO₃)₂·6H₂O as precursors. The reagents were dissolved in water and then ethylenediaminetetraacetic acid (EDTA) was added as complexing agent to prevent precipitation in a 1:1 ligand:metal molar ratio. The pH of the solutions was adjusted at 7-8 by adding aqueous ammonia. The solutions were flash frozen dropwise into liquid nitrogen and dried in a freeze-dryer for 3 days. The amorphous precursors were calcined at 300 °C for 2 h to prevent rehydration and to eliminate the organic matter. Finally, the powders were calcined at 400 °C for 4 h [5]. The catalysts were labeled as XCUCE and XCOCE, where X denoted the loading of copper or cobalt wt.% of each catalysts. The catalytic systems were studied by X-ray diffraction (XRD), hydrogen temperature-programmed reduction (H₂-TPR) and X-ray photoelectron spectra (XPS).

Catalytic Results

Catalytic tests were carried out in a fixed bed reactor at atmospheric pressure controlled by interior place thermocouple in direct contact with the catalysts. The samples were pretreated in-situ under flowing air for 30 min at 400 °C, followed by cooling to rt in He flow. The contact time W/F was 0.18 g s cm⁻³ (GHSV = 22,000 h⁻¹). The reaction mixture composition was 1.25% CO, 1.25% O₂, 50% H₂, balanced with He. The effect of CO₂ and H₂O was examined with the addition of 15% CO₂ and 12% H₂O. The temperature was varied in the 65-190 °C range, and measurements were carried out till a steady state was achieved. The carbon monoxide and oxygen conversions and the selectivity toward CO₂ were calculated as described elsewhere [6]. The excess of oxygen factor (l) used was 2 because this value was previously found optimal for CO-PROX [6].

Figure 1A compiles XRD diffractograms of fresh and used Co₃O₄-CeO₂ catalyst. The samples with Co show broad diffraction lines, which indicate a low particle size located at 2Θ 28.5, 33.4, 47.5 and 56.5° assigned to cerianite. Moreover it is not noticeable the presence the diffraction lines assigned to Co₃O₄, which suggests a high dispersion of this phase in the cerianite phase. In the other side, the redox properties of these materials were tested through H₂-TPR (Figure 1B). H₂-TPR profiles reveals four reduction peaks denoted as α_1 , α_2 , β_1 and β_2 . The first peak located at lower temperature has been ascribed to the reduction of Co³⁺ dispersed in close contact with CeO₂ surface to Co²⁺. The second peak is attributed to the reduction of Co³⁺ forming small clusters with ceria phase to Co²⁺. The third peak has been assigned to the reduction from Co²⁺ dispersed to Co⁰ and finally the fourth peak can be attributed to the reduction of the Co²⁺ species agglomerates in small clusters to Co⁰[7].

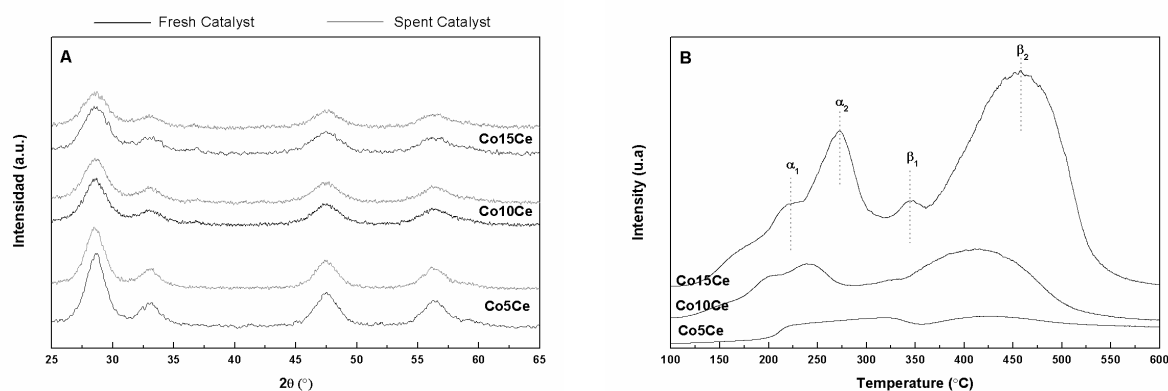


Figure 1 A) XRD diffractograms of fresh and spent CoXCe catalysts and B) H₂-TPR of CoXCe catalysts.

The catalytic results of the CuO-CeO₂ and Co₃O₄-CeO₂ systems show which the CO conversion (Figure 2A) increases with the reaction temperature, being more evidence for catalyst with the higher spinel cobalt content. The sample with copper is more active than all the cobalt systems and the conversion of CO to CO₂ is total from 115°C. With regards to the selectivity (Fig. 2B), CO₂ selectivity decreases at higher temperatures due to the competitive oxidation of H₂. The resistance to CO₂ and H₂O of these catalysts were also evaluated. Catalytic data reveals that the catalyst with

the highest cobalt content presents a high resistance to the CO₂ requiring a low cobalt content that previous researchers show in literature [8]. In Cu catalyst, the presence of CO₂ reduces the CO conversion possibly for competitive adsorption of CO and CO₂ and the formation of carbonates on the catalyst surface [9]. However, all catalyst suffer a hard blocks of the active centers by the presence of water in the reaction obtaining high CO conversion out of the temperature range of PEMFCs cells.

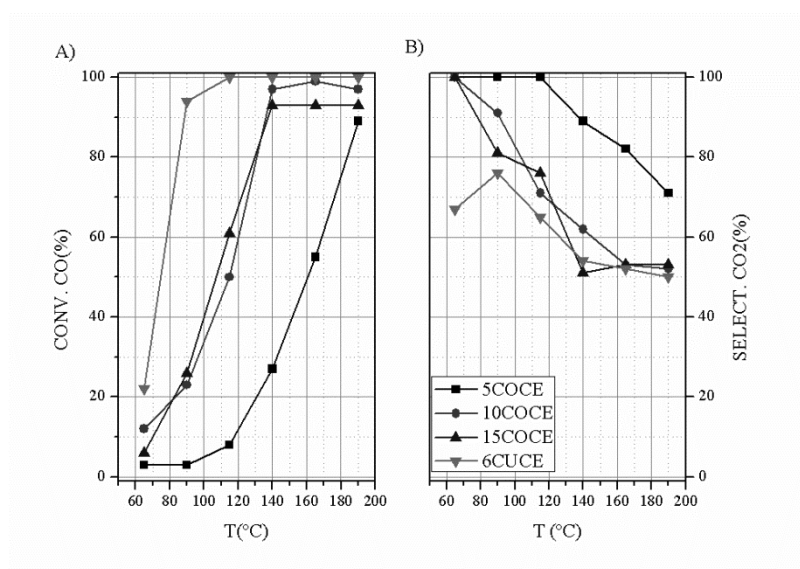


Figure 2. A) CO conversion and B) Selectivity to CO₂ as function of the temperature over the XCOCE and XCUCE catalysts. Operating conditions: GHSV = 22,000 h⁻¹, $\lambda = 2$, 1.25% CO, 1.25 %O₂, 50% H₂, He balance (%vol).

References

- [1] A.F. Ghenciu, *Curr. Opin. Solid State & Materials Science*. 6 (2002) 389.
- [2] J.D. Morse, *International Journal of Energy Research*. 31 (2007) 576-602.
- [3] P.C. Hulteberg, J.G.M. Brandin, F.A. Silversand, M. Lundberg, *International Journal of Hydrogen Energy* 30 (2005) 1235-1242.
- [4] A. Mishra, R. Prasad, *Bulletin of Chemical Reaction Engineering and Catalysis* 6 (2011) 1-14.
- [5] D. Pérez-Coll, P. Nuñez, J.R. Frade, J.C.C. Abrantes, *Electrochimica Acta* 48 (2003) 1551-1557.
- [6] E. Moretti, M. Lenarda, L. Storaro, A. Talon, T. Montanari, G. Busca, E. Rodríguez-Castellón, A. Jiménez-López, M. Turco, G. Bagnasco, R. Frattini, *Applied Catalysis A: General* 335 (2008) 46-55.
- [7] T. Bao, Z. Zhao, Y. Dai, X. Lin, R. Jin, J. Guiru, G. Wang, T. Muhammad, *Applied Catalysis B: Environmental* 119-120 (2012) 62-73.

[8] P. Gawade, B. Bayram, A.M.C. Alexander, U. S. Ozkan, Applied Catalysis B: Environmental 128 (2012) 21–30.

[9] D. Gamarra, A. Martínez-Arias. Journal of Catalysis 263 (2009) 189–195.

Effects of preparation method, carriers and promoters on the reactivity of cadmium and zinc sulfide systems in the water splitting reaction under visible light irradiation (HP04-1)

Francesco Arena a,b, Elena Balentseva c, Gloria Berlier c, Enrico Boccaleri d, Giorgio Gatti d, Lorenzo Spadaro b, Giuseppe Trunfio a

a) Department of Electronic Engineering, Industrial Chemistry and Engineering, University of Messina, Viale F. Stagno D'Alcontres 31, 98166 Messina, Italy

b) CNR-ITAE Institute "Nicola Giordano", Salita S. Lucia 31, 98126 S. Lucia, Messina, Italy

c) Department of Chemistry and Interdepartmental Centre of Excellence "Nanostructured Interfaces and Surfaces-NIS", University of Torino, via P. Giuria 7, 10125 Torino, Italy

d) Department of Science and Technological Innovation, University of the Eastern Piedmont "A. Avogadro", Viale T. Michel, 11 – 15121 Alessandria, Italy

Abstract

The effects of preparation method, carriers and dopants on the reactivity of CdS and ZnS materials in the water splitting reaction under visible light irradiation (WSR) have been investigated. The influence of textural and structural properties on the WSR performance of bare sulfide systems has been assessed. Physico-chemical characterization by TEM, XRD, XPS and Uv-vis spectroscopic techniques shed lights into the main structural requirements promoting the WSR activity of sulfide systems.

Introduction

As world population growth placing more demand on fossil fuels, the exploitation of renewable energy sources becomes crucial as solution to current energy and environmental dilemmas. Indeed, the continuously rising concentration of CO₂ in the atmosphere, expected to double current levels (≈400 ppm) before 2050, represent to date a major environmental threat, owing to the unpredictable consequences of the greenhouse effect, responsible of the global warming and climate changes in place [1]. Therefore, the middle-long term availability of renewable energy sources is compulsory to shift toward a sustainable development pattern. In this context, hydrogen is destined to play a pivotal role, since established "hydrocarbons-free" hydrogen manufacture processes would allow a series of environmental benefits, such as: i) the use for fuel-cells and automotive engines systems; ii) a systematic CO₂ recycle for "clean" fuels manufacture iii) and a strong CO₂ emissions cut from industrial ammonia and methanol synthesis loops [2]. This because currently employed fossil-fuels reforming processes cause huge CO₂ emissions and depletion of raw materials, while the hydrogen production by the catalytic water splitting under solar light irradiation (WSR) represents a very attractive potential way solving, at once, energy and environmental problems having also the advantage of a worldwide availability without any geographic restriction of raw materials location [3,4].

Since the pioneering work of Fujishima and Honda [5], plenty of systems have been shown to drive the WSR, though whatever industrial scale application is hindered by the lack of stable photo-

active materials for water reduction-oxidation [3]. Then, cadmium sulfide is still one of the most efficient water photoreducing materials under visible light irradiation, although relevant corrosion problems and environmental threat due to its high toxicity toward living species. This prompted a big research concern on alternative materials, being generally known that composition, crystallinity and particle size control the functionality of whatever WSR system [3,4,6,7].

Therefore, this study is aimed at providing a systematic assessment of the WSR activity of CdS in comparison to ZnS based systems, obtained via different synthesis routes. In addition, the effects of high surface area inorganic matrices carriers and dopants on the reactivity of CdS and ZnS phases, respectively, are highlighted.

Experimental

Bulk CdS and ZnS catalysts were prepared by the following three different synthesis procedures:

the classical precipitation method, involving the addition of an aqueous solution (0.2 L) of Cd(CH₃COO)₂·2H₂O or Zn(CH₃COO)₂·2H₂O precursors to Na₂S solutions (0.2 L) under vigorous stirring. After precipitation, the solids (LL) were filtered, washed with hot distilled water and dried at 100°C (12h).

a gas-liquid synthesis (GL) was performed by flushing aqueous solutions (0.3 L) of the above precursors with a constant flow of H₂S until the complete precipitation of sulfides. The precipitated samples were, then, subjected to the same treatments same of the LL ones.

a gas-solid synthesis (GS) was finally attained by flushing solid beds of the CdCO₃ and ZnCO₃ precursors put into a linear glass reactor kept at 90°C with a H₂S flow. At the end of the sulfidation process, the samples were washed with hot acidic water (H₂SO₄) to eliminate residual carbonate traces.

In addition, mesoporous silicas (SBA 15 and MCM-41) were also used to synthesize supported CdS systems, while various nanostructured composite MexZn1-xS systems (Me: Cu, In, Co, Ni; 0≤x≤0.1) with particle size of 2-4 nm were obtained by co-precipitation of the acetate precursors dissolved in ethanol, using thioacetamide as sulfur source.

The composition of the samples was determined by XRF analysis, using a Bruker AXS-S4 Explorer Spectrometer. Surface Area (SA) values were determined by the BET elaboration of N₂-adsorption isotherms (77K), obtained using a ASAP 2010Micromeritics Instrument). X-ray diffraction (XRD) analyses were performed by a Philips X-Pert diffractometer, operating with Ni β-filtered Cu Kα radiation (40 kV; 30 mA) and a scan rate of 0.05°/min. Catalytic tests were performed in a jacketed quartz reactor, loaded with 0.2 g of catalyst and a 0.25 L solution of Na₂S/Na₂SO₃ (0.1 M), flushed with Ar flow (20 mL/min) and kept in isothermal conditions (25°C) by the external recirculation of cooling water. The produced H₂ was periodically analyzed by a GC equipped with a TCD.

Results and Discussion

XRF analyses generally confirm the stoichiometric composition of the catalysts, according to XRD measurements showing very small peaks of the octavite (CdCO₃) phase only on the CdS(GS) sample

(Fig. 1). In addition, the preparation method strongly influences the catalyst structure and texture, as the CdS(LL) and CdS(GL) samples feature an analogous SA value (135 m²/g), much greater than that of the CdS(GS) catalyst (13 m²/g). This is in agreement with the considerably broader and poorly resolved XRD pattern of the former samples, denoting a much smaller particles size in comparison to much sharper diffraction peaks of the CdS(GS) material, which are diagnostic of a high degree of crystallinity.

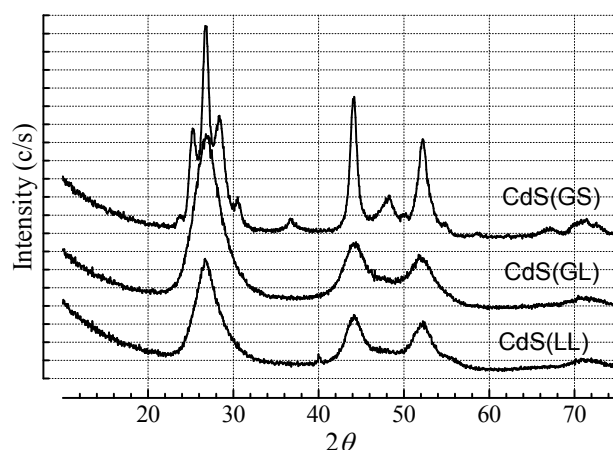


Figure 1. XRD patterns of the various CdS samples.

Bulk, composite and supported sulfide materials were characterized by TEM and diffuse reflectance UV-Vis spectroscopy, to assess the presence of nanocrystalline semiconductor particles and to highlight the related electronic features, respectively.

UV-Vis measurements confirm the quantum-confinement effect on both the reference CdS(GS) and supported CdS systems, with energy gap values of 2.47-2.48 eV.

The results of preliminary WSR tests, shown in Figure 2, indicate that the physico-chemical properties induced by the preparation method play a crucial influence on the photocatalytic activity of the bulk CdS system (Fig. 2A). Indeed, the CdS(GS) sample features a twofold higher activity level than the CdS(GL) one resulting, in turn, more than two times active than the CdS(LL) material. Notably, Figure 2B also shows that environmental-friendly Zn-based systems, like Zn_{0.95}Ni_{0.05}S and Zn_{0.95}Cu_{0.05}S, feature activity levels comparable with that of the most reactive CdS(GS) sample.

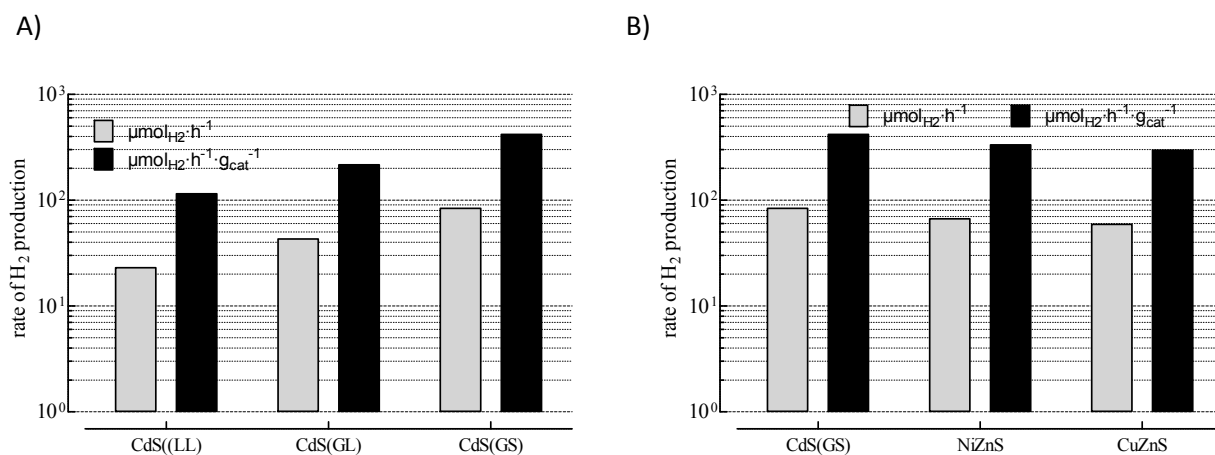


Figure 2. (A) WSR data of bulk CdS samples obtained via different synthesis routes and (B) comparison of the WSR performance of different bulk sulfide systems.

Conclusions

The preparation method strongly affects the physic-chemical and photocatalytic activity of the bulk CdS system. A new gas-solid sulfidation method, strongly enhancing the photocatalytic efficiency in comparison to conventional gas-liquid and liquid-liquid precipitation routes, has been disclosed. The influence of carriers and dopants on the performance of CdS and ZnS has been ascertained. Studies in progress disclose that synthesis route and chemical composition are key factors that could allow an effective replacement of toxic CdS with more environmental-friendly materials.

Acknowledgements

Italian Ministry for University and Research (MIUR) is gratefully acknowledged for funding through the program PRIN2009.

References

- [1] Our earth in 2050 (2013) <http://greenphysicist2.blogspot.it>
- [2] G.A. Olah, A. Goepfert, G.K. Surya Prakash, J. Org. Chem., 74 (2009) 487.
- [3] A. Kudo, Y. Miseki, Chem. Soc. Rev., 38 (2009) 253.
- [4] K. Maeda, K. Domen, J. Phys. Chem. C, 111 (2007) 7851.
- [5] A.K. Fujishima, K. Honda, Nature, 238 (1972) 37.
- [6] K. Maeda, K. Domen, Chem. Mater., 22 (2010) 612.
- [7] K. Maeda, K. Domen, J. Phys. Chem. Lett., 1 (2010) 2655.

Effect of temperature used in the solvothermal synthesis on the structure and photoactivity of CdS for hydrogen production under visible light (HP04-2)

F. Vaquero*¹, R.M. Navarro*¹, J.L.G. Fierro¹

*1 Institute of Catalysis and Petrochemistry (CSIC), Sustainable Energy and Chemistry Group (EQS)
C/Marie Curie 2, 28049, Madrid, Spain*

() corresponding author: f.vaquero@csic.es; r.navarro@icp.csic.es*

Keywords: Cadmium sulfide, Water Splitting, Hydrogen, Solvothermal method, Nanostructures

1 INTRODUCTION

The conversion of solar energy into hydrogen via the water splitting process assisted by photoconductor is one of the most interesting ways of achieving clean and renewable energy systems [1]. Among photocatalysts able to decompose water under visible light, cadmium sulfide (CdS) is an interesting photocatalyst material, since it has a narrow band gap (2.4 eV) and a valence and conduction band a suitable potential to effectively produce hydrogen and oxygen from aqueous solutions. However, it presents a series of disadvantages as their toxicity and photocorrosion under visible light irradiation, which limits their photocatalytic use. The utilization of a suitable sacrificial agent reduces the photocorrosion and increases the photocatalytic efficiency of the CdS. There are different strategies to improve the photocatalytic properties, stability and activity of CdS catalysts, including control of the structure and morphology of CdS, directly related with the method of preparation of photocatalyst. Various methods, such as coprecipitation, sol-gel, hydrothermal/solvothermal method, chemical vapour deposition process, template method, thermal decomposition method, and thermal evaporation have been explored to prepare CdS nanostructures with various morphologies. The solvothermal method allows obtaining nanoparticles of CdS using a solvent different from water at moderate temperature and pressure [2]. It is well known that the size and shape of nanocrystals synthesized by solvothermal methods depend on the solvent agent, the metal sources, temperature and time [3]. However, few reports have been concerned on the effect of preparation variables in the solvothermal method applied to formation of CdS nanostructures [4]. With this background, the present work aims to study the influence of the temperature used in the solvothermal synthesis on the characteristics of the CdS nanocrystals, analysing the consequences on their photophysical properties as well as in their photoactivity for water splitting under visible light.

2 Experimental/methodology

CdS nanocrystals were prepared by solvothermal method using a Teflon-lined stainless steel autoclave charged with 0.0104 mol of cadmium nitrate tetrahydrate ($\text{Cd}(\text{NO}_3)_2 \cdot 4\text{H}_2\text{O}$), 0.0312 mol of thiourea (NH_2CSNH_2) solved in ethylenediamine (en). Finally, was added 0.0208 mol of water to promote the total hydrolysis of the thiourea. The autoclave was tightly closed, heated at the selected temperatures (120, 150 and 190 °C) for 12 h and left to cool down to room temperature in an oven. The yellow precipitates were collected by centrifugation, washed with distilled water several times, washed with absolute ethanol to remove the excessive thiourea and other byproducts, and then dried under vacuum at 70 °C for 2 h. CdS samples were characterized by chemical analysis (TXRF), N2

adsorption-desorption isotherms at 77 K, UV-Vis spectroscopy, X-ray diffraction (XRD), Scanning electron microscopy (SEM), transmission electron microscopy (TEM) and high resolution TEM (HRTEM). Photocatalytic activities will be evaluated in a closed Pyrex glass reactor working at room temperature under Ar at atmospheric pressure. The photocatalyst powder (0.05 g) was dispersed by magnetic stirring in an aqueous solution (150 mL) containing 0.05 M Na₂S/0.02 M Na₂SO₃ as sacrificial reagents. The photocatalyst is irradiated for 5 h with a 150 W Xe OF arc lamp.

3 Results and discussion

Table 1 shows the atomic percentages of Cd and S obtained from TXRF analyses of CdS samples. As observed in Table 1, all the prepared CdS samples have similar surface coordination of Cd with S irrespective of the temperature used during the synthesis. Textural data of CdS samples show that the surface area of CdS decreases with the increase of the synthesis temperature. This fact is indicative of changes in the size and morphology of the CdS particles induced by the temperature used in the synthesis. SEM and TEM-HRTEM images presented in Figure 1.2 corroborated this fact. Morphological analysis of CdS samples by SEM showed changes in the agglomeration of CdS crystallites synthesized at different temperatures. Samples prepared at 120 and 150 °C showed irregular clusters of particles heterogeneous in size, ranging from 0.7 to 12 μm, while the sample prepared at 190 °C showed filamentous structures of few microns of length. TEM images of CdS samples (Figure 1.2) presented the formation of nanorods with different degree of crystallinity, length and width depending on the temperature of synthesis. The increase in the temperature of synthesis leads to nanorods with higher degree of crystallinity, more defined shape and greater length and width (Table 1).

Table 1. Surface composition (atomic percentage from TXRF analyses), textural data (from N₂ adsorption), band gap (from UV-Vis spectroscopy), nanorods properties (from TEM-HRTEM) and hydrogen production of CdS 120, 150 and 190 °C photocatalysts.

Catalyst	Cd (%)	S (%)	BET (m ² /g)	BG (eV)	TEM Length (nm)	TEM Width (nm)	H ₂ production (μmol/g cat)
CdS-120	46.7	5.3	75.5	2.5	32 - 69	5.8 - 10.4	142,7
CdS-150	48.2	5.1	49.7	2.5	56 - 141	8.3 - 17.8	91,9
CdS-190	46.7	5.3	25.7	2.5	292 - 1334	- 22.9 - 42.4	46,9

XRD patterns of the CdS samples (Figure 1.1) displayed reflections corresponding to the formation of CdS with a hexagonal crystal structure (JCPDS. 77-2306). As the solvothermal temperature increase, the crystallinity of the samples improves. In the samples prepared at lower temperature the relative intensity of the (002) peak was more intense than expected for the hexagonal phase. This

indicates that there is a relatively high crystalline order along the c-axis, whereas the order in the x-y plane is poor at low temperature. As the solvothermal temperature increases the intensities of (100) and (101) peaks increases while the (200) peak decreases. This represents the development of crystallinity in the x-y plane and the preferential orientation along the c-axis of nanorods formed at higher temperature as was showed previously by HRTEM analysis (Figure 1.2). The structural and morphological changes associated with solvothermal temperature did not cause differences in the optical properties of photocatalysts. Band gap for each sample, calculated from absorbance spectra, is given in Table 1. The UV-Vis results show similar band gap size in samples irrespective of the temperature used in the synthesis. Samples showed a band gap energy of 2.5 eV which is higher than that of bulk CdS (2.42 eV) probably due to a band tail due to disorder effects.

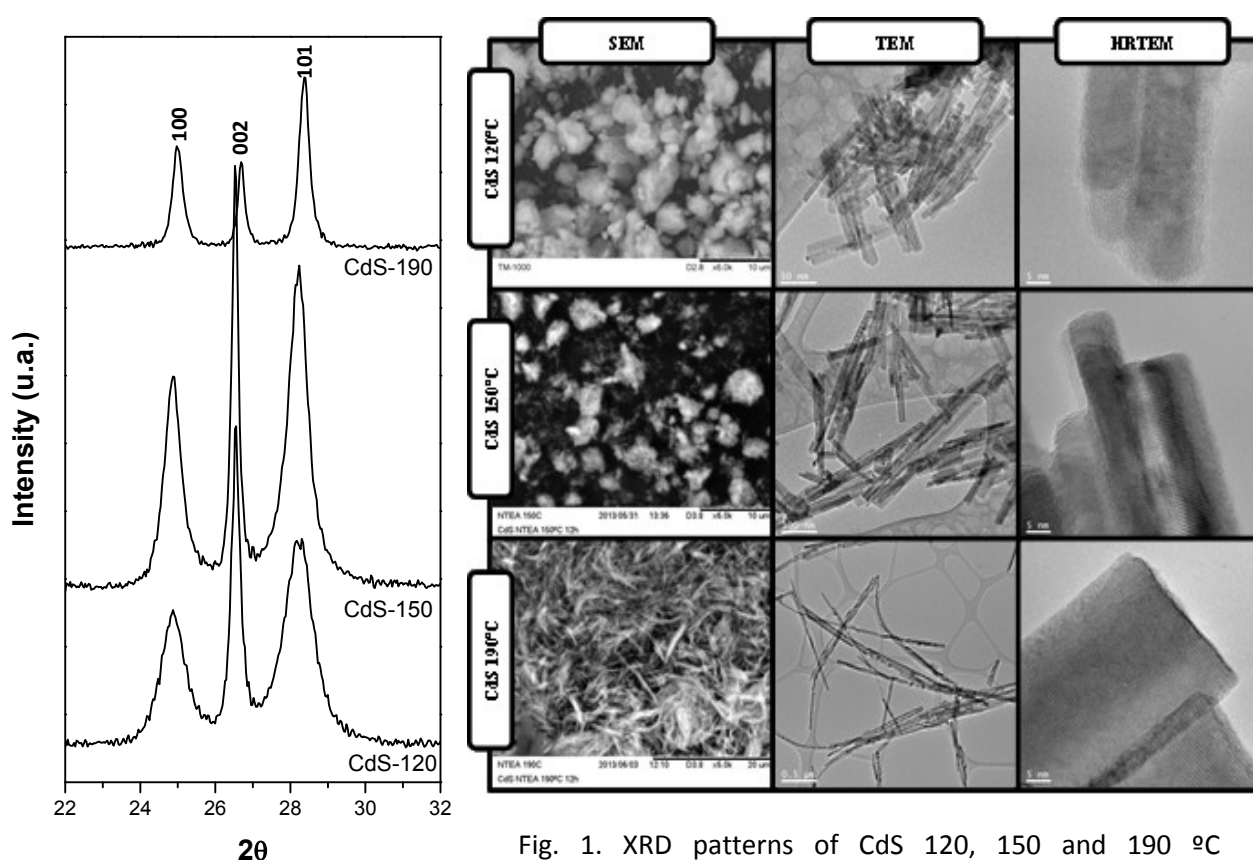


Fig. 1. XRD patterns of CdS 120, 150 and 190 °C photocatalysts (1). SEM, TEM and HRTEM images of CdS 120, 150 and 190 °C photocatalysts (2).

Table 1 shows the hydrogen production under visible light irradiation over CdS samples synthesized at different solvothermal temperatures. It is observed a decrease in the hydrogen production with the increase in the temperature used in the synthesis. It is known that photoactivity of catalysts is influenced by the process of generation, separation, recombination and migration of photogenerated charge carriers. In general, high photoactivity of catalysts is associated with well developed surface area and well defined crystallinity. The comparison of activity data with the structural characterization showed that the variation in the surface area of the CdS samples, more than crystallinity that follow an opposite trend, influences notably in the activity. Therefore, under

our preparation conditions, the negative effect of lower surface area seems dominant over the positive effect of increased crystallinity associated to the higher solvothermal temperature used in the synthesis of CdS.

4 Conclusions

CdS nanorods obtained from solvothermal synthesis were investigated for the hydrogen production from aqueous solutions containing $\text{SO}_3^{2-}/\text{S}^{2-}$ as sacrificial reagents under visible light. The temperature used in the solvothermal synthesis has influence on the surface area, shape, length and degree of crystallinity of CdS nanorods synthesized. Higher synthesis temperature favours the formation nanorods of higher crystallinity and length and lower surface area. It is observed a decrease in the hydrogen production with the increase in the solvothermal temperature used in the synthesis that indicates that effect of decrease surface area seems dominant over the increase in crystallinity in the definition of the photoactivity of catalysts synthesized by solvothermal method.

Acknowledgements

The authors would like to express appreciation for the financial support of the Secretaría de Estado de Investigación, Desarrollo e Innovación of Spain through the project ENE2010-21198-C04-01. F.Vaquero also acknowledges Secretaría de Estado de Investigación, Desarrollo e Innovación of Spain for its FPI grant.

References

- [1] R.M. Navarro, F. del Valle, J.L.G. Fierro, *Int. J. Hydrogen Energy*. 33 (2008) 4265-4273.
- [2] P. Dalvand, M.R. Mohammadi, *J. Nanopart Res.* 13 (2011) 3011-3018.
- [3] B.Xu, X. Wang, *Dalton Trans.* 41 (2012) 4179.
- [4] M.A. Mahdi, J.J. Hassan, S.S. Ng, Z. Hassan, *J. Crystal Growth*. 359 (2012) 43-48.

Solar Hydrogen Production from Cellulose Biomass with Enzymatic and Artificial Photosynthesis System (HPO4-3)

Yutaka Amao,^{1,2} Yuka Sakai,³ Satomi Takahara³

In the environmental science and the energy source development, hydrogen gas production from renewable resources of timber waste, including cellulose, lignin, etc. is important. We have previously reported the enzymatic photoinduced hydrogen production from sucrose or maltose as the renewable bio-resources using the light-harvesting function of Mg Chl-a. And the photoinduced hydrogen production from water-soluble methylcellulose using the light-harvesting function of Mg Chl-a, also has been accomplished. However, soluble cellulose derivative, methylcellulose is used as a renewable resource in this hydrogen production system. Thus, photoinduced hydrogen production from renewable resources of timber waste, including insoluble cellulose is not accomplished yet.

In this paper solar hydrogen production system by coupling the waste paper including cellulose biomass with cellulase and GDH, and hydrogen production with platinum colloid via the photoreduction of MV²⁺ using the visible light-harvesting function of Mg Chl-a is developed.

The reaction is started by adding cellulase (1110 units) to a solution containing news paper broken into pieces including cellulose (5.0 g) in potassium phosphate buffer (pH 7.0) in 300 mL of Erlenmeyer flask at 30 °C for 18 h. After reaction, a filtrate was collected by suction filtration. The reaction is started by adding NAD⁺ (18.5 mM) to a solution containing filtrate (120 mL) and GDH (50 units) in phosphate buffer (pH 7.0) in 300 mL of Erlenmeyer flask at 30 °C for 5 h. This solution is defined as NADH formed solution.

Photoinduced hydrogen production is tested in a reaction mixture containing the NADH formed solution (120 mL), Mg Chl-a (9.6 μM), MV²⁺ (2.0 mM) and platinum colloid (5.0 units) in potassium phosphate buffer (pH 7.0) in 300 mL of reaction vessel. The solution is deaerated by nitrogen gas and irradiated with a 200 W halogen lamp at a distance of 3.0 cm. Wavelengths less than 390 nm are removed with a Toshiba L-39 cut-off filter. The amount of hydrogen produced and the other produced gases are measured with a Shimadzu GC-14B gas chromatography (detector: TCD, column temperature: 40 °C, column: active charcoal with the particle size 60-80 mesh, carrier gas: nitrogen gas, carrier gas flow rate: 24 ml min⁻¹).

Figure 1 shows the time dependence of the hydrogen production in the system containing NADH formed solution, Mg Chl-a, MV²⁺ and platinum colloid by the visible light. When the sample solution is irradiated, the hydrogen production is observed as shown in Figure 1. Hydrogen produces continuously and the amount of hydrogen production is estimated to

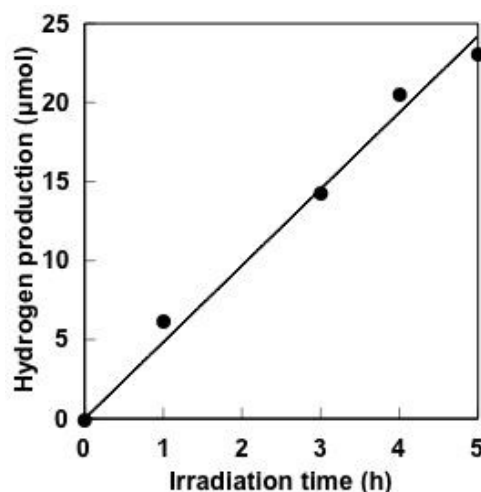


Figure 1. Time dependence of hydrogen production under steady state irradiation with visible light using 200 W halogen lamp at a distance of 3.0 cm. The sample solution is consisted of the NADH formed solution (120 mL), Mg Chl-a (9.6 μM), MV²⁺ (2.0 mM) and platinum colloid (5.0 units) in potassium phosphate buffer (pH 7.0) in 300 mL of reaction vessel.

be 23 μmol after 5 h irradiation. From the result of gases analysis using gas chromatography, hydrogen and argon gases are detected and the other gases such as carbon dioxide is not detected.

This work was partially supported by the Environment Research and Technology Development Fund (ERTDF) (No. K113016), Ministry of Environment, Japan.

Photocatalytic water splitting using CNT-inorganic hybrid materials (HP04-4)

A. Moya¹, A. Cheveran², S. Marchesan³, M. Prato³, D. Eder², J.J. Vilatela¹

¹ IMDEA Materials Institute, Madrid, Spain

² Institute of Physical Chemistry, University of Münster, Germany

³ INSTM, Italy

There is a continuously increasing plethora of new nanostructured hybrid materials with potential application in photovoltaics, energy storage and photocatalysis, etc (1). In the latter, the combination of an inorganic semiconductor with a nanocarbon such as carbon nanotubes (CNT) or graphene, often increases photocatalytic efficiency compared to the semiconductor (2). The increase in efficiency is mainly due to: the presence of the nanocarbon extending the light absorption range of the semiconductor by acting as a photosensitiser; the nanocarbon accepting photoexcited electrons from the semiconductor, therefore separating them from holes and increasing their lifetime. So the hybrid creates a highly conductive network for a more efficient electron transport between the electrodes. The hybrid can also act as substrate and stabilise small semiconductor particles crystallisation with larger specific surface thanks to their growth on the nanocarbon surface (Figure1).

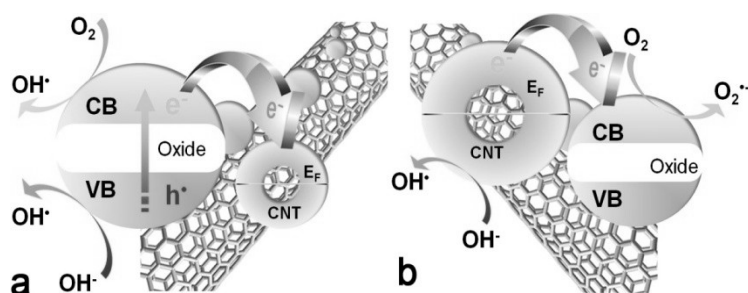


Figure 1. Scheme for possible charge-transfer reactions in nanocarbon–inorganic hybrids: nanocarbon as a) electron donors (i.e., “photosensitisers”) and b) electron acceptor (i.e., “charge separation”).(1)

The main challenges are the optimisation of the nanocarbon/inorganic semiconductor interface, the evaluation of synergistic effects based on interfacial charge and energy transfer processes and the development of novel hybrid architectures with controlled morphologies and pore structures.

Here we present results on the production, characterisation and photocatalytic activity of new hybrids consisting of CNTs and different inorganic semiconductors (e.g. TiO₂, Ta₂O₅, etc.) with superior interfacial properties. The hybrids are produced in-situ by electrospinning of a polymer solution containing the CNTs and metal oxide precursors, followed by thermal annealing to remove the polymer and crystallise the metal oxide (Figure 2). The final fibres have an average diameter of 250nm, with hybrid fibres having a narrower diameter distribution than the pure inorganics. X-ray diffraction and high-resolution transmission electron micrographs show that the inorganic particles in

the hybrid are highly crystalline and have a small size (~ 10 nm). High surface area and very good integration between the CNT and the crystalline metal oxide is achieved. Therefore, the adsorption in the CNT-inorganic interface is improved in order to study the charge and energy transfer processes.

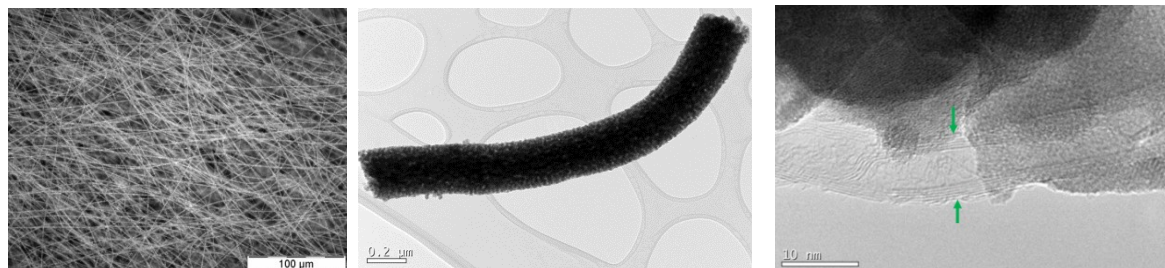


Figure 2. SEM and TEM images of the CNT-TiO₂ hybrid after heat treatment at 500°C/2h.

Finally, we present preliminary data on the efficiency of these new materials for photocatalytic water splitting. Hydrogen evolution data are related to the hybrid final structure and to the degree of chemical functionalisation of the CNTs. The effects of chemical functionalisation on CNT dispersion and on the charge transfer processes at the nanocarbon-inorganic interface are discussed.

1. Vilatela JJ, Eder D. Nanocarbon Composites and Hybrids in Sustainability: A Review. *ChemSusChem*. 2012 Mar 12;5(3):456–78.
2. Ren Z, Kim E, Pattinson SW, Subrahmanyam KS, Rao CNR, Cheetham AK, et al. Hybridizing photoactive zeolites with graphene: a powerful strategy towards superior photocatalytic properties. *Chem. Sci*. 2012;3(1):209–16.

Dynamic Model of a Solar Water Splitting Process based on a Two Step Thermochemical Cycle (HPO4-5)

M. Lange, M. Roeb, C. Sattler, R. Pitz-Paal

Deutsches Zentrum für Luft- und Raumfahrt (DLR), Linder Höhe, 51147 Köln, Germany

A hydrogen production method which is very well suited for the combination with solar energy is to split water in a thermochemical cycle. The core of the cycle is a metal oxide (MO) which is reduced and oxidized in two different steps, generating hydrogen in one step and oxygen in the other step. The equations describing the two steps are:



(index red: reduced; index ox: oxidized)

The water splitting step is slightly exothermic and takes place at temperatures typically below 1200 °C. The reduction step is endothermic and temperatures of 1400 °C are required. During the reduction step, the partial pressure of oxygen needs to be reduced. That is typically realized by sweeping the reactor with an inert gas such as N₂ or Ar.

The Hydrosol project [1, 2] has pursued the development of such a process by designing and testing reactors in the lab and small pilot scale in the range of 3 kW to 100 kW thermal input. The reaction chamber of the reactors consists of a honeycomb structure composed of silicon carbide, which is coated with the reactive metal oxide.

To generate the high required temperatures, the reactor is placed on a solar tower. Concentrated sunlight from a heliostat field is focused directly on the honeycomb structure, which heats up accordingly. During operation, the reactor temperature has to swing repeatedly between the levels that are required for the two reaction steps. The temperature is adjusted by changing the degree of concentration of the solar energy.

To better understand the influence of the redox material properties on the process efficiency, a dynamic process model was established with the software Aspen Plus Dynamics. As the library of unit operations in Aspen Plus does not contain a suitable reactor model to describe the Hydrosol reactor type, a new dynamic reactor model was written in the Aspen Custom Modeler language. It describes the thermal and chemical behavior of the reactor according to the input solar flux and inlet gas stream condition.

For validation reasons, first a model of a lab scale reactor was created and the results were compared to measured data from the solar furnace at DLR, Germany. In a second step, the model geometry was changed to the most recent reactor design which is foreseen to be applied in a 1 MW plant.

This paper describes the reactor model formulation and presents the results that are obtained from different simulation runs. In a first set of simulations, the upper limit of the process efficiency

was calculated. Those runs showed, that the metal oxide which was used in the previous reactors (NiFe₂O₄) does not allow for satisfying performance. The material parameters of the redox material were changed in the model to show what should be regarded when selecting a more suitable redox material. The kinetics of the reduction reaction as well as the oxygen uptake capacity of the metal oxide were identified as two crucial parameters which both need to be improved.

In another set of simulation runs, a realistic process model was simulated, including real solar data and an extensive heat recovery section. The results revealed that besides the aforementioned material characteristics, especially the maximum oxygen partial pressure at which the reduction reaction still takes place dominates the overall efficiency of the plant.

[1] M Roeb, J-P Säck, P Rietbrock, C Prah, H Schreiber, M Neises, L De Oliveira, D Graf, M Ebert, W Reinalter, et al. Test operation of a 100kw pilot plant for solar hydrogen production from water on a solar tower. *Solar Energy*, 85(4):634-644, 2011.

[2] Martin Roeb, Martina Neises, Jan-Peter Säck, Peter Rietbrock, Nathalie Monnerie, Jürgen Dersch, Mark Schmitz, and Christian Sattler. Operational strategy of a two-step thermochemical process for solar hydrogen production. *International Journal of Hydrogen Energy*, 34(10):4537-4545, 2008.

Water-gas shift activity over catalysts based on ceria-copper inverse configurations and influence of the presence of O₂ in the reactant mixture (HP04-6)

A. López Cámara ¹, L. Barrio ^{1,2}, G. Zhou ², R. Si ², J.C. Hanson ², J.A. Rodríguez ², V. Cortés Corberán¹, A. Martínez-Arias ^{1,*}

¹ Instituto de Catálisis y Petroleoquímica, CSIC, Marie Curie 2, 28049 Madrid, Spain.

² Department of Chemistry, Brookhaven National Laboratory, Upton, New York 11973, USA.

At present, hydrogen is mainly produced from the reforming of crude oil, coal, natural gas, wood, organic waste and biomass. However, an important amount of CO (1-10% content) is present in the reforming stream and degrades the performance of Pt-based electrodes used in low temperature fuel cell systems. The water-gas shift (WGS) reaction is a critical process for procuring clean hydrogen. In particular, for mobile applications, novel WGS catalysts tolerant to redox cycles, oxygen presence and steam condensation are required and ceria-based ones display promising properties in this sense. Among the latter, catalysts combining copper and ceria in inverse configuration (initially CeO₂/CuO) are most interesting from an economical point of view while they can apparently show a superior behaviour in comparison with traditional systems.

In this context, the present work examines catalytic properties for WGS of catalysts prepared by microemulsion method, as detailed elsewhere. In addition to CeO₂/CuO catalyst with Ce:Cu atomic ratio of 4:6, another two catalysts were prepared in which the copper-containing phase is doped with either Mn or Zn at Cu:M (M = Mn or Zn) atomic ratio of 9:1. **Error! Marcador no definido.** In any case, the catalysts are finally calcined at 773 K under air and atomic composition of the final catalysts is similar to nominal ones, according to ICP-AES chemical analysis, while SBET is around 100 m²g⁻¹. WGS catalytic tests were performed under CO (5 %) + H₂O (15 %) diluted in inert gas with a tubular reactor employing 1 g of catalyst and 250 ml min⁻¹ flow. A second set of catalytic tests was dedicated to explore O₂-assisted WGS by using CO/O₂ ratios between 20 and 5 in the reactant mixture. Similar conditions were employed during tests by XANES or XRD (synchrotron source), as well as DRIFTS under reaction conditions (operando tests).

Characterization of the catalysts by XRD or HRTEM is available elsewhere. Briefly, the catalysts are constituted by CeO₂ and CuO nanocrystals (about 4.5 and 10.5 nm average size, respectively) in inverse configuration. No hint of Mn- or Zn-containing phases could be obtained by these techniques. XPS shows copper and cerium appear in fully oxidised states in

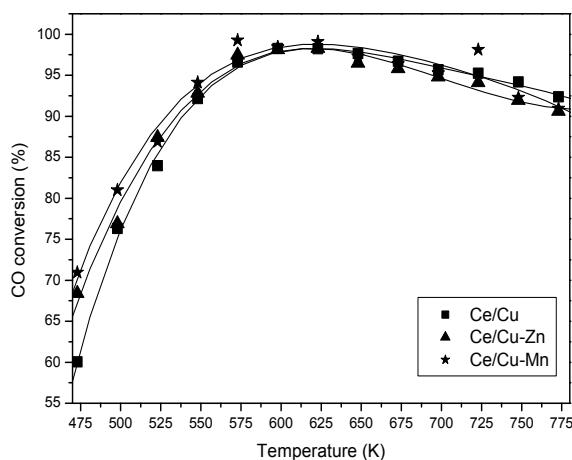


Fig. 1. WGS catalytic activity over the indicated catalysts.

the initial calcined catalysts while dopants of the copper oxide phase appear as Zn^{2+} and Mn^{4+} - Mn^{2+} states, respectively. Doping of the copper oxide component is confirmed by Rietveld analysis of the X-ray diffractograms as well as by Raman spectroscopy. Concerning the catalytic behaviour, as displayed in Fig. 1, doping of the copper oxide phase with either Zn or Mn cations apparently enhances WGS performance of the inverse catalyst. Such behaviour can be explained by the

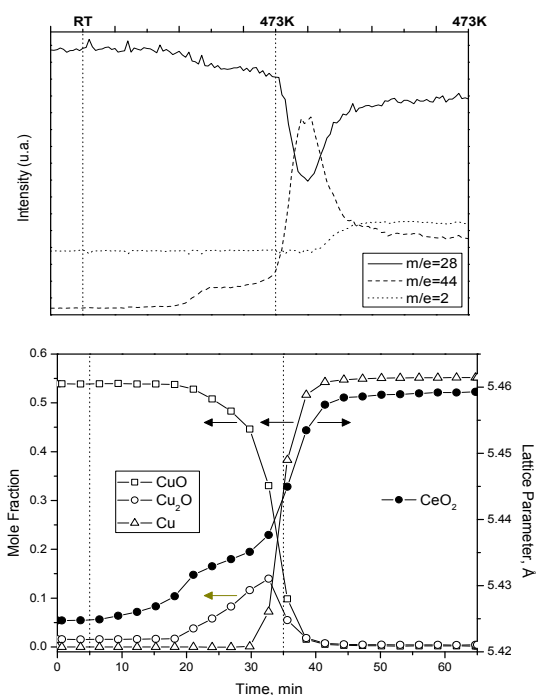


Fig. 2. Evolution of gases at reactor outlet (top) along with Rietveld-refined molar fraction of copper-containing phases and CeO₂ lattice parameter (bottom)

influence of the dopants on the morphological properties of the catalysts in terms of enhancing the amount of interfacial active sites as well as on the basis of differences in the facility for achieving active states of the catalytic centres in each case. This has been investigated by operando-XANES or -XRD, as illustrated in Fig. 2. The catalysts are shown to pass through an induction step below 473 K during which both CeO₂ and CuO become reduced, the latter in a sequential way with Cu₂O being intermediately formed. Only CO is observed to be consumed (with CO₂ being produced) in the reactant stream during such induction step, CO thus acting as reductant of both catalysts components. Then, only when both components achieve a significant reduction level and copper becomes fully reduced to metallic copper, WGS activity starts. This is in line with a previous hypothesis indicating that catalytic activity of this type of systems

is related to active sites combining metallic copper and reduced ceria, most likely following a redox reaction mechanism.

Concerning the analysis of O₂-assisted WGS, with the CeO₂/CuO and the Zn-containing catalysts a small enhancement in H₂ production is detected only at relatively low reaction temperature and at high CO/O₂ ratios. Nevertheless, interesting balance between CO oxidation and WGS activity leading to full CO elimination in a single step (i.e. without need of a second CO-PROX reactor) is shown to be generally achievable with this type of catalysts.

Experimental assessment of the cyclability of the Mn₂O₃/MnO thermochemical cycle for solar hydrogen production (HP05-1)

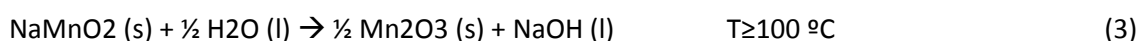
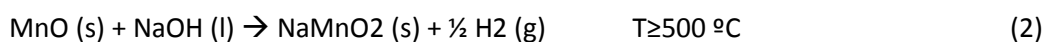
Javier Marugan¹, Juan Angel Botas², Raúl Molina¹, Carolina Herradón²

¹Department of Chemical and Environmental Technology, Universidad Rey Juan Carlos, Spain

²Department of Chemical and Energy Technology, Universidad Rey Juan Carlos, Spain

INTRODUCTION

Nowadays, the world faces an energy crisis mainly caused by the depletion of conventional resources and increasing environmental problems produced by fossil fuels. This fact has promoted the study of alternative fuels and energy sources [1]. In this context, hydrogen has been proposed for decades as a promising energy carrier for a future low carbon energy economy. Hydrogen could be a solution to store and transport renewable energy in a chemical form, helping to solve the problem of greenhouse gas emissions and releasing the world from the current fossil fuel dependence [2]. However, hydrogen is mainly generated by reforming of natural gas or gasification of coal, fossil fuel dependant, and being a massive use of hydrogen linked to the development of production techniques based on renewable energy sources. In this way, water splitting by solar-driven thermochemical cycles represents a promising technology for this purpose [3]. Sturzenegger and Nüesch proposed in 1999 a new manganese-oxide-based cycle for the production of solar hydrogen [4]. This cycle consists of three steps (reactions 2 - 4).



The thermal reduction of Mn₂O₃ into MnO occurs actually through two consecutive reactions (reactions 4 and 5):



Temperatures as high as 1500-1600 °C are possible to be achieved in modern solar concentrating systems with concentration factors in the range of 1500-5000 [5]. The use of a renewable energy source and the fact that the overall reaction process is the decomposition of water in hydrogen and oxygen, make the thermochemical cycle a renewable and environmental friendly process for hydrogen production.

Most reports of manganese oxide thermochemical cycle have been focused on the individual steps, mainly the high temperature reduction (reaction 1) and the hydrogen production step (reaction 2). However, studies about cyclability of the system as well as the evolution of hydrogen production with subsequent cycles of reaction and recovering of reactants are a lack in the current

literature. For those reasons, the aim of this work is to study the efficiency of the Mn-oxide thermochemical cycle for hydrogen production in subsequent operation cycles.

EXPERIMENTAL

The reduction of Mn₂O₃ and the hydrogen formation by reaction of MnO with NaOH was studied in a high temperature furnace capable to reach 1800 °C. A Pt/Rh (90/10) crucible resistant to temperatures up to 1500 °C and NaOH corrosion was placed inside as support for the Mn₂O₃ in the first step and the MnO/NaOH mixture in the second step. In a typical run, 1.15 g of Mn₂O₃ were placed in the reactor, starting the first step of the cycle by heating at 10 °C/min until temperature of 1450 °C is reached. After that, the furnace is uncontrolled cooled down to room temperature. The resultant material was moltured with NaOH in a ratio of NaOH/solid corresponding to twice NaOH respect to the stoichiometry of reaction 2. After that, the temperature was increased up to 1300 °C at 10 °C/min, finishing the second step of the cycle. The O₂ and H₂ released from the reactions were removed with a purge of nitrogen (50 L/h). The gas flow from the reactor goes through a moisture trap in order to remove traces of condensed water that could interfere in the hydrogen detection. Then, the gas flow was analyzed in a coupled paramagnetic and thermal conductivity gas analyzer (Emerson Xtream). The resultant solid from step 2 was treated with water at 80 °C during 30 min, filtered, and dried overnight at room temperature. Finally, it was used in up to three subsequent cycles. Small amounts of sample were removed after each step for XRD analysis by X-Ray diffractometry using a PW3040/00 X'Pert MPD/MRD equipment.

RESULTS AND CONCLUSIONS

The results obtained in each of the 3 cycle, in terms of hydrogen release and efficiency respect to the theoretical production according to reaction 1 are shown in Table 1.

Table 1. Hydrogen production results in three cycles with the Mn₂O₃ as initial solid

Cycle	H ₂ production (mmol H ₂ /cycle)	Efficiency	
		(mmol H ₂)theoretical*	H ₂)experimental/(mmol
1	5,84	0.922	
2	6,05	0.956	
3	6,08	0.960	

*Assuming that all the initial solid is Mn₂O₃ in each cycle

The theoretical mmolH₂/gMn₂O₃ ratio is 6.33, obtaining values of 6.05 and 6.08 for the last two cycles. It means an efficiency of 95.6 and 96 %, respectively. The lower hydrogen production for the

first cycle has been also reported for two step cycles based on ferrites [6]. This effect must be related to chemical, structural or morphological modifications in the material during the process. XRD diffraction of the initial Mn_2O_3 material and the resultant solid after each cycle is shown in Figure 1-a. It is clearly evident that the initial manganese oxide is not recovered after the third step of the thermochemical cycle. The solid is a mixture of Mn_3O_4 , different Mn_xO_y phases, mainly MnO_2 , and residual $NaMnO_2$. However, after the first step of each cycle, only MnO was detected (results not shown) indicating a transformation of all the phases towards the reduced manganese oxide. It should be pointed out that the oxygen production in the first step of the cycles was increased from 3.1 mmol/g initial solid (corresponding to the theoretical oxygen production according to reaction 1) to 7 mmol/g solid after the 3 cycles, which is in accordance with the thermal reduction of MnO_2 and other oxidized phases of manganese oxides, such as Mn_5O_8 . It should be pointed out that the thermal reduction of MnO_2 towards MnO has been widely reported in literature, occurring by formation of Mn_2O_3 in the range of 450-550 °C, Mn_3O_4 in the range of 700-800 °C and finally MnO at temperature higher than 1300 °C [7]. Additionally, the combination of traces of water and temperature simulates the third step of the cycle (reaction 3) washing out the residual $NaMnO_2$ of the material.

A high increase in the hydrogen production rate was also observed in cycles 2 and 3 respects to the first cycle (Figure 1-b). Although the solid obtained after the first step was MnO in all the cases, the smaller sizes obtained after each step, due to the amount of solid withdrawn for XRD measurements can be influenced heat and mass transfer phenomena in the solid bed formed in the crucible during the experiments. Actually, preliminary experiments demonstrate a remarkable influence of both physical processes in the overall reaction rates, especially with solid masses above 0.75 g in the experimental set-up. In this work, the initial Mn_2O_3 mass for the first cycle was 1.15 g, being 0.713 and 0.153 g for the subsequent cycles. Thus, the reaction rate shown in Figure 1-b for the first cycle could be highly influenced with mass and heat transfer phenomena, controlling the overall hydrogen production rate.

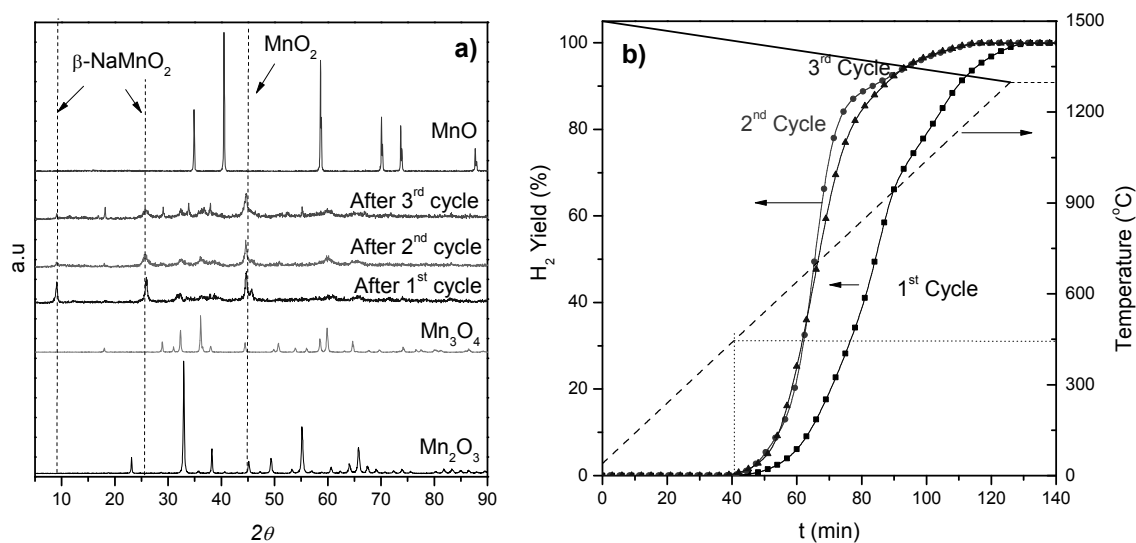


Figure 1. a) XRD diffractions for the resultant solids after each cycle and b) Results of the hydrogen production step time for each cycle

ACKNOWLEDGEMENTS

The authors wish to thank “Comunidad de Madrid” and “European Social Fund” for its financial support to the SOLGEMAC Project through the Programme of Activities between Research Groups (S2009/ENE-1617). Financial support of Ministerio de Ciencia e Innovación of Spain (Plan Nacional de Investigación Científica, Desarrollo e Innovación Tecnológica 2008-20) and Fondo Europeo de Desarrollo Regional (FEDER) through the program PSE-H2RENOV SP4-HYTOWER (PSE-120000-2009-3) is also gratefully acknowledged. C. Herradón also thanks Universidad Rey Juan Carlos for its PhD grant

REFERENCES

- [1] Campen A., Mondal K., Wiltowski T., Separation of hydrogen from syngas using a regenerative system, *Int. J. Hydrogen Energy*, 33, pp. 332-339, 2008
- [2] Pregger T., Graf D., Krewitt W., Sattler C., Roeb M., Möller S., Prospects of solar thermal hydrogen production processes, *Int. J. Hydrogen Energy*, 34, pp. 4256-4267, 2009
- [3] Perkins C., Weimer A.W., Likely near-term solar-thermal water splitting technologies, *Int. J. Hydrogen Energy*, 29, pp 1587-1599, 2004
- [4] Sturzenegger M., Nüesch P., Efficiency analysis for a manganese-oxide-based thermochemical cycle, *Energy*, 24, pp 959-970, 1999
- [5] Baykara SZ. Experimental solar water thermolysis. *Int. J. Hydrogen Energy*, 29, pp. 1459-1469, 2004
- [6] Fresno F, Fernandez-Saavedra R, Gómez-Mancebo MB, Vidal A, Sánchez M, Rucandio MI, Quejido AJ, Romero M. Solar hydrogen production by two-step thermochemical cycles: Evaluation of the activity of commercial ferrites. *Int. J. Hydrogen Energy*, 34, pp.34:2918-2924, 2009
- [7] Dose WM, Donne SW, Manganese dioxide structural effects on its thermal decomposition. *Mat. Sci. .Eng. B*, 176, pp. 1169– 1177, 2011

Hydrogen From Synthetic Biogas Via Sip Using NiAl_2O_4 Catalyst: Reduction Stage (HP05-2)

M. Herrer, J. Plou, P. Durán, J. Herguido, J.A. Peña

*Catalysis, Molecular Separations and Reactor Engineering Group (CREG).
Aragón Institute of Engineering Research (I3A). Universidad Zaragoza.
Zaragoza. 50018 Spain. E-mail: jap@unizar.es*

INTRODUCTION

Due to its high methane content, biogas can be envisaged as suitable feedstock for hydrogen production. Biogas is the product of the anaerobic digestion of solid municipal wastes, sewage sludge or livestock wastes. Sweetened biogas consists mainly of a mixture of methane and carbon dioxide, and constitutes the ideal composition to carry out the reaction of methane dry reforming (MDR). The products resulting from this process constitute a stream of hydrogen and carbon monoxide that could be further purified in order to obtain high purity hydrogen (e.g. PEMFC quality).

Present study plans the combination of the dry reforming of a synthetic biogas with steam-iron process (SIP) in order to generate high purity hydrogen [1]. SIP is a cyclic redox process divided in two steps. In the first one, biogas (in this case, MDR products) reacts with iron oxide reducing it to metallic iron. In the second step, iron is reoxidized with steam generating pure hydrogen and the former iron oxide completing the cycle.

EXPERIMENTAL

The experiments were carried out in a packed bed reactor. The solid used (2.5 g) was a mixture of 67.5%w “triple” oxide, 7.5%w nickel based catalyst and 25%w silica. The solid called “triple” was synthesized in lab via citrates. It is composed of Fe_2O_3 (98 %w) additivated with Al_2O_3 (1.75 %w) and CeO_2 (0.25 %w). Alumina provides structural stability and ceria enhances reaction rates where oxygen migration is involved [2]. On the other hand, the catalyst is a non-stoichiometric nickel aluminate with nickel oxide excess (10%w NiO over NiAl_2O_4). It was synthesized by co-precipitation with ammonia using increasing pH method [3].

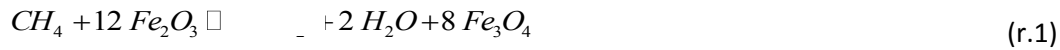
The gas flowrate fed was 250 NmL/min, containing equimolar flows of CH_4 and CO_2 (0.125 bar each) diluted in Ar. The reactor operates close to atmospheric pressure. This composition emulates a real sweetened poor biogas stream with low methane content (e.g. low heating value) [4].

Exhaust gases were analysed by gas chromatography and a mass spectrometry operating in parallel. The main purpose was to sample gases composition in a real time basis (mass spectrometer) with in-situ calibration (gas chromatograph).

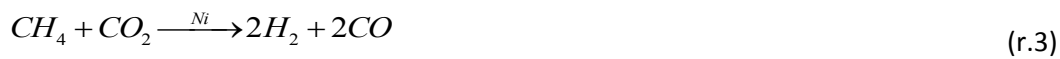
RESULTS

Experiments were carried out at temperatures from 600 °C to 750 °C (isothermal conditions). Figure 1 represents the gas composition evolution during the reduction step with synthetic biogas at

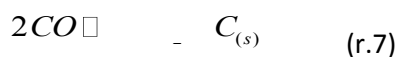
750 °C. During the first 5 minutes methane reacts with the lattice oxygen transforming Fe₂O₃ in Fe₃O₄ (r.1), producing a maximum of CO₂ and H₂O at approximately 2.5 minutes after beginning. Also during this stage, NiO (in 10%w excess respecting the stoichiometric of NiAl₂O₄) is reduced to Ni (r.2). This is the active species which will catalyse the dry reforming reaction. These results are in agreement with previous TGA observations [5].



The second stage shows a plateau in molar flows of the different species. In-situ MDR catalysed by emerging Ni produces hydrogen and carbon monoxide (r.3). Reduction of magnetite (Fe₃O₄) to metallic iron takes place at the expense of H₂ and CO (r.4 and r.5). The conversion keeps nearly constant values along this stage due to thermodynamic restrictions between Fe₃O₄ and Fe.



After approximately 20 minutes, iron oxide is fully converted into iron. From then on, only catalytic MDR takes place and the exhaust gas composition is governed mostly by the Water Gas Shift (WGS) equilibrium (r.6).



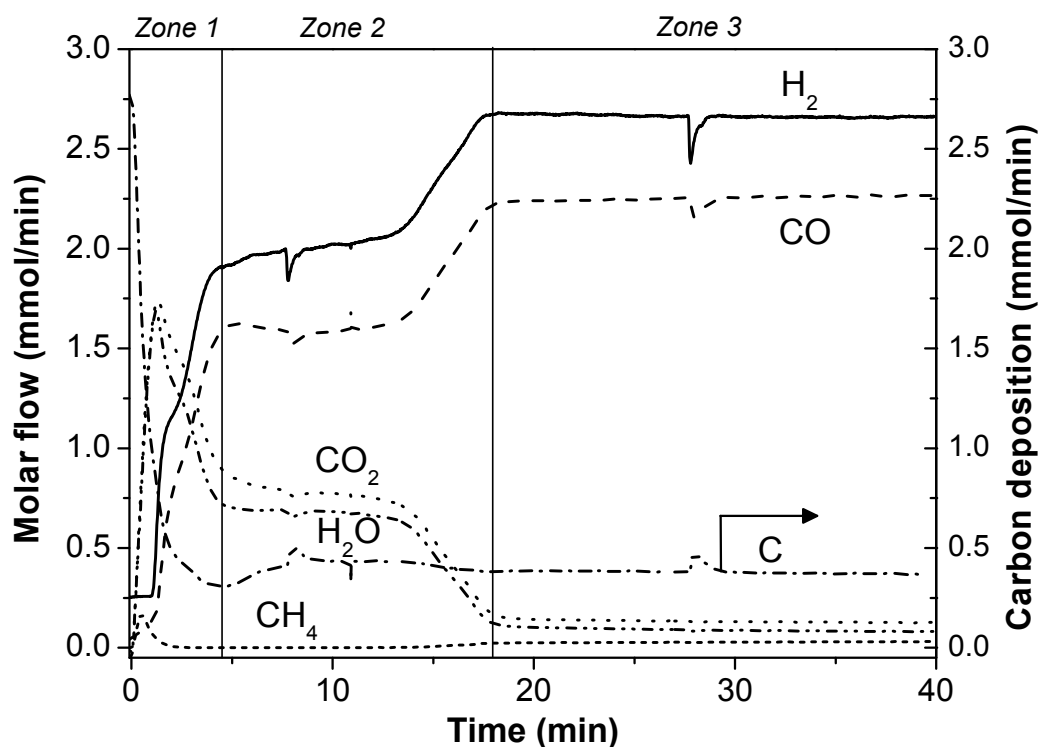


Figure 9. Product distribution for the reduction step at 750 °C.

In addition to these, also carbon formation has been evidenced along time due to side reactions such as the Boudouard reaction (r.7). A continuous carbon deposition was calculated from elemental balance (Fig. 1), nevertheless gas composition is kept constant along time. The explanation could be based on the iron oxide presence, which would reduce coke deposition over the catalyst.

Regarding the effect of reduction temperature on time product distribution (not shown), it should be noted that a similar behaviour is found but with faster reactions involved than that for 750°C (Fig.1). However, as lower is the temperature, the higher the time to complete the reduction, and also lesser the constant conversion in the second zone. When iron oxide is completely reduced reaching the third zone, the gas composition varies according to WGS reaction (r.6).

Figure 2a (inserted figure) represents experimental and theoretical methane conversion values as a function of the reduction temperature. The conversion of CH₄ is roughly equal to the theoretical one for temperatures above 650 °C. Below this temperature methane is not completely reacted. Meanwhile, subfigure 2b shows the effect of coke deposition (overpressure profiles in the bed) along a reduction step at different temperatures. Overpressure has been chosen as the parameter that allows following the total carbon deposited on the bed. This figure shows that the lower the temperature, the higher the carbon formation corresponding to an increase in the Boudouard disproportionation (r.7). However, an exception was found at 600 °C, because of the limited methane conversion at such a low temperature.

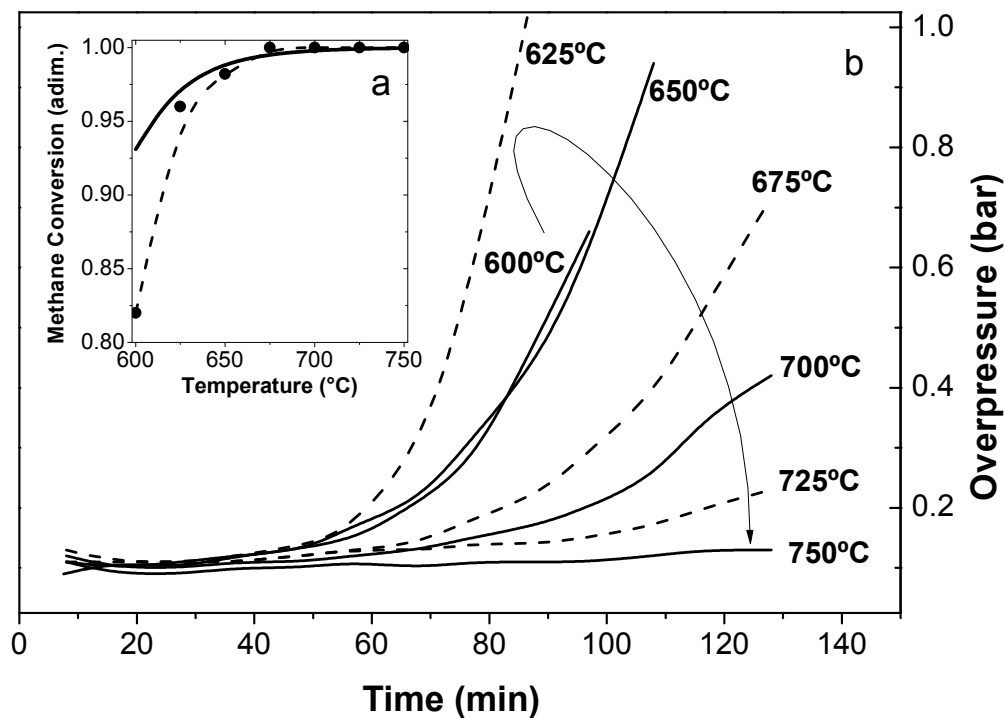


Figure 10: Experimental (symbols) versus theoretical methane conversion (a), and overpressure in the bed (b), for reductions at different temperatures.

Oxidation step involves the reaction between metallic iron and steam with pure hydrogen generation. Its behaviour in experimental conditions was widely explained in previous works of the research group [6]. In summary, the exhausted gases were constituted by hydrogen and unreacted steam. Neither CO nor CO₂ were detected. Respecting the effect of the reduction temperature on the subsequent oxidation step at 500 °C, the conclusion is that the higher the reduction temperature the lower the apparent oxidation rate.

Consequently, the optimal reduction temperature must be set at a value sufficiently low to avoid carbon deposition, but high enough to keep a reasonable reaction rate.

CONCLUSIONS

Hydrogen production by steam iron process using biogas is a feasible alternative to generate pure hydrogen. The process consists of a combination of methane dry reforming and steam-iron process where production and purification occur within the same vessel giving a step forward in the process intensification.

Even though carbon deposition in reduction step could be a drawback, hydrogen purity is maintained in the oxidation step. Coke deposition could be subsequently removed from the solid in an additional combustion step after several redox cycles.

Optimal reduction temperatures have been established between 650 and 700 °C, at which maximum methane conversion and low carbon formation take place. Temperatures up to this interval provoke important sintering effects over the solid, while below imply increasing amounts of coke deposition.

ACKNOWLEDGEMENTS

Financial support for this research has been provided by the Spanish Ministerio de Ciencia e Innovación (MICINN), through project ENE2010-16789. J. Plou also thanks the same institution for the grant BES-2011-045092. Financial aid for the maintenance of the consolidated research group CREG has been provided by the Fondo Social Europeo (FSE) through the Gobierno de Aragón (Aragón, Spain).

REFERENCES

- [1] A. Messerschmitt. Process of producing hydrogen. U.S. Patent 971,206 (1910).
- [2] E. Lorente, J.A. Peña, J. Herguido. *Journal of Power Sources*. 192 (2009) 224.
- [3] A. Al-Ubaid., E.E. Wolf. *Applied Catalysis*, 40 (1988) 73.
- [4] T. Bond, M. R. Templeton. *Energy for Sustainable Development*, 15 (2011) 347.
- [5] J. Plou, P. Duran, J. Herguido, J.A. Peña. *Fuel*. In press (2013).
- [6] R. Campos, P. Duran, J. Plou, J. Herguido, J.A. Peña. *Journal of Power Sources*. 242 (2013) 520.

Acceleration of Redox Reaction of Metal Oxide with Oxide Ion Conducting Support Materials and Application to Hydrogen Production (HP05-3)

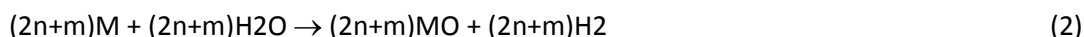
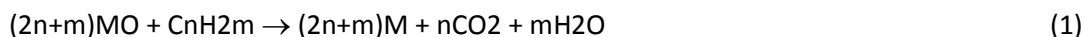
Junichiro Otomo,¹ Syunsuke Isogai,¹ Fumihiko Kosaka,¹ and Hiroyuki Hatano²

¹Department of Environment Systems, Graduate School of Frontier Sciences,
The University of Tokyo, 5-1-5 Kashiwanoha, Kashiwa, Chiba 277-8563

²Department of Integrated Science and Engineering for Sustainable Society,
Faculty of Science and Engineering
Chuo University, 1-13-27 Kasuga, Bunkyo-Ku, Tokyo 112-8551

INTRODUCTION

Redox reaction of metal oxide has been widely used in various energy conversion and storage systems, e.g., high grade heat generation in chemical looping combustion (CLC), hydrogen production in chemical looping reforming (CLR) and in the steam-iron reaction. Reduction of a metal oxide (MO) by hydrocarbon fuel (C_nH_{2m}) and subsequent oxidation process with water vapor involve the following reactions:



In the energy conversion systems, the reduction process of metal oxide such as Fe_2O_3 is often rate-determining and governs the kinetics of redox cycles. Therefore, the reduction kinetics of metal oxides should be improved. In this study, to develop new chemical energy conversion and storage systems using metal oxides, the kinetics of iron oxide (Fe_2O_3) reduction by methane or hydrogen using oxide ion conductors (OICs) as supports were investigated. In our previous studies [1, 2], Gd-doped ceria ($Ce_{1-x}Gd_xO_{2-\delta}$: GDC) support can improve the reduction kinetics of metal oxide such as NiO and Fe_2O_3 by methane. Quite recently, we have also reported that Fe-doped calcium titanate ($CaTi_{1-x}Fe_xO_{3-\delta}$: CTFO), which is also an oxide ion conductor, improves Fe_2O_3 reduction kinetics when CTFO is used as a support for Fe_2O_3 [3]. Such improvements may be induced by fast oxide ion transport at the interface between Fe_2O_3 and the oxide ion conductors. The detailed mechanism is, however, still unknown. Furthermore, subsequent oxidation process with water vapor may be also influenced by the oxide ion conducting supports. In this study, we investigate the redox reaction processes of MOs on GDC and CTFO in terms of interfacial oxide ion transport between MO and OICs. In this abstract, we demonstrate the improvements of Fe_2O_3 reduction rate and lattice oxygen utilization using GDC as a support, in comparison with different support materials of CeO_2 and Al_2O_3 .

EXPERIMENTAL

Oxygen carrier compounds were prepared by solid-state synthesis. GDC powder supplied from Daiichi Kigenso Kagaku Kogyo (Osaka, Japan), α - Al_2O_3 powder supplied from Kanto Kagaku (Tokyo, Japan), Fe_2O_3 and CeO_2 powders supplied from Wako Pure Chemical Industries (Osaka, Japan) were used. To prepare pelletized porous cermet samples of Fe_2O_3 /GDC, Fe_2O_3 / Al_2O_3 and Fe_2O_3 / CeO_2 ,

desired amounts of each powder were mixed by ball-milling using graphite carbon powder to form pores and ethyl cellulose as a binder. The mixtures were then pressed to form disks. The disks were calcined in air at 1373 K for 3 h to form porous cermet samples, which were characterized by scanning electron microscopy (SEM) and X-ray diffraction spectroscopy (XRD). The specific surface areas of the metal oxides were examined using the Brunauer-Emmett-Teller (BET) method with a surface area analyzer.

To evaluate the Fe₂O₃ reduction process, the weight changes of prepared porous cermet samples were measured by thermogravimetry (TG-DTA) in wet methane at ambient pressure. Gaseous mixtures (CH₄/H₂O/Ar; typical molar ratio = 1:2:17; steam-to-carbon ratio S/C = 2) were delivered continuously to the cermet sample using a water bubbler positioned in a water bath.

RESULTS AND DISCUSSIONS

The formations of Fe₂O₃/GDC, Fe₂O₃/Al₂O₃ and Fe₂O₃/CeO₂ composites were confirmed by XRD. Any other phases were not observed in the samples. To evaluate the reduction rates in Fe₂O₃/GDC, Fe₂O₃/Al₂O₃ and Fe₂O₃/CeO₂, the kinetics of reduction of Fe₂O₃ by wet methane at fixed temperatures were investigated. The conversion over time at 1123 K is plotted in Fig. 1. The conversion, X, of Fe₂O₃ reduction is defined as:

$$X = 1 - \left(\frac{m - m_{\text{red}}}{m_{\text{oxi}} - m_{\text{red}}} \right), \quad (3)$$

where m is the mass of a sample, m_{oxi} is the mass of the fully oxidized sample, i.e., Fe₂O₃, and m_{red} the mass of the reduced sample, i.e., Fe. The value of X formally changes through the following reaction steps:

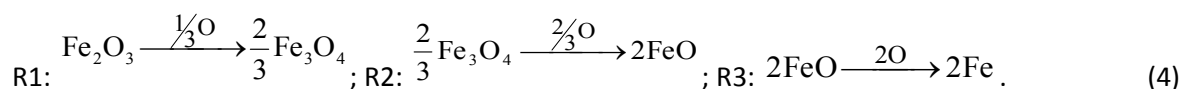


Figure 1 clearly demonstrates that reduction of Fe₂O₃ in Fe₂O₃/GDC is significantly faster than that in Fe₂O₃/CeO₂ and Fe₂O₃/Al₂O₃. Even taking the difference in the specific surface areas of Fe₂O₃/GDC, Fe₂O₃/Al₂O₃ into account, the GDC support has a considerable ability to enhance the reduction rate of Fe₂O₃. To view the extent of the reaction, the corresponding values of X for R1 and R2 are shown in Fig. 1 as dotted lines. Notably, Fe₂O₃ reduction in Fe₂O₃/GDC reached R2 under the present conditions, whereas that in Fe₂O₃/Al₂O₃ and Fe₂O₃/CeO₂ did not. Therefore, lattice oxygen utilization is also improved in Fe₂O₃/GDC compared with that in Fe₂O₃/Al₂O₃ and Fe₂O₃/CeO₂.

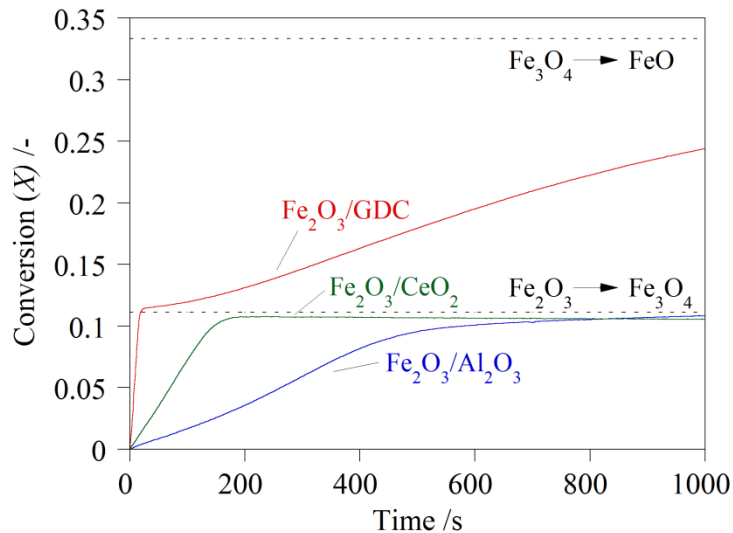


Fig. 1. Time profiles of Fe₂O₃/support (GDC, CeO₂, Al₂O₃) reduction by wet methane (S/C = 2) at 1123 K.

The higher reduction rate for Fe₂O₃/GDC also suggests that the reactor size for the Fe₂O₃ reduction process can be downsized effectively. Comparing the results of Fe₂O₃/GDC and Fe₂O₃/CeO₂, fast oxide ion transport at the interface between Fe₂O₃ and GDC may induce the observed fast Fe₂O₃ reduction kinetics (note: oxide ion conductivity: GDC > CeO₂). A three-phase boundary involving Fe₂O₃, GDC and gas may act as an initiation point to activate methane and subsequently reduce Fe₂O₃.

As stated above, oxide ion conducting materials can play a key role in MO reduction kinetics. Further observation of the interface between MO and OICs in terms of reactivity and changes in morphology should be performed to determine the mechanism of MO reduction in the presence of OICs.

CONCLUSION

To develop new chemical energy conversion and storage systems using metal oxides, the kinetics of iron oxide (Fe₂O₃) reduction by humidified methane using an oxide ion conductor, Ce_{1-x}Gd_xO_{2-δ} (GDC), as a support was investigated. The present result clearly showed that significant improvements in Fe₂O₃ reduction rate and lattice oxygen utilization were observed using GDC. Comparing with the reduction kinetics of Fe₂O₃/CeO₂ and Fe₂O₃/Al₂O₃, this result may be induced by fast oxide ion transport at the interface between Fe₂O₃ and GDC.

ACKNOWLEDGEMENTS

This work was supported by a Grant-in-Aid for Scientific Research (B) (25281061) from the Japan Society of the Promotion of Science, which is greatly appreciated.

REFERENCES

- [1] J. Otomo, Y. Furumoto, H. Hatano, T. Hatanaka, Y. Oshima, *Fuel*, 104, 691 (2013).
- [2] F. Kosaka, N. Kikuchi, H. Hatano, Y. Oshima, J. Otomo, *Proc. of International symposium on IMPRES, Chemical Science & Engineering Series 3*, 582 (2013).
- [3] S. Isogai, F. Kosaka, I. Takimoto, H. Hatano, Y. Oshima, J. Otomo, *Chem. Lett.*, (in press).

Techno-environmental evaluation of Steam-Iron as an alternative process for hydrogen storage or purification (HPO5-4)

Abel Sanz¹, Diego Iribarren¹, Javier Dufour^{1, 2, *}

¹ Instituto IMDEA Energía, 28935 Móstoles, Spain

² Rey Juan Carlos University, 28933 Móstoles, Spain

* Corresponding author: Javier Dufour (javier.dufour@imdea.org)

BACKGROUND

There is an increasing interest in hydrogen as a clean energy resource with a wide range of applications such as the production of ammonia and fertilizers, the upgrading of fuels, methanol synthesis and metallurgical processes. Moreover, there is a growing interest in hydrogen as an energy carrier [1].

The Steam-Iron process is one of the oldest commercial methods for hydrogen production [2], but it was replaced by the more economical and efficient steam reforming of natural gas, which is currently the main route for hydrogen production. However, the Steam-Iron process is gaining interest due to its simplicity, the high purity of the hydrogen obtained and, especially, the possibility of using renewable energy sources such as biomass. In this way, it would be possible to obtain green hydrogen. In this work, the techno-environmental performance of Steam-Iron as an alternative method for hydrogen storage or purification is evaluated.

PROCESS DESCRIPTION

Steam-Iron is a two-stage process (Figure 1). The reduction step involves the reaction of iron oxides with a reducing stream which can be syngas from different sources. In this step, iron oxide is reduced from Fe₂O₃ to Fe₃O₄, FeO and even metallic Fe. The final product depends on the reducing power of the gas stream. The oxidation step involves the reverse reaction, i.e. the oxidation of metallic Fe or metal oxides to a higher oxidation level. This step is carried out by treating the reduced solid with steam in excess. As a result, the output stream is a mix of hydrogen and water that can be separated by condensation, thus obtaining high-purity hydrogen. The reduction step is endothermic, but the oxidation is strongly exothermic, covering the energy needs of the first step.

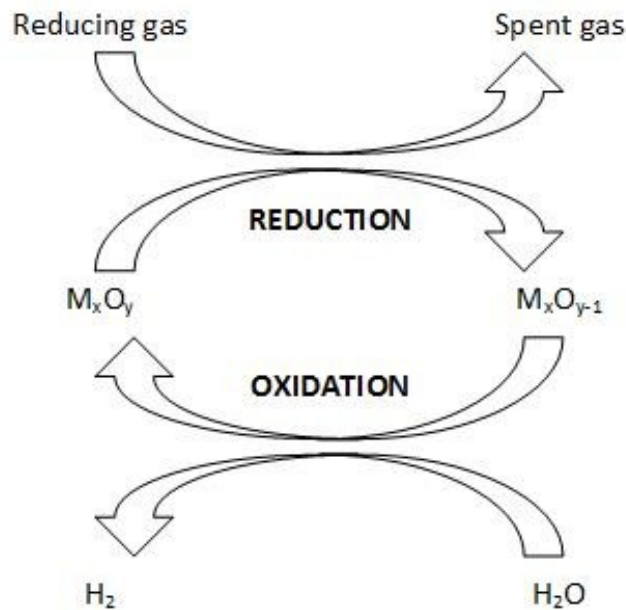


Figure 11. Steam-Iron process.

The Steam-Iron process can be used as a hydrogen-production method, since hydrogen is obtained in the oxidation step. Alternatively, it can be used as a hydrogen-storage method, since the reduced solid can act as a hydrogen carrier. Then, hydrogen can be generated in situ from this solid by means of a treatment with steam.

TECHNO-ENVIRONMENTAL EVALUATION

The goal of this work is to evaluate the techno-environmental performance of both alternatives of the Steam-Iron process: hydrogen purification and hydrogen storage. The data required for the analysis are obtained by process modeling with Aspen Plus™.

The operational assessment focuses on the energy balance and global energy consumption of both systems. Additionally, the environmental performance of each alternative is evaluated following the Life Cycle Assessment (LCA) methodology. Key inventory data for this LCA study are derived from the previous simulation of the processes, while background data are taken from the ecoinvent™ database. The environmental profile of the evaluated systems is calculated by implementing the life cycle inventories into SimaPro 7. A relevant set of impact potentials is considered, including global warming, abiotic depletion, cumulative energy demand, ozone layer depletion and photochemical oxidant formation. Life-cycle indicators are used to identify the most contributing elements within each system, also providing a basis for comparison between both alternatives.

REFERENCES

[1] Rydén, M.; Arjmand, M. Continuous hydrogen production via the steam-iron reaction by chemical looping in a circulating fluidized-bed reactor. *International Journal of Hydrogen Energy*, 37 (2012) p. 4843-4854.

[2] Peña, J.A.; Lorente, E.; Herguido, J. "Steam-Iron" Process for Hydrogen Production: Recent Advances. *Proceedings WHEC2010*, 78 (2010) p. 318-322.

High Temperature water gas shift reaction over catalysts containing one activity promoter (HP05-5)

Carmen Martos¹, Javier Dufour^{1,2}, Aida Ruiz¹ and Alfredo Lameiro¹

¹Department of Chemical and Energy Technology, ESCET, Universidad Rey Juan Carlos, Móstoles, Madrid, Spain, ²Instituto IMDEA Energía, Móstoles, Madrid, Spain.

ABSTRACT

The WGS reaction ($\text{CO} + \text{H}_2\text{O} \leftrightarrow \text{CO}_2 + \text{H}_2$) is an important step in the industrial manufacture of hydrogen. This is a reversible and exothermic reaction that is usually carried out in two stages to maximize CO conversion. The first step is performed at high temperatures (310-420 °C) with a catalysts based on Fe₃O₄-Cr₂O₃ under favourable kinetic conditions. The active phase of the catalyst is magnetite and Cr₂O₃ is added as a textural promoter. Moreover, small amounts of other metal are added to increase the activity of the material [1]. The catalysts based on Fe₃O₄-Cr₂O₃ have environmental and safety problems related to chromium compounds [2]. Furthermore, exposure to liquid water originated from condensation in catalytic reactors should be avoided, because of possible chromate leaching [3]. Therefore, the search for non-toxic catalysts that could be easily handled and discarded is much needed. There are several studies to replace chromium by other promoters like V, Al, Mo, Th and Mn [4–6]. The aim of this work is to study the replacement of Cr by molybdenum with two different precursors on the activity of magnetite-based catalysts prepared by oxiprecipitation method. Ferrous sulfate and chloride were the precursors selected and the Cu was the activity promoter selected.

Catalysts were prepared by oxiprecipitation method and they were characterized by X-ray powder diffraction, X-ray fluorescence, transmission electron microscopy, temperature programmed reduction and N₂ adsorption–desorption. The catalytic activity was tested in a fixed bed reactor using a feed gas composition of 72.5 % N₂, 16 % CO and 11.5 % CO₂ and a steam/CO molar ratio of 2.

Table 1.- Catalytic activity results

Sample	Precursor	X _{CO} (%)	S _{H₂} (%)
Commercial	--	54	98,13
ClFeCrCu	Chloride	68	78
SFeCrCu	Sulfate	79,32	89,81
ClFeMoCu5	Chloride	62,38	97,35
SFeMoCu5	Sulfate	78,10	97,16

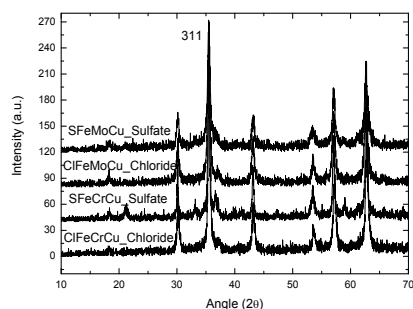


Figure 1.- XRD patterns of fresh catalysts

All the materials were composed of magnetite and independent phases of chromium, molybdenum and copper were not detected, as can be observed in the XRD patterns (Figure 1). In the case of chromium and molybdenum, this could suggest that these metals may be incorporated into magnetite lattice. Copper did not appear in the diffractograms, probably because of the low amount of this dopant (1%) in the materials.

Table 1 shows the catalytic activity results. All the samples showed higher catalytic activity than the commercial catalyst indicating that the oxiprecipitation synthesis method yields materials with better catalytic performance. Higher CO conversion were obtained for the samples prepared with sulfate (79,32% and 78,10%) showing that this precursor is more adequate. On the other hand, the properties of molybdenum and copper-doped catalysts synthesized by oxiprecipitation were similar to that of FeCrCu materials in terms of conversion but presents higher selectivity towards H₂. All these factors indicate that the replacement of Cr by Mo is a good option to avoid environmental and safety problems due to chromium compounds.

ACKNOWLEDGEMENT

The authors acknowledge to the Ministry of Science and Innovation, the Ministry of Economy and Competitiveness of Spain, and Comunidad de Madrid for funding through the projects CTQ2010-21102-C02-01 and S2009/ENE-1743.

REFERENCES

C. Ratnasamy, J.P. Wagner. "Water Gas Shift Catalysis". *Catalysis Reviews*, 51(3) (2009), pp. 325-440.

Carneiro de Araújo G, Rangel MC. "An environmental friendly dopant for the high-temperature shift catalyst". *Catal Today* 2000; 62:201-7.

Trimm D. L. "Minimisation of carbon monoxide in a hydrogen stream for fuel cell application". *Appl Catal Gen* 2005; 296(1):1-11.

Natesakhawat S, Wang X, Zhang L, Ozkan UM. "Development of chromium-free iron-based catalysts for high-temperature water-gas shift reaction". *J Mol Catal Chem* 2006; 260:82–4.

Rangel Costa J, Marchetti GS, Rangel MC. "A thorium-doped catalyst for the high temperature shift reaction". *Catal Today* 2002; 77:205–13.

J. Dufour, C. Martos, A. Ruiz, F.J. Ayuela. "Effect of the precursor on the activity of high temperature water gas shift catalysts". *International Journal of Hydrogen Energy*, In Press, <http://dx.doi.org/10.1016/j.ijhydene.2012.07.120>.

Enhancement of CO conversion in a novel Electroless Pore-Plated Pd membrane reactor for H₂ production via Water Gas Shift (HPO5-6)

D. Alique *, J. A. Calles, R. Sanz, L. Furones

Department of Chemical and Energy Technology, Rey Juan Carlos University, Móstoles, 28933, Spain

*E-mail: david.aliq@urjc.es

KEYWORDS: Pd membrane; pore-plating; membrane reactor; WGS

1. INTRODUCTION

Hydrogen separation is a key factor for economical optimization of global hydrogen production processes and control of CO₂ emissions. The combination of hydrogen production and separation processes in a unique unit by using hydrogen selective membranes is a good alternative in order to reduce capital assets and operating costs, enhancing the global efficiency of the process and the environmental performance [1]. Actually, the majority of H₂ is industrially obtained from natural gas via steam reforming, producing a mixture of CO and H₂ that is so-called syngas. In this context, the combination of reforming or water gas shift processes with hydrogen selective Pd membranes has received increased interest for last years.

Nowadays, the cost of membrane preparation and stability of the system are the most important barriers in order to scale-up this technology to the industry [2]. In this context, great efforts have been made to obtain thin Pd layers onto appropriate supports in order to maximize the permeate flux and save costs, maintaining a good stability and mechanical resistance. Among different alternatives, the preparation of composite membranes over porous stainless steel supports is one of the best options due to their similar thermal expansion coefficient and the increase of both thermal and mechanical resistance.

The aim of the present study is the integration of novel Pd-composite membranes prepared by ELP "pore-plating" [3] in a WGS tubular membrane reactor, analyzing the effect of several operational parameters such as temperature, pressure, H₂O/CO molar ratio and space velocity.

2. EXPERIMENTAL SECTION

2.1. MEMBRANE PREPARATION

Tubular stainless steel supports (PSS) of grade 0.1 μm were provided by Mott Metallurgical. Pd deposition over these supports has been performed by electroless pore plating [3]. First, the support was cleaned by sequential washing with HCl, NaOH and ethanol solutions under ultrasonic irradiation at 333 K. Then, an intermediate layer of Fe₂O₃-Cr₂O₃ was formed by oxidation of the support in a furnace with static air at 600°C for 12 h (heating and cooling rates of 1.8°C/min). After that, an activation of the pore area was carried out by direct reduction of Pd complexes and finally the Pd layer was incorporated by feeding the Pd source and hydrazine from opposite sides of the support. Several recurrences of the plating (last step) were carried out. Finally, the membrane was rinsed with deionized water and dried at 110 °C for 8 hours.

2.2. REACTION DEVICE

WGS reactions and permeation tests were performed in a home-made membrane reactor. The reactor contains a dense tube (for packed-bed reaction) or the above described Pd membrane (for membrane reactions and control permeation measurements) placed between two graphite o-rings to ensure the seal between the retentate and permeate sides. This assembly is placed into a furnace for achieving the desired temperature in each experiment.

The reaction tests were carried out using a feed gas with molar composition of 12% CO, 18% CO₂ and 70% H₂ (dry base), simulating a typical reformat feed. A commercial Fe/Cr High Temperature WGS catalyst provided by Süd-Chemie were use in the lumen side of the membrane. Temperature (350-450°C), pressure (1-3 bar), H₂O/CO molar ratio (1-3) and space velocity (h⁻¹) were the main parameters analyzed to evaluate the enhancement of CO conversion in the membrane reactor.

3. RESULTS & DISCUSSION

A completely dense Pd composite membrane was prepared with a Pd thickness of c.a. 13 μm, obtaining a permeance of 1-3·10⁻⁴ mol·m⁻²·s⁻¹·Pa^{-0.5}, total hydrogen selectivity and an activation energy of 13.1 kJ/mol. Moreover, the permeation experiments showed a high reproducibility after several thermal cycles, ensuring a good stability of the system. The membrane was combined with a HT-WGS commercial catalyst in a membrane reactor obtaining a significant improvement of the CO conversion (XCO) related to the previous experiments carried out in a conventional fix bed reactor, maintaining both complete hydrogen selectivity and membrane stability. So, the CO conversion values obtained at T=400°C, P=2 bar, GHSV=5000 h⁻¹ and H₂O/CO=1 were 59 and 32% for the membrane reactor and the traditional packed-bed reactor, respectively.

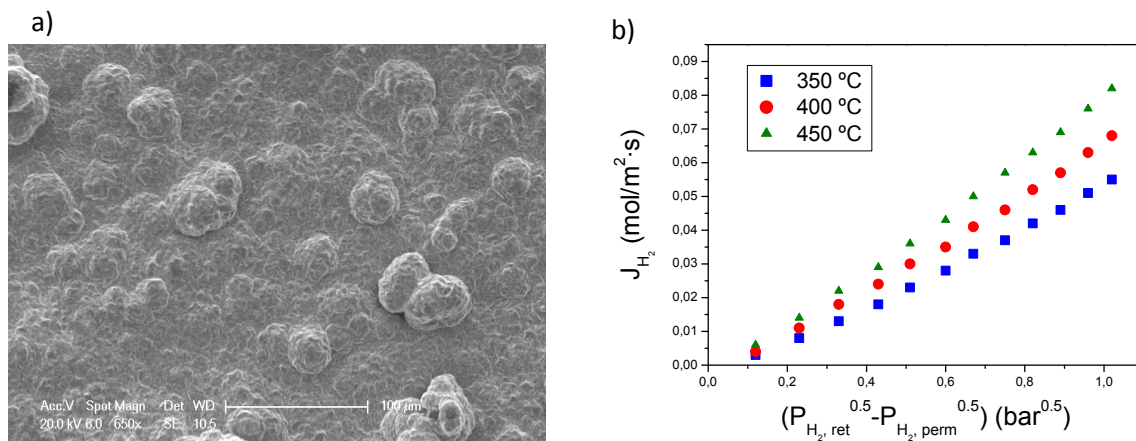


Fig. 1 (a) SEM micrograph of PSS-OXI-Pd external surface and (b) Permeation results with pure H₂ for temperatures 350-450°C

4. ACKNOWLEDGEMENT

We gratefully acknowledge the financial support provided by The Ministry of Education and Science through projects ENE2007-66958 and CTQ2010-21102-C02-01.

5. REFERENCES

- [1] D. Xie, F. Wang, K. Wu, E. Zhang, Y. Zhang, *Sep. Purif. Technol.*, 2012, 89, 189–192.
- [2] R. Sanz, J.A. Calles, D. Alique, L. Furones, S. Ordoñez, P. Marín; *Int. J. Hydrogen Energy*, 2011, 36, 15783–15793.
- [3] R. Sanz, J.A. Calles, D. Alique, L. Furones; *Int. J. Hydrogen Energy*, 2012, 37, 18476–18485

Hydrogen storage

Hydrogen storage by sodium borohydride: Development of versatile and fast responding reactors for the release of Hydrogen in mobile applications (HS1-1)

D.HUFSCHMIDT1, G.ARZAC1, G.ADAME2, M.A.JIMENEZ2, A.FERNANDEZ1

1Institute of Material Science of Sevilla (CSIC-Univ.Sevilla), Avda Américo Vespucio 49, 41092 Sevilla, Spain; 2Abengoa Hidrógeno, Campus Palmas Altas, Sevilla.

Email: dirk@icmse.csic.es

INTRODUCTION

In the recent years a large amount of investigation was carried out in order to establish Hydrogen as a future energy carrier. Many studies dealt with the production of Hydrogen from natural resources and also various applications were developed and improved. As from the economical point of view the production of Hydrogen and its consumption are rarely taking place the same time and at the same site, Hydrogen storage has become an important issue. Besides the classical ways of storing hydrogen in highly pressurized tanks or in liquid state, the storage by compounds, which bind Hydrogen chemically, has drawn the interest of many works. Most prominent among these compounds are the metal hydrides, which are formed by precursors with hydrogen and release under suitable conditions controllably Hydrogen.

SODIUM BOROHYDRIDE AS SUITABLE STORAGE COMPOUND OF HYDROGEN

Sodium borohydride (NaBH_4 , SBH) is a compound known since the 1940 and is studied now for several years for its ability to release Hydrogen under certain conditions. Opposite to many metal hydrides, it is a stable, non-flammable, non toxic and relatively cheap hydride. Although SBH is releasing reversibly Hydrogen at elevated temperatures, the hydrolysis according to: $\text{NaBH}_4 + 2 \text{H}_2\text{O} \rightarrow 4 \text{H}_2 + \text{NaBO}_2 + \text{Heat}$, is of high interest. Aqueous SBH solutions at high pH (fuel) are stable and only produce hydrogen when in contact with suitable catalysts (on demand H_2 generation). Cheap, but efficient catalysts are Co or CoB deposited on different carrier materials. The release of hydrogen can be carried out controlled under ambient conditions, which makes it suitable for small scale and portable applications.

SMALL SCALE REACTORS FOR HYDROGEN PRODUCTION

Many mobile and portable applications require small scale reactors for the immediate Hydrogen production. A reactor generating Hydrogen by the hydrolysis of SBH must fulfill several requirements. The reactor must be versatile and easily controllable, that means it must rapidly provide a stable defined Hydrogen flow rate. As the hydrolysis of SBH is a highly exothermic reaction, elimination of heat must be provided in order to prevent overheating. Finally, the reactor must be small, of light weight and safe during its use. Two different reactors types have been developed for the generation of Hydrogen by the hydrolysis of SBH.

A semicontinuous reactor was designed as shown in Figure 1a. A fuel solution of 19 wt% of SBH was added continuously to a catalyst present in the reactor. As seen in Figure 1b a constant and

defined hydrogen generation rate (HGR) depending on the flow rate of fuel could be obtained and reduced to 0 by stopping the flow of the fuel into the reactor. The temperature in the system remained constant after reaching a characteristic value. The generated Hydrogen left the system through an opening for further use, while the other product, Sodium metaborate (NaBO_2) remained in the reactor.

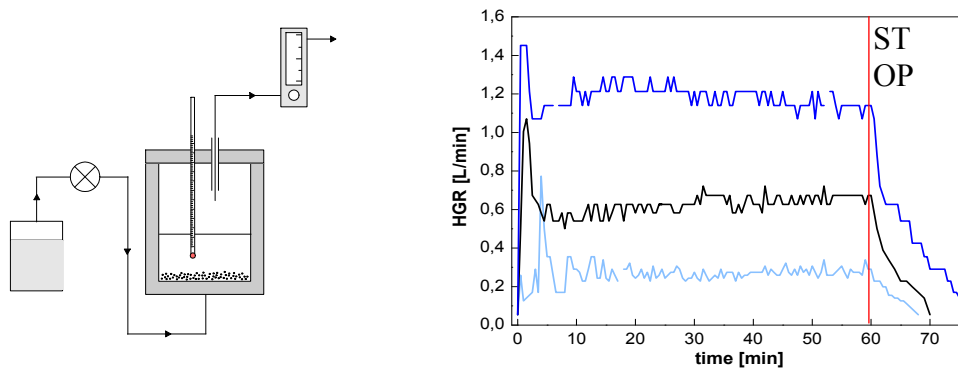


Figure 1a: Scheme of the semicontinuous reactor system; Figure 2b: HGR at different flow rates of 19 wt% of SBH, Flow rate a) 0.52 b) 1.2 c) 2.5 mL/min

As a second system a continuous reactor was designed as shown in Figure 2a. The fuel solution of 19 wt% of SBH was pumped into the reactor containing the catalyst with a flow rate of 2.8 mL/min, where the hydrolysis takes place, resulting in a HGR of 1 L/min. The entire mixture of products leaves the reactor into a separator, which also serves as disposal for the residues. As seen in Figure 2b the reactor is fast responding provides a determined and stable flow of Hydrogen necessary for many applications. A reaction temperature of more than 95 °C was achieved, which prevented the product Sodium metaborate from crystallizing inside the reactor. Thus long constant working times of production of Hydrogen could be obtained.

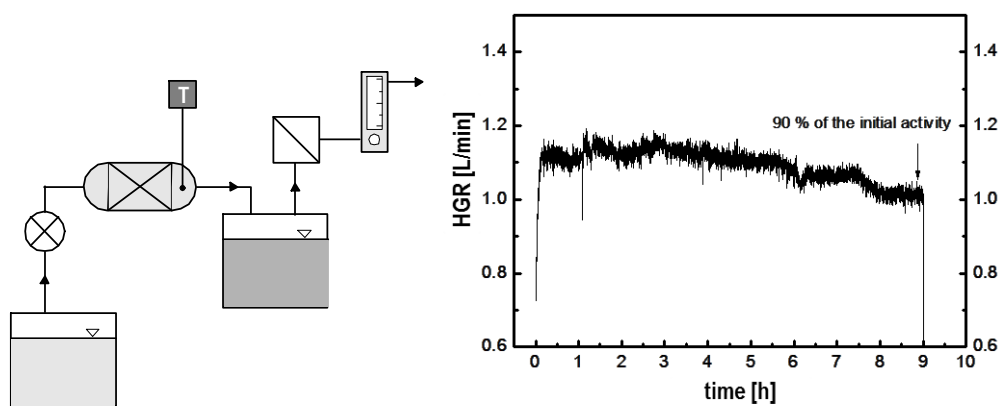


Figure 2a: Scheme of the continuous reactor system; Figure 2b: HGR at a constant flow rates of 19 wt% of SBH

CONCLUSIONS

The hydrolysis of Sodium borohydride permits the controlled and safe release of Hydrogen, making SBH to a promising option for Hydrogen storage. The two reactor systems developed fulfill the requirements to produce Hydrogen in the range of 1L/min for mobile and portable applications. The advantages of this process are its high safety during the use, the low toxicity of SBH and the residues and the economic price of the SBH. Unfortunately the hydrolysis is not a reversible reaction, so that the SBH only can be recovered by a recycling process of the residue.

ACKNOWLEDGEMENTS

Financial supports by the Spanish MINECO (CTQ2012-32519), the Junta de Andalucía and Abengoa Hidrógeno are acknowledged

Understanding the role of additives/catalysts in H₂ storage processes based on borohydride materials (HS1-2)

A.FERNÁNDEZ, E.DEPREZ, G.ARZAC, D.HUFSCHMIDT

*Institute of Material Science of Sevilla (ICMS),
CIC Cartuja (joint center of University of Sevilla and CSIC),
Avda Américo Vespucio 49, 41092 Sevilla, Spain
Email: dirk@icmse.csic.es*

INTRODUCTION

In the life cycle of hydrogen production-storage-use, a key topic under research is the hydrogen storage in solid hydride compounds. The main advantage of this method is its high storage capacity per volume unit, as compared to liquid or pressurized gas storage. Special attention has been paid on lightweight metal hydrides and complex hydrides, in particular borohydrides like LiBH₄ and NaBH₄ (see Fig.1 for a comparison among various hydride materials).

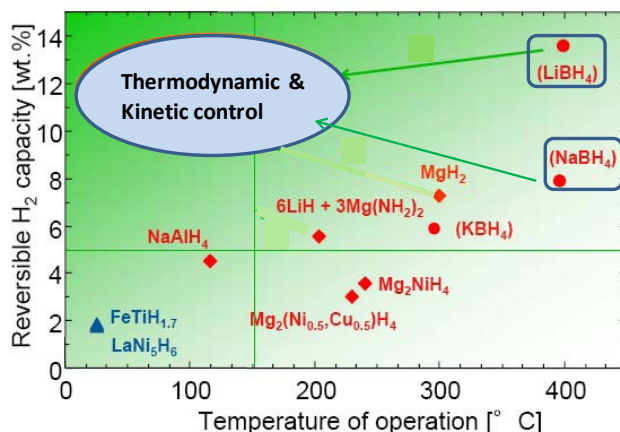


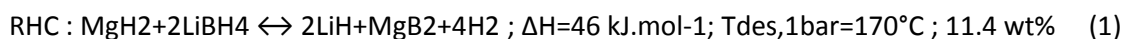
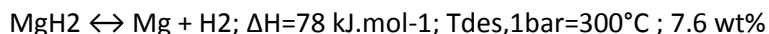
Figure 1: Materials for solid state hydrogen storage. Gravimetric storage capacity.

In the present work we will discuss how the adequate design of thermodynamics and the control of kinetics have been used to develop improved processes for possible applications of these complex borohydrides in hydrogen storage. The role of adequate additives/catalysts will be presented as a key factor for improved process design.

THE REACTIVE HYDRIDE COMPOSITE CASE. THE ROLE OF TI-BASED ADDITIVES

As we can see in Fig.1, LiBH₄ (LBH) is rather stable and the dehydrogenation reaction proceeds only at elevated temperatures. Destabilization of the complex hydride can be achieved, for example, by coupling with a metal hydride like MgH₂[1]. The overall reaction enthalpy is, therefore, lowered and allows for lower reaction temperatures keeping a high hydrogen storage capacity. The

concept of this “reactive hydride composite (RHC) system” has been proposed first based on thermodynamic concepts[1]:



Additionally reaction (1) was found to be reversible. The formation of MgB₂ appears to stabilize the dehydrogenated state and therefore decreases the total reaction enthalpy of the system. The pure LiBH₄ has been shown to be reversible but at much higher temperature than the RHC.

In spite of this thermodynamic strategy still the kinetic aspects must be considered and improved. The RHC system shows a two-step desorption mechanism. First, MgH₂ desorbs and forms Mg; thereafter the LBH decomposes forming LiH and MgB₂ whereby more hydrogen is released. The appearance of an incubation period between the two steps[1,2] makes the overall reaction very slow. However, kinetics could be enhanced by suitable additives, such as transition metal chlorides or oxides[2]. Particularly, the metal organic compound Titanium isopropoxide (Ti-iso) has shown to significantly improve the kinetics of the RHC system and especially the desorption of LiBH₄. The main contribution of the present work is the microstructural and chemical characterization of such Ti-iso additive during H₂ desorption and absorption. A combination of techniques like X-ray photoelectron spectroscopy (XPS), X-ray diffraction (XRD), X-ray Absorption spectroscopy (XAS) and the electron microscopy (TEM and SEM) analysis coupled to EELS and EDS are presented to elucidate the evolution of the additive during first cycles. The evolution of the Ti-isopropoxide additive to form Ti boride phases, which are in fact the active species for kinetic improvement, was found[3]. Our work postulates that the small (1.8%) lattice misfit between the {0001} basal plane of MgB₂ and the {0001} plane of TiB₂ is favouring the heterogeneous nucleation of the MgB₂ phase which is in fact the kinetic limiting step[3]. The reaction mechanism proposed for the desorption of H₂ in the RHC system is a random nucleation of the MgB₂ phase (promoted by the additive) followed by a Johnson-Mehl-Avrami growth mechanism.

THE HYDROLYSIS REACTION OF SODIUM BOROHYDRIDE. THE Co-B CATALYST

NaBH₄ (SBH) dehydrogenation also occurs at elevated temperatures (see Fig.1.). An alternative strategy for destabilization are the solvolysis reactions[4]. In particular the hydrolysis according to reaction (2):



In this case the reaction is highly exothermic although it is not reversible. Recycling strategies are needed to process the borate reaction products. From the thermodynamic point of view the release of hydrogen could now occur spontaneously and the kinetic control is therefore needed to make the reaction suitable for applications under controlled ambient conditions. In this sense aqueous SBH solutions at high pH (fuel) are stable and can produce hydrogen only when in contact with suitable catalysts (on demand H₂ generation) and have been foreseen in this work for low-scale portable applications[5].

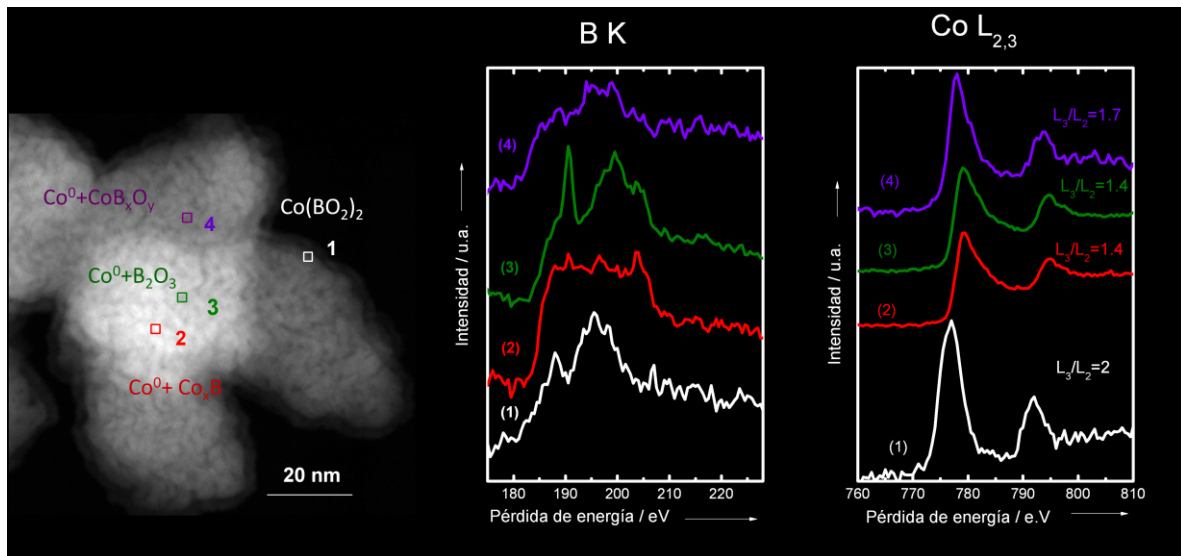


Figure 2: STEM/EDS study on the prepared Co-B catalyst. Left) HAADF image, centre) EELS B K-edge spectra, and right) EELS Co L_{2,3} spectra for the zones as defined in the left figure.

Cheap, but efficient catalysts are Co-B materials. In this work the Co-B based catalyst was prepared by chemical methods in powder form and also supported on pre-treated stainless steel homemade monoliths. The monoliths were prepared for its use in a continuous working reactor designed and built to allow a constant and adaptable generation of hydrogen (in the range of 0.3-1.7 L/min) over a long period of time[5]. The main contribution of the present work is to show the capabilities of the scanning TEM (STEM) with high angle annular dark field detector (HAADF), as well as, the electron energy loss spectroscopy (EELS) and X-ray fluorescence (EDS) with subnanometer resolution, to elucidate the role of boron compounds as stabilizers of the complex microstructure of Co-B catalysts[6] (see Fig.2). Such microstructural study, coupled to SEM-EDS, also elucidates the mechanism for the catalyst deactivation, reactivation and durability showing that the complex microstructure of the catalyst stabilizes the size of the catalytic active particles under operation conditions. In addition the long term sustainability can be improved by design of the reactor to self-stabilization of temperature over the melting point of borates (>90°C), this enhancing the removal of borates under operation and avoiding deactivation of the catalysts.

CONCLUSIONS

Thermodynamic considerations are the first step for progressing towards the use of light metal borohydride materials for solid-state hydrogen storage. In addition the kinetic improvement and the kinetic control of the processes need of the development of adequate additives and/or catalysts for each particular process. The use of powerful microstructural and chemical characterization techniques have been shown to strongly contribute to understand the behavior of catalysts and to draw-up the best operation conditions.

ACKNOWLEDGEMENTS

Financial supports from EC (AL-NANOFUNC, REGPOT-CT-2011-285895), the Spanish MINECO (CTQ2012-32519), the Junta de Andalucía and the CSIC (201260E006) are acknowledged.

REFERENCES

- [1] (a)Vajo, J. J.; Skeith, S. L.; Mertens, F. *Phys. Chem. Lett. B* 2005, 109, p.3719. (b)Barkhordarian, G.; Klassen, T.; Dornheim, M.; Bormann, R. *J. Alloys Compd.* 2007, 440, L18.
- [2] (a)Bösenberg, U.; Doppiu, S.; Mosegaard, L.; Barkhordarian, G.; Eigen, N.; Borgschulte, A.; Jensen, T.; Cerenius, Y.; Gutfleisch, O.; Klassen, T.; Dornheim, M.; Bormann, R. *Acta Mater.* 2007, 55, p.3951. (b)Vajo, J. J.; Salguero, T. T.; Gross, A. F.; Skeith, S. L.; Olson, G. L. *J. Alloys Compd.* 2007, 446-447, p.409. (c)Barkhordarian, G.; Jensen, T. R.; Doppiu, S.; Bösenberg, U.; Borgschulte, A.; Gremaud, R.; Cerenius, Y.; Dornheim, M.; Klassen, T.; Bormann, R. *J. Phys. Chem. C* 2008, 112, 2743.
- [3] (a)Deprez, E.; Muñoz-Márquez, M.A.; Roldán, M.A.; Prestipino, C.; Palomares, F.J.; Bonatto Minella, C.; Bösenberg, U.; Dornheim, M.; Bormann, R.; Fernández, A. *J. Phys. Chem. C* 2010, 114, p.3309. (b) Fernández, A.; Deprez, E.; Friedrichs, O. *International Journal of Hydrogen Energy*, 2011, 36, p. 3932.
- [4] B.H. Liu, Z.P. Li, *J. Power Sources* 2009, 187, p.527.
- [5] Arzac, G.M; Hufschmidt, D.; Jiménez de Haro, M.C.; Fernández, A.; Sarmiento, B.; Jiménez, M.A.; Jiménez, M.M. *International Journal of Hydrogen Energy* 2012, 37, p.14373.
- [6] Arzac, G.M.; Rojas, T.C.; Fernández, A. *Chem. Cat. Chem.* 2011, 3, p.1305.

Electrochemical Hydrogen Compressor Performance Based On Speak And Nafion Membranes (HS1-3)

S. Rivasa., J. L. Pinedab., A. Carbonec., A. Saccà., E. Passalacqua., Bamdad Bahard., J. Ledesma-Garcíaa., A. U. Chávez-Ramírezb., L.G. Arriagab.

aUniversidad Autónoma de Querétaro, División de Investigación y Posgrado, Facultad de Ingeniería. 76010. Querétaro, México.

bCentro de Investigación y Desarrollo Tecnológico en Electroquímica S. C., Parque Tecnológico Querétaro s/n, Sanfandila, Pedro Escobedo, C.P. 76703. Querétaro, México

cCNR-ITAE, Institute for Advanced Energy Technologies "N. Giordano" Via Salita S. Lucia sopra Contesse, 5-Messina, Italy

dXergy Incorporated. 310 North Race Street, Georgetown. DE 19947, USA.

An energy vector is any solid, liquid or gas that is capable of storing energy to be released in a controlled mode as needed. For instance, 1 Kg of H₂ contains the same energy as 2.5 Kg of gasoline (680 g/L), without the inconvenience of generating polluting side products [1]. The major challenges for an economic scheme based on hydrogen as an energy carrier are: reduction of production costs, more efficient storage methods and distribution systems, hydrogen fuel cells with higher conversion performance and certainly, public acceptance.

Proton exchange technologies are well suited to the needs of the hydrogen economy, since they are used to produce hydrogen in a solid polymer electrolyzer (SPE), to produce clean energy in a proton exchange membrane fuel cell (PEMFC), and recently to purify or compress hydrogen in an electrochemical hydrogen compressor (EHC). The heart of all these systems is the Membrane Electrode Assembly (MEA), and the essential differences are the electrocatalyst used for PEMFCs and SPEs, and the mechanical stress to which it is submitted in an EHC. In any case it is required that the polymer electrolyte has high ionic conductivity in varying operating conditions, since this capability affects largely the performance of the electrochemical device of interest.

Traditional hydrogen compression technologies have several drawbacks mostly related to the high energy demand to get low compression efficiencies, the EHC system turns out to be an interesting alternative in research due to its low energy demand to reach high compression rates, it is free noise, low maintenance and unpolluted hydrogen can be obtained. As can be seen in Figure 1., the main difference between a PEMFC and a EHC is the absence of oxygen to be reduced, therefore, is the hydrogen again that gets reduced at the cathode. The EHC can also be perfectly adapted to an SPE or even a Unitized Regenerative Fuel Cell (which is capable of operating as SPE or PEMFC) and the energy required for compression can be obtained from renewable sources (solar or wind). Challenges in EHC are cell design and Proton Exchange Membranes capable of withstand a high pressure between anode and cathode.

Nafion[®], a commercial perfluorosulfonic acid membrane, has been the most used and studied due to its excellent thermal and chemical properties in PEMFCs systems, even at 80 °C. However, its high production costs and low mechanical resistance have opened a research field towards the development of ionic conducting polymers with better general properties. A promising competitor

against Nafion® are the Sulphonated Poly(Ether Ether Ketone) (S-PEEK) membranes, since have shown a good proton conductivity, thermal and chemical stability, besides a low production cost [2-3].

The aim of this work was to evaluate the performance of S-PEEK, Nafion 112 and Nafion 115 membranes in an Electrochemical Hydrogen Compressor.

An Electrochem PEMFC (5 cm²) was used as compressor. The MEAs were made by Hot Spray deposition of the electrocatalytic ink, which was prepared by mixing Pt (E-Tek) and Vulcan Carbon XC-72 at proportions 30/70%, with Nafion solution (5%). As gas diffuser SIGRACET® 35BC by SGL Carbon were used. As well as in PEMFCs, the membrane must be highly hydrated; therefore water saturated hydrogen was passed through the ECHC during the whole set of tests. Potential pulses from 100 to 800 mV were applied to the ECHC while the pressure increase in the compression chamber was monitored. As expected, the highest the potential applied, the fastest the pressure increases, but this can be also limited by mass transfer and the ECHC sealing issues.

Pressure and current increments were followed as function of the applied potential, as can be seen in Figure 2., a 500 mV potential is enough to reach the highest pressure (20 psi) with Nafion® 115 after 400 seconds. The S-PEEK membrane reaches a steady pressure at 400 mV in 200 seconds but much lower than Nafion®. This low compression capacity could be caused by diffusion at a high pressure difference (between anode and cathode), since we expected a similar compression although at an inferior rate, in spite of its lower proton conductivity compared to Nafion®. Current density is related to the amount of hydrogen that passes from anode to cathode by a redox reaction, but this is not related to the highest pressure difference that every membrane is able to withstand, it means that it will reach its compression capacity faster at a higher potential applied, but it also means more power invested in the compression process.

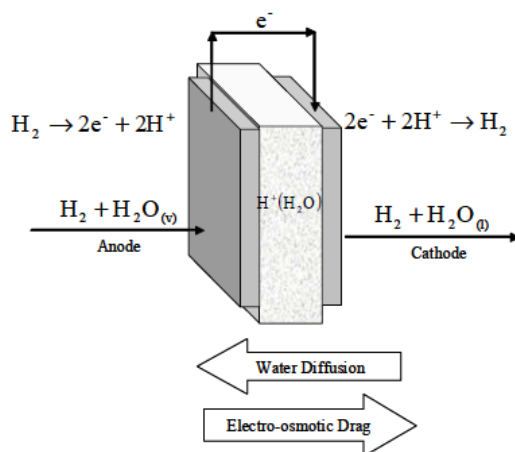


Figure 1.- Electrochemical Hydrogen-Compressor.

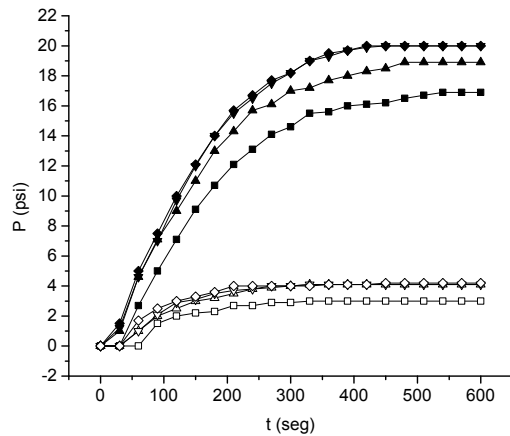


Figure 2. increasing pressure in function of the potential applied.

■ -300 mV, ▼ -400 mV, ▲ -500 mV, ◆ - 600 mV. Full symbols are for N15, empty are for S-PEEK.

[1] http://www1.eere.energy.gov/hydrogenandfuelcells/pdfs/fct_h2_storage.pdf

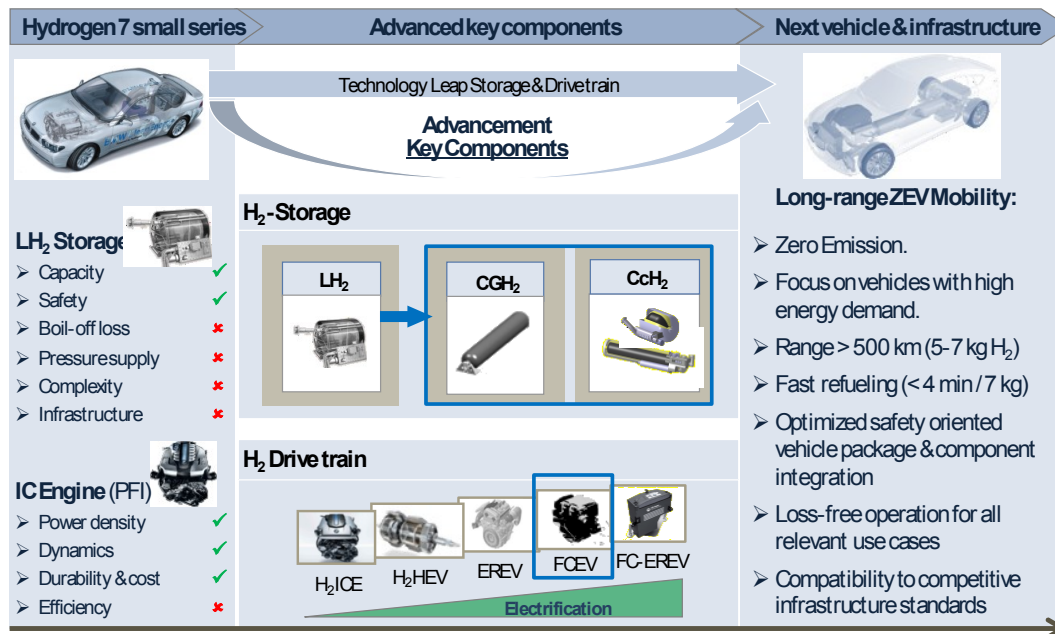
[2] Iulianelli A, Basile A. Sulfonated PEEK-Based polymers in PEMFC and DMFC applications: a review. *Int J Hydrogen Energy* 2012; 37:15241-55.

[3] Carbone A., Pedicini R., Portale G., Longo A., D'Ilario L., Passalacqua E. Sulphonated poly(ether ether ketone) membranes for fuel cell application: Thermal and structural characterisation. *J. Power Sources* 2006; 163:18-26.

BMW Hydrogen Storage Technology – Current Status and Future Trends (HS1-4)

Dr. Klaas Kunze, BMW, Dr. Oliver Kircher, BMW

Based on the successful demonstration of the Hydrogen 7 vehicle the BMW Group has entered into a new phase of intensive qualification of core components for future hydrogen vehicles. A special focus is set on onboard hydrogen storage, which has been identified as one of the main issues on the way to a customer oriented commercially viable hydrogen vehicle.



Advancement of core components


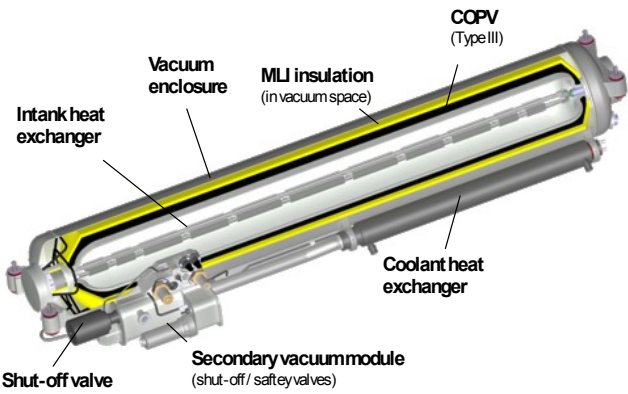
Due to its promising potential to overcome the challenge of thermal endurance of liquid hydrogen storage while retaining a higher system energy density than any other available hydrogen vehicle storage system and while minimizing other issues of liquid and high-pressure gaseous storage systems, cryo-compressed hydrogen storage (CcH₂) is BMW's preferred physical storage solution, in particular for use in larger passenger vehicles with high energy and long range requirements, whereas gaseous compressed hydrogen (CGH₂) is considered as an option for smaller vehicles with moderate range requirements. As a consequence the BMW Group has started a thorough component and system level validation of CcH₂ vehicle storage.

The presentation on BMW's hydrogen storage development and demonstration program will show BMW's ongoing hydrogen storage activities as a part of the efficient dynamics strategy and the perspective of the first vehicle integration of a CcH₂-storage in a vehicle for public road use.

The value of CcH₂ storage as a future hydrogen vehicle storage system option with reference to the best-fit solution for different vehicle applications will be highlighted. Based on the high density of

cryo-compressed storage, cruising range in hydrogen vehicles with high efficiency could be the same as that of today's gasoline vehicles. Beyond that, the ability of filling a cryo-compressed storage with either low-density compressed gaseous hydrogen (up to 5000 psi) at hydrogen stations with gas supply or high-density cryo-compressed hydrogen at stations with liquid hydrogen supply and cryogenic compression guarantees high refueling flexibility in an evolving infrastructure. In particular at stations, where liquid truck-in and liquid storage at the station are least-cost, a cryo-compressed hydrogen fill enables high vehicle range combined with fast and cost-efficient refueling. Due to its significantly reduced energy demand compared to warm gas compression, compression of liquid hydrogen via a cryogenic high-pressure pump enables very efficient cold and warm gas refueling and a scalable hydrogen station layout with a reasonable footprint.

Recent experiments with BMW's liquid hydrogen high-pressure cryo-pump and the CcH2 storage system prototype revealed a high refueling density of more than 70 g/L in a CcH2 single-flow refueling without pre-cooling when the CcH2 tank is continuously operated in the cryo-compressed mode. Switching from an initially warm tank in compressed gas (CGH2) mode to a cold tank in cryo-compressed mode with up to three times higher density has also been experimentally demonstrated and the results correspond well to simulation results.

Modular Super-insulated Pressure Vessel (Type III)		
Max. usable capacity	CcH ₂ : 7.1 kg (237 kWh) CGH ₂ : ≥ 2.3 kg (76 kWh)	+ Active tank pressure control + Double layer safety and leak detection + Engine/fuel cell waste heat recovery
Operating pressure	15 - 350 bar	
Vent pressure	≥ 350 bar	
Refueling pressure	CcH ₂ : 300 bar CGH ₂ : 320 bar	
Refueling time	< 5 min	
System volume	~ 235 L	
System weight (incl. H ₂)	~ 160 kg	
H ₂ -Loss (Leakage max. loss rate infr. driver)	<< 3 g/day 3 - 10 g/h (CcH ₂) < 1% /year	

System Layout BMW Prototype 2015

The presentation will summarize the current status of BMW's CcH2 storage component and system level validation, describe the key milestones that have already been successfully passed, indicate the first implementation of a CcH2 vehicle storage system in a passenger car and will finally extract the remaining challenges of CcH2 vehicle storage on its way to a commercial product.

Hydrogen as a solution for storing intermittent renewable energy (HS1-5)

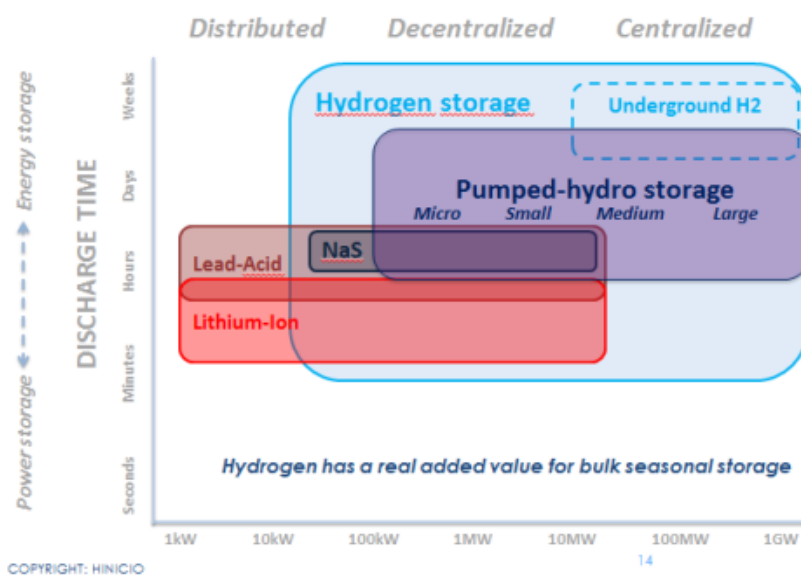
Jean-Christophe Lanoix, senior consultant, Hincio.

The recent rise of renewable electricity is rapidly creating new constraints on the electricity grid, which was initially mostly designed on a top-down model relying on predictable sources (mostly large-scale and fossil-based) as opposed to the more decentralized architecture imposed by intermittent renewable energy sources such as wind or solar. Electricity storage is one of the options at our disposal to meet those new flexibility needs at the power system level and is increasingly considered as a key enabler on a low or even zero carbon electricity pathway.

Many different technologies are already competing on this new market ranging from conventional pumped-hydro storage to batteries such as lead-acid, lithium-ion or sodium-sulfur accumulators. Within this technology portfolio, hydrogen enjoys very unique features. Beyond the conventional “re-electrification” scheme, which is common to all storage technologies, it can be utilized in other high added-value markets, including in the transport sector to supply fuel cell vehicles or in many industrial processes (electronic, ammonia, refineries, etc.). Hydrogen can even be injected into the natural gas grid to lower the carbon footprint of downstream applications or combined with captured CO₂ to produce synthetic methane in a “power-to-gas” scheme.

This presentation will focus on large-scale hydrogen underground storage. First, the various geological options for storing hydrogen in underground formations will be presented, ranging from salt cavern (which are often the preferred option), to rock caverns, depleting oil and gas field and abandoned mines. A detailed map of the European geological potential for hydrogen underground storage will be discussed.

Then, the key features, advantages and disadvantages of hydrogen versus other storage technologies, will be compared between each other, in particular in terms of rated power, storage capacity, discharge time, response time, investment costs, operational costs, etc.



The presentation will then highlight the potential role of large-scale hydrogen underground storage in tomorrow's energy system, in particular in a context where fuel cell vehicles and the necessary hydrogen infrastructure are being deployed while at the same time intermittent renewables are on the rise. Innovative business models will be discussed. Finally, the presentation will outline the key role played by regulation and public incentives to kick-start the energy storage market, for both hydrogen and other competing technologies.

This presentation will be mostly based on the preliminary results of the on-going European FCH-JU project "HyUnder" which aims at assessing the European potential for large-scale hydrogen underground storage. This project brings together key players in the hydrogen sector, including Shell, E.On Gas, Solvay, ECN, Hincio and LBST.

About HyUnder

HyUnder is a European project financed by the Fuel Cell and Hydrogen Joint Undertaking. HyUnder will provide the first complete assessment of the potentials for large scale storage of fluctuating renewable electricity in underground salt caverns for hydrogen, with specific focus on using synergies with its application as transport fuel and other markets. The project will also consider issues of public acceptance and regulatory obstacles. The project will run for a period of two years and will develop six case studies across Europe and an EU Implementation Plan on large scale underground hydrogen storage, with particular focus on salt caverns. The HyUnder consortium comprises 12 leading organizations from 7 different European countries including large industrial representatives, Small Medium Enterprises and research institutes.

For further information, please visit: www.hyunder.eu.

About Hincio

Hincio is a strategy consulting firm focused on sustainable energy, covering renewable energy technologies, fuel cells and hydrogen, smart energy storage, energy efficiency and clean transport technologies. Its multinational team consists of engineers, economists, environmentalists and policy experts in sustainable energy.

Hincio's services cover four practice areas: strategy, investments, policy and project management. We aim to provide clients with the necessary knowledge on sustainable energy and the understanding of the related markets to help them make informed decisions. Hincio also facilitates investment in clean energy technologies, advising clients on investment strategies, helping investors analyze opportunities and risks linked to regulatory and policy changes, and assisting project developers in accessing private investors and public funds. Hincio's policy experts help understand the challenges ahead and analyze the impact on businesses.

For further information, please visit: www.hincio.com

Energy evaluation of a solar hydrogen storage facility (HS1-6)

Eduardo López González^{1*}, Fernando Isorna Llerena¹, Manuel Silva Pérez² and Felipe Rosa Iglesias²

1Instituto Nacional de Técnica Aeroespacial (INTA), Ctra. S. Juan-Matalascañas, km. 34, 21130, Mazagón (Huelva), España

2Universidad de Sevilla, Escuela Técnica Superior de Ingeniería, Camino de los Descubrimientos, s/n, 41092, Sevilla, España

() lopezge@inta.es*

ABSTRACT:

Storage of electricity from renewable energy sources is one of the main challenges to be overcome in order to ensure a proper integration of these technologies into the power grid, paving the way for their gradual introduction into future energy scenarios.

The use of hydrogen as an energy carrier is a potential and promising option among the different technologies that can be used to store electrical energy from renewable sources on a large scale.

Typical hydrogen facilities used to store renewable electricity are currently based on electrolysis systems connected to the power source, mainly wind or photovoltaic, responsible for producing hydrogen and oxygen from the decomposition of water. Hydrogen is stored in accordance with the facility requirements for its use in stationary fuel cells for electric power production.

Nowadays, there are solutions and options for large-scale hydrogen storage adapted from the chemical industry, the main consumer of this gas as raw material for processes. Nevertheless, for medium and small-scale applications, the challenges to design and build up suitable hydrogen storage systems are different. In this context, the requirements related to energy performance are particularly important when assessing the performance of the overall system, and especially if such performance has to be compared with other potential methods for electrical energy storage, such as batteries.

This paper presents the evaluation, in terms of energy-related parameters, of a solar hydrogen storage system connected to a PV generator. The system is located at INTA R&D facilities in Huelva. These parameters will be representative of the real performance of the system, and can be used as indicators to compare different electrical energy storage systems based on hydrogen and other technologies. Main indicators of the solar hydrogen storage plant are:

- Specific energy consumption.
- Energy density, both gravimetric and volumetric.
- Energy efficiency.

A comparison with typical values of electrical energy storage systems based on lead-acid and lithium ion batteries is also provided.

The plant is able to produce 1.2 Nm³/h of hydrogen, while the capacity of the storage system has been designed to store the production of one week, around 30 Nm³. Hydrogen storage facility comprises a high pressure gas storage system and a metal hydride container, sharing both systems a common low pressure buffer. This storage system supplies hydrogen to different PEM fuel cells available at the INTA facility. The hydrogen storage facility was operated for one year, jointly with the solar hydrogen production system, considering four possible operation modes. The experimental results were used to calculate the above-mentioned parameters.

Specific energy consumption, in terms of kWh/Nm³ of stored hydrogen, includes both thermal and electrical energy consumption, and it has been estimated for the whole hydrogen storage plant under four operation modes of the facility.

The gravimetric and volumetric energy densities have been calculated at component and overall installation levels, showing that the volumetric energy density of metal hydride storage is significantly higher than those of the high and low pressure hydrogen storage systems. Regarding the gravimetric energy density, high pressure and metal hydride systems offer similar values, which are much higher than the corresponding value for the low pressure buffer.

Considering the use of hydrogen in a commercially available PEMFC system, the obtained energy density values have been compared with other electrical energy storage systems, such as those based on lead-acid batteries and lithium ion. This comparison shows that the gravimetric energy density of the overall hydrogen storage system is only slightly lower than the typical values for lithium ion batteries, achieving much higher gravimetric energy density than lead acid batteries. The volumetric energy density for the overall installation is inferior to that provided by lithium ion batteries, but similar to that of wet lead acid batteries. A consequence of the energy density analysis of the facility is that the energy density values of the overall installation can be adjusted by an adequate distribution of the hydrogen storage capacity in the different storage methods considered (low pressure, metal hydride and high pressure).

The energy efficiency was calculated for the overall system and the different operation modes of the facility. Regarding the annual energy efficiency by operation mode, the most efficient option is to use low pressure hydrogen in the fuel cells directly from the buffer tank (96% of energy efficiency). Most inefficient option is to use high pressure hydrogen, delivered to compression unit from metal hydrides, in the fuel cells (43%).

Experimental and simulated results for the desorption process in a complex hydride hydrogen storage reactor with addition of metal hydride (HS2-1)

INGA BÜRGER, CHRISTIAN BRACK, MARC LINDER;

German Aerospace Center, Pfaffenwaldring 38-40, 70569 Stuttgart

MOTIVATION

In the majority of studies concerning tank design for metal hydrides, the absorption process is in the focus due to the desired fast fuelling rates and the required heat removal [1–4]. However, for storage reactors of complex hydrides, also the desorption process can be crucial. Due to the conversion type reaction of these materials, hydrogen desorption rates at HT-PEM exhaust gas temperatures and above fuel cell H₂ supply pressures (170 °C and 1.7 bar) are quite slow [5]. Therefore, it is a challenge to discharge a significant fraction of hydrogen from the material. In this presentation, a new prototype reactor is introduced that is based on the addition of some MeH material to a complex hydride reactor. As this metal hydride material is able to desorb H₂ at a very fast reaction rate, the system pressure during the desorption process does not fall below the equilibrium pressure of the metal hydride material, that has been selected 3 to 5 bar above the fuel cell supply pressure. In the framework of the EU project SSH2S, this reactor concept is used for a 6.8 kg prototype tank that is couple with a HT-PEM fuel cell.

METHODOLOGY

The complex hydride material that has been used in the present study is Li-Mg-N-H (2LiNH₂ 1.1MgH₂ 0.1LiBH₄ 3wt.%ZrCoH₂, and for the according metal hydride material LaNi_{4.3}Al_{0.4}Mn_{0.3} has been selected. The final tank consists of 12 identical tubes, which are each filled with 282 g of both materials. The outer diameter of a single tube is 42.2 mm and the wall thickness is 1.65 mm. For the separation of the two materials, a perforated copper tube with 14 mm and 1 mm thickness has been used that is covered with a thin stainless steel mesh. The metal hydride is filled in the center and the Li-Mg-N-H material in the outer annulus. Furthermore, outside of the tube there is a 2 mm gap, where the heat transfer fluid is circulating.

For the 2D modeling, 1/8th of a perpendicular cut to the tube axis has been considered. For the domains of the MeH and Li-Mg-N-H material, mass balances of the gas and the solid as well as a total energy balance have been implemented, while for the copper and the steel wall just an energy balance has been modeled. The properties of the two materials have been determined in the SSH2S project or taken from the literature.

RESULTS

Constant flow rate

The basic desorption scenario that is considered in the present study can be described as follows. In the beginning, the pressure in the system refers to the hydride charging pressure of 70 bar. Then, hydrogen is removed from the system (to the fuel cell) at a constant mass flow rate. Due to this flow

rate, the pressure is continuously decreasing. As soon as the system pressure falls below the equilibrium pressure, the Li-Mg-N-H material starts to desorb hydrogen at a slow rate. Thus, the pressure continues to decrease, but less steep. When the pressure finally reaches the equilibrium pressure of the MeH material, this material desorbs hydrogen fast and sufficient, thus the pressure reaches a plateau. At this plateau, the Li-Mg-N-H material is desorbing at its own rate and the MeH material is desorbing the required amount that is released from the system. Finally, when the MeH material is completely desorbed, the pressure decreases again and as soon as a pressure of 1.7 bar is reached, the experiment is terminated.

Figure 1 shows the simulated and experimental results for 3 different experiments at a heat transfer fluid temperature of 170 °C. As expected, in the beginning of the experiment, the pressure decreases linearly. Then, according to the flow rates different plateau pressures are reached. For the highest flow rate of 2 NLmin⁻¹, the lowest plateau pressure of ~ 3 bar is reached, in contrast to the experiment with the lowest flow rate of 0.5 NLmin⁻¹ that shows a plateau at 10 bar. The reason for the different pressure levels is the difference in required thermal power for the endothermic desorption reaction that causes different temperatures inside of the tube. As mentioned before, as soon as the pressure falls below the fuel cell supply pressure of 1.7 bar, the desorption is terminated. In case of the experiment with the flow rate of 1 NLmin⁻¹, the reactor is able to desorb hydrogen for 122 min. This refers to an operation time of 2h for a 1 kWel HT PEM fuel cell system.

Additionally to the experimental data, in Figure 1 the simulated results for the according experiments are shown. In the beginning of the experiment, the simulation deviates from the experimental data. This behavior can be explained when the material is actually desorbing above the modeled equilibrium pressure of the material, and it refers to less than 10 % of the hydrogen capacity of the Li-Mg-N-H material. However, during the main part of the desorption process where the plateau pressure is formed, the simulation agrees very well with the experiment.

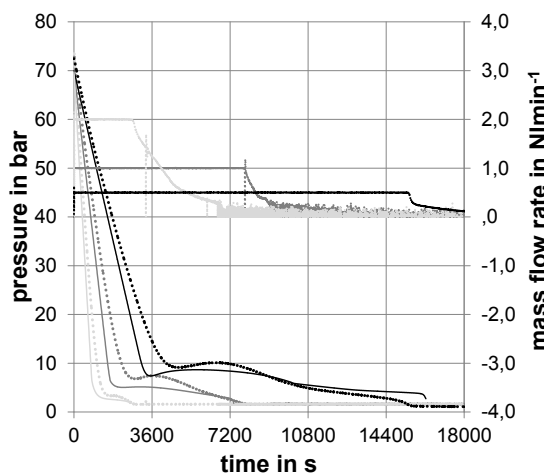


Figure 1: Pressure and mass flow rate versus time for three experiments at different mass flow rates. Light grey: 2 NLmin⁻¹, dark grey: 1 NLmin⁻¹, black: 0.5 NLmin⁻¹. Experiment: dotted line, simulation: solid line.

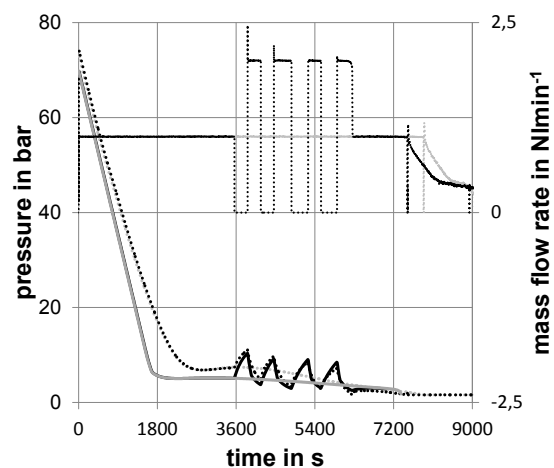


Figure 2: Pressure and mass flow rate versus time for one experiment with constant (1 NLmin⁻¹, grey) and one with periodic (0-2 NLmin⁻¹, black) mass flow rate. Experiment: dotted line, simulation: solid line.

Periodic flow rate

Besides the stabilization of the plateau pressure, the reactor concept for complex hydrides based on the addition of a metal hydride shows another effect. This effect can just be observed when the flow rate is not constant but periodically changing (s. Figure 2). In this case, during low loads, the pressure in the system increases, while during peak loads the pressure decreases. As the pressure even during peak loads will not fall below the equilibrium pressure of the MeH material, it exceeds this equilibrium pressure during low loads. Thus, in these phases the Li-Mg-N-H material is still desorbing while the MeH material “reabsorbs” hydrogen.

CONCLUSION

The new prototype reactor that is presented in this paper shows an improved desorption performance of a pure CxH reactor when a MeH material is added. On the one hand, the MeH material stabilizes the system pressure during desorption at a level above the fuel cell supply pressure. On the other hand, when periodic flow rates are applied, the MeH material can actually be recharged by the CxH material. Therefore it can be stated that this concept enables the utilization of CxH materials, even when the pure reaction rates are insufficient for the required dynamics of automotive applications.

ACKNOWLEDGEMENTS

The research leading to these results has received funding from the European Union's Seventh Framework Programme (FP7/2007-2013) for the Fuel Cells and Hydrogen Joint Technology Initiative under grant agreement n. 256653.

LITERATURE

[1] Mohan G, Prakashmaiya M, Srinivasamurthy S, Prakash Maiya M, Srinivasa Murthy S. Performance simulation of metal hydride hydrogen storage device with embedded filters and heat exchanger tubes. *Int J Hydrogen Energy* 2007;32(18):4978–87.

[2] Bhourri M, Goyette J, Hardy BJ, Anton DL. Honeycomb metallic structure for improving heat exchange in hydrogen storage system. *Int J Hydrogen Energy* 2011;36(11):6723–38.

[3] Hardy BJ, Anton DL. Hierarchical methodology for modeling hydrogen storage systems. part ii: detailed models. *Int J Hydrogen Energy* 2009;34(7):2992–3004.

[4] Garrison SL, Hardy BJ, Gorbounov MB, Tamburello D a., Corgnale C, VanHassel B a., et al. Optimization of internal heat exchangers for hydrogen storage tanks utilizing metal hydrides. *Int J Hydrogen Energy* 2012;37(3):2850–61.

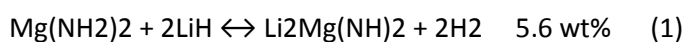
[5] Fichtner M. Conversion materials for hydrogen storage and electrochemical applications—concepts and similarities. *J Alloys Compd* 2011;509:S529–S534.

Modified Hydrogen Storage Performance Of Mg(NH₂)₂/LiH Composite (HS2-2)

Hujun Cao, Yao Zhang, Han Wang, Teng He, Zhitao Xiong, Guotao Wu, Ping Chen

Dalian National Laboratory for Clean Energy, Dalian Institute of Chemical Physics, Chinese Academy of Sciences, Dalian 116023, P. R. China.
caohujun@dicp.ac.cn; pchen@dicp.ac.cn

The demand for on-board hydrogen store is the driving force behind the tremendous efforts in materials research and development. Among those systems, amide-based composite system has the potential to meet the needs of onboard hydrogen storage for fuel cell vehicles due to its relatively high hydrogen capacity and tunable kinetics and thermodynamics [1]. A large number of amide-hydride and amide-complex hydride composites have been developed in the past decades. In particular Mg(NH₂)₂/2LiH system [2] has a favorable reaction thermodynamics (39 kJ/mol-H₂) and relatively high capacity (5.6 wt% H₂) [3]. Hydrogen desorption from Mg(NH₂)₂/2LiH system proceeds according to the reaction (1).



Although with suitable thermodynamic properties that allows it to achieve 1 bar equilibrium hydrogen pressure at ~80 °C, the majority of hydrogen desorption can only be achieved at temperatures above 180 °C even if the Mg(NH₂)₂/2LiH composite has been milled intensively, showing the presence of severe kinetic barrier. Previous studies indicate that the kinetic barrier was probably resulted from the relocation of atoms across amide/imide and imide/hydride phase boundaries, and also from the mass transport along the imide layer [4]. Numerous attempts have been made to overcome the barrier in recent years. Doping additives appears to effectively tune the hydrogenation/dehydrogenation kinetics, and therefore, lowers the operating temperature [5]. Our focus is to narrate the effect of Li₃AlH₆ on Mg(NH₂)₂/2LiH system [6]. Experimental results show that 3.2 mol % Li₃AlH₆-modified Mg(NH₂)₂/2LiH sample releases hydrogen at a rate ca. 4.5 times as fast as that of the Li₃AlH₆-free sample at 140 °C. The enhancement of desorption kinetics is reflected also by the reduction of activation energy (E_a) from 127 to ca. 96.3 kJ/mol. The interaction of Li₃AlH₆ and Mg(NH₂)₂ during ball milling results in the formation of LiAl(NH)₂, LiNH₂ and Mg₃N₂. LiAl(NH)₂ is actually the active species for the enhancement of dehydrogenation/re-hydrogenation kinetics of the system.

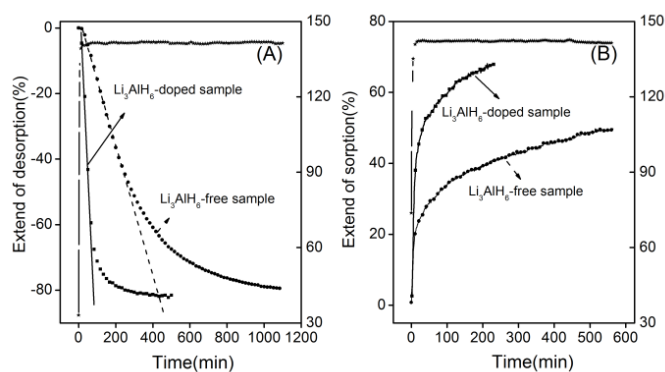


Fig. 1 Isothermal hydrogen desorption (A) and sorption (B) at 140 °C for the Li₃AlH₆-doped and the Li₃AlH₆-free samples.

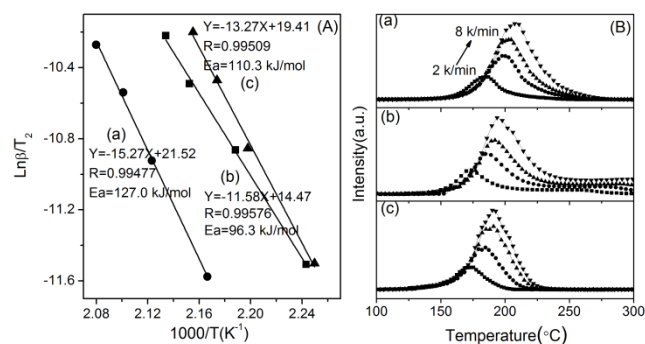


Fig. 2 Kissinger plots (A) and TPD profiles (B) for the Li₃AlH₆-free sample (a), Li₃AlH₆-doped Sample (b), and LiAl(NH)₂-doped Sample (c).

References

- [1] P. Chen, Z. Xiong, J. Luo, J. Lin, K. L. Tan, *Nature* 2002, 420, 302; P. Chen, Z. Xiong, G. Wu, Y. Liu, J. Hu, W. Luo, *Scripta Materialia* 2007, 56, 817.
- [2] W. Luo, *Journal of Alloys and Compounds* 2004, 381, 284; Z. Xiong, G. Wu, J. Hu, P. Chen, *Advanced Materials* 2004, 16, 1522.
- [3] Z. Xiong, J. Hu, G. Wu, P. Chen, W. Luo, K. Gross, J. Wang, *Journal of Alloys and Compounds* 2005, 398, 235.
- [4] P. Chen, Z. Xiong, L. Yang, G. Wu, W. Luo, *Journal of Physical Chemistry B* 2006, 110, 14221.
- [5] H. Cao, Y. Zhang, J. Wang, Z. Xiong, G. Wu, P. Chen, *Progress in Natural Science: Materials International* 2012, 22(6), 550.
- [6] H. Cao, Y. Zhang, J. Wang, Z. Xiong, G. Wu, J. Qiu, P. Chen, *Dalton Transactions* 2013, 42, 5524.

Long-Term Atomistic Simulation of Hydrogen Diffusion in Metals (HS2-3)

K. G. Wang¹, M. P. Ariza², and M. Ortiz¹

¹ Division of Engineering and Applied Science, California Institute of Technology

Pasadena, CA 91125, USA

² Escuela Técnica Superior de Ingeniería, Universidad de Sevilla

Sevilla 41092, Spain

ABSTRACT

The effective and efficient storage of hydrogen is one of the key challenges in developing a hydrogen economy. Recently, intensive research has been focused on developing and optimizing metal-based nanomaterials for high-speed, high-capacity, reversible hydrogen storage applications. Notably, the absorption and desorption of hydrogen in nanomaterials is characterized by an atomic, deformation-diffusion coupled process with a time scale of the order of seconds to hours – far beyond the time windows of existing simulation technologies such as Molecular Dynamics (MD) and Monte Carlo (MC) methods. In this work, we present a novel deformation-diffusion coupled computational framework which allows the long-term simulation of such slow processes and at the same time maintains a strictly atomistic description of the material. Specifically, we first propose a theory of non-equilibrium statistical thermodynamics for multi-species particulate solids based on Jayne's maximum entropy principle and the meanfield approximation approach. Unlike in MD and MC, now the individual hops of atoms are not explicitly tracked, but instead accounted for in the theory in a statistical sense. This non-equilibrium statistical thermodynamics model is then coupled with novel discrete kinetics laws, which governs the diffusion of mass – and possibly also conduction of heat – at atomic scale. Finally, this thermo-chemo-mechanical coupled system is solved numerically using a staggered procedure. The salient features of this computational framework are demonstrated in the simulation of a specific hydrogen diffusion problem using palladium nanofilms, which comes with a simulation time of one second. More generally, the proposed computational framework can be considered as an ideal tool for the study of many deformation-diffusion coupled phenomena in hydrogen-storage-related applications including, but not limited to, hydrogen embrittlement, grain boundary diffusion, and various cyclic behaviors.

1. INTRODUCTION

Hydrogen is an ideal energy carrier and considered as a potential substitute of fossil fuels for future transport, such as automotive applications. It can be stored as chemical compounds with metals (e.g. magnesium) in the form of metal hydrides. Recently, a great deal of effort has been made on the development of more advanced metal-based hydrogen-storage media, particularly nanomaterials such as nanofilms and nanoparticles. In this area of research, a number of challenging problems are characterized by the strong coupling of – possibly plastic – lattice deformation and the kinetics of hydrogen atoms. One example is hydrogen embrittlement, that is, the material becomes brittle and fracture following cyclic absorption and desorption of hydrogen. This type of problems requires deformation-diffusion coupled analysis at atomic scale; however, the typical time range is of the order of seconds to hours. Molecular Dynamics (MD) and Monte Carlo (MC) methods are

powerful techniques to study deformation and diffusion mechanisms in systems of particles, but they are limited to small time windows of microseconds at best. Considerable effort has been devoted to accelerating MD and MC methods and notable successes have been recorded in this direction (cf. [1]). However, no atomistically-based computational methods appear to be as yet available to study slow phenomena over time scales of the order of seconds to hours while maintain a strictly atomistic description of the material. In this work, we present an atomistic, deformation-diffusion coupled computational framework which is capable of long-term simulation of hydrogen diffusion in metal-based nanomaterials. This computational framework is an extension of HotQC, a maximum entropy scheme for finite temperature solids ([2], [3]), to multi-species materials with diffusion of mass.

2. THEORETICAL MODELS

We extend the maximum-entropy formalism of classical equilibrium thermodynamics to establish thermodynamic relations in non-equilibrium, multi-species solids where the thermodynamic state is allowed to vary from atom to atom. More specifically, we consider a system consisting of N atoms, each of which can be of one of M species including, in this context, hydrogen and the species of the hydrogen-storage material. For each particle $i=1,\dots,N$, and each species $k = 1,\dots,M$, we introduce the occupancy function

$$n_{ik} = \begin{cases} 1, & \text{if site } i \text{ is occupied by species } k, \\ 0 & \text{otherwise} \end{cases} \quad (1)$$

in order to describe the occupancy of each atomic site. In order to avoid explicitly resolving each individual hops of atoms, i.e. each discrete jump of $\{n\}$, we resort to statistical thermodynamics and require that the probability density function $\rho(\{q\}\{p\}\{n\})$ maximizes the information-theoretical entropy of Jaynes with respect to localized constraints in terms of macroscopic variables including atomic temperature and atomic molar fraction (e.g. $\langle n_i \rangle = x_i$).

In order to obtain explicit formulations of thermodynamic potentials suitable for computations, we apply the meanfield approximation theory [4] with a carefully designed trial Hamiltonian, and model the interatomic potential energy using the embedded-atom method. As a result, the thermodynamics of the solid is characterized by Gaussian distribution and atom-wise macroscopic variables including atomic temperature and molar-fraction ($\{x\}$). In particular, now the diffusion of hydrogen is characterized by the change of $\{x\}$ over both space and time, whereas the microscopic variable $\{n\}$ is no longer involved. The localized equilibrium conditions can be obtained by enforcing stationarity of free entropy with respect to parameters characterizing the meanfield trial Hamiltonian.

This thermodynamics model is then coupled with discrete kinetic models of Onsager type which governs mass transport and possibly also heat conduction. This in practice defines the evolution of atomic temperature and molar-fraction. In this work, we consider linear models of the form

$$\dot{x}_i^l = \sum_{\langle i,j \rangle} B_{ij}^l x_{ij}^l k_B (\gamma_j^l - \gamma_i^l), \quad i = 1, \dots, N; \quad l = 1, \dots, M \quad (2)$$

where γ denotes non-dimensionalized chemical potential, and k_B denotes the Boltzmann constant. $B_{i,j}^l$ denotes the bondwise diffusion coefficient between the $\langle i,j \rangle$ atom pair; in practice it can be obtained by fitting to experimental measurement.

3. COMPUTATIONAL METHODS

We solve the coupled deformation-diffusion problem in a staggered procedure. The optimal thermodynamic state is obtained by maximizing free entropy, where thermodynamic potentials and generalized forces are evaluated conveniently using Gaussian quadratures. The kinetic equations are integrated in time using variational time-integrators. To further accelerate computations for larger samples, we may recourse to the quasicontinuum (QC) method to schematically coarsen the computational sample in the elastic region / farfield. We parallelize all the spatial operations using MPI.

4. EXAMPLES AND RESULTS

In this work, we simulate hydrogen desorption in a series of Pd (111) nanofilms, which has been studied experimentally by Li and Cheng using an electrochemical stripping method [5]. We apply the Johnson-type EAM potential of [6] for palladium hydride. With a linearized version of this potential and for fixed temperature ($T=300$ K), the localized equilibrium conditions can be obtained in closed form formulation (Fig. 1).

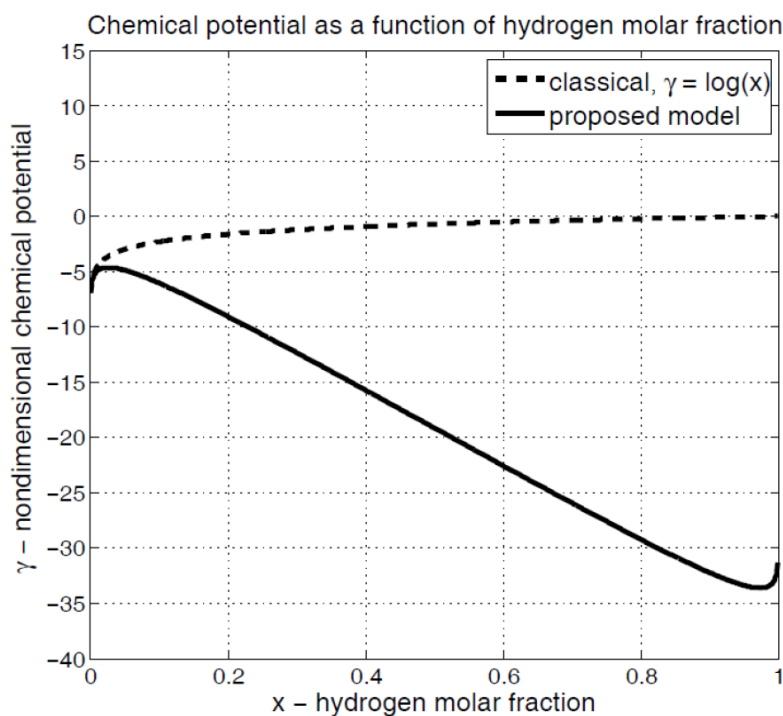


Figure 1: the localized equilibrium condition (a relation between $\{x\}$ and $\{\gamma\}$) for hydrogen diffusion in Pd.

Because of the specific geometry of the nanofilms under consideration, computation can be reduced to one-dimensional, in the thickness direction. We have simulated two cases from [5] with film thickness $L_{Pd}^{(1)} = 46\text{nm}$ and $L_{Pd}^{(2)} = 135\text{nm}$. In both cases the predicted time-history of hydrogen desorption is in good agreement with the experimental data (Fig. 2). It is notable that in both cases the computational time step is around $1\mu\text{s}$ and the total simulation time is 1.5s – far beyond the capabilities of the MD and MC methods.

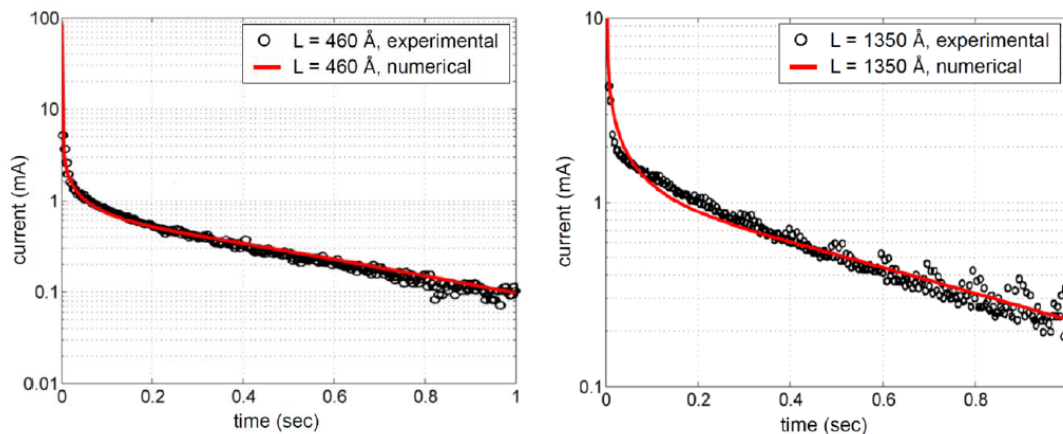


Figure 2: history of electric current (proportional to the gradient of hydrogen molar fraction x) at film surface: comparison of experimental and numerical results.

REFERENCES

- [1] Voter, A. F., Montalenti, F., Germann T. C. Extending the time scale in atomistic simulation of materials. *Annu. Rev. Mater. Res.* 2012; 32:321-346.
- [2] Kulakrni, Y., Knap, J., Ortiz, M. A variational approach to coarse graining of equilibrium and non-equilibrium atomistic description at finite temperature. *J. Mech. Phys. Solids* 2008; 56:1417-1449.
- [3] Ariza, M. P., Romero, I., Ponga, M., Ortiz, M. HotQC simulation of nanovoid growth under tension in copper. *Int. J. Fracture* 2012; 174:75-85.
- [4] Yeomans J. M. *Statistical mechanics of phase transitions*. Oxford University Press, Oxford, UK.
- [5] Li, Y., Cheng, Y.-T. Hydrogen diffusion and solubility in palladium thin films. *Int. J. Hydrogen Energy* 1996; 21:281-291.
- [6] Zhou, X. W., Zimmerman, J. A., Wong, B. M., Hoyt, J. J. An embedded-atom method interatomic potential for Pd-H alloys. *J. Mater. Res.* 2008; 23:704-718.

Thermal decomposition of ammonia borane impregnated in the pores of activated bentonite (HS2-4)

Binayak Roy^{1,a}, Joydev Manna^{1,b}, Pratibha Sharma^{1,c}

*1Department of Energy Science and Engineering, Indian Institute of Technology Bombay
Mumbai-400076, Maharashtra, India*

aroy_binayak@iitb.ac.in, bjoydev@iitb.ac.in, cpratibha_sharma@iitb.ac.in

Chemical hydrides (cf. borohydrides and ammonia borane) provide good means as eligible hydrogen storage material due to their relatively higher gravimetric hydrogen storage capacity compared to metal hydrides. The high decomposition temperature of borohydrides is the main disadvantage towards their PEM fuel cell application. Among all the chemical hydrides ammonia borane exhibits the lowest decomposition temperature. Ammonia borane releases two equivalent of hydrogen at ~ 120 °C and ~ 175 °C, respectively, which are still higher compared to operating temperature of PEM fuel cell (~ 90 °C). Along with the high decomposition temperature, ammonia borane also undergoes uncontrolled decomposition leading to formation of unwanted gaseous by-products (B₂H₆, Borazine etc.). Due to weakness of B-N bonding, when subjected to rapid heating, ammonia borane dissociates uncontrollably and leads to formation of borazine which is particularly detrimental for fuel cell applications. Gutowska et al first demonstrated that application of high surface area material, such as SBA-15, may successfully decrease the decomposition temperature of ammonia borane to a great extent [1]. The same effect was also reported for another high surface area material, MCM-41 by Lai et al [2]. It was also observed that when impregnated on the support material, the peak temperature of first stage decomposition of ammonia borane is decreased by

~ 16 °C compared to the pristine material [2]. It is also noteworthy from work of Gutowska et al [1], that the peak corresponding to borazine (m/e = 80) release is observed at a temperature, which corresponds to the second step of decomposition.

In the current work activated bentonite (Ben_act), with very high pore volume was employed as a support material to facilitate the decomposition of ammonia borane (AB). The Ben_act was prepared from bentonite clay by using urea as a blowing agent through two step impregnation-decomposition process. At first urea was chemically impregnated into the pores of bentonite using aqueous solution. Then the slurry was dried at 90°C to remove the water content and further heated at 132°C for 2h to decompose the urea. Ammonia borane was incorporated into the obtained Ben_act via chemical impregnation method using methanolic solution. The solvent was removed from the slurry by vacuum evaporation and the as prepared sample (AB+Ben_act) was used for experimentation.

The Ben_act and AB+Ben_act samples were characterized using XRD, FEG-SEM, FTIR and N₂ adsorption desorption (BET) isotherm. The thermal characterization of the AB+Ben_act and pure AB was performed with NETZSCH Jupiter TG-DTA analyzer. The evolved gases were analyzed using Aeolos Mass spectrometer. The temperature ramp was intentionally chosen to be 10°C/min to maximize the effect of uncontrolled decomposition of AB. Ben_act was observed to leave a profound effect on the decomposition of ammonia borane both in order to decrease the decomposition temperature and to suppress the unwanted excessive decomposition. The TGA curve (Fig 1a) showed

~20% and ~46 % of wt. losses of pure ammonia borane at first and second stage of decomposition, respectively. The wt. loss (~46%) corresponding to the second stage of decomposition was mainly attributed to the uncontrolled decomposition, which was a prime factor for borazine release. When incorporated in Ben_act the first stage of decomposition was appeared to undergo ~6% of wt loss and the second step was totally eliminated, and hence the possibility of borazine release completely eradicated. The absence of any exothermic peak in the DTA profile (Fig

1b) corresponding to the second stage decomposition further proves the observation. Additionally the peak temperature corresponding to the first stage decomposition was also observed to be decreased by ~21°C. Therefore it may be stated that Ben_act was able to both decrease the

decomposition temperature of ammonia borane and completely eliminate the possibility of borazine release.

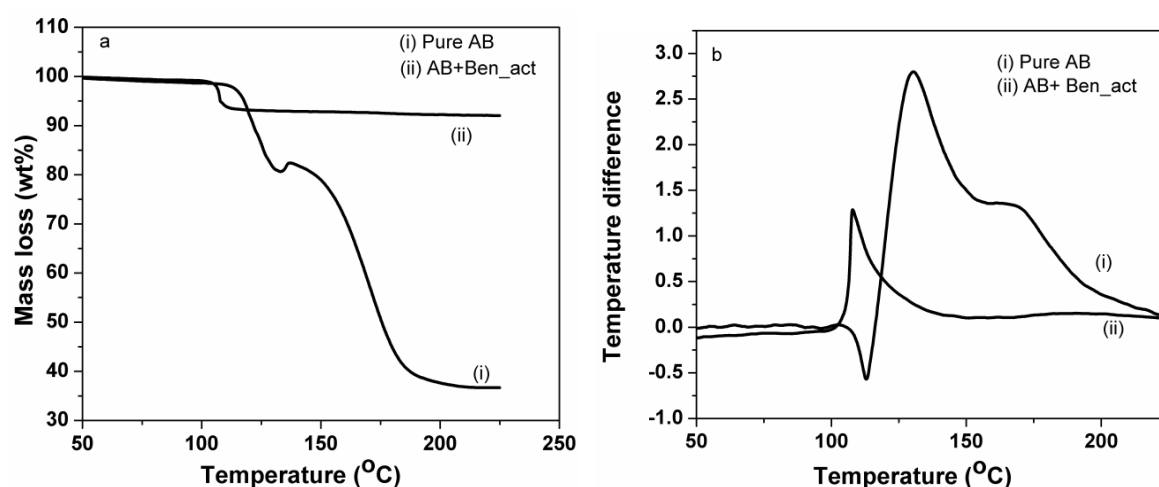


Figure 1: (a) TGA and (b) DTA profile of Pure AB and AB+Ben_act (Heating rate 10°C/min)

References:

- [1]. A. Gutowska, L. Li, Y. Shin, C. M. Wang, X. S. Li, J. C. Linehan, R. S. Smith, B. D. Kay, B. Schmid, W. Shaw, M. Gutowski, and T. Autrey: "Nanoscaffold Mediates Hydrogen Release and the Reactivity of Ammonia Borane", *Angew. Chem. Int. Ed.*, 44, pp. 3578–3582, 2005
- [2] S.W. Lai, H. L. Lin, T. L. Yu, L.P. Lee, B.J. Weng, "Hydrogen release from ammonia borane embedded in mesoporous silica scaffolds: SBA-15 and MCM-41", *Int. J. of Hydrogen Energy*, 37, pp. 14393-14404, 2012

Synthesis of trimetallic core-shell catalysts composed of transition metals for the hydrolysis of ammonia borane (HS2-5)

FANGYUAN QIU, LI LI, YING WANG, CHANGCHANG XU, CHENGCHENG CHEN, YIJING WANG*,
YONGMEI WANG, HUATANG YUAN

Co-Innovation Center of Chemistry and Chemical Engineering of Tianjin, Key Laboratory of Advanced Energy Materials Chemistry (MOE), Institute of New Energy Material Chemistry, Tianjin Key Lab on Metal and Molecule-based Material Chemistry, Nankai University, Tianjin, 30007 (P.R. China)

ABSTRACT: With the emergency of petrochemical energy, hydrogen is considered to be an ideal alternative. Ammonia borane (AB) is believed to be a prominent candidate owing to its high hydrogen content (19.6 wt %), excellent solubility and stability in water. Because of the low kinetic performance of the hydrolysis of AB without the presence of a suitable catalyst, synthesis of efficient catalysts with low cost and high catalytic activity is essential to facilitate the hydrolysis of AB. Therefore, in this work, triple-layered [Ag@Co@Ni](#) core-shell nanoparticles (NPs) were formed to be used in the hydrolysis of AB. It was found that [Ag@Co@Ni](#) core-shell NPs contained a Ag core, a Co inner shell and a Ni outer shell. The thickness of CoNi double shells varied with different contents of Co and Ni. [Ag_{0.04}@Co_{0.48}@Ni_{0.48}](#) core-shell NPs showed the distinctest core-shell structure and displayed a preferable catalytic activity towards the hydrolysis of AB. In order to further reduce the cost, trimetallic [Cu@FeCo](#) core-shell NPs with a Cu core and FeCo shells were synthesized. They exerted composition-dependent activities towards the catalytic hydrolysis of AB. Among them, [Cu_{0.3}@Fe_{0.1}Co_{0.6}](#) core-shell NPs showed the best catalytic activity. Kinetic studies demonstrated that the max hydrogen generation rates of AB catalyzed by [Ag_{0.04}@Co_{0.48}@Ni_{0.48}](#) and [Cu_{0.3}@Fe_{0.1}Co_{0.6}](#) core-shell NPs were 2481.4 and 6674.2 mL min⁻¹ g⁻¹, respectively, at 298 K. And the hydrolysis reactions were both the first order with respect to the catalyst concentration. The activation energies (E_a) of the hydrolysis of AB catalyzed by [Ag_{0.04}@Co_{0.48}@Ni_{0.48}](#) and [Cu_{0.3}@Fe_{0.1}Co_{0.6}](#) core-shell NPs were calculated to be 39.37 and 38.75 kJ mol⁻¹, respectively. It demonstrated that [Cu_{0.3}@Fe_{0.1}Co_{0.6}](#) core-shell NPs displayed much better catalytic activity than that of [Ag_{0.04}@Co_{0.48}@Ni_{0.48}](#) core-shell NPs. Furthermore, the TOF value (mol of H₂ · (mol of catalyst · min)⁻¹) of [Cu_{0.3}@Fe_{0.1}Co_{0.6}](#) core-shell NPs was 10.5, which was one of the best catalysts in the previous reports. For the sake of increasing the catalytic activity of [Ag_{0.04}@Co_{0.48}@Ni_{0.48}](#) core-shell NPs, graphene (rGO) was employed as an ideal support to improve the surface condition of the catalysts. It was interesting to note that the particle size of [Ag_{0.04}@Co_{0.48}@Ni_{0.48}](#) core-shell NPs can be effectively controlled by employing rGO with different reduction degree as supports and the catalytic activities of the composite catalysts were largely enhanced. The number of C=O and C-O functional groups on rGO played a major role in controlling the growth of the NPs. The strong steric hindrance effect of C=O resulted in the growth of large particles, while C-O contributed to the formation of small particles. The particle size of the NPs supported on rGO with different reduction degree decreased with the reduced number of C=O functional groups (solvothermal>NaBH₄>high temperature). The decrease in the particle size probably led to the increase in the catalytic activity towards the hydrolysis of AB. The smallest [Ag_{0.04}@Co_{0.48}@Ni_{0.48}](#) core-shell NPs supported on rGO reduced by high temperature method showed the highest catalytic activity towards the hydrolysis of AB. It demonstrated that rGO with different reduction degree was an appropriate support for

controlling the particle size of catalysts in the on-board application for hydrogen storage. These promising catalysts may make AB to have a bright future in the field of fuel cells.

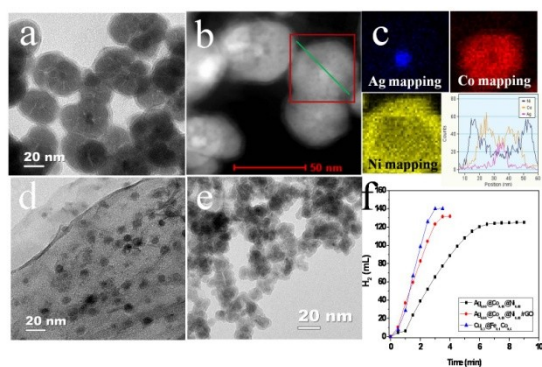


Figure 1. (a) Bright-field, (b) dark-field TEM images of Ag_{0.04}@Co_{0.48}@Ni_{0.48} core-shell NPs, (c) elemental mapping of Ag, Co, Ni and elemental distribution along a single NP indicated by the green line in part b, TEM images of (d) Ag_{0.04}@Co_{0.48}@Ni_{0.48}/rGO (high temperature) NPs and (e) Cu_{0.3}@Fe_{0.1}Co_{0.6} core-shell NPs and (f) catalytic hydrolysis of AB at 298 K.

Type Approval of Composite Gas Cylinders - Probabilistic Analysis of rc&s Concerning Minimum Burst Pressure (HS2-6)

Georg W. Mair, Martin Hoffmann, Florian Scherer

BAM Federal Institute for Materials Research and Testing

Gas cylinders made from composite materials receive growing popularity in applications where light weight is advantageous. At the same time, manufacturers are interested in cutting cost and weight through material reduction which requires a better understanding of safety relevant properties.

Current standards base safety determination mainly on demonstration of minimum amounts of endured load cycles and minimum burst pressure of a small number of specimens. Various research projects were conducted aiming at reducing minimum burst pressure requirements without compromising safety. No satisfying results were found.

This paper refers to the criterion of burst pressure. This can be considered as primarily valid instead of cycle fatigue aspects if a design type withstands more than 50,000 load cycles and if the burst test is performed with a very small pressure increase ratio. A performance chart is introduced which plots the average strength of a sample over its scatter. Various considerations are undertaken regarding the distribution of failure of composite pressure receptacles. The "relative scatter spread" is introduced as a universal key figure. For a rough assessment of the investigated test results the GAUSSian normal distribution (ND) is assumed as being sufficient if some precautions are taken. Hints are given that similar probabilistic methods can be applied to cycle fatigue sensitive receptacles, too.

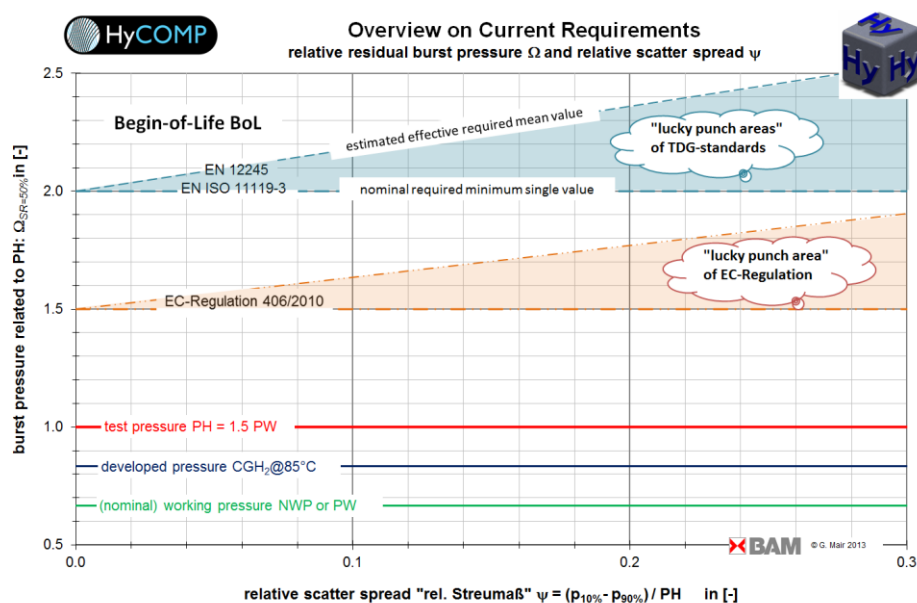
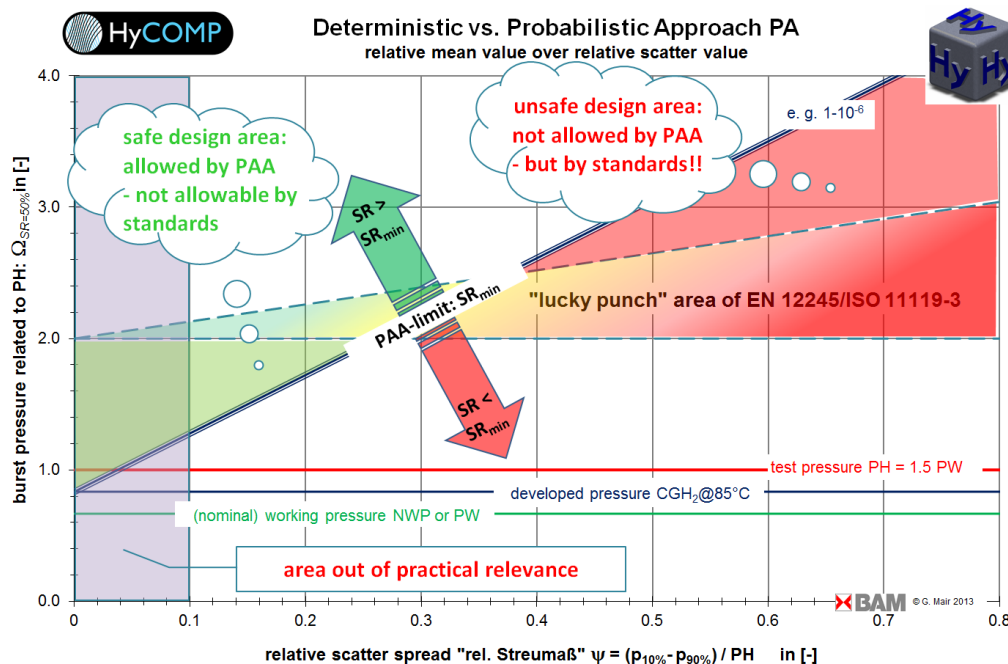


Figure 1: Visualization of requirements derived from standards

The importance of precise definitions of boundary conditions for burst tests is elaborated and reference is given for a well-proven sample standard regarding this issue. Tests according to these guidelines are called "Slow Burst Tests". The results of such burst tests, performed within the research project HyCube and others, are employed to investigate probabilistically the safety resulting from current standards.

The influences of applicable pressure levels on safety ratios are discussed. Differences between standards for automotive use inside the EU and international transport of dangerous goods are pointed out in Figure 1. This Figure is based on the mentioned performance chart developed by BAM for the rough estimation of survival rates for the assessment of tested samples of gas cylinders. Justifications for differing safety ratios are discussed.

The survival probability resulting from current RC&S, assuming ND as sufficiently precise is derived and visualized in Figure 2. On the one hand, cases in which potentially dangerous design types would be approved according to current RC&S are found. They are shown by two red triangular areas to the right of the large arrows in Figure 2. The upper one shows designs, which will get an approval with high probability. The right half of the lower one shows an area, which needs a little bit of luck for a successful approval process.



Figure

2: Areas of diverging assessment results

On the other hand there are again two green triangular areas placed in the left of these arrows which represents design types considered safe in the meaning of a probabilistic assessment. Especially design types represented by the lower triangular are not approvable according to current RC&S though, due to failing the required minimum stress ratios or burst ratios. For this reason it has

to be concluded, that the minimum burst pressure of specimens is not a satisfying criterion for safety – neither for new specimens nor for the behaviour during service life.

Criteria for the assessment of safety over lifetime according to probabilistic analysis are discussed based on the introduced performance chart for generic assessment and for a specific application.

Effects of degradation during service life are investigated. Current RC&S are based mainly on experiments with cylinders right off the production line. Artificial aging effects are only investigated with the approach of reducing mandatory strength when testing single pre-conditioned specimens. Currently no probabilistic analysis about the development of degradation is performed or required by relevant RC&S. It is known that fatigue in composite gas cylinders is not only dependant on the number of load cycles, but also on the time under load and the temperature. The correlations are not yet fully understood and proven. Additionally there are some service conditions improving the burst strength properties in the first years of service. The specific probability of potentially unsafe design types, approved according to current RC&S, is pointed out. Criteria useful for the determination of safety towards the end of service life (EoL) of composite pressure receptacles are developed. The topic of artificial aging, employed for the simulation of service life degradation, is discussed briefly.

Suggestions are made for future legislation to incorporate and apply probabilistic considerations. Possible potentials for saving material cost while granting a higher safety level than the current method are pointed out for the case of reduced and surveyed scatter of production.

Overall, the deficits of the sole criterion of minimum burst pressure for approval of gas cylinders as currently employed in RC&S are elaborated. It is concluded, that a potential for materials savings - as looked for in the research project StorHy - cannot be found in a discussion about demanded minimum strength values within the limits of their current definition. Instead of this, the safety assessment has to be changed over to a probabilistic procedure to make the potentials shown accessible and limit uncertainties. If a high design quality and reduced scatter during manufacturing can be assured, reduced burst strength would be acceptable, which represents gas cylinders not approvable according to current standards. The potential is presented by the green area in the performance chart Figure 2.

Open for further investigation is the collection of data regarding the comparison of artificial aging and degradation during real service life. This is inevitable to evaluate the current procedures for life time simulation to EoL. Another subject of future investigations has to be the confirmation of the universal applicability and conservativeness of the general approach introduced by both performance charts – one for the logarithm scale of load cycles and one for the burst strength. This is linked with the validation of the type of density function, the required confidence level and the acceptable samples size. Based on this, the potential of determining the individual reliability of each design type of gas cylinders by employing larger samples during the approval process has to be elaborated.

Fuel cell components and stacks

Enabling low temperature fuel cells via improved Pt-alloy cathode catalysts (FCC1-1)

M. Escudero-Escribano*, P. Malacrida, U. Grønbjerg, A. Verdaguier-Casadevall, J. Rossmeisl, I.E.L. Stephens, I. Chorkendorff

Department of Physics, Technical University of Denmark, 2800 Kgs. Lyngby, Denmark
 Maria.Escudero@fysik.dtu.dk

Proton exchange membrane fuel cells (PEMFCs) are a potentially zero emission source of power, which are expected to play a key role in a future society based on sustainable energy. The main obstacle to the development of PEMFCs as a commercially competitive reality is the high overpotential required for the oxygen reduction reaction (ORR) to proceed at an adequate rate. In order to improve the kinetics for the ORR and reduce the Pt loading, we need to develop more active, selective and stable catalysts [1-3]. This can be achieved by alloying Pt with other metals [1,3,4]. Alloys of Pt and early transition metals, such as Pt₃Y, have shown very promising ORR activity [3,4]. Herein, we present experimental and theoretical studies concerning the activity and stability of novel cathode catalysts based on alloys of Pt and lanthanides.

Rotating disk measurements show that sputter-cleaned, polycrystalline alloys of Pt and lanthanides present an enhancement over pure Pt, Pt₅Gd showing a five-fold increase in ORR activity [5], relative to Pt at 0.9 V in 0.1 M HClO₄, as shown in Fig. (A). For all the electrocatalysts, angle-resolved X-ray photoelectron spectroscopy (AR-XPS) measurements taken after the ORR show that a Pt overlayer with a thickness of few Pt layers is formed [5], as represented in Fig. (B). Accordingly, the effect of alloying Pt is to impose strain onto the Pt overlayer. Fig. (C) shows that alloys of Pt and lanthanides present a big ORR activity enhancement over pure Pt. Not only are the catalysts highly active, but also very stable [5], which make these materials very promising for the development of highly active and stable cathode catalysts.

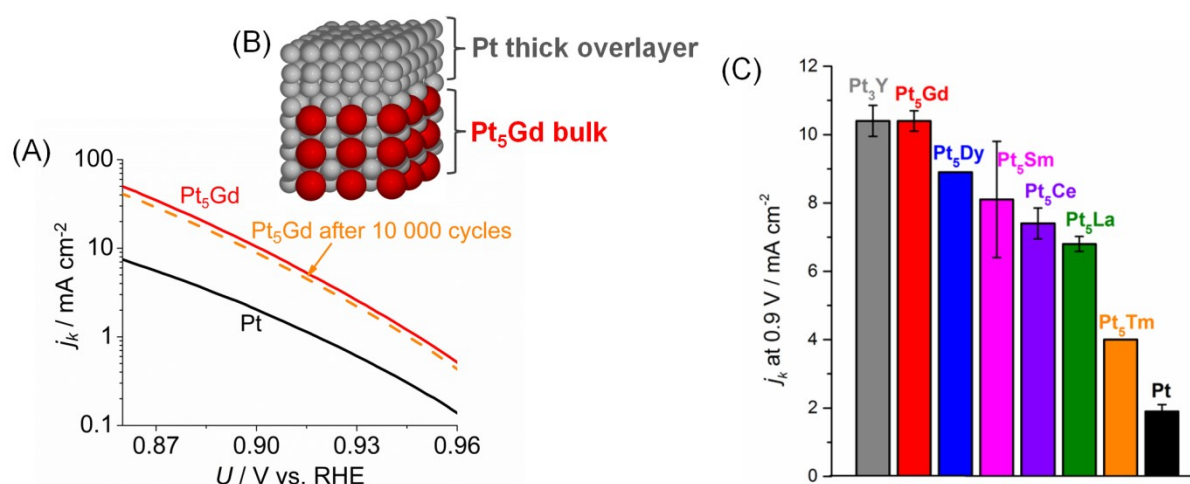


Fig. (A) ORR kinetic current densities at 1600 rpm and 50 mV s⁻¹ on Pt₅Gd before (red curve) and after (orange curve) 10 000 cycles between 0.6 and 1.0 V vs. RHE in comparison with pure Pt (black curve). (B) Schematic three-dimensional view of the Pt₅Gd structure. (C) Overall ranking of activity for Pt₃Y, Pt₅Gd, Pt₅Dy, Pt₅Sm, Pt₅Ce, Pt₅La, Pt₅Tm, and Pt.

-
- [1] H. A. Gasteiger, S. S. Kocha, B. Sompalli, F. T. Wagner, *Appl. Catal. B* 2005, 56, 9.
- [2] D. Strmcnik, M. Escudero-Escribano, K. Kodama, V. R. Stamenkovic, N. Markovic, *Nature Chem.* 2010, 2, 880.
- [3] I. E.L. Stephens, A. S. Bondarenko, U. Grønbjerg, J. Rossmeisl, I. Chorkendorff, *Energy Environ. Sci.* 2012, 5, 6744.
- [4] J. Greeley, I. E.L. Stephens, A. S. Bondarenko, T. P. Johansson, H. A. Hansen, T. F. Jaramillo, J. Rossmeisl, I. Chorkendorff, J. K. Nørskov, *Nature Chem.* 2009, 1, 552.
- [5] M. Escudero-Escribano, A. Verdager-Casadevall, P. Malacrida, U. Grønbjerg, B. P. Knudsen, A. K. Jepsen, J. Rossmeisl, I. E.L. Stephens, I. Chorkendorff, *J. Am. Chem. Soc.* 2012, 130, 16476.

Array of Self-Supported Platinum Nanotubes as PEM fuel cell electrode (FCC1-2)

Arnaud Morin, CEA/Liten/LCPEM
Samuele Galbiati, CEA/Liten/LCPEM
Nicolas Pauc, CEA/DSM/INAC
17 rue des Martyrs
38054 Grenoble Cedex 9

In the search for new and green sources of energy, proton exchange membrane fuel cell (PEMFC) is considered as a promising candidate for electric power generation in transportation and stationary applications. In order to be commercially viable, this energy conversion system requires several breakthroughs. Among them, a significant decrease in the global cost and an improvement of durability are necessary [1,2]. This absolutely requires a better use of the precious metal involved in the catalysis of the electrochemical reactions, i. e. platinum (Pt). Pt metal cost is high and its resources are limited. As a consequence, many efforts have been put on lowering the loading of Pt metal in PEMFC electrodes and especially at the cathode. Dramatic reduction by a factor of 10 of the Pt amount presently used in fuel cells seems to be the target that will allow mass production, e.g. a Pt loading of 0.1 g Pt/kW [3]. The conventional structure of active layers made of carbon supported platinum (Pt) nanoparticles (Pt/C) is inadequate for the combined cost, performance, and durability requirements. The Pt/C catalyst shows limited specific activity toward ORR due to the small size of the particles. The durability of Pt/C is limited by the degradation of the carbon support and the loss of Pt surface area through potential driven dissolution [4]. The tortuosity of the active layer induces strong limitations to the transport of reactants and products and consequently, leads to a misuse of platinum. As a consequence, new electrode architectures must be developed in order to try to reach this ultimate objective.

We developed a process to obtain an array of oriented platinum nanotubes supported onto Nafion membrane. Its fabrication pathway includes several steps (Figure 1). The catalyst is first deposited by Atomic Layer Deposition onto a sacrificial porous aluminium oxide template. The Nafion membrane is then stuck onto the template which is etched by a chemical route to obtain the supported platinum nanotube array. The array is finally coated with a thin proton conducting film of Nafion (Figure 2).

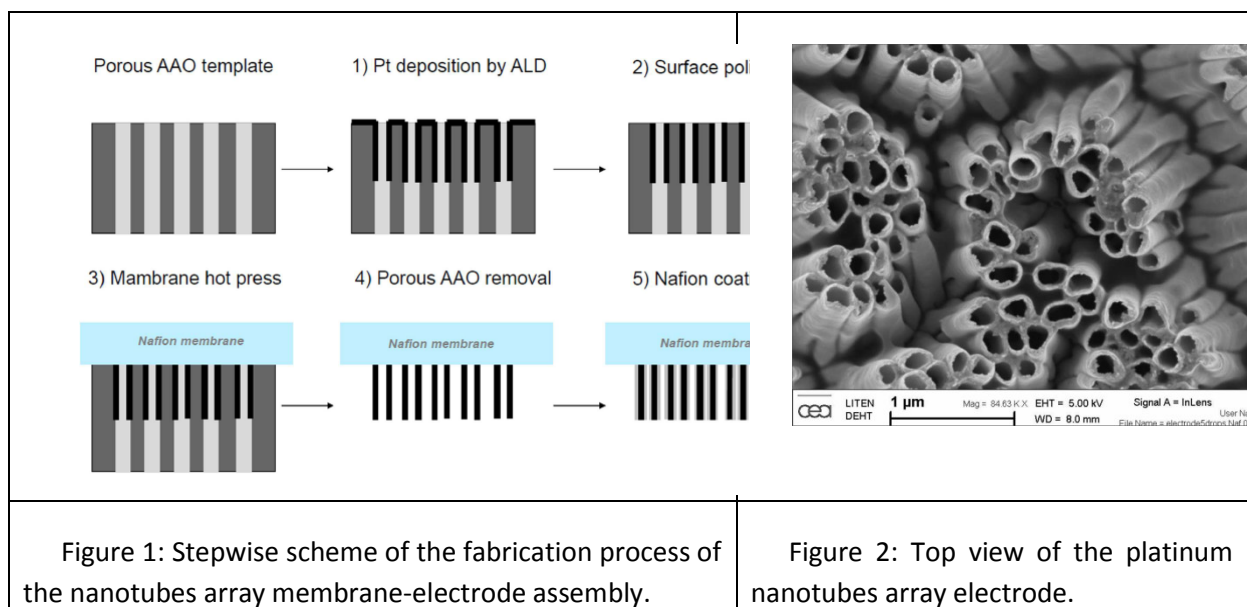
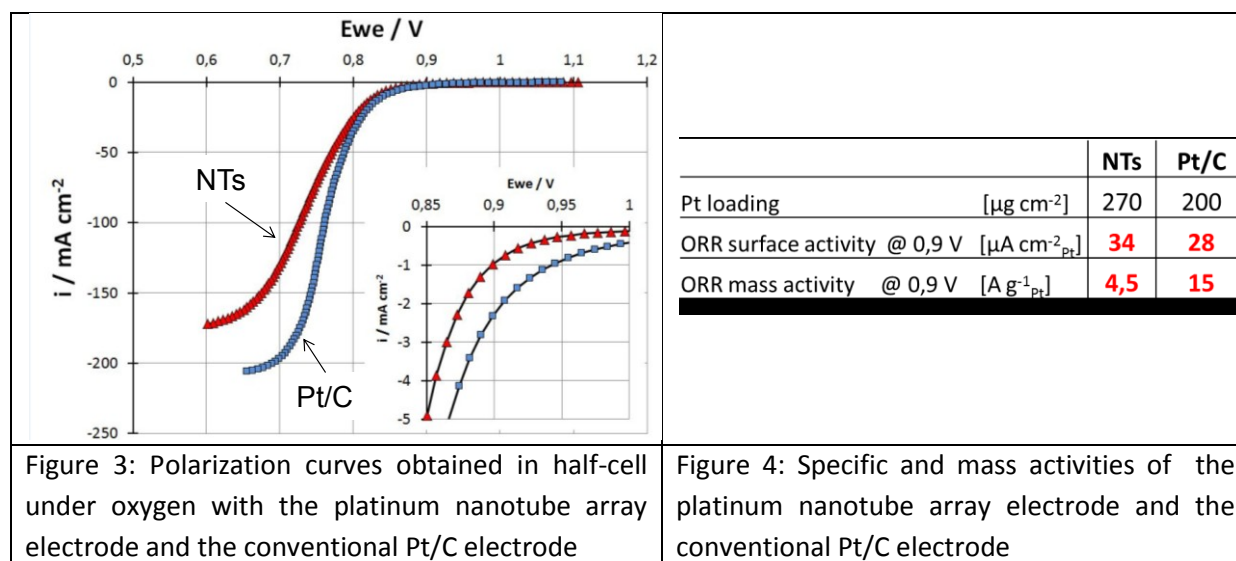


Figure 1: Stepwise scheme of the fabrication process of the nanotubes array membrane-electrode assembly.

Figure 2: Top view of the platinum nanotubes array electrode.

The nanotubes array electrode shows a limited value of specific surface ($23 \text{ cm}^2/\text{cm}^2_{\text{geo}}$ vs $190 \text{ cm}^2/\text{cm}^2_{\text{geo}}$ for the Pt/C), but very high values of surface utilization under both CO and N₂. These measurements confirm that the surface of the nanotubes is rough and that it is almost completely in contact with protons, electrons, water and gas.

The response of the nanotubes array to Oxygen Reduction Reaction ORR was also investigated in half cell configuration. Such a response does not equal the present performance of Pt/C dispersion electrodes in terms of mass activity (3 A/g vs 15 A/g) due to the high catalyst loading and to the limited surface of the nanotubes. Nevertheless it shows interesting values of surface specific activity ($34 \mu\text{A}/\text{cm}^2_{\text{Pt}}$ vs $28 \mu\text{A}/\text{cm}^2_{\text{Pt}}$) which can be related to the dense and bulky structure of the walls (Figure 3 and Table 1). Work is in progress to improve the performance of the electrode by decreasing the thickness of the wall of the nanotubes and by alloying the platinum with non-noble metal. Preliminary fuel cell tests will be done in the coming weeks on a 20 cm^2 electrode and will be presented during the conference.



REFERENCES

Borup, R.; Meyers, J.; Pivovar, B.; Kim, Y. S.; Mukundan, R.; Garland, N.; Myers, D.; Wilson, M.; Garzon, F.; Wood, D.; Zelenay, P.; More, K.; Stroh, K.; Zawodzinski, T.; Boncella, J.; McGrath, J. E.; Inaba, M.; Miyatake, K.; Hori, M.; Ota, K.; Ogumi, Z.; Miyata, S.; Nishikata, A.; Siroma, Z.; Uchimoto, Y.; Yasuda, K.; Kimijima, K. I.; Iwashita, N. Chem. Rev. 2007, 107, 3904.

Gasteiger, H. A.; Kocha, S. S.; Sompalli, B.; Wagner, F. T., Appl. Catal. B 2005, 56, 9.

« Cost analysis of PEM Fuel Cells Systems for Transportation December 2005 » -September 30, 20005- E.J. Carlson, P. Kopf, J. Sinha, S. Sriramulu, and Y. Yang –TIAX LLC Cambridge, Massachusetts NREL/SR-560-3910.

Stamenkovic, V.; Mun, B. S.; Mayrhofer, K. J. J.; Ross, P. N.; Markovic, N. M.; Rossmeisl, J.; Greeley, J.; Nørskov, J. K., Angew. Chem. 2006, 118, 2963.

Scaling-up and characterization of ultralow-loading MEAs made-up by electro spray (FCC1-3)

B. Martinez-Vazquez¹, D.G. Sanchez², J.L. Castillo¹, K.A. Friedrich², P.L. Garcia-Ybarra¹

¹UNED, Dept. Fisica Matematica y de Fluidos, Senda del Rey 9, 28040 Madrid, Spain

²DLR, Institute of Technical Thermodynamics, Pfaffenwaldring 38-40, 70569 Stuttgart, Germany

1. INTRODUCTION

The electro spraying of liquid suspensions containing catalytic nanoparticles is being successfully used in the production of nano-structured porous catalytic layers for proton exchange membrane fuel cell (PEMFC) electrodes [1–3]. The aim of these works is to reduce the platinum loading by increasing the platinum utilization without compromising the fuel cell performance.

Several methods, especially those based on sputtering [4], have been used to reduce the platinum loading on the electrodes. But these methods require a strict atmosphere control and vacuum conditions that make them relatively expensive and not easily adaptable to mass production. The benefits of electro spraying are the simplicity of the experimental set up (only a pump-needle system and a high voltage power supply), the high platinum utilization due to the small electro sprayed particle size and the easy scale-up suitable for industrial production [5–6].

Electrospray deposition enables the generation of nanostructured catalytic layers whose building blocks are clusters (of a few catalyst particles each) with a characteristic size of approximately 100 nm disposed in a dendritic arrangement. This nano-structuration produces catalytic deposits with the appropriated morphology for PEMFC electrode preparation. On the one hand, the small size of the catalyst clusters leads to a high dispersion of the catalyst. On the other hand, the dendritic arrangement of the catalyst clusters results in a highly porous deposit with an enhanced permeability and increased electrochemical active surface area [7].

So far, electrodes with 0.01mgPtcm⁻² loading have been characterized under some suitable conditions and shown to reach a platinum utilization in the interval 30-35 kWgPt⁻¹ [5] what, to the best of our knowledge, represents the maximum platinum utilization reported up to now for any catalyst deposition method.

We report here a series of experiments aimed to assess the behavior of these catalytic layers under a broad range of different operational conditions and materials.

2. EXPERIMENTS

Catalyst inks were prepared by dispersing Pt/C nanopowders (Pt 10 wt.% on Vulcan XC-72R) in ethanol mixed with Nafion. Electrodes with 0.01 mgPtcm⁻² Pt loading were prepared by electro spraying the catalyst ink. The substrate consisted of a 25 cm² square size TorayTM carbon paper coated with a Carbon Micro-Porous Layer (TP-CMPL). Nafion 212 and Nafion 211 were used as membranes, sandwiched between two equal electrodes to make a MEA without the need of hot-pressing.

Two series of experiments were performed on two different test-stations. First, to assess the effects of membranes with different thickness, MEAs with Nafion 212 and Nafion 211 membranes were compared by running experiments at different pressures, temperatures and degrees of humidification of the hydrogen-oxygen feeding gases. Secondly, a segmented cell [8] was used to visualize the drying effects [9] experienced by a N212 MEA fed with hydrogen and air at atmospheric pressure and low humidification.

3. RESULTS Y DISCUSSION

Figure 1 compares the performance of the 25 cm² MEA with N212 and previous results conducted with a 5 cm² MEA. In both cases, the operation conditions were the same, absolute pressure: 4.4 bars, temperature: 70 °C, feeding gases: dry H₂/O₂. Both MEAs show very similar performances without any sign of penalty due to the scaling-up. The maximum performance reaches up to near 600 mW/cm² that accounting for the overall 0.02 mgPt cm⁻² (cathode plus anode) loading leads to a platinum utilization of 30 kW/gPt as reported above.

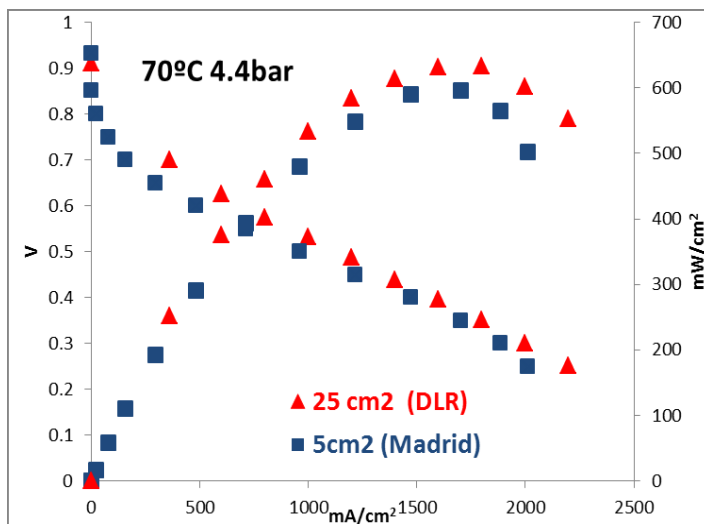


Figure 1

The study was also extended to humid feeding gases with a relative humidity ranging from 10% to 50%. In all cases, the EIS analysis was also performed and revealed that the ohmic resistance was almost not altered by the humidity.

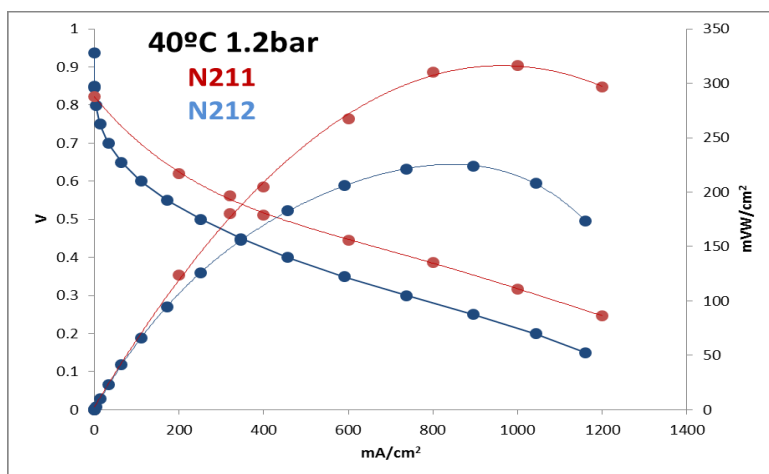


Figure 2

MEAs with membrane N211 were also tested under similar conditions. Comparison with the results of the membrane N212 shows that the performance of both membranes are quite similar at the larger values of the pressure (4.4 bars) but displayed interesting differences during the test conducted at 40 °C and 1.2 bar. In fact, the maximum performance of the N211 membrane in this case exceeds by more than 50% the maximum obtained with the membrane N212.

Finally, the segmented cell has been used to get the polarization curve when the oxidant gas was air, under two pressure conditions, 4.4 and 1.5 bars, and 70 °C. It is remarkable that to get a stable operation a sufficient degree of humidification was needed. Under some drying conditions, even sustained oscillations were observed, a behavior reported previously also on other PEMFC operating also under drying conditions [10].

ACKNOWLEDGMENTS

The characterization experiments were performed at DLR (Deutsches Zentrum für Luft und Raumfahrt) during a three-month stay of one of the authors (B. M-V) supported by a grant from UNED (Universidad Nacional de Educación a Distancia).

REFERENCES

- [1] S. Martin, P.L. Garcia-Ybarra, J.L. Castillo, *J Power Source* 195 (2010) 2443-2449.
- [2] S. Martin, P.L. Garcia-Ybarra, J.L. Castillo, *Int J Hydrogen Energy* 35 (2010) 10446-10451.
- [3] S. Martin, A. Perea, P.L. Garcia-Ybarra, J.L. Castillo, *J Aerosol Sci* 46 (2012) 53-63.
- [4] M. Cavarroc, A. Ennadjaoui, M. Mougnot, P. Brault, R. Escalier, Y. Tessier, J. Durand, S. Roualdes, T. Sauvage, C. Coutanceau, *Electrochem. Commun.* 11 (2009) 859-861.
- [5] S. Martin, B. Martinez-Vazquez, P.L. Garcia-Ybarra, J.L. Castillo, *J Power Source* 229 (2013) 179-184.

- [6] P.L. Garcia-Ybarra, J.L. Castillo, S. Martin, Patent Application No. P201200341.
- [7] J.L. Castillo, S. Martin, D. Rodríguez-Perez, A. Perea, P.L. Garcia-Ybarra, KONA Powder and Particle J. In Press.
- [8] M. Schulze, E. Gülzow, S. Schönbauer, T. Knöri, R. Reissner, J Power Sources 173 (2007) 19-27.
- [9] Sanchez, P.L. Garcia-Ybarra, Int J Hydrogen Energy 37 (2012) 7279-7288.
- [10] D.G. Sanchez, D. Guinea Diaz, R. Hiesgen, I. Wehl, K.A. Friedrich, J Electroanal Chem 649 (2010) 219-231.

Impact of PTFE content in GDLs on PEFC performance evaluated by neutron radiography combined with pulsed helox analysis (FCC1-4)

Johannes Biesdorf¹, Pierre Oberholzer¹, Thomas J. Schmidt¹, Pierre Boillat^{1,2}

¹ Electrochemistry Laboratory, Paul Scherrer Institut (PSI), 5232 Villigen PSI, Switzerland

² Neutron Imaging and Activation Group (NIAG), Paul Scherrer Institut (PSI), 5232 Villigen PSI, Switzerland

**Presenting author, email: Johannes.Biesdorf@psi.ch, Tel.: +41 56 310 57 27*

Polymer electrolyte membrane fuel cells (PEFCs) have attracted much attention during the last decade for their potential to replace combustion engines with low emissions and high power densities. However, before its commercialization, the efficiency of PEFCs must be increased by reducing the occurring performance losses (activation-, ohmic- and mass-transport-losses). In order to minimize mass-transport-losses (MTL), gas-diffusion layers (GDL) are attached between the electrodes and gas supply [1, 2], facilitating a homogeneous access of the reactant gases to the electrodes.

Neutron radiography (NR) is a suitable technique to investigate water inside fuel cells [3-5]. It offers the advantage of good transparency of usual fuel cell materials, as well as high contrast for liquid water. Based on a high resolution setup (FWHM: 35 μ m) [6], time dependent water distributions (exposure time of 15s) can be investigated inside the flow fields (FF) and GDLs. In order to understand the implications induced by different water distributions, occurring mass transport losses can be investigated by pulsing Helox (mixture of 79% He and 21% O₂) and pure Oxygen during the continuous operation with air [5]. By comparing the resulting voltages during the gas pulses, the pulsed gas analysis (PGA) delivers specific estimators of mass transport losses caused by bulk and non-bulk diffusion losses.

Using a the multicell setup [6], we are able to operate six differential fuel cells (active area of 1cm²) under identical operation conditions (temperature, humidification, pressure, and currents). In order to study the influence of the amount of hydrophobic coating (PTFE) on mass transport losses, different cell assemblies with GDLs (Sigracet 24 with MPL, SGL) having 0% or 5% PTFE on the anode side and 0%, 5% or 20% on the cathode side have been investigated.

During the measurements at the ICON beamline at PSI [7], various operation conditions with different cell temperatures, relative humidities, pressures, and currents have been investigated.

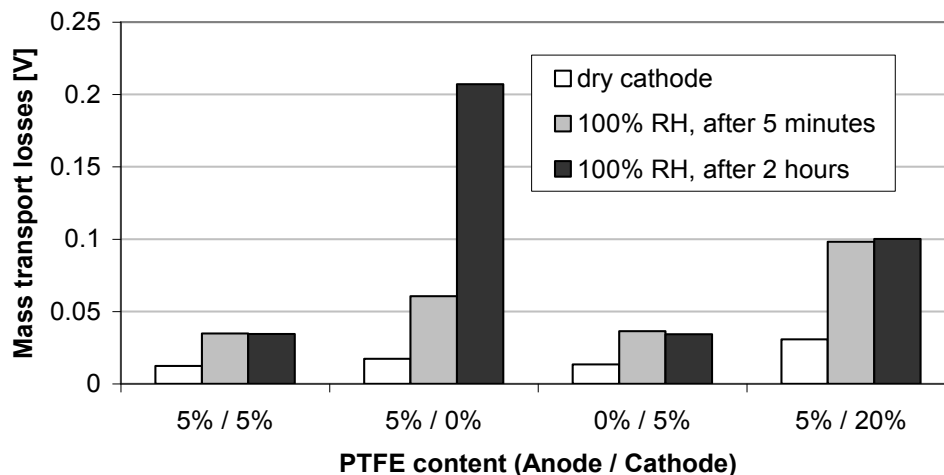


Figure 1: Mass transport losses at 1A/cm² measured with the PGA method for different cells and operating conditions. Anode relative humidity is 100%.

In Figure 1, it can be seen that the amount of PTFE in the cathode GDL has an important impact on the mass transport losses. A high amount of PTFE results in increased losses, in particular at high humidity. If no PTFE is used on the cathode, the losses are initially moderate, but increase dramatically after 2 hours of operation at full humidity. Consequently, moderate PTFE concentrations seem to be the optimal composition for an effective reduction of the mass transport losses.

Neutron imaging can be used to identify the relations between the observed losses and the accumulation of liquid water in the GDL. The GDL with 20% PTFE was observed to hold less water than the other GDLs, which contrasts with the increased mass transport losses it induces. The probably reason for this discrepancy is a different distribution of water on the microscopic scale. The very large mass transport losses in the GDL without PTFE after 2 hours of operation cannot be related with an important increase of the average GDL water quantity. However, a detailed observation (Figure 2) shows that water tends to be retained in the GDL-channel interface, identifying this region as a critical point.

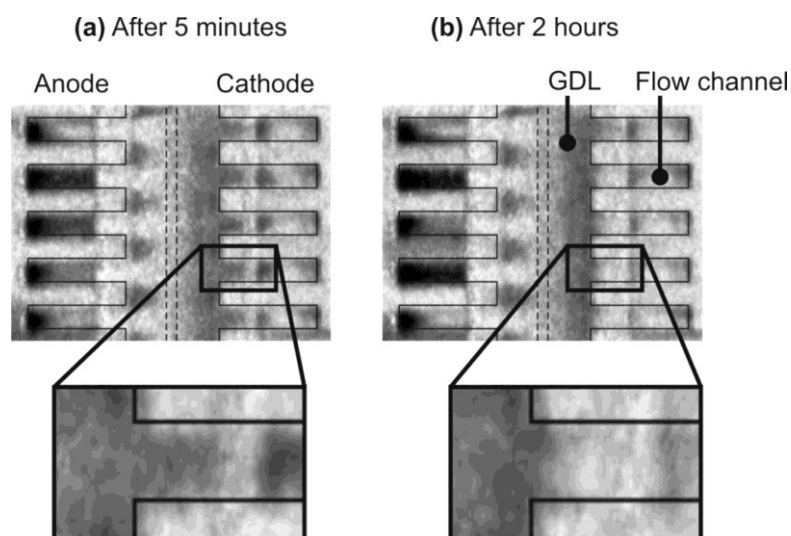


Figure 2: Water distribution in the cell without PTFE on the cathode side. (a) After 5 minutes of operation at full humidity. (b) After 2 hours of operation at high humidity.

- [1] G.-G. Park, Y.-J. Sohn, T.-H. Yang, Y.-G. Yoon, W.-Y. Lee, and C.-S. Kim, *J. Power Sources* 131, 182 (2004).
- [2] L. R. Jordan, A. K. Shukla, T. Behrsing, N. R. Avery, B. C. Muddle, and M. Forsyth, *J. Power Sources* 86, 250 (2000).
- [3] P. Boillat et al., *Electrochem. Commun.* 10, 546 (2008).
- [4] P. Oberholzer, P. Boillat, A. Kaestner, E. H. Lehmann, G. G. Scherer, T. J. Schmidt, and A. Wokaun, *J. Electrochem. Soc.* 160, F659 (2013).
- [5] P. Boillat, P. Oberholzer, A. Kaestner, R. Siegrist, E. H. Lehmann, G. G. Scherer, and A. Wokaun, *J. Electrochem. Soc.* 159, F210 (2012).
- [6] P. Oberholzer, P. Boillat, R. Siegrist, A. Kastner, E. H. Lehmann, G. G. Scherer, and A. Wokaun, *Electrochem. Commun.* 20, 67 (2012).
- [7] A. P. Kaestner, S. Hartmann, G. Kuhne, G. Frei, C. Grünzweig, L. Josic, F. Schmid, and E. H. Lehmann, *Nucl Instrum Meth A* 659, 387 (2011).

A Dissipative Particle Dynamics Approach to Evaluate Structures and Transport Phenomena (FCC1-5)

in Nafion Membranes with Different Equivalent Weights

*Erik O. Johansson, Bengt Sundén, and Jinliang Yuan
Department of Energy Sciences, Faculty of Engineering,
Lund University, P.O. Box 118, SE-221 00 Lund, Sweden*

The nano-scale structure of the Nafion membrane is first reconstructed using dissipative particle dynamics (DPD). The impact of different equivalent weight of the membrane is evaluated based on the equilibrated structure of the membrane by using the radial distribution function to estimate water pore sizes and the distances between water pores. Transport properties within the membrane are further investigated by calculating the mean square displacement of water within the equilibrated membrane. The equivalent weight is found to have a large impact on the transport properties of the membrane; the diffusivity decreases by several orders of magnitude from the lowest EW investigated to the highest.

Dissipative Particle Dynamics (DPD), Nafion Membrane, Modeling, PEMFC

Introduction

Nafion is the industry standard membrane material commonly applied in proton exchange membrane

fuel cells (PEMFCs) [1]. The Nafion membrane has been used since the 1960's, because the membrane shows good mechanical and chemical strength, as well as good proton conductivity as compared with competing membrane materials available on the market [2]. Besides from being used in the membrane, Nafion is also used in the anode and cathode catalyst layers in order to enhance the supply of protons to the reaction sites [3]. How well the Nafion material conducts ions is intimately linked with its structure on a nano-scale. In order to better understand the transport phenomena inside the material, it is also of pivotal importance to analyze how the material looks and functions on the nano-scale. In this paper, dissipative particle dynamics (DPD) models and simulations are developed and carried out to investigate how the equivalent weight (EW) of the membrane affects the general structure of the equilibrated membranes, as well as transport of liquid water within the membranes.

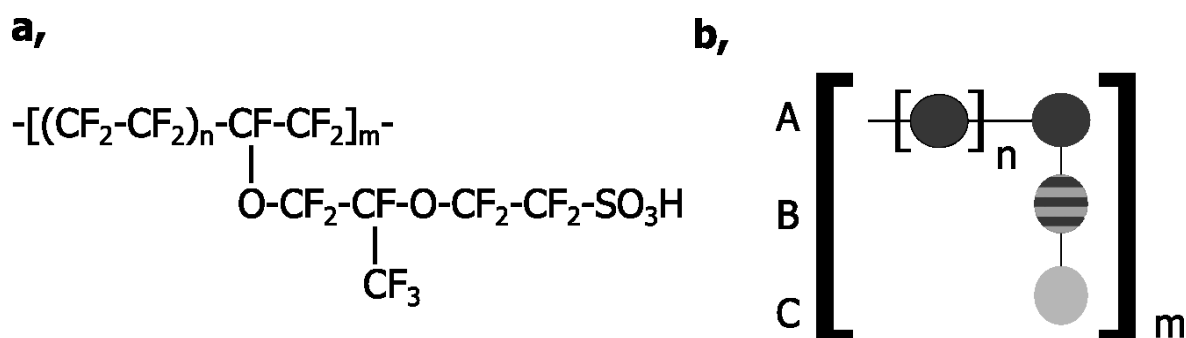


Figure 1: a) Chemical formula of the Nafion polymer. b) The Nafion molecule represented by the three kinds of coarse-grained beads: A (dark grey), B (striped), and C (light grey).

Method

The microscopic structure of the Nafion membrane is obtained using the dissipative particle dynamics (DPD) method [4], with the Nafion molecule represented by coarse-grained beads as shown in Fig. 1. The three bead-types in Fig. 1 represent hydrophobic backbone, side-chain, and hydrophilic side-chain, respectively. In the coarse-grained molecule, two repeating units are used, m , and n . m is the number of side-chains presented in every polymer. In this study m is set to 5 for all studied cases. The second repeating unit, n , represents the length of the hydrophobic backbone as compared to the number of side chains. A large n value gives a membrane with a high equivalent weight (EW), and vice versa. The equivalent weight is the molecular mass of the molecule divided by the number of sulfonic acid groups. Evaluation of the membrane structures are carried out by simulating the equilibration of the polymer in a water solution. The most important parameter in this evaluation is the ratio between the number of water particles in the domain and the number of sulfonate groups in the membrane, i.e., the so-called λ -value. The higher the λ -value is the more water is present in the membrane.

The structure of the membrane is evaluated by using the radial distribution function (RDF) [3]. By computing the RDF for interactions between water beads, the size of water clusters can be evaluated, as well as the distances between different water clusters.

Finally, the diffusivity of water beads within the structure can be evaluated by first freezing the polymer at an equilibrated state, and then allowing the water beads to randomly displace within the membrane. From the trajectory of the water beads, the mean square displacement method (MSD) can be used to evaluate the diffusivity of the water beads.

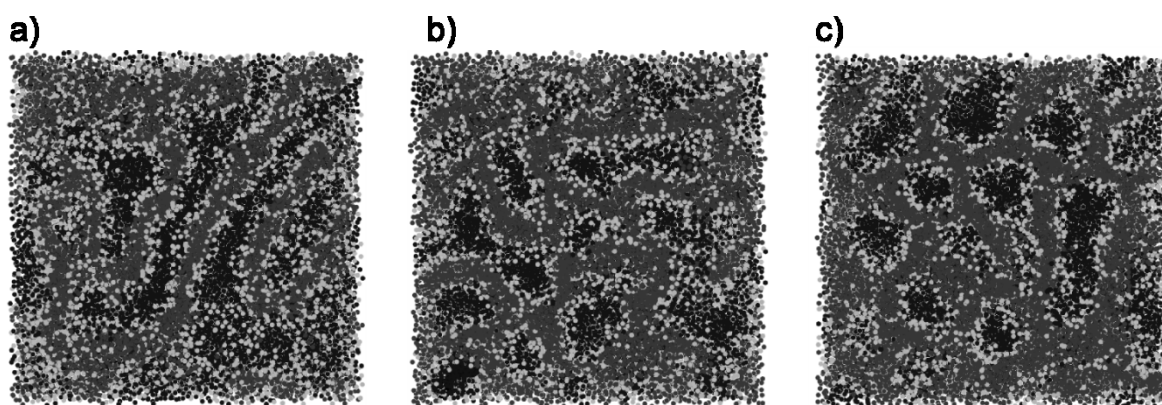


Figure 2: Equilibrium configurations for three different lengths of the repeating unit n with the same degree of water saturation. The colors represent: black – water beads; light grey - hydrophilic side chains; dark grey - hydrophobic side chains and backbone.

Results and Discussion

Figure 2 shows snapshots of the equilibrated structure for $n = 2, 3,$ and $4,$ respectively. All simulations are run within a simulation box of $V=403$ DPD units, corresponding to $30 \text{ nm}^3,$ and a water saturation of $\lambda = 10.$ It can be seen that the microscopic structures vary quite significantly: the highest values of n shows almost spherical water clusters (Fig. 2c) whereas the lowest values for n gives a more chain-like structure. To explain this behavior we need to look at the EW of the molecules. Since only the C bead contains a sulfonic acid group, the equivalent weight of the membrane will increase with an increase in the value of n repeating unit, from $\text{EW} = 960$ grams for $n = 2,$ to $\text{EW} = 1360$ grams for $n = 4.$ A higher EW means that more hydrophobic backbone particles are present at an equivalent λ -value.

The nanometer scale structures of the membrane have been evaluated by calculating the radial distribution function (RDF) for the water beads within the membrane. From this evaluation, it is shown that a higher EW produces larger water clusters, and that the distance between the water clusters increases, which makes it difficult for the water to transport from one pore to the next. This behavior is highlighted by the calculated diffusivities, which shows a decrease with several orders of magnitude when the largest EW is applied.

Conclusions

Dissipative particle dynamics models and simulations are developed and performed, with coarse-grained beads of water and polymer and different repulsion parameters, to acquire the structure of the Nafion membrane. The equivalent weight of the membrane material has been investigated in terms of nano-scale structure and transport properties within the membrane. It is found that the equilibrated structure of the membrane varies significantly with the equivalent weight: higher equivalent weights produces larger water clusters within the membrane, and the water diffusivity within the membrane decreases significantly with equivalent weight.

Acknowledgment

The financial support from the European Research Council (ERC) is gratefully acknowledged.

References

1. K. Jiao and X. Li, "Water transport in polymer electrolyte membrane fuel cells", *Progress in Energy and Combustion Science*, 37, 221 – 291, 2011
2. Smitha, B.; Sridhar, S. & Khan, A., "Solid polymer electrolyte membranes for fuel cell applications - a review", *Journal of Membrane Science*, 2005, 259, 10 - 26
3. Malek, K.; Eikerling, M., Wang, Q., Liu, Z., Otsuka, S., Akizuki, K. & Abe, M.,
"Nanophase segregation and water dynamics in hydrated Nafion: Molecular modeling and experimental validation", *The Journal of Chemical Physics*, AIP, 2008, 129, 204702
4. Groot, R. D. & Warren, P. B. "Dissipative particle dynamics: Bridging the gap between atomistic and mesoscopic simulation" . *The Journal of Chemical Physics*, AIP, 1997, 107, 4423-4435

Electrically Induced Thermal Evolution Of Graphene-Based Vanadium Oxide Semiconducting Films For Self-Thawing Of Fuel Cell Engines (FCC1-6)

Hye-Mi Jung and Sukkee Um†

1School of Mechanical Engineering, Hanyang University, 222 Wangsimni-ro, Seongdong-gu, Seoul 133-791, Republic of Korea

†Corresponding author: Tel./Fax. +82-2-2220-0432, sukkeeum@hanyang.ac.kr

Cold-start strategies of fuel cell engines are of great importance for long-term reliability and stable operation of automotive fuel cells in subfreezing environments. Until recently, either an internal or external heat supply (e.g. wire heating, hydrogen combustion, coolant heating, and hot-air blowing) available to overcome the formation of ice at subzero temperatures has been one of the significant considerations for the successful cold starting of fuel cell engines. Although these methods have been very useful in improving cold-start performance and capability of fuel cell vehicles at subzero temperatures, they require a significant amount of fuel and power consumption. Therefore, a more energy-efficient alternative method for supplying thawing-heat at sub-freezing temperatures is needed to achieve the rapid start-up of fuel cell engines and avoid excessive energy consumption by auxiliary heat supply units (e.g. burner, heater, and thawing tank) of fuel cell systems, compared with the conventional methods. In this regard, this study presents a new self-thawing heat-up strategy relating to effective use of fundamental thermo-physical characteristics of heat generation and thermal dissipation by Joule self-heating of highly electrically resistive semiconductors with negative temperature coefficients (NTC). In our proposal, crystalline graphene-based vanadium oxides with NTC-type semiconducting behavior are effectively introduced in the form of composite films on the surface of key components of fuel cell engines (i.e., compression retention units) as a self-sufficient Joule-heating source for thaw-heating (Figure 1).

The present research is focused on the technical applicability of the suggested scheme under simulated cold-start conditions by considering the electrically induced thermal evolution effects of graphene-based vanadium oxide composite films on the sub-freezing start-up of fuel cells. For this purpose, combined experimental and numerical studies were performed to investigate the intrinsic thermo-electrical properties and thermal dissipation characteristics of graphene-based vanadium oxide films coated onto compression retention units of fuel cells below the freezing temperature.

To achieve this, graphene-based vanadium oxide nanostructured films were preferentially fabricated from well-mixed 0.17M precursor solutions of vanadium alkoxide and graphene oxide dispersed in water using a sol-gel based dip-coating technique. Then, experimental evaluations were carried out to obtain the temperature-dependent electrical properties and the time-resolved surface temperature profiles of the composite films coated onto the fuel cell compression units (i.e., electrically insulating plates) in the operating temperature range of automotive fuel cells. During the measurements, the temperature effects on electrical properties of the as-obtained films were carefully measured over the temperature range from -20 °C to 140 °C using a four-point probe method. In addition, the instantaneously transient thermal response of the as-prepared films was precisely measured using a thermocouple embedded in the center of the sample under cold starting conditions (i.e., -20 °C). The temperature-dependent electrical resistance measured on the as-

deposited films clearly demonstrated that the graphene-based vanadium oxide semiconducting films thermally grown on electrically insulating substrates act as a non-linear Joule heating source inversely proportional to the operating temperature, thereby resulting in the self-sufficient thaw-heating capabilities at low temperatures (Figure 2). Then, the Joule heating rise of the as-fabricated films was approximately 32.6 °C at a current density of 0.25 A · cm⁻² at -20 °C.

On the basis of the experimental results, a finite-volume-based dynamic thermal modeling was performed to estimate thermal evolution and temperature build-up characteristics of a fuel cell engine enclosed with the graphene/vanadium-based semiconducting films formed on compression retention units at a sub-zero freezing temperature (i.e., -20 °C). Extensive modeling efforts were conducted to explore the strong time-dependent temperature variations and the average thermal response time over a 10-cell sub-stack during cold startup. For effective prediction on the time-dependent thermal characteristics over the entire fuel cell stack domain, a fully three-dimensional heat conduction model was developed using a modified effective thermal conductivities of the individual fuel cell components. In the present model, various heat sources such as irreversible reaction heat, Joule heating, and sensible/latent heat of phase change were included in a governing differential equation of transient heat transfer, in which the additional heat source by Joule self-heating of the composite semiconducting films was adapted from the experimental data. Numerical results showed that the 10-cell sub-stack model surrounded by the semiconducting films onto the electrically insulating planar strip of compression retention units can reach normal operating temperature in less than 30 seconds considerably faster than the conventional case without the films (i.e., more than 60 seconds) at sub-freezing temperatures.

All experimental and numerical studies revealed that the as-fabricated films formed on the electrically insulating plate can be applied as considerable self-thawing sources in order to enhance the cold-start operation of automotive fuel cells under the subzero temperatures.

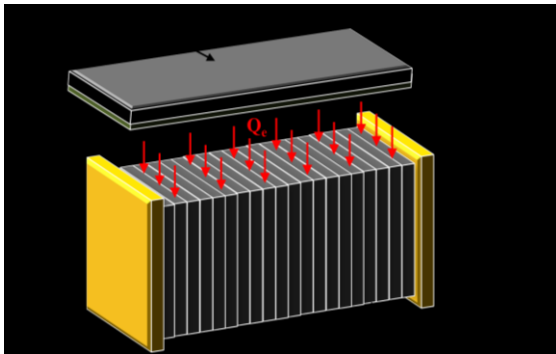


Figure 1

Figure 1 Schematic illustration of a cold-start strategy for self-thawing a fuel cell engine in a sub-freezing environment

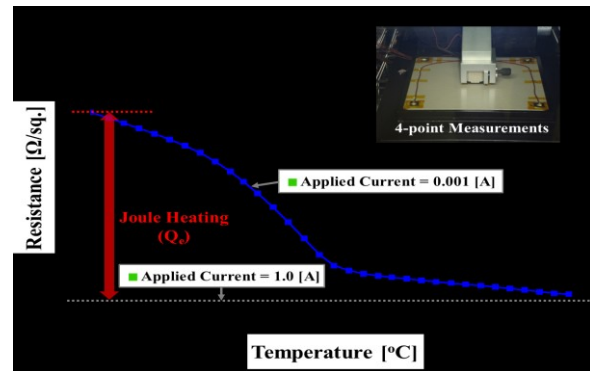


Figure 2

Figure 2 A typical experimental result of indirect Joule heating by graphene-based vanadium oxide semiconducting films coated onto electrically insulating substrate in the temperature range of -20 to 140 °C measured by a 4-point probe method

Order Reduction of a Distributed Parameter PEM Fuel Cell Anode Gas Channel Model (FCC2-1)

M.L. Sarmiento-Carnevalia,b, C. Batllea, I. Massanaa, M. SERRAb

aDepartament de Matemàtica Aplicada IV, Universitat Politècnica de Catalunya, EPSEVG, Av. V. Balaguer s/n, 08800, Vilanova i la Geltrú

bInstitut de Robòtica i Informàtica Industrial (CSIC-UPC), C/ Llorens i Artigas 4-6, 08028, Barcelona

INTRODUCTION

Distributed parameter modeling is required to accurately consider space variations, which are important regarding the performance and durability of the Proton Exchange Membrane Fuel Cells (PEMFC) [1-3]. However, the number of differential and algebraic equations (DAE) obtained from the discretization of a set of partial differential equations (PDE) is very large, and this not only slows down the numerical simulations, but also complicates the design of online model-based controllers.

The inclusion of complex DAE models within model-based control schemes requires a previous simplification. A method to simplify complex models consists of reducing the order while preserving the relationship between certain input and output variables, determined from the control objectives. These Model Order Reduction (MOR) techniques have been extended to DAE systems [4].

This work focuses on obtaining an order reduced model, from a PEMFC anode gas channel PDE model, which incorporates the effects of distributed parameters that are relevant for the proper functioning and performance of PEMFC. The original model is an in-house MATLAB® code, flexible enough to manipulate the underlying model equations and apply MOR techniques. The obtained order-reduced model is suitable to perform numerical simulations and design efficient controllers for the original nonlinear PDE model.

DESCRIPTION OF THE SYSTEM

The case study is the anode gas channel of a single PEM fuel cell (Fig. 1). The length of the channel is 0.4 m. A 10-segment grid has been considered to study spatial variations of hydrogen and water concentrations, flow velocity, channel pressure and temperature. The inputs to the system are hydrogen and water inlet flows, and the selected outputs for future control purposes are concentrations of each species at the end of the channel. All variables are indicated in Fig. 1.

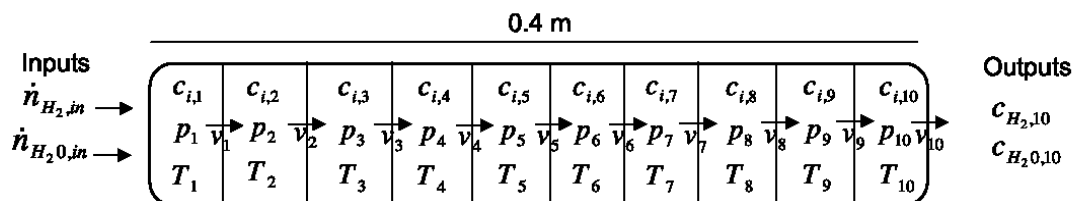


Figure 1: Single PEMFC anode gas channel

ANODE GAS CHANNEL MODEL EQUATIONS

In the following equations, k denotes segment number ($k = 1 \dots MZ$, $MZ = 10$ in this case) and i refers to gas components ($i = H_2, H_2O$). The total number of states is 30, which is the number of differential equations, and there are 30 algebraic variables and corresponding relations. The complete discretization process was presented in [5], which led to the following discretized equations. The general mass conservation equation for component i and segment k is:

$$\frac{dc_{i,k}}{dt} = -\frac{v_k c_{i,k} - v_{k-1} c_{i,k-1}}{\Delta z} - \frac{\dot{n}_{i,k}}{\delta}, \quad (1)$$

where Δz is the segment size, δ is the channel height and $\dot{n}_{i,k}$ is the flow rate of component i from segment k to the Membrane Electrode Assembly (MEA). The $\dot{n}_{i,k}$ values are set from a current density profile assumed. The boundary condition remains an algebraic equation as follows

$$v_0(t) c_{i,0}(t) = \dot{n}_{i,in} \quad (2)$$

This algebraic equation is used to calculate concentrations in the first segment of the gas channel. Calculation of flow velocity, using forward differencing is:

$$v_k = -K \frac{p_{k+1} - p_k}{\Delta z} \quad (3)$$

considering a boundary condition for the end segment

$$v_{MZ} = -K \frac{p^{amb} - p_{MZ}}{\Delta z} \quad (4)$$

where p^{amb} is the ambient pressure. The ideal gas law gives the pressure in the gas channel

$$p_k = RT_k \sum_i c_{i,k} \quad (5)$$

Accumulation of internal energy ρu in the gas channel is

$$\begin{aligned} \frac{d(\rho u)}{dt} = & -\frac{1}{\Delta z} \left(\sum_i v_k c_{i,k} h_{i,k}(T_k) - \sum_i v_{k-1} c_{i,k-1} h_{i,k-1}(T_{k-1}) \right) \\ & + \lambda \frac{T_{k+1} - 2T_k + T_{k-1}}{\Delta z^2} + \frac{\alpha_1}{\delta} (T_k^s - T_k) - \sum_i \frac{\dot{n}_{i,k}}{\delta} h_{i,k}(T_k) \end{aligned} \quad (6)$$

where h is gas enthalpy, λ is the heat conductivity coefficient and α_1 is the heat transfer coefficient.

The corresponding boundary equations are $T_{Mz+1} = T_0 = T^{amb} = 298.15 \text{ K}$. Temperature in the gas channel is given by the thermodynamic relation

$$(\rho u)_k + p_k = \sum_i c_{i,k} h_{i,k}(T_k) \quad (7)$$

MODEL ORDER REDUCTION

The method used to reduce the order of the case study nonlinear DAE model requires linearizing the original DAE model around an equilibrium point of interest, then computing the corresponding controllability and observability functions. The final step is finding an appropriate model realization that reveals which states of the original system can be truncated without considerably affecting the original input-output behavior [6]. Consider a nonlinear DAE model, as the one presented in the previous section

$$\begin{aligned} F_1(\dot{x}_1, x_1, x_2, u) &= 0 \\ F_2(x_1, x_2, u) &= 0 \\ y - h(x_1, x_2, u) &= 0 \end{aligned} \quad (8)$$

where $x_1 \in \mathbb{R}^d$ is the state vector, $x_2 \in \mathbb{R}^a$ are algebraic variables, $u \in \mathbb{R}^r$ are the control inputs, and $y \in \mathbb{R}^q$ are the outputs. Assuming that this DAE model has an underlying ODE description,

$$\begin{aligned} \dot{x}_1 &= \mathcal{L}(x_1, x_2, u) \\ x_2 &= \mathcal{R}(x_1, u) \end{aligned} \quad (9)$$

it follows that

$$\begin{aligned} \dot{x}_1 &= \mathcal{L}(x_1, \mathcal{R}(x_1, u), u) \\ y &= h(x_1, \mathcal{R}(x_1, u), u) \end{aligned} \quad (10)$$

4.1 COMPUTATION OF THE CONTROLLABILITY FUNCTION

The controllability function $L_c(x_{1,0})$ measures the minimal amount of energy in the control signal u , required to reach a specific state x . It is defined as the solution to the optimal control problem [4]:

$$L_c(x_{1,0}) = \min_{u(\cdot)} Jc$$

s.t.

$$\begin{aligned}
\dot{x}_1 &= L(x_1, x_2, u) \\
x_2 &= R(x_1, u) \\
x_1(0) &= x_{1,0} \in \Omega_x \\
0 &= \lim_{t \rightarrow \infty} x_1(t)
\end{aligned} \tag{11}$$

where J_c is a measure of the control signal energy

$$J_c = \frac{1}{2} \int_0^{\infty} u(t)^T u(t) dt \tag{12}$$

Due to the original model complexity, a local solution of the controllability function is computed, valid in a neighborhood of a specific equilibrium point. The result expressed as a convergent power series expansion up to some desired order is

$$L_c(x_1) = \frac{1}{2} x_1^T G_c x_1 + L_{ch}(x_1) \tag{13}$$

where G_c is a positive definite matrix, which is the inverse of the controllability Gramian, and $L_{ch}(x_1)$ contains terms of order three or higher. In this case study, $L_{ch}(x_1) = 0$. Therefore, the controllability function is approximated by a quadratic form that corresponds to a linear approximation of the original nonlinear model around a desired equilibrium point (section 4.3). The G_c matrix is derived from solving the Lyapunov equation

$$G_c A + A^T G_c + G_c B B^T G_c = 0 \tag{14}$$

where A and B are the resulting state and input matrices of the previously linearized DAE system.

4.2 COMPUTATION OF THE OBSERVABILITY FUNCTION

The observability function measures the energy in the output signal for certain initial state conditions. It is defined as

$$\begin{aligned}
L_o(x_1(0)) &= \frac{1}{2} \int_0^{\infty} y(t)^T y(t) dt \\
x_1(0) &= x_{1,0} \in \Omega_x \\
u(t) &= 0, \quad 0 \leq t < \infty
\end{aligned} \tag{15}$$

Considering a DAE model in the form of (8), the goal is to find $L_o(x_1)$ as a convergent power series on some neighborhood of $x_1 = 0$, up to a desired order

$$L_o(x_1) = \frac{1}{2} x_1^T G_o x_1 + L_{oh}(x_1) \tag{16}$$

where G_o is the observability Gramian (positive definite matrix) computed by solving the following Lyapunov equation

$$G_o A + A^T G_o + C^T C = 0 \quad (17)$$

and A and C are the resulting state and output matrices of the linearized DAE system. The observability function is approximated by a quadratic form as well, which corresponds to a linear approximation of the original nonlinear model.

4.3 COMPUTATION OF AN APPROPRIATE COORDINATE CHANGE

Once the controllability and observability functions are computed up to order two in this case study

$$L_c(x_1) = \frac{1}{2} x_1^T G_c x_1 \quad (18)$$

$$L_o(x_1) = \frac{1}{2} x_1^T G_o x_1 \quad (19)$$

a linear change of coordinates is used to simultaneously diagonalize G_c^{-1} and G_o as

$$\Sigma = G_c^{-1} = G_o = \text{diag}(\sigma_1, \sigma_2, \dots, \sigma_n), \quad (20)$$

where $\sigma_1 \leq \sigma_2 \leq \dots \leq \sigma_n > 0$ [4]. These σ_i values ($i = 1, \dots, n$) are denoted Hankel singular values and σ_1 is the Hankel norm of the system. A representation where the two Gramians are equal and diagonal is called balanced. A small σ_i means the amount of control energy required to reach the state $z = (0, \dots, 0, z_i, 0, \dots, 0)$ is large, while the output energy generated by the same state is small (Z being the new set of states). Computing this balanced realization requires performing Cholesky factorizations of the Gramians:

$$G_c = X X^T, \quad G_o = Y Y^T, \quad (21)$$

$X > 0$ and $Y > 0$. Then, the singular value decomposition (SVD) of $Y^T X$ is computed

$$Y^T X = U \Sigma V^T \quad (22)$$

where U and V are orthogonal. Finally

$$\Sigma = \text{diag}(\sigma_1, \sigma_2, \dots, \sigma_n) \quad (23)$$

The balancing transformation is given by

$$T = X\sqrt{\Sigma}^{-1/2}, \text{ with } T^{-1} = \Sigma^{-1/2}U^T Y^T \quad (24)$$

The balanced realization is given by the linear system

$$\tilde{A} = T^{-1}AT, \quad \tilde{B} = T^{-1}B, \quad \tilde{C} = CT \quad (25)$$

and

$$\Sigma = \tilde{G}_c^{-1} = \tilde{G}_o \quad (26)$$

4.4 TRUNCATION

The reduced model is obtained finding a major gap between two Hankel singular values, i.e., if $\sigma_k \gg \sigma_{k+1}$ for some k . The last z_{k+1} to z_n states of the balanced realization are left out without considerably affecting the input-output behavior, compared to the original system [4]. Recalling the original DAE model of (10), the balanced realization can be expressed as

$$\begin{aligned} \dot{z} &= \hat{L}(z_a, z_b, u) \\ y &= \hat{h}(z_a, z_b, u) \end{aligned} \quad (27)$$

where $z = (z_a, z_b)$ is the new set of states divided into two subsets determined by the Hankel singular values. The reduced order model would be

$$\begin{aligned} \dot{z}_a &= \hat{L}(z_a, 0, u) \\ y &= h(z_a, 0, u) \end{aligned} \quad (28)$$

SIMULATION RESULTS

In order to test the reduced-model behavior, step and sinusoidal input-output responses from the original model, linearized model (full order) and reduced model were simulated and compared. Fig. 2 (a) shows the response of output 1 (hydrogen concentration at the end of the channel) to unitary step changes (both inputs) at time 1. Fig. 2 (b) shows the response of output 2 (water concentration at the end of the channel) to unitary step changes (both inputs) at time 1. Fig. 2 (c) shows the response of both outputs to a sinusoidal input type at the hydrogen inlet flow. Fig. 2 (d) is the plot of Hankel singular values, which is important in order to decide how many states will be left out to reduce the order of the original model. This figure shows that approximately 5 states out of 30 are necessary.

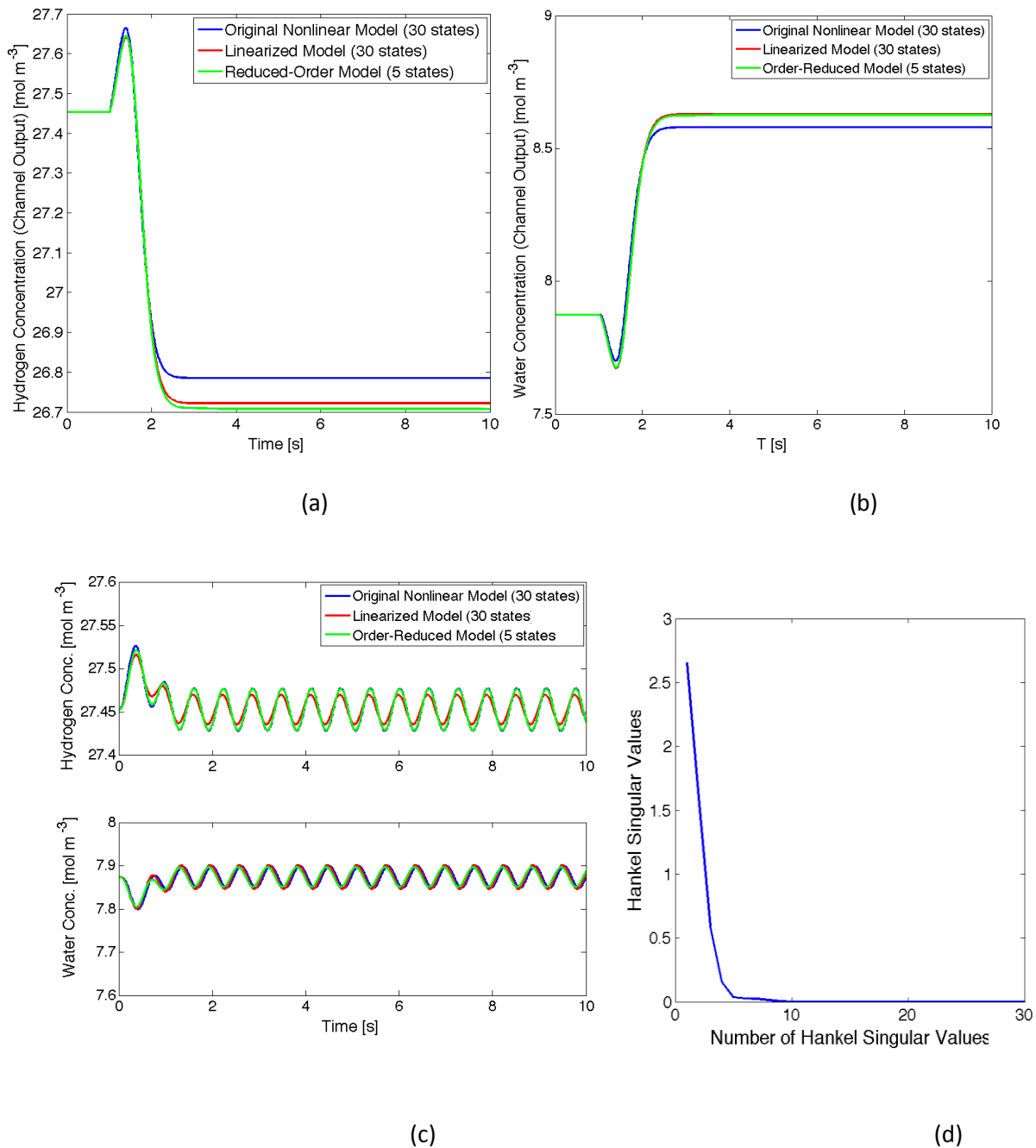


Figure 2: (a) Step change at time $t = 1s$ (Hydrogen Output) (b) Step change at time $t = 1s$ (Water Output) (c) Sinusoidal input (both outputs) (d) Hankel Singular Values

CONCLUSIONS AND ONGOING RESEARCH

Promising results have been found by applying an order reduction technique to a complex distributed parameter model of a PEM Fuel Cell Anode Gas Channel. The methodology consists of finding the controllability and observability functions of the original nonlinear model, computing a

change of coordinates to obtain a balanced realization that reveals the important states, and truncating less important states to approximate the original model. For the analyzed case study, a quadratic form of the controllability and observability functions has been used. Results have shown that reducing the order of the distributed parameter model from 30 states down to 5 states gives a very good approximation.

An interesting next step is to study the range of operating conditions (around the equilibrium) for which the reduced model is valid. In this moment, this model reduction technique is being applied to reduce an entire single PEMFC distributed parameter 1+1D model of approximately 100 states. The goal is to obtain an order-reduced model appropriate to design model-based controllers for PEM Fuel Cells.

Acknowledgements

This work has been supported by National Project DPI2011-25649 and European Project PUMA MIND FP7-303419.

REFERENCES

- S. A. I. C. Parsons, Fuel Cell Handbook. U.S. Department of Energy, 2000.
- D. Bernardi and M. Verbrugge, "Mathematical model of a gas diffusion electrode bonded to polymer electrolyte," *AIChE*, vol. 37, no. 8, 1991.
- C. Siegel, "Review of computational heat and mass transfer modeling in polymer-electrolyte membrane (PEM) fuel cells," *Energy*, vol. 33, no. 9, pp. 1331–1352, 2008.
- J. Sjöberg, Optimal control and model reduction of nonlinear DAE models. PhD thesis, Linköping University, Sweden, 2008.
- M. Sarmiento-Carnevali, M. Serra, and C. Batlle, "Distributed parameter model simulation tool for PEM fuel cells," *International Journal of Hydrogen Energy*, 2013.
- B. Moore, "Principal component analysis in linear systems: Controllability, observability, and model reduction," *Automatic Control, IEEE Transactions on*, vol. 26, no. 1, pp. 17–32, 1981.

Investigation of the liquid water distribution in a 50 cm² PEM Fuel Cell: effects of reactants relative humidity, oxygen/air feed, and current density. (FCC2-2)

Alfredo Iranzo a, Pierre Boillat b, Johannes Biesdorf b, Antonio Salva a, Felipe Rosa c*

a AICIA, School of Engineering, Sevilla, Spain

b Electrochemistry Laboratory (ECL), Paul Scherrer Institut (PSI), Switzerland

c Thermal Engineering Group, Energy Engineering Department, School of Engineering, University of Sevilla, Spain

INTRODUCTION

Neutron imaging of PEM Fuel Cells is a powerful instrument for the research and development of PEMFCs, as it allows the visualisation and quantification of the local water content within the cell. Liquid water is especially present at the cathode side, promoting mass transport losses and restricting the operation at high current densities. Also an excess of liquid water or a dry-out membrane will result in significant durability issues. Therefore, in order to ensure a successful performance and durability an appropriate water balance must be achieved within the cell.

In this work, a 50 cm² commercial PEM Fuel Cell has been used to investigate the effects of a set of different operating conditions on the resulting liquid water distributions in the cell. In particular, reactants relative humidity, cell current density, and the use of oxygen or air as oxidant, were investigated. Neutron imaging was used to determine the liquid water distributions in the cell for each case.

EXPERIMENTAL

Cell description.

The cell used in the experiment was a 50 cm² active area cell from ElectroChem Inc., with metallic Bipolar Plates (five-channel serpentine flow field). The Bipolar Plates layout is cross-flow, with horizontal channels in the anode and vertical channels in the cathode.

A set of Gas Diffusion Layers from SGL Group (Sigracet 24BC) were used. The GDL contains 5% of PTFE and a Micro Porous Layer (MPL) for enhanced performance of the GDL-catalyst layer interface. A Catalyst Coated Membrane (CCM) from Baltic Fuel Cells was used, with catalyst loading at anode and cathode electrodes 0.3 mg Pt/cm² and 0.6 mg Pt/cm² respectively. The membrane material is Nafion-117.

Experimental procedure.

The SINQ-NEUTRA beam-line at PSI (Boillat et al. 2008, Lehman et al. 2009), with 10 s exposure time, was used for the neutron imaging experiments. Before starting each of the tests the cell was dried out by flowing dry nitrogen through anode and cathode. Then the cell operation was performed in galvanostatic mode at 10 A and 25 A setting the anode and cathode flows to the

desired conditions. The matrix of operating conditions is shown in Table 1. The cell was operated at 2.0 bar and 60 C. The cell current density, voltage, cell resistance (HFR), and neutron imaging data were logged during the entire operation.

P = 2.0 bar T = 60 C I _a = 1.5 I _c = 5.0, Air				P = 2.0 bar T = 60 C I _a = 1.5 I _c = 3.5, Air		P = 2.0 bar T = 60 C I _a = 2.0 I _c = 10.0, O ₂	
i (A/cm ²)		RH _{a,c}		i (A/cm ²)		RH _{a,c}	
0.2	0 - 35	0 - 60	0 - 90	0.2	60 - 60	0.2	90 - 90
0.2	35 - 0	60 - 0	90 - 0	0.5	60 - 60	0.5	90 - 90
0.2	35 - 35	60 - 60	90 - 90	0.7	60 - 60	0.7	90 - 90
0.5	0 - 35	0 - 60	0 - 90				
0.5	35 - 0	60 - 0	90 - 0				
0.5	35 - 35	60 - 60	90 - 90				
0.7	0 - 35	0 - 60	0 - 90				
0.7	35 - 0	60 - 0	90 - 0				
0.7	35 - 35	60 - 60	90 - 90				

Table 1: Operating conditions used in the experiment

Once steady-state operation was achieved for each condition, the procedure described by Owejan et al. (Owejan et al., 2009) for distinguishing water in the different components of the cell was applied. First, the anode compartment was depressurized (2.0 bar to 1.0 bar) so that liquid water in anode channels is flushed out of the cell, and the cell remains in such condition during 60 s. Afterwards the anode compartment is also depressurized flushing out the liquid water in the cathode channels, maintaining the cell in such condition during 240 s. Images are recorded during the entire process. Therefore three different states of the cell water content are identified during the sequence:

- Cell with steady-state water content distribution within the entire cell, corresponding to the operating conditions defined.

- Cell with steady-state water content distribution, without liquid water in the anode channels.

- Cell with steady-state water content distribution, without liquid water in the anode and cathode channels (thus only water in GDLs and MEA is present).

- Cell with steady-state water content distribution, without liquid water in the anode and cathode channels and GDL (thus only water in MEA is present).

EXPERIMENTAL RESULTS

After performing the necessary corrections in the resulting images (detector background, change of beam intensity, neutrons scattered by the setup), the radiograms were referenced pixel-wise by dividing the obtained image by a reference image of the dry cell before operation. Therefore the attenuation corresponding to water only is obtained. The thickness of water δw is calculated from the relative neutron transmission (I / I_0) by inverting the Lambert-Beer law:

$$\delta w = -\ln(I / I_0) / \Sigma \quad (1)$$

where Σ is the attenuation coefficient of neutrons in liquid water, with a value of 3.5 cm⁻¹ for the given setup. The obtained water volume was converted into volume fraction by dividing by the depth of the active area in the beam direction (through-plane direction). Thus, the volume fraction obtained corresponds to the fraction of total volume.

The sequence of the neutron images recorded was analysed, and the differences in the liquid water distribution within the cell for the operating conditions tested were studied (reactants relative humidity, air or oxygen feed, and current density). In Figure 1 the increase in the cathode liquid water content can be observed, for increasing relative humidity of the cathode air inlet.

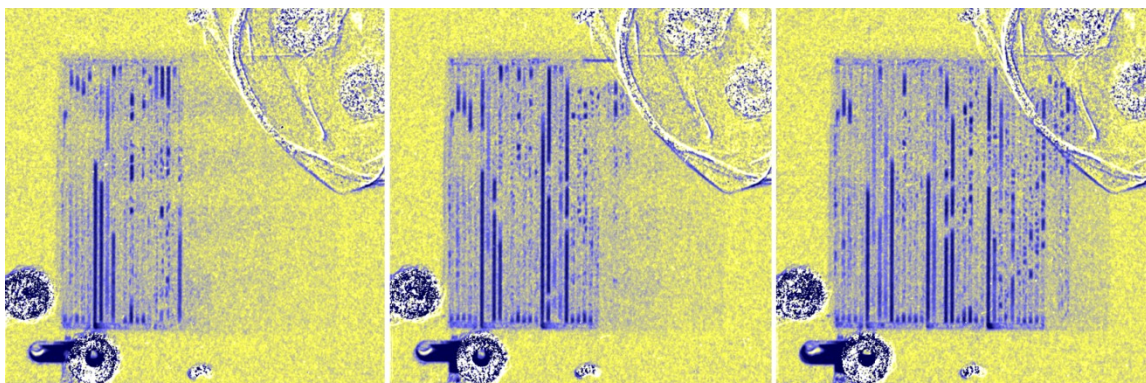


Figure 1: Liquid water content distributions in the cell at 10 A with H₂/Air (60 C, 2bar). Cathode flow field channels are vertical in the setup, anode flow field channels are horizontal. Left: RH_a 35%, RH_c 39%. Middle: RH_a 35%, RH_c 49%. Right: RH_a 35%, RH_c 59%.

The evolution of the cell resistance (HFR) for the different conditions was also analysed. The cell resistance is a direct indicator of the MEA water content (Tajiri et al. 2008). Figure 2 shows the cell resistance for the conditions depicted in Figure 1, where a decrease in the resistance (due to the larger membrane protonic conductivity) is observed as the cell water content increases.

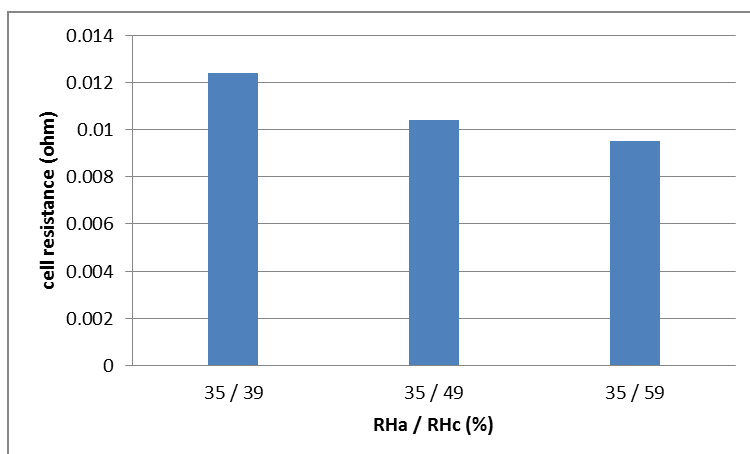


Figure 2: cell resistance at 10 A with H₂/Air (60 C, 2bar) for RH_a/c 35/39, 35/49, 35/59.

Neutron images were correlated with HFR (MEA resistance) where a direct correlation was found between liquid water content and cell resistance.

ACKNOWLEDGEMENTS

This work was carried out with the support of the European Community. We appreciate the support of the European Research Infrastructure project “H₂FC European Infrastructure” (funded under the FP7 specific programme Capacities, Grant agreement Number FP7-284522) and its partner Paul Scherrer Institut.

Alfredo Iranzo also gratefully acknowledges the support of the Spanish Ministry of Economy and Competitiveness under the program INNCORPORA, Torres-Quevedo PTQ-11-04703, co-funded with the European Social Fund.

REFERENCES

Boillat P, Kramer D, Seyfang BC, Frei G, Lehmann E, Scherer GG, Wokaun A, Ichikawa Y, Tasaki Y, Shinohara K. In situ observation of the water distribution across a PEFC using high resolution neutron radiography, *Electrochemistry Communications* 10, 546 (2008).

Lehmann EH, Boillat P, Scherrer G, Frei G. Fuel cell studies with neutrons at the PSI's neutron imaging facilities. *Nuclear Instruments & Methods in Physics Research Section A-Accelerators Spectrometers Detectors and Associated Equipment*, 605, 123 (2009).

Owejan, J.P., Gagliardo, J.J., Falta, S.R., Trabold, T.A. Accumulation and removal of liquid water in proton exchange membrane fuel cells. *Journal of the Electrochemical Society* 156 (12), B1475-B1483 (2009).

Tajiri, K., Wang, C-Y., Tabuchi, Y. Water removal from a PEFC during gas purge. *Electrochimica Acta* 53, 6337–6343 (2008).

Fuel cell current density distribution analysis: comparison between a 3D model and experimental data (FCC2-3)

F. Mariana³, M. Lakrouf^{1,2}, A. Picot^{1,2}, O. Rallières^{1,2}, H. Vergnes³, C. Turpin^{1,2}

1 Université de Toulouse; INP, UPS; LAPLACE (Laboratoire Plasma et Conversion d'Energie); ENSEEIHT, 2 rue Charles Camichel, BP 7122, F-31071 Toulouse cedex 7, France.

2 CNRS; LAPLACE; F-31071 Toulouse, France.

3 Laboratoire de Génie Chimique UMR 5503, Université Paul Sabatier, 118 route de Narbonne, 31062 Toulouse Cedex, France

Proton exchange membrane fuel cell (PEMFC) is an alternative energy source that doesn't generate undesirable by-product normally associated with the oxidation of fossil based fuel. However, its application still faces many challenges to overcome. These challenges include the need of uniform current distribution and careful water management. Careful water management is needed to avoid water flooding and at the same time to keep the membrane well hydrated. It appears indeed that inhomogeneity on the active area can be a sign of instability and can generate premature ageing of the PEMFC. A better understanding of phenomena implied in the active area homogeneity deterioration such as drying and flooding, and their impact on current density distribution (CDD) is crucial in order to assess and diagnose PEMFC state of health.

In this work, the CDD of an H₂/Air fuel cell has been studied. The fuel cell used is composed of a single cell that has an active area of 25cm² and a nominal current density of 1A/cm². The gas-supplying geometry used on both cathode and anode is a four-channel serpentine flow field. The CDD is assessed thanks to a Baltic S++ sensor plate placed on the cathode. The Baltic S++ sensor plate is a CDD measurement device composed of a 7x7 measurement cells' matrix. Each cell has an area of 50mm² and measures current density using Hall effect with a resolution of 0.1A.

A 3D computational fluid dynamics (CFD) model has been developed using Ansys Fluent fuel cell module. Ansys Fluent is a flow modeling software. The model is steady-state and integrates three-dimensional, multiphase, and non isothermal effects. The computational domain is a complete single fuel cell. This consists of two plates with carved gas channels transporting reactants and products, two porous gas diffusion layers, and two active layers and the membrane. The model was built using the chemical, physical, and geometrical characteristics of the experimental setting in order to be able to compare the two. The CFD model takes into account the activation losses, ohmic losses and mass transport phenomena that lower the theoretical power of the PEMFC. Besides these losses, PEMFC operation also has various issues affecting its performance. These issues include water management and current distribution.

The PEMFC has been studied along its whole voltage-current curve with an experimental gas setup of $\lambda_{air}=3$ for the air inlet and $\lambda_{H_2}=1.5$ for the hydrogen inlet, except for low current densities. The temperature and pressure conditions were set to $T=70^{\circ}C$ and $P=4bars$, and controlled thanks to a Baltic "quickCONNECTfixture" system including a compression device and a heating system. The air humidity is saturated to 100% using a bubble humidifier. The PEMFC current is controlled thanks to an active load. During the experiment, the PEMFC current has been varying from 0A to the maximal

current I_{max} () in 8min with CDD recordings every 5s. This protocol has been designed in order to observe CDD variations depending on the current while avoiding drying of the membrane.

The analysis of the current density maps obtained shows the current density is not homogeneously distributed over the fuel cell. The current density seems to be concentrated on the middle of the cell rather than on the edges. Moreover, CDD seems to be very dependent on the current imposed to the fuel cell. The current density is less homogenous on high current points and seems to be migrating to the H₂ outlet. This fact can be observed in Fig. 1 which shows the CDD recorded for a load current of $I=16A$. This figure presents the current density measured by the 7x7 sensors of the Baltic S++ measurement device. Dark colors correspond to high current density values. The arrows display the air and hydrogen inlets and outlets. It is clear in Fig. 1 that in this case, the current density is not homogeneously distributed but concentrated around the hydrogen outlet.

The comparison between experimental CDD and CDD computed through the CFD model shows that these results were predictable. Modeled CDDs show non-homogeneity over the cell with current density mainly concentrated on the center of cell. It can also be seen that CDD is less homogeneous for high load currents. Fig. 2 presents the distribution for the highest working current $I=25A$. In this figure, dark colors are linked to higher current density and arrows indicate hydrogen and air inlets and outlets. The same phenomenon is observed in Fig. 2 than in Fig. 1: the current density concentrates near the hydrogen outlet. The mesh of the modeled CDD is finer which allows studying the current distribution with more details than in experimental conditions. Nevertheless, comparison between experimental and modeled data enlightens the same current density behavior with non-homogeneity increasing with the working current. This comparison validates, at least qualitatively, the CFD model. The good correlation between the experimental and the model system helps to analyze the observed data.

The 3D modeling of a PEMFC using computational fluid dynamics software is an interesting tool to assess information about inhomogeneity of current density distributions. Model correlates with experimental Baltic S++ observations and helps the understanding of the phenomena implied. The next step of this work is to compare experimental and modeled current density distributions in case of flooding and drying. This work seeks to understand better the process inside a fuel cell and simulate the process parameters, especially in terms of current distribution and water management inside the cell. The main goal is the ability to predict the occurrence of water flooding. Accurate prediction then would be advantageous for a good water management.

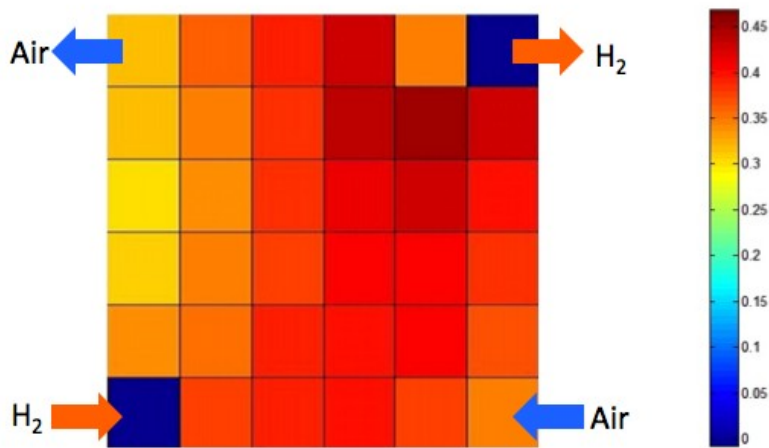


Fig. 1: Experimental current density distribution for $I=16A$

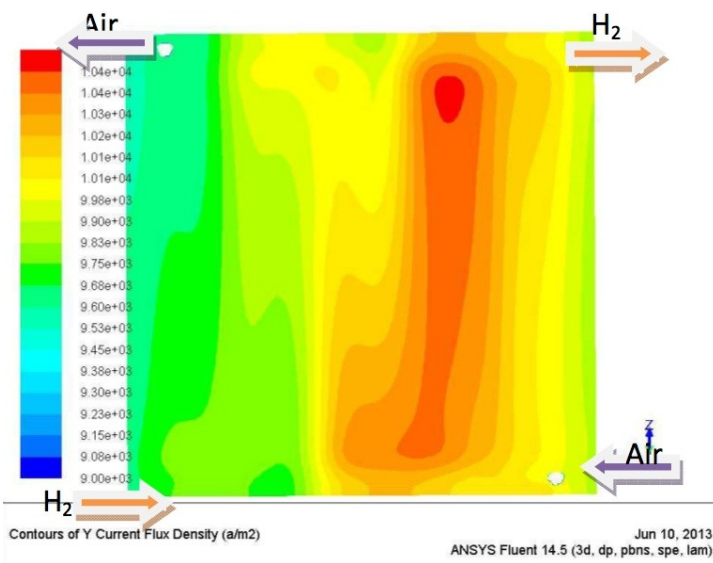


Fig. 2: Modeled current density distribution for $I=25A$

Ageing studies of PEM Fuel Cells developed for reformat fuel operation in μ CHP units (FCC2-4)

Sylvie Escribano, Laure Guétaz, Pierre-André Jacques, Fabrice Micoud
CEA/LITEN/DEHT – CEA/Grenoble - sylvie.escribano@cea.fr

Proton Exchange Membrane Fuel Cells (PEMFC) durability as well as their cost reduction are two objectives to be reached for large scale development and systems commercialization. Premium Act is an ambitious project on the durability of PEMFC, targeting one of the main hurdles still to overcome before successful market development of stationary fuel cell systems: durability, for which the target is several tens of thousands of hours.

Premium Act proposes an approach, combining experimental work, with both in-situ and ex-situ characterizations, and modelling work. The approach is applied for Direct Methanol and for reformates fuel PEFC technologies: the results presented here will concern the micro Cogeneration of Heat and Power (μ CHP) systems fed by reformat. The aim is to improve degradation understanding in order to propose operating strategies enhancing lifetime of given MEAs (Membrane Electrodes Assembly), and to design specific accelerated tests experiments. This presentation will be focused on the experimental results obtained about performance and MEAs degradation during aging tests of PEM fuel cells stacks or single cells.

Tests have been conducted with IRD components and stacks with load cycles and conditions representative for the considered μ CHP application (1). MEA tested contain respectively pure platinum (Pt) and platinum/ruthenium (PtRu) catalysts cathode and anode side and a mechanically reinforced membrane. In-situ tests have been conducted using operating conditions ranges (for temperature, pressure, relative humidity) and a smooth load profile, with steps at low and high current densities, defined based on the systems considered by the project. One major issue has been to evaluate the impact of various fuel compositions. Particularly accelerating impact of a CO concentration increase has been studied on both single cells and stack. Typically carbon monoxide (CO) concentration has been varied between zero and 50 ppm in the reformat fuel, and air bleeding has been also used in order to identify accelerating or slowing down features for these fuel cells degradation.

During fuel cell stacks and single cells ageing tests, in-situ electrochemical diagnostics are applied for both performance and components degradations analysis to identify the causes for fuel cell failure, particularly related to anode and cathode catalysts. Since these diagnostics only give averaged information on the electrodes and MEA status whereas the degradation is not homogeneous, in-situ results are completed with local ex-situ analyses to get better insights on modifications of the microstructure, particularly thanks to advanced electron microscopy techniques applied on samples degraded in different zones (like gases inlet or outlet, or more active zones like the middle of the cell).

One particular point was to check and compare the impact of the different operating conditions on the degradation mechanisms, and in the other way round to check the impact of the components degradation on the performance stability for the different conditions.

Results will show durability tests of hundreds of hours (up to 2000 hrs) conducted on stack or single cells and the subsequent modifications of the MEAs electrochemical properties and microstructure. Important conclusion concerns the impact of the PtRu degradation that appears to be acceptable for these durations when operating under pure Hydrogen but which becomes significant after only few hundred of hours when willing to operate the fuel cell continuously under reformat. It has been confirmed that in addition to common electrochemical Ostwald ripening and Pt dissolution able to occur at the cathode side during load cycles (2) the ruthenium dissolution is the degradation mechanism that leads to the acceleration of performance degradation in the case of reformat. Some added values of this work are to show that the accepted reversibility of CO poisoning impact is not true when operating with reformat; to enable getting in-situ information cell by cell at stack level about fuel impact; to show that increasing temperature increases CO tolerance and also stabilizes the performance, on the contrary to using air bleeding which does not reduce the voltage degradation rate; to enhance knowledge about Pt and Ru degradation mechanisms thanks to advanced TEM associated with EDX elemental chemical mapping, which allowed to detect particles dissolution at very early stage. As final output of the Premium Act project, these understanding investigations are used to develop specific accelerated tests with the aim to allow relevant ranking of MEAs versus long term durability, thanks to ageing tests of only few hundreds of hours.

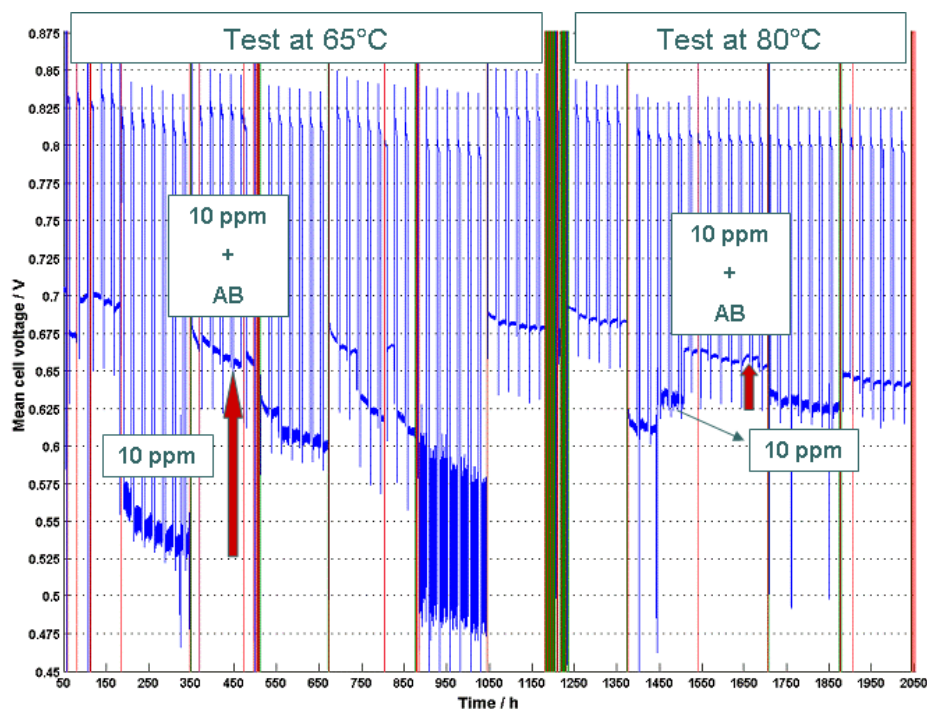


Figure: Average cell voltage during load cycles (6h at $0.065\text{A}/\text{cm}^2$ and 18h at $0.400\text{A}/\text{cm}^2$) applied on a 10 cells stack at 65 and then 80°C with different fuel compositions (pure H_2 or reformat with 76% of H_2 + 24% of CO_2 and CO concentrations of 5, 10 or 20 ppm; without or with Air Bleeding)

(1) Acknowledgements: this work is conducted in the frame of the project Premium Act supported by the FCH JU in FP7 program. Authors would like to thank IRD for providing the reference PEMFC

MEAs and stacks studied in this project; and also ICI and Soprano partners for their contributions in defining the operating parameters.

(2) L. Guétaz, S. Escribano, O. Sicardy, J. Power Sources 212 (2012) p.169-178

Lanthanide nickelates: advanced oxygen electrode materials for solid oxide cells (SOFC/HTSE) (FCC3-1)

J.C. Grenier^a, J-M. Bassat^a, A. Brevet^b, F. Mauvy^a, J. Mougín^b, A. Rougier^a

^a CNRS-ICMBC-CNRS, Univ. Bordeaux I, 87. Av. du Dr Schweitzer, F-33608 Pessac cedex, France

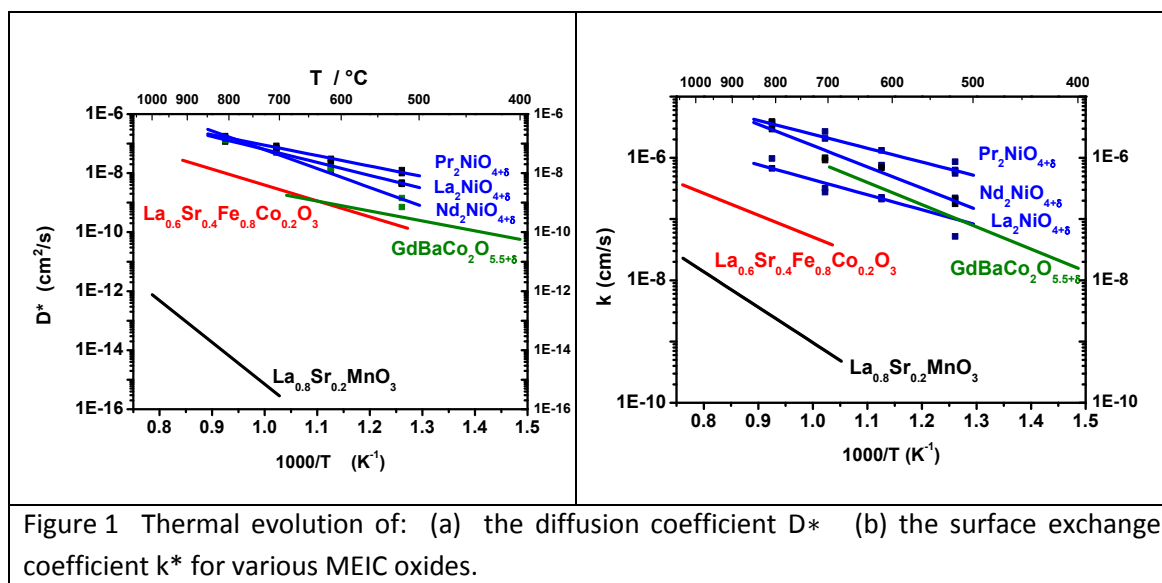
^b CEA-Grenoble, DRT/LITEN/DTBH/SCSH/, 17 rue des martyrs, F-38054 Grenoble Cedex 9, France
grenier@icmcb-bordeaux.cnrs.fr

High temperature ceramic solid oxide cells (SOC), based on an ion conducting solid electrolyte are of great interest in many energy conversion systems. These technologies are based on ceramic electrolytes with either ion oxide conductivity (Intermediate Temperature Solid Oxide Fuel cell, ITSOFC, High Temperature Steam Electrolysis (HTSE)) or protonic conductivity (Protonic Ceramic Fuel Cell, SOFC-H+). Nowadays, a lot of work is devoted to the development of such systems operating at intermediate temperatures (500 - 750 °C). One of the major problems is to decrease the high overpotential at the air electrode, which has required developing new oxide materials, the Mixed Electronic and Ionic Conducting (MEIC) oxides exhibiting simultaneously high electronic and ionic conductivities.

During the last two decades, most studies have been devoted to perovskite-type MEIC compounds, formulated $(A, A')(M, M')O_{3-\delta}$. These oxides show oxygen deficiency as well as a mixed valence of the metallic cation. Compounds, such as $\text{La}_{0.6}\text{Sr}_{0.4}\text{Co}_{0.2}\text{Fe}_{0.8}\text{O}_{3-\delta}$ (LSCF), are considered as excellent SOFC cathode materials, due to their high surface exchange kinetics and high oxygen diffusivity [1]. At the operating temperature, the oxygen vacancies are 3D randomly distributed.

More recently, new families of oxides have been evidenced to exhibit oxide ion conductivity with a 2D character. The first one, the so-called double perovskites are characterized by oxygen vacancies located in the lanthanide (LnO) layer. Typical compounds are: $\text{GdBaCo}_2\text{O}_{5+\delta}$, $\text{PrBaCo}_2\text{O}_{5+\delta}$ [2]. The second one, namely the Ruddlesden-Popper family, is formulated $\text{A}_2\text{MO}_{4+\delta}$ (A = La, Nd, Pr, Sr and M = Ni, Cu, Co). The main feature of these compounds is that they show oxygen overstoichiometry as well as a mixed valence of the transition metal cation, M [3-4].

Compared to the 3D perovskite compounds, these materials exhibit larger oxygen bulk diffusion (D^*) and surface exchange (k) coefficients than classical perovskite compounds (Fig.1). The electrochemical experiments as well as cell tests confirm these promising basic properties.

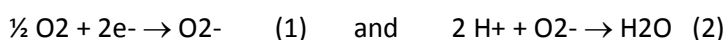


Cathodes of SOFC

Preliminary electrochemical measurements performed on symmetrical cells $Ln_2NiO_{4+\delta}/8YSZ/Ln_2NiO_{4+\delta}$, under air, had shown that values of area specific resistances (ASRs) at 600 - 700°C might agree with the requirements for an application in complete cells, the Pr compound exhibiting the lowest ASR value at 600 °C when using an interfacial CGO layer [5]. Indeed, high current densities have been reported, up to $1.31 A \cdot cm^{-2}$ @ 0.70 V, at 800 °C. Experiments on a 5-cell stack (250 cm^2) have led to a power density of $0.31 W \cdot cm^{-2}$ above 0.7 V average cell voltage, at 700°C, with an electrical efficiency of 33 % (fuel flow: 5 ml/min/ cm^2). Excellent performances have also been reported with composite cathodes ($La_2NiO_4-Sm_{0.2}Ce_{0.8}O_{1.90}$), more than $2 W \cdot cm^{-2}$ at 800 °C.

Cathodes of PCFC

Contrary to SOFCs, a peculiar feature of Protonic Ceramic Fuel Cells is that water vapor is formed at the cathode side, which requires some specific characteristics for the cathode material. Indeed, the reaction occurring at the cathode can be decomposed into two steps as follows:



If the cathode is a mixed electronic – oxygen ion conducting oxide, obviously reaction (1) may occur all over the surface, but the water is produced (reaction (2)) only near the electrolyte surface, i.e. at the three-phase boundary (TPB). But, using a mixed electronic - proton conducting oxide would allow the water to be formed mainly over the surface of the whole cathode and from a practical viewpoint, it would lead to faster electrode processes.

The behaviour of various Ln_2NiO_4 nickelates has been studied. Physical properties under moist air show that all these materials are stable, even during a long time in such conditions; even, some (OH) species seem to be present at temperatures as high as 600 °C.

Impedance spectroscopy measurements on symmetrical cells using the protonic electrolyte BaCe_{0.9}Y_{0.1}O_{3- δ} (so called BCY10) have been performed under air/3% H₂O atmosphere. The values of Area Specific Resistances (ASR) show these materials to be promising cathodes, especially

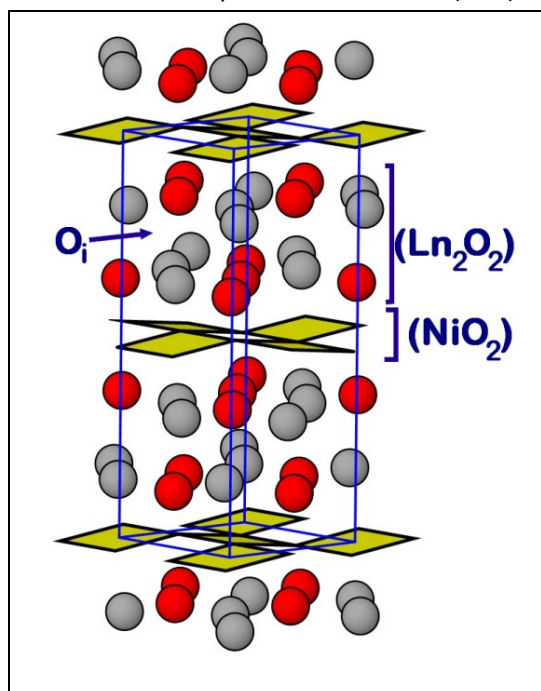


Figure 2 Structure of Ln₂NiO_{4+ δ} compounds showing the NiO₂ and Ln₂O₂ layers.

Pr₂NiO_{4+ δ} . A Ni-BCY10/BCY10/Pr₂NiO_{4+ δ} single cell has been operated at 550–650 °C, the power density value being about 200 mW.cm⁻² at 600 °C [6].

Anodes of HTSE

One of promising ways for the massive and clean production of hydrogen is the high temperature steam electrolysis (HTSE). Highly efficient electrolyzers are then required, which implies that the components of the solid oxide electrolysis cell (SOEC) should be optimized. Up to now, most studies have considered reversible solid oxide cells (fuel cell / electrolysis cell) based on commercial cells, the oxygen electrode (anode in this mode) being a perovskite-type oxide. Again, the Ln₂NiO₄ nickelates have been proposed as alternative materials because of their aptitude to accommodate a large oxygen overstoichiometry, especially under oxidizing conditions. Typical current-voltage curves of symmetrical cells show that Ln₂NiO_{4+ δ} materials can operate both under cathodic

and anodic polarization, but obviously, they appear more efficient for the water electrolysis, which is confirmed by the results obtained with a single complete cell [7]. The praseodymium nickelate appears again the most performing anode material.

Flexibility of the Ln₂NiO_{4+ δ} compounds

All these examples do point out the interest to use the Ruddlesden-Popper compounds, Ln₂NiO₄ nickelates as air electrode in different configurations. However, one can wonder why these materials are so efficient.

Based on TGA results and Thermal Expansion Coefficients under various oxygen partial pressures, on coulometric experiments as well as high temperature XRay Diffraction, the structural features of these compounds are examined. More especially, the 2D structure made of (NiO₂) layers of square planar sites and Ln₂O₂ rock salt-type layers can explain the exceptional flexibility of this structure. It will be discussed.

Finally, it appears that these compounds are really flexible for being used in different systems, which is illustrated by the good reported performances.

Acknowledgments: the authors gratefully acknowledge the European Community for supporting this work through the RAMSES project (#256768) as well as the French Research Agency (ANR) through the FIDELHYO project (# ANR-09-HPAC-005).

References

1. F. Tietz, V. A. C. Haanappel, A. Mai, J. Mertens, D. Stöver, *Journal of Power, Sources*, 156 (1), 20-22, (2006).
2. A.Tarancon, M. Burriel, J. Santiso, S. J. Skinner and J. A. Kilner, *J. Mater. Chem.*, 2010, 20, 3799–3813
3. E. Boehm, J.-M. Bassat, P. Dordor, F. Mauvy, J.-C. Grenier, Ph. Stevens, *Solid State Ionics*, 176 (37-38) 2717-2725 (2005).
4. P. Stevens, E. Boehm, J-M. Bassat, F. Mauvy and J-C. Grenier, France Brevet FR 2868211. 2005-09-30 and International Patent WO 2005099003 (2005-10-20).
5. C. Ferchaud, J-C. Grenier, Y. Zhang-Steenwinkel, M. A. van Tuel, F. P. F. van Berkel, J-M. Bassat , *Sol. State Ionics*(submitted)
6. G. Taillades, J. Dailly, M. Taillades-Jacquín, F. Mauvy, A. Essouhmi, M. Marrony, C. Lalanne, S. Fourcade, D. J. Jones, J-C. Grenier, J. Rozière, *Fuel Cells*, in press (2009).
7. F. Chauveau, J. Mougin, J. M. Bassat, F. Mauvy, J. C. Grenier, *J. Power Sources*, 195 (2010) 744–74922.

Advanced Solid Oxide Cells For Fuel-To-Power And Power-To-Fuel Conversion (FCC3-2)

Byung-Kook Kim

Korea Institute of Science and Technology, Seoul 136-791, Republic of Korea

High-temperature solid oxide cells based on ceramic membrane offer numerous advantages over the conventional energy systems such as high efficiency, low environmental impacts, fuel flexibility and modularity. To establish a foundation for a secure energy future and address the environmental concerns associated with the extensive use of fossil fuel, Korea Institute of Science and Technology (KIST) has carried out wide range of research activities in the field of high-temperature solid oxide fuel cells (SOFC) and solid oxide electrolysis cells (SOEC) for fuel-to-power and power-to-fuel conversion, respectively, over the past decades.

The SOFC research is aimed at achieving the high-performance, low-cost, modular, and robust cell, stack and system technologies suitable for various power generation applications. We have developed materials and fabrication techniques to enhance the performance and stability. Recently, we demonstrated 1 kW-class stacks with excellent long-term stability at 650oC with H₂ and CH₄ fuel through collaboration with Ssangyong Materials. Because the high-temperature operation of SOFCs increases the material costs and deteriorates the long-term stability, we are developing the next-generation SOFCs for the intermediate-temperature operation (500~600oC). There are two major approaches to reduce the operating temperature without sacrificing the performance. First approach is to improve the structure of the cell based on the conventional material system. We have developed the advanced fabrication techniques such as the pulsed laser deposition (PLD) and chemical solution deposition (CSD) processes to manufacture the thin-film electrolyte and nano-scaled electrodes because the reduction of the electrolyte thickness lowers the ohmic resistance and nano-scaled electrode enhances the electrocatalytic activity at the reduced operating temperatures. Second approach is to develop the novel materials such as proton conducting ceramics. The proton conducting fuel cells (PCFC) can potentially lower the operating temperature because the proton conduction is more facile than the oxygen ion conduction at the intermediate- and low-temperature range. It is extremely difficult to densify the proton conducting electrolytes due to the poor sinterability, and we have developed the bi-layer electrolyte structure to enhance the sintering behavior using the constraining effects. Consequently, we achieved decent performance and stability under the practical operating conditions with the maximum power density of 400 mW cm⁻² at 600oC.

For power-to-fuel conversion, high-temperature SOEC, which offer inherent advantages in thermodynamics and kinetics over the conventional low-temperature electrolysis, are actively investigated for energy storage via steam electrolysis and CO₂/H₂O co-electrolysis. Electricity and unused heat supplied from the renewable energy sources, nuclear power plants and high-temperature industrial processes can be effectively stored in the forms of hydrogen or syn-gas by high-temperature electrolysis, which can possibly overcome the limitations of conventional energy storage systems, such as pumped hydro, compressed air, batteries and supercapacitors, in costs, capacity, runtime and geographic restrictions. Because the SOEC reaction is the reverse of the SOFC reaction, the SOFC technology can be directly applied to SOEC development. On the contrary, there

are fundamental differences between SOFCs and SOECs in direction of mass and current flow, operating environments, and heat requirements. In general, dedicated SOFCs exhibit inferior performance and stability in SOEC operation, which emphasizes that materials and microstructure should be optimized for SOEC operating conditions. We have identified and tackled the critical challenges associated with the performance and long-term stability of SOEC, and this presentation will discuss the up-to-date progress in research activities at KIST.

Development and performance analysis of a metallic passive Micro Direct Methanol Fuel Cell for portable applications (FCC3-3)

D.S. Falcão^{a*}, J.P. Pereira^a, C.M. Rangel^b, A.M.F.R. Pinto^{a*}
^aCEFT, ^bLEPAE

*Departamento de Eng. Química, Universidade do Porto, Faculdade de Engenharia,
Rua Dr. Roberto Frias, 4200-465 Porto, Portugal*

^cLNEG

Estrada do Paço do Lumiar, 22

1649-038 Lisboa

Portugal

#corresponding author, E-mail: dfalcao@fe.up.pt, apinto@fe.up.pt

Phone: +351225081675, Fax: +351225081449

Fuel cells have great potential: high efficiency, minimization of moving parts and low emissions. Direct Methanol Fuel Cells (DMFC) has attracted much attention due to the facility of fuel (methanol) transport and storage, suitable for potential applications as a power source for portable electronic devices. With the advances on micromachining technologies, miniaturization of power sources became one of the trends of evolution of research in this area. Considering the advantages of the scaling laws, miniaturization affiances higher efficiency and performance of power generating devices, so, Micro DMFC is an emergent technology. There has been a growing interest in the development of this type of micro cells in the last years, mainly on experimental area. There are two ways of operate a Micro DMFC, considering the different concepts of fuel delivery: active and passive mode. On active mode, reactants supply is forced, needing moving parts to feed oxidant or fuel to the cell, requiring power to operate. A passive system requires no external power relying on diffusion and natural convection to deliver the fuel and oxygen. There are also cells that need a dispositive to supply the fuel but are passive at the cathode side, i.e., working in air-breathing operation. Most of the works on Micro DMFC are based on active systems but there is an increasing interest in the passive cells exhibiting higher volumetric energy density and more design flexibility mainly when miniaturization is needed. In this work, a passive (on both sides) Micro DMFC was “in house” designed and constructed, except the Membrane Electrode Assembly (MEA). The basic cell design consists in two acrylic terminal plates (the cathode with an open area to enter the air and the anode with a reservoir to contain the methanol solution) and two stainless steel current collectors with open circles (the circles diameter are different on both sides). The thickness of stainless steel plate is 300 μ m. The cell is presented in Fig. 1.

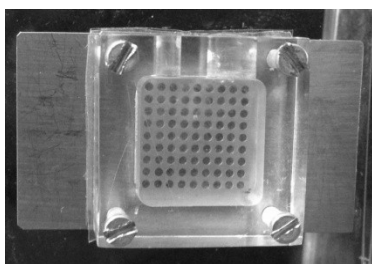


Figure 1 – Passive Micro DMFC picture.

The experimental rig avoids the necessity of auxiliary devices to supply the fuel and oxygen, so, it was only used an electrochemical station (Zahner) to obtain polarization curves. Several commercially available materials for MEA, the central part of a Micro-DMFC, are tested and the effect of methanol concentration on the cell performance is evaluated. The experiments with a passive Micro DMFC with 2.25 cm² active area were performed at room temperature, a condition of special interest taking in mind portable application. The maximum power density, 19.2 mW/cm², was obtained using a Nafion 117 membrane, 3 mg/cm² Pt-Ru and 0.5 mg/cm² Pt as, respectively, anode and cathode catalyst loading, carbon paper as anode gas diffusion layer (GDL) and a special Sigracet carbon paper with micro porous layer (MPL) as cathode GDL at methanol feed concentration of 3 M. This result demonstrates that membranes with low catalyst content could be used in passive MicroDMFC with success. Passive Micro DMFC performances are compared with the ones obtained using an active Micro DMFC already developed and tested by the team. For some MEAs tested the maximum power output obtained with the MicroDMFC is even superior to the one obtained with the active one. Research efforts should be directed to obtain high performances making a careful selection of MEAs materials and properties and also to choose adequate operating conditions.

Noble metal oxide and valve metal oxide promoters of Pt for methanol oxidation (FCC3-4)

V. Baglio¹, R.S. Amin², K.M. El-Khatib², S. Siracusano¹, A. Stassi¹, D. Sebastián¹, A.S. Aricò¹

¹ CNR-ITAE Institute, via Salita S. Lucia sopra Contesse, 5 - 98126 Messina, Italy

² Chem. Eng. & Pilot Plant Dept., National Research Center, Dokki, Giza, Egypt

Fuel cells represent an important technology for a large variety of applications including micro-power, auxiliary power, transportation, stationary power for buildings and other distributed generation applications, and central power [1]. Several types of fuel cells are in advanced stage of development. The direct methanol fuel cell (DMFC) is a promising power source for portable applications [2]. Yet, DMFCs are characterized by two slow reactions, i.e. methanol electro-oxidation and oxygen reduction with the further drawback of the presence of a mixed potential at the cathode determined by methanol crossover. On the other hand, there are specific advantages in using methanol as a direct fuel especially with regard to costs, simplicity of design, large availability, easy handling and distribution. In the last few years, a significant number of investigations have been carried out in the field of the electro-oxidation of methanol at low temperature [3]. Literature studies have underlined the importance of both nature and strength of adsorbed oxygen species in the methanol oxidation process. Unfortunately, water discharging occurs at high potentials on Pt surface. Since the role of Pt as catalyst for methanolic species adsorption and dehydrogenation appears almost unique, it is quite difficult to replace Pt with a similar active catalyst at the anode. However, there are several transition metals such Ru, Sn, W; Os etc. that may promote water displacement at low potentials. Pd may represent an alternative to Pt for dehydrogenation but the reactions rates are significantly lower.

In this work, we have investigated metal oxide modifications of Pt to individuate a guideline for the development of a multifunctional catalyst. As a basis for our work, we have focused on metal oxide used for the oxygen evolution from water in acidic environment such as “valve metal” oxide (SnO_x, VO_x) or active phase catalysts (RuO_x, IrO_x). There is an important analogy among the methanol oxidation and oxygen evolution since both processes require water discharging on the electrode followed by the adsorption of active oxygen species that give rise to a surface reaction with adsorbed methanolic residues or desorbs as oxygen molecule in the electrolysis mode. Of course, these processes occur in a quite different potential window and water displacement at very low potentials, as required for the methanol process, is a quite slow step.

The catalysts were prepared using a simple polyol method involving precursor reaction in ethylene glycol. Structure, chemistry and morphology of these catalysts were analysed together with the electrochemical behavior.

Acknowledgements

The research leading to these results has received funding from the European Community's Seventh Framework Programme (FP7/2011-2014) for the Fuel Cells and Hydrogen Joint Technology Initiative under grant agreement DURAMET no. 278054. The authors also acknowledge the support of bilateral CNR (Italy) – ASRT (Egypt) joint agreement 2013-2014.

References

- [1] M. Neergat, D. Leveratto, U. Stimming, Fuel Cells 2 (2002) 25.
- [2] R. Dillon, S. Srinivasan, A.S. Aricò, V. Antonucci, J. Power Sources 127 (2004) 112.
- [3] A.S. Aricò, V. Baglio, V. Antonucci, Direct Methanol Fuel Cells; Nova Publishers: New York, NY, USA, (2010).

Catalytic electro-activation of the Pt-Ti interphase for CO and metanol oxidation (FCC3-5)

M. Roca-Ayats¹, G. García², J.L. Galante¹, Miguel A. Peña¹ and M.V. Martínez-Huerta¹

1 Instituto de Catálisis y Petroleoquímica. CSIC. C/Marie Curie 2. 28049 Madrid, Spain.

2 Departamento de Química Física. Universidad de La Laguna. c/ Astrofísico F. Sánchez. 38071- La Laguna, Tenerife, Spain.

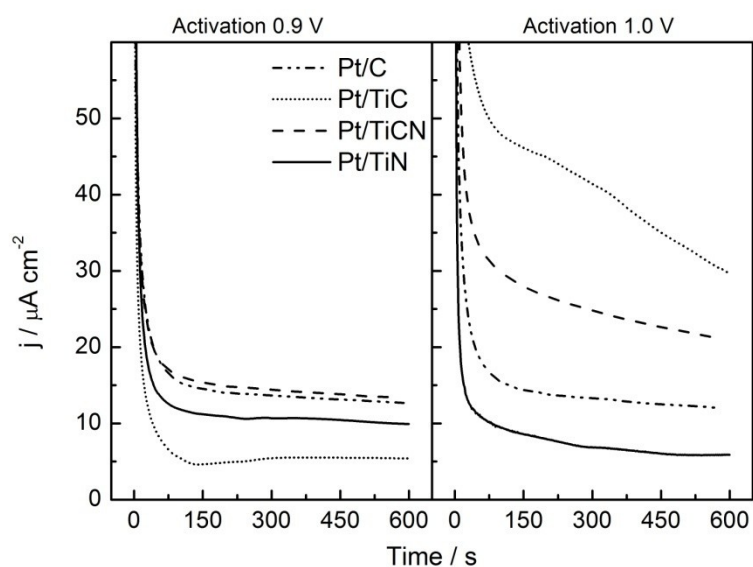
Direct methanol fuel cells (DMFC) seem to be promising devices for portable energy applications due to its low cost and easy manipulation. However, there are still some problems regarding the anodic catalyst that must be solved for a viable commercialization. At present, the catalysts employed contain a large amount of noble metals (platinum, ruthenium...) and a quite sluggish kinetics. In consequence, one of the principal tasks is to develop new cheaper materials with high activity [1]. To fulfil this purpose, the concept of “active site” must be taken into consideration.

In gas phase catalysis, it is quite usual to use solid catalysts made of reducible metals supported in transition metals and rare earth oxides (ZrO₂, CeO₂, TiO₂...) for application in reactions such as water gas shift reaction and oxidation of CO and hydrocarbons [2]. Part of the activity of those catalysts is related to the promoting effect of the support, which favours the formation of oxygenated species through a bi-functional mechanism. However, the utilization of metal oxides as support in electrocatalysis has been hindered by the low electric conductivity of this type of materials. Recently, the utilization of transition metals carbides and nitrides (TiC, WN, Mo₂C...) as supports has been developed due to their high electric conductivity and good physical and chemical properties [3]. For those materials, a synergetic effect of the support has been observed, with a positive effect on CO and methanol electrooxidation. Both, bi-functional and electronic effect, were proposed as responsible.

In the present work, four different catalysts made of platinum nanoparticles supported on different materials (TiC, TiCN, TiN and C-black) were synthesised by the ethylene glycol method [4] and thermally treated under helium flow. The catalysts were characterized by transmission electron microscopy (TEM), X-Ray diffraction (XRD), inductively coupled plasma atomic emission spectroscopy (ICP-AES) and X-Ray photoelectron spectroscopy (XPS). Results show an electronic charge transfer from the titanium-based supports to the platinum nanoparticles. This charge transfer appears to be stronger the nitrogen content in the catalyst support. The activities of the catalysts through CO and methanol electrooxidation after two different activation treatments (cycling up to 0.9 V or up to 1.0 V versus RHE), as well as the behavior of the catalyst supports, were evaluated by cyclic voltammetry and chronoamperometry and Fourier transform infrared spectroscopy (FTIRS). A significant enhancement of the activity toward CO and methanol electrooxidation reactions was observed for those carbide-based catalyst supports when the activation step arrived to 1.0 V instead of 0.9 V. This catalytic enhancement is associated to the generation of oxygenated species onto the interphase sites of platinum and titanium carbide.

ACKNOWLEDGEMENTS

This work has been supported by the Spanish Science and Innovation Ministry under projects CTQ2011-28913-C02-02 and ENE2010-15381. MR acknowledges to the FPU-2012 program for financial support.



Current transients recorded in 2M CH₃OH + 0.5 M H₂SO₄ at 0.55 V after activation at 0.9 (left) and 1.0 V (right).

REFERENCES

1. Zhao, X., et al., Recent advances in catalysts for direct methanol fuel cells. *Energy & Environmental Science*, 2011. 4(8): p. 2736-2753.
2. Campbell, C., et al., Model oxide-supported metal catalysts: energetics, particle thicknesses, chemisorption and catalytic properties. *Topics in Catalysis*, 2000. 14(1-4): p. 43-51.
3. Wang, Y.J., D.P. Wilkinson, and J. Zhang, Noncarbon support materials for polymer electrolyte membrane fuel cell electrocatalysts. *Chem Rev*, 2011. 111(12): p. 7625-51.
4. Bock, C., et al., Size-Selected Synthesis of PtRu Nano-Catalysts: Reaction and Size Control Mechanism. *J Am Chem Soc*, 2004. 126(25): p. 8028-8037.

Vibrating Wire Method With Semi-Circle Wire For Measuring Hydrogen Viscosity (FCC3-6)

Tatsuya HISATSUGU¹, Temujin UEHARA¹, Kan'ei SHINZATO²
Naoya SAKODA^{1,3}, Masamichi KOHNO^{1,3}, Yasuyuki TAKATA^{1,3}

¹Dept. of Mech. Eng., Kyushu Univ., 744 Motoooka, Nishi-ku, Fukuoka 819-0395, Japan

²Research Center for Hydrogen Industrial Use and Storage (HYDROGENIUS), Kyushu Univ., 744 Motoooka, Nishi-ku, Fukuoka 819-0395, Japan

³International Institute for Carbon-Neutral Energy Research (WPI-I2CNER), Kyushu Univ., 744 Motoooka, Nishi-ku, Fukuoka 819-0395, Japan

The measurement of thermal properties in the region of high pressure (~100 MPa) and high temperature (~500 °C) is necessary for the realization of society with fuel cell vehicle. In the refueling process of fuel cell vehicle at hydrogen station, pressure of hydrogen will rise up to 70 MPa and temperature will rise up to 470 °C. In order to refuel hydrogen with high efficiency, transport properties of hydrogen in high pressure and high temperature region are necessary. In our study, we focused on measuring viscosity of hydrogen which is an important transport property. In our previous study, we employed capillary method for measurement. Capillary method[1] is the most accurate method for the measurement of viscosity of fluid. However, the size of capillary method becomes big when measuring fluid with low viscosity. In order to minimize the size of device, we employed vibrating wire method with semi-circle wire for the measuring method of hydrogen. Vibrating wire method[2] which with linear wire is the popular way for the measurement of viscosity. However because of the demand for the viscosity measurement data in the high pressure and high temperature region, existing method is too large for the measurement (about 5 cm length of size of wire). Also, in the vibrating wire method with the linear wire, it is necessary to apply constant tensile force to the wire for the prevention of twisting of wire. Moreover, there is possibility of vibrating in two dimensional directions. In semi-circle wire vibrating method, radius of semi-circle is 1 cm as shown in Fig. 1 and it doesn't need tensile force for the prevention of twisting because of the force of restitution from the wire itself. Also, the possibility of vibrating in two dimensional directions is quite small because of the shape of the wire. Semi-circle wire uses Lorentz force for the driving force for vibrating. The wire is settled in the magnetic field of SmCo magnet, and the alternative current is applied to the wire by lock-in amplifier. Fig. 1 shows the schematic view of semi-circle vibrating wire viscosity probe. Lock-in amplifier also detects the induced voltage from wire by four terminal method. Alternative current is applied to the wire with transition of frequency. From the data of relationship between the frequency of applied alternative current and induced voltage, resonant curve can be obtained. Fig. 2 shows the example of resonant curve. In Fig. 2, horizontal axis shows the frequency of alternative current and vertical axis shows the induced voltage. Plots are the raw data and solid line is fitted curve. V_{max} shows the peak of resonant curve and V_{middle} shows half value and V_{offset} shows the bottom of curve. Also, f_0 is resonant frequency and f_{1} and f_{2} are frequencies at half value and $2\Delta f$ is half bandwidth. From these data, viscosity of fluid can be measured. In vibrating wire, mainly four forces are applied. There are Lorentz force, dumping force of fluid, dumping force of internal friction and elastic restoring force of wire. Viscosity of fluid causes dumping force of fluid. By detecting the amplitude of these forces and parameters, viscosity of fluid can be calculated. Specially, internal friction coefficient which is needed for calculation is important

factor to be measured accurately. It can be calculated from half band width 2Δ . The uncertainties in this method can be determined by calculating uncertainty of each parameter and sensitivity. Combined uncertainty is 2.3 % with the coverage factor, k , to be 2. In the parameters, the effect from wire's diameter and density are large. For the accurate measurement, accurate measured data for these two values are necessary. For the evaluation of measured data, we compare with estimate equation made by Yushibani et al[3]. The uncertainty of this estimate equation is 2 % in low density region and 4 % in high density region. Recently, we measured viscosity of nitrogen and hydrogen in region of ~ 0.7 MPa and ~ 500 °C before applied in the high pressure region in order to confirm the adequacy of measuring method. In the measurement of nitrogen, the deviations from Lemmon estimate equation[4] are ± 2 % in the ~ 400 °C temperature region, the uncertainty of Lemmon estimate equation is ± 2 %, and it can be concluded that this method is adequate in the ~ 400 °C region. However, in 500 °C temperature condition, the deviation from Lemmon estimate equation is near to 4 %. In the temperature region more than 350 °C, the magnetic force of SmCo decays with the increase of temperature even though its Curie point is 700~800 °C. By measuring density of magnetic flux of SmCo magnet before experiences 500 °C temperature condition and after experiences 500 °C temperature condition, density of magnetic flux is around 200 T in former condition. However it is around 80 T in latter condition. The density of magnetic flux depressed to 40 % of initial condition. Because of the loss of magnetic force, it can be concluded that accurate resonant curve cannot be attained from measurement. In fact the shape of resonant curve is different in higher temperature region. Therefore, it can be concluded that the vibrating wire method is not adequate for measuring viscosity of fluid in the condition of over 350 °C temperature condition data with SmCo magnet. In the measurement of hydrogen, the deviation from Yushibani estimate equation is ± 4.3 % in ~ 300 °C condition. It is out of uncertainty of Yushibani estimate equation. The improvement of method and solution for applying in high temperature measurement are necessary. In this paper, we report the principle of vibrating semi-circle method and results of measurements of fluids (nitrogen and hydrogen) with comparing to the calculated value by existing estimate equation and evaluation of the adequacy of this measurement to high temperature viscosity measurement.

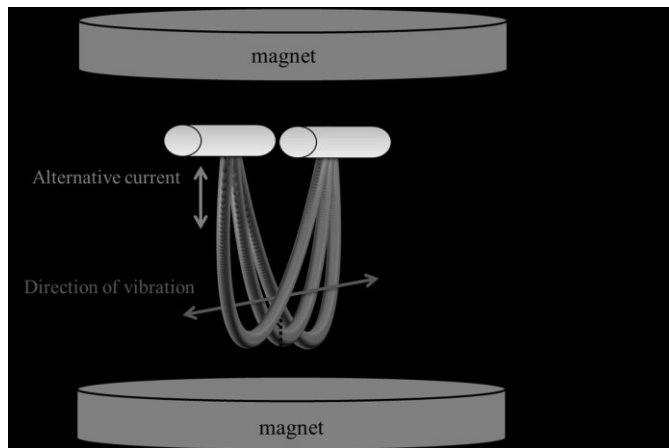


Fig. 1 Semi-circle vibrating wire method

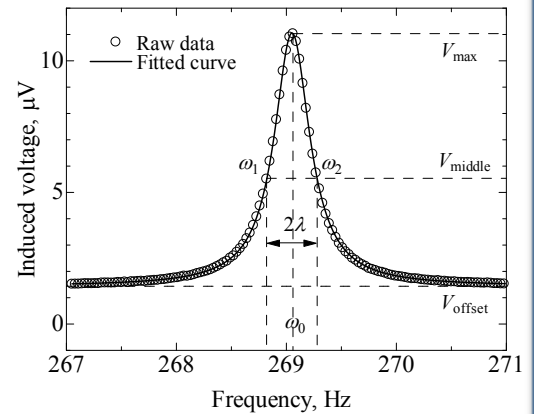


Fig. 2 Example of resonant curve

REFERENCES

- [1] J.Kestin, M.Sokolov, W.Wakeham; Theory of Capillary Viscometers, Appl. Sci. Res. 27, 1973, pp. 241-264
- [2] M. J. Assael, S. K. Mylona; A Novel Vibrating-Wire Viscometer for High-Viscosity Liquids at Moderate Pressures, Journal of chemical & engineering, 2013, pp. 993-1000
- [3] E. Yushibani; Measurement of Hydrogen Viscosity under High Pressure with Capillary Tube Method, D KYUSHU UNIVERSITY, 2010, pp. 26-51
- [4] E. W. Lemmon, R. T Jacobsen; Viscosity and Thermal Conductivity Equations for Nitrogen, Oxygen, Argon, and Air, Int. J. Thermophys, 2004, pp. 21-69

Advanced Electrodes for SOFCs – a PhD approach (FCC4-1)

Vicente B. Vert*, José M. Serra

Instituto de Tecnología Química (Universitat Politècnica de València – Consejo Superior de Investigaciones Científicas); Av. Los Naranjos, s/n; 46022 Valencia (SPAIN)

** corresponding author: viverbe@itq.upv.es*

The global raising energy demand, the high cost associated with conventional fuels and the generalized increasing environmental consciousness require, all together, using techniques and devices for energy generation being of more efficient, less polluting and capable of operating in a distributed manner.

Under this premise, fuel cells have very interesting features for a wide range of applications, from portable devices and automotive applications to electricity production on a stationary/larger scale. From the standpoint of overall efficiency, fuel flexibility, power ranges and materials handling, solid oxide fuel cells (SOFCs) are proposed as the most appropriate among the different fuel cells types.

The high electrical efficiencies, assorted to fuel cells, can rise up to 80% when using SOFCs highquality surplus heat in turbines, as they operate at temperatures above 800 °C.

However, this high operating temperature entails a high cost of the kilowatt-hour produced with these systems, due to the elevated price of building materials, connections and sealing. Thus, economically viable commercialization of these SOFCs needs for reducing their operating temperature to the range of 500-700 °C, but preserving energy efficiency and power densities.

Conventional SOFCs are based on oxygen ion conduction in the electrically insulating electrolyte, which separates the fuel combustion chemical reaction in the electrochemical half-reactions, thereby generating electrical energy. Electrodes in SOFCs are responsible for electrochemical activation of both oxygen and hydrogen, i.e., fuel. By lowering the operating temperature conductivity and catalysis are reduced dramatically in both electrolyte and electrodes.

Reducing electrolyte thickness, through advances in ceramic fabrication technology, makes plausible to use the same electrolyte materials, widely studied and characterized, used so far.

By contrast, increasing electrodes performance when lowering operation temperature needs to develop new materials, which improve electrocatalysis of oxygen reduction in cathodes and hydrogen activation/oxygen conductivity in anodes.

One of the main objectives of this PhD thesis was to obtain electrocatalytic materials with reduced polarization resistances for the oxygen reduction reaction, i.e., cathodes. These materials should be thermochemically compatible with the other component materials of the fuel cell for being used as cathodes thereof. Hence throughout this PhD thesis it has been projected the preparation and characterization of advanced cathodes for solid oxide fuel cells, whose structural optimization is proposed according to two strategies:

a. based on the wide-used cathode perovskite structure, multiple chemical elements (mainly lanthanides) are combined together, assuming that the resulting multimetallic compound may improve the electrocatalytic performance, as stated by previous studies with compositions containing these elements separately, and

b. based on the novel cathode swedenborgite structure, different compositions have been synthesized, because thermal compatibility with the rest of materials of the cell is presumably adequate according to the parent compound low thermal expansion coefficient, and then they were electrochemically tested

The most extensive study was carried out for the first material system (i.e., perovskite), for which it has been proposed a combinatorial experimental design. Results have been analyzed as a comprehensive package. Specifically, the combination of several lanthanides and barium, in the $(LaPrPmSmBa)_{0.58}Sr_{0.4}Fe_{0.8}Co_{0.2}O_3$ perovskite structure, has generated compounds with electrode polarization resistances lower than the state-of-the-art $La_{0.6}Sr_{0.4}Fe_{0.8}Co_{0.2}O_3$ cathode in the 450-650°C temperature range. The improvement in oxygen activation and diffusion, of these materials, has been associated with cooperative processes derived from the combination of two or three elements in the same position of the crystal structure. Results confirm that the increase of oxygen surface exchange and oxygen diffusion are responsible for the enhanced electrocatalysis of these multielement cathodes.

The novelty of the swedenborgite structure as a suitable material for acting as solid oxide fuel cell cathode, has been for the first time analyzed. The electrochemical studies carried out in crystal structures based on the $MBaCo_3ZnO_7$ swedenborgite, with Y, Er and Tb in the M position, revealed an activity for oxygen activation comparable to the $La_{0.6}Sr_{0.4}Fe_{0.8}Co_{0.2}O_3$ cathode in the 500-650 °C range. Besides, thermal expansion coefficient (TEC) values are low enough for the proper matching with state-of-the-art SOFC materials. Furthermore, chemical compatibility of the $TbBaCo_3ZnO_7$ compound with the $Ce_{0.8}Gd_{0.2}O_{1.9}$ electrolyte material, combined with its CO₂-tolerance, make this material a good candidate for acting as solid oxide fuel cell cathode.

On the other, the applicability of solid oxide fuel cells is greatly influenced on the availability of fuel to be used therein. Hydrogen produces only water as combustion by-product, but it should be previously generated because it is not a primary energy source. The versatility of solid oxide fuel cells allows operation with other types of fuels based on carbon (methane, syngas, biogas or even alcohols). However, this electrochemical reaction occurring on SOFC anodes with conventional materials is limited by the formation of carbon deposits that decrease the overall efficiency of the cell. Also, regeneration of these anodes is unfeasible due to the mechanical instability problems coming from redox cycling. Conventional anodes are based on nickel oxide (NiO), which also showed long-term problems due to particle coarsening under reducing atmospheres. In addition, NiO handling should be done carefully due to its intrinsic toxicity.

Therefore, another objective addressed along the PhD study was to develop non-NiO-based ceramic materials capable of acting as anode fuel cells and that can operate not only with hydrogen, but with carbon-based fuels. The added value for this study was their redox regeneration capability, then increasing the life of the cell. To do so a new series of materials based on ceramic perovskite structure, whose elements are selected to be stable and electrocatalytically active in reducing

atmospheres, have been developed. $\text{La}_{1-x}\text{Sr}_x\text{Cr}_{1-y}\text{Ni}_y\text{O}_3$ perovskites remained structurally unchanged under reducing atmospheres and after redox cycling. These perovskites are able to electrocatalytically activate methane. Moreover, anode nickel content is reduced and activity towards fuels activation is maintained. Indeed, methane steam reforming has been performed using this type of electrocatalytic and regenerative compounds, achieving 30% methane conversion at 900 °C. In addition, this material has been proposed and tested as promising anodes for proton conducting solid oxide fuel cells (PC-SOFC) since it possesses some protonic conductivity.

High performance microtubular Solid Oxide Fuel Cells for portable applications (FCC4-2)

M. Torrell¹, A. Meadowcroft³, R. Campana^{1,2}, A. Morata¹, D. Pla¹, K. Kendall³, M. Kendall^{4,*}, A. Tarancón^{1,*}

¹ Catalonia Institute for Energy Research (IREC) Jardins de les Dones de Negre, 1, 08930-Sant Adrià del Besòs, Barcelona, Spain; atarancon@irec.cat

² Centro Nacional del Hidrógeno, Prolongación Fernando el Santo s/n, 13500, Puertollano, Spain

³ Chemical Engineering, University of Birmingham, Edgbaston, Birmingham B15 2TT, UK

⁴ Adelan, 10 Weekin Works, Station Road, Birmingham, B17 9HD, UK; michaela@adelan.co.uk

Improved ceramic quality is required to overcome commercialization barriers typically present in Solid Oxide Fuel Cells (SOFCs). Portable applications have been largely discounted for SOFCs since quick start-up is often required and planar technology lacks good thermal shock resistance. However, recent progress in SOFC technology has demonstrated that this issue can be addressed by the implementation of microtubular [1] or thin film technologies [2]. These results open markets like Auxiliary Power Units (APUs) or Consumer Electronics (CE) typically restricted to Polymer Electrolyte Membrane (PEM) and Direct Methanol Fuel Cells (PEMFC).

Microtubular SOFCs (mSOFCs) have shown an astonishing thermal shock resistance many orders of magnitude better than planar SOFCs [1]. Kendall et al. recently proved that this thermal resistance can be controlled by reducing the tube diameter allowing faster start-up times for 2 mm tubes [3]. A 6-mm diameter microtubular SOFC is considered sufficient to give around 10 minute start-up times in typical Balance of Plant (BoP) systems.

This work presents the microstructural, electrochemical and cell performance analyses of single mSOFCs fabricated by high shear extrusion in the intermediate-to-low range of temperatures ($T < 700^\circ\text{C}$). These mSOFCs are being used in the FCH JU funded SAPIENS project which aims to develop a 200W portable system for a recreational vehicle [4].

Figure 1 shows a cross-section SEM image of the mSOFC device under analysis. Homogeneous and porous electrodes of Ni-YSZ (anode) and LSCF (cathode) are clearly observed. The anode support has a thickness of approximately $575\mu\text{m}$ and a conductivity of $\sigma_{RT} = 6000\text{ S/cm}$, ensuring good mechanical and electrical current collection. On the cathode side, the LSCF layer presents a thickness of approximately $30\mu\text{m}$ and a conductivity of $\sigma_{700^\circ\text{C}} = 220\text{ S/cm}$, in accordance with the literature. In order to improve the cathode current collection, silver paste and wires were applied. A YSZ-SDC bi-layer of $15\text{-}2\mu\text{m}$ in thickness is employed as electrolyte. The YSZ layer shows almost full density with closed porosity that ensures gas tightness between the anode and cathode sides while guaranteeing chemical stability under highly reducing atmospheres (anode). The SDC layer is employed as a barrier to avoid reactivity between YSZ and LSCF. This SDC-LSCF combination is commonly used to prevent the formation of the insulating $\text{La}_2\text{Zr}_2\text{O}_7$ and SrZrO_3 phases at typical fabrication/operating temperatures. However, a limitation of 1200°C in the fabrication process is still fixed to avoid extensive inter-diffusion between SDC and YSZ to form a resistive $\text{CeO}_2\text{-ZrO}_2$ solid solution. This limitation makes it difficult to obtain a full dense SDC layer. A low porosity SDC layer can be observed

in the cell under analysis in Figure 1. The SDC layer also plays an important role in improving the adhesion of the cathode to the electrolyte. In this sense, it is important to point out the excellent connectivity between the electrolyte and electrode layers shown in the picture.

This good adhesion is crucial for the low contact resistance shown by impedance spectroscopy. The contribution of the electrodes to the total area specific resistance is $0.75 \Omega\text{cm}^2$ at 700°C in OCV conditions (pure H_2/air) for SOFCs with an active area of 20 cm^2 . The performance at 700°C of the 20cm^2 -SOFC is shown in the I-V curve presented in Figure 2. OCV values of 1.1V , close to the theoretical value, confirm fully-dense electrolytes and good sealing between the tubes and the test rig. A maximum power of ca. 6W is achieved under pure H_2 and air atmospheres for a 20cm^2 -SOFC (power density of $300\text{mW}/\text{cm}^2$). According to the measurements, a total current of 15 A at 0.4V can be provided by a single cell with a fuel utilization over 35% .

The excellent performance shown by the mSOFCs, together with the excellent thermo-mechanical properties presented in previous papers, opens a new avenue for the realization of SOFCs in portable applications, unachievable up-to-now.

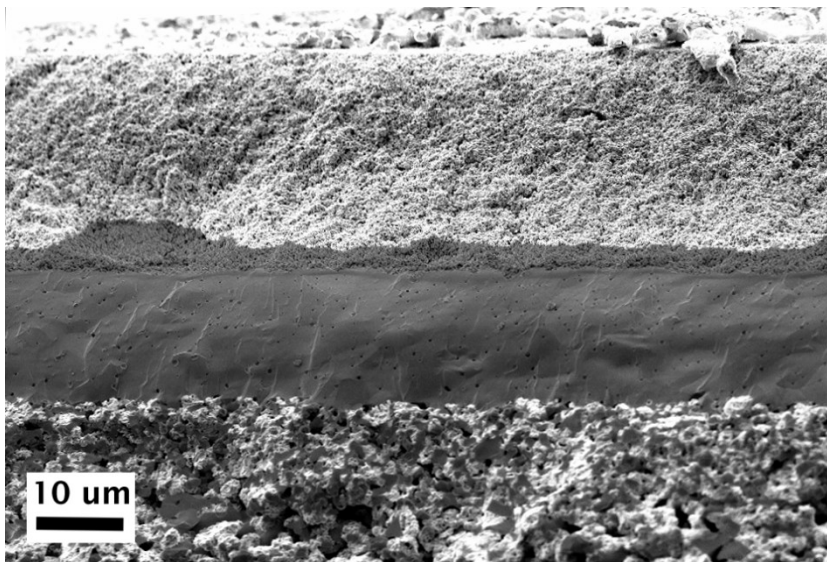


Figure 1. Cross-section SEM image of a single mSOFC cell. Four layers can be distinguished from the top to the bottom, namely, LSCF (cathode), SDC (Sr-diffusion barrier layer), YSZ (electrolyte) and Ni-YSZ (anode).

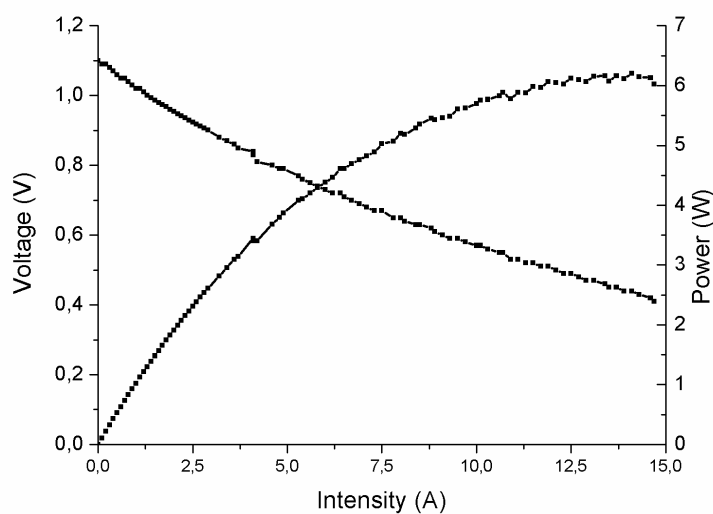


Figure 2. V-I curve for a 20cm²-mSOFC operated at 700°C under pure H₂ and synthetic air atmospheres (flows of 300 ml/min). Power is presented in the right y-axis.

REFERENCES

- [1] K. Kendall, Progress in Microtubular Solid Oxide Fuel Cells, *Int. J. Appl. Ceram. Technol.* 7 (2010) 1
- [2] I. Garbayo, A. Tarancón, J. Santiso, F. Peiró, E. Alarcón-LLadó, A. Cavallaro, I. Gràcia, C. Cané, Neus Sabaté, Electrical characterization of thermomechanically stable YSZ membranes for micro solid oxide fuel cells applications, *Solid State Ionics* 181 (2010) 322
- [3] K. Kendall, A. Meadowcroft, Improved ceramics leading to microtubular Solid Oxide Fuel Cells (mSOFCs), *Int. J. Hydrogen Energ.* 38 (2013) 1725.
- [4] SAPIENS project web-page: <http://www.adelan.co.uk/sapiens/>

ACKNOWLEDGEMENTS

The SAPIENS project funded the acquisition of these results. SAPIENS received funding from the European Union's Seventh Framework Programme (FP7/2007-2013) for the Fuel Cells and Hydrogen Joint Technology Initiative under grant agreement no [303415]. Information contained in the paper reflects only view of the authors. The FCH JU and the Union are not liable for any use that may be made of the information contained therein.

Infiltrated cathode materials for microtubular solid oxide fuel cells (FCC4-3)

M. A. Laguna-Bercero¹, V. M. Orera¹, H. Monzón¹, A. R. Hanifi², J. Cunningham², T. H. Etsell² and P. Sarkar³

*1Instituto de Ciencia de Materiales de Aragón (ICMA), CSIC- Universidad de Zaragoza
C/ Pedro Cerbuna 12, E-50009, Zaragoza, Spain*

*2Department of Chemical & Materials Engineering, University of Alberta, Edmonton, Alberta T6G
2V4, Canada*

*3Environment & Carbon Management, Alberta Innovates - Technology Futures, Edmonton, Alberta,
T6N 1E4, Canada*

Microtubular Solid Oxide Fuel Cells (MT-SOFC) have recently attracted much interest as they are more resistant to thermal cycling, and they present shorter start-up/shut-down times and higher volumetric power densities in comparison with the traditional planar geometry. Standard NiO-YSZ (yttria stabilized zirconia) tubes used in our laboratory are fabricated by either extrusion or cold isostatic pressing (CIP) of NiO, YSZ and pore former powders, followed by spray coating or dip-coating of the YSZ electrolyte. Both components are then co-sintered at 1400 °C. Typical oxygen electrodes such as LSCF (lanthanum strontium cobalt ferrite) or LSM (lanthanum strontium manganite) are deposited by dip-coating and sintered at 1150 °C. Thermo-mechanical matching of cell components, catalyser coarsening and quality of interfaces are important issues in cell fabrication.

Fabrication of electrodes by infiltration may contribute to reduce some of these problems as the cathode sintering stage is no longer needed. In this case we fabricate the oxygen electrode by infiltration of different cathode materials into a porous YSZ structure. One of the advantages of this fabrication method is an increased of TPB (triple-phase boundary) length compared with the standard cathode due to the smallest size of the dispersed catalyser particles having a higher surface area. In addition, since no sintering process of the cathode is needed the formation of non-conducting secondary phases such as non-conducting zirconates, and also the coarsening of the catalyser during sintering is eliminated.

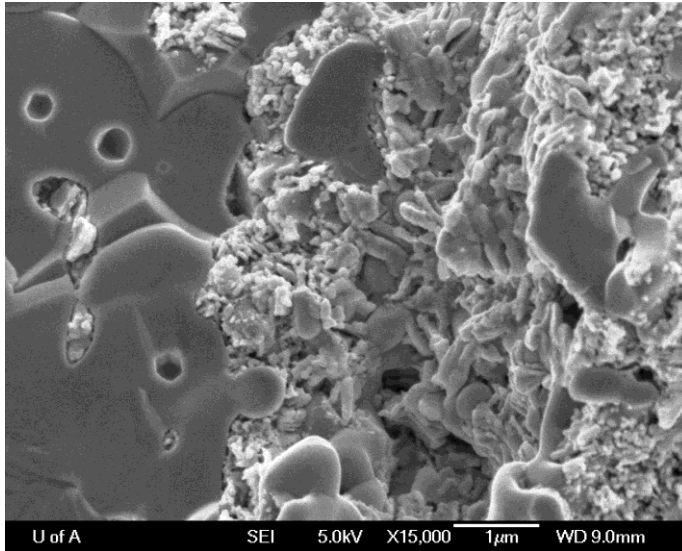


Figure 1. SEM image showing the cathode/electrolyte interface showing the $\text{Nd}_2\text{NiO}_{4+\delta}$ infiltrated cathode into porous YSZ.

In the present work, results about infiltrated LSM cathodes using different LSM concentrations will be shown. The j-V (current density-voltage) measurements showed an increase of near 20% in terms of power density: 700 mW cm^{-2} at 0.7V and $850 \text{ }^\circ\text{C}$ for a standard cell and 720 and 825 mW cm^{-2} at 0.7V and $850 \text{ }^\circ\text{C}$ for similar tubular cells but with non-optimised and optimised LSM infiltrated cathodes, respectively.

In addition, we will also present results on $\text{Nd}_2\text{NiO}_{4+\delta}$ cathodes infiltrated into porous yttria stabilized zirconia (YSZ). In order to obtain nickelate single phase, calcination times and temperatures of the salt precursors will be discussed. Anode supported microtubular cells using this cathode showed power densities of about 760 mW cm^{-2} at $800 \text{ }^\circ\text{C}$ and a voltage as high as 0.8 V. No degradation was detected after 24 hours under current load, assuring reasonable stability of the cell. Preliminary solid oxide electrolysis cell (SOEC) results showed slightly better performances in comparison with SOFC operation. It is believed that infiltration of nickelate salt precursors followed by calcination proposed in this work avoids high temperature sintering of the nickelate phase with the electrolyte and as a consequence, prevents their reaction. For this reason, infiltrated nickelates are very attractive for their use as intermediate temperature (IT) SOFC cathodes.

Preparation And Characterisation Of Sulphonated Composite PBI-TiO₂ Membranes For High Temperature PEMFCs (FCC4-4)

Justo Lobato^a, Manuel A. Rodrigo^a, Sara Mateo^a, Sonia Molina^a, Hector Zamora^a, Hector Rodrigo^b, Thomas Steenberg^b, and Hans A. Hjuler^b.

^a *Chemical Engineering Department, Enrique Costa Building, n 12. Camilo Jose Cela Av. University of Castilla- La Mancha, Ciudad Real, 13071, Spain.*

^b *Danish Power System, Bldg. 207, DTU, 2800 Lyngby, Denmark*

In recent years, special attention has been paid to high temperature PEMFCs (HT-PEMFCs) because of their numerous advantages as enhanced reaction kinetics, performance independent of humidity, elimination of cathode flooding, increased catalytic activity for both electrodes, easier water and thermal management due to the operational temperatures above 120 °C. Operating at high temperatures, the cooling system for ease the heat dissipation is simplified and allows heat recovery and, for that reason, the efficiency of the cell is increased. Another benefit is the reduced poisoning effect of the catalysts by fuel impurities, for example, carbon monoxide. This effect is very temperature-dependent, inasmuch CO adsorption is less pronounced with increasing temperature.

Polybenzimidazole (PBI) membranes have been studied as a promising electrolyte for HT-PEMFCs. The most desirable feature for the PBI is its proton conductivity, which depends on the amount of phosphoric acid retained in its structure. The following features are also important: water uptake, low gas permeability, minimal water drag coefficient, oxidative and thermal stability, good mechanical flexibility at elevated temperatures. In previous works, TiO₂-PBI based membranes have demonstrated to be serious candidates for being used as electrolytes in HT-PEMFCs¹ because of its low-cost and great conductivity obtained at high temperatures, in addition to the performance of the traits previously mentioned.

In this work, composite PBI membranes with 2 % of TiO₂ have been sulphonated in order to improve their characteristics as electrolytes for HT-PEMFCs. The operation conditions to sulphonate the composite PBI-TiO₂ membranes were optimized. It was found that one hour in a bath of 10 wt % of sulphuric acid is enough to obtain a high sulphonation degree. The membranes were characterized by XRD, FTIR, SEM and thermal analysis. Conductivity measurements were performed at three different temperatures under harsh conditions. Fenton analyses were performed in order to evaluate the chemical stability of the membranes. One of the main drawbacks of the phosphoric acid doped PBI membranes is the leaching of acid. Thus, leaching tests were also performed to evaluate the acid retention capability of these membranes.

Finally, in order to assess the performance of these membranes, single fuel cell tests were carried out at different temperatures and a preliminary long term assessment was also performed.

Acknowledgments

The authors further thank the European Commission as this work was supported by the Seventh Framework Programme through the project CISTEM (FCH-JU Grant Agreement Number 325262).

References

J. Lobato, P. Cañizares, M.A. Rodrigo, D. Úbeda, F.J. Pinar, *Journal of Membrane Science* 369 (2011) 105-111.

Influence of ammonia as contaminant on high temperature proton exchange membrane fuel cell performance (FCC4-5)

Fernando Isorna Llerena^{1}, Eduardo López González¹, Jaime Luis Sáenz Cuesta¹, Felipe Rosa Iglesias² and Juan Pedro Bolívar Raya³*

1Instituto Nacional de Técnica Aeroespacial (INTA), Ctra. S. Juan-Matalascañas, km. 34, 21130, Mazagón (Huelva), España

2Universidad de Sevilla, Escuela Técnica Superior de Ingeniería, Camino de los Descubrimientos, s/n, 41092, Sevilla, España

3Universidad de Huelva, Departamento de Física Aplicada, Campus de El Carmen, 21071, Huelva, Spain

() isornaf@inta.es*

ABSTRACT:

Proton exchange membrane fuel cells (PEMFCs) are a promising technology to produce electricity from hydrogen, for stationary power generation or for transportation applications. However, their performance can be severely affected by the presence of contaminants. Impurities in the fuel feed act as a barrier to the hydrogen oxidation. These impurities arise from the use of hydrogen from reformat as fuel. Most used reforming method is autothermal fuel reforming (ATR) which the outlet major components are H₂, H₂O, N₂, CO₂ and CO. An alternative method, partial oxidation (POX) reforming, produces the same major outlet components as ATR. Both processes yield CO as the most important impurity, but the coexistence of H₂ and N₂ at high temperatures and the presence of catalysts also may produce traces of NH₃.

Hydrogen used as fuel in the research, development and demonstration of fuel cells comes mainly from commercially available sources and in situ production. The reforming of natural gas (methane) and methanol obtained from biomass are the predominant methods for producing hydrogen. In the reforming process for hydrogen production is unavoidable impurities appearance. The result is a rich in hydrogen gas called "reformat gas" which typically contains between 40 and 70% of H₂, 15 to 25% of CO₂, from 1 to 2% of CO, small amounts of inert gases (water vapor and nitrogen) and sulfur impurities. Ammonia can be formed during these processes reformed at levels up to 150 ppm.

In spite of the fact that some studies have been published covering the effects of potential hydrogen contaminants (basically CO, CO₂ and H₂S), only a few of them have shown the effect of NH₃ on low temperature PEM fuel cells (LT-PEMFC) performance and there is a lack of research works covering the effect of NH₃ on high temperature PEM fuel cells (HT-PEMFC).

There are several reasons for operating H₂/air PEM fuel cell at temperatures above 100° C. Rates of electrochemical kinetics are enhanced, water management and cooling are simplified, useful waste heat can be recovered, and lower quality reformed hydrogen may be used as fuel.

Traces of NH₃ in the anode feed stream cause a decrease in cell current. The severity of the effects depends on NH₃ concentration and time of exposure of the anode to the contaminant. High concentrations and long time of exposures can result in irreversible disability. This paper presents the

evaluation of the effect of NH₃ on high temperature proton exchange membrane fuel cells, as well as possible mechanisms to recover the original performance. Steady-state tests were performed with different NH₃ mixtures: 50 ppm NH₃/H₂; 150 ppm NH₃/H₂; 300 ppm NH₃/H₂ and 500 ppm NH₃/H₂. Also, transient tests were performed with same concentrations. Data show that poisoning and recovery rates with NH₃ are in close relation not only with NH₃ concentration but with time of exposure. Longer times of exposure decrease the cell performance to impractical levels, and the cell is never recovered to original levels anymore.

Oxidation Behavior Of Ashless Coal In A Direct Carbon Fuel Cell (FCC4-6)

C.-G. Lee, W.-K. Kim, D.-L. Vu

*Department of Chemical Engineering, Hanbat National University
125 Dongsuh-Blvd, Dukmyung-dong, Yuseong-gu, Daejeon Korea 305-719*

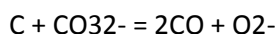
An ashless coal extracted from a bituminous coal was served as fuel in a direct carbon fuel cell and its oxidation behavior was investigated in terms of carbon species, coal to carbonate ratio, and gas compositions in the cell. The open circuit voltage and voltage at a polarization state were definitely dependent on the carbon species, and high carbon to carbonate ratio showed higher performance. Dominant product gases from the coal were H₂ and CO in the tested range.

Coal is relatively abundant energy source compared with other fossil fuels. Regardless of its abundance and long history of usage, inconvenience of its use reduces coal consumption at present. Coal as a solid fuel has a big problem of remaining ash in its use. Ashless coal has been attempted to overcome the problem. So far, ashless coal can be produced by two ways; one is removing ash compounds in the coal with acids and alkalines, and another one is extracting organic compounds from the coal with organic solvents.

In this work, an ashless coal was produced by a microwave method with a polar solvent of NMP. The solvent extracts the organic components in the coal. The electrochemical oxidation behavior of ashless coal was investigated with respect to carbon species, coal to carbonate ratio, and gas compositions in a coin type direct carbon fuel cell (DCFC).

The raw coal used in this work was Berau bituminous supplied by KEPRI in Korea. A coin type direct carbon fuel cell was fabricated by molten carbonate fuel cell technology. The diameter of electrodes was about 3 cm. The anode was porous Ni-Al alloy, and the cathode was porous Ni. The matrix was made of LiAlO₂. The long alumina tube at the upside of the cell was installed for the coal supply to the anode. A mixture of 62 mol% Li₂CO₃ and 38 mol% K₂CO₃ was served as electrolyte. The cathode gas was 70 % air and 30 % CO₂. More details of the DCFC operation was described in a previous work [1]. The normal H₂ fuel for the anode was H₂:CO₂ = 0.125 L min⁻¹: 0.025 L min⁻¹ with ca. 5 % of H₂O. Temperature ranged from 923K to 1123K. Coal to carbonate ratios were 3g to 3g, 3g to 1g, and 1g to 3g. Gas compositions in the cell were analyzed with a gas chromatography (HP 5890II).

Figure 1 compares thermo gravimetric analysis of several carbon species up to 1000oC under N₂ environment. The carbon was a commercial one made from bamboo at 1200oC. Therefore organic compounds except carbon were almost decomposed, so the stable behavior was obtained at the temperature range. On the other hand, the carbon and carbonate (62 mol% Li₂CO₃ + 38 mol% K₂CO₃) mixture shows steep decrease over 700oC. The behavior represents carbon reacts with carbonate. A previous work suggested following chemical reaction between carbon and carbonates [2].



Lee et al. confirmed above behavior with gas analysis, and they reported that ca. 62 mol% of CO, ca. 15 mol% of H₂ and ca. 6 mol% CO₂ were produced from carbon and carbonate mixture at 800 °C [3]. More drastic decrease is observed at ashless coal sample. Significant decomposition occurs from around 150°C. It implies that the ashless coal has organic components mostly of hydrocarbon species. This was confirmed that the gas species from the ashless coal was ca. 45 mol% of H₂ and ca. 50 mol% of CO [4].

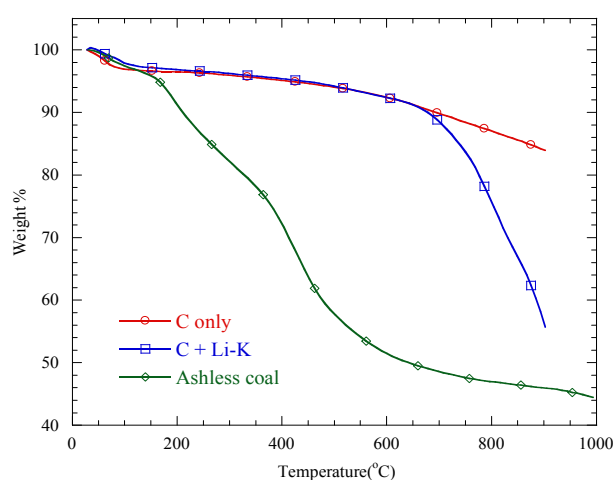


Fig. 1 Results of thermo-gravimetric analysis (TGA) with carbon only, carbon and carbonate mixture (C: carbonates = 1: 1 mass ratio), ashless coal only. The temperature was scanned by 20°C min⁻¹ under nitrogen environment.

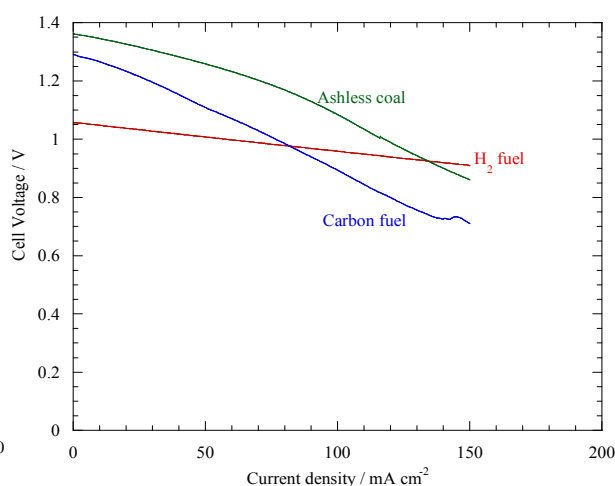


Fig. 2 Current-voltage behaviours of ashless coal only, carbon fuel (C: carbonates = 3 g: 3 g), and H₂ fuel at 850 °C.

Figure 2 shows current-voltage behaviors of conventional H₂ fuel, ashless coal only, and carbon fuel at 850°C. The H₂ fuel is the most active for the fuel cell, thus very flat slope is observed. On the other hand, carbon sources show much steeper slopes than H₂ fuel. It implies that carbon fuel has much larger resistance in their oxidation. In general, the oxidation rate of CO is much slower than H₂. Therefore the steepness of carbon would be resulted from the slowness in the oxidation. The carbon sources are generally gasified to CO, and the gas composition determines the open circuit voltage (EOCV) according to the following relation;

$$E_{OCV} = E_{0,CO/CO_2} + \frac{RT}{2F} \ln \left(\frac{[CO]}{[CO_2]_{an}} [O_2]^{0.5} [CO_2]_{ca} \right)$$

Thus the high EOCV represents very low amount of CO₂ in the anode compared with CO.

Different carbon to carbonate ratio represents the catalytic activity of carbonate on the gasification of carbon to CO. The carbon requires carbonates for its gasification; however the ashless coal shows independence in the gasification.

ACKNOWLEDGEMENT

This research was supported by Basic Science Research Program through the National Research Foundation of Korea (NRF) funded by the Ministry of Education, Science and Technology (2011-0009748).

C.-G. Lee, H. Hur, M.-B. Song, J. Electrochem. Soc., 158, B410 (2011).

K. Nagase, T. Shimodaira, M. Itoh, Y. Zheng, Phys. Chem. Chem.Phys., 1, 5659 (1999).

C.-G. Lee, H. Hur, Korean J. Chem. Eng., 28, 1539 (2011).

C.-G. Lee, W.-K. Kim, The 224th ECS meeting, #747, San Francisco (2013).

Supercritical synthesis of fuel cell catalysts on high surface area carbon substrates (FCC5-1)

Patricia Hernandez-Fernandez¹, Peter Brilner Lund¹, Christian Kallesøe¹, Henrik Fanø Clausen¹, Leif Højslet Christensen¹

¹ Danish Technological Institute (DTI), Nano- and micro-technology department, Gregersensvej1, 2630 Taastrup (Denmark)

Electrocatalysts for proton exchange membrane fuel cells (PEMFCs) are based on nanosized Pt particles. The widespread commercialization of this type of technology is severely hampered by the high loading of Pt required to catalyze the electrochemical reactions occurring at their electrodes. For instance, the oxygen reduction reaction (ORR) taking place at the cathode involves many intermediates species (O^* , HO^* , HOO^*), displaying a kinetic 6-fold slower than hydrogen oxidation [1]. If we move to fuel cells feeding with methanol (DMFCs), not only the cathode side requires high Pt loading to electro-reduce the O_2 to H_2O , but also the kinetic of the methanol oxidation reaction (MOR) at the anode is strongly impeded, which implies the use of even higher catalytic loadings, usually up to ten times higher than for hydrogen oxidation [2].

In this context, the synthesis of active and stable catalysts is highly important in order for this technology to become viable. A lot of parameters affect the performance of a catalyst in a particular electrochemical reaction. The particle size is one of the most important, and its effect has been studied for many years. Recently, Pérez-Alonso et al. concluded that the specific activity of the ORR of unsupported Pt nanoparticles decreases with decreasing particle size, with a maximum in mass activity around 3 nm [3]. On the other hand, Nesselberger et al. studied high surface area carbon supported Pt nanoparticles of different sizes, showing an increase of the ORR mass activity with decreasing particle size, stemming from the higher electrochemical surface area, ECSA [4]. They measured a mass activity 2-fold higher on 1.5 nm Pt particles compared to those of 5 nm. This fact underlines the importance of having a perfect control of the particle size.

At the Danish Technological Institute we are developing passive direct methanol fuel cells (DMFCs) to be used in hearing aids as well as larger systems in the 1-5 W range, with focus on pilot production of advanced passive fuel cell encapsulations. This includes the development of a synthesis method for the fabrication of catalyst structures for both anode and cathode of the DMFC. We present here catalytic structures fabricated using an up-scalable synthesis method with a very precise control of the particle size and spatial distribution onto high surface area substrates. Supercritical fluids are interesting because they share properties from gaseous as well as liquid phases, where molecules will mix freely in the supercritical phase, and chemicals may dissolve easily. They offer the opportunity to manipulate different properties of the reaction media as density, viscosity or diffusivity by controlling the pressure and temperature [5]. The supercritical flow synthesis (SCFS) has allowed us to synthesize particles directly onto different support materials with a high control of the size, particle distribution and composition.

The equipment required for SCFS is not readily available; therefore we have designed and build our own custom process line to handle the extreme environment of the supercritical fluid (minimum

pressure of 63 bar and temperature of 241 °C for scEtOH). A scheme is shown in Figure 1. The metallic precursors dissolved in ethanol as well as a suspension containing the carbonaceous support are introduced in the system by means of pumps. Both solutions reach the reactor at the desired pressure, where they are mixed with a heated solvent (scEtOH). Once there, the metallic nanoparticles will be directly formed onto the substrate and further matured through additional heating before they are cooled down and the product is tapped. The current process is capable of high volume production at 5 g/h, and is being developed towards even higher volume output.

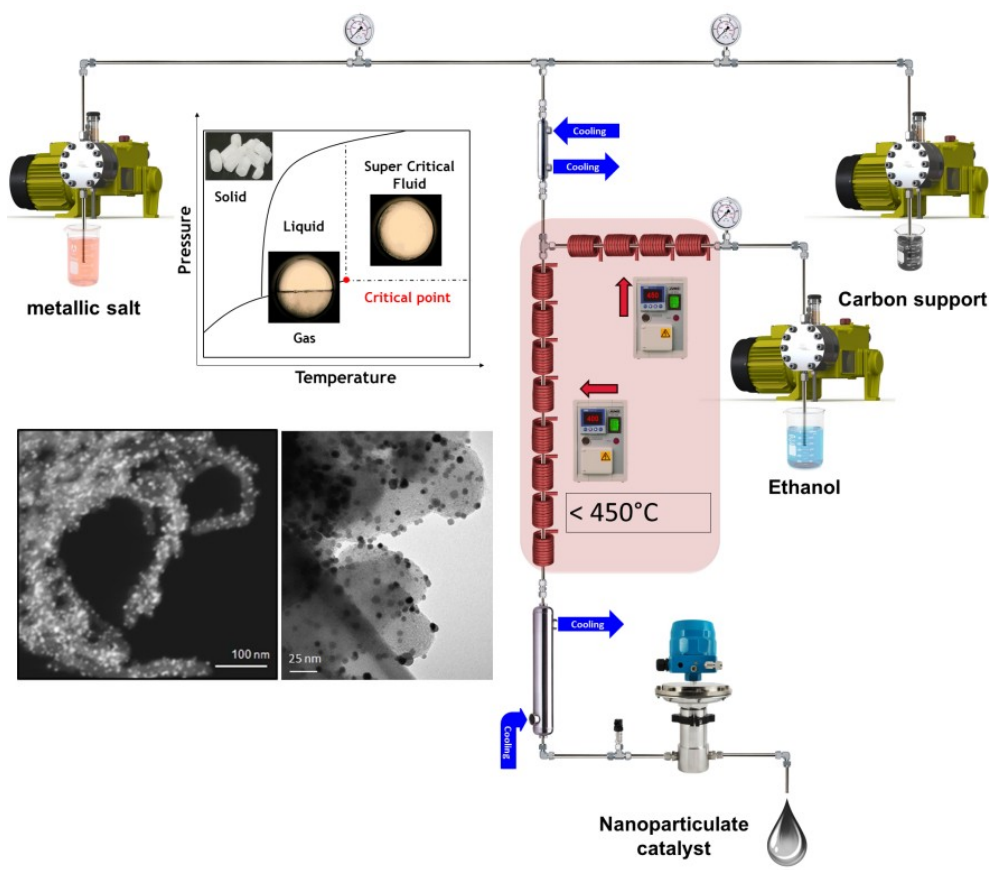


Figure 1- SCFS reactor scheme. Representative SEM and TEM pictures are also provided in the figure.

As previously mentioned, SCFS allows us to produce catalysts with the desired particle size and composition by changing the temperature and pressure conditions in our reactor. We have investigated the dependence of the Pt particle size with such parameters. This is illustrated in Figure 2A, where the particle size vs the temperature and pressure is plotted. We have produced Pt nanoparticles ranging from 1.3 ± 0.5 nm to 3.1 ± 0.5 nm by increasing the temperature from 250 to 425 °C while the pressure was kept at 300 bar. Furthermore, we have observed an increase in particle size when decreasing the pressure at a constant temperature of 400 °C. It should be mentioned that we have measured the metallic content of our catalysts by thermo gravimetric analysis, being 50 wt % in all the samples, which means that we are able to have a perfect control of the metallic loading avoiding Pt losses during the synthesis.

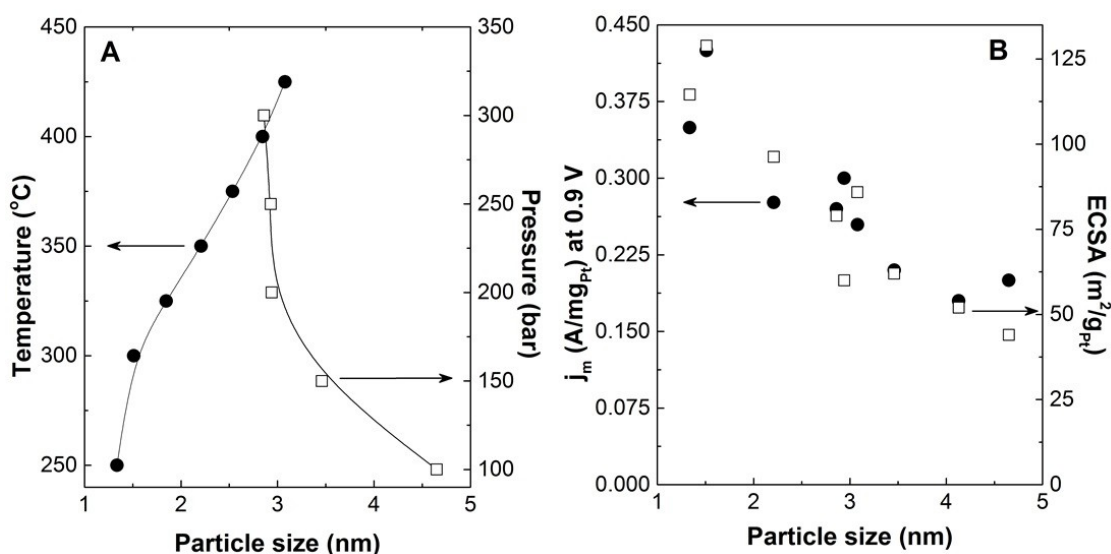


Figure 2- (A) Dependence of the Pt particle size with the temperature (●) and pressure (□). The line is to guide the eye. The temperature was kept at 400 °C for the pressure data points, whereas the pressure was 300 bar for the temperature experiments. (B) ORR mass activity (●) and electrochemical surface area (□) vs particle size. The experiments were carried out in 0.1M HClO₄ electrolyte. The mass activity corresponds to the anodic cycle measured at 50 mV/s and has been corrected for the capacitive effects of the substrate. The ECSA has been calculated from the electro-oxidation of pre-adsorbed CO at 0.05 VRHE, using the area under the CO-stripping peak and assuming that CO linearly binding on Pt provides a charge equivalence of 420 μC/cm²Pt.

We have tested our catalysts in the oxygen reduction reaction. Both the electrochemical surface area (ECSA) and the mass activity at 0.9 VRHE of the synthesized catalysts are shown in Figure 2B. As expected, the smaller particles possess higher surface area, and consequently higher mass activity. The figure highlights the importance of having a good control of the particle size during the synthesis process. Small changes in the particle size are translated in high differences in the ECSA and ORR mass activity. For instance, the catalysts with particles sizes around 4 nm display surface areas of ca. 50 m²/gPt, whereas the ones between 1.3-1.5 nm possess ECSA values of ca. 120 m²/gPt. Consequently, the mass activity is almost the double in the later catalysts.

Not just the activity but also the stability of the catalysts under reaction conditions is very important. Hitherto, we have proved that the supercritical flow synthesis lead to the formation of catalysts with high surface area and high activity in the ORR. The next step of our investigation has been to test the stability of these materials. For that purpose, we have carried out different accelerated stress tests (AST) [6]. Our first AST consists of 30,000 potential cycles in O₂-saturated electrolyte between 0.6 and 1 VRHE, showing no degradation. A more aggressive test with 30,000 cycles up to a potential of 1.05 VRHE showed a remaining mass activity approximately 90 % of the initial activity for particles sizes varying from 1.3 to 3.2 nm. Taking into account the US Department of Energy (DOE) requirements regarding mass activity losses for 2015 (< 40 % of the initial mass activity) [7], our results highlight the advantage of our synthesis method.

To sum up, we have successfully applied the supercritical flow synthesis to the fabrication of active and stable supported Pt nanoparticles in the ORR. The SCFS allows us to have a very precise control of the particle size, particle distribution and metallic content of our catalysts, avoiding losses of material during the fabrication process, and consequently reducing costs. We are currently developing the SCFS towards mass production, being able to produce more than 10 g of catalyst per hour, which makes this method very promising for commercial applications, our ultimate goal. We are currently fabricating different alloyed materials such as Pt-Ru nanoparticles with high surface area for applications in methanol oxidation reaction. Furthermore, we are also investigating the effect of different supports including graphene and carbon nanotubes, both of which are showing promising results. For instance, we have fabricated graphene supported Pt nanoparticles displaying an ORR mass activity of 0.3 A/mgPt with particles sizes of 5.3 nm. Furthermore we have not observed any mass activity loss after AST.

[1] V.R. Stamenkovic, B. Fowler, B.S. Mun, G. Wang, P.N. Ross, C.A. Lucas, N.M. Markovic, *Science* 315 (2007) 493

[2] A.S. Aricò, S. Srinivasan, V. Antonucci, *Fuel Cells* 1 (2001) 133.

[3] F.J. Perez-Alonso, D.N. McCarthy, A. Nierhoff, P. Hernandez-Fernandez, C. Strebler, I.E.L. Stephens, J.H. Nielsen, I. Chorkendorff, *Angew. Chem. Int. Ed.* 51 (2012) 4641.

[4] M. Nesselberger, S. Ashton, J.C. Meier, I. Katsounaros, K.J.J. Mayrhofer, M. Arenz, *JACS* 133 (2011) 17428.

[5] C. Aymonier, A. Loppinet-Serani, H. Reverón, Y. Garrabos, F. Cansell, *J. Supercrit. Fluids* 38 (2006) 242.

[6] A. Ohma, K. Shinohara, A. Iiyama, T. Yoshida, A. Daimaru, *ECS Trans.* 41 (2011) 775.

[7] J.S. Spendelov, D.C. Papageorgopoulos, *Fuel Cells* 11 (2011) 775

On the relationship between the amount of N and ORR performance of N/Carbon nanotube electrodes (FCC5-2)

Carlota Domínguez^{1*}, Francisco J. Pérez-Alonso¹, Mohammed A. Salam², Shaeel Ahmed Al-Thabaiti², Abdullah Yousif Obaid², José L. Gómez¹, J.L.G. Fierro¹, M.A. Peña¹ and Sergio Rojas¹.

¹Grupo de Energía y Química Sostenibles (EQS), Instituto de Catálisis y Petroleoquímica, CSIC, C/ Marie Curie, 2, L10. 28049 Madrid, Spain.

² Chemistry Department, Faculty of Science, King Abdulaziz University, P.O Box 80200-Jeddah 21589, Kingdom of Saudi Arabia.

Non-precious metal catalysts (NPMCs) are strong candidates for replacing Pt in the cathode of polymer electrolyte membrane fuel cells (PEMFCs). This is because they are less expensive and more abundant than noble metals [1] and their lower kinetics for the oxygen reduction reaction (ORR) as compared to Pt electrodes, can be compensated by using higher amounts of such NPMCs. Many approaches have been studied in order to improve the activity of NPMCs for ORR. Most of works suggest that the active site is formed by MN₄ moieties within carbon matrix structures [2, 3]. In general, the preparation of NPMCs comprises the use of carbon matrix (active carbon, carbon black, carbon nanotubes, graphene...), transition metal (M) and N precursors. Recently, it has been reported that nitrogen incorporation into the carbon matrix is related to the amount of defects into carbon nanotubes [4]. On the other hand, carbon nanotubes are endowed with improved stability during ORR measurements [5]. In this work, we have used carbon multiwalled nanotubes (CNTs) as support. The aim of this work is to study the relationship between the amount of defects on CNTs and the incorporation of nitrogen onto CNTs, and its repercussion for the ORR. We try to elucidate whether the active sites are created at the edges of CNTs or, in line with previous works, inside the micropores formed during the synthesis process [1, 2].

NPMCs were synthesized by a mechanical method. CNTs were ball-milled for different periods of time from 0 to 150 h. In principle, the amount of defects will increase with ball-milling time (the suffix before CNTs indicates the time under ball milling). Next, nitrogen was incorporated into the CNT-t by means of ball-milling of urea with the corresponding CNT-t. It should be noted that in all preparation the relative amount of urea to CNT-t was 1:2 molar ratio. The actual incorporation of the N atoms into the carbon matrix was obtained by pyrolysis at 800°C under inert atmosphere. The synthesized N/CNTs were thoroughly characterized by N₂ adsorption/desorption isotherms, Raman spectroscopy, X-ray photoelectron spectroscopy and chemical elemental analysis. Raman spectroscopy of N/CNTs shows that the amount of defects increased with ball-milling time. Remarkably, the amount of nitrogen actually incorporated into the carbon structure increases linearly with the amount of defects of the CNTs reaching a value of ca. 4 wt% of N for the CNT-150. Clearly, the amount of nitrogen incorporated to carbon support increases in parallel with the amount of CNTs defects. XPS analyses show that the nitrogen is actually being incorporated into the carbon network. N 1s core-level spectra have been fitted to four components corresponding to pyridinic-N, pyrrolic-N, graphitic-N and N-oxide species. The BET specific surface area increases with ball-milling time. Remarkably, the increase of the BET areas accounts to the formation of micropores in the samples which were subjected for ball-milling for more than 72 h.

The ORR was evaluated by electrochemical means using a RDE (rotating disk electrode) in 0.1 M HClO₄. Table 1 shows the ORR onset potentials for all electrocatalysts studied. Onset potentials range between 0.83V for N/CNT-150 and 0.72V for N/CNT-0. Samples obtained after longer ball-milling times show higher ORR activities. Raman and BET results indicate that an increase of ball milling time leads to an increase of the number of defects/edges at the CNTs. This in turn leads to a higher amount of nitrogen incorporated into the carbon matrix resulting in a higher amount of active sites for the ORR. Figure 1 shows ORR mass activities (IM) of the N/CNT-t confirming a higher activity with higher ball-milling times. Remarkably, longer ball-milling times of 72 and 150 h lead result in the formation of micropores. In fact, nitrogen can be incorporated both onto CNT defects and into the micropores. Noticeably, the ORR performance of the N/CNT-t triggers after the creation of micropores, i.e. with N/CNT-72 and N/CNT-150. It appears like the N located within the micropores results in more active sites for the ORR. The results obtained in this work indicate that there is a direct relation between defects formed after ball-milling, nitrogen incorporation to the catalyst and ORR activity.

Table 1. N content by elemental analysis, textural properties and faradaic current.

Sample	N (wt.%)	BET Surface area/ m ² g ⁻¹	Micropore Surface area/ m ² g ⁻¹	Onset potential ^a /V
N/CNT-0	0.66	229	3	0.723
N/CNT-12	0.84	239	4	0.742
N/CNT-24	1.23	237	9	0.759
N/CNT-48	1.20	229	13	0.783
N/CNT-72	1.75	392	109	0.800
N/CNT-150	3.94	483	195	0.830

a The onset potential has been defined as the potential at which a current density of 0.1 A·cm⁻² is generated [6].

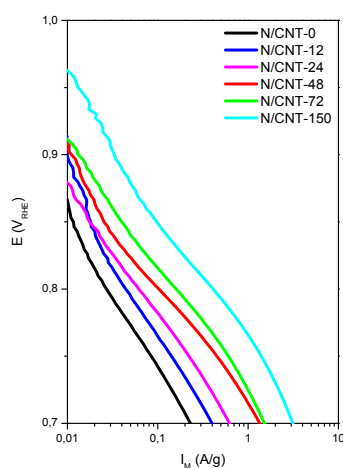


Figure 1. Mass activity (IM) of N/CNT-t electrocatalysts at different ball-milling times recorded during the positive going sweep in oxygen saturated 0.1 M HClO₄ at 10 mV·s⁻¹, 1600 rpm. Sample loading 0.6 mg·cm⁻².

Acknowledgements

This research work was funded by the Deanship of Scientific Research (DSR), King Abdulaziz University, Jeddah, under grant number (D-6-432). The authors, therefore, acknowledge with thanks DSR technical and financial support. Economic support from projects ENE2010-15381 from the Spanish Ministry of Science and Innovation and Project 201080E116 from the CSIC is also acknowledged.

1. Jaouen, F., et al., Recent advances in non-precious metal catalysis for oxygen-reduction reaction in polymer electrolyte fuel cells. *Energy & environmental science*, 2011. 4(1): p. 114-130.
2. Jaouen, F., et al., Cross-laboratory experimental study of non-noble-metal electrocatalysts for the oxygen reduction reaction. *ACS Appl Mater Interfaces*, 2009. 1(8): p. 1623-39.
3. Ferrandon, M., et al., Multitechnique Characterization of a Polyaniline–Iron–Carbon Oxygen Reduction Catalyst. *The Journal of Physical Chemistry C*, 2012. 116(30): p. 16001-16013.
4. Perez Alonso, F.J., et al., Effect of carbon nanotube diameter for the synthesis of Fe/N/multiwall carbon nanotubes and repercussions for the oxygen reduction reaction. *Journal of power sources*, 2013. 240: p. 494-502.
5. Wu, G., et al., A carbon-nanotube-supported graphene-rich non-precious metal oxygen reduction catalyst with enhanced performance durability. *Chem Commun (Camb)*, 2013. 49(32): p. 3291-3.
6. Wu, G., et al., High-performance electrocatalysts for oxygen reduction derived from polyaniline, iron, and cobalt. *Science*, 2011. 332(6028): p. 443-447.

Cation and anion binding effect on the oxygen reduction activity of Fe/N/C based catalysts (FCC5-3)

Francisco J. Pérez-Alonso^{1*}, Carlota Domínguez¹, Mohammed Abdel Salam², Abdulrahman O. Al-Youbi², Sulaiman N. Basahel², José L. Gómez¹, J.L.G. Fierro¹, M. A. Peña¹ and Sergio Rojas¹

¹Grupo de Energía y Química Sostenibles (EQS), Instituto de Catálisis y Petroleoquímica, CSIC, C/ Marie Curie, 2, L10. 28049 Madrid, Spain.

² Chemistry Department, Faculty of Science, King Abdulaziz University, P.O Box 80200-Jeddah 21589, Kingdom of Saudi Arabia.

Proton exchange membrane fuel cells (PEMFCs) have the potential to be widely implemented in the transportation sector and in portable devices [1] but some economic and technological challenges must first be solved. In particular, high loadings of Pt at cathode, which are used to compensate for the sluggish kinetics of the oxygen reduction reaction (ORR), are amongst the most significant obstacles preventing the massive utilization of PEMFCs.

Non-precious metal catalysts (NPMCs) are strong candidates for replacing Pt in the cathode of PEMFCs. NPMCS have recently shown significant ORR activity and very promising results [2]. This family of materials could potentially replace Pt in PEMFCs if their ORR activity is further improved.

It is well known that in order to obtain active NPMCs for ORR in acid electrolytes a pyrolysis step above 600 °C, in the presence of a nitrogen precursor, a transition metal (Fe or Co) precursor and a carbon matrix, is needed, resulting in nitrogen-coordinated iron or cobalt moieties. Graphene-coordinated FeN₄ and CoN₄ or FeN and CoN₂ moieties been proposed as the actual active sites in NPMCs [3].

However, their intrinsic activity and durability in acid media must be improved. Very little is known about the nature of the active site and their fate during the catalytic cycles; in fact, there is a lack of fundamental studies about the activity of NPMCs for the ORR and the relationships between the catalyst and the reaction media. Besides, electrolyte adsorption is in fact a key issue for the detailed understanding of the fine adsorption processes of different species on these catalysts that determine their final catalytic activity on ORR.

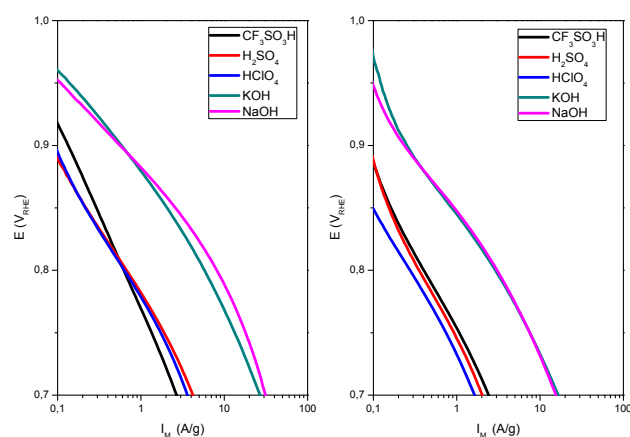


Figure 1. Diffusion corrected mass activities (i_M) of Fe/N/C (left panel) and L-Fe/N/C (right panel) electrocatalysts in oxygen saturated 0.1 M of different electrolytes studied at $10 \text{ mV}\cdot\text{s}^{-1}$, 1600 rpm. Sample loading $0.6 \text{ mg}\cdot\text{cm}^{-2}$.

In this work we try to investigate systematically anion and cation binding effect for Fe/N/C based catalysts in several acid and basic mediums and their repercussions for the ORR.

We prepared and characterized a Fe/N/C based electrocatalysts and we have evaluated their performance in the oxygen reduction reaction in different electrolytes (HClO_4 , H_2SO_4 , $\text{CF}_3\text{SO}_3\text{H}$, KOH and NaOH). The electrocatalysts were synthesized by ball milling of a mixture of active carbon or carbon nanotubes, urea and Fe-phthalocyanine. Finally, the active sites were created by pyrolysis at 800°C under N_2 atmosphere. An aliquot of the obtained solid was treated in 0.5 M H_2SO_4 to removing the acid-soluble phases resulting in the catalysts denoted by the prefix L-.

The ORR for the samples before and after acid washing was evaluated by electrochemical means using a RDE (Rotating Disk Electrode) in the different electrolytes described above.

Figure 1 shows the mass transport corrected mass ORR activities (i_M) in the kinetically controlled region of Fe/N/C (sample obtained using active carbon after pyrolysis step) and L-Fe/N/C (sample obtained using active carbon after pyrolysis step and treatment in 0.5 M H_2SO_4) electrocatalysts. The ORR performance varies with the pH. As observed, higher ORR rates are recorded in alkaline electrolytes. Moreover, at a given pH value, the ORR performance is not affected by the nature of the anion (acid electrolytes) or the cations (alkaline electrolytes). Moreover, the activity of Fe/N/C decreases remarkably after treatment in 0.5 M H_2SO_4 . In line with previous studies [4], the decreasing for the ORR activity could be related to the blockage of the active centers by the presence of adsorbed sulfates and/or the removing of fraction of the active sites that are not resistant to the strong acid environments typically employed for the acid-washing of Fe/N/C, e.g. 0.5 M H_2SO_4 . Physicochemical characterization by XRD and XPS indicates an important loss of Fe phases after acid-washing. This result would support the hypothesis that ORR activity decrease is due to the elimination of part of active sites. However, XPS and elemental analysis show that an important

amount of sulfates remain on the catalyst surface after acid-washing. Moreover, acid treatment produces an important decrease of BET surface area (275.7 m²/g for Fe/N/C electrocatalyst vs. 173.9 m²/g for L-Fe/N/C one) due to an important decrease of micropore volume. These results could indicate that at least part of decay in the ORR activity is also related to the blockage of micropores albeit it is not possible to discriminate whether sulfate is bonded to active center or just is physically adsorbed inside the micropore. To corroborate this hypothesis we prepared a reference catalyst using a non-microporous carbonaceous support such as multiwalled carbon nanotubes instead of active carbon (labeled as Fe/N/CNT).

Figure 2 compares the mass activities of Fe/N/CNT and L-Fe/N/CNT with those of Fe/N/C and L-Fe/N/C for the ORR in 0.1 M HClO₄. Both Fe/N/CNT and Fe/N/C record identical performances for the ORR indicating that the ORR activity of NPMC based upon Fe/N/C materials is independent of nature of carbon support.

In line with the results discussed above, the ORR activity after acid-washing of L-Fe/N/CNT is lower than that of Fe/N/CNT confirming that the 0.5 M H₂SO₄ treatment results in a suppressed ORR activity. However, the negative impact of the acid treatment for the ORR is significantly less severe for the catalyst prepared with CNTs than for the catalyst prepared with active carbon. This effect is remarkable since the decay in the ORR activity of Fe/N/C was ascribed both to the blockage of micropores by sulfates and to the elimination of a fraction of the active sites. Since as stated above, Fe/N/CNT lacks of micropores the observed decreasing of the ORR activity of Fe/N/CNT cannot be ascribed to the blockage of such micropores during 0.5 M H₂SO₄ washing. In fact, only a marginal decreasing of the BET surface area is observed from 157.6 m² g⁻¹ (Fe/N/CNT) to 135.1 m² g⁻¹ (L-Fe/N/CNT).

These results clearly indicate that micropore blockage is an important source of ORR activity loss when microporous carbons are used but it is not the only reason for the observed decay of the ORR performance of NPMCs.

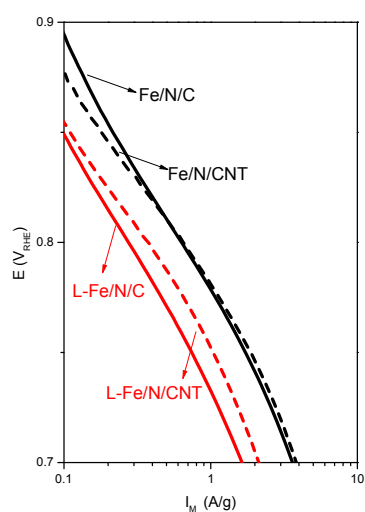


Figure 2. Mass activities (I_M) of Fe/N/C, L-Fe/N/C, Fe/N/CNT and Fe/N/CNT-L electrocatalysts in oxygen saturated 0.1 M HClO₄ at 10 mV s⁻¹, 1600 rpm. Sample loading 0.6 mg cm⁻².

Summarizing, Fe/N/C based electrocatalysts exhibit superior performances for the ORR in the alkaline electrolytes. However, their performance for the ORR is strongly affected by the actual pH of the reaction medium but not by the ultimate nature of the electrolyte. This observation is indicative of the lack of ion binding effects for the ORR with Fe/N/C based catalysts. In addition, the current densities of Fe/N/C are higher than those recorded with L-Fe/N/C when measured in the same electrolytes. The ORR decay after acid washing is ascribed to the blockage of micropores by sulfates and to the removal of a fraction of the active centers that are not resistant to the strong acid environments typically employed for the acid-washing step with H₂SO₄. The use of a different support (CNTs) with no presence of micropores produces a less severe ORR activity decay after acid washing due to the no blockage of micropores.

The choice of carbon support with optimal textural properties and the optimization of acid washing step appear to be crucial to increase ORR activity of this type of materials

Acknowledgements

This research work was funded by the Deanship of Scientific Research (DSR), King Abdulaziz University, Jeddah, under grant number (D-6-432). The authors, therefore, acknowledge with thanks DSR technical and financial support. Economic support from projects ENE2010-15381 from the Spanish Ministry of Science and Innovation and Project 201080E116 from the CSIC is also acknowledged.

1. H.A. Gasteiger, S.S. Kocha, B. Sompalli, F.T. Wagner, Applied Catalysis B-Environmental 56 (2005) 9-35.
2. F. Jaouen, E. Proietti, M. Lefèvre, R. Chenitz, J.P. Dodelet, G. Wu, H.T. Chung, C.M. Johnston, P. Zelenay, Energy and Environmental Science 4 (2011) 114-130.
3. M. Lefèvre, J.P. Dodelet, P. Bertrand, Journal of Physical Chemistry B 109 (2005) 16718-16724.
4. J. Herranz, F. Jaouen, M. Lefèvre, U.I. Kramm, E. Proietti, J.P. Dodelet, P. Bogdanoff, S. Fiechter, I. Abs-Wurmbach, P. Bertrand, T.M. Arruda, S. Mukerjee, Journal of Physical Chemistry C 115 (2011) 16087-16097.

Effect of reformat H₂ fuel and Air bleed mitigation on the durability of low temperature PEFCs for μ -CHP applications (FCC5-4)

G. Papakonstantinou, A. Pilenga, T. Malkow, G. Tsotridis

European Commission, Directorate-General Joint Research Centre, Institute for Energy and Transport, Westerduinweg 3, 1755 LE Petten, The Netherlands

Understanding the degradation and failure mechanisms in low temperature Polymer Electrolyte Fuel Cells (PEFCs) for stationary applications is of paramount importance for the effective commercialization of this technology. Meanwhile, the hydrogen fuel quality dictates its cost through the reformer design, a significant parameter for the commercialization of PEFCs for micro – combined heat and power (μ -CHP) applications. In the present communication, the effect of H₂ fuel quality on the performance and durability of low temperature PEFCs was studied at single cell level under steady load accelerated testing to simulate winter μ -CHP profile. The main pollutant of reformat based H₂ fuel is CO. As low as 10 ppm CO in H₂ increase the anode overpotential and consequently the FC voltage losses significantly, even for PtRu anode electrocatalysts, which are considered the state-of-the-art CO tolerant electrocatalysts [1]. The high anode overpotential may result in selective Ru dissolution from the anode electrode decreasing the CO tolerance. The air bleeding has appeared as an effective way to mitigate the CO poisoning voltage losses [2], however little is known about the long term effects of continuous air presence in the anode feed stream. Air bleed can introduce hot spots due to the evolving heat from the reaction of O₂ with H₂ and/or CO.

Table 1: Set and variable test conditions adopted in the sequence of steady load accelerating testing.

Input	Anode	Cathode
Gas supply	20 ppm CO in neat H ₂	Air
Relative humidity	80%	
Stoichiometry	1.5	3.0
Backpressure	Ambient (no backpressure)	
Variables	Low Setting	High Setting
Operation mode	Continuous steady load	
Current density	200 mA/cm ²	600 mA/cm ²
Air bleed	0	3%
Cell temperature	65°C	
MEA characteristics		
GDL	SGL Sigracet 35 DC, 325 μ m, 20% PTFE, MPL	
Cathode	Tanaka, TEC10F60TPM, 60 % wt Pt on C Black	
Anode	HiSPEC 10000, 60% wt PtRu on C Black	
Membrane	Composite Fumion® F940-rf, 40 μ m	

The testing conditions and the variables chosen to study the effect of CO and Air bleeding in the anode feed stream on single cell performance and durability are summarized in Table 1. The measurements were performed using a commercial test station to control T, P and electric parameters, equipped with Fuel Cell Technologies, Inc. humidification system to tune RH at the inlets. The single cell of 25 cm² active area was purchased from Baltic FuelCells on which the cell compression force could be tuned accurately. The flow fields design was 5th parallel serpentine channels in order to minimize the pressure drop and to simulate stack conditions where the pressure drop is very low, but in the expense of flooding events, while the flow configuration of anode and cathode was counter flow to provide for even distribution of the reactants. The polymer electrolyte membrane (PEM) was provided by FuMA-Tech and the MEAs were provided by IRD. The characteristics and materials compositions are summarized in Table 1. The testing sequence consisted of initial MEA activation/conditioning under voltage cycling, Beginning of test (BoT) in-situ characterization, Accelerated Stress Testing (AST) protocol with approximately 200 hrs duration and End of Test (EoT) characterization. The in-situ characterization consisted of I-V curves and EIS measurements under neat H₂/Air supply, CV measurements on both anode and cathode electrodes and H₂ crossover measurements. The AST protocol was frequently paused to collect I-V curves under the AST conditions. A representative experimental sequence is depicted in Fig. 1. The least squares regression fit is also depicted for the evaluation of the voltage decay vs. test duration.

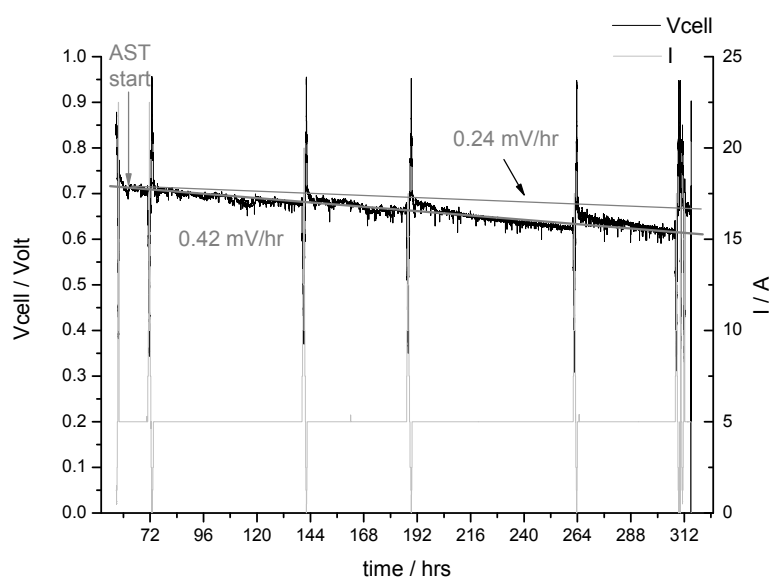


Figure 1: Evolution of cell voltage vs. test duration during steady load operation of 200 mA/cm² under 20 ppm CO in neat H₂ and 3% Air bleed in the anode. Cell T = 65°C, 80% RH at the inlet of both anode and cathode, H₂ stoich. = 1.5 and Air stoich. = 3.

The experimental protocol and the testing sequence enabled the discrimination of reversible from irreversible voltage losses, i.e. H₂O accumulation effect vs. permanent (irreversible) degradation. Irrelevant to the gas inlet mixture, the durability was mostly affected at high current densities, implying the degrading effect of increased humidity levels (H₂O produced by the reaction) on the MEA components. By comparing the results between the presence of CO only and CO with Air

bleeding in the anode feed stream, it is concluded that CO presence deteriorates the cell performance, which recovers readily upon Air introduction in the anode feed stream. However, the irreversible degrading effects are stronger under Air bleeding conditions, seen as increased absolute voltage decay vs. time. CV measurements revealed that the anode electrode was severely affected in all cases, seen as dramatic decrease of the double-layer/pseudo capacitance currents and under-potential deposited hydrogen (Hupd) charge. The cathode electrode electrochemical surface area (ESA) showed moderate losses (in the order of 10%), which increase with the current density. Interestingly, CV measurements on the cathode electrode after the Air bleeding tests revealed negative potential shift of the oxygen containing species reduction during the cathodic sweep. A positive shift of the oxygen containing species reduction peak should be expected based on the Pt ESA decrease (Pt particles size increase) [3]. The present trend implies that Ru species dissolved from the anode are migrating through the membrane and are deposited on the cathode electrode provoking the negative potential shift of the oxygen containing species reduction peak [4] and inhibiting the oxygen reduction reaction activity.

Acknowledgements:

The research leading to these results has received funding from the European Union's 7th Framework Programme (FP7/2007-2013) for the Fuel Cells and Hydrogen Joint Undertaking Technology Initiative under Grant Agreement Number 245113.

[1] N.M. Markovic, P.N. Ross Jr., *Surf. Sci. Rep.* 45 (2002) 117.

[2] S. Gottesfeld, J. Pafford, *J. Electrochem. Soc.* 135(10) (1988) 2651.

[3] K.J.J. Mayrhofer, B.B. Blizanac, M. Arenz, V.R. Stamenkovic, P.N. Ross, N.M. Markovic, *J. Phys. Chem. B* 109 (2005) 14433.

[4] A.N. Gavrilov, E.R. Savinova, P.A. Simonov, V.I. Zaikovskii, S.V. Cherepanova, G.A. Chirlina, V.N. Parmon, *Phys. Chem. Chem. Phys.* 9 (2007) 5476.

Polimerization of protic ionic liquid for HTPEMFCs: study of ionic moieties and crosslinking effects (FCC6-1)

F.J. Lemus; A. Eguizábal; M.P. Pina

Chemical Engineering Department, Nanoscience Institute of Aragón (INA); Edif. I+D, Campus Rio Ebro, c/Mariano Esquillor s/n, 50018 Zaragoza, Spain.

INTRODUCTION

Ionic Liquids (ILs) are organic salts commonly encountered as liquids at room conditions or below 298 K. They exhibit unique physicochemical properties such as no-volatile, no-flammability, high thermal stability, tunable electrochemical and ion conduction properties. Unlike traditional organic media, IL's properties can be adjusted via chemical alteration of the cation or anion to produce application specific compounds. Low symmetry organic cations such as ammonium, sulfonium or imidazole anions are usually combined with poly or mononuclear anions. As a matter of fact, these organic salts have been the subject of many experimental and theoretical investigations over the past decade 1-3. Among their potentialities for industrial applications 4-5, gas separation 1, 6-8, catalysis 9-13 and electrochemistry 14-15 are the most outstanding.

The deployment of ionic liquids (ILs) as proton transport carriers in the polymer membrane is emerging as an attractive alternative to overcome the operational limitations above 100°C¹⁶. These organic salts are able to transport protons⁴ due to their acid-base character and their capability to form complex or intermolecular hydrogen bonds. In spite of the exhibited benefits in terms of conduction properties, the number of publications dealing with ionic liquids as intrinsic conductors in PEM is scarce, and the ionic liquids tested are limited to a few. The main challenge hindering the use of ionic liquids as proton conductor in PEMFCs is the phase separation process that takes place between the polymer phase and ionic liquids resulting in inhomogeneous membranes. Polymer Ionic liquids (PILs), as solid-state polymeric electrolytes, may avoid some disadvantages of liquid conductors related to leakage, safety issues, mechanical stability and processing. However, the reported conductivity values remain low for practical applications¹⁷⁻¹⁸. In the present study, we analyze the effect of ionic moieties and UV assisted polymerization conditions on the proton conductivity and mechanical properties of the corresponding Polymer Ionic liquids (PILs) films.

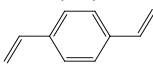
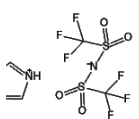
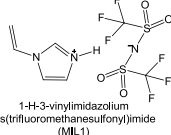
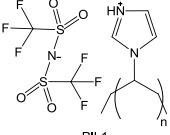

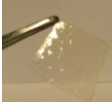
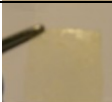
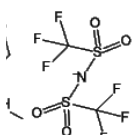
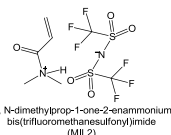
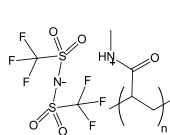


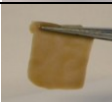
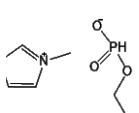
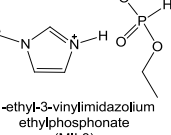
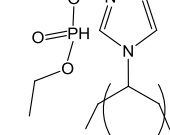



EXPERIMENTAL RESULTS

Three room temperature protic ionic liquids (RTILs) based on imidazolium and ammonium cations were selected based on our previous work¹⁹. Pure and cross-linked polymer ionic liquids (PILs) films were prepared from their corresponding monomers as follows: i) 5 g of monomer salt (MIL) was heated at 50°C under stirring; ii) desired amount of cross linker (divinylbenzene) was added (0%-1%-3% wt.) to the monomer (and kept under stirring at 50°C; iii) a respective amount of photo-initiator (2-hidroxy-2-methylpropiophenone) was added to achieve a mixture 1 % wt of photo-initiator in monomer; iv) the prepared solution was casted on preheated Teflon plates at 50°C; and, finally v) the film was irradiated by UV lamp (365nm; 2,4 mW/cm²) for 15 minutes.

Proton conduction performance was studied by Electrochemical Impedance Spectroscopy (EIS) using an Agilent 4294A Precision Impedance Analyzer from 40 Hz to 110 MHz. The ionic

conductivities were measured in a home-made stainless-steel conductivity cell according to procedures described in our previous works²⁰. TGA-DTA analyses from room temperature up to 900°C under N₂ flow and using 1°C/min as heating rate, were performed with a Q5000 IR. Differential Scanning Calorimetry (DSC) analyses were performed with a Mettler Toledo DSC822e equipment. Table 1 summarizes the main features of the as prepared films and also the proton conductivity properties of the starting materials, i.e. protic room temperature ionic liquids and monomeric derivatives.

Table 1. Main properties of the ILs and PILs films studied in this work.

Protic IL	RTIL proton conductivity at 120°C (mS/cm)		Monomer IL	Polymer IL	% Crosslinker (wt.) 	PIL proton conductivity at 0% RH (mS/cm)		T _{decomposition} (°C)	
	0% RH	100% RH				120 °C	200 °C		
	140	295	 1-H-3-vinylimidazolium bis(trifluoromethanesulfonyl)imide (MIL1)	 PIL1		0	182·10 ⁻³	1139	422
						1	347	371	409
						3	21	98	418
	100	500	 N,N-dimethylprop-1-ene-2-enammonium bis(trifluoromethanesulfonyl)imide (MIL2)	 PIL2		0	737	857	392
						1	257	294	392
						3	182	184	366
	200	560	 1-ethyl-3-vinylimidazolium ethylphosphonate (MIL3)	 PIL3		0	196	629	375
						1	96	313	296
						3	158·10 ⁻²	187	289

For PEMFC applications the most important feature of RTILs is proton conductivity. As it can be observed, proton conductivity values are over 100 mS/cm at 120°C at non-humidified conditions. All the selected RTILs are protic, i.e. have an H-Bond donor either on cation or anion. RTIL3 exhibits the best conductivity values at high temperatures under dry conditions due to H-bond donor character of the phosphonate anion facilitating the proton-hopping mechanism. RTIL1 and RTIL 2 seem to be stable either under wet or dry conditions due to the trifluoromethanesulfonyl imide based anion exhibits the greatest amount of H-bond acceptor sites. Cation nature, i.e. imidazolium (RTIL1 and RTIL3) or ammonium (RTIL2); seems to have a negligible effect on the proton conductivity measurements. On the contrary, anion nature, number H-bond acceptor sites on the anion and aliphatic chain of the cation have a more significant effect on conduction properties.

The polymer ionic liquids (PILs) obtained from the commercial monomeric derivatives by ultraviolet-induced radiation were the following: poly[1-(3H-imidazolium)ethylene] bis(trifluoromethanesulfonyl)imide (PIL1), poly[N,N-dimethylprop-1-one-2-enammonium]bis(trifluoromethanesulfonyl)imide (PIL2) and poly[1-(3-ethylimidazolium)ethylene] ethylphosphonate (PIL3) (see Table 1). As it was expected, the cross-linker (CL) addition is negatively affecting the proton conductivity: from 1139 mS/cm to 98 mS/cm at 200°C for PIL1-0% CL and PIL1-3% CL, respectively. On the other hand, the mechanical properties of the resulting films are notably improved. According to TGA-DSC analyses (not shown here), PIL1 based films are the only characterized by well-defined crystallization and melting events, and decomposition temperatures above 400°C whatever the % of CL used.

CONCLUSIONS

The poly[1-(3H-imidazolium)ethylene] bis(trifluoromethanesulfonyl)imide films prepared by UV assisted polymerization have demonstrated highly attractive possibilities to be deployed as solid electrolyte membranes for high temperature PEMFCs applications. However, further studies with time on stream under real FC operating conditions have to be performed to ensure their capabilities.

The authors would like to acknowledge financial support from the European Commission through the FP7 funded project ZEOCELL Grant Agreement 209481.

CITED REFERENCES

1. P. Wasserscheid and T. Welton, *Ionic Liquids in Synthesis*, 2003.
2. J. F. Wishart and E. W. Castner, Jr., *Journal of Physical Chemistry B*, 2007, 111, 4639-4640.
3. M. Deetlefs and K. R. Seddon, *Chimica Oggi-Chemistry Today*, 2006, 24, 16-+.
4. T. L. Greaves and C. J. Drummond, *Chemical Reviews*, 2008, 108, 206-237.
5. N. V. Plechkova and K. R. Seddon, *Chemical Society Reviews*, 2008, 37, 123-150.
6. L. A. Blanchard, D. Hancu, E. J. Beckman and J. F. Brennecke, *Nature*, 1999, 399, 28-29.
7. R. D. Noble and D. L. Gin, *Journal of Membrane Science*, 2011, 369, 1-4.

8. J. E. Bara, T. K. Carlisle, C. J. Gabriel, D. Camper, A. Finotello, D. L. Gin and R. D. Noble, *Industrial & Engineering Chemistry Research*, 2009, 48, 2739-2751.
9. D. Zhan and J. B. Fenn, *International Journal of Mass Spectrometry*, 2002, 219, 1-10.
10. H. Olivier-Bourbigou, L. Magna and D. Morvan, *Applied Catalysis A: General*, 2010, 373, 1-56.
11. D. Zhao, M. Wu, Y. Kou and E. Min, *Catalysis Today*, 2002, 74, 157-189.
12. M. Iglesias, R. Gonzalez-Olmos, I. Cota and F. Medina, *Chemical Engineering Journal*, 2010, 162, 802-808.
13. P. Kubisa, *Progress in Polymer Science*, 2009, 34, 1333-1347.
14. H. Ohno, *Electrochemical Aspects of Ionic Liquids*, John Wiley & Sons, Inc., 2005.
15. H. Ohno, H. Iwasaki, T. Eguchi and T. Tanaka, *ChemInform*, 2005, 36.
16. J.A. Asensio, E.M. Sanchez, P. Gomez-Romero, *Chem. Soc. Rev*, 2010, 39(8), 3210-3239.
17. D. Mecerreyes. *Progress in Polymer Science*, 2011, 36(12), 1629-1648.
18. Y. Jiayin, D. Mecerreyes, M. Antonietti. *Progress in Polymer Science*, 2013, 38, 1009-1036.
19. <http://ina.unizar.es/zeocell>
20. A. Eguizábal, J.Lemus, A.M. Moschovi, S. Ntais, V. Nikolakis, J. Soler, M.P. Pina, *Journal of Power Sources*, 2011, 196, 4314-4323.

Development of anodic materials for HT-PEMFCs with higher tolerance to H₂S (FCC6-2)

*María S. Rau, Carsten Cremers, Jens Tübke.
Fraunhofer ICT, Pfinztal – Germany*

INTRODUCTION

In the last few years the proton exchange membrane fuel cell or polymeric electrolyte fuel cell (PEMFC) has been considered one of the most suitable candidates for mobile and portable applications. Nevertheless, there are many uncertainties regarding the technological development of this electrochemical device. One aspect of interest for the present discussion is the presence of impurities in the H₂ which is used as fuel. In this context it should be considered that in a “hydrogen challenged” economy the fuel for the PEMFC is produced by hydrocarbon reforming [1], so the presence of contaminants such as carbon monoxide and hydrogen sulfide in small amounts (ppm) is inevitable. In connection with this, platinum, which is for the moment the best electrocatalytic material for the hydrogen oxidation reaction (occurring in the anode of the FC), has a high capability to adsorb CO and H₂S, generating different adsorbed species over the electrodic surface. For this reason, low quantities (in the order of ppm) of contaminant in the fuel can significantly reduce the performance of the FC electrodes.

There are numerous articles regarding the inhibition of the electrode surface due to the presence of diverse carbon species. The electrochemical oxidation of adsorbed carbon monoxide (CO(ad)) on Pt and bimetallic Pt-M electrodes (where M = Ru, Rh, Sn, etc) has been widely studied. It should be mentioned that an evaluation of the kinetic parameters of the reaction was recently presented for the first time, and it was also demonstrated that the reaction proceeds according to the Gilman’s mechanism [2]. In order to diminish the effect of the CO(ad), the researchers proposed two options, one is to weaken CO-Pt bonding, and the other is to provide the adsorbed hydroxyl species (OH(ad)) from oxyphilic surface atoms. Binary electrocatalysts Pt-M were developed, generally using Ru as M metal [3-5]. The role of the second metal was studied on alloys [6, 7], as well as on Pt (or M) surfaces partially covered, or decorated, by the metal M (or Pt) islands [8, 9].

In contrast to the CO poisoning effect on FCs, little information is available regarding the contamination of the PEMFC electrodes in the presence of H₂S at elevated temperatures. It is well known that H₂S has a high affinity for metals - especially metal oxides - thereby making the PEMFC sensitive to H₂S. For this reason, very small quantities of sulfur impurities (ppb) in the fuel may degrade the fuel cell performance. What is even worse, for the moment all the results seem to agree that the degradation is an irreversible process. Nevertheless, some authors [10] probed that once the anode of the FC is poisoned by S-species it is possible to obtain a partial recovery of the FC performance, while the cell is fed with pure H₂ and clean air.

The first antecedents related to the S contamination were presented by Loučka [11], who studied the kinetics of H₂S adsorption and oxidation on single crystal platinum electrodes in aqueous solution at 25°C. He found that the H₂S became completely dehydrogenated on adsorption and that the complete removal of the adsorbed species by oxidation could not be attained by holding the poisoned electrode at 1.6V vs. DHE unless the surface inhibition is very low. Unfortunately the type

of materials used in the FC anodes (nanoparticles of the electrocatalyst deposits on carbon particles) cannot withstand this kind of cleaning treatment. For this reason it is important to focus the research on the development of other types of anodic materials, with higher tolerance to H₂S contamination.

As in the case of CO, the bimetallic materials represent a good alternative to investigate in order to increase the tolerance of the fuel cell to the presence of H₂S in the hydrogen used as fuel. In the case of the sulfur species the authors suggest the use of Pt-M electrodes, where M could be: Pd, Cu, Ru, Rh, Ir, Co, etc. [12 - 18]. In the specific case of the Pt-Ru electrode (that was proved to be the best alternative proposed in the case of CO inhibition) Mohtadi et. al [12] demonstrated that these kind of electrocatalytic materials do not have a promising performance. To reach to this conclusion the authors evaluated the steady-state polarization curves after exposure to 50 ppm H₂S at 70°C. With these experiments it was possible to affirm that the Ru has no effect in improving the tolerance of the MEA. Considering all these aspects, this paper covers the evaluation of the electrocatalytic activity of alternative anodic materials under simulated HT-PEMFC conditions [18]. The behavior of Pt and other Pt-M electrodes will be studied during the hydrogen oxidation reaction under steady state conditions, using pure hydrogen and hydrogen contaminated with hydrogen sulfide.

EXPERIMENTAL PROCEDURES

To evaluate the inhibition of the anodic material of the FC in the presence of H₂S a three electrode cell was used. This had previously been developed in our group, and allows the simulation of the HT-PEMFC and also the detection of the outgoing gases by DEMS. The electrolyte used in the measurements was H₃PO₄ 85% (Carl Roth). In all the experiments a RHE in the same medium was used as a reference electrode, and a large area Pt electrode as counterelectrode. The measurements were carried out at a temperature of 145°C and at ambient pressure. The working electrodes tested in the present study consist of homemade Pt, Pt-Pd, Pt-A (where A is a platinum group metal) and Pt-B (where B is a base metal) supported on carbon and deposited on a GDL H2315 (FREUDENBERG FCCT SE & CO.KG9). Phosphoric-acid-doped polybenzimidazole (PBI) membranes were used in all the experiments.

The electrochemical oxidation of hydrogen was studied through the dependence of the steady state current on the overpotential. Before the experimental measurement the different tested electrodes were cycled at 10 mV / s in the cell until a stable cyclic voltammetric (CV) signal was obtained. The potential window of the CV was set in between 0.0 V and 1.1 V (vs. RHE), in order to avoid massive H₂ generation (at lower overpotentials) and

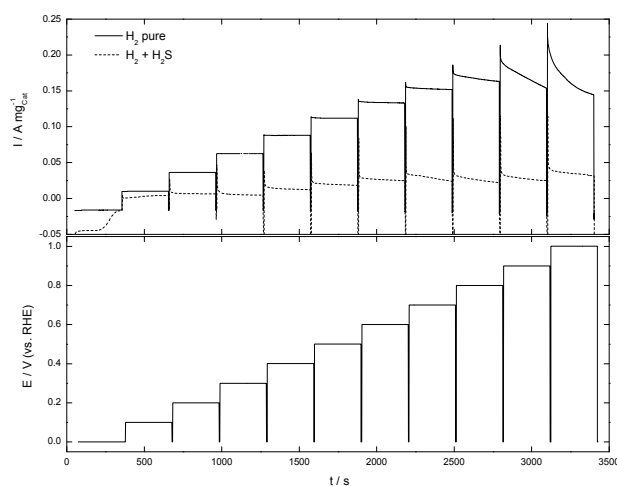


Figure 1: Evaluation of the hydrogen oxidation reaction over a Pt electrode with H₂ pure and with a mixture of H₂+H₂S. (Down) applied potential, (Up) current measure for each potential.

corrosion of the electrode (at higher overpotentials).

RESULTS AND DISCUSSION

Figure 1 shows the steady state current response of a Pt electrode at 145 °C with H₂ pure and with a mixture of H₂ and H₂S, when the different overpotential pulses were applied. It can be seen that in the presence of H₂S the currents are drastically diminished. The same response was obtained with the other materials. It should be noted that at potentials higher than 0.7 V the inhibition effect due to the presence of H₂S is reduced.

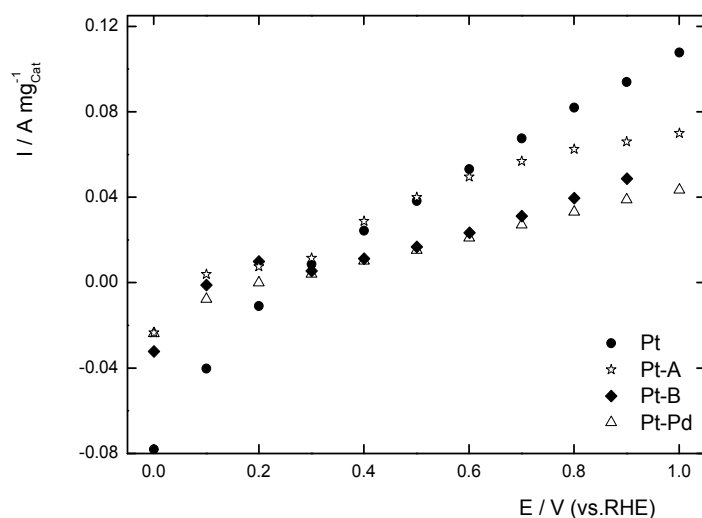


Figure 2: Dependence of the current with the overpotential for the hydrogen oxidation reaction in presence of H₂S for different materials.

Using the media of the values of the current measured for each overpotential applied, it was possible to show (Figure 2) the dependence of the current (in A mg⁻¹Cat) on the overpotential for all the anodic material tested. This graph shows the evaluation of the hydrogen oxidation reaction in different anodic materials, when the hydrogen used was contaminated with a high amount of H₂S (more than 10ppm).

From the analysis of Figure 2 it is important to note that in the region of lower overpotential (< 0.5 V vs. RHE) the inhibition effect of the H₂S is more significant than at higher overpotential (> 0.6 V vs. RHE).

Regarding the behavior of the different materials at lower overpotential, which is the range of interest for the operating FCs, Pt-A and Pt-B have presented the better performance. In this sense it is also remarkable that in both of them the amounts of SO₂ detected by DEMS were higher than for the other materials (these results will be presented in other publication).

CONCLUSIONS

In the present work different alternative anodic materials were tested in the presence of H₂S under HT-PEMFC. This paper evaluated for the first time the hydrogen oxidation reaction in the presence of H₂S over Pt-B. Investigations were furthermore carried out to determine whether Pt-B and Pt-A represent good alternatives to increase the tolerance of H₂S.

ACKNOWLEDGEMENT

This work was financially supported by the German Federal Ministry for Economics under contract N° 01MX12006A and by the European Commission through the ERANET+ Electromobility+.

REFERENCES

1. B.M. Besancon, V. Hasanov, R. Imbault-Lastapis, R. Benesch, M. Barrio, M.J. Møltnvik, *Int. J. Hydrogen Energy*, 34 (2009), 2350-2360.
2. M. S. Rau, M. R. Gennero de Chialvo, A. C. Chialvo, *J. Solid State Electrochem.*, 16 (2012) 1893.
3. F. Maillard, G. Q. Lu, A. Wieckowski, U. Stimming, *J. Phys. Chem. B*, 109 (2005)16230.
4. A. Czerwinski, A. Sobkowski, *J. Electroanal. Chem.* 91 (1978) 47.
5. A. Couto, M. C. Perez, A. Rincon, C. Gutierrez, *J. Phys Chem* 100 (1996) 19538.
6. R. Gisbert, G. García, M. T. M. Koper, *Electrochim. Acta*, 56 (2011) 2443.
7. N. M. Markovic, B. N. Grgur, C. A. Lucas, P. N. Ross, *J. Phys. Chem. B*, 103 (1999) 487.
8. M. Bergelin, E. Herrero, J. M. Feliu, M. Wasberg, *J. Electroanal. Chem.*, 467(1999)74.
9. E. A. Batista, T. Iwasita, W. Vielstich, *J. Phys. Chem. B*, 108 (2004) 14216.
10. V. A. Sethuraman, L. A. Wise, S. Balasubramanian, J. W. Weidner, *ECS Transactions* 8 (2006) 111.
11. T. Loučka, *J. Electroanal. Chem.*, 31 (1971) 319.
12. R. Mohtadi, W-K. Lee, S. Cowan, J. W. Van Zee, *Electrochem. and Solid-States Letters*, 6 (2003) A 272.
13. T. Lopes, V. A. Paganin, E. R. Gonzalez, *Int. J. of Hydrogen Energy* 36 (2011) 13703.
14. G. Ma, H. Yan, J. Shi, X. Zong, Z. Lei, C. Li, *J. of Catalysis* 260 (2008) 134.
15. J. Mbah, S. Srinivasan, B. Krakow, J. Wolan, Y. Goswami, E. Stefanakos, N. Appathurai, *Int. J. of Hydrogen Energy* 36 (2010) 10094.
16. J. A. Rodriguez, T. Jirsak and S. Chaturvedi, *J. Chem. Phys.* 110 (1999) 3138.
17. W. Shi, B. Yi, M. Hou, Z. Shao, *Int. J. of Hydrogen Energy* 32 (2007) 4412.

Performance of a High-Temperature PEM Fuel Cell Operated with Oxygen Enriched Cathode Air and Hydrogen from Synthetic Reformat (FCC6-3)

F. Javier Pinar, Nadine Bruns, Maren Rastedt, Peter Wagner

NEXT ENERGY • EWE Research Centre for Energy Technology at the University of Oldenburg, Carl-von-Ossietzky Str. 15, 26129 Oldenburg, Germany

The polymer electrolyte membrane fuel cell (PEMFC) is a very promising alternative for electricity production for automotive, stationary and mobile applications due to its high efficiency and low poisoning emissions. However, cost and durability of materials are nowadays two barriers for large-scale production of PEMFCs. There are three different PEMFC technologies; acidic low temperature (LT-) PEM, acidic high temperature (HT-) and alkaline LT-PEM.

Recent progress in PEMFC has been focused on achieving efforts in the development of HT-PEMFC systems. High temperature technology shows some desired features that low temperature does not have. Some of these features are improved kinetics for the oxygen reduction reaction (ORR), high tolerance to fuel impurities and simple system design as no humidification of reactant gases is needed [1-3]. The typical operation temperature range of this technology is 120-200 °C which allows its implementation preferably in combined heat and power systems (CHP). Thus, the overall energy efficiency of the system would be improved by utilization of the produced heat in housing or with larger systems in district heating. Among the different kind of electrolyte membranes used as proton conductors in HT-PEMFC, phosphoric acid polybenzimidazole (PBI) based membrane stands out due to its efficient proton conduction mechanism and high thermal and chemical stabilities [3]. However, PBI based membrane technology shows a few limitations that need to be overcome for commercialization purposes. These are: fast degradation under high temperature and acidic operation conditions, membrane-electrode assembly (MEA) exposed to high electrical potentials and phosphoric acid losses from the membrane into the gas diffusion electrodes.

The present work is under the work plan of the European Project CISTEM which is supported by the Fuel Cell and Hydrogen Joint Undertaking (FCH-JU grant agreement no. 325262) and whose consortium involves a total of eight Companies, Research Institutes and Universities within the European Community. The purpose of the CISTEM project is to show a proof of concept of HT-PEMFC technology being also ready for mini CHP systems up to 100 kWel of power range. Moreover, the system will be designed to be fuel flexible by utilization of hydrogen from reformat natural gas or pure hydrogen and oxygen which can be provided by electrolysis. Thus, utilization of oxygen from an electrolyser, which is normally wasted, will be of benefit to increase the electrical efficiency and performance of the fuel cell. In this work, experimental results with oxygen enriched cathode air are shown and different oxygen concentrations in the enriched air are studied. Figure 1 shows polarization curves with different oxygen concentrations in cathode side. It can be seen, the higher the oxygen concentration, the better the performance is due to an increase on the oxygen partial pressure in the cell. Thus, performance enhancement of 7.7% is observed when the fuel cell is operated with 75% v/v oxygen enriched air instead of air at a current density of 0.5 A/cm². Moreover, a long-term degradation test (~1,000 h of operation or end of life) is carried out with 75% v/v oxygen enriched cathode air and hydrogen in order to investigate the effects of a higher oxidizing

environment in the general behavior of the fuel cell. In parallel, another long-term degradation test is performed running with hydrogen in synthetic reformat. This second study is also quite interesting because it provides information how the fuel cell behaves under reformat fuel and it will deliver an update to literature with new experimental results from a HT-PEMFC fuel cell system. In both studies, state of the art PBI based MEAs are used. Therefore, this work can be considered as the basis and starting point for the development of the CISTEM project.

The results from different electrochemical techniques (electrochemical impedance spectroscopy, polarization curves, linear sweep voltammetry and cyclic voltammetry) are going to be shown for the performed tests. Thus, the electrochemical characterization methods selection will allow us to identify and classify the different mechanisms that may influence the degradation of the MEAs under investigation as for example, catalyst active surface reduction, hydrogen crossover enhancement, short circuit formation and proton transport deterioration in the membrane. Constant contact pressure mode has been selected as the standard operation mode in the cell compression unit, so that MEA thickness changes during characterization will be also monitored, recorded and shown.

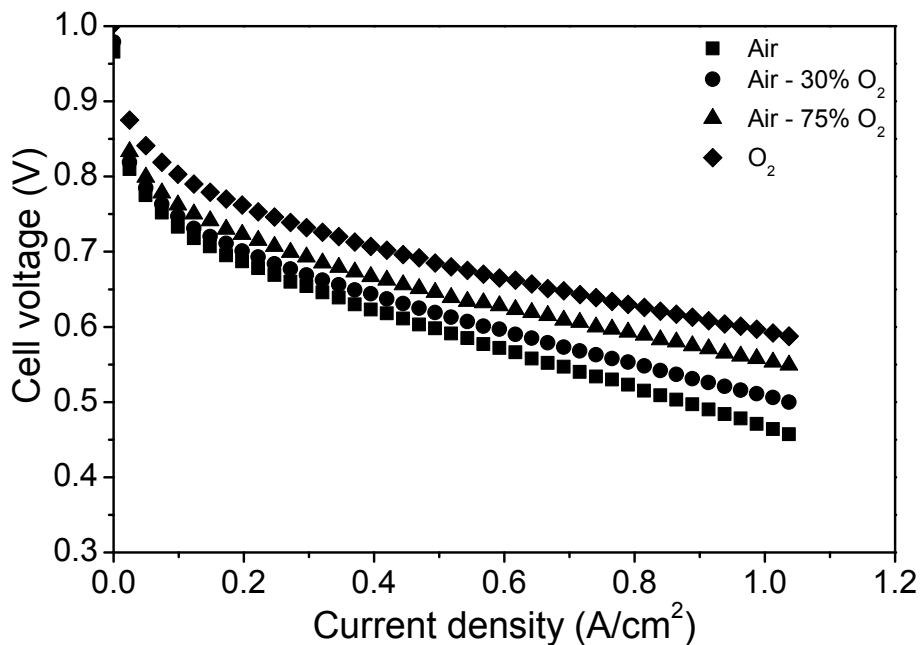


Figure 12 Polarization curves for the fuel cell operating with H₂/Air* and H₂/O₂*. 5-fold serpentine flow field, T=160 °C, p=1 atm. * λH₂=1.2; λAir=2, λAir-30% O₂=2.85, λAir-75% O₂=7.1, λO₂=9.5.

References:

- [1] Li Q, He R, Jensen JO, Bjerrum NJ. PBI-based polymer membranes for high temperature fuel cells - preparation, characterization and fuel cell demonstration. *Fuel Cells* 2004; 4:147-59.
- [2] Lobato J, Canizares P, Rodrigo MA, Linares JJ, Aguilar JA. Improved polybenzimidazole films for H₃PO₄-doped PBI-based high temperature PEMFC. *J. Membr. Sci.* 2007; 306: 47-55.
- [3] Ma YL, Wainright JS, Litt MH, Savinell RF. Conductivity of PBI Membranes for High-Temperature Polymer Electrolyte Fuel Cells. *J. Electrochem. Soc.* 2004, 151:A8-16.

Electrochemical performance of a HT-PEM fuel cell with bi-functional electro/reforming anode (FCC6-4)

George Avgouropoulos^{1,2,*}, Alexandra Paxinou^{1,2} and Stylianos Neophytides¹

1 Foundation for Research and Technology-Hellas (FORTH), Institute of Chemical Engineering Sciences (ICE-HT), P.O. Box 1414, GR-26504 Patras, Greece

2 Department of Materials Science, University of Patras, GR-26504 Rio Patras, Greece

ABSTRACT

The low energy densities of current battery systems contribute to the excessive weight and bulk of portable equipment, and severely limit the duration of military or commercial operations using portable electronic devices. While much progress has been made in battery technology, this power source still has limited energy density as compared with advanced H₂ fuel cells which could offer energy densities ranging from 500 to 1000 Wh/kg. Methanol may offer much higher energy densities than either batteries or fuel cells operating on stored H₂, making it an attractive source for advanced portable power. Methanol can be easily stored, transported and dispensed, and, at the same time, it can be efficiently produced from a wide variety of (renewable) sources. However, a methanol fuel cell would be the preferred energy source for a portable power system if a rugged, reliable and lightweight fuel processor was available to efficiently convert the alcohol to H₂ and drive a polymer electrolyte membrane (PEM) fuel cell, in a small volume.

Recent advances in the design/development of materials, such as polymer electrolyte membranes, electrocatalysts and methanol reforming catalysts, with respect to innovative features of IRAFC, allow the operation of PEMFCs at temperatures in the range 200-220°C [1-3]. The technological/commercial reasons for operating PEMFC at high temperatures are: (i) enhanced electrochemical rates, (ii) simplified water/cooling management, (iii) recover useful waste heat, (iv) lower quality reformed hydrogen containing up to 2% CO may be used as the fuel.

Recently, Avgouropoulos et al. [1-3] demonstrated the functionality of an Internal Reforming Alcohol Fuel Cell (IRAFC), where the methanol gets reformed by a catalyst incorporated into the anode compartment of PEM fuel cell (internal reforming) (Fig. 1, Direct IRAFC configuration). Integration of the reformer into the fuel cell eliminates the need for additional heat exchangers and a separate WGS and PrOx fuel processors. Thus, the design of the fuel processor-fuel cell system offers room for simplification, increase of efficiency and minimization of system weight and volume.

The heart of IRAFC unit is the Reformer Electrode Membrane Assembly (REMA). A high temperature membrane electrode assembly (HT-MEA), being able to operate at 200-220°C has been already demonstrated and is based on the high temperature H₃PO₄-imbibed HT-MEAs developed by ADVENT Technologies S.A. in close cooperation with FORTH/ICE-HT and University of Patras [1-3,6,7], which have proven operation on a long term basis at 210°C with minimal H₃PO₄ loss. However, the characteristics of the IRAFC significantly change in the presence of methanol in the H₂ stream, implying a poisoning effect of adsorbed methanol on the electrocatalyst and the proton conductivity of the membrane [8]. The second drawback of IRAFC configuration concerns the H₃PO₄ poisoning of methanol reformer (Fig. 2). In this work, the HT-PEMFC will have a bi-functional electro/reforming

anode, which consists of two layers separated with a thin graphite plate (Fig. 2, Indirect IRAFC configuration). The first layer's function is to reform methanol, and the second layer's function is to catalyze H₂ oxidation. The methanol reformer will be incorporated in the anode side of fuel cell and will be based on a novel engineering technology with respect to classical IRAFC configuration [1-3] based on a foam reformer, yielding voluminous cells.

In the proposed configuration (Fig. 1), a highly active Cu-based methanol reforming catalyst is deposited on the gas diffusion layer of a carbon paper and is separated from high temperature polymer electrolyte membrane electrode assembly (MEA) with an additional thin plate that enables (i) uniform reactants/reformate distribution to benefit the MEA operation [8] and (ii) protection from H₃PO₄ poisoning [9]. The advantages of this new IRAFC with a bi-functional anode are: lighter weight to ultra-thin catalytic layer as compared with voluminous foam-based reformers, simpler system configuration and higher power and energy efficiencies. There is no heat loss between the methanol reforming layer and the hydrogen oxidation layer.

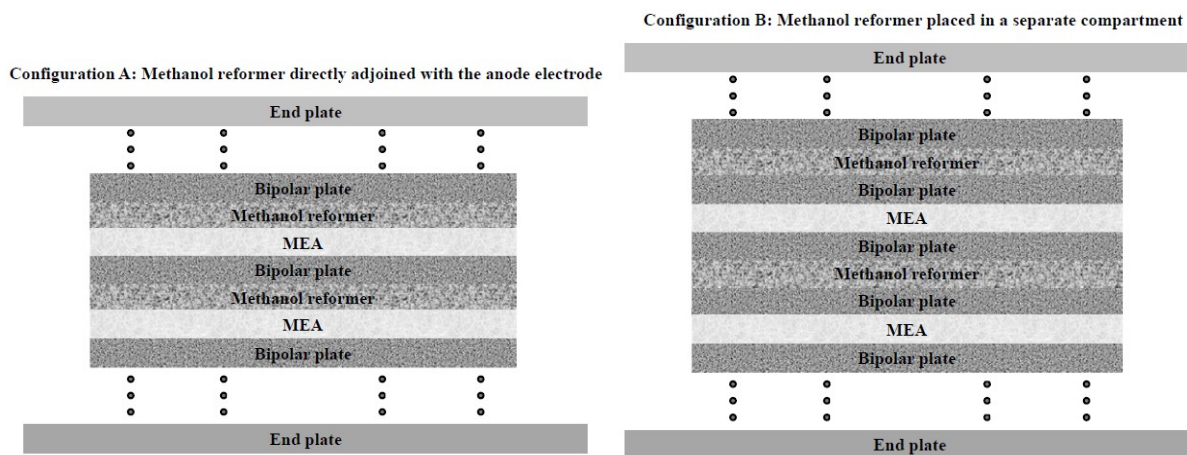


Figure 1. Direct (A) and indirect (B) IRAFC configuration

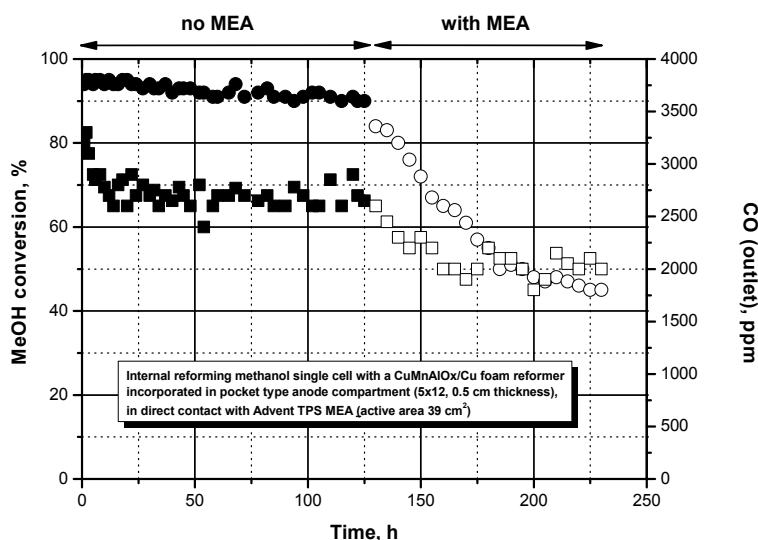


Figure 1. Long term testing of methanol reforming catalyst in direct contact with Advent TPS® MEA (Direct IRAFC configuration)

The corresponding bipolar plate anchoring the reforming catalyst will be machined with interdigitated flow fields forcing the methanol/water feed stream to flow and react uniformly across the whole volume of the catalytic layer. In this way the H₂-rich gas stream will flow internally to the flowfield of a thin graphite plate and distributed across the MEA area eliminating the risks of (a) phosphoric acid back diffusion and poisoning of reforming catalyst, (b) blocking the electrocatalyst active sites by excessive unreacted methanol. Preliminary results showed promising catalytic behaviour of Cu-based methanol reformer. Methanol conversions higher than 98% (less than 2000 ppm of CO in the outlet) were obtained at 210°C, under concentrated methanol/water feeds (30% MeOH/45% H₂O), while the hydrogen production rate was high enough to give 0.600 V at 0.2 A/cm², with an Advent TPS® MEA. The polarization curves and the characteristics of the impedance spectra of the proposed internal reforming methanol fuel cell will be presented and discussed. An optimization study will be presented with respect to the formulation process of highly active Cu-based low-temperature methanol reforming catalysts operating at 210°C with high stability, activity and selectivity towards H₂ production. The catalyst was mixed with carbon powder for conductivity purposes and deposited on the surface of the gas diffusion layer of a carbon paper via an advanced vacuum/heating table technique designed to be applied in scale-up synthesis, too. Preliminary tests in our lab showed that this route yields a uniform thin catalytic layer of less than 500 µm with exceptional activity/selectivity under concentrated feeds of MeOH/H₂O. Synthesis procedure is being optimized with respect to the catalyst mechanical integrity, improved gas distribution, low contact resistance, activity and stability with respect to H₃PO₄ poisoning. The design of the flowfields takes into consideration the integration of the methanol reformer into the anode compartment so that it ensures (i) uniform distribution of the methanol/water reactants flow through the reforming catalyst, (ii) elimination of phosphoric acid back diffusion, (iii) minimum MEA's exposure to unconverted methanol and (iv) excellent current collector functionalities.

REFERENCES

- G. Avgouropoulos, T. Ioannides, J.K. Kallitsis, S. Neophytides, *Chem. Eng. J.* 176-177 (2011) 95.
- G. Avgouropoulos, J. Papavasiliou, M.K. Daletou, J.K. Kallitsis, T. Ioannides, S. Neophytides, *Appl. Catal. B: Environ.* 90 (2009) 628.
- G. Avgouropoulos, J. Papavasiliou, M. Daletou, M. Geormezi, N. Triantafyllopoulos, T. Ioannides, J. Kallitsis, S. Neophytides, US Patent 200861/095779, September 10 (2008).
- J.A. Asensio, E.M. Sánchez, P. Gómez-Romero, *Chem. Soc. Rev.* 39 (2010) 3210.
- Y.L. Ma, J.S. Wainright, M.H. Litt, R.F. Savinell, *J. Electrochem. Soc.* 151 (2004) A8.
- M.K. Daletou, N. Gourdoupi, J.K. Kallitsis, *J. Membr. Sci.* 252 (2005) 115.
- K.D. Papadimitriou, F. Paloukis, S.G. Neophytides, J.K. Kallitsis, *Macromolecules* 44 (2011) 4942–4951.
- G. Avgouropoulos, S. Neophytides, *J. Appl. Electrochem.* 42 (2012) 719.
- J. Papavasiliou, G. Avgouropoulos, T. Ioannides, *Int. J. Hydrogen Energy* 37 (2012) 16739.

Multi-scale modeling to boost fuel cell performance: From pore-scale simulations to better efficiency and durability (FCC6-5)

U. Salomov, P. Asinari

Multi-Scale Modeling Laboratory (SMaLL), Dipartimento Energia, Politecnico di Torino, Corso Duca degli Abruzzi 24, 10129, Torino, ITALY

Polymer electrolyte membrane fuel cells (PEMFC) have received attention as new power sources for residential, transportation, as well as portable applications. Despite the tremendous progress in PEM fuel cell technology, namely development of the phosphoric acid doped PBI-based high temperature (> 100 oC) PEMFC with improved properties, like simplified system, reduced production cost, high efficiency and sufficient tolerance of Pt based hydrogen oxidation catalysts to CO impurity in hydrogen fuel (up to 2% at 180 oC) [1], degradation issues still remain. Loss of phosphoric acid, especially in high current density and elevated temperature (> 160 oC), through different processes like capillary transport, diffusion, membrane compression, evaporation and leaching by condensed water during shutdown and cold start, is thought to be one of the major mechanisms of degradation [2].

Deep insight into this degradation mechanism, leading to irreversible or reversible performance loss and the relation with other degradation mechanisms and the operating conditions, comes through pore-scale modeling of the mass transport phenomena, which provides the detailed information available at the microscopic scale. The morphological model presented in [3] was developed as the first step towards modeling of such degradation mechanisms in pore-scales.

In this work, we investigate how a parameter of a morphological model, namely distribution of catalyst (Pt) particles can change flow field at the catalyst layers and how this manipulation by flow field near membrane can be used as a mitigation strategy for phosphoric acid loss and crossover of reagents through membrane. The main idea behind the mitigation strategy is to manipulate flow field through catalyst layer by realizing different setups of morphological parameters, like distribution of catalyst particles, clusterization and so on. While velocity gradient is directly related to the component of pulling stress on phosphoric acid, by probing different distributions we have found the optimal configuration where this stress is zero at the interface between CL and membrane. For this purpose we have performed direct numerical pore-scale Lattice Boltzmann simulation of the fluid flow through catalyst layer for different distribution of catalyst particles. Moreover, a three-dimensional macroscopic model of the membrane electrode assembly (MEA) has been developed to analyze how the proposed mitigation strategy affects the polarization curve and hence the performance. The proposed distribution of ECSA may greatly improve durability by mitigating the phosphoric acid loss, at the price of only 9.3% reduction in efficiency at high current densities.

This work is part of the on-going European ARTEMIS project, within the Fuel cells and Hydrogen Joint Undertaking (FCH-JU). The purpose of ARTEMIS is to develop and optimize alternative materials for a new generation of European membrane electrolyte assembly, while reducing cost and increasing durability.

[1] Q. Li, J.O. Jensen, R.F. Savinell, N.J. Bjerrum. High temperature proton exchange membranes based on polybenzimidazoles for fuel cells. Prog. Polym. Sci. 34 (2009) 449.

[2] S. Yu, L. Xiao, and B. C. Benicewicz. Durability Studies of PBI-based High Temperature PEMFCs. FUEL CELLS 08, 2008, No. 3–4, 165–174

[3] U. R. Salomov, E. Chiavazzo, P. Asinari, Pore-scale modeling of fluid flow through gas diffusion and catalyst layers for high temperature proton exchange membrane (HT-PEM) fuel cells, [COMPUTERS & MATHEMATICS WITH APPLICATIONS](#), 67, 2014, 393-411

Optimization of HT-PEM fuel cells (FCC6-6)

*Hans Aage Hjuler, Héctor García, Thomas Steenberg
Danish Power Systems, Bldg. 207, 2800 Lyngby, Denmark*

*Qingfeng Li, Jens Oluf Jensen and Lars N. Cleemann
Department of Energy Conversion and Storage, Technical University of Denmark, 2800 Lyngby,
Denmark*

High temperature polymer electrolyte membrane fuel cells (HT-PEMFC) provide an attractive alternative to the Low Temperature (LT) PEM fuel cells that are only operational below 100 °C. Advantages include flexibility of using reformat fuels, efficient cooling, elimination of humidification and higher value of heat recovery. Polybenzimidazole (PBI) membranes doped with phosphoric acid have been demonstrated to be the most successful electrolyte system to achieve high temperature operation. Fuel cell systems based on this type of membranes have demonstrated the feasibility and potential of the technology.

A number of ongoing projects in Denmark and Europe aim at demonstrating the technology for various applications. Among these are fuel cells for combined heat and power (CHP) purposes in both micro-systems and larger systems as well for energy supply in buildings. A number of challenges have been recognized to improve the performance, including slow kinetics of oxygen reduction at the cathode, strong adsorption of acidic anions on catalysts, platinum utilization and ohmic resistance losses. Addressing these issues is of fundamental and technological importance for HT-PEMFCs. Our recent efforts are focused on optimization of single cell performance with the aim of demonstrating a 5 kW unit that can be modularly scaled up to 50-100 kW.

In this communication we update the progress we have achieved in the last few years. In addition to optimization of manufacturing processes for the polymer synthesis, catalyst preparation and MEA fabrication, further efforts are made to quantify and reduce losses within the MEAs of HT-PEMFCs. Ohmic losses related to the membrane electrolytes and electrodes have been determined by electrochemical impedance spectra and polarization measurements. The Pt utilisation particularly at the cathode is investigated and correlated to the overpotentials of MEAs. Single cell performances of more than 700 mV of cell voltage at a current density of 200 mA/cm² have been achieved. An operating point of 500 mV at 500 mA/cm² has been demonstrated. Long term durability at a constant current density of 200 mA/cm² has been achieved of more than 8.000 hours with a strong indication to reach 20.000 hours. Finally perspectives and future development of the HT-PEMFC technology will be outlined in the presentation.

Acknowledgements

The authors thank the European Commission for the support within the Seventh Framework Programme through the project CISTEM (FCH-JU Grant Agreement Number 325262). The Danish national program Energinet.dk is also thanked for financial supports.

Hydrogen and fuel cell systems and applications

HyLIFT: projects on hydrogen powered fuel cell materials handling vehicles in Europe (FCA1-1)

Hubert LANDINGER, Ludwig-Bölkow-Systemtechnik GmbH

THE PROJECT

Over the last three years the EU Fuel Cells and Hydrogen Joint Undertaking co-financed two fuel cell materials handling vehicle projects, HyLIFT-DEMO and HyLIFT-EUROPE that together plan to deploy more than 200 vehicles in daily operation in various sites in Europe. The overall aim of the two HyLIFT projects is to conduct large scale demonstration of hydrogen fuel cell materials handling vehicles to accelerate commercial market introduction of this technology.

A hydrogen-powered materials handling vehicle with a fuel cell combines the advantages of diesel / LPG and battery powered vehicles. Hydrogen provides the same consistent power and fast refuelling capability as diesel and LPG, whilst fuel cells provide energy efficient and zero emission electric propulsion similar to batteries.

The HyLIFT projects will see the demonstration of the 2.5 ton STILL forklift RX 60-25 and other STILL trucks, and the MULAG airport tow tractor Comet 3 FC. In total the demonstration of more than 200 vehicles is planned. HyLIFT-DEMO involves the partners LBST (coordination), H2 Logic (fuel cell system supply), DTU (R&D of future product generations), Linde (hydrogen competence), JRC (fuel cell system laboratory testing), SINTEF (accelerated durability tests), FAST/EHA (dissemination) and TÜV SÜD (certification support) whereas HyLIFT-EUROPE involves the partners LBST (coordination), STILL (forklifts and warehouse trucks), MULAG (airport tow tractors), Air Products (relocatable fuelling station supply and hydrogen competence), CHN (hydrogen stations), Element Energy (total cost of ownership calculations), FAST/EHA (dissemination), JRC (validation tests), Heathrow Airport (support vehicle usage) and H2 Logic (fuel cell systems and refuelling hardware).

An initial success of the projects is that first vehicles have clocked over 1,500 hrs of operation at an end-user site while the number of refuelling procedures at the corresponding hydrogen refuelling station has amounted to 2,000 to date.

This shows that fuel cell drive trains are a feasible and sustainable alternative for customers using either diesel or LPG today.

Market introduction has already begun in the USA where customers are increasingly opting for fuel cell material handling vehicles offering an attractive value proposition whilst providing energy efficient and zero emission electric propulsion.

SUCCESS FACTORS OF FUEL CELL MATERIALS HANDLING VEHICLES IN NORTH AMERICA

The presentation will initially provide some insights into the success of materials handling vehicles in North America and will elaborate on the facts that have encouraged this success. These success factors are e.g. constant operating power, increased productivity per vehicle and the availability of cheap hydrogen. Cost reductions could be achieved by reduced labour costs for hydrogen refuelling

instead of battery charging and by reduced costs of infrastructure warehouse space. Additional enablers are the funding support from the U.S. Department of Energy (DOE) and from the Defence Logistics Agency (DLA) as well as the federal tax credits for fuel cell purchases.

WHERE DO WE STAND IN EUROPE?

First of all it can be stated that the HyLIFT projects – HyLIFT-DEMO and HyLIFT-EUROPE – are one of the leading demonstration projects in Europe. Currently 11 vehicles are in demonstration – 10 STILL fuel cell forklifts and 1 MULAG fuel cell airport tow tractor.



Source: STILL GmbH

In the project tests, trials and demo operations helped significantly to overcome some childhood diseases. Nevertheless, it turned out that it is a real challenge to achieve a Total Cost of Ownership (TCO) equal to the conventional technology even taking the financial support into account. This is, beside the still high technology costs, caused by a better performance of conventional vehicles and more expensive hydrogen compared to North America. In addition the high availability requirements for materials handling vehicle operations in logistics centres allow near zero downtime.

Key to lowering technology costs (fuel cell system) is the implementation of series production for the fuel cell systems and significant cost reductions in the supply chain enabled by increased lot sizes. (It has to be noticed that currently the small lot sizes disable noteworthy cost reductions!) Batch production of the fuel cell systems is already in place, series production is under preparation.

Further large scale demo projects, such as HyLIFT-EUROPE, where 200 vehicles will be demonstrated, are already started or are under preparation.



Source: H2 Logic A/S

LESSONS LEARNED

There are numerous lessons learned from the ongoing projects, the most relevant are listed here:

Required supply chains able to provide significant numbers at competitive prices are far from being fully established

Customers of materials handling vehicles are operating in a fully commercial and industrial area where Total Cost of Ownership (TCO) is main criteria for purchase decision

Test trials for potential customers are inevitable and therefore easy approaches need to be developed to enable these test trials at potential customer sites

The hydrogen price delivered to the demo sites is of high relevance as this is one of only a few variables to enable cost reductions for the overall package

Deployment support mechanisms are required beyond HyLIFT-DEMO and the upcoming large scale demos and have to be reflected in the FCH JU 2.0 in the context of Horizon 2020

HOW TO PROCEED?

The demonstration of 200 vehicles in real world applications at end-user sites is secured in the project HyLIFT-EUROPE (2013-2016), the follow-up project of HyLIFT-DEMO, where also the vehicle OEMs STILL and MULAG are participating. Beside the identification of cheap hydrogen sources improvements have to be implemented in order to enlarge the opportunities for test trials at customer sites and to establish economically attractive supply chains. The commercialisation efforts need to be strengthened comprising the development of full-service packages with attractive Total

Cost of Ownership (TCO) for the end-users. Furthermore, additional large scale demo projects as well as adequate deployment support mechanisms need to be initiated and started. Test sites where some downtime is acceptable need to be identified to ensure testing in real life environments without compromising key future customers.

Finally, the topic of hydrogen powered materials handling vehicles needs to be anchored in the FCH JU 2.0 in the context of Horizon 2020. Furthermore, a joint USA – Europe fuel cell materials handling vehicle project might help to identify additional synergies and innovative solutions.

Cost-efficient fuel cell hybrid systems for inner-city transport (FCA1-2)

Manfred Limbrunner

Proton Motor Fuel Cell GmbH, Benzstrasse 7, D-82178 Puchheim

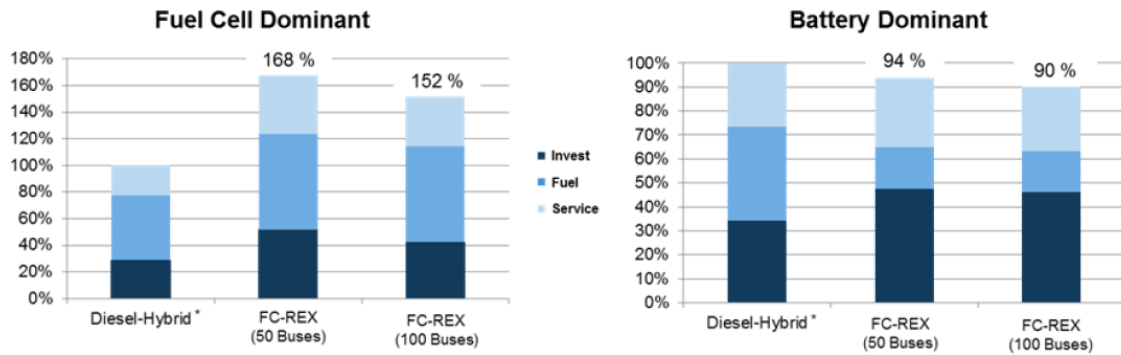
Proton Motor Fuel Cell GmbH was founded 1998 as a spin-off of Magnet Motor, a company focused on electrical drive systems. The ambition was to create a new and independent framework for development and sales of fuel cells. Proton Motor develops and distributes Proton Exchange Membrane (PEM) fuel cell systems for mobile, maritime and stationary applications. Through years of research and development Proton Motor furthermore gained well-founded expertise in hybrid systems with batteries and fuel cells. In addition to selling complete fuel cell systems, the company offers supporting services, therefor providing turnkey solutions to their customers. During operating time of installed systems, Proton Motor (PM) offers maintaining and repairing by their own customer service team.

Today PM offers high power systems for maritime applications, Range Extender systems for utility vehicles and modular stationary systems for (uninterruptable) power supply. The company focuses on the business sector, providing solutions for high power demands from 3 up to 200kW.

The mobile market is facing some upcoming challenges, making development and implementation of new solutions and technical systems essential. In their efforts for environment protection and antipollution, cities are implementing environment zones, in which emissions are restricted, and other guidelines to accelerate the progress to 'green cities'. To cope with these new requirements, new drive systems are designed, implemented and tested. The ideal case is a 'zero emission vehicle', realized with serial hybrid systems. Due to the restrictions of only battery-driven systems, hybrid systems with fuel cells could be the key.

The market of electric driven commercial vehicles for inner-city transport as well as electric driven buses grows. The balance between the operators requests for more shift operation (16...20 h/d at 300 d/a) with sufficient heating, ventilation and air conditioning at prices accepted by the market and emission free propulsion systems can not be achieved with either pure battery driven vehicles as well as with the conventional fuel cell hybrid systems. Vehicles nowadays are designed for multifunctional use (interurban as well as pure inner-city use). This makes it, according to conventional concepts, necessary to design fuel cell systems and battery systems to the maximum peak loads and the energy demand for a specified driving range. In practice vehicles serve a special application area. Therefore it is possible do design the propulsion system to these special demands. This is also taken care of with standardized drive cycles for buses "Standardised On-Road Test Cycles" (SORT). Especially the cycles SORT1 and 2 for inner-city traffic show clearly that a "small" fuel cell system in combination with an electric energy buffer (battery, super caps or battery + super caps) can achieve the operators requests more cost efficient than the conventional emission free solutions. Proton Motors standardized, modular range extender system with well-defined interfaces allows it on one hand to substitute existing battery driven concepts without big engineering effort and to reduce the battery capacity and therefore the costs, as well as to design new downsized propulsion concepts and to limit the costs of a fuel cell system to the absolute minimum to achieve a cost optimized emission

free propulsion system. Additional benefit and therefore additional cost savings can be achieved by using the waste heat of the fuel cell for heating of the passenger compartment or the battery.



A Compelling Value Proposition For Fuel Cell Buses (FCA1-3)

Daljit Bawa, ME

Ballard Power Systems

Hydrogen fuel cell technology has come a long way from the days of laboratory experiments – this working technology delivers exciting opportunities today. And, much like the commercialization path of diesel hybrid buses before it, clean energy hydrogen fuel cell bus technology is maturing rapidly while moving rapidly along a descending cost curve.

Highly-innovative, zero-emission fuel cell buses will play a critical role in the future of transit - preserving non-renewable energy sources, substantially reducing our environmental footprint and improving our quality of life. Fuel cell-powered buses deliver economic, operational as well as environmental benefits, when compared to traditional diesel or diesel hybrid systems.

We will review recent operational performance data regarding the deployments of the BC Transit Olympic Bus, Transport for London & Oslo bus fleets. We will discuss how those hybrid fuel cell-powered buses are offering reduced operating cost, lower noise levels, higher reliability, improved performance together with an effective fuelling solution.....all the while generating zero tailpipe emissions (aside from water, of course).

A compelling value proposition – from economic, operational and environmental perspectives – is emerging with the evolution of fuel cell hybrid buses. Ballard Power Systems is recognized as a world leader in the design, development and manufacture of clean energy fuel cell products. The company's FCvelocity™ family of motive fuel cell products are used effectively in mass transit buses today.

CHIC – Clean Hydrogen In European Cities: demonstration of 55 FC hydrogen buses (FCA1-4)

*MARIA DEL MAR ARXER, Carbueros Metálicos – Air Products
CHIC coordinator of the Infrastructure WP*

CHIC, the Clean Hydrogen In European Cities Project, is the essential next step leading to the full market commercialisation of Fuel Cell Hydrogen powered (FCH) buses.

The project will provide results from demonstrations of 55 hydrogen buses. Of these, 26 FCH buses are directly funded by European Union Joint Undertaking for Fuel Cells and Hydrogen (FCH JU) and started to operate in daily public transport operations in five locations across Europe - Aargau (Switzerland), Bolzano (Italy), London (UK), Milan (Italy), and Oslo (Norway) (Phase 1 cities). The CHIC project has 25 partners from 9 countries worldwide. The project is based on a staged introduction and build-up of FCH bus fleets and the supporting hydrogen refuelling stations and infrastructure, in order to facilitate the smooth integration of the FCH buses in Europe's public transport system.

The CHIC project forges partnerships with similar projects in Berlin, Cologne, Hamburg and Whistler (Canada) (Phase 0 cities), which have previously gained experience with operating 34 hydrogen powered buses (in the previous project HyFLEET:CUTE), and new cities and regions in Europe which are considering moving into the field. These partnerships will facilitate the effective and smooth introduction and expansion of the new systems now and into the future. During the project, "Phase 0" cities already deployed a further 29 buses through separately funded programs.

The buses in the CHIC project are supplied by three different manufacturers, and the hydrogen refuelling infrastructure involves the main industrial players active in hydrogen infrastructure development around the world. Five new hydrogen refueling stations have been built in Phase 1 cities alone, and in total 9 refueling stations are operated in the regions involved, with high average availabilities (>98%).

An important part of the project is to assess the environmental, economic and social impacts of the use of hydrogen powered buses. Hydrogen can be produced by different methods, including using renewable energy. Fuel cells use hydrogen to produce electricity while emitting only water vapour. Hydrogen and fuel cells can therefore play an important role in the reduction of local air pollutants, as well as in the decarbonisation of Europe's transport system. Hydrogen powered transport has the potential to meet the normal operational requirements of buses, light passenger and commercial vehicles without generating the harmful emissions and noise of conventional fuels.

The objectives of the CHIC project are to tackle the remaining obstacles the technology faces and move these demonstration vehicles to commercialization starting in 2017.

PROGRESS TO DATE

In London, five vehicles have been servicing the main touristic route RV1 since 2010. 2 other buses entered service in summer 2013, while the final one was delivered in December 2013.

In Aargau (Switzerland), five buses have been in operation since December 2011. Two hydrogen buses participated at the 41st and 42nd editions of the World Economic Forum (WEF) in Davos (in January 2013 and January 2014 respectively) transporting dignitaries and proving that buses can successfully run on high altitude areas and in harsh climate conditions.

Five FCH buses and a new H2 station have started operating in 2012 in Oslo. Operation hours have increased since April 2013.

In Milan, 3 buses along with the refuelling station are operating since beginning of August 2013.

Bolzano has received 5 hydrogen buses to service the main routes of the cities by the end of 2013. The H2 refuelling station is being set up and tested by now.

Two examples of the CHIC achievements so far:

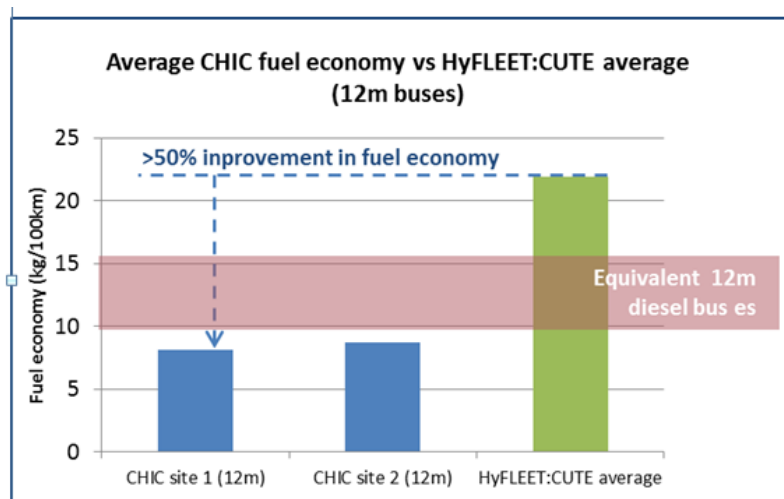
- Key improvements on the FC bus architecture:

Component	CHIC range (Phase 0 and phase 1 cities)	Key improvements over HyFLEET:CUTE
Fuel cell system	75 – 150 kW (rated peak output)	<ul style="list-style-type: none"> • Smaller and cheaper systems; • Higher power density; • Extended life.
Battery system	90 – 250 kW (Ni-MH or Li-ion)	The CHIC buses are characterised by a hybridised powertrain . The HyFLEET:CUTE buses had an electric drivetrain exclusively powered by a fuel cell system.
Supercapacitor system	180 - 240 kW (peak power)	In a hybridised powertrain, the energy storage systems (battery, supercapacitors or both) can: <ul style="list-style-type: none"> • Buffer peak loads; • Boost acceleration; • Allow energy recovery from braking.
Energy recuperation system	Brake resistors or wheel-hub motors	Benefits: <ul style="list-style-type: none"> • Greatly improved fuel efficiency (e.g. up to ~ 50% better than HyFLEET:CUTE); • Improved FC system life.
H ₂ storage system	4-8 tanks, 350bar 33 to 55 kg	<ul style="list-style-type: none"> • Lower number of tanks at parity of mileage (better fuel efficiency).

- Dramatic fuel economy improvement:

One of the most significant results of the trial program is the improvement in fuel economy which has been observed. The chart compares the fuel economy observed in the CHIC cities using 12m buses with the average from HyFLEET:CUTE and some benchmark diesel vehicles.

The reason for the >50% improvement is the use of fully hybridized powertrains, smaller and more optimized FC systems.



FUTURE OBJECTIVES

The success of CHIC will drive the focus of industry, governments and communities at local, regional, national and European level. It will increase the deployment of fuel cell buses in larger quantities.

- Fuel cell buses show many advantages for communities and transport authorities:
- Zero emission vehicles
- Technology that is efficient and proven to be capable for public transport
- Flexible in use as it does not show range limitations
- Fueling stations necessity for fuel cell buses is limited.

Fuel Cell Control Unit – employ automotive reliability for fuel cell systems (FCA1-5)

Dipl.- Ing. Dipl.-Wirt.-Ing. Nils Kaiser, Bosch Engineering GmbH

INTRODUCTION

Beginning high volume series production in the fuel cell industry poses new challenges: Tolerances for components apply, maintenance concepts have to be established and safe operation under a vast variety of conditions must be guaranteed. The automotive industry has established a lot of methods during recent years to cope with these challenges. Some of these methods, included in the AUTOSAR standard, are introduced by using the Fuel Cell Control Unit (FCCU) as an example. Purpose of this presentation is to show the benefits of employing important automotive concepts to fuel cell applications.

FUEL CELL CONTROL UNIT

The FCCU hardware is based on a state of the art engine control unit from Bosch (see exhibit 1). It offers analog and digital inputs and outputs as well as CAN and direct control of throttle valves.



Exhibit 1: Fuel Cell Control Unit Hardware

The software is implemented using automotive standards regarding tolerances, maintenance and safety. These will be shown in the following paragraphs.

TOLERANCES FOR COMPONENTS

If not every part is chosen manually, you will have to accept tolerances in components. This applies to mechanical features as well as electronic behavior. Another source for tolerances is ageing.

Therefore it is customary in the automotive business to have adaptable characteristic fields and self learning algorithms. Therefore a compensation of a fluctuating supply voltage is included in the

FCCU. If a sensor becomes too inaccurate it has to be changed. The new part might be of a different kind or even if it is of the same kind there might be another characteristic. That is why the software should offer flexibility by application of characteristic fields. This use case is shown as a practical demonstration.

MAINTENANCE CONCEPTS

In the automotive industry it is best practice to compartmentalize the whole car into smallest replaceable units (SRU) that are repaired if a malfunction occurs. The control software implementation should take this into consideration. To identify the impaired part the Diagnostic Safety Manager is used in the FCCU. The function of the SRU is monitored either by direct measurement (e.g. short circuits of sensor lines) or by diagnostic models (e.g. a running coolant pump would create a rise in pressure – missing rise indicates malfunction). In case of error detection the diagnosis is validated to exclude short term effects. A validated error will be transmitted to the error memory. The maintenance crew can access the error memory and gets error codes in return. A troubleshooting guide allows identifying the defective SRU. The presentation will show this approach as a live presentation with the FCCU in a hardware-in-the-loop simulation.

SAFE AND RELIABLE OPERATION

To implement a safety concept that ensures safe operation in all likely scenarios you have to compile a list of possible malfunctions. This can be achieved by performing a failure mode and effects analysis. Key parameters will be severity, occurrence probability and detectability. Errors can be classified as mechanical failures, misuse or wrong control software implementation. Mechanical failures have to be detected and their occurrence minimized by quality standards. Misuse has to be detected by the software and handled accordingly. The software itself could include programming errors or could reach instable states due to unsafe input values or component defects. In the automotive industry there is a three level concept employed. Level 3 ensures correct calculations in the electronic control unit. It looks for dead locks, memory distortion and wrong instruction sets. Depending on the safety goal it will offer increasing levels of redundancy. Level 1 detects malfunctions in the system components by using model based comparison between measurement and calculation. Level 2 checks the calculations of level 1 by using simplified models with less accuracy.

A simple example for visualization of the level concept would be the addition of $3 + 4$. If the result would be 12, level 3 would detect that the wrong instruction set, multiplication, had been used. This could occur by tampering with the instruction memory via EMC. If the result would be 8.5 level 2 would detect a larger than expected result, as level 2 model would say that the result would lie between 6 and 8. If the result is 7.01 level 1 would detect an error, because its model would expect 7.00.

Reliability means that a system is highly available, i.e. in case of minor malfunction the system should implement fallback levels. These will depend on error severity and best way to reach a safe state. Fatal errors, e.g. large hydrogen leaks, would require an immediate shutdown without regard to damaging the system further. Critical errors, e.g. nonoperational cooling, would allow a slower shutdown that helps to prevent secondary damages. Minor errors like loss of a not so important sensor could lead to activating a sensor model that calculates a replacement value. The operation might not be impaired at all or the operation strategy is slightly modified. It has to be carefully considered how an error is healed so the healing does not lead to unsafe conditions. The presentation will show the error handling as a live presentation with the FCCU in a hardware-in-the-loop simulation.

Aeronautical Auxiliary Power Unit (APU) based on Fuel Cell (FCA1-6)

Daniel Martínez Bastida; Antonio Ayuso Barea – SENER Ingeniería y Sistemas S.A., Madrid (Spain)

Jorgen Lundsgaard – IRD (Denmark)

Flemming Helsted Pedersen – Flemming Electronic Company (Spain)

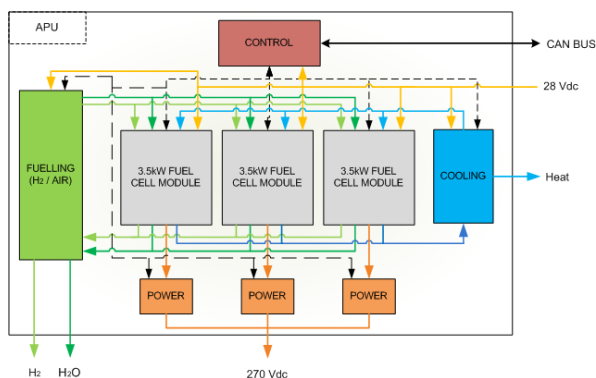
The purpose of the project has been to design, build and test an Auxiliary Power Unit (APU) based on proton exchange membrane fuel cells (PEMFC) for aeronautical applications with a Technology Readiness Level (TRL) of 5 (equivalent to a functional demonstrator). According to the new aeronautical levels of voltage, the output voltage of the system is 270Vdc.

Considering the new restricted regulation regarding CO₂ emissions in airports and the continuous increase of fuel prices, a system based on fuel cells represents an interesting alternative to replace the conventional APUs providing environmental and acoustic advantages.

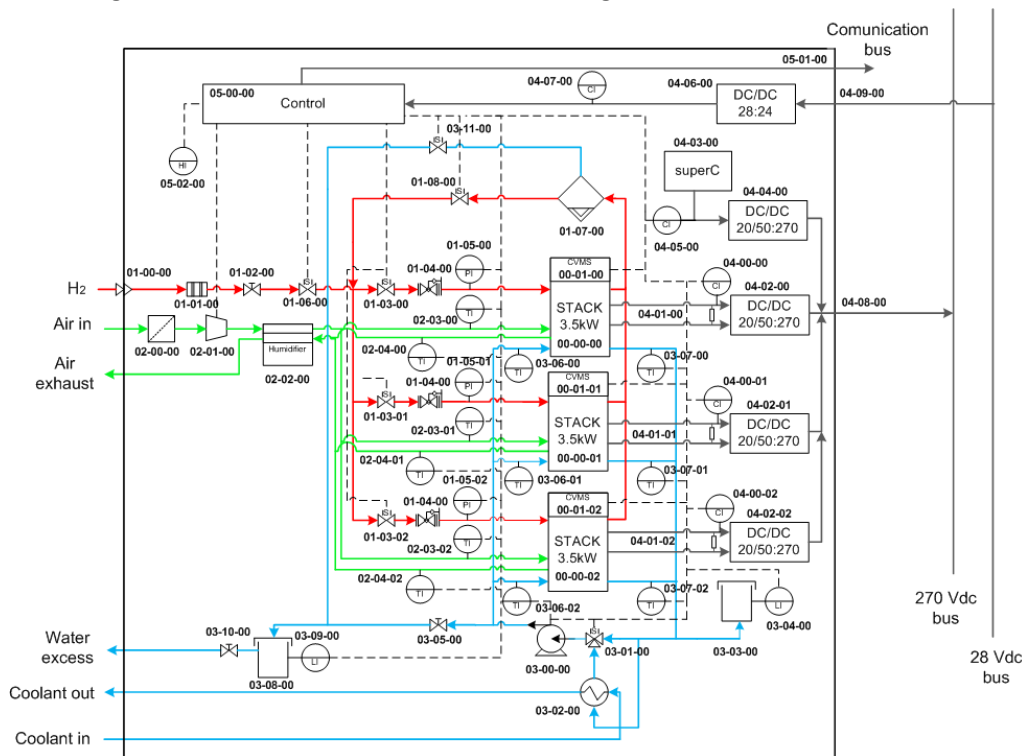
Moreover, there is a trend towards an increasing demand of electrical power in aircrafts due to two main reasons: in the new aircraft designs the mechanical, pneumatic and hydraulic equipments are being replaced by electrical systems and the continuous incorporation of new and more powerful electrical elements in certain areas such as communications, control or security. This issue would also justify the use of these APUs based on fuel cells in existing aircrafts without APU or with limited availability of electrical power to incorporate new equipment.

Thanks to its multi-functionality, an APU based on fuel cell could provide other benefits: It can be used as an energy generator source when the plane has landed and it can re-use the heat and water generated to feed other aircraft subsystems.

The first step of the project was to develop a technical specification. From this activity a preliminary design was created. The concept is a modular and redundant system. According to this, the APU consists of individual modules of fuel cells, each one with its own low level control system, cooling and fuelling circuit and power converter. These individual modules would be integrated in a common structure with a high level control unit that would interface with the low level controllers, the power electronics, the rest of the airplane electrical system and the high level cooling and fuelling circuits.



The figure below shows more in detail the design:



The next step was the design and development of a module of 3.5kW, in order to demonstrate and validate the concept. The fuel cell implemented is a PEMFC of the company IRD. The selected technology presents the best features. The proposed fuelling is pure hydrogen and air.

The DC/DC converter has been developed by Flemming Electronic Company in collaboration with SENER. The specific design has been necessary in order to fulfill the complexity of increasing the lower voltage output level up to 270Vdc with an efficiency over 90%.

Other components are commercial and they are not optimized neither in weight nor dimensions.

Finally the system was tested, being the most significant results shown here below:

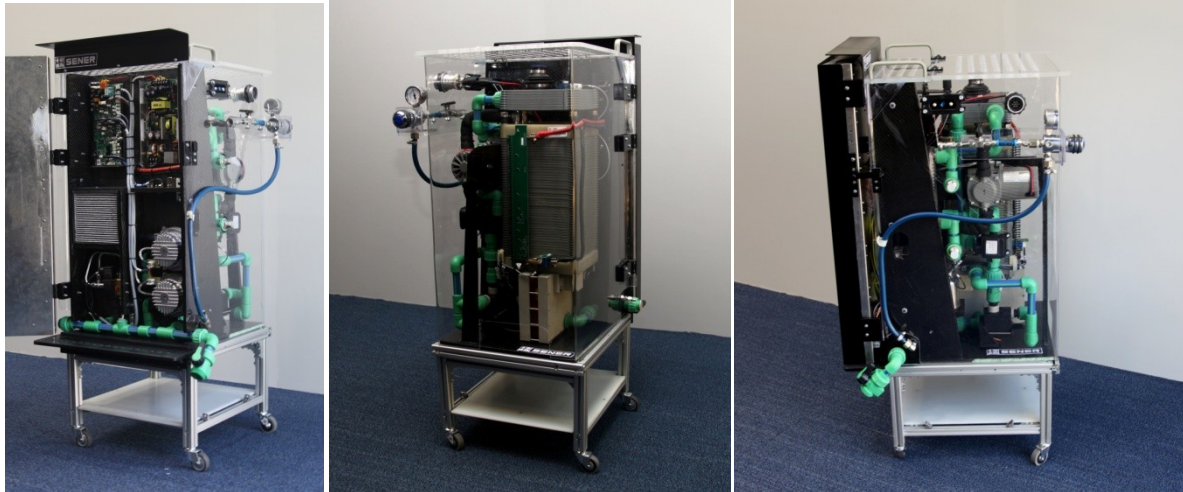
DC/DC converter performance: 90%

DC/DC converter power density: 1.6kg/kW

APU performance (Fuel cell + DC/DC converter): up to 40% without considering the heat generated.

APU power density: 14kg/kW

Output voltage: 270Vdc



The first conclusion is that the project has met the objectives as a functional demonstrator of the technology. APUs based on fuel cells are to be an alternative to conventional systems in order to solve the CO₂ emissions problems and the increasing demand of electrical power.

Other relevant conclusions would be the following:

In the medium term it could be possible to develop a competitive APU based on fuel cell.

The cost of fuel cells and reliability are the main challenges of the technology.

Structural, environmental and safety requirements are imperative for the product development. The investment needed to manufacture a certifiable system according to aeronautical regulations is very significant.

The reuse of heat generated by the fuel cell increases the power density close to 50%.

Apart from electrical power and heat it is possible to use the water generated.

The power electronic stage is critical in applications of 270Vdc.

Other significant issue is that the fuel cell dynamics is low, hence a battery or supercap would be necessary for specific transients.

Experimental results of a gasoline engine converted to run on hydrogen-rich synthetic gases (FCA2-1)

Jorge Arroyo¹, Francisco Moreno¹, Mariano Muñoz¹, Carlos Monné¹

1 Department of Mechanical Engineering

E.I.N.A., University of Zaragoza

María de Luna s/n. ed. Betancourt – Zaragoza, 50018 Zaragoza (Spain)

*Phone/Fax number: + 34 876555082, e-mail: jarroyo@unizar.es, fmoreno@unizar.es,
mmunoz@unizar.es, cmmb@unizar.es*

This work presents the processes of conversion, test and performance results of a spark ignition gasoline engine running on synthetic gases containing hydrogen. These gases are obtained from the catalytic decomposition of a biogas extracted from biomass gasification. This biogas, which has a composition of 60% CH₄ /40% CO₂ is processed through a catalyst at different temperatures and with different residence times. Catalytic decomposition produces hydrogen-rich fuel blends with a reduced fraction of CO₂. The decrease in CO₂, which actuates as diluent and deteriorates combustion, together with the increase of the proportion of combustible gases like CO, CH₄ and especially H₂, improves the quality of the blends, making them a good alternative to use as a renewable engine fuel.

The adaptation of the engine to run with liquid and gaseous fuel has supposed modifications in some engine components and the adaptation of the test facilities where the tests have been performed. The design of the modifications has been performed taking into account the special properties of flammability and diffusivity of hydrogen compared with other gaseous fuels. A new gaseous fuel supply line has been mounted and a safety system which prevents for leakages or fire has been installed. The gaseous fuel supply line is connected to a new gaseous injection circuit which comprises a new fuel ramp, an additional port where the gases are injected and new injectors designed to avoid problems with gaseous fuels. Modifications in the engine include the installation of a new engine control unit, a wideband oxygen sensor and a spark ignition system adapted to the characteristics of gaseous fuels.

The experimental tests were carried out using gasoline, methane, and three fuel blends. The first blend has a similar composition that the biogas from which the synthetic gases are extracted. The other two blends have the same composition that the synthetic blends obtained by decomposition of this biogas at 600°C and 700°C for 15 minutes. First synthetic gas composition is 23% H₂, 23% CO, 26% CH₄ and 28% CO₂, and the second blend composition is 40% H₂, 39% CO, 11% CH₄ and 10% CO₂. The presence of H₂ in synthetic blends suggested that the use of lean conditions could result in an increase in efficiency and a decrease in pollutant emissions. That is why two lean equivalence ratios ($\phi=0.85$ and $\phi=0.7$) were tested in addition to stoichiometric conditions. Tests were performed at full load (wide open throttle) and a wide range of speeds. The ignition timing was fixed for each speed, so that the only variable affecting each point tested was the fuel type used.

Results showed that efficiencies obtained with synthetic gases improve efficiencies obtained with raw biogas and even methane at lean conditions. The increment in the fraction of H₂ allows

obtaining good efficiencies at leanest conditions tested ($\phi=0.7$). However, the combination of air excess and high fraction of H₂ resulted in a big increment in NO_x compared with other fuels without H₂. The decrease in the fraction of CO₂ in synthetic blends supposed a decrease in emissions of CO₂ compared with biogas, although CO₂ levels remained high compared with gasoline and methane. CO is also a component of synthetic gases, so high CO emissions were expected. Nevertheless, elevated CO fractions are measured just at stoichiometric conditions. The combination of air excess and H₂ made that good combustion was maintained at lean conditions, so the fraction of unburned components was low at these conditions. Hydrocarbons presented a similar behaviour of CO. In gaseous blends, hydrocarbons in exhaust correspond to the fraction of methane that remains unburned. The low proportion of CH₄ in synthetic blends compared with pure methane and raw biogas implied low values of unburned hydrocarbons.

The study of pressure inside the cylinder allowed verifying the combustion behaviour of the synthetic blends. The combination of CO₂ and H₂ made that similar pressure curves were obtained with synthetic blends than with CH₄. Combustion results showed that, because of the presence of H₂ in synthetic blends, the combustion is advanced, even at lean conditions and consequently, adjustment of the ignition timing is needed in order to operate at optimal conditions. The study of the mass burning fraction and heat release confirmed this fact. Moreover, the improvement in combustion produced by H₂ resulted in low cyclic variability compared with gaseous fuels.

Methanol Reformer - The next milestone for Fuel Cell powered submarines (FCA2-2)

Stefan Krummrich

ThyssenKrupp Marine Systems GmbH

Werftstr.112-114

24143 Kiel

Germany

Javier Llabres

SENER Ingeniería y Sistemas, S.A.

Severo Ochoa 4

28760 Tres Cantos

Espana

INTRODUCTION

The market introduction of fuel cells for submarines at ThyssenKrupp Marine Systems was a major step for air independent propulsion (AIP) systems of submarines. The enormously increased submerged endurance of fuel cell submarines compared to conventional submarines is still inspiring submariners all over the world, with the result of a high market share of ThyssenKrupp Marine Systems GmbH in the field of non-nuclear submarines.

All submarines with fuel cells built until today are based on hydrogen storage in metal hydride storage cylinders. This technology offers many advantages regarding the special requirements of submarines, but the AIP energy that can be stored onboard is limited due to the high weight of the metal hydride storage cylinders – a submarine can only carry a limited.

Therefore, to overcome this limit and to further strengthen the market position and the technical leadership in the field of AIP systems application, ThyssenKrupp Marine Systems has signed an agreement with the Spanish engineering group SENER Ingeniería y Sistemas S.A., for the finalization of the development and the industrial production of an AIP system based on a methanol reformer.

This abstract and the corresponding presentation give an overview about the development goals, the status and the further steps to achieve a fully submarine-proven system layout.

CHOICE OF FEEDSTOCK

The choice of the best fuel for a reformer system for submarines has great influence not only on the system design, but also on submarine design and performance. Generally the feedstock for a reformer system can be hydrocarbon or alcohol. Compared to the storage of pure hydrogen, this implies the production of CO₂ on board. As CO₂ cannot be stored on board like e.g. the product water of the fuel cell, it has to be discharged into the surrounding sea. To ensure a weight balanced system (principle of Archimedes) the lost weight of the CO₂ has to be compensated with sea water.

The reformer has to be operated with fuel + oxygen (+ water). The oxygen is stored on board in liquid form in a cryogenic tank. This LOX tank is the dominant component defining system size. Consequently, the oxygen consumption of the AIP system is very important and should be kept as low as possible. With a view to the entire AIP system, the chemical products are water (H₂O) and carbon dioxide (CO₂). Therefore, the ratio of H to C in the chemical structure should be high, because the oxidation of C requires more oxygen than the oxidation of H. Furthermore the overall system efficiency is of importance for the oxygen consumption, and of course for the fuel consumption.

Further factors important for the choice of feedstock are worldwide availability, safety (handling etc.), purity (avoidance of additional reactors/absorbers etc.) and the reforming temperature to keep the reformer going.

ThyssenKrupp Marine Systems has considered three feedstocks for submarine reforming: Diesel (C_{13.57}H_{27.14}), Ethanol (C₂H₅OH) and Methanol (CH₃OH). The final choice was in favour of Methanol for the following reasons:

- H/C ratio is highest for Methanol
- highest efficiency of reforming process
- very easy reformation (T app. 250°C; for Diesel > 850°C, for Ethanol >700°C required)
- worldwide availability
- high purity (no sulphur etc.)

SYSTEM CONFIGURATION

At the beginning of the development the requirements for the reformers were defined. A major requirement was operation based on the existing and proven Siemens Fuel Cells. Furthermore the exhaust gas (CO₂) pressure should be high, to enable the discharge of exhaust gas into the surrounding seawater without the need for an additional exhaust gas compressor. Of major importance were the overall system efficiency and the reliability and availability of the system.

Based on these requirements, the choice was a methanol steam reformer system operated at elevated pressure. Hydrogen purification is performed with a membrane purification unit. The required thermal energy is produced in a high-pressure oxygen burner. An overview of the process is shown in Figure 1.

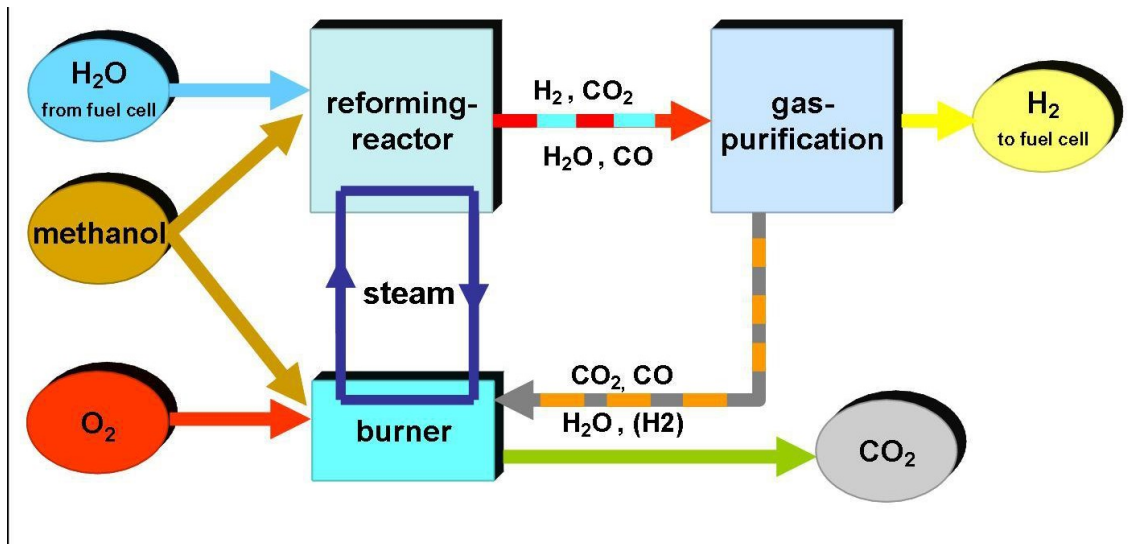


Figure 1: Overview of Methanol Reformer System

The methanol is mixed with water, evaporated and fed to the steam reformer. The reforming reactor is heated by a boiling water cycle operating between 60 and 100 bar. The methanol-water mixture is converted into a hydrogen-rich gas mixture at a temperature between 250-300°C. This reformat gas is further processed in a gas purification unit based on hydrogen-permeable membranes. The major fraction of hydrogen passes through the membrane and can be fed directly to the SIEMENS fuel cell. The rest of the reformat gas is burned with pure oxygen in the burner, under the addition of methanol, to provide the required heat for the reforming process. The only product gas from the reformer is CO₂, the H₂O in the exhaust gas is condensed and reused internally.

The methanol reformer itself will be operated in an encapsulation comprising several safety features, to protect the crew from any harmful gases and liquids.

EXHAUST GAS TREATMENT

One of the systems of highest importance is the exhaust gas treatment system. The reformer system produces CO₂, which must be given overboard silently, and without producing any gas bubbles in the seawater – a bubble cloud in the seawater would make the submarine detectable even in submerged conditions. For this purpose SENER has developed an exhaust gas treatment system. The first part of this system can compress the exhaust gas to the required pressure level of the surrounding seawater. This exhaust gas compressor only has to be operated at very high depth, because the reformer is even operated at elevated pressures.

The second part dissolves the exhaust gas of the reformer completely into the seawater. This system utilizes the seawater that is required also for cooling purposes onboard, so no additional seawater has to be pumped through the submarine. The exhaust gas is mixed and dissolved with the seawater and routed through a specially designed device.

STATUS AND OUTLOOK

The first Methanol reformer at ThyssenKrupp Marine Systems has been operated for years now. It has been operated together with the SIEMENS fuel cell successfully as well as with the exhaust gas treatment system of SENER. The hydrogen produced by the reformer meets the high purity requirements of the fuel cell, no difference could be observed compared to operation on pure hydrogen from liquid hydrogen storage. Furthermore the reformer exhaust was completely dissolved in seawater – no bubbles in the seawater could be observed.

Currently a new methanol reformer system is being built up based on the final submarine design of the system. This new reformer will be operated starting in 2014 in the test field of ThyssenKrupp Marine Systems with all peripheral systems which are also required onboard like Oxygen supply system, Methanol / Reaction water tank system, Methanol supply system and the exhaust gas treatment system. All these systems are being developed by SENER.

The development schedule implies elevated testing periods to show the high availability and reliability of the reformer system.

With this step in fuel cell AIP ThyssenKrupp Marine Systems and SENER Ingeniería y Sistemas, S.A. offer a unique and superior technology for future submarines, based on proven technology combined with years of experience in the field of fuel cell technology.

Developments in the context of the hydrogen and fuel cell-based AIP system of the Spanish S-80 submarine (FCA2-3)

África Castro, Abengoa Hidrógeno

INTRODUCTION

The world's different shipyards and navies are currently interested in submarines that, while being conventional (non-nuclear), can remain submerged longer. This requires the use of what is known as an anaerobic propulsion system (AIP system), that allows the vessel to remain submerged longer, thereby reducing its indiscretion.

A conventional submarine operating with an AIP system is a small, manageable, and not too costly vessel with extended capabilities for underwater navigation that make it attractive in many circumstances and applications.

When developing AIP systems, different shipyards are considering various technologies; thus we have the French Mesma system, the Swedish Stirling system, and the systems based on a closed cycle diesel engine (CCD). But, without a shadow of a doubt, fuel cells and hydrogen are playing a key role in the development of future AIP systems.

AIP SYSTEMS BASED ON FUEL CELLS

The idea of using fuel cells to generate electrical power on board a submarine is, obviously, attractive for its efficiency, reliability and energy density. This is, in short, an AIP system consisting of a fuel cell, an oxygen tank (usually in cryogenic state), a hydrogen tank or production system, a system that suits the electrical power output from the fuel cell to that required by the submarine, and a control system that governs the AIP system.

In fact, at present, the German shipyard ThyssenKrupp is already developing submarines with an AIP system based on fuel cells, in which the hydrogen is transported stored in metal hydrides.

However, there are disadvantages to transporting the hydrogen on the submarine when compared to its production on-board from another fuel; the possibility of producing the hydrogen as it is needed, using a feedstock such as a hydrocarbon or an alcohol in a reforming process, can facilitate logistics, increase autonomy, and enhance the overall security of the AIP system.

DEVELOPMENT OF THE AIP SYSTEM FOR THE SPANISH S-80 SUBMARINE

Abengoa has been working jointly, since 2001, with the Spanish Navy and the Spanish Navantia shipyards on the development of an AIP system based on fuel cells and bioethanol reforming. The AIP system on-board the S-80 submarine features the following subsystems:

- A Bioethanol Processing System (SPB): it is responsible for reforming bioethanol in a hydrogen-rich stream, using the reaction of steam reforming (SR), followed by water gas-shift (WGS) reactions and by preferential oxidation (COProx).

- A Fuel Cell System (SPC): a polymeric fuel cell transforms the flow of hydrogen from the SPB and oxygen from a cryogenic tank into water and electricity. It operates in open anode, which allows it to operate with reformed gas. The water produced at the outlet of the SPC is condensed and re-circulated to feed the SPB.
- A Power Conditioning System (SAP): it is the block responsible for suiting the electrical power produced by the SPC to the conditions required by the power bus of the submarine.
- A CO2 Evacuation System (SECO2): it collects the CO2 evacuated by the SPB (once the fuel cell has used the hydrogen the reformed gas contained) and dissolves it in seawater, in a low energy consumption and minimal acoustic signature process.
- An AIP Control System (SCAIP): it is the system responsible for controlling the whole process of the AIP system.
- Abengoa is responsible for the development of the SPB, the SAP and the SCAIP, having developed and tested different scale prototypes that have been used to validate the technologies used. It is currently developing and will supply the three units to Navantia, which will be then be installed on-board on the first of the S-80 submarines the Navantia shipyards is building for the Spanish Navy.

The fact that the SECO2 is being supplied by another Spanish company – Bionet – is also of note. The polymeric fuel cell is being supplied by the American company Hamilton Sundstrad, part of United Technologies Corporation.

DMFC and PEMFC/H₂ performance under unmanned aerial vehicles environmental flight conditions (FCA2-4)

OSCAR GONZALEZ-ESPASANDIN. Universidad Politécnica de Madrid, Spain.

oscar.gonzalez.espasandin@alumnos.upm.es

TERESA J. LEO. Universidad Politécnica de Madrid, Spain. teresa.leo.mena@upm.es

MIGUEL A. RASO. Universidad Complutense de Madrid, Spain. marg@quim.ucm.es

EMILIO NAVARRO. Universidad Politécnica de Madrid, Spain. emilio.navarro@upm.es

The increasing interest in finding power systems that use fuels other than oil derivatives has promoted in recent decades the study of fuel cells, being in general the aircraft industry one of the fields that has shown outstanding interest. Even if air traffic is responsible for only 3% of the total greenhouse emissions, aircraft manufacturers are working to achieve a more efficient aircraft, which is leading to more electric or all-electric aircraft concepts. The unmanned aerial vehicles (UAV) represent a case of particular interest from the point of view of the fuel cells incorporation into aircraft propulsion systems. This is especially true for the small size UAV, with low maneuverability and long operation time, which are currently the most developed, with interest in both military and commercial civil applications. Airships are also a new field of application potential of fuel cells.

Besides causing low environmental impact, the use of fuel cells in unmanned aircraft presents clear benefits that are intrinsic to this type of devices, which include its low noise level and its modularity. After the study of the state of the art and the feasibility of the implementation of different types of fuel cells in UAV, a sensitivity study of two types of fuel cells (hydrogen PEMFC and DMFC direct methanol) has been dealt with, compared to the same environmental conditions. The PEM/H₂ fuel cell working at low temperatures (65-80 °C) have a quick start, provide high current, high specific energy density and low specific power density. The fuel used is hydrogen stored in different ways. On the other hand, fuel cells of DMFC's have a lower power density and efficiency than the PEMFC, but they present greater simplicity and also higher energy density. Virtually all fuel cells are designed for operation on earth, so it is of capital interest to study how variation of environmental conditions during the flight of an aircraft affects the fuel cell performance. To do this, polarization curve models for both type of fuel cell that allow later use when studying 'stacks' have been defined. Thus, the analysis of the results obtained by varying parameters such as pressure, humidity and temperature of operation through the numerical simulation of these systems allows reaching conclusions about the influence of those parameters on the fuel cell performance for different cases.

The atmosphere model used in the simulation is the ISA international standard atmosphere. In the PEMFC H₂/air fuel cell simulations a 1-D model has been used to obtain the curve of polarization and the concentration overvoltage has not been taken into account. The model used to obtain the polarization curve of the DMFC fed with an aqueous solution of methanol and air gives the output voltage of the single cell by using the expression:

$$V = E + V_{\text{act}} + V_{\text{ohm}} + V_{\text{conc}}$$

where E is the Nernst's potential, V_{act} is the activation overvoltage, V_{ohm} is the ohmic overvoltage and V_{conc} is the concentration overvoltage. The developed models have been implemented in Simulink®. Different altitude values have been considered, according to the standard atmosphere conditions corresponding to the usual operating altitudes of various types of commercial UAV. Figure 1 shows the results obtained for the DMFC, when considering the influence that has the cathode pressure variation for a fuel cell operating at 353.15 K.

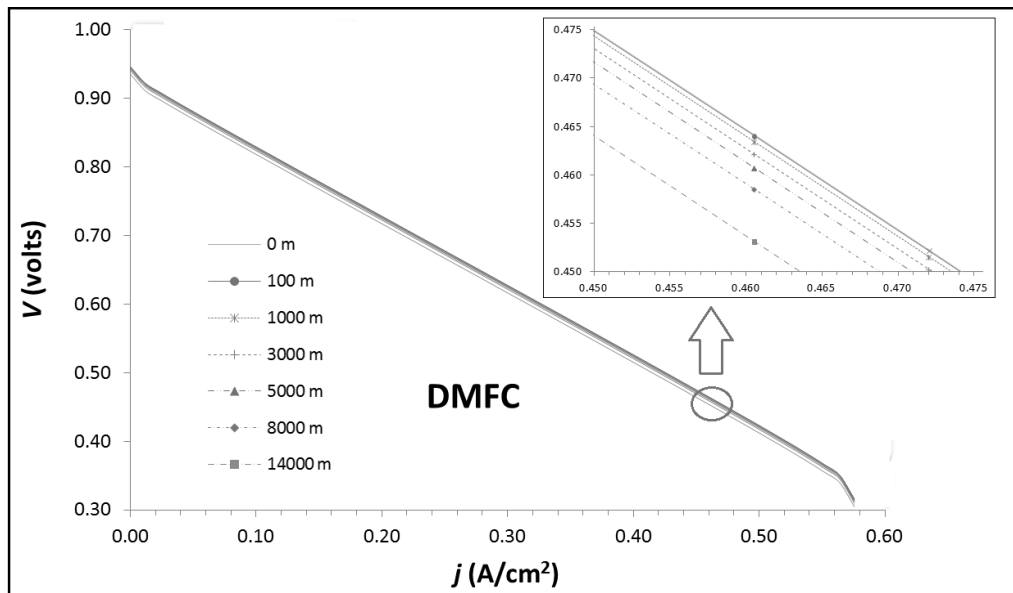


Figure 1. Influence of the supply pressure of the cathode in a DMFC fuel cell behavior.

The operating temperature of the studied fuel cells (PEMFC and DMFC) is a determining factor in their performance, so the output voltage decreases when the temperature does due to an altitude increment. Therefore, the obtained results show that if it is compatible with the weight and autonomy requirements, it is more appropriate to design a system on board an aircraft that maintains a constant optimal operating temperature regardless of the altitude. Moreover, the pressure decrement with the altitude has a harmful effect on the operation of both types of battery, PEMFC and DMFC, being more important on the PEMFC than in the DMFC. For the DMFC case, the temperature influence is by far the most important since it makes the battery voltage practically constant if it remains constant, regardless of the value of the atmospheric pressure, while the PEMFC H₂/air battery behavior is more affected by the value of the atmospheric pressure.

Fuel Cells for UAV(Unmanned Aerial Vehicle) applications (FCA2-5)

María P. Argumosa, INTA

Guillermo Gomez, ISDEFE

Jesús Maellas, INTA

In the last years UAV (Unmanned Aerial Vehicle)-systems have become relevant for civil and military applications. Nowadays there are several research programs in order to deploy new concepts about UAVs. The name UAV covers all vehicles, which are flying in the air with no person onboard with capability controlling the aircraft, so the UAVs concept includes the remote controlled aerial vehicles too.

Although currently civilian UAVs applications, as precision farming, infrastructures maintenance,... , are being rapidly increased, the development of UAVs has been and is strongly motivated by military applications as surveillance, reconnaissance and penetration of hostile terrain without the deployment of human beings in areas of high risk, and for these applications the UAVs need a reduce radar, sound and thermal footprint, so in much cases electric engines are a good solution, but unfortunately batteries and generators – the typical sources of remote power – are not ideal for meeting the UAVs requirements. The batteries have a lower energy-mass rate than other technologies like fuel cells. So the fuel cells could be an available solution to power the UAVs' propulsion system for applications where the endurance will be the main restriction while cost would be a secondary issue, for example the use of UAVs for military surveillance missions.

But not always the fuel cell systems have advantages over the conventional technologies; the vehicle size, power requirements and missions are variable parameters that can affect the challenge of using this rising technology.

In this article the use of the PEM fuel technology to power a mini UAV is analysed, offering a more efficient solution in small size unmanned vehicles with greater endurance. The airplane used in this research is an aircraft of 4 kg MTOW and a wingspan of 4 meters and with an infrared and visible camera, radio modem and video transmitter as payload. Once the electric engine was sized, four energy systems to the engine were simulated and compared between them to a surveillance flight at low altitude. The four studied energy systems were compound of the following elements:

- First system: Only batteries
- Second system: Small battery used to start the aircraft systems and respond to demand peaks, an ultra-light and efficient PEM fuel cell and a hydrogen pressure vessel of 200bar
- Third system: Small battery used to start the aircraft systems and respond to demand peaks, an ultra-light and efficient PEM fuel cell and a hydrogen pressure vessel of 300bar
- Fourth system: Small battery used to start the aircraft systems and respond to demand peaks, an ultra-light and efficient PEM fuel cell and a hydrogen chemical generator.

TRNSYS computer program was used to do the simulations. TRNSYS is a graphically based software environment used to simulate the behavior of transient systems. The vast majority of TRNSYS simulations are focused on assessing the performance of thermal and electric energy systems, but TRNSYS can equally well be used to model other dynamic systems such as traffic flow,

or biological processes too. In this case TRNSYS was used to calculate the energy consumption of an aircraft for a flight at low altitude and calm weather and simulate its energy supply system behavior. The results of the simulations for the four proposal systems justify the use of a PEM fuel cell system in this specific application.

A Polymer Fuel cell stack breadboard development for lunar manned exploration mission (FCA2-6)

Giacoppo Giosue' 1, Matera Fabio¹, Passalacqua Enza¹, Mailland Filippo², Hovland Scott³, Barbera Orazio¹*

¹National Research Council of Italy Institute for Advanced Energy Technologies, Italy

²Compagnia Generale per lo Spazio CGS Spa, Italy

³European Space Agency – ESTEC, The Netherlands

**e-mail: giosue.giacoppo@itae.cnr.it*

A pure hydrogen/oxygen polymer electrolyte of 1 kW power fuel cell stack has been designed manufactured and tested in the framework of an European Space Agency (ESA) study, conducted by an Italian consortium (CGS spa and CNR – ITAE). This fuel cell stack has been envisaged to be applied for lunar manned exploration missions as the primary energy source for both Mobile Vehicles (Pressurized Lunar Rovers, PLR) or Power Plants (Lunar Base, LB), and has been bread boarded in order to demonstrate the technology, measure the performance and test under representative power loads. The following constraints have been considered during the study: i) operation with pure hydrogen and oxygen ii) low humidification level (about 50%) iii) use of commercial MEAs. Developed fuel cell breadboard has been made by two module of 500 W nominal power each @ 80A, connected in series electrically but in parallel from the fluidic point of view. Each module is made up of 10 cells with an active area of 160cm²

As regarding the internal distribution of fluids, the gas and coolant fluids are distributed to the single cells by internal manifolds. Z-shape manifolds were used for the reactants and coolant distributions, for a more homogenous distribution of fluids.

A parallel serpentine flow path was adopted to distribute the reactants over the electrode surface. The geometrical parameters of the serpentine, were calculated using an own developed worksheet. It can determine the geometry of channels (channels width, channels height, land width, number of parallel serpentine) by respecting some geometrical (such as active area dimensions, electrical/open area ratio) and fluid dynamic constraints (flow path pressure drop and channel to channel crossover ratio). Conventional (polarization curves and time test) and specific electrochemical tests (inclined plane tests and 14 days load cycles) were performed to measure the stack performance, evaluate its robustness and define its operative limits.

Regarding the specific tests, they were performed with the aim to verify the compatibility of the developed Breadboard with the reference lunar applications. In particular, the inclined plane tests, were intended to study how the gravity affects the fluid/gases management of the cell. In fact, in a PEM fuel cell, the water is produced at the cathode side and, in a conventional configuration, the water motion direction is perpendicular to the gravity vector. The water, produced on the catalyst surface, that is parallel to the flow field plane, naturally moves towards the flow field channels through the GDL. Depending on the orientation of the flow field plate with respect to the gravity vector, this water motion can be enhanced or inhibited by gravity.

Because the designed fuel cell should operate in an environment with a reduced gravity at variable attitudes (due to the terrain slopes and obstacles, which do not allow for an always flat surface where to move on), it is important to measure the fuel cell sensitivity to the gravity orientation. Therefore, a set of tests at four inclinations has been performed (45°, 90°, -45°, -90°).

Another set of tests, namely 14 days load cycles, were necessary to demonstrate the ability of the breadboard to operate in accordance with some typical PLR load cycles during a of a 14 days mission. During this test the response of the FC stack, in terms of voltage and power, has been evaluated at sudden current load variations. This test comply with a typical PLR 14 days operative mission, complemented by 2 contingency days performed during night, accounting for a total of 16 days operative plan. Three load profiles have been selected taking into account the time spent during travelling could be longer, without interruption, or even shorter with several “starts and stops”.

The developed fuel cell breadboard (fig.1) showed good performance along the whole test campaign (0.75V per cell @500 mA/cm²), even if some failure were observed during the inclined plane tests. The Stack operated well at -45/+45° without significant changes in the overall performance, while some failure happened at -90/+90, where the perforation of some MEAs have been recorded.

The study has demonstrated the high performances of the developed stack and the potential of fuel cell technology for use in future lunar human exploration missions. At the same time, it has highlighted serious criticalities related to the reliability and robustness against the specific space environment of commercially available MEAs, which need to be further investigated in order to push the current technology level to the next step.

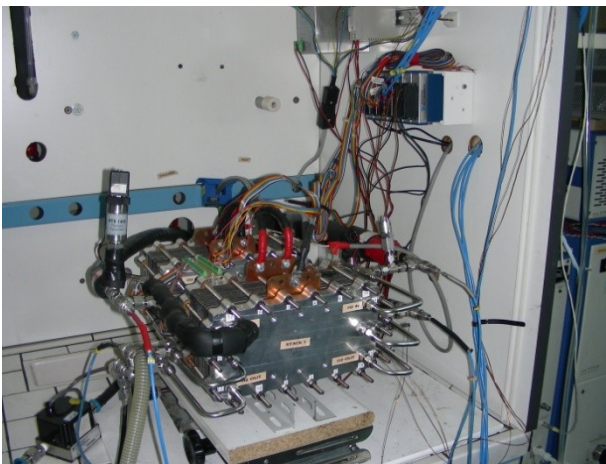


Fig. 1 Developed fuel cell breadboard under testing.

Challenges in PEMFC stack development for mobile and stationary applications (FCA3-1)

Mathias Reum

Proton Motor Fuel Cell GmbH, Benzstrasse 7, D-82178 Puchheim

Proton Motor Fuel Cells is a company designing Polymer Electrolyte Fuel Cell (PEMFC-) stacks and systems since more than 18 years. Besides OEM- and turnkey solutions in the mobile sector and standardized plug-in modules for stationary application, Proton Motor develops and certifies its own fuel cell stack products, the PM200 in the power range of 2 to 9 kW, and the PM400 in the power range of 9 to 30 kW. The tension field connected with the R&D of fuel cell stacks is characterized by performance, lifetime and costs, rendering the release of standardized stack products for our wide field of application a difficult task.

Classically, PEMFC stack development needs to be attended to the application of the fuel cell system. This means that PEMFC stacks will be designed differently when contemplated for a mobile or for a stationary application, respectively. Reasons for this are mainly the very different requirements on lifetime and size (i.e. volume and weight). In mobile fuel cell systems, on the one hand the constrictive packaging limits the dimensional measures of the stack and thus makes high demands on space-efficient cell design in terms of the partitioning between active cell area and media manifolds. Furthermore certain weight restrictions may apply due to the application of the fuel cell system in standard vehicle bodies. Hence, high-performance materials for nominal operation at high power densities are needed to save volume and weight per kilogram. This refers e.g. to metal bipolar plates or membrane electrode units with higher catalyst loading to achieve current densities of more than 2 A/cm². On the other hand, the lifetime requirement in automotive systems is usually lower than in stationary applications. Especially in the field of individual mobility 6'000 h may be enough as a specification, in trucks, light duty vehicles and busses this number might be higher by a factor of three. In the case of non-mobile and non-portable stationary applications, size and weight are not so much compelling parameters than the costs and high endurance of the fuel cell stack. This leads to the picture that fuel cell stacks currently available on the market for stationary power generation are designed for operating at a much lower nominal current density (often below 0.5 A/cm²), which goes ahead with the possible use of much simpler and cheaper stack components. However, stationary current generation is not uniform in its requirement pattern: while lifetimes up to 40'000 h have to be achieved in some cases (e.g. CHP applications), uninterruptible power supply (UPS) applications are connected with long standstill time but very little operating hours. Figure 1 elucidates this context in a graphical display of the tension field connected to PEMFC stack development.

This leads to the conclusion that a company producing PEMFC stacks for mobile and stationary applications should at least design two different product lines adapted to each of the application fields. However, in the current market situation – which is characterized by purchase quantities not even close to the long run marginal costs – it might be advantageous to not split up the quantities ordered from suppliers in different types of membranes, electrodes and different types of bipolar plates. This way it is possible to bring the costs down due to higher order numbers of one stack

product line. This is due to the fact that price degression with the ordered lot is yet the dominating factor on fuel cell stack costs. Proton Motor has shown that it is possible to successfully operate mobile and stationary applications with one stack product line (the PM200 for the smaller power range, and the PM400 for the high power range, respectively), whereas the design modifications on the stack are so insignificant that strong synergies are existing when this stack is going to be used for this or the other application field. Besides providing the opportunity of a better price policy due to higher margins, these synergies furthermore are keeping the R&D expenses down. The result is an affordable, reliable and cost effective fuel cell stack design to bring the fuel cell technology from the demonstration phase to the mass market.

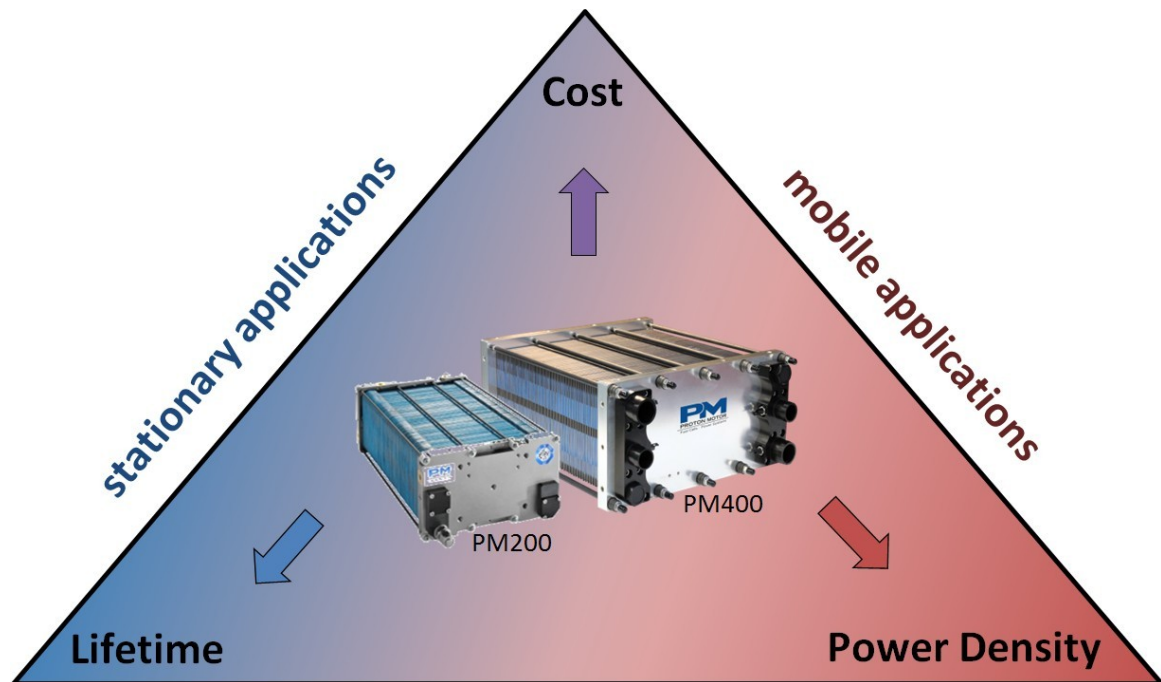


Figure 1: The tension field of Lifetime, Performance and Cost issues with the areas connected to the development of PEMFC stacks for stationary and mobile applications.

Variable Configuration Converter In Stacked Microbial Fuel Cells (MFC) For Optimised Energy Harvesting And Cell Reversal Prevention (FCA3-2)

G. PAPA HARALABOS*, A. STINCHCOMBE*, J. GREENMAN**, C. MELHUI SH* and I. IEROPOULOS*.

* Bristol Robotics Laboratory, University of the West of England and University of Bristol, BS16 1QY, (UK)

** Faculty of Health & Applied Sciences, University of the West of England, Bristol, BS16 1QY, (UK)

Introduction

A microbial fuel cell (MFC) is a bioelectrochemical device that converts biomass into electrical energy. The maximum theoretical open circuit voltage that a MFC can produce is 1.14 V, while the operating voltage is approximately 0.7 V [1]. Stacking of multiple MFC units is one viable way towards maximising electrical energy harvesting [2]. Connecting MFCs in series is the approach to achieve the highest voltage level from a given stack. However, a phenomenon that can occur is the change in the fuel cell's polarity when the internal resistance increases rapidly and the anode's potential becomes positive. This results in cell reversal and becomes a limiting factor on the overall performance of the stack. On the other hand, parallel connection allows for maximum current utilisation without the risk of potential imbalance, but restricts the operational voltage to ~0.7 V and requires amplification from voltage boosting circuitry [3, 4].

An alternative approach is the shifting of electrical configurations during charging by combining a range of all physical electrical connections within a stack. The present study illustrates how a sequential "variable configuration switching" allows to increase charging times and avoid cell reversal by gradually switching from parallel connections to serial connections. Such an approach progressively increases the voltage whilst maintaining a high charge transfer.

Methodology

Small-scale MFC stack

Eight small-scale MFC single chamber reactors with a volume of 6.25 mL each were fabricated from RC25 Nanocure (ceramic-filled photo curable resin) as previously described [5]. Each anode consisted of a 154.8 cm² non-modified carbon fibre veil electrode 5-times folded so as to fit in the chamber. A proton selective membrane (Membranes International, NJ) was used as a separator between the anode and the cathode. Cathode electrodes were prepared with commercially available activated carbon (AC) powder (60±2 mg cm²) mixed with PTFE (20%wt) and then suffused on a 6 cm² 30%wt PTFE treated carbon cloth (Fuel Cell Earth) followed by hot-pressing. The impregnated carbon cloth with AC was then heated to 80 °C. MFC anodes were inoculated with activated sewage sludge (pH 6.9) obtained from Wessex water Scientific Laboratory (Saltford, UK) for the first 14 days of the maturing period and then transitioned to urine. MFCs were operated in fed-batch mode for the whole duration of the experiment and replenished with anolyte (5mL) every 24h.

Variable switching parameters

For configuring the electrical connections between the stack of 8 MFCs, a digital switchbox without any boosting circuitry was developed. The output from the switch box was connected to a super capacitor with ultra-low leakage current (4.2 Volts, 1 Farad) (Murata Electronics, UK) which was charged from 0 to 3 Volts. The controlling and the shifting of connections was manually performed using LabView (NI instruments, UK) software under specific voltage changing points.

8 in parallel from 0 to 0.5 V.

4 parallel elements x 2 in series from 0.5 to 1 V.

2 parallel elements x 4 in series from 1 to 2 V.

8 in series from 2 to 3 V.

The shifting points were chosen based on the maximum voltage that each configuration can provide. Time between switching was approximately 300msec. All experiments were repeated 3 times.

Results and Discussion

Charging under a fixed configuration (8 in series)

Figure 1 shows individual voltages from all 8 MFCs connected in series in the stack whilst charging the supercapacitor from 0 to 3 V. The duration of the charging was approximately 4 hours and 3 MFCs went into reversal for the first 40 minutes of the experiment. After that, the reversed MFCs balanced back to positive voltage and continued to increase their voltage output. Throughout the charging process, current maintained an average level of 135 μ A.

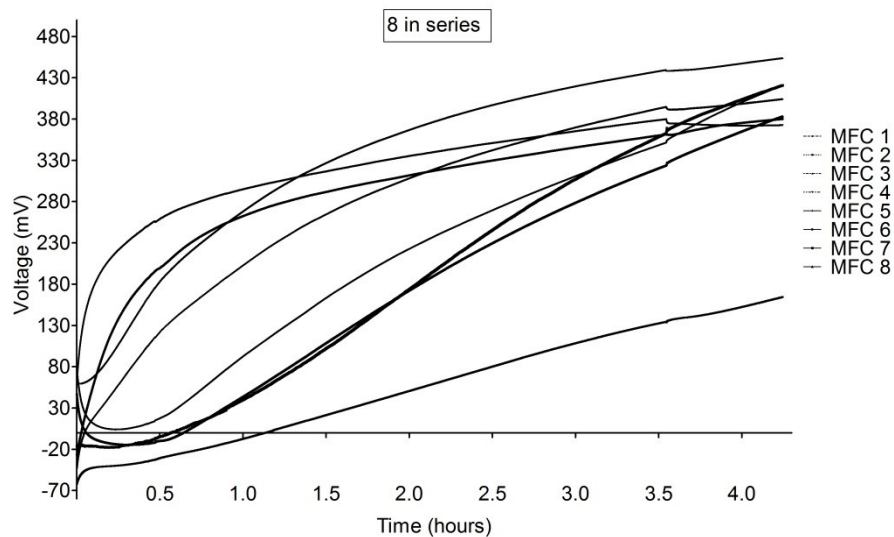


Fig.1. Voltage from individual MFC units connected in series

Charging via variable switching of configurations

When all MFCs were under variable switching mode, the charging lasted approximately 2 hours, twice as fast as the serial formation (Figure 2). The initial charging configuration from 0 to 0.5 V had 8 MFCs in parallel to maximise the current of the stack since the supercapacitor's potential was zero. Configuration was switched to 4 parallel x 2 series and continued charging until 1 V. Then, the configuration was switched to 2 parallel x 4 in series and left charging all the way up to 2 V. From that point all MFCs were connected in series and continued charging until 3 V were reached. Voltage readings showed that all MFCs maintained positive voltage values whilst charging and no cell reversal was observed as in fixed configuration. The average current was $190\mu\text{A}$, 29% higher than that of the serial configuration.

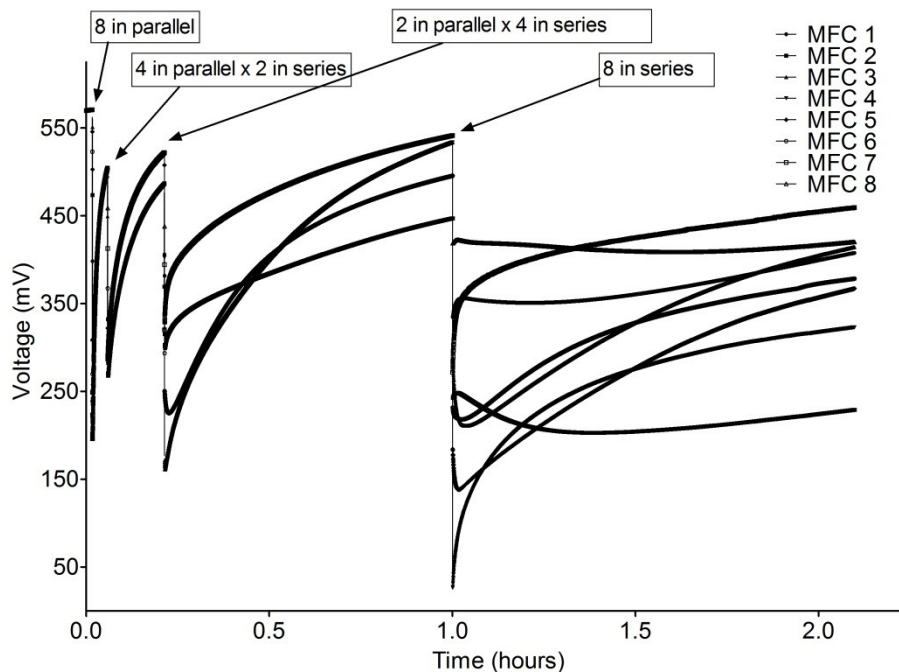


Fig.2. Voltage from individual MFC units during charging, in variable configuration regime

The theory behind the variable switching is to maximise the transfer of the generated charge from the MFC stack into the supercapacitor, by substituting parallel elements for serial gradually within the stack. This leads to faster current flow to the supercapacitor, by maintaining a potential disparity between the stack and the supercapacitor. Furthermore the method of variable switching enhances MFC stacks' robustness by minimising cell reversal without the use of complicated electronics. On-going work is focusing on the development of a MFC stack powered digital switch box, that can automate the stack configuration according to the performance of individual units so as to optimise charging times and maintain the MFCs' performance. Furthermore, it is examining the efficiency of variable switching compared to other means of energy harvesting tools currently available in the literature.

M. T. Madigan, J. M. Martinko, J. Parker, J. Brock *Biology of Microorganisms*; Prentice Hall: Upper Saddle River, NJ, 2000.

P. Aelterman, K. Rabaey, H. T. Pham, N. Boon and W. Verstraete, Continuous Electricity Generation at High Voltages and Currents Using Stacked Microbial Fuel Cells. *Environ. Sci. Technol.*, 2006, 40, 3388–3394.

Y. Kim, M. Hatzell, A. Hutchinson and B. Logan, Capturing power at higher voltages from arrays of microbial fuel cells without voltage reversal. *Energy Environ. Sci.*, 2011,4, 4662-4667

M. Alaraj, Z.J. Ren, J.-D. Park , Microbial Fuel Cell Energy Harvesting using Synchronous Flyback Converter, *Journal of Power Sources* (2013), doi: 10.1016/j.jpowsour.2013.09.017.

I. Ieropoulos, C. Melhuish, J. Greenman, I. Horsfield, EcoBot-III: a robot with guts. In: Fellersmann H, Dorr M, Hanczyc M, Laursen LL, Maurer S, Merkle Daniel, et al., editors. *Proceedings of the Alife XII Conference*; 2010 Aug 19e23; Odense, Denmark. London: MIT Press; 2010. p. 733e40.

Electrolyser real-time control using the techno-economic optimization software Odyssey (FCA3-3)

C. Bourasseau¹, B. Guinot¹, A. Chatroux¹, P. Mayoussier¹, M. Lopez¹

1CEA-LITEN/DTBH/ L2ED, 17 rue des Martyrs, 38054 Grenoble, France,

INTRODUCTION

Hydrogen from water electrolysis powered by renewable energy is a promising alternative for electricity storage, automotive fuel or for industrial applications. Due to the diversity of renewable power sources, applications and technologies, the control strategies of H₂ production and storage systems plays a critical role in the technical and economical (TE) optimization of such systems.

In order to test and compare storage technologies and control strategies for hybrid systems, CEA-LITEN has recently developed its own modeling and simulation tool called Odyssey for Optimization & Design of hYbrid Storage Systems for rEnewable energy. This software was proven of a great interest for the fine TE evaluation of storage systems, in particular when it comes to quickly compare several control strategies for a 20 year operation period of time. However, although it is necessary to identify the best strategy for an electrolyzer, it is essential to make sure that the real system is operated accordingly.

DESCRIPTION OF WORK

The approach in this contribution was to create a direct link between a long term TE evaluation and a system operational command by using the same software tool for both functions. To do that, the techno-economic evaluation software Odyssey was upgraded to be also used as a real-time control tool for a commercial 5 Nm³/h PEM electrolyzer. The methodology (illustrated in fig.1) to demonstrate the functionality of this control consisted in the following four steps: (i) experimental characterization of the electrolyzer, (ii) modeling, (iii) simulation and (iv) experimental validation.

First, the electrolyzer, specifically instrumented for this purpose, was finely characterized in order to model it within the software. A great care was taken to identify and dissociate energy consumption from auxiliaries and from the production stacks. Then, a H₂ system composed of a Renewable Energy source, the PEM Electrolyzer and a Hydrogen Storage was modeled to represent a specific application of green hydrogen production by water electrolysis for industrial use. Once the system was fully modeled, three different control strategies were implemented and simulated behaviors of the system were compared. For this specific application (green hydrogen production), the objective was to fill an industrial hydrogen storage in a given period of time (1week) while optimizing the revenues of the installation obtained by selling electricity on the EPEX Spot Day Ahead market. Electricity prices and available power fluctuating over time, the optimal control strategy has to maximize both on-time hydrogen storage delivery and revenues from injected electricity into the grid when prices are high. The first strategy would give priority to the hydrogen production. The second strategy would give priority to the electricity sell when price is above 65€/MWh and third strategy would be an advanced strategy based on storage state of charge and time to delivery. Besides the electrolyzer model, the important entry data were the intermittent power source profile,

three different strategies. The first strategy, which was giving priority to H₂ production, was able to deliver full storage on-time but electricity sell revenues were limited because the electricity usage (H₂ production vs. grid injection) was not optimized. For the second strategy, which imposed electricity sell when market price is above a threshold value, higher revenues were observed but the strategy was not able to ensure full filling of the storage. Finally, the third strategy, more advanced because taking into account the state of charge of H₂ storage, the time to delivery and the electricity market price, showed good revenues and ensured on-time delivery of hydrogen.

Following the simulation work, the techno-economic software was used to directly control the 5 Nm³/h electrolyzer based on the calculations realized for each algorithm.

To make the simulation software able to send set point commands to the electrolyzer, a specific communication network was built in order to allow data exchange between the different systems. Then, for the three different control algorithms, real-time control of the electrolyzer was realized and comparison between experiment and simulation was done. It was shown that behavior of the electrolyzer was in agreement with the simulation and that measured experimental data were very close to simulated data. The observed error between experimentation and simulation and for both power consumption and hydrogen flowrate was less than 2%. Simulated and experimental evolutions of SOC (state of charge) are represented in Fig.2. In this figure, the available power is represented on the left axis and the H₂ storage state of charge evolution for the three strategies is shown is represented on the right axis. Three different evolutions of state of charges are represented for the three implemented strategies.

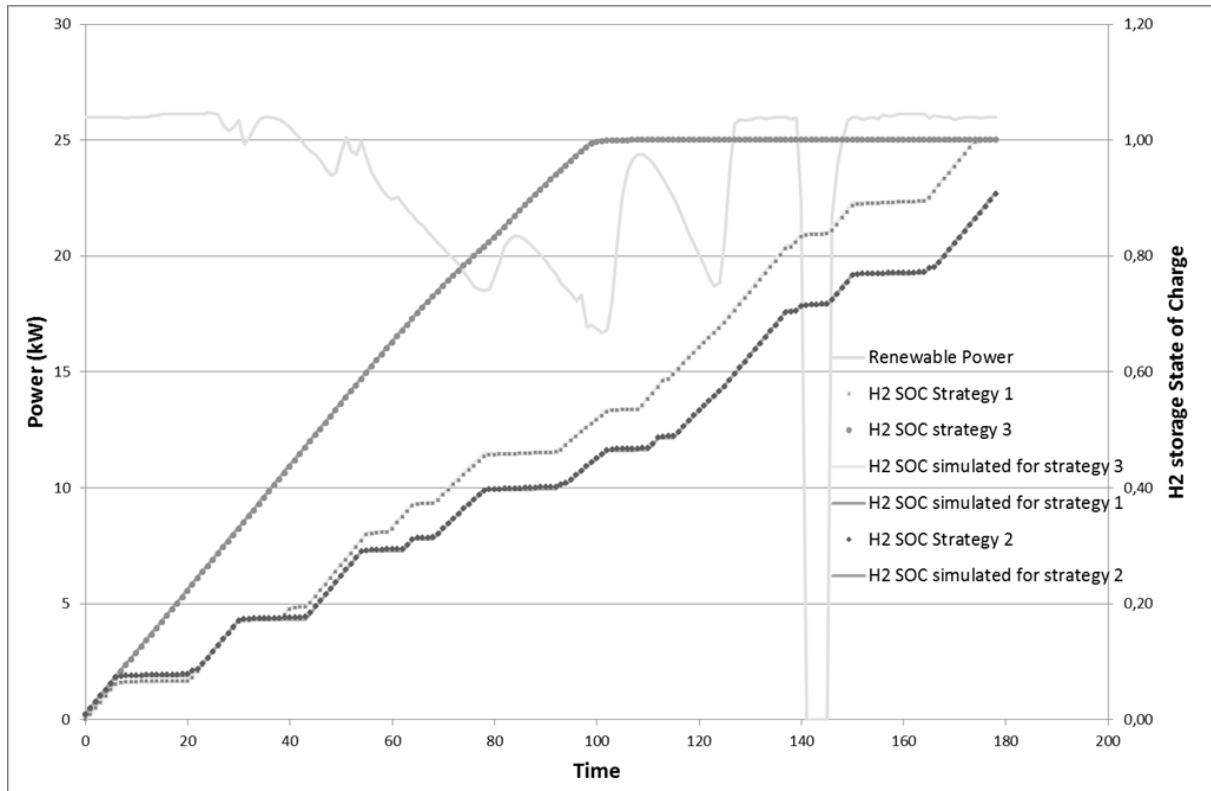


Figure 14 - Experimental results: H₂ storage SOC evolution

CONCLUSION

The four-step approach used here consisting in (i) characterization, (ii) modeling, (iii) simulation and (iv) experimental validation could be generalized to any industrial hybrid system in order to ensure that it is controlled as imagined by TE studies. In this work also, operational command of the electrolyzer using the well proven TE software Odyssey was demonstrated and good correlation between experimentation and simulation data was shown. Using the same software for both long term techno-economic evaluation and real-time control allowed for quick validation of strategies and this gave great confidence in the simulation results. Finally, this work also confirmed the important impact of electrolyzer control strategy on TE optimization for a specific industrial hydrogen application.

Investigations on a solid oxide cell after 6100 h operation in electrolysis mode (FCA3-4)

F. Tietz^a, M. Al Daroukh^{a,*}, J. Schefold^b, A. Brisse^b, D-N. The^c, M. Schröder^c

^a Institute of Energy and Climate Research (IEK-1), Forschungszentrum Jülich GmbH, D-52425 Jülich, Germany

^b European Institute for Energy Research (EIFER), Emmy-Noether-Strasse 11, D-76131 Karlsruhe, Germany

^c Institute of Physical Chemistry, RWTH Aachen University, 2 Landoltweg, 52056 Aachen, Germany

* Corresponding author. Tel.: +49 2461 614440; fax: +49 2461 612455; E-mail address: m.al.daroukh@fz-juelich.de (M. Al Daroukh)

Abstract

An electrode-supported solid oxide cell (SOC) was operated for 6100h with a current density of -0.75 A/cm² at a temperature of 780 °C indicating high stability and low voltage increase of 11 mV/kh. The cell consists of a 10 μm thick solid electrolyte (yttria-stabilised zirconia; YSZ) and a diffusion barrier layer of gadolinia-substituted ceria (CGO), a Ni/YSZ cermet as hydrogen electrode and as mechanical support, and a La_{0.58}Sr_{0.4}Co_{0.2}Fe_{0.8}O₃ perovskite (LSCF) as oxygen electrode. The electrodes as well as the YSZ and CGO layers were deposited on the electrode support by screen-printing.

Post-test analyses were performed showing no significant changes in microstructure compared to the initial state. Investigations by means of scanning electron microscopy (SEM), transmission electron microscopy (TEM), energy dispersive X-ray spectroscopy (EDS) and selected area electron diffraction (SAED) indicate material transport from the oxygen electrode into the diffusion barrier layer and pore formation at the cathode/electrolyte interface.

Keyword: SOEC, degradation, post-test analysis

Introduction

Climate change and production of clean energy will play more and more a major role in the near future. High prices of conventional energy sources associated with high contamination level from carbon dioxide emissions push renewable energy to the focus of research. Solid oxide electrolysis allows high electrical-to-chemical energy conversion which makes it very attractive for hydrogen production in the case waste heat is available and high temperatures can be achieved without significant additional system costs.

Although the technology is already well established for solid oxide fuel cells, the opposite current flow for solid oxide electrolysis causes a higher voltage difference between anode and cathode and hence higher driving forces for degradation processes.

In the recent years, many efforts were made to understand the degradation mechanisms occurring in solid oxide electrolysis cells (SOECs), e.g. [1]. Knibbe et al. [2] already reported

degradation phenomena like pore formation along grain boundaries in the electrolyte and Tietz et. al. [3] in addition, mass transport and formation of a dense layer at the CGO/YSZ interface, partial decomposition of anode particles and destabilization of the cathode.

In this present work an SOEC operated for of 6100 h has been analysed after the test and its degradation mechanism will be discussed.

Results

Fig. 1 shows the voltage curve during operation applying a current density of -0.75 A.cm^{-2} . The voltage increases over the entire experiment with a rate of 11 mV/kh , i.e. with a degradation rate of $1\%/kh$. This degradation value corresponds to the needed low voltage increase which makes solid oxide electrolysis stable enough for commercial application. The microstructure of the cell (Fig. 2) revealed the high stability of all layers after 6100 h of operation. Compared to the initial state, only the SrZrO_3 formation in the interlayer between electrolyte and CGO-layer seem to be extended, which might have increased the resistance and thus caused the degradation value of the cell.

Compared with former long-term tests as reported earlier [3], no pore formation at the grain boundaries of the electrolyte or within the electrolyte grain could be detected here. This means that even short electrolysis periods without steam supply cause more severe degradation phenomena than long operation periods with permanent steam supply.

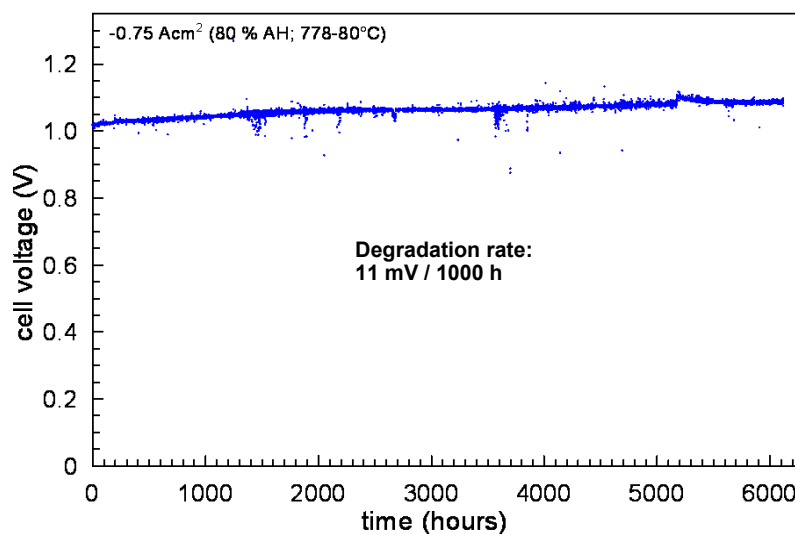


Fig. 1: Cell voltage during operation with $j -0.75 \text{ Acm}^{-2}$.

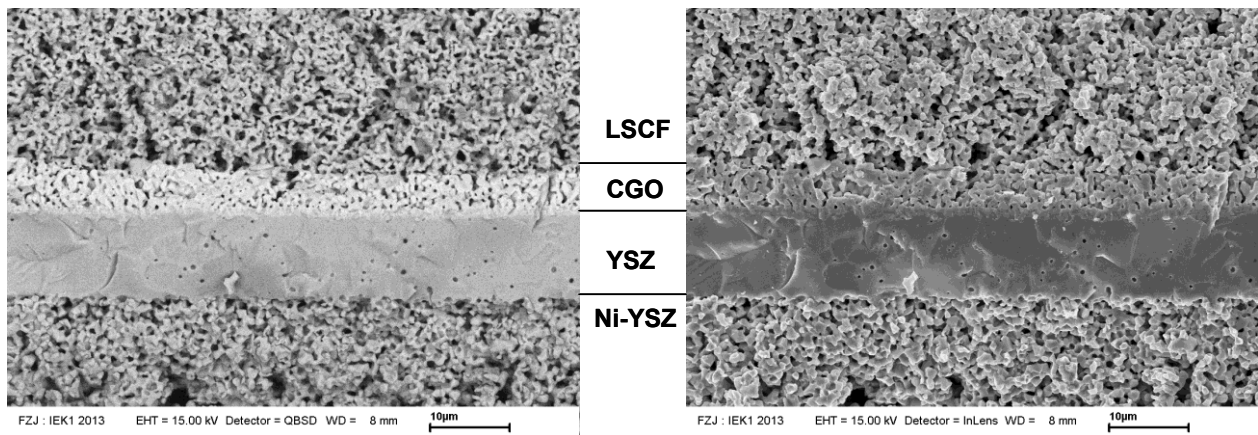


Fig. 2: Microstructure of the tested SOEC. From top to bottom: LSCF anode, CGO diffusion barrier layer, YSZ electrolyte, Ni/YSZ cathode.

References

- [1] R. Knibbe, A. Hauch, J. Hjelm, S. D. Ebbesen, M. Mogensen, *Green 1* (2011) 141-169
- [2] R. Knibbe, M. L. Traulsen, A. Hauch, S. D. Ebbesen, M. Mogensen, *J. Electrochem. Soc.* 157 (2010) B1209-B1217
- [3] F. Tietz, D. Sebold, A. Brisse, J. Schefold, *J. Power Sources*, 223 (2013) 129-135

Hydrogen Thermophysical Properties Database Compiling a New Equation of State and Correlations Based on the Latest Experimental Data at High Temperatures and High Pressures (FCA4-1)

Naoya Sakoda^{1, 2, 3}, Ryo Akasaka⁴, Satoru Momoki⁵, Tomohiko Yamaguchi⁵,
Kan'ei Shinzato³, Masamichi Kohno^{1, 2, 3}, and Yasuyuki Takata^{1, 2, 3}

¹ Department of Mechanical Engineering, Kyushu University, Fukuoka, Japan

² International Institute for Carbon-Neutral Energy Research (WPI-I2CNER), Kyushu University,
Fukuoka, Japan

³ Research Center for Hydrogen Industrial Use and Storage (HYDROGENIUS), Kyushu University,
Fukuoka, Japan

⁴ Department of Mechanical Engineering, Kyushu Sangyo University, Fukuoka, Japan

⁵ Graduate School of Engineering, Nagasaki University, Nagasaki, Japan

Accurate thermophysical properties of hydrogen over wide temperature and pressure ranges are essential in the coming hydrogen society. The development of fuel cell vehicles (FCVs) is one of the most promising key technologies for hydrogen utilization in order to reduce greenhouse gas emission, and the storage pressure of FCVs has been increased up to 70 MPa to expand the cruising range. Hydrogen refueling stations and infrastructures for FCVs requires higher-pressure hydrogen, and for the efficient design of them, accurate thermophysical properties of hydrogen at temperatures and pressures up to 500 °C and 100 MPa are of great importance. The thermophysical properties of hydrogen are sometimes roughly calculated from the ideal-gas equation of state (EOS), $P = \rho RT$, where P , ρ , R , and T denote the pressure, density, gas constant, and temperature, respectively. However, for instance, at 50 °C and 70 MPa, the difference of density calculated from the ideal-gas EOS and the latest multi-parameter EOS for hydrogen developed based on experimental data reaches 40 %, and the ideal-gas EOS is not applicable to the design of FCVs and hydrogen stations. The coefficients of multi-parameter EOSs are generally determined by fitting existing experimental data. However reliable experimental data of hydrogen are insufficient at high temperatures and high pressures, and at present the thermophysical properties in the range are extrapolated from the data at low temperatures.

In the present study, PVT (Pressure-Volume-Temperature) property, viscosity, and thermal conductivity of hydrogen up to 500 °C and 100 MPa were measured with originally developed apparatuses, and based on the obtained data, a new EOS and correlations were developed [1-3]. The EOS is a virial type, and the functional form is formulated as $Z(T, \rho) = 1 + B(T)\rho + C(T)\rho^2 + D(T)\rho^3$, where Z is the compressibility factor. B , C , and D denote the second, third and fourth virial coefficient, respectively, and they are functions of temperature. The other thermodynamic properties such as internal energy, enthalpy, entropy, and heat capacity are derived from the EOS according to the thermodynamic relations, but the calculations are usually hard to be performed because of complicated differentials and integrals. Moreover, in the actual calculations, the known properties are not always the independent variables of the EOS, temperature and density. For instance, it is necessary to derive temperature from known pressure and entropy for a calculation of compression work when hydrogen is compressed by a booster. In this case, many iterative

computations are required to find the solution. Therefore, an easy platform to calculate the thermophysical properties is desired for industries.

We developed a hydrogen thermophysical properties database based on a thermophysical properties database of PROPATH [4]. The developed database compiles not only a new EOS and correlations but also previous EOSs as a reference. Figure 1 summarizes the relationship among the measured data, EOS, and database. The database is available via Website, MS Excel, and Mathcad. Figure 2 shows an example of an application of the database working in MS Excel for a calculation of the compression work in the hydrogen station in Kyushu University. When the database is installed, original functions to calculate the thermophysical properties are added, and are easily available for users without any difficulties.

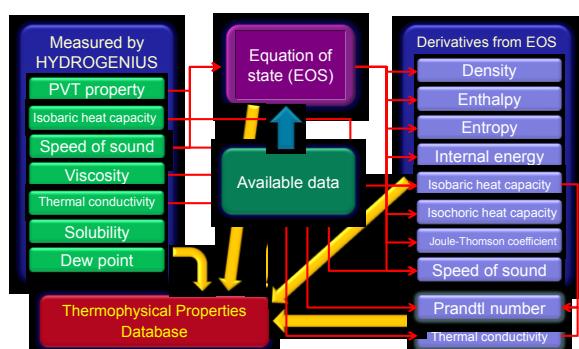


Fig. 1 Relationship among the measured data, EOS, database.

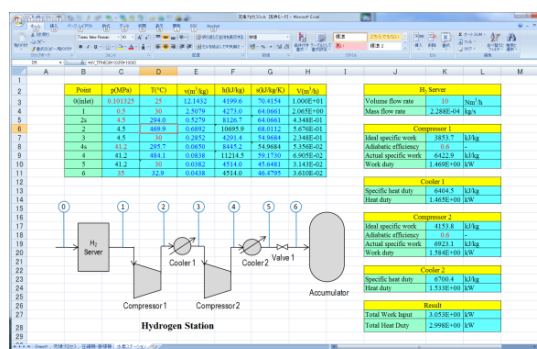


Fig. 2 Application for a calculation of the compression work in the hydrogen station in Kyushu University.

Acknowledgement

This research has been conducted as a part of the "Fundamental Research Project on Advanced Hydrogen Science" funded by New Energy and Industrial Technology Development Organization (NEDO).

References

- [1] N. Sakoda, K. Shindo, K. Motomura, K. Shinzato, M. Kohno, Y. Takata, M. Fujii, Int. J. Thermophys., 33, 381 (2012)
- [2] E. Yusibani, P. L. Woodfield, K. Shinzato, M. Kohno, Y. Takata, M. Fujii, Jpn. J. Thermophys. Prop., 24, 21 (2010)
- [3] S. Moroe, P. L. Woodfield, K. Kimura, M. Kohno, J. Fukai, M. Fujii, K. Shinzato, Y. Takata, Int. J. Thermophys., 32, 1887 (2011)
- [4] PROPATH Group, A Program Package for Thermophysical Properties of Fluids (PROPATH) Version 13.1 (2008)

Back-Up Systems For Telecommunications Installations Using Fuel Cells (FCA4-2)

Enrique García García, Luis Muñoz Sebastián

Iberdrola

One of the main problems facing those responsible for guaranteeing the continuity of telecommunications services is keeping the telecommunications network in operation in the event of lack of electricity supply in the public grid.

Stationary batteries and Diesel Groups have been used traditionally to allow communications systems to continue operating in the event of lack of power supply. The former supply the stored energy as direct current for a period of time limited by their capacity and charge level, while the latter keep all the AC-supplied equipment running, generally for long periods of time, based on the capacity of their fuel tanks. In this case, communications equipment, which is mostly supplied with alternating current, relies on the operation of the rectifiers.

This type of solution cannot be applied directly to installations with space limitations, and therefore alternative solutions need to be found to guarantee the conditions of supply and, consequently, service continuity.

As an alternative solution, five years ago IBERDROLA opted for the use of fuel cells (PEM) at major radio repeater stations with reduced space and up to 1 kW of direct current electricity usage. Because of the importance of keeping in operation the access repeaters that guarantee the power distribution grid's operation through the remote control system, we put in place an implementation plan that has resulted in 19 installations in operation today, with one or two units being added every year.

Compared to the alternative solutions, they offer competitive advantages such as small dimensions, direct DC supply, service availability and the capacity to maintain the power supply for days.

The drawbacks include power limitation and the difficulty in supplying hydrogen.

Power limitation is closely related to the cost of both implementation and operation of installations of more than 1 kW, and in the case of radio stations the use of this technology is, in our opinion, impracticable due to the associated costs.

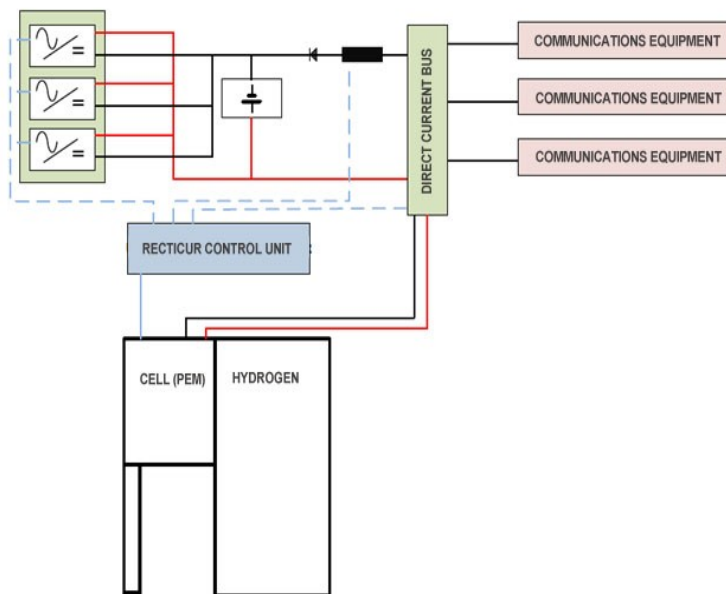
Supply difficulty associated on the one hand with the small distribution network of gas manufacturers, and on the other hand with the difficulty in accessing many sites where supply is needed, which in many cases increases the operation costs, since as a matter of prudence the cylinders need to be replaced while they still contain a significant amount of gas.

The PEM open-cathode cell technology used has proved to be an ideal solution for application at stations where the requirements are similar to those of IBERDROLA:

- Minimum runtime of 72 hours.
- Power up to 1 kW.
- Occupied space less than 4 m².
- Supply voltage – 48 Vdc.
- Switching on/off through external contact.



As a complement to the operation of existing commercial cells, all of which offer the possibility of voltage start, IBERDROLA, in partnership with the company RECTICUR, has developed a control unit external to the cell that enables its operation to be controlled based on the electrical parameters of the station where it is located, optimising the operation of both the batteries and the cell, while supervising the condition of the battery and of the associated rectifier.



Autonomous solar-hydrogen-battery power supply for remote emergency telecommunication stations (FCA4-3)

Bahman Shabani, John Andrews

School of Aerospace, Mechanical, and Manufacturing Engineering, RMIT University, Melbourne, Australia

This paper investigates the feasibility of using hydrogen storage in conjunction with a photovoltaic (PV) array and batteries to provide a robust and reliable standalone power supply for remote wireless telecommunications stations used in southeastern Australia by the Victorian Government's fire and other emergency communication system. Electrical load profiles on an hourly basis throughout a year were constructed for three typical remote installation configurations as follows: Minimal sites: peak demand 0.11 kW; average daily demand 0.077 kW; Medium sites: peak demand 0.18 kW; average daily demand 0.147 kW; and Full remote radio communication sites: peak demand 0.20 kW; average daily demand 0.156 kW, used in a real Fire Contingency Network (FCN). These profiles were assembled using available data on the power demand and hours of usage of the equipment installed at each of these sites during the off-season, burn and fire season, and during large incidents.

Four different standalone energy supply systems to meet these demands at the three types of FCN sites were investigated using the HOMER software: A solar-hydrogen system, with PV panels as the main source of electricity supply and hydrogen used to store energy on both a short-term and long-term basis; A solar-battery system, with a battery bank used for short and long-term storage; A solar-battery-diesel system, with a diesel generator plus a smaller battery bank used to provide the back-up supply to the PV array; and A solar-hydrogen-battery system, as for system 1, but with the addition of a small energy capacity battery bank to complement the hydrogen storage, particularly in meeting short-term energy storage needs. The hydrogen storage subsystem modelled in this study utilised a solid-state PEM electrolyser and fuel cell, and low-pressure hydrogen gas storage (up to 20 bar) in LPG type gas cylinders.

Cost, reliability and greenhouse gas emission impact are three key factors considered in order to determine a suitable stand-alone power supply system for the FCN sites studied. In particular, considering the critical role of these sites in emergency burn and fire events an uninterrupted year-round supply has to be guaranteed. Clearly the lowest cost option that meets all the operational requirements is advantageous. In addition, it is the low greenhouse gas emission option is always favourable from the environmental perspective.

Table 1 summarises the key findings from the analyses performed on different power supply systems that can be used (or currently in use) in FCN sites investigated in this study. The findings help compare these different systems and facilitate a guide through choosing the suitable system to be employed in such sites. This table clearly suggests that using hydrogen-based energy storage arrangement will make the whole power supply system to be considerably cheaper than those using batteries as both long-term and short-term energy storage. The maintenance costs was found to be a key factor in determining the overall cost of both solar-battery and solar-hydrogen systems. Basically

the loads to be normally supplied in such FCN sites are quite small (e.g. ~ 4 kWh per day with 0.2 kW peak in full sites); however, the sites, which are usually located in remote areas with no easy access, have to be regularly visited for maintenance purposes, disregarding the size of the load to be supplied. Hence the high costs of these visits would appear in the cost of the small daily load to be supplied and considerably adds to the unit cost of electricity supplied in such sites. Solar-battery systems are assumed to be visited at least four times per year (as suggested by the current operator) while hydrogen-based energy storage systems are inherently of lower maintenance such that the required annual maintenance visits of four (for battery systems) can be reduced to two or even one visits per year (two visits per year was assumed in these analysis). Considering 10-15 days of autonomous operation (e.g. due to unexpected weather condition, or fire events), the study is also suggesting that the battery bank is another element which considerably contributes in the high costs of solar-battery systems compared to solar-hydrogen systems. By using hydrogen as the energy storage medium the need for such a large battery bank is eliminated and the hydrogen system may costs about half of that needed to purchase such an oversized battery bank.

Reliability is another essential factor to be considered in choosing a suitable power supply system for FCN sites. Battery health status is always difficult to predict, that is why the sites using batteries as energy storage solution should be frequently monitored and visited in order to confirm the health status of the batteries in use. Moreover, batteries performance is very sensitive to the climate condition such that their charge and discharge pattern can be considerably affected in very cold or hot climate conditions; and this adds to the unpredictability level of their already unpredictable lifetime expectancy. Due to this problem and also in order to cope with unpredicted period of PVs' output unavailability (e.g. extended period of cloudiness), some sites use back-up diesel generators to ensure uninterrupted power supply in case of batteries' failure and the PVs' output absence. However, there are also some degrees of unreliability associated with these generators, mainly due to the fact that diesel fuel has to be supplied to the sites and the supply of fuel cannot be guaranteed at all times (e.g. harsh climate condition or fire events). The hydrogen equipment lifetimes (i.e. fuel cell and electrolyser) are much reliably-predictable than batteries. This is the main reason that hydrogen-based energy storage system has to be visited less frequently than batteries. Apart from the economic benefit of this life expectancy reliability, which has just been discussed, such a lifetime predictability will make the system more reliable than batteries (with or without diesel generator back-up).

Table 1. Cost and reliability comparison between the FCN power supply systems analysed

System		Average unit cost of electricity (\$/kWh) based on NPV	Reliability Rating	GHG emission Impact	Additional notes
Solar-Battery	Minimal	18.2	*	Zero emission	About 55% of the total annual load is supplied through the fuel cell and the rest by the PVs
	Medium	12.1			
	Full	11.3			
Solar-Battery-Diesel Gen	Minimal	18.8	**	Emissions from diesel fuel	About 55% of the total annual load is supplied through the fuel cell and the rest by the PVs. The diesel generator is an extra degree of reliability to cover unexpected period of PVs' unavailability
	Medium	11.9			
	Full	10.9			
Solar-H2	Minimal	10	***	Zero emission	Just above 50% of the total annual load is supplied through the fuel cell and the rest by the PVs
	Medium	6.7			
	Full	6.4			
Solar-H2-Battery	Minimal	11.2	****	Zero emission	About 20-25% of the annual load is supplied through the batteries and about 30% and 45-50% is supplied by the fuel cell and PVs respectively
	Medium	7.1			
	Full	6.7			
Reliability Rating Guide:					
*	Satisfactory		***	Very Good	
**	Good		****	Excellent	

On the basis of the HOMER simulation modelling conducted, and the unit cost assumptions made for the system components and annual maintenance, it was found that the solar-hydrogen would yield lower average unit cost of electricity over a 25 year period (e.g. 6.4 \$/kWh for full FCN sites) than the solar-battery (11.3 \$/kWh for full FCN sites) and solar-battery-diesel systems (10.9 \$/kWh for full FCN sites), in present value terms at 5% real discount rate. However, the findings are suggesting (Table 1) that adding a small battery bank (just to meet the diurnal storage demand of the system as shown in Figure 1 and provide no more than three days of autonomous operation), can make the system more reliable while adding to the overall cost of the system negligibly (e.g. 6.7 \$/kWh for full FCN sites compare to 6.4 \$/kWh for solar-hydrogen systems). In case of the PV array's output unavailability the solar-hydrogen-battery system can rely on both batteries and hydrogen system which in turn this is more reliable than when there is only hydrogen system to cover the PVs' unavailability. Moreover, by adding a small battery to the solar-hydrogen system, the fuel cell and electrolyser would need to operate for less number of hours (45% and 75% for the FCN cases respectively) which prolong their lifetime and hence makes the system more reliable.

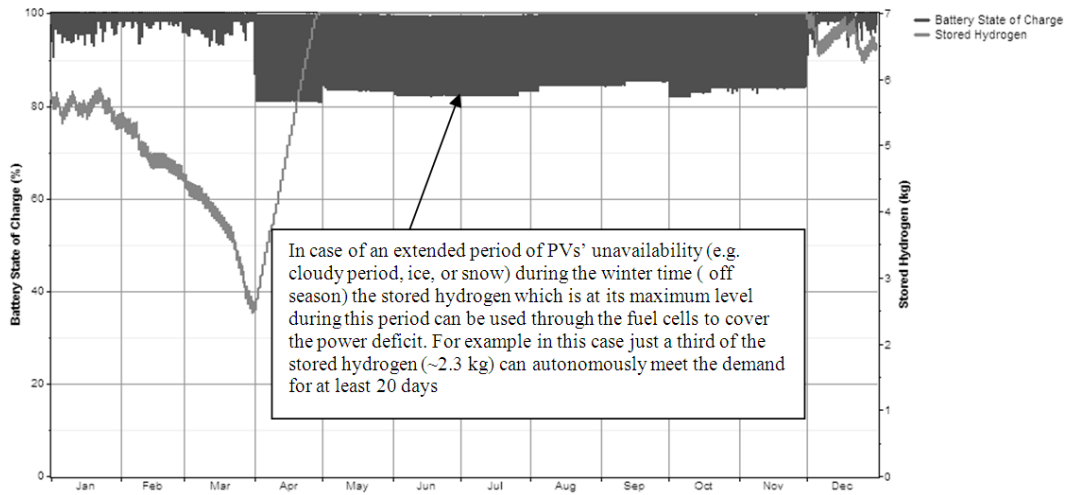


Figure 1. The variation of hydrogen level and battery state of charge in a solar-hydrogen-battery system sized for a full FCN site

Hydrogen storage in the geological underground – a first analysis of options for erection and operation (FCA4-4)

*Dr. Maurice Schlichtenmayer (ESK GmbH, Freiberg, Germany) and
Dr. Sebastian Bohnes (RWE Power AG, Essen, Germany)*

Hydrogen is a highly attractive energy carrier for storing renewable energies and is currently used as a resource in a number of industrial applications. Depending on its intended usage different forms of hydrogen storage are required, which are currently in various stages of research or implementation. Especially for the long-term storage of large amounts of hydrogen the storage in the geological underground is widely regarded as a highly attractive option due to its inherently large capacities, low estimated costs and a high level of technological maturity. Open questions, however, remain in terms of the eligibility of geological structures for hydrogen storage and the available equipment for underground and surface installations and in terms of the economic viability. In this context the conversion of existing gas storages for hydrogen storage can be a technologically challenging task with a great cost reduction potential. This work compares several options for the erection of an underground hydrogen storage facility with respect to the technological and economic viability in order to support an efficient implementation of large-scale, long-term hydrogen storage capacities.

In the present work, first, a context is defined in which an underground hydrogen storage facility is operated. It includes a variable hydrogen inflow (based on the market-driven operation of a hypothetical electrolyzer with a power of 500 MW_{el}) and a constant hydrogen demand, both at individually specified temperature, pressure and purity. In a second step, the main geological parameters are derived for the three major geological structures used for underground gas storage, aquifers, depleted hydrocarbon deposits and salt caverns, in order to meet this demand. Critical factors are identified that may inhibit to realization or safe operation of a storage facility on specific locations. Additionally, the surface facilities including compressor, pre- and post-conditioning and station piping are designed for hydrogen as a corrosive and highly diffusive storage medium compared to natural gas. Three major scenarios are possible for the erection of a complete storage facility: Green field (undeveloped location, requires extensive geological surveying and erection of infrastructure before building of the plant), brown field (developed location, requires less geological surveying, infrastructure already existent) and the conversion of an existing underground gas storage (like developed location, additionally, some existing facilities can be reused, is mainly relevant for salt caverns). Finally, the cost and time for the erection of a hydrogen storage facility designed according to the defined requirements are compared for the types of suited geological structures with respect to these three scenarios.

In general, hydrogen can be stored underground either in porous rock formations

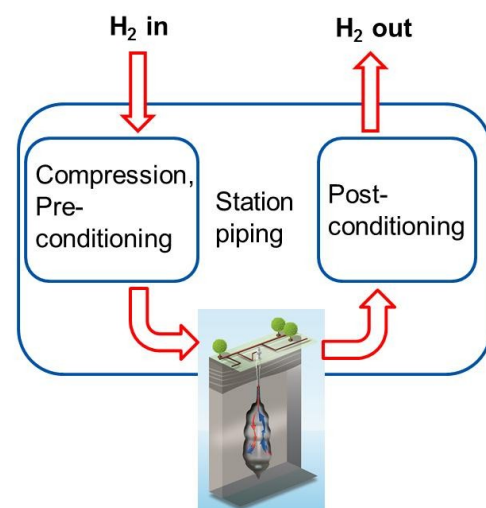


Figure 1: General layout of a hydrogen storage cavern

(mainly aquifers and depleted hydrocarbon deposits) or in large underground cavities like salt caverns and abandoned mines. Of all these options salt caverns seem to be most suited for hydrogen storage, since they best fulfill the requirements for gas tightness and possess a low risk for microbiological or geochemical reactions. Especially, microbiological activity in the formation fluids can pose a significant threat to all installations, since they usually are highly vulnerable to hydrogen sulfide, which can never be fully excluded in the presence of pure hydrogen as soon as a certain level of activity is reached.

It is shown that the needs of the generated hydrogen storage load curve can be met by either a single cavern or a two-cavern storage system depending on the geological possibilities for the size and depth of the caverns. The expected costs of the complete storage facility vary heavily depending on the existing infrastructure and the possibilities for conversion of an existing gas storage cavern. The option with the lowest costs is the conversion of an existing cavern in a well-developed location including necessary modifications on existing surface facilities. Costs can more than double in a non-developed location. Similar variations occur in the time demand for the erection of a storage facility, ranging from 4 years for the cavern conversion on a developed location to 11 years for the erection of a new facility including cavern leaching and erection of the leaching infrastructure.

The results of this analysis show that especially the conversion of decommissioned natural gas caverns for hydrogen storage is a highly cost and time efficient option to create large storage capacities for a future hydrogen market.

Simulation And Experimental Evaluation Of Operating Modes In A Hydrogen-Based Microgrid (FCA4-5)

L. Valverde-Isorna, F. Rosa, F.J. Pino, J. Guerra

Grupo de Termotecnia, Dpto. de Ingeniería Energética, Universidad de Sevilla

Abstract

The aim of this paper is to study and evaluate operating modes in a renewable energy microgrid with hydrogen as intermediate energy storage medium. The operating modes are conceptually defined based on the literature review. A simulation tool developed by the authors in a previous work is performed over three scenarios chosen for their representative value (clear day, intermittent irradiance and moderate wind). By a set of key performance indicators defined in this paper, we evaluate and quantitatively analyze the operating modes. The conclusions drawn from the simulation stage allow determining which modes are more appropriate from technical and practical standpoint when implementing in a “real” microgrid. Finally, selected operating modes are evaluated in a pilot plant.

INTRODUCTION

Government enacted rules are driving the adoption of Renewable Energy Sources (RES) in major countries. Twenty-nine states in USA have established electricity mandates to produce between 20 to 33% from renewables by 2020 according with [1] while EU's 20-20-20 mandate is leading the adoption in Europe. Wind and solar energy, in particular, are the most mature technologies. However, the inherent intermittence of any RES can further hinder the economic competitiveness of those resources. Then, energy storage will become an integral element of the removable adoption strategy in order to mitigate the instability of grid.

Although R&D strategies are funding a wide range of solutions, hydrogen as a storage medium has received much attention because of its flexibility along excellent chemical properties. Hydrogen differs from the conventional idea of energy storage, it separates the hydrogen production, storage and use. In the so-called Hydrogen Based Energy Systems (HBES), electrolyzers provide wind/solar peak shaving producing hydrogen from water, becoming the main solution to RES penetration. Later a fuel cell uses the hydrogen to quickly respond to load demand. In addition of being used in fuel cells, hydrogen production can be used for other purposes, such as fueling vehicles or it can be distributed through gas pipelines network.

A critical point in HBES is the Operating Mode (OM). Recent works focus the attention in the importance of control strategies and operating modes [2], [3], [4], [5]. Indeed, HBES efficiency is strongly dependent on the manner through which the equipment are operated. Moreover, the experience gained from demonstration projects around the world draws the conclusion that OM strongly affects the equipment lifetime. Then, in order for the technology to mature and scale up, a deep study in system operation is needed. Key performance indicators and experimental tests presented in this paper, attempt to address this gap.

DEFINITION OF OPERATING MODES

This section deals with the definition of the operating modes for hybrid hydrogen microgrids with hydrogen and batteries as intermediate storage. Some of the OM have been found in the literature and the rest have been defined in this work. OM can be classified according to technical criteria or economic criteria.

The operating modes defined here are:

MODE 1: Power demand tracking (MINDIFF) [6]. In this mode, the control minimizes the difference between power produced and demanded. Efficiency, operational constraints or economic criteria are not taken into account.

MODE 2: Hydrogen production priority (MAXH2). In this mode, any surplus power is directed to the electrolyzer. More common for long-term storage facilities or hydrogen refueling stations.

MODE 3: Battery protection (PROTEC BAT). This operating mode attempts to protect the batteries from intensive use by holding the drawn power constant. Electrolyzer and fuel cell work at variable power

MODE 4: Fuel Cell (FC) protection (PROTEC FC). In this case, the fuel cell operates at rated power. The system seeks to protect this equipment while the electrolyzer and batteries operate at variable power.

MODE 5: Electrolyzer (EZ) protection (PROTEC EZ). The electrolyzer works at rated power, protecting the equipment from intensive use. Therefore, the fuel cell and batteries absorb the wind/solar variability.

MODE 6: Maximum efficiency (MAX EFF). This mode attempts to operate the electrolyzer and fuel cell at their maximum efficiency, neglecting to absorb the whole energy excess and other factors. The maximum efficiency set-point is calculated taking into account both, the dc/dc power electronics and electrolyzer/fuel cell efficiency curves.

Thus, the different modes have advantages and disadvantages. Their pros and cons are studied by means of simulations and experimental tests.

KEY PERFORMANCE INDICATORS

Due to the literature gap in assessing the performance and operating quality of hydrogen microgrids, in this work, we have defined the following Key Performance Indicators (K.P.I) which enables a quantitative benchmark of the different operating modes.

- Percentage of non-satisfied demand (%NSD)
- Fuel Cell and Electrolyzer number of start-stop events (START-STOP ez|fc)
- Percentage of unused energy from renewables (%UNE)
- Hydrogen storage level (MHL)
- Batteries state of charge (SOC)

- Fuel Cell and Electrolyzer running time (tfc,tez)
- Hydrogen produced/consumed ratio (rH2)
- Fuel Cell and Electrolyzer operating constraint alarm event (e-Alarm ez|fc)
- Fuel Cell and Electrolyzer average efficiency (η_{ez} , η_{fc})
- Efficiency of the energy path (η_{path})
- Plant operating cost (O&M C)

SIMULATION TOOL

An overall system-scope model which includes all the interconnected equipment for HBES long/medium-term calculations was developed in [7]. This model was validated with experimental data gathered from a pilot microgrid plant designed, built and operated by the authors and described in 0. The experimental results demonstrated a good fitting with the model outputs. This tool has been used in the present work for the simulation stage. Table 1 is shown as example of the numerical results obtained.

SIMULATIONS

In this section we present the numerical simulations carried out to study the plant behavior under different external conditions (weather and demand). The results are summarized in tables for convenience, showing the key performance indicators.

Simulation conditions:

- Generation profile: “clear day”.
- Energy produced by the renewable energy: 15.93 kWh
- Energy demanded by the load: 14.77 kWh
- Simulation time: 24 hours.
- Initial conditions of storage devices: SOC=50%, MHL=50%

Table.1. Simulation results for photovoltaic source in high irradiance conditions. 24 hours of operation.

Indicator	%NSD	START-STOP (ez fc)	%UNE	MHL (%)	SOC (%)	Tez Tfc (h)	rH2	e-ALARM (ez fc)	η_{ez} , η_{fc}	η_{path}	O&M C (€)
MIN DIFF	0	2 1	0.85	36.5	40	5.02 4.62	0.488	4 1	67.41 50.75	79.20	4.422
MAX H2	0	2 1	0	24.5	40	8.38 7.05	0.429	8 4	68.2 50.19	74.70	4.707
PROTEC BAT	6.753	2 7	5.099	31.55	40	6.75 7.46	0.481	7 5	68.01 54.14	63.89	8.734
PROTEC FC	0	2 3	0.8	31.08	40	5.021 3.19	0.401	4 4	67.41 48.88	68.28	7.3
PROTEC EZ	0	2 1	0.8	30.81	40	5.23 5.69	0.438	2 4	66.44 48.87	67.51	4.69
MAX EFF	8.6	2 1	16.11	39.47	40	6.78 5.28	0.416	2 2	72.57 53.59	65.44	3.460

The results drawn from the quantitative comparison allow to obtain a set of OM with better performance. The selected OM are then tested in the experimental platform.

EXPERIMENTAL INVESTIGATION

Experimental set-up

Figure 1 shows the lab-scale hydrogen-based microgrid installed at the School of Engineering (University of Sevilla, Spain). The system was specifically designed for testing control strategies and operating modes. This MG comprises a 1 kW PEM electrolyzer, a 1.5 kW PEM fuel cell, 7Nm³ metal hydride for hydrogen storage and a 367 Ah battery bank as main components. An electronic load and electronic power source are used for emulating generation and demand profiles. Finally, a PLC manages the whole plant while a commercial computer allows implementing the diverse OM.

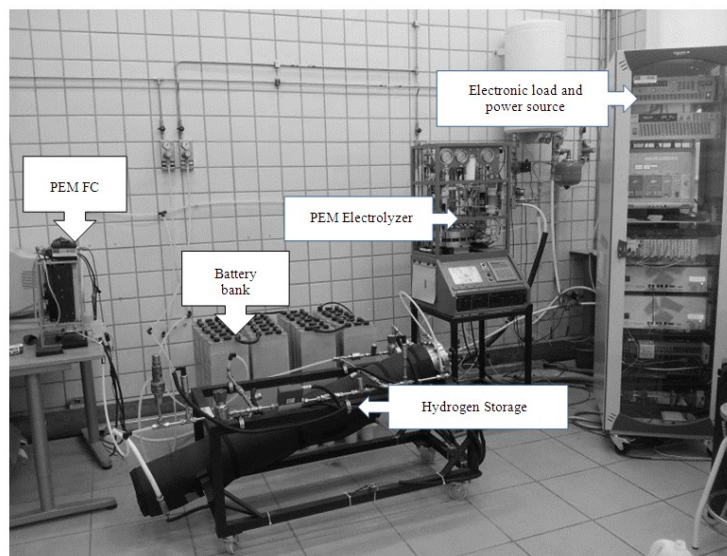


Figure 15. Laboratory-scale microgrid comprising electrolyzer, fuel cell, hydrogen storage (metal hydride), battery bank and the electronic power source and load.

Experimental results

In this section the experimental results gathered from the plant operation through the selected operating modes are shown and discussed. Every test was schedule for 24 hours operation time. The data were sample at every 41 seconds. Figure 16 shows a sample of the experimental results obtained from the plant operation. In this case, the graph shows the results under the operation mode called “Maximum Efficiency” in a windy day.

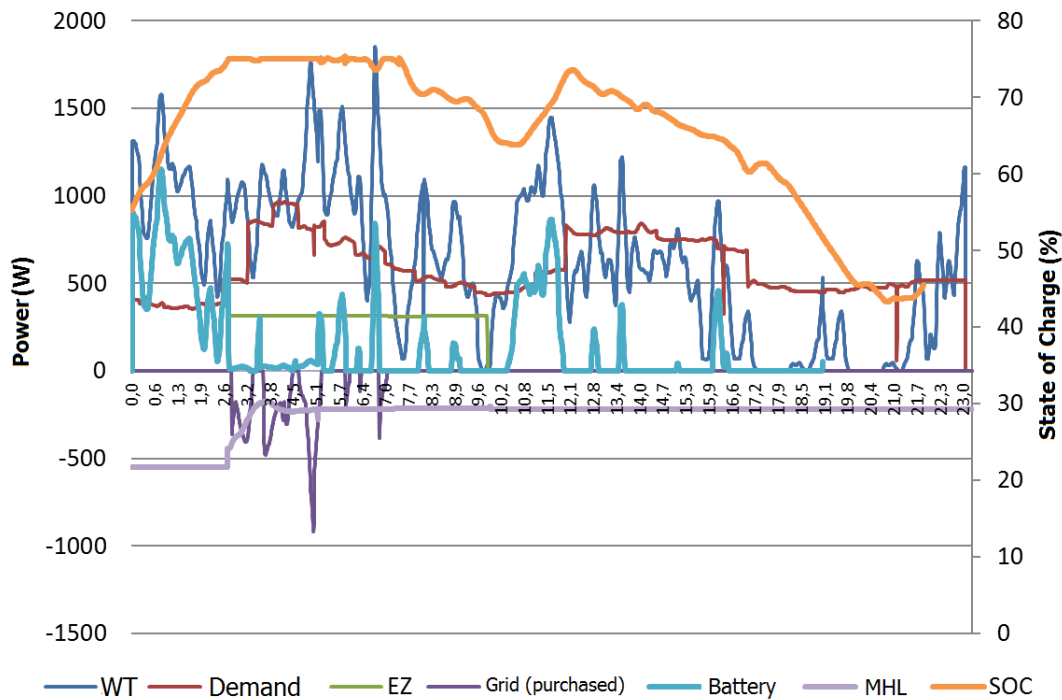


Figure 16. MG operation under MAX EFF operating mode over windy day. Electrolyzer/power converter working at maximum efficiency set-point (300 W).

CONCLUSIONS AND FUTURE WORK

According to the study results, depending on the external conditions certain modes have improved performance than others. External conditions such as weather, energy demand and the state of charge of storage devices among others. The analysis of KPI leads us to conclude that some OMs are better for certain “situations” and others mustn’t be used. The results were conclusive: modes that operate with variable power reached better efficiency rates but required an intensive use of the equipment. On the other hand, operation modes that work with steady power achieved better economic indicators as a result of reduced equipment intensive use, but the drawback is lower efficiency in the plant operation.

These experimental results are coherent with the simulation predictions. As future work, a new “multi-mode” control system which would operate the plant under selected operating modes, depending on the external/internal status, would be advisable.

REFERENCES

- [1] Institute for Energy Research, “The Status of Renewable Electricity Mandates in the States” 2011.
- [2] Ulleberg Ø., “The Importance of Control Strategies in PV-hydrogen Systems,” *Solar Energy*, n^o 76, pp. 323-329. 2004

- [3] Ulleberg Ø et al., "Hydrogen Demonstration Project Evaluations," IEA-final report, 2007.
- [4] Valverde L., Ali D., Abdel-Wahab M., Guerra J., Hogg D., "A technical evaluation of Wind-Hydrogen (WH) demonstration projects in Europe" POWERENG2013, Istanbul, 2013.
- [5] Ipsakis D., Voutetakis S., Seferlis P., Stergiopoulos F., Elmasides C., "Power management strategies for a stand-alone power system using renewable energy sources and hydrogen storage," International Journal of Hydrogen Energy, nº 34, Pages 7081-7095, 2009.
- [6] Pino F.J PhD dissertation, Análisis de Sistemas Integrados de Producción de Hidrógeno a partir de Energía Eólica. Aportaciones al modelado dinámico de sistemas., Sevilla: Universidad de Sevilla, 2010.
- [7] Valverde L., Rosa F, del Real A.J., Arce A., Bordons C. "Modeling, simulation and experimental set-up of a renewable hydrogen-based domestic microgrid," International Journal of Hydrogen Energy,, vol. 38, nº 27, pp. 11672-11684, 2013.

Assessment of Sustainability of the Direct Peroxide/Peroxide Fuel Cell (FCA4-6)

Ayşe Elif SANLI; Turgut Ozal University, Engineering Faculty, Electric&Electronics Engineering, Ankara, TURKEY

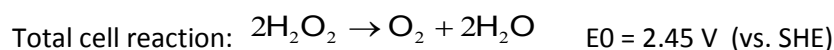
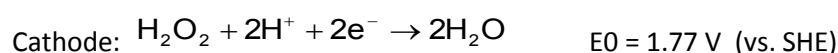
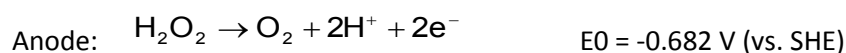
Aylin AYTAÇ, Gazi University, Faculty of Science, Department of Chemistry, Teknikokullar, Ankara, TURKEY

ABSTRACT

FCs have been considered one way to achieve sustainable development in the world because of a) their high efficiency, b) low emission of pollutants, c) effective reduction of greenhouse gas (CO₂), d) process simplicity regarding energy conversion, e) few moving parts and f) extremely low noise. Proton-exchange-membrane fuel cells (PEMFCs) have the disadvantage of being expensive, which makes commercialization difficult. The greatest contribution to the cost of the fuel-cell stack comes from the electrodes. Platinum electrodes constitute approximately 77% of the cost of fuel-cell stacks.

Additionally, the use of pure hydrogen is relatively difficult in transportation and electronic equipment due to transport and storage safety concerns in both small and large quantities. However, fuel-cell systems that use liquid fuels have been recognised as having the potential to complement batteries and show promise in becoming a useful technology for mobile and portable power supplies. Liquid fuels can be directly used as anode fuels to power fuel cells and provide higher theoretical electrochemical potentials and reactivities compared with gaseous hydrogen (Table 1). These competitive technologies therefore provide an important benchmark in terms of cost and performance.

The liquid fuels currently used in fuel cells and their by-products are hazardous to humans and to the environment. However, if safe and reliable liquid fuels can be developed, fuel-cell technology would be considered relatively 'green'. Fuel choice is a critical issue because fuels should be non-toxic and easily handled, generate minimal pollution, and be produced from renewable resources under mild conditions. An even more desirable outcome would be if the by-products could be removed, recycled or converted to safer materials. Hydrogen peroxide is non-toxic, does not bioaccumulate and does not deplete finite resources. We believe that 'low-concentration basic peroxide' should therefore be called a 'green fuel'. The renewability of liquid fuels is also an important principle of green-fuel-cell design. Aside from exhibiting favourable performance properties and manageable waste products, fuel-cell systems must be cost-effective, reliable, made from readily available materials, sustainable, and broadly applicable. Hydrogen peroxide, as a basic fuel and oxidant, and direct peroxide/peroxide fuel cells (DPPFCs), as a novel electricity-production system, come very close to meeting these challenges of green technology. The cell reactions and standard potentials for a direct peroxide/peroxide fuel cell are as follows:



Fuel cells using peroxide present unique advantages and features as summarised in Table.2 [1].

In our study, a power density of 10 mWcm⁻² at a cell potential of 0.55 V have been achieved with a direct peroxide/peroxide fuel cell (DPPFC) composed of carbon-paper-supported nickel (Ni/CP) as the anode catalyst and carbon-paper PbSO₄ (PbSO₄/CP) as the cathode catalyst. The catalysts have been prepared by electroless deposition. Using non-precious metals rather than platinum in our fuel cell makes the cell cost effective comparable to that of PEMFCs. Additionally, as a low-price fuel, hydrogen peroxide reduces the cost of this fuel cell.

Table I. Comparison of fuels for fuel cells in terms of their theoretical free energies, efficiencies and energy costs.

FUELS	Theoretical free energy	Fuel cost		Electrical efficiency	Energy cost
Hydrogen	32.9 kWh kg ⁻¹	6.9 \$/kg	H ₂ /O ₂ FC	91% *	² 200 \$/kW
H ₂ /H ₂ O ₂	3000 kWh kg ⁻¹		H ₂ /H ₂ O ₂ FC	40-55 ¹ %	
Hydrazine	5.4 kWh kg ⁻¹	³ 3 \$/ton	DHFC	100% *	-
Hydrazine/peroxide ⁴	2272 kWh kg ⁻¹		DHPFC		
Methanol	3.3 kWh kg ⁻¹	10.2 \$/kg	DMFC	97% *	⁵ 6 \$/kW
Methanol/peroxide	9.2 kWh kg ⁻¹		DMPFC	40 ¹ %	
NaBH ₄	9.3 kWh kg ⁻¹	55 \$/kg	DBFC	91% *	⁵ 10.2 \$/kW
NaBH ₄ /H ₂ O ₂	2800 kWh kg ⁻¹		DBPFC	⁶ 60%	
Hydrogen peroxide	478 Wh kg ⁻¹	1.8 \$/ton	DPPFC	⁷ 6 %	⁸ 1.84 \$/kW

* Theoretical conversion

¹ From Spakovsky [8]

² From Eaves [9]

³ Wuhan Xingzhengshun import & export trade Co

⁴ From Luo [10]

⁵ From J.W.We [11]

⁶ From Miley [12]

⁷ From Sanlı [6]

⁸ From Disselkamp [13]

Table II. Advantages and disadvantages of DPPFCs.

		Description
Advantages of DPPFCs	1. Green fuel/oxidant	H ₂ O ₂ used in fuel-cell applications is a safe and environmentally friendly oxidant. It is a liquid at standard temperature and pressure. H ₂ O ₂ has none of their associated environmental problems such as fast vaporisation, extreme toxicity, toxic waste, exploitation. H ₂ O ₂ can be considered a 'green fuel/oxidant' because of its stable, non-toxic by-products and ease of handling in plastic containers at a concentration of 35 wt% in water
	2. Abundant chemical	Hydrogen peroxide is an abundant and inexpensive chemical (< \$1/kg). Auto-oxidation is the most widely used method for the synthesis of H ₂ O ₂ . It can be generated by electrolysis using solar-panels as an environmentally method.
	3. Cost-effective fuel	The direct peroxide/peroxide fuel cell does not need platinum in its anode or cathode. DPPFC is cost-effective due to the low cost of its fuel and catalyst material.
	4. Simple system design	The advantages of using liquid fuels are the ease of engineering, low system size and weight, and simple membrane hydration [5]. Because of using the liquids in the system, there is no need to air, compressors, humidifiers, cooling plates.
Disadvantage of DPPFCs	1. Fuel cell performance	The only disadvantage of this system is the low performance of the peroxide/peroxide fuel cell due to <ul style="list-style-type: none"> • the anodic reaction kinetic • limited peroxide concentration

REFERENCES

- C.Song, Catalysis Today, vol. 77, pp. 17-49, December 2002.
- H.J. Stone, Ph.D. Thesis, Batelle Memorial Institute, May 26, 2005.
- E.J. Carlson, P.Kopf, J.Sinha, S.Sriramulu, Y. Yang, (Subcontract Report) TIAX LLC December 2005, Cambridge, Massachusetts.
- A. Kundu, J.H.Jang, J.H.Gil, C.R.Jung, H.R. Lee, S.H.Kim, B.Ku, Y.S.Oh; J. Power Sources, vol. 170, pp. 67-78, June 2007.
- Umit B. Demirci, J. Power Sources, vol. 169, pp. 239-246, June 2007.
- M. R. von Spakovsky, B. Olsommer, Energy Conversion and Management, vol.43, pp. 1249-1257, 2002.
- S. Eaves, J. Eaves, J. Power Sources, vol. 130, pp. 208–212, May 2004.
- N.Luo, G.H. Miley, K.J.Kim, R.Burton, X.Huang, J. Power Sources, vol.185, pp.685-690, 2008.

Recuperation of Exhaust Energy via Hydrogen Production Using a Steam Reforming Process – Fuel Saving Strategies for Natural Gas Combustion Engines (FCA5-1)

Dipl.-Ing. Ulrich Dehof 1; Dr.-Ing. Sven Wenzel1; Dipl.-Ing. Joerg vom Schloss1 ; Dipl.-Ing. Dominik Pennings2; Dr.-Ing. Kurt Imren Yapici2

1 Oel-Waerme-Institut, Kaiserstr. 100, 52134 Herzogenrath, Germany

2 ECC Automotive, Tulpenweg 4, 52249 Eschweiler, Germany

The increase of electrical efficiency is an important development task for CHP unit design. In order to optimize the energetic and economic fuel exploitation, thermal energy of exhaust gas can be used for hydrogen production. Steam reforming highly qualifies to recuperate thermal energy of flue gas. Being used as a heat sink, the reformer generates a hydrogenous fuel gas, in which thermal energy is chemically bound within reactions of the reforming process. Therefore the rejected heat of internal combustion engines can be used in parts to energetically enrich the combustible gas before being consumed in the engine. In combination with the reforming process, the exergetic efficiency of the engine enhances significantly. By running the combustion engine at duty points of constant exergetic output, more than 20 % fuel gas can be saved.

The Oel-Waerme-Institut and ECC Automotive collaborate in order to exploit this potential for natural gas combustion engines. Applied as CHP, it cogenerates heat and power to supply apartment houses or small districts. The system, being set up for testing, consumes 60 to 80 kW of combustible gas. General aim of design is to gain a maximum power-to-heat ratio.

The focus of the presented work lies within the macroscopic analysis of system components and their arrangement to each other. An analysis tool has been set up to simulate mass- and energy-flows of diverse system designs. Constrains such as operating conditions of the combustion engine or material strength data pile up to fixed boundarie, in which system designs are simulated. Parameter variations of temperature, pressure and specified effectiveness factors help to compare and evaluate the system design.

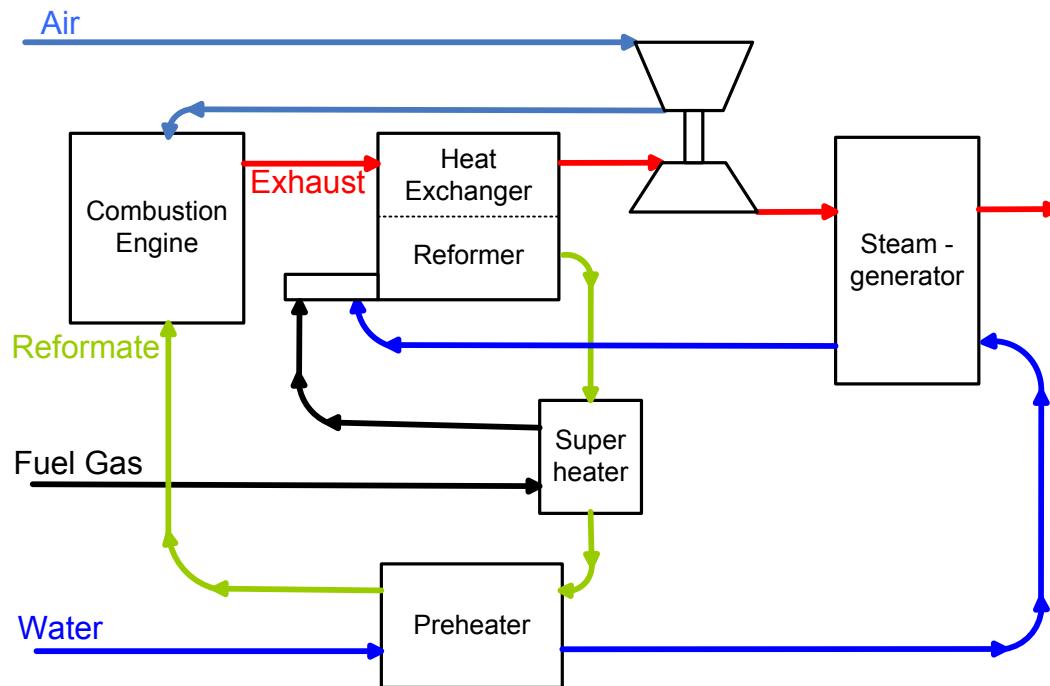


Figure 17: Fuel gas conditioning for combustion engines using steam reforming

The system design presented in the figure appears rather promising. Within simulations of conservative adjusted conditions, it still provides a 15 % fuel saving potential at minimum. Getting mixed with a water steam flow, the fuel gas reaches the reactor, in which a heat flux is extracted from the exhaust gas and partly bound within the reactions of the reforming process. In order to maximize the exergetic performance of the combustion engine, a turbo charger should be integrated into the system. The residual thermic potential of the exhaust gas suffices to generate steam out of water and can be used for further heating matters beyond. Thus, the energy balance is closed.

During further project-procedure components such as the reformer and the especially designed combustion engine get tested on test facilities, which are to be completed to a thoroughly integrated system step by step. Results of detailed performance tests will be compared with those of the simulation model.

Exergy analyses of hydrogen-based energy storage systems comparing utilization of pure and methanated hydrogen in combined cycle power plants and fuel cell μ -CHP units (FCA5-2)

Mario Ludwig¹, Christoph Haberstroh^{1,2}, Ullrich Hesse^{1,2}, Antonio Hurtado^{1,3}

1 TU Dresden, Boysen-TUD-Graduiertenkolleg, 01069 Dresden

2 TU Dresden, Bitzer-Stiftungsprofessur für Kälte-, Kryo- und Kompressorentchnik, 01069 Dresden

3 TU Dresden, Professur für Wasserstoff- und Kernenergietechnik, 01069 Dresden

The goal of a sustainable energy infrastructure in Germany requires the dominant sources of electric power to be hydro, biomass, wind or sun. Since hydro power and biomass are limited by Germany's landscape and amount of arable land, wind and sunlight need to provide the majority of electricity. But they provide their energy intermittently and independently of need and therefore require long term and high capacity storage systems. A favorable energy carrier to provide this appears to be hydrogen generated through electrolysis.

In this work an exergy analysis of five thinkable storage systems is executed. The hydrogen is considered to be generated by large scale, central polymer electrolyte membrane (PEM) electrolyser plants. Afterwards there are four different paths to be considered: direct on-site storage in a salt cavern, injection into the natural gas grid up to a certain volume percentage, reaction with carbon dioxide to methane and following injection into the natural gas grid and establishing a hydrogen gas grid. The generated gas is then used as fuel in a combined cycle gas turbine or it is used in a PEM fuel cell micro combined heat and power unit.

Since the storage system is supposed to be used for fluctuating wind and solar power, the plants will rarely operate at their maximum capacity. Instead they will have to follow the load curves for both excess and lack of power in the grid. To account for this the conducted exergy analysis is considering one year of part-load operation.

Simulation

The process chains are simulated in MATLAB. Electrolysis, compression, methanation, reforming and the fuel cell are simulated with self-programmed code while the combined cycle is simulated with Thermoflows programs GTPro and GTMaster.

The PEM electrolysis and fuel cell (PEMFC) are simulated using their respective polarization curves calculated with characterizing parameters [1]. Both operate at 80 °C while the electrolysis cell is pressurized at 30 bar and the fuel cell operates at atmospheric pressure. The optional reformer is considered to use catalytic partial oxidation and the following reformat cleaning is done by single-stage water gas shift and preferential oxidation to reduce carbon monoxide content [2] [3].

For Methanation CO₂ is considered to be used as reactant. The reactor is simulated using zero dimensional mass and energy balances given by the Sabatier reaction. It is considered to be catalyzed by Ru nanoparticle-loaded TiO₂ which gives 100 % yield already at a low temperature of only 200 °C [4].

The compression of hydrogen and methane is considered to be done with multi stage reciprocating compressors.

The amount of admixing hydrogen in the natural gas grid in Germany is defined as 2 vol% (volume percent). This limit needs to be raised in order to use the grid for energy storage. In the following analysis a gas turbine operated with 30 vol% hydrogen and 70 vol% methane is considered.

To simulate the CCGT the Siemens SGT5-4000F is chosen due to its high power and efficiency. In general in order to use hydrogen as a gas turbine fuel the burner needs to be adjusted, the NOx emissions need to be kept below the allowed legal limits and the turbo machinery needs to be operated in its operating envelope [5] [6]. Since conventional NOx flue gas treatment was shown not to be sufficient, steam injection from the low pressure steam turbine into the burner is considered.

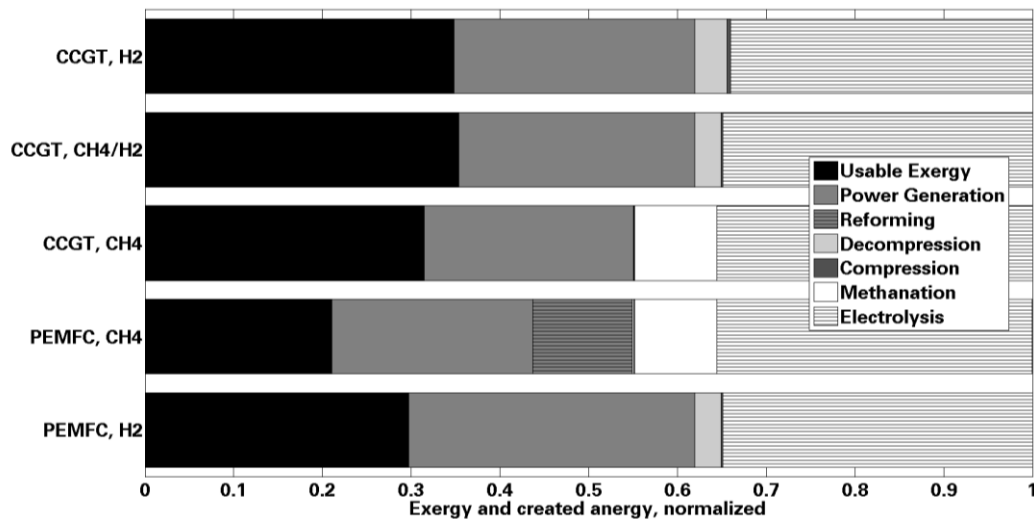


Figure 1: normalized exergy and energy for the single energy conversion steps at full load

CCGT, H2: hydrogen storage on-site in 200 bar salt-cavern, no district heating;

CCGT, CH4/H2: injection of hydrogen into 80 bar grid, fossil methane not included, district heating;

CCGT, CH4: methanation and injection into 80 bar grid, district heating;

PEMFC, CH4: methanation and injection into 80 bar grid, district heating;

PEMFC, H2: injection into 80 bar hydrogen grid, district heating

To keep the turbo machinery in its operating envelope the nozzle area of the turbine guide vanes was increased.

The load profiles needed to simulate operation over one year of operation were deduced from the solar and wind power feed-in and the vertical load of the four transmission grid operators in

Germany in 2012. The renewable power was extrapolated linearly to values given by a 100 % renewable energy scenario for 2050 of the German association of electrical engineers VDE. The vertical load was considered to be the same in 2012 and 2050. The excess power was curtailed at 70 % of the maximum to cut off the rare high peaks.

Results and discussion

The results of the exergy analysis for both full load and using the load profiles are given in figures 1 and 2, respectively. The bars indicate the normalized relative amount of anergy created in the single steps and the remaining usable exergy.

At full load the systems containing combined cycle gas turbines are more efficient than the fuel cells due to higher full load efficiencies. The main sources of anergy are the electrolysis and the power generation. Methanation also decreases the overall efficiency by around 10 % for the combined cycle while the combined methanation and reforming consume over 20 % of exergy. The pure hydrogen and hydrogen injected into the natural gas grid efficiencies with following utilization in a combined cycle are around the same. The storage and distribution of hydrogen converts around 3-5 % of fed exergy into anergy. The exergy efficiency increase when operating a district heating system is very small due to the low temperature of the provided heat. Overall 35 % power-to-power efficiencies can be reached at best and only 21 % in the worst case. The complete chain efficiency of the μ -CHP fuel cell units using a hydrogen gas grid is around 30 %.

When operating the systems in part-load different tendencies occur. The efficiency of the electrolysis and fuel cells increases while the efficiency of the combined cycles decreases. The efficiency of the electrolyser increases from 66 % at full load to 70 % when considering the load profile due to the reduced resistance at lower currents i.e. loads. The electrical efficiencies of the gas turbines are very close with around 55 % for full load and 47 % overall load profile efficiency. This shows the

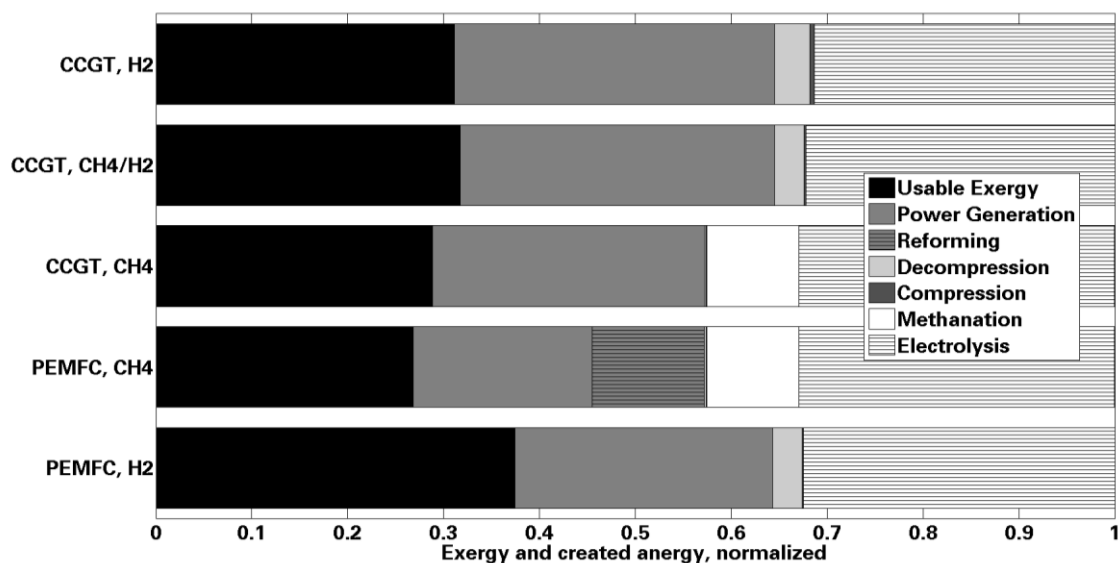


Figure 2: normalized exergy and energy for the single energy conversion steps over one year of operation

marginal influence of the change of fuel. The reason is that when using hydrogen as fuel, despite injecting steam for NO_x abatement which reduces the efficiency of the bottoming steam cycle, the efficiency of the topping gas turbine cycle is increased. The fuel cells efficiency drastically increases from 48 % at full load to 58 % when using the load profile due to similar effects as seen in the electrolyser. All other processes efficiencies are assumed to not change at part-load.

When comparing the whole chain load profile efficiencies, the opposing trends of increasing efficiency of electrolysis and fuel cell and decreasing efficiency of combined cycles result in substantially different overall results, showing the pure hydrogen fuel cell as the best option with about 38 % exergy efficiency, even outperforming the full load CCGTs with 30 % to 33 %. The fuel cell operated with methane and a reformer is still the worst option with 28 % exergy efficiency. It has to be noted that the efficiencies are highly dependent on the profile used and the maximum current considered for the electro-chemical devices.

Sources

[1] Ludwig, M.; Haberstroh, C.; Hesse, U. & Hurtado, A.; Hydrogen-Based Peak Power Management Unit for a Residential Application; European Fuel Cell Forum, 2013

[2] Navalho, J.; Frenzel, I.; Loukou, A.; Pereira, J.; Trimis, D. & Pereira, J.; Catalytic partial oxidation of methane rich mixtures in non-adiabatic monolith reactors; International Journal of Hydrogen Energy, 2013, vol. 38, pp. 6989 – 7006

[3] O'Connell, M.; Kolb, G.; Schelhaas, K.-P.; Schuerer, J.; Tiemann, D.; Ziogas, A. & Hessel, V.; The development and evaluation of microstructured reactors for the water gas shift and preferential

oxidation reactions in the 5 kW range; International Journal of Hydrogen Energy, 2010, vol. 35, pp. 2317 – 2327

[4] Abe, T.; Tanizawa, M.; Watanabe, K. & Taguchi, A.; CO₂ methanation property of Ru nanoparticle-loaded TiO₂ prepared by a polygonal barrel-sputtering method; Energy Environmental Science, 2009, vol. 2, pp. 315 – 321

[5] Chiesa, P.; Lozza, G. & Mazzocchi, L.; Using Hydrogen as Gas Turbine Fuel; Journal of Engineering for Gas turbines and Power, 2005, vol. 127, pp. 73 – 80

[6] Chacartegui, R.; Sanchez, D.; de Escalona, J. M.; Jimenez-Espadafor, F.; Munoz, A. & Sanchez, T.; SPHERA project: Assessing the use of syngas fuels in gas turbines and combined cycles from a global perspective; Fuel Processing Technology, 2012, vol. 103, pp. 134 – 145

A multi-fuel processor test bench based on reforming coupled to a fuel cell as a previous stage to industrial scale-up (FCA5-3)

A.J. MARTIN¹, T. GONZÁLEZ-AYUSO^{1,2}, C. MONTORO³, J.L. SERRANO¹, J.A. DAZA⁴, A. BALBÍN³, L. DAZA⁴

1. Centro de Investigaciones Energéticas, Medioambientales y Tecnológicas, CIEMAT.

Avenida Complutense 40, 28040 Madrid (Spain)

2. Olea Madrid S.L

3. Comberla Ingeniería, S.L.

4. Instituto de Catálisis y Petroleoquímica, Instituto de Catálisis y Petroleoquímica (CSIC),

Marie Curie 2 L10, 28049 Madrid (Spain)

INTRODUCTION

Electricity generation from hydrogen is a highly convenient alternative to incumbent fossil fuels electricity generation plants and is made possible either through fuel cells, internal combustion engines, or turbines. Fuel cells show the best theoretical yield due to the fact that, even though constrained by Thermodynamics' laws, they are not subject to limitations affecting thermal cycles when exchanging heat from/to high and low temperature reservoirs, respectively. Even if direct hydrogen production from renewable sources is the most desirable option, its current state-of-the-art does not allow implementation at an industrial scale. Integration of electrolyzers into windfarms and solar plants are nowadays at a demonstration stage. On the other hand, biomass is a renewable energy source and can be utilized, after adequate treatments, to produce H₂-rich compounds, such as hydrocarbons or alcohols. Many of them may undergo reforming. Reforming is a well-known process which has been used for more than a century to obtain hydrogen from a variety of substances. Remarkably, obtaining electricity by fuel cells from fossil fuels through reforming is more efficient, in theory, than direct using of fossil fuels in turbine-based power generation plants [1]. This fact closes the circle about the convenience of designing a reliable electricity generation system composed of a fuel processor coupled to a fuel cell capable of transforming H₂-rich compounds into electricity.

Some commercial products from domestic use (see successful Japanese Ener-Farm program [2]) up to 400 kW systems [3] based on natural gas reforming coupled to different types of low temperature fuel cells are already available and have been working for 20.000+ hours.

This communication describes the main features of a multi-fuel processor test bench coupled to a 5 kW low-temperature fuel cell. It is based on a previous 3 kW prototype fed by biogas currently installed in a waste water treatment facility in Murcia (Spain) under European LIFE project [4, 5]. Fuel flexibility, burner operation under a number of fuels and the capability of coupling/decoupling fuel processing from burner are novel features. We hope it helps us to learn more about integration of its components at a pre-industrial size as a previous stage for further scale-up and engineering optimization. Operation is expected to commence into first quarter, 2014.

DESCRIPTION

A simplified scheme of the system is depicted in the figure. Its main subsystems are:

A fuel processor set up including the reforming reactor followed by hydrogen purification stages, namely water-gas shift (WGS) and CO preferential oxidation (COProx). Water conditioning system is also included.

A 5 kW commercial low temperature fuel cell (PEMFC). PEMFC require a highly purified hydrogen inlet stream, including CO concentration at the ppm level.

An automatically controlled burner that can be operated under several fuel compositions including CH₄, CO₂, bioethanol and H₂.

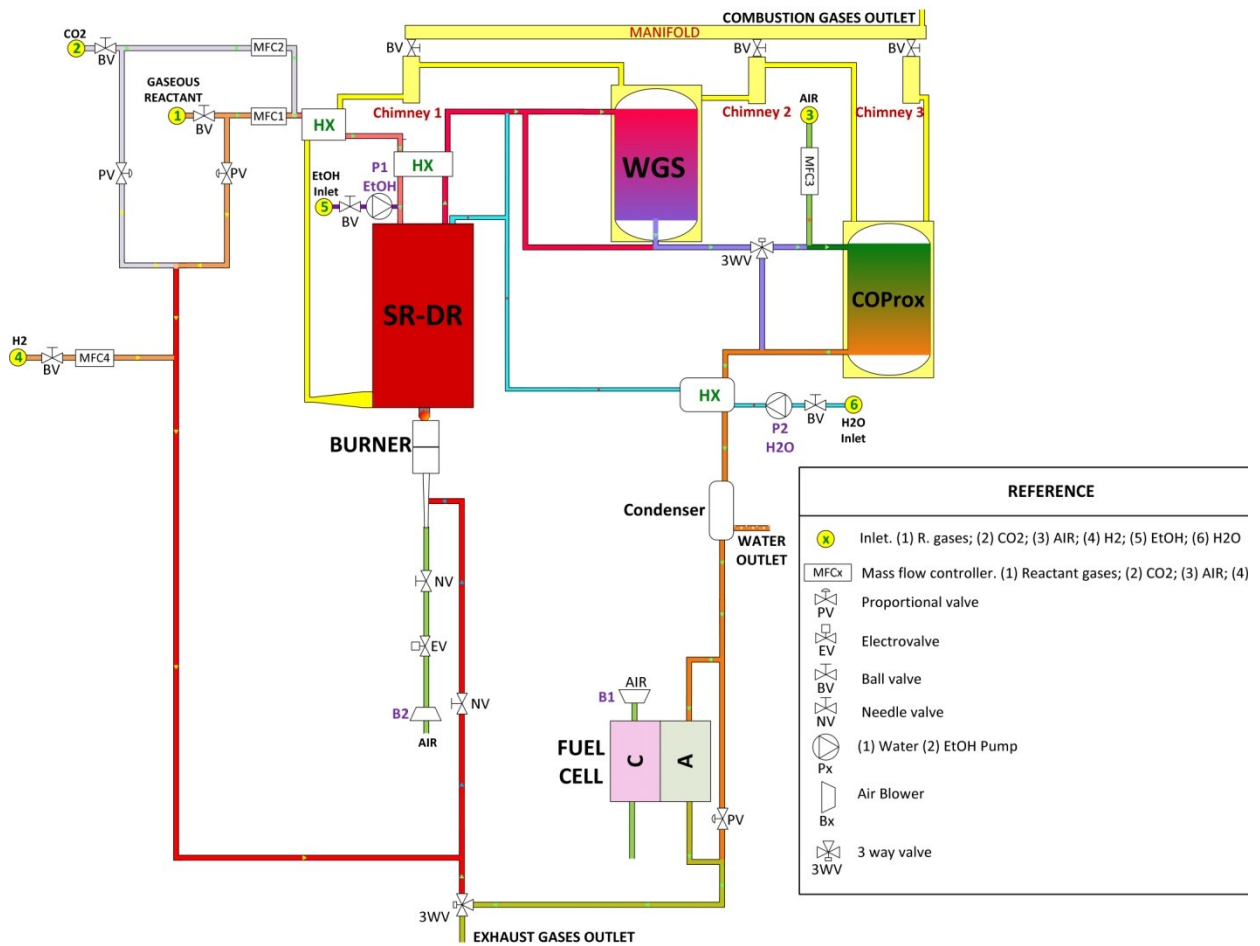


Figure 1. Fuel processor and fuel cell scheme.

Fuel Processor

The fuel processor is designed to allow some types of reforming of different fuels:

- Biogas under dry reforming ($\text{CH}_4 + \text{CO}_2$) or combined reforming ($\text{CH}_4 + \text{CO}_2 + \text{H}_2\text{O}$)
- Steam reforming of methane or heavier gaseous hydrocarbons ($\text{C}_x\text{H}_y + \text{H}_2\text{O}$)
- Steam reforming of liquid fuels, such as bioethanol ($\text{C}_2\text{H}_5\text{O} + \text{H}_2\text{O}$)

At this stage, the system is capable of operating using one of the above-mentioned processes at the same time. Reforming reactor has been designed for an easy catalyst replacement if needed. Further improvement includes in-parallel operation with different fuels in separated catalytic chambers. Water is evaporated through several stages and injected along the process scheme at different places depending on the type of reforming process selected. It is worthwhile mentioning that excess water not reacted into the reformer and/or WGS passes through the CO preferential oxidation reactor in order to obtain a more stable temperature distribution along the catalytic bed as well as to hinder hydrogen oxidation. Excess water is eliminated before entering the fuel cell. First tests include biogas dry reforming and steam methane reforming. During these tests, all three catalytic stages will work using patented catalysts by Instituto de Catálisis y Petroleoquímica (CSIC).

Burner

Thermal energy required to accomplish endothermic reforming as well as for water and inlet gases conditioning comes from a commercial biogas burner. It is adapted to allow expected hydrogen concentrations at the fuel cell's anodic outlet stream. External electrical energy is only used to feed monitoring, control, and burner's ignition (spark) equipments. The burner may be fed: (i) independently, (ii) by exhaust gases abandoning fuel cell's anodic compartment or (iii) by a combination of (i) and (ii). Our system also allows independent burner tests with no real fuel processing ongoing. Combustion gases keep the desired reforming temperature and overheat process water. Right after, gases may be either driven to jacket-type WGS and/or COProx reactors to speed up warming up process or released into the atmosphere. The burner is either controlled by the master software to obtain a stable reforming temperature or manually. An auxiliary system consisting of H_2 and O_2 streams allows, under certain set up parameters, reduction or oxidation treatments of the reforming catalyst, respectively.

Fuel Cell

The fuel cell unit is composed of a 5 kW commercial PEMFC stack which must be operated into certain pressure and temperature ranges. This system does not include a previous hydrogen separation stage in order to study the effect of reforming gases into this type of fuel cells. This fact diminishes the electrical yield since inlet anodic gas is not pure hydrogen. Expected hydrogen content is expected to reach ca. 60 % operating with biogas and dry reforming

Control and operation

Operation is mainly automatic. Control and monitoring are carried out by a home-made program based on Labview that controls main operation parameters through control loops developed at CIEMAT. Some critic parameters such as CO concentration at COProx outlet are continuously monitored and trigger protection protocols in case their value is out of a programmed range. As an auxiliary tool to control catalytic processes, a gas chromatographer fed by an automatic sample selector provides the composition of the three reforming, WGS, and COProx outlet streams every 5 minutes approximately.

This lay out may be easily transformed to integrate high temperature fuel cells, such as solid oxide fuel cells by bypassing WGS and COProx reactors. HT PEMFC may also be integrated by bypassing COProx reactor. Both cases would give rise to simpler schemes.

NOMINAL OPERATION PARAMETERS

The Table 1 provides information about some of the main physical magnitudes we expect our system to operate at when using biogas as a fuel and dry reforming as the first catalytic stage. Thermal and electrical magnitudes are within the kW range. This is appropriate for domestic use. External electrical input can be easily reduced since our system includes monitoring and analysis equipment not needed in a commercial plant. Further scaling up to a few hundreds kW would allow small industries and large commercial buildings to benefit from this electrical energy generation system.

Table 1. Design operation parameters for biogas operation under dry reforming

Consumptions		Nominal parameters	
Biogas	5 Nm ³ ·h ⁻¹	Produced H ₂	3.9 Nm ³ ·h ⁻¹
Water	12.6 kg·h ⁻¹	Nominal electric power	5 kW
Air	32.3 m ³ ·h ⁻¹	Inlet biogas to burner	0%
External electric power	0.6 kW	Burner thermal power	15.5 kW

This system is therefore helpful to test, from isolated catalysts or burners, to complex strategies based on combination of several fuels and/or reforming processes to reach cost-effective operation conditions with optimum reliability and performance.

ACKNOWLEDGMENT

Financial support from Comunidad de Madrid (DIVERCELCM, S2009/ENE-1475) is gratefully acknowledged.

REFERENCES

- [1] Hydrogen and Fuel Cells Program Plan, U.S. Department of Energy, 2011.
- [2] Dan Carter, Latest Developments in the Ene-Farm Scheme, Fuel Cell Today, February 2013.
- [3] ClearEdge Power product brochure, see www.utc.com
- [4] A.J.Martín, T. González Ayuso, J. Mielgo, J.L. Serrano, L. Daza, Analysis of a Biogas Processing Plant Coupled to a 5 kW Fuel Cell. Abstract 205, Fuel Cell Seminar and Exposition, Orlando, October 31st-November 1st, 2011.
- [5] Project LIFE07 ENV/E/000847 - BIOCELL

How to Put in Work a Fuel Cell System. Design, Implementation, Control and Cost Analysis of the Balance of Plant (FCA5-4)

Francisca Segura Manzano, francisca.segura@diesia.uhu.es, University of Huelva
José Manuel Andújar Márquez, andújar@diesia.uhu.es, University of Huelva

Abstract—Fuel cells appear to be the best option between conventional power generators and renewable energy sources. Fuel cells produce electricity directly from fuel via electrochemistry, which is inherently more efficient than combustion and minimizes the adverse characteristics associated with combustion process (e.g., excessive noise, emissions, and maintenance). In relation to renewable energy sources, fuel cells can operate for as long as fuel is available, so power production is independent from weather conditions as solar and wind energy happen. However, in order to be widely accepted, fuel cells must prove that they are more reliable and cost competitive than the conventional solutions. This will require that fuel-cell systems have a simple design and are no more expensive than actual combustion engines. This paper describe the whole sequence to put in work a fuel cell system, from the individual devices which integrate the balance of plant (BoP) up to the final assembly. Moreover, in basis on a cost/power comparative between comercial fuel cells the cost reduction is justified.

Key words: Fuel cell, balance of plant, design, control, cost comparative.

INTRODUCTION

Fuel cells features are widely known as their high efficiency, low maintenance and noise and null harmful emissions. But against these advantages their high cost supposes a drawback for fuel cells to be widely accepted. Most comercial fuel cells systems include balance of plant whose control system increases the price besides the high price of the own stack. Then simplifying the BoP keeping security, the final cost could be reduced.

Regarding PEM fuel cell (PEMFC) requirements to work, most systems need four subsystems: 1) a hydrogen fuel delivery system, 2) an air delivery system, 3) a thermal management system, and 4) an electrical power supply system. In principal, each of these sub-systems should be relatively simple; however, these sub-systems are complex due to the added complexity of managing water in the system. Water is not only the product of the PEMFC reaction it is also critical to ensure effective and stable operation [1]. Therefore removing the thermal management system, cost and complexity will be reduced [2].

This paper presents the design, building and control of the BoP for an air-cooled PEMFC (FC1020-ACS from Ballard). Watching the final result, it could be argued that fuel cell system is simpler and cheaper than comercial fuel cells systems.

Next section is dedicated to explain the design and building of the BoP for the air-cooled fuel cell, the control system is developed in Section III, and Section IV is dedicated to discuss and compare prices between comercial fuel cell systems. Main concluisons are gathered in Section V.

BoP: DESIGN and IMPLEMENTATION

The FCgen-1020ACS fuel cell stack is a 80 cells proton exchange membrane (PEM) fuel cell stack designed to provide stable electrical power while operating over a wide range of power and environmental conditions. It is air cooled, so no external humidification of the air is required. Moreover, the stack is designed to in a dead-ended configuration using dry hydrogen. The fuel cell stack has no moving parts and produces clean DC power with low thermal and acoustic signature. The number of cells is 80 and can reach up to 3.4 kW with 45.3 V and 75 A. Hence FCgen-1020ACS is a single stack, it needs BoP to be designed and built. The BoP can be divided into three sub-systems: Oxidant/Cooling Subsystem, Fuel Subsystem and Electrical Subsystem.

The Oxidant/Cooling Subsystem (Figure 1a, blue line) delivers oxidant agent to fuel cell cathode for the fuel cell reaction and the cooling subsystem maintain the stack at the proper temperature. Then, to configure this subsystem, the following devices are needed: a temperature sensor for fuel cell (T_{fc}), another one to measure the ambient air temperature (T_{amb}) and a fan with flow adjustment to control the oxidant flow and the stack temperature. Additionally an oxygen sensor (O_2) is included to prevent low concentration of oxygen in the surrounding atmosphere.

The Fuel Subsystem (Figure 1a, yellow line) delivers hydrogen fuel to the stack at the appropriate flow and pressure. The components' list for the inlet line include: the hydrogen bottle to store the fuel, a pressure regulator to condition the high hydrogen bottle pressure downstream to low fuel inlet pressure in the stack, a supply valve to control the hydrogen flow and a pressure sensor (P) to measures the stack anode pressure. In the outlet line, a purge valve will be needed to exhaust the hydrogen to environment and a hydrogen sensor (H_2) to avoid beating security limits.

On Electrical Subsystem (Figure 1a, red line), a relay is added to isolate the fuel cell from the electrical load and a blocking diode to avoid reversal currents which would damage the fuel cell. Additionally, current (I) and stack voltage (V_s) sensors will be connected on electrical terminals, and cell voltage monitoring system (V_c) on cells.

To get these three subsystems works simultaneously, a Control Unit will be the responsible for receive all the information from sensors and decide what to do every moment. And finally, with the aim to build an isolated non-polluting source, a Battery supplies all the devices from the BoP.

Once the BoP has been designed, we proceed to implement it, selecting the proper components in basis of fuel cell stack operation requirements and cost saving criteria. Figure 1b shows an image of the instrumentation and control board developed for the BoP. Table 1 describes the top level bill of materials in the final design.

Additionally, once the BoP building has been finished, authors have designed a virtual interface for the voltage monitoring system (Figure 1c). This interface allows us to know the 80 cells voltage instantaneously. These values are represented in different ways: amplitude versus cell number diagram, amplitude versus time diagram and typical values like average, peak and minimum values.

CONTROL SYSTEM

FCgen-1020ACS operating procedure has been designed to guarantee manufacturer's requirements: performance, durability and safety. This procedure is established by the Control Unit,

and is made up four steps (Figure 2): Off, Start-up, Run, Shutdown and Shutdown by Failure. In Off state, battery is disconnected so no one device receives electrical supply, sensors don't send information to controller nor actuators don't receive order. During the Start-up state, fuel cell is warming-up and controller guarantees fuel cell reaches optimal operating temperature, and electrical power could be drawn from fuel cell in Run state. After normal operation period, fuel cell can be stopped staying in Shutdown state. If during Start-up or Run state some sensor sends to controller a measure which means wrong and/or unsure performance of the fuel cell, the Shutdown by Failure happens. In this state, battery will be disconnected and the fuel cell could be restarted only if the fault has been corrected.

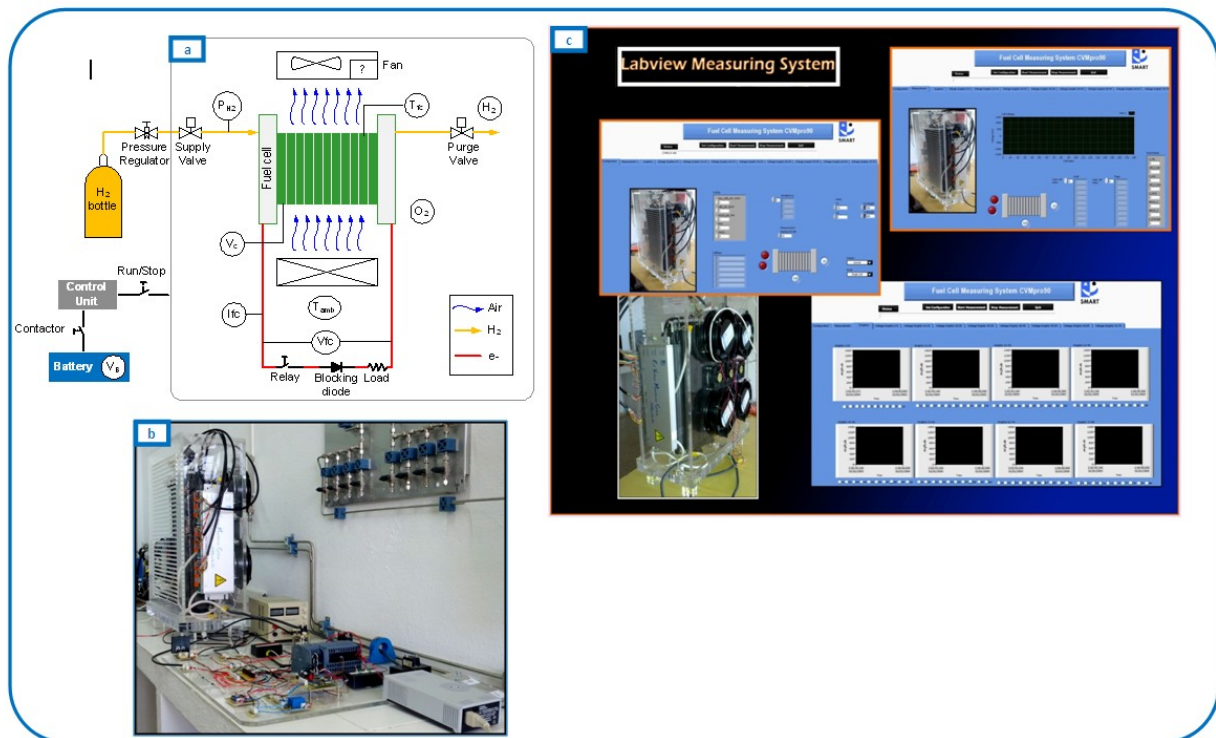


Figure 1: Fuel cell system developed. (a) BoP scheme. (b) BoP implementation. (c) Virtual interface for cell voltage monitoring.

Table 1. High-level bill of materials showing major fuel cell system	
Component	Quantity
Fuel cell stack	1
Oxidant/Cooling Subsystem	
Fan	4
Inlet air temperature sensor	1
Fuel cell temperature sensor	Included in stack
Oxygen sensor	1
Fuel Subsystem	
Valve supply	1
Purge valve	1
Pressure sensor	1
Hydrogen sensor	1
Electrical Subsystem	
Current sensor	1
Stack voltage sensor	
Cell voltage monitoring system	1
Blocking diode	1
Relay	1
Control system	
PLC	1
Battery	2

PRICES COMPARATIVE

In quantitative terms, a study from Fuel Cell Today [3] projects that a PEMFC back-up power product that costs – 1500 €/kW can be cost competitive, on a lifecycle basis. According to Alternative Energy Systems Consulting [4] actual PEM system costs for portable applications (military, remote generation and UPS and Telecom) are estimated between 1500-7500 €/kW. Table 2 shows a price comparative of fuel cell systems classified by power (from kilowatts to thousands of kilowatt), including the fuel cell system developed by authors and taking into account some of the most representative manufacturers. Regarding cost/kilowatt column we can advance the fuel cell system developed by University of Huelva is a cost competitive proposal (it has the lowest price compared to others) which approaches to boundaries established international organism: 2100 €/kW against 1500 €/kW threshold.

CONCLUSIONS

This paper presents a fuel cell system which reaches the two issues required for fuel cell will be widely accepted: simplicity and cost effectiveness. The fuel cell system in basis on FC-1020ACS Ballard stack and the BoP has been designed, implemented and controlled according to stack manufacturer recommendations. Simplicity has been achieved thanks to FC-1020ACS stack is air-cooled so no humidification system is needed and cost effectiveness because a throughout market study has been done to choose most suitable and lowest cost devices for BoP building.

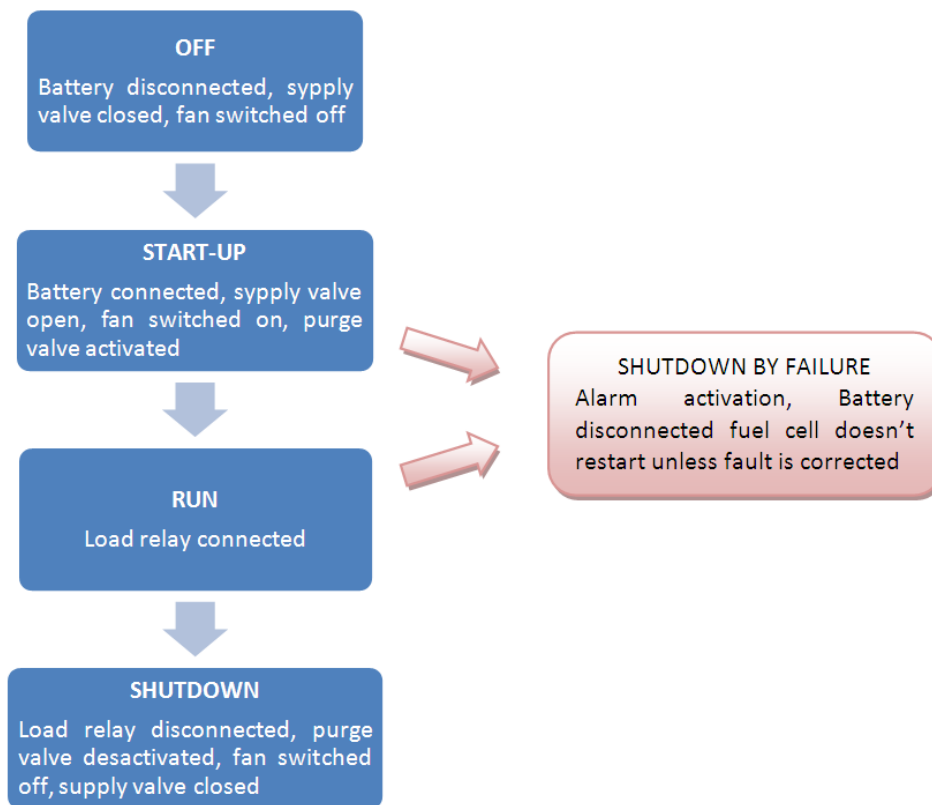


Figure 2: FCS-1020ACS operation sequence.

Table 2. Price comparative from fuel cell systems.

Fuel cell system (stack+BoP)	Power (kW)	Stack's Manufacturer	Cost (€)	€/kW
FC-42 / 360	0,36	Schunk	7000	19444
FC-42 / 720	0,72	Schunk	10200	14166
Nexa	1,2	Ballard	7000	5800
FC-1020ACS-University of Huelva	3,4	Ballard	7280	2100
Powerflow	5	Nuvera	30000	6000
IRG04 (Imperial Race Green)	19	NedStack	48000	2500
DFC300	300	FuelCellEnergy	900000	3000
PureCell	400	UTC Power	1,2 million	3000

REFERENCES

[1] M. L. Perry, E. Strayer, "Fuel-Cell Based Back-Up Power for Telecommunication Applications: Developing a Reliable and Cost-Effective Solution", 28th Annual International Telecommunications Energy Conference, INTELEC '06, 2006.

[2] M. Corder, M. Matian, G.J. Offer, T. Hanten, E. Spofforth-Jones, S. Tippetts, A. Agrawal, L. Bannar-Martin, L. Harito, A. Johnson, R. Clague, F. Marquis, A. Heyes, Y. Hardalupas, N.P. Brandon,

“Designing, building, testing and racing a low-cost fuel cell range extender for a motorsport application”, Journal of Power Sources, vol. 195 (23-1), pp. 7838-7848, 2010.

[3] Fuel cell Today Report 2013: <http://www.fuelcelltoday.com/analysis/event-reports/2013/hydrogen-plus-fuel-cells-2013>

[4] Alternative Energy Systems Consulting Report, First International Conference on Energy Efficiency & Conservation, 2003. Online: http://www.aesc-inc.com/download/AESC_HK_Fuel_Cell_Presentation.pdf

Residual heat use generated by a 12kW fuel cell in an electric vehicle heating system (FCA5-5)

Lucía Alberdi-Jiménez¹, Lorenzo Nasarre Cortés¹, Joaquín Mora Larramona¹, Luis Carlos Correas Usón¹

*¹ Foundation for the Development of New Hydrogen Technologies in Aragon
Walqa Technology Park, Ctra. 330A, km. 566, 22197 Huesca (Spain)
Phone number: +0034 974 215 258, Web: www.hidrogenoragon.org*

The current energy model based on fossil fuels is unsustainable; high dependence on these fuels located in exclusive regions, high pollution and rising prices are clear examples. There is a real need of change, where mobility represents a significant portion because it is the major consumer of these fuels.

Nowadays, a new fleet of low or zero emission vehicles have been developed: hybrid and electric vehicles, either pure batteries or fuel cell powered.

From the governments of various countries are encouraging the purchase of these vehicles; at the public level are being introduced into the transport companies. In the EU, several mobility demonstration projects are promoting and testing the use of these vehicles. Within these projects are CUTE, CHIC, HyTransit, HyTech, High V.LO City, H2Moves Scandinavia. This shows the commitment that exists to reduce dependence on fossil fuels and the emission of CO₂ to the atmosphere, in favor of sustainable transport fleet.

Electric and hybrid vehicles are technologically developed and the performance comparable to internal combustion vehicles. Despite their many similarities, internal combustion vehicles have an efficiency of 20-30%; this value increases up to 85-90% in an electric motor.

The heating system of internal combustion engine vehicles is based on the heat exchanging between the coolant and the engine. This liquid, at the outlet, has an approximate temperature of 90 °C, which is used to warm the air in the radiator, and then heating the vehicle cabin. In this case, the use of the heating system do not need additional energy input.

The energy consumption increase that involves the use of heating in electric and hybrid vehicles may reduce the overall performance of the drive system and the autonomy of electric and hybrid vehicles.

Because of the large amounts of energy lost as heat in the internal combustion engine vehicles, they do not need additional energy for heating because they use that heat. However, due to high efficiency of the electric motors, about 90%; electric vehicles do not have that energy lost as heat what has a serious impact on autonomy, and consequently on the efficiency of the vehicle as sometimes an electric car might need as much energy to heat as used to move it.

The standard solution to the heating system of these vehicles is based on a set of electrical resistors that are used to heat the air and after that, transferring this heat air to the inside of the vehicle.

Other solutions are the use of infrared lamps to heat the occupants directly removing cycle transmitting medium (air). These types of lamps are known technology, low cost and high efficiency, but are still in the research phase for this application and are not implemented in any vehicle in the market. Another option is to incorporate a small bioethanol engine responsible for supplying the necessary energy to the heating system.

The purpose of this study is part of the project to convert an electric vehicle to a fuel cell electric vehicle (lithium-ion batteries and fuel cell) funded by the LIFE + Zero-HyTechPark.

The LIFE +, is an instrument of the European Union to fund environmental projects. The main objective of the LIFE + Zero - HyTechPark is to implement the total capacity of sustainability in technology parks through an optimal power management based on hydrogen technologies and renewable energies. This project is coordinated by the Foundation for the Development of New Hydrogen Technologies in Aragon and the following partners are involved: Zamudio Technology Park (Vizcaya), Andalucía (Málaga) and Walqa (Huesca).

In this paper, it is presented the use of waste heat generated by the fuel cell to the heating system by removing the electrical resistance, to improve the overall efficiency of the system, and consequently the range of the vehicle.

On the vehicle in study, the conversion of a pure electric vehicle into a hybrid vehicle has been carried out by adding a 12 kW PEM fuel cell (Polymeric Exchange Membrane) to the propulsion system. This fuel cell has an optimum operating temperature around 50 °C. This temperature also depends on the current demanded to the fuel cell.

First of all, considering that the fuel cell operating point is about 125 A, with a corresponding temperature of 65 °C, this ensures that heat generated in the fuel cell reaction can be harnessed to heat the cabin of the vehicle.

Taking into account that the temperature reached by the fuel cell; a system to take advantage of that heat has been designed. The system is based on the fuel cell, its related cooling system and heating radiator.

Development of a Combined Heat and Power Plant Based on Molten Carbonate Fuel Cell Technology (FCA5-6)

Mariana Martín Betancourt, Rocío Palomino Marín, Juan Fernández García, Noelia Ibáñez Lirio.

There has been a resurgence on the interest in combined heat and power (CHP) technologies in recent years due to the efficiencies involved in the use of fuel, the reduction of the impact on greenhouse emissions and the possibility of grid independent operation. This interest has occurred in a wide variety of sectors, such as commercial buildings, industrial sites, rural and agricultural applications, etc. A properly sized CHP plant can provide the thermal needs of the end user and supply electricity required to the process with excess to sell to the utility grid.

The development of different technologies for the use in CHP plants has advanced along many different paths. One that has produced important results in the last years, has been the use of high temperature fuel cells as the core of the CHP plant. Fuel cells have many technological advances that make them very attractive for use as stationary CHP systems, including: high fuel efficiency, ultra-clean emissions, improved reliability, quiet operation, scalability, operation from readily available fuels and the ability to provide both electricity and heat.

Of the different types of high temperature fuel cells, molten carbonate fuel cells (MCFC) are the prime candidate to commercial use due to their current development. This type of fuel cell operates at temperatures higher than 550 °C at which the salts used as the electrolyte are in a molten state and conduct the ions between the electrodes. Stationary MCFC power plants typically process natural gas, and release fewer environmentally harmful emissions than those produced by a combustion cogeneration plant. With a fuel cell, carbon dioxide emissions may be reduced by up to 49%, nitrogen oxide by 91%, carbon monoxide by 68%, and volatile organic compounds by 93%. The high temperature of operation creates an exhaust that can be used in a variety of CHP applications.

As part of this emerging market, Abengoa Hidrógeno is developing a stationary MCFC power plant that will produce 300 kWe that will be located in Seville. The plant consists of three major components: a fuel cell stack where the electrochemical conversion of energy takes place, a mechanical balance of plant which processes the fuel, water and air for use in the fuel cell stack and an electrical balance of plant which converts the DC power output of the fuel cell into AC power. The MCFC stack will be supplied by FuelCell Energy, one of the top world leaders in this type of fuel cell technology, who has developed the Direct Fuel Cell (DFC®). The mechanical and electrical modules as well as the plant integration are being developed by Abengoa Hidrógeno.

The first power plant prototype will process natural gas from the pipeline and must be robust enough to withstand changes in natural gas composition, especially sulphur compounds that may differ depending of the gas source. However, the power plant should have the possibility to be adapted to operate with biogas generated from a number of industrial, agricultural plants and wastewater treatment facilities manufacturing processes.

According to the timetable of the project, the plant construction will start this year finalizing at the beginning of 2014 and the commissioning will be finished next year. The plant should be able to

work during 24 hours per day under different conditions prior its installation in the definitive location.

This project has been funded by Corporación Tecnológica de Andalucía (CTA). It also has been funded by the IDEA Agency and has been co-funded by the European Regional Development Fund, FEDER, within the Technology Fund Operational Programme 2007-2013.



Hydrogen distribution and filling stations

Infrastructure Readiness For Hydrogen Fleet Deployments (DFS1-1)

MARIA DEL MAR ARXER, *Carbuos Metálicos – Air Products*

Are we still facing a chicken and egg dilemma? The lack of hydrogen refueling infrastructure is seen as one of the major challenges to attract potential buyers of fuel cell hydrogen vehicles. With the aim to overcome this dilemma, in January 2013 the European Commission published a Proposal for a Directive to ensure the setting-up of infrastructure for the use of alternative fuels (among them the hydrogen) for road, sea and in-land water transport across the EU. Concerning the hydrogen fuel, publicly accessible hydrogen refueling stations within distances not exceeding 300 km will have to be set in place by the end of 2020 at the latest, to allow the circulation of hydrogen vehicles on the entire national territory of a member state. One would say that the chicken and egg dilemma is coming to an end.

In the past years new hydrogen refueling stations have been built and are being built every day around the world. Air Products has been involved in over 150 hydrogen fueling projects in 19 countries in 3 continents. The use of the company fueling technology has now reached >850,000 refuelings per year.

However vehicle deployment is still scarce. There are initiatives in place in several countries where a consortium of stakeholders (such as vehicle manufacturers, infrastructure suppliers, related industries, also Government Departments) has been formed, to joint develop the hydrogen energy emerging market. These consortiums pursue the reduction of the first-mover disadvantage due to the initially low utilisation of the stations by a small number of fuel cell electric vehicles.

As a first step towards standardisation of the hydrogen refueling technology, Air Products has developed a SmartFuel® fueling station concept, modular and expandable, which offers significant flexibility and reliability. At the same time that this modular concept can be replicated leading to an increase of the capacity and redundancy of the stations, it can also be as simple as possible, avoiding even the compression for 350 bar refuelings. The pressure only needs to be increased at the station for 700 bar refuelings. The compression-less SmartFuel® hydrogen fueling technology offers additional advantages at the point of use, such as minimizing the station maintenance costs as well as station footprint requirements. This concept relies on two new hydrogen distribution systems, developed and owned by Air Products: the Dual Phase hydrogen tanker and the High Pressure tube trailer.

The Dual Phase hydrogen tanker transports the hydrogen in liquid state and enables hydrogen to be delivered to fuelling stations as a liquid or as a gas at a set pressure (up to 500 bar). It is in operation in the US and Europe. The High Pressure tube trailer for its part transports and delivers gaseous hydrogen up to 500 bar. It features specialised composite cylinders. It has been deployed in California, and the first one of the European fleet now also in the UK. The compression-less SmartFuel® concept offers the opportunity to reduce distribution costs, because greater quantities of hydrogen can be transported from central production plants, in comparison with 200 bar tube trailers, the current industrial standard.

Both delivery vehicles can be connected directly to the onsite fueling system, making them an integrated part of the fueling station. They can be dropped at fueling station or used to refill storage at station, serving respectively as a hydrogen storage or distribution system. As mentioned before, this type of fueling station offers reduced overall site maintenance costs and its minimized footprint enables it to be used at existing retail gasoline stations, which significantly lowers the initial cost of infrastructure. It matches the projected rollout of fuel cell electric vehicles to serve the automotive market as it grows, as opposed to the installation of large stations that may be underutilized for longer periods of time, and provides a model for a fueling infrastructure which relies on existing production capabilities.

The presentation at the EHEC 2014 will describe some examples of the SmartFuel® fueling station concept implementation (Hamburg, Cologne, London). It will also discuss the options to serve the increasing refueling demand in the transition period: bus stations that could be designed to refuel also cars or the other way around, car stations that could also serve small fuel cell bus fleets, with the objective in mind to refuel large fleets of 200 fuel cell buses with dedicated stations.



SmartFuel® fueling station at Transport for London, featuring the Air Products Dual Phase hydrogen tanker and serving a fleet of 8 fuel cell buses.

Hydrogen Infrastructure for Transport – Hitting the road together (DFS1-2)

Floris Mulder

BACKGROUND AND OBJECTIVE

The vision of the EU [White Paper “A Roadmap to a Single European Transport Area – Towards a competitive and resource efficient transport system” (COM 2011/144)] aiming at growing transport and supporting mobility while reaching the 60% emission reduction target, will require a portfolio of low carbon transport solutions.

In view of the ambition of the Clean Power for Transport Package, in which hydrogen refuelling station networks are mentioned in paragraph 5, significant efforts will be necessary in the coming seven years to match the roll out of commercial fuel cell electric vehicles and hydrogen refuelling locations.

Over the last decade several large fuel cell electric vehicles (FCEV) R&D projects and market studies throughout Europe have demonstrated technical and economic feasibility and established the European industry’s role as market leader in several critical areas of fuel cell and hydrogen production and distribution development.

Major car manufacturers have announced that the first series’ produced FCEVs will be available on the European roads as of 2014 – 2015. On 30 September 2013, major OEMs and oil and gas companies announced a €350 million investment in 400 hydrogen refuelling stations in Germany by 2023. The need for an economical and environmentally sustainable network of hydrogen refuelling stations (HRS), enabling the first customers to travel between Europe’s emerging hydrogen hubs, is therefore becoming more prominent.

The first FCEV roll out initiatives have demonstrated the need to harmonise the roll out of HRS installations as well as authorisation procedures. These initiatives have also highlighted the need for strategic and coordinated planning of efficient and sustainable hydrogen production as well as distribution solutions. By linking national hydrogen corridors with sensibly spaced hydrogen stations, enabling first customers to travel between major European cities, HIT seeks to enhance the appeal of FC vehicles and to start market deployment.

The HIT project will further facilitate the pan-European build-up of economically and environmentally sustainable hydrogen production and distribution networks - where possible linked to local zero- or low carbon energy sources. HIT is a crucial step to next level involvement of the Netherlands, Denmark, France and Sweden. Furthermore, active support by Germany will secure direct dissemination of developments in Germany (CEP, H2Mobility, NOW) and to ensure sensible linking of national hydrogen corridors. HIT includes EU wide dissemination activities.

In addition active engagement of national and local authorities is needed to ensure effective planning to avoid higher costs at a later stage. A steep learning curve and an adaptive learning network – across national boundaries – is desirable.

HIT provides the means and tools for these needs and is instrumental to reach hydrogen's potential to fuel a large part of Europe's vehicles fleet with a low carbon alternative fuel.

HIT @ EHEC2014

The HIT project at EHEC 2014 will give an update of the following activities undertaken during the first year:

- NIP (National Implementation Plans): National/regional/local studies & preparatory actions
- Pilot installations: The HIT pilot stations are important locations in allowing the first long distance trips from Sweden, via Denmark and Germany into the Netherlands
- Synchronising Implementation Plan (SIP): The results and recommendations of the NIP will be integrated in a SIP and include descriptions of how to best link national hydrogen corridors across borders and fleet development schemes along these corridors

THE CONSORTIUM

The HIT consortium consists of the Dutch Ministry of Infrastructure and the Environment, HyER (Hydrogen, Fuel Cells and Electro-Mobility in European Regions), Air Liquide (FR), Copenhagen Hydrogen Network A/S (DK), AFHYPAC (FR) Hydrogen Sweden (SE) and Hydrogen Link Denmark Association (DK).

HIT is sponsored by NOW (Nationale Organisation Wasserstoff- und Brennstoffzellentechnologie, DE) and supported by the German Ministry of Transport.

The next phase of Hydrogen infrastructure in Norway (DFS1-3)

Ulf Hafselid, CEO, HYOP as, P.O.Box 102, 2027 Kjeller, Norway

Norway has been operating a hydrogen refuelling infrastructure since 2006 and has gained valuable experience which will be used in defining the way forward. The stations are being supplied in different ways with hydrogen, but all the hydrogen sold at the stations is made from water electrolysis and renewable power. Five stations for cars and one for buses are now in operation, supplying a small fleet of FCEVs from Daimler, Hyundai and Think, in addition to the five buses from Van Hool that operates in the EU CHIC project. One of the car stations is the H2Moves Scandinavia station, funded in a EU project from the FCH-JU.

The experience gained so far, has led to fully automated stations that are open 24/7 with very high availability. However, they are built as single-line units, and are thereby too vulnerable for stable supply of large volumes over longer periods of time. It is therefore necessary to start building more robust stations with higher capacities as larger fleets of FCEVs can be expected to arrive over the next few years. The stations will be built with a modular design, starting with a smaller unit and being capable of multiplying in size as demand grows.

Linking the hydrogen fuel infrastructure with electrolytic production of hydrogen using renewable power has become a priority in Norway. The hydrogen can either be produced on-site or trucked in from centralized production units. The amount of renewable electricity in the grid today is >97 %, and more renewable power will be phased in during the next decade, meaning that all hydrogen for the entire car fleet in Norway could be made from renewable power.

A nation-wide hydrogen station network is currently being planned based on extensive use of on-site production with electrolysis. The business model shows that profitability can be obtained when the hydrogen stations becomes closer in size with current petrol stations.

Hydrogen-Compressed Natural Gas Refueling Infrastructure in India (DFS1-4)

Sauhard Singh, Reji Mathai, Ved Singh, A K Sehgal, B Basu, R K Malhotra

*Indian Oil Corporation Ltd., Research & Development Centre,
Sector-13, Faridabad, Haryana, INDIA*

Hydrogen is receiving considerable attention worldwide as an energy carrier and clean fuel. For accelerating the development of hydrogen energy technologies in India, a National Hydrogen Energy Roadmap (NHERM) was prepared under the guidance of the National Hydrogen Energy Board constituted by Ministry of New and Renewable Energy (MNRE), Govt. of India. The road map envisages ambitious targets of putting one million hydrogen fuelled vehicles and deployment of an aggregate hydrogen based power generation capacity of 1000 MW in the country by 2020. The NHERM envisages an expenditure of US \$ 5 billion. It is estimated that one million vehicles will require about 7000 tonnes of hydrogen per day.

Till such time that the hydrogen is available in large quantities at economical rate, it has been proposed to use the same in admixture with CNG (HCNG) which will enable gaining experience with the supply, distribution and dispensing of hydrogen to automotive vehicles. For this IndianOil had set up India's first hydrogen dispensing station at Faridabad and another at commercial retail outlet in New Delhi. These dispensing stations comprise of high efficiency electrolyser for producing hydrogen with 99.999% purity (capacity of electrolyser – 11 kg/day), hydrogen compressor, hydrogen storage, HCNG blender, dual hose dispenser one for dispensing HCNG blends varying from 5 to 50 % H₂ in CNG at 200 bar pressure and another for dispensing hydrogen @ 350 bar. These hydrogen dispensing stations provide public awareness of using HCNG as automotive fuel.

Presently these stations are used for refueling the HCNG fleet of three-wheelers, passenger cars, LCVs and heavy duty vehicles. This paper aims to cover the current status on hydrogen production, storage, distribution and its application / use in transport sector in India. Also the paper highlights the various safety norms as per Indian & International standards followed during setting up of these hydrogen dispensing stations. Apart from highlighting the advantages of using and promoting HCNG as an automotive fuel in India, the initiatives taken by IndianOil for converting, testing and optimizing the vehicles running on HCNG will also be discussed in this paper.

Keywords : Hydrogen, HCNG blends, Electrolyzer

An optimization approach for evaluating subsidies in the initial location of hydrogen refueling stations (DFS1-5)

Carlos Fúnez^{a,b}, Doroteo Verastegui^b, Ricardo García^c, Eusebio Ángulo^c

^a National Center of Hydrogen, Technical Department. C/ Prolongación Fernando el Santo s/n - 13500, Puertollano (Ciudad Real) Spain, phone +34 926 420 682. carlos.funez@cnh2.es

^b Universidad de Castilla-La Mancha, Escuela Universitaria Politécnica de Almadén, Departamento de Matemáticas. / Plaza Manuel Meca, 1 - 13400, Almadén (Ciudad Real) Spain, phone +34 926 264 007. doroteo.verastegui@uclm.es

^c Universidad de Castilla-La Mancha, Escuela Superior de Informática, Departamento de Matemáticas. / Paseo de la Universidad, 4 - 13004, Ciudad Real, Spain, phone +34 926 264 007. Ricardo.Garcia@uclm.es, Eusebio.Angulo@uclm.es

INTRODUCTION

The proposal for a Directive of the European Parliament and of the Council, dated 24 January 2013, on the build-up of an infrastructure for alternative fuels, establishes a common framework of measures for the deployment of alternative fuel infrastructures in UE in order to break the oil dependence of the transport. This proposal sets out minimum requirements on alternative fuel infrastructures and the common technical specifications, including recharging points for electric vehicles and refuelling points for natural gas (LNG and CNG) and hydrogen [1].

In particular, article 5 of the above proposal requires to install enough hydrogen refueling stations in the territory of the Member States such that a hydrogen-powered vehicle can move on the whole national territory with a maximum of 300 km between recharging points. Moreover, it must be achieved no later than 31 December 2020. Also defines the common technical specifications that must meet this infrastructure.

A ROADMAP FOR REFUELLING STATIONS OF HYDROGEN

As indicated in the proposal for a European Directive commented previously, each Member State shall adopt a national policy framework for the market development of alternative fuels and their infrastructure, that will contain at least the following elements:

- Assessment of the state and future development of alternative fuels;
- Assessment of the trans-border continuity of the infrastructure coverage for alternative fuels;
- The regulatory framework to support the build-up of alternative fuels infrastructure;
- Policy measures to support the implementation of the national policy framework;
- Deployment and manufacturing support measures;
- Research, technological development and demonstration support;
- Targets for the deployment of alternative fuels;
- Number of alternative fuel vehicles expected by 2020;

- Assessment of the need for LNG refuelling points in ports outside the TEN-T core network that are important for vessels not engaged in transport operations, in particular fishing vessels;
- Where appropriate, cooperation arrangements with other Member States according to the second paragraph.

AN OPTIMIZATION APPROACH TO EVALUATE POLICIES ON SUBSIDIES

There have been projects related to service stations of hydrogen, as for example the HyWays project, which may be a reference point of interest, but has not come to grips with the problem of the location of filling stations to cover the demand at the country level.

The models proposed in the existing literature dealt with the dissemination process of hydrogen fueling stations, describing the interaction between the demand for hydrogen (depending on the number of journeys and of hydrogen-powered vehicles) and the location of hydrogen fueling stations (decided its location in terms of the benefits) [3]. In this communication the role of State, via subsidies, is added to this supply/demand equilibrium.

In literature, the effect so-called "who was first the chicken or the egg" has been described as critical in the process of implantation of hydrogen fueling stations. That is, the demand for hydrogen is going to generate new stations and the installation of these will cause the purchase of new vehicles of this type. The current equilibrium of supply equal to 0 and demand equal to 0 must be broken by external mechanisms, that through some initial subsidies, encourage the installation of these facilities.

An optimization model is proposed to decide which types of subsidies and their timing are optimal (minimum investment for State) will obtain a network of hydrogen fueling stations with a coverage given in 2020. The essential elements of the model are a nested logit model that describes the behavior of users compared to the acquisition of this type of vehicles depending on certain attributes, such as the percentage of coverage, the costs of acquisition, etc., a gravity model to describe from where to where traveling users and mechanisms to describe the commissioning/closure of hydrogen fueling stations in terms of the benefit. The benefit of these filling stations depends on its location, the number of trips, their used routes and the subsidies.

A heuristic algorithm is used to solve the proposed model. The solution provides the optimal plan of location, its timing and the optimal way of implementing a policy of subsidies given.

CONCLUSIONS

This communication proposes an optimization tool to support the decision making for holding the draft European Directive (for Spain). The model incorporates subsidies and this element is novel in Literature.

BIBLIOGRAPHY.

[1] European Parliament and Council directive on the creation of an infrastructure for alternative fuels. Brussels, January 24 2013.

[2] Communication from the Commission to the European Parliament, the Council, the Economic and Social Committee and the Committee of the Regions. Brussels, January 24 2013.

[3] Schwoon, M. (2007), A tool to optimize the initial distribution of hydrogen filling stations. Transportation research Part D, 12, 70-82.

[4] Melendez and A. Milbrandt, (2005). "Analysis of the Hydrogen Infrastructure Needed to Enable Commercial Introduction of Hydrogen- Fueled Vehicles", Proceedings of the National Hydrogen Association (NHA) Annual Conference, Washington, D.C.

Location of hydrogen fueling stations in urban areas (DFS1-6)

J. Javier Brey; Abengoa Hidrógeno, S.A.

Ana F. Carazo, Department of Economics, Pablo de Olavide University

Macarena Tejada, Department of Geography, History and Philosophy, Pablo de Olavide University

Raúl Brey, Department of Economics, Pablo de Olavide University

INTRODUCTION

The rollout of hydrogen fueling stations within a region, in a manner that creates sufficient infrastructure with minimum investment is, without doubt, one of the main problems hydrogen as a fuel will have to face. Users demand an infrastructure that allows them to refuel at their convenience, prior to venturing into buying a vehicle that runs on hydrogen. Moreover, the current high cost of hydrogen fueling stations makes it necessary to reduce the initial infrastructure to the minimum possible.

Given that the main objective in the initial stage is to supply the largest possible volume of potential users, planning the rollout of stations in major urban areas becomes a very important issue.

The problem of intra-city rollout requires a different approach to the rollout of stations to allow inter-city travel. In the case of a city we find a large population concentrated in a smaller area and, therefore, the location of the stations cannot be performed based solely on criteria of distance between them.

MODEL

When dealing with locating fueling stations two different approaches can be distinguished: optimization methods (operations research) and GIS based approach. The optimization approach makes use of optimization models to attain an efficient infrastructure design according to some specific criterion or criteria. These optimization-based approaches can be classified into two groups depending on the geometric representation of demand: models for point-based demands, and flow-based demands. In this paper the authors propose a multiobjective programming model that combines these two representations of demand when locating a preset number of refueling stations from a set of potential candidate sites

On the one hand, the first objective (f_1) is to locate the stations so as to minimize the travelling time from the different areas of the city to the stations. The different areas would be weighted by their population, so that the model tends to locate the stations closer to the more highly populated areas. The second objective (f_2) is to maximize traffic flow captured by the filling stations. Thus, the first objective locates the stations on the basis of the residence of the inhabitants while the second locates them attending to their travels.

Generally, this multiobjective problem can be written as:

$$\begin{aligned} & \text{Opt } (f_1(x), f_2(x)) \\ & \text{s. t. } x \in X \end{aligned}$$

where X represents the feasible region.

This vector optimization problem is generally solved by reducing it to a scalar optimization problem. Several scalarization methods exist. One of the best known is the weighted sum method. According to this method, the optimization problem can be written as:

$$\begin{aligned} & \text{Min } \alpha f_{1_{norm}}(x) - (1 - \alpha) f_{2_{norm}}(x) \\ & \text{s. t. } x \in X \end{aligned}$$

where $f_{1_{norm}}$ and $f_{2_{norm}}$ are the corresponding normalized objective functions, and α and $(1 - \alpha)$ are the weights associated with each of the objectives. This optimization problem can be solved for different values of α , thereby obtaining the set of possible solutions for the different values of α .

Finally, the optimization problem can also be solved for different values of the number of stations to locate, thereby enabling analysis of the trade-off between the number of stations and the average time required to reach them and captured flow.

APPLICATION

The authors are currently working on applying this model to the city of Seville, the fourth most populous city in Spain with a population of around 700,000 inhabitants and an area of approximately 140km². The importance of this city makes it a candidate for consideration as a major urban agglomeration with a view to locating hydrogen fueling stations in compliance with the Draft Directive the European Parliament and Council are currently discussing.

As a first step, we have divided Seville into a number of areas (census units), we have established their population, and we have located the gas stations that existed in Seville in 2012 (see Figure 1); we are using these stations as potential candidate sites. In addition, the traffic gauges in Seville have been located to establish the levels of traffic flow in the different areas of the city (see Figure 2). With all this information, it is now possible to calculate distances and solve the aforementioned model.

Figure 1.- Population per census unit. Red squares indicate the location of current gas stations.

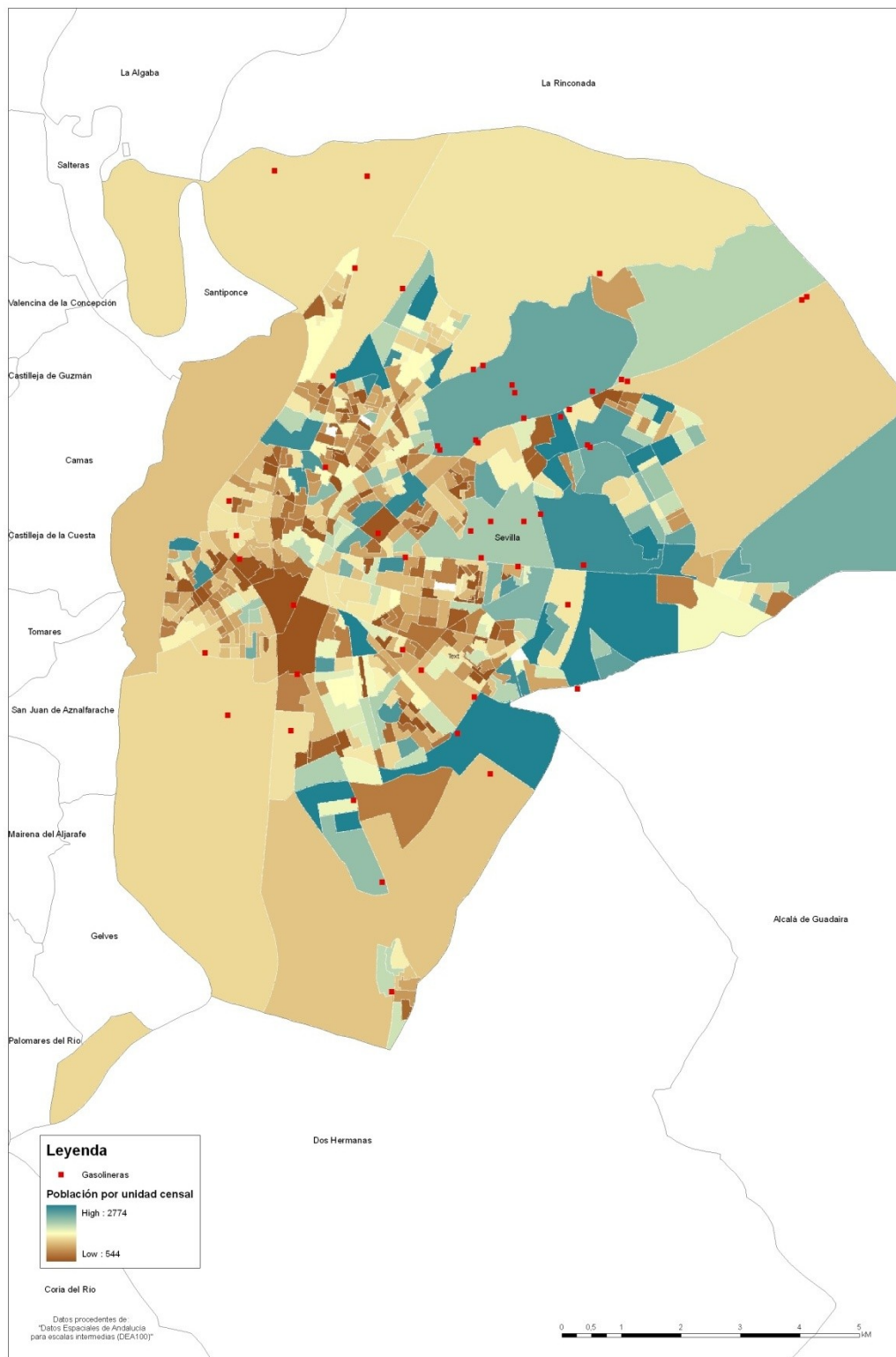
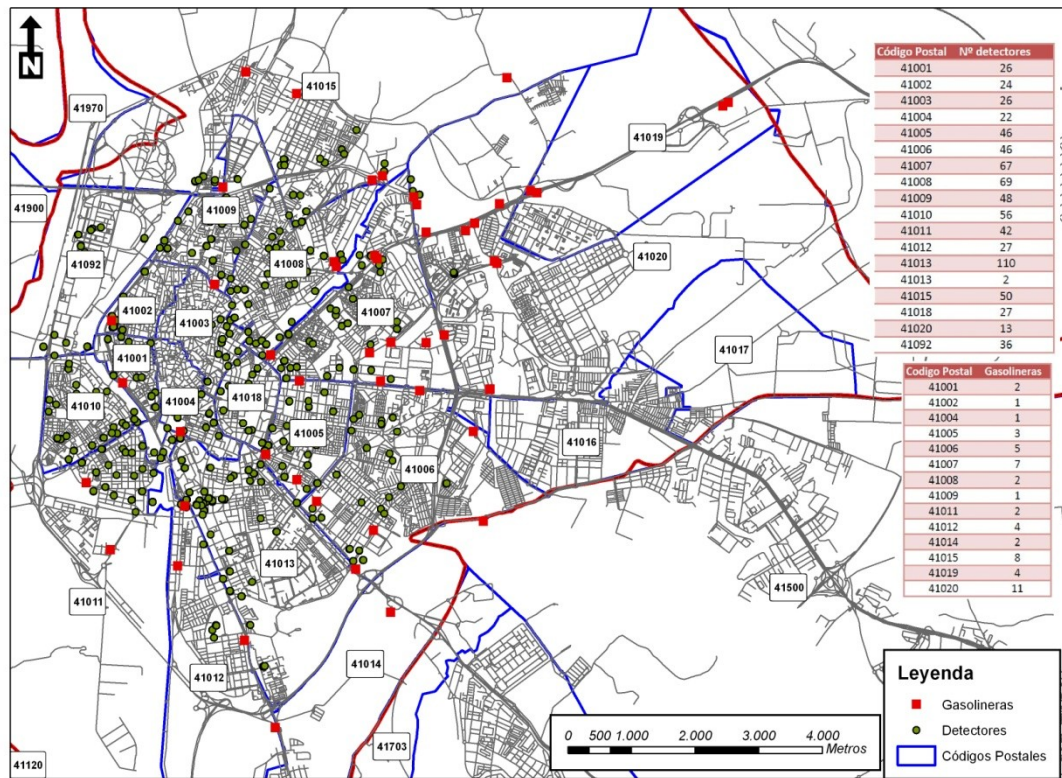


Figure 2.- Green circles indicate the location of traffic gauges. Red squares indicate the location of current gas stations.



Assessment of a hydrogen refueling station (DFS2-1)

C.WULF, M. KALTSCHMITT

*Hamburg University of Technology, Institute of Environmental Technology and Energy Economics,
Eißenendorfer Straße 40, 21073 Hamburg, Germany,
christina.wulf@tuhh.de; kaltschmitt@tuhh.de*

INTRODUCTION

The introduction of hydrogen as a fuel in the mobility sector requires a sufficient extension of hydrogen refuelling stations (HRS). In the beginning, these stations will probably be supplied with surplus hydrogen, e.g. from chemical processes, and hydrogen produced from natural gas due to economic reasons. But only the use of hydrogen from renewable sources, e.g. electrolysis with electricity from wind power, develops the full potential of hydrogen, i.e. reduction of greenhouse gas emissions, storage of surplus electricity, locally zero emissions and reduction of mineral oil imports. This can be accomplished either with big centralized electrolyzers or with smaller ones directly at the HRS.

The new HRS in Hamburg HafenCity, Germany is dispensing self-produced hydrogen from alkaline water electrolysis with electricity from renewable sources. To build and operate a highly efficient HRS according to the latest state of technology for private vehicles and buses is the main goal of this HRS. In this way more experience with this technology will be gained and the existing challenges can be mastered. Furthermore, the station can be used for demand side management for electricity coming from renewable sources of energy characterised by strong fluctuations, which in Hamburg is mainly wind power.

In this paper data from the HRS in Hamburg is taken to model and analyse this system. The focus is the energy consumption to verify if the high goals in respect of efficiency can be achieved and at which spots difficulties have to be tackled. Furthermore different load profiles are assessed to look at the energetic behaviour as well as the costs.

HYDROGEN REFEUILLING STATION

Technically this HRS is mainly constructed to serve fuel cell busses. They need 35 MP hydrogen and at the moment a special fuelling protocol for them it does not exist. That is why only the capacity of the system is defined. Additionally, fuel cell passenger vehicles can be refuelled according to the fuelling protocol SAE J2601 with 70 MP. For this, advanced framework conditions apply to the dispenser. Those include a specific fuel temperature at the dispenser nozzle, maximum fuel flow rate, maximum rate of pressure increase and other performance criteria.

Each of the two electrolyzers installed can produce 60 Nm³/h. The renewable electricity comes from the German electricity grid as alternating current (AC). Before it can be used in the electrolyser it has to be transformed to direct current (DC) in an inverted rectifier. Also the water has to be prepared before it can be split into hydrogen and oxygen. The normal tap water contains too many ions that could harm the electrodes. That is why it has to be deionised by a reverse osmosis unit.

Afterwards the water has to be alloyed with potassium hydroxide (KOH) to get the right conductivity for the electrodes.

The electrolyzers can run either in full or in part load (range of 40 to 100 %). This flexibility as well as the big sized middle pressure storage tank (4.5 MP) enables the system to serve as electricity storage. During the night hydrogen is produced and stored until it is needed during the day. When the electricity consumption is high the electrolyzers is operated at a minimum hydrogen production without shutting them down. Each electrolyser consists of four stacks that can be maintained individually. As fuel cells need very pure hydrogen (at least 99.999 % H₂) the hydrogen leaving the electrolyser needs to be cleaned. Even though electrolyzers produce very pure hydrogen, electrolyte can come out of the system. To get rid of this water the hydrogen needs to be cleaned by several gas separators and a drier.

In order to use a HRS for demand side management a more advanced storage and compression system is needed. The produced hydrogen flows from the electrolyser in the low pressure storage tank of a very small size of 1 m³ which is operated at 1.6 MP. Afterwards – if no vehicles receive hydrogen – it is compressed to 4.5 MP and stored in the two middle pressure tanks. These storage facilities have a capacity of 95 m³. In a last compression step hydrogen reaches 85 MP. The high pressure storage comprises four tanks from 1.2 to 0.6 m³.

The 70 MP storage tank of the vehicle makes a compression of the hydrogen to over 80 MP at the station necessary. For this, a new compressor, the so-called ionic liquid piston compressor, has been developed especially for hydrogen. Instead of a metallic piston, this compressor type has a nearly incompressible ionic fluid that compresses the hydrogen like a normal piston in vertical cylinders. The application of an ionic liquid piston compressor requires special fluid conditions. These are enhanced by using an organic salt that is not volatile, non-combustible, and environmentally friendly, inhibits corrosion and offers good lubrication. The long term usage of this compressor will show if the promised advantages as the lower energy demand, longer lifetime, less costs for operation and maintenance as well as low noise development are fulfilled.

Before the hydrogen can be dispensed to the vehicles it needs to be precooled down to -40 °C to achieve the SAE J2601 standard. Therefore a so called ultra low cold fill is installed.

APPROACH

According to the method introduced by Ulleberg in 2003 the electrolyser is modelled in Modelica an object-oriented modelling language that can carry out dynamic processes. The other components, i.e., rectifier, reverse osmosis, gas separators, drier, compressor, storage, cooling system and dispenser, as well as the electrolyser are built to a system with primary data from the actual HRS in Hamburg. If no sufficient data is available reasonable literature values are used. With this model two different load profiles for the system will be calculated. On the one hand a profile following the wind production in Germany will be assessed regarding the efficiencies and the costs. Furthermore on other load profile with allows a more constant production will be analysed.

Rollout of hydrogen refuelling stations employing a strategy of fixed nodes and maximum flows (DFS2-2)

J. Javier Brey; Abengoa Hidrógeno, S.A.

Ana F. Carazo, Department of Economics, Pablo de Olavide University

Raúl Brey, Department of Economics, Pablo de Olavide University

INTRODUCTION

The European Parliament and Council are currently discussing a proposal for a Directive to promote the use of alternative fuels in the Member States of the European Union. This Directive will require said Member States to take steps to increase the use of these clean and sustainable fuels. Among these fuels, hydrogen is of note, and has been included for the first time ever in regulations of this nature.

The proposal for a Directive, as regards hydrogen, requires the Member States to begin to define a strategy for a rollout of hydrogen refuelling stations that allows each nation to have a sufficient supply, thereby enabling potential users to purchase fuel cell vehicles.

In this regard, the proposal for a Directive indicates that hydrogen refuelling stations will have to be located:

In the large “major urban agglomerations”,

and ensuring a maximum distance between stations that, initially, has been set at 300 km.

However, the proposal for a Directive does not provide any further information on how to realize this rollout strategy and, most certainly, the manner in which this strategy is managed will have much to do with the success or failure of the rollout of hydrogen as fuel for transportation.

This paper suggests a strategy for the rollout of hydrogen refuelling stations in a given area or region, based on the criteria established by the aforementioned proposal for a Directive.

The procedure will be particularized for the case of Spain, to enable better appreciation of the potential of the algorithm.

PROPOSED METHOD

Objective:

The aim of this method is the location of hydrogen refuelling stations in a geographical area, beginning with a set of nodes that are the “major urban agglomerations” and which are, therefore, already set in advance, while establishing a maximum distance on “main motorways” between refuelling stations to ensure adequate supply. Obviously, the goal is to minimize the number of refuelling stations to be installed, to ensure maximum possible efficiency of investment.

Definitions:

The proposed method starts from the selection of what the proposal for a Directive refers to as “major urban agglomerations”; in this paper we will define every area whose population is more than 1% of that of the country or region to be considered as a “major urban agglomeration”. They will be referred to as MUA_i in the algorithm.

The second aspect is the definition of “main motorways”; for us, “main motorways” will be deemed to be all those with a category of highway or motorway, local, regional or national, operated publically or privately.

Lastly, the maximum distance we will allow between refuelling stations on a “main motorway” will be indicated as D_{max}. It is our understanding that the coverage of the refuelling stations must be done by linking the “major urban agglomerations” and also by linking these same areas to the borders of the region or country in question, thereby ensuring not only adequate interconnection within the area, but also with the neighbouring areas.

Algorithm:

After considering all these definitions, the algorithm is as follows:

- For all the “main motorways” that link MUA_i with MUA_j without going through MUA_k:

If the distance between MUA_i and MUA_j along any of the “main motorways” that link said nodes is equal to $d_{ij} < D$, then it conforms.

If all the “main motorways” that link MUA_i and MUA_j are longer than $d_{ij} > D$, then select the “main motorway” with the heaviest flow.

- For the “main motorway” with the heaviest flow that links MUA_i and MUA_j:

Position N_{ij} refuelling stations in such a way that the minimum possible are positioned while ensuring that the distances between stations is less than D.

These refuelling stations must be positioned at the points with the heaviest flow on the “main motorway” while ensuring compliance with the previous point.

- For all the “main motorways” that link MUA_i with a border of the area in question with another region or area without going through MUA_k:

If the distance between MUA_i and the border along any of the “main motorways” that link said node with the border in question is equal to $d_{ij} < D$, then it conforms.

If all the “main motorways” that link MUA_i and the border in question are longer than $d_{ij} > D$, then select the “main motorway” with the heaviest flow.

- For the main motorway with the heaviest flow that links MUA_i and the border:

Position Nij refuelling stations in such a way that the minimum possible are positioned while ensuring that the distances between stations is less than D.

These refuelling stations must be positioned at the points with the heaviest flow on the “main motorway” while assuring compliance with the previous point.

APPLICATION FOR THE CASE OF SPAIN

With a 2011 census population of 43.78 million, 1% of the Spanish population stands at 437,000 inhabitants. With that number of inhabitants, or more, in Spain we have:

Madrid	3,265,038
Barcelona	1,615,448
Valencia	798,033
Seville	703,021
Zaragoza	674,725
Malaga	568,030
Murcia	442,203

That gives us a total of 7 “major urban agglomerations” that would be, at the outset, provided with hydrogen refuelling stations.

The application of the abovementioned algorithm with $D = 300$ km would result in the following map:

Electrochemical hydrogen compression and purification (DFS2-3)

Wiebrand Kout, Peter Bouwman - HyET

The company Hydrogen Efficiency Technologies (HyET) has expanded greatly the abilities of electrochemical hydrogen compression, presenting this technology as a solution for logistical issues surrounding hydrogen usage.

Advantages include:

- Exceptionally high compression up to 1000 bar ΔP single stage
- Accurate, bi-directional control over hydrogen flow rate
- Purification of the hydrogen stream
- No noise
- Less maintenance
- More compact and lightweight than a mechanical compressor

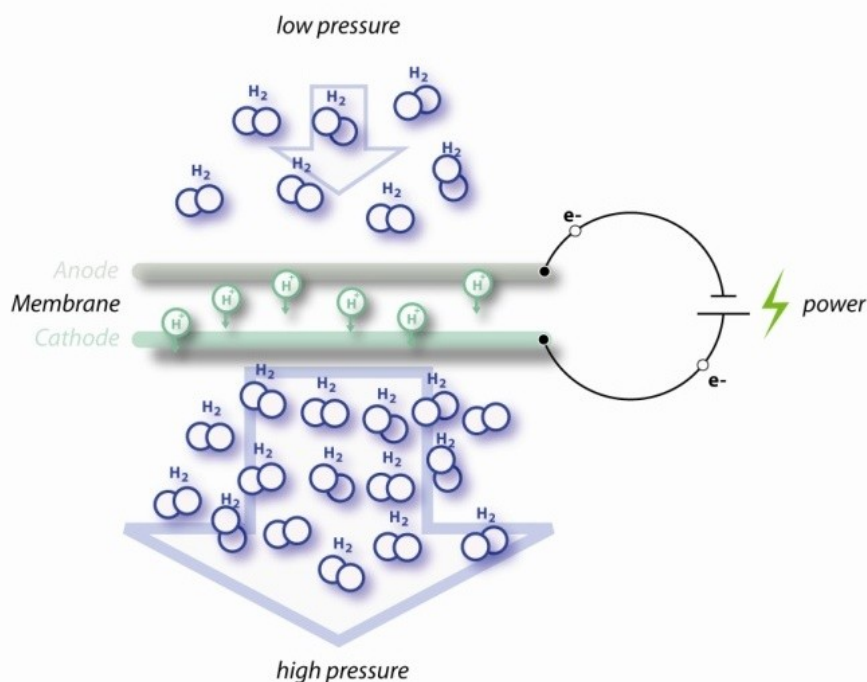


Figure 18 – Principle of Electro-chemical Hydrogen Compression using an external driving current, where electrodes convert hydrogen gas to protons and vice versa on either side of the acidic membrane.

These abilities, together with the modular scalability of the EHC, make this technology commercially attractive for several market applications such as automotive, energy buffering, and recycling respectively.

The working principle behind the EHC is driving (dissociated) hydrogen ions through a solid polymer, proton-conducting membrane by forcing a current through an external circuit. The membrane is the key component.

HyET has been working since 2009 on Research and Development of the electrochemical hydrogen compressor (EHC) technology for market introduction of related products. Our facilities are well equipped for realizing bespoke cell hardware and 'software' (i.e. Membrane Electrode Assemblies, MEA) designs, thanks to the transfer of surplus resources from the Energy research Centre of the Netherlands (ECN). Having both elements under one roof has proven critical to achieve mutual compatibility and successfully reach 1000 bar compression successfully in 1 single stage. The components in the MEA aimed at hydrogen compression are in principle similar to those in fuel cell applications, but their material composition and properties are different.

It was found that the well-known PFSA proton conductive membranes that are used in PEM fuel cells are not suitable for electrochemical compression. The reason is that the standard materials show too much hydrogen back-diffusion at pressure differences greater than 20 Bar. This back diffusion of molecular hydrogen directly reduces the main advantage of electrochemical compression: its high energy efficiency per quantity of pumped hydrogen (kWh/kg).

The logical approach to reduce back-diffusion is by using thicker membranes. The obvious downside of this approach is that also the cell resistance increases with membrane thickness, again resulting in reduced efficiency. Proprietary membranes have been developed at HyET to minimize passive permeation of all gases. Our bespoke membranes have a structure that allows protons to pass from anode to cathode, but prevents to a great extent the transport of hydrogen molecules in the opposite direction.

The electrodes used by HyET are different compared to electrodes used in fuel cells in two areas. HyET has developed electrically conductive materials that retain adequate porosity even at high working pressures. The superior mechanical strength ensures the access of the reactant gas to the catalyst is maintained, even under high pressures up to 1000 bar. In contrast, a typical fuel cell experiences a combined assembly and working pressure of less than 10 bar. The second difference is that the catalyst loading can be greatly reduced compared to fuel cells, due to the high reaction rate of Hydrogen Oxidation Reaction and Hydrogen Reduction Reaction. HyET has successfully tested electrodes with a catalyst loading of less than 10 $\mu\text{g}/\text{cm}^2$ of Precious Group Metals (PGM), thus reducing the component cost

HyET has made advances in the mechanical engineering of the electrochemical cell hardware. The stack cell pitch has already been reduced from five to two millimeters, and a further reduction to less than one millimeter is anticipated. The use of nontraditional machining technologies has enabled a simultaneous reduction of bipolar plate size and manufacturing tolerances. Controlling these tolerances has proven to be vital for a reliable sealing of high pressure hydrogen gas.

Experimentally the feasibility of electro-chemical hydrogen compression of hydrogen has been demonstrated up to a pressure of 1000 bar single stage under potentiostatic control as shown in Figure 2:

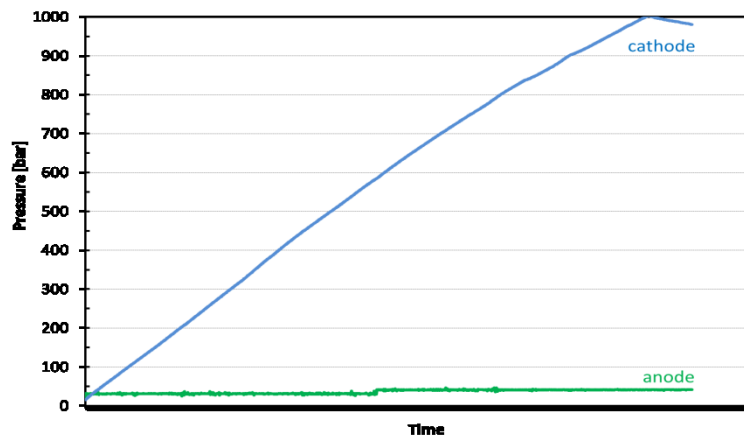


Figure 2 – Compression of hydrogen gas from 20 bar to 1000 bar single stage

The HyET technology has surplus value besides transporting hydrogen upon demand. The solid state electrochemical process generates no friction or heat like a mechanical compressor. As a result the energy use can be less than 3 kWh/kg of compressed hydrogen from 20 to 1000 Bar. Another major advantage is that the hydrogen is filtered, because contaminants cannot pass through the proton-conducting membrane like hydrogen does. Since hydrogen is actively and selectively extracted from the gas supply, it has proven possible to use sources containing less than 10% hydrogen and yet deliver pure hydrogen (>99.99%). The technology creates new market opportunities for (biological) hydrogen production, lower cost reformer systems and industrial hydrogen recycling. The ability to inject and extract hydrogen gas into/from natural gas pipelines creates a novel path for hydrogen distribution.

HyET is the project coordinator of the PHAEDRUS project, which is funded under the Seventh Framework Programme (SP1-JTI-FCH.2001.2.7). The project consortium will develop an all electrochemical 700 Bar hydrogen refueling station for fuel cell cars. PHAEDRUS will demonstrate the applicability of electrochemical hydrogen compression technology in combination with self-pressurizing Polymer Electrolyte Membrane (PEM) electrolyser technology. The partners will develop a station with modular dispensing capacity in the range of 50-200kg/day, ready for roll-out from 2015 onwards. Key objectives include the validation of the safety aspects of the system, its efficiency and the economic viability of the modular design concept. HyET is responsible for the development of an electrochemical compressor design capable of delivering 200kg/day of hydrogen at a pressure of 700 Bar.

Experimentally the feasibility of electrochemical compression of hydrogen has been demonstrated up to a pressure of 1000 bar single stage. The HyET technology features significant advantages over the conventional mechanical compression such as instant response, high efficiency, large compression factor and intrinsic purification. Dedicated materials and components are developed by HyET specifically towards this high pressure application, making use of advancements in fuel cells. HyET anticipates a surge in demand for its technology with increasing use of hydrogen as

energy carrier to link distributed, renewable energy sources with local storage and automotive power demand.

Acknowledgements

We gratefully acknowledge that the research leading to these results has received funding from the European Union Seventh Framework Programme under grant agreement n° FCH JU 303418 “Phaedrus”. For more details on this project please visit www.phaedrus-project.eu .

Effect of precooled inlet gas on temperature evolution during refueling (DFS2-4)

Rafael Ortiz Cebolla, JRC-IET, Rafael.ortiz-cebolla@ec.europa.eu

Nerea de Miguel Echevarria, JRC-IET, Nerea.de-miguel-echevarria@ec.europa.eu

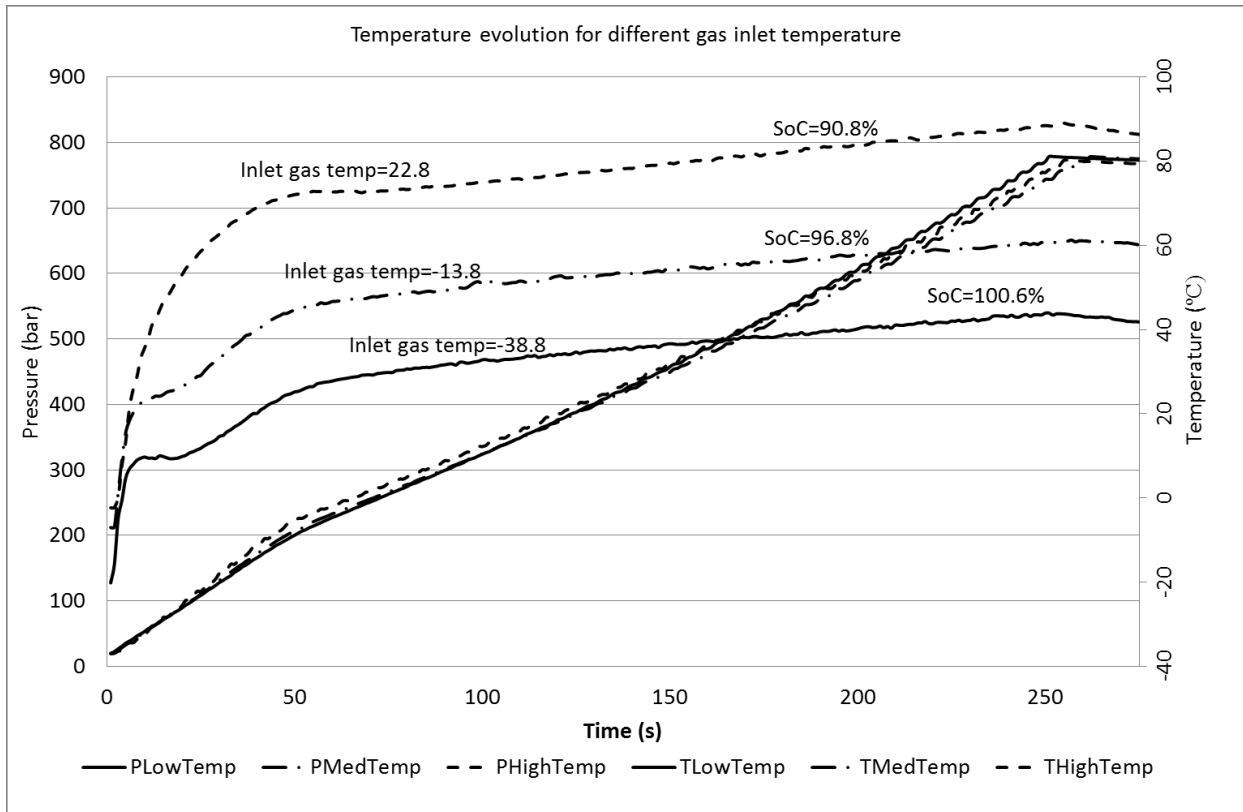
Beatriz Acosta Iborra, JRC-IET, beatriz.acosta-iborra@jrc.nl

Pietro Moretto, JRC-IET, Pietro.moretto@ec.europa.eu

Christian Bonato, JRC-IET, Christian.Bonato@ec.europa.eu

Frederik Harskamp, JRC-IET, Frederik.Harskamp@ec.europa.eu A number of car manufacturers (Toyota, Honda, General Motors...) have established 2015 as the starting year for the introduction of commercial Fuel Cell Vehicles (FCV) in the Japanese, European and USA markets. To have a successful introduction of these FCVs, a network of hydrogen stations should be deployed. These hydrogen stations have to ensure compliance with several safety requirements, one of them being not exceeding a temperature higher than 85°C inside the tank during the refuelling. Temperature limit of 85°C is set for two reasons, to protect the materials of the tank from thermal degradation, and to be able to fill the tank (100% state of charge) without exceeding the maximum working pressure (125% of the nominal working pressure). In addition, refuelling time should not exceed 3-5 minutes, to be competitive with conventional petrol stations and attractive for the potential costumers. To perform a refuelling within these two limits represents a technological challenge, since the faster the filling the higher the increase of temperature. For this reason it is necessary to study this process and try to figure out which are the important parameters affecting temperature evolution during refuelling.

The JRC-IET has developed a facility, GasTeF, for carrying out tests on full-scale high pressure vehicle tanks for hydrogen or natural gas. This facility is unique in Europe and it allows performing permeation tests and fast filling tests at a maximum pressure up to 850 MPa (with helium, hydrogen or methane). The facility allows performing tests with different environmental temperatures, flow rates and gas inlet temperatures. A big amount of data is collected during the tests through the different sensors installed in the facility. In this paper we show the effects of precooled inlet gas on temperature evolution, depending on several parameters as type of tank or flow rate. The type of tank (metallic liner, type 3 or plastic liner, type 4) affects temperature evolution during the filling, resulting in lower temperatures in type 3 tanks due to their higher heat transfer coefficient. This different thermal behaviour implies different precooling needs depending on the type of tank, which are studied and included in this paper. The flow rate plays an important role in the temperature evolution during refuelling, with higher temperature increase obtained with higher flow rates. The importance of the precooling regarding the flow rate is considered in this study. The test results will be compared with the fuelling protocols shown in the SAE J2601, where several inlet gas temperatures (-40°C, -20°C, 0°C, and not precooled gas) are considered. Furthermore a discussion based on the comparison between the energy used to cool down the gas and the additional amount of hydrogen mass introduced in the tank due to the precooling (to reach a 100% of state of charge) is included in this study.



Market strategies

Analysis of the general public and stakeholder awareness and acceptance on hydrogen technologies (MS-1)

Carolina García¹, Guillermo López²; Laura Vega², Daniel Esteban Bechtold¹

¹ Centro Nacional de Hidrógeno

² IPLUSF

PUBLIC AWARENESS AND ACCEPTANCE

Social acceptance of new technologies could be conceptualized as a three dimension issue, including socio-political, community and market acceptance (Wüstenhagen, Wolsink & Bürer, 2007). Deep social research on hydrogen acceptance are providing insight into the state of public and stakeholder acceptance (including socio-political and market actors), and about relevant factors affecting those levels of awareness and acceptance.

This will result in useful information to understand better how society and stakeholders respond to innovative technologies and applications. Therefore, research will focus in understanding influencing factors to the acceptance process (tacking into account a certain technology, project or system specification) during the different phases in hydrogen implementation. The aim is to achieve a better knowledge that helps to optimize the management of hydrogen transition.

The following questions are considered in order to understand the acceptance process' implications to the transition phase of hydrogen energy and FCH technologies:

a) *What has to be accepted?* Idea, technology, project, system set up...

b) *Who has to accept?* Core project (project manager, employees), project environment (regional partners, administration, politics, neighborhood, research groups), general public, interest groups and media...

c) *What level of acceptance is needed?* Tolerance (neutral/ "wait and see"), sympathize (passive acceptance), support (active acceptance)

d) *When is acceptance needed?* Project (initial, planning, implementation phase), transition phase, daily life.

Implementation process



Awareness and acceptance vary along the different phases of hydrogen implementation process, and also influencing factors and relevant actors. So, it is important to identify what

level of acceptance is needed and when; e.g. general public support and attitude during the transition phase could be a passive acceptance (“wait and see”) as long as people won’t be able to buy the technologies... Perhaps the stakeholders will keep on being supportive (investing money, setting up strategies) when the general public does not express enthusiasm... So far research has shown that a supportive acceptance will be necessary in the transition phase of hydrogen energy and FCH projects from people involved in the development and demonstration of technologies and the strategies.

WHY MEASURING AND INFLUENCING ACCEPTANCE

There is increasing realisation amongst policy makers and industry that public acceptance is a key consideration for any attempts to deploy and extend hydrogen technologies and infrastructures. The development of hydrogen technologies in Europe will involve small-scale applications as well as large-scale infrastructures that may be influenced by the acceptance of the general public, stakeholders groups, the local community and the potential customers and users.

Previous research on social acceptance has investigated the general levels of public understanding of HFC technologies in specific countries, but there is limited systematic evidence on the social acceptance of FCH technologies throughout Europe.

THE CONTRIBUTION OF HYACINTH PROJECT

HYACINTH is a project financed by the European Commission whose overall purpose is to gain a deeper understanding of the social acceptance of hydrogen technologies across Europe as well as to develop a communication and management toolbox to be used in ongoing and future activities aiming at introducing hydrogen into mobility, stationary and energy or backup power supply systems.

To reach these purposes the project consortium, led by the Spanish Centro Nacional de Hidrógeno, and supported by other nine organisations of five different countries, is working in the following objectives:

- Identify and understand awareness and acceptance of hydrogen energy and FCH technology and perceived potential benefits (added value) in the general public and at selected stakeholders, expected to be relevant to the implementation of FCH projects and activities in the transition phase (industry supplier, industry and private customer, administration and politics, interest groups and media),
- Identify the main drivers of social awareness and acceptance of FCH technologies in order to provide recommendations on how and what to best communicate and engage general public and stakeholders involved in regional hydrogen energy and FCH projects and activities,
- Support stakeholders (industry, project managers, policy makers...) by providing a social acceptance research toolbox, enabling a regional understanding of the acceptance process and providing tools to manage expectations to keep or increase acceptance at selected stakeholder groups and the general public.

These objectives will be achieved by the completion of the following tasks:

-Collection of relevant information in the target countries:

Identification of European existing hydrogen projects

Collection of hydrogen policy around Europe

Identification of hydrogen stakeholders

-Identification of methodological experiences to measure social acceptance in the Hydrogen and Fuel Cells Field: theoretical framework.

-Identification of the most meaningful factors affecting awareness and acceptance.

-Survey research with representative panels across Europe (up to 7.000 European citizens)

-Semi-structured interviews with 650 selected stakeholders in 7 countries.

HYACINTH TOOLBOX: A TOOL FOR ACCEPTANCE MANAGEMENT

The design of the data gathering instruments will build upon the methodological and conceptual developments in the research of social acceptance of new technologies. The toolbox will provide the necessary background information and understanding of the current state of awareness and acceptance of HFC technologies by the general public and by stakeholder groups (industry, municipalities, researchers, fleet operators ...). It will further provide the necessary tools to understand and manage expectations of future HFC projects and products in the transition phase, to identify regional challenges to the projects and to determine effective policy support measures.

Together the results from the research on the social acceptance of FCH technologies across Europe and the toolbox will support future projects in setting up under through consideration of the acceptance processes influenced by their activities; i.e. identifying regions of supportive acceptance, bottlenecks and challenges to be tackled, communication strategies and other means to actively manage the acceptance process FCH technologies.

Hydrogen Transport in European Cities (HyTEC) (MS-2)

¹Marieke Reijalt on behalf of ²Emma Guthrie, project coordinator

¹HyER; ²Air Products

The Hydrogen Transport in European Cities (HyTEC) project is creating two new European hydrogen passenger vehicle deployment centres in London and Copenhagen - cities widely recognised as leaders in developing ultra-low carbon urban transport solutions. The overall goal of HyTEC is to implement a demonstration programme that specifically address the challenge of transitioning hydrogen vehicles from exemplars to fully certified vehicles driven by end-users and facilitating the build of a network of Hydrogen Fuelling Stations (HRS). The project consortium consists of 15 organisations¹ from five member states, working together to:

The Hydrogen Transport in European Cities (HyTEC) project is creating two new European hydrogen passenger vehicle deployment centres in London and Copenhagen - cities widely recognised as leaders in developing ultra-low carbon urban transport solutions. The overall goal of HyTEC is to implement a demonstration programme that specifically address the challenge of transitioning hydrogen vehicles from exemplars to fully certified vehicles driven by end-users and facilitating the build of a network of Hydrogen Fuelling Stations (HRS). The project consortium consists of 15 organisations¹ from five member states, working together to:

- - Demonstrate the commitment of the two cities in integrating solutions in a cleaner air and a better and healthier lifestyle for their citizens
- - Demonstrate new fleets of hydrogen vehicles in different vehicles classes
- - Deploy new hydrogen refuelling facilities to support operation of the vehicles, which together with existing refuelling stations will lead to two new city based networks for hydrogen fuelling. These networks work on two different concepts, one based on on-site hydrogen production (Copenhagen) and the other on hydrogen delivery (London), allowing different pathways to be compared.
- - Produce a set of analytical results from the project, with an expert pan-European research team. The analysis is intended to consider the full well to wheels life cycle impact of the vehicles and associated fuelling networks, establish the technical performance of the vehicles and uncover non-technical barriers to wider implementation.
- - Plan for future H2 vehicle commercialisation, and provide an approach for the rollout of vehicles and infrastructure, building on the HyTEC demonstration activities.
- - Disseminate the results of the project widely to the public to improve awareness of hydrogen transport activity as user-friendly and good for the health. This is supported by targeted dissemination to other regions, key industrial stakeholders and policy makers.

In achieving these aims, the HyTEC project will create a genuine link between new and existing hydrogen passenger vehicle demonstration projects across Europe, thereby informing ongoing strategic planning for hydrogen rollout and also ensuring a 'common voice' towards the expansion of the hydrogen vehicle fleets in Europe.

The main project objectives addressed during this first period were:

- - Identify and evaluate HRS sites and select practical locations to install new HRS into the cities of London and Copenhagen and put fleets of vehicles into operation in both cities
- - Collect and analyse operational data from the HRS and vehicles
- - Capture qualitative data from the vehicle users in both cities.
- - Start work looking at hydrogen infrastructure expansion in both cities.
- - Create links with other cities and transfer learnings to regional and political stakeholders.

Consortium

Air products, Element Energy, HyER, hydrogen, fuel cells and electromobility in European regions), Cenex – centre of excellence for low carbon and fuel cell technologies, Greater London Authority, HySOLUTIONS GmbH, Matgas 2000 A.I.E., Ludwig-boelkow-systemtechnik GmbH, City of Copenhagen, Copenhagen Hydrogen Network, Hydrogen Link Denmark, Intelligent Energy Ltd, Heathrow Airport Ltd, London bus services Ltd, Fraunhofer-gesellschaft zur foerderung der angewandten forschung e.v

H2FC European Infrastructure; Support Opportunities to Hydrogen and Fuel Cell Research (MS-3)

*Olaf Jedicke; Karlsruhe Institute of Technology, Institute for Nuclear- and Energie Technologies
76366 Eggenstein-Leopoldshafen, Germany*

Introduction

The European Strategy Forum on Research Infrastructures (ESFRI) recognizes in its roadmap for Research Infrastructures that “in the near future hydrogen, as an energy carrier derived from various other fuels, and fuel cells as energy transformers, are expected to come into a major role for mobility but also for different other mobile and stationary applications” [1]. Actually it appears, that such modern hydrogen driven society lags far behind the reality. So it is allowed to question the current situation. The belief, that already most is comprehensively investigated and developed concerning hydrogen technology is incorrect. In fact, the hydrogen technology is market ready only partial and not prepared in a sufficient way to get finally included and adopted in a modern hydrogen driven society. Nevertheless it is possible to foster furthermore science and development on hydrogen technology. The “Integrating European Infrastructure” was created to support science and development of hydrogen and fuel cell technologies towards European strategy for sustainable, competitive and secure energy. Its acronym is H2FC European Infrastructure and was formed to integrate the European R&D community around rare and/or unique infrastructural elements that will facilitate and significantly enhance the research and development of hydrogen and fuel cell technology.

Research Infrastructure Project

H2FC European Infrastructure is a European Infrastructure Project funded by the European Commission. The project combines Europe’s leading R&D institutions together supporting research and development on i.e. hydrogen production technologies, pureness of hydrogen, storage materials and systems, storage and distribution possibilities, final use through fuel cells in a safe manner in stationary and mobile systems etc. The project is coordinated by Karlsruhe Institute of Technology (KIT) and consists of 19 European partners, collected from European’s research centers, universities and industry. With a total cost of € 10.147.583,60, H2FC European Infrastructure activities are subdivided into 25 work packages, fully interrelated, devoted to network activities, transnational access activities and joint research activities and oriented towards the resolution of identified scientific bottlenecks.

Main support to European’s hydrogen and fuel cell community will be given through the transnational access activities of the project, while opening very different technical and experimental facilities to external users. A further strong international support will be given to scientists and also to students by a continuous researchers exchange program and four technical schools. The prospects, education and the user access, will be announced by continuous calls through the H2FC European Infrastructure consortium.

Furthermore main objective of the project will be to generate a coordinated and integrated alliance based on complementary, state-of-the-art, or even beyond state-of-the-art unique infrastructures to serve the needs of the scientific hydrogen and fuel cells community and facilitate world class research. The current key research topics identified are:

- - Reducing degradation and increasing performance of electrolyser, hydrogen storage systems and fuel cells
- - Assessing and reducing hazards and risks associated with the use of hydrogen or hydrogen blended fuels and thereby ensuring the appropriate safety level of systems
- - Improving current storage technologies, in particular through advanced materials research.
- Objectives of the project are to provide:
 - - A single integrated virtual infrastructure accommodating H2FC communities' test and analysis facilities;
 - - Transnational access for the H2FC R&D communities to member state infrastructures
 - - Expert working groups to enhance work at the provided facilities and coordination in the aspects of safety, performance, durability
 - - Central databases and libraries of safety, performance and durability data and modelling codes
 - - Coordination of relevant education and training actions;
 - - Integration, enhancement and improvement of the existing infrastructures
 - - Coordination with national and international bodies as well as academic and industry demands.

Conclusion

The structure proposed in H2FC European Infrastructure will realize an alliance of the European scientific community for serving the necessities of the scientific community itself. Over the next 4 years, duration of the project, the H2FC consortium expects that external European experts will take up the opportunity to collaborate concerning identified scientific and technical bottlenecks, to strengthen hydrogen and fuel cell technologies, to support the adoption by industry and at least, to enlarge related knowledge.

ACKNOWLEDGEMENT

We like to acknowledge, that the H2FC European Infrastructure Project is support by the European Commission within the 7th Framework Programme under Capacities.

References

- [1] ESFRI, European Road Map for Research Infrastructures (Report 2006)

[2] EC, DG RTD. "European funded research on Fuel Cells and Hydrogen: review, assessment and future outlook". Report from the conference Hydrogen and Fuel Cell Review Days – 2007, Bruxelles, 10th-11th 2007

European Electro-mobility Observatory-compiling and presenting EV data (MS-4)

Jos Streng, Marieke Reijalt

HyER (the European Association for Hydrogen and fuel cells and Electro-mobility in European Regions, hyer.eu)

BACKGROUND AND OBJECTIVE

Electro-mobility is considered to become an important pillar of local transport systems. A lot of attention is currently given to these technologies and plenty of demonstration and evaluation projects are ongoing worldwide. Most of them include some form of data collection. Public awareness as well as expectations has increased significantly as the car industry worldwide is preparing the market roll out of EVs.

Therefore setting the right course for a successful and reliable commercialisation of EVs and the build-up of an appropriate energy infrastructure to recharge and refuel the first vehicles is crucial. Relevant decisions and measures have to be taken on European, national and regional/local level following the different jurisdictions of decision makers. The need to “translate” or “compile” recent scientific, technical and economical experiences and findings of ongoing R&D and demonstration activities into robust and practicable policy recommendations for different addressees is becoming increasingly urgent as recognised in the EU Clean Power for Transport Communication: “the Commission will facilitate information exchange and coordinated regional action across the EU with the European Electromobility Observatory.”

HyER with the support of the European Commission (DG MOVE) and a knowledge team consisting of TNO, ECN Vrije Universiteit Brussel and TÜV Nord and with the dissemination support of POLIS and AVERE, in December 2012 launched the European Electro-mobility Observatory (EEO) to become the central reference point for electro-mobility in Europe, evaluating and disseminating data and bringing together experiences from all relevant electro-mobility projects and programs across Europe.

The aim of the EEO is to be a central reference point, evaluating and disseminating data and bringing together experiences from all relevant electro-mobility projects and programs across Europe in a consistent way including:

- - Collection of technical and non-technical data from participating regions;
- - Gathering technology updates from industry and research institutions;
- - Conducting thorough data analysis and evaluation;
- - Providing policy recommendations;
- - Stimulating information exchange

By enabling:

- - Provision of basic statistics on electro-mobility in Europe;
- - Monitoring of progress and trends in electro-mobility;
- - Identification of best practices;
- - Identification of bottlenecks;
- - Fact-based, adaptive policy making in the field of introduction and deployment of electric vehicles and accompanying energy infrastructure at EU, national, regional and local level.

The EEO as an EU-wide monitoring framework of EV data and experiences will also organize a number of workshops and coordinate the number of surveys that are being conducted by different EU and national projects in order to avoid duplication and reduce the number of surveys sent of project managers.

APPROACH AND STATUS OF WORK

The HyER EEO pilot has established the scientifically sound and validated basis to take a much larger step towards the development of the general EU-wide observatory structure. The observatory has identified and collected lessons learned and results of a large number of national, regional and local users, i.e EV operators. Also is identified what the current knowledge needs are on the different governmental levels on the EU member countries.

On the basis of this inventory a practical and implementable structure for permanent collection, processing and analysis of appropriate data has been set up. The objective was to develop on the one hand a highly automated and standardized data collection system, maintaining however the greatest possible flexibility to adjust to new developments and needs for certain critical data.

A combination of web based surveys, bilateral exchanges and technical workshops are being organised to facilitate rapid recognition and visibility of the EEO. Currently the data collection system has been developed and a first inventarisation of the national and regional experts/contact points has been made.

The EEO monitoring framework for the data collection consists of a number of topics on which the requested information can be filled in:

- - Data on numbers of vehicle and energy delivery infrastructures
- - Financial and non-financial policy measures
- - National programs which include EV deployment activities
- - Knowledge needs and needs for exchange of experiences

The EEO has conducted a number of issue-based interactive workshops and webinars, to cover issues which cannot be handled via the general, standardized data collection. An example of such a workshop is the recently organised one on electric charging infrastructure

business models during the sustainable energy week in Brussels. These workshops are prepared by the research team by analysing available data and reports.

Coming months we expect to receive the data collection responses of the national and regional contact points providing us the data to analyse. During the EVS27 these outcomes and analyses will be presented.

THE CONSORTIUM

In order to face the above described challenges a multi-disciplinary and well-experienced consortium has been established to develop such a European Electro-mobility Observatory. The consortium is led by HyER (the European Association for Hydrogen and fuel cells and Electro-mobility in European Regions, hyer.eu) in association with TNO, ECN, VUB, TÜV Nord, POLIS and AVERE.

The heart of the consortium was involved in the HyER EEO pilot project that was conducted the year before the EEO started (2012). Coordinated by technical experts of TNO, ECN and Vrije Universiteit Brussel the EEO pilot identified, collected and analysed data and experiences of major electric mobility projects in 10 European key regions.

Commercialization and strategies

Pre-investigation of Water Electrolysis for Flexible Energy Storage at Large Scales: The Case of the Spanish Power System (CS-1)

F. GUTIERREZ-MARTIN,

E.T.S.I.D.I. Universidad Politécnica de Madrid (Spain)

This report aims to analyze the basis of hydrogen and power integration strategies, by using water electrolysis processes as a means of flexible energy storage at large scales; we consider two main aspects: 1) the state-of-the-art & development for electrolyzer techniques, and 2) the potential for introduction in utility systems.

We focus in the Spanish system, holding a surplus capacity which means a poor utilization ratio of the technologies ($\approx 30\%$), whereas the coverage with conventional utilities is near 50% over the peak demands. The load variations along the year make grid operations a challenging task to maintain the equilibrium in real time; this is complicated further by the geographic asymmetries of generation and demand, the penetration of renewable electricity and the limited interconnections. All of this means an inefficient use of infrastructures (both conventional and renewable), which suggests load leveling options to improve the efficiency based on more holistic energy approaches.

In this context, the production of hydrogen by electrolysis using the power grid mix is considered an option to increase flexibility and integration of renewable energy. Thus, we explore a novel aspect of the hydrogen economy which is based in the potentials of existing power systems and the properties of hydrogen as an energy carrier; the strategy is to control the power inputs, taking into account the efficiency and dynamics of electrolyzers, to show the benefits that can be reached by using surplus electricity at low prices, as well as the leveling effects on the energy balances of the plants.

ELECTROLYZER PERFORMANCE

Several factors affect the performance of electrolyzers: namely, the water dissociation potential, the kinetic parameters, the cell resistance and the Faraday efficiency; then, the energy yield is obtained from the voltage, current and BOP efficiencies using the equations:

$$V = [J + 2K (J \cdot r + E_0) + (J^2 + 4K \cdot E_0 J)^{1/2}] / 2K \quad \eta_F = f_1 \cdot J^2 / (f_2 + J^2) \quad E = 26.8 \cdot V / (\eta_F \cdot \eta_{BOP})$$

Focus is on alkaline water electrolyzers (AWE) which are the only currently available for large scales; fig. 1 show voltage, current and energy efficiency curves for AWE using representative parameters.

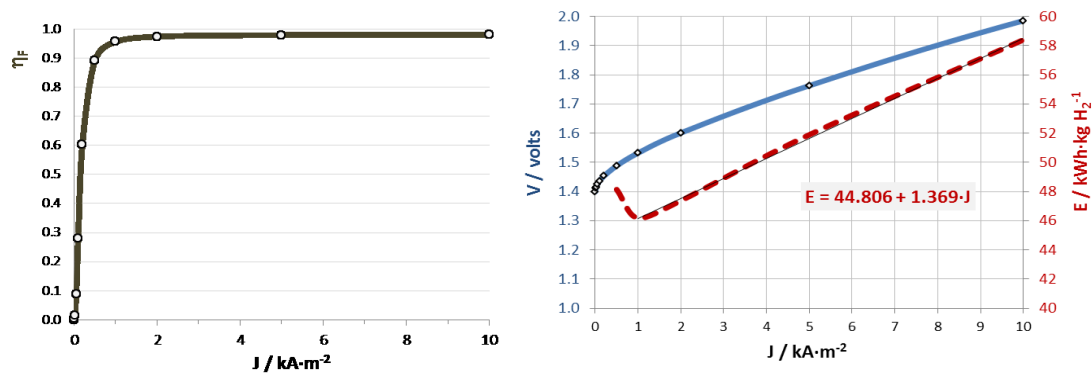


Fig. 1: Current-voltage and energy efficiency curves for an advanced alkaline water electrolyzer (AWE) with $E_0 = 1.4$ volt, $K = 120 \text{ m}\Omega\cdot\text{l}\cdot\text{m}^{-2}$ and $r = 0.020 \text{ m}\Omega\cdot\text{m}^2$, $f_1 = 0.98$ and $f_2 = 0.025 \text{ kA}^2\cdot\text{m}^{-4}$ (at 80°C), and $\eta_{\text{BOP}} = 0.93$

Capital costs can be anticipated between 200-400 €/kW, for large electrolyzers at increased current densities; this excludes BOP cost (like electronics, purifiers or handling the hydrogen).

$$\text{CEL (€)} = a \times Q_0 \text{ (kgH}_2\text{/h)} b \times J_0 \text{ (kA/m}^2) - c$$

The cost production of hydrogen is then estimated using expressions that include: the capital costs of electrolyzers+BOP (by a recovery factor and O&M rate), the inputs of electrolysis (from the power of the plants, their availability in h/year and the prices of electricity and water); the production of H₂ is the power input by the energy yield of electrolyzers.

$$\text{CH} = (\text{CCC} + \text{CO\&M} + \text{CE} + \text{CW}) / \text{QH}$$

$$\text{CCC} + \text{CO\&M} = (\text{F} + \text{OM}) \cdot \text{CEL} + \text{BOP} \quad \text{CE} + \text{CW} = 8760 \cdot \text{P} \cdot \text{u} \cdot \text{CAE} + 9 \cdot \text{QH} \cdot \text{CAW} \quad \text{QH} = 8760 \cdot \text{P} \cdot \text{u} / \text{E}$$

With this model we analyze electrolytic production, e.g. for big capacity plants, running part periods at increased current densities and using low priced power: the results are large installations with high hydrogen production, diminished efficiency (due to the high intensities) and reduced costs of energy. We simulated four parameters by a 2nd order design, where the regression shows significant effects of the utilization ratios and electricity prices, with relevant interactions of P/u , J_0/u , J_0/CAE ; concluding that the cost of hydrogen can be reduced using low priced electricity in long enough surplus periods, with larger capacities as u decreases, and rising the current densities as CAE , u , P become lower.

Summing up, reducing the voltage reduces the cost of energy, while increasing the intensity reduces investment costs; however, cell voltage increases with current density: in new advanced electrolyzers this conflict of interest is being optimized by new catalysts, new cell configurations and increasing the conductivity of electrolytes, till a point that there are not strong reasons to await for much more efficient processes to start business development; the relative high cost of equipment is still a barrier, but developing cheaper units (e.g. large plants for energy use) is just an engineering matter and not a feasibility question.

BALANCING THE GRID LOADS

An interesting system aspect of electrolytic processes is the possibility of power management; in this case, the choice of equipment has influence on the control capabilities of the system (range & times); The proposed model requires a holistic approach to the generating systems, the demand profiles, and their variations in space and time, together with an evaluation of electrolysis technologies that are applicable for managing the grid loads at large scales.

For the analysis, several power generation scenarios are superimposed to the load curves to estimate the H₂ producible in the valleys and the H₂ consumable in the peak hours; looking at the maximum surplus power values, we calculate the number/size of the plants, and using the electrolyzer model and parameters we approximate the production of hydrogen by:

$$Q_p = \sum P_t / E_t = \sum u_t P_0 / (k_0 + k_1 \cdot J_t)$$

where we regulate current densities according to the utilization ratios in each period (within a defined range): $J_t = u_t \cdot J_0$ $u_t = P_t / P_0$ ($0.10 \leq u_t \leq 1.20$)

The hydrogen for power regenerators (e.g. fuel-cells) is estimated from the peak imbalances, using a typical energy efficiency ($\eta = 0.60$): $Q_c = P_c / (\eta \cdot \text{LHV})$

Finally, the hydrogen available for other uses is obtained as: $Q_a = Q_p - Q_c$

The analysis illustrates how variation of generation scenarios serves the purpose to get a balance of the efficiency, economy and easiness of operations; the capacity of the installations and the power consumption determine the costs, whereas there are returns by selling energies and savings in fuel utilities. Such approach is completed with the whole analyses of the loading curves and the hydrogen operations annually, fixing a base-load power that is added to the production of the non-manageable resources and compared with the actual energy demands: the 'net surpluses' represent the electricity theoretically available for other uses (fig. 2a). If this energy is utilized in relation with the hydrogen technologies for electric grid load balancing, the model has to include: the maximum power surplus, which determines the capacity and utilization of electrolyzers (we use a limiting value); the hydrogen production, by taking into account the inputs, the efficiency and dynamic range of electrolyzers; and the deficits of electricity, due to the power imbalances and electrolyzers' operation, that account for the hydrogen consumed by e.g. fuel-cells (fig. 2b).

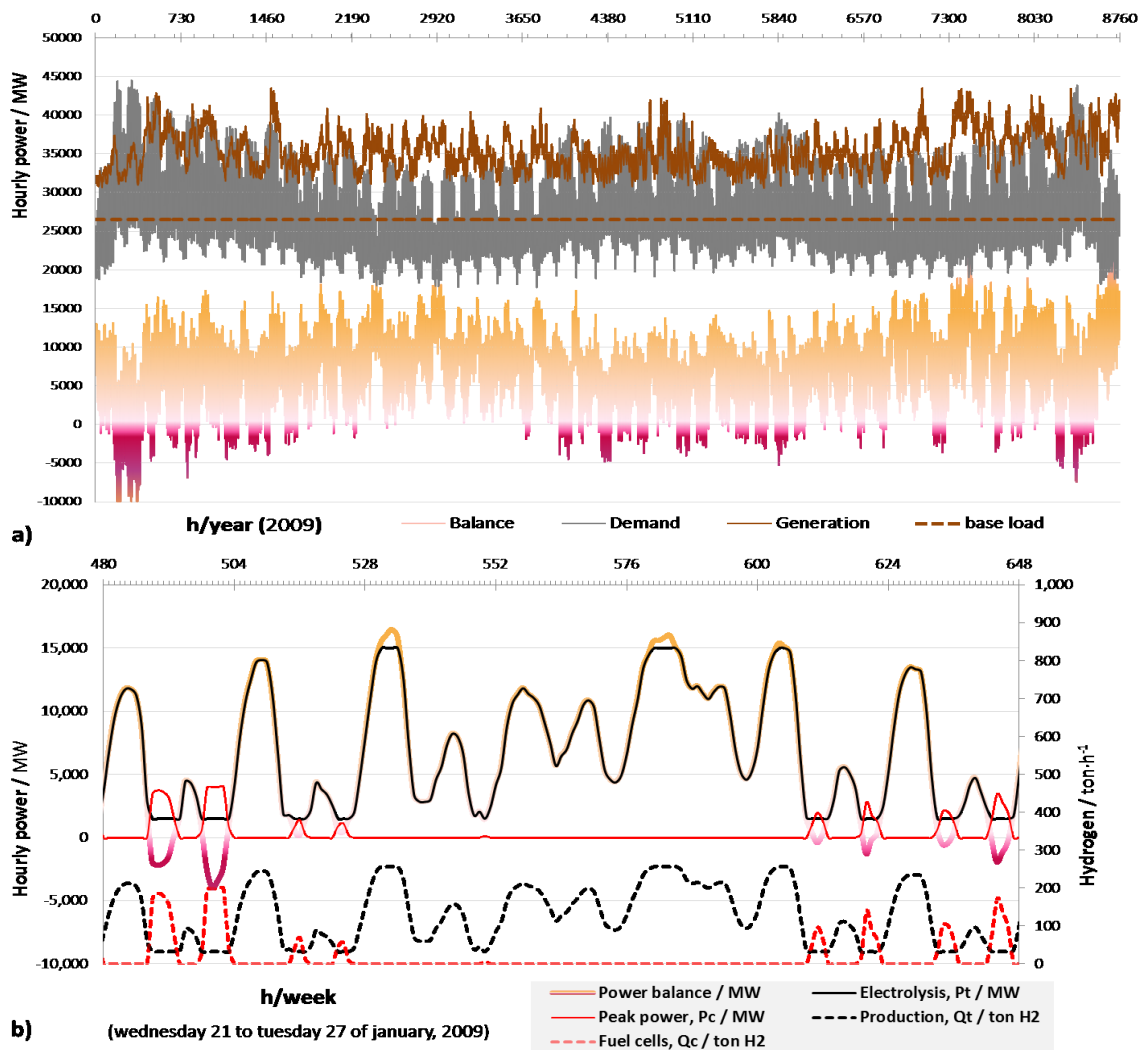


Fig. 2: a) Power generation scenario and load curves with a disaggregation of hours (Spain, 2009) b) Weekly balance of electricity and hydrogen using the electrolyzer and fuel-cell system

Finally, we simulate distinct scenarios -using all the model variables- to analyze their sensibility on the size, operation and economy of 'electricity and hydrogen processes': most significant factors are related to the efficiency and cost of electrolysis, power to electrolyzers and fuel-cells, but particularly electricity and hydrogen prices which are the only capable to render the systems cost effective within the ranges of values studied.

As we focus in the 'Spanish case', this is a good example for planning the transition from a power system holding large reserve capacity, high renewable energy and limited interconnections, to a more sustainable energy system being capable to optimize the size, the regulation modes, utilization ratios and impacts of the installations. Barriers for implementation can arise from political willingness, economical priorities or technical limitations; but whether this option is more feasible, when enough power surplus or grid

constraints exist, as an alternative to other operating procedures or exporting the electricity, is the prime question we are trying to answer in this report.

CONCLUSIONS

The electricity systems in many countries hold an excess of capacity that show the failures of the current liberalized energy markets to appoint resources efficiently.

The power industry is in probably a unique position, if the economy converts to hydrogen, to increase energy efficiency and avoid pollution.

Hydrogen production by electrolysis using the power grid mix could be an option, depending of the prices of energy in the different periods, if sufficient electrolyzer efficiencies and cost reductions are achieved.

The analyses show the effects of all factors relevant, and feasible results can be anticipated in some scenarios, e.g. for base load with power surplus at low price, running large electrolyzers in dynamic-range mode.

As concluding remark, with a large fraction of renewable in future power systems electrolysis is probably unavoidable even technology is not perfect; we can discuss efficiency, costs, etc., however a more fundamental question could be: what is the alternative, if business as usual is not an option?

REFERENCES

- Gutiérrez, F., Atanes, E. (2010) Power management using electrolytic hydrogen. SciTopics. Retrieved June 27, 2012, from: http://www.scitopics.com/Power_management_using_electrolytic_hydrogen.html.

- KI-Risø DTU, DONG Energy (2008) Pre-investigation of water electrolysis. Energynet 2006-1-6287.

- Shen, M., Bennett, N., Ding, Y. (2011) A concise model for evaluating water electrolysis. International Journal of Hydrogen Energy 36, No. 22, pp.14335-14341.

- Ursúa, A., Gandía, L.M., Sanchis, P. (2011) Hydrogen production from water electrolysis: current status and future trends. Proceedings of the IEEE (ID: 0016-SIP-2011-PIEEE).

- NREL (2006) Electrolysis: Information and opportunities for electric power utilities. TP-581-40605.

- NREL (2009) Current state-of-the-art hydrogen production cost estimate using water electrolysis. Independent Review BK-6A1-46676.

- REE (2012). The Spanish power system: http://www.ree.es/ingles/sistema_electrico/informeSEE.asp.

- Power demand tracking in real time:
http://www.ree.es/ingles/operacion/curvas_demanda.asp (on-line).

- Elygrid. Improvements to integrate high pressure alkaline electrolyzers for electricity/H₂ production from renewable energies to balance the grid. Retrieved July 18, 2012, from: <http://www.elygrid.com/>.

Water electrolysis as key enabler for power to gas accelerating renewable energy integration (CS-2)

Jan Vaes, jvaes@hydrogenics.com

Hydrogenics Nijverheidslaan 48c, B-2260 Oevel,

Hydrogen has a long standing history as a feedstock gas or process medium in industrial applications, whenever small to medium flows are required, and often the technology of choice when high purity streams are needed. Currently there is an increased demand for electrochemical hydrogen because it gives an answer to the growing practical issues related to the integration of renewable energies in today's energy mix. In the power-to-gas concept (Fig. 1), that provides a realistic route for a carbon-free economic future, water electrolysis is the key technology to store renewable energy, allowing the crossover between different energy vectors; electricity on the grid, natural gas as chemical energy storage and fuel for transport applications.

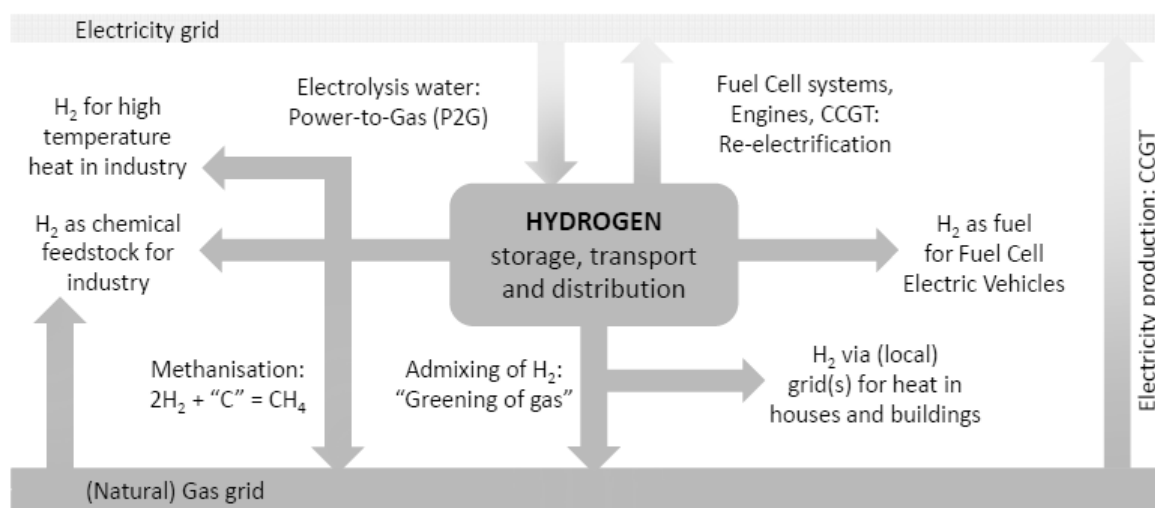


Figure 1: Schematic illustrating the role of water electrolysis in the power-to-gas concept. Hydrogen provides the link between the electricity and natural gas grids while it can also directly be used for transport applications or a feedstock gas for industry.

This contribution aims at illustrating how Hydrogenics further develops water electrolysis and fuel cell technologies, complements them with additional technologies in order to demonstrate different power-to-gas energy applications in real life. These projects study efficiencies and pinpoint bottlenecks therefore allow defining the business models that can be adopted to steer the tomorrow's energy mix. Three funded projects are illustrated, all shifting power along different energy vectors:

(1) Excess wind energy that is converted via water electrolysis and stored at high pressure for fueling utility vehicles and re-electrification via fuel cells (Don Quichote FCH-JTI project). A

60 kg per day fueling station was installed at one of Belgium's largest FMCG distribution center in the course of 2011 for fueling forklifts and, occasionally, buses and passenger cars up to 350 bar. After nearly two years of operation, the station is being expanded with a 60kg per day PEM electrolyzer and additional storage. In a later phase of the project a novel electrochemical compressor will be implemented. The hydrogen is used either for to assure the supply to the increasing fleet of forklifts at the customer's site, or by re-electrification through a 100 kW fuel cell rack peak demand. This project provides a unique setting to compare two electrolysis technologies, fuel cell equipped applications, resulting in directly comparable field data.

(2) A power controlled 1MW electrolyzer is deployed for grid stabilization in the Puglia region in the south of Italy where the high density of wind and solar plants puts a lot of stress on the transmission lines (Ingrid project –DG energy FP7). By constantly producing hydrogen but ramping up and down the production rate, the electrolyzer is helping to stabilize the local grid. The produced hydrogen is stored in both stationary and mobile metal hydride packages. The local stored hydrogen can be re-electrified, charging electric vehicles or put to back on the grid. The mobile hydride package can be moved at a consumer's site and where the hydrogen is freed and used as feedstock gas.

(3) In the Danish Biocat project Hydrogenics has teamed up with a consortium to use a similar electrolysis based grid stabilization technology, with the distinct difference that the hydrogen is further converted into methane with the aid of bacteria in a bio-reactor. This has the advantage of unlimited storage capability in the natural gas grid. Furthermore it expands the application range, since the consumption of chemically stored energy in CH₄ is spread worldwide and does not need (H₂-) specific infrastructure.

Homologation of Fuel Cell Electric Vehicle (CS-3)

Lorenzo Nasarre Cortés, Joaquín Mora Larramona, Marcos Rupérez Cerqueda and Luis Carlos Correas Usón, Lucía Alberdi

Aragon Hydrogen Foundation

With the famous "climate change" appear the figure of "electric vehicle", the mobility of this vehicle does not produce any emissions.

The main problems in the electric vehicle are the autonomy and the recharge time. Using a hydrogen fuel cell, able to increase autonomy and reduce the time to recharge electric vehicles. The fuel cell would be responsible for recharging the battery (REEV: "Range extended electric vehicle") or directly from the electric motor power (FCEV: "Fuel Cell Electric Vehicle").

We performed a model of the vehicle powertrain, in Simulink, to simulate different powertrain configurations for later with the optimal configuration of power train perform different tests on the test bench hybrid drive, available at the Aragon Hydrogen Foundation.

With the transformation of BEV (battery electric vehicle) in an FCEV (Fuel cell electric vehicle). The autonomy is increase; With FCEV you can drive this car during more kilometers approximately twice. Moreover with the change in the power train of vehicle, the time to recharge is reducing. In the BEV, the time to charge is eight hours and in the FCEV the time to charge hydrogen tanks is five minutes.

The performance of fuel cell electric vehicle is like that the performance of battery electric vehicle; because the electric motor is the same and the hydrogen fuel cell is able to produce energy enough to move the electric vehicle.

The objective of this project is demonstrate the advantages of a fuel cell electric vehicle against battery electric vehicle and get the homologation of FCEV an so, we use this vehicle for roads without any problem.

For the homologation of this vehicle will be a reality, the construction of fuel cell electric vehicle reach with a Regulation (EC) N79/2009 THE EUROPEAN PARLIAMENT AND OF THE COUNCIL of 14 January 2009 on type-approval of motor vehicles powered by hydrogen and amending Directive 2007/46/EC and Annex V of Regulation 110.

This table shows the components of the power train of the fuel cell electric vehicle with the location that it occupy and the points that the regulations have been taken into account so that the installation is correct and comply with the premises indicating the regulation .

COMPONENT	LOCATION	REGULATION POINTS
Li-ion batteries	Rear	8,13,15
Hydrogen tank	Under seats	4,8,10 (1)
FC (Hydrogenics 12 kW)	Rear	8,10,13,15
DC/DC Converter	Rear	8,13,15
Receptacle fitting	Left Rear	4,8,10
Hydrogen fittings	Cabin	5,8
Valves	Cabin	5,8

Applying this regulation our vehicle is recognized by the European Union countries and it is possible driving for all roads or streets of our continent. In this way, we could carry out technical inspection as if it were a conventional vehicle and get over it without any problems. In the picture below you can see how the technical inspection to fuel cell electric vehicle is equal to that performed conventional vehicles except the test of greenhouse gas emissions, because as you know, these vehicles do not emit any polluting emissions, the only emission is water.



Illustration 1: Technical inspection of fuel cell electric vehicle. ITV

In conclusion, the modification of a battery electric vehicle (or conventional internal combustion engine) to fuel cell electric vehicle is possible and moreover is covered by European legislation and is a process which although not easy or quick, is entirely feasible and therefore true. And so we can get the approval of the same and use the streets and highways of our country.

The International Energy Agency Hydrogen Implementing Agreement (IEA HIA): Collaborative R,D&D to 2015 and Beyond (CS-4)

Ms. Mary-Rose de Valladares; Manager Mr. Jan K. Jensen, IEA HIA Chairman; Mr. Antonio G. Garcia-Conde, former IEA HIA Chairman

The International Energy Agency Hydrogen Implementing Agreement (IEA HIA) is the world's largest and longest-lived collaborative organization in hydrogen research. The IEA HIA (www.ieahia.org) now has 25 members, consisting of 20 countries, the Commission of the European Union, and the UN Industrial Development Organization (UNIDO) and three

(3) sponsors. The member countries are Australia, Denmark, Finland, France, Germany, Greece, Iceland, Israel, Italy, Japan, Korea, Lithuania, The Netherlands, New Zealand, Norway, Spain, Sweden, Switzerland, the United Kingdom and the United States. The IEA HIA recently welcomed its first sponsor members: the International Association for Hydrogen Safety ("HySafe"): the Nationale Organisation of Wasserstoff und Brennstoffzellentechnologie (NOW): and Shell Global Solutions BV.

In its 30+-year history of international cooperation, the IEA HIA's tasks and activities have achieved much technical progress in hydrogen (H₂) production, storage, conversion, safety, integrated systems and infrastructure. The IEA HIA's core business is hydrogen R, D&D. It offers members an established, global network and acts as a catalyst and framework for collaboration. With a new Strategic Plan for 2009-2015, the IEA HIA expanded its commitment to analysis and outreach to advance introduction and commercialization of H₂ energy technology. The IEA HIA Strategic Plan for 2009-2015 has three themes, each associated with a series of portfolios: 1) Collaborative R, D&D that advances hydrogen science and technology; 2) Analysis that positions hydrogen for technical progress and optimization for market preparation and deployment for support in political decision-making; and 3) Hydrogen Awareness, Understanding and Acceptance that fosters technology diffusion and commercialization.

The collaborative R, D&D theme features four portfolios: Hydrogen Production, Hydrogen Storage, Integrated Hydrogen Systems, and Hydrogen Integration in Existing Infrastructure. The Analysis theme is comprised of three portfolios: Technical Analysis, Market Analysis, and Support for Political Decision-Making. The final theme, Hydrogen Awareness, Understanding, and Acceptance, includes three portfolios: Information Dissemination, Safety, and Outreach.

The IEA HIA is now engaged in planning for the next five year Strategic Plan, which will cover the period 2015-2020.

All IEA HIA tasks are initiated and developed on a democratic "bottom-up" basis by members. An Operating Agent (OA) manages each task and Subtask Leaders (STL) typically coordinate components of the task work packages. On the basis of a single (annual) Common Fund Fee, all Members are eligible to participate in any and every task at no extra charge. Rather IEA HIA Members contribute "expert" labor to each task in which they participate.

Of 33 tasks created by the IEA HIA, some 26 have been completed. Recently approved Final Reports for Task 23 – On Site Supply of Hydrogen, Task 24 – Wind Energy and Hydrogen Production, and Task 26 – Advanced Materials for WaterPhotolysis with Hydrogen are available on the IEAHIA website. The table below lists current and completed tasks active during the 2009-2015 planning cycle, noting tasks and topics that are expected to be the subject of future work.

TASK #	TASK NAME	DATES	STATUS
18	Integrated Systems Evaluation	2004-2009	Completed
19	Hydrogen Safety	2004-2010	Completed
21	BioHydrogen	2005-2010	Completed
21	BioInspired and Biological Hydrogen Production	2010-2014	Continuing
22	Fundamental & Applied H ₂ Storage Materials Development	2006-2012	Continuing
23	Small-Scale Reformers for on-Site H ₂ Supply	2006-2011	Completed
24	Wind Energy and Hydrogen Production	2006-2011	Completed
25	High Temperature Production of Hydrogen	2007-2011	Completed
26	Advanced Materials for Waterphotolysis with H ₂	2008-2012	Completed
27	Near-Term Market Routes to H ₂ via Co-Gasification with Biomass	2009-2011	Completing
28	Large-Scale Hydrogen Delivery Infrastructure	2010-2013	Continuing
29	Distributed and Community Hydrogen (DISCO H ₂)	2011-2014	Continuing
30	Global Hydrogen Systems Analysis	2010-2014	Continuing
31	Safety	2010-2013	Continuing
32	Successor to Task 22 – H ₂ Based Energy Storage	2013-2016	Continuing
33	Successor to Task 23 – Local H ₂ Supply for Energy Applications	2013-2016	Continuing
Anticipated successor tasks	Safety (Task 31);		
	Advanced Materials for Waterphotolysis		
	(Task 26) will expand to include renewables;		
	Power 2 Gas/Flexible Multi-sectoral H ₂		
	Plus: H ₂ in Marine Sector		

To carry out their work programs, all but one task meets for 2-3 days on a semi-annual basis at rotating locations determined by task members. Task 22 meets for 4-5 days at a nine-month interval. Sometimes the task meetings are held in conjunction with related conferences.

The IEA HIA believes that if the question concerns sustainability, the answer involves hydrogen. Our vision is one of a hydrogen future based on a clean sustainable energy supply of global proportions that plays a key role in all sectors of the economy. Our mission is to accelerate hydrogen implementation and widespread utilization to optimize environmental protection, improve energy security and promote economic development internationally while establishing the IEA HIA as a premier global resource for expertise in hydrogen. This presentation is an overview of the IEA HIA's work-in-progress and planned work and will include a discussion of themes and portfolios and their respective tasks.

Countries and assessments

Hydrogen as a Fuel and Energy Storage: Success Factors for the German Energiewende (CA-1)

Dr. Oliver Ehret, Dr. Klaus Bonhoff

National Organization Hydrogen and Fuel Cell Technology

In various countries and regions across the world, hydrogen receives growing recognition as a transport fuel and medium for energy storage. Hydrogen produced from renewable energies and used as a fuel promises substantial cuts in green house and other emissions, and reduced dependency from imports of mineral oil and other fossil fuels. The market introduction of fuel cell vehicles (FCVs) has started and is set to gain further momentum in the next few years; initiatives to build up extensive hydrogen infrastructure are taking shape around the globe. Especially countries shifting their energy systems from reliance on fossil energies to an energy supply based on renewables face the challenge to integrate wind, solar and other fluctuating power into existing energy systems. Hydrogen has become recognized as one of the most promising options for energy storage; often larger-scale R&D and demonstrations project are running or are firmly planned. A growing number of companies and governmental bodies act upon the results of economic analyses, showing that a hydrogen-based road transport offers significant potential for financial returns in the not too distant future; likewise hydrogen storage is increasingly regarded indispensable for the future viability of the energy sector also in economic terms. Synergies between applications in different sectors are of substantial promise; hydrogen produced from renewable sources may both be used as fuel and energy storage, facilitating clean transport and greater energy system stability at the same time. Economies of scale are amongst the forces promising much improved economic performance in the future. Germany is amongst the countries taking a lead position in the market preparation and introduction of hydrogen and fuel cell technologies for transport and energy storage; this paper discusses several key initiatives.

The German Energiewende aims at the almost complete replacement of fossil by renewable energies in the energy and transport sector by 2050, setting ambitious intermediate targets for the next few decades. Emission reductions and efficiency improvements are key enablers for achievement; both hydrogen and fuel cell technologies are most promising in these regards. Thus the German federal government set up the National Innovation Programme Hydrogen and Fuel Cell Technology (NIP), running from 2006 to 2016 and supporting market preparations for hydrogen and fuel cell technologies. The National Organization Hydrogen and Fuel Cell Technology (NOW) coordinates the € 1.4 billion programme, in close collaboration with the Project Management Organization Jülich and the ministries NOW works for. The central Lighthouse Project in the realm of transport NIP part-funds is the Clean Energy Partnership (CEP). In the steadily expanding CEP, 15 public hydrogen fuelling stations (HFSs) and about 130 fuel cells cars and buses are operating in 2013; funding has been secured for additional 35 HFSs to enter into operation by 2015, supporting the running of planned-for larger volumes of FCVs. Reflecting the growing commercial relevance of FCVs, the industrial initiative H2 Mobility was set up and is planning for the roll-out of a Germany-wide hydrogen infrastructure supporting the expected market introduction of growing FCV fleets.

Remarkable is the close collaboration between - otherwise often competing - vehicle manufacturers and infrastructure operators, ensuring a close alignment indispensable for successful coordinated FCV and HFS roll-out. Within NIP, hydrogen is primarily regarded as a transport fuel and to be produced from renewable energy sources, mainly wind and biomass. Thus, relevant demonstration projects and studies are running or have been completed.

Given the challenge to integrate the large and growing volumes of fluctuating renewable energies within the context of the Energiewende, hydrogen has also assumed crucial importance as a storage leveling out fluctuations and thus integrating renewables in the energy sector. Within NIP, a large wind-hydrogen-system ensuring constant power supply for a large wind park even at times of calm went into operation; another project focusing on large-scale PEM-electrolysis and injection of hydrogen into the natural gas grid started site construction. Electrolyzers run in several HFSs of the CEP, generating valuable operation experience. A study investigating the status and potential for development of water electrolysis showed both challenges and prospects; another study regarding the Integration of Wind-Hydrogen-Systems in the Energy-System found that in several cases wind-hydrogen may well compete at transport and storage markets in the future. Synergies between both applications exist and benefit the overall system, thus help to align the transport and energy sector and contribute to the aimed-for success of the Energiewende. Much progress in terms of technology improvement and validation as well as cost reduction has been achieved within the running NIP. Experts from industry and science advising NOW still point to further challenges needing to be overcome and recommend the continuation and expansion of NIP beyond 2016.

The Fuel Cell and Hydrogen Network North Rhine-Westphalia (CA-2)

Dr. Thomas Kattenstein, Dr. Frank Koch, Dr. Michael Weber

Fuel Cell and Hydrogen Network NRW

North Rhine-Westphalia (NRW) is a highly populated German state with 18 million inhabitants. Climate protection is a main target in NRW's policy. Hydrogen is regarded as being one of the most important factors in future energy supply.

The aim of the Fuel Cell and Hydrogen Network North Rhine-Westphalia, which was founded in 2000, is to establish hydrogen and fuel cell technology as a permanent component of the future energy supply, at the same time exploiting fully the technology's economic opportunities for NRW as an industry region. With a view to the challenges presented by the energy turnabout, climate protection, increased energy efficiency and the expansion of renewable energies, hydrogen and fuel cell technology is seen as a major key technology in all segments of the energy system.

More than 400 members from industry and science are already actively engaged in the Network and use the numerous services the Network offers. The Network is the largest of its kind in Europe. Major companies such as Ceramic Fuel Cells (Australia), Hydrogenics, Dynetek, and Ballard (Canada) have established bases here. The Network also represents NRW within the Clean Energy Partnership (CEP), a lighthouse project of the Federal Government for mobility with hydrogen and fuel cells.

The principal feature of the Network's activities is the initiation of co-operative projects, although the focus of the project work has shifted increasingly from research and development in the direction of testing and market preparation. The Network is at its members' disposal as a contact point for concretising project ideas and identifying suitable funding programmes, and as a two-way channel of communication with policymakers. Since 2000 the state government and the European Union (European Regional Development Fund - ERDF) have provided around 115 million euros for about 110 hydrogen and fuel cell projects under the program frame "NRW Hydrogen HyWay". The total investment volume is a good 190 million euros. The Network's members are also closely involved in national and European funding activities.

As a consequence of the expansion of renewable power generation following the energy turnabout, hydrogen will play an ever growing role as a storage medium in the future energy supply. Surplus wind power can be converted by water electrolysis into hydrogen both centrally and, in particular, on a decentralised basis. Hydrogen can then be stored without difficulty using various technical methods. As required it can, for example, be turned back into electricity using fuel cells with a high degree of efficiency or used as a "domestic fuel" in fuel-cell-powered vehicles to provide emission-free mobility. Projects to try out this approach are a current focus of the Network's activity.

Companies and institutes who have to date not operated directly in the field of fuel cell, battery and hydrogen technology, but who are able to make a valuable contribution with their expertise both to the development of fuel cell and battery systems with the related components and to the area of production, storage and transport of hydrogen, are expressly invited to become involved in the Network.

Aragon bet on Hydrogen and Fuel Cells (CA-3)

ARTURO ALIAGA LÓPEZ; JAVIER NAVARRO ESPADA; MARIA ALAMAN HERBERA; FERNANDO PALACÍN ARIZONA

*Government of Aragon and Aragon Hydrogen Foundation]
Aragon bet on Hydrogen and Fuel Cells*

The Aragon bet on renewable energy is not new. The first wind farm in Spain was installed near Zaragoza in the eighties. The region has always been at the forefront of wind energy development and there were over 1,800 MW installed power.

The Government of Aragón included the research and the technological development on hydrogen in its commitments for the term 2007-2011, which has placed the region as one of the benchmark territories in this matter.

In addition, the initiative of hydrogen technologies development in Aragon was recorded as a key strategic guideline not only in in the 2nd Research, Development and Knowledge Transfer Regional Plan of Aragon 2005-2008, but also in the Energety Plan of Aragon 2005-2012 and nowadays in the lines of action of the Aragonese Climate Change and Clean Energies Strategy (EACCEL).

To development this initiative, the principal instrument implemented by the Government of Aragon is the Foundation for the Development of New Hydrogen Tecnhonologies in Aragon (FHa) whose main objective is the development of new hydrogen technologies integrated with renewable energies and the promotion of the Aragon's incorporation to economic activities related to the use of the hydrogen as an energy vector.

The patronage of the Foundation formed by more than 60 members, key for the aragonese economy: Companies, entities from all sectors and research centers support this initiative, and new supports are being added year upon year

All the activities that have been carried out by the Hydrogen Foundation in Aragon are aligned to the strategic guidelines defined in the previous Hydrogen Master Plan in Aragon 2007-2010 and the new activities defined in this new Plan 2011-2015 will allow us to continue working for the creation of new innovative products and services on a regional level in a coordinated way and towards a European scope.

The Foundation line of action answers with the aim of favouring the positioning of the regional big companies capable of developing hydrogen technologies thanks to its path in the industry, the knowledge obtained during the last number of years and its bet for the new trends in the energy, industry and automobile sector. The foundation actions contribute to the international projection of the companies, research centers and other entities.

The General aims of the Plan 2011-2015 are:

- To have a tool for the identification of opportunities of the new hydrogen technologies detected in Aragon which will allow decisions to be taken on an institutional, business and academic level.
- To identify the strategic lines for the region and establish a time scale and actions plans for the deployment of these lines.
- The Specifics aims of the Plan 2011-2015 are:
- To review the state of technology, current development, projects, sector companies, research centre potential, incipient markets and to define opportunities.
- To identify strategic lines and specific projects for Aragonese SMEs, which represent the foundations for employment in Aragon.
- To set across-the-board and general support actions: training, dissemination, awareness, financing and policies needed to guarantee the success of the deployment of these strategic lines.
- To carry out a survey with longer temporary horizons 2020-2050, defining the continuity of the strategic lines drawn and setting the bases to reach these horizons.

The work methodology carried out to develop the evaluation of the previous Master Plan and to define the strategy to follow in its next review is: There is a part related to the technical state of the art, a thematic SWOT analysis, a conclusion summary and a few strategy lines.

Meanwhile, a worldwide SWOT analysis has been carried out on the potentiality in these technologies of the Aragonese companies, as well as other additional analyses.

The Plan strategy focuses on taking advantage of the existing strengths and opportunities so that developments and activities on a regional, national and international level can be carried out creating new markets.

Aragon is part of HyER the Hydrogen Fuel Cells and Electro-mobility in European Regions, whose main aim is to provide regions and municipalities with distinguishable legal status and with aptitude to exert influence on the Hydrogen Joint Technology Initiative. At this time, the region of Aragon has assumed one of the vice presidencies of the Partnership, by means of Mr Javier Navarro Espada, General Director of Industry and SME of the Government of Aragon. The regions that belong to the HyER are at an investing level in these technologies which is at the same level of magnitude as that the FCH JTI.

Numerical analysis of hydrogen safety issues (CA-4)

Daniele Melideo, Daniele Baraldi, Rafael Ortiz-Cebolla,

Joint Research Centre European Commission]

INTRODUCTION

Hydrogen is expected to play an important role in the energy mix of a future low carbon society. Hydrogen safety issues must be addressed in order to ensure that the wide spread deployment and use of hydrogen and fuel cell technologies can occur with the same or lower level of hazards and associated risk compared to the conventional fossil fuel technologies.

Computational Fluid Dynamics (CFD) methods are increasingly used to investigate safety issues related to the production, storage, delivery and use of hydrogen. CFD techniques can provide a wealthy amount of information on the consequences of potential hydrogen accidents in terms of dynamics of pressure and thermal loads. Therefore CFD simulations can provide a valuable contribution to the engineering design of safer hydrogen infrastructure and development of innovative mitigation measures and procedures. In order to apply CFD techniques to real-scale industrial problems, the accuracy of the numerical tools must be assessed by comparison between experimental data and simulation results.

The results from CFD validation benchmarks for two relevant safety issues are shown in the paper: accidental hydrogen release in closed environment and fast filling of hydrogen tanks.

HYDROGEN RELEASE IN CONFINED ENVIRONMENTS

One of the most important safety issues is related to the use of hydrogen systems in confined environments, such as a hydrogen powered vehicle in a garage or in a tunnel or a fuel cell power system in an industrial installation. If hydrogen is released in a closed environment, it can accumulate and reach more dangerous concentrations than in an open configuration. In this context the mixing mechanisms of a low density gas in air during a release from an accidental leak must be fully understood and the distribution of hydrogen concentration must be quantified. The concentration distribution of gas in the enclosure depends on many parameters e.g. the release rate, the volume of the enclosure, and the position and orientation of the leak. In the framework of the HyIndoor FCH JU co-funded project 0 several CFD simulations have been performed reproducing the experiments that were carried out at the CEA-GAMELAN facility. Several release rate (i.e. 4 NL/min and 60 NL/min) were simulated in a closed box (around 1 m³). For practical reasons, helium was used instead of hydrogen in the experiments.

Many computational grids in term of type of cells (tetrahedral or hexahedra or hybrid mesh) have been generated and different modeling approaches for turbulence have been applied (the laminar approach, the standard κ - ϵ model, and the Shear Stress Turbulent model). An example of comparison between the CFD results and the experimental data is illustrated in Figure 19. The release direction is vertical, the rate is 4 NL/min, the source is located at the bottom of the box and the release diameter is 20 mm. The results from the CFD code ANSYS

CFX 14.0 0 with a hexahedral computational mesh are shown in Figure 19 and compared with the experimental data at 980 s after the beginning of the release. The concentration is plotted at the sensor positions along a vertical line that goes from the floor to the ceiling of the facility. The laminar model produces a significant overestimation of the maximum concentration close to the ceiling while both turbulent models (the standard κ - ϵ model, and the Shear Stress Turbulent model) are capable of better describing the maximum concentration in that region. The maximum concentration is a very important parameter because in case of ignition, the over-pressure that is generated by the explosion depends on several parameters including the concentration field and the maximum concentrations.

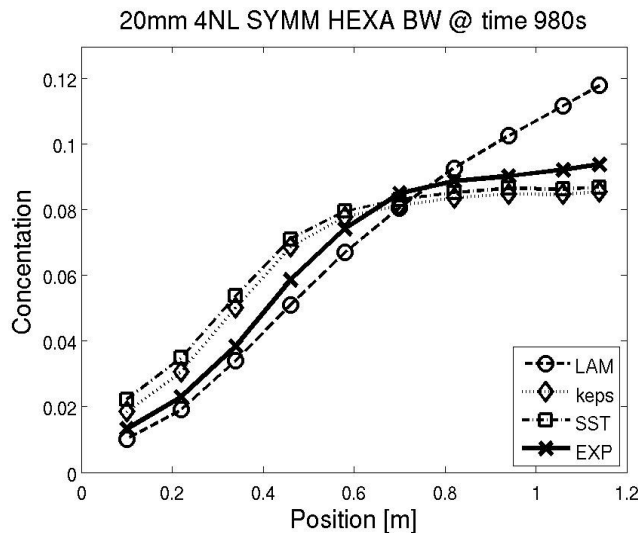


Figure 19 – Hydrogen release. CFD results vs. experimental data

FAST FILLING OF HYDROGEN TANKS

Drivers are used to re-fill the vehicle tank in few minutes with conventional fuels like gasoline and diesel. They have similar expectations towards a new technology like hydrogen powered vehicles. The requirement of a reasonable short filling time introduces a new challenge since the increase of temperature due to the quick compression inside the tank (e.g. from low pressure up to 700 bars) could affect the mechanical properties of the tank material and even jeopardize the structural integrity of the tank. Because of that reason, the maximum allowed temperature inside tanks is set to 358 K in international standards and regulations (e.g. the European regulation O, the SAE 00 and the international standard ISO 15869 0).

The main strategy to reduce the temperature increase is to pre-cool the hydrogen before injecting it into the tank. The selected experiment was carried out at JRC Institute for Energy and Transport (IET) in the compressed hydrogen Gas Tanks Testing Facility (GasTeF), an EU reference laboratory for safety and performance assessment of high-pressure hydrogen storage tanks 0 0. In the test the fast filling process from 2Mpa up to 77.5 MPa occurs in a type IV tank with a 29 L volume. The tank is made of an internal plastic liner in contact with the gas, the external composite carbon fiber wrap and two stainless steel bosses. The hydrogen is pre-

cooled to -40 C before entering into the tank. Compressibility effects were taken into account considering a real gas equation of state for the evaluation of hydrogen properties (Redliche-Kwong). The turbulence closure of the fluid governing equations was achieved through a modified $\kappa\text{-}\epsilon$ model 0 which includes a correction that limits the jet spreading rate over-prediction typical of the standard model.

Several types of computational grids and turbulence models have been tested in order to validate the model. As an example, the results of a CFD simulation are shown in Figure 20. The temperature history of the gas inside the tank from the experiment is well reproduced by the simulation results. The most relevant parameter that has to be taken into account is the maximum temperature that occurs at the end of the filling process. For that parameter, the difference between the simulation and the experiment is only few degrees and that is an acceptable discrepancy for the purpose of the simulation.

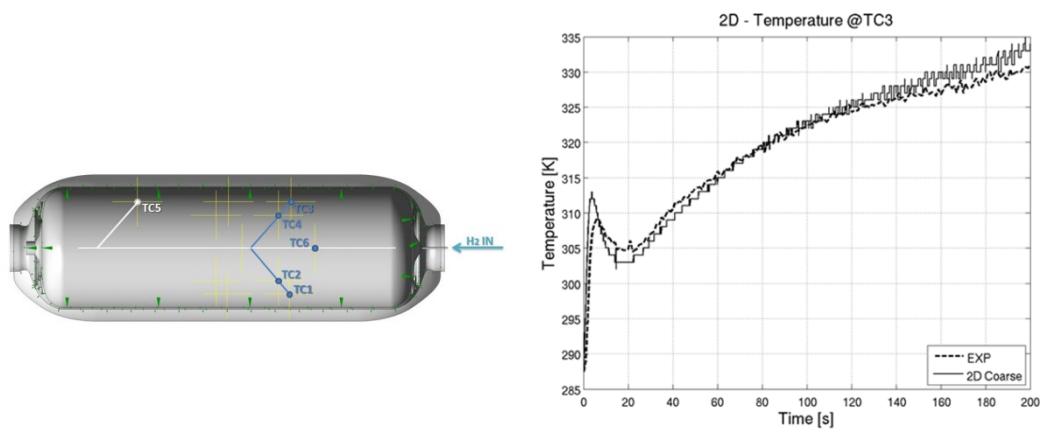


Figure 20 – Fast filling. Type IV tank on the left hand side. CFD results vs. experimental data on the right hand side.

CONCLUSIONS

A series of CFD benchmark calculations were performed for 2 relevant safety issues: hydrogen release in closed environments and fast filling of hydrogen tanks. By comparison between experimental data and simulations results, it was demonstrated the necessity of validation calculations in order to identify the correct modeling strategy (in term of computational mesh and turbulence model) to well capture the experiments.

REFERENCE

<http://www.hyindoor.eu/>

ANSYS CFX user manual.

Commission Regulation (EU) No 406/2010 of 26 April 2010 implementing regulation (EC) No 79/2009 on type-approval of hydrogen-powered motor vehicles. Off J Eur Union 18.05.2010. L122/1e107.

SAE J2579. Technical information report for fuel system in fuel cells and other hydrogen vehicles, revised; SAE International. March 2013.

SAE J2601 – Fueling Protocols for Light Duty Gaseous Hydrogen Surface Vehicles. SAE International.

International Standard Organization. Gaseous hydrogen and hydrogen blends e land vehicle fuel tanks. ISO/TS 15869; 2009.

Acosta, B., Moretto, P., Frischauf, N., Harskamp, F., GASTEF: The JRC-IE Compressed Hydrogen Gas Tanks Testing Facility, Proceedings of the Eighteenth World Hydrogen Energy Conference, 16-21 May 2010, Essen.

Galassi M. C., Acosta-Iborra B., Baraldi D., Bonato C., Harskamp F., Frischauf N., Moretto P., Onboard Compressed Hydrogen Storage: Fast Filling Experiments and Simulations. Energy Procedia 29, 2012, pp 192 – 200.

Ouellette P, Hill PG. Turbulent transient gas injections. J Fluids Eng 2000;122:743e53.

Application of Accident Modeling and Prediction Methodology to a Hydrogen Fuelling Station (CA-5)

Al-shanini A.1, Ahmad A.2, Khan F.3*

1,2Institute of Hydrogen Economy, Faculty of Chemical Engineering, Universiti Teknologi Malaysia, 81310 Johor Bahru, Malaysia,

3Faculty of Engineering and Applied Science, Memorial University of Newfoundland, St. John's, NL, Canada, A1B 3X5

Abstract

One of the most important aspects in realizing the hydrogen and fuel cell technology is safety. In addition to the safety standards in designs, construction and operations of hydrogen generation and supply systems, it is also important to develop methods to estimate risks associated with these facilities so that preventive and mitigating measures can be formulated. In this paper, an accident modeling methodology is applied to a hydrogen fuelling station. The modeling framework is represented by five prevention barriers, which may fail due to operational and technical failures, human factors, management and organizational failures, and natural phenomena. Failure probabilities of these barriers are estimated by using Fault Tree Analysis (FTA) based on plausible failure modes of individual components comprised in each barrier. The barriers include release prevention (RPB), dispersion prevention (DPB), ignition prevention (IPB), escalation prevention (EPB), and damage control & emergency management (DC&EM) prevention barriers; which are typical layers of protection normally employed in process industries in addition to plant operation facilities such as process control, alarm and interlocks.

Depending on the failures or successes of the prevention barriers, the outcome resulting from the initiating event such as a release of material and energy will take the form of one of the six end-state events (C1, C2, C3, C4, C5, and C6). These end-state events are safe, near-miss, mishap, incident, accident, and serious accident respectively. Note that for a serious accident to occur, all prevention barriers must fail. The probability of occurrence for each of the end states is estimated using Event Tree Analysis (ETA). The scheme is integrated with dynamic risk assessment methodology to update failure probabilities of barriers, thus providing dynamic adjustments to support risk-based decisions based on the trends of failure probabilities for each of the prevention barriers with time.

The modeling approach is applied a hydrogen station with a hypothetical number of end-state event occurrences in 11 time intervals. Using published frequency data for component failures, the failure probabilities of the barriers are calculated based on the constructed FT models. Then by considering the frequency of the initiating abnormal event in the ET as unity, the estimated posterior failure probabilities of the prevention barriers are computed. As shown in Fig.1, the results show that the posterior probabilities for the DPB, EPB, and DC&EMB barriers are lower than their priors. For the RPB the posteriors are higher than the corresponding priors for all cases, while for the IPB, the results show increasing probability of occurrence for the intervals from 4 to 7. This information facilitates the formulation of

maintenance plan by the management, and provides useful guides for further study to identify the root causes.

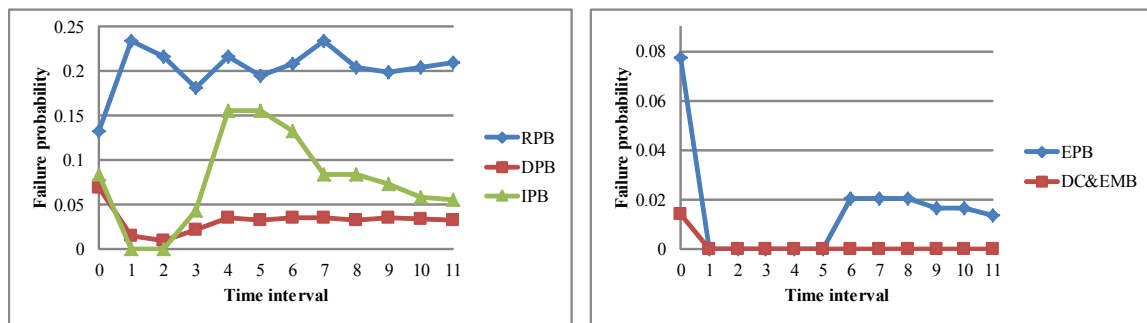


Fig. 1: Prevention barriers posterior failure probability

In addition, the framework also includes capability to predict future deviations that can serve as a useful guide for preventive maintenance activities. The Poisson-Gamma model (PGM) normally used in this methodology, is good in predicting future events with limited number of data. To further improve the prediction ability for data-scarce conditions that is typical in accident modeling, two additional models are considered. These are the Grey Model (GM) and Dynamic Bayesian-Grey Model (DBGM). As shown in Fig.2, the result shows that both the DBGM and GM are more accurate than the PGM.

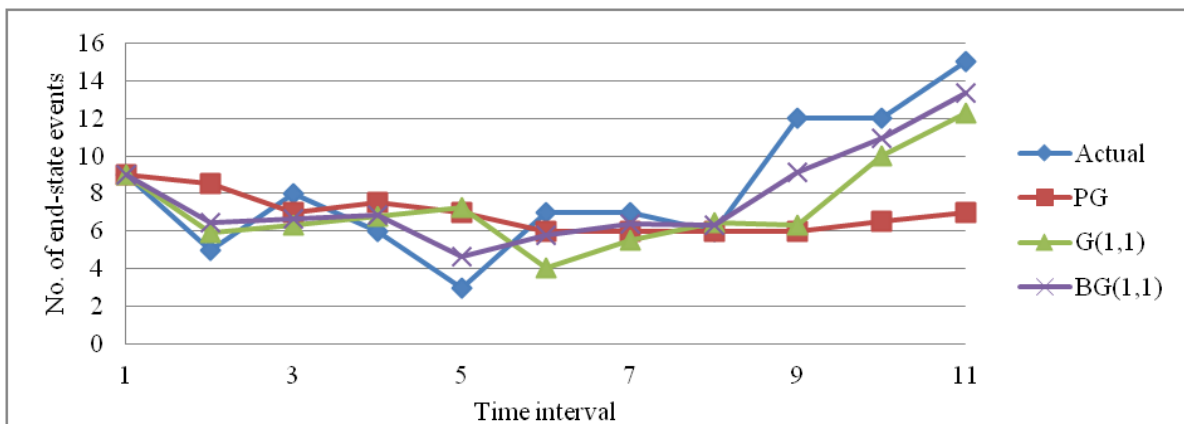


Fig. 2: Prediction of end-state occurrence

Results from the study have proved the suitability of the accident modeling strategy to be applied for the cases study considered. Both the dynamic updating and the prediction models can be used to prioritize facility plans of maintenance and management of change as required by the plant conditions. By using the information obtained, maintenance and repair plan can

be organized focusing on components with highest priority based on predicted urgency, thus offering savings to the plant.

Keywords: Accident modeling, On-site hydrogen filling station, Fault Tree Analysis (FTA), Event Tree Analysis (ETA), Dynamic Risk Assessment (DRA), Dynamic Bayesian-Grey Model (DBGM).

Life-cycle performance of hydrogen production via biofuel reforming (CA-6)

Ana Susmozas¹, Diego Iribarren¹, Javier Dufour^{1,2,*}

1 Systems Analysis Unit, Instituto IMDEA Energía. 28935 – Móstoles, Spain.

*2 Department of Chemical and Energy Technology, ESCET, Rey Juan Carlos University. 28933– Móstoles, Spain. * Corresponding author: Javier Dufour. E-mail: javier.dufour@imdea.org*

Hydrogen is mainly produced from natural gas via steam methane reforming (SMR). However, the environmental concerns associated with the use of fossil fuels have led to investigate other alternatives for hydrogen production. Among the numerous methods for green hydrogen production, thermochemical processes are being widely studied, focusing mainly on thermochemical water-splitting cycles, biomass gasification and the steam reforming (SR) of biofuels. The present work evaluates the environmental performance of hydrogen production via biofuel reforming using the Life Cycle Assessment (LCA) methodology. Furthermore, the environmental profile of these biohydrogen products is compared with that of fossil-derived hydrogen from conventional SMR. The functional unit (FU) of the LCA of each hydrogen-production system is defined as 1 kg of hydrogen produced (at plant). Capital goods are excluded from the study.

The four reforming systems evaluated are conventional SMR to produce fossil hydrogen (SMR-H₂) and three SR-based systems for the production of biohydrogen from ethanol (ESR-H₂), glycerol (GSR-H₂) and bio-oil (BSR-H₂). Figure 1 shows a general flowchart of these systems since all of them involve similar processes. The hydrocarbon feedstock is compressed and heated before entering the SR reactor, which operates at around 850 °C and 25 bar and uses a commercial Ni-based catalyst. The SR unit consists of a reformer surrounded by a combustion chamber in which a fuel is burnt to provide the heat required for the process. A tubular reactor is used for conventional SMR-H₂, while fixed bed reactors are considered for the case studies of biofuel reforming. The systems are designed to produce internally the steam required for the process. The syngas produced is cooled down and sent to a high-temperature-shift (HTS) reactor in order to increase the amount of hydrogen. Finally, the output stream is cooled and H₂ is recovered in a pressure swing adsorption (PSA) unit with 85% efficiency (40 °C and 23 bar). The PSA off-gas, together with natural gas, is used as the fuel of the combustion chamber that surrounds the reformer. The cooling water needs of the plant are satisfied by a cooling tower that requires a water makeup to offset the losses that occur in the tower.

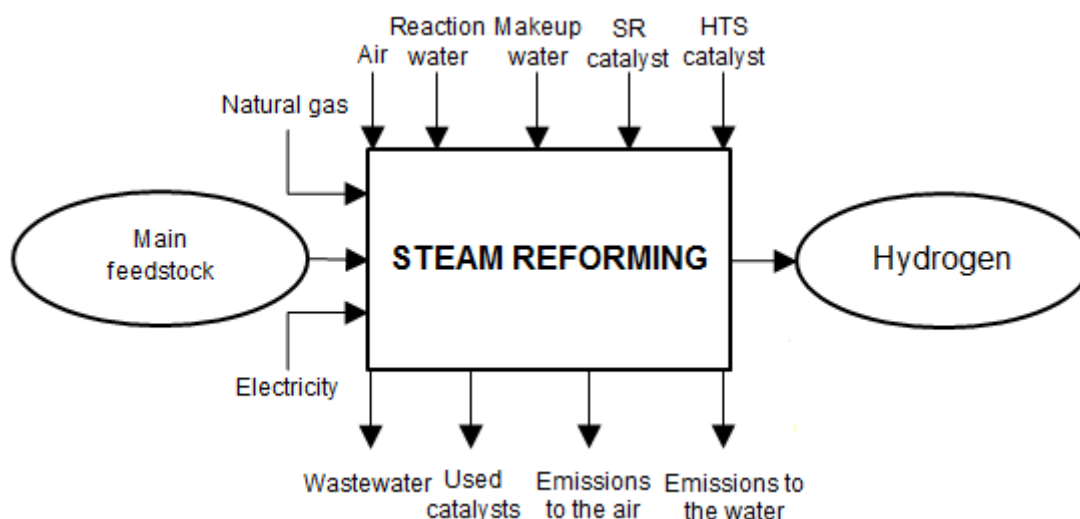


Figure 1. General flowchart of the SR-based systems for hydrogen production.

Foreground inventory data for the energy conversion systems are derived mainly from process simulation in Aspen Plus[®]. Additional life-cycle data for the production of the main feedstock are based on the ecoinvent[®] database for natural gas and corn bioethanol, and on specific literature in the case of glycerol from the esterification-transesterification of waste vegetable oils and bio-oil from the fast pyrolysis of poplar biomass. Data for background processes are taken from the ecoinvent[®] database. Background processes include waste management and the production of chemicals and energy carriers.

The life-cycle inventories of the hydrogen-production systems are implemented into SimaPro[®] 7. The evaluated environmental impact potentials include: abiotic depletion (ADP), global warming (GWP), ozone layer depletion (ODP), photochemical oxidant formation (POFP), land competition (LC), acidification (AP), and eutrophication (EP). Additionally, the cumulative (non-renewable) fossil and nuclear energy demand (CED) of each system is quantified. The subsystems and processes contributing most to the environmental impacts are identified. Figure 2 shows the comparison of the environmental profile of the hydrogen products evaluated. As can be observed in Figure 2, the suitability of a specific hydrogen fuel depends on the impact categories under study. In this respect, even though SR-based biohydrogen (especially, BSR-H₂) could lead to a favorable performance in terms of ODP, ADP, CED and GWP, conventional SMR-H₂ could still perform better in other impact categories such as LC, EP, AP and POFP.

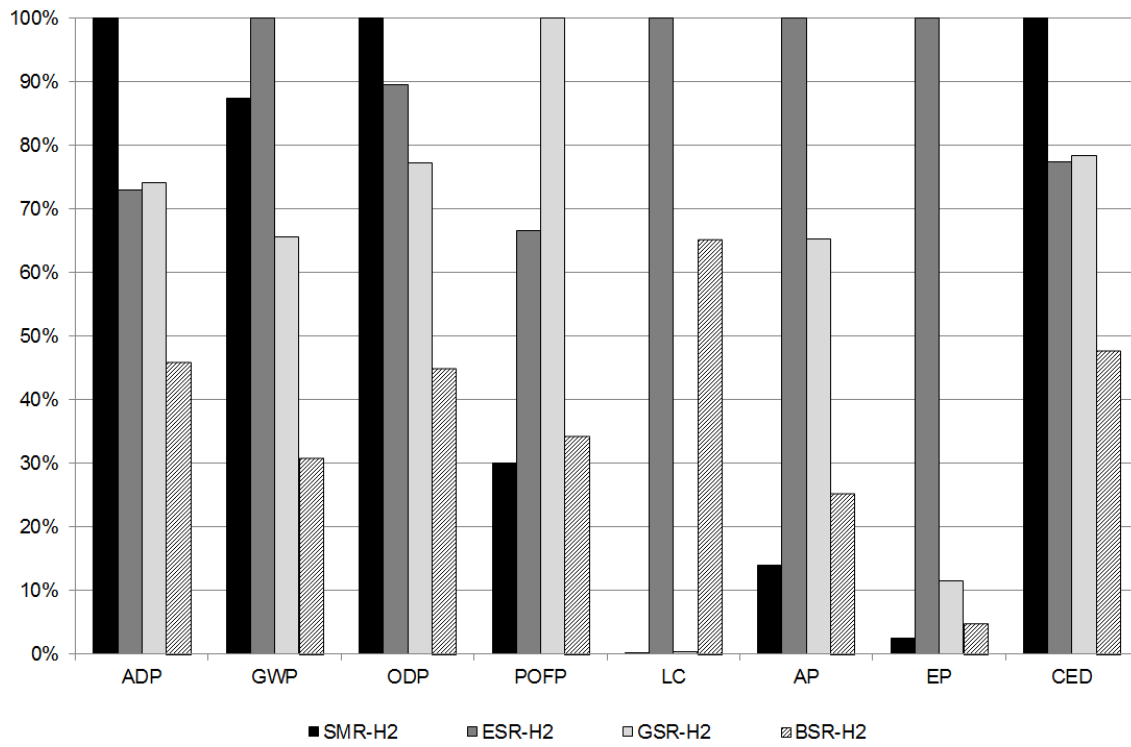


Figure 2. Comparison of the environmental impacts of SR-based hydrogen fuels.

Posters

State of Regulatory Framework for Hydrogen Infrastructures (P-3)

Gonzalo Manjavacas^a, Beatriz Nieto^b

^aCentro Nacional del Hidrógeno, Technical Department, gonzalo.manjavacas@cnh2.es

^bCentro Nacional del Hidrógeno, Technical Department, beatriz.nieto@cnh2.es

a,b C/ Prolongación Fernando el Santo s/n - 13500, Puertollano (Ciudad Real) España, phone +34 926 420 682

INTRODUCTION

It is expected that world's energy demand will be increasing continuously, being more intense in today's developing countries [1]. Nowadays, hydrogen, as an energy carrier, is considered as the element which can assume the role played during the last century by fossil fuels.

The generation, storage and transformation of hydrogen into energy are known as hydrogen technologies. Regulations, Codes and Standards (RCS) could become a barrier to the early introduction into the market if aspects such as the amendment of existing Regulations and Standards or creation of new ones are not appropriately considered [2].

In the above context, the Centro Nacional del Hidrógeno (CNH2) develops its activity, which main aim is scientific and technologic research about all aspects related to hydrogen technologies, being at scientific and technologic national and international service.

The present work is meant to give an overview of the development of hydrogen RCS and to provide an assessment and basis for the progress to date. It has to be taken into account that the commercialization of hydrogen energy technologies requires a regulatory framework to ensure that all of their applications are introduced in a coordinated fashion, complying with the highest safety standards.

DEVELOPMENT OF HYDROGEN REGULATIONS NOWADAYS

Safety parameters were established for the industrial use of hydrogen and were not designed for the volume and uses needed in an economy based on hydrogen. Regarding the use of hydrogen as an energy carrier, new constraints appear, so different aspects relating with these technologies may have an own regulatory framework. To support these new applications there is a clear need for a new safety culture to deal with hydrogen systems [3].

The existence of a non-harmonized framework for a given product in different countries or regions contributes to the so-called Technical Barriers to Trade (TBT). So, the importance of such joint efforts is clear, being to show it one of the main targets of the present work. Thus and first of all, it has to be noted the differences between Regulations, Codes of practice and Standards:

- Regulations are mandatory and reflect legal constraints translated into safety objectives, being set by governments.

- Codes of practice.- They provide advice on how to meet regulatory requirements, explaining the basic functions for safe handling (design, fabrication and inspection) and problem-preventive maintenance.
- Standards.- A standard is a document that provides requirements, specifications, guidelines or characteristics that can be used consistently to ensure that materials, products, processes and services are fit for their purpose.

Whereas a regulation is developed at the initiative of concerned regulatory bodies (i.e. European Commission), standards are developed mostly through the contribution of industry, considering the essential requirements set out in a regulation.

From an international point of view, certain technical committees from International Organization for Standardization (ISO) and International Electrotechnical Commission (IEC) are the main agents in developing these kinds of documents. On the other hand, there are national entities per country which develop standards too related with hydrogen infrastructures. Next, the main entities which draft codes of practice and standards related with hydrogen are summarized. The first one, it's the only one which develops codes of practice according European definition.

- European Industrial Gases Association (EIGA).- It's a safety and technically oriented organization representing the vast majority of European and also non-European companies producing and distributing industrial, medical and food gases.
- National Fire Protection Association (NFPA).- It publishes codes and standards that are designed to minimize the risk and effects of fire by establishing criteria for building, processing, design, service and installation in the United States, as well as many other countries.
- Compressed Gas Association (CGA). It promotes safe, secure... disposal of industrial and medical gases and containers, developing, publishing, and globalizing the technical information as standards and practices for the safe, environmentally responsible and efficient practices in the manufacture, transportation, storage, transfilling, and disposal of industrial and medical gases and their containers.
- Society of Automotive Engineers (SAE).- It's a American professional association and standards organization for engineering professional in various industries.
- Canadian Standards Association (CSA).- It's the largest standards development organization (SDO) in Canada. They work with other SDOs around the world as a key contributor to international and harmonized standards activities, being accredited in Canada by SCC and in USA by ANSY.

Nowadays, the main compulsory documents available are only proposals. If Europe is taken as example, it has to be noticed the "Proposal for a Directive of the European Parliament and of the council on the deployment of alternative fuels infrastructure, [COM(2013),18, Final]", which aims at ensuring the build-up of alternative fuel infrastructure and implementation of common technical specifications for this infrastructure.

The following sections are focused on standards from ISO and IEC bodies and codes from EIGA which documents are identified as IGC. It's resorted to American standards, i.e. from SAE, in some

cases because there are no standards from ISO/IEC which cover a specific topic. Codes and Standards referred to common elements like pipelines or everything related with explosive atmospheres (electrical apparatus, safety distances...) doesn't appear.

CODES AND STANDARDS FOR TRANSPORT

For transport applications, the costs for refueling sites are also major hurdle and will require the development of RCS and planning laws which treat hydrogen like conventional fuels and not as a hazardous industrial product [4].

In this way, it can be distinguished between documents related with Hydrogen Refueling Stations (HRS) and means of transport. The main codes of practice and standards available can be looked up next:

- ISO 15916 Basic considerations for safety of hydrogen systems.
- ISO/TS 20100 Gaseous hydrogen fuelling stations.
- ISO 1114-4 Transportable gas cylinders. Compatibility of cylinder and valve materials with gas contents. Part 4: Test methods for selecting metallic materials resistant to hydrogen embrittlement.
- ISO 17268 Gaseous hydrogen land vehicle refueling connection devices.
- ISO 14687-2 Hydrogen fuel – product specification-Part 2: Proton exchange membrane (PEM) fuel cell. Applications for road vehicles.
- ISO 16111 Transportable gas storage devices-Hydrogen absorbed in reversible metal hydride.
- ISO/TS 15869 Gaseous hydrogen and hydrogen blends-Land vehicle fuel tanks.
- ISO 13984 Liquid Hydrogen-Land vehicle fuelling system interface.
- IGC DOC 15/06/E Gaseous hydrogen stations.
- IGC DOC 100/11/E Hydrogen cylinders and transport vessels.
- SAE J 2601 Fueling Protocols for light duty gaseous hydrogen surface vehicles.
- SAE J 2799 – 70 MPa- Compressed hydrogen surface vehicle fuelling connection device and optional vehicle to station communications.
- SAE J2578 Recommended practice for general fuel cell vehicles- Safety.
- SAE J2579 Technical information report for fuel systems in fuel cell and other hydrogen vehicles.
- CSA HGV2 Standard hydrogen vehicle fuel containers.

CODES AND STANDARDS FOR STATIONARY APPLICATIONS

In this case, in which the smartgrid concept can be included, the main codes of practice and standards are summarized next:

- ISO 22734-1 Hydrogen generators using water electrolysis process. Part 1: Industrial and commercial applications.
- ISO 16110-1 Hydrogen generators using fuel processing technologies. Part 1: Safety.
- ISO 1114-1 Gas cylinders. Compatibility of cylinder and valve materials with gas contents. Part 1: Metallic Materials.
- ISO/FDIS 14687-3 Hydrogen fuel-product process- Part 3: Proton exchange membrane (PEM) fuel cell applications for stationary appliances.
- ISO 22734-2 Hydrogen generators using water electrolysis process. Part 2: Residential applications.
- ISO 16110-1 Hydrogen generators using fuel processing technologies-Part 1: Safety.
- IEC 62282-2 Fuel Cell Technologies – Part 2: Fuel cell modules.
- IEC 62282-3-100 Fuel Cell Technologies – Part 3-100: Stationary fuel cell power systems – Safety.
- IEC 62282-3-300 Fuel Cell Technologies – Part 3-300: Stationary fuel cell power systems – Installation.
- IGC DOC 06/02/E Safety in storage, Handling and Distribution of liquid hydrogen.
- IGC DOC 171/12/E Storage of hydrogen in systems located underground.
- IGC DOC 75/07/E Determination of safety distances.

CONCLUSIONS

Specific standards within the called Hydrogen Technologies are available although new documents are being or will be developed continuously. However, there are no current and applicable regulations, meanwhile different efforts are being made from international institutions.

To ensure a safe transition to a hydrogen economy, a common RCS framework must be available in order to comply with the highest safety requirements.

BIBLIOGRAPHY

[1] Elzinga D, Fulton L, Heinen S, Wasilik, O. ADVANTAGE ENERGY. Emerging Economies, Developing Countries and the Private-Public Sector Interface. Information paper from the International Energy Agency (IEA), 2011. 64 p.

[2] European Commission, Introducing hydrogen as an energy carrier. Safety, Regulation and public acceptance issues, Directorate-General for Research sustainable energy systems, EUR 22002, 2006.

[3] Saffers JB, Molkov V. Hydrogen safety engineering framework and elementary design safety tools, International Journal of Hydrogen Energy, In press, Corrected proof, Available online 17 July 2013.

[4] Apak S, Atay E, Tuncer G. Renewable hydrogen energy regulations, codes and standards: Challenges faced by an EU candidate country. International J Hydrogen Energy Apr 2012; 37(7): 5481-97.

SMR Integration and Increase of CO₂ Production (P-4)

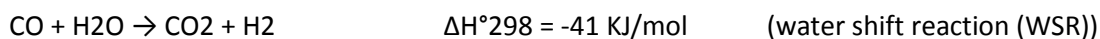
MARCELO TAGLIABUE, *Air Liquide Argentina S.A.*

The present work is a study of the efficiency optimization of a H₂ production plant through natural gas reforming, and to contribute to preserving the environment.

In recent years, H₂ has been attracting great interest as a clean fuel for combustion engines and fuel cells.

H₂ can be produced using several routes. The main route is the catalytic reforming of methane which includes, among others, steam-methane reforming (SMR) and dry-methane reforming (DMR), as may be seen in next reactions:

SMR reactions:



DMR reaction:

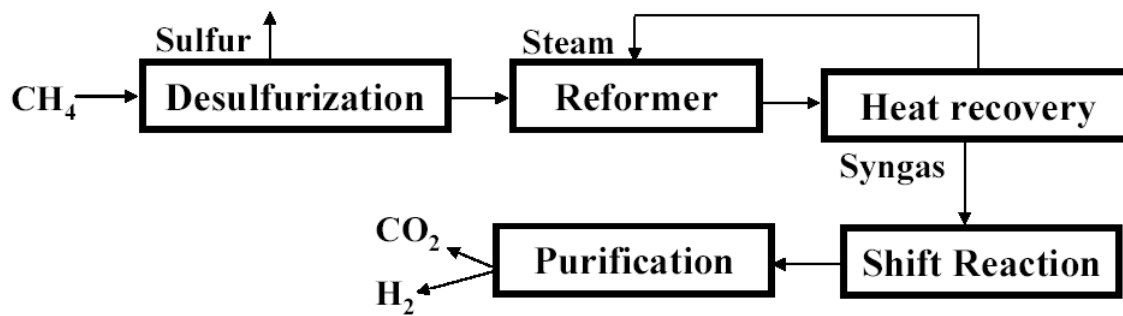


In the SMR plant used to make the test, reactions (1) and (2) are carried out.

The plant is a side fire type, with 52 tubes and 72 burners distributed in 6 rows, with a feeding of natural gas with about 95% of CH₄. This SMR plant consists of a high temperature shift plant (HTS), a CO₂ capture plant through an absorption process with amines, and a CO₂ liquefaction plant (for its later sale). In Figure 1 a plant scheme may be seen.

In its first stage this work was a theoretical study with the objective to see how a stream of non-condensable usually vented to the atmosphere (rich in CO₂ (reaction (3)) and H₂) and coming from the stripper of the CO₂ liquefaction plant could be added to the feed of the SMR plant, in order to reduce the emissions of CO₂ and other compounds responsible of the greenhouse, and to reduce the consumption of natural gas, keeping hydrogen production.

In the second stage, once made the theoretical study of the impact on the SMR when this feed is added, it was decided to proceed to the experimental work to learn how the major variables of the process were affected.



- Figure 1. SMR plant scheme

Literature shows that in the cases of syngas production by dry reformation, CO₂ is added after the hydro-desulfurization process (HDS). The reason to do this is that streams with high CO₂ and CO content are temporary poisons for cobalt/molybdenum catalysts. On the other hand, it is present the risk of occurrence of the reverse shift reaction inside the reactor. Moreover, it is generally agreed in the matter that there is a possibility of formation of coke on the catalyst due to the presence of CO₂ in the feed to the reformer, although the problems appear at higher CO₂/CH₄ ratios, usually 1 or bigger. In our case this ratio is about 0.04 so no problems of this kind are expected, but as a precautionary action the ratio S/C was increased.

In our case, the non-condensable stream should be added only before the HDS. For this fact, after studying the issue, the conclusion was that the maximum allowable CO₂ concentration for HDS catalyst for our plant is the about 16%. In the practical test this value was below of 5% (a safe operating range).

The practical results of the test were very encouraging. As dry reforming is more endothermic than the conventional reforming, initially the natural gas consumption increases because of the necessity of a bigger input of combustible and a lower flow of Off Gas from the pressure swing adsorption (PSA) due to the bigger conversion of CH₄. When the tubes wall cool down the excess air could be diminished (which in addition to provide the O₂ for the complete combustion is used to cool down the tubes), and so could be reduced the consumption of natural gas.

The H₂ produced is maintained approximately constant, because even if dry reforming produces less H₂, this is compensated because there is no need to recycle H₂ for the natural gas desulfurization reactions. This occurs because the H₂ present in the composition of non-condensable stream satisfies the necessary requirements for the desulfurization reaction.

In the case of CO₂ production -one of the most important issues of this work- although dry reforming is well known to produce syngas with a lower H₂/CO ratio, the plants that use it don't have WSR. In this case the extra moles produced of CO were transformed in CO₂, increasing it production.

On the other hand when reducing excess air to burners, the amount of steam exported diminished but the energetic efficiency of the reformer was preserved in all cases, as may be seen in next formula:

Energetic efficiency = Kcal provided by NG / (Kcal H₂ + Kcal steam + Kcal CO₂)

And, another fundamental objective was achieved due to 6 Tn/day of CO₂ stopped to be vented to the atmosphere, preventing the emanation of gases responsible of causing greenhouse effect and preserving the environment.

Alkali and Alkaline-Earth Metal Borohydride Hydrazinates: Synthesis, Structures and Dehydrogenation (P-21)

Teng Hea, Hui Wu^b, Guotao Wu^a, Zhitao Xiong^a, Ping Chen^{a,*}

^a Dalian Institute of Chemical Physics, Chinese Academy of Sciences, Dalian, China.

^b NIST Center for Neutron Research, National Institute of Standards and Technology, United States.

*corresponding author: pchen@dicp.ac.cn

Efficient storage of hydrogen onboard is one of the challenging technical issues for the so-called "hydrogen economy". Alkali and alkaline earth metal borohydrides are recognized as potential candidates for hydrogen storage due to their high hydrogen content. However, because of high chemical stability, dehydrogenation of those hydrides occurs at elevated temperatures. Considerable effort has been devoted to improve the thermodynamic and kinetic properties of those borohydrides. One of the strategies is to search for $H\delta^+$ rich compounds, such as $LiNH_2$, NH_3 , guanidinium or methylguanidinium, to complex with borohydrides to create an environment of coexisting protic $H\delta^+$ (N-H) and hydridic $H\delta^-$ (B-H), which may allow releasing molecular hydrogen via the combination of those two oppositely charged hydrogens. In this research, hydrazine, a $H\delta^+$ rich compound, was employed to complex with borohydride with the aim of synthesis of new hydrogen storage materials: borohydride hydrazinates.^{1,2}

Structural analysis reveals that $NaBH_4 \cdot NH_2NH_2$ crystallizes into a monoclinic P21/c cell with lattice parameters of $a=7.6307 \text{ \AA}$, $b=6.6135 \text{ \AA}$, $c=9.1099 \text{ \AA}$, $\beta=107.399^\circ$ and $V=438.70 \text{ \AA}^3$. $Mg(BH_4)_2 \cdot 3NH_2NH_2$, crystallizes into a trigonal P-31c cell with lattice parameters of $a=13.8385 \text{ \AA}$, $c=7.8284 \text{ \AA}$, and $V=1298.32 \text{ \AA}^3$. Whereas, $LiBH_4 \cdot 2NH_2NH_2$, $LiBH_4 \cdot NH_2NH_2$, $LiBH_4 \cdot 1/2NH_2NH_2$ and $LiBH_4 \cdot 1/3NH_2NH_2$ samples exhibit, respectively, an orthorhombic Pca21 cell, a monoclinic Cc cell, an orthorhombic P212121 cell and a monoclinic P21 cell.

Experimental results show that the retention of hydrazine in the vicinity of borohydride is in the order of $Mg > Li > Na$. $Mg(BH_4)_2$ hydrazinate can directly generate hydrogen instead of releasing NH_2NH_2 upon heating. Reducing hydrazine content improves dehydrogenation properties so that purer hydrogen delivers at lower temperatures. Isotopic labelling study indicates hydrogen desorption is via combination of $H\delta^+$ (N) and $H\delta^-$ (B) in borohydride hydrazinate system.

Reference:

1- T. He, H. Wu, G. Wu, J. Wang, W. Zhou, Z. Xiong, J. Chen, T. Zhang and P. Chen, Energy Environ. Sci., 2012, 5, 5686.

2- T. He, H. Wu, J. Chen, W. Zhou, G. Wu, Z. Xiong, T. Zhang and P. Chen, Phys. Chem. Chem. Phys., 2013, 15, 10487.

Hydrogen Production Technologies - Operational Challenges Of A Pressurized Alkaline Electrolyzer-Prototype (P-22)

Tannert D., Ziems C., Krüger P., Fischer U., Krautz H.J.

*Brandenburg University of Technology Cottbus-Senftenberg, Chair of Power Plant Technology,
Universitätsstraße 22 (MZG), 03046 Cottbus, Germany*

INTRODUCTION

Germany's energy transition policy aims to supply up to 80 % of the country's electricity demand exclusively from renewable energy sources by the year 2050. Given the fluctuating nature of renewable energy, this political goal will steadily increase the need to develop technologies able to match the electricity supply and demand. Even when measures like regulating medium load power plants and reducing output in full-load power plants are adopted, there is still the need to cut wind turbines from the grid to prevent grid instability. An important drawback is that reducing the output from full-load power plants results in efficiency losses and resources wastage.

Enabling high availability of the energy production coupled together with a reliable long-term storage technology could be a key factor for the smooth integration of renewable energy sources into the power grid.

A hybrid power plant with wind and hydrogen resources would be well suited for this purpose. This plant uses an electrolyzer, which operates with the electricity generated from wind turbines, to separate hydrogen from water. Hydrogen could then be stored for its use during peak load to generate electricity as the chemical energy in the fuel, can be converted into electricity.

As the use of renewable energies increases the production of green hydrogen and initiate future markets like green mobility, large-scale renewable energy storage and green hydrogen for industries could be fostered.

The BTU Cottbus-Senftenberg, within the framework of the joint research project, "Production of hydrogen from renewable energy sources" is developing an approach for the storage of surplus wind energy in the form of hydrogen, as well as its integration into the power grid.

STATE OF THE ART

As state of the art electrolyzers are mainly designed for stable operations, they become unsuitable for its use in hybrid power plants given the highly variable load produced by renewable energy sources e.g. wind energy. The system dynamics along the base load and overload conditions are crucial. In order to be considered reliable, an electrolyzer should be able to respond to load changes in minutes.

Regarding the product gas pressure, the current state of the art are electrolyzers operated at either atmospheric pressure or at pressures of up to 30 bar. This demands the gas to be further compressed before being stored. In order to avoid the compression stage and enabling the direct

storage of the hydrogen, an innovative electrolyzer prototype has been designed to operate at pressures up to 58 bar. Opposed to conventional systems, there is the potential to save energy by means of isothermal volume change.

Within this research, the operating life and part load capacity are major parameters. These parameters do not depend on basic process parameters e.g. cell temperature and current density, which themselves depend on and must be optimized for anticipated cell loading.

HIGH PRESSURE ALKALINE ELCTROLYSER PROTOTYPE

A pressure-resistant capsule, in which the stack is located, enables the pressure regulation in the system. Current standards and guidelines classify the design system as "permanently and technically tight". It is not able lead to an explosive atmosphere in the surrounding area.

The stack is composed of 24 single cells interconnected in series using bipolar cell construction and the filter press design. Each plate serves as the anode for one cell and as the cathode for the neighboring cell. Within the electrolysis system, explosive gas mixtures formation is avoided by the separation of the anolyte from the catholyte through a membrane. The power consumption of the stack is ca. 140 kW under a maximum current density of 6 kA/m². The gas formed within the cell is carried along with the electrolyte, where the flow is separated into anolyte and catholyte and sent to the subsequent separators.

The separators are located just above the pressure capsule. Advantage is taken from the density differences and the gases are separated from the electrolytes in the upper part of the separators. Small amounts of oxygen can still be found in the hydrogen and vice versa due to increased lateral diffusion of the product gases resulting from increased pressure. The volatile nature of renewable energies with minimum load feeds additionally leads to an increase in foreign gas concentrations in the product gases. A hydrogen gas quality of 3.0 (99.9 %) can be reached even without further treatment. After the separation process, the remaining electrolyte flows are recombined and cooled down to limit the maximum operation temperature to 75 °C.

A good dynamic behavior of the electrolyzer is an important criterium for the wind-electrolyzer coupling. This research project is greatly focused in this subject matter. Temperature influence on stack voltage and the influence of the pressure are among other research objectives. Figure 1 shows one part of the performed test runs.

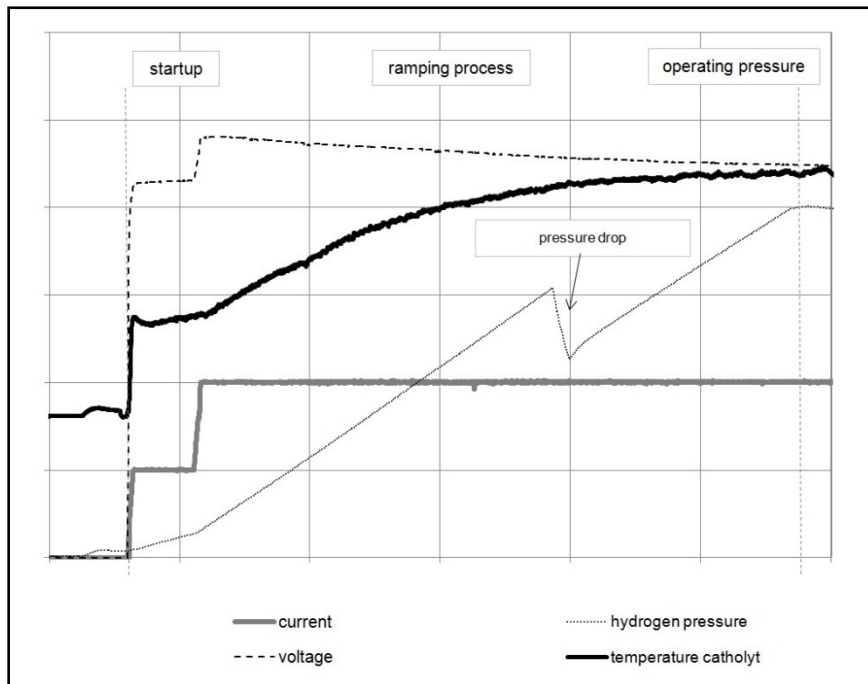


Fig. 1: Ramping process to build up the operating pressure

During the initial stage, the temperature gradient and the gradient of the voltage followed the applied current. During the ramping process, the stack heats up and when the operating temperature is reached, a drop in the cell voltage takes place and thus an increase in stack efficiency. The pressure drop of the system seen in Figure 1 during the pressure building results from the response of the automatic process control and which are as well used to improve the startup-behavior.

The time required to achieve optimum operating conditions vary according to the desired operating mode, and the target pressure. If the electrolysis unit is operated under direct coupling of wind turbines and PV systems, a system response is necessary within minutes.

In contrast, if the mode of operation sought is constant hydrogen production from renewable sources, much lower requirements for the startup behavior are required.

Several test runs have been carried out at different temperatures and under constant and fluctuating power input in order to assess the influence of both the over-potential of the electrodes and the ohmic over-potential due to the resistance of the KOH solution. Some of these measurements can be seen in Fig. 2.

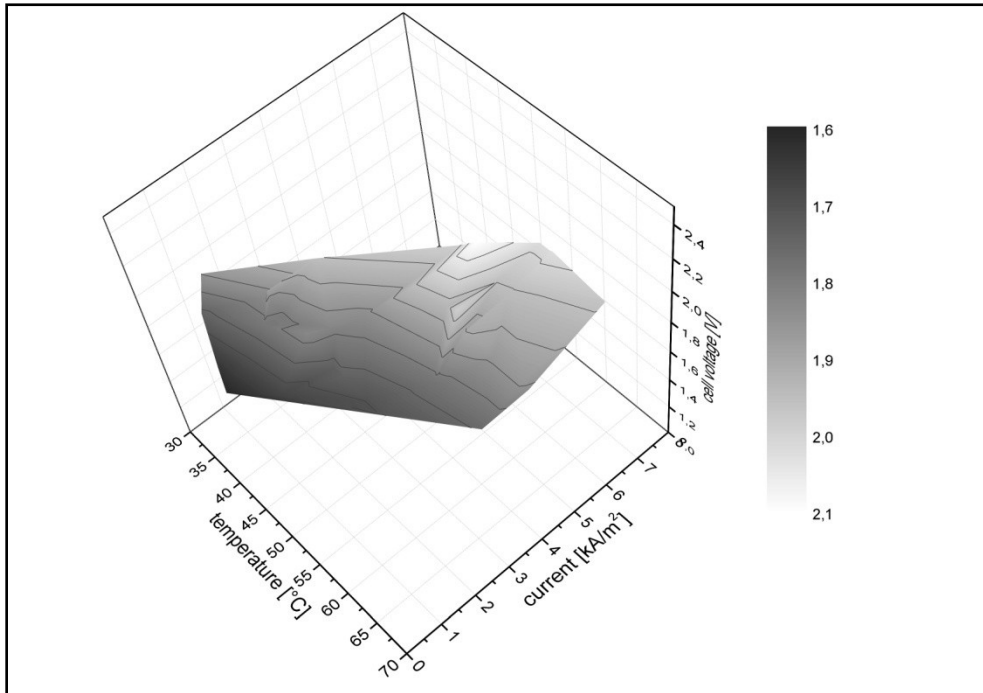


Fig. 2: cell voltage vs. current at different temperatures

By increasing the catalytic activity of the electrodes, a significant decrease in the activation overpotentials of the electrodes and thus of the cell voltages can take place. For this purpose, cathodes coated with Raney-nickel by vacuum plasma spraying (VPS) technique are used. Nickel, molybdenum and aluminum are the main components within this alloy are. An activation treatment is necessary prior to the first electrolyzer operation to remove the aluminum content in order to obtain a high porous nickel layer with a great specific surface area.

Improvement of the desorption kinetics and thermodynamics from CaH₂+AlB₂ system by NbF₅ doping (P-23)

Pasquale Rispoli^a, Benedetto Schiavo^b, Onofrio Scialdone^b, Alessandro Galia^b

^a Istituto per le Tecnologie Avanzate (ITA), Trapani Italy

^b Dipartimento di Ingegneria Chimica, Gestionale, Informatica, Meccanica – Università degli Studi di Palermo

Development of transport vehicles powered by fuel cells require hydrogen storage systems that have a high capacity (> 7% weight H₂), fast kinetics of absorption and release of the fuel, and regeneration temperature and pressure not too much far from ambient conditions. Hydrogen storage in solid materials has long been recognized as one of the most promising approaches to match these requirements. Among these materials, interesting candidates are constituted by composite systems [1], in which complex hydrides (with high hydrogen density) are mixed with other substances (usually metallic hydrides). These systems usually show better performances compared to those of the single complex hydrides. In a previous work [2], we showed the improvement of sorption properties of the composite system, CaH₂+MgB₂, by full substitution of magnesium with aluminum. In light of these results we looked for a possible catalyst to enhance sorption/desorption kinetics of the CaH₂+AlB₂ system. To this purpose, we tested the addition of different halides such as TiF₃, NbF₅ and TiCl₃+AlCl₃ [3], to the system. All of these additives improved both thermodynamics and kinetics of the hydrogen desorption rate with respect to the undoped systems and the best performance was obtained with the NbF₅-doped system, that showed the fastest kinetics and the lowest enthalpy of dehydrogenation. Moreover in the perspective of feeding fuel cell, mass spectrometry measurements indicated that the gas released from the doped samples does not contain any poisoning or corroding agent of the electrochemical converter.

[1] G. Barkhordarian, T.R. Jenssen, S. Doppiu, U. Bösemberg, A. Borgshulte, R. Gremaud, Y. Cerenius, M. Dornheim, T. Klassen, R. Bormann, Formation of Ca(BH₄)₂ from Hydrogenation of CaH₂+MgB₂ Composite, *J. Phys. Chem. C* 112 (2008) 2743–2749.

[2] B. Schiavo, A. Girella, F. Agresti, G. Capurso, C. Milanese. Ball-milling and AlB₂ addition effects on the hydrogen sorption properties of the CaH₂ + MgB₂ system. *J. Alloys Compd.* 509S (2011) S714–S718

[3] J.-H. Kim, J.-H. S., Y.W. Cho, On the reversibility of hydrogen storage in Ti- and Nb-catalyzed Ca(BH₄)₂, *J. Power Sources* 181 (2008) 140-143.

Advanced Alkaline Electrolyzer For Hydrogen Production; Design And Manufacturing (P-26)

AUTHORS: Agustín Merlos, Rubén Beneito, Lorena Rey, Joaquín Vilaplana, Julián Fortes, Juan Carratalá

AIJU, Avda./ de la Industria 23, Ibi, Spain, energia@aiju.info

Water electrolysis has been the most important technology to produce pure hydrogen for chemical processes. Nowadays, since societies are focusing increasingly on renewable and clean energy due to environmental reasons, electrolysis is becoming more relevant for energy use since it paves the way for effective long-term energy storage and for compensation of intermittent energy generation from renewables. In terms of application, hydrogen is widely considered as the most viable energy carrier for future energy technologies, particularly in the transport sector. [1]

Considering the hydrogen high demand forecasts and its great potential for future applications, the present work describes the development of an alkaline electrolyzer able to produce 5Nm³/h of hydrogen in ideal conditions. The prototype consists of a hydrogen production plant pressurized up to 20 bar and a fully automatic control system. The system includes all the necessary equipment for the safe production of hydrogen gas. In particular, all the components of the electrolyzer comply with directives ATEX (94/9/EC), PED (97/23/EC), EMC (2004/108/EC) and LVD (2006/95/EC) all included in the Machinery Directive (2006/43/EC).

The production plant could be roughly divided into three subsystems: i) stack or electrolysis unit, ii) hydrogen purification system and iii) control and monitoring system.

The electrolysis unit or stack is the key to obtain a balance between production and cost and also the size and weight of the stack limiting the transport and handling of the production plant. Design studies (CAD) of the stack have been performed on the electrodes since these allows the production of water inside the stack. A simulation (CAE) study has been performed on the bipolar plates in real working conditions from the viewpoint of fluid-dynamics, structural and thermal behavior. The simulations focused on the mechanical strength of the assembly at pressures and temperatures of real work parameters in stack. These studies have been accomplished with NX Nastran and its design with NX Unigraphics.

A process of manufacturing the electrodes has also been developed by electroplating. In this study investigated electroplating on the bipolar plates for obtaining an optimum performance and obtain a low-cost electrolyzer design has been carried out the bipolar plate and the electrodes are the same component.

The electroplating study was carried out with several coatings (Ni/Fe/Zn, Ni/Zn, Ni/Co/Zn) and several working conditions aiming to obtain a high-performance electroplating. In order to increase the surface area, a post-treatment was carried out on the Ni/Zn layer achieving current densities up to 500 mA/cm². The membranes used in the reactor are a high performance polymeric membranes which can operate at high temperatures and high concentrations of KOH with a very small thickness (50-60 μm) improving the efficiency by increasing the conductivity of the cell. Efficiencies that have

been achieved with developed electroplating and membranes are within 60% and 70% HHV (Hydrogen Higher Heating Value). The results are shown in Figure 1:

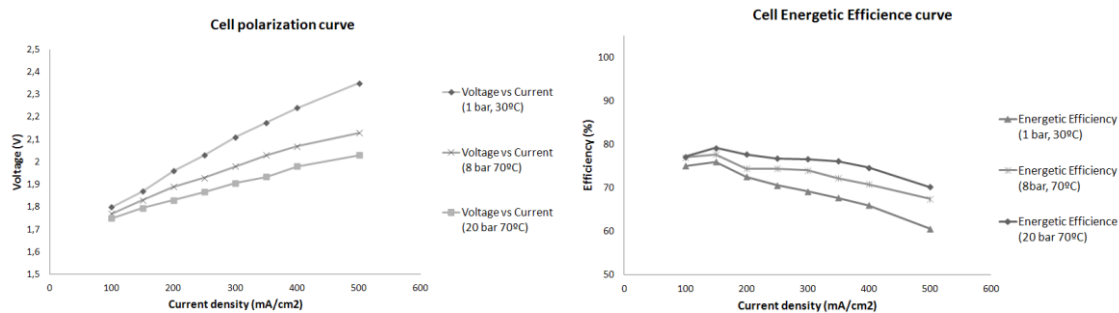


Figure 1: Polarization curve and efficiency curve of cell stack.

The purification and drying system aims to remove the humidity and oxygen traces in the hydrogen gas stream. The purification system contains; a deoxo unit with a palladium based catalyst, a condenser, a cooler and a drying unit with molecular sieve. The hydrogen produced in the electrolysis unit is conducted through the purifying system obtaining a purity of 99.99% downstream.

The control and monitoring system has been implemented using a SCADA application. A high performance industrial PC, a PLC and a display "touch screen" allow monitoring and control all relevant system parameters of electrolyzer. The interface allows to access all control and safety parameters of the electrolyzer under user access permissions (password) ensuring a safe control of the Hydrogen production plant. All security alarms and possible failures are based on a hazard and operability study (HAZOP) of the production plant.

Once determined the complete design all the components were manufactured and assembled to integrate the hydrogen production plant. Finally, hydrogen production of 4.65 Nm³/h at nominal power and 5.35 Nm³/h at peak power, have been achieved, at a pressure of 20 bar and with a purity of 99.96%. Figure 2 shows the complete system.

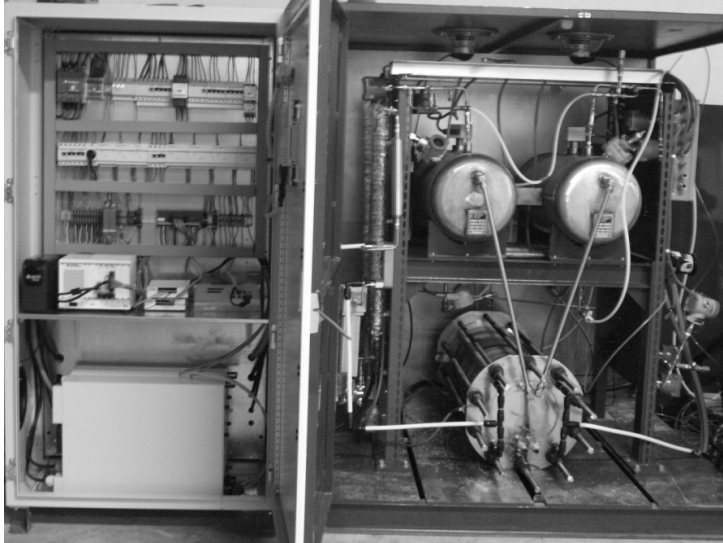


Figure 2: Hydrogen production plant with control system.

Acknowledgements: The research leading to these results has received funding from the European Union's Seventh Framework Programme (FP7/2007- 2013) for the Fuel Cells and Hydrogen Joint Technology Initiative under grant agreement n° [256837], Sustainable Hydrogen Evaluation in Logistics (SHEL) project.

References:

[1] Detlef Stolen, Hydrogen and Fuel Cells: Fundamentals, Technologies and Applications, Wiley-VCH Verlag GmbH & Co (2010).

[2] J.Kerres, G. Eigenberger, S. Reichle 1, V. Schramm, K. Hetzel, W. Schnurnberger, and I. Seybold, Advanced alkaline electrolysis with porous polymeric diaphragms; Desalination 104 (1996) 47-57, ELSEVIER

Water Management Studies In A Pem Fuel Cell: Fuel Cell Stack Design (P-28)

Agustín Merlos, Rubén Beneito, Lorena Rey, Juan Carratalá, Joaquín Vilaplana.

AIJU, Avda./ de la industria, 23, 03440-Ibi (Alicante), Spain.

Since the energy demand increases and with that the price of fossil fuels, it is becoming essential to develop alternative energy sources with minimum negative impact on the environment. The polymer electrolyte membrane fuel cell (PEMFC) is one of the most promising technologies for future automotive propulsion applications due to its high efficiency and zero gas emissions [1]. Water and thermal management are key factors to achieve better performance of PEMFC and therefore the design and simulation of the transport phenomena with their cells is of high relevance [2]. In the present work the design and simulation of the theoretical behavior of a cell operation at high current density has been studied, as well as the validation of the assembly and characterization of the fuel cell stack. Design studies (CAD) of the fuel cell are performed on the bipolar plates due to they carry the water drainage and cool the heat generated in the stack during its operation. The design of the bipolar plates has been carried out using NX Unigraphics. Two different configurations of the circuit with an active area of 45 cm² has been proposed: square design (with coil channel with bends at 90 degrees) and the second one a rectangular design (with linear channels and open angles)

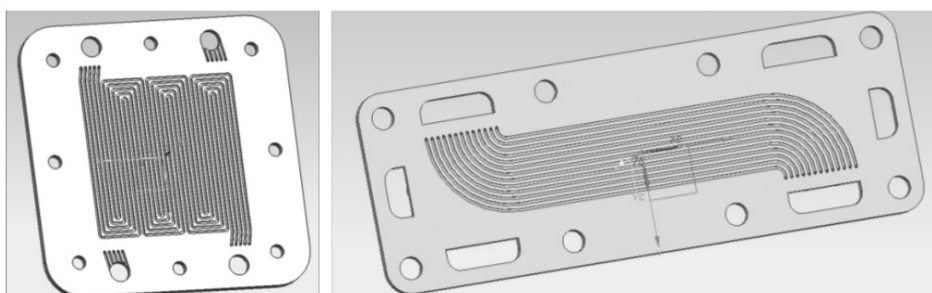


Figure 1: Designs of bipolar plates. Left; coil channel. Right; linear channel

Fluid dynamic and thermal simulations (CAE) were performed on designed bipolar plates to evaluate the behavior of water inside the channels and the heat transfer of the plates by themselves. In these simulations, temperature gradients, distribution of water inside the channels, gas pressure drops and shear stress during gas collision with the channel walls, were studied. The results of simulations disclosed that the rectangular channel open angles evacuated water better than the design with square channels with bends at 90 degrees. That means that the first on designed plate, has a lower pressure drop of the gas inside the bipolar plate and the gas shear stress on its collision with the walls is higher. Once the most optimal channel design was frozen, bipolar plates were manufactured and a stack with 18 cells was assembled obtaining a performance of 0.8-1.2 A/cm² at 700-600mV respectively and was achieved to obtain 550W of peak power. Finally, electrochemical characterization was carried out in order to obtain its polarization curve and dynamic response curve (Figure 2). The enhanced flow channels are designed for operation at high current densities, with lower cost, weight and size.

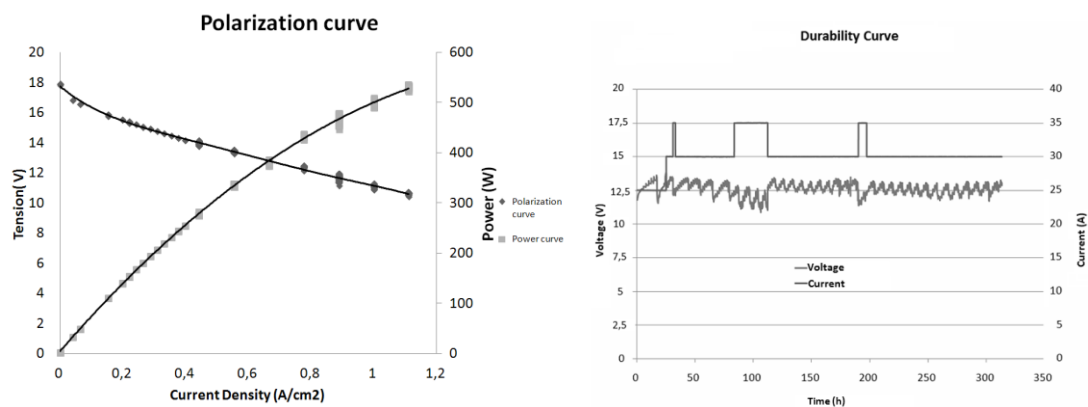


Figure 2. Polarization curve and response curve of PEM fuel cell developed.

Acknowledgements. The authors want to thank IMPIVA (Institute of Valencian SMEs) for financial support through its program of R&D for technological centers in the framework of project (ENERVANZA III).

References.

- [1] Detlef Stolen, Hydrogen and Fuel Cells: Fundamentals, Technologies and Applications, Wiley-VCH Verlag GmbH & Co (2010).
- [2] Jon P. Owejan, Jeffrey J. Gagliardo, Water management studies in PEM Fuel Cells, Part I: Fuel Cell design and in situ water distribution, International Journal of Hydrogen Energy 34 (2009) 3436-3444.

Investigation on water distribution patterns featuring back-diffusion transport in a Polymer Electrolyte Membrane Fuel Cell with Neutron Imaging (P-47)

Alfredo Iranzo ^{a*}, Pierre Boillat ^b, Johannes Biesdorf ^b, Antonio Salva ^a, Felipe Rosa ^c

^a AICIA, School of Engineering, Sevilla, Spain

^b Electrochemistry Laboratory (ECL), Paul Scherrer Institut (PSI), Switzerland

^c Thermal Engineering Group, Energy Engineering Department, School of Engineering, University of Sevilla, Spain

INTRODUCTION

Neutron imaging of PEM Fuel Cells is a powerful instrument for the research and development of PEMFCs, as it allows the visualisation and quantification of the local water content within the cell.

The mass transport losses in Polymer Electrolyte Fuel Cells (PEFCs) are the major restriction for the operation at high current densities. This is limiting the required reduction of stack size, weight, and cost of current PEFCs. In addition to the oxygen diffusion limitations in dry GDLs, water produced by the cathode electrode at high current densities is known to block the GDL pores and electrode reaction sites, causing the flooding of the cell and preventing oxygen from reaching the catalyst active sites. Also an excess of liquid water or a dry-out membrane will result in significant durability issues. Therefore, in order to ensure a successful operation of the cell an appropriate water balance must be achieved.

In this work, liquid water patterns identified in a 50 cm² cross-flow PEM Fuel Cell by means of Neutron Imaging are presented. A clear liquid water transport by back-diffusion (cathode to anode) was observed in the neutron radiographs, despite the high thickness of the membrane (N-117). These liquid water patterns are presented and discussed.

EXPERIMENTAL

Cell description.

The cell used in the experiment was a 50 cm² active area cell from ElectroChem Inc., with metallic Bipolar Plates (five-channel serpentine flow field, Figure 1). The Bipolar Plates layout is cross-flow, with horizontal channels in the anode and vertical channels in the cathode.

A set of Gas Diffusion Layers from SGL Group (Sigracet 24BC) were used. The GDL contains a Micro Porous Layer (MPL) for enhanced performance of the GDL-catalyst layer interface. A Catalyst Coated Membrane (CCM) from Baltic Fuel Cells was used, with catalyst loading at anode and cathode electrodes 0.3 mg Pt/cm² and 0.6 mg Pt/cm² respectively. The membrane material is Nafion-117.

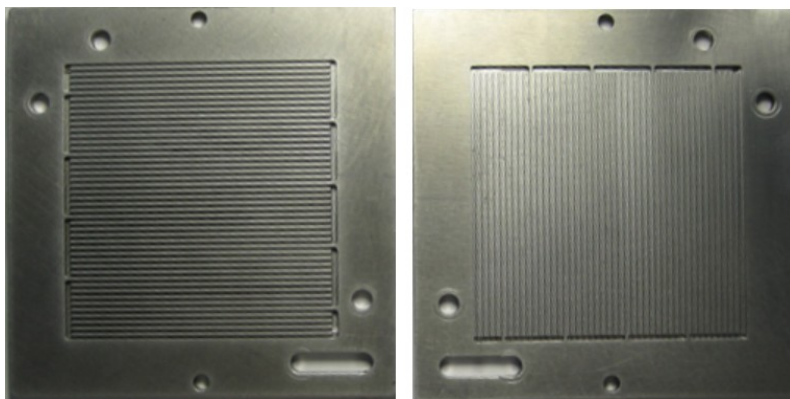


Figure 1: Flow field design used in the experiment. Left: anode side. Right: cathode side.

Experimental procedure.

The SINQ-NEUTRA beam-line at PSI (Boillat et al. 2008, Lehman et al. 2009), with 10 s exposure time, were used for the neutron imaging experiments. Before starting any test the cell was dried out flowing dry nitrogen through anode and cathode. Then the cell operation was performed in galvanostatic mode at 10 A and 25 A setting the anode and cathode flows and relative humidity to the desired conditions. The cell was operated at 2.0 bar and 60 C. Cell current density, voltage, resistance, and neutron imaging data were logged during the entire operation.

EXPERIMENTAL RESULTS

After performing the necessary corrections in the resulting images (detector background, change of beam intensity, neutrons scattered by the setup), the radiograms were referenced pixel-wise by dividing the obtained image by a reference image of the dry cell before operation. Therefore the attenuation corresponding to water only is obtained. The thickness of water δw is calculated from the relative neutron transmission (I/I_0) by inverting the Lambert-Beer law:

$$\delta w = -\ln(I/I_0) / \Sigma \quad (1)$$

where Σ is the attenuation coefficient of neutrons in liquid water, with a value of 3.5 cm⁻¹ for the given setup. The obtained water volume was converted into volume fraction by dividing by the depth of the active area in the beam direction (through-plane direction). Thus, the volume fraction calculated corresponds to the fraction of total volume.

The neutron images recorded indicated clear evidences of liquid water interferences between the anode and cathode sides, despite the high thickness of the membrane (N-117). A representative image is presented in Figure 2, together with an image of the cell structure.

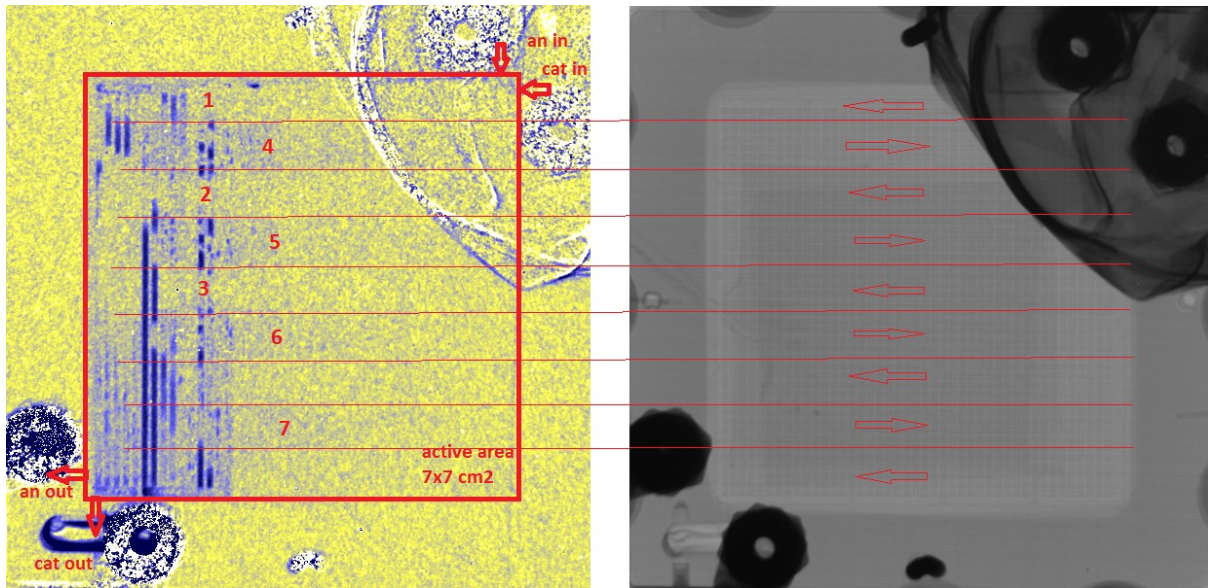


Figure 2: Neutron imaging of the cell. Left: liquid water distribution obtained in the experiment. Right: dry cell showing the cell structure.

The first observation is that liquid water is accumulated in the outlet region of the cell (vertical channels of the cathode close to the outlet), which is a very well-known pattern for serpentine flow fields (Li and Sabir, 2005). Liquid water is clearly present in cathode channels (vertical direction in Figure 1 and 2) with a much larger quantity than in the anode side of the cell, as water is being produced in the cathode side and transported towards the cathode outlet.

The gas flow in the anode channels follows the arrows marked in Figure 2 (right side). There is a clear correspondence with the liquid water distribution in the left side of Figure 2. Anode gas enters the flow field and flows towards the left, then bending at the end of the plate and flowing towards the right. This serpentine flow is repeated from the inlet to the outlet. It can be seen that every time the anode gas flows through a region with liquid water at the cathode channels, two linked phenomena occurs:

- First, a drying process in the cathode occurs (see points 1,2,3 in Figure 2, left side).

- Secondly, water is transported from the anode side to the cathode side, and the anode side increases its water content with the clear directionality of the anode gas flow (see points 4,5,6,7 in Figure 2, left side).

Therefore a fraction of the liquid water produced in the cathode is transported to the anode, where the only possible mechanism for this is the back-diffusion mechanism. Once in the anode side, the gas flow along the channels forces water to be distributed in the GDL with a preference in the along-the-channel direction. This water distribution profile demonstrates a relevant water transport between the cathode and anode sides of the cell, with a strong contribution of the back-diffusion mechanism in the final distribution observed within the cell. This pattern can be better observed in

the particular cell used in the experiments, as in the cross-flow layout of the bipolar plates the water in anode and cathode sides can be better determined.

ACKNOWLEDGEMENTS

This work was carried out with the support of the European Community. We appreciate the support of the European Research Infrastructure project "H2FC European Infrastructure" (funded under the FP7 specific programme Capacities, Grant agreement Number FP7-284522) and its partner Paul Scherrer Institut.

Alfredo Iranzo also gratefully acknowledges the support of the Spanish Ministry of Economy and Competitiveness under the program INNCORPORA, Torres-Quevedo PTQ-11-04703, co-funded with the European Social Fund.

REFERENCES

Boillat P, Kramer D, Seyfang BC, Frei G, Lehmann E, Scherer GG, Wokaun A, Ichikawa Y, Tasaki Y, Shinohara K. In situ observation of the water distribution across a PEFC using high resolution neutron radiography, *Electrochemistry Communications* 10, 546 (2008).

Lehmann EH, Boillat P, Scherrer G, Frei G. Fuel cell studies with neutrons at the PSI's neutron imaging facilities. *Nuclear Instruments & Methods in Physics Research Section A-Accelerators Spectrometers Detectors and Associated Equipment*, 605, 123 (2009).

Li X, Sabir I. Review of bipolar plates in PEM fuel cells: Flow-field designs. *International Journal of Hydrogen Energy* 30, 359 (2005).

Hydrogen production system by steam reforming integrated in a solar parabolic disc (P-48)

Marta T. Escudero, Belén Sarmiento, María Maynar, Rocío Domínguez

Abengoa Hidrógeno, Campus Palmas Altas, C/Energía Solar nº1, 41014 Sevilla

Introduction

Solar energy can contribute changing the current energetic model, ensuring the energetic independence of Europe and contributing with this to a sustainable development. Concentrated solar energy can be efficiently stored with a reasonable cost, enabling its adaptation to energetic markets connected to the power grid as well as to distributed generation grids.

Nowadays, the most important difference between solar energy plants and conventional thermal plants -focused on electricity generation- is the possibility to operate 24/24 hours. Storing of solar energy captured during off-peak hours -when the electricity consumption is low and the sun is shining-, and its posterior conversion into electricity allows injecting this electricity to the power grid during peak hours, when electricity price is more economically beneficial. For this reason, thermal storage is an essential requirement that it is becoming necessary in terms of profitability for solar plants.

Taking into account this scenario, hydrogen could be considered as a good choice for storing electricity due to its character of energy vector. Hydrogen has a big potential because it is a clean fuel whose combustion product is mainly water. In order to replace gradually fossil fuels, the hydrogen is considered as one of the most valuable candidates to be used as renewable fuel in the future, thanks to its ability to store energy that can be subsequently used in several applications, standing out among others the electricity production in fuel cells.

However, because of the fact that hydrogen cannot be found in the nature, it has to be produced using several methods, some of them with higher maturity level than other ones. To choose the most convenient method to produce hydrogen, the high quantity of energy available in a solar plant has been taken into consideration, because it is possible to reach high operating temperatures.

Hydrogen production by steam reforming of hydrocarbons or alcohols is a well-known and developed process; the use of biofuels instead of hydrocarbons -for example, the bioethanol-, makes the storage of solar energy environmentally friendly.

Objective and scope of work

Hydrogen production by bioethanol reforming integrated in a solar parabolic disc has been carried out in the framework of a national project, SolH2 (project reference: IPT-2011-1323-920000; participants: Imdea Energía, Ciemat, University of Seville and Abengoa Hidrógeno). This project has been created in order to demonstrate the technical feasibility of employing hydrogen to store energy in a solar plant, as well as to validate the hydrogen production by biofuel reforming integrated in a solar parabolic disc.

“Solar hydrogen” production presents problems and challenges associated to the high temperatures reached, the materials employed, the catalyst needed in the process as well as unexpected problems that may arise during the operation of the solar plant. These and other difficulties have been addressed in SolH2, a project partially funded by The Ministry of Economy and leaded by Abengoa Hidrógeno that could help to develop emerging solar technologies.

Design the solar receptor/reactor is the main challenge of this project that has been carried out from the point of view of industrial research. Because of this, the objective is testing the integration between reforming process and solar technology as well as achieving an optimal thermal integration of the process, making the scale-up of the prototype possible in the future.

In this context, the complete process have to be designed, developed and built during the timeline of the project.

Work developed: engineering phase

During the conceptual design -first phase of the project- the hydrogen production process was developed. As it is well known, steam reforming is an endothermic process. In industrial processes energy required for the reaction is generally obtained using a boiler, but in this case, solar energy can be used. For this, it was necessary to calculate and design the solar receptor in order to collect the maximum solar power. A detailed analysis of solar reactors from the point of view of thermal integration between solar receptor and reactor was carried out 0, 0. For this project, an indirect exchange tubular reactor has been chosen due to its high maturity level - among other factors-.

A complete thermal integration has been considered in order to provide the thermal energy required to heat the fuel (bioethanol and water in this case) as well as to keep constant the temperature reaction. A simple scheme of the process is shown in Figure 21.

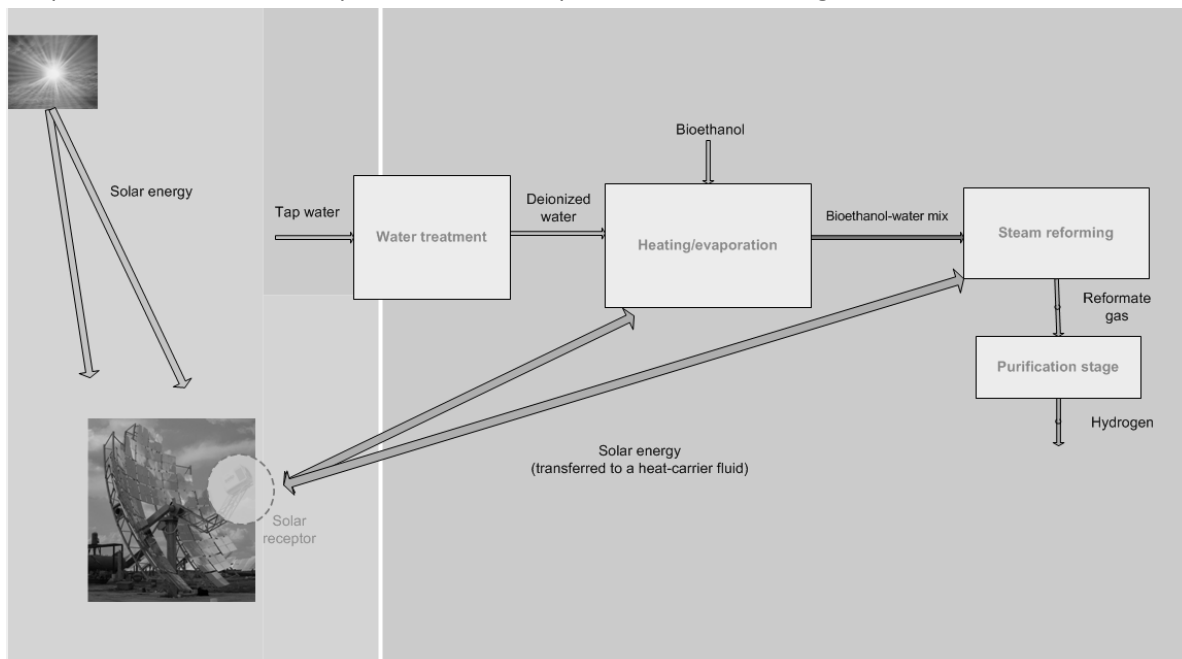


Figure 21.- Scheme of hydrogen production system by steam reforming integrated in a solar parabolic disc.

Hydrogen production process was designed taking into account the option to feed a fuel cell with the hydrogen stream produced; so it was necessary to adapt the reformat gas stream to achieve the strict requirements, (hydrogen purity, temperature, pressure...).

An innovative integration proposal has been developed by Abengoa Hidrógeno exclusively for this project. The biggest difficulty was to adapt the size of the equipment to install it on the solar disc. This problem was solved separating hydrogen production process; that is to say, reforming process is carrying out by the equipment placed over the solar disc, and the purification phase and the auxiliaries were placed at floor level.

In the following phases of the project -Preliminary Design Review (PDR) and Critical Design Review (CDR)- the complete hydrogen production plant was designed including required utilities and auxiliary equipment.

Current results

Engineering phase has been finished, now SolH2 project is under construction. Abengoa Hidrógeno is undertaking in parallel equipment construction and civil works.

Future works

Hydrogen production plant will be finalized integrating equipment on the solar disc; after that and before the start up, pre-commissioning and commissioning tests will be carried out.

The last phase of the project will consist on executing functional and performance tests. In the first case, the objective is to carry out the required tests to validate the correct operation of the system -according to design specifications-. Moreover, during performance tests, the optimization of the system will be carried out analyzing operational data compiled in nominal operation, as well as validating control strategies in different operational modes.

References

Hogan Jr., et al. 1990. A direct absorber reactor/receiver for solar thermal applications. Chemical Engineering Science 45, 2751–2758.

Diver, R.B. 1986. Receiver/reactor concepts for thermochemical transport of solar energy. SNL; ERA-11-040256; EDB-86-126746.

Eliminating hydrogen inventories for green energy storage using liquid metal technology (P-50)

Amalio Garrido-Escudero

Drage&Mate International, SL

The social and economic pressure on hydrocarbons promoted the study for clean and renewable energy applications. Such energy sources are highly variable and geographically distributed, so the control of availability is difficult. In order to store the generated energy and to facilitate the transport and use, the existence of a vector or "currency" that allows energy exchanges is required. This type of vector will decouple supply from demand.

During last seven years a research project team has developed the patented METALIQ process (Patent EP2394953). An innovative technology, currently unique, which provides a simple and effective solution for high efficient energy storage in a clean and safe way is now available using hydrogen for power generation.

This technology enables the energy storage in a self-sufficient way, with very low energy consumption during generation, without greenhouse gases emission, no waste generation, no carbon combustion reactions involved and using recyclable reagents available anywhere in the world. This technology is applicable to self-sufficient stationary applications like UPS, smart renewable energy management, APUs, automotive, aviation, etc.

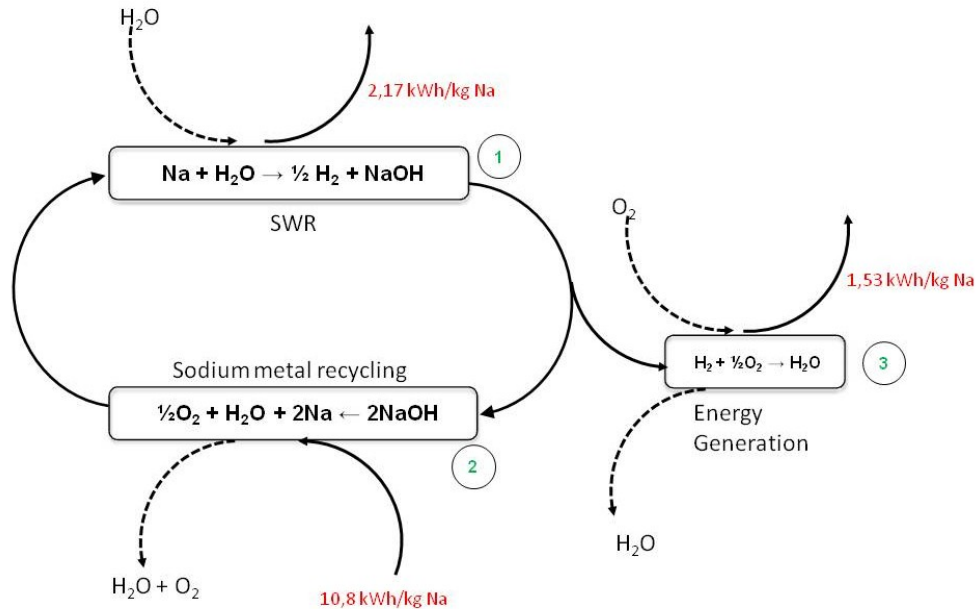
The METALIQ proposal is based on the direct energy to material conversion (DEMEC) using high energy density compounds like alkaline metals, alkaline-earth metals and alloys between themselves. The complete energy-material-energy cycle shows a theoretical yield higher than 33%.

Therefore METALIQ allows:

- - self-sufficient energy storage
- - low power needs during energy generation
- - free in greenhouse gas emission
- - no waste generation
- - without combustion reactions
- - with fuel obtainable anywhere in the world
- - able to be recycled using renewable energy
- - reduced volume and weight needs in comparison with batteries or capacitors
- - Long life (equivalent to industrial plants and utilities)
- - Low operating and maintenance cost
- - Modular and scalable

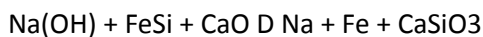
Sodium metal shows different chemical reactions suitable to be used as energy generation candidates. One of them is the very well known as Sodium Water Reaction (SWR)(1). This reaction

generates hydrogen gas (H₂) that can be use immediately as is produced. Hydrogen can be easily converted to mechanical or electrical energy by internal combustion engine or Fuel Cell in reaction with oxygen (3).



Once sodium metal reacts with water then sodium hydroxide is generated. Sodium hydroxide can be recycled(2) following different routes in order to generate sodium metal taking the energy to be stored. Sodium metal can be stored as energy storage up to 3,61 kWh/kg. Complete cycle can perform at 33,4% theoretical yield. This is METALiq Process.

METALiq works in a close loop using different recycling reactions as new silicothermal route:



or molten hydroxide or salt electrolysis (commercial technologies).

The innovative process works in very stable conditions thanks to a homogeneous phase continuous pipe reactor (HPCPR). The special liquid metal injectors design avoids chain reaction. Mathematical modeling of chain reaction and hydrogen detonation was key in development.

Energy density for alkaline metal used in this new technology is up to 1000 times higher than a lead-acid battery and up to 500 times less in cost per kWh stored.

References

DoE. (n.d.). Solar Glossary. Retrieved May 27, 2010, from http://www1.eere.energy.gov/solar/solar_glossary.html#E

Escudero, A. G. (2010). Patent No. EP2394953. Spain.

Kevin G. Gallagher, D. D. (May 2011). PHEV Battery Cost Assessment. Washington: Argonne National Laboratory.

P.A. Nelson, K. G. (September 2011). Modeling the Performance and Cost of Lithium-Ion Batteries for Electric-Drive Vehicles. Chicago: P.A. Nelson, K.G. Gallagher, I. Bloom, and D.W. Dees, Modeling the Performance and Cost of Lithium-Argonne National Laboratory.

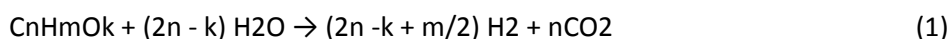
Hydrogen from biomass derived oxygenates: Thermodynamic comparison between bio-oil and ethanol steam reforming (P-56)

C. Montero, L. Oar-Arteta, B. Aramburu, A. Remiro, J. Bilbao, A.G. Gayubo

Chemical Engineering Department. University of the Basque Country UPV/EHU. P.O. Box.644, 48080. Bilbao-Spain. carodromontero@gmail.com

INTRODUCTION

Hydrogen is considered the clean fuel of the future because its combustion only produces water and CO₂. Nowadays nearly 90% of the hydrogen is obtained by steam reforming (SR) of natural gas or naphtha, but the need to reduce CO₂ emissions has promoted H₂ production from renewable raw materials, such as biomass [1]. Hydrogen can be obtained from biomass directly (gasification, high temperature pyrolysis, catalytic pyrolysis and biological processes) and by intermediate routes for obtaining oxygenated hydrocarbons followed by a reforming process [2]. Ethanol (obtained by biomass fermentation) and bio-oil (a complex mixture of more than 300 oxygenates compounds obtained by flash pyrolysis of biomass), are considered promising feeds for obtaining H₂ by SR [3, 4]. The steam reforming of oxygenates is a highly endothermic process which includes oxygenates reforming reaction to form CO and H₂, and the WGS reaction, the overall reaction being as follows:



The thermodynamics of ethanol steam reforming (E-SR) has been widely studied [3,5], but there are scarce information concerning the thermodynamics of bio-oil steam reforming (B-SR) due to the complex nature of this feed. A thermodynamic analysis of SR of a mixture of three model compounds of bio-oil (acetic acid, acetone and ethylene glycol) has been recently published [6].

In this paper, the thermodynamic analysis of SR of a “simulated bio-oil” is performed. The simulated bio-oil is composed of model compounds representative of the main families of components in bio-oil (acids, esthers, ketones, ethers, alcohols, phenols). The results corresponding to E-SR are also presented in order to compare the operating conditions required for obtaining high hydrogen yields from different biomass derived oxygenates.

METHODOLOGY

The thermodynamic analysis was performed considering a non-stoichiometric method (minimization of the Gibb’s free energy) by using Pro II-Simsci® 8.3 software, Gibb’s reactor and Soave-Redlich-Kwong equation of state, which allows obtaining the equilibrium composition of the gaseous products (H₂, CO₂, CO and CH₄), the coke-free operation zone and the energy requirements for the process. The simulation conditions were: atmospheric pressure; temperature = 300-1000 °C and steam/carbon ratio (S/C) =1-16. The amount of each model compound in the “simulated bio-oil” (Table 1) was based on the composition of a real raw bio-oil obtained by fast pyrolysis of pine sawdust, and determined by GC/MS in a Shimadzu QP2010S device [7]. The resulting molecular formula of the mixture is C_{4.86}H_{8.26}O_{1.92} and the molecular weight is 97.27 g/mol.

RESULTS

Figure 1 shows the effect of S/C ratio in the feed upon the maximum H₂ yield which can be obtained in the steam reforming of both feeds (ethanol or bio-oil). For both processes, the maximum H₂ yield increases continuously with S/C ratio, these increase being very noticeable below S/C=5 (at which H₂ yield reaches 90% for both E-SR and B-SR) and subsequently the increase is attenuated. The maximum H₂ yields obtained from both feeds is very similar, and only small differences are observed for S/C ratios below 2. For each S/C ratio, H₂ yield goes through a maximum with reaction temperature, and the temperature required for attaining this maximum (also shown in Figure 1) decreases as S/C increases, and it is slightly higher for E-SR than for B-SR.

For the processes, temperatures above 700 °C and S/C ratios higher than 2 are required for minimizing coke formation, which is higher for B-SR than for E-SR, probably due to the higher concentration of CO (which produces coke through Boudouard reaction).

The standard reaction enthalpy for both E-SR and B-SR increases noticeably with temperature up to 700 °C and it tends asymptotically to a constant value for higher temperatures. Under the conditions required for attaining H₂ yield higher than 80% (T>600 and S/C > 4) both processes are clearly endothermic, with enthalpy values in the 180-240 kJ/mol range for E-SR, and in the 350-520 kJ/mol range for B-SR.

Table 1. Composition of the simulated bio-oil.

Family of Compounds	Compound	% Mol
Ketones	Cyclohexanone	18.16
	Hydroxy acetone	11.06
Carboxylic Acids	Acetic acid	17.63
	Levulinic acid	5.45
Aldehydes	Vanillin	10.39
Alcohols	Propylene glycol	9.05
	Heptanol	10.07
Phenols	Methoxyphenol	8.94
Ethers	Trioxane	4.09
Esters	Ethyl propionate	5.17

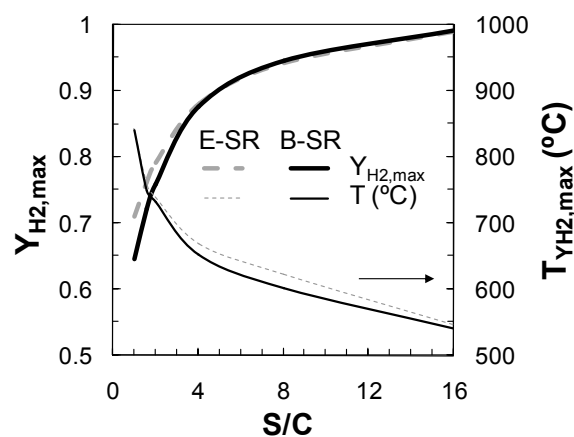


Figure 1. Evolution with S/C ratio of the maximum H₂ yield and of the temperature required for attaining this maximum, for E-SR (dashed lines) and B-SR (continuous lines).

CONCLUSIONS

The maximum H₂ yield attainable for both E-SR and B-SR is similar, the temperature required for the maximum H₂ yield being slightly higher for E-SR. Coke formation, which is higher for B-SR, can be avoided above 700 °C and for S/C ratio higher than 2. B-SR is more endothermic (by approximately 250 kJ/mol) than E-SR, which must be considered for the estimation of the energy requirements at industrial scale.

ACKNOWLEDGEMENTS

This work has been carried out with the financial support of The National Secretariat of Higher Education, Science, Technology and Innovation of Ecuador SENESCYT (Contract 20110560) and the Ministry of Science & Technology of the Spanish Government (Projects CQT2009-13428 and CTQ2012-35263).

REFERENCES

1. Y. Kalinci, A. Hepbasli, I. Dincer, *Int. J. Hydrogen Energy*, 34, 8799-8817, 2009.
2. A. Tanksale, J.N. Beltramini, G.M.Lu, *Renew. Sust. Energy Rev.*, 14,166-182, 2010.
3. S. Sun, W. Yan, P. Sun, J. Chen, *Energy*, 44, 911-924, 2012
4. A.A. Lemonidou, P. Kechagiopoulos, E.Heracleous, S. Voutetakis, *The Role of Catalysis for the Sustainable Production of Biofuels and Bio-chemicals*; Elsevier: Amsterdam, 2013.
5. G. Rabenstein, V Hacker; *J Power Sources*, 185:1293-1304, 2008
6. E. C. Vagia, A. A. Lemonidou, *Int. J. Hydrogen Energy*, 32, 212-223, 2007
7. B. Valle, A. Remiro, A. T. Aguayo, J. Bilbao, A.G. Gayubo, *Int. J. Hydrogen Energy*, 38, 1307 2013.

Preparation and Characterization of Sulfonated Poly(phenylene)s Containing Cis/Trans Mixture of Bis(4-chlorophenyl)-1,2-diphenylethylene for Proton Exchange Membrane (P-63)

HOHYOUN JANG, YOUNGDON LIM, SOONHO LEE, MD. AWLAD HOSSAIN, SEONGYOUNG CHOI,
HYUNHO JOO, FEI DAN, WHANGI KIM*

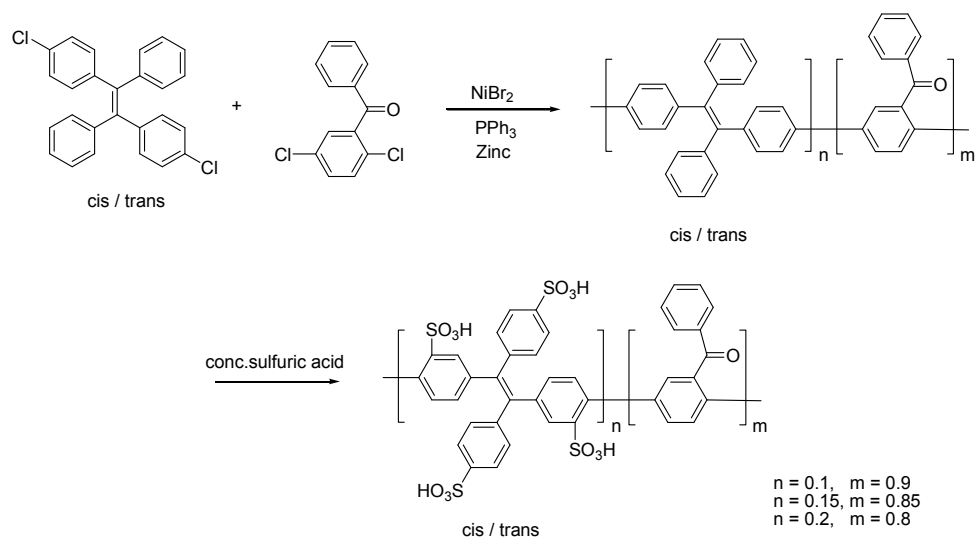
Department of Applied Chemistry, Konkuk University, Chungju, Korea

**Corresponding author: wgkim@kku.ac.kr*

ABSTRACT

Proton exchange membrane fuel cells (PEMFCs) are a promising future energy source due to their high power densities, efficiencies, and eco-friendliness. The commercial perfluorinated copolymer membranes, such as Nafion® and Flemion® have high proton conductivity with good chemical and mechanical stability. However, these membranes have some disadvantages for extensive applications, like poor performance at high temperatures, high cost, high methanol permeability, etc. These problems demand to the development of sulfonated aromatic hydrocarbon polymers as alternative proton exchange membranes. But hydrocarbon membranes have some drawbacks, particularly low chemical stability and proton conductivity compared to perfluorinated acid polymers and also low mechanical stability. They are easily exposed to nucleophile attack by hydrogen peroxide or peroxide radicals generated during PEMFC operation. To overcome these hindrances, an effort has been studied with the structure of sulfonic acid groups on the side chain of the nickel-catalyzed carbon-carbon coupling polymers. The chemical modification to sulfonic acid attached pendant aromatic rings of polymer provides better stability due to less reactive to nucleophilic substitution of main chain and also improve proton conductivity due to well phase separation between the hydrophilic and hydrophobic domains with microstructure. In addition, nickel-catalyzed carbon-carbon coupling polymers without ether linkages are presumably stable against nucleophilic attack by hydrogen peroxide or peroxide radicals generated by PEMFC operation system. Generally, nickel-catalyzed carbon-carbon polymerization is performed in dry aprotic polar solvent using catalytic amount of nickel chloride/bromide, triphenylphosphine or bipyridyl ligands, and excess zinc powder. The reaction mixture must be prepared under an inert atmosphere and the absence of water, as the catalysts are very sensitive to air. In this study, poly(phenylene)s without ether linkage in the main chain were synthesized via nickel-catalyzed carbon-carbon coupling polymerization of bis(4-chlorophenyl)-1,2-diphenylethylene (BCDPE) and 2,5-dichlorobenzophenone (Scheme1). The BCDPE is consisted of a 4:6 ratio of cis and trans forms. Conjugated cis/trans isomer based BCDPE has a non-planar conformation containing the peripheral four aromatic rings which facilitate the formation of π - π interactions. Moreover, polymers with pendant benzoyl group has some advantages, such as good solubility, durability and thermooxidative stability. Post sulfonation process was carried out to add sulfonic acid groups by using concentrated sulfuric acid. The number of sulfonic acid groups were controlled by varying the mole ratio of BCDPE monomers in synthesized poly(phenylene) copolymer. Sulfonic acid groups were attached both on the side-chain and main-chain phenyl groups simultaneously. A series of sulfonated poly (bis-chloro diphenylethylene)s, S-PBCDPE 10, 15 & 20 were prepared by controlling the mole ratios of BCDPE as 10%, 15% and 20%. The S-PBCDPE membranes' structures were characterized by ¹H NMR spectroscopy and FT-IR.

Membranes' thermal properties were investigated by thermogravimetric analysis (TGA). Water uptakes (WUs) were measured to observe the interaction of sulfonated polymer with water. The ion exchange capacities (IECs) of sulfonated polymers were evaluated with increasing degree of sulfonation. The IEC values of the sulfonated polymer membranes were achieved in the range of 1.56-2.51 meq/g. The proton conductivities of the membranes were measured as a function of the mole percentage of the sulfonic acid group. S-PBCDPE membranes exhibited proton conductivity results as 75.3-113.4 mS/cm, compared with 103.7 mS/cm for Nafion 211[®]. Furthermore, membrane's durability will be assessed by Fenton's reagent and also surface morphologies of polymer membranes will be studied by atomic force microscope (AFM).



Scheme1. Synthesis of S-PBCDPE polymer

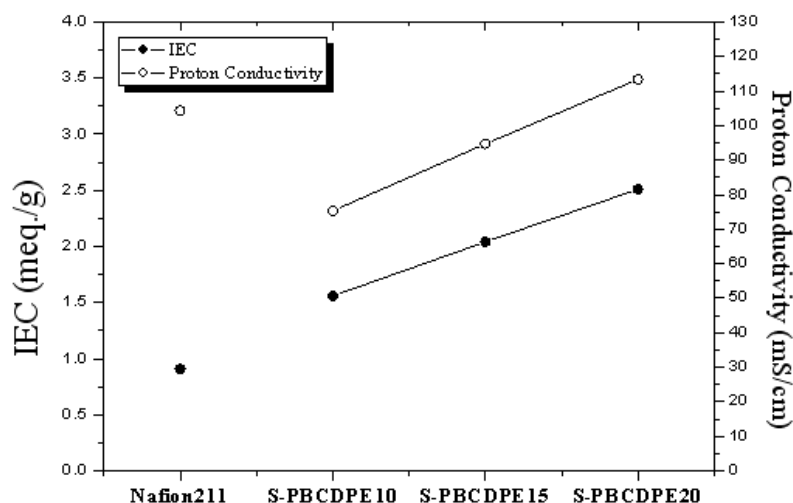


Figure1. IEC and proton conductivity of S-PBCDPE 10, 15, 20 and Nafion 211[®] at 80 °C under 90 % relative humidity

Synthesis and properties of sulfonated grafting copolymer via superacid-catalyzed polyhydroxyalkylation reaction (P-64)

Soonho Lee, YOUNGDON LIM, HOHYOUN JANG, YOUNGTAE JEON, JINSEONG IIM, IEI JIN and Whangi Kim*

Department of Applied Chemistry, Konkuk University Chungju, Korea

**Corresponding author: wgkim@kku.ac.kr*

ABSTRACT

Polymer electrolyte membrane fuel cell (PEMFC) can efficiently generate high power densities and thereby making it an attractive technology for automobile and portable applications. At present, perfluorinated polymer membranes, such as Nafion® and Flemion® are widely used for PEM materials because of their excellent physical & chemical stability, and high proton conductivity. Their characteristics are derived from fluoro atoms and carbon-carbon bonded chemical structures which attribute relatively long lifetime compared to hydrocarbon membranes. Most hydrocarbon membranes generally show lower ionic conductivities at comparable ion exchange capacities than Nafion®, and more susceptible to oxidative or acid-catalyzed degradation than Nafion® by structural ether linkage. Chemical degradation of the membranes is usually thought to play the most important role for abating fuel cell performance. Research in the field of hydrocarbon membranes has made great strides throughout the years. Performances (like- proton conductivity, power density, etc.) of hydrocarbon membranes are close to those of perfluorinated sulfuric acid membranes, and also their cost is low. However, the durability of hydrocarbon membranes is not as high as that of Nafion®. To overcome these kinds of drawbacks, the carbon-carbon backbone structured polymers were studied. Sulfonated poly(p-phenylene)s and their derivatives which are generally synthesized by Ni-catalyzed coupling copolymerization. The carbon-carbon bonded polymers were also prepared by the Diels-Alder polymerization. These carbon-carbon backbone based polymer membranes have excellent oxidative and chemical stability and good performance. However, they are very expensive regarding monomers, catalyst, and demanding reaction conditions. Olah and co-workers have explained the high reactivity of electrophilic species in superacid media and therefore numerous reactions have been carried out using superacid as a reaction medium.

The purpose of this work is to prepare the sulfonated grafting polymer containing 2,2,2-trifluoroacetophenone and pendant sulfonic acid groups for good chemical stability, solubility in polar organic solvents, low water uptake and improving proton mobility because of well phase separation. We synthesized copolymer from 2,2'-dihydroxybiphenyl and diphenylether with trifluoromethane sulfonic acid as a superacid.

A typical polyhydroxyalkylation procedure was as follows (Scheme 1): Trifluoromethane sulfonic acid was added to a mixture of 2,2,2-trifluoroacetophenone, 2,2'-dihydroxybiphenyl and diphenyl ether in dichloromethane. The resulting reaction mixture was decanted dropwise into methanol. After drying, white fibre like polymer was obtained. Sulfonated graft polymers were synthesized by condensation reaction with 3-bromopropane sulfonic acid potassium salt using sodium hydride base in dimethylacetamide. The resulting mixture was poured slowly into distilled water and the

precipitate was washed several times with water and dried under vacuum at 80 °C for 24 h. Finally, the acidification was carried out in concentrated hydrochloric acid to afford the sulfonated membranes. A series of sulfonated poly(phenylene ether)s, S-PPE 40, 50 & 70 were prepared by controlling the mole ratios of 2,2'-dihydroxybiphenyl as 40%, 50% and 70%.

These polymers are flexible, good soluble in polar organic solvents and also demonstrate good proton mobility because of well phase separation. High molecular weight polymer was achieved by superacid-catalyzed polyhydroxyalkylation. All these membranes were casted from dimethyl sulfoxide (DMSO). The resultant polymer membranes were studied by ^1H NMR, FT-IR, thermogravimetric analysis (TGA), ion exchange capacity (IEC), water uptake, dimensional stability and proton conductivity assessment. The chemical stability was also investigated by Fenton's reagent, and compared with Nafion 211.

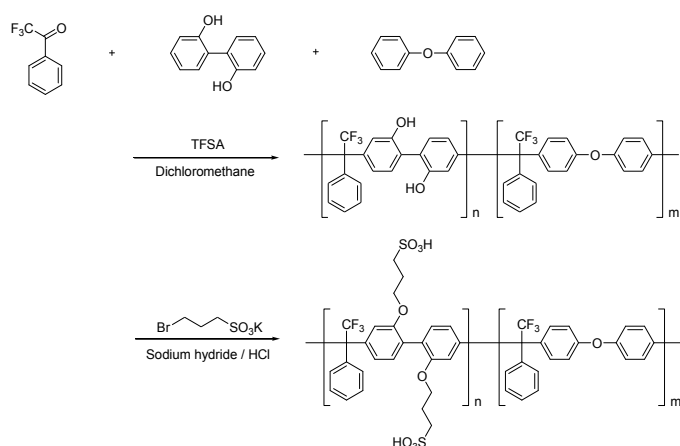


Figure 1. Preparation of sulfonate-grafted poly(phenylene ether).

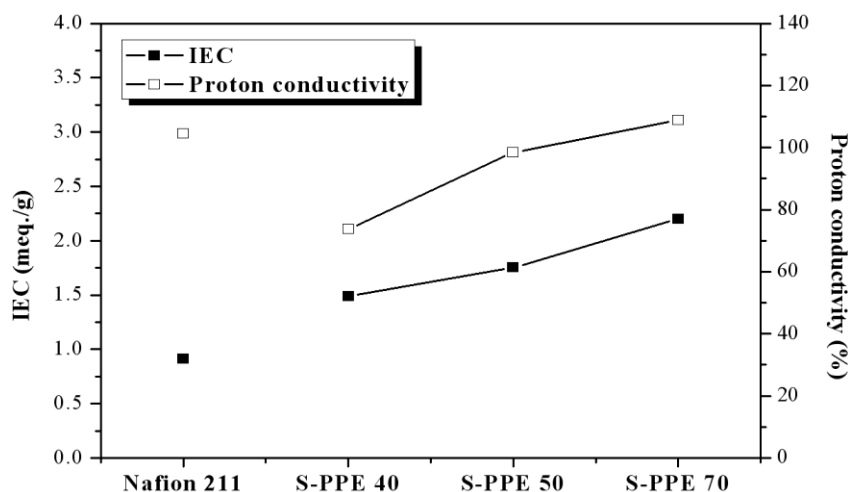


Figure 2. IEC and proton conductivity of S-PPEs and Nafion 211®

Hydrogenation Behaviors of MgH_x -Graphene Composites by Reactive Mechanical Grinding (P-70)

Young-Sang Lee, Tae-Whan.Hong*

**Department of Materials Science and Engineering/Research Center for Sustainable ECo-Devices and Materials (ReSEM), Korea National University of Transportation, 50 Dae hak ro, Chungju, Chunbuk, Korea*

Email: twhong@ut.ac.kr

In order to overcome the crisis of fossil fuel based modern society, the development of various renewable energy has been actively. As for the clean energy mediation and no discharge energy source, Hydrogen is able to solve an environmental matter and a volunteering war at the same time. It is now generally believed that hydrogen storage which cuts across the production, distribution, safety and application, forms the key factors for "hydrogen economy" [1, 2].

There are four main methods for hydrogen storage which are liquid hydrogen, compressed hydrogen, metal hydrides and adsorbent packed bed. Presently, only liquid hydrogen storage method is close to the requirement. Recently, metal hydride was considered that it may be providing suitable materials for hydrogen. Because it can be help hydrogen stable in the lattice structure of metal atoms crystal under the damage. And it should be able to absorb efficiently hydrogen compare with density of liquid hydrogen [3].

Magnesium and Magnesium-based alloys are considered to be promising storage media because of their hydrogen storage capacity (7.6wt.% for pure Mg), low density, low cost and high availability. However, commercial applications of the Mg hydride are currently hindered by its high operating temperature, and very slow reaction kinetics [4].

To overcome these disadvantages, many researchers studied techniques such as catalysing, nanostructuring and alloying. Furthermore, milling used as a hydrogen storage material has positive effects on hydrogenation behavior because a high surface area can be obtained by milling. A few studies were conducted for MgH_x intermixed with carbon [5]. Hydrogen storage capacities of various carbon absorption have been summarized in several papers. various nanostructured and microporous carbon-based materials have been studied intensively because of their light weight, high surface areas, and relative chemical stabilities.

The common kind of carbon adsorbents are activated carbons, carbon nanofibers, single-walled carbon nanotubes, multiwalled carbon nanotubes, and graphene. The two-dimensional structure of graphene consists of hexagonal cells constructed from sp^2 -hybridised carbon atoms. It is a promising material because of its high electron mobility and atomic thickness. Graphene is composed of a monolayer of carbon atoms packed into a dense honeycomb crystal structure [6]. They concluded that the interactions between carbon and metal hydride should be enhanced by increasing pore size, surface area and some surface modification studies in order to improve absorption capacity. The recent theoretical calculation results indicate that graphene may also work as a sorbent for hydrogen storage [5]. And graphene generally require cryogenic temperatures to adsorb significant amounts of hydrogen.

In this work, we are aimed at improving the operating temperature and slow reaction kinetics of the MgHx with addition of graphene powder. MgHx was prepared by reactive mechanical alloying under 2MPa hydrogen atmosphere for 96hrs MgHx synthesized with 5,10wt.% graphene milled for 96hrs using the Planetary ball mill. The synthesized powder was characterized by X-ray diffraction analysis (XRD), scanning electron microscopy (SEM), transmission electron microscope(TEM) energy dispersive spectroscopy (EDS), and simultaneous thermo gravimetric (TG), differential scanning calorimetric (DSC) analysis. The hydrogenation behaviors were evaluated by using a sievert's type automatic pressure-composition-temperature (PCT) apparatus. From the characteristics of the absorption kinetics and curves observed the role of graphene as catalyst in hydrogen absorption. The effect of added amount of graphene has been shown operating temperature of dehydrogenation that reduced.

The specific surface area of MgHx-5, 10wt.% graphene was identified using BET apparatus. The specific surface area of MgHx was 5.840m²/g, that of graphene flake 87.211m²/g, MgHx-5wt.% graphene 3.6567 m²/g, and MgHx-10wt.% graphene 3.9051m²/g respectively.

TG analysis results, the starting temperature of dehydrogenation and dehydrogenation amount of specimens on 5wt.% graphene composites were 613K and -2.11mg. Those of MgHx-10wt.% graphene were 579k and -1.9mg, respectively. Dehydrogenation amount can be estimated using the change of mass reduction.

DSC analysis, the starting temperature of reaction was similar to that in TG analysis. ΔH , the enthalpy change in reaction, was -947J/g for 5wt.% graphene and -841.9J/g for MgHx-10wt.% graphene composites.

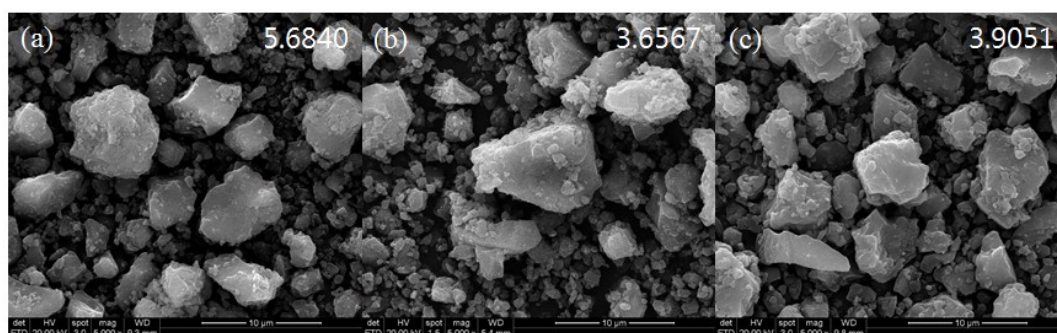


Fig.1 SEM image of (a) MgHx, (b) MgHx-5wt.%graphene and (c) MgHx-10wt.%graphene composites

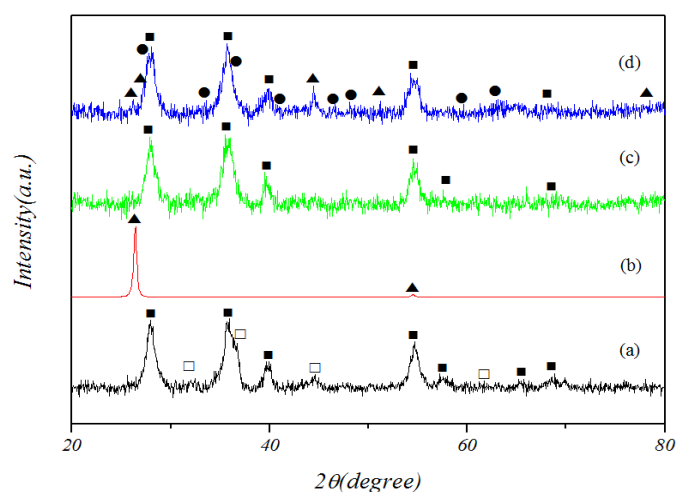


Fig. 2 XRD patterns of MgHx and MgHx-graphene composites after HIMA (a) MgHx (b) graphene (c) MgHx-5wt.% graphene (d) MgHx-10wt.% graphene (\square :Mg, \blacksquare :MgH₂, \blacktriangle :graphene, \bullet :Mg₂C₃)

References

- [1] S.K.Pandey, R.K.Singh, and O.N.Srivastava "Investigations on hydrogenation behavior of CNT admixed Mg₂Ni", *Int.J.Hydrogen Energy*, vol. 34, no.23, pp. 9379-9384, September. 2009.
- [2] C.A. Grimes, O.K.Varghese, and S.Ranjan "Light, Water, Hydrogen", Springer, 2008, ISBN: 0387331980.
- [3] A.Sigal, M.I.Rojas, and E.P.M.Leiva "Interferents for hydrogen storage on a graphene sheet decorated with nickel : A DFT study", *Int.J.Hydrogen Energy*, vol. 36, no. 5, pp 3537-3546, march, 2011.
- [4] F.J.Castro, V.Fuster, and G.Urretavizcaya "Hydrogen sorption properties of a MgHx-10wt.% graphite mixture", *J. Alloy & Compounds*, vol. 509, pp 595-598, January, 2011.
- [5] L.Wang, N.R.Stuckert, and R.T.Yang "Unique Hydrogen Adsorption Properties of Graphene", *American Institute of Chemical Engineers*, vol. 57, no. 10, pp 2902-2908, November. 2010.
- [6] W.Yuan, B.Li, and L.Li "A green synthetic approach to graphene nanosheets for hydrogen adsorption", *Applied surface science*, vol. 257, no. 23, pp 10183-10187, July, 2011.

Evaluations of Hydrogen Permeability on SCZY/SHP/Ni Composites Membrane (P-71)

Young-Sang Lee¹, Hyunchul Ju², Dong-Min Kim³, Whan-Gi Kim⁴ and Tae-Whan Hong¹

1Department of Materials Science and Engineering, Korea National University of Transportation, 50 Daehak-ro, Chungju, Chungbuk, 380-702, Republic of Korea

2School of Mechanical Engineering, Inha University, 253 Yonghyun-dong, Nam-gu, Incheon, 402-751, Republic of Korea

3Department of Materials Science and Engineering, Hongik University, 300 Shinan, Jochiwon, Chungnam, 339-701, Republic of Korea

4Department of Applied Chemistry, Konkuk University, Chungju, Chungbuk, 380-701, Republic of Korea

Email: twhong@ut.ac.kr

Keywords: SCZY-SHP, proton conductivity, ionic conductivity, perovskite, gas diffusion layer (GDL)

The nafion as known that can rapidly transfer proton. It used PEMFCs in a part of membrane. And the perovskite ceramics can transfer proton in high temperature [1]. Meanwhile, structures of energy consumption contain petroleum in industry field at present. However, petroleum will reach to resource exhaustion in addition generating climate pollution. Therefore many scientists will approach study in alternative and clean energy source. One of many ways is gasification of coal but this step is fault because coal is petroleum resource. The coal has low octane number rather than low energy efficiency and more wake climate pollution as this reason. The gasification coal can use clearly, such as separation membrane [2, 3]. It can separate to hydrogen from gasification coal. In the membrane science, this phenomenon had introduced three mechanisms, such as solution diffusion, Knudsen diffusion and molecular sieving [4]. Most of high quality hydrogen gas was gotten from solution diffusion method.

Palladium and its alloyed membranes have come to occupy an important position in hydrogen separation from gaseous mixtures, because they have high hydrogen permeability, chemical compatibility, and excellent hydrogen selectivity. However, there are certain disadvantages to using such palladium compounds, including high cost, thermal instability and brittleness resulting from formation of PdH caused by the strong interaction of palladium and hydrogen [5]. To mitigate these drawbacks, research has recently been conducted on other metals to substitute for palladium and on membranes with composite metal supports. One ceramic material, Al₂O₃, has proven itself attractive for a variety of uses because of its high melting point, degree of hardness, and anti-corrosive and thermal resistance properties. It is widely used as a catalyst or catalyst support due to its high surface area and chemical stability. Therefore, SCZY(Sr(Ce_{0.9}Zr_{0.1})_{0.95}Yb_{0.05}O_{3-δ}) was selected by ceramic material [6, 7].

The SCZY is consisted of perovskite structure and it could proton conducting in high temperature. Proton conducting ceramics of perovskite structure are exposed to hydrogen atmosphere at elevated temperatures, the electronic conductivity decreases and protonic

conduction appears. Their conductivities in hydrogen atmosphere are of the order of 10^{-2} – 10^{-3} S/cm at $1000-600^{\circ}\text{C}$ [8]

The sulfonated hexaphenylbenzene polymer (SHP) is proton conducting polymer [9]. If these materials were combined, composite membrane will be having a good hydrogen separation and decreasing ohmic contact in GDL of PEMFCs. This membrane is recommending use for low temperature range because of including polymer material. For the production of hydrogen from mixed gas by membrane, the probability of high and low temperatures make available a proto type membrane. This membrane is a good separation because property of proton conducting.

In this study, The SCZY was synthesized using the sol-gel process and SHP was made in Konkuk univ., this laboratory was co-working. The fabrications of SCZY-Ni composites has been prepared by high energy mill (vibration mill). The SCZY-Ni composites was fabricated to membrane using hot press sintering. The membrane was coated using SHP.

The prepared membrane was characterized by impedance analyzer, scanning electron microscopy (SEM), energy dispersive spectroscopy (EDS) and Brunauer-Emmett-Teller (BET). The membrane was evaluated and calculated to hydrogen permeability using our hydrogen permeation apparatus.

In result of BET analysis, SCZY-30SHP composite was measured specific surface area, it was $6.0810 \text{ m}^2/\text{g}$. And SCZY-46SHP composite was calculated to $4.1994 \text{ m}^2/\text{g}$. SCZY-30, 46SHP composites were measured to total pore volume and average pore diameter, their value was $0.0134, 0.0081 \text{ cm}^3/\text{g}$ and $8.8276, 7.6697 \text{ nm}$, respectively. If hydrogen separation membrane has a pore size of upper 12nm , hydrogen separation mechanism is Knudsen diffusion [10].

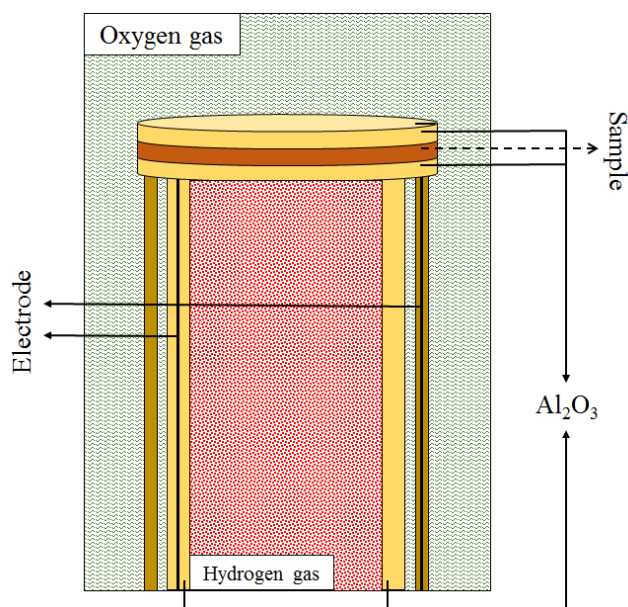


Fig. 1. The schematic of impedance test cells.

Table 1. Resistance and proton conductivity of SCZY-30, 40SHP composites

	T (K)	R (M Ω)	σ (μ S/m)
SCZY-30SHP	298	1.03 x 10 ²	2.63 x 10 ⁻²
	373	1.08 x 10 ²	2.51 x 10 ⁻²
	473	6.67 x 10 ¹	4.07 x 10 ⁻²
SCZY-46SHP	298	2.67 x 10 ²	1.02 x 10 ⁻²
	373	2.05 x 10 ²	1.33 x 10 ⁻²
	473	9.44 x 10 ¹	2.88 x 10 ⁻²

References

- [1] Hiroyasu Iwahara, *Solid State Ionics*, Vol. 125 (1999) 271.
- [2] Yu-Ming Lin, Guo-Lin Lee, Min-Hon Rei, *Catalysis Today*, Vol. 44 (1998) 343.
- [3] Truls Norby, *Solid State Ionics*, Vol. 125 (1999) 1.
- [4] G.Q. Lu, J.C. Diniz da Costa, M. Duke, S. Giessler, R. Socolow, R.H. Williams, T. Kreutz, *J. Colloid Interface Sci.*, Vol. 314 (2007) 589.
- [5] M.D. Dolan, *J. Membr. Sci.*, Vol. 362 (2010) 12.
- [6] G.B. Sun, K. Hidajat, S. Kawi, *J. Membr. Sci.*, Vol. 284 (2006) 110.
- [7] Linsheng Wang, Ryo Yoshile, Shigeyuki Uemiya, *J. Membr. Sci.*, Vol. 306 (2007) 1.
- [8] Hiroyasu Iwahara, Yamato Asakura, Koji Katahira, Masahiro Tanaka, *Solid State Ionics*, Vol. 168(2004) 299-310.
- [10] Y.D. Lim, D.W. Seo, S.H. Lee, H.Y. Jang, Hyunchul Ju, Arae Jo, D.M. Kim, W.-G. Kim, *Int. J. Hydrogen Energy*, In press (2012).
- [11] Aaron W. Thornton, Tamsyn Hilder, Anita J. Hill, James M. Hill, *J. Membr. Sci.*, Vol. 336 (2009) 101.

Non-Platinum Electrocatalysts for Hydrogen Oxidation in Alkaline Media (P-75)

*F. Tzorbatzoglou, A. Brouzgou and P. Tsiakaras**

*Department of Mechanical Engineering, School of Engineering, University of Thessaly, Pedion Areos,
38334, Volos, Greece.*

**email: tsiak@uth.gr*

Abstract

In the present work non-platinum electrocatalysts are investigated for hydrogen oxidation in alkaline media. Alkaline media [1] offer at least two advantages over acid ones: the use of non-platinum electrocatalysts, since they present higher activity than platinum-based electrocatalysts and consequently lower cost electrodes for fuel cells. Palladium-based electrocatalysts are considered the best candidates for replacing platinum-based ones in alkaline media, presenting higher activity in hydrogen and direct alcohol fuel cells [1, 2]. Here, we report the preparation of carbon Vulcan XC-72R supported PdRh and PdSn nano-electrocatalysts via a modified pulse microwave assisted polyol method and their study for hydrogen electrooxidation in alkaline media. The as-prepared electrocatalysts have been characterized by X-ray diffraction (XRD), Transmission Electron Microscopy (TEM), Linear Sweep Voltammetry (LSV) with rotating disk electrode (RDE) and Chronoamperometric measurements (CA). The electrochemical results have shown that the addition of Rh higher catalytic activity (1.5 mA cm^{-2}) than pure Pd over hydrogen oxidation, while the addition of Sn did not have any important influence on Pd's hydrogen electro-oxidation activity. The catalytic activity of PdRh/C was examined also for different electrolyte's concentration values (0.5, 1, 2 and 3M of KOH). Moreover for further kinetic analysis the hydrogen oxidation reaction was examined under 600, 1200, 1600, 2000 and 3000 rpm. As the rotation speed increases the current density also increases. Acknowledgments

F. Tzorbatzoglou, is grateful to the Research Funding Program: Heracleitus II which is co-financed by the European Union (European Social Fund – ESF) and Greek national funds through the Operational Program “Education and Lifelong Learning” of the National Strategic Reference Framework (NSRF) -Investing in knowledge society through the European Social Fund. A. Brouzgou and P. Tsiakaras are grateful to the Research Funding Program: Bilateral R&D cooperation between Greece and China 2012-2014 co-funded by the European Union and Ministry of Education, Lifelong learning and religious affairs.

References

- [1] A. Brouzgou, A. Podias, P. Tsiakaras, *Journal of Applied Electrochemistry* 43 (2013) 119-136.
- [2] B. Xing, O. Savadogo, *Electrochemistry Communications* 2 (2000) 697-702.

Low Temperature Hydrogen Oxidation over Platinum Free Electrocatalysts: PEMFC vs AEMFC (P-76)

F. Tzorbatzoglou, A. Brouzgou and P. Tsiakaras*

Department of Mechanical Engineering, School of Engineering, University of Thessaly, Pedion Areos, 38334, Volos, Greece.

*email: tsiak@uth.gr

Abstract

It is well-known that one of the main challenges as far as concerns the development and commercialization of H₂-PEMFCs is the reduction of amount of platinum at the anode compartment [1]. Moreover, very recently has been proved that alkaline membranes (AEM) offer greater conductivity than acid (PEM) membranes [1, 2]. In the present work, we report the preparation of platinum (2, 5 and 10 wt.% Pt loading) on carbon Vulcan XC-72R prepared via a modified pulse microwave assisted polyol method and their investigation over hydrogen electrooxidation reaction in acid and alkaline media. The as-prepared electrocatalysts have been characterized by X-ray diffraction (XRD), Transmission Electron Microscopy (TEM), Linear Sweep Voltammetry (LSV) with rotating disk electrode (RDE) and Chronoamperometric measurements (CA). The hydrogen oxidation reaction was studied under 600, 1200, 1600, 2000 and 3000 rpm conducting LSV measurements in order to study kinetically the reaction in both alkaline and acidic media. The electrocatalytic activity was also studied under different temperature values (25, 40, 50 and 60°C) as well as electrolyte's concentration values. The current density was observed at ~5 mA cm⁻² for the 10 wt.% Pt/C electrocatalyst in acidic media with almost the same activity in alkaline media.

Acknowledgments

F. Tzorbatzoglou, is grateful to the Research Funding Program: Heracleitus II which is co-financed by the European Union (European Social Fund – ESF) and Greek national funds through the Operational Program “Education and Lifelong Learning” of the National Strategic Reference Framework (NSRF) -Investing in knowledge society through the European Social Fund. A. Brouzgou and P. Tsiakaras are grateful to the Research Funding Program: Bilateral R&D cooperation between Greece and China 2012-2014 co-funded by the European Union and Ministry of Education, Lifelong Learning and Religious Affairs.

References

- [1] A. Brouzgou, S.Q. Song, P. Tsiakaras, Applied Catalysis B: Environmental 127 (2012) 371-388.
- [2] B. Xing, O. Savadogo, Electrochemistry Communications 2 (2000) 697-702.

A review of electrocatalysts for PEM water electrolysis applications (P-78)

P. Millet

Université Paris-Sud 11

ICMMO, bâtiment 410, 15 rue Georges Clémenceau, 91405 Orsay cedex France

pierre.millet@u-psud.fr

Abstract. Proton exchange membrane – based water electrolysis (PEM-WE) is a key process for transforming zero-carbon electricity sources into the supply of zero-carbon hydrogen and oxygen for miscellaneous end-uses. In a PEM-WE cell, a thin ($\approx 200 \text{ }\mu\text{m}$ thick) proton-conducting membrane is used as solid electrolyte and the gaseous production (H_2 and O_2) is released at the rear of membrane – electrode assemblies (MEAs), outside current lines (figure 1). In conventional PEM-WE cells [1], iridium oxide is used at the anode for the oxygen evolution reaction (OER) and carbon-supported platinum is used at the cathode for the hydrogen evolution reaction (HER). Capital expenses can be reduced by increasing operating current densities and operational expenses can be reduced by developing more efficient active layers (figure 2). Over the last years, several attempts have been made to reduce and/or suppress platinum group metal catalysts and make these cells more attractive for commercial applications. For example, cobalt-containing molecular compounds have been successfully tested in place of platinum for the HER [2].

The purpose of this communication is to provide a review of main electrocatalysts used in PEM-WE cells. Results obtained with both conventional (platinum group metal) and unconventional (non-platinoides) catalysts are presented. HER and OER mechanisms are analyzed (using Tafel and EIS measurements) and compared. Exchange current densities are determined. The roles of the structure of active layers (thickness, porosity, composition) and of the roughness of the electrodes (roughness factors were determined from cyclic voltametry experiments using internal reference electrodes) are analyzed and some perspectives for better performances are also discussed.

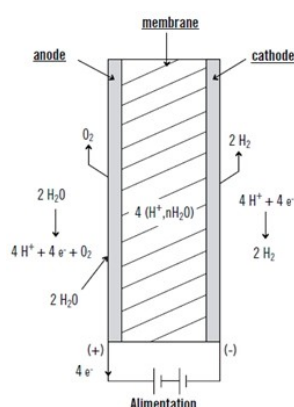


Figure 1: Schematic diagram of a PEM-WE cell showing half-cell reactions.

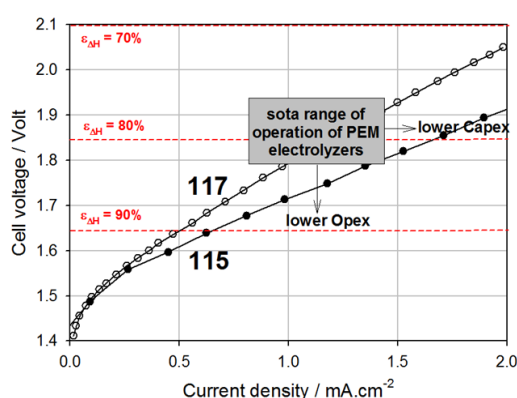


Figure 2: Typical polarization curves measured at 80°C using Nafion115 and Nafion 117 membranes.

References

[1] I. Cerri, F. Lefebvre-Joud, P. Holtappels, K. Honegger, T. Stubos, P. Millet, in : 'Hydrogen and Fuel Cells', Scientific Assessment in support of the Materials Roadmap enabling Low Carbon Energy Technologies, JRC Scientific and Technical Reports, May 2012.

[2] M-T. Dinh Nguyen, A. Ranjbari, L. Catala, F. Brisset, P. Millet and A. Aukauloo, Implementing Molecular Catalysts for Hydrogen Production in Proton Exchange Membrane Water Electrolyzers, Coord. Chem. Review, 256 (2012) 2435 – 2444.

Hydrogen production from methane steam reforming in combustion heat assisted novel micro-channel reactor with catalytic stacking: A CFD simulation study (P-83)

Chun-Boo Lee^{1,2}, Min-Ho Jin², Sung-Wook Lee^{1,2}, Dong-Wook Lee², Shin-Kun Ryi², Jong-Soo Park²,
Sung-Hyun Kim^{1,2}, Kyung-Ran Hwang³

*1Energy Materials and Convergence Research Department, Korea Institute of Energy Research (KIER),
102 Gajeong-ro, Yuseong-Gu, Daejeon 305-343, South Korea*

*2Department of Chemical and Biological Engineering, Korea University, 145 Anam-ro, Sungbuk-gu,
Seoul 136-701, South Korea*

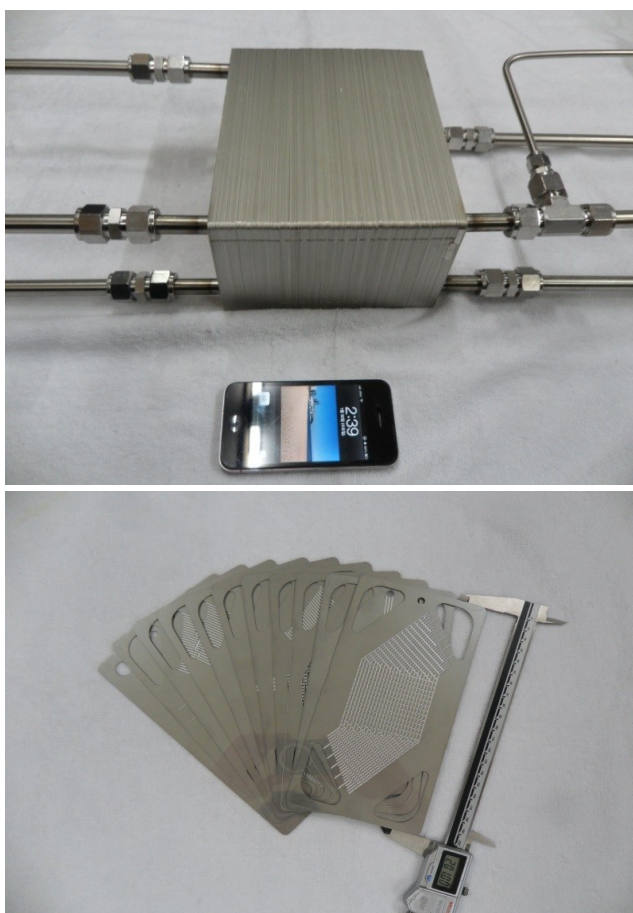
*3Clean Fuel Department, Korea Institute of Energy Research (KIER), 102 Gajeong-ro, Yuseong-Gu,
Daejeon 305-343, South Korea*

Hydrogen is a very important industrial gas with many chemical reactions and future applications. It is a promising clean fuel that can be produced from sources such as natural gas, coal and biomass. Hydrogen energy is drawing attention as an upcoming alternative energy source. It is mostly produced from the hydrocarbon reforming process. Methane steam reforming (MSR) is a well-known industrial hydrogen production process. Recently, it has been studied in mesoscale reactors and portable and on-board fuel processors. Fuel cells are a very promising technology for electrical power generation in stationary, mobile and portable applications. However, use of a conventional fixed-bed reactor for MSR has some problems: because the reaction is highly endothermic and heat transfer is typically poor, a substantial amount of heat transfer surface is usually needed, and hence, large reactors are required. In addition, deactivation of Ni-based catalysts is a concern. Several investigators have recently reported on the high activity and stability of Ni catalysts.

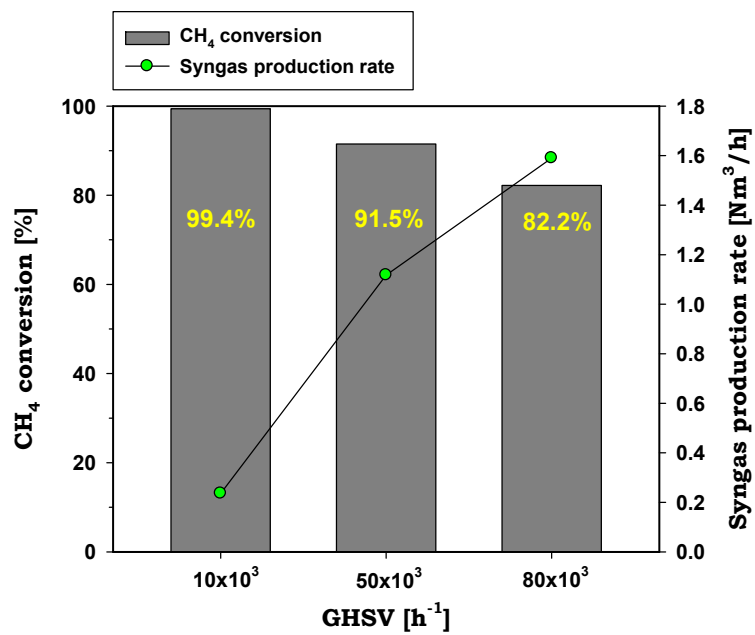
The micro-channel reactor (MCR) has been recognized as a promising technology for small scale, compact and mobile hydrogen production systems offering easy integration into existing installations, along with high heat and mass transfer coefficients, a high surface area to volume ratio, higher conversion and selectivity, as well as a fast response. However, there is still an issue which remains to be solved, namely the catalyst coating on the metal surface. Many different catalysts have been used to evaluate the steam reforming of hydrocarbons in an MCR. Casanovas et al. developed an MCR can be used to produce hydrogen from ethanol steam reforming. The results revealed that ethanol has been processed independently in separate zones of a MCR for total oxidation and steam reforming. Cai et al. studied the ethanol steam reforming reaction over a supported Ir/CeO₂ catalyst in a micro-channel structured reactor. They obtained a hydrogen yield exceeding 40 LH₂/gcat h with an ethanol conversion of 65 %. Their research used a catalytic coating inside the micro-channels. However, when coating micro-channel plates, a thin layer and homogenous film with stable adhesion over the surface of the micro-channels is needed to inhibit the peeling of the catalyst at the relatively high temperature required. For this reason, a different method is needed for loading the catalysts into the MCR.

In our previous studies, we developed a porous nickel metal catalyst for the MSR reaction which exhibited a high methane conversion and stable hydrogen production. This nickel metal catalyst has various advantages, such as good catalytic performance for the MSR reaction. It is easy

to prepare and the number of stacks can be modulated. Moreover, we prepared and tested a multi-membrane reformer for the direct production of hydrogen via MSR. We developed high hydrogen permeation flux and perm-selectivity membranes and tested them in several situations. In particular, we designed and prepared an MCR containing a nickel metal catalyst and investigated the potential application of an on-board MSR for hydrogen production using an assisted combustion reaction. In the present work, we further investigate the application of an MCR containing a nickel metal catalyst with variable number of stacks for hydrogen production via MSR. Micro-channels were contained in the MCR one side of the nickel metal catalyst with variable number of stacks for producing hydrogen to generate the necessary heat for the endothermic MSR and the combustion reaction was performed on the other side of the MCR. Here, we focus on the possibility of highly hydrogen production concurrently with highly methane conversion by using a MCR.



<Fig. 1> The micro-channel reactor; (a) Photographs of the micro-channel reactor (MCR); (b) photograph of the plates.



<Fig. 2> Methane conversion and syngas production rate as a function of GHSV at S/C = 3.0.

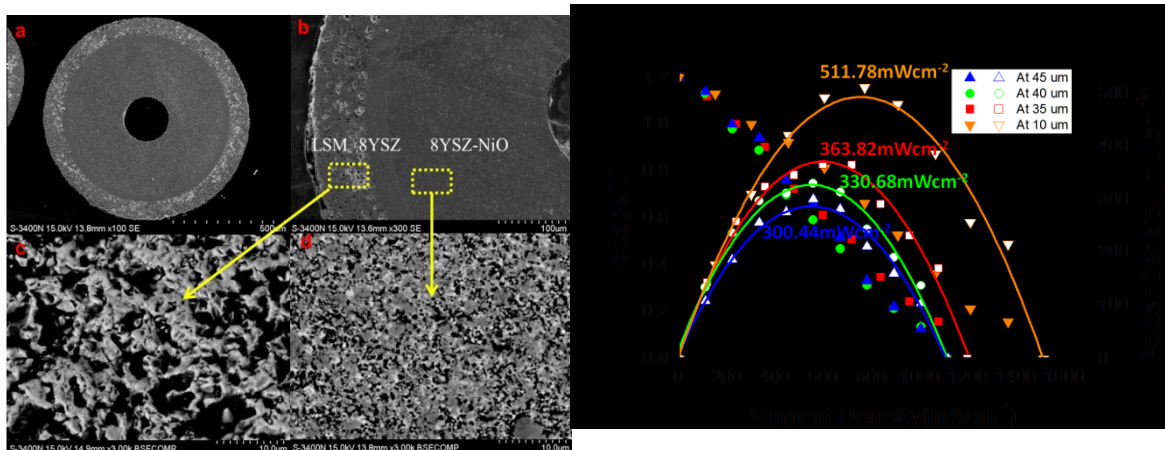
Effects of Electrode/Electrolyte Thickness on the Performance of Micro-tubular Solid Oxide Fuel Cells Made by Sequential Aqueous Electrophoretic Deposition (P-85)

J.S. Cherng,¹ F.A. Yu,¹ C.C. Wu,¹ T.H. Yeh²

¹Department of Materials Engineering, Ming Chi University of Technology, Taipei 24301, Taiwan
²Center for Thin Film Technologies and Applications, Ming Chi University of Technology, Taipei 24301, Taiwan

*E-mail: cherng@mail.mcut.edu.tw

A Series of anode-supported micro-tubular solid oxide fuel cells (SOFCs) are manufactured by sequential aqueous electrophoretic deposition (EPD). The process of these micro-tubular SOFCs includes sequential aqueous EPDs of an anode layer (8YSZ-NiO), an electrolyte layer (8YSZ), and a cathode layer (LSM) onto a thin wire electrode, followed by stripping, drying, and a single-step co-sintering at 1250°C. The microstructure of the resultant micro-tubular SOFCs, including the thickness and porosity of each layer, is controlled by the processing parameters such as solid loading, current density, deposition time, and sintering temperature. In particular, the effects of the electrode/electrolyte thickness on the cell resistance and electrochemical performance of such micro-tubular SOFCs are investigated and discussed based on the microstructural, AC-impedance and voltage-current-power analyses. It is found that the area specific resistance is proportional to the electrolyte thickness while the cell resistivity increases with electrolyte thickness at lower temperature but remains about the same at higher temperature. On the other hand, the effect of anode thicknesses on the cell performance is negligible, due possibly to the poor continuity of 8YSZ in the anode.



Effects of the filler compositions of micro porous layer for anode on the performance of direct highly concentrated methanol fuel cell (P-88)

Yeong-Soo Kim ^(a,b), Dong-Hyun Peck ^(a), Sang-Kyung Kim ^(a,b), Seongyop Lim ^(a,b), Doo-Hwan Jung ^(a,b,*)

a Fuel Cell Research Center, Korea Institute of Energy Research (KIER), 152 Gajeong, Yuseong, 305-343 Daejeon, Republic of Korea

b Advanced Energy Technology, University of Science and Technology, 217 Gajeong, Yuseong, 305-350 Daejeon, Republic of Korea

For the successful market entry of direct methanol fuel cell (DMFC), it is imperative to overcome the sluggish kinetics of methanol as well as solve methanol crossover. In this study, the functional layer as called micro porous layer (MPL) was introduced between anode gas diffusion layer (GDL) and catalyst layer to inhibit methanol crossover and minimize the performance decreases of fuel cell.

To prepare anode MPLs, various carbon like carbon black (Vulcan XC-72R, CB), spherical activated carbon (AC), platelet carbon nano fibers (PCNFs) and multi-walled carbon nano tubes (MWCNTs) or meso-porous silica materials were used. They have different specific surface area and tapped density each other and those are shown in Table1. They are coated on anode GDLs only or by mixture and some binders like poly-tetrafluoroethylene (PTFE) are used. Physical properties of GDLs with MPL such as thickness, surface image, hydrophobic/philic porosity and gas permeability were measured and compared with bare GDL without MPL. Also, membrane electrode assemblies (MEAs) with various anode MPLs were prepared of 9cm² and then tested using electrochemical analysis e.g., current-voltage polarization, electrochemical impedance spectroscopy (EIS), voltammetric curves. Current-voltage test was carried out in condition of 1M, 3M, 5M and 7M at 60oC. Methanol and air was fed into the anode and cathode at a flow rate of $\lambda = 6$ (λ denotes the stoichiometric ratio of the methanol and air for an electrochemical reaction under operation at 4 A), respectively.

Through the observation of the surface of MPLs, it was figured out that the use of carbon materials with lower tapped density like CB and MWCNF causes to the occurrence of cracks in anode MPL. Cracks in MPL structure increased gas permeability and hydrophilic pore volume of MPLs. On the other hands, cracks were hardly displayed in the SEM images of AC MPL. But the measurement result of hydrophilic pore volume was similar to those of CB and MWCNT. Considering the results of SEM images and physical properties of MPL, physical properties of MPL had more correlation with the tapped density than the surface area of fillers. From current-voltage tests, it was demonstrated that the performances of MEAs with a cracked MPL were higher than the results of MEAs with a crack-free MPL in 1M and 3M condition whereas the performances of MEAs with crack-free MPL was superior to those of MEAs with a cracked MPL, when 5M and 7M methanol into fuel cell. From the EIS results, it was found that while a porous MPL in anode was more effective to mass transfer in anode electrode than a dense MPL, it was ineffective to decreasing methanol crossover than dense MPL. The anode MPL consisting of only PCNFs (PCNF-MPL) with the specific surface area of 48m²/g and the tapped density of 156.25mg/mL demonstrated the crack-free and dense surface.

Accordingly, we prepared the modified anode MPL combining PCNF with CB materials to reduce electric resistance of MPL. Consequently, the MEA having a modified anode MPL (PCNF 50vol %, CB

50vol %) showed the highest maximum power density of 67.7mW/cm² at 60oC and 7M methanol condition.

Table 1. The Specific Area and the Tapped Density of the Powders for the MPLs

	Vulcan XC 72R	Spherical Activated Carbon	SBA-15	Multi carbon tube	walled nano	Platelet carbon nano fiber
Specific area (m ² /g)	220	1800	762	198		48
Tap density (mg/mL)	75.21 ±5	384.61 ±5	208.33 ±5	54.05 ±5		156.25 ±5
Denotement of prepared MPL	CB	AC	SBA	MWCNT		PCNF

DMFC for auxiliary power supply in a river buoy (P-90)

Delia Muñoz Alé, Javier Brey Sánchez, María Duque López, Manuel Rodríguez Pérez and Rocío Domínguez Jiménez

Abengoa Hidrógeno, Campus Palmas Altas, C/ Energía Solar 1, 41014(Sevilla)

Currently, buoys installed in the Guadalquivir River in Seville (Spain) have a dual function: the maritime traffic signaling and environmental control.

Today, the use of renewable energy, backed by a storage system, represents the most common method used for supplying electrical power to the buoys equipment. The most common combination is solar or wind power and batteries.

However, the fact that buoys increasingly incorporate more features makes it necessary to increase their generation autonomy. But it is not always possible to increase the size of the solar panels and / or wind turbines, due to limited space availability.

Therefore, the implementation of alternative renewable power sources makes sense as it would cover the energy deficit, which will significantly affect positively on the operating regime of the buoys. The improvement could be such that would even allow the installation of new metering equipment in the buoys due to overproduction of electrical energy.

The project “ECO-boya: Design and construction of an intelligent and efficient device for maritime signaling”, emerges from this idea.

The first aspect developed by the project ECO-boya is the characterization of available energy resources in the Guadalquivir River. This will quantify potential solar and marine energy (waves and currents) available along the river and its estuary, creating a resource map to serve as reference for the development of other project activities.

After that, the ECO-boya will be developed. Major aspects to be addressed in this phase of the project will be:

- Device for the use of currents energy to be used as the main energy supply for the equipment installed in the buoy.
- Design of an alternative energy supply system. Since the currents action is variable, a fuel cell system will be developed as an alternative to power the equipment when the currents don't provide sufficient power.
- Measuring and communications equipment to improve the current system and incorporate new applications.
- Integration of the different equipment that comprise the ECO-boya for energy optimization, maximizing the performance of the device and reducing energy consumption.

- Structural design adapted to the new internal layout derived from the improvements implemented, and adaptation of the float and the anchors that allow maximum use of the current energy resource.

Once the buoy is constructed, it will be tested for operation in a location where the energy resources available allows the evaluation of the device performance in similar conditions.

As part of this project, Abengoa Hidrógeno is developing the fuel cell system, based on a 280 W DMFC, that will be installed in a buoy in the Guadalquivir River as part of the power supply system. The advantage provided by the use of methanol is the logistics of the fuel. The transportation of methanol has much less complexity than the transportation of hydrogen gas, especially for this particular application because of the location of the fuel cell system.

The complexity of the design is given by the particular operational environment, with a high humidity and the risk of water in critical parts of the system. This fact has forced an innovative mechanical design that protects the system from the water and humidity while allowing airflow.

This project has been funded by the IDEA Agency and has been co-funded by the European Regional Development Fund, FEDER, within the Technology Fund Operational Programme 2007-2013.



Development of degradation and optimization model for PBI based high temperature PEMFCS (P-97)

Taegon Kang^{1, 2}, Minjin Kim^{1, 2, *}, Jintae Kim¹, Young-jun Sohn^{1, 2}

¹Hydrogen and Fuel Cell Research Center, Korea Institute of Energy Research, Daejeon, Republic of Korea

²Advanced energy technology, University of Science & Technology, Daejeon, Republic of Korea

* corresponding author (minjin@kier.re.kr)

Fuel cells are more eco-friendly and substantial energy technology than conventional fossil energy sources. The fuel cells are widely used in the stationary, portable and transportation applications due to high energy conversion efficiency and excellent load conformability. Proton exchange membrane fuel cells (PEMFC) mostly use perfluorosulfonic acid (PFSA) polymers in the membrane. This system has high conductivity, chemical stability, mechanical strength and potentially long term durability, but it has material problems such as poisoning of carbon monoxide (CO) and difficult water and heat management. To solve these problems, a high temperature PEMFCs (HT-PEMFCs) based on polybenzimidazole (PBI), which is operated from 393.15 K to 473.15 K, has been developed. The HT-PEMFCs system is relatively simple because of a high tolerance to CO and sulfur as well as no humidification.

The aim of this work is the development of numerical model that consider the degradation of the performance during the long term operation, and to achieve the operating optimization of PBI based HT-PEMFCs for the high performance. The developed stack model includes activation and ohmic over-potential that are including the effect of the agglomeration of platinum in the catalyst layers and the spilling of phosphoric acid (PA) in the membrane that are the cause for the degradation of the performance. These over-potentials are expressed as exchange current density and doping level of PA in the developed model. We implements two step parameter estimation methods. First, steady state parameter estimation is conducted in order to find out kinetic parameters of the MEAs like activation energy for catalyst, charge transfer coefficient and reference exchange current density in Butler-Volmer equation by comparing I-V curve data. Second, dynamic parameter estimation is conducted in order to express degradation of voltage according to time by comparing durability data at 0.2 A/cm² current density. After dynamic parameter estimation, we find out coefficients of reference exchange current density as a result of increasing activation over-potential in accordance with time. Also, ohmic over-potential is calculated by using resistance data in the membrane.

Following the previous researches, the degradation ratios of the high temperature membrane electrode assemblies (MEAs) are significantly differed according to the condition of operating factors such as operating temperature, pressure, relative humidity and flow rate during over thousands of operations. But, we focus only on the operating temperature and relative humidity because the pressure and flow rate are linear correlation with the performance. The relative humidity affects the performance in a negative way caused by decreasing molar fraction of a fuel. Reformed gas from a reformer includes the high relative humidity. So, the high relative humidity in the reformed gas is removed. This is to hinder efficiency of the fuel cell system. Therefore, we find out steady state optimum condition of the operating factors that are the operating temperature and relative humidity

for maximized voltage at a given time because the relative humidity is closely connected with the operating temperature. The performance and lifetime are compared at the arbitrary operating condition and the optimum ones. The results show correlation between the operating factors and change of each of the over-potentials according to time.

Durability analysis of high temperature PEM fuel cell for DSS test using EIS (P-98)

Jintae KIM¹, Bong-gu LEE^{1,2}, Minjin KIM^{1,2,*}, and Young-Jun SOHN^{1,2}

¹Hydrogen and Fuel Cell Research Center, Korea Institute of Energy Research, Daejeon, Korea

²Advanced Energy Technology, University of Science and Technology, Daejeon, Korea

Proton exchange membrane (PEM) fuel cells are considered one of the most promising zero emission power sources. However, the commercialization of PEM fuel cells faced many challenges these challenges are; (1) the impurities in fuel stream tend to absorb on the active site of catalyst; (2) water in the electrode exists in liquid state, which is easily to be flooded; (3) transport of proton through the electrolyte and it means that external humidification is needed. As the best substitute traditional low temperature proton exchange membrane fuel cells, phosphoric acid doped poly-benzimidazole (PBI) based high temperature PEM fuel cells have been focused. However, it has been reported that their performance drops more rapidly than low temperature PEM fuel cells. Particularly, deterioration accelerates when reformed gas which contains excessive impurities (especially CO) is supplied in the fuel stream or they undergo a great fluctuation of temperature and exposure to high voltage through shut down and start up procedure. We confirmed the effect of the composition of the gas supplied to the anode on the performance characteristics of high temperature PEM fuel cells. It was observed that CO₂ and CO made the cell voltage reduced while CH₄ had an insignificant effect. Gas 1 (H₂ 80 %, CO₂ 20 %) made voltage drop 8 mV and it was caused by dilution of H₂ at the anode catalyst layer. Besides, voltage with gas 2 (H₂ 80 %, CO₂ 19.5 %, CO 0.5 %) was 14 mV lower than voltage with pure hydrogen because CO adsorbed on the Pt surface of the anode and active area was significantly decreased. On the other hand gas 3 (H₂ 80 %, CO₂ 17.5 %, CH₄ 2 %, CO 0.5 %) made voltage additionally declined only 1 mV. After that, in order to investigate the degradation of high temperature PEM fuel cells according to the composition of the simulated reformat, daily based start up and shut down (DSS) tests were carried out at 0.2 A cm⁻², 150 °C for 12 hours a day with changing the composition of the simulated reformat and to analyze their degradation causes. Degradation rates with pure hydrogen, gas 3, and gas 4 (H₂ 80 %, CO₂ 16 %, CH₄ 2 %, CO 2 %) were 170, 160, and 270 μV h⁻¹, respectively. Degradation rate of the gas including CO of 0.5 % is lower than it of H₂ and it is supposed to result from variation of each MEA and experimental error. The electrochemical impedance spectroscopy (EIS) analyses and polarization curves are recorded every 5 days to check the deterioration of performance and the change for some kinds of resistances during the DSS test. Activation resistance at the cathode increased to 44.1 mΩ cm⁻² from 36.2 mΩ cm⁻² (21.6 %) while activation resistance at the anode increases to 19.6 mΩ cm⁻² from 18.4 mΩ cm⁻² (6.8 %) after DSS tests with H₂. However, activation resistance of anode increased to 33.7 mΩ cm⁻² from 18.4 mΩ cm⁻² (83.4 %) while activation resistance of cathode increased to 57.0 mΩ cm⁻² from 36.2 mΩ cm⁻² (53.8 %) after DSS tests with reformed gas including CO of 2 %. We verified that reformed gas including small amount of CO didn't have a major impact on the decrease in the durability of high temperature PEM fuel cells but cell voltage diminished when CO concentration increased.

Excellent catalytic effects of Ni- and graphene-based catalysts on hydrogenation/dehydrogenation of magnesium hydride (P-101)

GUANG LIU, LI LI, FANGYUAN QIU, YING WANG, YIJING WANG*, YONGMEI WANG, HUATANG YUAN

Co-Innovation Center of Chemistry and Chemical Engineering of Tianjin, Key Laboratory of Advanced Energy Materials Chemistry (MOE), Institute of New Energy Material Chemistry, Tianjin Key Lab on Metal and Molecule-based Material Chemistry, Nankai University, Tianjin, 30007 (P.R. China)

ABSTRACT: One of the most technically challenging obstacles to face the anticipated future hydrogen economy is the development of safe and efficient onboard hydrogen storage materials. Many materials have been studied to find out the most suitable one for a hydrogen storage system to satisfy both a high storage density, keeping beneficial thermodynamics, kinetics as well as low cost. Magnesium hydride has proposed to be one of the most promising candidates due to its high volumetric and gravimetric hydrogen storage capacity (110 g H₂ L⁻¹ and 7.6 wt% H₂ for MgH₂). In our present works, Ni- and graphene-based catalysts were synthesized to catalyze hydrogenation/dehydrogenation of MgH₂ and the hydrogen storage properties of MgH₂ are systematically investigated. Firstly, the desorption temperature and the desorption kinetics of MgH₂ have been improved by doping with NiB nanoparticles. MgH₂-10 wt.% NiB mixture started to release hydrogen at 180 °C, whereas it had to heat up to 300 °C to release hydrogen for the pure MgH₂. In addition, a hydrogen desorption capacity of 6.0 wt.% was reached within 10 min at 300 °C for the MgH₂-10 wt.% NiB mixture, in contrast, even after 120 min only 2.0 wt.% hydrogen was desorbed for pure MgH₂ under the same conditions. Further cyclic kinetics investigation using high-pressure differential scanning calorimetry technique (HP-DSC) indicated that the composite had good cycle stability. Secondly, highly crumpled graphene nanosheets (GNS) with a BET surface area as high as 1159 m² g⁻¹ was fabricated by a thermal exfoliation method. It was found that the as-synthesized GNS exhibited a superior catalytic effect on hydrogenation/dehydrogenation of MgH₂. A systematic investigation was performed on the hydrogen sorption properties of MgH₂-5 wt.% GNS nanocomposites acquired by ball-milling. The graphene layers were broken into smaller graphene nanosheets in a disordered and irregular manner during milling. It was confirmed that these smaller graphene nanosheets on the composite surface, providing more edge sites and hydrogen diffusion channels, prevented the nanograins from sintering and agglomerating, agglomeration, thus leading to enhanced hydrogen storage properties. The composites MgH₂-GNS milled for 20 h can absorb 6.6 wt% H₂ within 1 min at 300 °C and 6.3 wt.% within 40 min at 200 °C, even at 150 °C, it can also absorb 6.0 wt% H₂ within 180 min. It was also demonstrated that MgH₂-GNS-20 h could release 6.1 wt% H₂ at 300 °C within 40 min. Finally, a porous Ni@rGO nanocomposite was successfully prepared by the ethylene glycol method followed by an annealing process. The desorption peak temperature shifted from 356 °C for pure milled MgH₂ to 247 °C for MgH₂-5 wt.% Ni@rGO. The MgH₂-5 wt.% Ni@rGO composite could desorb 6.0 wt.% H₂ within 10 min at 300 °C even after nine cycles, in contrast, only 2.7 wt% H₂ was desorbed even after 120 min for undoped MgH₂. It is found that the Ni particles contained in Ni@rGO are mainly responsible for the kinetics improvement, while rGO nanosheets have beneficial effects on the hydrogen capacity and increase and prevent the hydride sintering and agglomeration during cycling, so as to enhance the cyclic stability. In addition, the as-synthesized NiB, GNS and Ni@rGO exhibit superior catalytic effects on

hydrogenation/dehydrogenation of MgH_2 . The activation energy (E_a) of MgH_2 decreased significantly after adding NiB, GNS and Ni@rGO compared to MgH_2 .

Valorization of biogas produced in WWTP by means of PEM fuel cells (P-103)

*M. Martín**, *M. Mar Castro***, *N.A. Moya****, *T.R.Serna****

**EMUASA, Plaza Circular, 9, 30008 Murcia, Spain (E-mail: mmartin@emuasa.es)*

*** Aqualogy Aqua Ambiente, Plaza de Cetina, 6, 2º, 30001, Murcia, Spain (mcastroq@aqualogy.net)*

****Aqualogy Medio Ambiente, Avda. De la Diagonal, 211, 08018 Barcelona, Spain (E-mail: nmoyasan@aqualogy.net, trserna@aqualogy.net)*

Mitigation of global warming is a major priority in energy and environmental policies of the European Union (EU). Besides contributing to these objectives, production and use of biogas allow to create many economic and environmental benefits.

Biogas is a mixture of mainly methane (CH₄) and carbon dioxide (CO₂) generated in Waste Water Treatment Plants (WWTP) as a byproduct of the process of sludge stabilization by anaerobic digestion.

The biogas valorization through different methods (boilers, cogeneration plants, micro-turbines and upgrading for its use as fuel or for injection to grid) is widely developed. Due to its high electrical efficiency and reduced environmental impact, fuel cells (FC) are destined to become an interesting alternative for implementation in biogas production facilities.

The project BIOCELL, funded by the LIFE+ program, has been carried out from 2009 to 2012 and aimed to demonstrate the feasibility and economic viability of energy production from biogas via Polymeric Exchange Membrane Fuel Cells (PEMFC) and Solid Oxide Fuel Cells (SOFC) adapted to WWTP, developing the adequate tools for its industrial implementation and assessing its environmental impact. The project consortium has been constituted by four companies: CETaqua (Spain), Aguas de Murcia (Spain), Suez Environnement (France) and Degremont (France).

The specific project developed by Aguas de Murcia has an innovative feature which is obtaining hydrogen through a dry reforming (DR) process. One of the most attractive features of DR is that the CO₂ of biogas can be used as oxidant during the reforming reaction, avoiding gas emissions entering the atmosphere.

The study has involved a high degree of technological innovation due to the absence of background information about industrial plants operating this kind of technologies such as the lack of commercial equipment suitable for integration into the demonstration plant.

As Figure 22 shows, the pilot plant installed in Murcia consist on: (1) pretreatment of biogas, made up: (i) caustic scrubbing (absorption of hydrogen sulfide (H₂S) by chemical washing with a solution of sodium hydroxide (NaOH)) and a polishing stage, make up of (ii) cooling, for removal of water (H₂O) and siloxanes (Si), and (iii) adsorption in a bed of activated carbon, to eliminate H₂O, H₂S and Si compounds; (2) a fuel processor to generate a hydrogen (H₂) rich stream by means of a specific catalyst, and (3) two commercial PEMFC manufactured by MES S.A. (2 x 1.5 kWe). The off gas

and the excess of reformat gas produced are recirculated to a burner, providing the thermal energy needed to carry out the process.

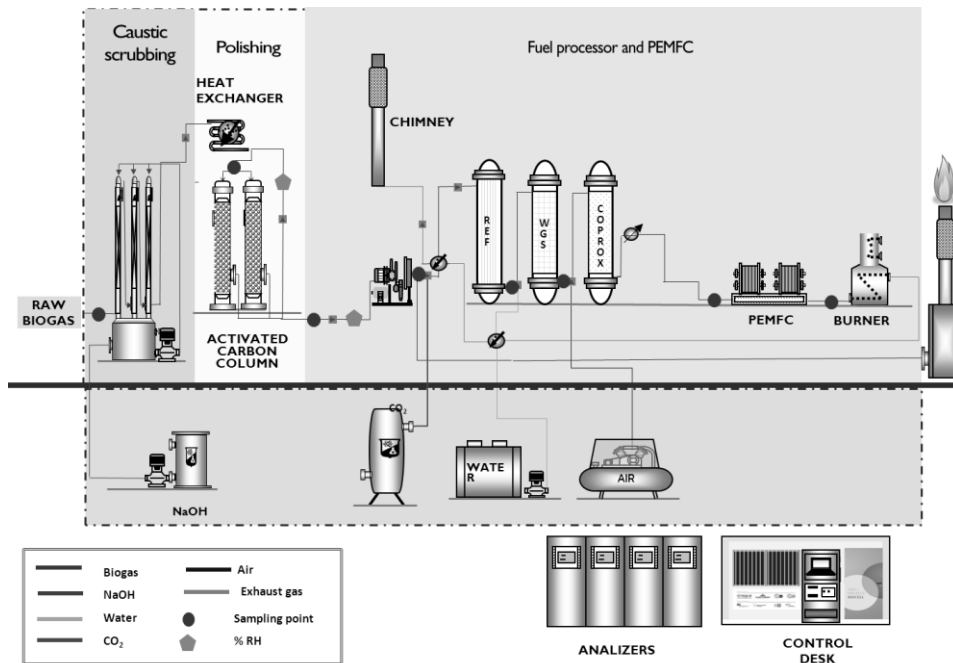


Figure 22. Layout of PEMFC pilot plant.

The biogas processor was designed to be feeding by CH₄:CO₂ 1:1, at nominal flow of 5 Nm³/h and is made up of three main stages: catalytic REForming (REF), and the oxidation of carbon monoxide (CO) in two steps: Water Gas-Shift (WGS) and CO PReferential OXidation (COPROX), aimed at eliminating, almost entirely, the CO in the stream feeding the stack because this compound is a poison for the PEMFC.

According to previous experiences developed by Aguas de Murcia and the recommendations of the manufacturers of reforming catalyst and FC, have been set the following quality limits: at pretreatment output biogas should contain less than 0.1 ppm of H₂S ([H₂S] <0.1 ppm) and less than 0.2 mg/Nm³ of Si ([Si] <0.2 mg/Nm³) and, at PEMFC input, the concentration of CO should be lower than 50 ppm ([CO] <50 ppm).

The innovative nature of this project has relied both on the difficulty in the processor design and operation and the use of reformed biogas to fuel a PEMFC.

The pretreatment stage has worked in a proper way, allowing obtaining a biogas clean stream fulfilling the quality requirements established to feed the reforming stage. The fuel processor has ran intermittently since its launch over 385 h, resulting in better performance of different reactors than expected in previous simulations or laboratory tests, but due to numerous problems, breakdowns and adjustments, have been unable to put the whole plant into operation, lacking the feeding of FC.

The PEMFC have been tested at laboratory scale fueled by several mixtures of H₂ and nitrogen (N₂) showing acceptable results. By using pure H₂ as fuel it is possible to achieve performances of 86.67% and fed by H₂:N₂, 1:1, at input pressure of 0.65 bar, a maximum power of 800 W has been achieved, which means a rate of 26.67% of nominal power.

The operational problems arisen at pilot plant and its on-progress solution provided useful knowledge for future projects. Outcomes show that the plant operation is feasible, although the process is energetically expensive and is in an early stage of development.

Further work is necessary to optimize the system, involving FC manufacturers, biogas producers and research centers in order to achieve a more reliable and efficient fuel processor, lower operational expenses, develop catalysts less sensitive and high capacity stacks that support reforming gas as feed.

Hydrogen adsorption on Co/Ni mixed-metal MOF-74-type materials (P-106)

Guillermo Calleja, Carmen Martos, Juan Ángel Botas, Gisela Orcajo and José Antonio Villajos

*Department of Chemical and Energy Technology, Universidad Rey Juan Carlos.
Tlf: 0034 914887601, Fax: 0034 914887068. E-mail: gisela.orcajo@urjc.es*

Metal-Organic Framework materials (MOFs) are promising candidates to overcome the technological challenge of efficient hydrogen storage based on physisorption. Some MOF structures are able to satisfy the gravimetric adsorption capacity targets required by the US Department of Energy (DOE), but in all cases at low cryogenic temperatures near 77 K, still far from the operation temperature in vehicles, being -40-60 °C [1]. This behavior is due to the weak interactions between hydrogen molecules and the adsorbent sites of the materials, showing too low values of the isosteric heat of H₂ adsorption [2]. By increasing these interactions, however, higher temperatures can be used for storing H₂ at applicable conditions. Among all known strategies for improving H₂-MOF affinity, the presence of a certain amount of Open Metal Sites (OMS) in the MOF structure (generated after guest molecules removal) is one of the most promising, since OMS directly provide stronger interactions with H₂ molecules, and therefore easier adsorption.

MOF-74 family of materials, also known as CPO-27 (M-MOF-74, M= Zn, Cu, Co, Ni, Mg, Fe) shows an interesting structure for examining the influence of the OMS on the hydrogen adsorption properties, since it exhibits one of the highest concentration of OMS and H₂ surface-packing density among MOF materials [3]. It is well-known that Ni-MOF-74 shows an isosteric heat of hydrogen adsorption of 13 kJ/mol, close to the well-established optimal range (15-20 kJ/mol) for hydrogen adsorption over solids [1]. Moreover, the isosteric heat of adsorption can be enhanced when the structural metal is partially substituted by another metal, producing mixed-metal clusters [4]. In this work, a partial substitution of Co for Ni in MOF-74 structure has been carried out using different metal ratios, in order to increase the isosteric heat of adsorption and to create network defects that could act as new adsorption sites.

Herein M-MOF-74 type materials were synthesized following the procedure already published [5] but adding different Ni/Co ratios in the synthesis medium, while keeping constant the total metal concentration. The samples obtained were named as Ni_xCo-MOF-74, where x is the theoretical Ni concentration respect to the 100 of total metal content. Physico-chemical characterization of the obtained materials was accomplished by powder X-ray Diffraction (XRD), Scanning Electron Microscopy (SEM), Inductively Coupled Plasma (ICP), Thermogravimetric analyses (TGA), and N₂ adsorption/desorption at 77K.

XRD patterns of as-prepared samples as well as the simulated from Single Crystal XRD technique, depicted in Figure 1-left, show that MOF-74 is the only crystalline phase present in all obtained materials. In addition, theoretical and experimental metal content of the samples can be observed in Figure 1-right down. So, it is confirmed a successful substitution of Co for Ni in different extensions in all samples, being the nickel incorporation extent in the framework lower than the theoretical value expected from the solution concentration. On the other hand, all materials exhibit the needle-shape

morphology, characteristic of MOF-74 structure, as can be seen in the SEM micrograph, Figure 1-right. Finally, H₂ adsorption isotherms at 77 K and 87 K were collected for those materials, confirming a positive effect of cobalt substitution by nickel in the MOF-74 structure.

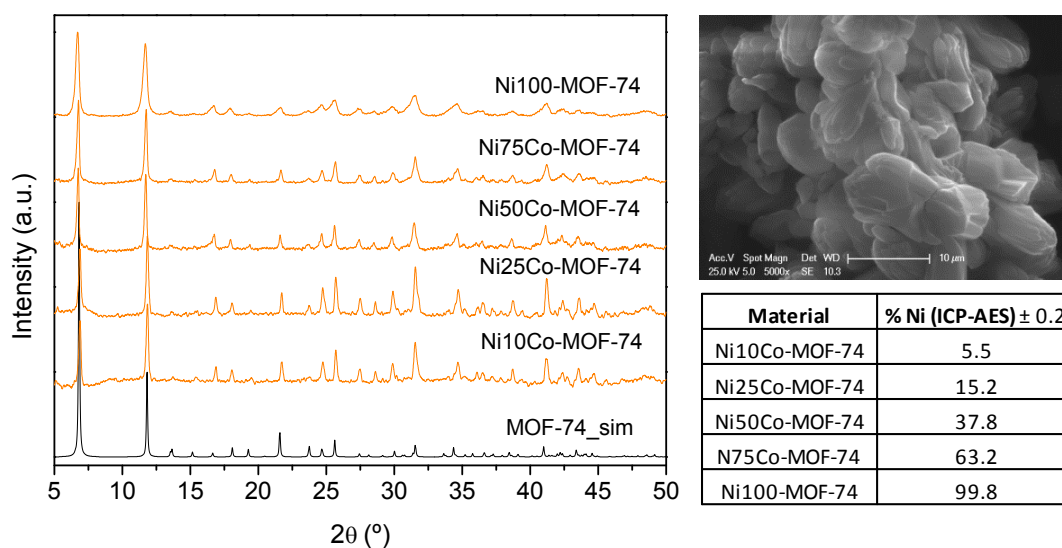


Figure 1: Left: Experimental and simulated XRD patterns for MOF-74-type materials; Right: SEM micrograph of the Ni50Co-MOF74 material and metal content for all obtained materials.

REFERENCES

Suh M. P., Park H. J., Prasad T. K., and Lim D.-W. "Hydrogen Storage in Metal-Organic Frameworks." *Chemical Reviews* 112, no. 2 (2012): 782-835.

Schlichtenmayer M, and Hirscher M. "Nanosponges for hydrogen storage." *Journal of Materials Chemistry* 22, no. 20 (2012): 10134-10143.

Liu Y, Kabbour H, Brown C. M, Neumann D. A., and Ahn CC. "Increasing the density of adsorbed hydrogen with coordinatively unsaturated metal centers in metal-organic frameworks." *Langmuir* 24, no. 9 (2008): 4772-4777.

Botas J. A., Calleja G. Sánchez-Sánchez M., Orcajo G. "Effect of Zn/Co ratio in MOF-74 type materials containing exposed metal sites on their hydrogen adsorption behavior and on their band gap energy." *International Journal of Hydrogen Energy* 36 (2011): 10834-10844.

Rowsell JLC, and Yaghi OM. "Effects of functionalization, catenation, and variation of the metal oxide and organic linking units on the low-pressure hydrogen adsorption properties of metal-organic frameworks." *Journal of the American Chemical Society* 128, no. 4 (2006): 1304-1315.

Synthesis and characterization of new nano-composites membranes based in polysulfone/ ZnAl-heptamolibdate LDH (P-107)

M. Herrero, A.M. Martos, F. Yepes, A. Varez, B. Levenfeld

Departamento de Ciencia e Ingeniería de Materiales e Ingeniería Química, Universidad Carlos III de Madrid, Avda de la Universidad 30, 28911 Leganés, Madrid. Spain

In the last years, great effort has gone into the fuel cells development in order to avoid the dependence on hydrocarbon fuel and the pollution release during the process which can be cause hazardous threat to the environment and human life. The most promising fuel cells are the polymer electrolyte membrane fuel cells (PEMFCs) due their modularity [1] and wide variety of applications. However, they have several handicaps to a greater commercialization, mainly related to their low-proton conductivity at a low relative humidity, to the high fuel crossover and to their poor mechanical properties. Also, the most utilized membranes are based on expensive perfluorinated polymers, which operate only under fully hydrated conditions. Many efforts are being done in order to replace this type of polymer, the alternatives could be: (i) modified perfluorinated composites membranes, (ii) functionalized non fluorinated polymers and related composite, and (iii) acid-base composite membrane [2,3].

The second approach includes polymers with high mechanical and chemical stability, relatively high proton conductivity, low cost and low permeability to the fuel. Some of them are: sulfonated polysulfone (SPSU), sulfonated poly (ether ketone) (SPEK), sulfonated poly (ether ether ketone) (SPEEK), etc [3]. Among these, the polysulfone is one of the preferred materials due to its low cost, high thermal stability, and easy availability. In addition, this polymer has been easily sulfonated with various sulfonating agents giving excellent proton conducting membranes.

Incorporations of inorganic fillers, such as, TiO₂, ZrO₂, heteropolyacids, clays..., leads to an increase in some properties of the virgin polymer [4,5]. Heteropolyacids are known to be strong Brönsted acids as well as solid electrolytes. Usually, they have unique discrete structures and exhibit high proton mobility, but, also, they show high solubility in aqueous media and larger particle size producing ineffective bridging between the inorganic filler and the polymer affecting membrane endurance and hence PEMFC performance [6].

On the other hand, organic and inorganic nanoclays are showing the most promising results due to the high reinforcement even at very small filler amount. They can be exfoliated to individual platelets inducing extremely large surfaces and interface between the filler and the polymer matrix. These lamellar solids are used to increase the mechanical properties, decrease the fuel and water permeability, and, due to their hygroscopic properties, maintain humidity inside the membrane [7]. In this sense, LDHs, also called anionic clays or hydrotalcite-like compounds, exhibit certain specific advantages (purity, crystallinity and particle size control, easy functionalization), which are lacking in layered silicates type nanoclays. LDHs constitute a large family of inorganic materials, with the general formula $[M_{2+1-x}M_{3+x}(OH)_2](An^-)_{x/n}mH_2O$, where M₂₊ is a divalent cation such as Mg, Ni, Zn, Cu, and M₃₊ is a trivalent cation such as Al, Cr, Fe, V or Ga; x is a value that determines the layer charge density and the anion exchange capacity, ranges between 0.2–0.4. An⁻ is an exchangeable

anion with formal charge n [8]. Recently we have demonstrated that conductivity of sulphonated polysulphone increases slightly with the LDH addition [9].

In this work, we report the synthesis of a Zn,Al-LDH intercalated with a heteropolyacid, heptamolibdate, in order to obtain the best properties of the individual inorganic particles, the heteropolyacid high proton mobility and the hydrotalcite water uptake and fuel barrier properties, to be used as filler in polymer with proton exchange membrane applications. The Zn,Al- heptamolibdate (HMo-LDH) was obtained by the anion exchange method. The polysulfone was sulfonated using trimethylsilyl chlorosulfonate ($\text{Si}(\text{CH}_3)_3\text{SO}_3\text{Cl}$, 99%) as sulfonating agent, different ratios PSU: chlorotrimethylsilane were used (1:1 and 1:3) [9]. Then, the HMo-LDH/SPSU membranes, with different HMo-LDH weigh percent (0, 1, 2 and 5%), were obtained by the casting method using dimethylacetamide as solvent. The degree of dispersion of the LDH particles and the type of the polymeric membranes obtained were studied by X-ray diffraction (XRD). The interactions between HMo-LDH and SPSU were discussed on the basis of the FTIR spectroscopy data. The Water Uptake Measurements were used as a quantitative measure of membrane performance in fuel cells application. High proton conductivity is supported by high level of water uptake; at the same time, it is also a sign of low-dimensional stability as water influences the polymer microstructure and mechanical properties. The water uptake measurements for different membranes are recorded in Fig. 1. It can be observed that the composites water uptake is higher than SPSU membrane, and the amount of absorbed water increase with the HMo-LDH content. These results are promising, because generally, the higher the water uptake of a given polymer film improves the proton conductivity, because the mobility of the ions in the membrane phase increases with increasing water content.

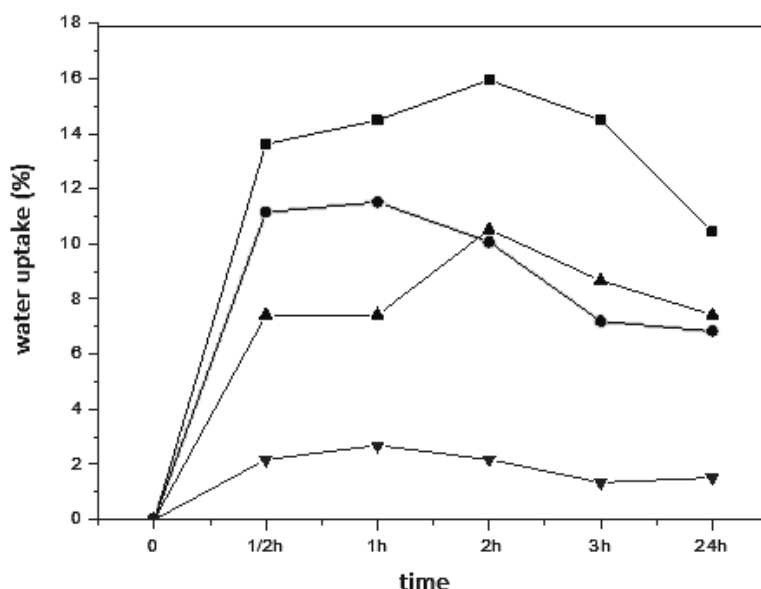


Figure 1- Water uptake measurements at different times at 25 °C for 11SPSU (▼) and SPSU_HMo-LDH at different HMo-LDH weight percent: 1% (▲), 2% (●) and 5% (■).

The thermal stability was determined by TGA analysis and electrochemical impedance spectroscopy (EIS) was used to study the membranes electrical properties. The EIS measurements

were carried out with the membranes in contact with HCl solutions at different concentrations [10]. Results showed a clear dependence of the membrane electrical resistivity with the sulfonation degree and the amount of the LDH added. We will determine for all the membranes prepared the polarization and the power density curves of the membrane electrode assembly (MEA).

Acknowledgments

Authors thank financial support received from the regional government (Comunidad de Madrid through MATERYENER S2009 PPQ-1626), and Spanish Government, MICINN (MAT2010-19837-CO6).

References

- [1] Peighambardoust SJ, Rowshanzamir S, Amjadi M. Review of the proton exchange membranes for fuel cell applications. *Int J Hydrogen Energy* 2010; 35: 9349-9384.
- [2] Jannasch P. Recent developments in high-temperature proton conducting polymer electrolyte membranes. *Curr Opin Colloid and Interface Sci* 2003; 8: 96-102.
- [3] Hickner MA, Ghassemi H, Kim YS, Einsla BR, McGrath JE. Alternative Polymer Systems for Proton Exchange Membranes (PEMs). *Chem Rev* 2004; 104: 4587-4612.
- [4] Unnikrishnan L, Mohanty S, Nayak SN, Singh N. Synthesis and characterization of polysulfone/ clay nanocomposite membranes for fuel cell application. *J Appl Polym Sci* 2012; 124: E309-E318.
- [5] Kim TW, Sahimi M, Tsotsis TT. Preparation and characterization of hybrid Hydrotalcite-Sulfonated Polyetheretherketone (SPEEK) cation- exchange membranes. *Ind Eng Chem Res* 2009; 48: 9504-9513.
- [6] Thanganathan U., Nogami M. Synthesis of mixed composite membranes based polymer/HPA: Electrochemical performances on low temperature PEMFCs. *J Mem Sci* 2012, 411: 109-116.
- [7] Unnikrishnan L, Madamana P, Mohanty S, Nayak SK. Polysulfone/ C30B nanocomposite membranes for fuel cell applications: Effect of various sulfonating agents. *Polymer: Plastics technology and Engineering* 2012; 51: 568-577.
- [8] Rives V. *Layered Double Hydroxides: Present and Future*. Nova Science Publishers, Inc., New York; 2001.
- [9] Herrero M., Martos A.M., Varez A., Galvan J.C., Levenfeld B. Synthesis and characterization of polysulfone/ layered double hydroxide nanocomposite membranes for fuel cell application. *Int J Hydrogen Energy* 2013; in press (doi: <http://dx.doi.org/10.1016/j.ijhydene.2013.06.041>)
- [10] Benavente J., Canas A., Ariza M.J., Lozano A.E., de Abajo J. Electrochemical parameters of sulfonated poly ether ether sulfone membranes in HCl solutions determined by impedance spectroscopy and membrane potential measurements. *Solid State Ionics* 2011; 145: 53-60.

Synthesis and characterization of quaternary ammonia polysulfone nanocomposite membranes for H₂/O₂ alkaline fuel cell applications: An electrochemical study (P-108)

M. T. PÉREZ-PRIOR, T. GARCÍA-GARCÍA, A. VÁREZ, B. LEVENFELD

Departamento de Ciencia e Ingeniería de Materiales e Ingeniería Química, Universidad Carlos III de Madrid, Avenida de la Universidad, 30, 28911 Leganés, Madrid, Spain

Fuel cells have been recognized as an alternative energy generation technique for many applications such as stationary, transportation, and portable electronics.[1] Among these systems, alkaline anion-exchange membrane fuel cells (AEMFCs) have received much attention in recent years with important progress related to the development of alkaline polyelectrolytes.[1,2] AEMFCs offer some advantages over other fuel cells, such as that they are easier to handle as the operating temperature is relatively low (typically between 23-70 °C) and the higher reaction kinetics at the electrodes than in acidic conditions.[3] This high electrical efficiency permits the use of a lower quantity of a noble metal catalyst, like platinum which is scarce and expensive. In this type of fuel cells, anion-exchange membranes (AEMs) are a key component and the charge carriers are hydroxide ions or other anions instead of protons. AEMs are solid polymer electrolyte membranes that contain positive ionic groups as quaternary ammonium (QA) functional groups.

In this work, quaternary ammonium polysulfone (QAPS-OH) has been used as electrolyte (Figure 1). Polysulfone (PS) has been employed as polymer backbone due to its excellent characteristics, such as solubility in a large range of aprotic polar solvents, high thermal resistance, chemical resistance on the whole pH range or high mechanical resistance of the films. The synthesis of QAPS-OH was then performed from PS by adding a chloromethyl pendant group to the polymer backbone, follow by reacting the chloromethyl group with amine to form quaternary ammonium pendant groups which act as the counter ion for the hydroxide ion. To avoid the use of hazardous materials, it has been used paraformaldehyde and chlorotrimethylsilane as chloromethylating agent and low toxicity solvents such as N-methylpyrrolidone and ethanol, instead of N,N-dimethylformamide and methanol, respectively.[4]

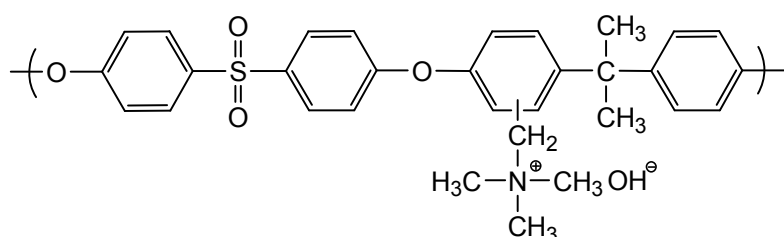


Figure 1. Chemical structure of QAPS-OH

Many research works reveal that the incorporation of inorganic additives into the anion exchange membranes improves the chemical properties of the membranes. In fact when ZrO₂ nano particles are incorporated into an anion exchange polymer matrix, this composite membrane exhibits better

electrochemical properties.[5] Recently, ionic conducting polymer composite membranes based on quaternary polysulfone/TiO₂ have been synthesized[6] and the results indicate that the introduction of TiO₂ enhances thermal resistance and improves water uptake. So, in the present work, the inorganic component added to the polymer membrane was Al₂O₃. Some studies related to solid polymer electrolytes containing Al₂O₃ have previously carried out[7] however, as far as we know, no reports on the use of Al₂O₃ as inorganic solid in QA-type membranes have been published. Therefore a novel composite polymer membrane based on the QAPS-OH and Al₂O₃ was prepared. Different loadings of Al₂O₃ (1-9 wt.%) have been used to prepare the QAPS-OH/Al₂O₃ composite membranes. The composite membranes were subjected into several characterization studies as ¹H-NMR, TGA, SEM or XRD and the membrane performance in a prototype fuel cell was also evaluated.

The electrochemical behavior of the QAPS-OH/Al₂O₃ composite membrane has been investigated by impedance spectroscopy. The test cell used was constituted by two half-cells separated by two O-rings where membrane was placed. A conventional electrochemical setup of four electrodes involving two saturated Ag/AgCl electrodes as reference electrodes and two graphite electrodes as secondary electrodes. The electrochemical measurements were performed in different KOH solutions. Prepared membranes were placed in contact with the KOH solution and they were equilibrated during a specific period of time in contact with the electrolyte, and, then, the measurements were carried out. As expected the resistivity associated to the membrane decreased as KOH concentration increased. Impedance plots as a function of the amount of Al₂O₃ added to the membrane were performed. The morphology of the resulting plots revealed an improving of the ionic conductivity with the percentage of the ionic solid. Thus QAPS-OH/Al₂O₃ composite membranes showed higher ionic conductivity than those based on QAPS-OH.

Evaluation of the performance of the fuel cell was carried out using membrane electrode assemblies (MEAs) composed by an electrolyte membrane coated by a catalyst on both the anode and cathode sides and sandwiched by a gas diffusion layer. The cell fuel tests were carried out in a H₂/O₂ fuel cell system. From the results obtained in this study, the possibility of using the QAPS-OH/Al₂O₃ composite membranes as electrolytes in fuel cell systems should be taken into account.

Acknowledgments

Authors thank financial support received from the regional government (Comunidad de Madrid through MATERYENER S2009 PPQ-1626) and Spanish Government, MICINN (MAT2010-19837-CO6).

References

- [1] Lu, S., Pan, J., Huang, A., Zhuang, L., Lu, J. Alkaline polymer electrolyte fuel cells completely free from noble metal catalysts. *Proc. Natl. Acad. Sci. USA* 2008, 105, 20611-20614.
- [2] Pan, J., Lu, S., Li, Y., Huang, A., Zhuang, L., Lu, J. High-performance alkaline polymer electrolyte for fuel cell applications. *Adv. Funct. Mater.* 2010, 20, 312-319.
- [3] Merle, G., Wessling, M., Nijmeijer, Anion exchange membranes for alkaline fuel cells: A review. *J. Membr. Sci.* 2011, 377, 1-35.
- [4] Pantamas, N., Khonkeng, C., Krachodnok, S., Chaisena, A. Ecofriendly and simplified synthetic route for polysulfone-based solid-state alkaline electrolyte membrane. *Am. J. Applied Sci.*, 2012, 9, 1577-1582.
- [5] Vinodh, R., Purushothaman, M., Sangeetha, D. Novel quaternized polysulfone/ZrO₂ composite membranes for solid alkaline fuel cell applications. *Int. J. Hydrogen Energy* 2011, 36, 7291-7302.
- [6] Nonjola, P. T., Mathe, M. K., Modibedi, R. M. Chemical modification of polysulfone: Composite anionic exchange membrane with TiO₂ nano-particles. *Int. J. Hydrogen Energy* 2013, 38, 5115-5121.
- [7] Mohamad, A. A., Arof, A. K. Plasticized alkaline solid polymer electrolyte system. *Mater. Lett.* 2007, 61, 3096-3099.

Study of Hydrogen production from wind power in Adrar (P-112)

Lilia Aiche-Hamane¹, Mustapha Hamane², Boumedienne Benyoucef³

1Department of mechanics, Faculty of technology, University Saad Dahlab Blida, Algeria

e-mail: l_aiche@yahoo.fr

2Centre for development of renewable energies (CDER), Algiers, Algeria

e-mail: m_hamane@yahoo.fr

3University Aboubakr Belkaid Tlemcen, Algeria

Abstract

Increasing the security of energy supply by reducing the dependency on imported fossil fuels, and reducing the emission of greenhouse gases have increased the need for developing sustainable energy sources based on renewable energy and low or zero emission energy conversion technologies. Among renewable energy sources, wind electricity in particular has become competitive in many markets around the world. Wind power has matured greatly over the last twenty years. Wind capacity has reached 282 275 MW in 2012 which represents an annual growth of 19.2%. However, the intermittency of the wind source makes necessary to develop efficient energy storage system. Hydrogen as an energy vector, together with electrolyser and fuel cell technologies can provide a technical solution to this challenge.

The aim of this study is to show the potentialities of Algeria to develop wind hydrogen systems and give a methodology for hydrogen production by a simplified efficient system proposed in this paper.

Algerian wind potentialities

Algeria is the largest country in Africa, located in the northern part sharing a vast coastline of about 1200 km along the Mediterranean Sea. A wind resource assessment has been carried out in Algeria [1]. The wind maps estimate the resource at 50 m hub height in terms of seven wind classes, ranging from the lowest class (<4 m/s), to the highest (> 9m/s) . Algeria has an interesting wind resource particularly in the southwest region which is remote area and where autonomous systems are more suitable. The region of Adrar with wind speeds greater than 8m/s is the most promising area for wind system installations in Algeria. A wind farm of 12 wind turbine of Gamesa type G52-850kW for a total capacity of 10 MW will be operating in 2014 at 75 kilometres from Adrar city.

Hydrogen production from wind

In the present paper, hydrogen production from wind power has been studied. A methodology is proposed to design wind hydrogen system. In order to reduce system losses and improve system efficiency, a direct coupling of the wind turbine to the electrolyser via AC/ DC converter has been proposed for hydrogen production [2](fig.1).

Wind turbine model

The wind power density delivered by a WT is given at standard conditions of 15 °C and 101.3 kPa by the following equation [3]:

$$\bar{P} = \sum_{i=1}^n P(V_i) f_i \tag{1}$$

Where P(Vi) is the wind turbine power produced at the wind speed Vi . It is given by the power curve of the wind turbine. fi is the wind speed frequency at the wind speed Vi. It is given by the weibull distribution function.

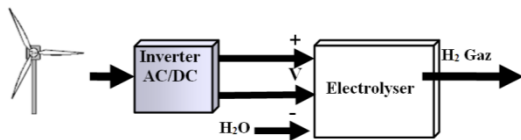


Fig.1.Wind hydrogen production system

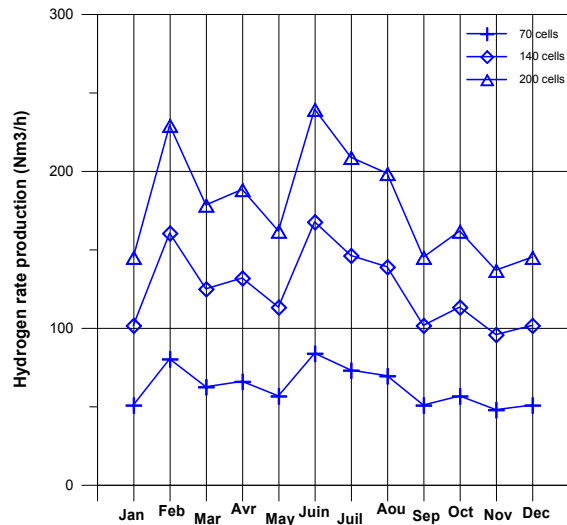


Fig.2. Hydrogen production according to electrolyser cells number

Power conditioning model

Power conditioners are devices that can invert AC power to DC power. The power loss (Ploss) for a power conditioner is mainly dependent on the electrical current running through it. The three-parameter expression is given by [4]:

$$P_{loss} = P_{in} - P_{out} = P_0 + (U_s / U_{out})P_{out} + (R_{ipn} / U_{out}^2)P_{out}^2 \tag{3}$$

A convenient relationship between the input power Pin and output power Pout can be derived by normalizing (3) with respect to the nominal power Pn of the power conditioner:

$$\frac{P_{in}}{P_{nom}} = \frac{P_0}{P_{nom}} + \left(1 + \frac{U_s}{U_{out}}\right) \cdot \frac{P_{out}}{P_{nom}} + \frac{R_{ipn}}{U_{out}^2} \cdot P_{nom} \cdot \left(\frac{P_{out}}{P_{nom}}\right)^2 \tag{4}$$

Electric efficiency is given by:

$$\eta = P_{out} / P_{in} \quad (5)$$

Where P_{in} is the Power entering the conditioner (W), P_{out} the Power leaving the conditioner (W), P_0 the Idling power (W), P_n the nominal (rated) power (W), U_s the setpoint voltage (V), U_{out} the Output voltage (V), R_i the internal resistance [Ω], R_{ipn} the internal resistance constant = $R_i P_n$ (V^2) and I_{out} the output current (A).

Electrolyser model

Alkaline electrolyser currently dominates global production of electrolytic hydrogen.

The model for a high pressure alkaline water electrolyser has been considered [4]. It is based on a combination of fundamental thermodynamics, heat transfer theory, and empirical electrochemical relationships. A dynamic thermal model is also included. A temperature dependent current-voltage curve for a given pressure and a Faraday efficiency relation independent of temperature and pressure form the basis of the electrochemical model. The electrolyser temperature can be given as Input, or calculated from a simple or detailed thermal model. The electrode Kinetics of an electrolyser cell has been modelled using the following empirical model (I-U) as:

$$U = U_{rev} + \frac{r}{A} I + s \log \left[\frac{t}{A} I + 1 \right] \quad (5)$$

Where U is the operating cell voltage (V), U_{rev} is the reversible cell voltage (V), r is the ohmic resistance of electrolyte (Ωm^2), s is the overvoltage coefficient on electrodes (V), t is the overvoltage coefficient on electrodes ($A^{-1} m^2$), A is the electrode area (m^2) and I is the current passing through the electrode (A).

The production rate of hydrogen in an electrolyzer cell is directly proportional to the transfer rate of electrons at the electrodes, which is equivalent to the electrical current in the external circuit. It can be expressed as [4]:

$$n_{H_2} = \eta_f \cdot N_{cel} \cdot \frac{I}{n \cdot F} \quad (6)$$

Where n_{H_2} is hydrogen production rate mol s⁻¹, N_{cel} is the number of cells in series, n is the number of moles of electrons per mole of water ($n=2$), F is the Faraday constant, $F= 96.485$ A s mol⁻¹. η_f is the Faraday efficiency defined as the ratio between the actual and theoretical maximum amount of hydrogen produced in the electrolyser, it is also called the current efficiency.

Case study

The simulation of the system presented in Fig.1. has been conduct using Hydrogen energy system modelling tools (HYDROGEMS) integrated in the transient system simulation program (TRNSYS) [5]. The design of the electrolyser has been proposed according to wind speed data available at Adrar and wind turbine system parameters. The wind turbine selected is of the type G52-850kW from Gamesa which starts the power production at 4m/s and reaches the maximum rated output power of 850 kw at 14m/s at 86 m hub height tower.The high pressure alkaline water electrolyser of GHW has been considered. It operates at 30 bars with a nominal temperature of 80°C. A monthly simulation of the electrolyser for different number of cells (70 cells, 140 cells end 200 cells) has been done. The results of the simulations are presented on fig.2.

Conclusion

This paper presents the results of simulation of hydrogen production from wind power in the site of Adrar. A correct sizing of electrolyser constitutes the most important step to obtain an optimal and efficient system. It has been found that the current limit in a stack do not allow an interesting production of hydrogen, therefore, the electrolyser may contains more than one stack in parallel in order to improve the system and increase its efficiency.

References

L. Aiche Hamane, "Contribution to the wind power potential assessment and mapping in Algeria". Master thesis, Mechanical engenneering department, Blida university, Algeria, 2003. [Contribution à l'élaboration de la carte du gisement énergétique éolien de l'Algérie].

L.Aiche-Hamane, M.Belhamel, B.Benyoucef, M.Hamane, 2010, "Study of hydrogen production from wind power in Algeria", 18th World Hydrogen Energy Conference WHEC 2010, 18th World Hydrogen Energy Conference 2010 - WHEC 2010.

L. Aiche-Hamane, M. Belhamel, B. Benyoucef and M.Hamane,"Feasibility study of hydrogen production from wind power in the region of Ghardaia", International journal of hydrogen Energy, Vol. 34, pp. 4947-4952, 2009.

O. Ulleberg,, "Modeling of advanced alkaline electrolysers: a system simulation approach", International Journal of Hydrogen Energy, Vol. 28, pp. 21-33, 2003.

SA Klein, WA Beckman, JW Mitchell et al, "TRNSYS—a transient system simulation program", Solar Energy Laboratory, University of Wisconsin, Madison, 2007.

Electrochemical analysis of WNi-CeO₂ cermet as sulphur tolerant SOFC anode (P-116)

M.J. Escudero*, I. Gómez de Parada*, **, A. Fuerte*

*CIEMAT, Av. Complutense 40, 28040 Madrid, (Spain)

** UAM, Ciudad Universitaria de Cantoblanco, 28049 Madrid, (Spain)

ABSTRACT

The solid oxide fuel cells (SOFCs) have great potential for direct utilization of hydrocarbons fuels such as natural gas, syngas and biogas. However, all fossil fuels contain certain amounts of contaminants, such as sulphur compounds, which degrade the anode of SOFCs such as Ni/YSZ cermet anodes. The conventional Ni/YSZ based cermet anodes show a very tolerance to fuel containing H₂S. Matsuzaki et al.(1) observed a significant poisoning with the H₂S concentrations of 0.05 and 2 ppm at 750 and 1000 °C, respectively. Therefore, the development of anode materials that can operate on sulphur-containing fuels is recognized as an important technical objective for SOFC development. Doped or undoped ceria oxides are commonly applied as sulphur-tolerant components in metal cermet anodes due to the good performance and lower cost relative to available alternatives, as well as CeO₂ is widely used in sulphur removal process. In the context, there are literature reports (2),(3) that support that the addition of ceria increases the sulphur-tolerance of the Ni-based electrodes. In addition, WS₂ has been studied as anode material in H₂S oxidation fuel cells to improve performance (4),(5), and the results revealed that was stable and active during the testing time of 36 h.

Based on these studies, doping with hexavalent W to Ni-CeO₂ could increase the sulphur tolerance. In this work a bimetallic W-Ni formulation combined with CeO₂, (WNi-Ce), has been prepared and studied as alternative SOFC anode material that could be operate with H₂S containing fuels. The effect of H₂S with different concentrations to an H₂ fuel on the cell performance and stability has been investigated in a SOFC single cell based on La_{0.9}Sr_{0.1}Ga_{0.8}Mg_{0.2}O_{2.85} (LSGM) as electrolyte and with WNi-Ce cermet as anode material at 750 °C.

The WNi-Ce compound was synthesized by coprecipitation within reverse microemulsion method with a nominal chemical formula of Ce_{0.7}Ni_{0.2}W_{0.1}O_{2+δ} (WNi-Ce) and showed a fluorite phase of CeO₂ together with a second of NiWO₄. After its reduction in 10%H₂ at 750°C for 50 h, additional diffraction peaks due to metal nickel were detected. Similar morphology was observed by SEM before and after its reduction. The powders showed a homogeneous microstructure with a particle size around 0.5 μm. The thermal expansion coefficients (TEC) were 9.8 K⁻¹ in air and 14.8 x10⁻⁶ K⁻¹ (200-450°C) and 18.5 x10⁻⁶ K⁻¹ (450-750°C) in 5%H₂/N₂. This formulation showed a semiconductor behavior in reducing atmosphere with an activation energy of 0.95 eV and a n-type electronic conduction. Reactivity studies carried out at 750 °C, under dry H₂ for 50 h, revealed no reaction between this material and LSGM electrolyte.

A single cell was fabricated with WNi-Ce as anode, La_{0.58}Sr_{0.4}Fe_{0.8}Co_{0.2}O_{3-δ} (LSCF) as cathode and La_{0.9}Sr_{0.1}Ga_{0.8}Mg_{0.2}O_{2.85} (LSGM) as electrolyte with an active area of 0.28 cm². A thin buffer layer of La_{0.4}Ce_{0.6}O_{4-δ} (LCD) between anode and electrolyte was used to avoid possible interfacial reactions due to the presence of Ni. The effect of H₂S in H₂ (10-500 ppm) on the performance has

been studied at on single cell at 750 °C under both open circuit voltage (OCV) and current load conditions using electrochemical techniques. The OCV values measured after one hour of the H₂S/H₂ introduction were 1037, 1030, 1028, 1025, 1022 and 1043 mV for 0, 10, 50, 100, 300 and 500 ppm of H₂S, respectively. It can be observed a decrease in the OCV values with an increasing H₂S (0-300 ppm) except for 500 ppm H₂S. There are two effects opposed each other in their influence on the voltage. The first one is a decrease in the OCV values with the sulfur electrochemical oxidation according to the thermodynamic calculation. The other one is an increase in the OCV values could be directly related to the differential partial pressures of H₂O (PH₂O). The anodic gas is a mixture of dry H₂S/H₂ with humidified H₂, except of 500 ppm H₂S/H₂ composition which is feeding without passing through bubbler. With increasing H₂S concentrations, the PH₂O became lower in the mixture gas, leading to slightly higher OCV values. This could be the main reason to the higher OCV value measured for 500 ppm H₂S which is dry H₂S/H₂.

Fig. 1a displays the cell voltage and power density as function of current density with varying H₂S concentrations (0-500 ppm) at 750 °C of the cell. These data were obtained after one hour of H₂S exposure for each concentration. As can be expected, the maximum current density (cell voltage=0V) and the maximum power density (MPD) decrease with increasing H₂S concentration. At the 500 ppm H₂S, the MPD decreased significantly by 52% (226 mW/cm² →108 mW/cm². This could be due to the adsorption of S on the Ni surface, blocking the active sites for hydrogen adsorption and oxidation.

The impedance spectra of the cell that were measured after IV curves are presented in Fig 1b. Nyquist diagrams show that the total internal resistance increased with increasing H₂S concentration, but the ohmic resistance remained constant, only the polarization resistance changed. The polarization resistance increased from 1.0.9 to 2.4 Ω·cm² between 0 and 500 ppm H₂S/H₂. Then, the adsorbed species did not form an insulating layer, but poisoned the activate sites for H₂ oxidation.

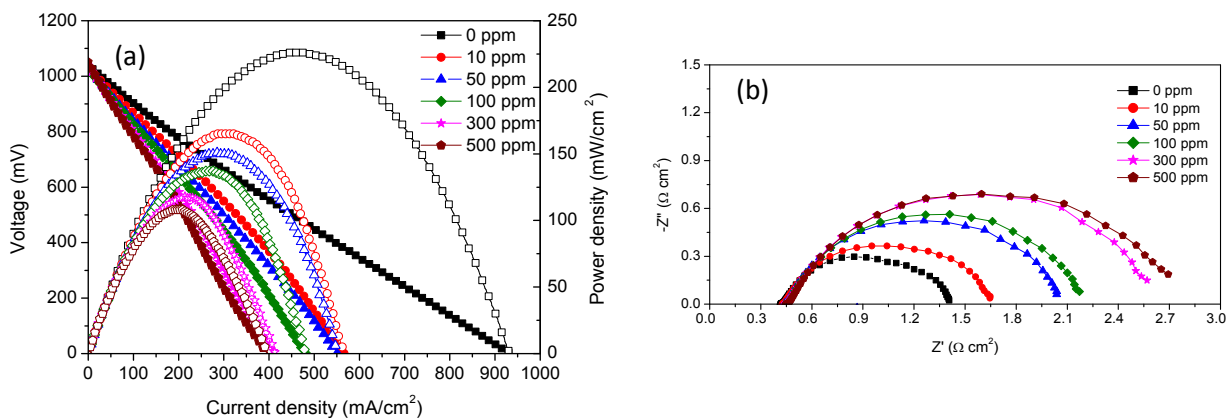


Fig. 1- Electrochemical characterization the WNi-Ce/LDC/LSGM/LSCF cell varying H₂S concentrations (0-500 ppm) at 750 °C. (a) IV curves; (b) Impedance spectra.

Short term stability of the cell was measured a constant current during 1 h in each H₂S concentrations (0, 10, 50, 100, 300 and 500 ppm H₂S/H₂). The current density demand varied in each

test and corresponded to the intensity required to achieve 90% of the maximum power. Each value was obtained of IV curves measurements in identical experimental conditions before the stability test. Note that the cell performance remained stable in all compositions. As it was supposed, the power density decreases with the increases of H₂S content in the feeding gas. The cell reached power densities from 224 to 107 mW/cm² for 0 and 500 ppm of H₂S, respectively. In all cases, similar IV curves and impedance spectra were measured before and after the stability tests.

Therefore, the excellent sulfur tolerance revealed by WNi-Ce could be attributed to the good catalytic activity for H₂ oxidation of the surface sulfides formed with the tungsten as well as the ability of desulfurization of CeO₂.

- (1) Y. Matsuzaki, I. Yasuda, *Solid State Ionic*, 132 (2000) 261-269.
- (2) J.P. Trembly, A. I. Marquez, T.R. Ohrn, D. J. Bayles, *J. Power Sources* 158 (2006) 263-273.
- (3) J.W. Yun, H.C. Ham, H.S. Kim, S.A. Song, S.W. Nam, S. P. Yoon, *J. Electrochem. Soc.*, 160(2) (2013) F153-F161.
- (4) N. U. Pujare, K. J. Tsai, A. F. Sammells, *J. Electrochem. Soc.*, 136 (1989) 3662-3678.
- (5) C. Yates, J. Winnick, *J. Electrochem. Soc.*, 146(8) (1999) 2841-2844.

Combined XPS and DRIFTS study of the reduction under CO of Cu/CeO₂ CO-PROX catalysts (P-117)

Manuel Monte¹, Guillermo Munuera², José C. Conesa¹, Arturo Martínez-Arias^{1,*}

¹ Instituto de Catálisis y Petroleoquímica, CSIC, Marie Curie 2, 28049 Madrid, Spain.

² Departamento de Química Inorgánica. Universidad de Sevilla, 41092 Spain.

CuOx/CeO₂ is a catalyst interesting for various processes involved during production-purification of hydrogen generated from hydrocarbons or biomass feedstocks. In particular, it shows promising characteristics for reactions involving CO oxidation like the water-gas shift (WGS) and preferential oxidation of CO (CO-PROX) [1,2]. Its catalytic properties for such processes has been shown to depend strongly on the characteristics of the interface formed between the two oxide components

[1,2]. Accordingly, we have found recently important catalytic differences for CO-PROX as a function of the face exposed in the CeO₂ [3]. This is illustrated in Figure 1 which exhibits the catalytic behaviour of two 1.0 wt.% Cu catalysts supported on CeO₂ supports differing in the type of face exposed at their surface. While the sample supported on CeO₂ nanospheres (NS) displays a higher oxidation activity for both CO and H₂ (the two competing reactions over this type of catalysts and whose relative respective activity determines the overall CO-PROX performance of the system), an important decrease of the H₂ oxidation activity is observed over the catalyst supported on CeO₂ nanocubes (NC). The latter results in an important widening of the maximum CO conversion window, as evidenced in Fig. 1.

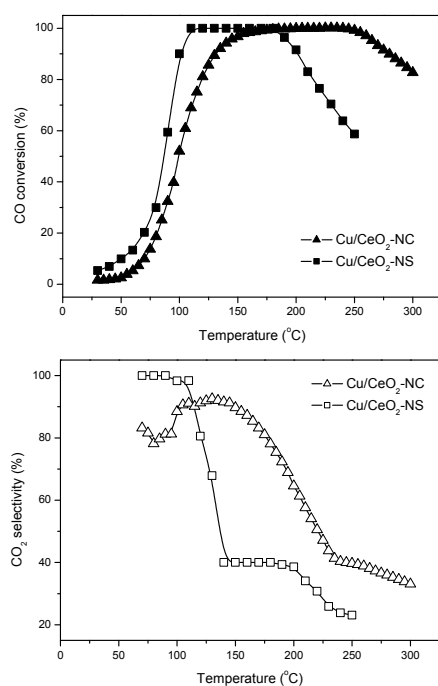


Fig. 1. CO conversion and selectivity to CO₂ under CO-PROX mixture of 1% CO + 1.25% O₂ + 50% H₂ (He balance) over the indicated

of establishing structure/chemistry/activity relationships, the present work examines the reduction properties under CO of the two mentioned 1.0 wt.% Cu catalysts supported on CeO₂ in the form of nanospheres (exposing mainly most thermodynamically stable (111) surfaces) and nanocubes (exposing (100) surfaces), respectively [4]. Details of the preparation and multitechnique (XRD, HREM, Raman, XPS, EPR, H₂-TPR, SBET) characterization of the two catalysts can be found elsewhere [3]. For the analysis of redox properties, the catalysts subjected to treatment under diluted CO between room temperature and 300 oC are examined by XPS spectra in gas environment obtained at

Within this context, in order to explore in detail the redox properties of the two catalysts, which could provide important details in terms

ISSS station of the BESSY II synchrotron in Berlin. In parallel, similar experiments were performed by DRIFTS. In any case, gases evolutions were analysed on-line by MS.

Important charging effects disallow extracting details in the synchrotron-XPS spectra of the samples in their initial oxidised states (after thermal pretreatment under diluted oxygen). Such initial condition was examined separately with a laboratory XPS equipment provided with electron gun which shows that both catalysts start from fully oxidised states in the two components (CuO and CeO₂). Partial reduction of the catalysts under CO at T > 60 °C allow diminishing the charging effects and shows predominant Cu⁺ state (according to joint analysis of Cu (2p) photoelectron and Cu L3VV Auger spectra) and slightly reduced ceria (according to Ce (3d) spectra) in both catalysts. The Cu⁺ state prevails up to 180 and 210 °C in the nanocubes and nanospheres configurations, respectively, temperatures above which the metallic state of copper begins to form. This is also in accordance with the evolution observed in Cu L edge XANES spectra obtained upon recording the total electron yield signal as well as with observation of H₂ evolution related to the WGS reaction, upon interaction of CO with surface hydroxyls, in the presence of metallic copper [1]. In turn, DRIFTS spectra show the formation of different types of carbonate and carbonyl species. The latter are related to the presence of interfacial Cu⁺ species (at ca. 2110 cm⁻¹), Cu⁺ species on top of the dispersed copper oxide particles (at ca. 2120 cm⁻¹) as well as stable carbonyls at 1975-1980 cm⁻¹ in the presence of metallic copper, in good correlation with the evolution of copper states observed by XPS. Such results are examined in conjunction with those obtained during CO adsorption/desorption experiments by synchrotron-XPS in the C (1s) region. The absence of CuO_x particle size effects on such results has been explored by examining by DRIFTS another sample supported on ceria nanocubes with similar surface copper coverage as the nanospheres supported one. The implications of these results on the catalytic properties of the systems for CO-PROX or WGS processes will be discussed in detail.

[1] X. Wang, J.A. Rodriguez, J.C. Hanson, D. Gamarra, A. Martínez-Arias, M. Fernández-García. *J. Phys. Chem. B* 110 (2006) 428.

[2] D. Gamarra, C. Belver, M. Fernández-García, A. Martínez-Arias. *J. Am. Chem. Soc.* 129 (2007) 12064.

[3] D. Gamarra, A. López Cámara, M. Monte, S.B. Rasmussen, L.E. Chinchilla, A.B. Hungría, G. Munuera, N. Gyorffy, Z. Schay, V. Cortés Corberán, J.C. Conesa, A. Martínez-Arias. *Appl. Catal. B* 130-131 (2013) 224.

[4] A. Martínez-Arias, D. Gamarra, M. Fernández-García, A. Hornés, P. Bera, Zs. Koppány, Z. Schay. *Catal. Today* 143 (2009) 211.

Synthesis of CuO/Al₂O₃ films onto stainless steel microgrids for CO preferential oxidation (P-123)

Zouhair Boukha, José L. Ayastuy, Ainara Iglesias-González, Beñat Pereda-Ayo, Miguel A. Gutiérrez-Ortiz, Juan R. González-Velasco

*Chemical Technologies for Environmental Sustainability Group,
Department of Chemical Engineering, Faculty of Science and Technology,
Universidad del País Vasco UPV/EHU, P.O. Box 644, E-48080 Bilbao, Spain*

() Corresponding author: zouhair.boukha@ehu.es*

Keywords: Stainless steel microgrids, copper oxide, alumina, COProx, COTox

INTRODUCTION

The design of new kinds of structured reactors for catalytic applications has attracted much attention in the last decade. According to some experimental studies, the miniaturisation of structured catalysts exhibits important advantages compared to conventional catalysts, thus becoming an interesting candidate to be used in industrial catalytic processes [1-2]. Due to their high surface areas, it was well established that the micro-structured reactors offer high heat/mass transfer coefficients and short contact time of the reactants which results in a better control of the reaction conditions. These characteristics are essential for a precise control of temperature and products distribution. Additionally, metallic micro-reactors have supplementary advantages such as high thermal conductivity, high mechanical resistance and the possibility to adopt different geometry and configurations.

On the other hand, the CO oxidation is an exothermic reaction with environmental interest. In the field of clean energy, CO must be removed from H₂ streams to be used in fuel cells (COprox). The conventional catalysts of CO oxidation reactions generally contain noble metals supported on oxides. Transition metals such as Cu and Co have also been investigated. They are active, less expensive than noble metals but very sensitive to the distribution of copper species [3]. For this reason search for new materials capable of developing suitable interactions with the loaded metal is essential.

The present work concerns the preparation, characterisation and activity for COTox and COProx reactions of CuO/Al₂O₃/SS316 microstructured reactors (micro-grid type) and their comparison with conventional catalytic systems. Their characterization involved BET, SEM, XRD, H₂-TPR, UV-visible-NIR and XPS.

EXPERIMENTAL

Several methods have been used for the washcoating of alumina on ceramic and metallic monoliths. In the present study the deposition of alumina film was prepared using a modified version of the methods mentioned in the literature. Then, the average particle size of the alumina (calcined at 850°C) was reduced to less than 3 μm by wet milling in a ball mill for 72h. The alumina milled slurry was mixed with polyvinyl alcohol (PVA) and colloidal alumina, used as binder, and stirred for 2 h. The pH was adjusted to desired value (3.5-4) by adding HNO₃ or NH₃. The final slurry composition was: 10.6% alumina, 1% PVA, 3.4% colloidal alumina and remaining water. The stainless steel

microgrids (AISI 316, wire: 100 μm and space: 150 μm), previously calcined at 900°C for 4h, were dipped in the suspension for 10 min and the excess suspension was evacuated by a flow compressed air. The samples were dried at 120°C for 30 min and the procedure was repeated until a 6 wt. % increase was obtained; and then calcined at 600°C in static air for 5 h with a temperature ramp of 1°C min⁻¹.

For the impregnation of the active phase the alumina-washcoated SS316 substrates were dipped into a stirred aqueous solution of 0.8 M Cu(NO₃)₂·3H₂O for 2 h. Then, the samples were dried at room temperature for 2 h and at 120°C for 2h. The impregnation and drying were repeated two and three times to obtain three catalysts with different Cu loadings (Table 1). Finally, the resulted microstructured reactors, labelled CuO(10)/Al₂O₃/SS316, CuO(14)/Al₂O₃/SS316 and CuO(18)/Al₂O₃/SS316 were calcined in air at 600°C for 10h with temperature ramp of 1°C min⁻¹.

The catalytic tests were performed, with flow/mass ratio of 660 ml min⁻¹ g⁻¹, in a tubular flow reactor operating at atmospheric pressure. To prevent a bypass flow the microreactor was rolled around a small stainless steel cylinder. For COTox the mixture was composed of 2% CO and 2% O₂ diluted in He and a total flow rate equal to 100 cm³ min⁻¹. In the case of COProx reaction the composition was 1% CO, 1% O₂, 12.5% H₂O, 12.5% CO₂ and 60 % H₂ in He balance. The temperature of reaction was increased from room temperature up to 360°C with a heating rate of 5 °C min⁻¹. The reaction products were continuously analysed by mass spectrometer which was calibrated using different mixtures of CO, H₂ and CO₂.

Results and discussion

SEM images showed that the preparation method used in this work for the synthesis of CuO/Al₂O₃ films onto stainless steel microgrids resulted in homogeneous and stable coatings with an estimated thickness of 8-10 μm . Microanalysis (EDS) of the washcoat showed that the copper was homogeneously dispersed on the internal and external middle zone of the film. Additionally, a good adherence of the deposited film was evidenced by ultrasonic tests for 1h (wt. loss < 1%).

Table 1 showed the textural characteristics of the CuO(x)/Al₂O₃/SS316 micro-structured catalysts. When the BET surface area for the CuO(x)/Al₂O₃/SS316 sample is referred to 1g of washcoated CuO(x)/Al₂O₃, a very slight decrease, from 122 m².g⁻¹ to 119 m².g⁻¹, may be noticed. As deduced from N₂ adsorption isotherms (not displayed) and the data reported in Table 1, all the samples may be considered as mesoporous materials exhibiting IV-type isotherms. We concluded that the deposition of alumina onto stainless steel microgrids did not significantly affect its textural properties.

Table 1. Characterisation results of the prepared catalysts

	Al ₂ O ₃ , %	CuO, wt. %*	SBET, m ² . g ⁻¹	Pore volume, cm ³ .g ⁻¹	Mean pore diameter, nm	CuO particle size, nm	Cu dispersion, %	T50CO
Alumina	-	-	123	0.500	13.5	-	-	-
Alumina/SS316	6	-	7.3 (122)*	0.019 (0.40)	11.2	-	-	-
CuO(10)/Al ₂ O ₃	-	10.5				30		247/248**
CuO(10)/Al ₂ O ₃ /SS316	6	10.5	8.0 (119)*	0.025 (0.37)	12.3	21	76	250/217**
CuO(14)/Al ₂ O ₃ /SS316	6	14.4	8.0 (114)*	0.025 (0.36)	11.6	30	57	250/242**
CuO(18)/Al ₂ O ₃ /SS316	6	18.3	8.0 (109)*	0.024 (0.33)	11.4	30	36	236/226**

(*) Referred to the washcoat weight

(**) Defined as the temperature required for 50% CO conversion (at the first and second catalytic run)

X-ray diffraction patterns of the alumina support calcined at 850°C showed a typical diffractogram for a transition alumina. Furthermore, despite its deposition onto stainless steel microgrids, the structural characteristics of the alumina remained unchanged. After copper impregnation two typical peaks belonging to CuO appeared at $2\theta = 35.5^\circ$ and 38.5° . Their intensity increases with copper loading. The average size of CuO particles was found to be around 21 nm on CuO(10)/Al₂O₃/SS316 and 30 nm on both CuO(14)/Al₂O₃/SS316 and CuO(18)/Al₂O₃/SS316.

The H₂-TPR diagrams of CuO(x)/Al₂O₃/SS316 microstructured catalysts showed three distinct peaks centred at 220, 275 and 340°C. The first one was assigned to the reduction of highly dispersed CuO particles. The two following peaks located at higher temperatures were attributed to the reduction of bulk CuO (275°C) and CuO strongly interacting with the substrate (340°C).

The UV-visible-NIR spectra of the CuO(x)/Al₂O₃/SS316 prepared catalysts showed the presence of bands in higher (1500 nm) and lower (600-800 nm) wavelength regions, consistent with both octahedral and tetrahedral coordination of cupric ions. Furthermore, the micro-structured catalysts spectra were characterized by the presence of additional bands in the UV-Visible regions around 350 and 450 nm. Iwamoto et al. observed analogous bands and ascribed them to Cu²⁺-O₂⁻-Cu²⁺ charge transfers [4]. Since these two bands were detected in the spectrum of bulk CuO (Fig. 4c), used as reference, their presence in the micro-structured catalysts spectra attested the presence of three-dimensional CuO.

Fig. 1 shows the light-off curves, in COTox reaction, over CuO(10)/Al₂O₃/SS316 micro-structured catalysts and CuO(10)/Al₂O₃ powder catalyst. The experiments were carried out using fresh catalysts. On CuO(10)/Al₂O₃/SS316 CO activation starts around 150°C. Its conversion increased rapidly to reach about 100% at 270°C, and then it stays constant up to 360°C. On CuO(10)/Al₂O₃ CO conversion begins at approximately 140°C but it did not reach 100% before 340 °C. A second catalytic run, performed on the same catalysts revealed a decrease of the temperature of CO activation on CuO(10)/Al₂O₃/SS316 catalyst. The conversion starts around 125°C and increased less abruptly than in the first increase. Moreover, the T₅₀ is lower by at least by 33°C from the first to second catalytic run (Table. 1). However on Cu(10)/Al₂O₃ powder catalyst the catalytic activity did not undergo any noticeable improvement.

The differences between of CuO(x)/Al₂O₃/SS316 and CuO(x)/Al₂O₃ probably result from the size of CuO particles and their interactions with the carrier. It is well established that the catalytic activities of copper based catalysts in CO oxidation reaction are related to both the highly dispersed CuO species and bulk CuO species [3]. Special attention was devoted to the determination of correlations between the catalysts activity and the copper distribution on the different sites of the carrier.

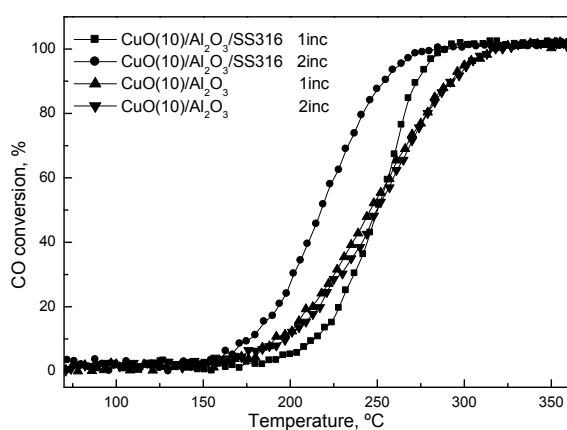


Figure 1. CO conversion in COTox reaction over CuO(10)/Al₂O₃/SS316 and CuO(10)/Al₂O₃ vs. the reaction temperature.

Acknowledgements

The financial support for this work provided by Gobierno Vasco (GIC IT-657-13) is gratefully acknowledged.

References

- [1] N. C. Pérez, E. E. Miró, J. M. Zamaro, *Appl. Catal. B.*, 129 (2013) 416
- [2] I. Yuranov, N. Dunand, L. Kiwi-Minsker, A. Renken, *Appl. Catal. B.*, 36 (2002) 183
- [3] M. Luo, P. Fang, M. He, Y. Xie, *J. Mol. Catal. A*, 239 (2005) 243
- [4] M Iwamoto, H Yahiro, N Mizuno, W.X Zhang, *J. Phys. Chem.*, 96 (1992) 9360

Optimizing the synthesis method of ZrO_2 -supported $NiFe_2O_4$ for solar hydrogen production by thermochemical water splitting (P-125)

*R.M. Navarro, L. Ruiz-Matas, J. Andrade, M.C. Alvarez-Galván, J.L.G. Fierro
Instituto de Catálisis y Petroleoquímica (CSIC)
c/ Marie Curie 2, Cantoblanco, 28049, Madrid (Spain)*

Introduction

Nowadays, increasing energy demand and elevated emissions of air pollutants and greenhouse gases strengthen research efforts on the conversion of solar energy into chemical energy carriers such as hydrogen using renewable resources as water. The most direct method for using solar energy to produce hydrogen from water is the one-step thermolysis of the water molecule. However, due to materials limitations at the high-temperatures required, direct water splitting is not expected to be economically viable in the near future being thermochemical multi-step water splitting cycles an alternative to reduce the temperature requirements of the thermal splitting of water. Thermochemical cycles are multi-step processes where water is decomposed into hydrogen and oxygen via two or more chemical reactions that form a closed cycle while other intermediate reactants and products are recycled [0,0]. Among the thermochemical cycles studied in literature, two-step water-splitting cycles using metal-oxide redox pair are one of the most attractive for practical solar applications due to its simplicity and efficiency. Two-step metal-oxide redox cycle proceed with the endothermic solar thermal dissociation of the metal oxide to the metal or to the lower-valence oxide, followed by a second non-solar exothermic step, corresponding to the hydrolysis of the metal/lower-valence oxide to form H_2 , regenerating the metal oxide. The net reaction is $H_2O + \text{thermal energy} \rightarrow H_2 + \frac{1}{2} O_2$. One of the two-step metal-oxide redox water splitting cycle uses iron oxide redox pair (Fe_3O_4/FeO) for thermal reduction and subsequent water decomposition. With this metal oxide, the temperature of the first thermal-reduction step, highly endothermic, can be decreased to around $1400^\circ C$ if it is performed under an oxygen partial pressure lower 10^{-6} bar. However, the use of this oxide presents a drawback associated with the low melting point of FeO that favor the rapid sintering by the formation of a very hard material [0]. The use of $NiFe_2O_4$, by substitution of Fe^{2+} by Ni^{2+} , increases the melting point of the material, enhancing the hydrogen productivity of the redox oxide [0,0]. Another approach to alleviate deactivation by sintering is supporting the active phase over a stable substrate, such as monoclinic ZrO_2 , which has a higher melting point than ferrite and is chemically inert at these high temperatures [0]. Taking into account the importance of controlling the contact of $NiFe_2O_4$ particles and ZrO_2 support as a way to minimize the thermal sintering of $NiFe_2O_4$, the preparation method is of crucial importance for directing the development redox materials with improved solar activities. With this background, this work aims to improve the efficiency of zirconia-supported nickel ferrite materials to produce renewable hydrogen by solar two-step thermochemical cycles, controlling the contact between both phases. In order to achieve this goal, two different synthesis methods (coprecipitation of all elements and coprecipitation of Ni and Fe over ZrO_2 particles) have been used, and the calcination temperature has been optimized. The prepared materials have been analyzed by several characterization techniques and relationships between H_2 production efficiencies and physicochemical properties have been established.

Experimental

Synthesis of materials

Two methods were used for the synthesis of ZrO₂-supported NiFe₂O₄ materials (25% weight of nickel ferrite): (i) joint coprecipitation of Ni²⁺, Fe³⁺ and Zr⁴⁺ cations (being NiCl₂, FeCl₃ and ZrOCl₂ the precursor salts) as their hydroxides using NaOH. The coprecipitation was carried out under stirring, under inert atmosphere (He flow) in order to prevent the oxidation of Ni²⁺ and with solvent refluxing. The temperature was set at about 60°C and the pH of the final suspension was adjusted to 8.5. The precipitate was aged under stirring for 2 hours and overnight without stirring. Then, it was deeply washed with deionized water and centrifuged three times. After, it was dried at 60°C overnight and calcined at different temperatures in N₂ flow (500, 600, 700 and 800°C) to achieve the transformation into spinel phase (ii) coprecipitation of Ni²⁺ and Fe³⁺ cations, using the same procedure described above and deposition as hydroxides over a commercial ZrO₂ powder or over ZrO₂ prepared by the method indicated above, but calcined in static air at 600°C.

Characterization methods

The BET surface area of the prepared materials was determined by N₂ physisorption measurements at 196°C (Micromeritics TriStar II 3020 apparatus). The bulk crystal structures of the different samples were analyzed by X-ray diffraction (XRD) technique (PANalytical X'pert PRO diffractometer equipped with a monochromator for Cu K α 1 radiation, $k = 0.15406$ nm). Surface texture and morphology of prepared materials was characterized by means of a scanning electron microscopy, SEM, using a HITACHI TM-1000 microscope coupled to an Energy Dispersive X-Ray analyzer, Oxford Instruments. The detailed morphology study at the nanometer scale of nickel ferrite particles deposited over zirconia was studied by using high-resolution transmission electron microscopy (TEM/STEM, JEOL 2100F, 200 kV, coupled to an EDX detector (INCA x-sight de Oxford Instruments). Oxygen release capability of prepared samples was investigated by H₂-temperature programmed reduction (TPR) with 50 mLN/min of 10% H₂/Ar mixture from 50 to 900°C and a heating ramp of 10°C/min, after cleaning the surface in helium flow at 800°C, to remove adsorbed water and carbonates.

Activity tests

Two-step water splitting cycles were carried out at laboratory scale in a fixed bed tubular horizontal reactor, made of recrystallized alumina, which was placed inside an electric furnace. Sieved grains (0.21-0.42 mm) of supported-zirconia nickel ferrite (0.5 g), contained in a Pt-Ir mesh frame, were placed in the middle of the reactor. For the activation step, helium gas passed through the reactor. For the hydrolysis step, water vapor was introduced by means of a saturator (gas bubbler) placed inside a heater at 343 K, bubbled with argon gas, being 0.31 the water mole fraction in the feed stream. For the activation, the reaction temperatures were set in the oven at 1500°C (1 hour) and, for the hydrolysis, at 1100°C (2 hours). The outlet gas was analyzed by means of a gas chromatograph (Varian 3800) equipped with a capillary column, a molecular sieve capillary column and a TCD detector. In both steps, a small flow of nitrogen was introduced together with helium and argon gases, as an internal standard for quantitation of O₂ and H₂.

Results and discussion

For samples prepared by joint coprecipitation of Ni^{2+} , Fe^{3+} and Zr^{4+} , the calcination temperature had a great influence on textural, structural and morphological properties (table 1). A decrease in surface area with calcination temperature rise is observed. This trend is the same than that observed in the SEM images, which indicate that an increase in the calcination temperature produce a growth of nickel ferrite grain size; together with a loss of sheet-shape particles, observed at low calcination temperatures. Concerning the samples prepared by coprecipitation of Ni^{2+} and Fe^{3+} over ZrO_2 and calcined at 600°C , the surface areas are lower than that prepared by joint coprecipitation of the three cations. SEM micrographs reveal a lesser contribution of zirconia particles to geometric surface area in samples prepared by coprecipitation-deposition of Ni^{2+} and Fe^{3+} over ZrO_2 .

Table 1. Mean crystallite sizes in samples after reaction and amount of H₂ produced per gram of nickel ferrite

Sample	Calcination temperature (°C)	BET Surface area (m ² /g) fresh sample	NiFe ₂ O ₄ (crystallite size, nm) fresh sample	ZrO ₂ (Crystallite size, nm) fresh sample	NiFe ₂ O ₄ (Mean Crystallite size, nm) after 1 cycle	ZrO ₂ (Crystallite size, nm) after 1 cycle	Milimol H ₂ /g NiFe ₂ O ₄
FZ-500-cop	500	79.0	very low crystallinity		17.0	19.8 (m)	0.83
FZ-600-cop	600	58.6	n.d.	7.9 (t)	16.3	29.9 (m)	1.00
FZ-700-cop	700	18.7	n.d.	8.2 (t)	16.1	17.2 (m)	0.78
FZ-800-cop	800	9.5	n.d.	majority (t), 22.2 (m)	18.2	21.3 (m)	0.65
FZcom-600-dep	600	11.6	22.5	60.1 (m)	56.8	57.4 (m)	0.58
FZlab-600-dep	600	29.7	22.7	18.3 (t), 22.7 (m)	43.9	41.3 (m)	0.38

(cop: coprecipitation of Ni²⁺, Fe³⁺ and Zr⁴⁺, dep (deposition-coprecipitation): coprecipitation of Ni²⁺, Fe³⁺ and deposition over ZrO₂) n.d. no detectable; t: tetragonal; m: monoclinic

X-ray diffractograms of freshly prepared materials reveal a higher crystallinity of samples prepared by deposition-coprecipitation method, with larger crystallite sizes, determined by Scherrer equation, for both nickel ferrite and zirconia phases. ZrO₂ phase type depends on the synthesis method and on the temperature and calcination atmosphere. Thus, a higher temperature favors the transition from tetragonal to the more stable monoclinic structure.

Representative HRTEM micrographs also evidence changes in morphology among the different samples, being observed smaller grain sizes of both support and nickel ferrite in samples prepared by coprecipitation (Figure 1).

The thermochemical two-step water splitting was examined on ZrO₂-supported ferrites. During the hydrolysis step, hydrogen production increases until reaching a maximum at around 3 hours of reaction. H₂ productions (shown in table 1) indicate a greater reactivity for those samples prepared by coprecipitation, being found the best performance, after 1 cycle of thermal reduction-hydrolysis, with the material calcined at 600°C (FZ-600-cop). Obtained results indicate that small crystallite sizes of both nickel ferrite and zirconia increase the efficiency of these supported materials for hydrogen production by water thermochemical cycles. As derived from SEM, XRD and surface area values of spent materials, sintering is the main cause of deactivation.

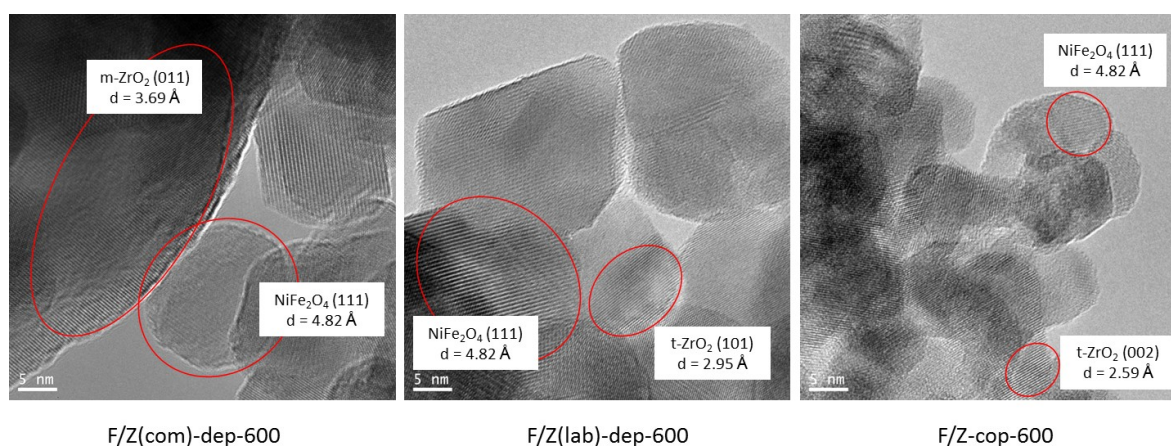


Figure 1. HRTEM micrographs of freshly prepared ZrO₂-supported NiFe₂O₄ samples

Conclusion

The ZrO₂-supported ferrite material prepared by joint coprecipitation of the cations and calcined in inert atmosphere at 600°C is found to be a promising material for hydrogen production by two-step water thermochemical cycle. Characterization of fresh and spent materials point out that an intimate contact of both support and active phase is essential to achieve high reactivity.

References

- T. Kodama, N. Gokon, Chem. Rev. 107 (2007) 4048-4077
- A. Steinfeld, Solar Energy 78 (2005) 603-615
- T. Kodama, N. Gokon, R. Yamamoto, Solar Energy 82 (2008) 73-79
- M.G. Rosmaninho, S. Herreras, R.M. Lago, M.H. Araujo, R.M. Navarro, J.L.G. Fierro, Nanosci. and Nanotech. Lett. 3 (2011) 705-716

Control and Monitoring Tools Developed for Hydrogen Based Systems (P-133)

José Manuel Andújar Márquez, andújar@diesia.uhu.es, University of Huelva
Francisca Segura Manzano, francisca.segura@diesia.uhu.es, University of Huelva

Abstract—This paper summarizes the work developed under the agreement signed between University of Huelva and Accadue enterprise. The agreement aims redesigning for optimization and performance improvement, including on-line monitoring via the Internet, of the instrumentation and control system for an alkaline electrolyzer.

Key words: Software tools, hydrogen systems, electrolyzer, fuel cell.

INTRODUCTION

This paper presents the work developed under the project whose aims are redesigning to optimize and improve the performance of an alkaline electrolyzer. For this purpose, authors should carry out three basic tasks:

1. Designing and implementing an instrumentation hardware/software system that allows acquisition, monitoring and processing all interesting variables in the operation of the electrolyzer.
2. Design and implement a control hardware/software system that allows optimize the electrolyzer operation.
3. Provide the electrolyzer of the possibility of on-line monitoring via Internet.

Next sections are dedicated to explain tasks described above. In Section II the alkaline electrolyzer operation mode is explained, and from here we can know the interesting variables to develop the instrumentation hardware/software system. Section III is centered on control hardware/software system implementation and Section IV describes the virtual interface for on-line monitoring. Main conclusions are gathered in Section V.

ELECTROLYZER OPERATION PRINCIPLE

The electrolysis unit consists of the following subsystems [1]:

Process section (or electrolysis) including assembly electrolytic stack, the delivery system of demineralized water and the temperature regulation system, the separation gas equipment and the circuitry needed for the production of hydrogen and oxygen at desired pressure.

Purification section is the unit to which the gas enters, is purified and then dried. This post-treatment allows obtaining purities greater than 5 ppm. Gas purification takes place in two phases: the first phase takes place in a drying tower, where in the presence of a catalyst, palladium is normally used at a temperature of about 100 °C, the oxygen existing in the flow of hydrogen is reacted with a fraction of hydrogen to form water, which is removed. The next stage of drying is performed in two filters working alternately as PSA (Pressure Swing Adsorption) technology. The

active element is constituted by activated carbon which is capable of removing traces of moisture entrained in the gas produced. For drying is usually used an alloy of alumina Al_2O_3 .

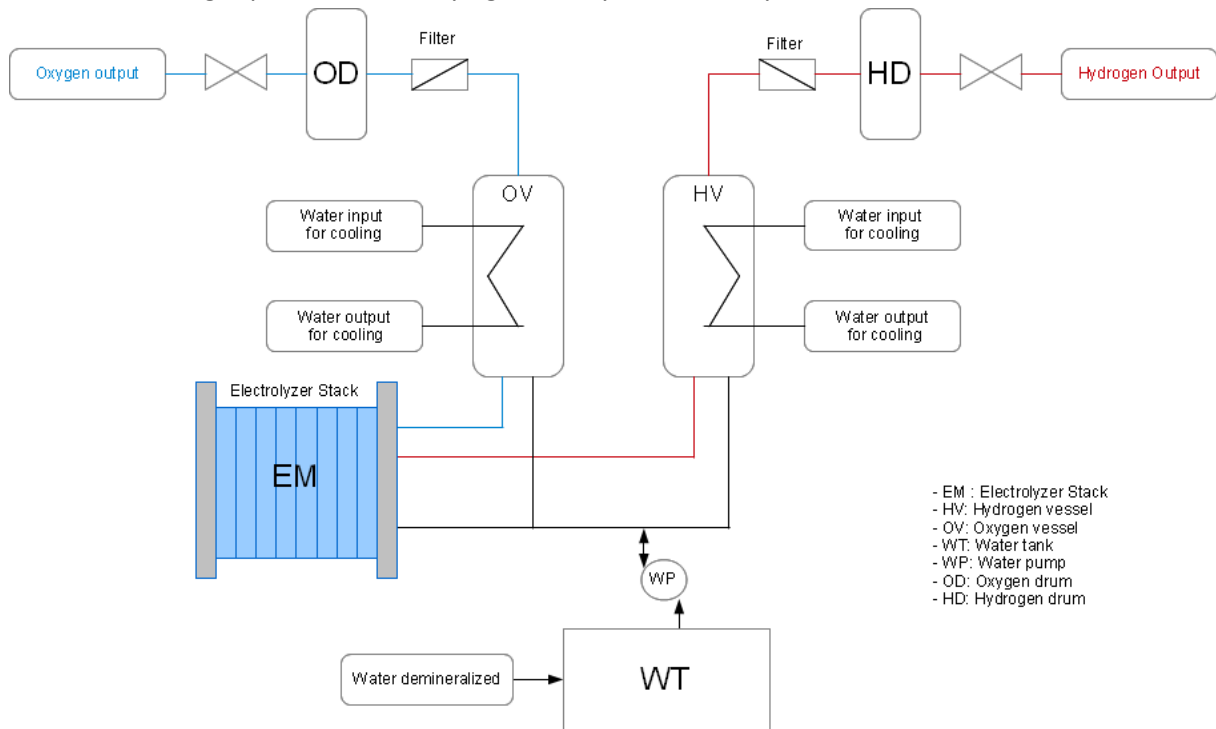


Figure 1a. Electrolyzer scheme: *process section*.

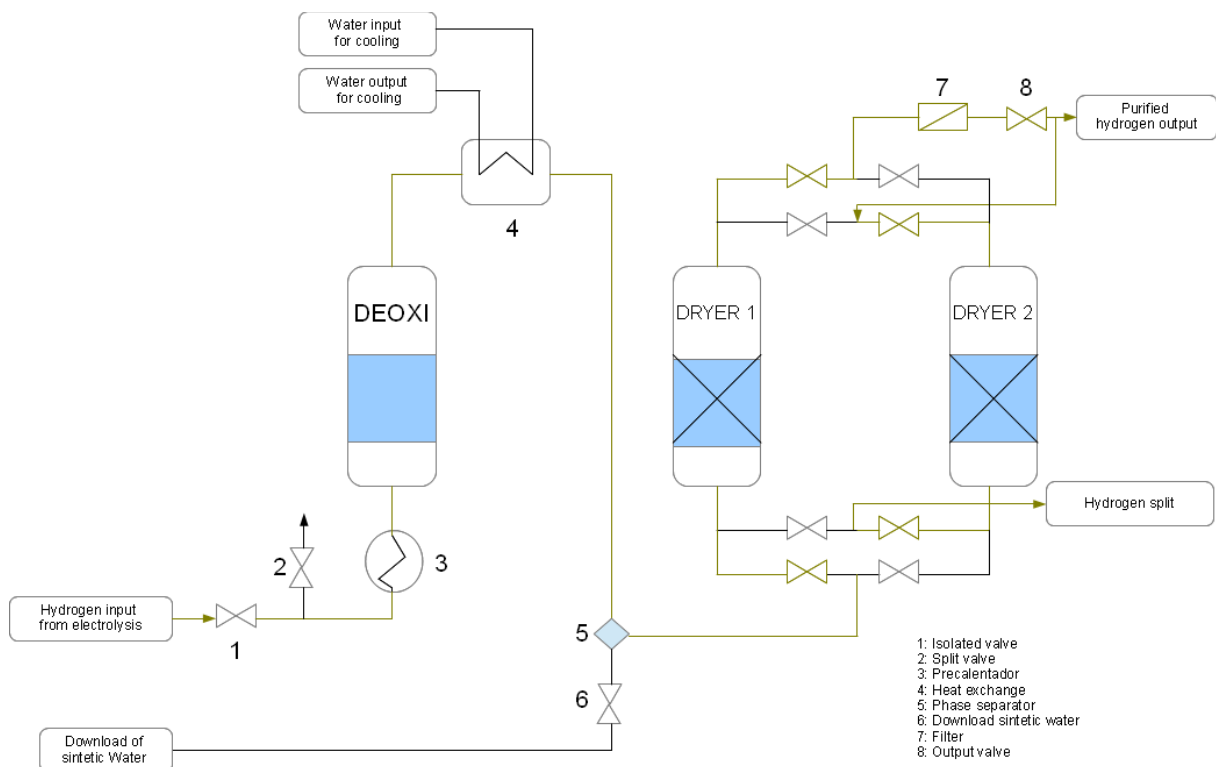


Figure 1b. Electrolyzer scheme: *purification section*.

These subsystems are represented on Figure 1. In Process section (Figure 1a) hydrogen and oxygen produced gas are separated from liquid electrolyte by gravity separators. Then three level

indicators (high, low and super-low) will inform the level of gas-liquid interface and then adjust the production ratio. Moreover, the difference between hydrogen and oxygen levels allow decide to open or no the purge valve to control the gas pressure. Next, Purification section (Figure 1b) is responsible for clean hydrogen from humidity. Dryers contain alumina and adsorb water excess that can be found in the hydrogen flow. In the circuit there are two dryer working in parallel and alternately (PSA technology), so that when the first one is filtering hydrogen, the other one is emptying the water contained in the alumina.

ELECTROLYZER CONTROL HARDWARE/SOFTWARE SYSTEM

The electrolyzer control sequence is shown is Figure 2. The operation status can be one of six possible states: Off, Standby, Purge, Production, Standby from production and Shutdown. Next, transitions between states are described.

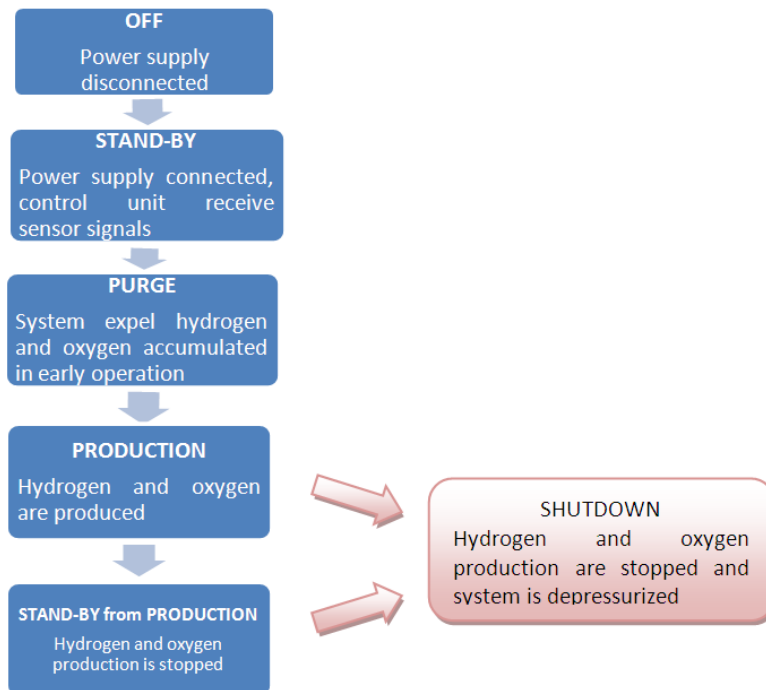


Figure 2. Electrolyzer control sequence.

- Off.- Electrolyzer doesn't receive electrical supply.
- Standby.- Electrolyzer receive electrical supply, and control unit receive sensors information.
- Purge.- System expel hydrogen and oxygen accumulated in early operations.
- Production.- Pressurized hydrogen and oxygen are produced.
- Stand-by from production.- Hydrogen and oxygen production are stopped.
- Shutdown.- Hydrogen and oxygen production are stopped (in case of production state) and system is depressurized.

Each state requires some variables to be controlled, so control system must guarantee transitions between states take place and moreover variables keep inside the admissible range

recommended by manufacturer. Table 1 shows the variable list to be controlled clasified by operation state.

Table 1. Variables list to be controlled.

State	Variables
Purge	Supplied Current (<20%) Electrolyte level on hydrogen and oxigen vessel (Figure 1a)
Production	Supplied Current (20% < current <100%) Electrolyte levels on hydrogen and oxygen vessel (Figure 1a) Hydrogen pressure (< 30 bar) Stack temperature (< 82 °C)
Shutdown	Electrolyte levels on hydrogen and oxygen vessel (Figure 1a)

Figure 3 shows an image of electrolyzer stack as well as purification section and the system control front panel.

ELECTROLYZER VIRTUAL INTERFACE

The virtual interface developed provides information about thermochemical variables like temperature, pressure and production ratio, and electrical variables like voltgae, current and power production. Additionally, the virtual interface (Figure 3) has been developed under three languages and is accesible by means the link: <http://172.16.183.115:8000/primera%20pantalla22.html>. Therefore a situation in which electrolyzer is running but it is not located at the same place where operator or technical supervisor is, the virtual interface allow knowing in real time the current electrolyzer state.



Figura 3. Virtual interface for electrolyzer monitoring.

CONCLUSIONS

This paper describes the operation principle of an electrolyzer and the operation sequence for the hydrogen and oxygen sequence. For a correct production, electrolyzer needs a control system where variable like electrical supply (power, current and voltage), temperature, pressure or even liquid electrolyte levels must be controlled. Additionally to tasks related to electrolyzer control, a virtual interface has been developed for monitoring the aforementioned variables.

The software tool developed has two main features which mean a contribution to hydrogen systems. These features are: 1) it is free and available for the whole scientific community, and 3) it offers a detailed description from producer hydrogen systems.

REFERENCES

- [1] T. Maeda, H. Ito, Y. Hasegawa, Z. Zhou, M. Ishida, "Study on control method of the stand-alone direct-coupling photovoltaic – Water electrolyzer", *International Journal of Hydrogen Energy*, Vol. 37(6), pp. 4819-4828, 2012.
- [2] S. Siracusano, A. Di Blasi, V. Baglio, G. Brunaccini, N. Briguglio, A. Stassi, R. Ornelas, E. Trifoni, V. Antonucci, A.S. Aricò, "Optimization of components and assembling in a PEM electrolyzer stack", *International Journal of Hydrogen Energy*, Vol.36(5), pp. 3333-3339, 2011.

High-purity hydrogen from acidic fractions of bio-oil by "steam-iron" (P-149)

J. Lachén, J. Plou, P. Durán, J. Herguido, J.A. Peña

*Catalysis, Molecular Separations and Reactor Engineering Group (CREG).
Aragón Institute of Engineering Research (I3A). Universidad Zaragoza.
Zaragoza. 50018 Spain. E-mail: jap@unizar.es*

INTRODUCTION

Bio-oil is one of the fuels embracing the philosophy of "Waste to Wheels" [1]. This is the liquid resulting from the fast pyrolysis of biomass. It is composed of a vast variety of hydrocarbons in different proportions; nevertheless there exist a general agreement in describing four different fractions according to its solubility in water and diethyl ether. These are labelled as alcoholic, aldehydic, phenolic and acidic fractions, being acetic acid the most abundant compound in the last of the above mentioned [2].

Present work explores the feasibility of simultaneously obtaining and purifying hydrogen (up to PEMFC quality) from the acidic fraction of a hypothetical bio-oil. For such purpose, acetic acid has been chosen as the most representative compound. The main novelty compared to other traditional methods such as steam reforming is that to carry out this task, it will be performed through the steam-iron process (or SIP) [3]. SIP is a cyclic process consisting of the reduction of an iron oxide to a lower oxidation state solid (e.g. metallic iron) by a reductive agent (e.g. acetic acid). The subsequent reoxidation of this metal with steam produces hydrogen as main gaseous product and the former iron oxide completing the cycle.

Previous works of this research group have demonstrated positively that the reduction of the iron oxide can be carried out with other components present in different fractions of bio-oil like methanol [4] and ethanol. In contrast with these alcoholic species, where iron oxide can be reduced with no extra aid at the reaction conditions, the reduction with acetic acid makes it necessary the presence of a catalyst in order to improve the reaction rate and adequate the distribution of products to maximize the yield to hydrogen minimizing the amount of coke deposited over the solid.

EXPERIMENTAL

The process has been carried out in a tubular lab-scale fixed bed reactor machined in quartz. The solid (see below), is supported in a porous plate made out of the same material than that of the reactor. During the reduction step, acetic acid is fed by a HPLC pump Shimadzu LC-20AT and vaporized by a 400W evaporator Tope®. Same equipment is used during the oxidation steps, in this case dosing water that enters the reactor as steam. At the exit of the reactor, a cold trap consisting in a Peltier cell operating at 10 °C retains the condensable species (mainly water and non-reacted acetic acid). Non-condensable gases are sampled by a micro-GC Agilent 490. The reactor operates at temperatures ranging from 550 to 800 °C heated up by a 10 kW oven Nabertherm (RHTV 120-300/16) that works at nearly isothermal conditions.

The solid, synthesized in our laboratory is composed of a mechanical mixture of iron oxide (reactant) and catalyst. Iron oxide is doped with minor quantities of ceria (1.75%w CeO₂) and alumina (0.25%w Al₂O₃) with the purpose of respectively, improving reaction rate and lower sintering. This solid accounts for the 90%w of the catalyst+oxide sample. Synthesis of the oxide is based in a sol-gel method (citrates) [5]. The catalyst is a non-stoichiometric nickel aluminate (NiO/NiAl₂O₄) with an excess of 10%w of NiO, precursor of the active metallic nickel. Synthesis of the catalyst is carried out by a co-precipitation method [6].

Once synthesized separately both solids are mixed up with silica (75:25 %w oxide+catalyst:silica) in order to reduce radial gradients of temperature inside the packed bed. The particle diameter is 160-200 μm for all the compounds.

RESULTS

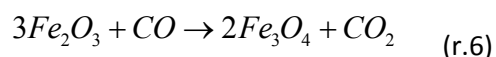
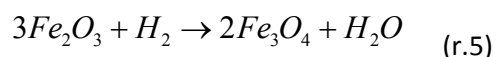
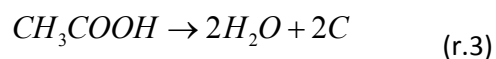
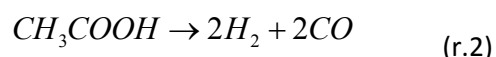
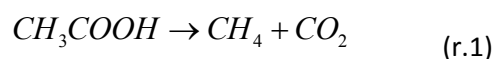
Reduction Step

The reduction step experiments were carried out at temperatures ranging from 650°C to 800°C. WHSV is approximately 1.6 g acetic acid / (g solid·h) and the total flow is 250 NmL/min.

Figure 1, shows the molar flows in the exhaust gases of H₂, CO and CO₂ coming out from the reactor for the reduction step. Methane was never detected and the acetic acid fed was fully converted into products.

The behaviour of the reaction can be divided into three stages:

Stage A: for the first 5 minutes the activation of the catalyst is accomplished through reduction of NiO to Ni. Also the reduction from Fe₂O₃ to Fe₃O₄ takes place during this stage, probably by means of hydrogen or carbon monoxide generated from acetic acid decomposition.



Stage B: The mix of gases is highly reductive during this stage. Reactions (r.7) and (r.8) are possible due to the high concentration of H₂ and CO. At 700°C, thermodynamic equilibrium (from the decomposition reactions, r.1, r.2 and r.3) predicts that the concentrations of gases are roughly [H₂] ~50%, [CO] ~40%, [H₂O] ~5%, [CO₂] ~5% and a very low quantity of CH₄. Also carbon is deposited on

the solid but in a low extent. Along this step, the iron oxide continues being reduced to metallic iron and an increment of H₂O and CO₂ is produced.



Stage C: The last period is easily noticed by a change in the gases distribution (e. g., from 25 minutes at 700°C). At this moment, the solid is mainly composed of Fe, Ni and SiO₂, so there is no possible reduction of any oxide. In parallel, gases distribution is governed by the Water Gas Shift equilibrium (r.4).

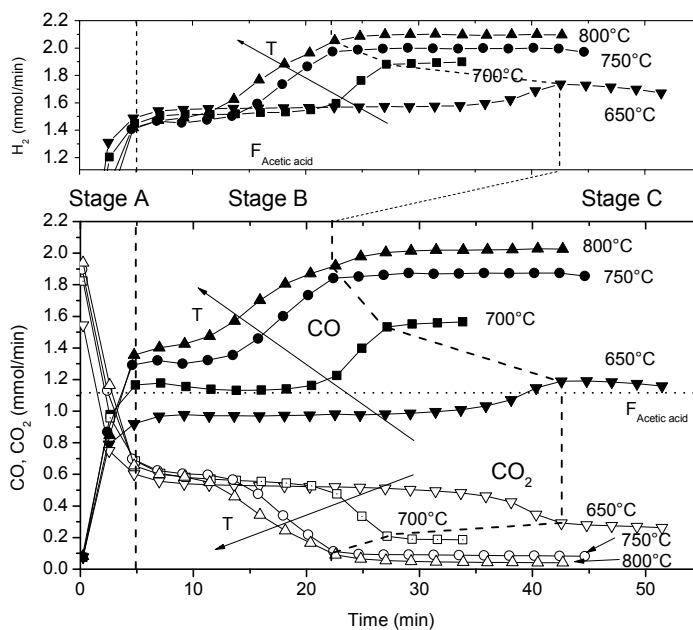


Figure 23 – Gaseous species distribution during a reduction step from 650°C to 800°C (F_{Acetic acid} = 1.117 mmol/min).

Oxidation Step

After the reduction described in the preceding section, and once the solid has been completely reduced to its metallic state, the following step of the process consists of the oxidation with steam to release high purity hydrogen and reoxidize the metal to a former oxidation state. To carry out this reaction, a working temperature of 550°C has been selected based on previous experience [7].

Figure 2 shows the amount of hydrogen released per 100 grams of iron depending on some operational variables such as the presence of catalyst and the number of redox cycles. It is remarkable that neither CO nor CO₂ were detected by GC. Consequently, high purity hydrogen (CO_x content lower than 1ppm) was obtained.

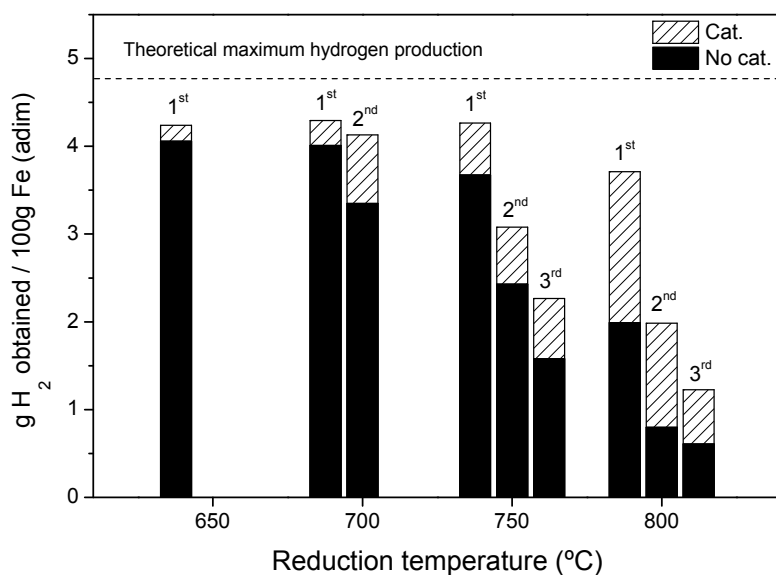


Figure 24 – Hydrogen obtained in the oxidation step for different operational variables (temperature and catalyst presence).

At low temperature only one cycle is evidenced because the amount of carbon deposited on the surface of the solid is too high. Consequently this favours the overpressure increase along the reactor up to a point in which it does not permit continuing the experiment. At high temperature the amount of carbon is lower but sintering reduces significantly the efficiency of the oxidation. As it can be evidenced, the presence of catalyst is positive because it not only reduces the time for complete reaction but because it also increases the amount of hydrogen produced (different product distribution).

CONCLUSIONS

It has been demonstrated the feasibility to produce high-purity hydrogen from acetic acid by steam-iron process. This information together with that obtained for other compounds also present in the organic fractions of a bio-oil (methanol, ethanol, acetaldehyde, phenol, etc.) could be used to determine a mathematical model capable of predicting the behaviour of a given bio-oil knowing only its composition.

During the reduction step there are two opposing effects: carbon deposition and thermal degradation of the solid (sintering). The first one is favoured with low temperatures not presenting an important effect on the stability of the solid along cycles. On the contrary, high temperatures inhibit the formation of significant amounts of coke, but inevitable provoke an important degradation of the solid that shorten its duty. As a consequence, an optimal reduction temperature of around 750 °C has been determined that favours the operation.

ACKNOWLEDGEMENTS

Financial support for this research has been provided by the Spanish Ministerio de Ciencia e Innovación (MICINN), through project ENE2010-16789. J. Plou also thanks the same institution for the grant BES-2011-045092. Financial aid for the maintenance of the consolidated research group CREG has been provided by the Fondo Social Europeo (FSE) through the Gobierno de Aragón (Aragón, Spain).

REFERENCES

- [1] Argonne National Laboratory, "Waste-to-Wheel Analysis of Anaerobic-Digestion-Based Renewable Natural Gas Pathways with the GREET Model". Energy Systems Division. ANL/ESD/11-6, 2011.
- [2] M.Bertero, G. de la Puente, U. Sedran. Fuel. 95 (2012) 263.
- [3] A. Messerschmitt. Process of producing hydrogen. U.S. Patent 971,206 (1910).
- [4] R. Campos, P. Duran, J. Plou, J. Herguido, J.A. Peña. Journal of Power Sources. 242 (2013) 520.
- [5] J.Kirchnerova, M. Alifanti, B. Delmon, Applied Catalysis A: General. 231 (2002) 65.
- [6] A. Al-Ubaid., E.E. Wolf. Applied Catalysis, 40 (1988) 73.
- [7] E. Lorente, J.A. Peña, J. Herguido, Int. J. Hydro. Energy 33 (2008) 615.

Hydrogen sensing properties of anodically synthesized porous TiO₂ film coated with Pd thin film and its mechanical enhancement by the bottom electrode configuration (P-151)

Jongyun Moon^{a*}, Hannu-Pekka Hedman^a, Marianna Kemell^b, Ermei Makila^c, Jarno Salonen^c, Aulis Tuominen^d, Risto Punkkinen^a

^a Department of Information Technology, University of Turku, Turku, FI-20014, Finland

^b Department of Chemistry, University of Helsinki, FI-00014, Finland,

^c Department of Physics, University of Turku, FI-20014 Turku, Finland

^d Department of Electrical engineering and automation, University of Vaasa

Summary

We report a hydrogen sensor having metal electrodes under the porous TiO₂ film, which was made by anodization of Ti film sputtered on SiO₂/Si substrate. Metal electrodes (Al, Au) were deposited on SiO₂/Si substrate before Ti deposition. After anodization using organic electrolyte, a thin Pd film was deposited on the surface of TiO₂ film. The material properties, such as pore structure, morphology and elemental composition were studied by FESEM and EDS. The response of the sensor based on the resistance change was measured at hydrogen concentrations ranging from 1 ppm to 10,000 ppm in ambient air at different temperatures.

Introduction

Due to the increasing needs of the renewable energies, the hydrogen fuel cell has been intensively studied to replace the traditional fossil fuels. Due to the explosive properties of hydrogen in air, highly sensitive hydrogen sensors are necessary in hydrogen fuel systems.

TiO₂ nanostructures, such as tubular structures synthesized by anodization of Ti foils, have shown an unprecedented sensitivity to hydrogen [1]. In spite of the incredible hydrogen sensing performance of nanostructured anodic TiO₂ film, the oxide film with a metal base can be mechanically vulnerable, thus more improvements are required regarding the electrical contact using wire-bonding. Some effort to produce more reliable and sensitive sensors has contributed to modifying the material structures, developing new sensor structures and synthesizing the sensor materials on different substrates, such as glass, alumina and silicon [2 - 3].

In our study, we succeeded in manufacturing a sensor that has an anodic TiO₂ film on a SiO₂/Si substrate using the bottom electrode configuration with a very thin Pd film deposited on the oxide film as a catalyst. Finally, its material and hydrogen sensing properties were studied.

Sensor preparation and material characteristics

Al was firstly sputtered in order to improve adhesion between the substrate and metal electrode, and Pt or Au were deposited through a shadow mask to form metal electrodes on a thermally oxidized silicon chip (TOX). Then, Ti film (99.9%) of ca. 500 nm was deposited by a DC magnetron sputter (BAL-TEC MED 020) in Ar at a pressure of 0.02 mbar at 150°C. As seen in Fig. 1 (a), the

schematic of the sensor imitates a traditional metal semiconductor sensor with the bottom electrode configuration that enhances the mechanical properties of the sensor based on anodic oxide film for the integration with micro-electric devices.

The anodization was performed in an organic electrolyte containing 0.25 wt.% of NH_4F in ethylene glycol. Electric potential of 20 - 60 V during the anodization was applied gradually with 1 V/s of a ramping rate. The anodization bath temperature was kept at 5°C by a refrigerated circulator (Neslab RTE-100). The current behavior during the experiment was monitored by a precision multimeter (Fluke 8846). Afterwards, a small amount of Pd (99.9%, approximately 2 nm) was deposited on the sensing area that covers both metal electrodes by the same sputtering method at room temperature.

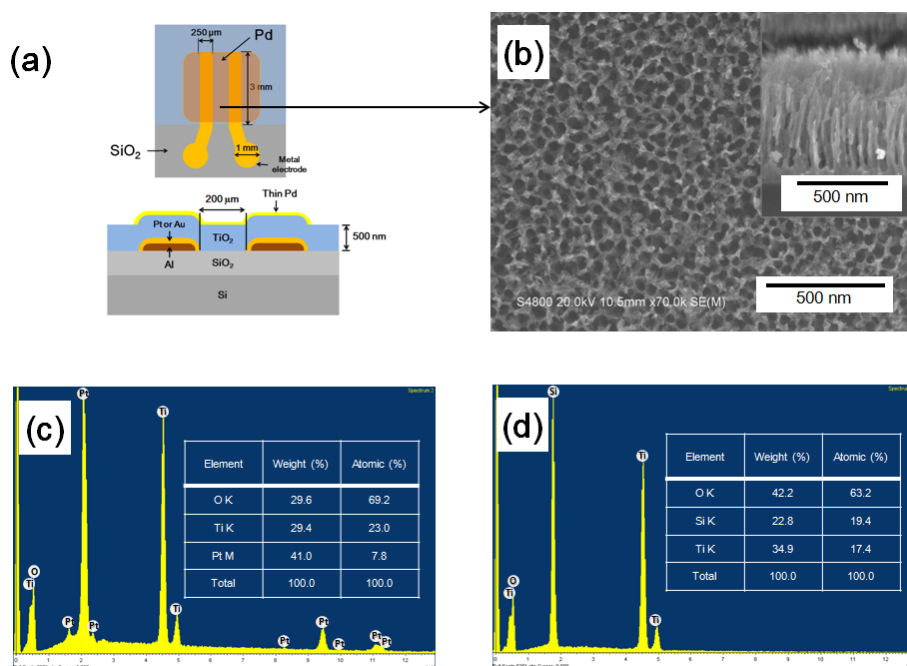


Fig. 1 - a) Schematic of the sensor configuration b) FESEM image of anodic TiO₂ film between the metal electrodes and inset; its cross sectional image, c) and d) EDS results of TiO₂ film on the metal electrode and SiO₂ substrate, respectively.

The surface morphology and the elemental composition analysis were performed by the field emission scanning electron microscopy (FESEM, Hitachi S-4800) equipped with the energy dispersive X-ray spectroscopy (EDS). The obtained TiO₂ film has porous structure with the average pore diameter of 20 nm and the average oxide thickness of 500 nm as seen in Fig. 1 (b). The porous TiO₂ film was formed uniformly on TOX substrate and the metal electrode. EDS result shows in Fig. 1 (c) and (d) that the relative intensity of the oxygen of TiO₂ film detected over Pt/Au metal electrode is smaller than the one on TOX. It is assumed because metal electrodes prevent to detect oxygen in SiO₂ layer. Thus, Si and Al elements were not visible. In addition, Pd peak was not detected on both areas.

The anodized sample was then annealed at 500°C for 6 h in ambient air with 1°C/min of the temperature ramping rate in a furnace (3-130 Furnace, Vulcan) for crystallization.

The sensor was attached on an alumina substrate and Cu wires were applied by using a silver paste to connect the electrodes to the coaxial cables of the measuring instrument.

Sensor characterization

The hydrogen sensing behavior of the sensor was monitored by the resistance change measured from the bottom electrodes by using a precision multi-meter (Keithley 6487 Picoammeter Voltage Source). The sensor was placed on a heater (15 mm × 15 mm, Ultramic 600, Watlow) to control the operating temperature.

Gas sensor measurement was performed in a closed 56 liter of glass test chamber and the air inside chamber was circulated by two wind pans. The hydrogen concentration in the chamber was created by adding a known volume of pure hydrogen.

The crystallized sensor was tested at hydrogen concentrations ranging from 1 ppm to 10,000 ppm at three different temperatures (140°C, 160°C and 180°C) in a humid ambient environment with ca. 50 % of a relative humidity. The response (S) of the sensor was calculated by the fomula

$$S = \frac{R_A - R_H}{R_A}, \quad (1)$$

where RA and RH are the resistance of the sensor in the air and the presence of hydrogen, respectively. The resistance change of the sensor during the hydrogen sensing measurement is described in Fig. 2 (a).

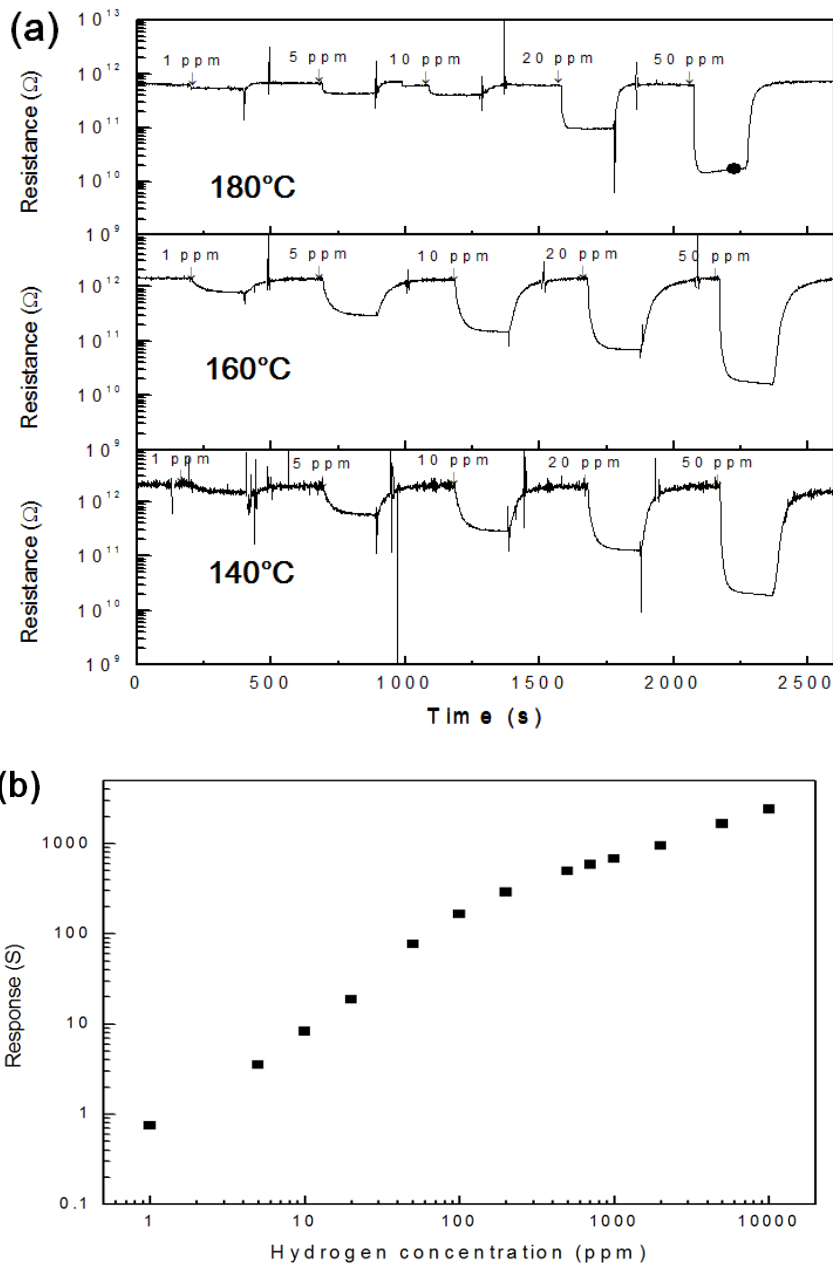


Fig. 2 - a) Resistance plot of anodic TiO_2 sensor upon exposure to hydrogen concentration (1 - 50 ppm) at different operating temperatures, b) Hydrogen sensing response as a function of hydrogen concentration (1 - 10,000 ppm).

The base resistance of the sensor decreases when the operation temperature increases. In addition, it is seen that the noise of the sensor signal was reduced at higher temperature. The highest response was observed at 160°C and their plot is described in Fig. 2 (b). The increase of the operating temperature improved the response/recovery time. The sensor was able to detect 1 ppm of

hydrogen concentration shown the response of 0.75 and any saturation phenomena was not observed up to 10,000 ppm of hydrogen with the response of 2400.

Conclusion and outlook

A gas sensor consisting of porous TiO₂ film with the bottom electrode configuration has been demonstrated to detect hydrogen in ambient air. Anodically prepared the oxide film with thickness of 500 nm is successfully formed with porous structure on both TOX and metal electrodes. Pd was sputtered on the oxide film as a catalyst, however, the elemental existence of Pd catalyst was not confirmed by our analysis method (EDS). The sensor shows a good response to hydrogen range from 1 ppm ($S = 0.75$) to 10,000 ppm ($S=2400$) at 160°C.

Further tasks will be laid on calibration of response and recovery time, in-dept material characteristics, such as crystalline structure, electrical property and catalytic properties.

Acknowledgement

J. Moon gratefully acknowledges Fortum Foundation (B2 grant number 12-118). Authors cordially thank Sensorex Oy, Finland, for the use of their facilities in hydrogen testing.

References

- [1] Paulose M, Varghese OK, Mor, GK, Grimes CA; Ong KG, Unprecedented ultra-high hydrogen gas sensitivity in undoped titania nanotubes. *Nanotechnology* 2006;17:398-402.
- [2] Moon J, Hedman H-P, Kemell M, Suominen A, Mäkilä E, Kim H, Tuominen A, Punkkinen R, A study of monitoring hydrogen using mesoporous TiO₂ synthesized by anodization. *Sens Actuators B Chem.* 2013; in Press:
- [3] Mor GK, Varghese OK, Paulose M, Ong KG, Grimes CA, Fabrication of hydrogen sensors with transparent titanium oxide nanotube-array thin films as sensing elements. *Thin Solid Films* 2006; 496: 42-48.

LIFE+ ZEROHYTECHPARK: “experiencie on low power pem fuel cell UPS systems for central servers” (P-153)

[AUTHORS: A. ARNEDO MONCAYO, Aragon Hydrogen Foundation; J. SIMON ROMEO, Aragon Hydrogen Foundation; L. ALBERDI JIMENEZ, Aragon Hydrogen Foundation; L. CORREAS USÓN, Aragon Hydrogen Foundation]

INTRODUCTION

The aim of the ZERO-HYTECHPARK project, part of the European LIFE+ program related to environment, is to achieve more sustainable technology parks. The project has a budget of 1.3 million Euros, 50% of which is financed by the European Union during four years (from 1 January 2010 to 31 December 2013).

The Foundation for the Development of New Hydrogen Technologies in Aragon coordinates this initiative with the participation of technology parks partners in Huesca, Andalusia and Bizkaia. ZERO-HYTECHPARK aims to achieve total sustainability in these areas via optimum energy management by means of systems based on hydrogen technologies and renewable energies.

The main project objectives are:

Achieve a building with virtually no CO₂ emissions.

Promote sustainable mobility.

Disseminate the technologies used to the general public and interested scientific and industrial sectors in particular.

This will be achieved by designing, simulating and starting up energy solutions in the headquarters building for the Development of New Hydrogen Technologies in Aragon, located in Walqa Technology Park in Huesca, whose results can be extrapolated to the rest of the buildings in the technology complex, as well as to other parks.

On this context a small 3kVAr peak power PEM fuel cell UPS systems for central servers has been installed and tested.

THE SYSTEM

Regarding a safe use of hydrogen it has been taking into account several hazards such as: the low amount of energy to ignite, the low percentage of hydrogen on air to create an explosive atmosphere and invisibility of the hydrogen and its flame. With these considerations installing a hydrogen UPS is more than “plug and play” a specific fuel cell.

The overall system is compound by:

- H2 PEM Fuel Cell (1.7kW nominal power)
- Power electronics (Online SAI) (3kVAR peak POWER)
- H2 storage (200 bar standard bottles)
- H2 leakage detection system
- Safety vented system



Illustration 1: Backup system, hydrogen storage and overall view with central server

The topology chosen for power electronics is the online UPS. This is an ideal topology for environments where electrical isolation is necessary or for equipment that is very sensitive to power fluctuations like servers and data centers. Although once previously reserved for very large installations of 10 kW or more, advances in technology have now permitted it to be available as a common consumer device, supplying all range from 500 watts or less.

The initial cost of the online UPS may be higher, but its total cost of ownership is generally lower due to longer battery life. The online UPS may be necessary when the power environment is "noisy", when utility power sags, outages and other anomalies are frequent, when protection of sensitive IT equipment loads is required, or when operation like in this case from an extended-run backup generator, (the fuel cell).

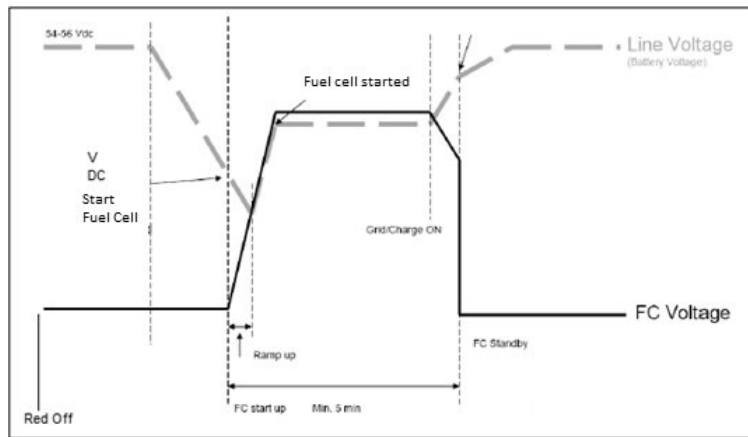


Illustration 2: system function graph

The system was firstly installed on April 2012, and since that date is being tested and used on the Aragon Hydrogen Foundation facilities. The three months first stage of test with electronics load was developed and successfully passed. Since June 2012 the UPS was connected to the server and supplying energy.

Hydrogen fuel cell power pack design (P-154)

Lorenzo Nasarre Cortés, Joaquin Mora Larramona, Alfonso Arnedo Moncayo, Lucia Alberdi Jimenez, Mariano Gomez and Luis Carlos Correas Usón for Aragon Hydrogen Foundation

With the requirements for reducing emissions, improving logistic investment and increase productivity, new markets as material handling have become attractive for hydrogen fuel cells technology, where there are battery-powered forklifts. This type of trucks has some serious drawbacks including:

- Vehicle and operator downtime for battery changes during shift
- Valuable warehouse floor space used for battery storage and recharging
- Decreased power as the battery discharges

Using hydrogen fuel cell power pack instead the battery pack, some impacts at distribution center are:

- \$0 invested in a battery charging and changing infrastructure
- Reduced operational costs
- Reduced carbon footprint
- Elimination of need to store and handle toxic lead-acid batteries.

Some fuel cell integrators are developing hydrogen fuel cell power pack for distribution center operators replacing on their forklift fleet the current battery pack to fuel cell power packs.



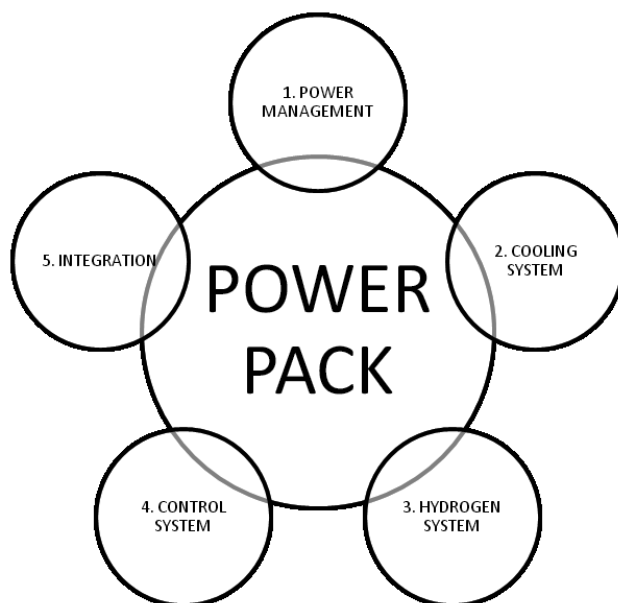
This paper introduces a complete system-level design and integration of a hydrogen fuel cell (PEM) power pack. We describe the entire design methodology in order to obtain an efficiency, reliable, robust, secure and low-cost industrial product, taking into consideration the health of people and the environment.

In this work the methodology has been developed. The methodology steps are: product requirements definition, system simulation and analysis, test program design, control and execution, control logic creation, reliability monitoring and forecasting, troubleshooting, commissioning and O&M engineering.

The system design has been created at two steps: stack balance of plan and power pack. Both have been designed by quality engineering applying the Excellence Methodology and Failure Mode and Effects Analysis (FMEA), systematic techniques for failure analysis for each component. The benefits of such a system can only be realized if the system is properly designed and sized, based on the technologies available and the application involved. Important task is the fuel cell stack balance of plant (BOP) that it is an ad-hoc design for forklift power pack application.

Fuel cell stack balance of plant consists of air supply subsystem (fan, intake filter, ducting, compressor, and humidifier), fuel supply subsystem (purge valve, anode recirculation blower) and controls (optimal stack operation). BOP behavior has been investigated in this study by an elaborated testing program, first each component separately way and then altogether.

A hydrogen fuel cell power pack has been designed. We have formulated all subsystems needed for a correct and safe operation. The power pack subsystems are power electronics (regulated DC power, battery or ultra-capacitors), coolant subsystem (coolant pump, radiator), hydrogen system (fuel storage, pressure regulator and supply valve), control subsystem (start-up, shut-down and hybrid systems) and final integration (packing, commissioning).



The strategy has been created for an optimal functioning of the stack, while ensuring the safety of your integrity, and end-user application. Also has been implemented in the Matlab/Simulink software

and its effectiveness is evaluated by the simulation results and experimental data from the testing power pack structure. The model developed here is able to predict nitrogen crossover issues, fuel starvation, pure recirculation, anode purge strategies, voltage and system efficiency and so on.

The control strategy has been loaded into the system ECU (electronic control unit). The ECU is designed to control all components of the BOP and the power pack: stack temperature, current and voltage, hydrogen and air pressure, lifeline, blower, fuel recirculation and more.

A GUI (graphical user interface) has been developed. Here the system is visualized and controlled a manual way because it is linked with the ECU, where also it is a data-logger, in order to make troubleshooting engineering by maintenance staff.

Using the hydrogen fuel cell power pack design methodology described in this work, we can provide a high-value way to industrial partners for promoting fuel cell development efforts towards commercialization; by creating industry-leading clean energy power solutions.

The Catalytic Activity of Carbon Nanotube Loaded Carbon Paper towards Oxygen Reduction Reaction in PEMFC (P-161)

Ki-Seong Lee¹, MinKu Lee², Tae-Whan Hong³, Whan-Gi Kim⁴, Hyun-Chul Ju⁵, Dong Min Kim^{1*}

¹Department of Materials Science and Engineering, Hongik University,
2639 Sejong-ro, Jochiwon, Sejong, 339-701, Republic of Korea

²Nuclear Material Development Division, Korea Atomic Energy Research Institute,
Yuseong, Daejeon, 305-353, South Korea

³Department of Materials Science and Engineering, Korea National University of Transportation,
50 Daehak-ro, Chungju, Chungbuk, 380-702, Republic of Korea

⁴Department of Applied Chemistry, Konkuk University,
322 Danwol, Chungju, Chungbuk, 380-701, Republic of Korea

⁵Department of Mechanical Engineering, Inha University,
253, Youghyun-dong, Nam-gu, Incheon, 402-751, Republic of Korea

The polymer electrolyte membrane fuel cells (PEMFCs) have been recognized as the efficient and environment friendly fuel cells that solely produce water as by-product without emitting any pollutants. It has received considerable attention because of its potential use in transportation and portable electronics. Since it was invented in 1839, Pt-based electro-catalysts have been used as electrode materials for the oxygen-reduction reaction (ORR) in PEMFCs. However, high price of Pt drives the researcher in this field to develop alternative electrode materials for example non-precious metal catalysts, which are potentially less expensive and more abundant. Many researchers have attempted to develop precious-metal-free cathode catalysts by employing alternative materials such as carbon nanotubes (CNTs). CNTs are carbon of a cylindrical nanostructure. These cylindrical carbon molecules have unusual properties which are valuable for nanotechnology, electronics, optics and other fields of materials science and technology. Owing to their extraordinary thermal conductivity, and mechanical and electrical properties carbon nanotubes find applications as additives to various structural materials.

In this study, we sprayed CNTs on carbon paper (CP). The prepared CNTs loaded carbon paper (CNT/CP) was investigated as an electrocatalyst for oxygen reduction reaction (ORR) in PEMFC using cyclic voltammetry (CV) and electrochemical Impedance spectroscopy (EIS).

Keywords: Spray, CNT, cyclic voltammograms, EIS, PEMFC

RF-Sputtered Gd-doped ceria (GDC) Thin Film as electrolyte for micro-SOFC (P-162)

*Young-Ku Jin, Ki-Seong Lee, Subrata Sarker, Dong Min Kim**

*Department of Materials Science and Engineering, Hongik University,
2639 Sejong-ro, Jochiwon, Sejong 339-701, South Korea*

Abstract:

Solid oxide fuel cells (SOFCs) convert chemical energy with high efficiency directly into electricity and heat, and can operate on a variety of fuels such as natural gas or hydrogen. Micro-SOFCs (MSOFCs), for low temperature operation, are suitable for portable electronic devices. Reducing the thickness of cell components with thin film process, especially for the electrolyte of high oxygen-ion conductivity, is needed to avoid the large Ohmic resistance at moderate temperatures (below 750 °C).

Here, we discussed the design, the fabrication process and the electrochemical performance of MSOFCs using GDC as an electrolyte. Electrochemical impedance spectroscopy (EIS) of Gd-doped ceria (GDC) as the electrolyte of micro solid oxide fuel cells (MSOFCs) is studied. The cells in this study were GDC sandwiched between two thin films of platinum (Pt) and SrRuO₃ (Pt/GDC/SrRuO₃) where GDC were deposited on SrRuO₃ by RF-sputtering method. The sputtering conditions for depositing GDC thin films were 100 W (RF power), 12/8 (O₂/Ar flow ratio) and pressure of 100 mTorr. The GDC sputter target was fabricated in laboratory using Gd/Ce (10/90). The microstructure was analyzed by X-ray diffraction and ionic conductivity was measured by Electrochemical Impedance Spectroscopy (EIS) in the quartz tube at high temperatures ranged from 300 to 750 °C. EIS study of the as deposited GDC allowed us to separate the individual electrode reaction and diffusion in the electrolyte and thus provided useful insight about the performance of GDC for micro-SOFCs. EIS spectra were interpreted assuming a porous electrode in contact with a solid electrolyte. Thus, the equivalent circuit model consists of a capacitor representing an electrode-electrolyte interface that is, an electric double layer paralleled with a resistor that corresponds to the polarization resistance.

The performance of the MSOFCs is limited by three loss mechanisms: Ohmic losses in the substrates and connecting wires; polarization losses through gas diffusion; and losses by activation polarization. EIS study of the Pt/GDC/SrRuO₃ system can successfully extract the information about activation polarization at the Pt/GDC interface. As a result, performance of GDC as electrolyte materials for MSOFCs could be inferred from the above study.

Ag-Modified Cu-Ceria Anode for SOFC directly fuelled with simulated biogas mixtures (P-164)

Araceli Fuerte¹, Rita Ximena Valenzuela¹, María José Escudero¹

¹ Centro de Investigaciones Energéticas Medioambientales y Tecnológicas (CIEMAT)
Av. Complutense 40, 28040 Madrid, Spain. Tel: +34 91 346 6622

ABSTRACT:

Traditionally, H₂ is a large-scale production by the reforming process of light hydrocarbons, mainly natural gas, used by the chemical industry. However, the reforming technologies currently used encounter numerous technical/scientific challenges, which depend on the quality of raw materials, the conversion efficiency and security needs for the integration of H₂ production, purification and use, among others. Biogas is a high-potential versatile raw material for reforming processes, which can be used as an alternative CH₄ source. The production of H₂ from renewable sources, such as biogas, helps to largely reduce greenhouse gas emissions. Within this context, the integration of biogas reforming processes and the activation of fuel cell using H₂ represent an important route for generating clean energy, with added high-energy efficiency.

Biogas is mainly constituted by CH₄ and CO₂ while containing a few percent of H₂, N₂ and trace contaminants such as NH₃, H₂S and halides. This composition fluctuates significantly during biogas production and it is highly dependent of the substrate used for the production process. It is well known that formation of carbon deposits on SOFC anodes can be minimize by anode morphology and operating parameters such as steam and current density [1]. Ammonia is not practically a problem in SOFC feeds, since it is oxidised to N₂ and H₂O in a two-stage process [2]. However, sulphur impurities can cause deactivation of most methane reforming catalysts or SOFC anodes, so they have to be removed from biogas feedstock before its use in fuel cell.

In this context, copper-ceria catalysts can be suggested as promising anodes for SOFCs directly feed by biogas. Several studies have demonstrated the ability of these materials to operate as SOFC anodes for direct methane oxidation [3,4] and good high sulphur tolerance. In this respect, previous work of our group demonstrated that co-doping of copper ceria induces changes in the redox properties and enhances the catalytic activity for methane oxidation. For example, the partial substitution of copper for cobalt reduced the carbon deposit formation [5]. On the other hand, doping these ceria based materials with an alkaline rare-earth (divalent cation Ca²⁺) increased the oxygen vacancy concentration and concomitant oxide ion conductivity that enhanced the anode performance [6]. Materials exhibited high sulphur tolerance and were able to operate at levels up to 500 ppm at 750 °C. Recently, we have demonstrated that the incorporation of a transition metal, such as silver, in these optimised formulations improves the catalytic properties of doped ceria for the complete oxidation of methane [7] as well as shows excellent thermal and chemical compatibility with electrolytes materials applied in SOFC. For that, this material can be considered a promising anode for SOFC directly fuelled with biogas.

The present work analyses a bimetallic Ag-Cu formulation combined with Ca_{0.2}Ce_{0.8}O_{2+δ} (AgCu-CaCe) focusing to its use as anode of SOFC directly fuelled with different simulated biogas mixtures,

at 750 °C. Its single cell evaluation, based on a La_{0.9}Sr_{0.1}Ga_{0.8}Mg_{0.2}O_{2.85} (LSGM) solid electrolyte and a LSM perovskite cathode, together with the electrochemical characterisation in a symmetric cell configuration have allowed to demonstrate the ability of this material to operate directly with simulated biogas mixtures without loss of single cell performance due to the formation of carbon deposits or sulphur anode poisoning. The results reveal significant modifications in the structural, catalytic/redox and electrical properties of the systems as a function of the presence of Ag Ag dopant in the formulation.

Reliable and stable single cell performance was achieved, under different atmospheres over a long term period (515 h) without evidence for sulphur or carbon poisoning of anode material (Fig. 1).

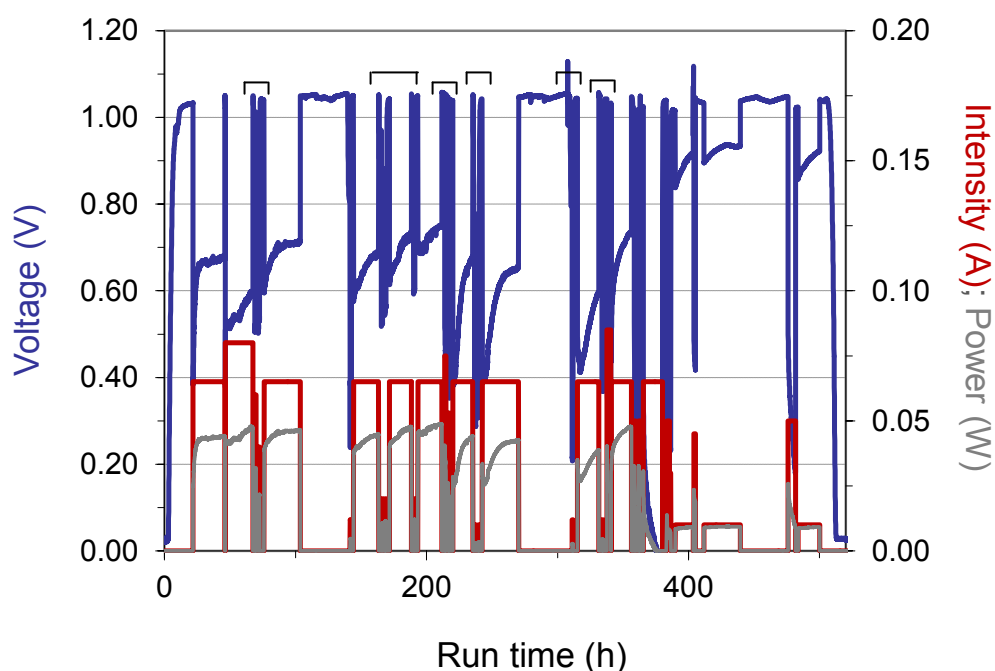


Fig.1. Global cell performance of AgCu-CaCe/LSGM/LSM single cell as function of time at several current densities and fuel composition. H₂ (without brackets); CH₄ (1); biogas (2); H₂/H₂S (3); biogas+H₂S (4); CH₄/H₂S (5)

The silver doping of basic copper-ceria formulation Cu-Ca_{0.2}Ce_{0.8}O_{2+ δ} (Cu-CaCe) enhances the catalytic activity for hydrocarbon oxidation, what improves the single cell performance using biogas as fuel, besides reduces the polarisation cell resistances (Fig. 2).

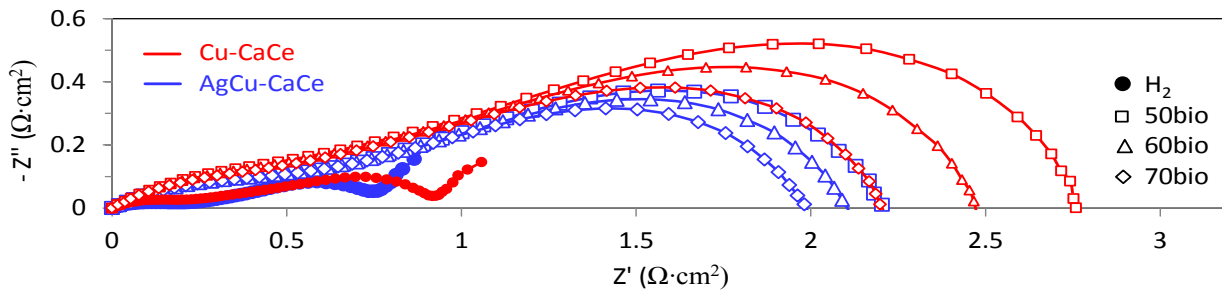


Fig. 2. Impedance spectra in symmetric cell configuration of Cu-CaCe (black line) and AgCu-CaCe (grey line) and LSGM electrolyte, in humidified H₂ and simulated biogas mixtures (50bio: 50CH₄:45CO₂:5H₂; 60bio: 60CH₄:35CO₂:5H₂; 70bio: 70CH₄:25CO₂:5H₂).

[1] Atkinson A, Barnett S, Gorte R.J, Irvine J.T.S, McEvoy A.J. et al., Nature 3 (2004) 17-27.

[2] Fuerte A, Valenzuela RX, Escudero MJ, Daza L. J Power Sources 192 (2009) 170-174.

[3] McIntosh S, Gorte RJ. Chem. Rev. 104 (2004) 4845-4865.

[4] Fuerte A, Valenzuela RX, Escudero MJ, Daza L. ECS Transactions 25 (2009) 2173-2182.

[5] Fuerte A, Valenzuela RX, Escudero MJ, Daza L. J Power Sources 196 (2011) 4324-4331.

[6] A. Fuerte, R.X. Valenzuela, M. J. Escudero, L. Daza. Proceedings of 9th European Solid Oxide Fuel Cell Forum 2010, 113-121.

[7] A. Fuerte, R.X. Valenzuela, M. J. Escudero, L. Daza, Proceedings of Fuel Cells 2012 Science & Technology, A Grove Fuel Cell Event, P71.

Photocatalytic hydrogen production from methanol over Cu-TiO₂ catalysts (P-166)

P.P.C. Udani, Eirik Djuve, Magnus Rønning

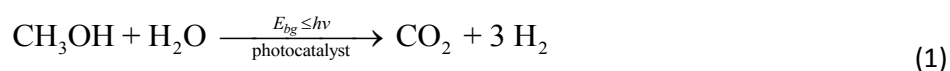
*Department of Chemical Engineering, Norwegian University of Science and Technology, NO-7491
Trondheim, Norway.*

1. Introduction

The photocatalytic hydrogen production is a challenging research topic which has received much attention in recent years for its potential to provide hydrogen as a clean and renewable energy carrier even on a large scale. Among the various fuels, methanol is identified as a promising candidate to produce hydrogen¹. Because it has a high hydrogen/carbon ratio and can be produced from renewable sources and, as a consequence, may be considered as a sustainable energy carrier.

Noble metal loaded TiO₂ has extensively been proved to be the best photocatalysts for hydrogen production, mainly because of their ability to enhance photoproduced electron–hole pair separation and photoinduced reduction processes²⁻³. However copper containing TiO₂ is cost effective compared with noble metal loaded TiO₂ and showed high photocatalytic activity in hydrogen generation⁴⁻⁶. Although Cu-TiO₂ catalysts have been used extensively in methanol photoreforming, the optimum composition of the catalysts for the reaction is still unclear and strongly depends on the reaction condition and preparation method. Moreover, there are relatively few reports dealing with continuous operation.

In this study, we have investigated photoreforming of methanol (Eq.1) with the use of UV light and Cu-TiO₂ photocatalysts in a semi-continuous reactor set up.



The effects of several parameters on the hydrogen production were studied, including copper loading, catalyst content in the suspension and initial methanol concentration. The photocatalysts were characterized by using XRD and N₂ physisorption before and after the activity measurement. The copper containing catalysts are compared with noble metal catalysts in terms of hydrogen production and stability.

2. Experimental

Catalysts were mainly prepared by using the incipient wetness impregnation method and TiO₂-P25 (Degussa) used as the photoactive support. In addition, other supports such as TiO₂-anatase have been used for comparison. The appropriate mass of nitrate salts of copper (Cu(NO₃)₂·3H₂O) was dissolved in deionized water to give the desired metal concentration. The volume added to the catalyst was just sufficient to fill the pores of the support. The impregnated support was then dried in an oven at 110 oC overnight, and was calcined in a muffle furnace at 200 oC for 4 h. The calcined catalysts were lightly ground and sieved before use. The copper content of the final catalyst was

determined by the concentration of the copper nitrate solution used in the impregnation, and was denoted by the weight percentage of copper in the catalyst: $\text{Wt \%} = (\text{wt Cu}/\text{wt (Cu+TiO}_2)) \times 100$

The photocatalytic reaction was performed in a homemade cylindrical quartz reactor (volume:~ 1.2 l) and was kept inside the photoreaction chamber. The chamber was equipped with 14 UVC (15 W, 254 nm) lamps and a magnetic stirrer. To maintain a constant reactor temperature, the exhaust tubing of the reaction chamber was connected to the ventilation system. Typically, 0.25 g powder of photocatalyst was dispersed in the reactor containing 500 ml of 50 vol.% methanol solution. Prior to the irradiation, the photocatalyst suspension in methanol solution was deaerated thoroughly for 30 min by a 100 ml/min flow of Ar. The reactor effluent was analyzed on-line with a TCD micro gas chromatograph (Agilent Technologies 3000) with a molecular sieve column. Ar was used as carrier gas and the GC response was first calibrated by introducing known flow of hydrogen into the system

X-ray Powder Diffraction (XRD) patterns were obtained using a Bruker D8 Advance X-ray Diffractometer with Cu-K α radiation ($K\alpha = 1.54 \text{ \AA}$) in the scanning angle (2θ) range of 20-80 $^\circ$. The specific surface area of the catalyst was measured by the BET method (Micromeritics Tristar II 3020). To remove traces of water and impurities from the catalyst surface, all samples were degassed overnight at 200 $^\circ\text{C}$ before the measurement.

3. Results and discussion

3.1 Photocatalytic activity

Photocatalytic activity increased with copper loading up to 5 wt% and then showed nearly constant hydrogen evolution as further increase in copper loading as showed in Figure 1. However different values are reported in the literature as optimum copper loading⁵⁻⁶. This is most likely due to reactor configuration and photon penetration depths. The catalysts supported on TiO₂-anatase showed lower hydrogen evolution compared to P25 supported catalysts. The TiO₂-anatase supported catalysts followed the same trend when changing the copper loading.

No significant hydrogen evolution is detected with pure TiO₂-P25 and pure CuO. Blank runs without photocatalyst, and also with absence of UV irradiation showed no hydrogen evolution, confirming the photo-induced reaction. This shows that the coexistence of TiO₂, CuO and UV-irradiation is essential to produce hydrogen from methanol.

The time course of photocatalytic hydrogen production from methanol over 10 wt% Cu-TiO₂ was studied under the conditions of initial methanol concentration being 50 vol.% at room temperature for 24 hours. The hydrogen evolution increases significantly at the beginning of the reaction and after approximately 5 hours, the hydrogen evolution reaches to a maximum level and then no significant change in hydrogen evolution observed. The results indicate that the Cu-TiO₂ photocatalyst is a relatively stable photocatalyst for the hydrogen production from methanol.

The photocatalytic activity of TiO₂ impregnated with different metals decreased in the order of Pd > Au > Cu according to the preliminary results in a comparative study of Cu-TiO₂, Au-TiO₂ and Pd-TiO₂. However, after 10 h of reaction, the hydrogen evolution activity changed to Au > Pd > Cu.

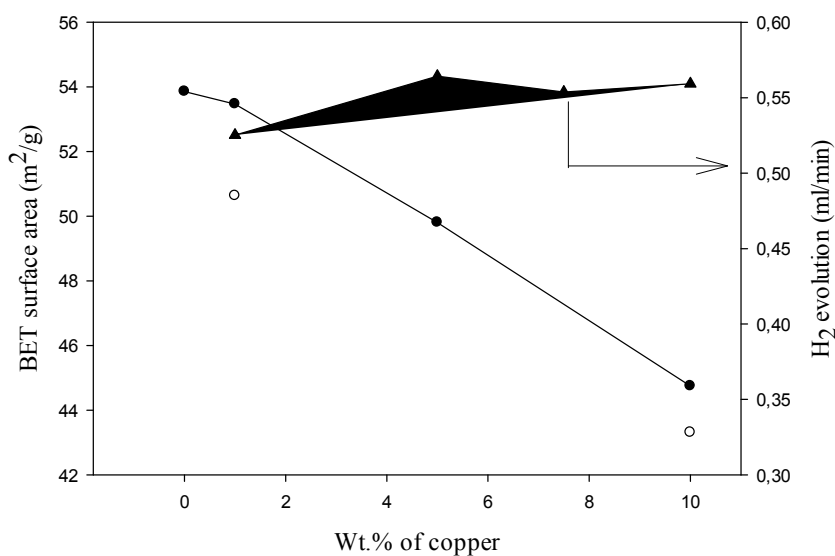


Figure 1. The effect of copper loading (▲) and BET surface areas of fresh (●) and used (○) photocatalysts.

3.2 Effect of catalyst loading

The effect of catalyst loading on hydrogen evolution over 10 wt% Cu-TiO₂ was investigated by varying the catalyst mass in the suspension. As shown in Figure 2A, hydrogen evolution increased when the mass of catalyst was increased from 0 mg to 500 mg. After that, no further increase in the hydrogen evolution was observed. This may be due to the excess of particles inhibiting the penetration of light through the reactor. When a higher mass of catalyst was used, it is observed that the catalyst particles tend to agglomerate forming larger particles. This may also prevent the accessibility of the UV photons.

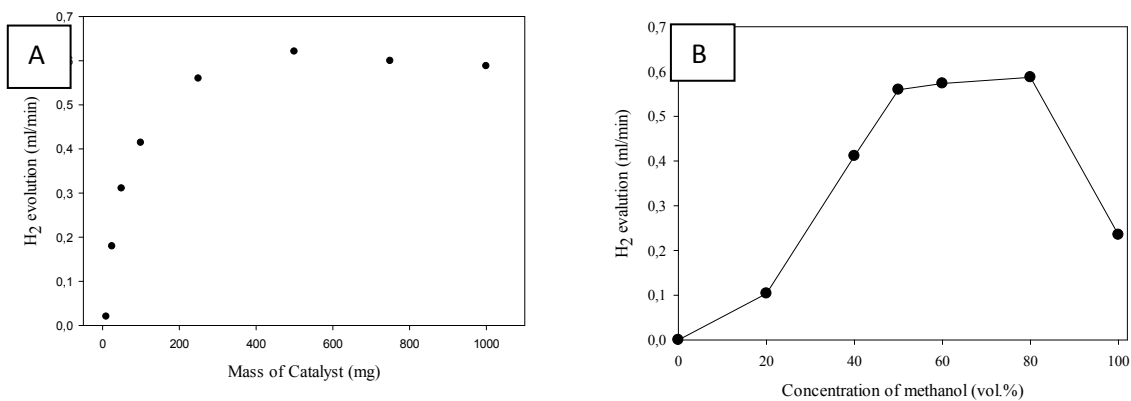


Figure 2. A. The effect of catalyst loading and B. The effect of initial methanol concentration.

3.3 Effect of initial methanol concentration

The effect of initial methanol concentration was also studied over 10 wt% Cu-TiO₂ catalyst and is shown in Figure 2B. Hydrogen production increased with increasing methanol concentration up to 50 vol.%. In the range of 50-80 vol.%, the hydrogen production was almost constant. However further increase in methanol concentration showed decrease in hydrogen production. When methanol concentration is low, the rate of photocatalytic reaction is limited by the mass transfer of methanol from the solution to the catalyst surface. As the concentration of methanol increases, more methanol molecules can be adsorbed on the surface of the photocatalyst. But the relative amount of reactive species formed on the surface of the catalyst will not increase, as the light intensity and catalyst amount remain constant.

3.4 BET surface area

The BET surface areas of both fresh and used catalysts decreased with increasing copper content as shown in Figure 1. The photocatalysts did not show any significant change in the surface area after being exposed to reaction conditions. As discussed in the previous section, photocatalytic activity increased with copper loading up to 5 wt% and then showed nearly constant hydrogen evolution as further increase in copper loading. However, the BET surface area of the catalyst with high copper loading is lower than those of lower copper loading catalysts, indicating the BET surface area may not be a critical parameter in the photocatalytic activity.

3.5 X-Ray Diffraction (XRD) analysis

In the XRD patterns of fresh catalysts, no detectable diffraction peaks of CuO crystallites could be distinguished for copper loadings less than 5 wt %. Lack of CuO peaks at low copper loading suggests that CuO particles are too small to be detected by XRD or present in a highly dispersed amorphous state. When the copper loading is above 5 wt%, the XRD peaks corresponding to CuO crystal phases were observed at $2\theta = 35.5$ and 38.7 and the intensity increased with increasing copper loading. The copper in all the fresh catalysts was in the form of CuO.

However, the state of copper was changed after exposure to reaction conditions. Copper was present as metallic copper and Cu₂O after the reaction. Furthermore, no significant changes in the characteristic peaks of TiO₂-P25 were observed for the fresh catalysts, indicating that there was no phase transformation in the TiO₂ support during the preparation.

4. Conclusion

Continuous photocatalytic hydrogen production from methanol and water has been demonstrated. The results indicate that the coexistence of Cu and TiO₂ was required to enhance the photocatalyst performance. The 5 wt.% Cu-TiO₂ catalyst showed the highest hydrogen production under the experimental conditions used in this study. In addition, Cu-TiO₂ can be considered as a promising photocatalyst to produce hydrogen from methanol by considering its' photoactivity, stability and cost when compared to noble metal loaded photocatalysts.

References

T. Miwa, S. Kaneco, H. Katsumata, T. Suzuki, K. Ohta, S. C. Verma, K.Sugihara, Int. J. hydrogen Energy 35 (2010) 6554.

G. Wu, T.Chen, W. Su, G. Zhou, X. Zong, Z. Lei, C. Li, Int. J. Hydrogen Energy 33 (2008) 1243.

S.S. Tan, L. Zou, E. Hu, Catal. Today 115 (2006) 269.

Y. Wu, G. Lu, Shuben Li, Catal. Lett. 133 (2009) 97.

S. Xu, D.D. Sun, Int. J. hydrogen Energy 34 (2009) 6096.

T. Sreethawong, S. Yoshikawa, Catal. Commun. 6 (2005) 661

High V.LO-City: speeding up fuel cell hybride bus deployment in European cities (P-168)

Paul Jenné (Van Hool) , Dalijt Bawa (Ballart)

Since 2002 several EU supported fuel cell bus programmes have successfully demonstrated the technical feasibility of operating fuel cell buses and refuelling hydrogen in public transport operations. Bus manufacturers consider the fuel cell hybrid (FCH) bus as the most promising technology to substitute the diesel hybrid bus in the coming years, as FCH technology will contribute significantly to reduce local transport emissions and to simplify operations. In order to facilitate a smooth integration of FCH buses, specific requirements with regards to maintenance, environmental and financial sound operations of public transport fleets need to be addressed, including:

- • Increase energy efficiency of buses
- • Reduce the total cost of ownership
- • Increase the life time of the fuel cells
- • Reduce life cycle costs and more specifically the cost of hydrogen
- • Define concrete economic early markets

Within the context of the 7th framework programme – Fuel Cells and Hydrogen Joint Undertaking (FCH JU), the High V.LO-City project has been in place since late 2011; this five-year project has a total budget of 31.5 million Euro. It involves three regions (Flanders, Liguria and Scotland), which were also the source of the name assigned to the project, High V.LO-City: V = Flanders, L = Liguria and O = ScOtlad. The choice of three different regions will allow to conduct the tests on different areas and climates.

High V.LO-City will operate III generation of hybrid fuel cell buses manufactured by Van Hool: Liguria and Flanders will have 5 buses each, while Scotland will have 4, all will be in operation in 2014. The project partners are Van Hool (project leader and vehicle manufacturer), Dantherm Power (fuel cell manufacturer), Ballast Nedam (manufacturer of refuelling infrastructures), Solvay (hydrogen producer), Waterstofnet (specialist in hydrogen refuelling and storage facilities), three Regions (Regione Liguria, Flanders and Aberdeen City Council), three transport operators (Riviera Trasporti, De Lijn and), one research body (DITEN Department of Electrical, Electronic and Naval Engineering, University of Genoa), a member body at the European level for fuel cell studies (HyER – European Association of Hydrogen, fuel cells and Electro-mobility in European Regions) and FIT Consulting (project management specialist).

The latest generation of FCH buses in the High V.LO-City project reaches efficiency levels that go far beyond those tested in previous fuel cell bus projects. In addition, experiences from past projects point to the importance of addressing public transport needs for more flexibility and for modular hydrogen capacity build- up, that have not been implemented so far. Last but not least EU regulations, as the EU Directive on the promotion of clean and energy efficient road-transport vehicles (COM 2009/33) require public authorities to include life cycle costs including energy consumption and CO2 emissions into their procurement decisions.

The High V.LO-City project aims at accelerating the integration of a new generation of FCH buses in public transport fleets by demonstrating the technical and operational quality, their value in creating a clean and highly attractive public transport service and in facilitating the modular shift that local transport policies are envisioning. By linking effectively previous and future demonstration sites, the project seeks to further broaden and consolidate a network of successful FCH bus operators that is able to widen the dissemination of FCH bus operations in Europe.

Reinforced Polymeric Ionic Liquid Membranes for HT PEMFCs (P-174)

F.J. Lemus; A. Eguizábal; M.P. Pina

Chemical Engineering Department, Nanoscience Institute of Aragón (INA); Edif. I+D, Campus Rio Ebro, c/Mariano Esquillor s/n, 50018 Zaragoza, Spain.

INTRODUCTION

The deployment of protic ionic liquid based membranes as electrolytes membranes for HT PEMFCs [1] could alleviate or eventually suppressed the common encountered problems in this field [2] (phosphoric acid catalyst poisoning, conductivity losses due to dehydration, acid oligomerization...). These organic salts are able to transport protons due to their acid-base character and their capability to form complex or intermolecular hydrogen bonds [3]. However, liquid electrolytes do present some disadvantages, such as need of encapsulation due to leakage under FC operation [1], [4], [5]. For these reasons, there is an increasing interest in designing polymer electrolytes composed of ILs [6], [7]. Polymer Ionic liquids (PILs), as solid-state polymer electrolytes, allow to improve mechanical stability, safety and simple processing.

In this work PILs based membranes have been synthesized by ultraviolet radiation-induced polymerization [8]. By this polymerization method, two different approaches have been developed for the preparation of reinforced electrolyte membranes [9]: pure PIL films and supported PIL on polybenzimidazole (PBI) porous matrix. In the first case, different cross-linker (CL) percentages (0, 1, 3, 5 and 10%) have been studied in order to find the optimum in terms of mechanical properties, chemical stability and conduction performance. The second approach, involves the preparation of porous PBI supports, the monomeric IL infiltration and the in-situ UV polymerization.

EXPERIMENTAL AND RESULTS

Poly[1-(3-H-imidazolium)ethylene] bis(trifluoromethanesulfonyl imide based films have been obtained by UV assisted polymerization (365nm, 2.4 mW/cm², 15 min) of commercial 1-H-3-vinylimidazolium bis(trifluoromethanesulfonyl)imide in presence of 2-hidroxy-2-methylpropiophenone (1% wt) as photo-initiator. By this polymerization method, two different approaches have been developed for the preparation of reinforced poly[1-(3H-imidazolium)ethylene] bis(trifluoromethanesulfonyl imide solid electrolyte membranes. The first one involves the copolymerization with divinylbenzene (from 1% to 10% wt.) as cross-linker (CL) agent. Pure PIL films exhibit proton conductivity values higher than 1000 mS/cm at 150°C. In general, the proton conductivity decreases with the cross-linker percentage (i.e., 1000 mS/cm for 0% of CL to 0.64 mS/cm for 10 % CL at 150°C). This behavior is related to the blocking of terminal conducting groups by crosslinking process. Thus, higher CL degree increases the rigidity/fragility of the membrane. The most distinguished feature of PILs proton conduction performance is the activation with temperature. The optimum CL range from mechanical and conduction properties is identified at 1% of CL.

PIL reinforcement has also been attained by supporting on preexisting porous polymer membranes.. In particular, PIL supported membranes have been successfully prepared by vacuum

assisted filtration of monomeric 1-H-3-vinylimidazolium bis(trifluoromethanesulfonyl)imide on polybenzimidazole (PBI) membranes 85% in porosity and circa 200 nm in pore size (prepared in the lab by delayed demixing method^{1,9-(1)}), followed by in situ UV polymerization (see Figure 1). Thus, the PIL supported onto porous PBI membranes will be easier to implement in the standard MEA procedures already developed for high temperature PEM based on PBI.

Figure 2.a comparatively shows the proton conductivity of the outperforming reinforced PIL electrolyte membranes. The conduction-temperature dependence is similar to the observed for pure PIL without CL. For reinforced PIL-PBI membranes conductivities values up to 250 mS/cm and 340 mS/cm at 150°C and 200°C respectively, are achieved in presence of 5% of water partial pressure. For such PIL based membranes, time on stream conduction measurements were carried out at 200°C for more than 1.000 h (40 days) (see Figure 2.b). After the initial losses in performance, the steady state values attained are 350 mS/cm and 275 mS/cm for PIL+1% CL and PIL/PBI respectively.

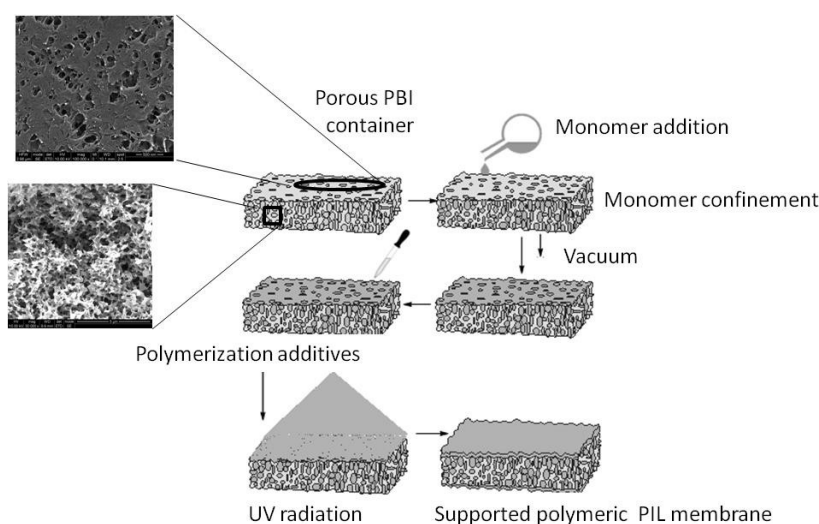


Figure 1. Preparation scheme for Supported Polymeric Ionic Liquids Membranes on porous polybenzimidazole (PBI) containers.

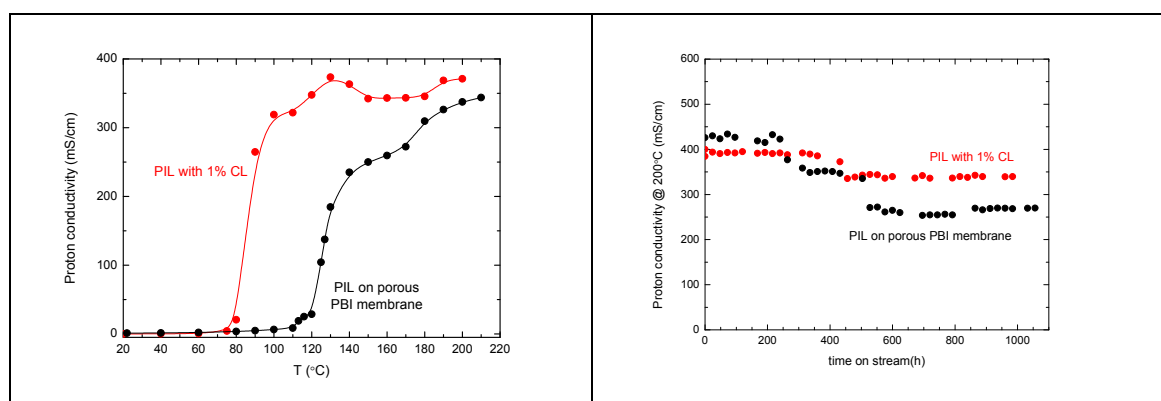


Figure 2. Proton conduction performance of reinforced PIL membranes in presence of 5% of water molar fraction: a) conductivity-temperature dependence; b) endurance properties.

CONCLUSIONS

Reinforced PIL films have been prepared either by copolymerization or embedding in a porous container. The physico-chemical and electrochemical characterization results have demonstrated their suitability as solid electrolyte membranes for HT-PEMFC applications. Our research efforts are focused on specific MEAs development for high H₂/O₂ single cell testing. The authors would like to acknowledge financial support from the European Commission through the FP7 funded project ZEOCELL Grant Agreement 209481.

CITED REFERENCES

[1] A. Eguizábal, J.Lemus, V. Roda, M. Urbiztondo, F. Barreras, M.P. Pina. International Journal of Hydrogen Energy, 2012, 37(8), 7221-7234.

[2] J.A. Asensio, E.M. Sanchez, P. Gomez-Romero, Chem. Soc. Rev, 2010, 39(8), 3210-3239.

[3] T. L. Greaves, C. J. Drummond, Chemical Reviews, 2008, 108, 206-237.

[4] A. Eguizábal, J.Lemus, A.M. Moschovi, S. Ntais, V. Nikolakis, J. Soler, M.P. Pina, Journal of Power Sources, 2011, 196, 4314-4323.

[5] A. Eguizábal, J.Lemus, M.P. Pina, Journal of Power Sources, 2013, 222, 483-492.

[6] D. Mecerreyes. Progress in Polymer Science, 2011, 36(12), 1629-1648.

[7] Y. Jiayin, D. Mecerreyes, M. Antonietti. Progress in Polymer Science, 2013, 38, 1009-1036.

[8] J.E. Bara, S. Lessmann, C.J. Gabriel, E.S. Hatakeyama, R.D. Noble, D.L. Gin. Industrial & Engineering Chemistry Research, 2007, 46(16), 5397-5404.

[9] F.J. Lemus, A. Eguizábal, M.P. Pina. Membranas reforzadas basadas en líquidos iónicos poliméricos para su aplicación en procesos de transporte de iones y métodos de fabricación de dichas membranas. 2012, P201231812.

[10] A. Eguizábal, J.Lemus, O. Garrido, M.Urbiztondo, J. Soler, A. Blazquez, M.P. Pina, Journal of Power Sources, 2011, 36(6), 813-843.

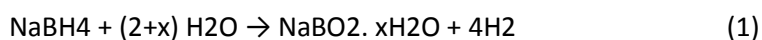
Hydrogen generation by hydrolysis of sodium borohydride with bentonite supported Co-B catalyst (P-175)

Joydev Manna^{1,a}, Binayak Roy^{1,b}, Devendra Pareek^{1,c}, Pratibha Sharma^{1,d}

¹Department of Energy Science and Engineering, Indian Institute of Technology Bombay, Mumbai-400076, Maharashtra, India

ajoydev@iitb.ac.in, broy_binayak@iitb.ac.in, cdevpareek@iitb.ac.in, dpratibha_sharma@iitb.ac.in

One of the current global challenges is implementation of hydrogen economy over the existing fossil fuel economy. A suitable hydrogen storage material with high storage capacity (7.5 wt%) at optimum condition (temperature and pressure) and low cost may fulfill the desire target. Pressurized and cryogenic liquid storage do not favor the aforementioned objectives. Metal hydrides give a great opportunity to store hydrogen in solid-state at moderate condition and also give an important safety advantage over the gas and liquid storage methods [1]. But heavy weight of metal reduces the gravimetric storage capacity. However, this problem is resolved in complex hydrides (e.g. LiBH₄, NaBH₄, NaAlH₄ etc.) due to their light weight and consequent high gravimetric hydrogen storage capacity but they suffer from high decomposition temperature and irreversibility [2]. Sodium borohydride is a potential hydrogen storage material with a hydrogen storage capacity of 10.8 wt%. Moreover hydrogen can be generated from sodium borohydride by means of hydrolysis at room temperature and atmospheric pressure. Hydrolysis of sodium borohydride follows the following reaction pathway [3]:



Self-hydrolysis of sodium borohydride occurs when NaBH₄ comes in contact with water. But the reaction is not spontaneous and stops after sometime due to increase in pH of the solution, owing to the formation of byproduct NaBO₂ [3]. Therefore a suitable catalyst is required to make this reaction spontaneous as well as extract all of the hydrogen from NaBH₄. There have been many catalysts tested to improve the sodium borohydride hydrolysis reaction. Noble metals (Pt, Rh, Ru etc.) being the most effective but their high cost limits their wide application [4], [5], [6]. Cobalt-based catalysts, especially cobalt boride alloy (Co-B), have potential catalytic activity to replace noble metals in NaBH₄ hydrolysis [7]. Co-B catalysts can be easily synthesized by reduction of cobalt(II) salts, but the Co-B particles so synthesized always are found to be in agglomerated state, due to high surface energy involved in the exothermic reduction process [8]. The effective surface area of the agglomerated Co-B particles is very less and consequently the catalytic activity also diminishes. Therefore, catalytic activity of Co-B can be improved by dispersing the particles in a suitable support material.

In the current work, low cost, abundant bentonite clay was used as a support material for cobalt boride catalyst. Cobalt boride was loaded into the bentonite clay by two step impregnation-reduction methods. The prepared catalyst was characterized by X-ray diffraction (XRD), Fourier transform IR spectroscopy (FTIR), Field gun emission scanning electron microscopy (FEG-SEM), Inductive coupled plasma atomic emission spectroscopy (ICP-AES) and N₂ adsorption-desorption (BET) isotherm. Hydrogen evolutions from stabilized alkaline (0.5 M NaOH) solution of sodium borohydride (0.02 M)

were measured in an indigenously assembled hydrolysis set-up by water displacement method. Hydrolysis reactions were performed at different temperature to calculate the activation energy of the reaction.

The obtained catalyst was found to be amorphous in nature with 15 wt% of Co-B loading into bentonite. From FTIR and BET surface area measurements successive loading of Co-B in bentonite was also confirmed. The hydrolysis results (Fig.1) demonstrated a much higher hydrogen generation rate (HGR) compared to hydrolysis reaction catalyzed by unsupported Co-B. For unsupported Co-B HGR was found to be 132 ml min⁻¹ g⁻¹Co-B, whereas for bentonite supported Co-B catalyst HGR was 602 ml min⁻¹ g⁻¹Co-B at room temperature. The effect of solution temperature on sodium borohydride hydrolysis is shown in Figure 2. From the figure it can be seen that with the increase in temperature rate of the reaction increases. Activation energy of the reaction is calculated using Arrhenius equation and it has been found that the activation energy (36.48 kJ mol⁻¹) in presence of bentonite supported Co-B is notably less compared to the activation energy (45 kJ mol⁻¹) with unsupported Co-B hydrolysis reaction.

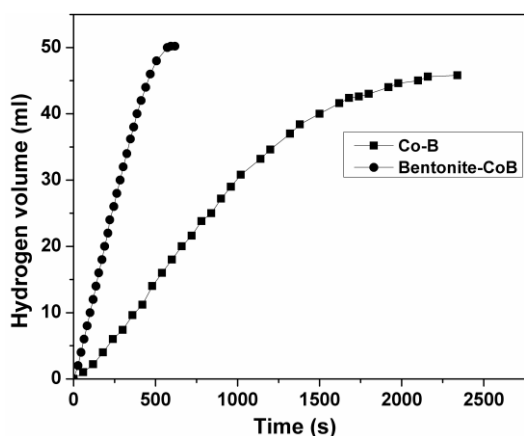


Figure 25: Hydrogen generation plots of pure Co-B and bentonite supported Co-B

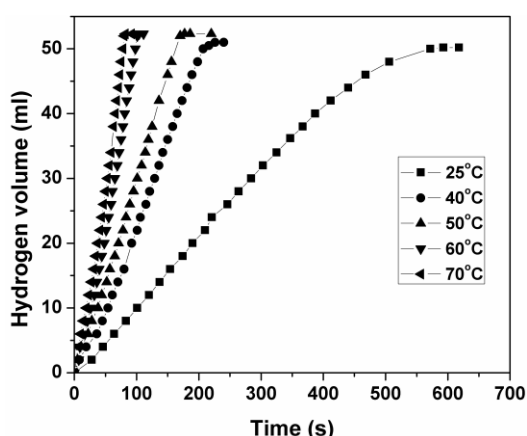


Figure 2: Hydrogen generation plots of bentonite supported Co-B catalysts at different solution temperature

References:

- [1] L. Schlapbach and A. Züttel. "Hydrogen storage materials for mobile applications" *Nature*, 414, pp. 353–358, 2001.
- [2] S. Orimo, Y. Nakamori, J. R. Eliseo, A. Zu, and C. M. Jensen. "Complex Hydrides for Hydrogen Storage" *Chem. Review*, 107, pp. 4111–4132, 2007.
- [3] H. I. Schlesinger, H. C. Brown, A. E. Finholt, J. R. Gilbreath, Hoekstra H R, and Hyde E. K. "Sodium Borohydride , Its Hydrolysis and its Use as a Reducing Agent and in the Generation of Hydrogen," *J. AM. CHEM. SOC*, 199, 1953.
- [4] P. Krishnan, T. Yang, W. Lee, and C. Kim. "PtRu-LiCoO₂ — an efficient catalyst for hydrogen generation from sodium borohydride solutions" *J. of Power Sources*, 143, pp. 17–23, 2005.
- [5] C. Salim, M. Zahmakiran, and O. Saim, "Zeolite confined rhodium(0) nanoclusters as highly active, reusable, and long-lived catalyst in the methanolysis of ammonia-borane" *Applied Catalysis*, 93, pp. 387–394, 2010.
- [6] Y. C. Zou, M. Nie, Y. M. Huang, J. Q. Wang, and H. L. Liu. "Kinetics of NaBH₄ hydrolysis on carbon supported ruthenium catalysts" *Int. J. of Hydrogen Energy*, 36, 19, pp. 12343–12351, 2011.
- [7] N. Patel, R. Fernandes, N. Bazzanella, and A. Miotello. "Enhanced hydrogen production by hydrolysis of NaBH₄ using Co-B nanoparticles supported on Carbon film catalyst synthesized by pulsed laser deposition" *Catal. Today*, 170, pp. 20–26, 2011.
- [8] C. Wu, F. Wu, Y. Bai, B. Yi, and H. Zhang. "Cobalt boride catalysts for hydrogen generation from alkaline NaBH₄ solution" *Materials Letters*, 59, pp. 1748–1751, 2005.

The grain size effects on stress assist hydrogen transport in polycrystalline Nickel (P-177)

**Sathiskumar Jothi, T.N.Croft, S. G. R. Brown, E. de Souza Neto*
College of Engineering, Swansea University, Singleton Park, Swansea SA2 8PP, UK
**S.Jothi@swansea.ac.uk*

ABSTRACT:

Underprivileged sympathetic of the role of hydrogen in the stress assist embrittlement of polycrystalline nickel passion the exertions to effects of grains sizes on stress assist hydrogen transport in polycrystalline material. Quantifying the actual precise behavior of stresses and hydrogen transport in material microstructure plays important role for the better understanding of hydrogen embrittlement mechanism. Stress assist hydrogen transport in polycrystalline materials has received considerable attention as a result of the material's unique structural embrittlement behavior. Microstructural grain size and grain boundaries play an important role in stress assists hydrogen transport in polycrystalline nickel. Experiments have indicated that stress assist hydrogen transport in nickel depends on the grain size and grain boundary density of material [1]. Multiscale microstructural polycrystalline model is required to steady the influence of stress assist hydrogen transport over the various average grains sizes of the polycrystalline material using finite element analyses. The proposed work is aimed to develop such a model by taking into account of grain size and grain boundary in the form of heterogeneous intergranular and intragranular polycrystalline microstructural degree of freedom. This microstructural region is used to investigate the behavior of stresses assist hydrogen transport mechanism. This 2D multiphase microstructural polycrystalline model increases the density of grain boundary as the grain size reduces. The multiphase polycrystalline model consists of two phases with grain interior and intergranular phases. The intergranular phase is the combination of grain boundary regions and triple junction regions. The results of this finite element analysis show that stress assist hydrogen transport enhanced at smaller grain size material. Consequently the grain size and grain boundary effects cannot be neglected when predicting stress assist hydrogen transport in a polycrystalline material.

Keywords: Stress assists hydrogen transport; grain size and grain boundary effects; polycrystalline nickel; Multiscale microstructural model;

Acknowledgements:

This work was supported by the Swansea University and MultiHy Project funded by the European Union's 7th Framework program under the theme "Nanosciences, Nanotechnologies, Materials and new production Technologies".

Reference:

A. Oudriss, J. Creus, J. Bouhattatte, E. Conforto, C. Berziou, C. Savall, X. feaugas (2012) Grain size and grain boundary effects on diffusion and trapping of hydrogen in pure nickel, Acta Materialia 60:6814-6828.

Porous Ni-YSZ and Ni-GDC anode buffer layers prepared by magnetron sputtering for Solid Oxide Fuel Cells (P-186)

Francisco J. Garcia-Garcia¹, Francisco Yubero¹, Agustín R. González-Elipe¹ and Richard M. Lambert^{1,2}

1. Instituto de Ciencia de Materiales de Sevilla, (CSIC, Univ. Sevilla), Av. Américo Vespucio 49, E-41092 Sevilla, Spain

1,2. Chemistry Department, Cambridge University, Lensfield Road, Cambridge, CB2 1EW, UK.

Solid Oxide Fuel Cells (SOFCs) are one of the main competitors among environmental friendly energy sources for the future due to low emission rates, high electric efficiency and a potential for a low operating cost. The development of SOFCs operating on hydrocarbon (HC) fuels is the key to their short to medium term broad commercialization, taking into account that (i) these fuels are available almost everywhere through the existing infrastructure (pipelines, gas stations), (ii) European Union identifies natural gas as a key energy vector and (iii) the role of biofuels becomes increasingly important.

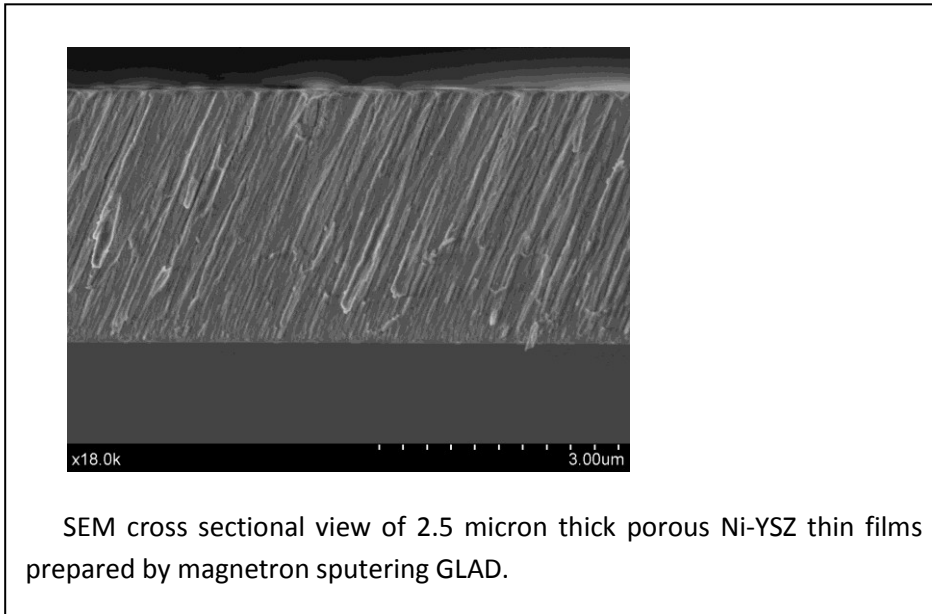
To utilize hydrocarbons, fuel cell power plants usually employ fuel reforming, which converts fuels into hydrogen, leading to additional plant complexity and volume, increasing the total cost. Based on this argument, the development of direct HC SOFCs, which operate directly on real hydrocarbon fuels, would substantially reduce the cost of fuel cell systems. However, practical implementation of direct HC SOFCs faces major challenges.

Conventional SOFC use either porous nickel-YSZ or nickel-GDC cermets about 100 microns thick for the anode due to its reasonable cost, good catalytic activity and electrical conductivity. However, the disadvantages are their poor redox stability, low tolerance to sulfur, carbon deposition when using hydrocarbon fuels and the tendency of Ni for agglomeration after prolonged operation. In particular, the low tolerance for carbon deposition makes these materials prone to degrade and thus inappropriate for long term operation with the available hydrocarbon fuels. To overcome this problem, doping the Ni cermets with Mo and Au has recently been proposed [1].

On the other hand, it is well recognized that improved performance of the SOFC due to the reduction of the operating temperature by reducing its ohmic losses. This can be achieved reducing the cell thickness using thin film technology in the manufacturing processing.

In this study, Ni-YSZ and Ni-GDC porous thin film materials have been prepared by magnetron sputtering (MS). Compared to other chemical synthetic routes, MS is a one-step process yielding directly the final formulation of the oxide that has the additional advantage of avoiding the production of undesirable byproducts. It permits to control the microstructure, density, and composition of the films (including doping with other minority elements) for thicknesses up to few microns. The novelty of this study lies in the use of glancing deposition configuration for the growth of Ni-YSZ and Ni-GDC thin films. Similar approach was recently considered for the growth of electrochromic of SixWyO thin films [2].

The GLAD thin films are characterized by a columnar microstructure with a high porosity (up to 40% void fraction) and a pore structure consisting of mesopores extending from the surface of the film up to the interface with the substrate (see figure). This opens the possibility of using this type of films as buffer-layers to improve the adhesion and the thermal compatibility between the electrolyte and anode layers of the SOFC device. Morphological, chemical, and structural properties of the films have been characterized. Furthermore, their ionic and electronic conductivities are measured.



[1] D.K. Niakolas et al., Applied Catalysis A: General 456 (2013) 223.

[2] F.J. Garcia-Garcia et al., Nanoscience and Nanotechnology Letters 5, 89-93 (2013)

EFFECT OF GAS CHANNELS FLOW PATTERNS ON COLD-START BEHAVIORS OF POLYMER ELECTROLYTE FUEL CELLS (PEFCs) (P-188)

Ahrae Jo and School of Mechanical Engineering, Inha University, 253 Yonghyun-Dong, Nam-Gu Incheon, 402-751, Republic of Korea

Johan Ko and School of Mechanical Engineering, Inha University, 253 Yonghyun-Dong, Nam-Gu Incheon, 402-751, Republic of Korea

Hyunchul Ju and School of Mechanical Engineering, Inha University, 253 Yonghyun-Dong, Nam-Gu Incheon, 402-751, Republic of Korea*

In order to successful self-startup of an automotive fuel cells, a variety of operating conditions and flow patterns of reactant gas channels has been considered for automotive fuel cells mainly owing to its cheaper fabrication cost, higher mechanical strength and better durability to shocks and vibration.

One of the issues to be resolved for the commercialization of automotive fuel cells is a successful startup of fuel cells in extremely cold weather. The major problem of polymer electrolyte fuel cell (PEFC) startup from sub-zero temperature is that produced water by oxygen reduction reaction (ORR) on cathode side of a PEFC freezes into an ice or frost. The ice/frost is formed in the cathode catalyst layer (CL) if an amount of accumulated water in the cathode CL is greater than the water vapor saturation pressure. If the water vapor saturation pressure increases rapidly due to increasing of temperature of a variety of conditions, ice/frost is not formed or only small amount of ice is formed due to rapidly increasing water vapor saturation pressure. Therefore, optimal cold start strategy should be developed to ensure fuel cell longevity and reliability under the sub-zero environment, which demands precise examination of ice formation/growth characteristics inside PEFCs during cold start.

In this study, the 3-D, transient cold-start model developed in the previous study is applied to large-scale PEFC geometry with the active area of 15 cm². In order to reduce the computational turnaround time involving a large numerical mesh with millions of grid points, the 3-D cold start code is parallelized for parallel computing. The cold-start PEFC model is applied to the straight and serpentine channels geometries with conventional graphite bipolar plate to analyze the effect of flow patterns on PEFC startup performance. In order to the impact of flow patterns between the anode and cathode streams that can be accurately examined only via large-scale cold start simulations, We considered four simulation(Fig.1) cases such as co- and counter flow, serpentine flow and cross flow configurations. We aim to numerically explore key cold start phenomena such as ice accumulation/melting, cell temperature rising, and electrolyte hydration/dehydration processes during a cold start period for a PEFC to reach normal operating temperature from subzero temperature.

The simulation results clearly show the evolution of ice, water content, temperature, and current density contours at different cold start stages characterizing freezing, melting, hydration, and dehydration processes. The effect of co- and counter flow patterns shows the opposite trend such as a current density and temperature distribution due to the difference location of cathode entrance. And the amount of ice accumulation indicates a similar trend in the case of co- and counter flow.

Therefore, we can be predicted that the impact of amount of ice accumulation is insufficient. Under the influence of the serpentine flow patterns, we know that the ice is accumulated near the U-turn channel region in the cathode CL. With elucidating the characteristics of ice distribution on large-scale cell under various cold start conditions, we show a capability to conduct large-scale transient cold start simulations, which is highly desirable for automotive fuel cell manufacturers to design and optimize their real-size PEFCs.

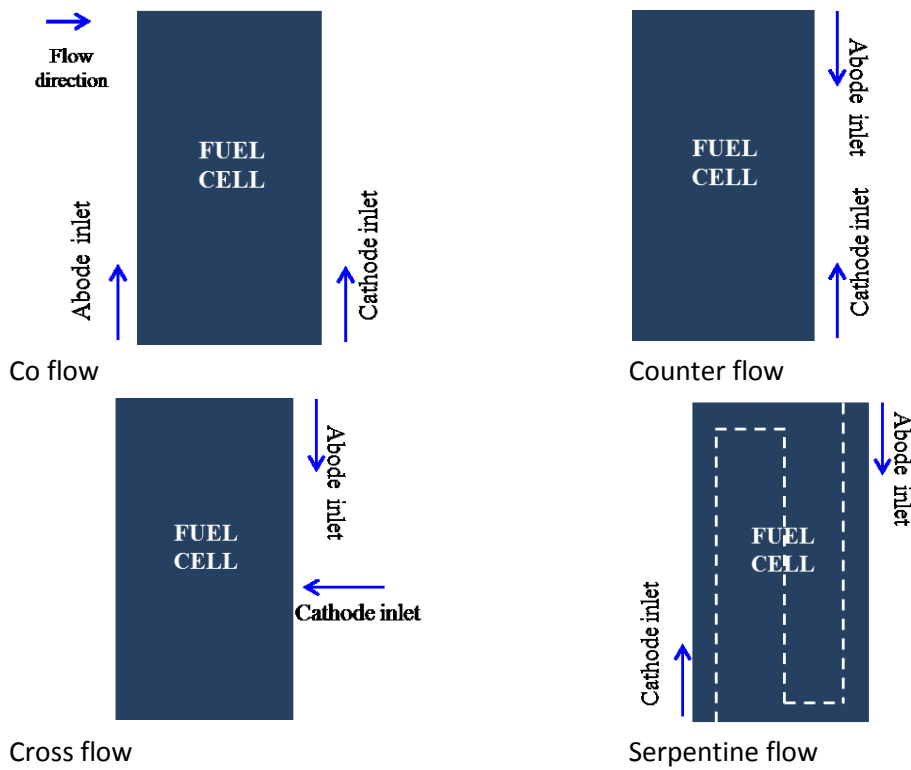


Fig. 1. Schematic of the simulation cases.

Development of ultralight and thin bipolar plate based on EPOXY-Carbon fiber prepregs-graphite composite (P-189)

Ahrae Jo and School of Mechanical Engineering, Inha University, 253 Yonghyun-Dong, Nam-Gu Incheon, 402-751, Republic of Korea

Sunghyun park and School of Mechanical Engineering, Inha University, 253 Yonghyun-Dong, Nam-Gu Incheon, 402-751, Republic of Korea

Geonhui Gwak and School of Mechanical Engineering, Inha University, 253 Yonghyun-Dong, Nam-Gu Incheon, 402-751, Republic of Korea

Kyungmun Kang and School of Mechanical Engineering, Inha University, 253 Yonghyun-Dong, Nam-Gu Incheon, 402-751, Republic of Korea

Hyunchul Ju and School of Mechanical Engineering, Inha University, 253 Yonghyun-Dong, Nam-Gu Incheon, 402-751, Republic of Korea*

A bipolar plate (BP) performs several crucial functions for fuel cell operations such as effective supply of reactant and removal of product, mechanical support of fuel cell stack and electrical path of electrons. In order to fulfill these functions, the material for BP must possess sufficient mechanical strength as well as high electrical conductivity. Therefore, appropriate choice of BP material is important to enhance fuel cell performance and durability. So far, the most common materials for BPs are metal alloys, graphite, and graphite-resin composites. The metal alloys based BPs exhibit excellent mechanical strength and electrical conductivity, whereas these have surface corrosion problems. On the other hand, pure graphite based BPs show excellent corrosion resistance but suffer from several disadvantages such as high manufacturing cost and low mechanical strength. As an alternative of aforementioned BPs, graphite-resin composites BPs have been extensively researched and presented in the literature. . Using the excellent mechanical strength and in-plane electrical conductivity of epoxy-carbon fiber prepregs, in this study, we design and fabricate ultrathin composite bipolar plates (BPs) for fuel cells. For the successful fabrication of prepreg-based BPs, it is essential to increase the through-plane electrical conductivity of pristine prepregs and reduce the electrical contact resistance due to excessive surface resin extruded during compression molding. In addition, the moldability of prepreg layers should be greatly improved for the proper construction of a serpentine flow field on the prepreg surface. To resolve all these technical issues, we suggest a multilayer BP structure in which prepreg layers, pure graphite layers, and graphite-resin composite layers are combined and compression-molded. The multilayered prepreg BP is approximately 0.6 mm thick and exhibits good electrical behavior with a high-quality serpentine flow channel configuration.

Fig. 1 shows the through-plane electrical conductivities for the cases in which 6-, 10-, 20-, and 40- μm particles were used. The through-plane conductivity increased with a decrease in the graphite particle size. The highest through-plane conductivity of 38 S cm^{-1} was achieved when using 6- μm graphite particles, which would cause negligible ohmic loss owing to the low thickness (0.6 mm) during fuel cell operation. In addition, we measured the through-plane conductivity of the pristine epoxy-carbon fiber prepregs, which turned out to be as low as 4.8 S cm^{-1} . This further indicated that the proposed BP design and fabrication, in which the carbon fibers were more tightly compacted under compression molding and the extruded resin during the prepreg compression was effectively absorbed by neighboring graphite layers, effectively reduced the through-plane electrical resistance of the prepregs.

Fig. 2 shows a three-pass serpentine flow field formed on the composite coated graphite-prepreg hybrid layer (Fig. 2a) and graphite-prepreg hybrid layer (Fig. 2b). Comparison of Figs. 2a and 2b clearly shows that the shape and quality of the serpentine flow channels on the composite coated graphite-prepreg hybrid BP (Fig. 2a) are much better, particularly near the U-turn region. The test results clearly demonstrate that the low through-plane electrical conductivity and poor moldability of pristine prepregs are greatly improved by our proposed BP design and fabrication.

The results demonstrate that the moldability of the prepreg plate was greatly improved by employing the additional outer layers made of natural graphite and epoxy resin composite, because these layers act as a buffer to prevent excessive resin extrusion on the channel surface. This study clearly demonstrates that the prepreg based BP technology can be applicable to fuel cell stack to reduce its volume and weight.

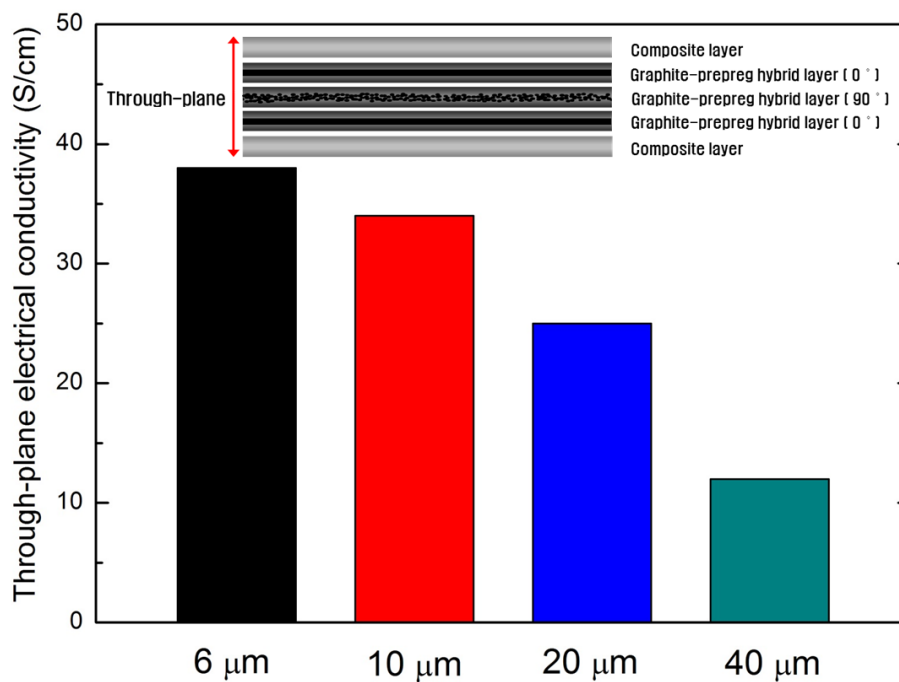
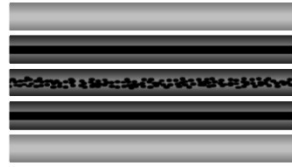


Fig. 1. Through-plane electrical conductivity of the composite coated graphite-prepreg hybrid BPs for graphite particle sizes of 6 μm, 10 μm, 20 μm, and 40 μm.



Composite layer
Graphite-prepreg hybrid layer (0 °)
Graphite-prepreg hybrid layer (90 °)
Graphite-prepreg hybrid layer (0 °)
Composite layer

(a)



Graphite-prepreg hybrid layer (0 °)
Graphite-prepreg hybrid layer (90 °)
Graphite-prepreg hybrid layer (0 °)

(b)

Fig. 2. Top view of a three-pass serpentine flow field formed on (a) the composite coated graphite-prepreg hybrid layer and (b) the graphite-prepreg hybrid layer.

Advanced Multi-Fuel Reformer for Fuel Cell CHP Systems (P-194)

José Luis Viviente

Fundación Tecnalia Research & Innovation

Distributed power generation via Micro Combined Heat and Power (m-CHP) systems, has been proven to overcome disadvantages of centralized plant since it can give savings in terms of Primary Energy consumption and energy costs. The main advantage is that m-CHP systems are able to recover and use the heat that in centralized systems is often lost. Wide exploitation of these systems is still hindered by high costs and low reliability due to the complexity of the system.

ReforCELL(www.reforcell.eu) aims at developing a high efficient heat and power cogeneration system based on: i) design, construction and testing of an advanced reformer for pure hydrogen production with optimization of all the components of the reformer (catalyst, membranes, heat management etc) and ii) the design and optimization of all the components for the connection of the membrane reformer to the fuel cell stack.

The main idea of ReforCELL is to develop a novel more efficient and cheaper multi-fuel membrane reformer for pure hydrogen production in order to intensify the process of hydrogen production through the integration of reforming and purification in one single unit. To increase the efficiency and lifetime of the reformer, novel stable catalysts and high permeable and more stable membranes will be developed. Afterwards, suitable reactor designs for increasing the mass and heat transfer will be realized and tested at laboratory scale. The most suitable reactor design will be scaled up at prototype scale (5 Nm³/h of pure hydrogen) and tested in a CHP system.

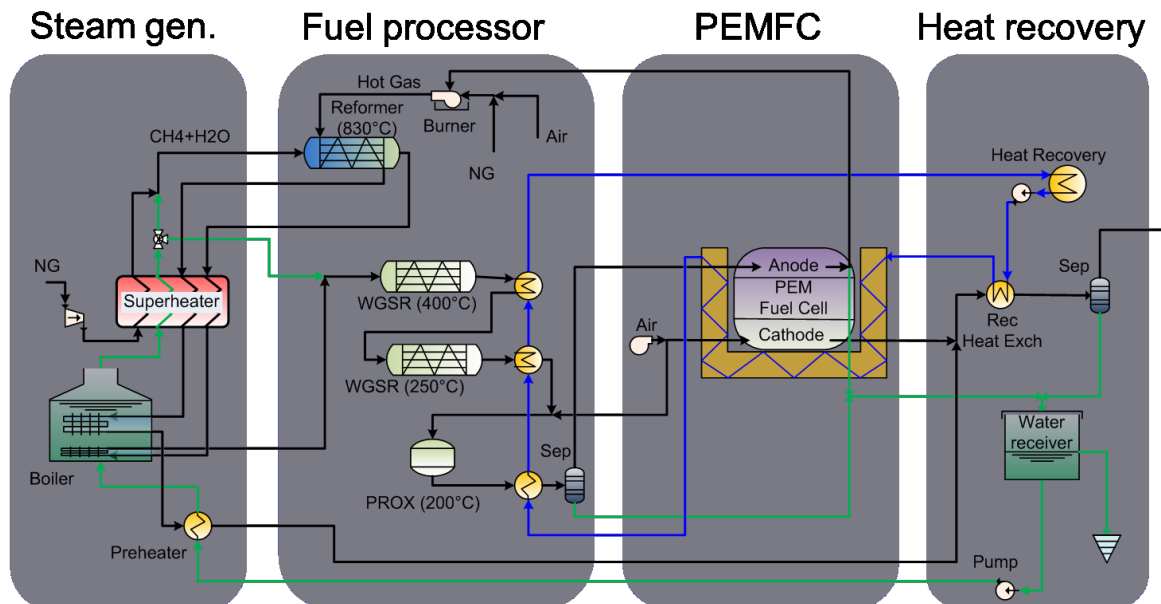


Figure 1. Layout of PEM m-CHP unit using traditional reforming (TR) for fuel processing

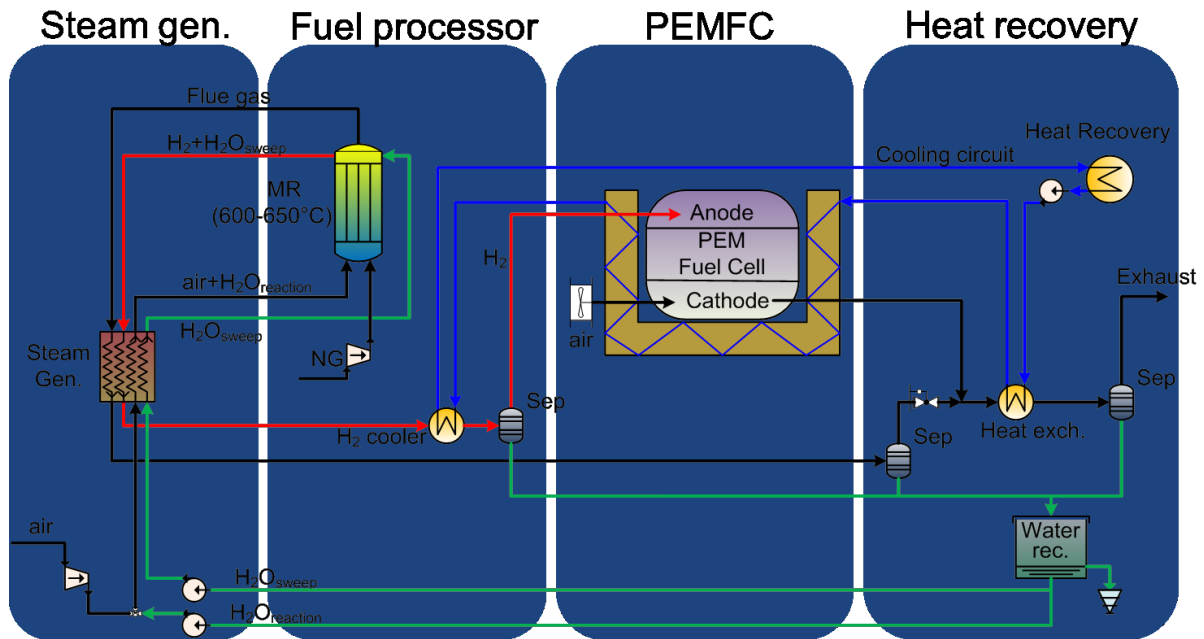


Figure 2. Layout of PEM m-CHP unit using membrane reformer (MREF) for fuel processing

The connection of the novel reformer within the CHP will be optimized by designing heat exchangers and auxiliaries required in order to decrease the energy losses in the system. The project aims to increase the electric efficiency of the system above 42% and the overall efficiency above 90%. Besides, a complete lifecycle analysis of the system will be carried out and cost analysis and business plan for reformer manufacturing and CHP system will be supplied.

This general objective is directly related to the development of a novel catalytic membrane reactor (CMR) for hydrogen production with:

- Improved performance (high conversion at low temperature for the autothermal reforming reaction)
- Enhanced efficiency (reduction of the energy consumption)
- Long durability under CHP system working conditions
- Clean environmental operating conditions (CO₂ emissions reduced from conventional reformer).
- and including a good recyclability of its individual components and safety aspects for its integration in domestic CHP systems.

The technical objectives needed to achieve these goals with the novel multi-fuel processor (based in CMR) are the following:

- Develop an advanced catalyst able to catalyse different reforming reactions under moderate (<700C) conditions and resistant to sulphur compounds and coke formation and at reduced cost.
- Develop new hydrogen permeable membrane materials with improved separation properties, long durability, and with reduced cost, to be used under reactive conditions.
- To assess the large scale production of the membrane developed.
- Understand the fundamental physico-chemical mechanisms and the relationship between structure/property/performance and manufacturing process in membranes and catalysts, in order to achieve radical improvements in membrane reactors.
- To design, model and build up novel more efficient (e.g. reducing the number of steps) multi-fuel catalytic membrane reactor configurations based on the new membranes and catalysts for small-scale pure hydrogen production.
- To validate the new membrane reactor configurations, and design a semi-industrial Autothermal Reforming (ATR) prototype for pure hydrogen production.
- To improve the cost efficiency of membrane reactors by increasing their performance, decreasing the raw materials consumption and the associated energy losses.

Other technical objectives are related to the integration and validation of the multi-fuel reformer into the PEM fuel cell CHP system:

- To design the optimum CHP system (aided by simulation tools) in order to achieve a complete system able to achieve the targets in performance and cost.
- To test the reliability of the novel reactor with a Fuel Cell CHP system
- To assess the health, safety and environmental impact of the system developed, including a complete Life Cycle Analysis (LCA), of the developed system.

The ReforCELL project structure is broken down in nine work packages following the focus on efficiency improvement of the overall m-CHP system based on PEM fuel cell and innovative multi-fuel processor. Furthermore, the novel materials and components will be implemented in a m-CHP system for proof of concept and validation.

For a maximum impact on the European industry this research, covering the complete value chain of micro-CHP fuel cell systems, can only be carried out with a multidisciplinary and complementary team having the right expertise, including top level European Research Institutes and Universities (6 RES) working together with representative top industries (4 SME and 1 IND) in different sectors (from materials to micro-CHP developers).

Acknowledgements

This project is supported by the European Union's Seventh Framework Programme (FP7/2007-2013) for the Fuel Cells and Hydrogen Joint Technology Initiative under grant agreement n° 278997.

Disclosure

The present publication reflects only the author's views and the FCH JU and the Union are not liable for any use that may be made of the information contained therein.

Numerical simulations of the two-phase flow in the anode channel of a PEMFC using the VOF method (P-196)

Rui B. Ferreira^a, D.S. Falcão^a, V.B. Oliveira^a, A.M.F.R. Pinto^a

^a*Centro de Estudos de Fenómenos de Transporte, Departamento de Engenharia Química, Faculdade de Engenharia da Universidade do Porto, Rua Dr. Roberto Frias, 4200-465 Porto, Portugal*

INTRODUCTION

Features like high efficiency, quick/cold start-up, easy scale-up, and low to zero emissions make proton exchange membrane fuel cells (PEMFCs) a viable, clean and efficient technology to generate power for various applications. In particular, these devices have a great potential as an alternative to the internal combustion engines for automotive applications. In a PEMFC, electricity is produced through the electrochemical reaction between hydrogen (fuel) and oxygen (oxidant), liberating only heat and water as by-products.

From several technical issues that still inhibit the wide commercialization of PEMFCs, water management is a major aspect. On the one hand, low water content causes the membrane dehydration which diminishes proton conductivity. On the other hand, due to the low operating temperature of a PEMFC (60-80°C), liquid water is unavoidable and a large amount of it can flood the cell, increasing the transport resistance of reactants to the reaction sites and consequently decreasing the cell performance. In particular, water transport along the gas flow channels is very important for fuel cell design and optimization since this is where the water formed in the electrochemical reaction leaves the cell.

Several mathematical models, namely Computational Fluid Dynamics (CFD) models, have been developed to simulate the gas-liquid two-phase flow in the channels of PEMFCs [1-3]. So far, these studies have focused exclusively on the cathode side as it is the water-generating electrode and flooding is more prone to occur. However, visualization experiments shown that, for certain operating conditions, flooding can also occur in the anode channels [4-6], and it could be even more significant than that on the cathode side [7, 8]. In addition, due to the lower gas flow rate, density and viscosity of hydrogen in the anode compare to those of air in the cathode, liquid water removal is more difficult in the anode.

This work presents numerical simulations of the two-phase flow in the anode channels of a PEMFC. The dynamic behavior of liquid water in the anode gas channels is studied and compared with that on the cathode side. The effects of the hydrogen flow rate and anode channel walls wettabilities on liquid water removal from the channel are also analyzed.

NUMERICAL SIMULATIONS

Simulations of the two-phase flow in the anode channels of a PEMFC are performed in the CFD commercial software Fluent 14.5, using the Volume of Fluid (VOF) method. A scheme of the computational domain considered is presented in Figure 1. A microchannel with 250 μm \times 250 μm cross section and 1000 μm length with a pore with 50 μm diameter on the gas diffusion layer (GDL)

surface is used. Hydrogen (or air) enters the channel through the square cross section while water emerges through the pore in the GDL. These features were already used in previous studies for modeling the two-phase flow in the cathode gas channel [2, 9] and are representative of the gas flow channels of PEMFCs.

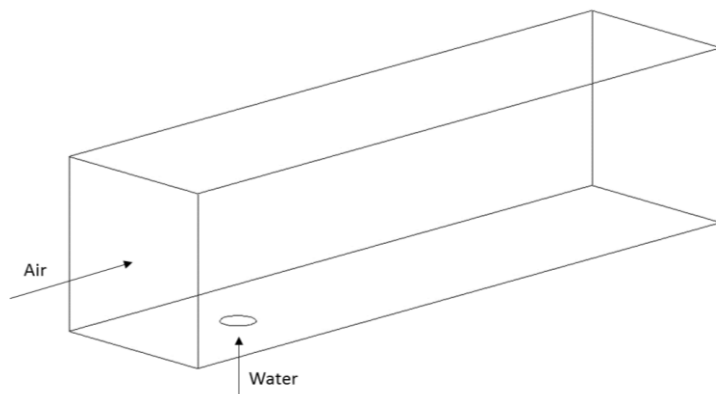


Figure 26. Schematic representation of the computational domain used for simulating the two-phase flow in the anode channel of a PEMFC.

OUTCOMES OF THE PRESENT WORK

This work enriches the literature related with the simulation of the two-phase flow in the channels of PEMFCs, which has been focused exclusively on the cathode side, by simulating the two-phase flow in the anode side for the first time. The results can be useful to optimize the design of the anode gas flow channels in order to prevent liquid water flooding and consequently increase cell performance.

REFERENCES

- [1] Quan P, Zhou B, Sobiesiak A, Liu Z. Water behavior in serpentine micro-channel for proton exchange membrane fuel cell cathode. *Journal of Power Sources*. 2005;152:131-45.
- [2] Zhu X, Sui P, Djilali N. Three-dimensional numerical simulations of water droplet dynamics in a PEMFC gas channel. *Journal of Power Sources*. 2008;181:101-15.
- [3] Ding Y, Bi H, Wilkinson D. Three dimensional numerical simulation of gas-liquid two-phase flow patterns in a polymer-electrolyte membrane fuel cells gas flow channel. *Journal of Power Sources*. 2011;196:6284-92.
- [4] Ge S, Wang C-Y. Liquid water formation and transport in the PEFC anode. *Journal of The Electrochemical Society*. 2007;154:B998-B1005.
- [5] Spornjak D, Prasad AK, Advani SG. Experimental investigation of liquid water formation and transport in a transparent single-serpentine PEM fuel cell. *Journal of Power Sources*. 2007;170:334-44.

[6] Rosli MI, Borman DJ, Ingham DB, Ismail MS, Ma L, Pourkashanian M. Transparent PEM fuel cells for direct visualization experiments. *J Fuel Cell Sci Tech.* 2010;7.

[7] Sergi JM, Kandlikar SG. Quantification and characterization of water coverage in PEMFC gas channels using simultaneous anode and cathode visualization and image processing. *International Journal of hydrogen energy.* 2011;36:12381-92.

[8] Lee D, Bae J. Visualization of flooding in a single cell and stacks by using a newly-designed transparent PEMFC. *International Journal of Hydrogen Energy.* 2012;37:422-35.

[9] Zhu X, Liao Q, Sui PC, Djilali N. Numerical investigation of water droplet dynamics in a low-temperature fuel cell microchannel: Effect of channel geometry. *Journal of Power Sources.* 2010;195:801-12.

Mo₂C electrocatalysts for hydrogen evolution: effect of carbon-support (P-199)

B. Šljukić^{a,}, D.M.F. Santos^a, L. Amaral^a, R.P. Rocha^b, C.A.C. Sequeira^a and J.L. Figueiredo^b*

^a ICEMS, Instituto Superior Técnico, Universidade de Lisboa, Av. Rovisco Pais, 1049-001 Lisbon, Portugal

^b Laboratório de Catálise e Materiais (LCM), Laboratório Associado LSRE/LCM, Departamento de Engenharia Química, Faculdade de Engenharia, Universidade do Porto, R. Dr. Roberto Frias, 4200-465 Porto, Portugal

Hydrogen (H₂) represents one of the most promising fuels for clean and renewable energy sources to be used in the future. It is a clean fuel due to its non-toxicity and no pollutants emission, such as greenhouse gases, during its usage. At present, industrial H₂ is mainly produced by steam reforming of natural gas (48%), and also by oil reforming (30%) and coal gasification (18%). Full advantage of H₂ as clean and efficient fuel means its production using only renewable energy sources with no pollutants evolution. Consequently, H₂ production by water is seen as one of the most promising methods for large-scale hydrogen production. At the moment, alkaline and proton exchange membrane electrolyzers are the dominant ones. Alkaline electrolysis is well-established technology; however, H₂ production by water electrolysis is limited to only 4 to 5% of its total production due to the high process cost. One way to lower the cost is employing more efficient electrocatalysts for hydrogen evolution reaction (HER).

Transition metal (Ti, V, Mo, Ta, W) carbides (TMCs) have been pointed out as materials that display comparable electronic and catalytic properties to Pt-group metals (Ru, Rh, Pd, Ir, Pt) because of their unique d-band electronic structures. Activity of electrocatalyst for HER is related to the hydrogen binding energy (HBE) whether it is monometallic or bimetallic alloy material. Pt-group metals have intermediate HBE values resulting in high activity for HER. TMC-based electrodes are expected to have similar values of HBE and to exhibit comparable activity to Pt electrocatalysts for HER. Thereafter, TMCs show great potential to be low-cost replacement for Pt in HER applications as they are several orders of magnitude more abundant and economical than Pt-group metals.

Low-cost molybdenum carbide (Mo₂C) nanoparticles anchored in carbon supports were recently shown to efficiently enhance hydrogen evolution. Furthermore, carbon-supported Mo₂C electrocatalyst were shown to have higher activity compared to the bulk electrocatalyst for water electrolysis in acidic media. Thereafter, Mo₂C electrocatalyst supported on carbon nanotubes (Mo₂C-CNT) and supported on carbon xerogel (Mo₂C-XG) were prepared herein. Synthesised electrocatalysts were characterised by thermogravimetric analysis (TGA), X-ray photoelectron spectroscopy (XPS) and X-ray diffraction analysis (XRD). Subsequently, the two electrocatalysts were studied in terms of their electrocatalytic activity towards HER and this was correlated to their physical properties. Electrodes were prepared by depositing the corresponding catalytic ink made using each of the catalysts, on the surface of a glassy carbon tip. The electrodes were tested using linear scan voltammetry (LSV) in 8 M KOH aqueous electrolyte in the 25 - 45 °C temperature range.

LSV studies used for evaluation of the two electrocatalysts activity for the HER made possible determination of several kinetic parameters, including Tafel coefficient, charge-transfer coefficient, and exchange current density. The analysis was performed using a potential region of 100 mV, between -1.38 and -1.48 V vs. SCE. Based on the values of determined parameters, performance for HER of the two types of carbon-supported Mo₂C electrocatalysts, i.e. influence of the carbon support, was directly compared. Tafel slope was found to be 212 and 98 mV dec⁻¹ for Mo₂C-CNT and Mo₂C-XG, respectively. Lower Tafel slope value associated with lower overpotential for hydrogen discharge indicated higher activity of the Mo₂C-XG for HER. The exchanged current density values were found to be similar, i.e. 1.18 and 1.12 mAcm⁻². The better performance of Mo₂C-XG electrocatalyst might be due to the lower size of its nanoparticles and its higher porosity.

The prepared Mo₂C-CNT electrocatalyst showed very good stability during measurements and reasonable electrocatalytic activity for the HER. The observed activity generally owes to the unique effects of the anchored structure coupled with the electronic modification. The increase in temperature, from ambient to 45 °C, lead to an enhancement of the Mo₂C-CNT activity for HER as evidenced by a decrease of the Tafel coefficient value from 212 to 172 mV dec⁻¹.

Mo₂C-XG electrocatalyst presented promising results, clearly overpassing the catalytic activity of Mo₂C-CNT. This behaviour is attributed to smaller particle size and higher porosity of the former. However, the preparation procedures need further improvements in order to increase the current activity of the catalysts.

Phosphoric Acid Doped Cross-linked Porous Polybenzimidazole Membranes for Proton Exchange Membrane Fuel Cells (P-201)

Steve Lien-chung Hsu*, Cheng-Hsun Shen, Li-cheng Jheng, , Jacob Tse-Wei Wang

Department of Materials Science & Engineering, Research Center for Energy Technology and Strategy
National Cheng-Kung University, Tainan, 701-01, Taiwan, R.O.C.

Proton exchange membrane (PEM) is one of the key elements for polymer exchange membranes fuel cells (PEMFC). In PEMFCs, the proton conducting polymer is used in the form of a thin film, and acts as an electrolyte. PEMs require chemical, thermal stability, and outstanding mechanical properties, as well as low cost fabrication for useful applications. Polybenzimidazole (PBI) membranes exhibit good these characteristics at temperatures up to 200 oC. In particular, PBI doped with phosphoric acid (PA) has stable proton conductivity at temperatures higher than 100 oC, which gives it the potential for use as high-temperature proton exchange membrane.

The proton conductivity of PA doped PBI membranes were dependent on the doping level. The conventional PA-doped PBI membranes were prepared by immersing the PBI membranes in a PA solution. Several different processes for preparation PA doped PBI membranes have been explored to improve the proton conductivity in recent years. Recently, Mecerreyes et al. proposed a method to increase the PA doping level in PBI membranes by incorporating the porosity with different porogens. Also, several research groups have developed new methods to generate PBI membranes to exhibit high conductivity, such as by direct casting methods. For example, PBI membranes were prepared by direct-casting from a PBI/methanesulfonic acid solution to obtain high acid doping levels. However, one of the drawbacks of PBI membranes doped with high amounts of PA is the extremely poor mechanical properties to fabricate membrane electrode assemblies. To solve this issue, covalent cross-linked PBI had been demonstrated to be a useful approach. Cross-linked PBI membranes with both outstanding mechanical stability and high proton conductivity have been successfully prepared.

In this study, we report the preparation of cross-linked and porous PBI membranes for PEM. Combining the porosity and cross-linking approaches, we were able to prepare new PBI membranes with high proton conductivity at high temperatures and useful mechanical properties after PA doping. The cross-linked porous polybenzimidazole (PBI) membranes were prepared by mixing a low-molecular-weight compound (porogen) and a crosslinker with the polymer to form cross-linked polymer membranes. SEM images of the cross-section of the porous polymer membranes show the pore size and morphology (Fig.1). The cross-linking by p-xylylene dichloride can effectively improve the mechanical properties of the porous PBI membranes after phosphoric acid doping. The good mechanical strength of the cross-linked porous PBI membranes makes them possible to hold more phosphoric acid, and consequently, higher proton conductivity. Fenton's test indicated that the covalently cross-linked structure played an important role in the radical oxidative stability of the porous membranes. The doping level of phosphoric acid in the cross-linked porous PBI membranes showed that the enhanced conductivity was due to the increase of porosity, which results in the increase of acid uptake. Impedance analysis showed that the conductivity of the cross-linked porous PBI membranes could reach 2.1×10^{-2} S/cm at 160 oC under anhydrous condition (Fig. 2). The cross-

linked porous PBI membranes have the potential for use as proton exchange membranes in high temperature PEMFC.

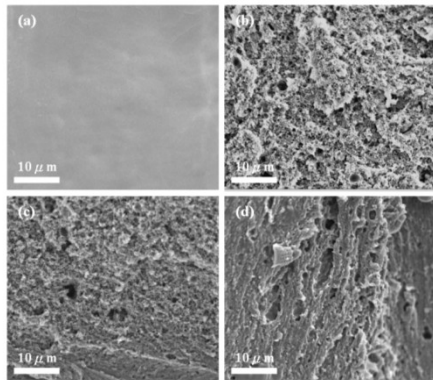


Fig. 1 SEM micrographs of porous PBI membranes prepared from various porogen contents: (a) zero DBP (b) 33 wt % DBP (c) 50 wt % DBP and (d) 67 wt % DBP.

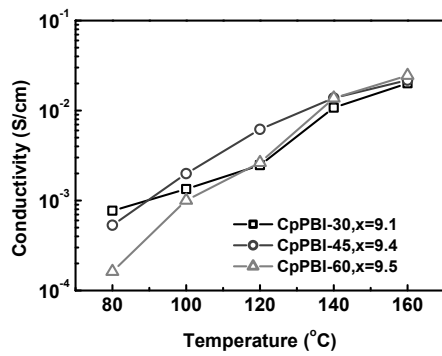


Fig. 2 Proton conductivity of cross-linked porous PBI membranes doped with different amounts of phosphoric acid at different temperatures.

Development of high performance membrane electrode assemblies using a non-platinum catalyst for alkaline membrane fuel cells (P-205)

Seok-Hee Park, Korea Institute of Energy Research

Chang-Soo Kim, Korea Institute of Energy Research

Tae-Hyun Yang, Korea Institute of Energy Research

The development of alkaline membrane fuel cells (AMFCs) will enable the use of non-platinum catalysts and hydrocarbon-based electrolyte membranes. Alkaline membrane fuel cells (AMFCs) offer potential advantages over PEMFCs because they can use transition metal catalysts, which can have an ORR activity similar to that of platinum [1-3], and a low-cost hydrocarbon anion-exchange membrane [4]. The use of a low-cost catalyst and a hydrocarbon-based electrolyte membrane would accelerate the commercialization of fuel cells, especially in applications such as back-up power systems for telecommunication [5]. AMFCs have many advantages over the conventional alkaline fuel cells; thermodynamically favorable kinetics at higher pH, easy electrolyte control, easy water management. But the performance and durability of the AMFCs are much lower than those of the PEMFCs. In this paper, to improve the performance of AMFC membrane electrode assemblies (MEAs), various conditions such as catalyst type, ionomer type, ionomer content, pretreatment, and cell humidification were investigated.

Acta's carbon-supported non-platinum catalyst, Hypermec 4020 (Cu-Fe/C, 3.5 wt% metal, Vulcan-XC72) was used for the cathode, Johnson Matthey's Pt/C catalyst HiSPEC 4000 (40 wt% Pt, Vulcan-XC72) was used for the anode or cathode, and Commercial AMFC ionomers were used for the preparation of the catalyst inks. The platinum loading was 0.5 mg cm⁻² in the anode or cathode, and the Hypermec 4020 loading was 2.0 mg cm⁻² in the cathode. The ionomer content of the Pt/C catalyst was, 25 wt%, as previously optimized. However, the ionomer content of the cathodes for the non-Pt catalyst was varied with different ionomer ratios from 20 wt% to 60 wt%. Well dispersed catalyst slurries were sprayed onto the anion-conducting membrane (in-house pore-filling membrane) which had an ion conductivity and a durability similar to those of a commercial membrane to prepare MEAs (active area: 25 cm²) [6]. The performances of the MEAs were measured at a single cell test station at various relative humidity (RH) from 50% to 110%, atmospheric pressure, and 50 °C when supplied with H₂ and CO₂-free air.

The AMFC MEA using non-platinum and platinum catalyst yields maximum current densities of 343 and 630 mA/cm² at 0.6V, respectively. For comparison, the performance of the MEA with platinum cathode catalyst was more than double the performance of that with non-platinum cathode catalyst. The maximum current density, 630 mA/cm² at 0.6 V, was acquired with 30 wt% ionomer content within electrode. And also 412 mW/cm² peak power at 0.47 V and 50 °C has been demonstrated. Increasing cell temperature is advantageous for higher MEA performance during short-term operation and 70°C is optimum temperature. Ionomer content of the catalyst ink is most sensitive factor for high performance AMFC MEA. Various kinds of optimized condition are affected by the materials used and preparation procedure of MEA, and also by the other single cell operating conditions. They will be presented in detail by the poster. MEA durability was confirmed by constant current technique at 300 mA/cm² over 200 hrs.

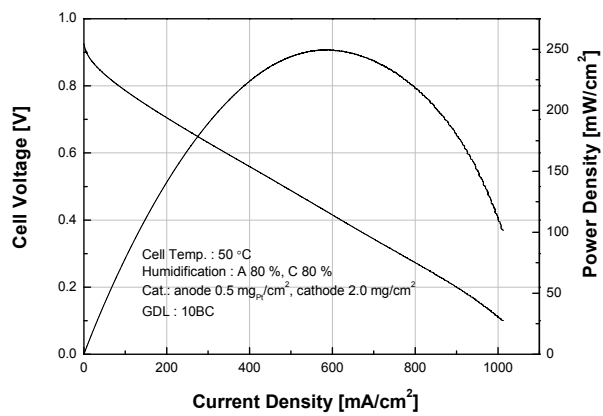


Fig. 1 Maximum AMFC MEA (active area: 25 cm²) performances measured with non-platinum cathode catalysts with clean air at 50 °C operation

References

- [1] Sawai K, Suzuki N (2004) J Electrochem Soc 151:2132-2137
- [2] Coutanceau C, Demarconnay L, Lamy C, Le'ger JM (2006) J Power Sources 156:14-19
- [3] Varcoe JR, Slade RCT (2005) Fuel Cells 5:187-200
- [4] Yu EH, Scott K (2004) J Power Sources 137:248-256
- [5] Gottesfeld S (2011) 2011 AMFC Workshop
- [6] Lee MS, Kim TY, Park SH, Kim CS, Choi YW (2012) J Mater Chem 22:13928-13931

H₂ uptake capacities on materials incorporating cyanometalate building blocks (P-209)

Dr. Ferdi Karadas

H₂ storage has seen a significant research and commercial thrust particularly over the past two decades due to rise in global energy needs and environmental concerns. Solid adsorbents have received intense interest because of the potential they have demonstrated in hydrogen storage field since no regeneration energy is required to remove H₂ and they are robust even at extreme conditions. Even though promising developments have been made with the means of both theoretical and experimental research groups, the field continues to lag because of a missing link between current research and near future commercialization of an efficient porous material that exhibits high H₂ storage capacities at ambient conditions. Thus, new systems should be designed, prepared, and studied systematically to achieve this goal. Herein this project, this issue will be addressed by introducing extended networks incorporating cyanide (CN⁻) bridging groups.

H₂ could be adsorbed on a surface either with a physisorption process, which is a result of Van der Waals forces between H₂ molecules and surface, or with a chemisorption process where H₂ molecule disassociates to bind chemically to the material surface. Given that H₂ storage technology requires a regeneration energy in the 0.1 - 1 eV range to work at ambient temperatures and pressures, both of these processes are not suitable for H₂ storage applications since the binding energy of the former process is very small (in the meV range) and that of the latter is high (in the 2 - 4 eV range). The approach applied in this proposal is to improve interactions in the physisorption process by introducing specific groups to the network that interacts strongly with H₂ such as exposed metal centers, cyanide, and ammonia functional groups.

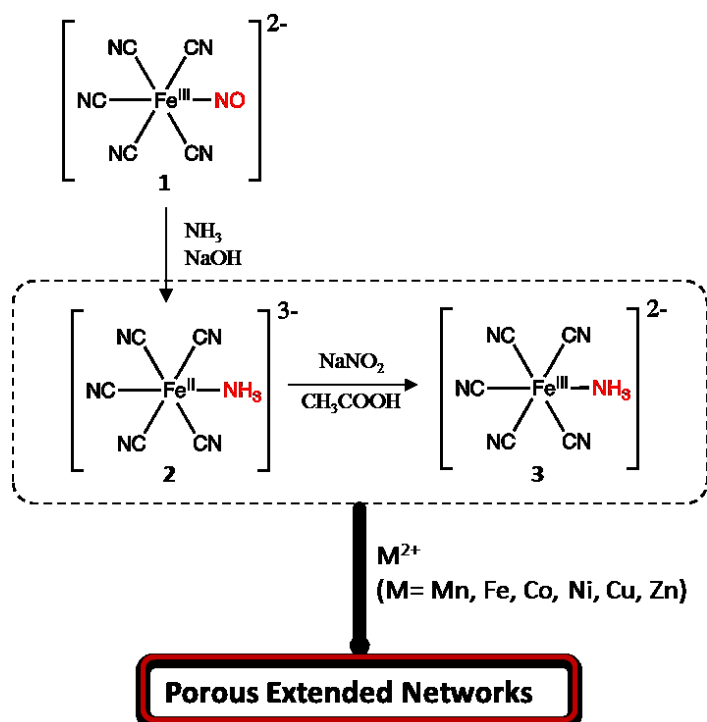


Figure. Synthetic methodology to prepare extended networks incorporating pentacyanometalate precursors.

all exist in the same cubic structure even when metal ions with different oxidation states are used,

since the binding energy of the former process is very small (in the meV range) and that of the latter is high (in the 2 - 4 eV range). The approach applied in this proposal is to improve interactions in the physisorption process by introducing specific groups to the network that interacts strongly with H₂ such as exposed metal centers, cyanide, and ammonia functional groups.

One of the well-known examples of cyanide clusters is Prussian Blue analogues (PBAs) that represent a large family of compounds based on a cubic $\text{M}'[\text{M}(\text{CN})_6]$ ($\text{M}' = \text{Cr}^{3+}, \text{Mn}^{2+}, \text{Fe}^{2+/3+}, \text{Co}^{2+/3+}, \text{Ni}^{2+}, \text{Cu}^{2+}, \text{Zn}^{2+}$, and $\text{M} = \text{Fe}^{2+/3+}, \text{Co}^{2+/3+}, \text{Cr}^{3+}, \text{Mn}^{2+}$) framework, in which metal ions are connected through cyanide bridging ligand. One of the remarkable structural properties of PB analogues is that they

which could be utilized in H₂ storage field due to two main reasons; a) the framework provides its charge balance by creating vacancies, which improves the porosity of network, b) exposed metal centers are generated that could interact with adsorbed H₂ molecule.

Contrary to the previously applied synthetic methods that include the reaction of hexacyanometalate complexes with transition metal ions, pentacyanometalate ions have been used to prepare novel extended networks. Pentacyanonitrosylferrate complex (1) is a commercially available complex, which could be reacted with ammonia in basic media to prepare the pentacyanoamminiferrous complex 2. Precursor 2 could easily be oxidized to 3 with NaNO₂ in acidic media. Several papers have been published in the 80s about the chemistry of pentacyanoferrate complex indicating that ammonia ligand could in fact be replaced with a variety of N-donor ligands such as pyridine-based ligands and aminoacids.

It is aimed to use this rich chemistry to prepare extended porous networks. Similar to the synthesis of PBAs, pentacyanometallate complexes have been reacted with divalent transition metal ions to prepare porous extended networks. It is aimed to improve the porosity of PBAs by introducing extra vacancies inside the framework due to the ability of ammine ligand to connect only one metal center. Clusters have been characterized with XRD, FTIR, TGA, CHNO elemental analysis, and ICP-MS techniques.

Pore analysis as well as the H₂ adsorption measurements have been performed with BET method to determine the surface area (m²/g) and pore volume (cm³/g) of clusters. Adsorption and desorption measurements have been performed in the 0 to 1 bar range at 77 K to compare H₂ storage capacities of family of clusters with those that have previously been studied.

Preparation and characterization OF Pd-Ag-Au alloy membranes for hydrogen separation (P-214)

Jon Meléndez^{1,2}, Ekain Fernandez¹, Pedro L. Arias², D. A. Pacheco Tanaka¹

1TECNALIA Research & Innovation, Materials for Energy and Environment Area

2 University of the Basque Country UPV/EHU, Chemical Engineering and Environmental Department

Palladium membranes have advantages of high hydrogen flux and exclusive perm-selectivity to hydrogen because of their unique permeation mechanism. Pd membranes can be integrated in membrane reactors where separation process is coupled with catalytic reactions such is in the production of hydrogen by steam reforming. Since the permeation flux is inversely proportional to the membrane thickness, development of supported Pd membranes with a thickness of less than 5 μm have been intensively studied in order to attain high hydrogen flux and to minimize the material cost. Among the methods for the fabrication of thin membranes electroless plating (ELP) technique provides advantages over other alternatives, such as PVD and CVD, particularly with respect to the operational flexibility, simple equipment, cost performance and applicability to non-conductive materials of any shapes. Pure Pd membranes are often damaged by: a) hydrogen embrittlement due to the α - β phase transition of palladium hydride which occurs at below the critical temperature (293 $^{\circ}\text{C}$) and pressure (2 MPa) and b) the sulphur poisoning leading to the deactivation of the membrane. Alloying Pd with Ag permits higher tolerance to hydrogen embrittlement. Besides, better tolerance to sulphur can be achieved by alloying Pd with Au. Galvanic displacement of Pd with Au is one of the procedures for Pd-Au membrane preparation; however the amount of Au deposited for this method is difficult to control because the amount of Au displaced with Pd depends on various factors, for example, surface area of the Pd membrane, treating time and temperature. In the present work, we describe the fabrication and characterization of thin Pd-Ag-Au membranes supported on porous alumina tubes by electroless plating technique.

Asymmetric porous alumina tubes (provided by Inopor), having 10 mm of outside diameter and surface pore size of 100 nm were used as support. Supported thin Pd-Ag membranes were prepared by the ELP technique described in [1]. An Au layer is deposited on the Pd-Ag membrane by the technique of ELP using $\text{K}[\text{Au}(\text{CN})_4]$ and hydrazine as Au source and reductant agent respectively [2]; using this technique, the amount of gold deposited can be accurately controlled since all the gold in the plating solution is deposited on the membrane. Various membranes with different metal composition will be prepared. The alloy Pd-Ag-Au alloy was formed by annealing the membrane at 550 $^{\circ}\text{C}$ for several hours and confirmed by XRD analysis. Hydrogen permeation characteristic were carried out using a shell-and-tube type apparatus detailed in [1] in order to measure the permeation of hydrogen and nitrogen through the membranes. The effect of the temperature and metal composition in the hydrogen permeation will be studied.

References

[1] D.A. Pacheco Tanaka, M.A. Llosa Tanco, S. Niwa, Y. Wakui, F. Mizukami, T. Namba and T. M. Suzuki, Preparation of palladium and silver alloy membrane on a porous α -alumina tube via simultaneous electroless plating, *J. Membr. Sci.* 247 (2005) 21– 27.

[2] J. Okazaki, D.A. Pacheco Tanaka, M.A. Llosa Tanco, Y. Wakui, T. Ikeda, F. Mizukami and T.M. Suzuki, Preparation and Hydrogen Permeation Properties of Thin Pd-Au Alloy Membranes Supported on Porous α -Alumina Tube, Materials Transactions 49 (2008) 449–452.

Acknowledgements

Jon Meléndez would like to thank University of Basque Country (UPV-EHU) for Zabalduz scholarship program. Besides, D.A. Pacheco Tanaka would like to thank People Programme (Marie Curie Actions) of the European Union's Seventh Framework Programme (FP7/2007-2013) under REA grant agreement n° 267200. Many thanks also to Jon Zuñiga and J.L. Viviente from Tecnalía for their support.

Comparison between electroless plating and PVD-magnetron sputtering techniques for preparation of Pd-Ag membranes for hydrogen separation (P-217)

Ekain Fernandez¹, José Angel Sanchez-García¹, Jon Meléndez¹, Alba Arratibel¹, D. A. Pacheco Tanaka¹

¹TECNALIA Research & Innovation, Materials for Energy and Environment Area

Palladium membranes have advantages of high hydrogen flux and exclusive perm-selectivity to hydrogen because of their unique permeation mechanism [1]. Pd membranes can be integrated in membrane reactors where separation process is coupled with catalytic reactions such is in the production of hydrogen by steam reforming. Since the permeation flux is inversely proportional to the membrane thickness, development of supported Pd membranes with a thickness of less than 5 μm have been intensively studied in order to attain high hydrogen flux and to minimize the material cost. The most important problem associated with the use of pure Pd membranes is the hydrogen embrittlement phenomenon. Operation with hydrogen at a temperature below 300°C and a pressure below 2 MPa, leads to the nucleation of the β -hydride phase from the α -phase resulting in severe lattice strains. In this case a pure palladium membrane becomes brittle after a few α - β cycles [2]. In order to avoid embrittlement, Pd77Ag23 alloy has been used for a while because it has the critical temperature (T_c) for formation of the β phase is around room temperature [3].

Common Pd-based layer deposition technologies include physical vapor deposition (PVD, including magnetron sputtering, thermal evaporation or pulsed laser evaporation), chemical vapor deposition (CVD or MOCVD), electroless plating (ELP), electroplating and diffusion welding [4]. Each technology has its strengths and weaknesses; therefore, there is a trend of tailoring the deposition technology to the features of the support in order to obtain a suitable composite membrane. The most widely used preparation technology for dense metal layers is ELP due to its ability of covering supports with complex geometries, the simplicity of the required equipment and its low cost (absence of electrodes or electrical source) [5]. On the other hand, PVD magnetron sputtering is a very attractive deposition technology because it could provide thinner uniform layers (down to only few nanometers), much lower than the thickness achieved with the ELP technique, with a controlled microstructure and composition across of these coatings. Other important advantage of PVD versus ELP is its environmental friendly operation, without producing waste liquids from chemical baths [6]. In the present work, we describe the fabrication and characterization of thin Pd-Ag membranes supported on porous alumina tubes prepared by electroless plating and PVD-Magnetron Sputtering techniques.

Asymmetric porous alumina tubes (provided by Inopor), having 10 mm of outside diameter and surface pore size of 100 nm were used as support. On one side, supported thin Pd-Ag membranes were prepared by the ELP technique described in [7]. On the other side, supported thin Pd-Ag membranes were prepared by PVD-Magnetron Sputtering technique using CemeCon® CC800/8 equipment. Manufactured membranes were characterized by e.g. SEM -EDX and XRD in order to analyze their morphology/structure and their alloy composition. Moreover, gas permeation properties of prepared membranes were evaluated for H₂ and N₂ as a function of differential pressure and temperature using a shell-and-tube type apparatus detailed in [7].

References

- [1] F. Gallucci, E. Fernandez, P. Corengia, M. Van Sint Annaland, Recent advances on membranes and membrane reactors for hydrogen production, *Chemical Engineering Science* 92 (2013) 40–66.
- [2] H.P. Hsieh, Inorganic membrane reactors – a review. *AIChE Symp. Ser.* 85 (1989) 53–67.
- [3] S.N. Paglieri, J.D. Way, Innovations in palladium membrane research. *Sep. Purif. Rev.* 31 (2002) 1–169.
- [4] N. Iniotakis, C.B. Von Der Decken, H. Fedders, W. Froehling, F. Semetz, Hydrogen Permeation Membrane. US Patent 4699637. 1987.
- [5] O. Mallory, J.B. Hajdu, Electroless Plating: Fundamentals and applications. American Electroplaters and Surface Finishers Society, Orlando, FL, ISBN: 9780815512776. 1990.
- [6] H. Klette, Thin Pd-Ag foil prepared by PVD, supported on porous SS. *Membrane Tech* 5 (2005) 7.
- [7] D.A. Pacheco Tanaka, M.A. Llosa Tanco, S. Niwa, Y. Wakui, F. Mizukami, T. Namba and T. M. Suzuki, Preparation of palladium and silver alloy membrane on a porous α -alumina tube via simultaneous electroless plating, *J. Membr. Sci.* 247 (2005) 21– 27.

Acknowledgements

The authors would like to thank Jon Zuñiga and J.L. Viviente from TECNALIA for their support.

Steam Reforming Process for manufacturing of Hydrogen in Solid Oxide Fuel Cell using Biogas (P-222)

Yu-Jin Han, Department of Semiconductor & Display Engineering, Hoseo University

Jin-Do Chung, Department of Environmental Engineering, Hoseo University

Jang-Woo Kim, Department of Display Engineering, Hoseo University

Eui-Woo Lee, Department of Environmental Engineering, Hoseo University

Hae-Yeul Ryu, Department of Environmental Engineering, Hoseo University

Byung-Uk Im, Department of Environmental Engineering, Hoseo University

Kyu-Yeol Kim, Department of Environmental Engineering, Hoseo University

Abstract

With the advent of the 3E age of the world in which environment, energy and economy must be taken into consideration at the same time and where the competition for the acquisition of resources has been intensified, the trend in response to this is to change the national policy paradigms on energy and resources from "stable implementation" to "autonomous development."

Fuel cells compose a new energy technological field. They are highly efficient and do not have a combustion process so the occurrence of pollutants and factors of pollution can be greatly reduced. For these reasons, fuel cells are being proposed as a measure of solution for the issues of global warming and the depletion of fuel energy. However, hydrogen fuel must be continuously supplied in fuel cell because fuel cells are energy conversion devices as opposed to batteries.

Nevertheless, the situation is that as the infrastructure for commercial hydrogen production and supply has not been set up yet.

Thus, this study is conducted to integrate the regeneration energy biogas with the high efficiency fuel cells. As part of the study, research is carried out with the purpose of reforming the biogas to achieve a stable supply of hydrogen.

The catalyst optimization for steam reforming. the applied commercial catalysts are Nickel supported by alumina, Ruthenium supported by alumina and a non-commercial catalyst which was used by supporting Ni with Ru was used.

By using a SEM (scanning electron microscope) and through a TGA (thermogravimetric analysis), the effects according to the catalyst reaction variables was analyzed and the gas modified by each of the other catalysts were used as fuel for solid oxide fuel cells and an analysis of the electrical characteristics.

Having compared the reaction activation, the activation was shown to be of greater in the order of $\text{Ru}(0.5)/\text{Ni}(20)/\text{Al}_2\text{O}_3 > \text{Ni}(20)/\text{Al}_2\text{O}_3 > \text{Ru}(2)/\text{Al}_2\text{O}_3$. The resistance to the carbon deposits at 750°C and S/C ratio 2.5 conditions, were shown to be higher in the order of $\text{Ru}(2)/\text{Al}_2\text{O}_3 > \text{Ru}(0.5)/\text{Ni}(20)/\text{Al}_2\text{O}_3 > \text{Ni}(20)/\text{Al}_2\text{O}_3$.

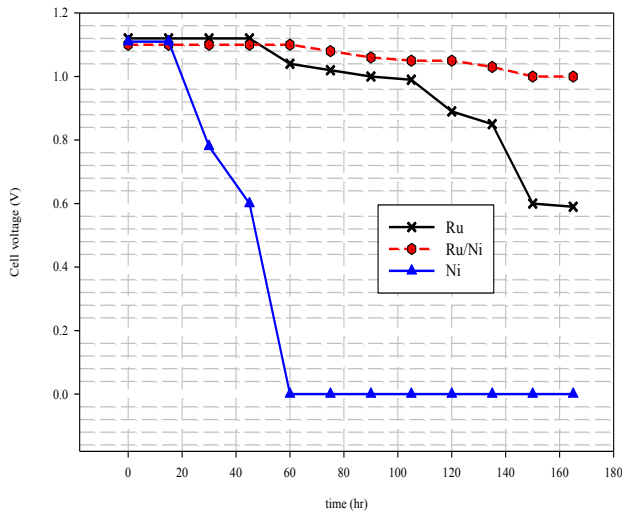


Fig. 1. Cell voltage at a variation of time (at 750°C, S/C=2.5)

As a result of running an electrical characteristic assessment at 750°C and S/C ratio 2.5 conditions, there were no change initially in the voltage value but, upon over 160 hours operation, the electrical characteristics were shown to be of good quality in the order of Ru(0.5)/Ni(20)/Al₂O₃ > Ni(20)/Al₂O₃ > Ru(2)/Al₂O₃.

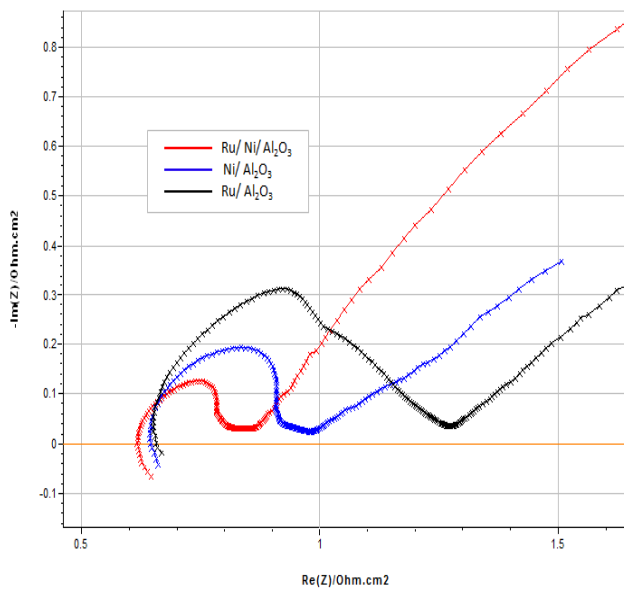


Fig. 2. Impedance spectra change at a variation of catalyst (at 750°C, S/C=2.5)

Thus, it is determined that when operating solid oxide fuel cells over a long period using biogas, for the steam reforming catalyst, the Ru(0.5)/Ni(20)/Al₂O₃ catalyst with precious metals showed

outstanding characteristics compared to the existing commercial reforming catalyst of Ni(20)/Al₂O₃ in reaction to carbon deposits and activation in high temperatures and the Ru(0.5)/Ni(20)/Al₂O₃ catalyst did not need pre-reduction as well.

Acknowledgment

This work was supported by the Human Resources Development of the Korea Institute of Energy Technology Evaluation and Planning(KETEP) grant funded by the Korea government Ministry of Knowledge Economy (No. 20114010203130)

Global hydrogen systems analysis. IEA HYDROGEN ANNEX 30 (P-223)

*Maria P. Argumosa, INTA
Susan Schoenung, Longitude 122 West, Inc
Jochen Linssen, Forschungszentrum Juelich
Thomas E. Drennen, Sandia National Laboratories*

The IEA Hydrogen Implementing Agreement covers several expert groups on hydrogen topics. The annex 30 has the target of: developing a consistent data basis and perform systems analysis of hydrogen resources, generation and demand scenarios considering sustainable low-carbon solutions.

This group has been working, trying to build a database on hydrogen production and applications technologies, since 2010 and it will present its results before spring 2014.

The specific objectives of this task are: to prepare authoritative analyses which can be used to answer questions about hydrogen sources and utilization; to update the assessment of hydrogen technology maturity and projections and to interface with other HIA tasks regarding data and RD&D progress.

The whole work has been structured in three subtasks:

Subtask A: Global Hydrogen Resources Study. It focuses on the analysis of the available hydrogen resources worldwide and the future hydrogen interregional trading; using a H2 simulation model developed by Sandia National Laboratories of United States. Ten country data have been gathered together about feedstock availability and prices (United States, Germany, Spain, Norway, Denmark, Sweden, France, Japan, Italy and UK).

The model uses the least cost option calculation of hydrogen production pathway and offers options for international trading (transport included) and carbon tax that may change the results.

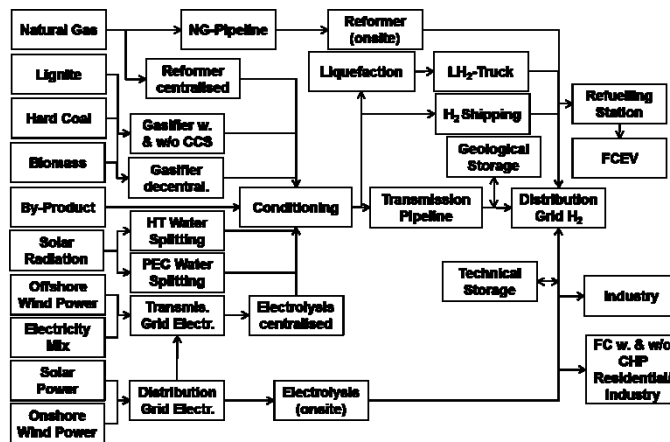
The Pacific Rim is being analyzed also.

The main results of this analysis and the Spanish specific data will be showed in the EHEC 2014 congress.

Subtask B: Hydrogen Technology Database. Upon this umbrella three activities has been carried out:

- The development of a DATABASE based on the consistency of technical parameters: Same definition of efficiency (balancing all energy inputs/ outputs) to defined conditions of hydrogen; and the consistency of economical parameter: price levels, calculation scheme of costs: interest rate, annuity factor, economical lifetime.
- The edition of a HANDBOOK for technology description and frame conditions of technical and economical data.
- A detailed DATA ANALYSIS of different hydrogen production costs based on resources data from Subtask A and technology description of Subtask B under consistent

assumptions (interest rate, economical lifetime etc.), comparison of national differences.



Selected technologies and pathways considered in Subtask B

Subtask C: Collaboration with IEA Analysis Group. The main target of this expert activity has been to start and not stop with collaboration between the HIA experts and the WEO and ETP responsible on the outlook and prospects analysis. The main job carried out by this group has been reviewing and making comments on the reports before their edition in order to check that the results are according to the real hydrogen technology facts.

A fourth subtask is being spun out of this task, this is called: Hydrogen for Smart Grid. It is dealing with the use of renewable generated hydrogen in three scenarios, using HOMER as an analysis tool:

- Hydrogen for second generation bio fuels production
- Power-to-gas (The idea is to avoid the use of a fuel cell)
- Power systems services

Preparation of Pd-Ag pore filled membranes for hydrogen separation (P-225)

Alba Arratibel^{1,2}, Ekain Fernandez^{1,2}, Jon Meléndez¹, M. A. Llosa Tanco, Fausto Gallucci², D.A. Pacheco Tanaka²

*¹TECNALIA Research & Innovation, Materials for Energy and Environment Area
²Eindhoven University of Technology, Department of Chemical Engineering and Chemistry, Multiphase Reactors Group.*

Membrane reactors are reactors integrating catalytic reactions and separation through membranes in a single unit. This combination of process steps results in a high degree of process integration/intensification, with accompanying benefits in terms of increased process or energy efficiencies and reduced reactor or catalyst volume [1]. Palladium membranes have been used in membrane reactors (generally reforming and water gas shift reactions for hydrogen production) due to their remarkable permeability and exclusive perm-selectivity of hydrogen. In order to attain high hydrogen flux and minimize the material costs, researchers have been motivated to fabricate thin palladium membranes. Pure palladium membranes are tended to be suffered from hydrogen embrittlement at lower than critical temperature and pressure (293 °C) and pressure (2 MPa). On the other hand, Pd–Ag alloy membrane has been recommended due to its better hydrogen permeability and improved mechanical strength against hydrogen embrittlement.

The surface of thin Pd based membrane is prone to become contaminated and mechanically damaged when the membrane is integrated in a reactor. The damage is even more serious when it is used as part of fluidized bed membrane reactors where the collision with the catalyst particles can erode and destroy thin Pd membranes. Improved mechanical stability and better adhesion of the palladium membrane can be expected by filling nanosized pores of a ceramic support with palladium particles.

Novel “Pore-filled” (PF) Pd membranes have been developed by the electroless plating technique [2,3]. Four steps are involved in the preparation of the “Pore-filled” membranes: a) coating of the surface of α -Al₂O₃ support tube (100 nm pore size) with a nanoporous (< 6 nm) ceramic layer b) seeding; nanoparticles of Pd are deposited inside the porous ceramic, they are used as catalysts for electroless plating (ELP) of Pd, c) coating with a nanoporous protecting ceramic layer and d) plating; forcing to pass a Pd plating solution through the pores, Pd(II) present in the solution will react with the Pd seeds increasing their size until the pore is completely filled with Pd. This “Pore-filled” membrane configuration provides advantages of membrane handling since palladium layer is not exposed directly on the top surface; the amount of Pd used is a fraction of the conventional Pd membranes and are stronger against hydrogen embrittlement. In this work, the preparation and characterization of Pd-Ag pore filled membranes will be for the first time reported.

References

[1] F. Gallucci, E. Fernandez, P. Corengia, M. Van Sint Annaland, Recent advances on membranes and membrane reactors for hydrogen production, *Chemical Engineering Science* 92 (2013) 40–66.

[2] D.A. Pacheco Tanaka, M.A. Llosa Tanco, T. Nagase, J. Okazaki, Y. Wakui, F. Mizukami, T.M. Suzuki, Fabrication of hydrogen-permeable composite membranes packed with palladium nanoparticles, *Adv. Mater.* 18 (2006) 630–632.

[3] D.A. Pacheco Tanaka, M.A. Llosa Tanco, J. Okazaki, Y. Wakui, F. Mizukami, T.M. Suzuki, Preparation of “pore-fill” type Pd–YSZ γ -Al₂O₃ composite membrane supported on α -Al₂O₃ tube for hydrogen separation, *J. Membr. Sci.* 320 (2008) 436–441.

Acknowledgements

The authors would like to thank Jon Zuñiga and J.L. Viviente from Tecnia and Prof. Martin Van Sint Annaland from Eindhoven University of Technology for their support.

Structural and electrical characterization of the novel $\text{SrCo}_{1-x}\text{M}_x\text{O}_{3-\delta}$ perovskites (M= Ti, V, Nb) : evaluation as SOFC cathode materials (P-232)

V. Cascos^{1,*}, R. Martínez-Coronado², J.A. Alonso¹

¹Instituto de Ciencia de Materiales de Madrid, CSIC, Cantoblanco 28049 Madrid, Spain

²Materials Science and Engineering Program/Mechanical Engineering, The University of Texas at Austin, Texas 78712, United States

*E-mail: vcascos@icmm.csic.es

An intermediate-temperature solid oxide fuel cell (IT-SOFC) is an electrochemical device that converts chemical energy directly into electrical energy at temperatures between 550 and 850 °C; these devices have a high energy-conversion efficiency, low environmental impact and good fuel flexibility [1,2]. The cathode is responsible for a significant drop in the cell potential at intermediate temperatures, thus one of the major improvements required for the commercialization of IT-SOFC is the development of new mixed ionic-electronic conductors with better performance at these temperatures. High-temperature $\text{SrCoO}_{3-\delta}$ phases with cubic 3C-like crystal structures are presented as mixed conductors with very high oxygen permeability and high electrical conductivity [3,4]. However, this phase is not stable below 900 °C where a 3C-cubic to 2H-hexagonal phase transition takes place when the sample is slowly cooled down.

The stabilization of a 3C perovskite framework in the $\text{SrCoO}_{3-\delta}$ system has been a widely used strategy to obtain an adequate mixed ionic-electronic conductor to be used as a cathode in intermediate-temperature solid oxide fuel cells. For this purpose, several substitutions have been performed in either the Sr (Ba, La, Sm) or in the Co (Sc, Fe, Ni, etc) positions. In a previous work, we have stabilized a 3C perovskite phase by doping the $\text{SrCoO}_{3-\delta}$ system with Mn^{2+} , Sb^{5+} or Mo^{6+} in $\text{SrCo}_{1-x}\text{M}_x\text{O}_{3-\delta}$ ($x = 0.05, 0.1, 0.15$ and 0.2) [5,6]. The aim of this work has been to introduce highly-charged cation at the Co sublattice, in order to avoid the stabilization of the 2H structure containing face-sharing octahedra, in perovskites of composition $\text{SrCo}_{1-x}\text{M}_x\text{O}_{3-\delta}$ with Mn^{4+} , V^{5+} and Nb^{5+} for moderate values of $x = 0.03, 0.05$. We have stabilized tetragonal 3C perovskite (corner sharing network) phases in all cases and we have studied the crystal structures by neutron diffraction. The structures were correctly refined in the $P4/mmm$ model as shown in the Fig.1, allowing to precisely characterize the defective oxygen network.

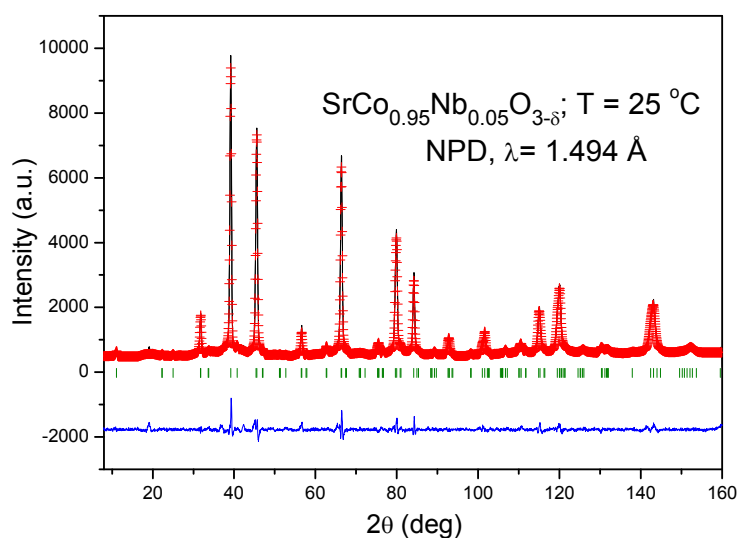


Fig.1: Observed, calculated and difference NPD Rietveld profiles at RT for $\text{SrCo}_{0.95}\text{Nb}_{0.05}\text{O}_{3-\delta}$.

Thermal expansion measurements show compatibility with LSGM electrolyte; the good values of conductivity (between 100-200 Scm^{-1} at 800°C) are adequate for cathodes in SOFC. Finally, single cells in electrolyte (LSGM) supported configuration yield reasonable current densities, with maximum output powers of $600\text{mW}/\text{cm}^2$ at 850°C with pure H_2 as fuel as shown in the Fig.2.

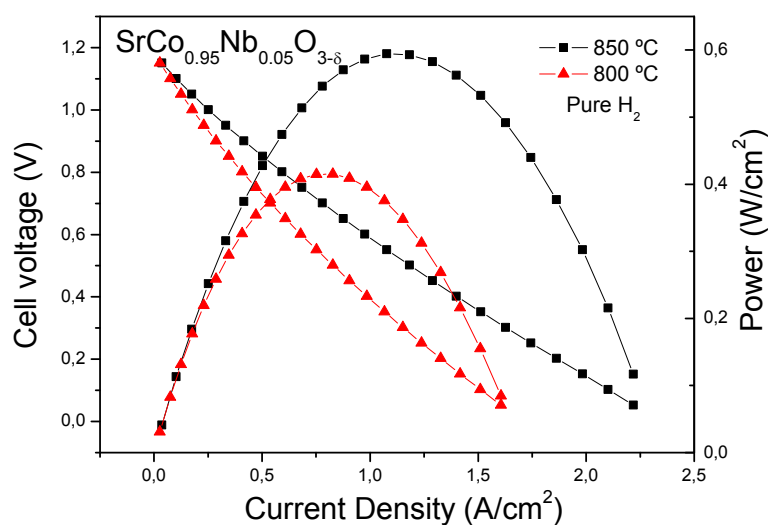


Fig.2: Cell voltage (left axis) and power density (right axis) as a function of the current density for the test cell with the configuration SMFO/LDC/LSGM/SCNO in pure H₂ measured at T= 800 and 850°C with Pt as current collector.

Keywords: solid oxide fuel cells, cathode materials, energy conversion, neutron powder diffraction

References

- [1] H.Y. Tu, Y. Takeda, N. Imanishi, O. Yamamoto, *Solid State Ionics* 117 (1999) 277–281.
- [2] M. Dokiya, *Solid State Ionics* 152 (2002) 383–392.
- [3] Deng, Z. Q.; Yang, W. S.; Liu, W. Chen, C. S. J. *Solid State Chem.* 2006, 179, 362.
- [4] De la Calle, C; Aguadero, A.; Alonso, J.A.; Fernández-Díaz, M.T. *Solid State Sciences* 2008, 10, 1924.
- [5] Aguadero, A.; De la Calle, C.; Alonso, J. A.; Escudero, M. J.; Fernandez-Díaz, M. T.; Daza, L. *Chem. Mater.* 2007, 19, 6437.
- [6] Aguadero, A.; Perez-Coll, D.; Alonso, J. A.; Skinner, S. J.; Kilner, J. *Chem. Mater.* 2012, 24, 2655-2663.

Acknowledgments. We are grateful to the Spanish Ministry of Economy and Competitiveness for granting the project MAT2010-16404, and SINQ (PSI-Switzerland) for making all facilities available for the neutron diffraction experiments.

Dehydrogenation kinetics of magnesium hydride under different experimental conditions (P-234)

Antonio Perejón, Pedro E. Sánchez-Jiménez, Luis A. Pérez-Maqueda, José M. Criado

Instituto de Ciencia de Materiales de Sevilla (CSIC-University of Seville), Américo Vesputio 49, 41092 Sevilla, Spain.

Hydrogen storage is one of most important issues for realization of hydrogen energy economy. Mg-based materials have been extensively studied as solid-state hydrogen storage candidates due to the large capacity of MgH₂ (7.7 mass%) and the relative high abundance of magnesium in earth. However, the kinetic and thermodynamic properties of Mg-based materials present problems for practical applications, because Mg needs temperatures above 300°C to absorb hydrogen and the dehydrogenation temperature of MgH₂ is even higher because of its high thermodynamic stability. These temperatures can be decreased by applying an activation process based on several cycles of hydrogenation and dehydrogenation, but it has been demonstrated that even after activation the absorption and desorption rates are low for practical applications. Nanostructure MgH₂ presents enhanced hydrogen absorption and desorption rates due to the presence of more nucleation sites and larger surface area.

Therefore, a deep knowledge of the kinetics of absorption and desorption processes is crucial for future applications of MgH₂. Most of the kinetic studies of absorption and desorption of hydrogen in MgH₂ are performed in isothermal conditions and assume an Avrami-Eroffev kinetic model (nth-order nucleation-growth model) for the analysis, in such a way that the model is used just as a fitting function without physical meaning. It is worth noting that the assumption of a kinetic mechanism produces a significant effect on the kinetic parameters, i.e. activation energy and pre-exponential factor, resulting from the kinetic analysis. Thus, if an incorrect kinetic model is assumed, the resulting parameters will also be erroneous.

In this contribution, dehydrogenation kinetics of commercial MgH₂ was studied by thermogravimetry (TG) and differential scanning calorimetry (DSC) under three different experimental conditions:

- high vacuum
- atmospheric pressure
- 20 bar of H₂

Experimental data was obtained from linear heating rate, isothermal and sample controlled thermal analysis (SCTA) experiments. The kinetic analysis was performed using the Combined Kinetic Analysis procedure, which allows the determination of the kinetic parameters from the simultaneous analysis of a set of experimental curves recorded under any thermal schedule. Moreover, this method does not require making any kind of assumptions about the kinetic models followed by the reaction.

Interestingly, the results obtained show that dehydrogenation kinetics of MgH₂ strongly depends on the experimental conditions used for the reaction. Thus, if the reaction is performed under high

vacuum, it follows a first order kinetics (F1), while in air it follows a two-dimensional diffusion model (D2) and a third-order nucleation-grow model (A3) when the experiment is carried out in 20 bars of hydrogen pressure. Moreover, the activation energy of the reaction is also influenced by the experimental conditions, and is higher as the pressure of the system increases, being 109 kJ mol⁻¹ for the experiment in vacuum, 148 kJ mol⁻¹ in air and 176 kJ mol⁻¹ in 20 bars of hydrogen pressure.

Thermal Integration possibilities with SOFC exhaust gases and heat transfer (P-237)

*Tamara Guerrero¹, Daniel Márquez¹, Marta T. Escudero¹ and Rocío Domínguez¹.
1Abengoa Hidrógeno, Campus Palmas Altas, C/Energía Solar nº1, 41014 Sevilla.*

INTRODUCTION

Nowadays, all kind of fuel cells are being studied because of the quality of the power produced by them, and because of the resources required to the feeding and the not noxious exhausts. Particularly, Solid Oxide Fuel Cells are considered in this work because it is a technology in continuous development because of the usefulness of high temperature fuel cells.

SOFC can be fed with different fuels as hydrogen, reformato gas, etc. and air or pure oxygen, and the optimum operating temperature is between 600 and 800 °C.

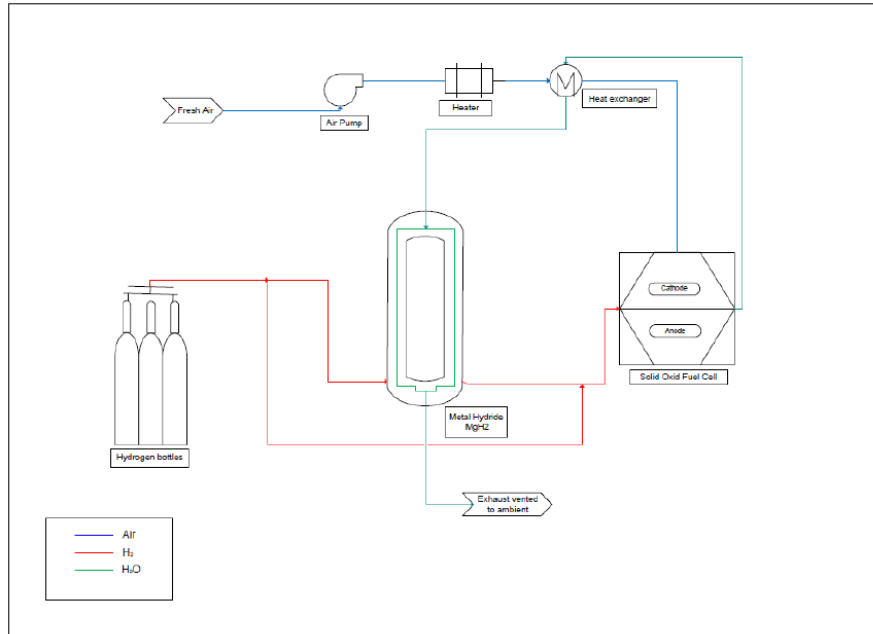
The aim of this work comes from the European project “Fast, reliable and cost effective boron hydride based high capacity solid state hydrogen storage materials” (Bor4store). The research leading to these results has received funding from the European Union's Seventh Framework Programme (FP7/2007-2013) for the Fuel Cells and Hydrogen Joint Technology Initiative under grant agreement n° 303428.

In this work, some possibilities of how to profit the high temperature in which this kind of fuel cell operates are presented. Depending on the power supplied by the SOFC selected, these possibilities have to be studied to find out the viability of these proposals.

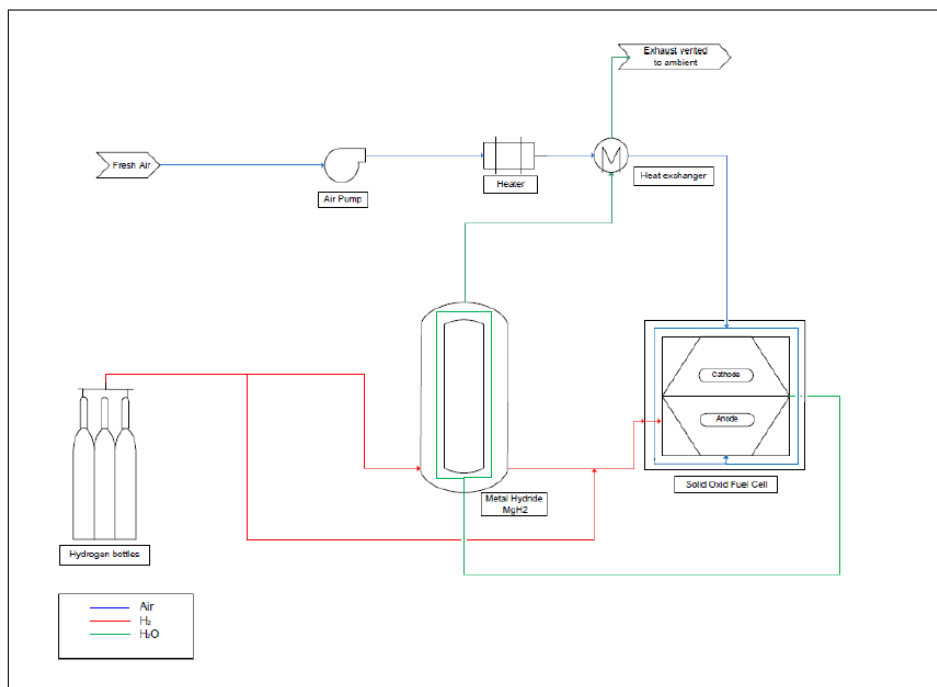
THERMAL INTEGRATION

Firstly, there are two possibilities of thermal integration presented that depend on the exhaust air flow of the Solid Oxide Fuel Cell.

The first possibility presented consists on the warm up of the air input with the exhaust gases from the cathode of the fuel cell. This exhaust flow goes out of the stack at a temperature around 600-700 °C and can be driven around the air input conduction to warm it up before going into the stack to make easier the operation of the fuel cell increasing the efficiency.



The second option presented consists on the warm up of the metal hydride to help the desorption of hydrogen and the warming up of the fuel flow too. The temperature required by the metal hydride tank to correctly desorpt has to be considered before calculating the viability of this thermal integration.



Secondly, there is an option of thermal integration presented that depends on the heat radiated by the chamber where the stack is contained in. That chamber reaches temperatures in a range between 600 and 700 °C.

Supposing a metal hydride as fuel supplier, for this case of thermal integration, the tank is proposed to be placed near or around the chamber, depending on the geometry of the tank, to directly be warmed up by radiation. To correctly desorpt the hydrogen of the metal hydride, the range of temperature supported by the tank and the borohydride has to be taken into account to correctly control the temperature, not to damage it physically or to interfere in the proper desorption of the metallic borohydride.

CONCLUSIONS

After regarding all the three possibilities of thermal integration presented in this work there are some requirements that have to be known for studying the viability of each one.

- The power supplied by the SOFC is required to correctly calculate the input and output flows of fuel and air.
- The temperature of the exhaust air flow.
- The temperature measured on the wall of the chamber where the stack is placed.
- If a metal hydride tank is used as hydrogen supplier, the range of operation temperature is required.

Once all these data is recovered, calculations and simulations can be done with all three different proposals to correctly decide which is the best one before building the system.

That way, not only the power supplied by the Solid Oxide Fuel Cell is useful, even the temperature and the heat can be profited for a better operation of the system and an increase of the efficiency.

Effect of carbon dioxide on proton exchange membrane fuel cell performance: Influence of the operating temperature (P-240)

Manuel Antonio Díaz a,*, Fernando Isorna b, Alfredo Iranzo c, Eduardo López d, Felipe Rosa e, Juan Pedro Bolivar f

a, b, d INTA-National Institute for Aerospace Technology, Ctra. San Juan del Puerto-Matalascañas, km 33, 21130 Mazagon, Huelva, Spain.

c, e Thermal Engineering Group, Energy Engineering Department, School of Engineering, University of Seville, Camino de los Descubrimientos s/n, 41092 Sevilla, Spain.

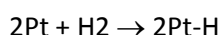
f Dept. Física Aplicada, E.P.S. La Rabida, Universidad Huelva, 21819 Palos de la Frontera, Huelva, Spain

*Corresponding author. Phone: +34 959208847; Fax: +34 959208828.

E-mail address: isornaf@inta.es.

Currently, approximately 95 % of hydrogen (H₂) is produced by the steam reforming of natural gas or methane. In the feed obtained using this process, besides H₂, there are different impurities like carbon monoxide (CO), carbon dioxide (CO₂), methane (CH₄) and nitrogen (N₂) which can be present, hence it is important to determine how they can affect the fuel cell performance. The presence of these impurities can have a highly negative effect on the fuel cell performance even at low concentration levels, decreasing the overall system efficiency and, depending of the type of impurity, the degradation of the different components which comprise a fuel cell can be highly irreversible. For this reason, the presence of impurities in the reacting flows will influence the durability and the efficiency of a fuel cell.

CO₂ is commonly considered as an inert gas. That means that the losses are typically only attributed to the H₂ dilution. However, a CO₂/H₂ mixture produces larger polarization losses than a N₂/H₂ mixture. This can be explained if it is considered the production of CO through the Reverse Water Gas Shift reaction (RWGS):



The RWGS can produce CO concentrations of about 10-100 ppm approximately. This reaction can take place under normal operating conditions of a PEMFC and with the presence of a catalyst. It means that even a non-containing CO fuel can produce a drastic degradation on the performance if enough concentration of CO₂ is present.

An experimental investigation of the performance of Low Temperature PEMFCs operating with different concentrations of CO₂ at the anode inlet is presented. 50 cm² MEAs are used in the investigation, with catalyst Pt loading 0.5 mg cm⁻² for both anode and cathode. An analysis of the effect of temperature is also presented in this work. The results show that the performance loss is larger than expected if only a dilution effect were considered, so that a real contamination process occurs in the cell when CO₂ is fed to the anode together with hydrogen. The contamination is attributed to the Reverse Water Gas Shift reaction (RWGS) which produces CO from the CO₂ fed to

the anode. This contamination effect is analysed and quantified by comparing the polarization curves of the contaminated cell with the ones corresponding to the cell operating with pure hydrogen. The overpotentials for different current densities, CO₂ concentrations, and cell temperatures are presented and discussed (Figure 27 and Figure 28).

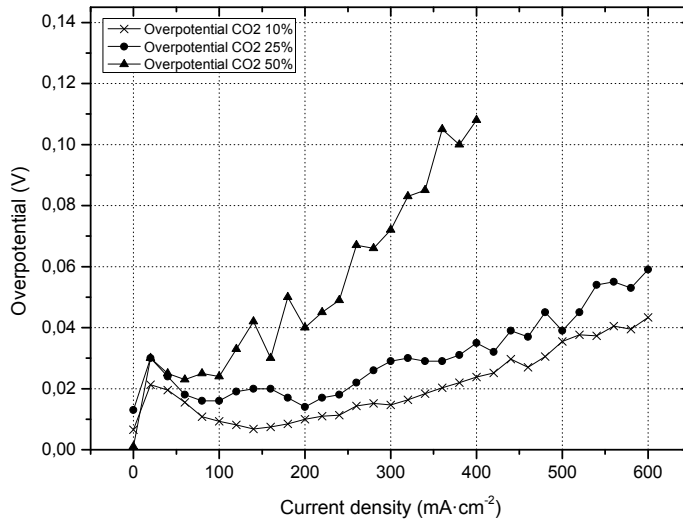


Figure 27: Overpotential due to the presence of CO₂ in the fuel (EH₂ – EH₂/CO₂). T=60°C. RH = 100 %. P = 3 bar (absolute).

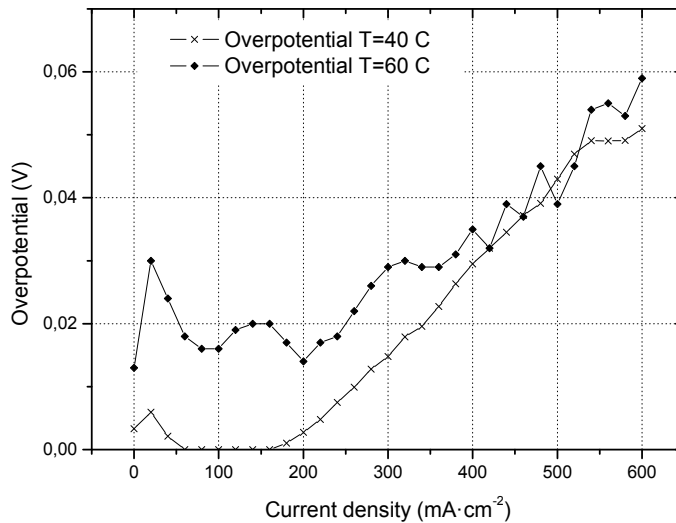


Figure 28: Comparison of the overpotential (EH₂ – EH₂/CO₂) at T=40°C and T=60°C with a 75/25 % mixture H₂/CO₂ of. RH=100 %. P=3 bar (absolute).

Two different regeneration processes (anode feeding with pure H₂ and with air) are also presented and discussed. The analysis of the effectiveness of each regeneration strategy also supports the conclusion that CO produced via the RWGS reaction is adsorbed onto the catalyst, so that CO₂ is producing a real contamination and not only a dilution effect.

Numerical modeling of the degradation rate for membrane electrode assembly in high temperature proton exchange membrane fuel cells and analyzing operational effects of the degradation (P-242)

*Taegon Kang^{1, 2}, Minjin Kim^{1, 2, *}, Jintae Kim¹, Young-jun Sohn^{1, 2}*

¹Hydrogen and Fuel Cell Research Center, Korea Institute of Energy Research, Daejeon, Republic of Korea

²Advanced energy technology, University of Science & Technology, Daejeon, Republic of Korea

** corresponding author (minjin@kier.re.kr)*

Fuel cells have taken center stage as more eco-friendly and substantial energy technology than conventional fossil energy sources. Fuel cells are widely used in stationary, portable and transportation applications due to high energy conversion efficiency and excellent load conformability. Proton exchange membrane fuel cells (PEMFC) mostly use perfluorosulfonic acid (PFSA) polymers in the membrane. This system has high conductivity, chemical stability, mechanical strength and potentially long term durability, but it has material problems such as poisoning of carbon monoxide (CO) and difficult water and heat management. To solve these problems, a high temperature PEMFC (HT-PEMFC) based on polybenzimidazole (PBI), which is operated from 393.15 K to 473.15 K, has been developed. The HT-PEMFC system is relatively simple because of a high tolerance to CO and sulfur as well as no humidification.

The aim of this work is to develop a degradation model for predicting the lifetime of HT-PEMFC. Because determining the durability performance data of HT-PEM require long-term experiments and a change of over-potentials, we utilized experimental data from references. Also, we directly experimented on the initial performance of HT-PEM using a Celtec-P1100 membrane electrode assembly (MEA) from BASF Company Ltd. in the Germany to increase the accuracy in predicting performance of model. The size of the active area of the used MEA was 23.92 cm². The cause of the increasing degradation is separated as activation, ohmic, and concentration over-potential at the initial, middle, and late times in a polarization curve. The activation over-potential is affected by the exchange current density, which is one of the kinetic parameters, the ohmic over-potential is affected by the PA doping level in ionic conductivity, and the concentration over-potential is affected by the molar fraction of oxygen at the cathode. Thus, novel equations that include the effects of over-potentials according to the operating conditions and time are proposed in the developed model. In this paper, the development of a degradation model including the effect of over-potentials is used to predict the long term lifetime with regard to various operating conditions, because the operating conditions significantly affect the lifetime of HT-PEM, which has been partially investigated through previous experiments. Thus, we develop a semi-empirical model that includes the effects of over-potentials to predict the lifetime of HT-PEM, for which it is hard to design an analysis of the degradation at various operating conditions, and to determine the initial performance and degradation rate using the developed model at various operating conditions. The agreement of experimental data with the results of the developed model is considerably good at the verification stage of the developed model. Based on the simulation results of the developed model, initial performance is not highly impacted, whereas the lifetime is strongly influenced by changing temperature, PA doping level and inlet gas pressure. The results show that the agreement of the

experiments with the results of the developed model is considerably good at the verification stage of the developed model. Based on the simulation results of the developed model, initial performance is not highly impacted, whereas the lifetime is strongly influenced by changing temperature, PA doping level and inlet gas pressure.

Study on the Sulfur adsorption properties of Mesoporous Material for Fuel Cell (P-247)

Jaedong Kim, kihoon An, Dalryung Park, Bongyu Kim,
Jinwook Kim, Wankeun Bang**, Jiman Kim**

*New Energy Technology Center, R & D Division, Korea Gas Corporation,
Ansan 426-790, Korea*

**Department of Chemistry, BK21 School of Materials Science and Department of Energy Science,
Sungkyunkwan University, Suwon 440-476, Korea*

***Coseal Co.Ltd. Research Center 493-2 Soryong-dong, Kunsan-city, Cheollabuk-do, Korea*

Abstract

Fuel Cell is the system which produces electricity and thermal power using natural gas. After 2010, the 1kW fuel cell systems have been distributed in Korea and recently, 5kW and 10kW fuel cell system also were distributed. Natural gas used as city gas in Korea contains organic sulfur compounds(3-4ppm) such as tert-butyl mercaptan(TBM) and tetrahydrothiophene(THT) as ordants to make it easy to detect leakage of the gas. However, Sulfur compounds easily poisoned steam reforming catalysts containing Ni. Therefore the sulfur compounds have to decrease to ppb level in fuel cell system.

Desulfurization of natural gas for fuel cells has been investigated using mesoporous materials. Mesoporous materials such as SBA-15, MCM-48, MCM-41 were synthesized using surfactants and

samples were characterized by N₂ sorption, X-ray diffraction and SEM. The sulfur adsorption properties were characterized by GC analyzer using standard gas (THT=10ppm, TMB=10ppm/ CH₄ balance). The peak of low angel in XRD patterns showed the stability of structure of SBA-15, MCM-41, MCM48. N₂ sorption shows surface area, pore volume, pore size of mesoporous materials.

The sulfur adsorption properties of mesoporous material were obtained from the breakthrough curves of TBM and THT using standard gas. The durability of mesoporous material was evaluated in natural gas for life time of mesoporous material.

In order to increase sulfur adsorption properties, metal were incorporated in the mesoporous material. Various metal were incorporated in the mesoporous material and the sulfur adsorption properties were evaluated. The Al grafting and Fe impregnation have effect on the sulfur adsorption due to increase of acid sites. Al grafting have more effect on the adsorption of THT than TBM and Fe impregnation have more effect on the adsorption of TBM than THT. The structure of Fe-SBA-15 was stable in the range of 5wt% to 15wt% Fe and sulfur adsorption of Fe-SBA-15 increased with Fe content. The sulfur adsorption of Al-SBA-15 increased with Al content. The adsorption amount of sulfur increased with metal incorporation due to increase of acid sites. Fe impregnation after Al grafting also was more effective on increase of sulfur adsorption properties. However, excessive addition of metal decreases the adsorption amount of sulfur due to removal of pore structure.

The pore size and pore structure of mesoporous material also have effect on sulfur adsorption properties. The structure of MCM-41 and SBA-15 is hexagonal and structure of MCM-48 is cubic. The pore size of MCM-41 and MCM-48 is 2-3nm and pore size of SBA-15 is about 6-8nm.

Fe-SAB-15 shows higher sulfur adsorption properties than Fe-MCM-41 because pore size of SBA-15 is larger than that of MCM-41. Fe-MCM-48 shows higher sulfur adsorption than Fe-MCM-41 because MCM-41 have 2D-hexagonal structure and MCM-48 have 3-D channel structure. This result indicates that sulfur compound can diffuse more readily through the larger pores in the mesoporous material for absorption on acid sites and lager pore volume increase sulfur adsorption.

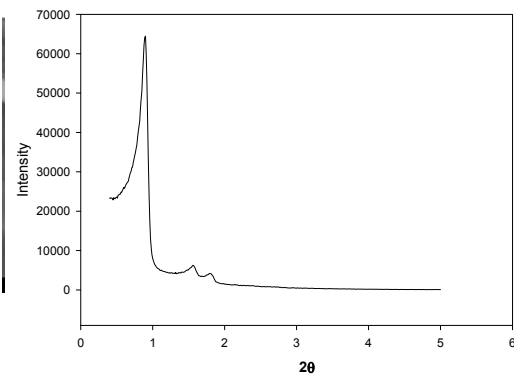


Fig. 1. XRD pattern of Fe-MCM-41.

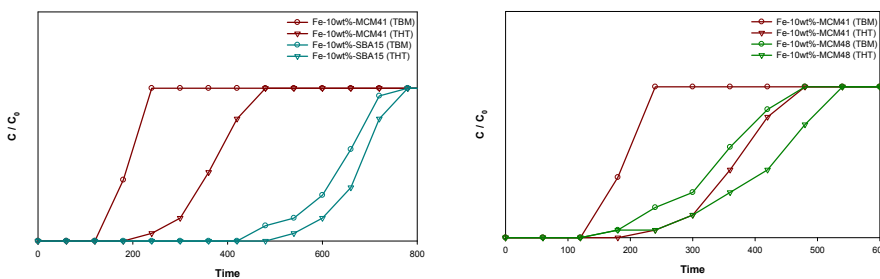


Fig 2. Breakthrough curves of mesoporous material

Development of Steam Methane Reformer for 5kW PEMFC Stationary Fuel Cell System (P-249)

Dalryung Park, Jaedong Kim, kihoon, Bongyu Kim, Jinwook Kim

*New Energy Technology Center, R & D Division, Korea Gas Corporation,
Ansan 426-790, Korea*

Hydrogen will be utilized as an important energy source in the future without the concern of pollution coming from various carbon based exhausted gases. Fuel cell is the energy conversion device that produces electricity directly from hydrogen through a simple chemical reaction. To the successful commercialization of fuel cell, it is important to establish efficient fuel reforming technology and related facility for smooth hydrogen production.¹

Depending on the chemical reactions involved, the hydrocarbon reforming technology has been classified as steam reforming, partial oxidation reforming, and autothermal reforming.² Steam reforming has been utilized widely over partial oxidation reforming, and autothermal reforming because it allows advantage to produce bulky hydrogen.

In steam reforming, much research efforts have been poured with special attention on some critical parameters that determine the overall efficiency of the reformer. Inflow gas ratio, flow rate and reforming temperature effects on the overall performance have been studied.⁴⁻⁵ These research outputs may be served as a tool for the design of baseline reformer, but do not reach the level of the commercialization, mainly due to the lack of heat control study. In this research, ideal thermal conditions were thought to find out that allows optimized overall system efficiency. By the help of well-constructed performance evaluation system, some dominant parameters on the overall performance are attempted to be appropriately analyzed.

This paper studied the development of steam methane reformer based on natural gas for 5kW polymer electrolyte fuel cell. The performance evaluated for natural gas based steam reformer with special attention on the operating conditions of internal combustor. In steam reformer in which strong endothermic process is involved, appropriate control of heat source is highly important that enables the efficient hydrogen production. In this study, experimental measuring device was setup to evaluate the performance of steam reformer for 5kW PEMFC.

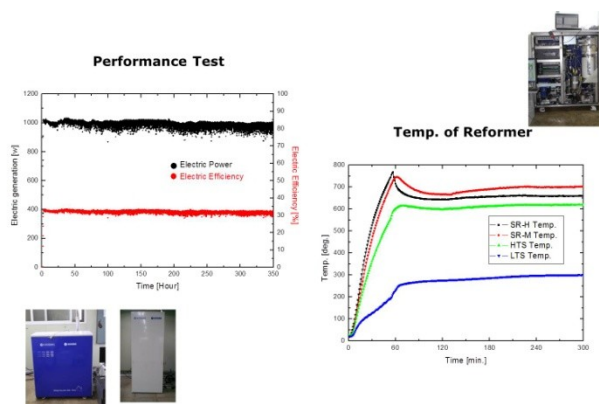
We investigated the dependence of the performance such as hydrogen reforming efficiency on the operation conditions such as inflowing mixed gas ratio and heat transfer through main reforming reactor and auxiliary combustor.

Experimental results showed that the hydrogen conversion rate can be improved through the temperature distribution control based on main reactor inlet gases ratio such as steam to carbon ratio (SCR) and air-fuel ratio at the auxiliary combustor. With the increment of the amount of fuel in the combustor, the overall internal temperature could increase generally, but the thermal efficiency does not always increase. The study shows that the thermal efficiency and the fuel conversion rate of

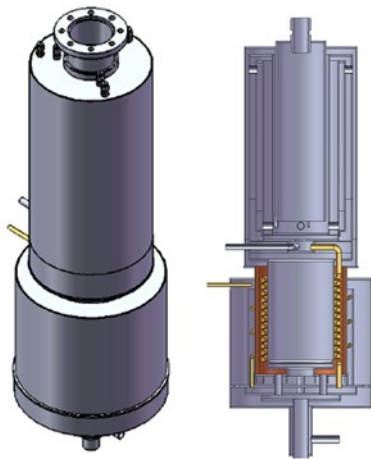
steam reformer could be improved by the effective heat transfer design and optimized parameter setup such as appropriate inlet gas mixed ratios.

The life and high performance for processing technologies are required for wide use of the fuel cell (PEMFC) using H₂ fuel as an alternative clean fuel.

The effects of Ru on the self-reducibility of Ru-doped Ni/MgAl₂O₄ catalysts, which do not need pre-reduction treatment with H₂, were investigated in the steam reforming of methane (SRM). The stepwise impregnated Ru/Ni/MgAl₂O₄ catalyst produced superior performance as compared to co-impregnated Ru-Ni/MgAl₂O₄ catalyst for SRM. KOGAS fuel Processor with Ru/Ni/MgAl₂O₄ has been evaluated by DSS(Daily Start up / Shut down) for durability of KOGAS fuel Processor and catalyst.



Performnace test



Compact reformer for 5kW HT-PEMFC
(Small temperature difference)

Hydrogen production from biogas through dry and steam reforming (P-250)

A. Serrano-Lotina¹, A. Balbín², J.A. Daza¹, C. Montoro², L. Daza¹

¹ Instituto de Catálisis y Petroleoquímica (CSIC); C/ Marie Curie 2 L10, 28049 Madrid (Spain)

² Comberla Ingeniería S.L.; C/ Utrech 3; 28232 Las Rozas de Madrid, Madrid (Spain)

INTRODUCTION

There is a growing interest in the development of power sources that use renewable fuels and reduce emission of pollutants. This interest is justified by the heightening concern about environmental degradation, energy security as well as the possible exhaustion of the fossil fuel resources. One example is the use of biogas (mainly composed by CH₄ and CO₂) which is generated from anaerobic digestion of sewage or wastewater [1]. In order to produce hydrogen from this renewable gas, it is necessary a reforming step. There are two alternatives: 1) carbon dioxide reforming (DR: CH₄ + CO₂ ⇌ 2H₂ + 2CO) and 2) steam reforming (SR: CH₄ + H₂O ⇌ 3H₂ + CO). The first reaction has two drawbacks: the deactivation of the catalyst due to carbon deposition [2] and the participation of reverse water-gas-shift (RWGS: H₂ + CO₂ ⇌ H₂O + CO) which decreases the amount of the produced hydrogen. On the other hand, steam reforming is the most extended way to produce hydrogen from CH₄, but it is necessary to eliminate the CO₂ from the feed.

Since previous studies [3] had reported good results when La-promoted catalysts, obtained from hydrotalcite-like precursor calcination, were used in dry reforming of methane, this catalyst will be used for these tests. The aim of this work is to study the influence of H₂O addition over dry reforming and the addition of CO₂ over steam reforming using a La-promoted catalyst obtained from hydrotalcite-like precursor.

EXPERIMENTAL

The tested catalyst was obtained after calcination at 750 °C of a hydrotalcite precursor, which was prepared by co-precipitation, according to a previously reported method [1,3]. The final measured Mg/Al molar ratio was 2.3 whereas Ni and La contents were 2.8 and 1.9%, respectively.

Catalytic tests were carried out in a tubular fixed-bed stainless steel (Ni free) reactor at 700 °C. The catalyst was reduced in situ at 650 °C for 1 h with 100 mL·min⁻¹ of H₂. Both tests were performed with the same sample (200 mg of catalyst). The CH₄:CO₂:H₂O feeding ratio was evaluated between 1:1:0 and 1:1:3 (influence of water addition to dry reforming) and 1:0:3 and 1:1:3 (influence of CO₂ addition to steam reforming). Each of the represented data is the average of the results obtained during approximately 2 h. The catalyst was stable during each step and when initial conditions were operated at the end of the test, same results were observed.

The results of these experiments have been obtained under non-equilibrium thermodynamic conditions, since the stability of the catalyst was also evaluated.

RESULTS AND DISCUSSION

The influence of water addition in dry reforming of methane is shown in Fig. 1. When H₂O/CH₄ ratio was below 0.5 methane conversion didn't change significantly but CO₂ conversion decreased while H₂/CO ratio increased. This may be explained by a lower participation of RWGS. In these conditions the main reaction is dry reforming of methane, as was also reported by Soria et. al. [4]. When H₂O/CH₄ ratio was higher than 0.5, methane conversion and H₂/CO ratio increased while CO₂

conversion decreased. An increase of CH₄ conversion seemed to indicate that steam reforming was predominant, which would explain the increase in H₂/CO ratio. When H₂O/CH₄ ratio was above 2.5, H₂/CO ratio was higher than 3 (theoretical value) which indicate that water-gas-shift reaction (WGS: H₂O + CO ⇌ H₂ + CO₂) was also taking place.

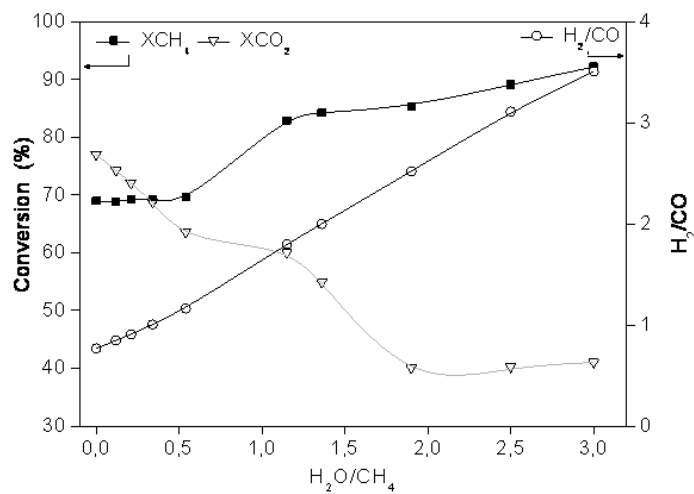


Fig. 1. Dry reforming of methane: Influence of water addition.

Fig. 2 shows the influence of carbon dioxide addition over steam reforming of methane. When there was no carbon dioxide, CH₄ conversion was near the equilibrium. H₂/CO ratio was much higher than theoretical (7.5 instead of 3) what indicated that WGS reaction was taking place in a high extent (according to theoretical calculations 50% of CO is being consumed by WGS). Contrary to what Huang et. al. [5] reported, when CO₂ was added to the feed, CH₄ conversion decreased, but not appreciable changes were detected between the different CO₂ concentrations. This decrease may be due to the competition of H₂O and CO₂ for the active sites. When CO₂/CH₄ ratio was above 0.6, CO₂ conversion increased, which may indicate that dry reforming was taking place. The increase of CO₂/CH₄ ratio produced a decrease of H₂/CO ratio what may be explained by a decrease in WGS participation.

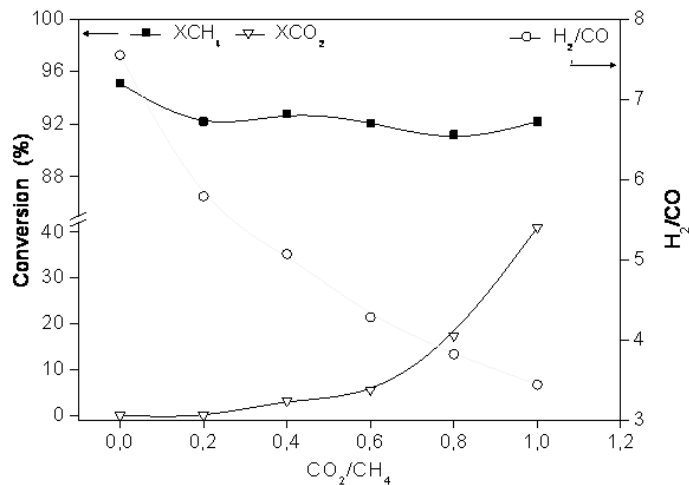


Fig. 2. Steam reforming of methane: Influence of CO₂ addition.

CONCLUSIONS

In this work, a Ni-based catalyst derived from hydrotalcite structure has been evaluated for the hydrogen production from biogas, transforming a waste into clean energy. Steam reforming of methane is the most extended way to produce hydrogen. Since biogas and other methane resources contain also CO₂, which is usually harmful for this process, it is previously eliminated, what raises the price of this technology. For that purpose, carbon dioxide presence was evaluated in steam reforming. The addition of carbon dioxide led to a decrease in methane and CO conversion, the latter consumed by means of WGS reaction. In all cases steam reforming was the predominant reaction. When CO₂ content increased, CO₂ conversion also increased what may indicate that combined reforming is taking place. An energy balance should be done in order to know the optimum ratio, taking into account the costs of CO₂ elimination and the costs of water addition and gasification.

The catalyst was also evaluated in biogas reforming. In order to minimize carbon deposition and increase H₂/CO ratio, water was added to the stream. When small amounts of water (H₂O/CH₄ ratio below 0.5) were added, dry reforming was still the predominant reaction with the participation of RWGS. When higher amounts of water were added, the predominant reaction was SR. When H₂O/CH₄ ratio was above 0.5, H₂/CO ratio > 3 what indicate that WGS was also taking place. Then, if high amounts of water are added the production of hydrogen will increase. An energy balance should be done in order to know the optimum ratio, taking into account the costs of water addition and gasification.

As a final conclusion, it can be said that an excellent catalyst has been obtained for combined reforming which can strengthen hydrogen production from a waste such as biogas.

ACKNOWLEDGMENT

Financial support from Comunidad de Madrid (DIVERCELCM, S2009/ENE-1475) is gratefully acknowledged.

REFERENCES

- [1] A. Serrano-Lotina, L. Rodríguez, G. Muñoz, A.J. Martín, M.A. Folgado, L. Daza, Catal. Commun. 12 (2011) 961-967.
- [2] V.R. Choudhary, K.C. Mondal, Appl. Energy 83 (2006) 1024–1032.
- [3] A. Serrano-Lotina, L. Daza, J. Power Sources 238 (2013) 81-86.
- [4] M. A. Soria, C. Mateos-Pedrero, A. Guerrero-Ruiz, I. Rodríguez-Ramos, Int. J. Hydrogen Energy 36 (2011) 15212-15220.
- [5] T-J. Huang, S-Y. Jhao, Appl. Catal. A 302, 2006, 325-332.

New catalysts based on chalcophanite promoted with Ni applied to steam reforming of bioethanol (P-255)

C. Fdez-Caballero, J.F. Da Costa-Serra, A. Chica*

Instituto de Tecnología Química (UPV-CSIC), Universidad Politécnica de Valencia, Consejo Superior de Investigaciones Científicas, Avenida de los naranjos s/n, 46022 Valencia, Spain

(*) corr. author: achica@itq.upv.es Fax: +34 96 387 78 13 Tel: +34 96 387 70 00 ext.: 78508

INTRODUCTION

The use of hydrogen as a fuel is an excellent alternative to the current problems associated with the use of fossil fuels (depletion, instability of production and prices, environmental pollution, etc.) [1]. However, the ecological benefits derived from its use can only be achieved if hydrogen is generated from renewable energy sources. One route with high potential for producing renewable

hydrogen is the reforming of alcohols from biomass fermentation processes. However, the effective use of this route requires the development of efficient reforming catalysts, especially for the steam reforming of ethanol (SRE). Many of these catalysts incorporate Ni as active phases [2-5] and both, the physicochemical characteristics of the support and the method of incorporation of Ni are crucial to prepare steam reforming catalysts with high activity, selectivity and stability.

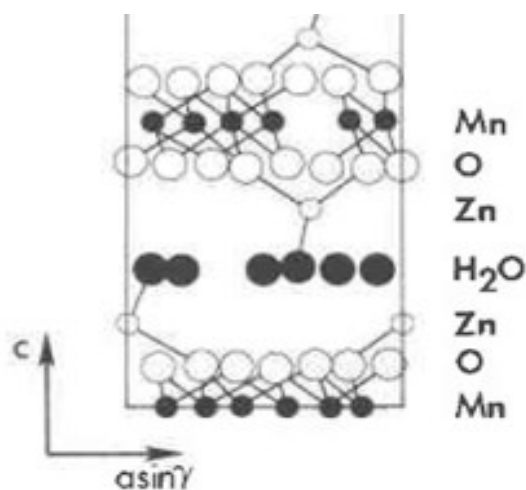


Figure 1. Chalcophanite projection structure along the axis a.

MOs with laminar structure are the most studied as catalytic materials [8-10]. This work shows for the first time the synthesis of chalcophanite, a laminar MO (Figure 1), with Ni and its use as active catalyst in the SRE.

EXPERIMENTAL

The preparation of chalcophanite material containing Ni, (Ni- CCFT), was conducted following the methodology described in [11] with the appropriate modifications for the Ni incorporation. The incorporation of Ni takes place in the last step of the chalcophanite synthesis by ion exchange using $\text{Ni}(\text{NO}_3)_2 \cdot 6\text{H}_2\text{O}$ (97% Aldrich) as nickel precursor. After the exchange the sample was filtered, washed, dried. Operating in this way is achieved a chalcophanite sample containing 8 wt.% of nickel. XRD-diffractograms of chalcophanite samples were recorder in a Philips 1060 diffractometer ($\text{Cu K}\alpha$ radiation). Textural properties were obtained by N_2 adsorption-desorption at 77 K in a Micromeritics ASAP 200 equipment. Chemical composition of the catalysts was determined by atomic absorption spectrometry using a Varian Spectra A-Plus apparatus. Catalytic studies were carried out in a fixed-

bed continuous reactor at atmospheric pressure, molar ratio H₂O/EtOH=13, GHSV=4700 h⁻¹ and a temperature range between 673-873 K. Before the reaction, the catalysts were calcined at 873 K and reduced "in situ" in H₂ flow (100 mL/min) at 873 K for 2 hours.

The analysis of the reaction products was conducted on-line using a gas chromatograph (Varian 3800) equipped with two columns (TRB-5, L = 30m, ID = 0.25 mm; Carbosieve SII, L = 3m, DI = 2.1 mm) and two detectors, thermal Conductivity (TCD) and flame ionization (FID).

RESULTS AND DISCUSSION

The diffraction patterns of chalcophanite containing Ni shows that it is a typical diffractogram of chalcophanite structure [11]. This is the first time that a chalcophanite containing Ni is synthesized. The level of Ni presents in our chalcophanite was found 8 wt.% (determined by chemical analysis).

Table 1 shows the ethanol conversion and products selectivity for the chalcophanite-based catalyst (Ni- CCFT) compared with a reference catalyst based on Ni/ZnO, which is described in literature as a good catalyst for the SRE [5,12]. As it can be seen chalcophanite based catalyst exhibits higher catalytic activity. It is important to note that the reference catalyst contains a high level of Ni, in particular 19.4 wt.%. It can be seen also that the hydrogen selectivity is significantly higher in chalcophanite based material. The distribution of other reaction products is also presented in Table 1. Specifically, it can be seen that the production of CO and CH₄ is lower in the Ni-CCFT catalyst, especially at low temperatures. Similarly, the formation of other products such as ethylene, a known precursor of coke, acetaldehyde and acetone is significantly lower in this catalyst. These results demonstrate the positive effect that the chalcophanite based material incorporating Ni has in the SRE.

Table 1. Ethanol conversion and products selectivity obtained with Ni-Ref. and Ni-CCFT catalysts in the steam reforming of ethanol. Catalytic data obtained after 5 hours on stream. Reaction conditions: H₂O/EtOH = 13, GHSV = 4700 h⁻¹ and atmospheric pressure.

		Ni-Ref. (Ni/ZnO)							
		Selectivity, mol %							
T ^a , K	Cov., mol %	H ₂	CH ₄	CO	CO ₂	C ₂ H ₄	C ₃ H ₆	C ₂ H ₄ O	C ₃ H ₆ O
673	85.71	57.46	15.84	7.38	16.43	0.26	0.03	2.54	0.05
773	92.24	65.54	8.19	4.57	20.56	0.14	0.02	0.83	0.15
873	93.29	69.12	4.19	5.85	20.52	0.07	0.00	0.22	0.04
		Ni-CCFT							
		Selectivity, mol %							
T ^a , K	Cov. %	H ₂	CH ₄	CO	CO ₂	C ₂ H ₄	C ₃ H ₆	C ₂ H ₄ O	C ₃ H ₆ O
673	91.03	62.59	11.61	2.89	22.25	0.12	0.00	0.45	0.00
773	97.78	72.42	4.93	1.81	20.62	0.07	0.00	0.15	0.00
873	99.97	73.76	3.76	4.13	18.22	0.00	0.00	0.13	0.00

Activity of Ni based catalysts in the reforming of hydrocarbons is related to the size of the metallic nickel particles since smaller Ni metallic particles would increase the number of active sites available to carry out the SRE. The size of the Ni metallic particles present in the Ni-CCFT catalyst was

determined by XRD and TEM and they were found significantly lower than in the reference material (17 nm and 33 nm, respectively).

Reducibility of the catalysts was studied by TPR. It would be expected that smaller particle sizes presented higher reduction temperatures due to their high interaction with the support. However, the Ni incorporated into chalcophanite reduced at lower temperatures (659 K and 728 K, respectively). This result seems to indicate that the reduction of Ni is favored in the chalcophanitic environment. The higher reducibility of nickel species and the smaller particle size of the metallic nickel could justify the observed catalytic results.

The results shown in this work reveal the interest that the chalcophanite material would have as support in the preparation of Ni catalysts with high activity in the SRE.

Currently, we are carrying out different studies related to the stability of this catalytic material. Specifically, we are completing studies about catalytic activity at long reaction times and coke deposition and sinterization of metallic particles of Ni after reaction.

CONCLUSIONS

This is the first time that a chalcophanite material containing Ni is prepared and studied in the SRE. The catalytic results show a better performance of the chalcophanite-based material compared with the reference. This work shows the interest that MOs with chalcophanite structure could have as Ni support for the preparation of efficient catalysts in the production of hydrogen by SRE.

ACKNOWLEDGEMENTS

Javier F. Da Costa and Carolina Fernandez-Caballero thank the CSIC the scholarship grant JAE-predoc and JAE-intro, respectively.

REFERENCES

- [1] H.W. Huber, S. Iborra, A. Corma, *Chem. Rev.* 106 (2006) 4044-4098.
- [2] A. Haryanto, S. Fernando, N. Murali, S. Adhikari, *Energy Fuels* 19, 2098 (2005).
- [3] M. Ni, D.Y.C. Leung, M.K.H. Leung, *Int. J. Hydrogen Energy* 32, 3238 (2007).
- [4] A. Chica, S. Sayas, *Catal. Today* 146 (2009) 37-43.
- [5] J. F. Da Costa-Serra, R. Guil-López, A. Chica, *Int. J. Hydrogen Energy* 13 (2010) 6709-6716.
- [6] S. L. Suib, *J. Mater. Chem.* 18 (2008) 16323.
- [7] K. A. Malingier, Y. S. Ding, S. Sithambaram, L. Espinal, S. Gomez, S. L. Suib, *J. Catal.* 239 (2006) 290.
- [8] S. Sithambaram, R. Kumar, Y. C. Son, S. L. Suib, *J. Catal.* 253 (2008) 269.

[9] R. Ghosh, X. F. Shen, J. C. Villegas, Y. Ding, K. Malinger, S. L. Suib, J. Phys. Chem. B 110 (2006) 7592.

[10] A. Fuertes, J.F. Da Costa-Serra, A. Chica, Energy Procedia 29 (2012), 181-191.

[11] B. J. Aronson, A. K. Kinser, S. Passerini, W. H. Smyrl, A. Stein, Chem. Mater. 11 (1999) 949-957.

[12] N. Homs, J. Llorca, P. Ramírez de la Piscina, Catal. Today 116 (2006) 361.

Oxidative steam reforming of methane over nickel catalysts supported on La₂O₃-CeO₂-Al₂O₃ (P-266)

Miletić N., Izquierdo U., Barrio V.L., Arias P.L.

Introduction

Hydrogen is considered as an interesting energy vector. Even if its sustainable production will imply the use of green electricity or renewable raw materials, natural gas reforming is the most common technology used for producing this gaseous compound. Many promising applications require decentralized hydrogen availability. Due to its physical properties hydrogen transport can be quite expensive and as a result decentralized production can be a clear alternative. The natural gas distribution network suits quite well the requirements for this hydrogen distributed production at small to medium size facilities. The comparatively small reforming plants must avoid very complex technologies to facilitate their robustness and competitive prices. Oxidative steam or autothermal methane reforming processes simplify hydrogen production avoiding the conventional steam reforming huge endothermicity, but require active and stable catalysts. This contribution will present the results obtained in these processes using nickel catalysts supported on Al₂O₃, CeO₂-Al₂O₃, La₂O₃-Al₂O₃, and La₂O₃-CeO₂-Al₂O₃.

Experimental

These catalysts were prepared by the sol-gel method (10 wt.% of nickel), and their catalytic performances for oxidative steam reforming of methane, combination of partial oxidation and steam reforming (CH₄/H₂O/O₂ = 1:1:0.3), were investigated in a continuous flow fixed bed reactor under atmospheric pressure operating at WHSV = 170.8 h⁻¹ and T = 550 °C. After the supports preparation and impregnation, the resulting particles were dried at 110°C overnight, grinded and sieved (mesh size between 420 and 500 μm) and calcined at 900°C for 2 hours in an air flow. Prior to the reaction, the catalysts were reduced in 20 vol% of hydrogen at 800°C for 4 hours. BET isotherms were used to measure surface area, pore volume and pore size distribution. TPR provided information about active phase reducibility and their interaction with the different supports. H-TPD was used to investigate Ni dispersion.

Results and discussion

The activity results proved that the Ni/La₂O₃-CeO₂-Al₂O₃ catalyst showed the highest catalytic activity and stability compared to the other catalysts (see Figure 1). Namely, the methane conversion was almost constant with no significant fluctuations or catalytic deactivation along 6 h of reaction time (methane conversion = 51.8 ± 0.9 %). On the other hand, significant deactivations were observed in the behavior of the other three catalysts. Interestingly, the highest degree of deactivation was observed for the Ni/La₂O₃-Al₂O₃ catalyst (39.4 ± 5.7 %), followed by Ni/CeO₂-Al₂O₃ (40.8 ± 4.5 %).

Deactivation of nickel catalysts during the methane reforming uses to be mostly due to coke deposition and active metal sintering. Nevertheless, in oxidative steam reforming of methane, carbon formation is hindered due to the presence of oxygen. It is well known that the addition of

ceria contributes to avoid active metal sintering, stabilizes the Al_2O_3 and stores and releases oxygen, while lanthana addition mostly enhances the thermal stability of alumina supported catalysts. In this case both oxides addition was required to end with a stable catalyst these. This very promising result can be explained in terms of oxygen dynamics and Ni dispersion stability.

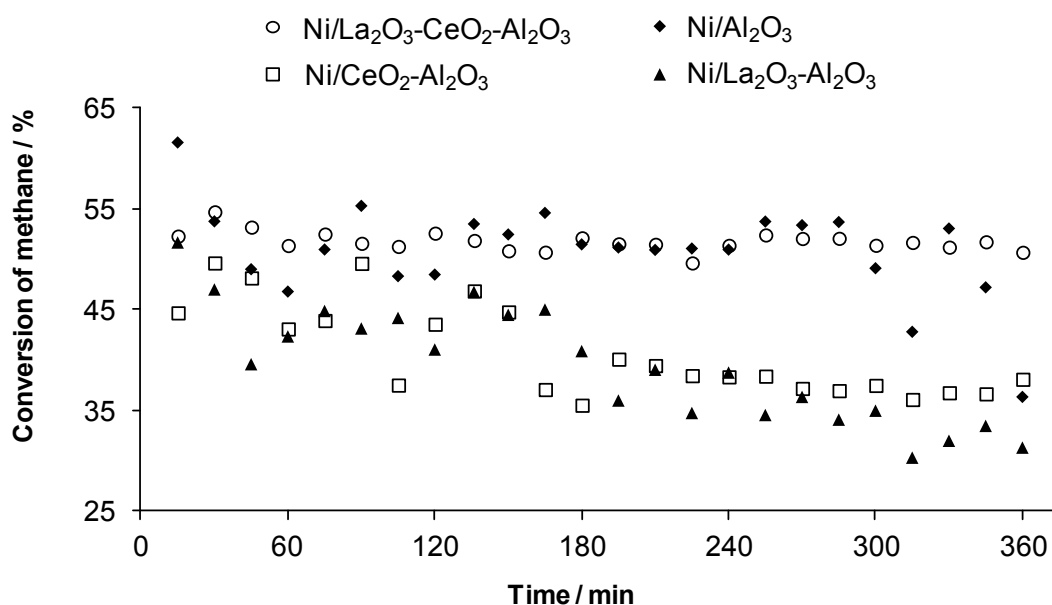


Figure 1. Conversion of methane over time during oxidative steam reforming (reaction conditions: $\text{CH}_4/\text{H}_2\text{O}/\text{O}_2 = 1:1:0.3$, $\text{WHSV} = 170.8 \text{ h}^{-1}$, $T = 550 \text{ }^\circ\text{C}$).

Catalytic performances of the synthesized catalysts were summarized in Table 1. As it can be noticed, Ni/La₂O₃-CeO₂-Al₂O₃ catalyst showed the highest H_2/CH_4 ratio, CO_2/CH_4 ratio, H_2/CO ratio and H_2/COX ratio, and the lowest CO/CH_4 ratio. The measures high H_2/CO ratios (between 3,8 and 5,8) may indicate all these catalysts are also quiet active for the water gas shift reaction during oxidative steam reforming of methane.

Table 1. Catalytic performances of catalysts (reaction conditions: CH₄/H₂O/O₂ = 1:1:0.3, WHSV = 170.8 h⁻¹, T= 550 °C).

Catalysts	H ₂ out /CH ₄ in	CO out /CH ₄ in	CO ₂ out /CH ₄ in	H ₂ out /CO out	H ₂ out /CO _x out
Ni/Al ₂ O ₃	1,041	0,183	0,198	4,716	2,098
Ni/CeO ₂ -Al ₂ O ₃	0,707	0,169	0,170	4,058	1,753
Ni/La ₂ O ₃ -Al ₂ O ₃	0,676	0,161	0,166	3,775	1,732
Ni/La ₂ O ₃ -CeO ₂ -Al ₂ O ₃	1,174	0,156	0,235	5,760	2,187

Conclusions

A promising catalyst for oxidative reforming of methane has been developed even if further experimental work is required to prove its stability under harsher conditions (T high enough to allow almost total methane conversion and longer times of reaction).

Open Source control in PEM Fuel Cells (P-268)

C. Merino¹

*1. Centro Nacional del Hidrógeno (CNH2). Unidad de Simulación y Control.
Prolongación Fernando el Santo, s/n. 13500 Puertollano (Ciudad Real), Spain.
e-mail: carlos.merino@cnh2.es*

INTRODUCTION.

Every time becomes more relevant and dissemination initiatives under alternative licenses intellectual property, as is the Open Source movement. This new trend is spreading also in the world of research and development which opens a new path for the collaborative development and dissemination worldwide, promoting technological advances.

Aware with this new change, the National Hydrogen Center (CNH2) commitment to this development alternative in research based on the use of software and hardware of Open Source and contributing to the research community in order to enhance the knowledge on fuel cells and hydrogen technologies.

Under the above criteria the National Hydrogen Center offers the challenge of developing hardware and Open Source software for monitoring and control of fuel cells in order to provide a low cost solution open to the scientific community and disclosing that allows demonstration and development of balances of plant (BOP) for small polymer technology fuel cells (PEMFC).

SETTING AND DESIGN.

It was necessary to review the tools available to successfully meet the proposed objective of developing a control PCB for polymer technology fuel cell. There are several steps. It is first necessary to select the development environment; including available alternative is selected initiative Arduino control boards by widespread at all levels that are getting this control platform.

Therefore a specific control board, shield, connected as an additional module that allows it and take advantage of all the features developed for the rest of the Arduino community.

Control PCB has an 8-bit microcontroller ATmega2560, 256KB and operating at 16 MHz. These features are sufficient to implement basic control strategies. Developed adaptation board comprises of instrumentation and basic control elements for controlling and monitoring of a small power fuel cell that is usually used in a didactic way. Electric current and cell voltage are measure and relay connection control are included. In the gas supply circuit is monitored operating temperature of the stack and stack cooling by use of PWM power fan, the solenoid control gas feed in both anode and cathode as control dead-end valve in the hydrogen circuit.

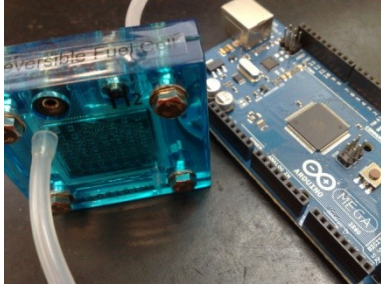


Figure 29. Fuel Cell and Arduino controller.

This acquisition and signal adaptation allows complete monitoring system providing information on the instantaneous power generated, an energy meter supplied, the operating time, estimated consumption based on performance models and taking data for representing the polarization curve of the cell in experimentation.

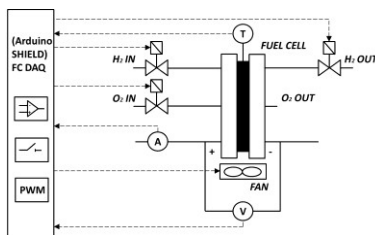


Figure 30. P&ID Fuel Cell and DAQ Arduino Shield.

For microcontroller programming has been used Open Source tool Arduino IDE. In this way is achieved have open to any user control strategies and they can be modified by any researcher in order to test different control techniques. Turn the PCB design and control board signal conditioning can be modified for any advanced user with knowledge in electronics design to include new features in it and contribute to the community with a version based on the original PCB.

CONCLUSION

The development and validation of the data acquisition and control system has been done on a small and reconfigurable didactic cell.

With the development of this low-cost solution, but with high potential, is intended to offer the scientific community a new tool for development and greater dissemination of knowledge in fuel cells and hydrogen technologies.

Advances in Hydrogen Production by Sorption Enhanced Reforming. Process and materials development (P-269)

Asunción Aranda*(1), Saima Sultana Kazi(1), Cristina Sanz Pinilla(1), Johann Mastin(1), Julien Meyer(1), Ramón Murillo (2)

(1) Institute For Energy Technology (IFE), Kjeller, Norway. * suni.aranda@ife.no

(2) Instituto de Carboquímica – Spanish Research Council (ICB-CSIC)

Sorption Enhanced Reforming (SER) is an emerging technology for the production of H₂ from hydrocarbons with in situ CO₂ capture. In an SER process, the addition of a solid CO₂ sorbent in the reforming reactor (to capture the CO₂ produced during the reforming and water-gas shift reactions) increases the H₂ yields and lowers the reaction temperature compared to conventional reforming process [1,2]. The use of internal sorbent results in a simplification of the H₂ production steps and reduces the needs for downstream purification stages. Since 2002, Institute for Energy technology (IFE) has worked on the development of the SER technology, both on the reactor technology and on process and material development [3,4]. ICB-CSIC has wide knowledge as well in Calcium Looping systems and has developed experimental sets and suitable materials for the SER technology [5,6].

One of the key issues of the process is the long term performance of the CO₂ sorbent and reforming catalyst. They can be used as two separate materials in the process, but an integration of the CO₂ capture and the catalytic reforming in one single high performance combined material will advance the technology and is expected to bring better reaction efficiencies and cost reductions.

The sorbents commonly used for this application are CaO-based natural sorbents (limestone and dolomite) for their availability and low cost. However, their CO₂ absorption capacity decreases rapidly with the increasing number of cycles, due to sintering and pore closure effects. Additionally, these sorbents often show poor mechanical properties, with significant attrition during long-term cyclic operation in circulating fluidized bed reactors. To overcome those problems, extensive efforts have been put on the development of synthetic CaO-based sorbents. Institute for Energy Technology (IFE) has patented a novel solid sorbent for high-temperature CO₂ capture applications. The developed sorbent shows a genuine composite structure made of stable nano-particles of CaO (~100nm) homogeneously distributed on the surface a calcium aluminate matrix. This layered structure has proved to significantly improve the chemical and mechanical stability of the sorbent [3,4].

Preliminary studies showed that the integration of a reforming catalyst with a synthetic sorbent is feasible by wet impregnation. Multi-cycle experiments were carried out on those CO₂ sorbents and hybrid particles in a thermogravimetric analyser to determine the variation of the CO₂ absorption kinetics (and, therefore, the nickel activity) along carbonation/calcination cycles due to the SER reaction.

Particles were also tested in SER cycles, using a fixed bed reactor. After an initial calcination, the dispersed Ni nanoparticles were reduced in hydrogen prior to reforming (25vol%CH₄ / 75vol% H₂O) at 625oC and atmospheric pressure. The gas outlet composition analysed by micro-GC during the experiment showed a yield of H₂>95vol% during the first 30 minutes, while the CO₂ and CH₄

concentrations remained low. These results showed that the combined material is suited for the SER. Based on those promising results, especially when the CO₂ sorbent material is combined with a nickel catalyst, standardized particle production methods were developed. The fine micropowder obtained by the patented synthesis method has been agglomerated (by shear agglomeration) into particles of suitable size to be tested in lab-scale fixed bed and fluidized bed reactors that can be alternatively operated in reforming and regeneration modes.

From this collaborative work, the chemical and mechanical properties of the new materials will be presented, including the results of the tests performed for hydrogen production by SER and the materials characterization.

In parallel to the R&D effort on materials, IFE is currently building the first medium scale SER prototype unit as part of the HyNor hydrogen station in Lillestrøm (Norway), which will be commissioned at the end of 2013 to produce hydrogen from upgraded biogas. The facility uses a Dual Bubbling Fluidized Bed reactor system and will provide a proof-of-concept for SER at prototype scale and under process conditions unavailable at laboratory scale. Advances in this unique demonstration project will be presented.

References

- [1] Harrison, D.P. Energy Procedia, Volume 1, Issue 1, February 2009, 675-681.
- [2] Johnsen, K., Ryu, H.J., Grace, J.R. and Lim, C.J. Chemical Engineering Science. 61, 2006, 1195-1202.
- [3] Mastin, J., Aranda, A. and Meyer, J. New synthesis method for CaO-based synthetic sorbents with enhanced properties for high temperature CO₂-capture, Energia Procedia4, 2011, 1184–1191
- [4] Mastin J., Meyer J. and Råheim A., Particulate, heterogeneous solid CO₂ absorbent composition, method for its preparation and method for separating CO₂ from process gases with use thereof. Patent Application WO/2011/005114
- [5] <http://www.caoling.eu/index.php>
- [6] García-Lario, A. L., Aznar, M., Grasa, G., García, T., Murillo, R. Study of nickel catalysts for hydrogen production in sorption enhanced reforming process Journal of Power Sources 242 (2013) 371-379

Effect of exposure time to organometallic precursors for the preparation of Pt Nanocatalysts on a Nafion-coated Carbon BLACK (P-270)

Woo-Kum Lee¹, Hyung-Ryul Rim¹, Gyu-Bum Joung², Sehui Lee², Eunsoo Jin²,
Jae-Young Lee¹, and Hong-Ki Lee¹

¹Hydrogen Fuel Cell RIC, Woosuk Univ., Wanju-gun, Jeonbuk 565-902, Korea

²Dept. of Electricity and Electrical Eng., Woosuk Univ., Wanju-gun, Jeonbuk 565-701, Korea

A gas diffusion layer (GDL) in a polymer electrolyte membrane fuel cell (PEMFC) stack has a thin microporous layer (MPL) made of carbon-based powder mixed with organic binder and hydrophobic dispersion agent, which is coated onto a macroporous sheet of carbon cloth, paper or felt, in order to form a microporous structure on a macroporous carbon backing. Then some large amount of Pt or Pt-based bimetallic nanocatalysts is dispersed on the membrane assembled side of the GDL. Generally, carbon-supported nanocatalysts are prepared in wet processes: carbon-based supporter and metallic precursors are vigorously mixed in a solvent and then reducing agent solution is dropped into the first solution in order to produce Pt or Pt-based bimetallic nanoparticles on the carbon-based supporter. However, it is very difficult to control the nanoparticle size and to disperse homogeneously on the carbon surface [1,2].

In this study, a drying process [3] developed by us was used to prepare Pt nanoparticles on a nafion coated carbon black, and the effect of exposure time to organometallic precursors for the preparation of Pt nanocatalysts on a Nafion-coated carbon black was studied.

As shown in Figure 1, firstly carbon black slurry might be prepared: deionized water (6.0 g) and a surfactant (0.1 mg) were well-mixed in a 10 ml vial bottle, and a carbon black (0.06 g) was poured into the bottle little by little under ultrasonic condition for 30 min. Then nafion solution (0.5 g) was dropped into the bottle while maintaining the ultrasonic mixing for 15 min, and finally well-dispersed carbon black slurry was prepared. All the slurry was evenly spray-coated on the GDL of 7×7 cm² and it was dried at 80°C for 24 hr. The loading weight of nafion coated carbon black was 3.6 mg/cm². And then, Pt nanoparticles were prepared by the following procedure: 10 mg of platinum(II) bis(acetylacetonato) denoted as Pt(acac)₂ in the glass reactor was sublimed at 180°C oil bath in vacuo and it was adsorpted on the nafion coated carbon black (1×1 cm²), and finally it was spontaneously reduced to form Pt nanoparticles on the carbon black without any reducing agent. The exposure time to the Pt(acac)₂ was 5, 15 and 30 min. The morphology of the nanocatalysts was observed by field emission scanning electron microscopy (FE-SEM, JMS-6701F, JEOL) at an acceleration voltage of 10 kV and the elemental analysis was carried out by energy-dispersive X-ray spectroscopy (EDS, JED-2300 Energy Dispersive X-ray Analyzer, JEOL), which was connected to the FE-SEM. The morphology of the nanocatalysts on the carbon black was also observed by high-resolution transmission electron microscopy (HRTEM, Hitachi JEM-2010) operated at an accelerating voltage of 200 kV.

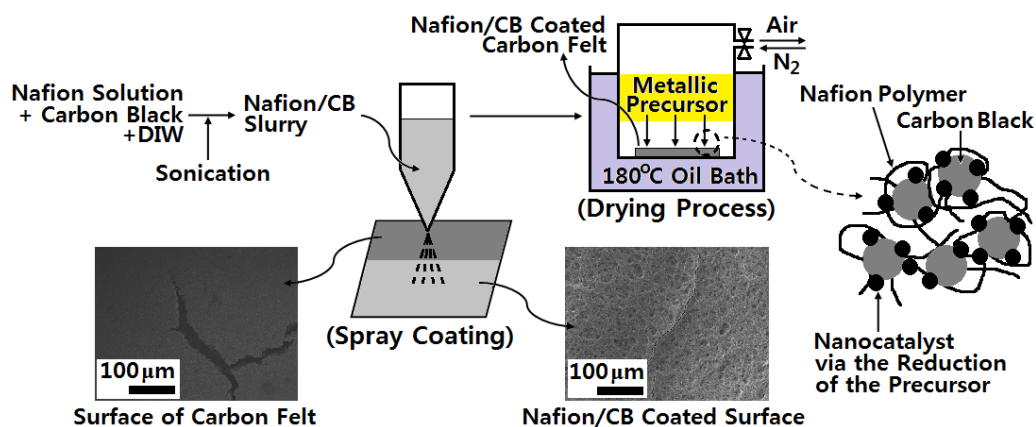


Figure 1. Schematic diagram for the preparation of Pt nanocatalysts on a nafion coated carbon black.

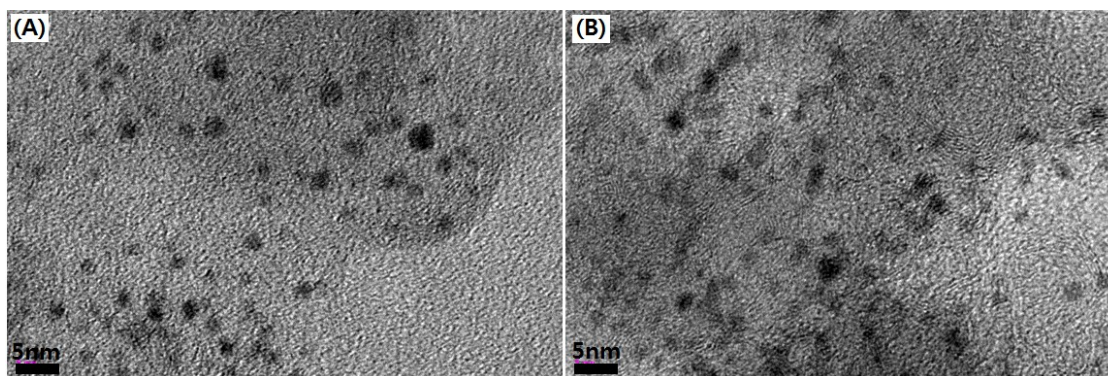


Figure 2. TEM images for Pt nanoparticles through the exposure time to Pt(acac)₂ for (A) 15 min and (B) 30 min.

Figure 2 showed TEM image of Pt nanoparticles prepared by the reduction of Pd(acac)₂ at 180°C for (A) 15 min and (B) 30 min, and it was found that Pt nanoparticles were evenly dispersed on the carbon black. The loading weight, number density and particle size of Pt nanoparticles increased with increasing exposure time at 180°C, Pt nanoparticle size at the exposure time of 15 min was 1.7 nm and that of 30 min was 2.1 nm. When loading time was 5 min, no particle was observed in TEM image and it meant 5 min was too short for the generated nucleus to grow.

References

- [1] I.T.Kim, H.K.Lee, and J.P.Shim, J. Nanosci. Nanotech., 8, 5302 (2008).
- [2] J.H.Choi, K.W.Park, and Y.E.Sung, J. Electrochem. Soc., 150, A973 (2003).
- [3] J.Y.Lee, D.Yin, and S.Horiuchi, Chem. Mater., 17, 5498 (2005).

Acknowledgement

This research was financially supported by the Ministry of Education (MOE) and National Research Foundation of Korea (NRF) through the Human Resource Training Project for Regional Innovation (NRF No. 2013032228).

Effect of graphite fiber on electrical conductivity of an epoxy/carbon composite used for a bipolar plate in a fuel cell (P-271)

Jae-Young Lee¹, Woo-Kum Lee¹, Hyung-Ryul Rim¹, Seung-Weon Yang², Gyu-Bum Joung³,
Sehui Lee³, Eunsoo Jin³ and Hong-Ki Lee¹

¹Hydrogen Fuel Cell RIC, Woosuk Univ., Wanju-gun, Jeonbuk 565-902, Korea

²Dept. of Computer Eng., Woosuk Univ., Wanju-gun, Jeonbuk 565-701, Korea

³Dept. of Electricity and Electrical Eng., Woosuk Univ., Wanju-gun, Jeonbuk 565-701, Korea

Bipolar plate is a repeated unit together with two gas diffusion layers (GDLs) and a membrane electrode assembly (MEA) separating the adjacent cell in a polymer electrolyte membrane fuel cell (PEMFC) stack. The main functions of the bipolar plate are: (i) distributing reactant gases (hydrogen fuel and oxidant gas) uniformly to the active areas, (ii) electronically connecting two adjacent cells, (iii) preventing leakage of reactant gases and coolant, and (iv) removing heat from adjacent cells. Therefore it should be required to satisfy the good electrical conductivity over 100 S/cm. It should also have good mechanical stability, corrosion resistance and low gas permeability [1,2]. To achieve these properties together with cost reduction and easy processibility, metallic materials or polymer/carbon composites have been used to substitute the conventional graphite raw material because graphite plate is so brittle and its manufacturing cost is too high [1]. To overcome the brittleness, carbon fiber filament (CFF) was incorporated into the epoxy/graphite power (GP) composite and graphite fiber (GF) was introduced in order to improve electrical conductivity.

The materials were as follows: a bisphenol-F type epoxy resin powder (YSLV-80XY) was purchased from Tohto Kasei Co., Ltd., Japan. Its epoxy equivalent weight was 190-200 g/eq, the melting point was 78°C and the molten viscosity was 0.1 Pa·S at 150°C. A phenol novolac-type curing agent (KPN 2110, Kangnam Chemical Co., Ltd., Korea) was used whose hydroxyl equivalent weight was 104 g/eq and its softening point was 105°C. The accelerator (triphenyl phosphine, TPP) was obtained from Arkema Inc., Canada. Graphite powder was purchased from TIMCAL Group, Switzerland under the trade name of TIMREX SFG6L. CFF and GF were obtained from Kureha Chemical Industry Co., Japan under the trade names of KCF-100 and KGF-200, respectively.

Epoxy matrix was prepared by mixing novolac epoxy, curing agent and accelerator, in which all were powder type, at a weight ratio of 100 : 53 : 1. And then, GP, CFF and GF were well-mixed into the epoxy matrix at a weight ratio of epoxy matrix : GP : CFF GF = 20~30 : 60~80 : 0.5~5 : 0.5~5 wt%. The formulation was poured into a mold and cured at 110°C for 2 hr under 80 kg/cm² pressure and post-cured at 180°C for 2 hr under the same pressure.

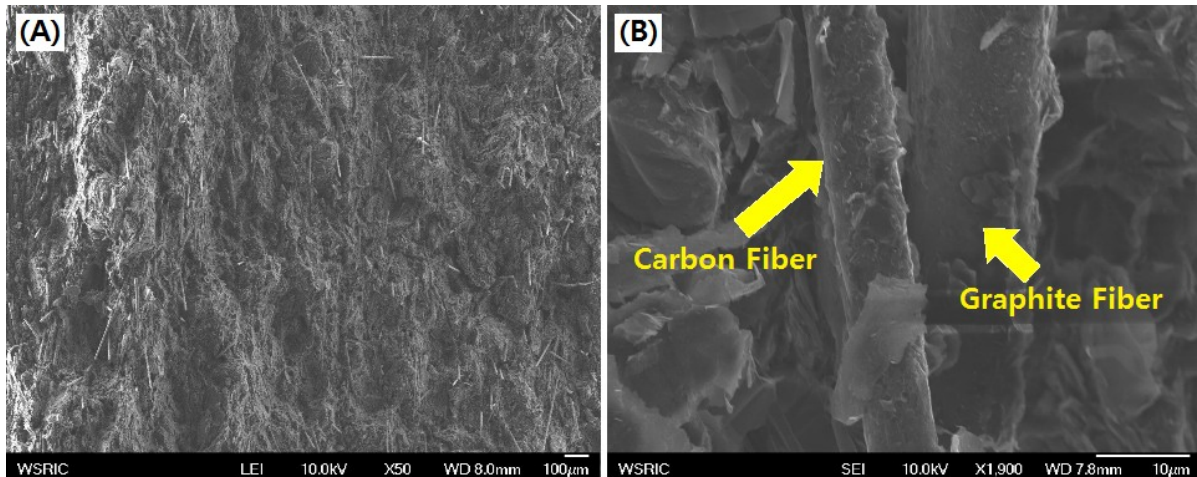


Figure 1. SEM image of fracture surface for epoxy(25 wt%)/GP(68 wt%)/CFF (2 wt%)/GF(5 wt%) composite after tensile test at a cross-head speed of 10 mm/min. (A) low magnification and (B) high magnification

Electrical conductivity was measured by using Keithley 2000 conductivity meter with 4-point probe method. Field emission scanning electron microscopy (FE-SEM, JMS-6701F, JEOL) was employed at an acceleration voltage of 10 kV in order to observe the morphology of CFF and GF dispersion and their surfaces being pulled out from the epoxy matrix after tensile test.

As was expected, electrical conductivity increased with increasing total carbon content, and especially, the value increased with increasing GF content in the same carbon content. The value of the epoxy/GP system without CFF and GF was 27.2 S/cm and that of the system with 3 wt% CFF 3 wt% and without GF decreased by 12%. In the epoxy(25 wt%)/GP(68 wt%)/CFF (2 wt%) system with GF(5 wt%) the conductivity was 98.4 S/cm, which was 3.6 times higher than that of the system without GF. In the epoxy/GP system, electrons transferred by hopping between the GPs which were separated by insulating epoxy barriers. Therefore if GFs with 0.3-1 cm length were added to the GP system, electrons conductively transferred through the GFs which could connect the GPs located far from each other. It was confirmed by scanning electron microscopy (SEM), as shown in Figure 1. CFF and GF were evenly dispersed in the epoxy matrix and they connect the GPs.

References

- [1] B. Cunningham and D.G. Baird: J. Mater. Chem. Vol. 16 (2006), p. 4385
- [2] A.J. Appleby and F.R. Foulkes: Fuel Cell Hand Book, Van Nostrand Reinhold, New York (1989)

Acknowledgement

This research was financially supported by the Ministry of Education (MOE) and National Research Foundation of Korea (NRF) through the Human Resource Training Project for Regional Innovation (NRF No. 2013032228).

Preparation of Pt Nanopatterning for PEMFC on a Self Assembled Copolymer Thin Film using a drying process (P-272)

Jae-Young Lee¹, Woo-Kum Lee¹, Hyung-Ryul Rim¹, Gyu-Bum Joung² and Hong-Ki Lee¹

¹Hydrogen Fuel Cell RIC, Woosuk Univ., Wanju-gun, Jeonbuk 565-902, Korea

²Dept. of Electricity and Electrical Eng., Woosuk Univ., Wanju-gun, Jeonbuk 565-701, Korea

Platinum (Pt) is the most effective catalyst for the hydrogen oxidation on an anode and the oxygen reduction on a cathode in a proton-exchange membrane fuel cell (PEMFC), but it has several critical issues to be modified before the commercialization. For example, the oxygen reduction reaction (ORR) is kinetically limited at the cathode, and the scale of the Pt crystallites leads to high costs for Pt-based electrocatalysts with sufficient surface area and activity. In order to overcome these barriers, many researchers have studied to maximize the activity of a Pt nanocatalyst. In general, the Pt catalysts size should be smaller and evenly distributed on the surface of carbon supporter in order to maximize the surface area of the catalysts. For this, many Pt-based bimetallic catalysts such as Pt-Au, Pt-Pd, Pt-RuO etc. have been studied to improve the performance and durability of the catalysts by solving the problems such as carbon monoxide (CO) poisoning, dissolution and aggregation of Pt nanoparticles.

In this study, we prepared Pt nanopatterning on a self assembled copolymer thin film using a drying process [1]. The symmetric diblock copolymer of poly((methylmethacrylate)-block-(2-hydroxyethylmethacrylate)) (P(MMA-b-HEMA)) ($M_n = 24,300/16,700$) (Polymer Source Inc., Japan) was solved in 1,4-dioxane, methanol or 2-methoxyethanol to make 0.5 wt% solutions. P(MMA-b-HEMA) thin film with about 20 nm was made on Si-wafer by using spin-coating and then it was dried in the air for 24 hr. And then, it was annealed at 180°C for 24 hr in order to get self-assembled nanopatterns. Pt catalyst nanopatterns were prepared by following procedure: about 10 mg of platinum(II) bis(acetylacetonato) denoted as Pt(acac)₂ in the glass reactor was sublimed at 180°C oil bath in vacuo and Pt(acac)₂ was selectively adsorbed on HEMA domain, and then it was spontaneously reduced to form Pt nanopatterns on the HEMA domain, as shown in Figure 1. The exposure time to the Pt(acac)₂ was 60 min and then it was pyrolyzed at 800°C in N₂ atmosphere to remove polymer components. Finally, the pattern was transferred on the nafion membrane and its catalytic performance was characterized by using fuel cell test station.

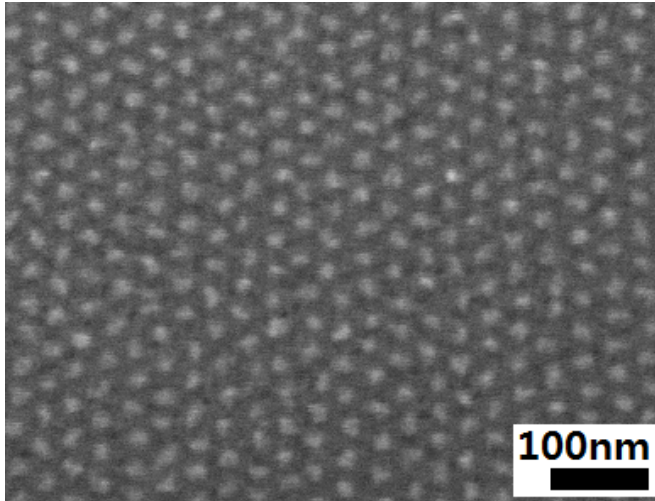


Figure 1. SEM image showing the Pt nanopattern on self-assembled P(MMA-b-HEMA) thin film.

Reference

[1]J.Y.Lee, D.Yin, and S.Horiuchi, *Chem. Mater.*, 17, 5498 (2005).

Acknowledgement

This research was financially supported by the Ministry of Education (MOE) and National Research Foundation of Korea (NRF) through the Human Resource Training Project for Regional Innovation (NRF No. 2013032228).

Multi factors influence analysis on the development and marketplace of hydrogen technologies. Students dissemination (P-277)

Gema M. Rodado^a, Gema Alcalde^b

^aCentro Nacional del Hidrógeno, CNH2 Scientific Culture and Innovation Unit (UCC+i- CNH2) Manager, gema.rodado@cnh2.es

^bCentro Nacional del Hidrógeno, Project Management Division Manager, gema.alcalde@cnh2.es

^{a,b} C/ Prolongación Fernando el Santo s/n - 13500, Puertollano (Ciudad Real) España, phone +34 926 420 682

INTRODUCTION

The use of molecular hydrogen as energy carrier and storage system began to be considered from the middle of the last century [1], since then, these technologies have been adapting and evolving to the needs and demands of society.

It is important to disseminate the uses and properties of hydrogen technology to society, but previously it must be studied, analyzed and directed to different public for achieving a greater impact. The National Hydrogen Centre (CNH2) develops many activities focused on training and dissemination of hydrogen technologies adapting the content of each one to different segments of society.

The technology requires of strong strategic plans [2] that promote and encourage the private and public investment. For this reason, the public policies have a fundamental role based on the general interest of society and the sustainability of the planet by decreasing the CO₂ emissions and getting lower energetic consumption.

The present work is based on dissemination and social acceptance of two major hydrogen and fuel cells applications, such as energy storage and energy generation from hydrogen respectively, a study of the dissemination and perception to primary and secondary students and finally, the influential factors and the way to improve the establishment of hydrogen technologies in the society.

HYDROGEN TECHNOLOGIES

As mentioned above, since the mid-twentieth century processes and equipment of production, storage and hydrogen transformation into electricity and heat have been researched and developed to adapt them to the most demanding applications in society: stationary and transport applications.

Stationary applications

One of the challenges of society is the opportunity that hydrogen offers such as energy storage system.

After studying the different sources and equipment for hydrogen generation, the sector is in the development stage of energy storage obtained from renewable sources by electrolysis and the possibility of installing smartgrids for power distribution in rural or isolated areas.

Transport applications

Given the need to reduce emissions and replace fossil fuels, practically, in all transport sectors, the use of electric vehicles with fuel cell powered by hydrogen is considered. The market launch of these vehicles is scheduled to begin in 2015, thanks to the increasingly competitive prices proposed by automotive companies and those projects that countries are implementing to develop infrastructure and a hydrogen refueling stations network, e.g. H2 Mobility or H2USA.

SOCIAL ACCEPTANCE

In order to achieve the acceptance and use of a technologically innovative product by society, it is necessary to disseminate their properties, advantages and disadvantages, to make it known worldwide so that more users demand products based on these technologies. . This would facilitate the inclusion of new companies in this sector promoting competitiveness, development and product improvement and also cost reduction.

There are many studies about social acceptance of hydrogen technologies, based on the demonstration and focused on the application of these technologies in different projects such as: PSEH2RENOV, HYSOCIETY, HYFLEET, CUTE, HYCHAIN, NEXTHYLIGHTS.

Social acceptance study

The acceptance of a new technology by the public depends on their training and their knowledge of the technology. To achieve this acceptance of hydrogen and fuel cells technologies, the CNH2, in addition to the development of R&D&I projects, is committed to society and general public by promoting training, scientific dissemination and social acceptance activities, among other.

Thus, it is conducting social acceptance studies which have begun to inform primary and secondary education students about these technologies by the development of educational talks and demonstration workshops titled “El Hidrógeno y la Energía” (Hydrogen and Energy) and “El Hidrógeno te mueve” (Hydrogen moves you), focusing on the following topics:

- Energy
- Hydrogen and its properties
- Hydrogen production
- Fuel Cells and their applications
- Hydrogen vehicle operation

The workshops consisted of activities based on hydrogen production from renewable energies, storage and processing in domestic applications, integrated hydrogen vehicle with reversible PEM fuel cell and the operation of Scalextric that integrates a fuel cell as power system.

Finally, participants received a questionnaire with simple questions related to the session explained, as well as an impact evaluation of it.

Results

The results of the sessions were analyzed using the questionnaires given to the participants. The following summarizes some of the results:

Hydrogen production: most of participants thought that hydrogen is obtained from water, although they did not consider the generation via hydrocarbons. This idea is probably obtained because the workshops were focused on hydrogen generation from renewable sources and its following storage, creating the opinion that hydrogen is a clean and no pollution energy.

Hydrogen properties: the general idea on hydrogen is a colorless, odorless and tasteless gas, and a very light element, but participants did not know any other properties.

Hydrogen storage: most students considered that hydrogen could be stored as a pressure gas, but they did not know other ways of storage, such as captured gas in very porous solid material due to its novelty.

Fuel cells: the results showed that participants know some of the properties of a fuel cell: silent, modular and expensive, but most of them were not aware that its main aim is to produce electricity. Most of the results showed that fuel cells are compared with batteries.

Workshops Impact: most of participants were more satisfied with workshops than any speech on hydrogen, although in general they had quite a good reception.

After analyzing the obtained results in the questionnaires about sessions, the conclusions were:

It would be necessary to emphasize in different hydrogen production methods, not only from water but also from other resources although underlining the benefits of hydrogen from water and its combination with renewable energies.

It would be recommended to remark the hydrogen properties like its advantages as a fuel, its boiling point and its storage capacity in different states, so hydrogen requires the same characteristics as other fuels to burn. Taking the correct measures of manipulation, as same as in other gases, hydrogen will be a secure gas.

Finally, it would be convenient to elaborate more extended explanations about fuel cells applications and properties, marking the production of electrical and thermal energy adapted to needs user, and explaining that fuel cell is no similar to a battery.

CONCLUSIONS

It is strategic to carry out scientific dissemination and the execution of approaching workshops about technologies to society, especially young people, as they will become our future researchers. Several reasons support this statement: on the one hand, the nowadays problems in the world related to the reduction of greenhouse effect and the use of fossil fuels are well known and on the other hand, the efforts made by stakeholders to achieve the progress in researching, demonstration projects and awareness addressed to the society with the goal to introduce "Hydrogen Economy".

Besides it is necessary to show to society the benefits of the hydrogen technologies and equipment which are used as storage energy system or as an alternative fuel to reduce emissions. It would ensure the penetration in market of hydrogen technologies favoring the creation of companies based on the aforementioned technologies and satisfying to user.

To improve the establishment of these technologies in the society it is necessary to remove some barriers such as the high costs of materials and processes, the development of a supply infrastructure or the frightened related to hydrogen security. Nevertheless thanks to researching advances, demonstration projects and consciousness activities directed to society, hydrogen and its technologies are being accepted step by step.

The hydrogen and fuel cells implementation depends on technological, economic, social, and training factors.

Since decades ago, there are different public policies and tools in the world, European, national and regional area whose target is the public and private investment promotion in the development of technology based on planet sustainability. The policies have been adapted to solve the necessities and social problems, mainly those related to energy and transport sector, environmental and reduction of the greenhouse effect.

But the development of technologies, its experimentation, introduction and market implementation and finally, its use, is a long process that requires a long period to be able to compete with other more mature and cheaper technologies for the users.

Finally, it would be interesting to be focused on students, as explained before, because they are our future. It is essential to approach the technologies through a dynamic way, justifying their researching and development and considering students part of these new technologies. On the other hand, it is also important to get involved teachers and educators in training, making training of trainers.

REFERENCES

[1] Asociación Nacional de Ingenieros de ICAI & Universidad Pontificia de Comillas. Madrid. Hidrógeno y Pilas de Combustible: estado actual y perspectiva inmediata. ISBN: 978-84-9359050-6-7.

[2] CNH2, «Manuel Montes_BoletínCNH2-Diciembre 2012,» Diciembre 2012.

The use of waste hydrogen for energy purposes in Poland (P-279)

Jerzy KALETA, Marek BRZEŹAŃSKI, Eugeniusz WOŹNIKOWSKI**, Pawel GAŚIOR
and Tadeusz PAPUGA**

*Institute of Materials Science and Applied Mechanics,
Wroclaw University of Technology, Wybrzeże Wyspiańskiego 27, 50-370 Wrocław, Poland*

**Institute of Automobiles and Internal Combustion Engines,*

Cracow University of Technology, ul. Jana Pawła II 37

31-864 Kraków, Poland

*** Skotan S.A.,*

ul. Uniwersytecka 13, 40 007 Katowice, Poland

INTRODUCTION

Many industrial processes like production of chlorine and caustic soda generates hydrogen as a by-product. Some of this hydrogen is reused in the production process, however significant amount that is wasted can be used as a fuel for transportation equipment and in stationary applications.

Worlds production of by-product hydrogen just in chlor-alkali industry is estimated at 16 billion m³ per year. Jet it is believed that 2.4 billion m³ of this hydrogen is released to the atmosphere every year and therefore wasted. This amount of H₂ would allow to generate 420 MWe in power cells with efficiency of 50 %.

In Europe about 23 billion m³ of by-product hydrogen is produced every year and between 2 and 10 billion m³ is wasted (in Poland about 0.4 billion m³, lack of accurate data). This amount of hydrogen would be enough to power up more than 1 million vehicles with hydrogen power cells or to produce heat and electrical power for industrial purposes.

Lately, about 100 projects and demonstrative installations were started aimed to present usefulness of the by-product hydrogen in production of heat and electrical power. So far in Poland there was no such installation.

BASIC ASSUMPTIONS

Project "The use of waste hydrogen for energy purposes" was started in 2012. The goal of the project was development of the technology for exploitation of by-product hydrogen in chosen chemical plant.

Additional assumption was that hydrogen is mixed with liquid and gas hydrocarbons and those hydrocarbons were meant to be used as a fuel as well. Technology of use of waste hydrogen required development of methods for its purification, transportation and combustion with taking into consideration safety factors.

The project is realized in ZAK S.A. company in Kędzierzyn-Koźle, one of the largest chemical plant in Poland. The company manufactures products for agriculture, construction, chemical industry and plastics industry. Skotan S.A. company is the investor of the project.

Realization of the project allowed for construction of small power plant with capacity of 1.2 MW (Fig. 1). It was assumed that the pilot investment will allow to gather know-how necessary to proceed with similar investments in other companies producing waste hydrogen.

Two pilot technological lines were planned:

- with hydrogen (+hydrocarbons) used as a fuel for generators based on the combustion engines (leading technology),
- with purified hydrogen used for fuel cells (complementary technology).

Investment was planned for construction new power plant from the ground. Cost of the investment estimated to be about 10 million €.



Fig. 1. General view of new by-product hydrogen power plant.

THE RESEARCH PROGRAM

The research was conducted by the consortium of Cracow University of Technology (CUT) and Wrocław University of Technology (WUT).

The main goal of the collaboration were:

- concept of method for purifying gas stream by extracting unwanted gas and liquid elements,
- selection of the liquid and gas fuel composition for combustion engines running generators,
- selection of power cells,
- application of Structural Health Monitoring System (SHMS) for gas installations, buffer tank, power and heat generators and for the construction of the building plant is situated in,

- testing of both technologies after commissioning of demonstrative power plant.

SAFTY INSTALATION

A great effort was put on safety aspects and structural health monitoring of the most critical elements. An innovative technology based on distributed optical fiber based sensors for hydrogen pipeline integrity and leakage detection was applied. Each of four supply gas pipelines (one with pure hydrogen to the fuel cell and three others with waste hydrogen to power generators, Fig. 2) is permanently monitored. In case of any fuel leak an operator is alarmed and proper safety procedures are started. The SHM system is based on distributed temperature measurements at the whole length. Each temperature event connected with fuel leak (by Joule's-Thompson effect) is detected and localized with a meter accuracy.

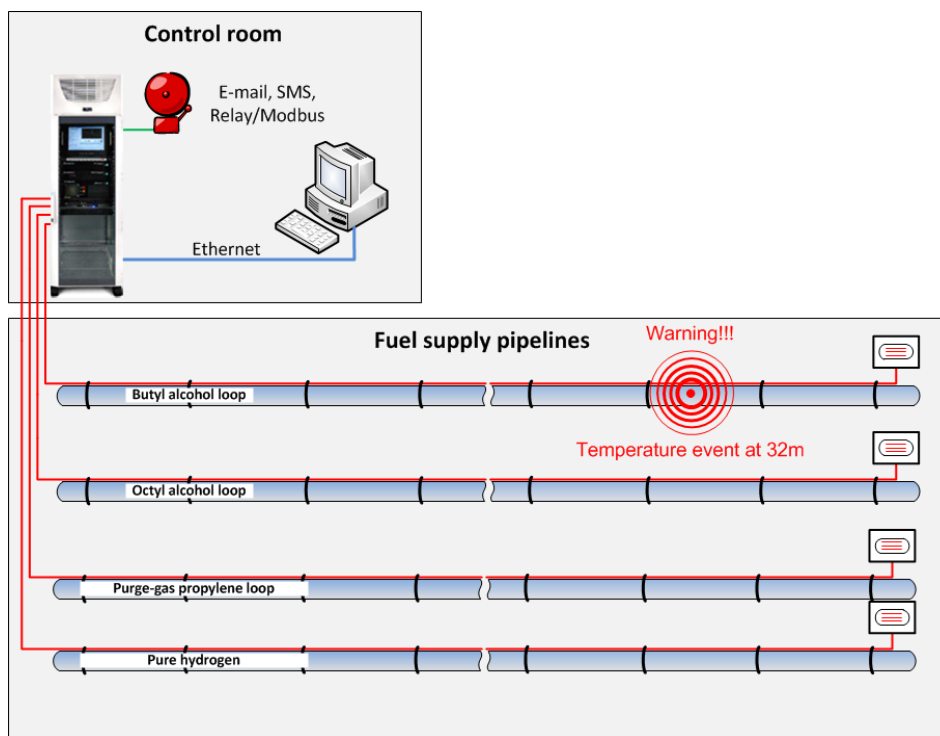


Fig. 2. Scheme of pipeline monitoring system.

CONCLUSIONS

Research, design and construction allowed start of the experimental power plant with capacity of 1,2 MW powered by by-product hydrogen. Two technologies were successfully tested:

- 1) combustion of hydrogen contacting hydrocarbons,
- 2) production of electric power with use of purified hydrogen and power cells.

Additional auxiliary technologies (like SHM system for fuel leakage detection) was also effectively implemented.

ACKNOWLEDGMENT

This work is supported under grant POIG.01.04.00-02-105/10, co-financed by European Regional Development Fund (Poland, The Innovative Economy Operational Program 2007-2013, Action No 1.4).

A semi-analytical model for droplet dynamics on the GDL surface of a PEM fuel cell cathode (P-281)

Alex Jarauta (CIMNE-UPC), Jordi Pons-Prats (CIMNE-UPC), Marc Secanell (University of Alberta), Pavel Ryzhakov (CIMNE-UPC), Sergio Idelsohn (CIMNE-UPC), Eugenio Oñate (CIMNE-UPC)

Water management is one of the key factors affecting Proton Exchange Membrane Fuel Cell (PEMFC) performance [1], [2], [3], [4]. The water produced within the fuel cell is evacuated through the gas channels, and at high current densities water can block the channel, thus limiting the current density generated in the fuel cell. Numerical models of a droplet emerging from a pore have high computational costs and are difficult to implement. Analytical models are easy to implement into Membrane Electrode Assembly (MEA) models and have a low computational cost.

A semi-analytical model of a water droplet emerging from a pore of the Gas Diffusion Layer (GDL) surface in a PEM fuel cell channel is developed. The current work expands a previous model of Esposito et al. [1] and is composed of a geometrical and dynamic model for the droplet that can describe its shape at any configuration. In this work, a more accurate representation of the forces is provided. The forces acting on the droplet are the drag force exerted by the air and the adhesion force between the water and the GDL surface. Figure 1 shows a water droplet emerging from a pore on the GDL surface, subjected to the drag force exerted by the airflow and the adhesion force. The adhesion force expression is developed from the integration of the surface tension force along the contact line, where the contact line has a particular configuration depending on the droplet deformation. The drag force is expressed with the classical formula. However, since the drag coefficient has been identified as one of the factors that take the numerical results away from the experimental results [1], the drag coefficient of the droplet is computed numerically for the working conditions and is characterized as a linear function depending on the droplet height (expressed as the dimensionless Reynolds number) and the hysteresis angle (difference between the advancing and receding angles). The computed drag coefficient is bigger compared with the drag coefficient computed with the equation found in literature. This is the main contribution of the present work, since it provides with an analytical expression for the drag coefficient that has been computed numerically for the considered conditions.

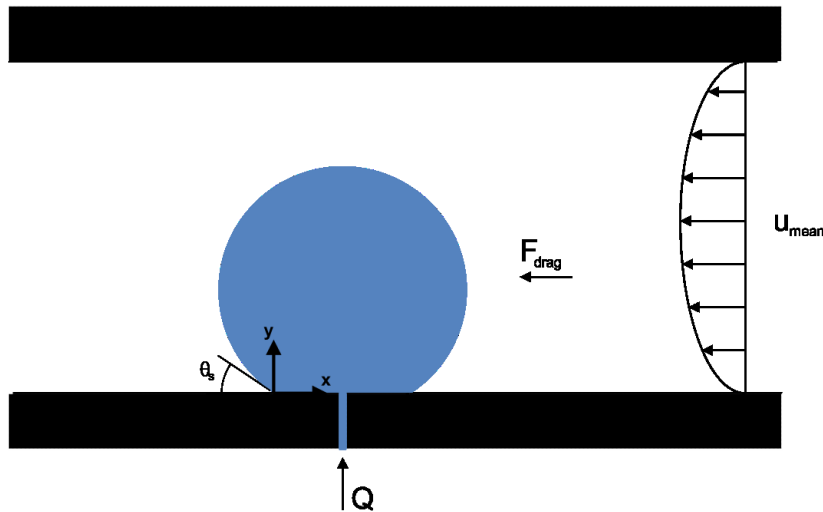


Figure 31 – Droplet emerging on the GDL surface subjected to the drag and adhesion forces

The analytical model is used to study the problem of a growing droplet in a gas flow channel to see the effects of: i) air velocity and liquid mass flow in droplet deformation and oscillation; and, ii) droplet height in frequency oscillation. The dynamic governing equation of the droplet is Newton's Second Law applied to the x-coordinate of the center of mass, and it is solved with fourth-order Runge-Kutta method. Figure 2 shows the evolution of the x-coordinate of the center of mass over time for the static and the dynamic case. The x-coordinate of the center of mass show the expected oscillations since the drag force unbalances the droplet and the adhesion force takes the droplet to a new balance state.

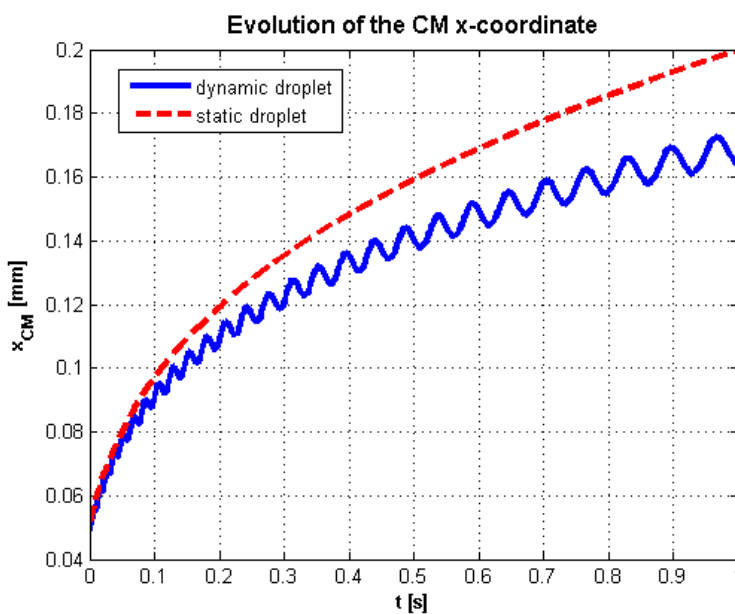


Figure 32 – Evolution of the x-coordinate of the center of mass over time for the static and the dynamic case

Results show that the predicted values for both drag and surface tension force are higher than the results found in literature. In other words, the air exerts more force on the droplet according to the present model, but the droplet is more rigid due to the higher value of the adhesion force and therefore it deforms less. As expected, increasing the air velocity leads to more deformation of the droplet and oscillation with lower frequency but higher amplitude [1], [2], [4]. Similar effects have been identified when the liquid mass flow is increased, leading to faster detachment of the droplet. The detachment of the droplet occurs later than the previous model predicted due to the higher values of the acting forces.

A frequency analysis has been done keeping the droplet with a constant mass. The predicted frequency oscillation values are significantly lower than the values from literature [1], but these results are obtained for different water injection conditions.

The presented model can have several applications. For instance, it can be integrated with a MEA model to have a full model of a fuel cell or it can be applied to fluid/structure interaction problems for the drag coefficient relationship.

REFERENCES

[1] A. Esposito, P. Polverino, C. Pianese, and Y.G. Guezennec. A lumped model of single droplet deformation, oscillation and detachment on the GDL surface of a PEM fuel cell. ASME 2010 8th International Fuel Cell Science, Engineering and Technology Conference, 2010.

[2] A. Theodorakakos, T. Ous, M. Gavaises, J.M. Nouri, N. Nikolopoulos, and H. Yanagihara. Dynamics of water droplets detached from porous surfaces of relevance to PEM fuel cells. *Journal of Colloid and Interface Science*, 300:673-687, 2006.

[3] X. Zhu, P.C. Sui, and N. Djilali. Numerical simulation of emergence of a water droplet from a pore into a microchannel gas stream. *Microfluid Nanofluid*, 4:543-555, 2008.

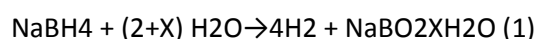
[4] K.S. Chen, M.A. Hickner, and D.R. Noble. Simplified models for predicting the onset of liquid water droplet instability at the gas diffusion layer/gas flow channel interface. *International Journal of Energy Research*, 29(12):1113-1132, 2005.

Hydrogen production through sodium borohydride ethanolysis (P-291)

G.M. Arzac and A. Fernández

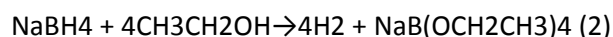
INTRODUCTION

Sodium borohydride (NaBH₄, SB) is a safe and easy to handle hydrogen storage material with a high gravimetric density (GHD, 20%). It produces hydrogen through solvolysis reactions. Water is definitely the most studied solvolytic agent and catalyzed hydrolysis reaction (1) has proven to be efficient in producing hydrogen at appreciable rates in small and high-scale reactors [1].



The theoretical gravimetric hydrogen density of reaction (1) is 10.8 % but the reaction product, sodium borate (NaBO₂) is water consuming to form hydrates which precipitate onto the catalyst reducing the total conversion [2]. For this reason, in practice the maximum GHD achieved was around 4% [2-3].

Alcohols are also advantageous solvolytic agents. In particular methanol (CH₃OH) and ethanol (CH₃CH₂OH) are the most promising because of their lightweight. Sodium borohydride ethanolysis (2) is interesting because of its high potential GHD (3.6 %) and safety. The use of sodium borohydride can be an advantageous method to extract hydrogen from bioethanol. Bioethanol can also be recovered by hydrolysis of the reaction by-product (NaB(OCH₂CH₃)₄).



In this paper, SB ethanolysis is studied as a hydrogen producing reaction to feed PEMFC (Polymer Exchange Membrane Fuel Cells). Reaction products are characterized by TEM (Transmission Electron Microscopy), SEM (Scanning Electron Microscopy) and XRD (X-Ray Diffraction).

RESULTS AND DISCUSSION

Sodium borohydride ethanolysis as shown to obey first-order rate law in ethanol and very slow (0.071 ml.min⁻¹). For this reason, a series of catalysts which have demonstrated high performance for sodium borohydride hydrolysis have been tested for reaction (2) [1]. Table 1 summarizes main results.

Catalyst	Activity (ml.min ⁻¹ .g ⁻¹)
CoCl ₂ ·6H ₂ O	403
Co-B (prepared as in Ref [4])	197
H ₂ PtCl ₆	352
Citric acid	604
RuCl ₃ ·3H ₂ O	1130
CoCl ₂ ·6H ₂ O+ RuCl ₃ ·3H ₂ O (30% atomic Ru)	480

Table 1. Activity for sodium borohydride ethanolysis for the studied catalysts.

For tested catalysts, the H₂ evolution curves (Fig.2) obey a pseudo first-order law. Metal salts have shown to be more active than the corresponding M-B materials. For metal salts, reactivity is Ru » Co ~ Pt. The mixture of Co and Ru metal salts does not produce synergistic effect as reported previously for sodium borohydride hydrolysis. Acid catalysis has also shown to be advantageous.

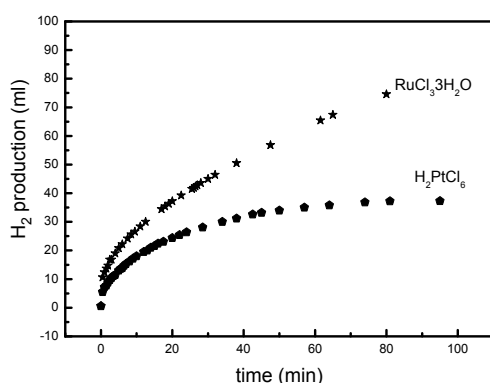


Figure 1. Hydrogen evolution curves for noble metal catalysed SB ethanolysis.

CONCLUSIONS

Sodium borohydride ethanolysis was studied as a method to produce hydrogen for PEMFC. Uncatalysed, the reaction has shown to be extremely slow. Catalytic reaction was studied and Ru as its metal salt has demonstrated to be the most efficient catalyst. More effort will be done to improve the catalytic activity of the Ru based catalyst by ex-situ reducing its metal salt and further supporting.

REFERENCES

- [1] S.S. Muir, X. Yao, Int J. Hydrogen Energy, 2011; 36: 5983-5997. References therein

[2]G.M. Arzac, A. Fernández, A. Justo, B. Sarmiento, M.A. Jiménez, M.M. Jiménez. Journal of Power Sources, 196, 2011, 4388-4395

[3]J.Hannauer et al, Energy Environ. Sci., 2010, 3, 1796-1803.

[4] G.M. Arzac, T.C. Rojas, A. Fernández, Chem Cat Chem, 2011; 3: 1305-1313

Evaluation of sepiolite-supported catalysts for biogas reforming to hydrogen production (P-292)

Serrano-Lotina, J.A. Daza, A. Dieng, A. Balbín, L. Daza

*Instituto de Catálisis y Petroleoquímica (CSIC)
C/ Marie Curie 2 L10, 28049 Madrid (Spain)*

INTRODUCTION

Biogas is a hydrogen source produced by the anaerobic digestion of organic matter present on waste. The utilization of this resource not only constitutes an alternative fuel that can reduce fossil fuel dependency and emissions of greenhouse gases, but also helps to reduce all the organic matter present on waste [1]. The hydrogen, obtained from biogas can be used to feed certain types of fuel cells, which offer the advantages of higher efficiencies and neither pollutants nor greenhouse gases generation. Since CH₄ and CO₂ are the main components present in biogas [2], CO₂ reforming of methane constitutes an interesting process to study. The major drawback of this reaction is catalyst deactivation, mainly produced by carbon deposition [3,4].

Sepiolite is a good material as catalytic support due to their fibrous structure and open porous network [5] but it has not been studied in dry reforming of methane. On the surface of the sepiolite there are both alkaline center (Mg, O tetrahedron) and acid center (Si, O tetrahedron). Since acidity seems to favor carbon deposition, two lanthanides has been added in order to see its influence in the Ni-based catalyst for biogas reforming.

EXPERIMENTAL

Natural sepiolite (Tolsa S.A.), whose chemical composition (expressed as oxides) is: 60.8 wt.% SiO₂; 20.3 wt.% MgO; 4.6 wt.% Al₂O₃; 1.2 wt. % Fe₂O₃; 1.2 wt.% CaO; 1.1 wt.% K₂O and 0.4 wt.% Na₂O, was used to prepare three Ni-based catalysts: NiSep (5% Ni), NiLaSep (5% Ni, 3% La) and NiCeSep (5% Ni, 3% Ce). Catalysts were synthesized by impregnation method. They were dried at 110 °C overnight and calcined at 550 °C for 2 h.

Chemical composition was determined by ICP-MS, chemical structure by X-ray diffraction (XRD) and BET area by N₂ adsorption-desorption isotherms. Catalysts were pre-reduced at an adequate temperature, which was determined by temperature programmed reduction (TPR). In order to test catalytic activity and stability, catalytic tests were performed in free-Ni stainless steel reactors at 700 °C, reactants feed of CH₄:CO₂ 1:1 and W/F of 1 mg·min·cm⁻³. Catalytic tests were performed under equilibrium conversion in order to ensure that deactivation was not hidden by an excess of catalyst mass.

RESULTS AND DISCUSSION

The results of the chemical analysis of the three catalysts were: 6.1% Ni (NiSep), 3.1 % La and 4.6% Ni (NiLaSep) and 3.1% Ce and 4,8% Ni (NiCeSep). XRD characterization showed that the addition of the promoters (La and Ce) and the nickel did not modify crystalline structure. No peak related to

NiO or La₂O₃ were observed. However, in NiCeSep catalyst, CeO₂ phase was detected. BET areas of the catalysts were 109, 89 and 95 m²·g⁻¹ for NiSep, NiLaSep and NiCeSep, respectively. Then, the addition of the promoters decrease superficial area.

The appropriate reduction temperature was evaluated from TPR characterization. Fig.1 shows the evolution of water signal since water is formed when NiO is reduced. The peak at approximately 100 °C is ascribed to physisorbed water. Two peaks at 550 and 810 °C approximately were detected in the three catalysts, what indicate that nickel is strongly interacting with sepiolite support. A peak at 380 °C was detected in NiLaSep and NiCeSep and it can be ascribed to reduction of free NiO. In order to reduce all the nickel present, the catalysts were reduced in situ at 850 °C for 1h with pure H₂ (100 mL·min⁻¹).

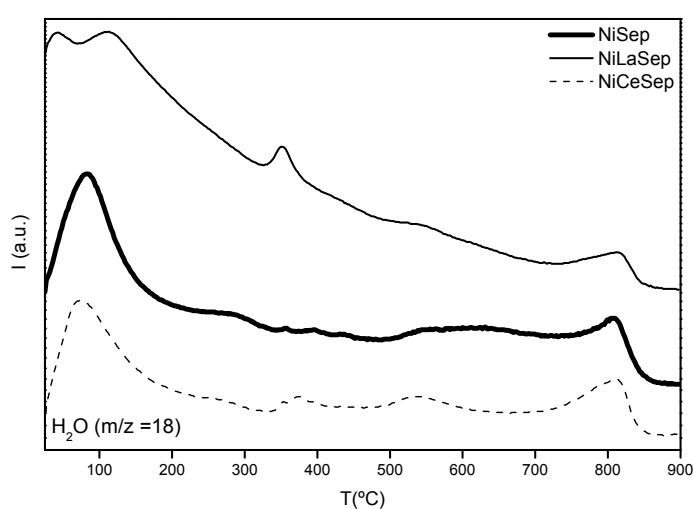


Fig. 1. TPR-MS of NiSep, NiLaSep and NiCeSep.

They were tested during 10 h, according to the conditions reported in the Experimental section. It can be seen that CO₂ conversion (XCO₂) was higher than CH₄ conversion (XCH₄) in all cases (Fig. 2). This is due to the occurrence of reverse water-gas-shift reaction ($\text{H}_2 + \text{CO}_2 \rightleftharpoons \text{H}_2\text{O} + \text{CO}$) [6]. The presence of water in the product distribution (NiSep: 5%, NiLaSep: 4% and NiCeSep: 7%) and the H₂/CO ratio below unity (NiSep: 0,6, NiLaSep: 0,6 and NiCeSep: 0,7) confirmed it.

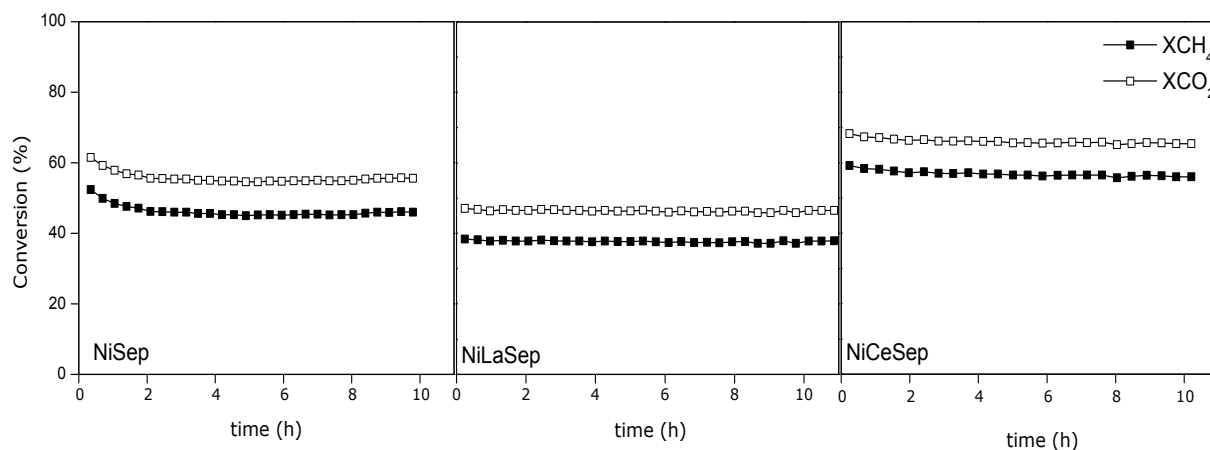


Fig. 2. CH₄ and CO₂ conversion vs. time in dry reforming of methane for catalyst NiSep, NiLaSep and NiCeSep.

Testing conditions: CO₂:CH₄=1, 700 °C and W/F = 1 mg·min·cm⁻³.

All the catalysts showed good stability during the tests. Catalytic activities were 9.1 mol CH₄·h⁻¹·gNi⁻¹ (NiSep), 10.1 mol CH₄·h⁻¹·gNi⁻¹ (NiLaSep) and 14.6 mol CH₄·h⁻¹·gNi⁻¹ (NiCeSep). The activity of NiSep is lower than the catalytic activity of NiLaSep, despite having a higher conversion. This is because this activity is related to Ni content which was higher in the former catalyst. Then, the addition of promoters leads to an increase in the activity of the catalysts as it has been previously reported [7,8] and this may be probably due to a higher Ni dispersion.

CONCLUSIONS

Sepiolite supported Ni-based catalysts have been characterized and tested in dry reforming of methane reaction. According to TPR characterization, there is a strong interaction between Ni²⁺ and sepiolite. Consequently, high reduction temperatures were necessary in order to reduce Ni²⁺ to Ni⁰. All the catalysts were stable in dry reforming of methane during 10 h. The addition of Ce or La increased catalytic activity, overall in NiCeSep.

These are interesting results since sepiolite is a cheap and fully available support in Spain and this technology could convert waste into renewable hydrogen.

ACKNOWLEDGMENT

Financial support from Comunidad de Madrid (DIVERCELCM, S2009/ENE-1475) is gratefully acknowledged.

REFERENCES

[1] D. Deublin, A. Steinhöuser, Biogas from waste and Renewable Resources. An introduction. Wiley-Vch, 2008. pp. 368.

[2] E. Turpeinen, R. Raudaskoski, E. Pongracz, R.L. Keiski, *Int. J. Hydrogen Energy* 33 (2008) 6635-6643.

[3] J. R. Rostrup-Nielsen, J. Sehested, *Adv. Catal.* 47 (2002) 65-139.

[4] A. Serrano-Lotina, L. Daza, *Appl. Catal. A: Gen.* (2013), <http://dx.doi.org/10.1016/j.apcata.2013.08.027>

[5] X-L. Zhai, M-Y. Jia, Y-S. Shen, *Chin. J. Chem.* 23, 2005, pp. 557

[6] A. Serrano-Lotina, L. Daza, *Int. J. Hydrogen Energy* (2013), <http://dx.doi.org/10.1016/j.ijhydene.2013.05.135>

[7] C.E. Daza, J. Gallego, J.A. Moreno, F. Mondragón, S. Moreno, R. Molina, *Catal. Today* 133–135 (2008) 357-366.

[8] A. Serrano-Lotina, L. Rodríguez, G. Muñoz, L. Daza, *J. Power Sources* 196 (2009) 4404-4410.

Experimental evaluation of cell components affecting the performance of an air-breathing PEM fuel cell (P-295)

Levent Akyalçın

Anadolu University, Department of Chemical Engineering, İki Eylül Campus, 26555, Eskişehir, TURKEY

Air-breathing PEM fuel cells (ABPEMFCs) are promising power generation devices both to charge the batteries and to supply power directly to portable electronics like smart phones, tablets, etc. Because of their simplicity of natural convection oxygen delivery, low weight, easy fuel charge and low operating temperatures make the ABPEMFCs attractive for near future portable power applications.

Performance of the ABPEMFCs depends on both structural and environmental conditions. Catalyst loading on the electrodes, membrane thickness and cathode opening geometry for air delivery are the main structural factors affecting the performance of the ABPEMFCs. Relative humidity and temperature of surrounding of ABPEMFCs are the other important parameters, which depend on the environmental conditions.

It is possible to find many researches on ABPEMFCs published in the literature. Some of those researches are focused on the mathematical modeling of ABPEMFCs either at cell component level or overall system level. The rest of the researches are mainly focused on experimental evaluation of parameters affecting the ABPEMFC performance either at cell component level and environmental conditions level. On the other hand, evaluating the individual effects of the cell components and environmental conditions on fuel cell performance may limit to recognize the overall picture.

In order to improve fuel cell performance, it is essential to understand these parametric effects on the fuel cell operations and optimize them. The optimization of the cell components affecting the performance of ABPEMFC and obtaining related data are very important in various applications, and especially for fuel cell producers to validate and improve their models. Therefore, doing large numbers of experiments are often needed to understand clearly the effects of the parameters on the performance of ABPEMFC and to optimize them. It is known very well that performing large numbers of experiments of systematic experimental studies to optimize the cell components of ABPEMFC are costly and time-consuming process. To overcome this challenge, Taguchi's orthogonal array (OA) analysis, known as experimental design methods, may be used in order to evaluate the respective impacts of those parameters on the performance of ABPEMFC, and to reduce the number of experiments when many parameters are studied. The main advantage of this method over other statistical experimental design methods is that the parameters affecting an experiment can be investigated as controlling and none controlling. Detail about the Taguchi's OA analysis can be found elsewhere. The advantage of the Taguchi method on the conventional experimental design methods, in addition to keeping the experimental cost at a minimum level, is that it minimizes the variation in product response while keeping the mean response on target. Its other advantage is that the optimum component combination determined from the laboratory work can also be reproduced in the real application of ABPEMFC.

In this study, the Taguchi method was applied to determine optimum structural combination of a membrane electrode assembly (MEA) and cathode current collector opening geometry in obtaining maximum power density of an ABPEMFC. Performing a variance analysis, in order to determine the optimum levels and relative magnitude of the effect of combinations, also followed performance measure analysis.

Experimental parameters and their levels given in Table 1 are determined in the light of literature and preliminary tests. The L9 (34) OA was accepted as the most proper method to determine the experimental plan, for four parameters of each three values. The performance of ABPEMFC can be affected by some factors known as controllable or uncontrollable (noise sources). In order to observe the effects of uncontrollable factors on this process, each experiment was repeated three times with same combinations of parameters.

Table 1. Experimental parameters and their levels.

Parameter	Level	1	2	3
A. Anode Pt loading, mgPt cm ⁻²		0.45	1.35	1.78
B. Cathode Pt loading, mgPt cm ⁻²		0.45	1.35	1.78
C. Nafion membrane		112	1135	115
D. Cathode current collector opening geometry		Vertical	Circular	Oblique

In the present work, the order of the experiments was obtained by inserting parameters into the columns of OA, L9 (34) selected to be the experimental plan given in Table 2. The order of experiments is randomized in order to avoid noise sources which had not been considered initially and which could take place during an experiment and affect results in a negative way.

Table 2. Experimental plan.

No. of Experiment	A	B	C	D
1	1	1	1	1
2	1	2	2	2
3	1	3	3	3
4	2	1	2	3
5	2	2	3	1
6	2	3	1	2
7	3	1	3	2
8	3	2	1	3
9	3	3	2	1

The optimum structural combinations of an ABPEMFC were found to be membrane, Nafion 112 with a thickness of 51 μm , amount of platinum loaded on anode, 0.45 mg Pt cm⁻², amount of platinum loaded on cathode 1.78 mg Pt cm⁻² and vertical cathode current collector opening. Under these conditions, the amount of maximum power density was predicted as 99 mWcm⁻² at 0.5 V by using experimental results obtained from the experimental plan. The verification experiment was

done for the same optimum structural combination and maximum power density at 0.5V was observed as 98 mWcm⁻². According to the results of this optimization, it was seen that amount of platinum loaded on cathode was the most effective parameter.

Integration of an electrolyzer into a minigrid (P-296)

T. GONZÁLEZ-AYUSO¹, B. MARTÍNEZ¹, J.L. SERRANO¹, L. DAZA²,

1. Centro de Investigaciones Energéticas, Medioambientales y Tecnológicas, CIEMAT.

2. Instituto de Catálisis y Petroleoquímica, ICP-CSIC

INTRODUCTION

Electricity generation plants from renewable sources are in continuously expanding due to the more than likely depletion of fossil fuels and increasingly demanding anti-pollution policy. New challenges each day to improve the utilization of the energy generated by these plants. One of the options to improve this utilization is the implementation of energy storage cycles during the more generation and lower consumption periods and the regeneration when a more amount of energy is needed. Conventional systems for these cycles are the batteries and different studies about the several electrochemical processes are being carried out to minimize its rate between the size and the storage capacity.

Another cycle to improve this energy excess is its conversion to chemical energy by water electrolysis, the storage of the generated hydrogen and its final reconversion to electricity through the corresponding electrochemical reaction into one of the types of fuel cells [1]. By this cycle the water electrolysis to generate hydrogen is the stage with lower efficiency. Fuel cells are not subject to limitations affecting thermal cycles when exchanging heat. On the other hand, hydrogen can be obtained also trough reforming of gas or liquid fuels to feed a fuel cell, but water electrolysis is a simply method and provides pure hydrogen that can be feed to a low temperature fuel cell.

The communication describes the behavior and main features of an electrolyzer as a part of a generation system and some operation data of experimental minigrid. The selected alkaline electrolyzer has been supplied by Claind and has been integrated on the EGA-1500 system (spanish initials of Autonomous Generation Station) [2].

EXPERIMENTAL

The main equipments of EGA-1500 are:

- Renewable sources. Two arrays of photovoltaic panels of 1.5 kWp each give a power of 3 kW. The system has also a wind generator emulator with a power capacity of 6 kW. These generators provide the energy that the integrated system will transform to electrical energy.
- Storage system. There are two different storage systems. A conventional system based on a group of lead-acid battery with a capacity of 600 Ah, and a second system that permits the storage of the hydrogen generated by electrolysis as chemical energy. This system includes a Claind electrolyzer to convert electrical energy on chemical energy, the hydride system to store de hydrogen in the form of metallic hydrides with a storage capacity of 5 kg of hydrogen, and a PEM fuel cell to reconvert the chemical energy to electricity when needed.

- Energy management system (EMS). The brain of system developed on labview language optimizes the operation of all equipments that form the integrated minigrig.
- Dynamic load. This load finishes the cycle. The EMS can change the set point of load to adjust generated energy to consumed energy depending on the all variables of the system.

A simplified scheme of the system is depicted in the figure 1.

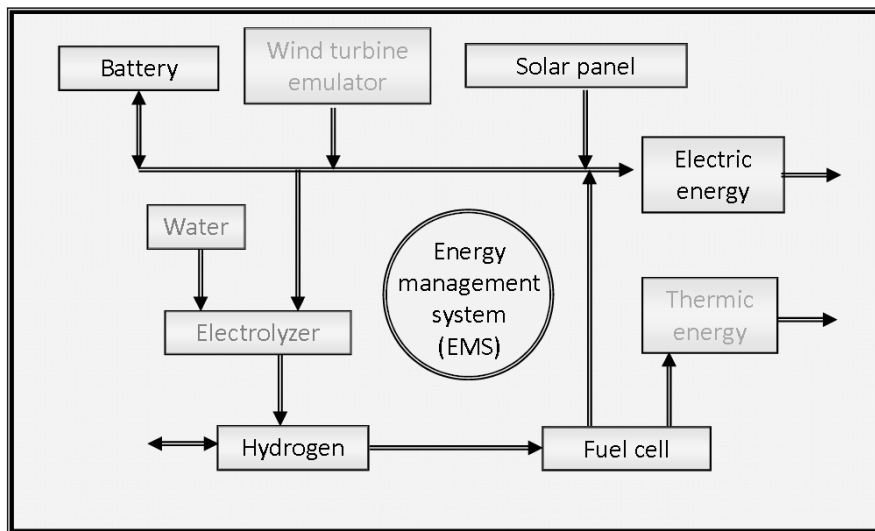


Figure 1.- EGA-1500 scheme.

OPERATION

The electrolyzer has an electrolytic stack with capacity to generate hydrogen until a rate of 1 Nm³h⁻¹. With the control panel is possible to fix the percentage of hydrogen production. The generated gases are separated from the electrolyte in two vessels. Hydrogen is then dried, the residual oxygen content is eliminated in a Deoxo stage and hydrogen is analyzed to ensure its purity. Electrolyte is maintained constant adding by means of a pump a volume of water stoichiometric to the liquid spent in electrolysis. The electrolyzer calculates the hydrogen generated from the power consumed.

In order to integrate the electrolyzer in the EGA system a first step has been carried out connecting the hydrogen generator to hydrogen storage system. A flowmeter has been installed in the exit of electrolyzer to measure the hydrogen flow supplied to the system and a series of tests have been made to measure the variation of the power consumption versus the hydrogen generation. The shape of line of power consumption, the influence of percentage of production set up and the pressure of storage system are studied and a control protocol is proposed to control the electrolyzer integration in EGA-1500 system.

ACKNOWLEDGMENT

Financial support from Community of Madrid (DIVERCELCM, S2009/ENE-1475) and Spanish Ministry of Economic and Competitiveness (MAT2010-20846 and MAT2011-27151) is gratefully acknowledged.

REFERENCES

- [1] P.L. Zervas, H. Sarimveis, J.A. Palyvos, N.C.G. Markatos. Journal of Power Sources 181 (2008) 327–338.
- [2] T. González-Ayuso, M. Labrador, J.L. Serrano, M.A. Folgado, L. Daza. CONAPPICE 2006, 237-240.

PEM fuel cell performance analysis: static and dynamic behaviour and its integration with a supercapacitor (P-298)

IDOIA SAN MARTÍN, ALFREDO URSÚA, PABLO SANCHIS

Department of Electrical and Electronic Engineering, Public University of Navarre, Campus de Arrosadía, 31006 Pamplona, Spain

ABSTRACT

This paper examines the proton exchange membrane fuel cell (PEMFC) performance and its integration with a supercapacitor (SC). Firstly, a complete experimental characterization of the PEMFC electrical behaviour was presented. Furthermore, the electrical behaviour during static regime was analyzed by means of the I-V characteristic curves and current-power curves for different operating temperatures. In turn, a detailed study of the hydrogen consumption and the efficiency took place. This was followed by the experimental characterization of the electrical behaviour in dynamic regime in different operating environments. Finally, a study was made of the system comprising a 1.2 kW PEMFC and a SC of 83.3 F and 48.6 V. To do so, a direct connection of both sub-systems in parallel was performed. The integration of FC with SC has resulted in an improvement on the system during the dynamic regime.

INTRODUCTION

In recent years, the development of FC has been spectacular motivated mainly by the growing demand of numerous sectors, such as the transport, the portable devices and the stationary applications sector. The PEMFC operates at low temperatures, generally under 80 °C and as a result allows a quick start up. At the same time, its response to load variations is relatively fast, it is compact, lightweight, and also contains a solid polymer as electrolyte, it is easier to manufacture than other types of FC. PEMFC has been validated in various applications such as transport, distributed generation, cogeneration and portable systems [1].

The FC dynamic characteristics are principally limited by the hydrogen and oxygen (or air) feed system. Rapid variations in the power output may cause a large decrease in voltage, and can be harmful for the FC by reducing its useful life [2, 3]. For that reason, in applications with significant power output variations, such as in microgrids or electric vehicles, it appears to advisable to integrate the FC with an auxiliary sub-system to respond to the power output faster dynamics. The SC can assume large variations of power, which makes them very attractive for use in combination with a FC system [4-7].

SYSTEM DESCRIPTION AND EXPERIMENTAL SET-UP

The experimental study was conducted at the Renewable Energies Laboratory of the Public University of Navarre. The laboratory is equipped with the PEMFC and the SC analyzed in this paper. Furthermore, it contains the hydrogen installation comprising four B50 hydrogen cylinders, with a total capacity of 35.2 Nm³.

The PEMFC, showed in the Fig. 1a, corresponding to model NEXA1200, is developed by Heliocentris. This FC obtains oxygen from the air and has a power output of 1200 W. The FC comprises a stack with 36 series connected cells and the voltage range is approximately between 20 and 36 V, and the maximum current is 60 A. In addition, it incorporates a relay and a diode in order to connect to the load.

Likewise, there is a module of SC corresponding to model BMOD0083 made by Maxwell, showed in the Fig. 1b. Each module has a capacity of 83.3 F, a voltage of 48.6 V and it is compound of 18 cells connected in series. Each cell has a capacity of 1500 F and a voltage of 2.7 V and it is compound of two porous carbon electrodes and an organic electrolyte.

Furthermore, the laboratory is equipped with a programmable electronic load made by Amrel. Its operating range is from 0 to 7500 W, and a maximum voltage and current input of 600 V and 400 A. The programmable electronic load has four operating modes and can reproduce current, power, voltage and resistance profiles.

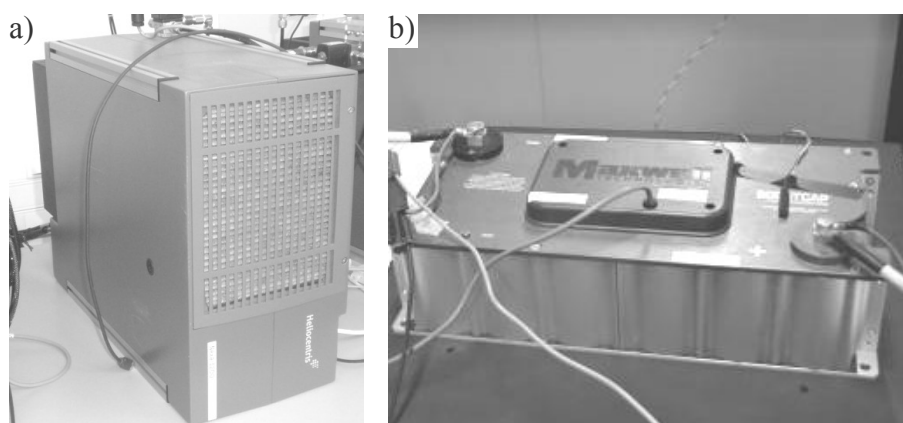


Fig. 1 a) Photo of the fuel cell and b) photo of the supercapacitor.

RESULTS AND DISCUSSION

The electrical characterization of FC during static operation regime is based on its I-V characteristic curves at different temperatures. To do so, the FC was required to supply a sinusoidal wave of 60 A peak-to-peak superimposed to a DC current. The DC current determines the operating temperature while the sine wave component allows to obtain the current - voltage relation and thus a point of the I-V curves. The sine wave component frequency must ensure that the FC operates at static regime and with a minimal temperature variation. The tests are carried out maintaining the same sine wave component and varying the DC current component, so the I-V curves are obtained at different operating temperatures. Fig. 2a shows the I-V curve corresponding at an operating temperature of 53.9 °C. Likewise, the hydrogen consumption and the current - power (I-P) curve have been plotted for the same operating temperature. On the other hand, an analysis was made of the efficiency of the stack (η_S) and the FC (η_{FC}). Fig. 2a shows η_S and η_{FC} for a current range from 0

to 60 A and for operating temperature of 53.9 °C. It can be seen that η_S decreases as the FC current increases. This is due to the fact that an increase in FC current causes an increase in the activation, ohmic and concentration losses. The difference between both efficiencies is due to the fact that a part of the electrical power generated by stack must cover the electrical consumption of the peripherals (fan, sensors, etc), in consequence, η_{FC} is lower than η_S .

This was followed by an analysis of the electrical behaviour of FC during dynamic operation regime. The realized tests are based on current, resistance and power steps demanded of the FC. Fig. 2b shows one of the tests, where upward and downward current steps are demanded of the FC. It can be seen that an instantaneous change of FC current (i_{FC}) causes a variation in the FC voltage (v_{FC}). Furthermore, other study was also carried out of the dynamic behaviour of the FC. To do so, the FC was required to supply a sine wave current of different amplitudes and frequencies superimposed to DC current. The results obtained with these tests allow us to analyze the phase difference between FC current and voltage. As the frequency of the sine wave current increases the dynamic behaviour of the FC appears, mostly caused by the double layer effect.

Finally, the integration of SC with the FC is successfully carried out. A direct connection is made of both sub-systems in parallel (FC-SC system). For the purpose of the analysis, the FC-SC system was subjected to the current and power step tests. Fig. 2c shows one of the step tests. In this case, the current demanded by the load (i_L) was covered by the SC (i_{SC}) and by the FC (i_{FC}). It was observed that the variation of i_L is initially covered by the SC, whilst the i_{FC} progressively increases according i_{SC} decreases. Comparing the tests conducted on the FC (Fig. 2b) and the FC-SC system (Fig. 2c), it can be observed that, in case of the FC-SC system, v_{FC} showed far less variation than for the system compound only of FC. The same happens with the i_{FC} due to the fact the rapid variations of i_L were covered by the SC in the case of the FC-SC system. In short, the integration of SC with FC achieves the FC operating conditions were less severe and apparently leading to a longer service life.

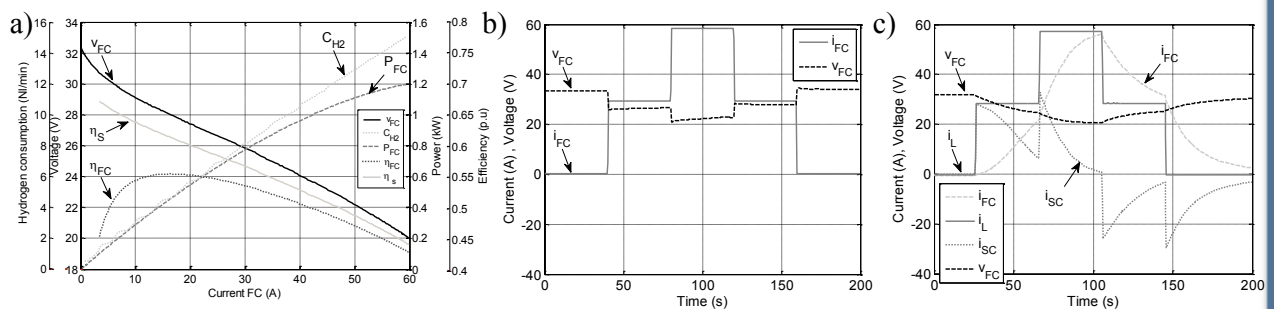


Fig. 2 a) Static regime test: hydrogen consumption (CH_2), voltage (v_{FC}), power (P_{FC}), fuel cell (η_{FC}) and stack (η_S) efficiency versus fuel cell current (i_{FC}) for an operating temperature of 53.9 °C. b) Current step test of FC: FC current (i_{FC}) and FC voltage (v_{FC}) and c) Current step test of system compound of SC and FC: load current (i_L), FC current (i_{FC}), SC current (i_{SC}) and voltage (v_{FC}).

SUMMARY AND CONCLUSION

This paper reports on the complete characterization of a PEMFC on static and dynamic regime. With regard to the static regime behaviour, the I-V curves, I-P curves and hydrogen consumption have been obtained for different temperatures. In addition, an analysis of the stack efficiency and the fuel cell efficiency was made for different temperatures. Likewise, the characterization of the FC on a dynamic regime was carried out by means of demanding current, resistance and power steps of the FC and sinusoidal demanding current of different amplitudes and frequencies superimposed to DC current. The methodology implemented made it possible to obtain a deep characterization of the PEMFC performance.

Finally, the integration of the FC and the SC was carried out by means of direct connection of both sub-systems, achieving an improvement in the dynamic behaviour respect to the system comprised only by FC. With the incorporation of the SC, the FC operates in less severe transient conditions and presumably leading to a longer service life.

ACKNOWLEDGEMENTS

We would like to acknowledge the support of the Spanish Ministry of Economy and Competitiveness (grant DPI2010-21671-C02-01) and the Government of Navarre and FEDER funds.

REFERENCES

- [1] Wang Y, Chen K S, Mishler J, Cho S. C, Adroher X C. A review of polymer electrolyte membrane fuel cells: Technology, applications, and needs on fundamental research. *Applied Energy*, 2011; 88(4):981-1007.
- [2] Zhang G, Shen S, Guo L, Hongtan L. Dynamic characteristics of local current densities and temperatures in proton exchange membrane fuel cells during reactant starvations. *Int J Hydrogen Energy* 2012; 37(2):1884-92.
- [3] Taniguchi A, Akita T, Yasuda K, Miyazaki Y. Analysis of degradation in PEMFC caused by cell reversal during air starvation. *Int J Hydrogen Energy* 2008; 33(9):2323-9.
- [4] Thounthong P, Rael S, Davat B. Analysis of supercapacitor as second source based on fuel cell power generation. *IEEE Trans Energy Conversion* 2009; 24(1):247-55.
- [5] Khaligh A, Li Z. Battery, ultracapacitor, fuel cell, and hybrid energy storage systems for electric, hybrid electric, fuel cell, and plug-in hybrid electric vehicles: State of the art *IEEE Trans Vehicular Technol* 2010; 59(6):2806-14.
- [6] Yalcinoz T, Alam M.S. Improved dynamic performance of hybrid PEM fuel cells and ultracapacitors for portable applications. *Int J Hydrogen Energy* 2008; 33(7):1932-40.
- [7] San Martín, I. Ursúa, A. Sanchis, P. Integration of fuel cells and supercapacitors in electrical microgrids: Analysis, modelling and experimental validation. *Int. J Hydrogen Energy* 2013; 38:11655-71.

Nanosized Fe-doped ceria samples synthesized by freeze-drying precursor method (P-300)

Mariano O. Mazan¹, Jassiel Marrero-Jerez², Pedro Núñez², Susana A. Larrondo^{1,3}

1: Departamento de Ingeniería Química, Facultad de Ingeniería Universidad de Buenos Aires. Pabellón de Industrias, Ciudad Universitaria, (1428) Buenos Aires Argentina

2: Departamento de Química Inorgánica, Universidad de La Laguna, E-38200 La Laguna, Tenerife, Spain.

3: Centro de Investigaciones en Sólidos CINSO-UNIDEF-CONICET, J.B. de La Salle 4397, 1603 Pcia. Buenos Aires, Argentina.

INTRODUCTION

Solid-oxide fuel cells (SOFCs) are promising candidates for stationary power generation due to the possibility of using syngas obtained from fossil fuels or biogas. Nowadays, the investigations are concern about the reduction of the operating temperature to the intermediate temperature range (500-700°C) in order to make this technology economically feasible. Reducing the operating temperature reduces the kinetics of the processes that occur at the interfaces gas/electrode increasing the associated polarization resistance. In this context, the use of nanomaterials is entirely feasible. These materials have special properties associated with the greatest contribution of the surface where it is possible to accommodate large number of defects, which can be beneficial increasing the electrochemical performance, either lowering the polarization resistance of the anode or by providing new active sites conferring resistance to coke formation, sulfur poisoning, etc.

Many materials have been tested as anodes with different structures (spinel, pyrochlore, perovskite, etc.). However, CeO₂-based materials with fluorite structure appear to be the most promising because the resistance to coke formation, their ability to oxidize the carbon that may be formed in reactions with hydrocarbons [1-4]. Despite the good characteristics mentioned, these materials have poor electronic conductivity and mechanical stability. Doping with aliovalent cations with higher ionic radius, like Gd³⁺ and with isovalent cations with lower ionic radius, like Zr⁴⁺, has been intensively studied. Therefore, it is interesting to study the effect of doping with an aliovalent cation like Fe³⁺, with a lower ionic radius, on the physicochemical properties with the objective to develop ceria-based materials with structural and redox properties appropriated for electrocatalytic application.

In this work the synthesis of nanosized Ce_{1-x}Fe_xO_{2- $\frac{x}{2}$} mixed oxides, with x = 0, 0.1 and 0.2, by the freeze-drying precursor method, as a potential electrode material for IT-SOFCs, is presented. The so-obtained solids were characterized by Scanning Electron Microscopy (SEM) with Energy Dispersive X-ray Spectroscopy (EDS), X-Ray Diffraction (XRD), Physisorption of Nitrogen at its normal boiling point (77 K) Temperature Programmed reduction (TPR) with hydrogen and electrocatalytic studies in different atmospheres using the Electrochemical Impedance Spectroscopy technique (EIS). The influence of the iron content in the physicochemical and electrical properties of the synthesized samples is studied.

EXPERIMENTAL

The precursors were synthesized by the freeze-drying method. The required amounts of Ce (NO₃)₃·6H₂O (Sigma-Aldrich, 99.99%) and Fe(NO₃)₃·9H₂O (Sigma -Aldrich, 99.99%) to obtain the desired stoichiometry and EDTA (Sigma-Aldrich 99.4 %) as complexing agent in the appropriate amount to get a 1:1 ligand to cation molar ratio were dissolved in distilled water. The pH of the solution, initially acid, was adjusted to 7-8 by adding aqueous ammonia. Droplets of the as-obtained solution were subsequently flash-frozen by pouring them into liquid nitrogen, retaining the cation homogeneous distribution of the original solution. Afterwards, the system is freeze-dried in a HetoLyolab freeze-dryer for 3 days. The obtained highly hygroscopic amorphous precursor was immediately pre-calcined at 350°C for 2 hours to prevent rehydration and to eliminate the organic matter by combustion.

SEM micrographies and EDS spectra were obtained with a Jeol JSM-6300, with acceleration potential in the 3-30 KV range, with LaB6 filament and 3nm resolution.

XRD experiments were collected with a PANalytical X'Pert Pro automated diffractometer, equipped with a primary monochromator Cu K α 1 radiation and the X'Celerator detector. The scans were performed within the 2 θ range 10–120° with a 0.02° step size.

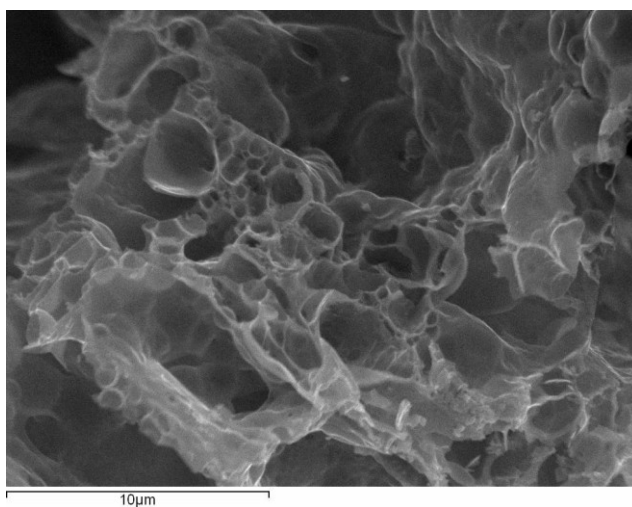


Figure 1. Ce_{0.9}Fe_{0.1}O_{2-d} SEM Micrographie

Specific surface areas were determined by the BET method using the N₂ adsorption isotherm, at (-196°C) in a Micromeritics Gemini 2365.

TPR profiles were obtained with a Micromeritics Autochem 2920 equipment, with a 5mol% H₂-Argon balance mixture, using a flow rate of 50 mL(STP).min⁻¹ and temperature ramp rate of 10°C.min⁻¹.

EIS measurements were carried out with a Solartron 1260 frequency response analyser, with 50 mV of AC perturbation, in the 1 MHz to 0.01 Hz frequency range. The impedance spectra were collected in air and 5mol%H₂ (Ar balance) flows, at isothermal conditions, beginning at 800°C and cooling down to 550°C in 50°C steps.

RESULTS AND CONCLUSIONS

In Figure 1 the SEM micrographie of sample Ce_{0.9}Fe_{0.1}O_{2-d} is presented. It is possible to observe that the sample has high porosity. The same characteristic was observed for the other two samples. Then, the synthesis process produces samples with high porosity, appropriate to catalysis applications. The EDS results indicated Fe to Ce atomic ratios compatible with the nominal composition of the samples.

XRD patterns showed only the main peaks corresponding to the ceria fluorite structure with no peaks corresponding to secondary phases. Besides, a reduction in cell parameter is observed. Therefore, it is possible to consider that iron was incorporated in the ceria structure. Nevertheless, further experiments should be performed in order to study the possibility of having an amorphous Fe₂O₃ phase over the ceria structure. The diffraction peaks are wide as an indication of nanometric crystallite sizes. In Table 1 results of BET and TPR characterization techniques are summarized.

Table 1. BET and TPR results

Sample	S_{BET} (m ² .g ⁻¹)	$D_p=6.(\rho.S_{\text{BET}})^{-1}$ (nm)	TPR (reduction %)
CeO ₂	20	42	34
Ce _{0.9} Fe _{0.1} O _{2-d}	38	23	55
Ce _{0.8} Fe _{0.2} O _{2-d}	40	22	62

The BET specific surface area increases with the increment in the iron content. Considering spherical particles it is possible to estimate particle sizes from BET results (D_p in Table 1) being the values obtained below 50nm. The reduction percentage of the sample increases with the increment in iron content indicating a better reducibility. Besides, the TPR peak corresponding to bulk Ce⁴⁺ moved to higher temperature consistent with the presence of an aliovalent cation (Fe³⁺). Influence of the iron content on polarization resistance was also observed. The synthesized solids possess structural, redox and electrochemical properties that make them potential candidates as electrode material for IT-SOFCs.

ACKNOWLEDGEMENTS

Mr. Mazan and Mrs. Larrondo gratefully acknowledge the financial support by Vicerrectorados de Internacionalización y de Investigación de la Universidad de La Laguna 2013, respectively. Mr. Mazan PhD scholarship granted by Fundación Peruilh, Facultad de Ingeniería, Universidad de Buenos Aires is also acknowledged.

The research work was supported by the financial contribution of projects MAT2010-16007 MINECO, Spain (Cofounded FEDER) and PIDDEF 2011-2013 N° 011/11, MINDEF, Argentine.

REFERENCES

[1] Ch. Chatzichristodoulou, P.T. Blennow, M. Sjøgaard, P.V. Hendriksen, M.B. Mogensen, Chapter 12 “Cerium and its use in Solid Oxide Cells and Oxygen Membranes” in “Catalysis by Cerium and Related Materials 2nd. Ed.”, A. Trovarelli (Ed.), (2013), 623.

[2] L. Fan, Ch. Wan, M. Chen, B. Zhu J. Power Sources 254 (2013) 154.

[3] A. J. Jacobson, Chem. Mater. 22 (2010) 660

[4] P. Blennow, K.K. Hansen, L.R. Wallenberg, M. Mogensen, Solid State Ionics 180 (2009) 63.

Development of simple method for measuring quantity of hydrogen permeation through thick metals using sensor gas chromatograph (P-301)

Ryosuke KUMAGAI¹, Ryusei ISHIDA¹, Kan'ei SHINZATO¹, Naoya SAKODA¹, Masamichi KOHNO^{1,2}, Yasuyuki TAKATA^{1,2}

¹Dept. of Mech. Eng., Kyushu Univ., 744 Motoooka, Nishi-ku, Fukuoka 819-0395, Japan

²International Institute for Carbon-Neutral Energy Research (I2CNER), Kyushu Univ., 744 Motoooka, Nishi-ku, Fukuoka 819-0395, Japan

Pressure decrease in the metal vessel which enclosed hydrogen is observed on measurements of PVT property of hydrogen at temperatures over 300 °C. But pressure decrease in the metal vessel which enclosed helium or nitrogen is not observed. It is seemed that hydrogen permeates into the wall of the metal vessel. The accurate measurements of the quantity of hydrogen permeation are important for safety used of high temperature hydrogen. For measurements of quantity of hydrogen permeation, an experimental apparatus has been developed. Fig. 1 shows schematic flow-chart of the experimental apparatus. The main components of the experimental apparatus consist of a measurement vessel, a detection vessel, an electric heater, a gas chromatograph and an internal pressure vessel. The measurement vessel is made of SUS316L which has a coiled shape, the inner diameter of 4.3 mm, the thickness of 1.0 mm and the length of 2.32 m. The measurement vessel is contained by the detection vessel which has the inner diameter of 50 mm, the thickness of 2.5 mm and the length of 128 mm. In addition to the main components of the experimental apparatus, there are some ancillary components that consist of feed charging and discharging of hydrogen gas, mass flow meter, thermal couple, pressure sensor, PC for recording experiment data. To improve the accuracy of the measurement, highly precise mass flow meter is used for measuring the flow rate of carrier gas. The mass flow meter can measure flow rate up to 5 liters per minutes. The measurement vessel which enclosed hydrogen is heated with an electric heater, and hydrogen permeates into the detection vessel. Permeated hydrogen is carried to the gas chromatograph by carrier gas. Carrier gas is nitrogen and heated with an electric heater in order not to lower temperature in the measurement vessel before flowing into the detection vessel. The gas chromatograph is measurable every five minutes, then measurement time is shorter than the general gas chromatograph. The general gas chromatograph measures using peak area, but the gas chromatograph that is used by this measurement measures using peak height. Therefore, it can reduce the influence of interference gas and noise. It uses the semiconductor as a detector. When hydrogen gas adheres to the surface of the semiconductor, the electrical resistance of the semiconductor changes. By using the change, the gas chromatograph can measure hydrogen concentration. Before measuring, calibration of the gas chromatograph using the standard gas is carried out to improve accuracy of measurement. Quantity of hydrogen permeation is expressed by multiplication of flow rate of carrier gas and hydrogen concentration. If hydrogen which permeates into the detection vessel is mixed enough by carrier gas, quantity of hydrogen permeation should maintain the same regardless of carrier gas flow rate. So, carrier gas of enough quantity to mix hydrogen which permeates into the detection vessel is necessary. Quantity of hydrogen permeation was measured under conditions of pressure up to 0.72 MPa and temperature from 573 K to 773 K. The permeability obtained is compared in Fig. 2 with reported values and shows similar tendency.

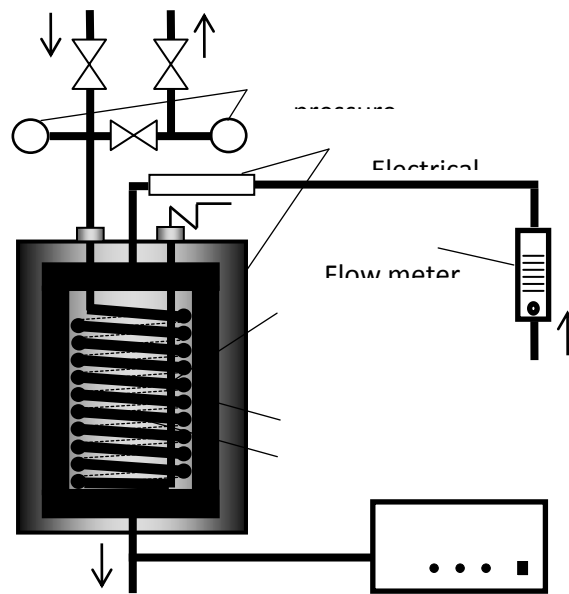


Fig. 1. Schematic flow-chart of the experimental setup

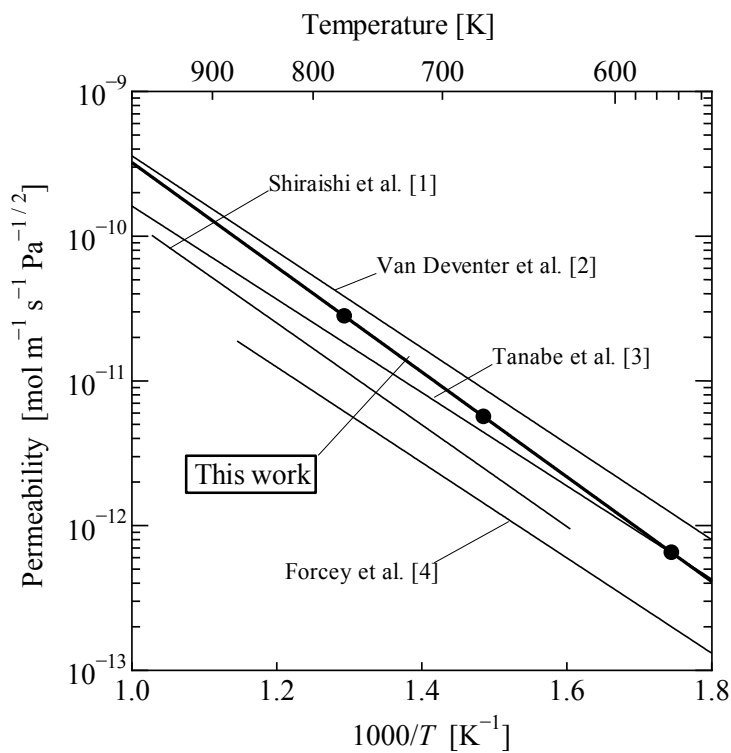


Fig. 2. Temperature dependence of hydrogen permeability through SUS316L

REFERENCES

- [1] T.Shiraishi, M.Nishikawa, T.Yamaguchi, K.Konmotsu, J.Nucl.Mater. 273 (1999) pp.60-65
- [2] E.H. Van Deventer, V.A. Maroni, J.Nucl.Mater. 92 (1980) pp.103-111

- [3] T.Tanabe, Y.Yamanishi, K.Sawada, S.Imoto, J.Nucl.Mater. 122&123 (1984) pp.1568-1572
- [4] K.S. Forcey, D.K. Ross, J.C.B Simpson, J.Nucl.Mater. 160 (1988) pp.117-124

Air-breathing pem fuel cell system for golf cart (P-305)

**E.H.Majlan, R.E.Rosli, S.A.A.Hamid, Dedi Rohendi, W.R.W.Daud, J.Sahari*

Fuel Cell Institute, Universiti Kebangsaan Malaysia, 43600 UKM Bangi, Selangor, Malaysia

**Email: edy@ukm.my Tel: +60389217078/6038 Fax: ±60389216024*

Today, the world needs a more reliable power source, and the fuel cell is one of the candidates for an alternative energy source based on its specific characteristics. The fuel cell is light in weight, offers fuel flexibility, and has the ability to provide energy to a range of diverse applications. In this paper, the development, manufacturing and assembly of the PEMFC as a power generator for golf cart. The fuel cell (FC) stack was manufactured in-house, and the supercapacitor (SC) was sourced from Maxwell™. The power management of the hybrid power and reactant control system for the fuel cell is performed using a LabVIEW™ program and applied using NI devices. The FC in this system serves as the primary power source to satisfy the load and to charge the SC. In contrast, the SC acts as the auxiliary power source to supply any load amount that exceeds the capability of the FC. This power management system contains two components, one of which is the controller circuit unit and the other is the power controller device. These two components are related to one another through the controller circuit, which carries out the power management strategy programmed in the power controller device.

Two stacks are built, each with 40 cells consisting of end plates, current collectors, bipolar plates, a gas diffusion layer, membrane electrode assemblies (MEA), and sealants sandwiched together. Bipolar plates are used instead of single plates in this stack to reduce the overall size. The unit is engraved using a computer numerical control (CNC) machine. Two stacks are connected in series to obtain a higher voltage value. The gas flow pattern and size of the bipolar plate (anode and cathode) are designed to produce an output power of 5 kW at a 48 Vdc net voltage. The stack is designed based on a fuel cell open system with an air-cooling system. For the anode side, the flow shape is constructed with a serpentine flow, but for cathode, a straight flow is engraved. The size of both plates is 30 cm in length and 11 cm in width with a plate area of 330 cm². The plate is built using a mixture of graphite and carbon materials.

As the heart of the fuel cell, the MEA consists of two electrodes (anode and cathode) and an electrolyte membrane. The electrode consists of a gas diffusion layer (GDL) and a catalyst layer (CL). The GDL material is made of Teflonized carbon paper P75T CPS (Ballard, USA) used as a backing layer (macro-porous layer) and a micro-porous layer (MPL) made from carbon black Vulcan-XC72 (Cabot, USA), a polytetrafluoroethylene (PTFE) solution (60 wt%, DuPont, USA), isopropyl alcohol (IPA) (Sigma-Aldrich USA) and ammonium bicarbonate (Sigma-Aldrich USA). The main ingredient of the catalyst layer is the Pt/C catalyst (20 wt%, PMC, USA) with 0.7 mg cm⁻² loading in the anode and cathode and a Nafion solution (5 wt%, DuPont, USA). A Nafion NR 212 (DuPont, USA) was used as the membrane. The resulting thickness of each MEA was approximately 0.23 mm, and Figure 1 shows an example of a stack as built.

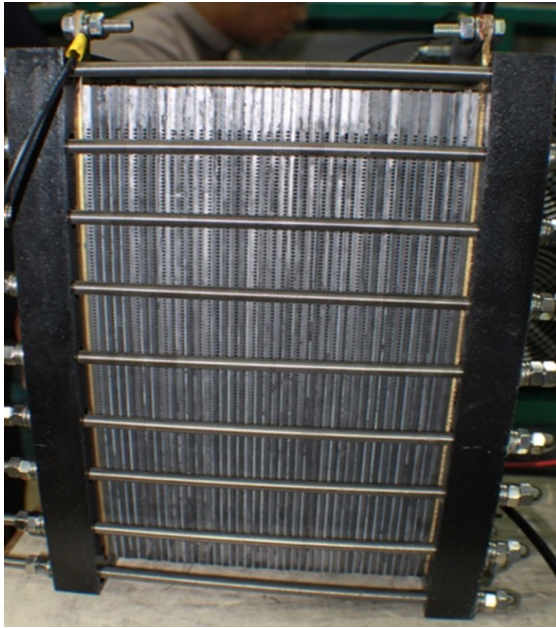


Figure 1. The Air-Breathing PEM fuel cell

As shown in Figure 2, the fuel management system is designed with the controller to prevent the occurrence of unsatisfactory fuel supply that will limit the ability of the fuel cell to deliver the power amount requested from the load.

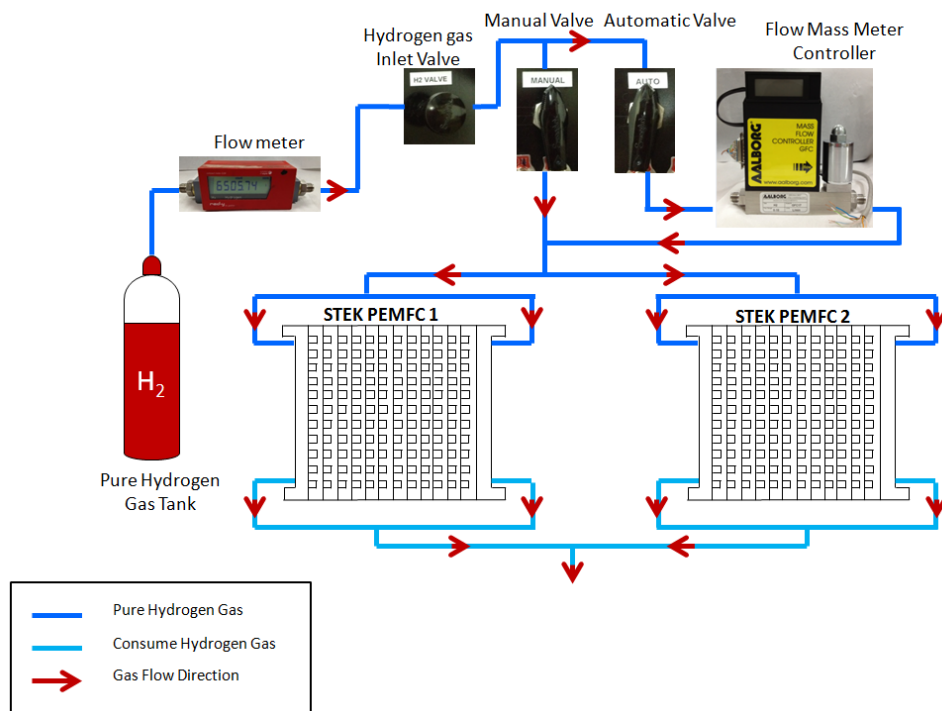


Figure 2. Flow diagram of the reactant controller for the PEM fuel cell stack

The reactant controller focuses on the flow rate of the hydrogen supply for adjustment according to the requested load power to meet the requirements of the reaction and reduce excess waste to the atmosphere. The power management controller manages the power flow of the FC and SC to meet the load demand. The controller programs operated successfully and satisfied the required load. The use of a PEMFC and supercapacitor in a hybrid vehicle appears to be an environmentally safe and sustainable option that can overcome the problem of environment pollution released by ICE vehicles.

A study on degradation of high-temperature PEMFC (P-308)

here Gisu Jeong, MinJoong Kim, Sung Jong Yoo, Jong Hyun Jang, Hyoung-Juhn Kim, EunAe Cho*

Fuel Cell Research Center, Korea Institute of Science and Technogloty
39-1 Hawolgok-dong Sungbuk-gu Seoul South Korea 136-791

Lifetime is one of the crucial issues for commercialization of high temperature-polymer electrolyte membrane fuel cells (HT-PEMFCs). As a frontier combined heat and power (CHP) generation system, low temperature- (LT-) PEMFC by Panasonic exhibits 39 % in electrical and 95 % in total efficiency with lifetime of 60,000 h. Although HT-PEMFC has various advantages over LT-PEMFC, such as system compactness and high quality of waste heat, lifespan of HT-PEMFC is much shorter than LT-PEMFC.

Degradation of LT-PEMFC has been extensively studied to develop components and system control technologies for durable LT-PEMFC. However, degradation of HT-PEMFC has not yet been elucidated clearly.

In this study, degradation phenomena of HT-PEMFC were investigated under a constant current condition and a daily start and stop (DSS) operating condition. Degradation of HT-PEMFC was correlated with loss of phosphoric acid from the cell. Based on the results, start and stop procedure was suggested to improve durability of HT-PEMFC.

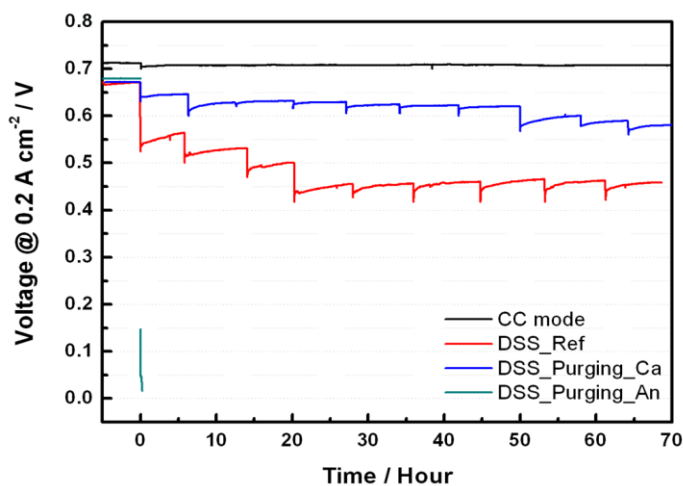


Fig. 1 Long-term stability of HT-PEMFC under a constant current, DSS, DSS with cathode-purging, and DSS with anode-purging at 150 oC.

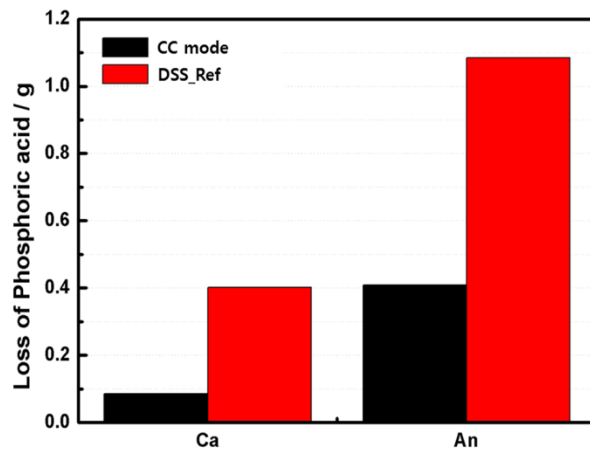


Fig. 2 Loss of phosphoric acid from HT-PEMFC during constant current and DSS operation.

Poisoning intermediates on the ethanol electrooxidation reaction over Pt-based catalysts (P-316)

José L. Gómez de la Fuente, Carlota Cobos, Carlota Domínguez, Francisco J. Pérez-Alonso, M.A. Peña, Sergio Rojas

Grupo de Energía y Química Sostenibles (EQS), Instituto de Catálisis y Petroleoquímica, CSIC, C/ Marie Curie, 2, L10. 28049 Madrid, Spain.

INTRODUCTION

Direct Ethanol Fuel Cells (DEFCs) have emerged as alternative energy transformation devices for portable applications. The main advantages of the use of ethanol as fuel are its easy storage, handling and distribution logistics as well as its high theoretical mass energy. Moreover, ethanol can be obtained from renewable sources and is less toxic than methanol. The complete oxidation of ethanol to CO₂ (in aqueous media) releases 12 e⁻, as compared to 6 e⁻ released by methanol. Alas, under typical reaction conditions of DEFCs (T<80°C, P<5 bar), ethanol is only partially oxidized to acetaldehyde (AAL) and acetic acid (AA), releasing 2 and 4 e⁻, respectively [1]. Pt is the best electrocatalyst for the ethanol oxidation reaction (EOR) in acid media at r.t. However, Pt is rapidly poisoned by adsorbed species coming from the dissociative adsorption of ethanol. Remarkably, the formation of C1 species is observed in the early stages of ethanol electrooxidation on Pt. This observation indicates that Pt is able to break the C–C bond. However, the very formation of such C1 species results in the suppression of the catalytic performance for the EOR. This is because C1 species, typically CH_{x,ad} and CO_{ad}, remain adsorbed at the catalyst surface under the EOR conditions.

The most accepted strategy to improve Pt tolerance to such poison species consists in the addition of a further catalytic function to favor the oxidation of such species. Typically, Pt is modified with oxophilic metals such Ru or Sn, which, by promoting the formation of OH_{ad}, lead to a more facile oxidation of C1_{ad} [2,3]. In this sense, Sn-modified electrocatalysts, in particular Pt₃Sn phase, are the most active electrodes for the EOR. In addition, Ru-modified Pt electrodes are known to improve methanol and ethanol electrooxidation. This study aims to understand the observed promotional effect of Sn for the EOR with Ru-Pt/C catalysts.

EXPERIMENTAL

SnRu-Pt/C was prepared by the polyol method. First, Pt colloids were obtained from H₂PtCl₆ by thermal reduction on a solution of ethylene glycol/NaOH. Afterwards, SnCl₂ and RuCl₃ salts were added and reduced with NaBH₄ at 60 °C. Metal particles were deposited on carbon black support, washed thoroughly by centrifugation and filtered with ethanol and hot water and dried overnight at 70 °C. Commercially available catalysts, 20wt.% Pt/C (Etek) and 30wt.% PtRu/C (Johnson Matthey, JM) were used for comparison.

Aliquots of the as prepared SnRu-Pt/C were subjected to a thermal treatment under an H₂/Ar at 300°C (ramp 10°C/min) and labeled as H-SnRu-Pt/C. All samples were characterized by TGA, XRD, TEM and SEM-EDS. The performance for the electrooxidation of CO_{ad}, ethanol and AAL was

evaluated by means of electrochemical tests in a three electrode cell using Ar purged 0.1M HClO₄ as electrolyte.

RESULTS AND DISCUSSION

The total metallic content of both SnRu-Pt/C and H-SnRu-Pt/C samples is of 24wt.% as determined by TGA. The atomic ratios obtained by SEM-EDS are of 1.9 : 1.8 : 1.0 for Pt : Ru : Sn. TEM images reveal a very high metallic dispersion over carbon, with an average particle size of 2.3 nm on the fresh sample. The mean particle size of H-SnRu-Pt/C is of 4.4 nm i.e, it agglomerates after thermal treatment in H₂. Moreover, the surface of H-SnRu-Pt/C is enriched in Sn as revealed by XPS.

The performance of the catalysts for the electrooxidation of CO_{ad} was evaluated by adsorbing CO onto the electrodes from CO-saturated electrolytes at 0.05 V during 15 min. After purging non-adsorbed CO, 3 consecutive cyclic voltammograms were recorded between 0-1 V at 10 mV/s. A broad CO_{ad} oxidation wave is recorded in the forward cycle of the first voltammogram for all catalysts. The onset potential for CO oxidation follows the order H-SnRu-Pt/C < SnRu-Pt/C < 30wt.% PtRu/C (JM) << 20wt.% Pt/C (Etek). Clearly, the electrodes containing Sn are the more CO tolerant catalysts in the series. In addition, the improved CO tolerance of the H-treated catalyst probably accounts to particle size effects. The EOR was studied by recording the variation of the intensity response (normalized to the amount of Pt on the electrodes, iM) with time at selected potentials. In addition the performance of the electrodes for the electrooxidation of AAL was also evaluated.

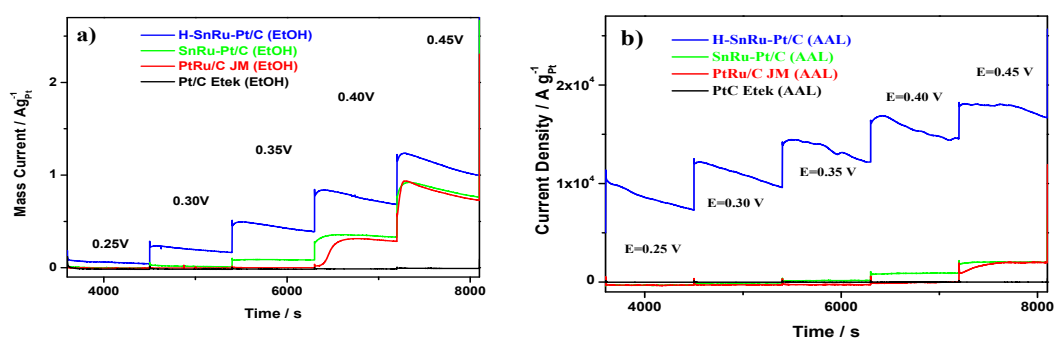


Figure 1. Chronoamperograms for Pt/C (Etek), PtRu/C (JM), RuSn-Pt/C and H-RuSn-Pt/C recorded at selected potentials in: (a) 0.2M EtOH/0.1M HClO₄; (b) 0.2M AAL/ 0.1M HClO₄.

As shown in Figure 1a, the Sn-containing electrodes, especially H-SnRu-Pt/C record the highest iM for the EOR for all potentials studied. This effect is even more evident at low E values which are the desired working potentials of anode electrodes of DEFCs. As stated above, AAL and AA are the major products of the EOR in acid medium. Therefore, in order to understand the superior performance of the Sn-containing electrodes the electrooxidation of AAL has been evaluated. Figure 1b shows the variation of the iM with time during the electrooxidation of AAL at selected potentials. Remarkably, only H-SnRu-Pt/C records visible activity for the AAL electrooxidation at all studied potentials, and in fact, the performance for the AAL oxidation of the rest of the catalysts is almost negligible and only residual oxidation currents are recorded at E > 400 mV for SnRu-Pt/C and at E > 450 mV for PtRu/C (JM). Taking into account that CO_{ad} oxidation on both Sn-containing electrodes is rather similar the

superior performance of H-SnRu-Pt/C cannot be merely ascribed to a higher CO_{ad} tolerance. This work shows that the ability for the oxidation of AAL can be directly related with the performance for the EOR. This in turn is a clear indication that AAL is produced during EOR and that AAL oxidation is a key step in the overall EOR.

Acknowledgements

Financial support from the Spanish Ministry of Science and Innovation under project ENE-2012-15381 is acknowledged.

1 Wang, H., Jusys, Z., Behm, R. J. J. Appl. Electrochem. 36 (2006) 1187-1198

2 Borbath, I., Gubán, D., Pászti, I. E. et al. Top. Catal. 56 (2013) 1033-1046

3 Beyhan, S.; Coutanceau, C.; Leger, J.-M.; Napporn T. W.; Kadirgan, F. Int. J. Hydrogen Energy 38 (13) 6830-6841

Numerical predictions and experimental validation of DEFC performance: AEM vs. PEM (P-322)

Andreas Podias and Panagiotis Tsiakaras

*Laboratory of Alternative Energy Conversion Systems,
Department of Mechanical Engineering,
University of Thessaly, Pedion Areos, 38334 Volos, Greece*

INTRODUCTION

Alkaline anion-exchange membranes (AEMs) conduct hydroxyl ions (OH^-) and represent the high pH equivalent to proton-exchange membranes (PEMs) employed in the acidic-type PEM fuel cells. AEM-based direct ethanol fuel cells (DEFCs) exhibit several advantages over the PEM-based ones, such as:

- (i) faster oxygen reduction reaction (ORR), thus introducing lower activation overpotentials;
- (ii) non-precious metal catalysts can be used effectively;

(iii) a potentially simplified water management, which is necessary to avoid either cathode flooding (high water crossover) or a high cathode activation loss (too low water crossover) is the case in AEM-based DEFCs (water is produced at the anode and consumed at the cathode); and

(iv) fuel crossover within the membrane is less severe in AEM-based DEFCs, because it takes place in the opposite way to the OH^- transport (cf. fig. 1).

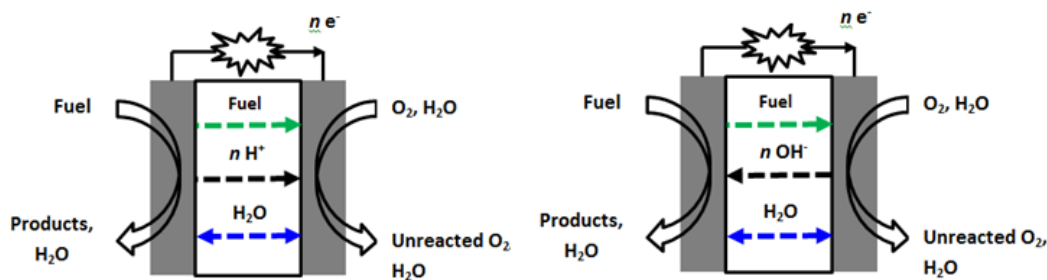


Figure 1. Schematic of the PEM-based (left) and AEM-based (right) DEFC

The present work focuses on modelling and simulating the performance of a DEFC considering the effect of water and ethanol crossover (cf. fig. 1) through the polymeric membrane. The predictions are verified against experimental single cell performance data for different low- and non-Pt anode catalysts.

PERFORMANCE PREDICTIONS vs. EXPERIMENTS

AEM-based polymer electrolyte fuel cells have been attracting attention worldwide, mainly due to the prospect of using Pt-free electrocatalysts. Recent progress and polarisation performance characteristics, such as, maximum area-, and mass-specific power densities, for PEM- and AEM-type DEFCs is critically reviewed in [1].

A significant drawback of the DEFC performance is the alcohol crossover via the membrane (either PEM, or AEM); crossover, adversely affects fuel efficiency (i.e., energy density) due to the wasteful oxidation on the cathode side leading to a mixed potential formation [2, 3]. However, in an AEM-type DEFC the direction of the electro-osmotic drag is from the cathode to the anode, which can reduce the rate of fuel crossover from the anode to cathode, improving the cell performance.

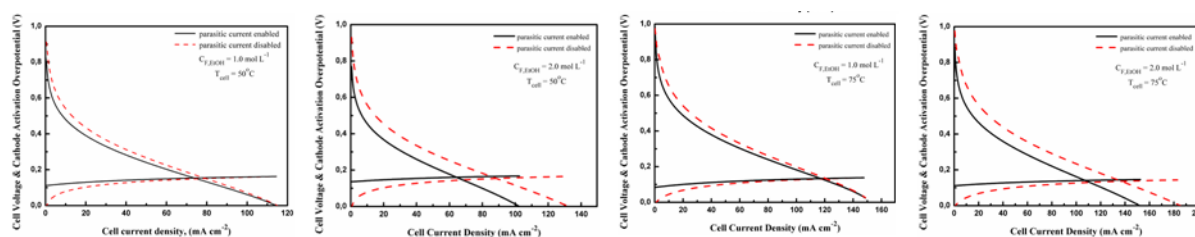


Figure 2. Effect of ethanol crossover on cathode overpotential and cell voltage of a PEM-type DEFC

The effect of ethanol crossover on cathode overpotential and cell voltage is predicted numerically (cf. fig. 2) for different ethanol feed concentrations and operation temperatures. Ethanol crossover gives rise to a parasitic current (j_{cross} or j_{leak} ; see e.g. [2, 3]). The net effect of this parasitic current loss is to offset the DEFC's operating current by an amount given by j_{cross} . This has a significant effect on the open circuit voltage (OCV) of the DEFC: OCV reduction below its thermodynamically-predicted value. The gross current produced at the DEFC electrodes then reads:

$$j_{\text{gross}} = j + j_{\text{cross}}.$$

Here, j is the actual DEFC operating current that we can measure and use. The activation, η_{act} , and concentration η_{conc} , overpotentials, are based on j_{gross} since the reaction kinetics and species concentrations are affected by the crossover current. The ohmic, η_{ohmic} , overpotential, should be based, however, on j , since only the operating current of the DEFC is actually conducted through the cell.

CONCLUSION

Alcohol crossover via the membrane (either PEM, or AEM) represents a significant drawback in terms of performance. Enhancing the anode alcohol electrooxidation rate is an important target towards reduction of the alcohol crossover rate. The higher reactivity of polycarbon alcohols, such as ethanol, in alkaline media as compared to acidic media, renders them potential candidates for fuelling AEM-based DEFCs for portable devices, yet breaking of the C-C bonds present in polycarbon alcohols is still an active research objective.

REFERENCES

Brouzgou A, Podias A, Tsiakaras P, PEMFCs and AEMFCs directly fed with ethanol: a current status comparative review, *Journal of Applied Electrochemistry*, Volume 43, 2013, 119-136.

Andreadis G, Podias A, Tsiakaras P. The effect of the parasitic current on the direct ethanol PEM fuel cell operation, *Journal of Power Sources*, Volume 181(2), 2008, 214-227.

Andreadis G, Podias A, Tsiakaras P. A model based parametric analysis of a direct ethanol polymer electrolyte membrane fuel cell performance, *Journal of Power Sources*, Volume 194(1), 2009, 397-407.

ACKNOWLEDGMENT

The work is partially supported by the “Bilateral R&D Co-operation between Greece-China 2012-2014”, which is co-financed by the European Union and the Greek Ministry of Education-GSRT.

Hybrid Chitosan-Carbon as New Electrocatalyst Support for Direct Methanol Fuel Cells (P-325)

B. Aghabarari^{1,2}, G. García^{1,3}, M. Ghiaci⁴, M.A. Peña¹ and M.V. Martínez-Huerta¹

1 Instituto de Catálisis y Petroleoquímica. CSIC. C/Marie Curie 2. 28049 Madrid, Spain.

2 Nano Material Division, Materials and Energy Research Center, P.O. Box: 14155-4777, Tehran, IRAN

3 Departamento de Química Física. Universidad de La Laguna. c/ Astrofísico F. Sánchez. 38071- La Laguna, Tenerife, Spain.

4 Department of Chemistry, Isfahan University of Technology, Isfahan, 8415683111, Iran

Fuel cells with methanol (CH₃OH) in the form of direct methanol fuel cell (DMFC), using a proton-exchange membrane, are been considered as alternatives to hydrogen [1]. The main advantage of both is that methanol is a liquid fuel, and the storage problems when hydrogen is used are solved, since their power density in terms of energy by volume of fuel at normal conditions is much higher. However, along with the rapid DMFCs' development, a series of challenging problems have emerged such as low alcohol electrooxidation kinetics. Therefore, the success of the DMFCs largely depends on the electrocatalysts. Based on the present development status of the electrocatalysts for alcohols oxidation, it is recognized that Pt-based catalysts are the most active anode catalysts for direct alcohol fuel cells. However, current fuel cell technology still suffers from the low Pt utilization, limited mass transport capability and limited electrochemical stability of the carbon-based support in the electrode structure. As a consequence, the development of new hybrid polymer-carbon materials has recently become a major focus for fuel cell applications [2]. Chitosan is a very abundant biopolymer which can be used as a stabilizer of metal particles for the preparation of heterogeneous catalysts [3]. Recently new hybrid chitosan derivative-carbon black was prepared and used as support for Pt nanoparticles. These catalysts improved the activity toward oxygen reduction reaction (ORR), compared with those of commercial Pt/C catalyst. The biopolymer chitosan provided an efficient and sustainable surface nitrogen source associated with the superior performance of the catalysts [4].

In the present work, electrocatalysts based on platinum nanoparticles supported of chitosan derivative-carbon support have been tested for alcohol electrooxidation. The work studies the effect of chitosan derivative presence on the resulting catalyst and the electrocatalytic activity towards CO and methanol oxidation. In order to gain higher nitrogen contents and higher affinity for Pt ions on the chitosan biopolymer, a new compound with a high atomic N/C ratio was incorporated. In the approach used, the chitosan derivative was prepared by a Michael reaction with methyl acrylate followed by an amidation reaction with diethylentriamine to obtain Chitosan- (N-(2-(2-aminoethylamino)ethyl) propanamide). The catalysts were characterized by transmission electron microscopy (TEM), X-Ray diffraction (XRD), inductively coupled plasma atomic emission spectroscopy (ICP-AES) and X-Ray photoelectron spectroscopy (XPS), as well as a number of electrochemical techniques like CO adsorption studies, cyclic voltammetries, current-time curves and in situ FTIR.

Results show a significant effect of the chitosan derivative on the catalytic activity. The catalysts obtained display higher CO tolerant and methanol oxidation than commercial carbon supported platinum catalyst provided by Johnson-Matthey. The in situ FTIRS technique has been employed for the further investigation of the oxidation process of CO and methanol over chitosan based catalysts at a molecule level in order to provide information over the nature of the intermediates and the oxidation products in acid media (0.5 M H₂SO₄). Integrated intensities of the CO₂ band for Pt supported on hybrid chitosan derivative catalyst (Pt.CSD.C.M2) and the commercial monometallic catalyst 20 wt.% Pt/C (JM) are shown in Fig. 1. It was observed higher band intensities at lower potential for Pt.CSD.C.M2 compared with commercial catalyst. This catalytic enhancement is associated to the presence of nitrogen, which may affect the electro-transfer rates and adsorption processes of the electrochemical reactions.

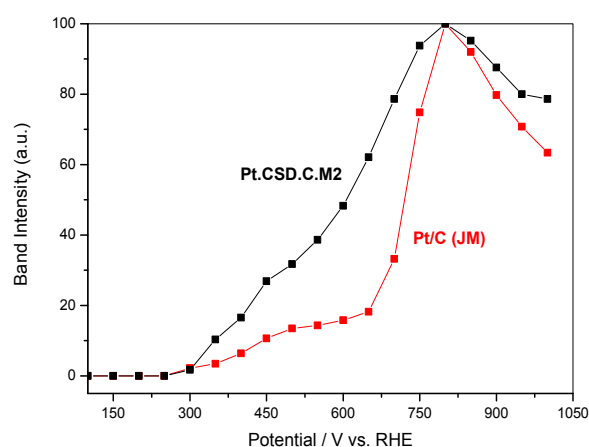


Fig. 1 Integrated intensities of the CO₂ band for Pt supported on hybrid chitosan derivative catalyst (Pt.CSD.C.M2) and the commercial monometallic catalyst 20 wt.% Pt/C (JM).

ACKNOWLEDGEMENTS

This work has been supported by the Spanish Science and Innovation Ministry under projects CTQ2011-28913-C02-02 and ENE2010-15381.

REFERENCES

- [1] Demirci UB. J Power Sources 169 (2007) 239.
- [2] G. Wu, K. L. More, C. M. Johnston, P. Zelenay, Science 332 (2011) 443.
- [3] R. Marguerite Prog Polym Sci 31 (2006) 603
- [4] B. Aghabarari, M.V. Martínez-Huerta, M. Ghiaci, J.L. G. Fierro and M.A. Peña, RSC advances 3(2013) 5378

The Unique Role of CaO in Stabilizing the Pt/Al₂O₃ Catalyst for the Dehydrogenation of Cyclohexane (P-327)

Jiafeng Yu,[a] Qingjie Ge,[a] Jian Zhang,[b] Hengyong Xu,[a,*] Dang Sheng Su[b,*]

[a] Dalian Institute of Chemical Physics, Chinese Academy of Sciences

[b] Institute of Metal Research, Chinese Academy of Sciences

Hydrogen is a clean and reproducible energy carrier, which only emits water, for both transportation and stationary applications. Cycloalkanes are good candidates for hydrogen storage (6–8% on weight basis and 60–62 kgH₂/m³ on volume basis). This kind of liquid hydrocarbons using catalytic reaction pair of dehydrogenation of cycloalkanes and hydrogenation of corresponding aromatics is a promising candidate for long-term storage and long-distance transportation of hydrogen. Moreover, dehydrogenation of hydrocarbons is an attractive alternative for hydrogen production due to its zero carbon oxides (CO_x) emission and low by-products. However, as a source of hydrogen, the liquid hydrocarbons have fallen out of favor because of poor performance. Thus, catalytic systems with high dehydrogenation activity and coke resistance ability are highly desirable. Moreover, coke-induced deactivation is one of the major challenges in the field of heterogeneous catalysis.

Herein, the performance of the Pt/Al₂O₃ catalyst for the hydrogen-free dehydrogenation of cyclohexane was improved by doping with a small amount of Ca. The Ca-modified Pt/Al₂O₃ catalyst exhibited a cyclohexane conversion of 97.0% and maintained a conversion above 75% after 48 h, whilst the unmodified catalyst was deactivated from 87.0 to 2.7% under the same conditions. A mechanistic study on the hydrogen-free dehydrogenation of cyclohexane with a Ca-modified Pt/Al₂O₃ catalyst was investigated.

Characterization techniques, including in situ diffuse reflectance Fourier-transform infrared (in situ DRIFT), X-ray photoelectron spectroscopy (XPS), thermal analysis and temperature-programmed techniques, revealed that the presence of Ca not only decreased the acidity of alumina support, but also changed the location and the type of coke deposition, from active metal to metal/support interface and from hydrogen-lack to hydrogen-rich carbonaceous, respectively. From the results of XPS, the promotion effect of Ca was also associated with neutralizing the residual Cl ions that were bonded onto the Al₂O₃ support as one of the coking sites and reducing the benzene-platinum interactions by electron transfer from Ca to Pt to efficiently recycle the active sites. Electron donation from Ca to Pt would afford both the efficient exposure of the active sites whilst simultaneously suppressing the deep dehydrogenation of H-rich coke into more-conjugated one. Moreover, there were C_xH_y type coke components at the beginning of the reactions on both the promoted- and unpromoted Pt catalysts. But the IntH₂O/IntCO₂ ratio decreased with reaction time on the unpromoted catalyst, while the trend was reversed on the Ca-promoted catalyst. Thus, we concluded that Ca could efficiently suppress the deep dehydrogenation of carbonaceous species to form the H-deficient coke and promote coke desorption by increasing the H/C ratio of H-deficient coke. Therefore, the high activity of the Pt nanoparticles was maintained over a long period of time. According to the result of in-situ DRIFT, Ca promoted the complete dehydrogenation of cyclohexane into benzene and inhibited the formation of coke precursors, which was in agreement with its

superior activity and stability but inferior amount of coke compared to the Pt/Al₂O₃ catalyst. The amount and components of coke that were deposited onto the Ca-modified Pt/Al₂O₃ catalyst remained unchanged throughout the reaction, thereby resulting in improved stability.

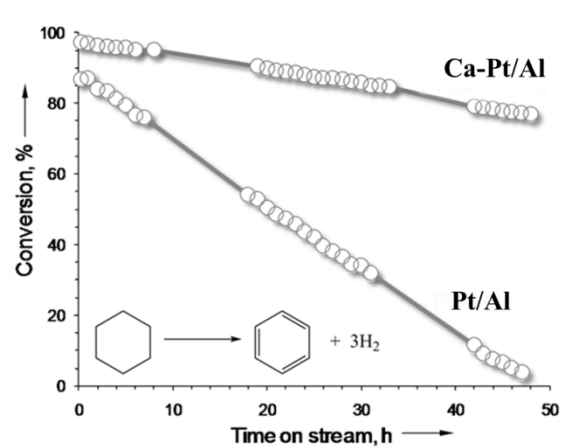


Figure 1. Catalytic activity of the supported Pt nanoparticles in the dehydrogenation of cyclohexane; conditions: 350 °C, 1 atm, catalyst (150 mg), N₂/ C₆H₁₂ (12:1), total GHSV=35000 mL/gcat-1 h⁻¹

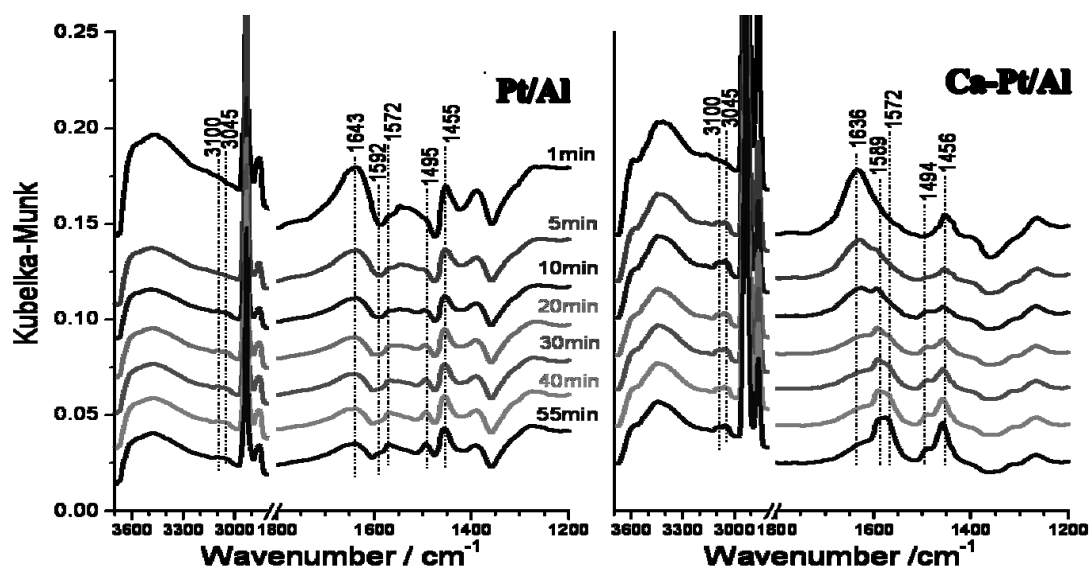


Figure 2. In situ DRIFT spectra of Pt-based catalysts in 5% cyclohexane/He at 350 °C with the time on stream

Photoinduced Hydrogen Production with Photosensitization of Zn Chlorophyll Analog Dimer as a Photosynthetic Special pair Model (P-329)

Masaharu Kondo¹, Shuichi Ishigure², Yuko Maki³, Takehisa Dewa², Mamoru Nango^{2, 4}, and Yutaka Amao⁴

¹ Center for Fostering Young and Innovative Researchers, Nagoya Institute of Technology, Gokiso-cho, Showa-ku, Nagoya, Aichi, Japan 466-8555,

² Materials Science and Engineering, Nagoya Institute of Technology, Gokiso-cho, Showa-ku, Nagoya, Japan, 466-8555,

³ Department of Applied Chemistry, Oita University, Dannoharu 700, Oita 870-1192

⁴ OCARINA, Osaka City University, 3-3-138 Sugimoto, Sumiyoshi-ku, Osaka, Japan 558-8585

In photosynthetic bacteria, bacteriochlorophyll dimer, which is so-called “special pair”, in the reaction centre protein (RC) plays an important role in the initial light reactions of photosynthesis. On the other hand, photoinduced hydrogen production from water, which is an attractive photosynthesis mimetic system, has been studied extensively by means of converting solar energy to chemical energy. Photoinduced hydrogen production systems containing an electron donor, a photosensitizer, an electron mediator, and a hydrogen production catalyst have been widely studied. In this system, the photosensitizer molecule is one of the important factors. Water soluble zinc porphyrins and chlorophylls are used as photosensitizer molecules. However, the photoinduced hydrogen production with the photosensitization of special pair model molecule has not been reported yet. In this study we describe a system for visible light-induced hydrogen production with colloidal platinum, and methylviologen (MV²⁺) photoreduction by the visible light photosensitization of dimer connected Zn pyropheophorbide-a molecules (ZnPyOH) by lysine, ZnPy-K(ZnPy)OH (chemical structure is shown in Figure 1) as a photosynthetic special pair in the presence of NADPH as an electron donor.

ZnPyOH and ZnPy-K(ZnPy)OH were prepared from chlorophyll a with several synthetic reaction steps, pyrolysis, hydrolysis, condensation and metallation. These compounds were characterized by UV-vis. absorption, ¹H-NMR, and MALDI-TOF mass spectroscopies. Colloidal platinum was prepared by refluxing hydrogen hexachloroplatinate (IV) hexahydrate and sodium citrate.

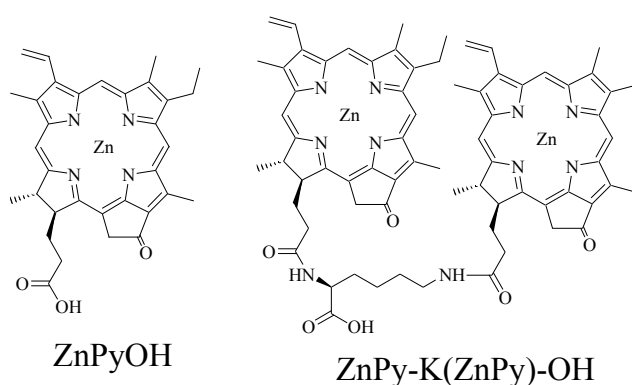


Figure 1. Chemical structures of ZnPyOH and ZnPy-K(ZnPy)-OH

Photoreduction of MV²⁺ is the most important step in photoinduced hydrogen production process. A solution containing ZnPyOH (10 $\mu\text{mol dm}^{-3}$) or ZnPy-K(ZnPy)OH (5.0 $\mu\text{mol dm}^{-3}$), MV²⁺ (2.0 mmol dm^{-3}), and NADPH (2.0 mmol dm^{-3}) in 3.0 mL of 10 mmol dm^{-3} potassium phosphate buffer (pH 7) was deaerated by freeze-pump-thaw cycles repeated 6 times. ZnPyOH and ZnPy-K(ZnPy)OH was dissolved in aqueous solution with 0.1 mmol dm^{-3} cetyltrimethylammonium bromide (CTAB) micellar. The sample solution was irradiated with a 200 W halogen lamp (Philips) at a distance of 3.0 cm with a Sigma 600 cut-off filter at 30 °C. The MV^{•+} concentration was determined by the absorbance at 605 nm using the molar coefficient 13 000 $\text{mol}^{-1} \text{dm}^3 \text{cm}^{-1}$. When the sample solution was irradiated, the accumulation of MV^{•+} was observed with irradiation time (Data not shown). For the system using ZnPyOH, the conversion ratio of MV²⁺ to MV^{•+} was estimated to be 9.0 % after 60 min irradiation. For the system using ZnPy-K(ZnPy)OH, in contrast, the conversion ratio was estimated to be 6.5 %. In both systems, the concentration of Zn pyrochlorophyllide moiety was almost the same. However, the accumulation rate of MV^{•+} in the system using ZnPy-K(ZnPy)OH was lower than that of ZnPyOH system. As the MV²⁺ photoreduction system using ZnPyOH or ZnPy-K(ZnPy)OH was achieved, the development of photoinduced hydrogen production system was attempted. The photoinduced hydrogen production with ZnPyOH or ZnPy-K(ZnPy)OH was carried out as follows. The sample solution containing ZnPyOH (10 $\mu\text{mol dm}^{-3}$) or ZnPy-K(ZnPy)OH (5.0 $\mu\text{mol dm}^{-3}$), MV²⁺ (2.0 mmol dm^{-3}), NADPH (2.0 mmol dm^{-3}) and colloidal platinum (0.5 units) in 3.0 mL of 10 mmol dm^{-3} phosphate buffer (pH = 7.0) was deaerated by freeze pump thaw cycle for 6 times, and substituted by argon gas. The amount of hydrogen evolved was detected by gas chromatography (detector: TCD, column: active carbon, carrier gas: nitrogen). When the sample solution was irradiated, the hydrogen production was observed as shown in Figure 2. By irradiation, hydrogen evolved continuously more than 120 min. After 120 min irradiation, the amount of hydrogen production with the system using ZnPyOH and ZnPy-K(ZnPy)OH were estimated to be c.a. 0.3 and 0.2 μmol , respectively. In MV²⁺ photoreduction and photoinduced hydrogen production, the system using ZnPy-K(ZnPy)OH was lower than that of ZnPyOH system. These reasons are as follows. In ZnPy-K(ZnPy)OH, the photoexcited state of ZnPyOH moiety will be quenched by the other ZnPyOH moiety due to the interaction between ZnPyOH moieties. The activity of photosensitization of ZnPy-K(ZnPy)OH was lower than that of ZnPyOH.

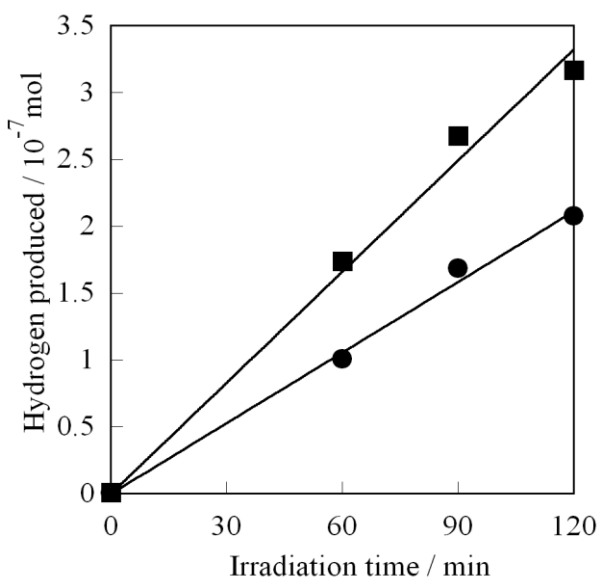


Figure 2. Time dependence of hydrogen production with the system consisting of ZnPyOH (10 $\mu\text{mol dm}^{-3}$) or ZnPy-K(ZnPy)-OH (5.0 $\mu\text{mol dm}^{-3}$), MV²⁺ (2.0 mmol dm^{-3}), NADPH (2.0 mmol dm^{-3}) and colloidal platinum (0.5 units) in 3.0 mL of 10 mmol dm^{-3} phosphate buffer (pH=7.0) under steady state irradiation at 30°C. Square: ZnPyOH, circle: ZnPy-K(ZnPy)-OH

The performance of an ionic liquid functionalized carbon supported Pt-Ru catalyst for pem fuel cells (P-335)

M.A. Esteves, A.I. de Sá, C.M. Rangel,

LNEG, Laboratório Nacional de Engenharia e Geologia,
Estrada do Paço do Lumiar 22, 1649-038 Lisboa, Portugal

Ionic liquid (IL) functionalization of carbon supports has been recognized as an alternative approach to improve the catalyst efficiency in polymer electrolyte membrane (PEM) fuel cells. The addition of an IL functionality by electrostatic or covalent interaction is thought to improve the stability and dispersion of metal nanoparticles such as Pt, Au, Rh, Pd, in the support, leading to better fuel cell performance. In particular, imidazolium-based ILs are favorable because of their air, water and electrochemical stability, wide-liquid range and easy methods of preparation [1].

In this work, the synthesis and the electrochemical behavior of an ionic liquid functionalized carbon supported Pt-Ru core-shell nanocatalyst are investigated regarding the methanol oxidation reaction (MOR) and oxygen reduction reaction (ORR). The new core-shell 10 wt % Ru – 20 wt % Pt-carbon supported catalyst, Ru@Pt/C_IL1 was synthesized by sequential Ru and Pt reduction with ethylene glycol [2] in a IL-functionalized support, C_IL1, previously prepared by covalent attachment of 1-(3-aminopropyl)-3-methylimidazolium bromide to oxidized Vulcan XC-72, Vulcan-COOH [3].

Preliminary characterization of the catalyst was undertaken by scanning electronic microscopy (SEM) and energy dispersive X-ray spectroscopy (EDX). The composition of the catalysts is similar to that of a commercial catalyst (EICHEM) also supported in Vulcan XC-72 with 20 wt % Pt - 10 wt % Ru, referred to as Pt-Ru/C_Com.

The catalyst activity for methanol oxidation reaction (MOR) was evaluated by cyclic voltammetry in acid medium. The catalyst ink was prepared by dissolving 10 mg of the catalysts in a Nafion + isopropanol solution followed by sonication for 30 min. A drop (10 μ L) of the catalyst ink was deposited on glassy carbon rods and dried at 50 $^{\circ}$ C, in order to prepare the electrodes for the voltammetric studies. The catalyst load is 1mg cm⁻². Before testing, the catalysts were previously activated by performing 30 cycles at 0.050 V s⁻¹ from -0.2 to +1 VAg/AgCl sat, in a N₂ saturated H₂SO₄ solution (0.5 M).

The stability of the catalyst was evaluated by potential cycling between -0.2 and +1 V for 350 cycles in 0.5 H₂SO₄ + 1 M CH₃OH (N₂ saturated) at a scan rate of 0.050 V s⁻¹ (Fig.2a). The cyclic voltammograms show that the highest current density for the forward peak (0.067 A cm⁻²) is achieved between the 40th and 50th cycle and after that there is a continuous decrease of the current.

Performance was compared with commercial catalyst, Ru-Pt/C-Com, (see Fig.2b). Voltammograms were obtained in the same experimental conditions. Similar peaks are displayed. A maximum current density of the forward peak (0.072 A cm⁻²) is practically maintained from the 50th to the 100th cycle and after that the decrease is less accentuated than the catalyst under test.

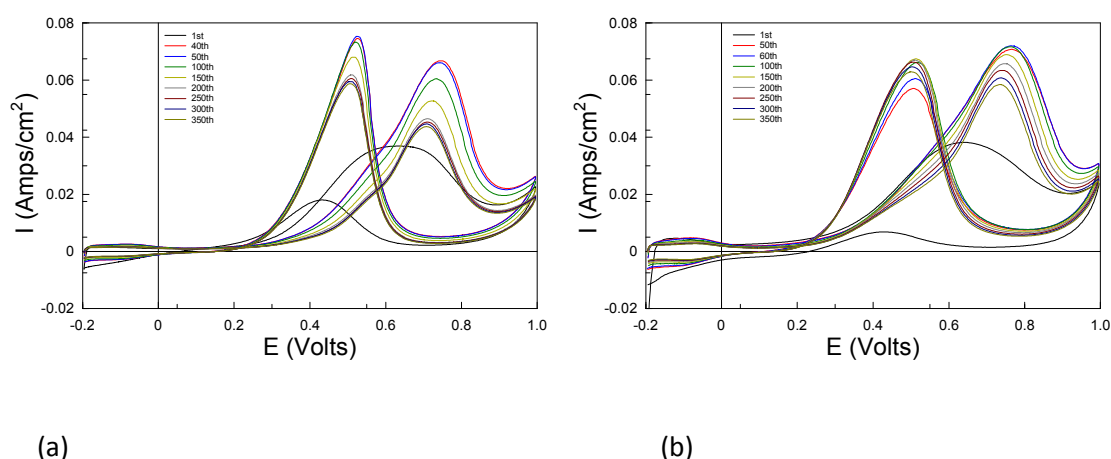


Fig. 2 Cyclic voltammograms obtained for the catalysts Ru@Pt/C_IL1 (a) Ru-Pt/C-Com (b) in 0.5 H₂SO₄ + 1 M CH₃OH at room temperature and a scan rate of 50 mV^s⁻¹.

Preliminary tests were also performed to evaluate the activity of this catalyst for the oxygen reduction reaction (ORR). Linear sweep voltammetry (LSV) was carried out at a sweep-rate of 1 mV^s⁻¹ in 0.5 M H₂SO₄ (O₂ saturated). The Tafel plot shows a linear region (Fig.2) corresponding to a Tafel slope of 0.044 V/dec and exchange current density of 8.51 x10⁻⁹A cm⁻².

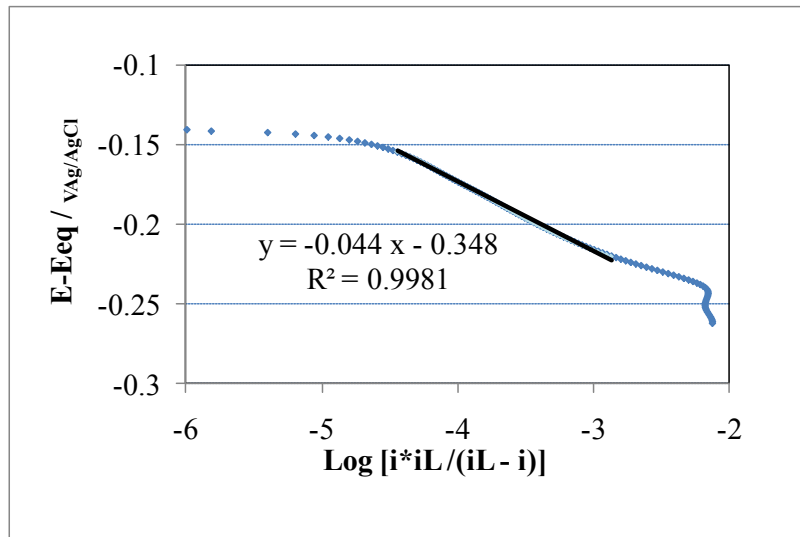


Fig.2 Tafel plot for ORR for the catalyst Ru@Pt/C_IL1 obtained in 0.5 M H₂SO₄ oxygen saturated solution at sweep-rate of 1 mV^s⁻¹ and at room temperature.

TEM studies are being conducted in order to characterize particle size and distribution and the core-shell character of the catalyst.

Acknowledgment

This research is partially funded by the Portuguese Fundação para a Ciência e Tecnologia (FCT), Project PTDC/CTM-ENE/1585/2012.

References

- [1] H. Zhang, H. Cui, *Langmuir*, 25 (2009), 2604-2612.
- [2] C. Li, Z. Shao, M. Pang, C. T. Williams, X. Zhang, C. Liang, *Ind. Eng. Chem. Res.* 51 (2012), 4934-4941.
- [3] Z. Wang, Q. Zhang, D. Kuehner, X. Xu, A. Ivaska, L. Niu, *Carbon*, 46 (2008), 1687-1692.

Temperature and Pressure effects on hydrogen separation from unconverted shift gas mixture using a Palladium Membrane Reactor (P-338)

M. M. Barreiro¹, M. Maroño, J. M. Sánchez

*1CIEMAT, Combustion and Gasification Division, Avenida Complutense, 40, 28040 Madrid, Tlf.
Contact: 0034 91 346 67 01. Spain email: mdelmar.barreiro@ciemat.es;
josemaria.sanchez@ciemat.es*

ABSTRACT:

Temperature and pressure influence on hydrogen permeation through a Pd-based membrane from unconverted shift gas mixture was investigated. The permeation of hydrogen when the catalyst was placed in the outer shell (catalytic membrane reactor CMR) has been compared to the hydrogen permeation for the void reactor case (membrane reactor, MR). Furthermore, the catalytic effect of the Pd layer on the water gas shift reaction (WGS) was also analyzed.

Keywords: Hydrogen, palladium membrane, gas separation, water-gas shift reaction, catalytic effect

INTRODUCTION

The interest toward the Pd membranes and its alloys has been increasing in the last two decades because it is known that this type of membrane is permeable only to hydrogen. This allows their use in those reactive processes that are favored by selective hydrogen removal, e.g. steam re-forming of hydrocarbons, water-gas shift and dehydrogenation reactions, among others [1].

This work examines operating conditions under which hydrogen permeation will take place when a synthetic unconverted shift gas mixture is considered. Those conditions could be subsequently applied to run the shift reaction in a CMR using such a mixture.

EXPERIMENTAL

Permeation experiments were conducted with a semi-commercial supported Pd membrane (O.D. = 2.54 cm; L=15 cm) housed in a single tube and shell membrane reactor from CRI Catalyst Co., U.S. In the bench-scale facility, synthetic gas blends can be prepared and fed, up to 2 Nm³/h, 793 K and 1200 kPa. In order to evaluate the hydrogen permeation behavior and compare with previous Catalytic Membrane Reactor Studies [2], a mixture of H₂/CO₂/CO/H₂O (17/19/7/57) (% v/v) was chosen.

Permeability data were collected at 593; 653 and 723 K, and at 500, 800 and 1000 kPa. The experiments were run at a space velocity (GHSV) of 5539 h⁻¹ for the MR studies and at 16771 h⁻¹ for the CMR studies. The GHSV values were calculated as:

$$\text{GHSVMR} = Q_{\text{feed}} (\text{L/h}) / \text{Annulus volume of the reactor (L)} \quad (\text{eq. 1});$$

$$\text{GHSVCMR} = Q_{\text{feed}} (\text{L/h}) / \text{Volume of the catalyst (L)} \quad (\text{eq. 2}).$$

RESULTS

Figure 1 shows the effect of pressure and temperature on hydrogen permeation for the void reactor case. As can be seen hydrogen permeation increased on increasing pressure, i.e. at higher driving force. An increase of temperature also led to higher permeation.

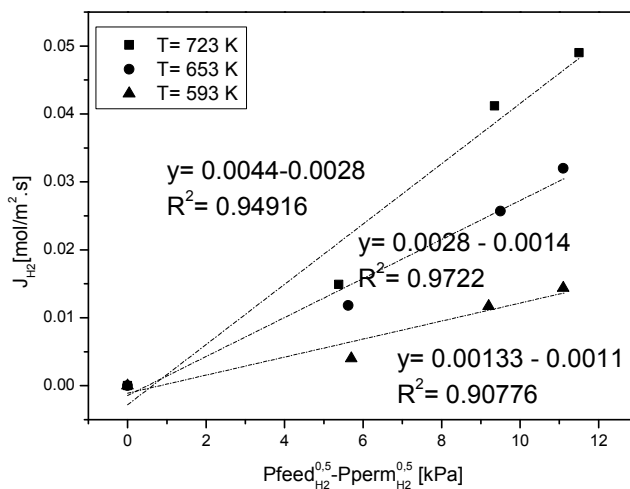


Figure 1 Effect of pressure and temperature on H₂ permeation. Operating conditions: $P_{\text{perm}} = 0$ kPa (rel); F_{feed} (dry gas) = 4.71 L/min; Gas composition (wet basis) = 18% v/v CO, 18% v/v H₂, 7% v/v CO₂; 57% v/v H₂O; GHSVMR = 5539 h⁻¹

It can be seen a slight deviation of the linearity at lower temperature. This behavior might be due to the presence of CO, CO₂, and H₂O which are able to adsorb on the surface of Pd. Due to this fact, those gases can compete with hydrogen for the active sites of the Pd layer producing a reduction of the hydrogen permeation. Moreover, as hydrogen permeates along the membrane length local pressure driving force decreases slightly which may also account for the deviation observed in linearity.

Additionally, in the case of void reactor the hydrogen flux for the full mixture and for pure hydrogen gas at 723, 653 and 593 K was compared. The hydrogen permeation for the mixture was 6.76; 8.31 and 14.36 times smaller than for pure hydrogen, which means that the presence of other gases inhibited heavily hydrogen permeation.

The activation energy and the pre-exponential values for pure hydrogen and for the mixture were determined from Arrhenius and Richardson equation.

For pure hydrogen, the value of activation energy was lower -11.53 kJ/mol- than for the mixture - 33.50 kJ/mol-. The reason is attributed to the fact that the hydrogen molecules find more resistance to pass through the palladium layer when CO, CO₂ and H₂O are present in the gas mixture. This result is also in agreement with our previous result regarding the effect of the pressure above discussed.

Figure 2 compares the hydrogen flux in the case of MR and CMR as a function of the driving force at 593 and 653 K. Permeance values were calculated using a linear regression analysis in accordance with Sievert's law. Although the coefficient of determination, R², was not close to 1, it can be seen that for both temperatures results show a reduction of the permeance on the CMR studies. The inhibition factors to hydrogen permeation were obtained by dividing the values of the permeance of the CMR by the values of the MR case for each temperature. The factors were: 0.29 at 593 K and 0.11 at 653 K. These results suggest that the presence of the catalyst had an unfavourable effect in terms of hydrogen permeation. This effect was more significant at higher temperature than at lower temperature.

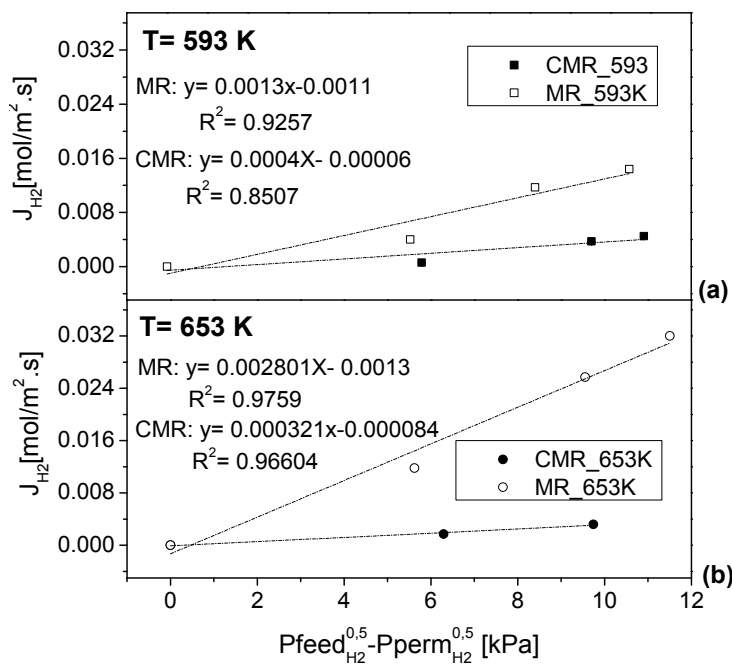


Figure 33 Hydrogen flux through the membrane for runs with catalyst (CMR) and without (MR) (a) 593 K (b) 653 K. Operating conditions: P_{perm} = 0 kPa (rel); F_{feed} (dry gas) = 4.71 L/min; Gas composition (dry basis) = 44% v/v CO, 40% v/v H₂, 16% v/v CO₂; R (H₂O/CO) = 3 mol/mol; GHSV_{CMR} = 16771 h⁻¹

In spite of the advantageous effect of the catalyst to convert the CO in H₂ which would lead to a higher content in the gas and therefore to a higher driving force [2], results shows that for the CMR case, the inhibition to hydrogen permeation created by the presence of the catalyst was stronger than the favourable effect caused by the increase of temperature found in the MR case. Actually, for the CMR case, instead of an increase of permeation on raising temperature, an almost constant value was obtained.

Furthermore, the potential catalytic effect of the Pd layer for the WGSR was studied in the MR case. Results show that the carbon monoxide conversion remained below 3 %. Equilibrium conversion predicted by thermodynamics at that temperature and for that gas composition, would be 12%. Therefore, the palladium layer did not have a significant catalytic activity. Hydrogen permeation did not seem to enhance carbon monoxide conversion either. Similar results can be found in literature. [3-4].

CONCLUSIONS

In the present study, permeation of hydrogen from unconverted shift gas mixture was evaluated. The presence of CO, CO₂ and H₂O reduced the hydrogen permeation and this effect was higher at lower temperature. Moreover, the increase of hydrogen permeation was directly proportional to pressure and temperature. Additionally, the presence of the catalyst had an unfavourable effect in terms of hydrogen permeation. Furthermore, it was found that the palladium layer did not have a significant catalytic activity towards the shift reaction.

REFERENCES

- [1] A. Caravella et. al. J. Phys. Chem. B 114 (2010) 6033-6047
- [2] J. M. Sánchez et. al. Biomass and Bioenergy 35 (2011) S132-S144
- [3] R. Killmeyer, FY 2004 Progress Report, DOE Hydrogen Program
- [4] N. Itoh et. al. Journal of Membrane Science, 66 (1992) 149-155

Renewable hydrogen production from steam reforming of glycerol using Ni-Cu-Mg-Al mixed oxides obtained from hydrotalcite-like compounds (P-340)

Robinson L. Manfro¹ and Mariana M.V.M. Souza^{1,*}

¹School of Chemistry, Federal University of Rio de Janeiro, Centro de Tecnologia, Bloco E, sala 206, Rio de Janeiro/RJ, Brazil. *mmattos@eq.ufrj.br

Introduction

Glycerol is a commodity chemical widely used by the pharmaceutical, personal care, food and cleaning industries. A detailed review on glycerol utilization can be found elsewhere [1]. One possible option for using of glycerol is in hydrogen production. Dumesic group [2,3] was the first to produce hydrogen from biomass-derived oxygenated hydrocarbons, including glycerol, through the aqueous phase reforming (APR). Although the catalyst has provided stability for a long period, the high pressure and low reaction rates have prevented its use as a commercially viable process. On the other hand, the steam reforming process can be performed at atmospheric pressure. The steam reforming is the most efficient technology available, and with greater profitability [4]. It is highly endothermic and should ideally be performed at high temperatures, low pressures, and high steam/glycerol ratios to obtain high conversions [5].

Catalysts based on noble metals have a lower sensitivity to carbon deposition and higher activity. However, commercial reforming catalytic systems are typically based on transition metals, especially Ni because of its low cost and wide availability. Nickel shows a good activity for C–C bond scission [3], and copper, on the other hand, is inactive for C–C bond cleavage but has high activity for the water-gas shift reaction, thus favoring the selectivity to hydrogen [3,6]. Hydrotalcites, a family of anionic clays, are lamellar compounds of aluminum and magnesium hydroxides with interlayer spaces containing exchangeable anions. A partial substitution of Mg²⁺ and/or Al³⁺ by other cations results in materials with isomorphous structures known as hydrotalcite-like compounds (HTLCs) [7]. An exceptional reason that increases the effort for the synthesis of these materials is that thermal decomposition of HTLCs precursors leads to the formation of mixed oxides exhibiting fine dispersion of metal cations and high surface area, compared with those obtained from direct methods as impregnation.

Due to these properties observed in the hydrotalcite-like compounds, Ni and Cu were selected to be included in a catalyst formulation applied to glycerol reforming. The Ni–Cu bimetallic catalysts have been extensively studied in ethanol steam reforming [8,9], showing that CO production and coke deposition are decreased with the addition of copper [8]. The objective of this work is to develop Ni–Cu catalysts derived from hydrotalcite-like compounds with high activity for steam reforming of glycerol, aiming a gas phase rich in hydrogen and low formation of liquid by-products. The effect of the Cu content (0–10 wt%) on the catalytic activity for reforming reaction and hydrogen selectivity was investigated.

Experimental

Three hydrotalcite-like derived catalysts were prepared with 20 wt.% of NiO and 0, 5 and 10 wt.% of CuO (Ni, Ni5Cu and Ni10Cu). The synthesis methodology used was based on Corma et al. [10]. The samples were calcined in flowing air at 500 °C for 3 h. The physical and chemical characterizations of the catalysts as X-ray fluorescence (XRF), X-ray powder diffraction (XRD), textural properties, temperature programmed reduction (TPR), temperature programmed desorption of ammonia (TPD-NH₃), as well as their respective discussion, are presented in Manfro et al. [11]. The catalytic tests were performed at atmospheric pressure in a fixed bed quartz reactor, at 500°C, with gas hourly space velocity (GHSV) of 50,000 h⁻¹. The catalysts were reduced in situ under 30 % H₂-N₂ flow (90 mL min⁻¹) up to 1000 °C for 30 min. The 10 vol.% glycerol aqueous solution was fed to the reactor using a pump and vaporized in He flow in a steel tube. The gas phase was analyzed online by gas chromatograph Shimadzu GC-2014. The liquid phase was analyzed by HPLC Shimadzu Prominence system.

Results and discussion

The glycerol conversion into gas for the three catalysts is presented in Figure 1 (A). The Ni catalyst showed higher values of glycerol conversion into gas (> 95 %) until 25 h, and then presented successive reductions reaching 83 % in 30 h of reaction. The Ni5Cu and Ni10Cu catalysts presented, after a short initial period of stability, a strong deactivation up to 24-26 h, stabilizing the glycerol conversion into gas at 23 % and 15 %, respectively, in the last hours of reaction. Figure 1 (B) shows the H₂ selectivity. Despite the fluctuation in glycerol conversions into gas, the H₂ selectivity remained relatively constant over time for all three catalysts. Analyzing the average H₂ selectivity displayed during 30 h of reaction, it is observed the following order: Ni5Cu > Ni > Ni10Cu (71.1 %, 68.8 %, 63.5 %).

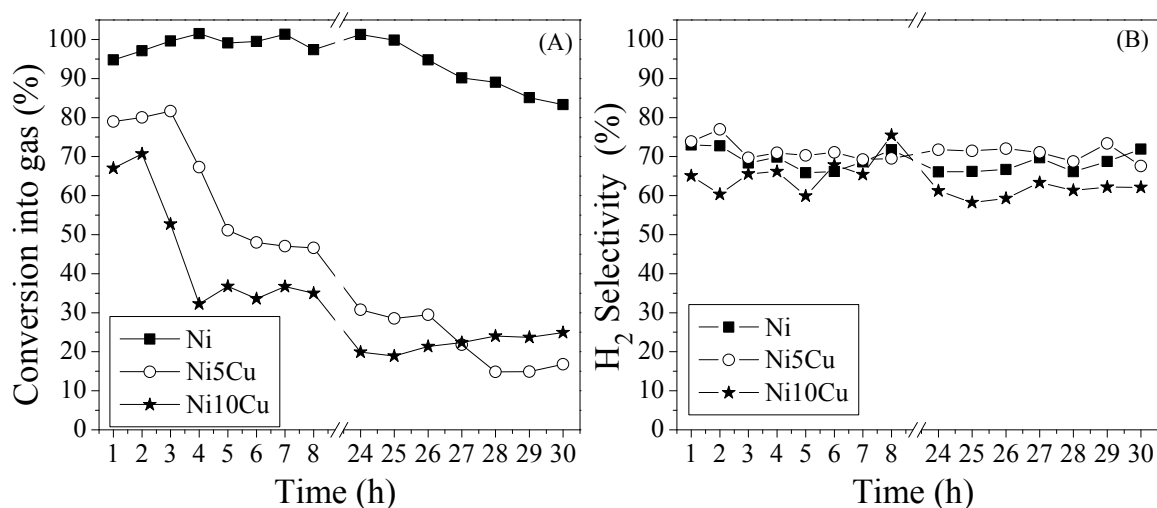


Figure 1: Glycerol conversion into gas (A) and selectivity to hydrogen (B) using Ni, Ni5Cu e Ni10Cu catalysts. Reaction conditions: temperature 500 °C, 0.250 g of catalyst, 50,000 h⁻¹ GHSV and 10 vol.% glycerol solution.

The selectivities to CO₂, CH₄ and CO obtained in the catalytic test showed good stability during 30 h of reaction. The average values are presented in Table 1. The CO₂ is the main gaseous carbon-

containing product obtained in the catalytic tests. However, it is observed that both CH₄ and CO selectivity increase in catalytic tests performed with copper containing catalysts, and increasing the copper content in the catalyst increases the selectivity to these compounds, consequently the selectivity to CO₂ is reduced. It is also observed an increase in the H₂/CO₂ molar ratio for copper-based catalysts, mainly for Ni10Cu catalyst, which showed H₂/CO₂ molar ratios higher than the theoretical value (7/3), indicating that there are reactions occurring in parallel to the reaction of steam reforming of glycerol, which are generating more H₂ and/or consuming CO₂.

The liquid by-products identified in the steam reforming of glycerol were lactic acid, acetol, acetaldehyde, acrolein and acetic acid. The chemical routes for the formation of these compounds have been shown in other works from our group [11,12]. Table 1 presents the average yield of liquid by-products in steam reforming of glycerol. As expected, due to high conversion of glycerol into gas, the tests conducted with Ni catalyst had lower yields to liquid by-products. In addition, it was not observed the formation of acetic acid and acetaldehyde in these reactions. The highest yields to liquid by-products were obtained with copper-based catalysts. In these reactions the main liquid by-product was lactic acid, followed by acetol, acetaldehyde, acrolein and acetic acid. The main difference between Ni5Cu and Ni10Cu catalysts involves acrolein and acetol, with an increase in both yields with increasing copper content. A reasonable explanation for this fact is related to the acidity of the catalyst and the greater proportion of strong acid sites on the Ni10Cu catalyst in relation to Ni5Cu [11].

Table 1: Average selectivities to CO₂, CH₄ and CO, average H₂/CO₂ molar ratio and average yields to liquid by-products achieved in the reaction of steam reforming of glycerol. Reaction conditions: 500 °C, 0.250 g of catalyst, 50,000 h⁻¹ GHSV and 10 vol.% glycerol solution.

Catalyst	Ni	Ni5Cu	Ni10Cu
Selectivity (%)			
CO ₂	94.5	71.6	52.7
CH ₄	1.7	2.9	4.3
CO	3.8	25.5	43.0
H ₂ /CO ₂ (molar)	1.7	2.3	2.9
Liquid by-products			
YAcetic acid (%)	-	0.54	0.9
YLactic acid (%)	0.12	9.02	9.0
YAcetol (%)	0.09	3.65	7.07
YAcrolein (%)	0.08	1.96	4.10
YAcetaldehyde (%)	-	3.40	5.43

Conclusions

The reactions performed with Ni catalyst showed the highest glycerol conversion into gas and high selectivity to CO₂ and low selectivity to CO and CH₄. However, higher selectivities to H₂ were

obtained with Ni5Cu catalyst. The addition of Cu to catalysts promoted an increase in selectivity to CO and CH₄ and this may be associated with parallel reactions to glycerol reforming that should be modifying the theoretical H₂/CO₂ molar ratio (7/3). It was identified the liquid by-products of steam reforming of glycerol, with the following order of yield: lactic acid > acetol > acetaldehyde > acrolein > acetic acid.

References

- [1] Zheng, Y., Chen, X., Shen Y., Chem. Rev., 2008; 108, 5253-5277.
- [2] Cortright, R.D., Davda, R.R., Dumesic, J.A., Nature, 2002; 418, 964-967.
- [3] Davda, R.R., Shabaker, J.W., Huber, G.W., Cortright, R.D., Dumesic, J.A., Appl. Catal. B Environ., 2005; 56, 171-186.
- [4] Adhikari, S., Fernando, S.D., Haryanto, A., Catal. Today, 2007; 129, 355-364.
- [5] Sehested, J., Catal. Today, 2006; 111, 103-110.
- [6] Davda, R.R., Shabaker, J.W., Huber, G.W., Cortright, R.D., Dumesic, J.A., Appl. Catal., B, 2003; 43, 13-26.
- [7] Cavani, F., Trifiró F., Vaccari, A., Catal. Today, 1991; 11, 173-301.
- [8] Vizcaíno, A.J., Carrero, A., Calles, J. A., Int. J. Hydrogen Energy, 2007; 32, 1450-1461.
- [9] Chen L.-C., Lin, S.D., Appl. Catal., B, 2011; 106, 639-649.
- [10] Corma, A., Fornes, V., Rey, F., J. Catal., 1994; 148, 205-212.
- [11] Manfro, R.L., Pires, T.P.M.D., Ribeiro, N.F.P., Souza, M.M.V.M., Catal. Science & Technol., 2013; 3, 1278-1287.
- [12] Manfro, R.L., Ribeiro, N.F.P., Souza, M.M.V.M., Catal. for Sustain. Energy, 2013; 1, 60-70.

Hydrogen production by bio oil reforming over nickel aluminates (P-342)

Lucas G. Carreira¹, Mariana M. V. M. Souza¹, Nielson F. P. Ribeiro^{1,2}*

*1Laboratório de Tecnologia do Hidrogênio (LabTech), Escola de Química-UFRJ, Centro de Tecnologia, Bloco E, sala 206, CEP 21941-909 Rio de Janeiro, RJ, Brazil, * nielson@eq.ufrj.br.*

2 Núcleo Multidisciplinar de Pesquisa (NUMPEX-Nano)-Polo Avançado de Xerém, Estrada de Xerém, 27 CEP.: 25.245-390 Duque de Caxias, RJ - Brazil

Introduction

Hydrogen has been considered a clean source of energy when applied to fuel cells for energy production. However, the main routes of hydrogen production today are based on fossil fuels, as the reforming /oxidation of natural gas, naphtha and coal. In addition to the environmental problems generated by the burning of fossil fuels, the current demand for energy has increased drastically caused mainly by the increase in world population and the greedy growth in emerging economies. This scenario, coupled with political issues related to dependence on imported oil and energy security, makes the production of sustainable fuels a key issue.

Power generation from biomass is the only sustainable source of organic carbon and is already being used in fuel substitution. Biofuels generate far fewer greenhouse gases than fossil fuels and can be considered carbon neutral. Bio- oils are produced from fast pyrolysis of biomass, which mainly produces a dark brown color liquid known as bio- oil (1,2). Vagia et al. (3) performed a thermodynamic analysis of the reforming of bio-oil compounds, represented by different models. The authors concluded that bio-oil can be reformed into hydrogen, carbon monoxide, carbon dioxide and methane, and the proportions depend on the process conditions and type of catalyst used.

In this context, the main objective of this work is the development of nickel catalysts with spinel structure doped with calcium, prepared by the method of combustion, for reforming the bio - oil and resistant to sintering and coking. The aim is to evaluate the effect of the proportion of fuel and presence of promoter on the catalytic activity and stability for reforming reaction of bio-oil using acetic acid as a model compound of soluble aqueous phase of bio-oil.

Materials and Methods

Nickel aluminate catalysts promoted with calcium were synthesized by the combustion method using urea as a fuel agent by varying the amount of urea from 0.25, 0.5 and 1.0 times the stoichiometric amount, calculated according to the propellant chemistry (4). The samples were prepared with different Ca ratios, $\text{Ni}_{0,67}\text{Ca}_{0,33}\text{Al}_2\text{O}_4$ and $\text{Ni}_{0,80}\text{Ca}_{0,20}\text{Al}_2\text{O}_4$, called respectively by Ni_2CaU_x and Ni_4CaU_x with $x = 25, 50$ and 100 depending of stoichiometric urea amount. One sample without calcium was also prepared as reference using the stoichiometric amount of urea (NiAlU_{100}). The characterization of the catalysts was performed using the techniques of X -ray diffraction (XRD) and temperature-programmed reduction (TPR). The reforming reaction of the bio - oil was carried out in a fixed bed reactor at 400-700 oC using acetic acid as a model compound and steam/carbon ratio of 2. Before reaction the catalysts were reduced at 750 oC with 20% H_2/N_2 for 1h.

Results and discussion

The sample Ni2CaU100 achieved the highest flame temperature, with rapid ignition during combustion synthesis. The reaction had a rapid temperature rise, reaching a maximum of 1206 °C in a short time, showing the occurrence of the combustion process. For Ni2CaU50 sample the ignition was more gradual and the temperature reached was much lower (641 °C), while for the Ni2CaU25 sample the temperature rise is very small and slow with no visible ignition. The results for the Ni4Ca series of catalysts showed similar behavior, in which the increase of the fuel / oxidant ratio provides increased flame temperature and faster ignition.

Figure 1 shows the XRD of the samples. Analysis of X-ray diffraction revealed that in all catalysts it was not obtained a pure spinel structure, with the presence of nickel oxide, which indicates the segregation of NiO that was higher in samples with a low content of fuel. Furthermore, one can observe an increase in crystallinity with increase of the fuel / oxidant ratio. Ribeiro et al. (5) studied the synthesis of nickel aluminate via the combustion method with urea and also noted the presence of small amounts of segregated nickel oxide when fuel/oxidant ratio stoichiometric was used. As pure nickel aluminate or mixed nickel and calcium aluminate phases have the same characteristic Bragg angles it is not possible to say what kind of spinel structure was formed. However, the absence of calcium secondary phases indicates that calcium is incorporated into the structure of the spinel.

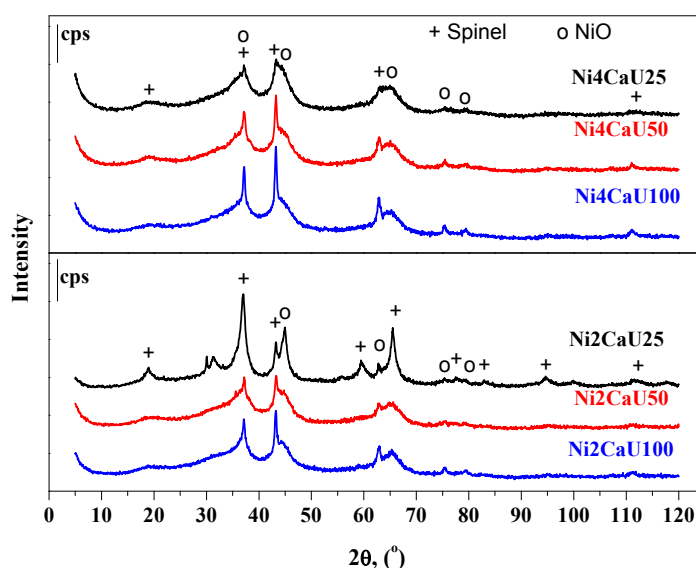


Figure 1. XRD of different catalysts.

From TPR profiles, there are two kinds of nickel species present in the samples: nickel oxide segregated with low interaction with the support, with reducing temperatures around 460 °C, and the nickel/calcium aluminate reduction at 1000 °C, for the Ni2CaU100 catalyst, or close to 750 °C, for the others. The results are consistent with those observed by the X-ray diffraction. It was observed that the amount of surface nickel oxide with less interaction with the support tends to increase for catalysts prepared with lower amounts of urea. The main reduction peak shifts to higher

temperatures with increasing amount of fuel, which may be associated with the maximum temperature reached during combustion, as described in Molina and Poncelet (6).

The synthesized catalysts were evaluated in the reaction of bio-oil reforming using acetic acid as model compound. Figure 2 shows the molar fractions of gaseous products for the NiAlU100 sample and the conversion of acetic acid for all catalysts. High conversions of acetic acid were observed for NiAlU100, around 80 % at 450 °C and complete conversion from 550 °C, showing the potential application of this catalyst for the process.

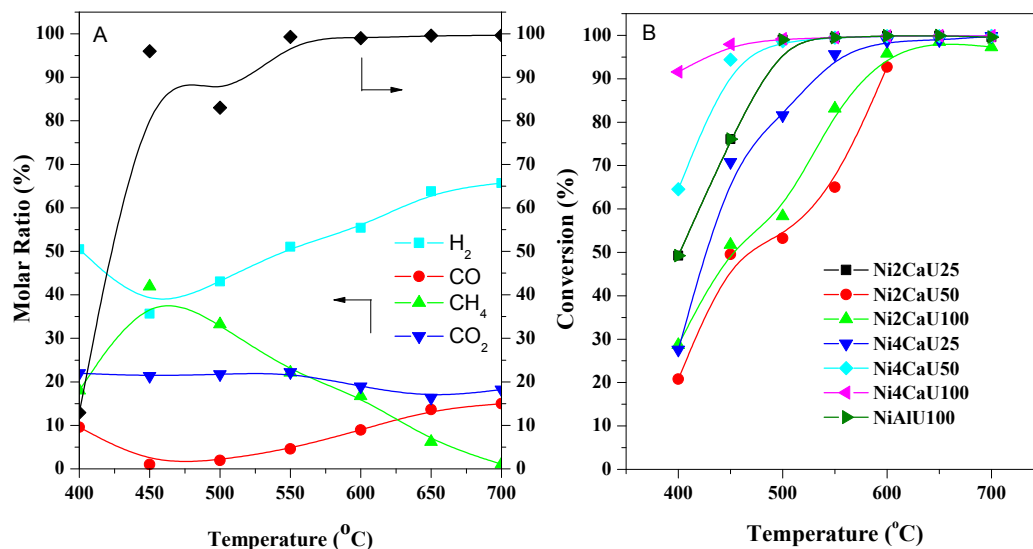


Figure 2. A) Catalytic evaluation in acetic acid reforming over NiAlU100 catalyst and B) Conversion of different catalyst.

The distribution of products in the gas phase can be understood by analyzing the reactions involved in the system. The reaction of the steam reforming of acetic acid is represented by Equation 1. However, in addition to H₂ and CO₂ found in the vapor phase, CO and CH₄ were also formed. The formation of CO is probably associated with the decomposition of acetic acid, as described in Equation 2 (7) or from the reverse reaction of water gas shift, Equation 3 (8). CH₄ formation can be due to decarboxylation of acetic acid, Equation 4 (8). The increased production of hydrogen from 450 °C and the concomitant decrease in methane production can be attributed to methane reforming, as described in Equation 5.





Evaluating the results of the conversion of acetic acid of the different catalysts, different behaviors are observed according to the calcium concentration in the samples. For Ni₂Ca series of catalysts, increasing content of fuel led to an increase of the catalytic conversion. Opposite behavior was observed for the Ni₄Ca series. This can be attributed to the different metal dispersions of the catalysts, since it is known in the literature that increasing the flame temperature during synthesis can cause significant changes in the metal dispersion (5). It was also observed that a smaller proportion of calcium in the synthesized catalysts causes an increase in catalytic activity, which is consistent with the higher content of the active phase present.

The distribution profile of the gaseous products of the samples synthesized with calcium showed similar behavior, but the evolution of the reactions was distinguished for reference NiAlU100sample. At low temperatures there was only the decarboxylation of acetic acid, Equation 4, followed by formation of methane and carbon dioxide, and then the reforming reaction of methane, Equation 5, which produces carbon monoxide and hydrogen. The inclusion of calcium in the sample caused the reduction of the coking process as observed with long-term testing.

Conclusions

The catalytic activity tests showed the best performance of the catalysts promoted with calcium compared with the traditional nickel aluminate for steam reforming of bio - oil using acetic acid as a model compound. The increase of the calcium content in samples significantly decreased the catalytic activity, and its inclusion provided significant differences in the distribution of gaseous products, moreover, a significant increase in catalyst stability with the reaction time. The catalyst with the best catalytic performance in the tests was the Ni₄CaU50.

References

- D. A. Bulusheva, J.R.H. Rossa, *Catalysis Today*, 2011, 171, 1–5.
- X. Hua, G. Lu, *Applied Catalysis B: Environmental*, 2009, 88, 376–385.
- E. Ch. Vagia, A. Lemonidou, *Journal of Catalysis*, 2010, 269, 388-396.
- A. Ringuedé; J. A. Labrincha; J. R. Frade, *Solid State Ionics*, 2011, 549, 141-150
- N.F.P. Ribeiro, R.C.R. Neto, S.F. Moya, M.M.V.M. Souza, M. Schmal, *International Journal of Hydrogen Energy*, 2010, 35, 1172- 1732
- R Molina, G. Poncelet, *Journal of Catalysis*, 1998, 173, 257-267.
- S. Thaicharoensutcharittham, V.Meeyoo, B.Kitiyanan, P. Rangsunvigit, T. Rirkomboon, *Catalysis Today*, 2011, 164, 257-261.
- Yu-He Wang, Hong-Mei Liu, Bo-Qing Xu, *Journal of Molecular Catalysis A: Chemical*, 2008, 299, 44-52

Novel materials for a HT-PEMFC stack for operation as automotive range extender (P-343)

[D.J. Jones, J. Rozière, N. Donzel, A. Kreisz (CNRS, Montpellier France)

A. Morin, C. Nayoze (Commissariat à l'Énergie Atomique et aux Energies Alternatives, France)

F. Alcaide Monterubio (CIDETEC, Spain)

M. Smit (Nedstack, Netherlands)

P. Asinari, U. Salomov (Politecnico Di Torino, Italy)

A. Piu (CRF, Italy)]

The purpose of the ARTEMIS (Automotive pemfc Range extender with high TEMperature Improves meas and Stacks) project funded by the Fuel Cell & Hydrogen –Joint Undertaking is to develop and optimise alternative materials for a new generation of European High Temperature MEAs which could be integrated into a 3 kWe high temperature PEMFC stack, while reducing cost & increasing durability. Hybridisation and specific use profile of the HT PEMFC stack versus the batteries will be defined.

The MEAs are based on new and alternative polybenzimidazole type membranes and improved catalytic layers providing low catalyst loading and high efficiency at high temperature as well as a high tolerance to pollutants. Due to their higher operating temperature range (160-180 °C), HTPEMFC are much more tolerant to CO, allowing few percent of CO without irreversible performances losses. Their use yields cheaper and smaller combined reformers. A HT-PEMFC-based electric generator could then possibly be integrated into a vehicle by using available liquid fuels (LGP, gasoline, methanol, etc.), allowing a more rapid access to the automotive market. The range extender option is a realistic and incremental introduction of fuel cell technology into the automotive sector.

New membrane, electrocatalyst, support, and bipolar plate materials are being developed specifically for HT PEMFC MEAs and their application as a range extender for transportation application.

The ARTEMIS project is in its early stage but promising results have already been obtained, with MEAs comprising project materials showing performance higher than state-of-the-art, and satisfactory durability, which validates the concept and justifies upscale to single cell testing at 200 cm² level and then to a short stack. Further improvements to the electrode structure, catalyst materials will be integrated progressively as they become available. Also, bipolar plate materials and their specific seals developed specifically to operate at high temperature under acidic conditions are developed and their properties further enhanced. In parallel to the performances achievement, ARTEMIS will go deep inside the range extender load profile with the definition of the best sets of batteries versus PEMFC stack hybridisation. Modeling tools have demonstrated reactant gas flows by pore scale simulation and their effect on phosphoric acid pull within the porosity and tortuosity of the catalytic layer, and a specific model on MEA performance simulation related to the catalyst distribution has been developed.

This poster will discuss the particular challenges for an automotive APU and representative use profiles for a HTPEMFC stack operated as range extender in a hybrid electric vehicle. It will discuss

the technology options for this type of application, and present the status of ARTEMIS - materials, cells and stack - in this context.

The research leading to these results has received funding from the European Community's Seventh Framework Programme (FP7/2010-2013) for the Fuel Cells and Hydrogen Joint Undertaking under grant agreement ARTEMIS no. 303482.

Improvement of fuel cells' cost and performance by application of nanotechnology: a review (P-345)

*Wan Ramli Wan Daud
Founding Director
The Fuel Cell Institute
Universiti Kebangsaan Malaysia]*

The world energy supply that consists of mostly fossil fuel will peak by 2020-2030, be depleted in 40-50 years time and precipitate an energy crisis because of widening fossil fuel production and demand gap that threatens the energy security of the world. Green house gases (GHG) emissions from human activities have been proven beyond doubt to be the main cause of global warming and climate change. Further deployment of nuclear energy is uncertain because of negative public opinion on Fukushima disaster. Large-scale biofuel deployment is slow because of conflict between fuel and food crops. Solar energy, wind and wave energy is constrained by high cost, low energy extraction efficiency, seasonal variability and weather unpredictability. On the other hand, hydrogen energy offers the best alternative clean energy, but is constrained by cost, durability and safety of hydrogen transport and storage. Fuel cell technology using hydrogen energy is an advanced energy technology that is green, sustainable, clean, environmental friendly, and emits only water. The priority of R&D in fuel cells is to develop cheaper and more durable fuel cell technology that can match the low cost and durability of conventional internal combustion engines (ICEs) and combined cycle power stations using fossil fuels. The fuel cell cost must be reduced to the target of \$30/kW that will be competitive enough with conventional power conversion technology. In addition, the fuel cell stack lifetime of 2500 h for transportation 20,000 hours for stationary application achieved in 2009 must be doubled to meet the target of 5000 h and 40,000 h for transportation and stationary application respectively. Both the cost and durability targets can be achieved by a greater fundamental understanding of the inter-related and complex processes occurring in the fuel cell stack and balance of plant. Application of nanomaterials, nanostructures and nanosystems in fuel cells will increase both performance and durability but at less cost by taking advantage of the enhanced ionic conductivity and electrocatalysis of nanomaterials and nanostructures. PEMFC's cost can be reduced and its durability can be improved by replacing the costly Pt electrocatalyst for oxygen reduction reaction and hydrogen oxidation reaction, with new cheaper more durable nanostructures, nanomaterials and nanosystems such as nitrogen doped CNTs (NCNTs), carbon nanofibers (CNF), carbon nanowires (CNW), carbon nanoshells (CNS) and carbon nanosheets or graphenes. Both cost reduction and durability improvement of membranes in PEMFCs can also be achieved by replacing expensive Nafion membranes with new high temperature inorganic/organic nanocomposite membranes containing nanostructures, nanomaterials and nanosystems as well as inorganic nanomaterials such as Nafion/Pd-SiO₂ nanofiber composite membranes. Cheaper DMFCs can be made by replacing expensive Pt with nanostructured electrocatalysts for methanol oxidation and oxygen reduction and expensive Nafion membranes with organic-inorganic nanocomposite membrane to prevent methanol crossover which degrades MFCs, using similar nanomaterials used to improve PEMFC performance such as NCNTs, CNF, CNW and graphenes. Since microbial fuel cells (MFCs) main application are in combined wastewater treatment and electricity generation, its cost can be reduced by using cheaper polymer electrolytic membrane nanocomposites that is impermeable to oxygen and nanostructured electrodes that are able to form more stable biofilm for

microorganism to transfer electron to anode easily. More conductive but cheaper bipolar plates can be made from nanocomposite polymers using oriented CNTs, CNFs and graphenes.

A multi dimension approach for fast analysis of Polymer Electrolyte Membrane Fuel Cells (P-346)

J. Dujc¹, J.O. Schumacher¹

¹ Zurich University of Applied Sciences, ICP - Institute for Computational Physics

ABSTRACT: We present a multi-dimensional approach for finite element method simulation of polymer electrolyte membrane fuel cells (PEMFC). In this approach, the PEMFC is divided into regions of 2D and 1D domains. Two parallel 2D domains represent the anode and cathode side flow fields (FF) and gas diffusion layers (GDLs). Anode and cathode sides are connected by the 1D domains, representing the membrane electrode assembly (MEA).

Keywords: polymer electrolyte membrane fuel cell, PEMFC, membrane electrode assembly, MEA, modeling, model reduction, FEM.

INTRODUCTION

When dealing with PEMFC modeling, we are faced with two significant challenges: (i) the large area to thickness ratio and (ii) numerous coupled physical and electrochemical processes. We treat the first obstacle (i) by reducing the 3D model into a combination of two parallel 2D regions, which are connected by the 1D regions, see [2]. The 2D regions capture all the significant in-plane phenomena, while the through-plane processes in the membrane electrode assembly are captured by the 1D regions. By carefully choosing the parameterization and which processes/fields are included in the model, we can also address the second obstacle (ii).

The paper is organized as follows. In Section 2, the 1D MEA model is briefly presented. 2D simulations are outlined in Section 3. The coupling 1D + 2D algorithm is discussed in Section 4, and conclusions are drawn in Section 5.

1D MEA SIMULATION

In Fig. 1 we present the geometry of the membrane electrode assembly composed of: the anode side gas diffusion layer Ω_1 , anode side catalyst layer Ω_2 , membrane layer Ω_3 , cathode side catalyst layer Ω_4 and cathode side gas diffusion layer Ω_5 . The boundaries between sub-domains are denoted with $\partial\Omega_i$, $i = 1, 2, 3, 4, 5, 6$. One can describe the MEA behavior with varying level of complexity, depending on the number of fields used and their type of parameterization. In our implementation we solve for the following seven field variables: the electrostatic potential of electrons ϕ_e and protons ϕ_p , the temperature field T , the dissolved water content of the membrane λ , the water vapor concentration c_v , the hydrogen concentration c_{H_2} and the oxygen concentration c_{O_2} . The general form of governing equation for each field can be described with the following partial differential equation

$$\nabla \cdot j_{field}^{\Omega_i} = q_{field}^{\Omega_i}, \tag{1}$$

where $j_{field}^{\Omega_i}$ is the flux, $q_{field}^{\Omega_i}$ is the source/sink term and the subscript field denotes the fields $\phi_e, \phi_p, T, \lambda, cv, cO_2, cH_2$. The Ω_i denotes the sub-domain as shown in Fig. 1.

The fields are significantly coupled through the sink/source terms in (1) and also through material and other parameters found in fluxes, which are generally not constants, but are rather functions of several field variables.

The partial differential equations (1) are solved for the prescribed boundary conditions. We assume the zero Neumann boundary condition at the following list of positions and accompanying fields

$$\begin{aligned} \partial\Omega_2: & \phi_p, \lambda, \\ \partial\Omega_3: & \phi_e, cv, cH_2, \\ \partial\Omega_4: & \phi_e, cv, cO_2, \\ \partial\Omega_5: & \phi_p, \lambda. \end{aligned} \tag{2}$$

The list of prescribed Dirichlet boundary conditions, which are also input parameters from the 2D simulation, is the following

$$\begin{aligned} \partial\Omega_1: & \phi_e, T, cv, cH_2, \\ \partial\Omega_6: & \phi_e, T, cv, cO_2, \end{aligned} \tag{3}$$

The 1D MEA finite element method simulations are carried out in a standalone routine written in C programming language.

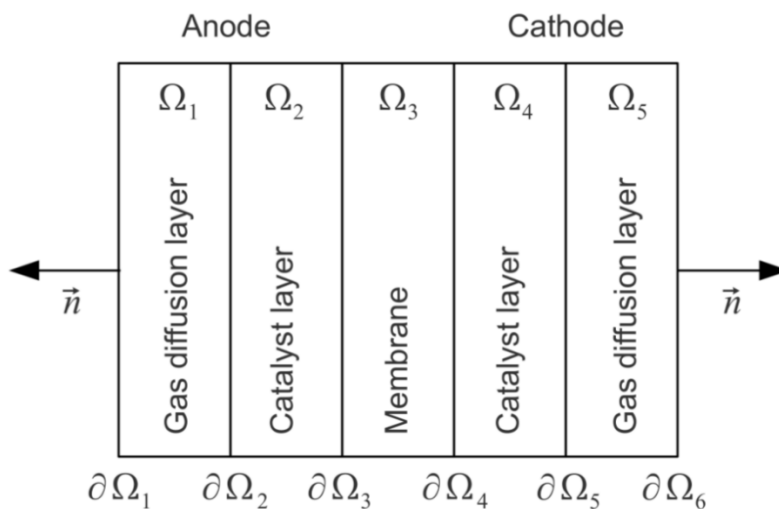


Figure 34: Geometry of the MEA model

2D ANODE AND CATHODE SIDE SIMULATIONS

The in-plane processes in flow fields and gas diffusion layers of anode and cathode side are simulated by SESES [1]. In the 2D simulations we solve for the field variables that are listed in the 1D Dirichlet boundary conditions (3): ϕ_e , T , c_v , c_{O_2} , c_{H_2} . Additionally we also solve for the velocity field u and pressure field P . For the free flow in the channels we assume the incompressible Navier-Stoke's equations, while Darcy's law is considered for the porous medium of GDLs.

COUPLING PROCEDURE

In Fig. 2 a schematics of the coupled 2D + 1D model is presented, where the blue and red regions denote the FE meshes for anode and cathode side in-plane simulations and perpendicular are the connecting through-plane 1D meshes. From an algorithm point of view we divided the 2D + 1D simulation into the global simulation steered by SESES and local simulation performed by the C routine. In every Newton-Raphson iteration of global simulation in SESES, a local simulation is performed for every node in the 2D mesh. The input parameters for the 1D simulations are the current anode and cathode side nodal values of field variables from the 2D simulation

$$\mathbf{v}^{2D} = [\varphi_e^{2D,A}, T^{2D,A}, c_v^{2D,A}, c_{H_2}^{2D,A}, \varphi_e^{2D,C}, T^{2D,C}, c_v^{2D,C}, c_{O_2}^{2D,C}] = [v_1, v_2, v_3, v_4, v_5, v_6, v_7, v_8] \quad (4)$$

For the given set of input parameters \mathbf{v}^{2D} , the C code performs the FEM simulation in order to determine the equilibrated configuration of the membrane electrode assembly. Once the converged state is achieved, the C code returns to SESES the values of boundary fluxes

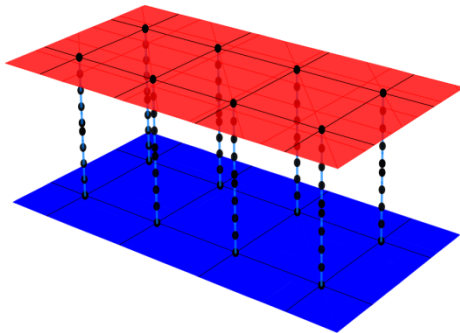


Figure 35: Schematics of the coupled 2D + 1D model

$$\begin{aligned} \mathbf{f}^{1D} &= [f_{\varphi_e}^{1D,A}, f_T^{1D,A}, f_{c_v}^{1D,A}, f_{c_{H_2}}^{1D,A}, f_{\varphi_e}^{1D,C}, f_T^{1D,C}, f_{c_v}^{1D,C}, f_{c_{O_2}}^{1D,C}] \\ &= [f_1, f_2, f_3, f_4, f_5, f_6, f_7, f_8], \end{aligned} \quad (5)$$

and the derivatives of fluxes with respect to the input parameters

$$df_{2D}^{1D} = \begin{bmatrix} \frac{\partial f_1}{\partial v_1} & \frac{\partial f_1}{\partial v_2} & \frac{\partial f_1}{\partial v_3} & \frac{\partial f_1}{\partial v_4} & \dots \\ \frac{\partial f_2}{\partial v_1} & \frac{\partial f_2}{\partial v_2} & \frac{\partial f_2}{\partial v_3} & \frac{\partial f_2}{\partial v_4} & \dots \\ \frac{\partial f_3}{\partial v_1} & \frac{\partial f_3}{\partial v_2} & \frac{\partial f_3}{\partial v_3} & \frac{\partial f_3}{\partial v_4} & \dots \\ \frac{\partial f_4}{\partial v_1} & \frac{\partial f_4}{\partial v_2} & \frac{\partial f_4}{\partial v_3} & \frac{\partial f_4}{\partial v_4} & \dots \\ \vdots & \vdots & \vdots & \vdots & \ddots \end{bmatrix} \quad (6)$$

The results of the local analysis, f^{1D} and df_{2D}^{1D} , are afterwards used in SESES to contribute to the global residual vector and the global tangent stiffness matrix. Once all the contributions of the 1D domains are considered, SESES performs an iteration to update the values of 2D nodal degrees of freedom.

CONCLUSION

A computationally efficient model of a PEMFC is presented. It is based on a 2D + 1D approach, where the flow-fields and the gas diffusion layers on the anode side and on the cathode side are discretized in two dimensions. The membrane electrode assembly is modeled in one dimension.

The 2D + 1D approach is suitable to take the high aspect ratio between the in-plane and the through-plane dimensions of a PEFC into account. This is essential to describe large-area fuel cells. The number of DOFs of the presented model is significantly smaller in comparison to a full 3D discretization of the model domain.

References

- [1] SESES Manual. <http://icp.zhaw.ch/seses/>, August 2013.
- [2] J.O. Schumacher, J. Eller, G. Sartoris, T. Colinart, and B. Seyfang. 2+1D modelling of a polymer electrolyte fuel cell with glassy-carbon micro-structures. *Mathematical and Computer Modelling of Dynamical Systems*, DOI:10.1080/13873954.2011.642390:1–23, 2012.

An overview of H₂FC SUPERGEN, the UK's inclusive Hydrogen & Fuel Cell research network and UK Hydrogen & Fuel Cell activities (P-348)

Chloe Stockford¹, Nigel Brandon¹, John Irvine², Tim Mays³, Ian Metcalfe⁴, David Book⁵, Paul Ekins⁶, Anthony Kucernak¹, Vladimir Molkov⁷, Robert Steinberger-Wilckens⁸, Nilay Shah¹

¹Energy Futures Lab, Imperial College London, SW7 2AZ, UK

²School of Chemistry, University of St Andrews, KY16 9ST, UK

³Department of Chemical Engineering, University of Bath, BA2 7AY, UK

⁴School of Chemical Engineering and Advanced Materials, Newcastle University, NE1 7RU, UK

⁵School of Metallurgy and Materials, University of Birmingham, B15 2TT, UK

⁶UCL Institute for Sustainable Resources, University College London, WC1H 0NN, UK

⁷Hydrogen Safety Engineering and Research Centre (HySAFER), University of Ulster, BT37 0QB, UK

⁸Centre for Hydrogen & Fuel Cell Research, School of Chemical Engineering, University of Birmingham, B15 2TT, UK

The Hydrogen & Fuel Cells SUPERGEN Hub (www.h2fcsupergen.com) was established in 2012 and is the UK's first inclusive Hydrogen and Fuel Cell Network. The Hub endeavors to bring together academia, industry and government in the areas of Hydrogen & Fuel Cells. Funded by a £4 million grant from Research Councils UK Energy Programme, the Hub is directed by Professor Nigel Brandon of Imperial College London. It has around 350 members including around 100 UK-based academics, and over 20 industrial partners and government organisations, which brings together the vast majority of the UK's Hydrogen & Fuel Cell Researchers.

The Hub has a core research structure, shown in the graphic above, which highlights the broad range of interests it covers, including PEMFC, SOFC, Hydrogen Storage, Hydrogen Production, Socio-economics. Additionally the Hub also distributes funding, arranges networking activities and will release four white papers including the role of Fuel Cells and Hydrogen in Low carbon heating systems (which is due for release in May 2014) which is designed to inform policy makers.



The research methodology within the Hub core programme consists of nine work packages, that cut across policy and socio-economics, systems, safety, and education and training, along with key aspects of underpinning science and technology, namely hydrogen production, hydrogen storage, PEM fuel cells, and solid oxide fuel cells/electrolysers, integrating these together in a final research synthesis work package. This structure is illustrated above.

H2FC SUPERGEN seeks to address a number of key issues facing the hydrogen and fuel cells sector specifically: (i) to evaluate and demonstrate the role of hydrogen and fuel cell research in the UK energy landscape, and to link this to the wider landscape internationally, and (ii) to identify, study and exploit the impact of hydrogen and fuel cells in low carbon energy systems. Such systems will include the use of hydrogen and of fuel cell technologies to manage intermittency with increased penetration of renewables, supporting the development of secure and affordable energy supplies for the future. Both low carbon transport (cars, buses, boat/ferries, forklifts, etc.) and low carbon heating/power systems employing hydrogen and/or fuel cells have the potential to be important technologies in our future energy system, benefiting from their intrinsic high efficiency and ability to use a wide range of low to zero carbon fuel stocks. One major drive for the Hub is to contribute to technology development that will help the UK to meet its ambitious carbon emissions targets. The Hub links the academic research base with industry, from companies with global reach through to SMEs and technology start-ups, to ensure effective and appropriate translation of research to support wealth and job creation for UK plc, and with local and national government to inform policy development. The Hub champions the complete landscape in hydrogen and fuel cells research, both within the UK and internationally, via networks, knowledge exchange and stakeholder (including outreach) engagement, community building, and education, training and continuous professional development.

The Hub champions the complete landscape in hydrogen and fuel cells research, both within the UK and internationally, via networks, knowledge exchange and stakeholder (including outreach) engagement, community building, and education, training and continuous professional development. The Hub represented the UKs H2FC community by signing an MOU with Korea for Hydrogen & Fuel Cells and endeavours to expand international collaboration.

This presentation aims to give an overview of H2FC SUPERGENs activities as well as to give an outline of the UKs active Hydrogen and Fuel Cell landscape.

Theoretical Study on the Effects of the Magnesium Hydride Doping with Cobalt and Nickel on the Hydrogen Release (P-354)

Hasan S. AlMatrouk¹ and Viorel Chihai²

¹Kuwait Institute for Scientific Research, PO Box 24885, Safat 13109, Kuwait, hmatrouk@kisir.edu.kw

²Institute of Physical Chemistry "Ilie Murgulescu", Romanian Academy, Splaiul Independentei 202, Bucharest, Romania, vchihai@icf.ro

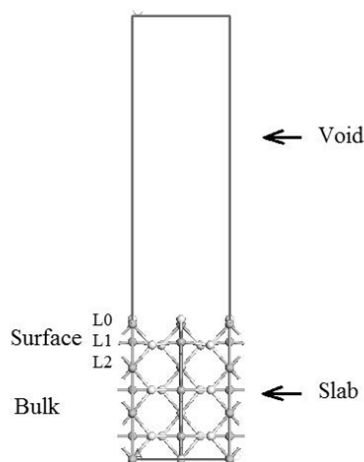
The design of new materials with a high hydrogen contain and the development of new and efficient methods for the controlling and the optimization of the hydrogen release by the manipulation of thermodynamic and kinetic conditions of the materials are essential in establishing the optimum and safe technological solutions for the production, storage, transportation and usage of hydrogen. The traditional couple theory - experiment enables us to understand the interaction mechanisms and the phenomena that take place in bulk, on the surface, at the interface of different materials or at the grain boundaries, as well as to establish the analytical equations and to characterize material properties. The computer simulations may help the scientists to understand how the atomic and molecular Hydrogen reacts with the surface, interface, grain boundaries and the bulk defects of the materials and how we may tune the material properties by reducing the size and changing their electronic structure by doping/alloying the base material. The atomistic and quantum simulations are essential in the thermodynamic and kinetic analysis of the bulk, surface and interface phenomena.

In the present contribution we present the results of our DFT-based investigations (using a PW91/USPP calculation scheme) of the effects of doping the Magnesium Hydrate with Cobalt and Nickel on the bulk properties and on the Hydrogen adsorption and desorption on the MgH₂(001) surface. We present the energetic and electronic aspects of these interactions and discuss the qualities of the calculation methods.

The bulk calculations indicate that the doping and the Hydrogen vacancy affect the electronic band structure of the Magnesium Hydride by the introduction of peaks or bands in the DOS of the Magnesium Hydride. The charges, the spins and the interatomic distances in the vicinity of the

defects are affected. The presence of the dopants and of the hydrogen vacancy is accompanied by the decreasing of the cohesive energy of the magnesium hydride. In order to avoid the effects of the defects periodicity large supercells that include disordered defects were used.

We continued our study with the calculations of the clean and Co- and Ni-doped surfaces (001) of the Magnesium hydride. The surface systems were represented by 3D periodic slab models, consisting in seven layers. The atoms in the two top layers L0 and L1 are completely relaxed and the



The slab model of the Magnesium Hydride surface (001).

atoms in the third layer L2 are relaxed only along the c-axis, perpendicular to the surface. The other atoms are fixed in their bulk optimized position. A void domain of 20 Å is included to separate the image slabs along the c-axis. The size (for lattice constants $a=b=6.4085$ Å and $c=29.0843$ Å) and the rectangular shape of the box are fixed during the optimization procedures.

The calculations predict the rumpling and relaxations of the first two layers of the Magnesium Hydride surface (001) and that the first layers are almost neutral, but they have an electric dipole. By removing a Hydrogen atom from the first layer, the nearest Magnesium atom in the first layer tries to compensate this missing partner by closer contacts with the other neighbor atoms. The adsorbed Hydrogen atom on top of a Magnesium atom prefers to form a bond with one Hydrogen atom bonded to the same Magnesium atom. The hydrogen-hydrogen distance (0.842 Å) is larger than the one predicted by the same calculation scheme for the free Hydrogen molecule (0.751 Å). Both Hydrogen atoms make covalent bonds with the two neighbor Magnesium atoms.

The surface structure is locally affected by the presence of the Magnesium substituent atoms $M = \text{Co}$ or Ni . The Cobalt atom accepts the local topology of the replaced Magnesium atom and slightly contracts its neighborhood. The Nickel atom is more aggressive, producing a rearrangement of its neighbor Hydrogen atoms and forming with them an almost planar cross. The same tendencies of the substituent atoms of Cobalt and Nickel are observed when a Hydrogen vacancy is created near them. The Cobalt atom contracts further its neighborhood by reducing its distance to the closest Magnesium atom in the second layer. In the case of the Nickel substituent a local rearrangement takes place and the Nickel atom forms again the same planar cross with four Hydrogen atoms. When a Hydrogen atom adsorbs on top of the substituent atom of Nickel a new arrangement takes place: the planar cross fragment is maintained with the fifth Hydrogen atom perpendicular on their plane. The adsorbed Hydrogen on top of the Cobalt substituent forms a bond of 1.600 Å with the Cobalt atom. Excepting the clean and the Ni-doped surfaces that are non-magnetic, all other surfaces are ferromagnetic.

The present study points out the merit of the Cobalt and Nickel dopants in the magnesium hydrate destabilization, which facilitates the hydrogen release. The doping of the surface (001) of the Magnesium hydride can change the structure and the properties of the surface, speeding up the Hydrogen desorption process. Further investigations are necessary to validate our findings, by using larger surface models and by considering various other faces of the Magnesium Hydride, other doping sites and other doping elements.

Hydrogen in Mobile Applications – the Path of Latvia to Carbon Free Economy (P-356)

J. Kleperis¹, B. Sloka², J. Dimants², I. Dimanta³, A. Starikovs¹, M. Gudakovska¹, J. Fricsons¹

1 – Institute of Solid State Physics, University of Latvia, Riga, Latvia;

2 - University of Latvia, Faculty of Economics and Management, Riga, Latvia;

3 - University of Latvia, Faculty of Biology, Riga, Latvia

In a low-carbon society we will live and work in low-energy, low-emission buildings with intelligent heating and cooling systems. We will drive electric and hybrid cars and live in cleaner cities with less air pollution and better public transport (1). Many of these technologies exist today but need to be developed further. Besides cutting the vast majority of its emissions, Europe could also reduce its use of key resources like oil and gas, raw materials, land and water. Currently the GHG emission of Latvia is considerably below the target of the Kyoto Protocol. That allows Latvia will be able to achieve the set target. Nevertheless, Latvia is strongly depending from imported energy resources. The most significant local energy resources used are fuel-wood and hydro-energy (Daugava HPP cascade). Solid fuel, oil products and electricity are imported from several countries and supply regions, but there is only one supplier for natural gas – Russia. The split of energy flows shows the relatively high dependence from energy import – only 33% of total energy consumption is covered by local energy resources. The large part of the fuel for the centralized heat supply to regions and cities are imported in Latvia – 63% of the natural gas, 3% of oil products, 0.6% of coal and the rest 33 % is only local biomass. The share of fossil fuels in transport sector is growing year by year and is above 99%. The traffic with average daily flow intensity 25,000 vehicles per day in typical street canyons (Brīvības, Valdemāra, Čaka-Marijas) located in Riga city center is major air pollution source (2). The number of days when particle PM10 concentrations exceeds EU and Latvian guidelines and annual average concentration on nitrogen dioxide are two main air quality problems arising from internal combustion engine propelled vehicles in Riga. Switch to electro-mobility and electro-hydrogen vehicles could solve air pollution problems in Riga. E-mobility is recognized as carbon-free transport in Riga Municipality and five charging points are already operating. Municipal Enterprise “Riga Traffic”, Energy Company “Latvenergo” are using commercial electric vehicles. First, experience shows that problems can result in cold winter days (energy capacity of batteries is falling markedly), and an increase of electric charging points and number of e-cars will increase uneven load on the central power grids significantly. A good solution is the integration of hydrogen as an energy carrier into electro-mobility, since hydrogen can be produced from domestic resources using grid energy in moments when consumption is minimal. Latvian Hydrogen Association together with Riga Energy Agency organized a conference on hydrogen for local energy and transport officials in Riga City Council for politicians, government officers, society inviting lecturers from University of Latvia and representatives from Hydrogen Fuel Cells and Electro-mobility in European Regions (HyER). It was recognized (3) that current knowledge and awareness levels of hydrogen and fuel cells in Latvia are still low in the general public, and misunderstandings of hydrogen properties continue to impart negative opinions about the safe use of hydrogen as a fuel. Latvia has not yet realized hydrogen technology projects in large scale, there are no also demonstration projects on hydrogen technologies, but researchers from main Universities and Institutes are involved in different research topics. Renewable energy technologies (hydrogen as energy carrier including) are taught at

University of Latvia, Riga Technical University, Latvia University of Agriculture. Hydrogen technology topics like as renewable energy always are interdisciplinary, including knowledge from natural sciences, technical sciences and social sciences.

(1) Europe`s Roadmap for moving to a competitive low-carbon economy in 2050: <http://ec.europa.eu/clima/policies/roadmap/>

(2) Iveta Steinberga, Janis Bikshe Jr., Karlis Kundzins, Janis Kleperis, Janis Bikshe. Evaluation of Local Scale PM Pollution Levels in Typical Street Canyon in Riga. Journal of Environmental Protection, , 2013, 4, 956-963

(3) Dimants J., Dimanta I., Sloka B., Kleperis J., Kleperis J. Jr. Renewable energy powered campus proposal for the University of Latvia. International Scientific Journal for Alternative Energy and Ecology ISJAE, No 9 (113) 2012, pp.81-89

Specific technical requirements for hydrogen storage systems on underwater vehicles intended for exploration of the world ocean (P-357)

[Ivanov R.; Denisova M.]

The paper considers various methods of hydrogen storage and generation in application to the powerplants of underwater vehicles (UV) intended for exploration of the world ocean. Hydrogen fuel is used in air-independent power systems based on electrochemical fuel cells. Particular features of various hydrogen storage systems are examined taking into account their specific technical requirements. Challenges in the field of hydrogen storage are highlighted in application to underwater vehicles designed for exploration of the world ocean.

In all cases under consideration the powerplant based on electrochemical hydrogen-oxygen fuel cells is examined which demands reliable solutions for hydrogen storage and supply. The physical and chemical properties of hydrogen are very different from those of hydrogen fuels traditionally used in shipbuilding.

Hydrogen is a very abundant element. It is a part of most compounds in living creatures and many non-organic substances. Currently, hydrogen compounds in the nature are more abundant than compounds of any other element. Pure hydrogen H₂ is a gas without colour, smell or taste. It is the lightest of all known gases, with density being about 1/14 of the air density. Melting and boiling temperatures of hydrogen (-259°C and -252.7°C respectively) are extremely low, being the second lowest after those of helium. Liquid hydrogen is the lightest fluid with specific weight of 0.07 g/cm³. Crystallized hydrogen with density of 0.088 g/cm³ is also the lightest crystalline substance. As compared to other substances, hydrogen is highly volatile in terms of critical temperatures, densities (in any state of aggregation) and evaporation heats. This is why hydrogen has not been much used so far as fuel for stationary and mobile power plants, although it has the higher caloric power than all the rest of known natural fuels.

There are also other properties of hydrogen impeding its active use as fuel for mobile power plants. Firstly, it is highly explosive. Hydrogen-chlorine mix (1:1) explodes in the daylight, whereas in the darkness hydrogen aggregation with fluor is accompanied by explosion, and the mix of hydrogen and oxygen (2:1) is a detonating gas. Explosivity limits of hydrogen are as follows: with air 4-75 vol. %, with oxygen 4.1-96 vol. %. Self-ignition temperature of hydrogen is 510 °C [1].

Liquid hydrogen is a fluid without colour and taste. It is not toxic but causes strong cold burns due to freezing of tissues.

To apply hydrogen in underwater vehicles for exploration of ocean resources and to meet strict requirements stated to such vehicles in terms of mass and size, it is required to develop a special approach to storage of hydrogen used as fuel for the power plant with electrochemical generators. One of the key requirements here is to make hydrogen storage system more compact than could be achieved by storing the hydrogen in one of its natural states (solid, liquid or gaseous), as well as to mitigate the amount of free hydrogen in the volume of fuel storage and supply system.

The most preferable ways of hydrogen storage aboard underwater vehicles are as follows:

- Balloons with high-pressure oxygen;
- Cryogenic tanks with fluid hydrogen at the temperatures not higher than 20 K;
- Bound hydrogen in alkali metals and hydrid compounds (to be extracted by hydrolysis);
- Bound hydrogen in intermetallic compounds.

Besides, there also exist such innovative and promising developments of hydrogen storage system as carbon tubes and microcapsules.

The most conventional method of hydrogen storage widely used in the industry is high-pressure hydrogen balloons. However, standard metal balloons for liquid hydrogen (even at increased pressures) are not always compact enough. Here, a very interesting solution could be using the balloons made of composite materials, with various volume, shape and design pressure. Such option would provide significant reduction in both weight and volume of underwater vehicles [2].

Despite all the challenges related to generating cryogenic temperatures (not higher than ~ 20 K for hydrogen), such approach remains interesting for shipbuilding application because it does not require any additional systems for generation of hydrogen and ensures at least the minimum amount of initial reagent aboard the vehicle.

Due to advanced heat insulation solutions, cryogenic hydrogen storage systems are better than conventional metal balloons in terms of specific mass. Application of liquefaction plants allows recovery of evaporating hydrogen into the initial tank. Along with it, such method is rather energy-consuming.

The main principles for extraction and storage of the bound hydrogen from hydric compounds are as follows:

- Hydrolysis of alkali metals;
- Hydrolisis of metallic hydrids;
- Conversion of diesel fuel.

Chemical reactivity of hydrogen is due to the following factors: low atomic radius, low ionization potential, relatively low energy necessary for breaking H-H link.

Hydrolisis of hydrogen from alkali metals is performed using water:

For example, overall reaction for magnesium is as follows:



The reaction requires temperature between 50 and 100°C and weak water solution of acid. Upon completion of hydrolysis, 1 kg magnesium provides about ~ 0.083 kg of hydrogen and 2.4 kg magnesium hydroxide Mg(OH)₂. Poor solubility of this hydroxide in water is a restriction for applying such method of obtaining hydrogen aboard ships.

If hydrolysis is performed on a metallic hydride, i.e., a compound of a metal and hydrogen, the amount of hydrogen per 1 kg of initial substance will grow because hydrogen will be extracted not

only from water but from the hydride, too. Table 1 provides mass fractions of hydrogen in various hydrides.

Table 1. Metallic, metalloid, aluminium and boron hydrides.

Hydride	Density, g/cm ³	Mass fraction of hydrogen, %	Hydride	Density, g/cm ³	Mass fraction of hydrogen, %
SiH ₄	0.68	22.22	Mg[AlH ₄] ₂	1.05	17.39
AlH ₃	1.45	18.75	Li[BH ₄]	0.681	33.33
BeH ₂	0.8	33.33	Na[BH ₄]	1.074	20.00
LiH	0.78	25.00	Mg[BH ₄] ₂	1.046	26.66
MgH ₂	1.42	14.28	Zr[BH ₄] ₄	1.13	21.05
Li[AlH ₄]	0.917	20.00	Al[BH ₄] ₃	0.544	30.00

Promising option here is using more complicated hydrides of metals and their alloys, such as sodium-aluminium (NaAlH₄) and lithium (LiAlH₄) hydride, as well as boron hydrides of lithium (LiAlH₄), aluminium (Al(BH₄)₃) and sodium (NaBH₄).

Using boron hydride of sodium is of particular interest because here hydrogen can be obtained by warming up the water solution of boron hydride up to the temperatures about 50-70 °C or by applying catalytic dissociation methods.

Boron hydride of sodium NaBH₄ is a colourless crystalline substance with density of - 1074 kg/m³. Upon completion of hydrolysis, 1 kg of boron hydride of sodium provides ~0.20 kg of hydrogen (H₂) and ~1.7 kg of sodium metaborate (NaBO₂). The reaction requires temperatures at least 50°C or a catalyst.

It should be noted that hydrogen storage in "hydrogenic" accumulators allows developing a reversible storage system for required amounts of hydrogen and, due to the properties of materials used for this purpose, provides the following advantages:

- Safe storage of significant amounts of hydrogen at normal operational conditions of an underwater vehicle;
- Required purity of obtained hydrogen due to deliberate hydrogen saturation of the intermetallic alloys that simultaneously purify the hydrogen from various inclusions.

Key and very important disadvantage of such hydride storage system is low mass fraction of hydrogen, i.e., real hydrogen output is not more than 10%.

Extraction of hydrogen from liquid hydrocarbons (i.e., diesel fuel widely used in shipbuilding) is becoming more and more popular. Two-stage oxidation of hydrocarbon fuel (in particular, diesel

fuel) is an advantageous way to obtain hydrogen (in terms of maximum possible output technically and economically achievable for electrochemical generators) with minimum fractions of carbonic oxide, carbon dioxide and sulfur compounds. At the first stage (partial oxidation), with deficit of oxidant (oxygen or air), hydrogen-bearing synthesis gas (mix of hydrogen and carbon monoxide) is generated in a once-through high-temperature reactor. To increase the fraction of hydrogen, this synthesis gas is sent to catalytic oxidation of carbon monoxide with water.

One of the drawbacks of obtaining hydrogen through conversion of diesel fuel, even using efficient catalysts, is that this process takes place only at rather high temperatures (between 400 and 1200°C, depending on selected way of conversion and initial substance), so the hydrogen extraction system must have an additional high-temperature power source with power depending on efficiency of conversion method applied and on required capacity of hydrogen generator.

Promising way of hydrogen storage is using carbon nanotubes that, along with metals and liquids, can be filled with gases and link a lot of hydrogen ensuring its safe storage.

Carbon nanotube is a material obtained through evaporation of a graphite rod due to very high current. To store hydrogen inside such carbon nanotubes, they must be opened, i.e., the lids closing them must be removed. For this purpose, the nanotubes must be put into acid so that the lid came off. Then the tube must be dried and filled with high-pressure hydrogen. The whole process takes places at the temperature of liquid nitrogen, although there exist some preliminary developments for building up the technology of hydrogen storage at room temperature.

Today, there are ongoing intense researches of the ways to increase hydrogen-carbon ratio with accumulation of practicable amounts of hydrogen to be used in fuel cells of vehicles or in large or small stationary power plants [3].

It could also be promising to store hydrogen in microspheres. For example, there is a known way to accumulate hydrogen in glass microspheres with diameter of 5-200 μm and wall thickness of 0.5-5 μm . At the temperature of 200-400 °C and increased pressure, the hydrogen actively diffusing through the walls fills the microspheres and stays inside them after cooling. Diffusion losses of hydrogen for such storage mode are about 0.5% per day. The losses at room temperature might be reduced by 10-100 times if microspheres are covered with metal films.

Considerable drawback of these hydrogen accumulation methods is that charging of carbon nanotubes and accumulators with microspheres requires high pressure and increased temperature of hydrogen. These methods are hardly practicable due to complicated technology of hydrogen extraction and insufficient development of real system parameters.

Fig. 1 provides specific volume and mass parameters for various hydrogen storage systems with electrochemical generators for underwater exploration vehicles.

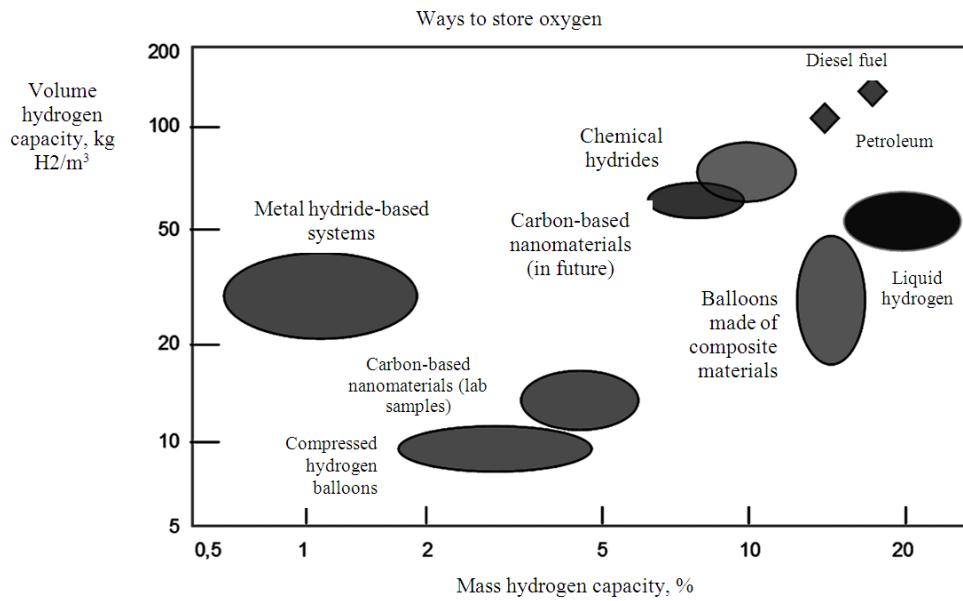


Fig. 1 – Specific volume and mass parameters of various hydrogen storage system in application to power plants with electrochemical generators

REFERENCES

GOST R 51673-2000. Hydrogen, gaseous, pure. Technical conditions. (in Russian)

2. A. Koroteev, V. Mironov, V. Smolyarov. Prospects of using hydrogen in vehicles // International scientific journal Alternative power and environment, issue No. 1, 2004, pp. 5-13. (in Russian)

3. R. Ivanov. Practicable areas of applying power plants with hydrogen-oxygen electrochemical generators for submarines. Transction of All-Russian Conference Fuel-cell and their application in power plants. Moscow, Chernogolovka, 2013 (in Russian).